



IMPERIAL INSTITUTE
OF
AGRICULTURAL RESEARCH, PUSA.

PROCEEDINGS

OF THE

ROYAL SOCIETY OF LONDON

SERIES A

CONTAINING PAPERS OF A MATHEMATICAL AND
PHYSICAL CHARACTER.

VOL. CXXXI.

LONDON:

PRINTED FOR THE ROYAL SOCIETY AND SOLD BY
HARRISON AND SONS, LTD., ST. MARTIN'S LANE,
PRINTERS IN ORDINARY TO HIS MAJESTY.

JUNE, 1931.

LONDON:

HARRISON AND SONS, LTD., PRINTERS IN ORDINARY TO HIS MAJESTY,
ST. MARTIN'S LANE

CONTENTS.

SERIES A. VOL. CXXXI.

No. 816.—April 21, 1931.

	PAGE
Explosions of Mixtures of Acetylene and Electrolytic Gas. By W. A. Bone, F.R.S., R. P. Fraser and F. Lake. (Plates 1-3.)	1
The Adsorption of Substances by Fuller's Earth. By H. J. Phelps. Communicated by C. N. Hinshelwood, F.R.S.	17
The Solution of the Torsion Problem for Circular Shafts of Varying Radius. By A. Thom and J. Orr. Communicated by R. V. Southwell, F.R.S.	30
The Diurnal Tide in an Ocean bounded by Two Meridians. By D. C. Colborne. Communicated by G. R. Goldsbrough, F.R.S.	38
The Pressure Exerted by Granular Material: an Application of the Principles of Dilatancy. By C. F. Jenkin. (Plate 4.) Communicated by Sir Alfred Ewing, F.R.S.	53
The Upper Limit of Energy in the Spectrum of Radium E. By F. R. Terroux. (Plate 5.) Communicated by Lord Rutherford, F.R.S.	90
The Arithmetically Reduced Indefinite Quadratic Form in n -Variables. By L. J. Mordell, F.R.S.	99
The Spectrum of Singly Ionised Antimony. By D. G. Dhavale. Communicated by M. N. Saha, F.R.S.	109
The Development of a High Speed Wind Channel for Research in External Ballistics. By Sir Thomas E. Stanton, F.R.S. (Plate 6.)	122
The Effect of Combined Electric and Magnetic Fields on the Helium Spectrum.—II. By J. S. Foster. (Plates 7 and 8.) Communicated by A. S. Eve, F.R.S.	133
✓ Stark-Effect in Molecular Hydrogen in the Range 4100-4770 Å. By J. K. L. MacDonald. (Plate 9.) Communicated by A. S. Eve, F.R.S.	146
Investigations on the Spectrum of Selenium. Part I.—Se IV and Se V. By K. R. Rao and J. S. Badami. (Plates 10 and 11.) Communicated by A. Fowler, F.R.S.	154
A Metrical Theory and its Relation to the Charge and Masses of the Electron and Proton. By H. T. Flint. Communicated by O. W. Richardson, F.R.S.	170

	PAGE
The Kinetics of Reactions in Solution. Part I.—A Comparison of the Decomposition of Chlorine Monoxide in the Gaseous State and in Carbon Tetrachloride Solution. By E. A. Moelwyn-Hughes and C. N. Hinshelwood, F.R.S.....	177
The Kinetics of Reactions in Solution. Part II.—The Decomposition of Trinitrobenzoic Acid in Various Solvents. By E. A. Moelwyn-Hughes and C. N. Hinshelwood, F.R.S.....	186
The Forces on a Solid Body Moving through Viscous Fluid. By S. Goldstein. With notes in the text by J. M. Burgers. Communicated by H. Jeffreys, F.R.S.....	198
The Magnetic Susceptibility of Binary Systems of Organic Liquids. By Miss V. C. G. Trew and J. F. Spencer. Communicated by W. Wilson, F.R.S.	209
The Study of the Magnetic Properties of Matter in Strong Magnetic Fields.—I. The Balance and its Properties. By P. Kapitza, F.R.S. (Plate 12.)	224
The Study of the Magnetic Properties of Matter in Strong Magnetic Fields. Part II.—The Measurement of Magnetisation. By P. Kapitza, F.R.S. (Plate 13.)	243
The Antiseptic and Trypanocidal Action of certain Styryl and Anil Benzthiazole Derivatives. By C. H. Browning, F.R.S., J. B. Cohen, F.R.S., S. Ellingworth and R. Gulbransen. (Abstract.)	273
Some Aliphatic and Aromatic Amino Derivatives of α -Quinoline Methiodide. By J. B. Cohen, F.R.S., K. E. Cooper and P. G. Marshall. (Abstract.)	274

No. 817.—May 1, 1931.

The Wave Resistance of a Spheroid. By T. H. Havelock, F.R.S.	275
On Twisted Cubic Curves which satisfy Twelve Conditions. By J. A. Todd. Communicated by H. F. Baker, F.R.S.	286
On the Transmission of Light by Thin Films of Metal. By S. Rama Swamy. (Plate 14.) Communicated by W. Wilson, F.R.S.	307
On the Thermal Conductivity of some Metal Wires. By W. G. Kannuliuk. Communicated by Lord Rutherford, F.R.S.	320
Material and Radiational Waves. By A. M. Mosharrafa. Communicated by O. W. Richardson, F.R.S.	335
The Chemical Constant of Chlorine Vapour and the Entropy of Crystalline Chlorine. By T. E. Stern. Communicated by R. H. Fowler, F.R.S.	339
The Velocity of Corrosion from the Electrochemical Standpoint. By U. R. Evans, L. C. Bannister and S. C. Britton. Communicated by Sir Harold Carpenter, F.R.S.	355
On a Night Sky of Exceptional Brightness, and on the Distinction between the Polar Aurora and the Night Sky. By Lord Rayleigh, For. Sec. R.S. (Plate 15.)	376

The Behaviour of Electrolytes in Mixed Solvents. Part III.—The Molecular Refractivities and Partial Molar Volumes of Lithium Chloride in Water-Ethyl Alcohol Solutions. By J. A. V. Butler and A. D. Lees. Communicated by J. Kendall, F.R.S.	382
Valve Methods of Recording Single Alpha-Particles in the presence of Powerful Ionising Radiations. By C. E. Wynn-Williams and F. A. B. Ward. Communicated by Lord Rutherford, F.R.S.	391
Viscosity and Rigidity in Suspensions of Fine Particles. I.—Aqueous Suspensions. By C. M. McDowell and F. L. Usher. Communicated by R. Whytlaw-Gray, F.R.S.	409
Optical and Equivalent Paths in a Stratified Medium, Treated from a Wave Standpoint. By D. R. Hartree. Communicated by E. V. Appleton, F.R.S.	428
The Scattering of Light by Turbid Media.—Part I. By J. W. Ryde. Communicated by R. H. Fowler, F.R.S.	451
The Scattering of Light by Turbid Media.—Part II. By J. W. Ryde and B. S. Cooper. Communicated by R. H. Fowler, F.R.S.	464
X-Ray Nondigram Lines. By G. B. Deodhar. Communicated by O. W. Richardson, F.R.S.	476
The Theory of Metallic Corrosion in the Light of Quantitative Measurements.—Part IV. By G. D. Bengough, A. R. Lee and F. Wormwell. (Plates 16–22.) Communicated by Sir Harold Carpenter, F.R.S.	494

No. 818.—June 3, 1931.

On the Periodicity in Series of Related Terms. By Sir Gilbert Walker, F.R.S.	518
Ethyl Alcohol, A Product of High Pressure Syntheses. By G. T. Morgan, F.R.S., and R. Taylor	533
The Decay Constant of Uranium II. By C. H. Collie. Communicated by F. A. Lindeman, F.R.S.	541
The Reflection of Vapour Molecules at a Liquid Surface. By T. Alty. (Plate 23.) Communicated by Sir Joseph Thomson, F.R.S.	554
Viscosity and Rigidity in Suspensions of Fine Particles. II.—Non-Aqueous Suspensions. By C. M. McDowell and F. L. Usher. (Plates 24–26.) Communicated by R. Whytlaw-Gray, F.R.S.	564
The Colloid Chemistry of Dyes : the Aqueous Solutions of Benzopurpurine 4B and its Isomer prepared from <i>m</i>-Tolidine.—Part I. By C. Robinson and H. A. T. Mills. Communicated by F. G. Donnan, F.R.S.	576
The Colloid Chemistry of Dyes : the Aqueous Solutions of Benzopurpurine 4 B and its Isomer prepared from <i>m</i>-Tolidine.—Part II. By C. Robinson and H. A. T. Mills. Communicated by F. G. Donnan, F.R.S.	596

The Molecular Symmetry of Hexa-aminobenzene in the Crystalline State, and certain other Properties of the Substance. By I. E. Knaggs. (Plate 27.) Communicated by Sir William Bragg, F.R.S.	612
An X-Ray Study of Mannitol, Dulcitol, and Mannose. By T. C. Marwick. (Plate 28.) Communicated by Sir William Bragg, F.R.S.	621
Some Investigations in Röntgen Spectra. Part I.—X-Ray Spark Lines. By G. B. Deodhar. (Plate 29.) Communicated by O. W. Richardson, F.R.S.	633
Some Investigations in Röntgen Spectra. Part II.—X-Ray Spectra and Chemical Combination. Sulphur. By G. B. Deodhar. (Plates 30, 31.) Communicated by O. W. Richardson, F.R.S.	647
Some Investigations in Röntgen Spectra. Part III.—Fine Structure of K-Absorption Edge of SiO_2 . By G. B. Deodhar. Communicated by O. W. Richardson, F.R.S.	654
The Spectrum of H_2 .—The Bands ending on $2p^3\Pi$ Levels. By O. W. Richardson, F.R.S., and P. M. Davidson	658
Analysis of the Long Range α -Particles from Radium C. By Lord Rutherford, F.R.S.	684

OBITUARY NOTICES.

Alfred Barnard Basset	i
Lord Melchett (with portrait)	ii
Sir Charles Parsons (with portrait)	v
Index	xxvii

PROCEEDINGS OF THE ROYAL SOCIETY.

SECTION A.—MATHEMATICAL AND PHYSICAL SCIENCES.

Explosions of Mixtures of Acetylene and Electrolytic Gas.

By W. A. BONE, D.Sc., F.R.S., R. P. FRASER, A.R.C.S., D.I.C., and F. LAKE,
B.Sc., A.R.C.S., D.I.C.

(Received October 27, 1930.)

[PLATES 1-3.]

In a previous paper from our laboratories* it was stated that successive additions of acetylene to electrolytic gas had been found on explosion to have a peculiar disturbing influence upon the uniformity of the initial flame movement, reaching a maximum when the percentage of acetylene in the medium amounts to 20, but subsiding with further additions and eventually disappearing when the acetylene exceeds 30 per cent. In the present paper the results of further investigations of the matter will be described.

EXPERIMENTAL.

A. *The Experimental $x\text{C}_2\text{H}_2/(100 - x)(2\text{H}_2 + \text{O}_2)$ Mixtures.*

These mixtures were made up accurately by adding highly purified acetylene (x being successively increased from 0 up to 65) to pure electrolytic gas in a gas-holder over mercury. Chemical analyses showed that in no case did any adventitious nitrogen present exceed 0.2 per cent. The mixtures were subsequently fired moist in the explosion tubes at 15° C. and barometric pressure.

Among the series of mixtures investigated, those corresponding with (i) $\text{C}_2\text{H}_2 + 5\text{H}_2 + 2\frac{1}{2}\text{O}_2$ ($\text{C}_2\text{H}_2 = 11.8$ per cent.), (ii) $\text{C}_2\text{H}_2 + 3\text{H}_2 + 1\frac{1}{2}\text{O}_2$ ($\text{C}_2\text{H}_2 = 18.2$ per cent.), and (iii) $\text{C}_2\text{H}_2 + 2\text{H}_2 + \text{O}_2$ ($\text{C}_2\text{H}_2 = 25.0$ per cent.) were especially interesting, because, assuming a preferential burning of acetylene, which in fact occurs, (i) contained just sufficient oxygen for completely

* 'Proc. Roy. Soc.,' A, vol. 114, p. 431-32 (1927).

burning all the hydrocarbon to carbon dioxide and steam, (ii) to burn it all to carbonic oxide and steam, and (iii) to burn it all to carbonic oxide and hydrogen.

B. *The Explosion Tubes and General Procedure.*

(1) Our usual procedure was to make two or more firing trials with each mixture in a horizontal tube (fig. 1) of 2.5 cm. uniform internal diameter and

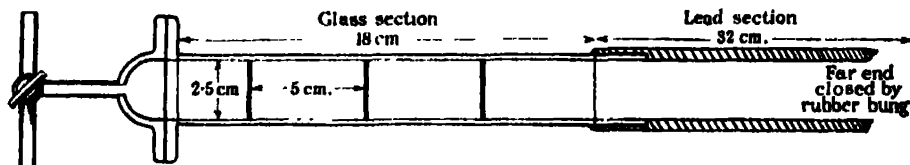


FIG. 1.—Explosion Tube.

50 cm. long, composed of a glass section 18 cm. and a lead section 32 cm. long, the former having a flanged open end, and the latter being closed at its far end with a rubber bung. There were the usual "reference marks" 5 cm. apart on the outside of the glass section.

At the outset of each trial the flanged open end of the glass section was closed by a glass mouth-piece carrying a 3-way glass tap of 3 mm. bore, through one branch of which connection was made by a glass tube to a "Hyvac" pump capable of quickly evacuating the tube down to 1/10 mm., and through the other with the mercury gas holder containing the experimental mixture. In each case the explosion tube was filled with the moist experimental mixture at a slightly higher (2 to 3 mm.) pressure than the barometric. Ignition was subsequently effected by gently sliding off the mouth-piece and applying a 2-cm. high coal-gas (batswing) flame, the utmost care being taken to do so without imparting any sensible impulse to the gaseous medium, which would thus be fired in a quiescent condition at atmospheric pressure and room temperature, the latter being almost uniform at 15° C.

The progress of the flame along the horizontal tube was photographed, by means of a Fraser high-speed photographic machine on a highly sensitive film rotated in a vertical plane, using a very fast Zeiss lens $f/1.4$, of 7 cm. focal length. In such-wise systematic photographic records of the explosion flames were obtained, two successive explosions with the same mixture usually being recorded on one and the same film.

(2) Concurrently with the foregoing "open tube" explosions, another series was made with corresponding mixtures in cylindrical closed tubes (fig. 2) —2 cm. internal diameter and 35 cm. long, fixed horizontally—each mixture

being fired moist at a pressure of about 400 mm. by means of a condenser discharge of 1 microfarad at 210 volts across the platinum balled electrode

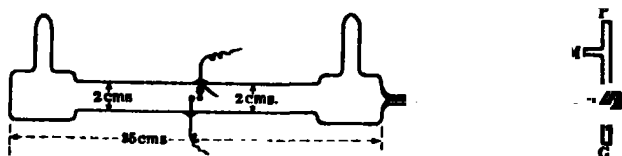


FIG. 2.—Explosion Tube.

situated mid-way along the tube. The course of each explosion was also followed photographically, and finally the cold gaseous explosion-products were withdrawn for analysis.

(3) *Records of Results.*—In what follows, experiments made under condition (1) will be referred to as the “open-tube,” and those under condition (2) as the “closed-tube,” explosions. The symbol *S* will be used to denote “flame-speeds” (S_1 = the initial speed, and S_2 , etc., subsequent speeds, those which were not uniform for an appreciable time, but only mean speeds between two selected points, being distinguished by an asterisk); while T.D. will be used to denote the total duration in milliseconds of the explosion luminosity so far as it affected the film. Where two or more explosions with the same mixture have been recorded on one film, they will be distinguished by the letters *a*, *b* and *c*.

C. *The Open-tube Explosions with $x\text{C}_2\text{H}_2/(100-x)(2\text{H}_2+\text{O}_2)$ Mixtures.*

Explosions were made of altogether 18 different mixtures of acetylene-content varying from 0 to 65 per cent. with results as shown in photographs Nos. 1 to 15 inclusive.* Throughout the first 11 of them—excepting No. 8, which was made with a 30 instead of a 50 cm. long tube—the vertical film speed was kept constant at 1450 cm. per second so that variations in the angles subtended in the photographs afford direct evidence of changes in the flame-speeds. For mixtures containing more than 22 per cent. of acetylene, however, the film-speed had to be adjusted to suit the flame-speed in each case.

Initial Flame Speeds.—In fig. 3 the observed initial flame speeds in centimetres per second are plotted against percentages of acetylene in the mixture fired; and, together with any subsequent flame speed observed and the total duration of luminosity in each explosion, they are also shown in Table I.

* Actually only the first 15 out of the whole 18 photographs taken are reproduced in this paper, the phenomena behind the flame fronts in Nos. 16, 17 and 18 being obscured by a copious deposit of carbon.

From the photographs (Plate 1 to 3), fig. 3, and Table I, it will be seen that, while the effect of adding the first 1 per cent. of acetylene to electrolytic

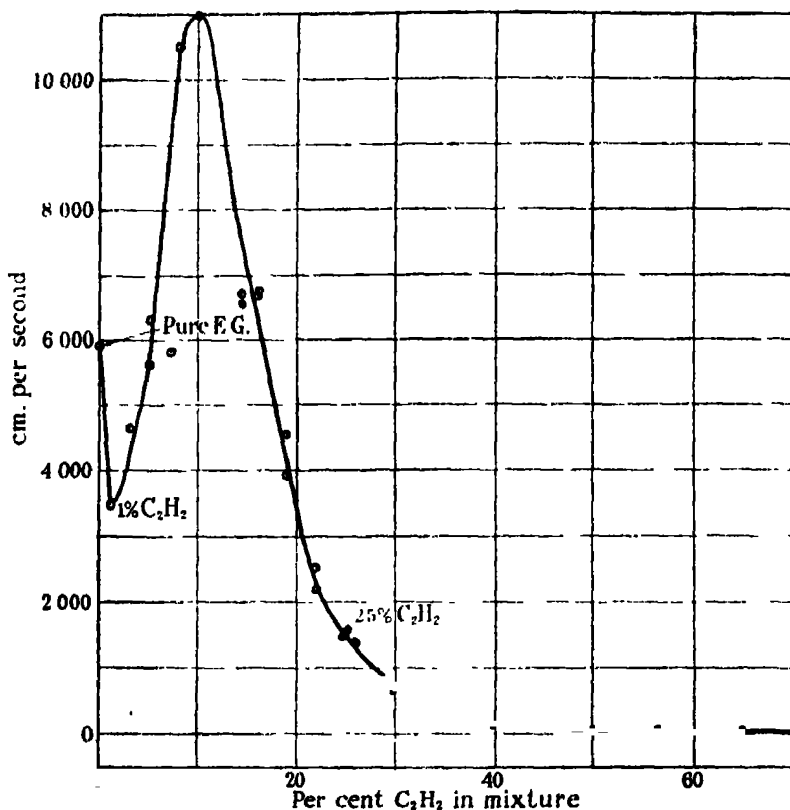


FIG. 3.—Initial Flame Speed in the $x\text{C}_2\text{H}_2/(100 - x)(2\text{H}_2 + \text{O}_2)$ "Open Tube" Explosion.

gas was to reduce the initial flame speed considerably, further additions up to about 11.8 per cent. had the opposite effect. The highest speeds were observed with the mixtures containing between 8 and 11.8 per cent. of acetylene, the maximum apparently being near the $\text{C}_2\text{H}_2 + 5\text{O}_2 + 10\text{H}_2$ composition ($\text{C}_2\text{H}_2 = 11.8$ per cent.)* when the oxygen present would just suffice to burn the hydrocarbon completely to carbon dioxide and steam. On further increasing the acetylene content, both the initial and the general flame speeds rapidly diminished until the 40- C_2H_2 /60-electrolytic gas mixture was reached, after which they diminished much more slowly.

* It is difficult to say precisely where the maximum speed occurred, because near the apex of the speed-composition curve (fig. 3) the mixtures are so very "sensitive" and fast-burning, that the observed initial flame speeds were rarely uniform enough for accurate measurements, and therefore towards its apex the curve becomes conjectural.

Table I.—Results of $x\text{C}_2\text{H}_2/(100-x)(2\text{H}_2+\text{O}_2)$ Explosions in Open Tubes.

Photograph No.	Percentage C_2H_2 in mixture.	S_x cm. per sec.		S_s cm. per sec.		T.D. milliseconds.	Remarks.
		(a)	(b)	(a)	(b)	(a)	(b)
1	nil	6,000	5,960	—	—	11.3	—
2	1.0	3,320	3,500	6,420	7,400	7.73	9.2 5.9 The first 1 per cent. of C_2H_2 caused a marked decrease in initial flame speed.
3	3.0	4,680	4,600	8,500	8,160	5.9	5.0
4	5.0	5,650	6,300	vibrational		6.7	5.5
5	8.0	5,810	10,500	—	16,750	—	4.0
6	11.8	12,230*	10,900*	—	—	4.1	4.1
7	14.3	7,840*	7,810*	—	—	5.65	5.5
8	15.0	[5590]	—	[8390]	—	—	—
9	16.0	6,780	6,700	—	—	—	6.4
10	19.0	4,570	3,940	irregular	—	—	7.6
11	23.0	2,530	2,200	—	—	—	10.0
		(a)	(b)	(c)			
12	25.0	1,530	1,566	1,590	irregular and strongly vibrational	—	—
13	26.0	1,390	1,400	—	irregular and strongly vibrational	—	—
14	30.0	685	728	—	—	—	58
15	40.0	134	111	—	—	—	405
	50.0	40	39.8	—	—	—	—
	57.0	36.5	36.2	—	—	—	—
	65.0	32	31.7	—	—	—	—

NOTES.—(1) Speeds shown in brackets [No. 8], are not in line with the others, because explosion was made in a 30, instead of a 50-cm. tube.

(2) No carbon separation in any of the explosions 1 to 12 inclusive.

(3) In No. 12 combustion occurred in accordance with $\text{C}_2\text{H}_2 + \text{O}_2 + 2\text{H}_2 = 2\text{CO} + 3\text{H}_2$.

Homogeneous flame-fronts, and uniform initial flame-speeds; thermal decomposition of excess C_2H_2 over 25 per cent., causes carbon separation, and prolonged and diffuse luminosity.

Flame front very thin and compact, with little or no after-burning. No carbon deposition.

Separation of carbon in flame front begins.

Flame speeds and luminosities progressively diminish with increasing C_2H_2 content. Flame front becomes heterogeneous, and develops pronounced feathery appearance.

Rapid increase in flame speeds and luminosity in flame front, with increasing C_2H_2 content. Flame fronts compact and fairly homogeneous.

Duration of Luminosity.—The total duration of luminosity progressively diminished with each successive addition of acetylene until it reached a minimum with mixtures containing somewhere between 8 and 11·8 per cent. of acetylene. Several of the photographs with mixtures containing up to 15 per cent. (but not higher) of acetylene show the highly luminous track of "compression waves" reflected from the far end of the tube, passing through the medium after the original luminescence had become feeble or in one or two cases (*e.g.*, Nos. 7 and 8) almost inappreciable.

Carbon Deposition.—It is important to note that no carbon deposition was ever observed on explosion of any mixture containing 25 per cent. or less of acetylene, *i.e.*, in any whose acetylene content was below the $C_2H_2 + O_2 + 2H_2$ proportion, the combustion of which was in accordance with the equation



As soon, however, as the acetylene content exceeded this limit, carbon deposition could be observed in a degree dependent upon the amount of acetylene in excess of 25 per cent.

Photographic Analyses.—The chief interest of the flame photographs lies in what they reveal concerning the character of the flame front in each case and the homogeneity or otherwise of the still-burning luminous medium behind it.

No. 1 (Plate 1).—The two photographs in No. 1 for pure electrolytic gas showed almost the same initial flame speeds (*circa* 6000 cm. per second) and general character of the first 13 cm. of the flame movements. In each case there was also an evenness about the luminosity, both in the flame front and in the medium behind it, indicative of a homogeneous and fairly prolonged combustion, although its total duration was only about 10 milliseconds. Combustion was not completed in the flame front, but continued behind it for about 0·01 second, this being about 10 times that observed in the explosion wave after detonation has been set up in electrolytic gas.*

No. 2 (Plate 1).—The addition of 1 per cent. of acetylene to the electrolytic gas caused not only a marked decrease in the general flame speed, but also a tendency for the initial uniform speed to be abruptly succeeded by another; this second speed, after remaining uniform for a while, subsequently became

* Dr. G. S. Turpin found 0·001 second as the maximum time during which the medium behind the flame front conducts electricity after detonation has been set up in electrolytic gas ('Studies from the Physical and Chemical Laboratories of the Owens College, 1893, p. 283 to p. 295); and in our laboratories 0·00075 second has been found as the total duration of luminosity under such conditions.

irregular. No. 2b shows a well-marked "reflection wave" extending to well outside the open end of the tube.

No. 3 (Plate 1).—Further increase in the acetylene-content to 3 per cent. caused a marked increase in the average flame velocity, together with a continued tendency to an abrupt change from a lower to a higher uniform flame speed; and in the case of No. 3b this tendency was accompanied by the development of greater luminosity in the flame front.

Nos. 4 to 6 inclusive (Plates 1, 2).—With still further increases in the acetylene content up to 11.8 per cent., the foregoing tendencies markedly increased. The flame front acquired a brilliant luminosity, and the medium immediately behind it became non-homogeneous, as shown by the appearance in the photographs of fine hair-like striæ, betokening backward movements of fine streams of incandescent matter originally in the flame-front. The initial flame speeds generally reached their maxima, and the total durations of luminosity their minima, at about the $C_2H_2 + 2\frac{1}{2}O_2 + 5H_2$ ($C_2H_2 = 11.8$ per cent.) composition, which apparently marked a "transition stage" in the series; for afterwards both the general flame speeds and the luminosity of the flame-front diminished, and the total duration of luminosity increased, as the acetylene-content of the medium was raised.

Nos. 7 to 11 inclusive (Plates 2, 3).—As more acetylene was added to the medium, and within the composition-range $C_2H_2 + 2\frac{1}{2}O_2 + 5H_2$ to $C_2H_2 + O_2 + 2H_2$, the hitherto homogeneous flame front became more or less heterogeneous, showing a tendency towards burning "in layers" with a pronounced "feathery" appearance behind it. Also, immediately after the 14.3 per cent. C_2H_2 -content had been passed, the actual flame front became decidedly less luminous. These features are particularly well marked in photographs Nos. 8 to 11 inclusive, namely for mixtures containing between 14.3 and 22 per cent of acetylene, whose compositions ranged equidistantly round $C_2H_2 + 1\frac{1}{2}O_2 + 3H_2$ ($C_2H_2 = 18.2$ per cent.). Other noteworthy features are the highly luminous "reflected waves" (from the far stoppered end of the explosion tube) passing through the medium in Nos. 7 and 8 long after the flame front had passed, and (in No. 8) after the original luminosity had almost ceased.

No. 12 (Plate 3).—In this photograph of three separate explosions in a $C_2H_2 + O_2 + 2H_2$ medium ($C_2H_2 = 25$ per cent.), each flame front appears very thin and compact, with remarkably little burning behind it. The initial flame speeds were nearly uniform and constant at a mean of about 1575 cm. per second, the mixtures burning without any separation of carbon or appreciable steam formation in accordance with the equation



N^o 6.

11.82
C₁H₂

N^o 8

152
C₁H₂

N^o 10

192
C₁H₂



N^o 5.

82
C₁H₂

7. 52
x

N^o 9

162
C₁H₂

N^o 13.
26 1/2 C.M.

N^o 14.
✓ 30 1/2 C.M.



N^o 15.
25 1/2 C.M.

N^o 16.
25 1/2 C.M.

N^o 17.
22 1/2 C.M.

N^o 18.
25 1/2 C.M.

N^o 19.
25 1/2 C.M.

N^o 20.
25 1/2 C.M.

Measurements were always made of the initial firing pressure, P_i , the final pressure of the cold products, P_f ; and after "correcting" these to "dry gas at 15° C." the ratio P_f/P_i in each case was calculated. Both the original mixtures and the final gaseous products were carefully analysed, and from the analytical results, combined with the pressure data, were deduced the carbon-hydrogen-oxygen balances for the original mixtures and cold gaseous products in each explosion. These balances enabled the relative proportions of steam as well as the ratios $\text{CO} \times \text{OH}_2/\text{CO}_2 \times \text{H}_2$ in the final combustion products (before condensation of steam) to be calculated.

Initial Flame Speeds.—It was also possible to deduce an approximate figure for the mean initial flame speed over the first 10 cm. run from the igniting spark in each case. These figures, while of relative value only, confirmed generally

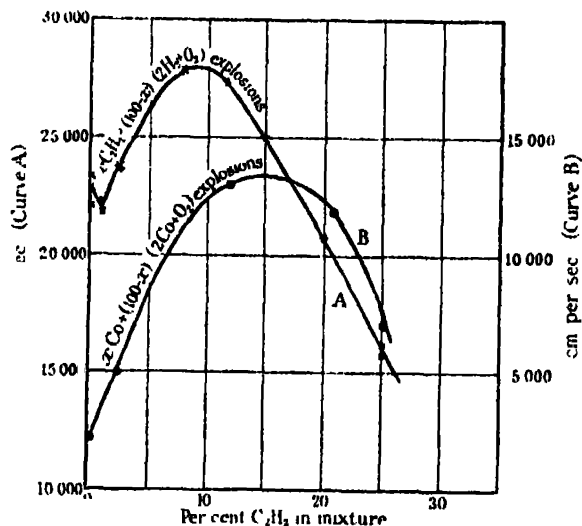


FIG. 4.—Initial Flame Speeds in "Closed Tube" Explosions.

the trend of the initial flame speeds in the corresponding "open-tube" explosions.

Analytical Data.—The chief value of the experiments lay, however, in the evidence afforded by the analytical data concerning the chemical features of the combustion as the amount of acetylene in the original mixture was progressively increased from 0 to 30 per cent.

First of all, they confirmed our previous observation that not until the acetylene present exceeded 25 per cent., or the $\text{C}_2\text{H}_2 + \text{O}_2 + 2\text{H}_2$ proportion, did any free carbon particles aggregate and separate out in the explosion. For it will be seen from the results shown in Table II that in every case up to

Table II.—Results of "Closed Tube" $x\text{C}_2\text{H}_2/(100 - x)(2\text{H}_2 + \text{O}_2)$ Explosions.

Percentage composition of original mixture.			Initial firing pressure P_f mm.		Pressure of dry gaseous products P_f/P_v mm.		Percentage composition of dry gaseous products.				C, H_2 and O_2 balances.			$\frac{O_2}{H_2} \times \frac{H_2}{O_2}$		Induction period milliseconds.	Mean flame speed, to first shoulder cm./sec.	T.D. millise.
C_2H_2	H_2	O_2	P_f mm.	Pressure of dry gaseous products P_f/P_v mm.	CO_2	CO	H_2	C_2H_2	(a) Units in initial mixture. H_2O in products mm. (b) Units in gaseous products.	C.	H_2	O_2						
—	66.6	33.3	396.0	—	—	—	—	—	—	—	—	—	—	—	—	0.058	22,060	5.65
1.00	66.0	33.0	391.6	28.7	0.073	no analysis made			{	{	{	{	{	{	{	{	{	{
1.25	65.8	32.9	391.7	27.4	0.070													
2.5	65.0	32.5	397.8	68.3	0.172	6.8	21.4	71.8	nil	(a) 19.8 (b) 19.3	268 49	130 12	227	{	14.6 (22.7)	—	23,820	3.9
8.1	61.2	30.6	390.3	169.3	0.432	9.5	27.5	62.9	nil	(a) 63.1 (b) 62.7	270 106	120 40	162	{	4.75	—	27,880	3.4
11.7	58.8	29.4	397.3	246.5	0.621	6.8	30.6	62.5	nil	(a) 93 (b) 92	280 154	117 55	125	{	4.05 (3.94)	0.07	27,420	2.9
14.4	57.0	28.5	401.8	298.2	0.743	5.0	33.0	61.9	nil	(a) 116 (b) 114	287 185	115 64	102	{	4.1	0.07	25,050	2.8
20.0	53.3	26.7	397.7	410.9	1.033	2.1	37.2	60.7	nil	(a) 159 (b) 162	291 249	106 85	42	{	3.95	0.04	20,700	2.75
25.0	50.0	25.0	391.8	490.1	1.252	0.4	39.55	59.9	nil	(a) 196 (b) 196	293 293	98 99	nil	{	—	0.137	15,720	1.65
29.8	46.7	23.3	413.9	510.0	1.23	0.5	36.8	60.0	2.4	(a) 246 (b) 215	317 318	96 96	nil	{	—	—	—	—

such limit the whole of the carbon originally contained as acetylene in the mixture fired appeared as oxides of carbon in the products.

Secondly, they confirmed the observation originally made in 1906 by W. A. Bone and J. Drugman* that in the explosion of a $C_2H_2 + O_2 + 2H_2$ mixture neither is carbon deposited nor steam formed, the combustion conforming to the equation



Finally they show that in the combustion of $x C_2H_2 / (100 - x)(2H_2 + O_2)$ mixtures, where x exceeds some small value very much below 8, (i) the acetylene is preferentially burnt in the flame front to carbonic oxide and hydrogen, (ii) any excess of oxygen is then distributed between the carbonic oxide and hydrogen in the medium behind it in accordance with the principle of "mass action," and (iii) only when acetylene is originally present in excess of the $C_2H_2 + O_2 + 2H_2$ proportion does any of it either escape combustion or deposit carbon in the flame.

It was only where x was smaller than a certain as yet undetermined value much below 8 that the relative proportion of hydrogen finally appearing as steam in the resultant products exceeded that corresponding with the $CO \times OH_2 / CO_2 \times H_2$ equilibrium, which in such circumstances was certainly not attained.†

E. Explosions of a $C_2H_2 + O_2 + 2H_2$ Mixture when Diluted with Argon or Nitrogen.

The fact that on exploding a $C_2H_2 + O_2 + 2H_2$ mixture the whole of the acetylene burns to carbonic oxide and oxygen leaving the hydrogen entirely intact—there being neither any carbon separation nor steam formation—is one of the most striking in the whole range of the science of combustion. It shows that in combustion "selective affinity" plays a part which cannot be ignored. For here acetylene monopolises the whole of the oxygen even in the presence of twice its own volume of hydrogen.

Being curious to know how this phenomenon might be affected by a lowering

* 'J. Chem. Soc.', vol. 89, pp. 669-676 (1906).

† In connection with this statement it should be remembered that when a system containing oxides of carbon, hydrogen and steam is cooling down after an incomplete combustion in gaseous explosions, the equilibrium ratio $CO \times OH_2 / CO_2 \times H_2$ adjusts itself automatically with the falling temperature until some point, usually between 1400 and 1600° C. (dependent upon the cooling powers of the walls of the containing vessel) is reached, when it "freezes out." In glass vessels this usually occurs when $CO \times OH_2 / CO_2 \times H_2 = \text{circa } 4.0$, corresponding with a temperature of *circa* 1650°.

of the general flame temperature by dilution with an inert gas, we asked Dr. D. S. Chamberlin, of Lehigh University, who was then working in our laboratories, to make experiments in which mixtures corresponding with $C_2H_2 + O_2 + 2H_2 + 4Ar$ and $C_2H_2 + O_2 + 2H_2 + 4N_2$, respectively, were exploded at atmospheric pressure by an electric spark in hermetically sealed glass bulbs of about 80 c.c. capacity.

We were surprised to find that, whereas such dilution with argon made not the slightest difference in the result—the mixture exploding with a bluish flame unaccompanied by any carbon deposition or steam formation—a corresponding dilution with nitrogen visibly caused both carbon separation and steam formation, whence it was evident that the nitrogen was no mere inert diluent but had exerted a chemical influence upon the end results.

Thus for example, (a) whereas in the $C_2H_2 + O_2 + 2H_2 + 4Ar$ explosion the final pressure (p_f) of the cold products was 10 per cent. higher than that of the original mixture at the same temperature, and the whole of the carbon and oxygen originally present was accounted for as oxides of carbon in the gaseous products (there being neither carbon separation nor visible steam formation), in accordance with the equation



(b) in the corresponding $C_2H_2 + O_2 + 2H_2 + 4N_2$ explosion, where both visible carbon separation and steam formation occurred, the final pressure (p_f) of the cold products was only 2 per cent. higher than that of the original mixture, and only about 90 per cent. of the carbon and 86 per cent. of the oxygen originally present appeared in the gaseous products, the remainder appearing as either free carbon or steam.

F. Comparative "Closed Tube" Explosions with Moist $x C_2H_2 / (100 - x) (2CO + O_2)$ Mixtures.

Before completing our experiments, we thought it advisable to carry out a comparative series of "closed tube" explosions with $x C_2H_2 / (100 - x) (2CO + O_2)$ mixtures, to see whether the replacement of the hydrogen of the electrolytic gas by carbonic oxide in a $x C_2H_2 / (100 - x) (2H_2 + O_2)$ explosion would materially affect the result so far as the "selective burning" of the acetylene was concerned.

Accordingly, starting with the explosion of a moist $2CO + O_2$ mixture, we studied the effect of gradually adding up to 30 per cent. acetylene to it, the

Table III.—Results of "Closed Tube" $x\text{C}_2\text{H}_2/(100 - x) (2\text{CO} + \text{O}_2)$ Explosions.

Percentage composition of original mixture.			Initial firing pressure P_f mm. dry.	Pressure of dry gaseous products $\frac{P_f}{P_f^*}$ mm.	$\frac{P_f}{P_f^*}$ free.	Percentage composition of dry gaseous products.					C, H ₂ and O ₂ balances.			Gaseous H ₂ O in products mm.	$\frac{\text{H}}{\text{HO}} \times \frac{\text{H}}{\text{O}}$	Mean flame-speed to first shoulder, cm./sec.
						CO ₂	CO	H ₂	O ₂	C ₂ H ₂	C	H ₂	O ₂			
	C ₂ H ₂	CO	O ₂													
	nil	66.2	33.1	369.9	270	0.688	97.0	0.2	nil	0.4	nil	(a) 262 (b) 262	—	525 526	—	2,200
	2.4	64.5	32.25	398.3	264.8	0.71	82.2	15.25	1.0	nil	nil	(a) 276 (b) 277	—	257 256	—	4,940
	11.96	53.2	29.1	405.5	343.8	0.857	33.3	60.0	5.6	nil	nil	(a) 325 (b) 326	—	237 221	4.0	13,080
	20.8	52.3	26.15	399.2	424.0	1.06	10.6	72.5	15.9	nil	nil	(a) 375 (b) 357	—	208 200	3.0	11,830
	24.75	50.0	25.0	400.5	492.7	1.22	3.0	75.5	20.5	nil	nil	(a) 399 (b) 386	—	100 100	—	7,210
	30.0	46.5	23.3	406.4	501.0	1.23	0.5	74.8	21.85	nil	2.5	(a) 246 (b) 215	—	96* 96	—	—

* Carbon visibly deposited in this experiment, but not in any other.

explosions all being carried out in our "closed tubes" at initial pressures between 370 and 406 mm.

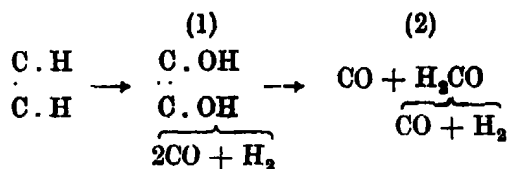
The results, which are detailed in Table III, did not differ materially in general character from those of the corresponding $x\text{C}_2\text{H}_2/(100-x)(2\text{H}_2 + \text{O}_2)$ series. The mean initial flame speeds (see fig. 4B) again were near their maximum at about the $\text{C}_2\text{H}_2 + 2\frac{1}{2}\text{O}_2 + 5\text{CO}$ composition, and no carbon separated until the $\text{C}_2\text{H}_2 + \text{O}_2 + 2\text{CO}$ composition had been passed, the last-named mixture exploding with a bluish flame, without any carbon separation or steam formation substantially in accordance with the equation,



Moreover, it will be seen from Table III that the ratios $\text{CO} \times \text{H}_2\text{O}/\text{CO}_2 \times \text{H}_2$ in the final explosion products of mixtures initially containing 11.95 and 20.8 per cent. of acetylene, respectively, were substantially those of a "frozen out" equilibrium.

Discussion of Results.

It has long been known that carbonic oxide and formaldehyde simultaneously arise at an early (if not the initial) stage in the slow combustion of acetylene, probably as the result of the decomposition of an unstable $\text{C}_2\text{H}_2\text{O}_2$, while in explosive combustion the formaldehyde at stage 2 (or possibly the dihydroxyacetylene at stage 1) is resolved into carbonic oxide and hydrogen thus:—



The most outstanding and significant feature of our present experiments is the fact that explosions of the $\text{C}_2\text{H}_2 + \text{O}_2 + 2\text{H}_2$ mixtures—where the oxygen present was just sufficient to burn either all the acetylene to carbonic oxide and hydrogen or all the hydrogen to steam—gave the thinnest and most compact flame of all (there being a minimum of "after burning"), and yielded nothing but carbonic oxide and hydrogen according to the equation



Therefore we conclude that in all but No. 2 of these explosions (this exception being the single case where only 1 per cent. of acetylene was present in the mixture exploded) there was in the flame front a selective burning of the hydrocarbon to carbonic oxide and hydrogen. This conclusion is supported

by the behaviour of the moist $C_2H_2 + O_2 + 2CO$ mixture, which on explosion also yielded practically nothing but carbonic oxide and hydrogen thus,



Standing in close relation with these facts are our observations that in none of the $x C_2H_2 + (100 - x) (2H_2 + O_2)$ nor the $x C_2H_2 + (100 - x) (2CO + O_2)$ series of explosions was there any separation of carbon or survival of acetylene until after x had exceeded 25, *i.e.*, the $C_2H_2 + O_2 + 2 (H_2 \text{ or } CO)$ proportion. As soon, however, as this limit was passed, there was carbon deposition and some survival of acetylene.

Another fact to be considered is the pronounced endothermic character of acetylene, which implies that certainly the CO (and possibly the H_2) produced by its primary combustion would be born in a highly "excited" and, therefore, most reactive condition.

Keeping all these facts in mind, and working backwards and forwards from photograph No. 12 as base, we may now review photographs Nos. 1 to 15 in conjunction with the data in Tables I and II, remembering also that, whereas in proceeding from No. 12 backwards to No. 1 the proportion of oxygen to total combustible in the flame front progressively increases, the reverse is the case in passing forwards from No. 12 to No. 15. Consequently, seeing that the primary, and only, chemical change involved in the explosion flame of No. 12 was



and that probably the carbonic oxide so arising was highly "excited," then as the available oxygen in the medium increased, as it did in proceeding backwards from No. 12, such "excited" carbonic oxide would immediately compete with the hydrogen for any excess oxygen that might be available, and in the first instance it would probably acquire a much larger share of it than the ultimate thermal equilibrium $CO \times OH_2 / CO_2 \times H_2$ ratio. Such competition is, we think, evidenced in the photographs Nos. 11 to 7 inclusive by the irregularity of the flame front, by its tendency to form "layers," and by the fine streams of highly luminous gas ("excited" CO in process of burning) issuing from the flame front, which imparted to the flame a pronounced "feathery" appearance. And it will be seen that this characteristic is at a maximum round about the $C_2H_2 + 1\frac{1}{2}O_2 + 3H_2$ ($C_2H_2 = 18$ per cent.) composition, *e.g.*, in No. 10.

On approaching the $C_2H_2 + 2\frac{1}{2}O_2 + 5H_2$ ($C_2H_2 = 11.8$ per cent.) composition, however, where there would be sufficient oxygen in the flame front to

burn all the carbon monoxide primarily resulting from the selective combustion of acetylene, the flame rapidly lost its "feathery" character, and the flame front became much more compact and brilliantly luminous, such condition culminating at the $C_2H_2 + 2\frac{1}{2}O_2 + 5H_2$ composition (No. 6). For here the further oxidation of the primarily-formed carbonic oxide was mostly concentrated in the flame front, which thus acquired maximum luminosity.

On passing further backward from No. 6 to No. 5, etc., the oxygen supply in the flame front much more than sufficed to burn all the carbonic oxide primarily formed by the combustion of acetylene in that region; consequently combustion of hydrogen occurred more and more there, whereby the luminosity of the flame front diminished, although its character became more homogeneous.

It should be understood, of course, that the foregoing suppositions are subject to the overriding condition that behind the flame fronts in Nos. 11 to 5 some "after burning" occurred, and the $CO \times OH_2/CO_2 \times H_2$ equilibrium came into play, and was adjusting itself automatically to the falling temperature. This accounts for the high luminosity of the "reflected waves" from the far (closed) end of the tube observed in Nos. 8, 7, 5, 4, 3 and 2.

With regard to the passage from No. 12 onwards to No. 15, it is fairly clear that as the available oxygen supply was progressively diminished from $C_2H_2 + O_2 + 2H_2$ to $2C_2H_2 + O_2 + 2H_2$, etc., as much of the acetylene as there was oxygen available for was burnt primarily to $2CO + H_2$ (via $C_2H_2O_2$) in the flame front, and that the remainder either decomposed into its elements, giving rise to the observed carbon-separation, or escaped combustion altogether, none of the hydrogen being burnt. Even a very small excess of acetylene over the $C_2H_2 + O_2 + 2H_2$ proportion caused a carbon separation and the yellowish luminosity of the flame in No. 13. Soon afterwards the flame front became perfectly regular (Nos. 14 and 15) with no tendency to form "layers"; the luminosity behind it depended partly upon the amount of separated carbon, and partly also upon the flame temperature, the total duration of luminosity (although not its intensity) increasing considerably.

While the foregoing is, we think, a reasonable and consistent view of the phenomena exhibited by photographs Nos. 3 to 15 inclusive of the "open tube" $x C_2H_2/(100 - x) (2H_2 + O_2)$ explosion, it does not explain the curious reduction in the flame speed resulting from the addition of the first 1 per cent. of acetylene to electrolytic gas. From the results obtained on exploding the $2.5 C_2H_2/97.5 (2H_2 + O_2)$ mixture in the "closed tube" series (Table II) obviously something unusual was happening with such a low acetylene-content;

because the "water gas" equilibrium was not nearly attained during the cooling behind the flame front. This is one of those puzzling points so frequently turning up in explosion research, for which at the time no explanation seems at hand, but whose further exploration often leads to some new discovery; and accordingly we desire to reserve its discussion for some future occasion.

In conclusion, our best thanks are due to the firm of Radiation, Ltd., under whose Research Fellowship at the Imperial College two of us have carried out the experimental part of the work, as well as to Dr. D. S. Chamberlin, of Lehigh University, U.S.A., for his help in connection with the $C_2H_2 + O_2 + 2H_2 + 4Ar$ or $4N_2$ experiments referred to on p. 12.

The Adsorption of Substances by Fuller's Earth.

By HAROLD JOHN PHELPS, B.A., B.Sc., Ramsay Memorial Research Fellow,
The Department of Biochemistry, Oxford.

(Communicated by C. N. Hinshelwood, F.R.S.—Received December 6, 1930.)

The utility of fuller's earth as a decolourising agent in the industrial preparation of oils has long been recognised. More recently also fuller's earth, in common with other powerful adsorbents has proved of the greatest use in the isolation of rare substances in the laboratory. Despite, however, the importance of fuller's earth both from the industrial and from the theoretical point of view, the ideas expressed in chemical literature as to its origin and nature, and the mechanism by which it acts as an adsorbent are diverse in the extreme. It was the object of the investigations here described to throw some light on the mechanism by which fuller's earth adsorbs organic acids and bases from aqueous solutions. In particular the influence of hydrogen-ion concentration upon the adsorption of these bodies was studied. The results indicate that two types of adsorption take place; that of unionised molecules and that of cations which displace calcium ions from the surface.

The Chemical and Geological Nature of Fuller's Earth.

Geologists seem to be agreed that fuller's earth consists essentially of aluminium silicate associated with a little free silica and smaller quantities of

iron, calcium and alkalis. It differs from ordinary clays in having a higher percentage of combined water. The exact nature of the silicates actually present in fuller's earth is necessarily uncertain as a rational analysis of so complex a mixture is obviously extremely difficult to obtain.

The chemical nature of fuller's earth suggests that it may take up substances from solution in a variety of ways. The presence of silica, alumina and calcium salts makes it probable that chemical combinations add to the true adsorption effects due to the very large surface that fuller's earth undoubtedly presents. The great variety of media, aqueous and non-aqueous, in which fuller's earth has been employed as an absorbent serve only to complicate the problem still further.

The conclusion of most workers who have used fuller's earth in its industrial sphere as an absorbent from oils, fats and petroleum, is that surface and capillarity effects are of predominating importance. Benedict* inclines to the view that fuller's earth may remove certain colouring matters by oxidative destruction, which is not out of harmony with the observation of Parsons† that some samples of fuller's earth are strong oxidising catalysts.

Workers investigating aqueous solutions have, however, been driven to postulate polar as well as apolar‡ adsorption. The characterisation of these two types of adsorption is due to Michaelis and Rona.§ It is very probable that normal (or apolar) adsorption proceeds through the medium of uncharged particles. The investigations of Fromageot|| and of Peters and myself¶ although on quite different lines, both point very strongly to this conclusion. In the case of "polar" adsorption, there is little doubt that an ionising element or group in the surface is replaced by a like-charged ion of the adsorbate.

It has been suggested by Michaelis and Rona** and by Freundlich†† that adsorption by kaolin is exclusively polar. Gibbs' generalisation, on the other hand, leads to the view that there must be some concentration, however slight, of all "surface-active" substances at any interface bounding their

* 'J. Oil & Fat Industry,' vol. 2, p. 62 (1925).

† 'J. Amer. Chem. Soc.,' vol. 29, p. 598 (1907).

‡ The adsorption of non-electrolytes and the adsorption of weak electrolytes in which the anion and cation are taken up in equivalent amounts is referred to as "apolar." When the ions of an electrolyte are taken up in different amounts the adsorption is called "polar."

§ 'Biochem. Z.,' vol. 102, p. 268 (1920).

|| 'C. R.,' vol. 179, p. 1404 (1924).

¶ 'Proc. Roy. Soc.,' A, vol. 124, p. 584 (1929); 'J. Chem. Soc.,' p. 1724 (1929).

** 'Biochem. Z.,' vol. 97, p. 57 (1919).

†† "Colloid and Capillary Chemistry."

solutions. The most reasonable conclusion from the available data for adsorption by fuller's earth is that both polar and apolar adsorption occur, one or other process predominating according to the nature of the adsorbate and the solution in which it is. Experimental evidence of the importance of silica in fuller's earth is provided by the work of Gretti and Williams,* who have determined the adsorption of a number of weak organic ampholytes and bases and also that of glucose. The adsorbents used were: silica, ferric oxide, alumina and fuller's earth. The results with fuller's earth were strikingly parallel to those obtained with silica. On the other hand Seidell, whose studies of fuller's earth as an adsorbent are well known, has come to the conclusion that, in the cases of methylene blue and quinine sulphate the cation is selectively adsorbed with the displacement of calcium from the fuller's earth.† It should be noticed that the greatest adsorption of quinine, observed by Seidell, demands the displacement of calcium representing more than 2 per cent. of the total weight of the earth. This implies that Seidell used an earth unusually rich in calcium. On the other hand the very exact relationship existing between the quinine absorbed by Seidell's fuller's earth and the calcium appearing in solution, shows how large a part the displacement mechanism plays.

More recently Salmon and Gueraint‡ have made a comprehensive study of the influence of hydrogen-ion concentration upon the absorption of certain substances by charcoal and various samples of fuller's earth. The results obtained by these workers on the adsorption of oxalic acid by charcoal are consistent with those obtained by Peters and myself (*loc. cit.*) using other organic acids and purified charcoal. Salmon and Gueraint found that fuller's earth adsorbed oxalic acid in solutions of "reaction" between p_H 3 and p_H 11, the adsorption falling to zero in more acid solutions. This result, which has been entirely confirmed in my own work, indicates that the oxalate ion is selectively absorbed. It is very significant, however, that Salmon and Gueraint found that fuller's earth which had been extracted with hydrochloric acid had practically no power of adsorbing oxalic acid. This suggests that fuller's earth takes up oxalic acid by virtue of small quantities of free basic substance (*e.g.* lime or alumina) which would naturally react preferentially with the oxalate ion.

* 'J. Amer. Chem. Soc.,' vol. 50, p. 668 (1928).

† 'J. Amer. Chem. Soc.,' vol. 40, p. 312 (1918).

‡ 'J. Biol. Chem.,' vol. 80, p. 67 (1923).

The General Technique of the Adsorption Experiments.

As in my work on charcoal adsorption (*loc. cit.*), attention was focussed upon a study of the influence of hydrogen-ion concentration upon the absorption of weak electrolytes. A study of these phenomena has led to a considerable simplification of our views on the mechanism of charcoal adsorption, and has in the hands of Salmon and Gueraint proved a valuable contribution to our knowledge of fuller's earth as an adsorbent. As it was intended that the present investigation should form a corollary to my previous work on charcoal adsorption, the general technique of the experiments was as far as possible similar to that previously employed. All the adsorbates investigated were used in approximately 0.2 per cent. solutions. A single experiment consisted in shaking 20 c.c. of such a solution, to which 2 c.c. of suitably diluted mineral acid or alkali had been added, with 200 mg. of fuller's earth for about 12 hours at 20° C. The fuller's earth was then centrifuged off and samples of the residual liquid were analysed. The equilibrium values of the hydrogen-ion concentration were determined electrometrically. The adsorption of propionic, hexoic (caproic) and oxalic acids was studied. The first two were purified by redistillation while the oxalic acid was a normal "analytical reagent" sample. Normal propylamine and butylamine, the two bases studied, were both purified by redistillation. One sample of English fuller's earth was used throughout. I am greatly indebted to Messrs. Boots, Ltd., for the gift of this sample and for the details of its composition* which they have given me.

** Analysis of Surrey Powdered Fuller's Earth.*

	per cent.			per cent.
Silica ...	61.21	(a) Loss on ignition	6.69
Alumina ...	16.37	Carbon dioxide	0.53
Ferrio oxide...	6.92	Titanium oxide	0.73
Ferrous oxide	1.02	Phosphoric anhydride	a trace
Magnesia ...	3.24	Alkalis (calculated as Na ₂ O)	...	0.33
Calcium oxide	3.45	(b) Sulphur	0.40
		Total	100.89

Hydroscopic Moisture 7.89 per cent.

(a) Loss on ignition less CO₂.

(b) It is assumed that the sulphur present is in the form of pyrite [FeS₂] as is probable from the circumstances of firing, the figure given above for ferrio oxide will be high and should read 6.42 per cent. Sulphur would then show as pyrite 0.75 per cent. and the total would amount to 100.74.

Methods of Estimation.

The monocarboxylic acids were estimated by the methods of titration between limits which has been described in detail previously (Phelps, *loc. cit.*). In the very acid regions which were explored in the present investigation the strong acid correction becomes rather considerable and the accuracy of the determination of the weak acid is rendered less good on that account. Control experiments were carried out to correct for the adsorption of the strong acid by the earth and also for the presence of any substances titrating between p_H 3 and p_H 11, which might have been liberated from the earth by the action of the strong acid.

The simple amines were determined as before by distillation in a micro-kjeldahl apparatus, the free amine being trapped in N/70 sulphuric acid which was "back-titrated" using methyl red as an indicator.

Oxalic acid was determined by the usual method of titration with permanganate in presence of excess sulphuric acid at 70° to 80° C. In the determination of these relatively small quantities of oxalate (about 5 mg. samples) the amount of sulphuric acid added and the temperature of titration had to be controlled with reasonable care. The error in the analysis of samples of about 10 mg. did not exceed 2 per cent.

Experimental Results.

Some typical results of experiments with propionic acid are shown in Table I. The adsorption is expressed as milligrams of propionic acid absorbed by 200 mg. of fuller's earth from a solution containing 1.89 mg. of propionic acid per cubic centimetre originally.

Table I.—Propionic Acid.

p_H	1.76	1.89	2.17	2.65	3.05	3.63
mg. adsorbed by 200 mg. F.E.	-0.5	±0.0	-3.2	-0.2	-0.2	-0.2
p_H	3.79	3.92	3.99	4.29	4.56	5.70
mg. adsorbed by 200 mg. F.E.	±0.0	-1.4	-0.3	-1.6	-0.8	-0.8

It will be seen that all the results show virtually no adsorption. All the negative values of less than 0.5 mg. are absolutely without any individual significance. Those showing a greater negative adsorption are very probably the result of carbon dioxide being taken up by the solutions during analysis. It may in any case be claimed with confidence that between the limits of

acidity of $p_H 1.6$ and $p_H 5.7$, propionic acid is not adsorbed by fuller's earth in the slightest degree.

The results with hexoic acid show that this acid also is not at all adsorbed by fuller's earth. The greatest adsorption measured amounts only to 2.0 mg. of acid absorbed by 200 mg. of fuller's earth. This represents less than 5 per cent. of the acid originally present, and is almost within the limits of experimental error when working with such small samples (5 c.c. samples of approximately N/70 solutions were analysed).

Oxalic Acid.

The adsorption of oxalic acid was found to be influenced by hydrogen-ion concentration in a manner very similar to that observed by Salmon and Gueraint for their samples of fuller's earth. The results are shown in fig. 1 in which the adsorption in milligrams of oxalic acid per 200 mg. of fuller's earth is plotted against the reciprocal of the logarithm of the equilibrium hydrogen-ion concentration.

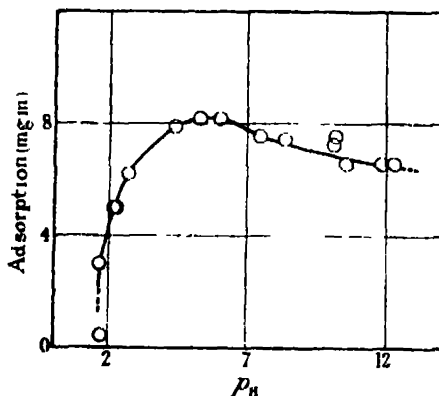


FIG. 1.—Oxalic Acid.

The adsorption of oxalic acid plotted against hydrogen-ion concentration. The adsorption is expressed as milligrams of oxalic acid adsorbed by 200 mg. of fuller's earth.

The Normal Amines.

In fig. 2 the adsorption of *n*-propylamine is plotted against p_H in the same way as that of oxalic acid. The results with *n*-butylamine were so exactly similar to those obtained with *n*-propylamine that they do not need detailed description. The curve of the adsorption of *n*-butylamine plotted against p_H is shown in fig. 3. The point of inflexion of the curve and the point of maximum adsorption both agree very nearly with the corresponding values for *n*-pro-

pylamine. The actual weight of *n*-butylamine adsorbed by a given weight of fuller's earth is slightly less than chemically equivalent to the weight of

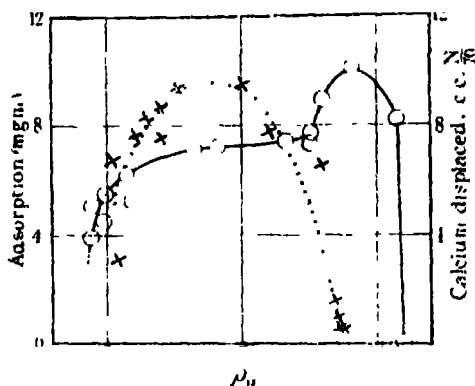


FIG. 2.—*n*-Propylamine.

The adsorption of *n*-propylamine plotted against hydrogen-ion concentration. The adsorption is expressed as milligrams of base adsorbed by 200 mg. of fuller's earth. The superimposed crosses and the dotted line represent the amounts of calcium displaced from fuller's earth during the adsorption of the amine. The calcium is measured as cubic centimetres of N/70 solution displaced from 200 mg. of fuller's earth.

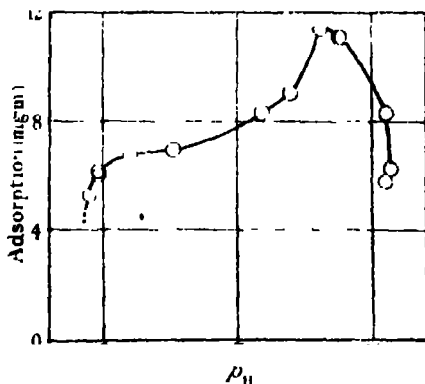


FIG. 3.—*n*-Butylamine.

The adsorption of *n*-butylamine plotted against hydrogen-ion concentration. The adsorption is expressed as milligrams of base adsorbed by 200 mg. of fuller's earth.

n-propylamine adsorbed under the same conditions (e.g., 8 mg. per 200 mg. of earth at p_H 7 and 11.8 mg. at p_H 10). It must be pointed out that the maximum adsorption of *n*-butylamine seems to be maintained between p_H 10 and p_H 11. This apparent slight difference from the behaviour of *n*-propylamine is in all probability due to the fact that the experiments on the latter have not chanced

to give equilibrium p_H values over this range. It must also be admitted that the adsorption of *n*-butylamine rises somewhat more between p_H 4 and p_H 8 than does the adsorption of *n*-propylamine.

The Importance of Calcium.

If Seidell's view is correct that the adsorption of bases proceeds by the displacement of calcium ions from the earth, it might be expected that the amount of the displaced calcium would show the same variations with hydrogen-ion concentration as are shown in the amount of amine absorbed.

A further series of experiments were therefore conducted in which *n*-propylamine solutions were allowed to come into equilibrium with fuller's earth under exactly the same conditions as before. The amount of calcium in the equilibrium liquid and the reaction of the solution were determined. The calcium analyses were performed by the usual method of precipitation as oxalate. The precipitate, after regulated washing with cold distilled water, was dissolved in hot dilute sulphuric acid and titrated with N/30 potassium permanganate.

It is very difficult to decide what correction should be made for the calcium salts dissolved out of the fuller's earth, or removed from it in some way not directly connected with the process of the adsorption of the amine. In fact, there has been subtracted from all the calcium determinations the amount of calcium which is removed from fuller's earth by shaking with distilled water under the same conditions. It is assumed that all additional calcium which appears in presence of *n*-propylamine has been displaced from the surface by the adsorbed amine. It is possible that in the presence of propylamine sulphate and the free base some additional calcium will be discharged into solution by processes not directly connected with the adsorption of the base; or alternatively that the presence of the base and its salt will depress the solution of free calcium from the earth. The results make it improbable that the error from this source is appreciable.*

The results are shown in Table II, and in fig. 2, in which the adsorption of *n*-propylamine (as previously described) is plotted as milligrams of base

* Propionic acid solution (more acid than p_H 3) displaces about four times as much calcium as is displaced by pure water at p_H 7. Even if a comparable amount of calcium were displaced by *n*-propylamine in neutral solution as a result of processes not directly connected with the adsorption of the base, the general agreement between the calcium displacement and the base adsorption is not seriously impaired. It is, of course, obvious that no significant results will be obtained in solution more acid than about p_H 2, as under such conditions calcium salts will be soluble *per se*.

adsorbed per 200 mg. of fuller's earth, while the superimposed crosses give the amounts of displaced calcium expressed as cubic centimetres of N/70 solution displaced from 200 mg. of fuller's earth. The shape of the calcium displacement curve is sufficient to show the close relation to the adsorption curve in solutions of reaction between $p_H 4$ and $p_H 9$. If the calcium displaced and the base adsorbed are both expressed as chemical equivalents, it is found that over the range $p_H 3$ to $p_H 8$ the calcium displaced is approximately chemically equivalent to the base adsorbed. In more alkaline solutions the calcium displaced falls to nil while the base adsorbed rises to a maximum.

Table II.—The Displacement of Calcium.

p_H	Ca displaced as c.c. N/70 solution per 100 mg. F.E.	n-propylamine adsorbed from fig. 2, as c.c. N/70 solution per 100 mg. F.E.
	c.c.	c.c.
10.79	0.25	5.75
10.53	0.25	5.65
10.52	0.51	5.65
10.46	0.76	5.60
9.95	3.22	5.05
8.05	3.85	4.45
7.13	4.72	4.40
4.67	4.70	4.20
4.03	4.35	4.00
4.03	3.77	4.00
3.49	4.18	3.90
3.12	3.20	3.85
3.01	3.82	3.80
2.44	1.50	3.50

(neutral water blank 0.47 c.c.)

Adsorption by Aluminium Silicate Gel.

The adsorption of the simple amines by fuller's earth in solutions more alkaline than $p_H 9$ is plainly a process quite distinct from the adsorption in more acid solutions. It would be expected that an adsorbent essentially similar to fuller's earth but containing no calcium would adsorb the simple amines very selectively at a reaction of about $p_H 10$, the adsorption falling off rapidly in more acid or more alkaline solutions.

Aluminium silicate gel was selected as the most suitable form of adsorbent which could be freed from impurities likely to give rise to replaceable cations. The gel was prepared from 30 per cent. aluminium nitrate solution and dilute (about twice normal) sodium silicate. The gel was washed repeatedly with very dilute ammonium acetate solution until free from nitrates. It was then washed with a few changes of distilled water. Finally the gel was dried in

an air current at room temperature and activated by heating in a current of air at 250° C. for a few hours.*

The adsorption of *n*-butylamine by this gel was studied. The technique of the adsorption experiments was identical with that employed previously. The results are shown in fig. 4.

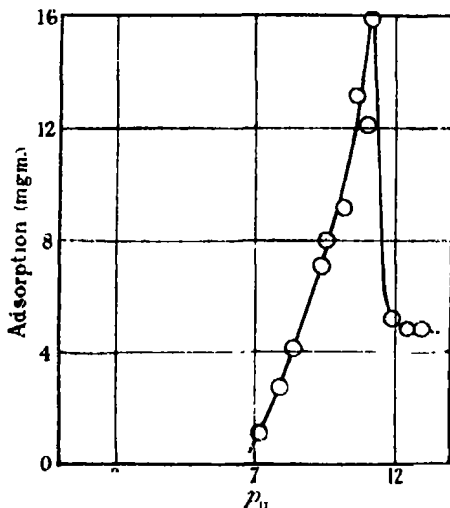


FIG. 4.—Adsorption of *n*-Butylamine by Silica Gel.

The adsorption of *n*-butylamine by aluminium silicate gel plotted against hydrogen ion concentration. The adsorption is expressed as milligrams of base adsorbed by 200 mg. of the gel.

It will be seen that the above anticipations were entirely fulfilled. The adsorption rises from zero at $p_H 7$ to a very sharp maximum at $p_H 10.5$. In more alkaline solutions there is a rapid fall in the adsorption. By a fortunate accident activity of the gel was of the same order as that of the sample of fuller's earth previously used, the maximum adsorption of *n*-butylamine being about 16 mg. on to 200 mg. of the gel and 11.8 mg. on to a similar weight of fuller's earth, these adsorptions taking place from solutions of approximately the same strength.

These results justify the belief that the adsorption of *n*-butylamine in alkaline solution, with a very sharp maximum between $p_H 10$ and $p_H 11$, is a property exhibited by a pure silicate surface. The adsorption exhibited by fuller's earth over the whole range of reaction $p_H 3$ to $p_H 13$ may be represented by the combined effect of the adsorption in alkaline solutions characteristic

* I am greatly indebted to Dr. B. Lambert for his help in the preparation of the aluminium silicate gel.

of aluminium silicate together with the adsorption in neutral solutions which has previously been demonstrated to proceed by the displacement of calcium ions. In fact, if the curve shown in fig. 4 be added to the curve representing the calcium displaced at various hydrogen-ion concentrations, the combination curve is of exactly the same form as those shown in figs. 2 and 3 representing the influence of hydrogen-ion concentration upon the adsorption of *n*-propylamine and *n*-butylamine respectively.

The adsorption of oxalic acid by fuller's earth in solutions more alkaline than $p_H 1.5$ must proceed through the medium of oxalate ions. In view of the apparent accessibility of the calcium in fuller's earth it seems probable that the adsorption of oxalate ions is really due to the formation of insoluble calcium oxalate at the surface of the earth.* This view is indirectly supported by the fact that aluminium silicate gel does not adsorb oxalic acid at all at any hydrogen-ion concentration. Table III shows actual figures obtained, showing in all cases very slight negative adsorption but hardly reaching the probable experimental error in any case. The oxalate solutions used were one-thirtieth normal.

Table III.—Oxalic Acid on Silicate Gel.

p_H	1.71	2.08	2.53	3.81	4.81	5.15	6.55	6.81
mg. adsorption by 200 mg. of gel	-0.4	-0.7	-0.6	-0.4	-0.6	-0.6	0.2	-0.3

Discussion of Results.

There seems to be very little doubt that for solutions of reaction between $p_H 3$ and $p_H 8$, the contention of Seidell, that the adsorption of bases by fuller's earth proceeded by the displacement of calcium, is substantially correct. The much greater adsorption of the base at $p_H 10$ has been shown to be a property of an aluminium silicate surface. All the adsorption that is observed may be accounted for by the displaced calcium in solutions more acid than $p_H 7$ to $p_H 8$. On the other hand, aluminium silicate gel will not adsorb the bases at all in solutions more acid than $p_H 7$. When one remembers that the true adsorption of unionised amine molecules by pure charcoal falls from a maximum value at $p_H 11$ to zero at $p_H 7$,† it seems quite probable that this "apolar"

* Salmon and Gueraint (*loc. cit.*) showed that when calcium was removed by acid treatment fuller's earth lost nearly all its power of adsorbing oxalic acid.

† Published experiments on the adsorption of the simple amines (Phelps and Peters, *loc. cit.*) showed a more gradual change, but recent experiments with a charcoal prepared from pure cellulose give the result described. (Phelps, *Proc. Biochem. Soc.*, "Chemistry and Industry," June 20, 1930.)

mechanism is responsible for the adsorption of the simple amines by aluminium silicate gel and by fuller's earth in alkaline solutions.

The very rapid fall of the adsorption in solutions of hydrogen-ion concentration between p_H 11 and p_H 13 has no parallel in charcoal adsorption, and, since no change in the state of the amine should take place over this range, must be attributed to some change in the surface itself. This change occurs both with the aluminium silicate gel and with fuller's earth, and is apparently, therefore, a property of a silicate surface. It may be suggested that the ionisation of silicic acid at the surface may begin at about p_H 11, and by giving the surface a charge this process may render it inoperative as an adsorbent for neutral molecules.

On the acid side of neutrality the adsorption of the simple amines and of oxalic acid are influenced by hydrogen-ion concentration in very similar ways. Both fall off to zero over the same range of reaction (p_H 4 to p_H 1.5). In the case of the normal amines adsorption has been shown to be due to the displacement of calcium ions from the surface, and in the case of oxalic acid adsorption is almost certainly due to the formation of calcium oxalate at the surface. It would seem therefore that calcium is not available to take part in these changes in very acid solutions. Remembering the fact that weak solutions of mineral acids have been found to remove considerable quantities of calcium from fuller's earth, it seems likely that at p_H 1.5 the strong acid necessarily present competes successfully for the calcium in the earth and so inhibits the polar adsorption of the normal amines or of oxalic acid.

Propionic and hexoic acids are not adsorbed by fuller's earth to any extent at any p_H . Oxalic acid is adsorbed in solutions more alkaline than p_H 1.5. The adsorption rises to a maximum at about p_H 4 and then falls off very gradually with increasing alkalinity. At p_H 12 the adsorption is about three-quarters of its maximum value.

The adsorption of *n*-propylamine and *n*-butylamine is influenced by acidity in almost exactly the same way. In both cases the adsorption rises from a vanishingly small value in very acid solution to about p_H 4.5. From p_H 4.5 to about p_H 8 the adsorption is almost independent of the hydrogen-ion concentration. In solutions more alkaline than p_H 9.5 there is a very rapid rise in the adsorption to a maximum at p_H 11, which is immediately followed by a rapid fall to a vanishingly small value at p_H 13.

It has been found that between p_H 4.5 and p_H 8, over which range the adsorption remains almost constant, an amount of calcium is displaced which is almost exactly chemically equivalent to the base adsorbed. In more alkaline solutions, the calcium displaced falls to zero. It is concluded, therefore, that the adsorption of these bases by fuller's earth is a true apolar process in very alkaline solutions, but that in solutions more acid than p_H 8 adsorption proceeds almost entirely by the displacement of calcium ions from the fuller's earth.

Further evidence in support of this view has been obtained by studying the adsorption of *n*-butylamine by aluminium silicate gel. In this case there is no calcium to be displaced. The adsorption of the base rises from nil at p_H 7 to a sharp maximum at p_H 11, followed by a rapid fall in more alkaline solution.

The fact that aluminium silicate gel does not adsorb oxalic acid at all at any hydrogen-ion concentration suggests that the adsorption of this acid by fuller's earth is due to the formation of insoluble calcium oxalate at the surface.

In conclusion, I would like to express my sincere thanks to Professor R. A. Peters for his kind interest and helpful advice throughout this work, and to express my indebtedness to the Ramsay Memorial Trustees for a Fellowship which placed me in a position to carry out these researches.

The Solution of the Torsion Problem for Circular Shafts of Varying Radius.

By ALEXANDER THOM, D.Sc., Ph.D., and JAMES ORR, B.Sc.

(Communicated by R. V. Southwell, F.R.S.—Received December 17, 1930.)

Introduction.—When a bar of circular section whose radius is a function of z , fig. 1, is subjected to terminal couples applied in a suitable way, the stresses and strains may be expressed* in terms of a function ψ .

This function satisfies the equation

$$\frac{\partial^2 \psi}{\partial r^2} - \frac{3}{r} \frac{\partial \psi}{\partial r} + \frac{\partial^2 \psi}{\partial z^2} = 0 \quad (1)$$

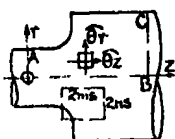


Fig. 1.

throughout an axial section, with $\psi = \text{constant}$ on the boundary. The stresses are

$$\widehat{\theta z} = \frac{\mu}{r^2} \cdot \frac{\partial \psi}{\partial r}, \quad \widehat{r\theta} = -\frac{\mu}{r^2} \cdot \frac{\partial \psi}{\partial z}$$

where μ is the modulus of rigidity of the material. The displacement, v , of any point is directed at right angles to an axial plane passing through the point, and is given by

$$r^2 \cdot \frac{\partial}{\partial r} \left(\frac{v}{r} \right) = -\frac{\partial \psi}{\partial z}, \quad r^2 \cdot \frac{\partial}{\partial z} \left(\frac{v}{r} \right) = \frac{\partial \psi}{\partial r}.$$

Equation (1) has been solved for certain boundaries by the usual analytical methods; for the general case (including boundaries of non-mathematical form) the only method so far developed is an approximate graphical one due to Willers.† The present paper describes an arithmetical trial and error method, applicable to the general case, which may be carried to any desired degree of accuracy. An appendix to the paper mentions other physical problems which can be treated by similar methods.

Method of Solution.—The boundaries are drawn to a suitable scale on squared paper, so that estimated ψ values may be written at the corners of the squares. To find the corresponding values of ψ at the centres of the squares we have, using Taylor's theorem

$$\psi_A = \psi_M + \frac{1}{2}S \cdot \frac{\partial \psi}{\partial r} + \frac{1}{2}S \cdot \frac{\partial \psi}{\partial z} + \frac{1}{8}S^2 \cdot \frac{\partial^2 \psi}{\partial r^2} + \frac{1}{4}S^2 \cdot \frac{\partial^2 \psi}{\partial r \partial z} + \frac{1}{8}S^2 \cdot \frac{\partial^2 \psi}{\partial z^2} + \dots,$$

and similar expressions for ψ_B , ψ_C , ψ_D , fig. 2, therefore

* Love, "Mathematical Theory of Elasticity," 4th ed., p. 325.

† Willers, 'Z. Math. Phys.,' vol. 55 (1907).

$$\psi_M = \frac{1}{4}(\psi_A + \psi_B + \psi_C + \psi_D) - \frac{1}{8}S^2 \cdot \nabla^2 \psi - \frac{1}{384} \cdot S^4 (\nabla^4 \psi + 4\partial^2 \psi / \partial r^2 \partial z^2). \quad (2)$$

Substituting from (1), $\nabla^2 \psi = 3/r \cdot \partial \psi / \partial r$, and neglecting the terms with fourth order and higher derivatives

$$\psi_M = \frac{1}{4}(\psi_A + \psi_B + \psi_C + \psi_D) - \gamma, \quad (3)$$

where

$$\gamma = \frac{1}{8}S^2 \cdot 3/r \cdot \partial \psi / \partial r.$$

The term γ is obtained from the estimated ψ values; it is a small correction, and in all cases which have been tried, it was sufficiently accurate to take $\partial \psi / \partial r$ at M (fig. 2) $= \frac{1}{2}(\psi_A - \psi_D)/S + \frac{1}{2}(\psi_B - \psi_C)/S$.

Hence, an approximation to the values of ψ at the centres of the squares may be found, and used, by applying (3) again, to find a new approximation to the original corner values. This approximation is in general better than the assumed values (see below), that is, the process is convergent. Continuing, the process is repeated until the values cease changing, when equation (1) is satisfied to the approximation of (3). An actual example of the method is given later in the paper.

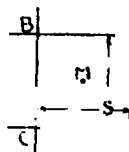


FIG. 2.

We have still to examine whether the neglected terms in (2) are in fact negligible. This is easily tested at any part of the section, when the values have settled, by enlarging that part, using smaller squares and finding if the values alter, for the neglected terms diminish in importance with the size of the square. Now the higher derivatives are, in general, greatest, near portions of the boundary which change direction quickly, so it is necessary in many cases to enlarge the section near these parts.

In estimating the preliminary ψ values, consider the regions where the boundary radius is constant, or varies slightly with z , such as OA, BC, fig. 1, some distance from positions where it is changing rapidly. For these regions $\partial^2 \psi / \partial z^2 = 0$, and (1) becomes $\partial^2 \psi / \partial r^2 - 3/r \cdot \partial \psi / \partial r = 0$, giving $\psi = kr^4$. The value of ψ is then calculated for corners of squares on OA and BC, noting that since it is constant on the boundary $\psi_A = \psi_C$. Also $\psi = 0$ on OB; therefore it is known completely on the boundary OACB. Intermediate values are guessed to give regular increases.

Where a boundary does not pass through the corner of a square, the adjacent ψ value must be found by interpolation. For about 1 per cent. accuracy this may be done graphically, but greater accuracy requires numerical interpolation.

Convergence.—This will be considered in two steps: (a) when the term γ in (3) is small and therefore changes in it are negligible, as in all examples yet solved by this method; and (b) when changes in this term are not negligible.

(a) Let the size of the square be such that neglected terms in (2) do not affect the last significant figure at any part of the section. Let ϵ denote the error in the assumed value of ψ ; the estimated values are then $\psi + \epsilon$.

Including ϵ in (3) we have

$$\psi_M + \epsilon_M = \frac{1}{4}\Sigma\psi + \frac{1}{4}\Sigma\epsilon - \gamma$$

since

$$\psi_M = \frac{1}{4}\Sigma\psi - \gamma$$

subtracting

$$\epsilon_M = \frac{1}{4}\Sigma\epsilon \quad (4)$$

where Σ denotes the sum of the corner values. ϵ_M is the error in the approximation to the centre value on applying (3).

Let fig. 3 give the variation of ψ and ϵ along a line, $z = \text{constant}$. Assume

for convenience of representation that ϵ does not vary with z . The successive approximations are shown in the lower figure, which gives ϵ alone, and it is seen that abrupt changes in it are smoothed out, while it creeps steadily to zero. In this diagram, $abcd$ is the error surface which alters, on applying (3) twice, to $efgd$.

This point is also illustrated by finding a relation between ϵ and δ , where δ is the difference obtained in the estimated ψ value by applying (3) twice, first to obtain the central

values and again from these, to obtain new corner values (a double round). If ϵ is the error at a corner, its value at the surrounding corners may be expressed by Taylor's theorem, in terms of its first and second derivatives as shown at the nine main corners in fig. 4.

The four centre values are then found from (4). Another application of (4) gives the new central error, which is then found to exceed the original by

$$\delta = \frac{1}{8}S^2 \cdot \nabla^2 \epsilon. \quad (5)$$

When the error surface is concave up, $\nabla^2 \epsilon$ and so δ are positive, that is, hollows fill up; similarly, peaks flatten. This formula shows that the first tendency

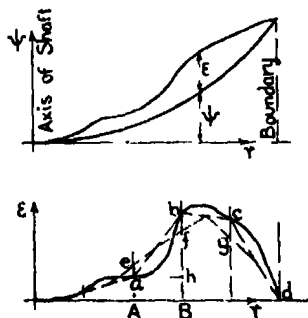


FIG. 3.

is to smooth out abrupt changes in ϵ , for in these regions $\nabla^2 \epsilon$ has a high value, and the second tendency is to diminish ϵ gradually over the section.

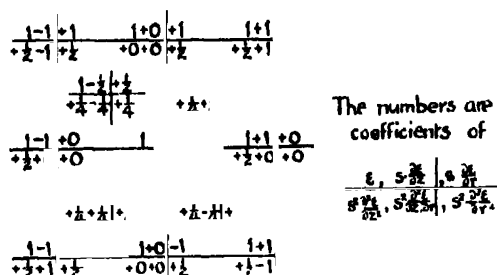


Fig. 4.

(b) When the changes in γ are not negligible, (4) becomes

$$\varepsilon_M = \frac{1}{2} \Sigma \varepsilon - \frac{1}{8} S^2 \cdot 3/r \cdot \partial \varepsilon / \partial r.$$

It will be shown that the effect of the second term is to hasten the convergence. Referring to fig. 3, the typical variation of the error along a line, $z = \text{constant}$, is shown; it is zero for some distance near the $r = 0$ end, since ψ there is small, and also irregularities in the boundary scarcely affect this region.

Consider the square, two of whose corners are A and B, fig. 3; here $S \cdot \partial \epsilon / \partial r$ is hb , giving $\frac{1}{8} S^2 \cdot 3/r \cdot \partial \epsilon / \partial r = \frac{3}{8} \cdot S/r (hb)$. Since $S/r < 1$ except for the first square, the effect of this term is never violent, and it decreases as r increases; it hastens the convergence where $\partial \epsilon / \partial r$ and ϵ have the same sign, which occurs in general at the smaller values of r ; it retards the convergence where they have different signs, which occurs in general at the higher values of r . Now, this term is less important at the higher values of r , the region where the convergence is retarded, hence the general effect is to hasten the convergence.

Shortening the Process.—If an approximate average value of the ratio ϵ/δ could be estimated for a part of the section, the slow creep of the successive approximations could be quickened. Consider a rectangular part of the section including $2m \times 2n$ squares of side S , fig. 1; assume that ψ is known on the sides so that the error there is zero. Let the error take the simple form

$$\varepsilon = \varepsilon_0 \left(1 - \frac{r^2}{n^2 S^2}\right) \left(1 - \frac{z^2}{m^2 S^2}\right),$$

where ε_0 is the error at the centre of the rectangle, the origin of co-ordinates. From (5)

$$\delta = \frac{1}{4} S^2 \cdot \nabla^2 \epsilon = -\frac{1}{2} \cdot \epsilon_0 \left(\frac{1}{m^2} + \frac{1}{n^2} - \frac{r^2 + z^2}{m^2 n^2 S^2} \right),$$

therefore

$$\varepsilon_0/\delta_0 = -2/(1/m^2 + 1/n^2),$$

and the average value of ε/δ is less than this. It is found that using

$$\varepsilon/\delta = -1.5/(1/m^2 + 1/n^2) \quad (6)$$

over the part of the section considered gives good results in practice. The best procedure is to take two double rounds, and apply (6) to the differences obtained by the second.

In actual cases, equivalent values of m and n are estimated; for example, in the case of a shaft enlarging to a greater diameter, fig. 1, the equivalent rectangle is usually as shown, enclosing the region of great error. This method gives better results than might appear at first sight, for, with the differences δ all over the section, obtained by applying a double round, the operator can tell, after a little experience, where the error is great and where it is nearly zero.

Further, if the multiplier (6) is incorrectly estimated, its general effect can be observed when the next double round is taken, and so may be altered to suit.

Example.—To illustrate the method, the example of a shaft with a collar is given in full (figs. 5 and 6).

First, the values are estimated; on the line $z = -1$, $\psi = kr^4$, so, taking any convenient number (in the example, 41), as the boundary value, intermediate values on this line are calculated. On the line at the centre of the collar, $z = 6$, the boundary value only is known; the others must be guessed. On the line $r = 0$, $\psi = 0$. Within these boundaries the values are guessed to give regular increases.

The term γ is calculated throughout the section from the estimated values, and is shown by numbers enclosed in circles in fig. 5.

Now the correcting process can proceed. By applying (3), the values are found at the centres of the squares, a comptometer proving very useful for this step; applying (3) again to the centre values a better approximation to the corner values is obtained. The differences between the second and first approximations are written down so that a double round may be repeated on them, the smaller numbers making this easier than the first round.

As the formula for shortening the process is applied at this stage, a rectangle is sketched in, which surrounds the region requiring much correction. In the example the rectangle is bounded by the lines $z = 3$, $z = 9$, $r = 6$, $r = 11$. From (6), $\varepsilon/\delta = -1.5/(1/9 + 1/6.2) = -6$. Hence the differences from

the last double round are multiplied by 6 to obtain the next approximation. The application to a few values is shown at (a), fig. 5; for the centre point

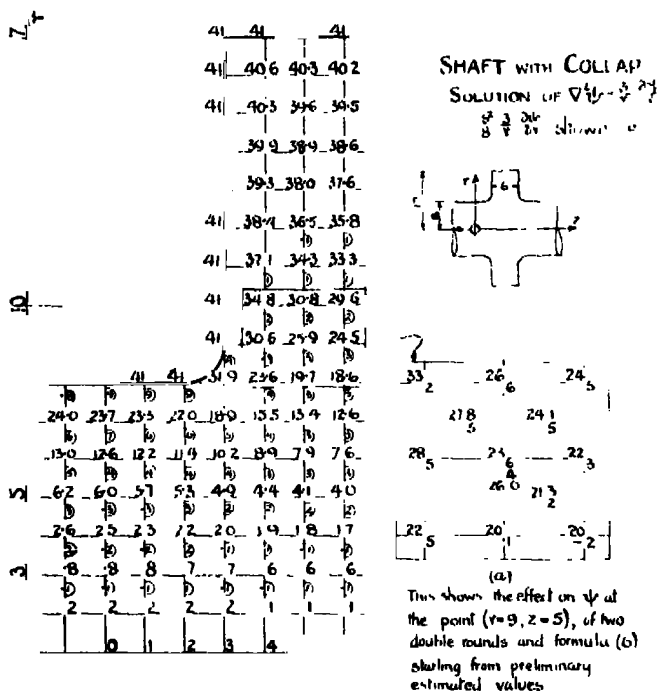


FIG. 5.

$\psi + \varepsilon_1 = 23$, the first double round gives $\delta_1 = 0.6$, the second gives $\delta_2 = 0.4$, therefore, the second approximation is $\psi + \varepsilon_2 = 23 + 0.6 + 6 \times 0.4 = 26.0$. The value at this point when the field has finally settled is 25.9.

Having settled the values on the section with this size of square, we next investigate the effect of the neglected terms in (2) by reducing the size of square to half at various parts, and finding if the values alter. In this case it is found that they alter only near the junction of shaft and collar, and this region is shown enlarged in fig. 6.

When the values cease changing, the problem is solved, and the final step of finding the stresses and strains may be taken. The maximum stress occurs on the boundary; it is equal to

$$\sqrt{(\partial \psi / \partial x)^2 + (\partial \psi / \partial y)^2} = \frac{\mu}{r^2} \sqrt{\left\{ \left(\frac{\partial \psi}{\partial r} \right)^2 + \left(\frac{\partial \psi}{\partial z} \right)^2 \right\}} = \frac{\mu}{r^2} \cdot \frac{\partial \psi}{\partial n},$$

where dn is the element of the normal to the boundary. The simplest and

most accurate method of finding these derivatives is to use difference formulæ. The stress on the boundary, from $z = 0$ to $z = 2.7$, is plotted in fig. 6; the

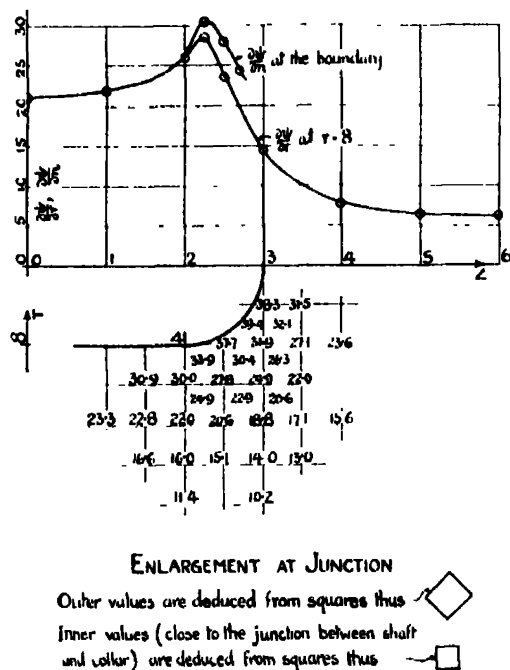


FIG. 6.

maximum stress occurs at $z = 2.25$, and $= 1.47 \times$ stress on the boundary at $z = 0$.

The angular position (v/r), of any point with reference to its unstrained position, is given by $\partial/\partial z (v/r) = 1/r^3 \cdot \partial\psi/\partial r$. So the twist of the cross section at $z = 12$, relatively to the section at $z = 0$, is found by integrating

$$\frac{1}{r^3} \int_0^{12} \frac{\partial\psi}{\partial r} \cdot dz$$

along a line, $r = \text{constant}$. Here $\partial\psi/\partial r$ is found along $r = 8$ and is shown plotted in fig. 6. The twist on this 12-inch length is the same as that for a length of 8.7 inches of an 8-inch radius shaft, subjected to the same torque.

The methods discussed in this paper have been developed in connection with experimental work, which is being carried out in the James Watt Engineering Laboratories, University of Glasgow, under the directorship of Professor J. D. Cormack.

APPENDIX.

Similar methods have been applied successfully to the solution of other physical problems, namely :—

- (a) Torsion of prisms with non-circular sections ; the equation to be solved is $\partial^2 \Psi / \partial x^2 + \partial^2 \Psi / \partial y^2 + 2 = 0$, with $\Psi = \text{constant}$ on each boundary. Actual cases for which a solution has been obtained include a shaft with keyway, several British standard structural sections, a hollow serrated shaft and a hollow square. In several of these cases, tests on specimens gave experimental verification.

- (b) *Perfect fluid flow in two dimensions ; the equation is

$$\partial^2 \psi / \partial x^2 + \partial^2 \psi / \partial y^2 = 0,$$

with $\psi = \text{constant}$ on a fixed boundary.

- (c) Viscous fluid flow in two dimensions ; the equations to be solved are

$$\begin{aligned} \nu \cdot \nabla^2 \zeta &= -\frac{\partial \psi}{\partial y} \cdot \frac{\partial \zeta}{\partial x} + \frac{\partial \psi}{\partial x} \cdot \frac{\partial \zeta}{\partial y} \\ \nabla^2 \psi &= 2\zeta. \end{aligned}$$

A solution* has been obtained for the flow past a cylinder at Reynold's number = 10, which was consistent with experimental results.

The solution in cases (a) and (b) is straightforward, and the remarks on convergence given above apply to these also. In case (c) it is necessary to solve two fields simultaneously, one for the stream function (ψ), the other for the vorticity (ζ). A consideration of the flow between parallel plates indicated that the process may not be convergent if the size of the chosen squares exceeds some limiting figure.

* Thom, 'Aer. Res. Com.' R. & M., No. 1194.

The Diurnal Tide in an Ocean bounded by Two Meridians.

By D. C. COLBORNE, M.A., Armstrong College, Newcastle-on-Tyne.

(Communicated by G. R. Goldsbrough, F.R.S.—Received January 2, 1931.)

§ 1. *Introduction.*

In a series of papers it has been shown by Goldsbrough how, by the introduction of a certain form of null-function, solutions of the general dynamical equations may be obtained for the tides in an ocean on a rotating globe bounded by two meridians from pole to pole. The method is described in Part I* of the series and in that and succeeding papers its application has been made to special cases. In particular in Part III† the method has been used to consider the lunar semi-diurnal tide M_2 in an ocean of uniform depth bounded by two meridians 60° apart. In the present paper solutions have been found in a similar way for the diurnal tide in the same type of ocean.

The results obtained show agreement with observations in that the amplitudes of the diurnal tide are considerably smaller than those of the semi-diurnal tide. Also, at points suitable for comparison, there is a close similarity in the values of the ratio of the heights of the two tides obtained theoretically and from observations. The wave represented by the solution is of an unusual type, the range of values of the phase over the whole ocean being exceptionally small. It is shown that the wave obtained is equivalent to the combination of a stationary wave and a progressive wave of much smaller amplitude, and that this type of combination can have only a limited range of phase angles. As a result there are periods during which neither high nor low tide occurs at any point of the ocean. The cotidal lines, when present, move across from one boundary to the other approximating more closely to the meridians as they approach the central meridian which is actually a cotidal line.

I wish to thank Professor Goldsbrough, F.R.S., with whom I have had the advantage of discussing the problem throughout and to whom I am much indebted, for his helpful suggestions. I also thank Dr. J. R. Airey for providing tables of Gauss functions, not available elsewhere, which were of considerable assistance in the calculations.

* 'Proc. Roy. Soc.,' A, vol. 117, p. 702 (1928).

† 'Proc. Roy. Soc.,' A, vol. 126, p. 1 (1929).

§ 2. The Null-Function.

In considering the diurnal tide it is again required to solve the equations

$$\begin{aligned}\frac{\partial u}{\partial t} - 2\omega v \cos \theta &= -\frac{g}{a} \frac{\partial}{\partial \theta} (\zeta - \bar{\zeta}) \\ \frac{\partial v}{\partial t} + 2\omega u \cos \theta &= -\frac{g}{a \sin \theta} \frac{\partial}{\partial \phi} (\zeta - \bar{\zeta}) \\ \frac{\partial \zeta}{\partial t} &= -\frac{1}{a \sin \theta} \left\{ \frac{\partial}{\partial \theta} (hu \sin \theta) + \frac{\partial}{\partial \phi} (hv) \right\}\end{aligned}\quad (1)$$

subject to the condition that the velocity component v should be zero at the boundaries.*

The type of ocean for which this solution will be worked out is the same as that considered in the case of the semi-diurnal tide, i.e., an ocean bounded by two meridians from pole to pole, 60° apart and of uniform depth 12,700 feet—the mean depth of the Atlantic Ocean. This gives the value 22.9 for β , where $\beta = 4\omega^2 a^2 / gh$. The tide producing potential now used, however, being that of the diurnal tide is of the form $gHP_1^1(\mu)e^{i(\phi + \sigma t)}$. It has also been assumed that $\sigma = \omega$ which is true for the lunar and solar constituents K_1 and also for the solar constituent P_1 if the orbital motion of the sun be neglected. It is only approximately true, however, for the lunar diurnal tide O_1 for which $\sigma = 0.927\omega$.

Since the above potential is an odd function of μ the null-function which is to be formed must consist of "associated Legendre functions" which are odd functions of μ . The null-function has therefore been taken to be of the following form, the denominators $P_{3\kappa+1}^{3\kappa+1}(0)$ being introduced to avoid the appearance of large coefficients in the expansions of $P_{3\kappa+1}^{3\kappa}(\mu)$ which are involved.

$$\begin{aligned}& \sum_{\kappa=1}^{\infty} E_{\kappa} [(e^{3i\kappa\phi} - e^{-3i\kappa\phi}) P_{3\kappa+1}^{3\kappa}(\mu) \div P_{3\kappa+1}^{3\kappa+1}(0) \\ & \quad - i \sum_r a_r^{\kappa} (e^{3ir\phi} + e^{-3ir\phi}) \sum_n b_n^{3r}(3\kappa) P_n^{3r}(\mu)] \\ & + \sum_{\kappa=0}^{\infty} F_{\kappa} [(e^{3i\kappa\phi} + e^{-3i\kappa\phi}) P_{3\kappa+1}^{3\kappa}(\mu) \div P_{3\kappa+1}^{3\kappa+1}(0) \\ & \quad + i \sum_r a_r^{\kappa} (e^{3ir\phi} - e^{-3ir\phi}) \sum_n b_n^{3r}(3\kappa) P_n^{3r}(\mu)].\end{aligned}\quad (2)$$

It is possible to obtain the terms of this null-function from the corresponding null-function composed of even functions of μ as used in the case of the lunar

* The notation used here and throughout agrees with that used by Goldsbrough.

semi-diurnal tide.* It would only be necessary to multiply the latter through out by μ and then apply the formulæ

$$(2s + 1) \mu P_s^s(\mu) = P_{s+1}^s(\mu).$$

$$(2n + 1) \mu P_n^s(\mu) = (n - s + 1) P_{n+1}^s(\mu) + (n + s) P_{n-1}^s(\mu).$$

This would simplify the calculation, but there is the disadvantage that in order to obtain a certain number of terms of the expansions in terms of odd functions of μ one more term is required of the corresponding expansion in terms of the even functions. A sufficient number of terms was not available from the previous calculations of the even null-function, and it was therefore found more convenient to evaluate the series for the null-function now required by the same method as used for the semi-diurnal tide. The two methods have, however, been combined in a later part of this paper thus reducing the amount of calculation to some extent.

The final form of the null-function used is given in the table which follows. The main terms are given in group (I) and the subsidiary terms of the corresponding double series in the groups (II). In the case of the latter the co-factors are obtained from the table by taking the quantity in the second column together with the appropriate coefficient from the remaining columns.

Table I.—Terms of the Null-Function.

(I) Co-factors of

$$E_1: (e^{3i\phi} - e^{-3i\phi}) P_4^3(\mu) + P_4^4(0).$$

$$E_2: (e^{6i\phi} - e^{-6i\phi}) P_7^6(\mu) + P_4^4(0).$$

$$E_3: (e^{9i\phi} - e^{-9i\phi}) P_{10}^9(\mu) + P_{10}^{10}(0).$$

$$F_0: 2P_1$$

$$F_1: (e^{3i\phi} + e^{-3i\phi}) P_4^3(\mu) + P_4^4(0).$$

$$F_2: (e^{6i\phi} + e^{-6i\phi}) P_7^6(\mu) + P_7^7(0).$$

(II) Co-factors of $iE_1 P_n^s(\mu)$.

		$n = s + 1.$	$n = s + 3.$	$n = s + 5.$	$n = s + 7.$
$s = 0$		$-3.75. 10^{-1}$	$2.92. 10^{-1}$	$-9.67. 10^{-2}$	$-1.28. 10^{-2}$
$s = 6$	$e^{6i\phi} + e^{-6i\phi}$	$4.45. 10^{-6}$	$2.59. 10^{-7}$	$3.06. 10^{-8}$	$5.43. 10^{-9}$
$s = 12$	$e^{12i\phi} + e^{-12i\phi}$	$2.00. 10^{-14}$	$1.19. 10^{-15}$	$1.20. 10^{-16}$	$1.69. 10^{-17}$

* 'Proc. Roy. Soc.,' A, vol. 126, p. 3 (1930).

Table I—(continued).

Co-factors of $iE_2P_n^s(\mu)$.

		$n = s + 1.$	$n = s + 3.$	$n = s + 5.$	$n = s + 7.$
$s = 3$ $s = 9$	$e^{3i\phi} + e^{-3i\phi}$ $e^{9i\phi} + e^{-9i\phi}$	$-5.13 \cdot 10^{-3}$ $9.87 \cdot 10^{-10}$	$-5.95 \cdot 10^{-4}$ $2.64 \cdot 10^{-11}$	$-2.43 \cdot 10^{-4}$ $1.58 \cdot 10^{-11}$	$-9.74 \cdot 10^{-7}$ $1.53 \cdot 10^{-13}$

Co-factors of $iE_3P_n^s(\mu)$.

		$n = s + 1.$	$n = s + 3.$	$n = s + 5.$	$n = s + 7.$
$s = 0$ $s = 6$ $s = 12$	$e^{6i\phi} + e^{-6i\phi}$ $e^{12i\phi} + e^{-12i\phi}$	$-4 \cdot 10 \cdot 10^{-3}$ $-4.26 \cdot 10^{-6}$ $8.27 \cdot 10^{-14}$	$9.23 \cdot 10^{-3}$ $1.74 \cdot 10^{-7}$ $1.26 \cdot 10^{-15}$	$-7.93 \cdot 10^{-2}$ $-2.98 \cdot 10^{-9}$ $4.55 \cdot 10^{-17}$	$1.75 \cdot 10^{-2}$ $-5.68 \cdot 10^{-11}$ —

Co-factors of $iF_0P_n^s(\mu)$.

		$n = s + 1.$	$n = s + 3.$	$n = s + 5.$	$n = s + 7.$
$s = 3$ $s = 9$	$e^{3i\phi} - e^{-3i\phi}$ $e^{9i\phi} - e^{-9i\phi}$	$2.34 \cdot 10^{-2}$ $1.55 \cdot 10^{-9}$	$4.76 \cdot 10^{-3}$ $1.77 \cdot 10^{-10}$	$1.56 \cdot 10^{-3}$ $3.22 \cdot 10^{-11}$	$6.54 \cdot 10^{-4}$

Co-factors of $iF_1P_n^s(\mu)$.

		$n = s + 1.$	$n = s + 3.$	$n = s + 5.$	$n = s + 7.$
$s = 6$ $s = 12$	$e^{6i\phi} - e^{-6i\phi}$ $e^{12i\phi} - e^{-12i\phi}$	$8.90 \cdot 10^{-4}$ $8.01 \cdot 10^{-14}$	$5.18 \cdot 10^{-7}$ $4.77 \cdot 10^{-15}$	$6.12 \cdot 10^{-3}$ $4.81 \cdot 10^{-10}$	$1.09 \cdot 10^{-3}$ —

Co-factors of $iF_2P_n^s(\mu)$.

		$n = s + 1.$	$n = s + 3.$	$n = s + 5.$
$s = 3$ $s = 9$	$e^{3i\phi} - e^{-3i\phi}$ $e^{9i\phi} - e^{-9i\phi}$	$-2.56 \cdot 10^{-3}$ $1.48 \cdot 10^{-9}$	$2.98 \cdot 10^{-4}$ $3.96 \cdot 10^{-11}$	$-1.22 \cdot 10^{-4}$ $2.38 \cdot 10^{-12}$

§ 3. *Solution of the Equations.*

We now proceed to solve the equations (1) of § 2, taking for $\bar{\zeta}$ the terms of the null-function together with the term corresponding to the tide producing potential, i.e., $HP_2^1(\mu) e^{i\phi}$. This solution contains the arbitrary constants E_n, F_n which may be determined later from the conditions at the boundaries.

The complete solution of the equations (1) will be the aggregate of the solutions corresponding to each term of $\bar{\zeta}$ taken separately, and these solutions are obtained by the same method as given in Part III* of Goldsbrough's papers. Since in the present problem $\sigma = \omega$ we have

$$\begin{aligned}
 x_r^s &= \frac{(r-s+1)(r-s+2)}{(2r+1)(2r+3)\{(r+1)(r+2)-2s\}} \\
 y_r^s &= \frac{(r+s+1)(r+s+2)}{(2r+3)(2r+5)\{(r+1)(r+2)-2s\}} \\
 \text{and} \\
 L_r^s &= -\frac{hg}{4\omega^2 a^2} + \frac{r(r+1)-2s}{4r^2(r+1)^2} \\
 &\quad - \frac{(r-1)^2(r-s)(r+s)}{r^2(2r-1)(2r+1)\{r(r-1)-2s\}} \\
 &\quad - \frac{(r+2)^2(r-s+1)(r+s+1)}{(r+1)^2(2r+1)(2r+3)\{(r+1)(r+2)-2s\}} \}
 \end{aligned} \tag{3}$$

Now let $\zeta = \sum_{r=-s}^{\infty} C_r^s P_r^s(\mu) e^{i(\sigma t + s\phi)}$, in which the time factor is included, be the solution corresponding to a typical term $\gamma_n^s P_n^s(\mu) e^{i(\sigma t + s\phi)}$ of $\bar{\zeta}$. Then writing

$$\frac{x_r^s C_r^s}{C_{r+2}^s} = H_r^s, \quad \frac{y_{r-2}^s C_r^s}{C_{r-2}^s} = K_r^s,$$

we have

$$C_{r-2}^s / C_r^s = H_{r-2}^s / x_{r-2}^s, \quad r < n+1,$$

$$C_{r+2}^s / C_r^s = K_{r+2}^s / y_r^s, \quad r > n-1.$$

Also

$$C_n^s = \frac{gh\gamma_n^s}{4\omega^2 a^2} / (H_{n-2}^s - L_n^s + K_{n+2}^s),$$

and

$$H_{r-2}^s - L_r^s + K_{r+2}^s = 0, \quad (r \neq n),$$

from which it follows that

$$H_r^s = \frac{x_r^s y_r^s}{L_r^s - H_{r-2}^s} \quad \text{and} \quad K_r^s = \frac{x_{r-2}^s y_{r-2}^s}{L_r^s - K_{r+2}^s}. \tag{4}$$

The requisite values of x_r^s , y_r^s and L_r^s having been calculated from (3) and taking into account the condition that $\lim_{r \rightarrow \infty} C_r^s = 0$, which is necessary in order that the coefficients of ζ should be convergent at the poles $\mu = \pm 1$, the values

* *Loc. cit.*, p. 3.

of H_1^2 and K_1^2 may be evaluated from (4). Hence the values of the coefficients C_1^2 are obtained.

In the case of an ocean of uniform depth covering the whole of a rotating globe or bounded by lines of latitude there is, as first established by Laplace,* no rise and fall due to the diurnal tide but only tidal currents. The solution of the equations corresponding to the potential $gHP_2^1(\mu)e^{i(\phi+\sigma t)}$ is thus zero. The complete expression for the solution ζ is therefore that given in the Table II below. To obtain any specified term, e.g., that containing $E_1P_8^3(\mu)$, take the entries corresponding to $s = 3$, $n = 8$ from the group for E_1 together with the factor given in the second column. The complete term is thus $E_1(1.82 \cdot 10^{-3} e^{3i\phi} - 1.64 \cdot 10^{-3} e^{-3i\phi})P_8^3(\mu) \div P_4^1(0)$.

Table II.—Series for ζ .

(1) Coefficients of $P_n^s(\mu)$ in terms with co-factor E_1 .

		$n = s + 1.$	$n = s + 3.$	$n = s + 5.$	$n = s + 7.$
$s = 0$	i	1.97	-1.86	$4.99 \cdot 10^{-1}$	$-8.48 \cdot 10^{-2}$
$s = 3$	$e^{3i\phi} \div P_4^1(0)$	$8.09 \cdot 10^{-1}$	$-4.17 \cdot 10^{-2}$	$1.82 \cdot 10^{-3}$	$-6.16 \cdot 10^{-4}$
$s = 3$	$e^{-3i\phi} \div P_4^1(0)$	-1.19	$4.49 \cdot 10^{-2}$	$-1.64 \cdot 10^{-3}$	$4.92 \cdot 10^{-4}$
$s = 6$	$i e^{6i\phi}$	$4.35 \cdot 10^{-2}$	$2.09 \cdot 10^{-7}$	$2.69 \cdot 10^{-9}$	$5.00 \cdot 10^{-9}$
$s = 6$	$i e^{-6i\phi}$	$4.71 \cdot 10^{-2}$	$2.27 \cdot 10^{-7}$	$2.78 \cdot 10^{-9}$	$5.09 \cdot 10^{-9}$
$s = 12$	$i e^{12i\phi}$	$2.02 \cdot 10^{-14}$	$1.17 \cdot 10^{-16}$	$1.18 \cdot 10^{-16}$	—
$s = 12$	$i e^{-12i\phi}$	$2.04 \cdot 10^{-14}$	$1.18 \cdot 10^{-16}$	$1.19 \cdot 10^{-16}$	—

(2) Coefficients of $P_n^s(\mu)$ in terms with co-factor E_2 .

		$n = s + 1.$	$n = s + 3.$	$n = s + 5.$
$s = 3$	$i e^{3i\phi}$	$-4.36 \cdot 10^{-3}$	$7.59 \cdot 10^{-4}$	$-5.57 \cdot 10^{-5}$
$s = 3$	$i e^{-3i\phi}$	$-6.30 \cdot 10^{-3}$	$8.25 \cdot 10^{-4}$	$-5.35 \cdot 10^{-5}$
$s = 6$	$e^{6i\phi} \div P_7^2(0)$	$9.92 \cdot 10^{-1}$	$-8.64 \cdot 10^{-2}$	$9.84 \cdot 10^{-3}$
$s = 6$	$e^{-6i\phi} \div P_7^2(0)$	-1.07	$6.90 \cdot 10^{-2}$	$-6.43 \cdot 10^{-3}$
$s = 9$	$i e^{9i\phi}$	$9.95 \cdot 10^{-10}$	$2.37 \cdot 10^{-11}$	$1.47 \cdot 10^{-12}$
$s = 9$	$i e^{-9i\phi}$	$1.02 \cdot 10^{-9}$	$2.46 \cdot 10^{-11}$	$1.50 \cdot 10^{-12}$

* Lamb, "Hydrodynamics," p. 320 (1924).

Table II—(continued).

(3) Coefficients of $P_n^s(\mu)$ in terms with co-factor E_s .

		$n = s + 1.$	$n = s + 3.$	$n = s + 5.$
$s = 0$	i	$2.97 \cdot 10^{-1}$	$-2.57 \cdot 10^{-1}$	$8.75 \cdot 10^{-2}$
$s = 6$	$ie^{6i\phi}$	$-4.27 \cdot 10^{-6}$	$2.06 \cdot 10^{-7}$	$-5.24 \cdot 10^{-8}$
$s = 6$	$ie^{-6i\phi}$	$-4.59 \cdot 10^{-6}$	$2.05 \cdot 10^{-7}$	$-4.86 \cdot 10^{-8}$
$s = 9$	$e^{9i\phi} + P_{10}^{10}(0)$	1.01	$-2.51 \cdot 10^{-3}$	$1.03 \cdot 10^{-3}$
$s = 9$	$e^{-9i\phi} + P_{10}^{10}(0)$	-1.04	$1.99 \cdot 10^{-3}$	$-6.70 \cdot 10^{-4}$
$s = 12$	$ie^{12i\phi}$	$8.39 \cdot 10^{-14}$	$1.18 \cdot 10^{-15}$	$4.32 \cdot 10^{-17}$
$s = 12$	$ie^{-12i\phi}$	$8.46 \cdot 10^{-14}$	$1.21 \cdot 10^{-15}$	$4.38 \cdot 10^{-17}$

(4) Coefficients of $P_n^s(\mu)$ in terms with co-factor F_0 .

		$n = s + 1.$	$n = s + 3.$	$n = s + 5.$	$n = s + 7.$
$s = 0$	1	-6.31	7.18	-2.24	$3.28 \cdot 10^{-1}$
$s = 3$	$ie^{3i\phi}$	$1.74 \cdot 10^{-2}$	$3 \cdot 10 \cdot 10^{-3}$	$1.25 \cdot 10^{-3}$	$5.81 \cdot 10^{-4}$
$s = 3$	$ie^{-3i\phi}$	$-2.61 \cdot 10^{-2}$	$-3.45 \cdot 10^{-3}$	$-1.32 \cdot 10^{-3}$	$-5.94 \cdot 10^{-4}$
$s = 9$	$ie^{9i\phi}$	$1.54 \cdot 10^{-9}$	$1.70 \cdot 10^{-10}$	$3.11 \cdot 10^{-11}$	—
$s = 9$	$ie^{-9i\phi}$	$-1.60 \cdot 10^{-9}$	$-1.74 \cdot 10^{-10}$	$-3.15 \cdot 10^{-11}$	—

(5) Coefficients of $P_n^s(\mu)$ in terms with co-factor F_1 .

		$n = s + 1.$	$n = s + 3.$	$n = s + 5.$	$n = s + 7.$
$s = 3$	$e^{3i\phi} + P_4^4(0)$	$8.09 \cdot 10^{-1}$	$-4.17 \cdot 10^{-2}$	$1.82 \cdot 10^{-3}$	$-6.16 \cdot 10^{-5}$
$s = 3$	$e^{-3i\phi} + P_4^4(0)$	1.19	$-4.49 \cdot 10^{-2}$	$1.64 \cdot 10^{-3}$	$-4.92 \cdot 10^{-5}$
$s = 6$	$ie^{6i\phi}$	$8.71 \cdot 10^{-6}$	$4.19 \cdot 10^{-7}$	$5.39 \cdot 10^{-8}$	$1.00 \cdot 10^{-8}$
$s = 6$	$ie^{-6i\phi}$	$-9.42 \cdot 10^{-6}$	$-4.54 \cdot 10^{-7}$	$-5.57 \cdot 10^{-8}$	$-1.02 \cdot 10^{-8}$
$s = 12$	$ie^{12i\phi}$	$8.09 \cdot 10^{-14}$	$4.67 \cdot 10^{-15}$	$4.71 \cdot 10^{-16}$	—
$s = 12$	$ie^{-12i\phi}$	$-8.17 \cdot 10^{-14}$	$-4.73 \cdot 10^{-15}$	$-4.75 \cdot 10^{-16}$	—

Table II—(continued).

(6) Coefficients of $P_n^s(\mu)$ in terms with co-factor F_s .

		$n = s + 1.$	$n = s + 3.$	$n = s + 5.$
$s = 3$	$ie^{3i\phi}$	$-2.18 \cdot 10^{-2}$	$3.79 \cdot 10^{-4}$	$-2.79 \cdot 10^{-5}$
$s = 3$	$ie^{-3i\phi}$	$3.15 \cdot 10^{-2}$	$-4.13 \cdot 10^{-4}$	$2.67 \cdot 10^{-5}$
$s = 6$	$e^{6i\phi} + P_7^7(0)$	$9.92 \cdot 10^{-1}$	$-8.64 \cdot 10^{-2}$	$9.84 \cdot 10^{-3}$
$s = 6$	$e^{-6i\phi} + P_7^7(0)$	1.07	$-6.90 \cdot 10^{-2}$	$6.43 \cdot 10^{-3}$
$s = 9$	$ie^{9i\phi}$	$1.49 \cdot 10^{-2}$	$3.55 \cdot 10^{-11}$	$2.20 \cdot 10^{-12}$
$s = 9$	$ie^{-9i\phi}$	$-1.54 \cdot 10^{-2}$	$-3.69 \cdot 10^{-11}$	$-2.25 \cdot 10^{-12}$

§ 4. Application of the Boundary Conditions.

It is now possible to determine the values of the coefficients E_n , F_n by making use of the boundary condition, *i.e.*, that v vanishes both when $\phi = 0$ and $\phi = \pi/3$. It may be deduced from equations (1) that it is therefore necessary that

$$\frac{\mu}{f} \sqrt{1-\mu^2} \frac{\partial \zeta'}{\partial \mu} + \frac{i}{\sqrt{1-\mu^2}} \frac{\partial \zeta'}{\partial \phi} \quad (5)$$

where $f = \frac{\sigma}{2\omega} = \frac{1}{2}$, should be zero for all values of μ when $\phi = 0$ and $\pi/3$.

The function ζ' to be substituted in (5) is $\zeta - \bar{\zeta}$ and is therefore made up of the terms in the series for ζ given in Table II together with the term $-HP_1^1(\mu)e^{i\phi}$. Before carrying out this substitution, however, the Legendre functions in ζ' which are of various orders are replaced by equivalent series of functions all of the same order. Then from the resulting identity, by equating to zero the coefficients of each of the Legendre functions in turn, we obtain equations from which the coefficients E_n , F_n may be determined.

As in the case of the semi-diurnal tide it has been found most satisfactory to expand the Legendre functions in ζ' as series of "associated functions" of order three, but of even degree, as they must be odd functions of μ . In obtaining these series use has been made of the corresponding series given in Table III of that paper,* in the manner already suggested in § 2. The logarithms of the coefficients in these expansions of $P_n^s(\mu)/P_7^7(0)$ are given below.

* *Loc. cit.*, p. 10.

Table III.

s .	n .	$P_4^s(\mu)$.	$P_6^s(\mu)$.	$P_8^s(\mu)$.	$P_{10}^s(\mu)$.
0	1	2.26500	3.57271	3.08724	4.71081
	3	π 2.01496	3.33646	4.98453	4.65031
	5	3.11263	π 3.54171	4.57252	4.49276
	7	4.10139	4.79518	π 3.19008	5.64048
	9	5.03743	5.88024	4.55023	π 4.91381
1	2	2.63205	3.77948	3.08884	4.61172
6	7	2.89482	π 3.95952	4.54369	π 5.37107
	9	1.10275	1.10037	π 2.52314	3.85974
	11	1.22635	1.30273	1.21800	π 2.94002
9	10	2.90857	π 2.19422	3.29907	π 4.13672
	12	1.47755	1.15527	π 2.90661	2.26553
	14	1.86106	1.74827	1.17232	π 1.35411
12	13	2.90406	π 2.28556	3.60638	π 4.79029
	15	1.68931	1.07841	π 1.08735	2.69897
	17	0.24533	1.99423	π 2.30940	π 1.54121

The result of the substitution of these series is to obtain an expression for ζ' which is of the form

$$\sum_{r=0}^{\infty} (A_r e^{2ir\phi} + B_r e^{-2ir\phi}) + H\alpha e^{i\phi},$$

where A_r and B_r are linear in E_r , F_r and, with α , are also linear in the functions $P_n^s(\mu)$. Putting $\phi = 0$ and $\phi = \pi/3$ after carrying out the operation (5) on this expression we obtain the identities:

$$\begin{aligned} \sum_{r=0}^{\infty} (A_r + B_r) + \sum_{r'=1}^{\infty} (A_{r'} + B_{r'}) + H\alpha &= 0, \\ \sum_{r=0}^{\infty} (A_r + B_r) - \sum_{r'=1}^{\infty} (A_{r'} + B_{r'}) + H\alpha e^{i\frac{\pi}{3}} &= 0, \end{aligned}$$

where r , r' are even and odd integers respectively. Taking half the sum and half the difference of these we have

$$\begin{aligned} \sum_{r=0}^{\infty} (A_r + B_r) + \frac{1}{2}H\alpha (1 + e^{i\frac{\pi}{3}}) &= 0 \\ \sum_{r'=1}^{\infty} (A_{r'} + B_{r'}) + \frac{1}{2}H\alpha (1 - e^{i\frac{\pi}{3}}) &= 0 \end{aligned} \tag{6}$$

Linear equations in E_r , F_r are then obtained by equating to zero the coefficients of $P_n^s(\mu)$ in each of the identities (6). Six equations were obtained in this way, the coefficients of $P_4^s(\mu)$, $P_6^s(\mu)$ and $P_8^s(\mu)$ alone being considered. This

reduces the calculations as far as possible consistent with what appears, as shown later, to be a sufficient degree of accuracy.

The left-hand members of these six equations are given below. Each of the numbers is to be multiplied by the quantity at the head of the column in which it appears and the sum of the terms in each row so obtained is equated to zero.

F_0i	E_1	F_1	E_2i	F_2i	E_3	$\frac{1}{4}(1-\sqrt{3}i)H$
-12.8	-2.81	+0.074	+0.066	-3.30	-3.90	+0.411
- 1.34	+0.212	-0.460	+0.087	+0.393	+0.778	+0.808
- 0.182	-0.007	+0.051	-0.051	-0.004	-0.107	+0.237
+ 1.75	+0.048	+8.48	-3.68	-0.530	-0.228	-0.713
+ 3.86	+1.250	-0.326	+0.492	-0.286	+0.131	-1.400
- 0.063	-0.070	-0.109	-0.032	+0.093	+0.027	-0.410

The solution of these equations gives the following values for the coefficients E_n, F_n :—

$$\left. \begin{aligned} F_0 &= -0.305(\sqrt{3} + i)H & E_2 &= 2.93(\sqrt{3} + i)H \\ E_1 &= -0.40(1 - \sqrt{3}i)H & F_2 &= 1.89(\sqrt{3} + i)H \\ F_1 &= -1.41(1 - \sqrt{3}i)H & E_3 &= 0.835(1 - \sqrt{3}i)H \end{aligned} \right\}. \quad (7)$$

§ 5. *The Final Form of ζ .*

If the values of the coefficients (7) are substituted in the expression for ζ of § 3 the final form for ζ is obtained representing the tidal elevation at each point of the ocean considered at each instant of time. Since the ratio of the real and imaginary parts of E_n, F_n is $\sqrt{3} : 1$ for κ even and $-1 : \sqrt{3}$ for κ odd the expression for ζ , with the time factor included is as follows :—

$$\begin{aligned} \zeta/H e^{i\sigma t} &= e^{i\frac{\pi}{6}} [3.79P_1 - 3.07P_3 + 1.03P_5 - 0.15P_7 \\ &\quad + ie^{2i\phi} (0.33P_1^3 + 0.09P_3^3 + 0.001P_5^3) \div P_1^4(0) \\ &\quad + ie^{-2i\phi} (0.05P_1^3 - 0.07P_3^3 - 0.02P_5^3) \div P_1^4(0) \\ &\quad + e^{4i\phi} (0.005P_7^3 - 0.03P_9^3 + 0.003P_{11}^3) \div P_7^4(0) \\ &\quad + e^{-4i\phi} (0.001P_7^3 + 0.001P_9^3 + 0.002P_{11}^3) \div P_7^4(0) \\ &\quad + ie^{6i\phi} (0.04P_{10}^3 - 0.014P_{12}^3 - 0.0005P_{14}^3) \div P_{10}^4(0) \\ &\quad + ie^{-6i\phi} (0.1P_{10}^3 - 0.005P_{12}^3 - 0.0002P_{14}^3) \div P_{10}^4(0) \\ &\quad + e^{12i\phi} (-0.01P_{13}^3 + 0.001P_{15}^3 + 0.0002P_{17}^3) \div P_{13}^4(0) \\ &\quad + e^{-12i\phi} (+0.05P_{13}^3 - 0.001P_{15}^3 - 0.0001P_{17}^3) \div P_{13}^4(0)]. \quad (8) \end{aligned}$$

Considered in the horizontal direction this double series shows fair convergence, but in the vertical direction this is not so obvious. That it does give a satisfactory representation of the function, however, may be shown by testing the degree of accuracy with which it satisfies the boundary condition for a particular value of μ . Subtracting $HP_1(\mu) e^{i(\phi + \pi)}$ from the expression (8) for ζ we have ζ' which substituted in the boundary condition (5) should give a result which vanishes for $\phi = 0$ and $\phi = \pi/3$ respectively. When $\mu = \pm 1$ this is true since the factor $1 - \mu^2$ occurs throughout and also for $\mu = 0$ since ζ' is an odd function of μ . Taking an intermediate value $\mu = \frac{1}{2}\sqrt{2}$ the following results are obtained :—

	Positive terms.	Negative terms.
$\phi = 0$	$8.35 + 7.05i$	$-7.80 - 7.4i$
$\phi = \pi/3$	$7.95 + 7.75i$	$-7.70 - 7.34i$

If account be taken of the approximations used in the process of obtaining ζ , the percentage differences of corresponding terms, in no case more than 7 per cent. may be considered satisfactory.

§ 6. Examination of the Results.

From the expression (8) for ζ the tide height at each point of the ocean may be obtained at each instant of time and the corresponding phase. First of all, since ζ is an odd function of μ the equator is a line of zero range and the phase angles at corresponding points north and south of this line differ by 180° . Further, the form of the expression for ζ shows that there is symmetry about the central meridian. The expression (8) is of the form

$$e^{i\frac{\pi}{6}} \{M_0 + i(M_1 e^{2i\phi} + N_1 e^{-2i\phi}) + (M_2 e^{4i\phi} + N_2 e^{-4i\phi}) + \dots\}, \quad (9)$$

where M_r and N_r are odd functions of μ . Thus writing $\phi = \pi/6 \pm \psi$ we have as the respective values for ζ

$$e^{i\frac{\pi}{6}} \{M_0 - (M_1 e^{2i\psi} - N_1 e^{-2i\psi}) - (M_2 e^{4i\psi} + N_2 e^{-4i\psi}) + \dots\}$$

and

$$e^{i\frac{\pi}{6}} \{M_0 - (M_1 e^{-2i\psi} - N_1 e^{2i\psi}) - (M_2 e^{-4i\psi} + N_2 e^{4i\psi}) + \dots\}.$$

The real parts of the expressions in the brackets are identical, while the imaginary parts differ only in sign. The range is therefore the same at points symmetrically situated about the central meridian $\phi = 30^\circ$. These results agree with the general results obtained by Proudman* for an ocean of the type considered.

* 'M.N.R.A.S. Geophysical Suppl.,' vol. 2, p. 98.

The actual tide heights have been calculated for numerous points and are given in the following table, the factor H being omitted.

Table IV.—Tidal Amplitudes.

ϕ	0°.	10°.	20°.	30°.
$\mu = 1$	0.76	0.76	0.76	0.76
0.9	1.02	1.53	1.91	2.05
0.8	1.92	2.20	2.40	2.45
0.7	2.89	3.10	2.61	2.58
0.6	3.74	3.14	2.92	3.04
0.5	4.27	3.30	3.12	3.52
0.4	4.36	3.17	3.00	3.62
0.3	3.90	2.73	2.05	3.11
0.2	2.96	2.07	1.75	2.18
0.1	1.58	1.08	0.89	1.10
0	0	0	0	0

From the symmetry already noted the values for $\phi = 40^\circ, 50^\circ$ and 60° are equal to those for $\phi = 20^\circ, 10^\circ$ and 0° respectively. It will be seen that the amplitudes increase from the equator up to about latitude 30° and then steadily diminish to the poles.

To compare these tide heights with the corresponding results for the semi-diurnal tide* it must be remembered that the value of H is not the same in the two cases. The comparison is therefore made by reducing both sets of results to feet. If the value of H for the diurnal tide is taken as that of the tide O_1 , denoting this value by H_1 and the corresponding value for the semi-diurnal tide M_2 by H_2 , we have $H_1 = 0.42H_2$ where

$$H_1 = \frac{3}{2} \frac{M}{E} \left(\frac{a}{c} \right)^3 a \times 0.19 \text{ feet.}$$

M and E are the masses of the moon and earth respectively, a the distance of the moon from the earth's centre and c the radius of the earth. The heights, expressed in feet, thus obtained at points along the boundary $\phi = 0^\circ$ are as follows :—

$\mu =$	0	0.1	0.2	0.3	0.4	0.5	0.6	0.7	0.8	0.9	1.0
O_1	0	0.53	1.0	1.31	1.46	1.43	1.25	0.98	0.64	0.34	0.25
M_2	27	26.1	25	21.5	18	14	9.3	5.1	2.2	1.25	0.37

* *Loc. cit.*, p. 14.

These heights are, for the most part, larger than those obtained by observation, but the amplitudes of the diurnal tide are seen to be much smaller than those of the semi-diurnal tide except at the poles. The ratio of the height of O_1 to the height of M_2 increases steadily from zero at $\mu = 0$ to $1/10$ at $\mu = 0.5$ and $2/3$ at $\mu = 1$. It is not to be expected that these results will be in very close agreement with the observed tides along the whole of the Atlantic coasts owing to the considerable divergences of the latter from the shape assumed in the theoretical method. Considering the western boundary of the North Atlantic Ocean, however, for points open to the sea on the coast of the United States, the ratio of the observed heights of the two tides obtained from tables of the harmonic constants show good agreement with the theoretical values at corresponding latitudes. Further north fewer observations are available, but at suitable points for comparison the ratio diminishes in much the same way as shown above. Along the eastern boundary of the northern half of the ocean similar agreement is not so apparent; the ratios, for the most part, being smaller than those obtained from the calculations. This is due to the fact that the observed heights of the lunar semi-diurnal tide M_2 are greater on the east side of the Atlantic Ocean than at corresponding latitudes in the west. The diurnal heights, on the other hand, are practically the same.

In order to determine the cotidal lines, the phase angles were calculated at the same time as the amplitudes. These angles were found to present an unusual feature. The central meridian of the ocean is a cotidal line, its phase in the northern half being 330° . There is an increase in this value as one boundary is approached and a decrease towards the other, but the greatest and least angles obtained are 355° and 305° respectively. The difference in phase at any two points in the northern half is thus never greater than 50° and in most cases considerably less. Similar conditions prevail in the southern half, since, as previously shown, the phase angles at corresponding points north and south of the equator differ by 180° .

The reason that the phase angles have such a small range of values is seen, from the calculations, to be due to the predominance in ζ of the terms involving Legendre polynomials. The latter terms arise mainly from the function $P_1(\mu)$ which occurs in the null-function. Now Hough* has shown that for an ocean covering a rotating globe and of uniform depth 14,520 feet the period corresponding to $P_1(\mu)$ is $25\frac{1}{2}$ hours. This depth gives $\beta = 20$, and since in the present problem $\beta = 22.9$ and the period is 24 hours, it is evident that the

* 'Phil. Trans.,' A, vol. 189, p. 233 (1897).

terms mentioned are outstanding owing to the function $P_1(\mu)$ appearing, as stated, in the course of solving the equations.

The wave represented by ζ is thus equivalent to that formed by the combination of a stationary wave given by the terms containing these ordinary Legendre functions and a progressive wave of considerably smaller amplitude. Harris* has considered the combination of a stationary wave and a progressive wave giving a formula from which the phase may be obtained. The combination now under consideration, however, is a particular case where one wave has a much larger amplitude than the other and produces an unusual result which requires a more detailed examination.

In the expression (8) for ζ among the terms which give rise to the progressive wave the coefficient of $e^{i(3\phi + \sigma t)}$ is much larger than any of the others. The latter may, therefore, be neglected without fundamentally affecting the nature of the result. Using the notation of (9) the expression for ζ is thus considered in the form

$$H(M_0 + iM_1 e^{3i\phi}) e^{i\sigma t},$$

where M_0 and M_1 are functions of μ . The factor $e^{i\frac{\pi}{3}}$ has been omitted as this increases all the phase angles by 330° and does not affect their relative values.

Since for high or low tide $\partial\zeta/\partial t = 0$ we have

$$-\sigma H [M_0 \sin \sigma t + M_1 \cos (3\phi + \sigma t)] = 0,$$

therefore

$$\tan \sigma t = \frac{-M_1 \cos 3\phi}{M_0 - M_1 \sin 3\phi}. \quad (10)$$

From the expression for ζ it will be seen that M_0 and M_1 are both positive for all values of μ and $M_0 > M_1$. The function on the right-hand side of (10) therefore increases with ϕ , and as ϕ varies from 0 to $\pi/3$ the value of σt increases from $-\alpha$ to $+\alpha$ where $\tan \alpha = M_1/M_0$ is less than unity. The range of values of σt given by (10) is thus $< 90^\circ$. But σt must take all values from 0° to 360° and it is necessary to consider what happens throughout this complete range. This may be done by means of the diagram below.

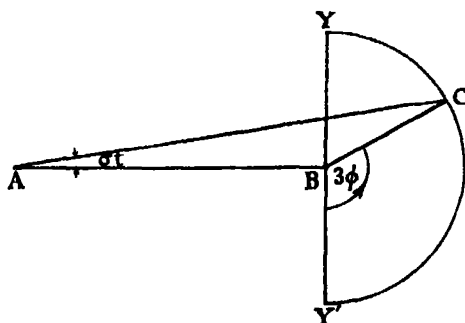
If AB and BC represent M_0 and M_1 , respectively, for the same value of μ and the angle $\pi + 3\phi$ is measured counterclockwise from BY the angle BAC is equal to σt since we may write (10) in the form

$$\tan \sigma t = \frac{M_1 \cos (\pi + 3\phi)}{M_0 + M_1 \sin (\pi + 3\phi)}.$$

* 'Manual of Tides,' Part IV B, p. 322.

52 *Diurnal Tide in an Ocean bounded by Two Meridians.*

As ϕ varies from 0 to $\pi/3$, which is its complete range of values, C moves along the semi-circle YCY' from Y' to Y and σt increases from $-\alpha$ to α .



During this range of values for σt high tide therefore occurs at points of the ocean, and the cotidal lines move across from one side to the other. Since μ varies from 0 to 1 along a meridian, M_0 and M_1 also vary and the cotidal lines do not, in general, coincide with the meridians. They approximate more closely to them as they approach the central meridian, which is a cotidal line and then deviate somewhat again towards the other boundary. There is no isolated point of zero range and the amphidromic point thus lies outside the ocean, i.e., is imaginary.

As AC continues to turn about A, i.e., σt increases from the value α , C leaves the semi-circle, the cotidal lines disappear and there are no points where high tide occurs. When σt reaches the value $\pi - \alpha$ we see from the diagram that CA produced will meet the circle in Y' ($\phi = 0$). Cotidal lines of low tide thus begin to appear in the ocean and continue to do so until $\sigma t = \pi + \alpha$, when $\phi = \pi/3$. There then arises another range of values of σt from $\pi + \alpha$ to $2\pi - \alpha$ during which cotidal lines disappear and neither high nor low tide occurs at any point of the ocean.

This explains the nature of the wave represented by the expression (8) for ζ . There are two equal periods of time during which there is neither high nor low tide at any point of the ocean. There are also two shorter periods, one when high tide occurs at points in the northern half of the ocean and low tide at corresponding points in the southern half, and the other when the reverse occurs in the two portions. During these latter periods the cotidal line moves across the ocean as stated above and the maximum value of 2α , which measures the greatest difference of phase, is in this case about 50° .

The Pressure Exerted by Granular Material: an Application of the Principles of Dilatancy.

By C. F. JENKIN.

(Communicated by Sir Alfred Ewing, F.R.S.—Received January 12, 1931.)

[PLATE 4.]

I. Introduction.

The author had spent about three years endeavouring unsuccessfully to obtain experimental confirmation of the recognised theories of earth pressure and was attempting to measure the "coefficient of friction" of sand (on which all the theories are based) when a research student engaged on this work, Mr. C. P. R. de Villiers, called his attention to a remarkable phenomenon. This was recognised as an example of Dilatancy as described by Osborne Reynolds, and quickly led to the recognition of dilatancy as the fundamental property of granular material on which its behaviour and the forces it exerts ultimately depend. Two well known methods were being used to measure the coefficient of friction; the apparatus is shown in figs. 1 and 2. The outer vessels contained sand and the couples to rotate the disc (fig. 1) and the

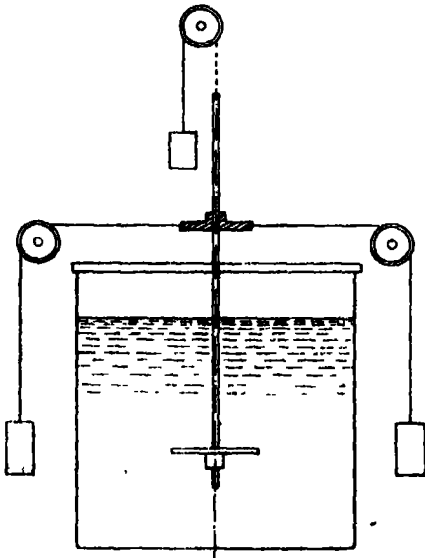


FIG. 1.—Friction measurement with Disc.

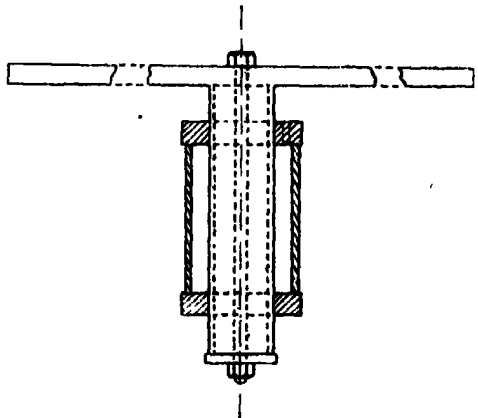


FIG. 2.—Friction measurement with Cylinder.

cylinder (fig. 2) were measured. With neither apparatus could repeat results be obtained. The impossibility of getting repeat results had been the fundamental trouble in all our work. But while making these tests Mr. de Villiers observed that the surface of the sand *heaved up* at the instant when rotation of the disc or cylinder began. This was particularly surprising in the disc apparatus (fig. 1) in which the moving disc was about 6 inches below the surface of the sand. To check whether the sand was really expanding, as it appeared to be, a simple experiment was made with the cylindrical apparatus (fig. 2). The cylinder was completely filled with sand while it was gently tapped ; no ramming was applied and the hole in the top through which it was filled was left open. When an attempt was made to rotate the inner cylinder it was found to be locked, and when the cylinder was finally forced round the couple required was 270 times the ordinary friction couple. When the sand was emptied out a lot of fine dust was found with it showing that rotation had not occurred until the sand was crushed. These experiments showed that the *closeness of packing* of the grains of sand was an essential factor in determining its behaviour and furnished the key to the irregular results of all our previous experiments. Small changes in packing may produce large effects.

To illustrate the magnitude of the effect of closeness of packing a simple experiment on foundation pressures may be quoted. A small flat plate was laid on the flat surface of sand in a large box, and the force was measured to cause the plate to sink into the sand. When the sand was loosely poured into the box and trickled off level the force was only about one-tenth of that required when the sand was shaken and rammed to get it into the close-packed condition. (The densities of the sand in the two conditions were about 91 and 110 lb. per cubic foot ; this small difference offers no explanation of the large difference in bearing pressure.)

As a consequence of these experiments the author set to work to investigate the bearing of dilatancy on the theory of earth pressure. The following paper describes the results which have so far been obtained and their experimental confirmation. The field for experiment offered by the new apparatus (described later) has turned out to be very wide ; the results given here are a mere outline which must be filled in later, but the author has been advised to publish them now rather than to wait for their completion ; and indeed he can see no end at present, for new points of interest are continually arising all of which call for investigation. Much of the work had been completed when the author had the opportunity of re-reading Osborne Reynolds' paper. It was printed in the 'Philosophical Magazine,' in December, 1885, and appears on p. 203

vol. 2, of Osborne Reynolds' "Scientific Papers" ('C.U. Press'). It is entitled "The Dilatancy of Media composed of rigid particles in contact." In it on p. 210 occurs this remarkable prophecy:—

"As regards any results which may be expected to follow from the recognition of this property of dilatancy: in a practical point of view it will place the theory of earth-pressure on a true foundation."

The author believes he could hardly have stronger support for the ideas here developed.

II. Theory and Model.

The principle involved in all that follows may be stated thus: The pressure in a granular mass depends on its weight, on the geometry of the boundaries and the geometry of all the points of contact between the grains, and on the coefficient of friction at the points of contact.

The term "geometry of the points of contact" is meant to include their positions and the inclinations of the minute surfaces of contact. *Changes in the geometry* is the fundamental fact of dilatancy, the most striking effect being an increase in volume; it might be called "changes of packing," but this expression does not call attention to the importance of the directions of the surfaces of contact.

To investigate the almost infinite complexity of the geometry of a mass of sand is clearly impossible, so a simpler material was chosen. The simplest granular material is made up of equal spheres, so the first step was to investigate the static forces between spherical balls, at rest in a box under the action of gravity. It was found that the problem in three dimensions was too complex, so it was reduced to a two-dimensional problem, the box becoming a vertical frame enclosing a single layer of circular discs. A model was made, shown in fig. 3, the essential parts being the base *b*, the "wall" *a*, and the back *c*, and the single layer of steel discs (1 inch diameter, $\frac{1}{4}$ inch long) which rest on the base and fill the space between the wall and the back. The wall *a* in many of the investigations is supposed to represent a retaining wall on which the "sand" (the steel discs) is pressing; it is made to slide on the base so that the motion of the discs may be observed while the wall slides away from them. To eliminate friction with the back board, a piece of cardboard is laid on it while the discs are stacked in position, and then carefully slipped out, leaving the discs free. Each disc is marked with an arrow on the face and has two small holes drilled in it, so that, by means of a two-pronged key, it may be turned to set the arrow in any desired position. By watching the motion of the arrows

as the wall was slipped forward some guide could be obtained as to the points where slipping or rolling occurred, but definite data could not be obtained

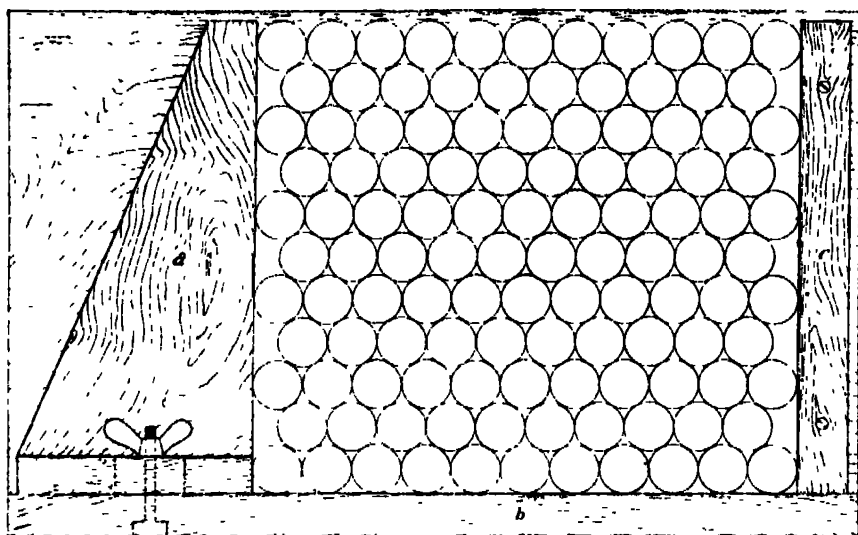


FIG. 3.—Model with Discs.

because very slight differences in diameters between the discs interfered with their ideal motions.

The discs can be arranged in the frame in an infinite number of patterns; the simplest, viz., closest packing, was chosen and the two simplest positions in the frame were chosen, as shown in figs. 4 and 5, these, called *a* and *b*, are

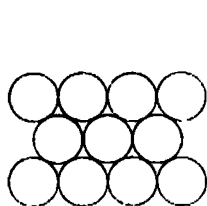


FIG. 4.—Arrangement *a*.

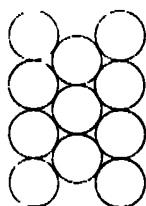


FIG. 5.—Arrangement *b*.

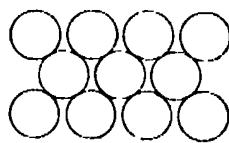


FIG. 6.—Imaginary gaps
arrangement *a*.

the only two arrangements which have been investigated up to the present time. The completely arbitrary nature of this choice must be borne in mind in all that follows. The forces between the discs in both arrangements are indeterminate, because each disc (except those on the boundaries) touches six others, and to make them determinate some further assumption is necessary. The forces in a mass of sand are also indeterminate. The most important

earth-pressure which the engineer has to deal with is the thrust on a retaining wall. As is well known this may have any value between the "active" and "passive" forces, the former (the most important) acting when the retaining wall moves slightly away from the soil behind it, and the latter when it is forced against the soil. To make the model problem determinate therefore it will first be assumed that the wall moves slightly away from the discs.

In arrangement *a* such a motion might be expected to leave small gaps in the horizontal rows of balls, as shown in fig. 6, but a trial with the model proved that these gaps did not appear; nevertheless it will be assumed that all horizontal forces at these points vanish,* and these points will be called "slack contacts" to distinguish them from actual "gaps" which appear under other conditions. By eliminating two forces from each disc the remaining forces have thus been made determinate in arrangement *a*.†

When the discs are put in the model in arrangement *b* and the wall is moved forward, one or two of the alternate columns of discs sink a little, leaving gaps as shown in fig. 7. There appears to be no reason why any one of the inter-

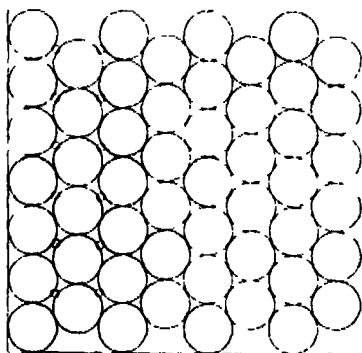


FIG. 7.—Real gaps, arrangement *b*.

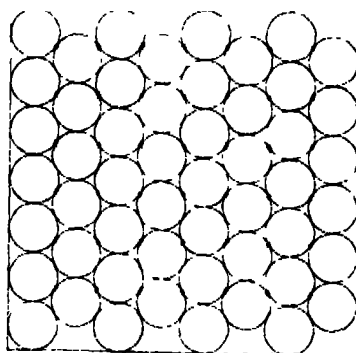


FIG. 8.—Slack contacts, arrangement *b*.

mediate columns should move rather than any other, but the condition is unstable and the moment one column begins to sink it wedges up the rest. It may be assumed therefore that when the motion is very small slack contacts occur at every point marked X in fig. 8. The problem is still indeterminate, but it will be shown that a sufficiently definite solution can be found.

The patterns for the discs having been chosen and the conditions made

* The other possible assumptions are that the forces vanish at the ends of one or other of the diagonal diameters; the results following from these assumptions are given on p. 68. A method of demonstrating the slack contacts is given in Appendix III.

† It is also assumed that the forces vary in a regular manner from the top row downwards and from the wall inwards.

determinate, a number of problems were investigated, only a few of which need be described.

Problem 1.—Neglecting friction, find the distribution of the forces on the vertical wall and horizontal base. The solution, for arrangement *a*, which is perfectly simple, is shown in fig. 9A. The force polygons, a few of which are

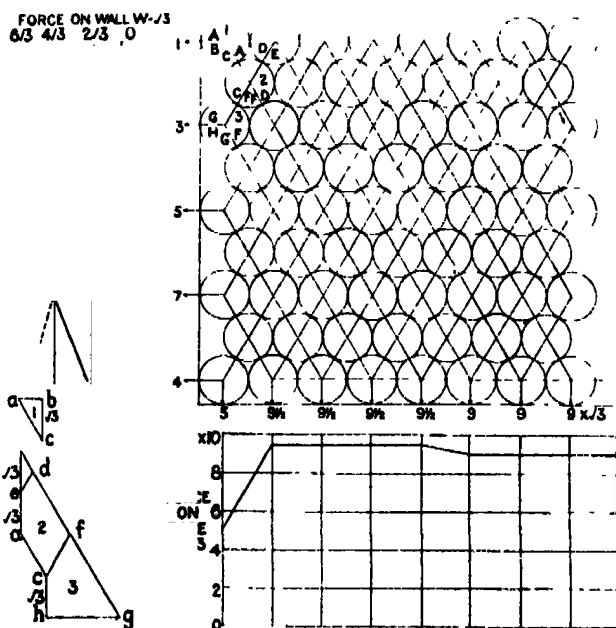


FIG. 9A.—Forces on Wall and Base, arrangement *a*, neglecting friction.

shown, are drawn in order, commencing with the triangle of forces for the left-hand top disc. The weight of the disc is taken to be $\sqrt{3}$, in order to avoid fractional values for the forces. The forces on the wall are proportional to the depth from the top (neglecting the bottom disc)* and the centre of pressure is one-third of the height of the wall from the base. These results agree exactly with the usual theories of earth pressure. The pressure on the base is uniform except for a small drop in the corner and a small hump extending a short distance from the wall. If the number of discs is supposed to be indefinitely increased, these irregularities decrease indefinitely. The addition of a uniform load on each of the top row of discs adds constants to all the forces.

The solution for arrangement *b*, shown in fig. 9B, is also perfectly simple.

* To avoid the trouble of the corner disc the device used in fig. 20 may be used.

The force polygons, a few of which are shown, are drawn in order, commencing with the triangle of forces for the top disc. The weight of the disc is again

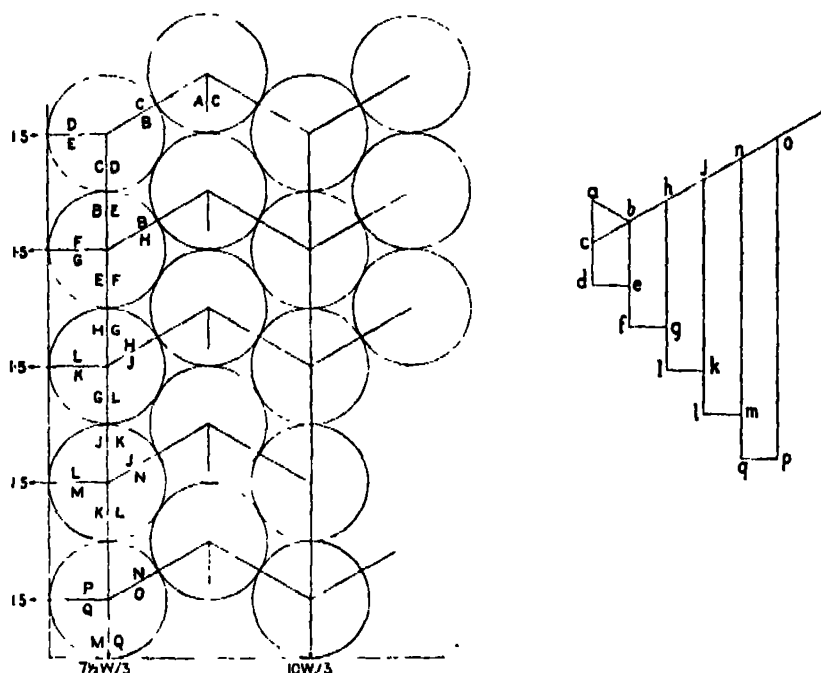


FIG. 9B.—Forces on Wall, arrangement b, neglecting friction.

taken to be $\sqrt{3}$. The weight is transmitted vertically down, only small forces being exerted on the wall, which become negligible at any depth. (The distribution of the small side force is indeterminate, but as it vanishes this point need not be discussed.)

Only those solutions are of use which can be shown to apply to an indefinitely large number of discs ; very misleading results may be obtained if this point is overlooked. For example the large variation of pressure on the base shown in fig. 9A becomes negligibly small when the number of discs is increased, but the corresponding distribution in fig. 11 does not become uniform ; the form of the curve in the figure is, however, greatly distorted by terms which vanish at great depth.

Problem 2.—Assuming friction to act between the discs and between the discs and the wall and base, find the distribution of forces. The solution of this problem for arrangement a is very difficult, because there is no guide to whether slipping or rolling will occur at any point of contact. Starting from the top row to draw the polygons of forces progress is easy, on reasonable

assumptions, for the first few rows of discs, but difficulties accumulate as the lower rows are reached. A solution was eventually found in the following way. A group of discs supposed to be at great depth was considered and a solution was hit upon, shown in fig. 10, which gave equal forces above and below them (their weight being negligible at this depth). The conditions are

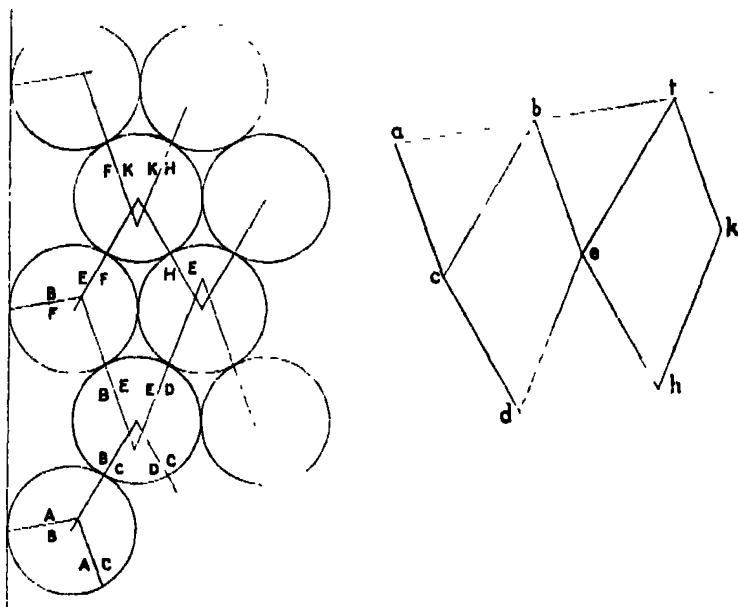


FIG. 10.—Forces on Wall. Solution at great depth, with friction.

different in alternate layers, since only alternate layers touch the wall. Considering the middle layer, all the downward forces EF, HE, etc., on this layer are radial, but all the upward forces on the same layer, BE, ED, etc., are inclined at the friction angle* to the radii. The forces FK, BE and AC are equal; also the forces KH and ED; also the forces BF and AB. Then a method of drawing the force polygons was found which, starting with the known forces in the top layer, gradually approached the conditions found for great depth. This solution is shown in fig. 11. It is believed to be a correct and possible solution but it is not certain whether it is a unique solution. In this figure the discs and polygons are numbered to correspond. The polygons are drawn in the order of the numbers, beginning with the triangle for the left-hand top disc. On each layer which touches the wall the downward forces, such as CF, FD, etc., are radial (as in the solution at great depth). The upward forces on these layers gradually approach the positions they reach

* The tangent of the "Friction Angle" is the coefficient of friction between the discs.

at great depth, i.e., at the friction angle with the radii. They cannot be at this angle near the top while complying with the conditions of static equilibrium;

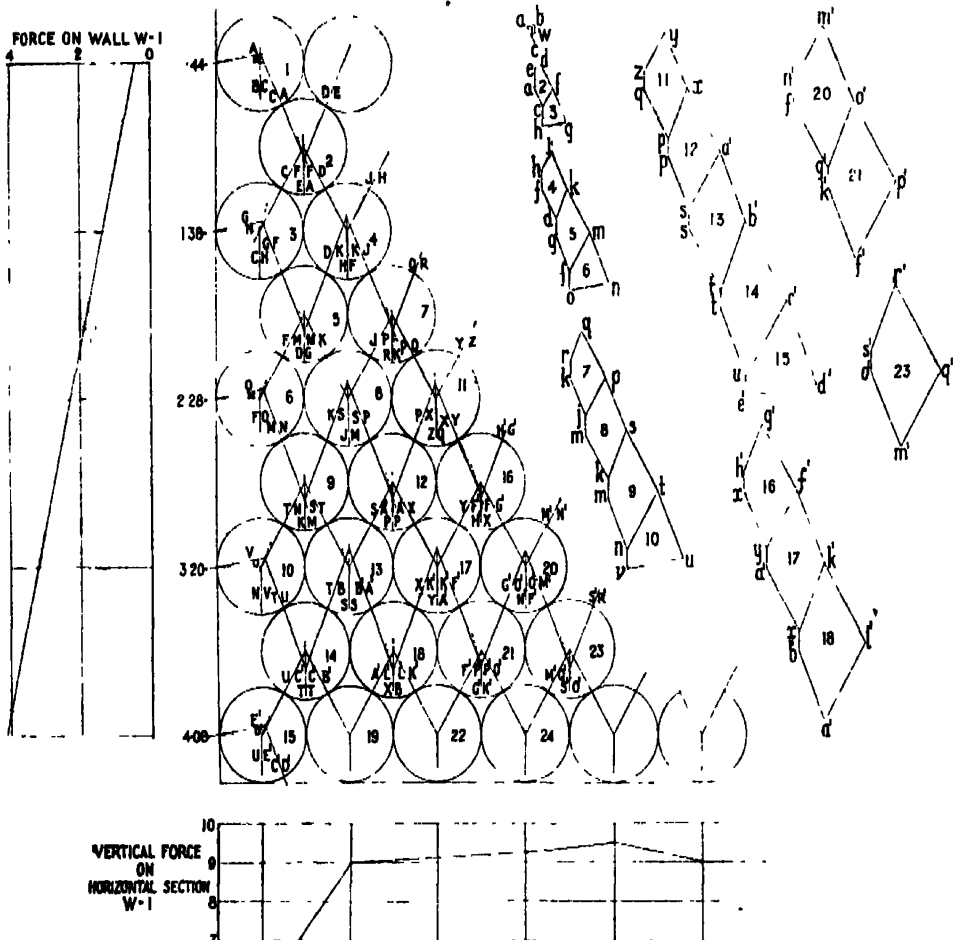


FIG. 11.—Forces on Wall. Complete Solution, with friction.

for example the force CA must pass through the intersection of AB (drawn at the friction angle with the wall) and BC, the line of action of the weight. In general there are five forces on each disc which must be shown in equilibrium. The intermediate resultants, used in the construction, are shown dotted. The results are interesting. The pressure on the wall no longer varies linearly, the curve (though nearly straight) is concave to the wall, so the centre of pressure is above one-third of the height of the wall. The resultant force is inclined to the horizontal by the friction angle. If the vertical component of the total force on the wall is called V , then the force on the base is reduced by \bar{V} and

the distribution on the base is no longer uniform. Fig. 11 shows that the alteration to the normal pressure distribution extends to a distance subtending an angle of 30° at the top of the wall.

These results also agree with the facts. The resultant pressure is known to be inclined (and not horizontal as Rankine supposed, when there is no surcharge). Experiments described later confirm this fact and that the centre of pressure is usually above the one-third point. The pressure distribution on the base is not uniform in reality; this fact has received very little attention as it is of hardly any importance to engineers, but it is interesting because the pressure distribution on the wall is intimately connected with that on the base.

The solution, including friction, for arrangement *b* is shown in fig. 12. The conditions are hardly different from those without friction. As the depth

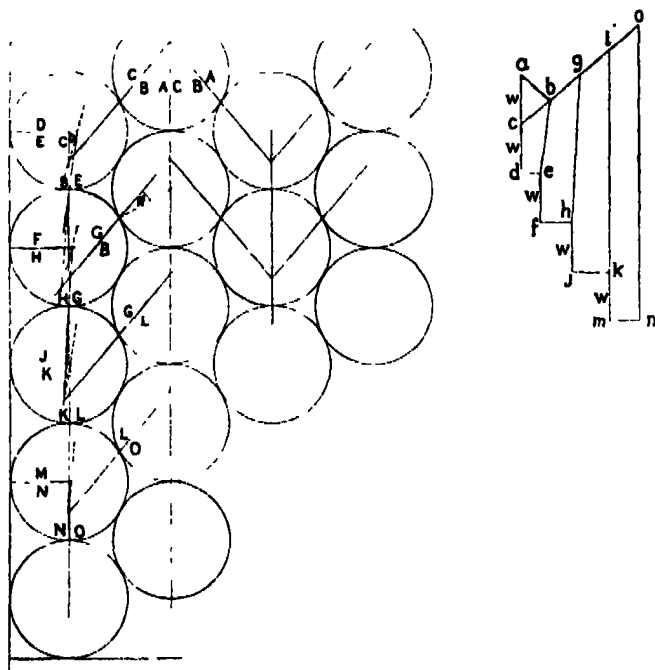


FIG. 12.—Forces on Wall, arrangement *b*, complete solution with friction.

increases the larger forces become almost vertical and for a large number of discs the pressure on the wall becomes negligible. The distribution of the pressure on the wall is indeterminate, but as it vanishes this point need not be discussed. These results have no apparent connection with sand pressures,

but may be found useful in the future in connection with the forces exerted by a material consisting of thin flat grains.

These results being satisfactory the next step was entered on. The most characteristic feature of sand pressure, in the author's opinion, is the phenomenon known as *arching*. It finds no place in the accepted theories of earth pressure, but is very well known and is the direct cause of the failure of many earth pressure tests. Three typical examples may be given of its action:—

- (I) If a small hole be bored in the bottom of a box containing sand, the pressure at the hole disappears and the sand only issues gently and can be stopped by a very slight obstruction. The sand "arches" over the hole.
- (II) If sand or any granular material such as corn be stored in a vessel whose depth is large compared with its diameter, such as a grain silo, the bulk of the weight is carried by the side walls and not by the base and the pressure at various depths is not proportional to the depth, as it is in a wide expanse of sand. The sand "arches" or rather forms domes, abutting on the sides, which carry the weight.
- (III) The Swedish engineer Stroyer has invented a new construction of steel retaining wall,* the essence of which is that it is slightly flexible and is tied back by a strong stay at the top, the base being securely driven into the soil. The wall bulges slightly and thereby throws the load on to the top tie and the bottom of the wall. The pressure is taken by arching between the top and bottom of the wall (both of which are secure).

Each of these three types of arching were investigated in the two-dimensional systems of discs.

(I) *A Hole in the Base.*—If a short length of the base of the model (representing the plug in the bottom of a box of sand) be slightly lowered as in fig. 13

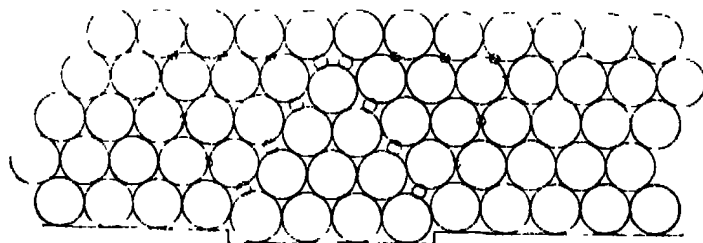


FIG. 13.—Arching over a Hole in the Base.

* 'Proc. Inst. Civil Engineers,' vol. 226, p. 116.

the discs automatically assume a very elegant new pattern.* Gaps appear at all the points marked with a small circle. The result is the removal of a series of diagonal forces, which cannot act across the gaps, and the introduction of a series of horizontal forces. The system of forces is determinate and is shown in fig. 14. The lines of action of the forces form a beautiful arch over

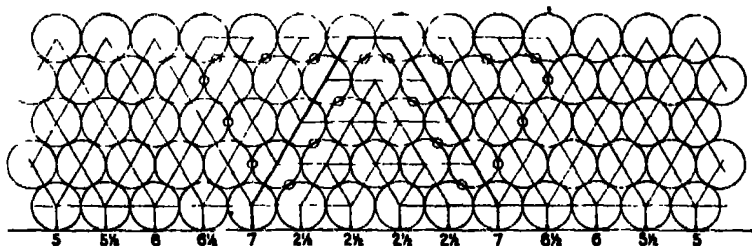


FIG. 14. Arching over a Hole ; solution without friction.

the hole, and the only load left on the plug is equal to the weight of the triangle of discs immediately resting on it. It should be noted that the discs forming the top of the arch do not descend, so no disturbance is propagated to any greater height. Any amount of surcharge may be added on the top layer without affecting the load on the plug, but if the plug is entirely removed the arch collapses. The behaviour of the two-dimensional system corresponds closely with that of sand. This type of arching is the cause of the uncertainty of all earth-pressure measurements made with small elastic plates or capsules buried in the soil, for the purpose of serving as pressure indicators.

(II) *Grain Silo*.—The model was arranged to show arching in a silo. To start the arching, the bottom was slightly lowered in the middle to represent the slackening which would occur if some grain were drawn off, but arching failed to appear and all attempts to draw a diagram of arching were also a failure. A more careful inspection of the model showed what was happening. A single arch formed at the bottom like that shown in fig. 13, but, as was pointed out in that figure, the crown of this arch does not descend, so the conditions to induce arching higher up were absent. Arrangement *b* was then tried, as shown in fig. 15. This was entirely successful. Gaps appeared at the points marked with small circles, and a possible distribution of forces is shown in fig. 16. This diagram represents the condition at great depth and may be compared with fig. 10 for the ordinary distribution at great depth. It is not

* The technical difficulty of drawing these diagrams is very great. The draughtsman has shown all the first order displacements correctly, but some of the second order displacements are not quite accurate.

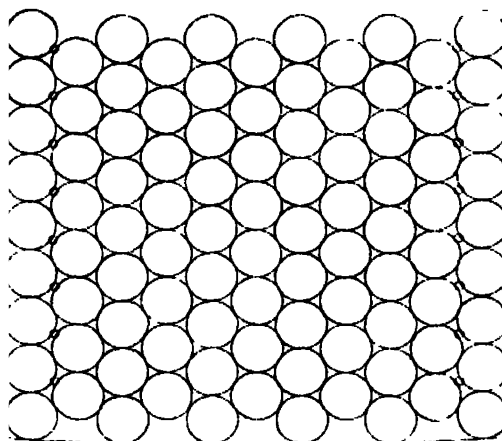


FIG. 15.—Arching in Silo.

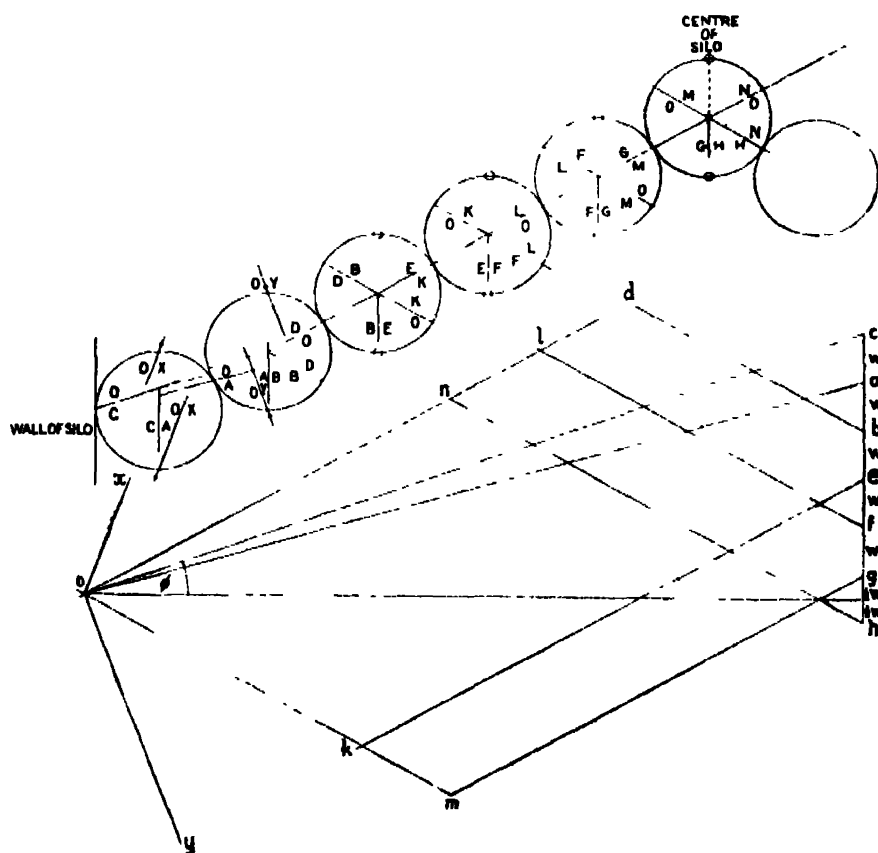


FIG. 16.—Arching in Silo ; solution at great depth, with friction.

certain whether this solution is unique. It has interesting points. The forces on the two outermost columns of discs are quite different from those on the rest; this is to be expected because the outermost column abuts on a vertical wall and the second column has a row of gaps. The central group of discs is assumed to have slack contacts at the points marked with a small circle, the lowering of the middle of the base has loosened the vertical contacts exactly as the sliding of the wall loosened the horizontal contacts, no new assumption has therefore been made. The gaps show that dilatation has taken place; the increase of volume occurs entirely sideways and may be regarded as the cause of the jamming and arching. The load on the base will be that due to the forces shown under the discs in the arch together with the weight of the discs filling the triangular space under the lowest arch. This load is independent of the height to which the silo is filled. Before the middle of the base was lowered, to induce arching, the whole weight was borne by the base.

(III) *Stroyer's Retaining Wall*.—Fig. 17 shows the positions assumed by the discs when the model is fitted with a flexible retaining wall. The tie rod is

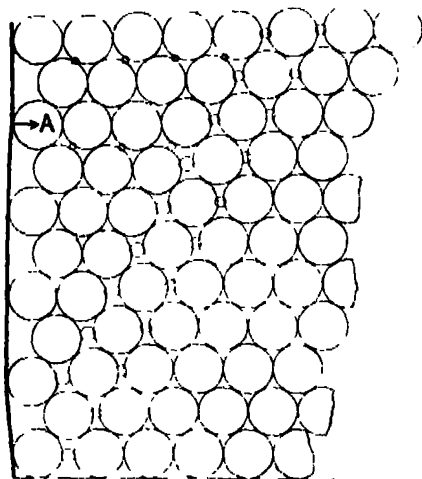


FIG. 17.—Stroyer's retaining wall.

supposed to be at A, and the upper part of the wall is supposed to be vertical. These conditions are quite arbitrary and are intended to represent more or less what might happen in practice. The gaps which appear are marked with a small circle. The solution is shown in fig. 18* (without friction). The hori-

* There is a small inconsistency in fig. 18 in the corner. This may be removed by the device used in fig. 20. It has not been thought necessary to redraw the figure.

zontal forces are shown on the margin in parallel columns with the forces on an ordinary retaining wall (without friction). Stroyer's claim that the force

3

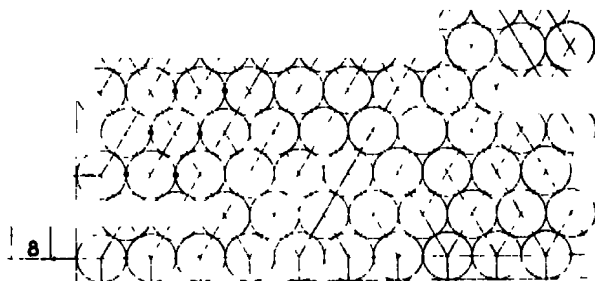


FIG. 18.—Stroyer's Retaining Wall ; solution, without friction.

is concentrated on the tie and the base of the wall is confirmed. But a point which may be of importance in practice is that the overturning moment on Stroyer's wall is greater than on an ordinary wall and the tie rod should be designed accordingly. Experiments described later in this paper prove that the position of the resultant may be far above the one-third height, and though the necessary conditions do not often occur, the model suggests that they will occur in Stroyer's wall.

In each of these examples of arching the slack contacts have shifted from the positions they occupied in the ordinary conditions previously described. This suggests that a second solution of the first problem (pressure on a wall) might be found if the slack contacts were assumed to be on one of the diagonal diameters of each disc, instead of on the horizontal diameter. To investigate this possibility it is first necessary to examine what happens in the model when the wall is moved a little forwards. The positions automatically assumed by the discs is shown in fig. 19. A double line of gaps appears (marked with small circles) along a line rising at 60° from the corner ; this corresponds with the " plane of rupture " in sand.* (In the sand used in the experiments the plane of rupture is at about 62° from the horizontal.) The double line of gaps and the special position assumed by the bottom corner disc are due to the model having a flat bottom board. If we assume (as would happen in a real

* This plane of rupture may be seen in fig. 17 also.

retaining wall) that the bottom row of discs is resting on more discs underneath them, only a single line of gaps appears, as is shown in fig. 20, where the

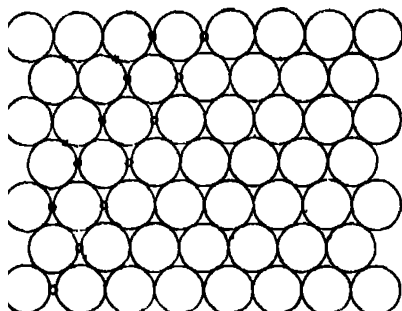


FIG. 19.—Plane of Rupture.

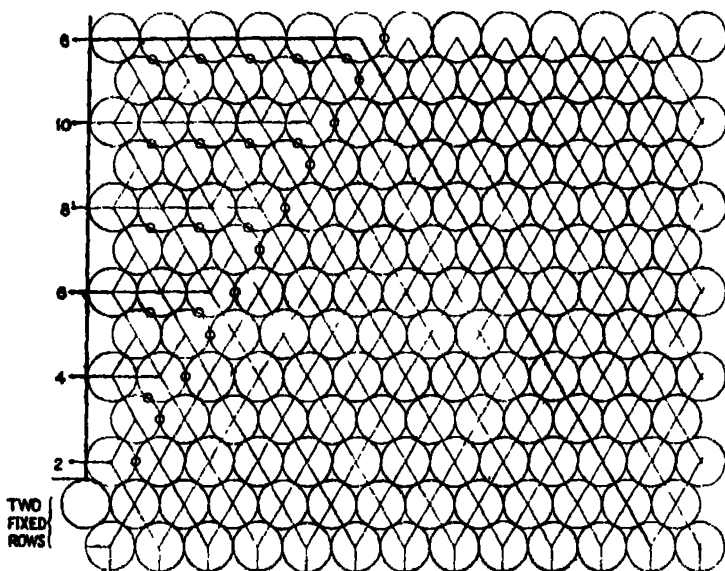


FIG. 20.—Arching against Wall. Solution without friction.

bottom two rows of discs are fixed and the foot of the wall is supposed to rest on them. It will now be assumed that slack contacts occur on the diagonal diameters (as shown at the points marked X in fig. 19 and by small circles in fig. 20) instead of on the horizontal diameters. This assumption makes the solution determinate* and the forces are shown in fig. 20 (neglecting friction). This solution represents the effect of *vertical arching from the base*. It may be compared with the normal solution already given in fig. 9 ; it will be seen that

* Cf. note on p. 57.

the total force on the wall is the same but the centre of pressure is now two-thirds up the wall instead of one-third.* The arching can only extend as far back from the wall as the plane of rupture, the gaps prevent horizontal forces extending further. But for these gaps the force would have been infinite, if the discs extended far enough to the right. It will be noticed that the top row of discs carries a large compressive force; this condition is extremely unstable and could not occur in real sand; in sand the stress is always zero at a free surface.

Considering the two solutions for the pressure on the wall, it may be said that the general solution is indeterminate, but must lie between the two. The force does not vary but it may act at any point between one-third and two-thirds up the wall. This result is strikingly confirmed by the experiments on sand described later.

It is now possible to summarise the results obtained with the model in more general terms.

The forces between the discs are at first indeterminate. Any small change in the shape of the surrounding frame (*e.g.*, sliding the wall forwards, lowering part of the base, causing a bulge in the base (silo), causing a bulge in the wall (Stroyer)) results in a geometrical change of pattern including always a series of gaps (this follows from Osborne Reynolds' theorem of dilatancy). A very small change of shape in the boundary is sufficient to produce these effects; it need only be of the same order of magnitude as the elastic strain in the discs.† The gaps are definite limits to the lines of action of the forces. Within the areas bounded by the gaps the forces may still be indeterminate, but two limiting solutions may be found by assuming slack contacts to occur on horizontal or diagonal lines. These two solutions correspond to the "ordinary" pressure distribution and that produced by "arching." Since dilatancy may be looked upon as the cause of the gaps and also of the slack contacts, its intimate connection with pressure distribution is apparent.

These results have been obtained with a model containing discs in closest packing. No attempt has been made to deal with loosest packing. Loosest

* When there is a surcharge the centre of pressure will go higher still.

† What great changes of pressure in sand are produced by minute changes of boundary may be illustrated by one of the results of very large scale tests recently made in the Massachusetts Institute of Technology on an experimental wall 14 feet long supporting sand 4.85 feet deep. The initial resultant force on the wall of about 6 tons was reduced to one-third of this value when the top of the wall was tipped forward by one-hundredth of an inch, and to one-eighth when the wall was tipped forward by five-hundredths of an inch. *Vide* 'Engineering,' vol. 129, p. 689 (1930).

packing between discs or spheres is extremely unstable, the slightest disturbance causing them to fall into closer packing. Osborne Reynolds suggests that granular material in general cannot be homogeneous and that the loosest packing which can persist occurs when the expansion due to any change of boundaries in some parts equals its contraction in other parts.

No attempt has been made to make a model to represent irregularly shaped grains; they can only be investigated experimentally.

III. *Experiments with Granular Material.*

The next step was to make use of the results already obtained to design a method of measuring sand pressure. The difficulty of measuring the pressure may be illustrated by fig. 13. If a spring balance were put under the plug in the base it obviously would not read the normal pressure, which would be transferred by the arch to the sides of the hole. But the same figure suggests how correct readings could be obtained. In that figure it will be noted that complete arching over a plug in a hole can only occur if the ratio of depth of sand to diameter of hole is greater than a certain value. If the sand is too shallow the arch will fall in, and any modification of pressure on the plug would then be confined to a narrow area round its edge. If a guard ring, having the same freedom of movement as the plug, be placed round the edge, the pressure measured on the plug should be correct. The same line of argument shows that if we want to measure the pressure on a vertical wall, the *length* of the wall must be great compared with the depth of sand, to avoid the errors due to horizontal arching from the ends, and the ends should be protected by an equivalent of the guard ring.

An apparatus shown diagrammatically in fig. 21* for measuring the force on a vertical wall was made on these lines, the length of the wall (21 inches) being seven times its depth (3 inches), proportions which are very different from anything which has been used hitherto. There is an extension at each end which moves forward with the wall, to form the guard. The wall is hung on three knife edges at the bottom of three vertical links so that it swings horizontally while remaining vertical. Three quantities have to be found, the magnitude of the force on the wall, its inclination to the horizontal and the height of its point of application. The three quantities observed are, the force exerted by the spring S which balances the horizontal force on the wall, the value of the counter-weights W_1 , which balance the vertical force on the

* The figure shows the wall as first made. Several modifications have been made since then.

wall, and the value of the back weight W_2 , which balances the tipping moment of the force about the knife edges. The motion of the wall is limited by

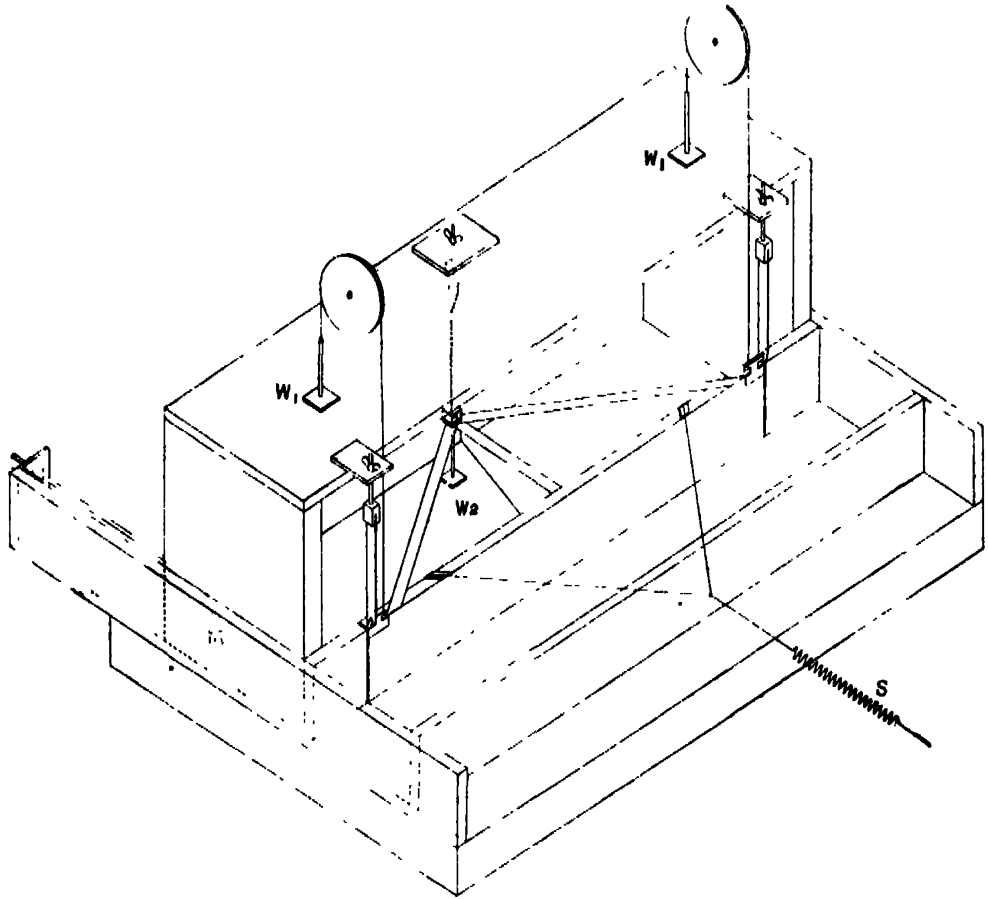


FIG. 21.—Experimental Hanging Wall.

horizontal and vertical stops (not shown), the vertical freedom being kept very small. A sand-tight joint at the bottom is secured by using a surface plate for the base and grinding the metal edge of the wall accurately straight. A clearance of about four-thousandths of an inch is allowed between them. (The sand grains are about 25-thousandths of an inch diameter.) The joints at the ends of the wall are covered with very thin sheet rubber, which does not prevent a small vertical motion. The three vertical links carrying the wall are suspended from the top of a wooden frame which also carries the guard walls; this frame can be moved slowly backwards by the fly nuts on two screws. The whole wall (including the guards) is moved slowly away from the sand while

the spring and weights are adjusted. By this means observations can be repeated again and again under identical conditions, the sand being filled in little by little as its level falls.

To test the effect of the friction between the wall and the sand as fully as possible one wall was prepared with its face covered with fine sand-paper which gave a friction angle* of about 30° , and a second with a polished steel face (sheets of very thin polished steel are sold under the name of music steel). When properly cleaned this gave a friction angle of about 10° .† The choice of a material with a very small friction angle turned out to be most fortunate; some of the most striking results have been obtained with the steel wall.

With this apparatus the author obtained the first series of measurements on sand pressures he ever got which could be repeated. After four years of failure this was encouraging.

As first made the extensions at the ends (guards) were only 1 inch wide, the width of the surface plate preventing the use of wider pieces. Slight evidences of end arching were observed when the apparatus had been got into good working order, so wooden extensions of the surface plate were made and the guard extended to 3 inches each side. As anticipated this modification slightly increased the observed forces on the wall. To make certain that end effects have been entirely eliminated a wider extension still will be made, but urgency of other tests has postponed this for the present.

The conditions under which earth pressure measurements are made must be carefully defined. The author measured the pressure on a wall, free to move parallel to itself, while it was very slowly moved away from the sand. The sand was loosely sprinkled into position and lightly strickled off level, the measurements being made without delay (to avoid any risk of gradual settlement). Under these conditions the sand is continuously in approximately

* The friction angle, i.e., the angle whose tangent is the coefficient of friction between the sand grains and the wall face, may be measured by laying the wall, face down, on a flat topped mound of sand and measuring the horizontal force required to make it slip. This method cannot be relied on to give very close results, and there is no doubt that the angles (indicated by the symbol ψ) in the tables found in the experiments with the new apparatus are more accurate.

† The friction angle between sand and the steel wall varies from 10° to 20° . The cause of the higher friction appears to be the presence of traces of oil, but it is not certain that moisture may not also have an effect. Rubbing with a rag soaked in ether and then swilling with ether has been the most successful of the various methods tried for cleaning the steel. Great confusion was caused in the earlier tests before this variation of the friction angle was discovered.

loosest packing and no general dilatation takes place as it gradually slips forward.

Before describing the results of the measurements on the experimental wall, it is necessary to discuss briefly the old theories. The three principal theories are Rankine's, based on conjugate stresses, *vide* "Civil Engineering," by W. J. M. Rankine (1867); the wedge theory (which has many modifications) based on the equilibrium of a large wedge of sand sliding down the plane of rupture; and Résal's theory based on the solution of a differential equation stating the conditions of equilibrium of an infinitesimal block of sand, *vide* "Poussée des Terres," par J. Résal (Paris, 1903). All these depend on the sliding of one part of the sand over another and therefore on the coefficient of friction between two surfaces of sand. The two latter theories also take account of the coefficient of friction between the sand and the wall. None of them takes any account of the packing of the sand (except in so far as it affects the density) or of the shape of the grains (except as this modifies the coefficient of friction) or of arching. Arching is so important in grain silos that a method of estimating its effect for practical purposes has been developed, but nothing which could be called a theory of arching has been formulated. In all three theories the centre of pressure is assumed to be at one-third of the height of the wall.*

A practical difficulty arises when an attempt is made to use these theories—there is no known method of measuring the coefficient of friction; the methods commonly used are open to serious objection. In the older statements of the theories, the angle of repose was used instead of the friction angle (*i.e.*, the angle whose tangent is equal to the coefficient of friction between two surfaces of sand), and this angle can easily be measured with sufficient accuracy. Osborne Reynolds points out that the angle of repose depends on dilatancy; it may therefore turn out to be a sound basis for calculations, and is more likely to give useful results than a coefficient of friction measured by an unreliable method.

Some results of the tests made with the hanging wall are given in Tables I to V. They are not offered as complete in any way; they are the beginning of investigations along a number of different lines. The field of investigation opened up by the new apparatus is so large that a full statement of results cannot be expected for a considerable time.

* German engineers appear to assume a higher position of the centre of pressure than is customary in England. Weyrauch assumes that it is at 0.4 times the height of the wall. (The author has failed to find the original authority for this statement.) In the 'Bauingenieur,' heft 38, p. 657, Dr. Ing. W. Drechsel proposes much higher positions for surcharged walls.

Most of the tests have been made on standard Leighton Buzzard sand as specified in the British Engineering Standards Association specification for Portland Cement No. 12, 1925. It passes a sieve with 20 meshes per inch and is retained on one with 30 meshes per inch. Its density is 91 lb. per cubic foot in loosest packing. Angle of repose $32\frac{1}{2}^\circ$. A few tests have been made on small glass spheres mean diameter 55 mils., sold under the name of Glistening Dew and used for decorating Christmas cards. The density of the glass spheres is 106 lb. per cubic foot in loosest packing. Angle of repose 25° . And a few have been made on ground glass, which is used in the manufacture of glass-paper; its density in loosest packing is 68 lb. per cubic foot. Angle of repose 40° . This was graded with the same sieves as those used for the sand. These two substances were chosen for the first experiments to investigate the effect of grain shape, the first being almost spherical and the other very angular, while the coefficient of friction between the grains was probably about the same for both.

Tables I to V.

In the tables :—

R is the resultant force in lbs. on the wall.

C is $2R/\delta h^2$, where δ = density of granular material; h = height of wall; l = length of wall. C is therefore independent of the size of the wall and of the density of the granular material.

ψ is the angle between the resultant force and the normal to the wall.

x is the ratio of the height of the centre of pressure to the height of the wall.

ϕ (used by Résal, *vide* tables in the Appendix) is the angle whose tangent is the "coefficient of friction" between two layers of sand (or approximately the angle of repose).

"Surcharge" is the angle between the surface of the sand and the horizontal, when the sand slopes up from the top of the wall.

Table I.—Sand. Vertical Sand-paper Wall.

	R.	C.	ψ .	x .
No surcharge..	1.41	0.27	31°	0.42
10° "	1.59	0.304	$30\frac{1}{2}^\circ$	0.37
20° "	1.85	0.354	$30\frac{1}{2}^\circ$	0.34
30° "	2.44	0.467	$30\frac{1}{2}^\circ$	0.54

Table II.—Sand. Vertical Steel Wall.

	R.	C.	ψ .	α .
No surcharge	1.33	0.254	11°	0.383
10°	1.50	0.287	11°	0.365
20°	1.98	0.379	10½°	0.519
30°	2.50	0.478	11°	0.57

Table III.—Sand. Inclined Sand-paper Wall.

Inclination 20°.*

		R.	C.	ψ .	α .
No surcharge	Maximum ..	2.34	0.447	29°	0.417
	Minimum ..	2.2	0.421	30°	0.443
	Filling	1.64	0.313	—9°	0.453
	Tapping	1.81	0.346	25°	0.397

Table IV.—Glass Balls. Vertical Steel Wall.

	R.	C.	ψ .	α .
No surcharge	2.36	0.387	15°	0.333

Table V.—Ground Glass. Vertical Sand-paper Wall.

	R.	C.	ψ .	α .
No surcharge	0.926	0.240	29°	0.45

Magnitude of the Resultant Force.—The values calculated by the old theories agree fairly well with the observed values, as was expected since the theories are based on the angle of repose which depends on dilatancy. The new observations and the values given by old theories are compared in Tables VI to X in the Appendix. The observations on vertical walls with sand are also compared with the theories in fig. 22. The best agreement is with the wedge theory (there are two wedge theory curves, one for the sand wall and one for

* See fig. 25, p. 79.

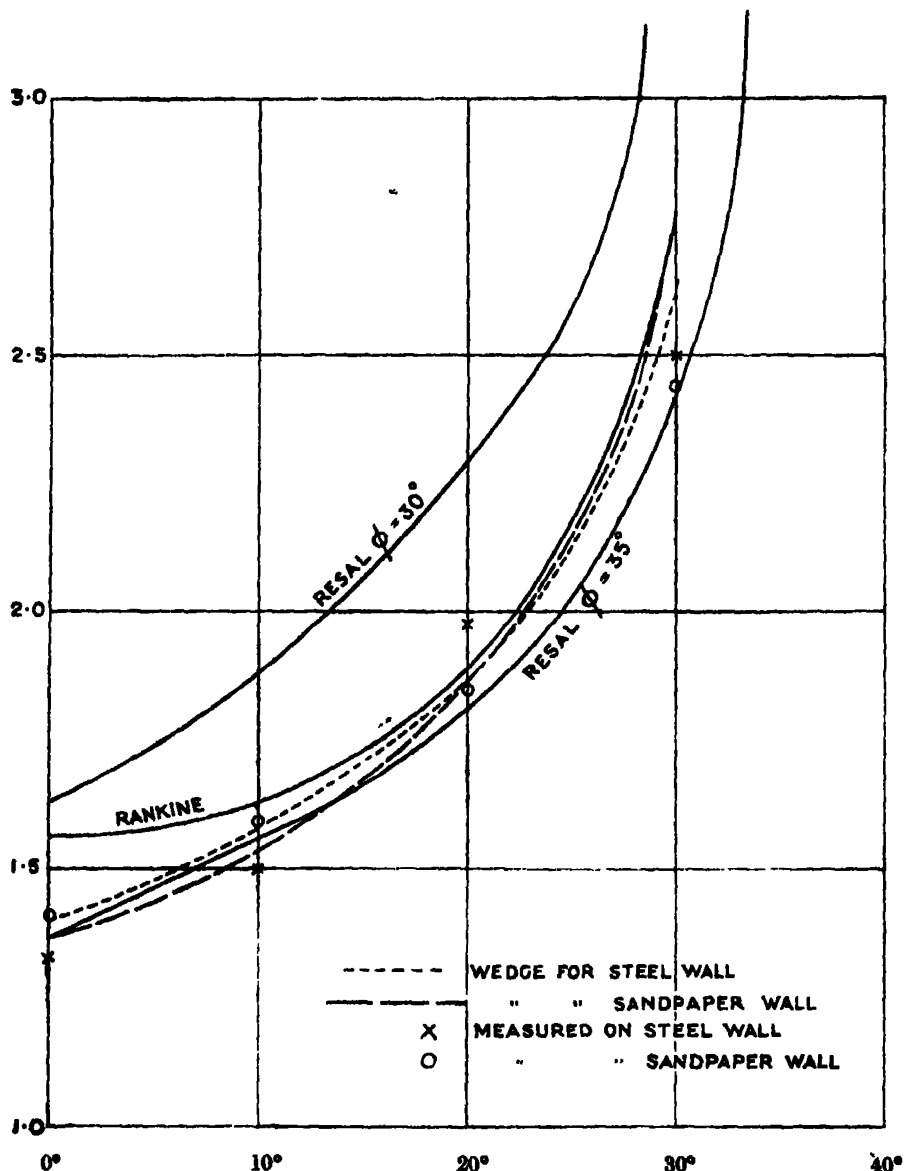


FIG. 22.—Resultant forces, Observed and Theoretical.

the steel wall, the other curves apply to both sand and steel walls). Rankine's curve gives rather too big forces with small surcharges.* A close comparison with Résal's theory unfortunately cannot be made, for the author has failed

* The surcharge is the angle at which the surface of the sand slopes upwards from the top of the wall.

to find any way of interpolating for an angle of repose of $32\frac{1}{4}^\circ$ between Résal's results for 30° and 35° , both of which are plotted. The observed values for 20° surcharge are decidedly above the curves; no reason can be suggested for this. The observed values for 30° surcharge are decidedly below the curves, but it will be observed that the curves are rising very steeply at this end, for example Résal's 30° curve goes up to 4.53, far above the top of the figure. Additional experiments are clearly needed at 15° and 25° surcharge.

If a more accurate method of calculation than the wedge theory is found necessary (as it may be for other conditions) the new principles suggest that the effects of grain shape and of friction between the grains must be separated. The angle of repose, on which the old theories all depend, indicates only their combined effect in a single test.

Inclination of Resultant Force.—The experiments show that the resultant force acts in the direction indicated by the new principles, namely, inclined to the normal to the wall at the friction angle, this angle depending on the smoothness of the surface of the wall. Rankine's theory is wrong, as has long been known. Résal assumes that the angle of friction with the wall is the same as the angle of friction between two sand surfaces, i.e., approximately the same as the angle of repose. This is generally true in practice but is shown by the experiments not to be true for the steel wall. In the form of the wedge theory employed in this paper, the author uses the correct assumption as to the direction of the resultant.

Height of the Centre of Pressure.—The measurements of the height of the centre of pressure are rather erratic; the tests do not repeat accurately. The variations are certainly not instrumental, and are probably caused by changes in the coefficient of friction between the grains of sand, due to variations in the humidity of the atmosphere. Reference has already been made to the large variations in the coefficient of friction between the sand and the steel wall, which could be measured. Variations in the intergranular friction cannot yet be measured; it is probable that relatively small variations in the friction have a considerable effect on the extent of the vertical arching and so on the height of the centre of pressure. The tests have been made in all sorts of weather from hot summer to foggy winter. The only case in which a serious difference has been found is in the tests on the sand wall with 30° surcharge: in the early tests made in June and July the height of the centre of pressure was found to be about 0.43 h., which is very different from the value given in the table, which was obtained in November.

The experimental figures, whose general accuracy need not be doubted,

are very remarkable and entirely in accordance with the results which have been obtained from the new principles. All the tests show that the centre of pressure is higher than one-third the height of the wall, and in the tests with the steel wall with 30° surcharge (Table II) it rises well above the middle of the wall. This result was so novel that considerable doubt as to its accuracy was felt, and a second method of finding the position was tried. For this purpose the wall was supported on knife edges at its foot, instead of at its top. With this arrangement the tipping moment alone could be measured (not the horizontal and vertical forces), but this tipping moment, with the magnitude of the force already found, gives the height of the point of application. The experiments were successful and confirmed the previous results. Accepting this position for the point of application of the resultant force, the distribution of pressure on the wall became a matter of great interest. It must differ widely from the distribution assumed in all three theories which is a simple triangle as shown in fig. 23a, with the centre of pressure one-third above the base. At the top of the wall there is a free surface and therefore the pressure must vanish, so possible distributions may be represented by a

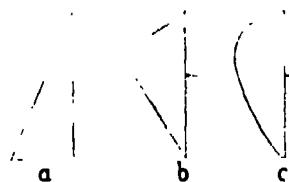


FIG. 23.—Distribution of Pressure on Wall.

triangle such as 23b or some curved line such as 23c, the centre of pressure in each case being at the observed height. These figures looked very improbable, but suggested a simple and striking test to check whether the distribution really was of this unexpected type. A shallow $1\frac{1}{2}$ inch wall was made, only half the height of the original 3-inch one. It could be hung just clear of the

base and tested in the ordinary way, or it could be hung as shown in fig. 24a above a second $1\frac{1}{2}$ -inch wall fixed in the sliding frame, the two together making up a 3-inch wall, the joint between them being made sand-tight by a thin rubber strip. According to accepted theories the pressure on the top half wall should be one-quarter that on the whole wall, and it should be the same as when tested in the ordinary way, but if the suggested type of pressure distribution

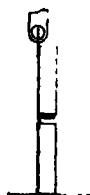


FIG. 24a.—Divided Wall.



FIG. 24b.—Pressure distribution on Divided Wall.

were true the pressure on the top half wall would be more than *half* that on the whole wall, and more than double that on the same wall tested in the ordinary way. These tests were successful and completely confirmed the reality of the remarkable pressure distribution. The approximate pressure distributions in the three tests are shown in fig. 24B.

There is no reason to doubt that the raising of the centre of pressure is due to vertical arching like that already discussed and shown in fig. 20, though the action in three dimensions with irregular grains must be far more complex. There are many reasons to expect that vertical arching will be more effective the greater the surcharge, but a really satisfactory proof that it must be so has not yet been found. If a complete solution of the arching forces in the model *with friction* could be found it would afford the explanation, but to find such a complete solution would be very difficult and laborious and the author has not attempted it. The difficulty of such problems was foreseen by Osborne Reynolds who writes:—

“The problem presented by frictionless balls is much simpler than that in the case of friction. In the former case the theoretical problem may be attacked with some hope of success. With friction the property is most easily studied by experiment.”

Sand Pressure on an Inclined Wall (Table III).—This test was the first of a series to be made on walls at different inclinations to the vertical. The wall, which sloped back at the top 20° , see fig. 25, was covered with sand-paper and the guard walls at each end were sloped at the same angle. The resultant force is still inclined at the friction angle to the normal to the wall, so that it makes an angle of 50° with the horizontal, as shown in fig. 25.

Glass Spheres and Ground Glass (Tables IV and V).—These are the first tests made to investigate the effects of grain shape. The glass spheres behaved just like sand. The angle of repose is much smaller and the theoretical forces based on this small angle agree well with the experimental values.

The ground glass behaved quite differently, as was expected in the light of the new principles, and brought to light a new phenomenon. The motion of

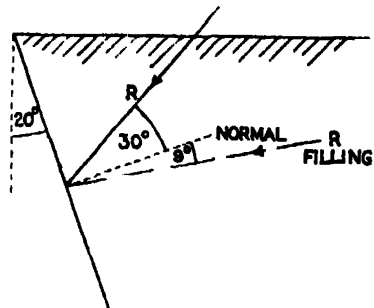


FIG. 25.—Inclined Wall.

the grains under the test conditions (and in other circumstances, as will be explained) was unstable and occurred in jerks. The tests were made with the improved measuring gear (described below) so that variations in the pressure could be watched continuously. As the wall was slowly pulled back by means of the screws in the regular manner, all the gauges gave rapid jerks, 9 or 10 jerks occurring during a single turn of the nut on the screw, which gives a displacement of 0.032 inch, so that slips occurred for every three- or four-thousandths of an inch motion of the wall. The gauges indicated that the pressure varied about one-third of the maximum for each slip. An attempt was made to stop this jerky motion by introducing springs between the wall and the gauges. The result was only to decrease the frequency of the jerks. The variation of the gauges was the same as before, so it was apparent that the slips depended only on the pressure on the wall, starting when the pressure fell to a certain minimum value and raising it to a certain maximum value. These maximum and minimum values were not very constant, which suggested that the slips were not necessarily occurring simultaneously over the whole area of the wall.

To explain these results the ground glass was tested in various simple ways ; the following facts bear on the subject. If a conical pile of ground glass is

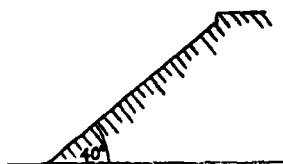


FIG. 26.—Angle of Repose of Ground Glass.

patted on the top and then scraped away at the base, the glass slips away and leaves the section of the pile in the form shown in fig. 26, with the top $\frac{1}{4}$ inch almost vertical and the lower slope at the angle of repose, 40° . This shows that the patting of the grains has consolidated it a little and caused it to "bind." Nothing of this sort occurs with the standard sand or glass spheres.

If a flat plate is pushed down into the ground glass, it enters with a pleasant scrunch, which is just like that made by fresh snow when trodden on. (Snow is far more spiky than the ground glass.) The noise made in this experiment is almost certainly due to the jerky nature of the slipping. It may be the beginning of the "singing" heard from some sands. Nothing of this sort occurs with the standard sand or glass spheres though the latter give a slight hissing or rasping sound under some conditions of motion. Bearing these two observations in mind, the behaviour of the ground glass against the testing wall may be explained as follows. When the grains slip they will be brought up with a blow against the wall ; this blow will cause them to bind and they will therefore not slip so soon next time ; the slip being delayed will result

in a harder blow on the wall and a firmer binding of the sand. Thus all the elements for unstable motion exist. This instability raises many difficulties of interpretation. It is useless to discuss these questions until further experimental results have been obtained.

Improved Measuring Gear.—Most of the tests were originally made with the apparatus as described, which is suitable for measuring constant, but not varying forces. While making the measurements some unexplained variations and difficulties of adjustment were noted and to investigate these direct reading apparatus was substituted for the original weighing devices. The horizontal forces, vertical forces and tipping moments are now all indicated by very stiff springs with optical levers, so that it is possible to watch their values continuously. This modification brought to light the fact that the forces were not constant but changed in a slowly recurring irregular cycle between a minimum and a maximum value, all three values varying together. The actual readings of the springs are plotted in fig. 27 for two of the tests. In these curves the abscissæ represent distances moved back by the wall, while the ordinates are the actual scale readings. The zeros are not shown and the vertical scales are arbitrary; they are only reproduced to show the type of fluctuation and the manner in which the readings all vary together. The magnitude of the variations may be taken from Table III which gives the values of R , C , ψ , and α for the maximum and minimum values of the curves, fig. 27a; also from Table VI which gives the corresponding maximum, minimum and mean values for curve 27b. The single points on the right of curve 27a show how the readings change after vibration (see below under the heading Vibration).

This discovery made all the measurements previously obtained unreliable and was very disconcerting. Three explanations appeared to be possible:—

- (1) That the irregularities were due to grains of sand jamming under the wall.

The fact that the horizontal and vertical forces decreased together, while the centre of pressure rose, was consistent with this explanation.

- (2) That the irregularities were due to the experimental wall being too small to give a constant average for a material known (as pointed out by Osborne Reynolds) to be non-homogeneous.
- (3) That the irregularities were due to the alternate building up and breaking down of vertical arching, i.e., to an indeterminacy in the force system between the grains.

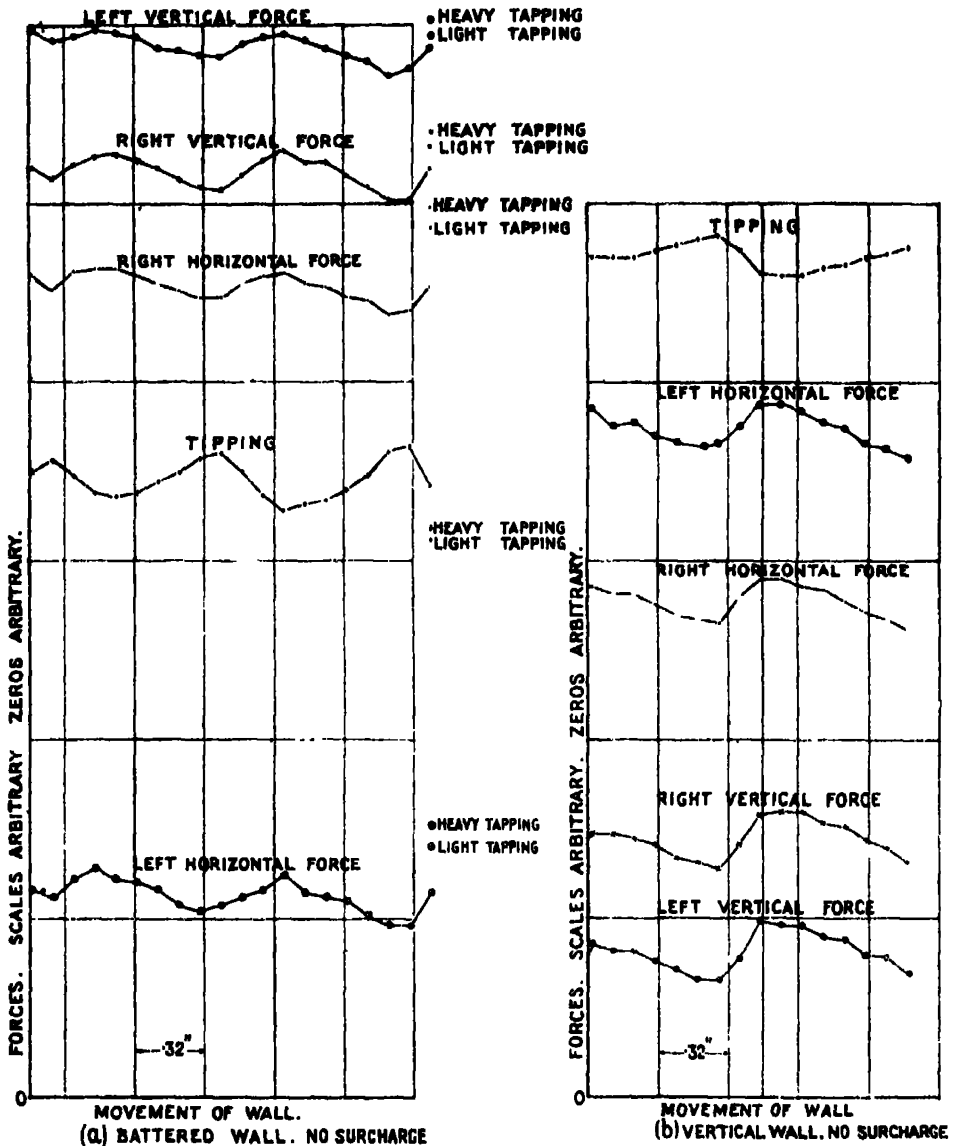


FIG. 27.—Variations of forces during tests.

The first explanation, which might seem the most obvious, was investigated first. Gaps of many widths under the wall were tried, from about 2 mils. to 35 mils. without producing any change. The stiff horizontal springs were removed and the original spiral spring put back. With this the wall moves backwards and forwards, perhaps a millimetre, between the stops, the idea

being that in each forward movement the wall would probably come off a grain of sand if it rested on one. But the results were unaltered. Finally a strip of felt was put under the wall to make the joint ; it was about $\frac{1}{8}$ -inch thick and projected about $\frac{1}{4}$ -inch below the steel face. The results were unaltered. After these experiments it appeared hardly possible that the variations were due to grains of sand, but a critical test was arranged. The horizontal springs were removed and the horizontal force on the wall taken by two small wire trunnions fixed on the bottom corners of the wall and bearing against the guard walls. The back spring was retained to measure the overturning moment. (This arrangement is in effect similar to one already described on p. 77.) As the wall was now pivoted in line with the bottom edge, no forces (such as would be produced by grains of sand) on the bottom edge, whether vertical or horizontal, could produce any moment. The test showed, however, that there was just the same cyclic variation of the overturning moment. This proved that sand grains were not the cause of the irregularity.

The second explanation cannot be finally tested until a larger wall is made. It is not likely that the variations in packing of the sand are on a large enough scale to make the average pressure vary, but the most serious argument against this explanation is that it does not account for the perfectly consistent way in which the height of the centre of pressure varies with the force on the wall.

The third explanation appears to be the correct one. This is supported by the fact that the whole phenomenon can only be observed if care is taken to avoid vibration. A very slight shake is sufficient to break down the arching and drop the centre of pressure ; for example, dropping a penny on the apparatus from a height of 8 inches has a big effect. If this explanation is correct, this new phenomenon affords a remarkable confirmation of the explanation of arching given on p. 69, where it is pointed out that in the model the conditions are indeterminate and that the centre of pressure may vary in position. The simple two-dimensional model without friction indicates that only the position of the centre of pressure should change, while the force remains constant, but it is hardly surprising to find that with sand the force varies also. Put more generally, the new principles have led to the conclusion that the force system will be indeterminate and experiment shows that it is so.

As a consequence of this discovery almost all the tests were repeated with the new springs and the readings plotted as illustrated in fig. 27. The figures given in the tables are the results calculated from the mean reading except in Table III where the maximum and minimum values are given. Until

all the conditions which determine the range of the fluctuations are known, no special importance can be attributed to the range which was observed under the particular conditions of the tests.

Initial Pressure on Pouring in the Sand. (Inclined wall.)—The sand was filled in from the back so that it slid down a slope against the wall. The initial conditions, before the wall began to move, are given in Table III. The inclination of the force is interesting, viz., -9° (see fig. 25). This corresponds to 11° above the horizontal, whereas the inclination after the wall begins to move is $+30^{\circ}$ which corresponds to 50° above the horizontal.

Vibration.—To ascertain what sort of effect vibration had and whether the apparatus was able to measure it, the base plate was given a number of taps with a wooden mallet at the end of the test on the inclined wall. The apparatus worked satisfactorily and the readings of the springs appeared to settle down to definite values which are given in Table III, and shown by single points at the right hand of fig. 27a. How to measure the violence of the vibrations has not yet been considered.

Movement of the Wall necessary to Establish a Steady Regime.—Only two experiments on this point have been made. The conditions chosen for the experiment were those likely to show the largest effect, viz., 30° surcharge on the sand-wall. In the first the sand was filled in at the back so that it slid down against the moving wall; in the second it was poured against the moving wall so that it slid back against the back wall. In both tests the pressure on the wall rose to about 3 lb., or 23 per cent. above the mean value, and did not fall to the mean value until the wall had been moved 1.6 inches back. The high initial pressures must be attributed to the initial packing being different from that finally assumed when a steady regime had been established. As both packings must be approximately equally loose, it appears to follow that when a steady regime is established the packing is not isotropic, whereas in the initial condition it is. The author had expected to find a marked difference between the experiments due to the different stratifications caused by the two methods of loading, but these particular experiments do not warrant any such deduction.

General Conclusions Drawn from the Tests.—The author believes that the results of the tests are sufficient to show that the new apparatus is capable of giving reliable data on granular pressures. The actual figures given are not yet entirely satisfactory, for they show that there is some unknown factor which influences the results; this is provisionally assumed to be the variable adsorbed film of moisture on the grains.

The experiments quoted confirm the following facts deduced from the new principles :—

The direction of the force on a wall is inclined to the normal at the friction angle.

The position of the centre of pressure is indeterminate and may be much higher than one-third of the height of the wall.

The distribution of pressure is consequently very different from the commonly accepted triangular distribution.

The pattern of the packing, which is the essence of dilatancy, is of fundamental importance ; this includes both closeness and geometrical arrangement. Two patterns have already been recognised in sand, viz., ordinary loosest packing and arched loosest packing, and the corresponding pressures on the wall have been shown to be different. Close packing has not been investigated yet, but two striking experiments illustrating its effect are quoted at the beginning of the paper.

Grain shape is of great importance—ground glass and glass spheres behave very differently.

None of the experiments contradict the results deduced from the principles of dilatancy in any way. They all show that the subject is far more complex than used to be supposed.

Engineers will note that all these investigations relate to dry granular material. Clay is quite a different matter.

A great deal remains to be done. The model will be used to investigate surcharges, and also loose packing and possibly the pressure on inclined walls. The gap between a simple two-dimensional model and a three-dimensional granular mass with irregularly shaped grains, packed at random and not homogeneously, is very wide, but, unless the forces in a three-dimensional model of spheres can be found, it may be doubted whether it is worth while attempting to get nearer reality with the theoretical investigation of stresses. The most profitable line for further work appears to be experimental.

Though there is no reason to doubt the results given by the small scale apparatus, a scheme is being considered for making a much larger one. With this it will be possible to determine whether any of the phenomena observed in the small apparatus depend on its giving an imperfect average and also whether any other scale effects exist.

The author has to thank the Department of Scientific and Industrial Research and the Director of the Building Research Station at Garston for the facilities

given him for carrying out this work, and his assistant at the Station, Mr. R. C. Bevan, for his constant help ; without his aid the long and laborious graphical work involved in seeking for the solutions to the various statical problems could not have been accomplished. He also has to thank the Earth Pressure Committee of the British Association for their encouragement.

APPENDIX I.

The wedge theory has many variants. In this paper it is used as follows :—

Let abc , fig. 28, represent the section of a wedge of sand slipping down an arbitrarily chosen plane of rupture cb and pressing on the wall ab .

Let G be its centre of gravity.

Draw GR making the friction angle ψ with the wall ab .

Draw $G\tau$ making the angle of repose ϕ with the plane bc .

Then R and τ represent in direction (not position) the forces exerted on the wedge by the wall and the rest of the sand.

Draw the triangle of forces ABC , in which $AB =$ weight of wedge.

Then CA represents the magnitude of the force R .

Let a number of lines bc be drawn at different inclinations and find the one which gives the largest value of R . That maximum R is the force on the wall by the wedge theory (in magnitude, not position).

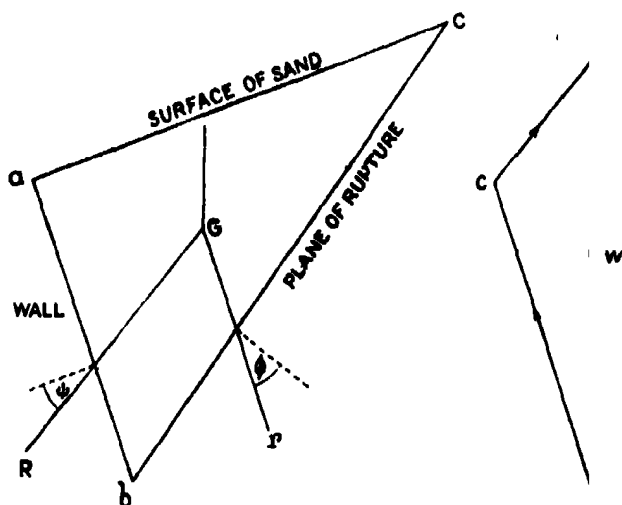


FIG. 28.—Wedge Theory.

APPENDIX II.—Tables.

In the following Tables the experimentally measured values are stated and compared with those calculated by Rankine's Theory, the Wedge Theory and Résal's Theory.

The meanings of the symbols are given at the head of Table I, p. 74.

Rankine's values are calculated by the formulæ given in Andrew's "Theory and Design of Structures," 3rd edition, 1921.

The wedge theory values are calculated in the manner described in Appendix I to this paper.

Résal's values are calculated from the tabular values given in the "Poussée des Terres"—*Deuxième partie*, by Jean Résal, Paris, 1910.

Table VI.—Sand. Vertical Sand-paper Wall. Angle of repose $32\frac{1}{2}^\circ$.

	Measured.			Rankine.	Wedge.	Résal.	
	Mini- mum.	Mean.	Maxi- mum.			$\phi = 30^\circ$.	$\phi = 35^\circ$.
No surcharge—							
C	0.257	0.27	0.278	0.298	0.262	0.311	0.261
ψ	32°	31°	32°	0°	30°	30°	35°
π	0.44	0.42	0.40	0.333	0.333	0.333	0.333
10° surcharge—							
C	—	0.304	—	0.311	0.396	0.361	0.296
ψ	—	$30\frac{1}{2}^\circ$	—	10°	30°	30°	35°
π	—	0.37	—	0.333	0.333	0.333	0.333
20° surcharge—							
C	—	0.354	—	0.362	0.358	0.439	0.347
ψ	—	$30\frac{1}{2}^\circ$	—	20°	30°	30°	35°
π	—	0.34	—	0.333	0.333	0.333	0.333
30° surcharge—							
C	—	0.467	—	0.532	0.537	0.866	0.463
ψ	—	$30\frac{1}{2}^\circ$	—	30°	30°	30°	35°
π	—	0.54	—	0.333	0.333	0.333	0.333

Table VII.—Sand. Vertical Steel Wall. Angle of Repose $32\frac{1}{2}^\circ$.

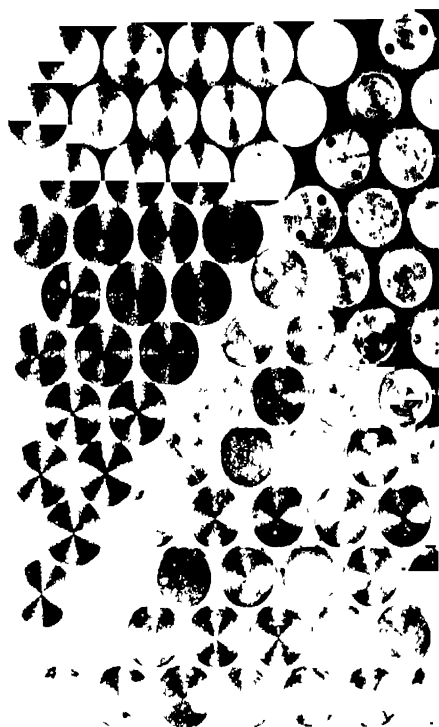
	Measured.	Rankine.	Wedge.	Réal.	
				$\phi = 30^\circ$.	$\phi = 35^\circ$.
No surcharge—					
C	0.254	0.299	0.268	0.311	0.261
ψ	11°	0°	10°	30°	35°
x	0.38	0.333	0.333	0.333	0.333
10° surcharge—					
C	0.287	0.311	0.301	0.361	0.298
ψ	11°	10°	10°	30°	35°
x	0.365	0.333	0.333	0.333	0.333
30° surcharge—					
C	0.379	0.362	0.360	0.439	0.347
ψ	$10\frac{1}{2}^\circ$	20°	10°	30°	35°
x	0.519	0.333	0.333	0.333	0.333
90° surcharge—					
C	0.478	0.532	0.507	0.866	0.462
ψ	11°	30°	10°	30°	35°
x	0.57	0.333	0.333	0.333	0.333

Table VIII.—Sand. Inclined Sand-paper Wall. $\alpha = + 20^\circ$ (fig. 25).
Angle of Repose $32\frac{1}{2}^\circ$.

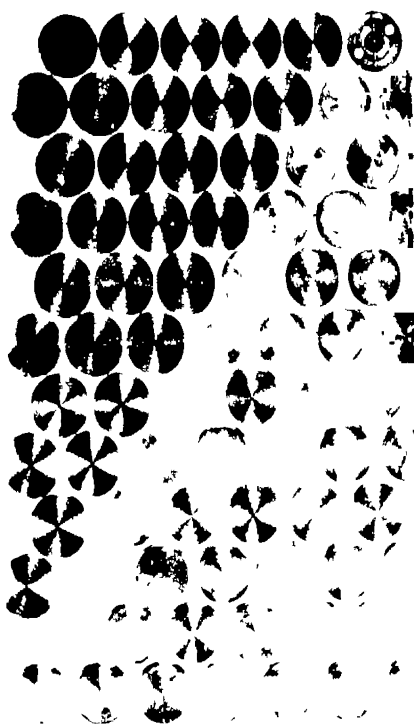
	Measured.				Rankine.	Wedge.	Réal.	
	Maxi- mum.	Mini- mum.	Filling.	Tapping.			$\phi = 30^\circ$.	$\phi = 35^\circ$.
No surcharge—								
C	0.447	0.421	0.313	0.346	0.494	0.387	0.497	0.468
ψ	29°	30°	-9°	25°	$27\frac{1}{2}^\circ$	30°	30°	35°
x	0.417	0.443	0.463	0.397	0.333	0.333	0.333	0.333

Table IX.—Glass Balls. Vertical Steel Wall. Angle of Repose

	Measured.	Rankine.	Wedge.	Réal. $\phi = 25^\circ$.
No surcharge—				
C	0.387	0.405	0.361	0.373
ψ	15°	0°	15°	25°
x	0.333	0.333	0.333	0.333



A — Ordinary Pressure Distribution



B - Pressure Distribution under Arching.

Table X.—Ground Glass. Vertical Sand-paper Wall. Angle of Repose 40°.

	Measured.	Rankine.	Wedge.	Réal.
No surcharge—				
C	0.240	0.218	0.202	0.219
φ	29°	0°	29°	40°
z	0.450	0.333	0.333	0.333

APPENDIX III.

(Plate 4.—*Added February 8, 1931.*)

A very simple method of demonstrating the slack contacts has been found. If the wall in the model be slightly tipped back at the top, as shown in photo A, the slack contacts, assumed to exist in the ordinary pressure distribution, appear as minute gaps. They may be seen in the photograph between all the discs on each horizontal line of discs to the left of the plane of rupture (which lies immediately above the discs marked by double black dots).

Again, if the wall be slightly tipped forwards, as shown in photo B, the slack contacts assumed to exist when vertical arching occurs, again appear as minute gaps. They may be seen in the photograph between alternate discs in each diagonal row of discs to the left of the plane of rupture.

The Upper Limit of Energy in the Spectrum of Radium E.

By F. R. TERROUX, 1851 Exhibition Scholar and External Research Student
of Emmanuel College, Cambridge.

(Communicated by Lord Rutherford, F.R.S.—Received January 24, 1931.)

[PLATE 5.]

1. *Introduction.*—The disintegration of radium E has for some years attracted considerable attention. It is distinguished from the majority of β -ray bodies by the fact that there are no traces of peaks, due to homogeneous radiation, superimposed on the continuous spectrum of the disintegration electrons. It seems clearly established from the work of Ellis and Wooster,* and of Meitner,† on the heating effect of radium E, that the β -rays from this body are initially inhomogeneous when emitted from the nuclei. It is obviously of considerable interest to determine the velocity with which the fastest of the particles emerge from the nucleus; in other words the “end point” of the β -ray spectrum.

The existence of such an upper limit in the case of radium E was first suggested by Gray,‡ who observed an end point or kink in the β -ray absorption curve. Madgwick§ investigated the continuous distribution of the particles by means of an ionisation chamber and magnetic deflection, and found a fairly definite end point, such as Gurney|| had observed in the case of radium (B + C). Madgwick gave this end point as 5000 Hp, corresponding to an upper limit of energy of 1,070,000 volts.

The work of Douglas, Sargent, and of Feather,¶ on the absorption curve of radium E, confirms the existence of a definite kink in this curve and this is taken to indicate a sharply defined end point in the continuous spectrum. The thickness of absorber corresponding to the kink in the absorption curve is called the effective range of the particles, and the values obtained by the above

* ‘Proc. Roy. Soc.,’ A, vol. 117, p. 109 (1928).

† ‘Z. Physik,’ vol. 19, p. 307 (1923).

‡ ‘Proc. Roy. Soc.,’ A, vol. 87, p. 487 (1912), and ‘Trans. Roy. Soc. Canada,’ vol. 16, p. 125 (1922).

§ ‘Proc. Camb. Phil. Soc.,’ vol. 23, p. 982 (1927).

|| ‘Proc. Roy. Soc.,’ A, vol. 109, p. 540 (1925).

¶ Douglas, ‘Trans. Roy. Soc. Canada,’ vol. 16, p. 113 (1922); Sargent, ‘Proc. Camb. Phil. Soc.,’ vol. 25, p. 514 (1929); Feather, ‘Phys. Rev.,’ vol. 35, p. 1559 (1930).

workers agree closely. Chalmers* has described a method, wherein the effective range of the particles is correlated with the upper limit of the continuous spectrum and this method gives an end point for radium E at about 5000 Hp.

In the course of an investigation on the passage of fast β -particles through gases,† by the cloud expansion method, and using a combined source of radium D, E, and F, evidence was found of the emission of a number of particles whose velocities were considerably in excess of the above limit for radium E. Since in the above source radium D emits only very slow β -rays of the order of Hp 740, whereas Polonium is an α -ray body, it seems reasonable to attribute these very fast particles to radium E.

This result, in direct contradiction to previous work, raised a point of considerable interest. The fast particles, observed to come from radium E, suggested that the distribution curve might in reality tend asymptotically to zero and that there might be a finite probability of an atom disintegrating with any energy. Evidence as to whether the distribution curve has a sharply defined end point at 5000 Hp, or whether it shows a gradual tailing off far beyond this limit, is clearly of the greatest importance in any attempt completely to describe the process of disintegration. The following work was accordingly undertaken to determine, by means of the cloud expansion method, the general form of the upper region of the radium E spectrum and the upper limit of velocity. The chief advantage of the cloud expansion method is that it is sufficiently sensitive to show clearly the presence of a single β -particle regardless of its velocity; this is of particular importance when dealing with very small numbers. It was actually found, in applying this method, that the radium E spectrum appears to show no trace of an end-point at 5000 Hp, and that there is evidence of particles emitted with an energy of the order of 3,000,000 electron volts (corresponding to Hp 12,000).

2. *Experimental Method.*—The use of the cloud expansion method for the measurement of α -particle velocities from their range is already well established. More recently the method has been applied to β -particles by Meitner, Petrova, Feather‡ and others.

The range of each particle is obtained by measuring the length of the track,

* 'Proc. Camb. Phil. Soc.,' vol. 25, p. 331 (1929).

† 'Proc. Roy. Soc.,' A, vol. 126, p. 289 (1930).

‡ Meitner, 'Naturwiss.,' vol. 14, p. 1199 (1926); Petrova, 'Z. Physik,' vol. 55, p. 628 (1929); Feather, 'Proc. Camb. Phil. Soc.,' vol. 25, p. 522 (1929).

and the velocity may be deduced by using the results of Nuttall and Williams,* who determined the relation between the range and the initial velocity experimentally. Fast β -particles cannot be dealt with in this way, since their range greatly exceeds the confines of an expansion chamber. Their velocity can, however, be measured quickly and conveniently from the curvature of the tracks in a magnetic field.

The expansion apparatus used in this work has already been described in detail.† The source employed for the greater part of the work was an old radon tube containing radium D, E and F, in equilibrium and was chosen for convenience. It was assumed that the fast β -rays obtained were emitted solely from radium E, for the reasons given above. This assumption was tested experimentally, by comparison with a newly prepared source of radium E alone. The source was placed outside the chamber at a distance of 1 cm. from the wall. The rays from the source were controlled by an automatic shutter, and entered the chamber through a cellophane window of surface density 2.6 mgm. per cm.².

The magnetic field was produced by a pair of Helmholtz coils, mounted symmetrically about the chamber, in a horizontal plane.

The field, of the order of 500 gauss, was uniform over the area of the chamber to less than $\frac{1}{2}$ per cent., and was calculated from the value of the current through the coils at the moment of the expansion.

The position of the source was so adjusted that about 10 tracks were photographed on each pair of plates; a greater number of tracks giving rise to confusion and difficulty in measurement. Attention was confined to the region between 3500 Hp and 10,000 Hp. With the magnetic field available it was difficult accurately to measure the curvature of tracks above the latter value. Tracks below 3500 Hp were rejected, because the relative number of such tracks appearing on the plates was reduced by their being to some extent prevented by excessive curvature from entering the apparatus. The region given above is perfectly satisfactory if only the upper end of the distribution curve is desired.

The tracks were photographed with a stereoscopic camera, mounted vertically above the chamber. The radii of curvature of the tracks were measured by the optical projection method described by Williams and Nuttall.‡ In this method, three adjustable needle points are made to coincide with three equi-

* 'Proc. Roy. Soc.,' A, vol. 121, p. 611 (1928).

† Williams and Terroux, *loc. cit.*

‡ 'Phys. Soc. Proc.,' vol. 42, p. 212 (1930).

distant points of an image in space, which exactly corresponds to the original track in all respects except orientation. The image of the set of needle points is then projected on a screen where the distances between the points can be accurately measured, and the radius of curvature calculated from these measurements.

In applying this method care is taken not to measure a section of track which includes a branch or a nuclear scattering of the β -ray, since, in both cases, the resultant deflection would affect the value of the radius of curvature obtained.

The straggling effect of the cellophane window (2.6 mgm. per cm.²) is negligible.*

In the present work, the probable error in the measurement of H_p for any single fast track is of the order of 9 per cent.

The cloud expansion method described above has several pronounced advantages over ionisation, photographic and absorption measurements. As previously mentioned, it is equally sensitive to rays of all velocities, and by using the stereoscopic method of viewing the tracks, it is possible to reject any track, such as that arising from the absorption of a γ -ray in the walls of the chamber, which does not enter the chamber via the source window.

Some 80 pairs of plates were taken, using the combined source of radium D, E and F, and on measurement yielded about 500 tracks. For comparison a few pairs of plates were taken, with a source of radium E alone, under identical conditions.

3. Results and Discussion.—It was found, on measuring the plates taken with the radium D, E and F source, that out of all the tracks in the region concerned about 15 per cent. of the tracks were above 5000 H_p , the previously accepted end point. Measurement of the eight pairs of plates taken with a source of radium E alone showed about 16 per cent. of the total to lie above 5000 H_p . The very close agreement between the two is doubtless fortuitous, but the result seems to justify the assumption made above, that the fast rays from the combined source are emitted by radium E.

The results obtained are shown in Table I. In this table the middle column gives N , the number of β -rays actually found, within an interval of 800 H_p . The value of H_p corresponding to the middle of the interval is given in the first column. The third column gives the probable error for N .

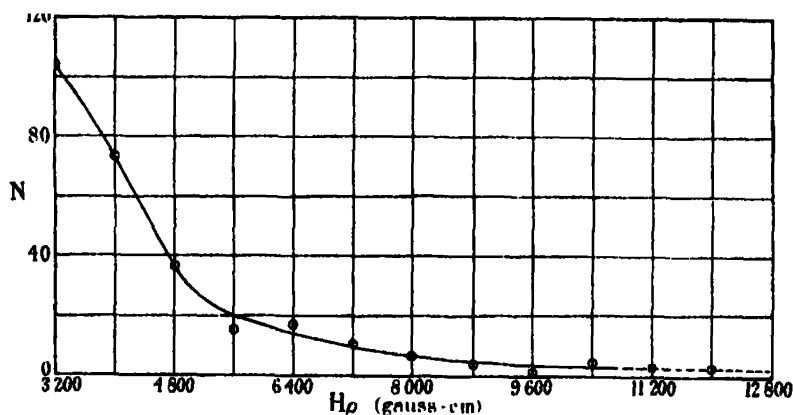
* White and Millington, 'Proc. Roy. Soc.,' A, vol. 120, p. 702 (1928).

Table I.

H_p (gauss-cm.).	N (interval 800 H_p).	Probable error (per cent.).
3,200	104	7
4,000	73	8
4,800	36	11
5,600	15	20
6,400	17	20
7,200	11	22
8,000	6	24
8,800	3	35
9,600	1	75
10,400	5	40
11,200	3	50
(12,000)	(2)	(50-100)

A few tracks were found above 11,000 H_p but they were difficult to measure and the values given in brackets serve merely to indicate the presence of a very small number in this region. A 12,000 H_p particle has an energy of about 3,000,000 volts. The results in the above table are incorporated in the distribution curve in fig. 1.

In this curve, as before, N is the number of particles found in an interval

FIG. 1.—Radium E; Velocity Distribution of fast β -rays.

of 800 H_p . Owing to the relatively small number of tracks involved, the statistical error is considerable.

The actual points, shown by circles, agree with the smooth curve within the limits of their probable error, and it seems reasonable to conclude that the curve represents the velocity distribution of the fast β -rays fairly accurately.

The curve descends steeply at the beginning and then flattens out very

definitely. It is clear that there is no indication of an "end point"; that is to say, a value of H_p beyond which no particles are to be found, within the region covered by the curve. The very small number of particles found in the neighbourhood of 12,000 H_p is indicated by the broken portion of the curve.

As stated in the introduction, a number of observers have fixed the end point at 5000 H_p , and Gray and O'Leary* have estimated that less than one atom in 25,000 emits a β -ray of 8000 H_p .

On the other hand, Danysz, Curie and d'Espine, and Yovanovitch and d'Espine† using magnetic deviation and photographic plates with a source of radium E alone, find a weak band extending from about 6000 to about 12,000 H_p . Such a band agrees rather well with the flatter portion of the curve in fig. 1. The work of Aston‡ renders it impossible to attribute the presence of the β -rays in this region to the effect of the weak γ -radiation associated with radium E. Aston found that only one quantum of γ -radiation was emitted per 30 disintegrations, and that the average energy associated with these quanta was of the order of 250,000 volts. It is evident that if this radiation is monochromatic it is of the wrong frequency to account for the above region of the β -ray spectrum. If, as appears more probable, these γ -rays form a continuous distribution with an average energy of 250,000 volts, then the number of β -particles which they eject in the above region could not account for more than 3 or 4 per cent. of the number actually found.

The general form of the continuous spectrum of radium E is given by Ellis and Wooster (*loc. cit.*) and is mainly based on the work of Madgwick (*loc. cit.*). It is difficult to estimate the accuracy of this curve, but the general form between 1000 and 4000 H_p is sufficiently reliable to combine with the curve of fig. 1 in order to estimate what proportion of the radium E emission consists of very fast rays.

The complete curve is shown in fig. 2 and was obtained by adjusting the data of fig. 1 to the curve given by Ellis and Wooster, at H_p 4000. This point is chosen because the probable error is small in this region, and because this is the point at which the slopes of the two curves agree most closely. The solid line shows the spectrum of radium E, while the previous curve is represented by the solid line as far as 4000 H_p , and beyond this by the broken line

* 'Nature,' vol. 123, p. 568 (1929).

† Danysz, 'Ann. Chim. Phys.,' vol. 30, p. 241 (1913); I. Curie and d'Espine, C. R., vol. 181, p. 31 (1925); Yovanovitch and d'Espine, 'J. Physique,' vol. 8, p. 276 (1927).

‡ 'Proc. Camb. Phil. Soc.,' vol. 23, p. 970 (1927).

which meets the axis at 5000 Hp. The scale of N , the number of particles, is arbitrary.

The relative numbers of particles emitted in different regions of the spectrum

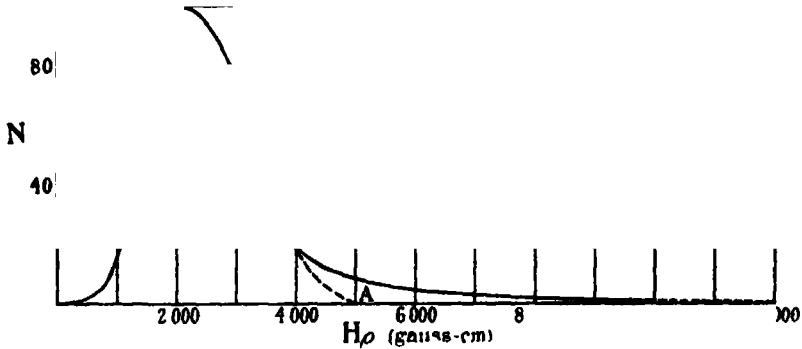


FIG. 2.—Radium E; β -ray Spectrum.

may be estimated from the relative areas beneath the curve. In this way it is found that about 4 per cent. of the total number emitted are above 5000 Hp and that about 1.5 per cent. of the total number are above 7000 Hp. (5000 Hp corresponds to an energy of 1,070,000 electron volts and 7000 Hp corresponds to an energy of 1,650,000 electronvolts.) The values of the relative numbers of very fast particles given above may be excessive if, as seems possible, a number of the slowest particles emitted from the source were absorbed in the window foil and are therefore not represented in the above curve.

The energy distribution curve for radium E is given in fig. 3, and was drawn from the data of Ellis and Wooster combined with the present observations.

The solid line represents the number of particles N plotted against the

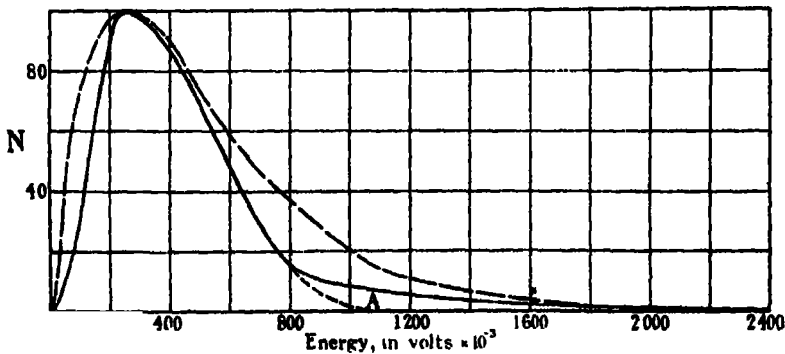


FIG. 3.—Radium E; Energy Distribution Curve.

Terroux.

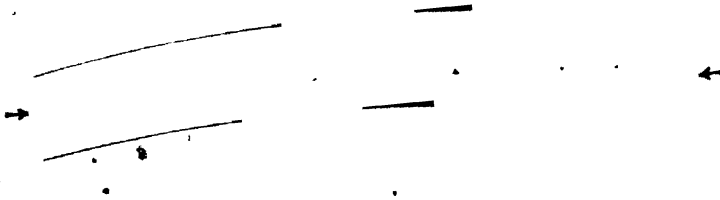


FIG. 4 Radium E H_p 10,160 gauss. cm.
(full lines correspond to H_p 5,000).

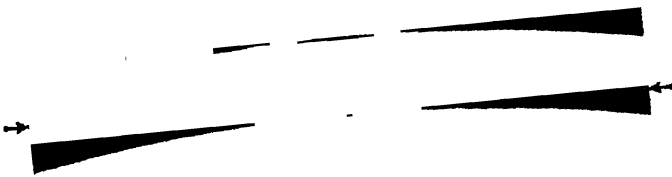


FIG. 5 Radium E H_p 9,030 gauss. cm.
(curvature of full lines corresponds to H_p 5,000).

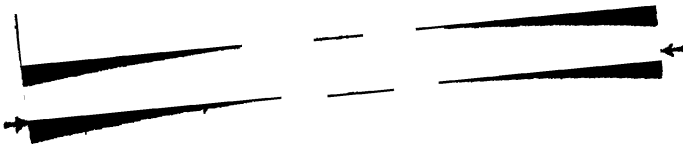


FIG. 6 Radium E H_p 7,000 gauss. cm.
(curvature of full lines corresponds to H_p 5,000).

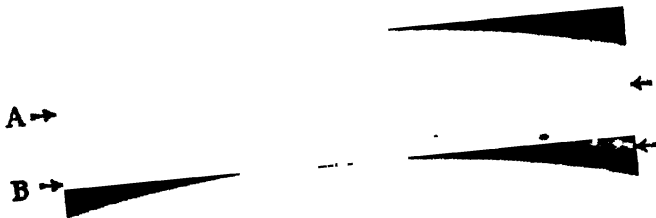


FIG. 7. - Radium E. H_p = 6,650 (A) and 5,530 (B) gauss. cm.
(curvature of full lines corresponds to H_p 5,000).

(Facing p. 96.)

energy expressed in electron volts. The point A, at 1,070,000 volts represents the upper limit of the previous curve.

It is possible to estimate, from the above curve, the average energy per disintegration. This was done by graphical methods and the value obtained was 473,000 volts. The value obtained in the same way from the previous curve is about 395,000 volts which is about 18 per cent. less. Since the accuracy of the above estimate depends not only on the part of the curve given in the present work but also on the previous curve, the probable error is considerable and is estimated at 20 per cent. Ellis and Wooster from their measurement of the heating effect, obtained a value for the average energy per disintegration of $344,000 \pm 40,000$ volts, which result is fully confirmed by the recent work of Meitner and Orthmann.* There is no reason to doubt the accuracy of this value and it is therefore probable that the above estimate is too high. This discrepancy may be attributed to the fact that the slowest particles emitted are inadequately represented in the above curve.

It was mentioned in the introduction that the end point of the continuous β -ray spectrum has been estimated from the effective range of the particles (in paper and aluminium). This procedure has been applied by Chalmers, Sargent and Feather (*loc. cit.*). When the absorption curve is plotted, a more or less sharply defined kink is shown in the curve. The position of this kink can be determined with fair accuracy by the methods described by the above observers. The position of this kink corresponds to a certain thickness of the absorber, which is taken as the effective range of the particles. By correlation with existing data on end points and effective ranges for other β -ray bodies an estimate is made of the end point of the element in question. This method gives an end point for radium E at 5000 Hp.

Reference to the spectrum curve given in fig. 2 suggests a possible explanation of this result. The curve shows a noticeable and fairly sudden inflexion in the region between 4000 and 5000 Hp. It is obvious, from the estimated probable error given in Table I, that the true curve may be much smoother in this region, or it may in reality show a more clearly defined inflexion or kink. In the latter case, one should expect a corresponding kink to appear in the absorption curve which would have no connection with the upper limit of the radium E spectrum. Should this kink in the spectrum actually exist, it is not necessarily due to a peculiarity in the β -ray emission but may be due to the superposition of two curves representing alternative modes of dis-

* 'Z. Physik,' vol. 60, p. 143 (1930).

integration. In any case the present results show no evidence of an end point in the region investigated.

There is no reason to doubt that the curve of fig. 3 gives the general form of the energy distribution of the β -particles as they emerge from the nuclei. The general shape of this curve with its gradual tailing off suggests a Maxwellian distribution. In order to test this, the curve represented by the broken line was drawn and its equation (since one is dealing with an energy distribution), is of the form

$$N = N_0 E e^{-KE},$$

where $N_0 = 1.098 \times 10^{-3}$, and $K = 4 \times 10^{-6}$, N is the number of particles and E is the energy expressed in volts. The constants were chosen to make the maxima of the two curves coincide. While the curves themselves do not coincide they do resemble each other in general form. A closer agreement could, of course, be obtained by using a different function of E in the non-exponential part, $N_0 f(E)$, of the above equation. This suggests that the β -particles from radium E are emitted initially from the nuclei of the source in a simple statistical distribution. This hypothesis if correct gives no picture of the state of the β -particles within the nuclei before emission, but it supplies a definite condition which any description of the mechanism of emission must fulfil.

Plate 5, figs. 4, 5, 6 and 7 show photographs of some of the very fast tracks obtained. Above and below each track, curved white lines are drawn whose curvature coincides with that of a track of 5000 Hp. The fast tracks shown are less curved by the magnetic field and the difference is clearly visible. The magnification is in every case about five times actual size.

Summary.

(1) The upper limit of the β -ray spectrum of radium E was investigated by means of a cloud chamber apparatus, and was found to extend as far as 12,000 Hp (corresponding to energy of about 3,000,000 volts).

(2) No evidence was found of an end point within the region investigated. The number of particles observed decreased very gradually with increasing Hp.

(3) The number of particles emitted above 5000 Hp is estimated to be about 4 per cent. of the total number.

(4) The average energy per disintegration is estimated at 473,000 volts with a probable error of 20 per cent.

(5) The form of the distribution curve obtained suggests the possibility that the β -particles from radium E are emitted from the nuclei according to a Maxwellian law.

The writer is deeply indebted to Dr. C. D. Ellis for his interest in this work, and to Lord Rutherford and to Dr. J. Chadwick for their constant encouragement.

The Arithmetically Reduced Indefinite Quadratic Form in n -Variables.

By L. J. MORDELL, F.R.S., the University, Manchester.

(Received October 4, 1930.)

§ 1. Let

$$f(x_1, x_2, \dots, x_n) = \sum_{r,s=1}^n a_{rs} x_r x_s, \quad (1)$$

or for brevity, say $f(x)$, where $a_{rs} = a_{sr}$ and a_{rs} is any real number, rational or irrational, be a quadratic form in n -variables. Suppose that the determinant

$$\Delta = |a_{rs}| \neq 0,$$

so that $f(x)$ cannot be expressed as a quadratic form with fewer than n variables. From (1) can be derived an infinity of forms

$$g(y_1, y_2, \dots, y_n) = \sum_{r,s=1}^n b_{rs} y_r y_s, \quad (2)$$

say $g(y)$, with $b_{rs} = b_{sr}$, by means of the linear substitutions

$$x_r = \sum_{s=1}^n \lambda_{rs} y_s, \quad (r = 1, 2, \dots, n), \quad (3)$$

where the λ 's are integers and the determinant $|\lambda_{rs}| = 1$. We consider throughout only such substitutions. All the forms $g(y)$ have the same determinant Δ . They are said to be equivalent to $f(x)$ and to define a class of forms, the class including all the forms equivalent to $f(x)$ and only these. The problem of selecting a particular form as representing the class, i.e., the so-called reduced form, is fundamental. There are several methods* of defining a

* Bachmann, 'Die Arithmetik der quadratischen Formen,' vol. 2, pp. 250-335, 350-358, 494-519 (1923), hereafter referred to as Bachmann.

reduced form due to Hermite (three methods), Korkine and Zolotareff, Minkowski, Voronoi, and Selling, and leading to some of the most beautiful investigations in number-theory. Thus when $f(x)$ is a positive *definite* form, a reduced form $g(y)$ of the class of $f(x)$ can be found such that, *inter alia*,

$$0 < b_{11} b_{22} \dots b_{nn} \leq k_n \Delta, \quad (4)$$

where k_n is a constant depending only on n , i.e., not on the particular form $f(x)$ in n -variables and of determinant Δ , e.g., $k_2 = 4/3$, $k_3 = 2$. The result (4) was given by Hermite with $k_n = (4/3)^{\frac{1}{2}n(n-1)}$. When* $n = 3$, definitions have been given by Seeber and Selling, and when $n = 4$ by Charve,† leading to a *unique* reduced form in each class; but this does not hold for the definitions given when $n \geq 5$. It is, however, easy to find out if two reduced forms (1) and (2), say, are equivalent, for there is only a finite number of representations of b_{rr} by $f(x)$, i.e., integer values of x_1, x_2, \dots, x_n for which

$$f(x_1, x_2, \dots, x_n) = b_{rr}.$$

Many arithmetical applications are concerned with the important case of forms with integer coefficients, i.e., when all the coefficients a_{rs} of $f(x)$ are integers. It is then an easy deduction from (4) that there exists only a *finite* number of classes of definite quadratic forms in n -variables of given positive, integer determinant Δ , or say for brevity, the class number is finite.

The theory of the reduced definite forms, then, is tolerably complete and satisfactorily developed.

§ 2. Suppose next that $f(x)$ is an indefinite form. The theory when $n = 2$ and $-\Delta$ is not a perfect square is of long standing; and when a_{rs} ($r, s = 1, 2$) are integers, the class number is finite. The last result also holds if $-\Delta$ is a perfect square so that $f(x)$ splits into linear factors with integer coefficients. Thus

$$f(x) = (p_1x_1 + p_2x_2)(q_1x_1 + q_2x_2),$$

and a linear substitution changes this into

$$g(y) = py_1(qy_1 + ry_2),$$

where p, q, r are integers, $p^2r^2 = -4\Delta$, $0 \leq q < r$. Hence there is only a finite number of values of p, q, r since $\Delta \neq 0$.

Many of the results for $n \geq 3$ are due to Hermite or had their origin in his

* Bachmann, pp. 175–224, 414–418. See also Dickson, 'Studies in the Theory of Numbers,' pp. 156–185 (1930), hereafter referred to as Dickson's studies.

† A brief summary of Charve's results is given by Dickson, 'History of the Theory of Numbers,' vol. 3, p. 230 (1923). This book will also be useful for other references and various details.

work, though Eisenstein* had previously given results, some conjectural, for the ternary form. Hermite† applies to indefinite forms one of his methods of reduction. There are, however, serious difficulties overlooked by him. He ignores the cases when the form assumes infinitesimal values, i.e., integer values of the unknowns exist such that $|f(x)| < \epsilon$ for arbitrary $\epsilon > 0$; and also when the form assumes zero values. But certainly an infinity of indefinite forms (whose coefficients are not integral multiples of some number) assume infinitesimal values. Also Meyer‡ proved in 1883 that every indefinite form in more than four variables, with $\Delta \neq 0$ and integer coefficients, always represents zero. It is unlikely that Hermite knew this result at the time his paper was written, nearly 30 years before.

Meyer's proof§ depended on the deeper arithmetical theory of the indefinite ternary quadratic form. I have found a very elementary proof which is being published shortly.||

Hence the case $b_{11} = 0$ in the reduced form with at least five variables is really the important one. Other writers also have not realised this fact, which, as will be seen, leads to a great simplification in the theory.

Finally, Hermite's method has the further great disadvantage that it does not give even a theoretical means of deciding if two reduced forms are equivalent or not.

These remarks may help to show that the subject was not originally, and perhaps is even not now, an easy one.

Other results for $n \geq 3$ were later given by Hermite, who discovered an exceedingly important method of reduction by the use of continuous parameters, i.e., those not restricted to integer or even rational values, but he did not give details of his proofs. Thus for $n = 3$, he stated¶ that a reduced form $g(y)$ exists for $f(x)$ such that its coefficients satisfy the five inequalities.

$$-2 \mid \Delta \mid \leq b_{11} b_{22}^2, b_{22} b_{31}^2, b_{33} b_{12}^2, b_{11} b_{22} b_{33}, b_{12} b_{23} b_{31} \leq 2 \mid \Delta \mid. \quad (5)$$

* 'J. R. Angew. Math.,' vol. 41, pp. 239-242 (1851).

† 'Œuvres,' vol. 1, pp. 122-127 (1905); Bachmann, pp. 350-354, does not note that Hermite gave the method for indefinite forms also. Hermite, p. 127, states that the number of reduced indefinite forms with integer coefficients and given Δ , is finite. My remarks suggest that his proof was incomplete.

‡ Cf. Bachmann, vol. 1, pp. 266-267 (1898). On pp. 551-553, reference is made to Minkowski's proof depending on the theory of the general quadratic form.

§ An account is given in Dickson's *Studies*, pp. 68-70.

|| On the condition for integer solutions of the equation $ax^2 + by^2 + cz^2 + dt^2 = 0$ ('J. R. Angew. Math.,' vol. 164, pp. 40-49 (1931).

¶ 'Œuvres,' vol. 1, p. 194 (1905).

He then says that if the coefficients a_r are integers, the class number is finite. It is not clear whether he took special note of cases such as $b_{11} = 0$. Then it does not follow from (5) that b_{23} is bounded, and so a new discussion is necessary. Probably he did not, as there was a similar omission* in dealing with binary forms of any degree, as has been noted by Julia.† I do not think that a proof of (5) has been published, though the theory for $n = 3$ was developed by Selling,‡ who gives bounds for the coefficients b_r of a reduced form different from Hermite's.

Hermite also stated§ that for $n > 3$ and integer coefficients a_r , the class number is finite. He says (in 1853) that the rigorous demonstration of this theorem had occupied him many times during the preceding six years. Again it does not appear that he considered forms representing zero, so that it is suggested, after what has been said, that his proof may not be satisfactory. A proof was published by Stouff in 1902, and an outline|| is given by Bachmann.

The proofs of Selling and Stouff of the finiteness of the class number are rather involved and do not make obvious why the method of reduction should succeed. It is therefore desirable to point out the great simplification possible in the proofs. It is, of course, also necessary to treat completely the case when the form represents zero, and this is done very simply. It is hard to realise that all this has not been done before. But even Dickson in his studies just published,¶ although he gives a table of non-equivalent reduced indefinite forms when $n = 3$ and an account of its construction (ultimately by tentative methods) never proves that the class number for an arbitrary integer Δ is finite.

It may be remarked that the method of reduction by continuous parameters does in theory enable one to find out if two reduced forms are equivalent. It means, however, a great deal of detailed work. Thus the form**

$$z^2 - 5x^2 + 4xy - 5y^2$$

* Hermite, *loc. cit.*, p. 178; also p. 90.

† 'Thèse. Étude sur les formes binaires non-quadratiques à indéterminées réelles, ou complexes, ou à indéterminées conjuguées,' Paris, p. 30 (1917).

‡ Bachmann, pp. 494-510 for a sketch of Selling's work.

§ 'Œuvres,' vol. 1, p. 227 (1905).

|| Bachmann, pp. 510-519.

¶ Dickson's Studies, pp. 146-151.

** 'Got, Thèse. Questions diverses concernant certaines formes quadratiques ternaires indéfinies et les groupes fuchsien arithmétiques qui s'y rattachent,' pp. 42-58 (1913), Toulouse. Cf. also the remarks made by Fricke and Klein in their "Vorlesungen über die Theorie der Automorphen Functionen," vol. 1, p. 523 (1897). The interesting account of ternary forms, pp. 519-532, is worth while reading.

is one of 54 equivalent reduced forms of determinant 21. The mere tabulation of the results requires 17 pages. The labour involved in finding in this way the reduced non-equivalent indefinite forms of any determinant would be enormous. There are ways of avoiding some of the calculations, but the general method may still have to be used as a last resort. Thus Dickson leaves undecided the question of the equivalence of the forms

$$x^2 - 3y^2 - 2yz - 23z^2, \quad x^2 - 7y^2 - 6yz - 11z^2$$

of determinant 68.

§ 3. We consider then the indefinite forms in n -variables with $n \geq 3$. Take first the case $n = 3$. The ternary form can be written in an infinity of ways in one of the two canonical forms

$$\pm f(x_1, x_2, x_3) = V_1^2 + V_2^2 - V_3^2, \quad (6)$$

where

$$V_r = \xi_r x_1 + \eta_r x_2 + \zeta_r x_3, \quad (r = 1, 2, 3)$$

are linear functions of x_1, x_2, x_3 with real coefficients, rational or irrational. Writing $-f$ for f if need be, it suffices to consider the positive sign. Then the index of $f(x)$ is 1, i.e., the number of negative signs on the right-hand side of (6), a number independent of the particular decomposition V_1, V_2, V_3 , is 1. The only condition to be satisfied by ξ_3, η_3, ζ_3 , or say, ξ, η, ζ , is that they should be real, and that

$$f(x_1, x_2, x_3) + (\xi x_1 + \eta x_2 + \zeta x_3)^2 \quad (7)$$

should split into factors. These will be imaginary giving real V_1, V_2 since the index of $f(x)$ is 1. On equating the determinant of (7) to zero,

$$F(\xi, \eta, \zeta) + \Delta = 0 \quad (8)$$

where

$$F(\xi, \eta, \zeta) = (a_{22} a_{33} - a_{23}^2) \xi^2 + \dots$$

is the contravariant of $f(\xi, \eta, \zeta)$.

Hermite's method of reduction by continuous parameters is to associate with the form $f(x)$ the definite form

$$f_1(x_1, x_2, x_3) = V_1^2 + V_2^2 + V_3^2, \quad (9)$$

$$= f(x_1, x_2, x_3) + 2V_3^2. \quad (10)$$

There are an infinity of forms $f_1(x)$ corresponding to the real values ξ, η, ζ satisfying (8). On reducing the definite forms (10), and it is immaterial which definition of a reduced form is adopted, we obtain an infinite family, say (f_1) of reduced definite forms with, in general, irrational coefficients. The sub-

stitutions reducing $f_1(x)$ change $f(x)$ into a system of forms all equivalent to $f(x)$, say (f) . He proves that if two forms $f(x)$, $g(y)$ are equivalent, the corresponding families (f) and (g) are identical. Thus let $f(x)$ be changed into $g(y)$ by (3) with $n = 3$, say, the substitution S . Then for any set ξ, η, ζ taken with $f(x)$ in (10), we need only take the set ξ', η', ζ' with $g(y)$, where

$$\xi x_1 + \eta x_2 + \zeta x_3 = \xi' y_1 + \eta' y_2 + \zeta' y_3,$$

i.e.,

$$\xi \lambda_{11} + \eta \lambda_{21} + \zeta \lambda_{31} = \xi'. \quad \text{etc.} \quad (11)$$

Clearly ξ', η', ζ' is also a solution of the equation corresponding to (8) formed from $g(y)$, since $g(y) + 2V_3'^2$ where $V_3' = \xi_3' y_1 + \dots$, splits into linear factors. Then $f_1(x)$ is equivalent to $g_1(y)$ and is transformed into it also by S . Hence if the substitution Σ reduces $g_1(y)$, then $S\Sigma$ reduces $f_1(x)$. The corresponding reduced forms in (f) , (g) can be written as $S\Sigma f(x)$, $\Sigma g(y)$ say, and are identical, and so every form of (f) is found in (g) and conversely. Clearly the two forms $f(x)$, $g(y)$ are equivalent if the families (f) , (g) have in common a quadratic form. If (f) , (g) each contain an infinity of forms, this may not be easy to find out, but it is very simple if each contains only a finite number of forms.

If $f_1(x)$ is reduced for any set of values ξ, η, ζ (i.e., even only one set), then $f(x)$ is called a reduced form. If $f(x)$ is not reduced, a reduced form for $f(x)$ is found by taking (10) with any set ξ, η, ζ satisfying (8) and reducing by the substitution (3) the definite form (10).

This becomes

$$g(y_1, y_2, y_3) + 2(\xi' y_1 + \eta' y_2 + \zeta' y_3)^2,$$

where ξ', η', ζ' are defined by (11) and are now a solution of the equation corresponding to (8) with $f(x)$ replaced by $g(y)$. Then $g(y)$ is equivalent to $f(x)$ and is a reduced form.

At first sight, this seems a surprising definition of a reduced form, since there are a doubly infinite number of values for ξ, η, ζ . The work of other writers does not make clear the reason for the success of the method. The key is, of course, the simple idea leading to the inequalities (5) of which the proof is immediate.

On comparing (6) and (9) it is clear that the determinant of the form $f_1(x)$ is $-\Delta$. From (6), $\Delta < 0$.

If $f_1(x)$ is a reduced form, we have from (4),

$$(\xi_1^2 + \xi_2^2 + \xi_3^2)(\eta_1^2 + \eta_2^2 + \eta_3^2)(\zeta_1^2 + \zeta_2^2 + \zeta_3^2) \leq 2|\Delta|. \quad (12)$$

Then $f(x)$ is equivalent to a reduced form $g(y)$ where

$$b_{11} = \xi_1^2 + \xi_2^2 - \xi_3^2, \quad b_{12} = \xi_1\eta_1 + \xi_2\eta_2 - \xi_3\eta_3.$$

Hence

$$|b_{11}| \leq \xi_1^2 + \xi_2^2 + \xi_3^2, \quad |b_{12}| \leq |\xi_1\eta_1| + |\xi_2\eta_2| + |\xi_3\eta_3|.$$

Then first

$$|b_{11} b_{22} b_{33}| \leq 2 |\Delta|.$$

Next since

$$(\eta_1^2 + \eta_2^2 + \eta_3^2)(\zeta_1^2 + \zeta_2^2 + \zeta_3^2) \geq (|\eta_1\zeta_1| + |\eta_2\zeta_2| + |\eta_3\zeta_3|)^2, \quad (13)$$

(12) clearly gives

$$|b_{11} b_{23}^2| \leq 2 |\Delta|.$$

Finally, on multiplying together the three inequalities such as (13), (12) gives

$$|b_{12} b_{23} b_{31}| \leq 2 |\Delta|.$$

This proves (5).

Suppose now the coefficients a_{rs} of $f(x)$ are all integers. The coefficients b_{rs} are also integers and (5) shows that if $b_{11} b_{22} b_{33} \neq 0$, then there are at most a finite maximum number, depending only on Δ , of values for the b 's. Hence the class number, excluding forms representing zero, is finite.

Suppose next that $b_{11} = 0$. Then the system (f) apparently may contain an infinity of forms reduced according to the definition, *e.g.*, from the inequalities (5), b_{22} may not be bounded if $b_{11} = 0 = b_{12}$. In fact, Stouff's lengthy investigation* for the indefinite form in n -variables shows that all the coefficients of the reduced indefinite form are bounded on selecting one of Hermite's methods of reducing a definite form and developing the theory. But we can dispense with all this in the present paper. For even if there are an infinity of reduced forms, it is easy to pick out a finite number of these such that any member of (f) is equivalent to at least one of them.

For $g(y)$ now becomes

$$2y_1(b_{12}y_2 + b_{13}y_3) + b_{22}y_2^2 + 2b_{23}y_2y_3 + b_{33}y_3^2. \quad (13A)$$

An appropriate linear substitution involving only y_2, y_3 , *i.e.*,

$$y_1 = z_1, \quad y_2 = r_1z_2 + r_2z_3, \quad y_3 = s_1z_2 + s_2z_3$$

changes this into

$$2c_{12}z_1z_2 + c_{22}z_2^2 + 2c_{23}z_2z_3 + c_{33}z_3^2, \quad (14)$$

* 'Annales scientifiques de l'école normale supérieure,' vol. 39, pp. 99-118 (1902)
A résumé is given by Bachmann, pp. 513-519.

or say $h(z)$. The determinant of $h(z)$ is

$$\begin{vmatrix} 0 & c_{12} & 0 \\ c_{12} & c_{22} & c_{23} \\ 0 & c_{23} & c_{33} \end{vmatrix} = c_{12}^2 c_{33}.$$

This gives a finite number of values for c_{12} , c_{33} . Replace then in (14) z_1 by $z_1 + \mu_2 z_2 + \mu_3 z_3$, where μ_2 , μ_3 are integers. Since c_{22} , c_{23} are replaced by $2c_{12}\mu_2 + c_{22}$, $c_{12}\mu_3 + c_{23}$, we may suppose μ_2 , μ_3 so taken that

$$|c_{22}| \leq 2|c_{12}|, \quad |c_{23}| < c_{12}.$$

Hence the class number for forms representing zero* is finite.

§ 4. The proof just given is perfectly general. Thus for an indefinite quaternary form, there are three distinct canonical types for $\pm f(x)$,

$$V_1^2 + V_2^2 \pm V_3^2 \pm V_4^2. \quad (15)$$

The case of two negative signs, so that $\Delta > 0$ may suffice as an illustration. In place of the three parameters ξ_3 , η_3 , ζ_3 connected by one equation, there are eight parameters, ξ_3 , η_3 , ζ_3 , τ_3 and ξ_4 , η_4 , ζ_4 , τ_4 , connected by two equations expressing the fact that

$$f(x_1, x_2, x_3, x_4) + (\xi_3 x_1 + \dots + \tau_3 x_4)^2 + (\xi_4 x_1 + \dots + \tau_4 x_4)^2$$

is a quadratic function of only two variables.

The associated definite form, on putting, $V_1 = \xi_1 x_1 + \eta_1 x_2 + \zeta_1 x_3 + \tau_1 x_4$, is

$$f_1(x) = V_1^2 + V_2^2 + V_3^2 + V_4^2,$$

whose determinant on noting (15) is seen to be Δ , the same as that of $f(x)$. If $f_1(x)$ is reduced for any set of values of ξ_3 , ξ_4 , etc., then from (4)

$$(\xi_1^2 + \xi_2^2 + \xi_3^2 + \xi_4^2)(\eta_1^2 + \dots + \eta_4^2)(\zeta_1^2 + \dots + \zeta_4^2)(\tau_1^2 + \dots + \tau_4^2) \leq k_4 \Delta. \quad (16)$$

Since for the reduced form $g(y)$ equivalent to $f(x)$,

$$b_{11} = \xi_1^2 + \xi_2^2 - \xi_3^2 - \xi_4^2, \quad b_{12} = \xi_1 \eta_1 + \xi_2 \eta_2 - \xi_3 \eta_3 - \xi_4 \eta_4,$$

$$|b_{11}| \leq \xi_1^2 + \xi_2^2 + \xi_3^2 + \xi_4^2, \quad |b_{12}| \leq |\xi_1 \eta_1| + |\xi_2 \eta_2| + |\xi_3 \eta_3| + |\xi_4 \eta_4|,$$

(16) gives at once

$$|b_{11} b_{22} b_{33} b_{44}| \leq k_4 \Delta. \quad (16A)$$

* It is conceivable that a form representing zero appears as a Hermite reduced form with $b_{11} \neq 0$. But it is not difficult to find out if a given indefinite quadratic form represents zero. See Bachmann, vol. 1, pp. 231-233, for Smith's result for the ternary form, pp. 259-266 for Meyer's result for the quaternary form, pp. 551-553 for Minkowski's result. See also my forthcoming paper to which I have already referred.

Since

$$(\zeta_1^2 + \dots + \zeta_4^2)(\tau_1^2 + \dots + \tau_4^2) \geq (|\zeta_1\tau_1| + \dots + |\zeta_4\tau_4|)^2,$$

(16) gives again

$$\left. \begin{aligned} |b_{11} b_{22} b_{34}^2| &\leq k_4 \Delta, \\ |b_{12}^2 b_{34}^2| &\leq k_4 \Delta. \end{aligned} \right\} \quad (16B)$$

These inequalities then, and those derived by permuting the letters, are satisfied by a reduced form, and appear to be new. Clearly, a glance at the canonical forms (15) shows that they still hold if the index of $f(x)$ is 1 or 3, and also 0, 4 when the form is definite. For definite forms, however, (16A) has already been assumed in (4), i.e., from only this property of reduced definite forms, there follow the inequalities (16B).

If now the coefficients a_{rs} are integers, (16A), (16B) show that if $b_{11} b_{22} b_{33} b_{44} \neq 0$, the class number is finite for forms not representing zero. This was also proved by Picard.*

If $b_{11} = 0$, $f(x)$ is equivalent to a form which can be written as

$$2c_{12}z_1z_2 + \sum_{r,s=2}^4 c_{rs}z_rz_s, \quad (17)$$

the terms multiplying y_1 , in the analogue of (13A) having been absorbed into the variable z_2 . The determinant of (17) is

$$\begin{aligned} \Delta = & \begin{vmatrix} 0 & c_{12} & 0 & 0 \\ c_{12} & c_{22} & c_{23} & c_{24} \\ 0 & c_{23} & c_{33} & c_{34} \\ 0 & c_{24} & c_{34} & c_{44} \end{vmatrix} = -c_{12}^2 \begin{vmatrix} c_{33} & c_{34} \\ c_{34} & c_{44} \end{vmatrix} = -c_{12}^2 \Delta_2, \end{aligned} \quad (18)$$

say. Hence there are at most a finite number depending only on Δ of values of c_{12} , Δ_2 . Then the form in two variables $\sum_{r,s=2}^4 c_{rs}z_rz_s$, whether definite, indefinite, or reducible, belongs to one of a finite number of classes. Finally, writing for z_1 , $z_1 + \mu_2 z_2 + \mu_3 z_3 + \mu_4 z_4$ where μ_2, μ_3, μ_4 are integers, we may suppose

$$|c_{22}| \leq 2|c_{12}|, \quad |c_{23}| \leq |c_{12}|, \quad |c_{24}| \leq |c_{12}|.$$

Hence the class number for the forms representing zero is also finite.

* 'J. Math. pures appl.,' vol. 1 (4), pp. 90-93 (1885).

The proof holds for $n \geq 5$. Thus for $n = 5$, the coefficients b_{rs} of the reduced form of any index (including definite forms) satisfy the inequalities

$$\begin{aligned} |b_{11} b_{22} b_{33} b_{44} b_{55}| &\leq k_5 \Delta, \\ |b_{11} b_{22} b_{33} b_{45}^2| &\leq k_5 \Delta, \\ |b_{11} b_{23}^2 b_{45}^2| &\leq k_5 \Delta. \end{aligned}$$

The same conclusions follow as before for forms with integer coefficients.

§ 6. For $n \geq 5$, a simple normal type can be deduced from Meyer's theorem. We can now always take $b_{11} = 0$ as part of the definition of a reduced form, and so $f(x)$ is equivalent to a form (cf. (14), (17))

$$z_2(2c_{21}z_1 + c_{22}z_2 + \dots + 2c_{2n}z_n) + \phi(z_3, z_4, \dots, z_n) \quad (19)$$

where $\phi(z)$ is a reduced form, definite or indefinite, in $n - 2$ variables and of determinant Δ/c_{11}^2 . Hence c_{11} has only a finite number of values, and we may clearly take

$$|c_{22}| \leq 2|c_{12}|, \quad |c_{33}| \leq |c_{12}|, \dots, \quad |c_{2n}| \leq |c_{12}|. \quad (20)$$

If the index of $f(x)$ is 1, then $\phi(z)$ is a definite form since the terms in z_2 considered as a difference of two real squares have an index 1. Nothing more need be done.

If the index of $f(x)$ is 2, then the index of $\phi(z)$ is 1, and so $\phi(z)$ is an indefinite form in $n - 2$ variables. If $n = 4, 5, 6$, the reduction of $\phi(z)$ has been dealt with, and the conditions (20), etc., can again be satisfied by writing $z_1 + \mu_2 z_2 + \dots$ for z_1 . If $n \geq 7$, $\phi(z)$ is an indefinite form in five or more variables. When reduced, it takes the form

$$z_4(2d_{43}z_3 + d_{44}z_4 + \dots + 2d_{4n}z_n) + \psi(z_5, z_6, \dots, z_n)$$

where $\psi(z)$ is a definite form in $n - 5$ variables. We may suppose $|d_{44}| \leq 2|d_{34}|$, etc., on writing $z_3 + \nu_4 z_4 + \dots$ for z_3 . Writing again $z_1 + \mu_2 z_2 + \dots$ for z_1 in the first term of (19) we may still suppose (20) holds.

Similarly the resulting normal form is obvious whatever be the index of $f(x)$ or the value of μ , and clearly it proves once more that the class number is finite.

The Spectrum of Singly Ionised Antimony.

By D. G. DHAVALÉ, M.Sc., Research Scholar, Department of Physics,
Allahabad University.

(Communicated by M. N. Saha, F.R.S.—Received October 27, 1930.)

There have been many investigations on the spectrum of antimony in different stages of ionisation during recent years. The arc spectrum of antimony has been experimentally investigated by Foote, Ruark, Mohler and Chenault in the Bureau of Standards* and by Malurkar in this laboratory. The complete classification has, however, not yet been given.

The spectrum of doubly ionised antimony has been recently investigated by Lang.†

No systematic work seems to have been done on the spectrum of singly ionised antimony, either experimental or theoretical. The following investigation was undertaken with a view to removing this gap in our knowledge.

Following the system adopted in this laboratory we begin with a general survey of the spectra of the following groups of elements :—

Table I.

I	In	Sn	Sb	Te	I	Xe	Cs
II	Sn ⁺	Sb ⁺	Te ⁺	I ⁺	Xe ⁺	Cs ⁺	Ba ⁺
III	Sb ⁺⁺	Te ⁺⁺	I ⁺⁺	Xe ⁺⁺	Cs ⁺⁺	Ba ⁺⁺	La ⁺⁺
IV	Te ⁺⁺	I ⁺⁺	Xe ⁺⁺	Cs ⁺⁺	Ba ⁺⁺	La ⁺⁺	Ce ⁺⁺
V	I ⁺⁺	Xe ⁺⁺	Cs ⁺⁺	Ba ⁺⁺	La ⁺⁺	Ce ⁺⁺	Pr ⁺⁺

These groups of elements have the electronic constitution

$$(1s^2 2s^2 2p^6 3s^2 3p^6 3d^{10} 4s^2 4p^6 4d^{10} 5s^2) 5p^x \dots 6s \dots 6p, \text{ etc.}$$

in their excited states, x having the value indicated at the head of the column.

* 'Bureau of Standards Sci. Papers,' p. 463 (1924).

† 'Phys. Rev.,' vol. 35, p. 445.

The light-electron runs through the higher levels $6s$, $6p$, etc., as graphically denoted in the following general diagram :—

	s	p	d	f	
5	2	x	(1)		
6		(1)	(1)	(1)
7			(1)	p	..

(considering the electrons outside the inert gas shell only).

In the normal state there will be $(x + 1)$ electrons in the $5p$ orbit.

LOCATION OF LINES DUE TO DIFFERENT TRANSITIONS.

(1) Transition $5p \leftarrow 5d$.

↑
 $6s$

Most of these lines lie in and beyond the Schumann region and need not be considered here.

(2) Transition $6s \leftarrow 6p$.

For some elements in Table I the lines due to this transition are known. They are shown in Chart 1 and plotted in fig. 1.

In plotting this chart I have made use of some unpublished results of Mr. Suresh Chandra Deb on the spectrum of iodine, and my best thanks are due to him for having kindly allowed me to make use of his data. Only the most important lines have been given in this chart. The reference is given under each element.

The diagram once more illustrates the use of the two empirical rules which are so successfully being used in this laboratory, viz., the arithmetic Progression Law* and the Method of Horizontal Comparison.† As these rules have been sufficiently explained in other papers published by workers in this laboratory it is not necessary to explain them again. In the above table they have been extended to elements with higher atomic weights than those considered by

* Saha and Kichlew, 'Ind. J. Phys.', vol. 2 (1928).

† Saha and Mazumder, 'Ind. J. Phys.', vol. 3, p. 67 (1928).

Chart 1.—Transition $5p^a$ ($6s \leftarrow 6p$).

$\pi \rightarrow$	0	1	2	3	4	5	6
1	—	$^3P_1 - ^3D_1$	$^4P_1 - ^4D_1$	—	$^4P_1 - ^4D_1$	$^3P_1 - ^3D_1$	—
2	$^3S_1 - ^3P_1$	$^3P_1 - ^3P_1$	$^4P_1 - ^4P_1$	$^3S_1 - ^3P_1$	$^4P_1 - ^4P_1$	$^3P_1 - ^3P_1$	$^3S_1 - ^3P_1$
3	—	$^3P_1 - ^3S_1$	$^4P_1 - ^4S_1$	—	$^4P_1 - ^4S_1$	$^3P_1 - ^3S_1$	—
I	In	Sn	Sb	Te	I	Xe	Cs
1	—	—	—	—	—	11335	—
2	7776	—	—	—	—	22094	11732
3	— Fowler "Report" (calc.)	—	—	—	—	22211 'B.S.J.R.,' vol. 3, p. 731 (1929)	— Fowler "Report" p. 107
II	Sn^+	Sb^+	Te^+	I^+	Xe^+	Cs^+	Ba^+
1	—	12863	—	—	—	—	—
2	15492	16715	—	161315	—	—	21952
3	— Green & Loring, 'Phys. Rev.,' vol. 30, p. 582	19992 Dhavale (this paper)	—	Deb (un- published)	—	—	— Fowler "Report," p. 137
III	Sb^{++}	Te^{++}	I^{++}	Xe^{++}	Cs^{++}	Ba^{++}	La^{++}
1	—	—	—	—	—	—	—
2	22970	—	—	26437	—	—	31520
3	— Lang, 'Phys. Rev.,' vol. 35, p. 445	—	—	—	—	—	— Gibb & White, 'Proc. Nat. A. Sc.,' vol. 12, p. 554
IV	Te^{+3}	I^{+3}	Xe^{+3}	Cs^{+3}	Ba^{+3}	La^{+3}	Ce^{+3}
1	—	—	—	—	—	—	—
2	—	—	—	—	—	—	40731 Gibb & White
3	—	—	—	—	—	—	do.

earlier workers. It can only be added that these rules are found to be of great use in the quick classification of the lines.*

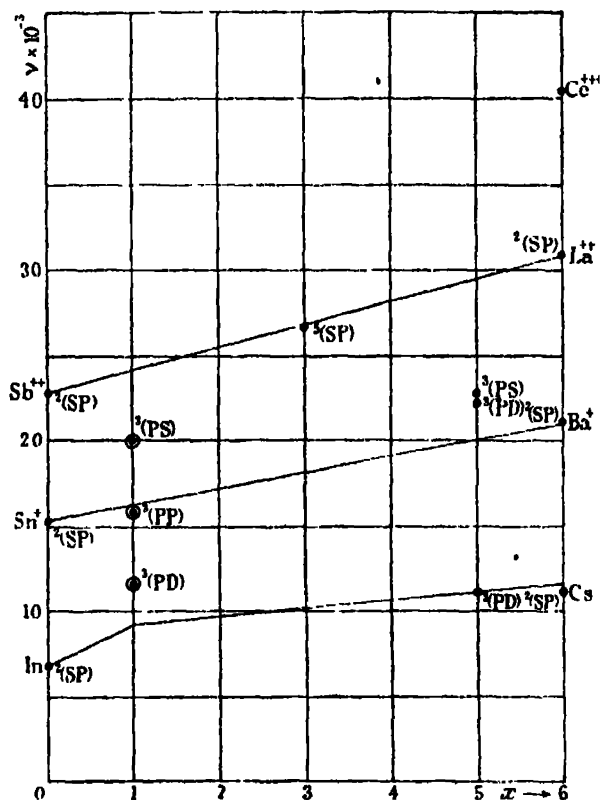


FIG. 1.—Transition $5p^2 (6s \leftarrow 6p)$.

(3) Transition $(6p \leftarrow 6d)$.

The two empirical laws hold not only for the transition $(6s \leftarrow 6p)$ but also for the transition $(6p \leftarrow 6d)$. The data for this transition is very scanty, but whatever is available has been collected in Chart 2. No graph has been plotted as there are not many points.

* It should, however, be noted that as the separations for the higher elements increase the different multiplets, which are grouped together about the line in fig. 1 in lighter elements, get wider and fall away from the line, so that only one of the multiplets may remain near the line. The others will be far away from it. Their positions can be located approximately by interpolating from data on similar multiplets of the other elements in the group. Also while the strongest line in one multiplet may be located in one the others go far off from it due to the large separations.

Chart 2.—Transition $5p^2$ ($6p \leftarrow 6d$).

$n \rightarrow$	0	1	2	3	4	5	6
1	—	$^3P_1 - ^3D_2$	$^4P_1 - ^4D_4$	—	$^4P_1 - ^4D_4$	$^3P_1 - ^3D_2$	—
2	$^3P_1 - ^3D_2$	$^3S_1 - ^3P_1$	$^4D_4 - ^4F_5$	$^3P_1 - ^3D_2$	$^4D_4 - ^4F_5$	$^3S_1 - ^3P_1$	$^3P_1 - ^3D_2$
3	—	$^3D_2 - ^3F_4$	$^4D_4 - ^4P_1$	—	$^4P_1 - ^4D_4$	$^3D_2 - ^3F_4$	—
I	In	Sn	Sb	Te	I	Xe	Cs
1	—	—	—	—	—	—	—
2	6950	—	—	—	—	—	11411
3	— Fowler "Report" (calc.)	—	—	—	—	—	— Fowler "Report," p. 107
II	Sn ⁺	Sb ⁺	Te ⁺	I ⁺	Xe ⁺	Cs ⁺	Ba ⁺
1	—	20498	—	—	—	—	—
2	17969	—	—	22674	—	—	24202
3	— Green & Loring, 'Phys. Rev.,' vol. 30, p. 582	24181.9 Dhvale (this paper)	—	— Deb (un- published)	—	—	— Fowler "Report," p. 137
III	Sb ⁺⁺	Te ⁺⁺	I ⁺⁺	Xe ⁺⁺	Cs ⁺⁺	Ba ⁺⁺	La ⁺⁺
1	—	—	—	—	—	—	—
2	28524	—	—	36788	—	—	—
3	— Lang, 'Phys. Rev.,' vol. 32, p. 740	—	—	— Dutt & Deb, 'Nature'	—	—	—

With a view to filling up the many gaps in the two charts I undertook to investigate the spectra yet unknown and began with the spark spectrum of antimony. The regularities manifested in these charts were used as guiding principles for analysing the spectra.

Experimental.

As it was found that the data available for antimony was not sufficient entirely new measurements were made over a wide range. The spark was produced between two electrodes cut from the pure metal supplied by Kahlbaum with the help of an induction coil. A parallel plate condenser made by piling

together alternate sheets of tin and glass was used. The fact that only a few of the strongest lines of Sb^{++} were brought out indicates that the excitation was very proper for Sb^+ lines. Photographs were taken in the first and second orders of a 1-metre concave grating mounted in this laboratory according to the Paschen-Runge mounting. Neon lines were used for comparison in the red and infra-red regions and copper lines in the visible and ultra-violet. Measurements were made from λ 8500 to λ 3000. The dispersion was about 15 to 16 Å. per millimetre in the first and 7 to 8 Å. in the second order. Photographs were taken on neocyanin, panchromatic and ordinary plates as required.

Classification.

Considering the structure diagram of singly ionised antimony given above the terms predicted by Hund's theory are given below.*

Structure outside inert gas shell.	Adopted prefix.	Terms (theoretical).						Terms (observed).					
$5s^2 5p 6s$	$6s$	3P						3P				1P	
$5s^2 5p 6p$	$6p$	3D	3P	3S	1D	1P	1S	3D	3P	3S	1D	1P	1S
$5s^2 5p 6d$	$6d$	3F	3D	3P	1F	1D	1P	3F	3D	3P	1F	1D	1P
$5s^2 5p 7s$	$7s$	3P						3P				1P	

The lines identified as belonging to the $6s \leftarrow 6p$ transition are given in Table II.

The Multiplet Differences.

Antimony being a heavy element the multiplet differences are rather large. It will be interesting to note how these arise. Lang† has found that for the $5p$ level of Sb^{++} the difference $^3P_2 - ^3P_1$ is 6576. Now in the case of Sb^+ the terms arising from the electron-combination $(5p) \cdot (6s)$ follow j-j-coupling

* The notation used in this paper is that recommended by Russel Shenstone and Turner in their report ('Phys. Rev.', vol. 33, p. 900) with minor differences necessitated by the nature of the particular case. The exact mode of representing every term will be clear from the table of configuration given here. The diagram that used to be given by workers in this laboratory to elucidate the structure and configurations of the running electron has also been modified in the above sense. It is hoped that the representation while retaining its originality will be found intelligible and useful.

† *Loc. cit.*

Table II.

	200	5031.9
	$6s\ ^3P_0$	$6s\ ^3P_1$ $6s\ ^3P_2$
$6p\ ^1D_1$ 830	(6) 16237.7	— —
$6p\ ^3D_2$ 1028	—	(7) 16865.6 (8) 11835
$6p\ ^1D_2$	—	— (12) 12863
$6p\ ^3P_0$ 404	—	(4) 20423.3 —
$6p\ ^3P_1$ 829.6	(3) 21117.9	(8) 20917.3 —
$6p\ ^3P_2$	—	(6) 21746.9 (10) 16715.0
$6p\ ^3S_1$	(3) 25226.0	(6) 25024.9 (8) 19992.0

(*vide* Pauling and Goudsmit, "Structure of Line-spectra," p. 106) and the resultant terms can be described as follows:—

$$\begin{array}{l}
 {}^3P_0 \\
 {}^3P_1 \text{ and } {}^3S_1 \text{ give } {}^3P_1 \\
 {}^3P_2 \\
 {}^3P_1 \text{ and } {}^3S_1 \text{ give } {}^1P_1
 \end{array}$$

The difference between ${}^3P_0 - {}^3P_1$ and ${}^3P_2 - {}^1P_1$ will be rather small whereas the difference ${}^3P_1 - {}^3P_2$ will be very large and comparable with 6576 of Sb^{++} . This is well brought out by the differences actually obtained.

We can compare this coupling with the analogous case of tin. For Sn^+

Table III.

	621.9		1540.2		697.4		1116.5		—1404.2		—1885.4	
	$6d^2P_2$	$6d^2P_1$	$6d^2P_2$	$6d^2P_1$	$6d^2D_1$	$6d^2D_1$	$6d^2D_1$	$6d^2D_2$	$6d^2P_0$	$6d^2P_1$	$6d^2P_2$	$6d^2P_2$
$6p^3D_1$ 830	(4) 23880.5	—	—	—	(4) 24306.1	—	—	—	(2) 30251.9	—	—	—
$6p^3D_2$ 1028	(2) 23049.4	(4) 23671.3	—	—	(3) 23562.4	(5) 24259.8	(3) 25376.3	—	—	(6) 28019.1	(4) 26133.7	—
$6p^3D_3$	—	(4) 22641.7	(7) 24181.9	—	—	—	(10) 24348.6	—	—	—	(8) 25105.6	—
$6p^3P_0$ 494	—	—	—	—	—	—	—	—	—	(3) 24467.3	—	—
$6p^3P_1$ 839.6	—	—	—	—	—	(4) 20207.8	—	—	(3) 25376.3	(4) 25972.1	—	—
$6p^3P_2$	—	(4) 18701.4	—	—	—	(5) 19379.3	(6) 20496.7	—	—	(3) 23140.2	(8) 21249.9	—
$6p^3S_1$	—	—	—	—	—	(4) 16103.5	—	—	(2) 21269.6	(3) 19862.9	—	—

$^3P_1 - ^3P_0$ of the $5p$ level is 4253* and the differences for the corresponding levels of tin are† are

$$\begin{array}{rcl}
 ^3P_0 & \left. \vphantom{\begin{array}{c} ^3P_0 \\ ^3P_1 \end{array}} \right\} & 273 \\
 ^3P_1 & \left. \vphantom{\begin{array}{c} ^3P_0 \\ ^3P_1 \end{array}} \right\} \dots\dots\dots & \\
 & & \left. \vphantom{\begin{array}{c} ^3P_0 \\ ^3P_1 \\ ^3P_2 \end{array}} \right\} 3714 \\
 ^3P_2 & \left. \vphantom{\begin{array}{c} ^3P_2 \\ ^1P_1 \end{array}} \right\} \dots\dots\dots & \\
 ^1P_1 & \left. \vphantom{\begin{array}{c} ^3P_2 \\ ^1P_1 \end{array}} \right\} & 628
 \end{array}$$

lines classified as belonging to the $6p \leftarrow 6d$ transition are given in Table III and the lines due to the $6p \leftarrow 7s$ transition in Table IV. The known differences found from the last classification facilitate this classification. The analysis is, of course, effected in the usual manner.

Table IV.

	1187.4	6241.9	
	$7s\ ^3P_0$	$7s\ ^3P_1$	$7s\ ^3P_2$
$6p\ ^3D_1$	(4) 20343.5	(5) 21530.9	(4) 27772.8
830			
$6p\ ^3D_2$	—	(8) 20702.5	(6) 26942.5
1028			
$6p\ ^3D_3$	—	—	(10) 25917.4
$6p\ ^3P_0$	—	—	—
494			
$6p\ ^3P_1$	(4) 15463.2	(9) 16649.3	(3) 22890.6
829.6			
$6p\ ^3P_2$	—	(5) 15820.4	(9) 22064.8
$6p\ ^3S_1$	—	—	—

It will be seen that the P-terms in the $5p\ 6d$ level are inverted. This has been found to be the case in $\dagger N^+$ as well as $\S P^+$.

* Green and Loring, 'Phys. Rev.', vol. 30, p. 582.

† Sur, 'Z. Physik,' vol. 41, p. 792.

‡ Fowler and Freeman, 'Proc. Roy. Soc.,' A, vol. 114, p. 662 (1927).

§ Bowen, 'Phys. Rev.,' vol. 29, p. 510 (1927).

The following two multiplets have been identified as belonging to the $5d \leftarrow 6p$ transition.

Table V.

	$5d\ ^3F_2$	$5d\ ^3F_3$	$5d\ ^3F_4$
$6p\ ^3P_1$	(7) 14543.9	—	—
$6p\ ^3P_2$	(5) 15374.5	(8) 14688.4	—
$6p\ ^3P_3$	—	(3) 15720.2	(10) 14748.9

Table VI.

	$5d\ ^3D_1$	$5d\ ^3D_2$	$5d\ ^3D_3$
$6p\ ^3P_0$	(8) 13895.2	—	—
$6p\ ^3P_1$	(5) 14390.1	(9) 13459	
$6p\ ^3P_2$	—	(7) 14289.1	(10) 12515

Singlet Lines.

The classifications thus far known in this group do not contain many singlet lines. Thus a few lines are given by Fowler in his work on N^+ . No singlet lines are discovered in the classification of P^+ , and As^+ has not yet been investigated. The following singlet lines were obtained from considerations based on the work of Fowler and Freeman on N^+ .

Table VII.

	$6s\ ^1P_1$	$7s\ ^1P_1$	$6d\ ^1F_3$	$6d\ ^1D_2$	$6d\ ^1P_1$
$6p\ ^1D_2$	—	(8) 27458.4	(7) 24140.7	(3) 25344.1	(5) 29997.6
$6p\ ^1P_1$	(9) 13742	(7) 24109.4	—	(5) 21997.4	(6) 26849.9
$6p\ ^1S_0$	(10) 17958.0	(7) 19893.8	—	—	(4) 22429.6

Ionisation Potential.

It will be seen that both the transitions $6s \leftarrow 6p$ and $6p \leftarrow 7s$ are known and that they form a Rydberg sequence. We can find out from this the term values of the actual terms $6s$, $6p$, $7s$, with the help of the table of Rydberg sequences given in Fowler's 'Report.' Knowing the value of $6p$ we can arrive at the term value of $5p$ which will give us the ionisation potential. Thus from Tables II and IV

$$6s - 6p = 16715 \text{ taking the line } {}^3P_2 - {}^3P_2$$

$$6p - 7s = 22065 \text{ taking the same line,}$$

therefore

$$6s - 7s = 38780.$$

Let $6s = 4N/(2 + \sigma)^2$ and $7s = 4N/(3 + \sigma)^2$, then from the table referred to above $6s = 77036$ and $7s = 38256$, from which $6p = 60321$.

Taking $6p = 4N/(2 + \pi)^2$ we have $5p = 4N/(1 + \pi)^2 = 152364$, which gives the ionisation potential of Sb^+ to be 18.8 volts. From these term values and the observed lines all the remaining term values will follow. They are given below in order of magnitude:—

Table VIII.—Triplet Term Table for Sb II.

Term.	Value.	Term.	Value.
$6s {}^3P_0$	82267.9	$6p {}^3P_2$	60321.0
$6s {}^3P_1$	82067.9	$6p {}^3S_1$	57044.0
$5d {}^3F_4$	80575.5	$7s {}^3P_0$	45685.3
$5d {}^3F_3$	79893.2	$7s {}^3P_1$	44497.9
$5d {}^3F_2$	78921.9	$6d {}^3F_4$	42151.6
$6s {}^3P_2$	77036.0	$6d {}^3D_1$	41638.6
$5d {}^3D_1$	75540.7	$6d {}^3F_3$	41539.7
$5d {}^3D_2$	74610.1	$6d {}^3D_3$	40941.2
$5d {}^3D_3$	72836.0	$6d {}^3F_2$	39989.5
$6p {}^3D_1$	68031.0	$6d {}^3D_1$	39824.5
$6p {}^3D_2$	65301.0	$6d {}^3P_2$	39068.7
$6p {}^3D_3$	64173.0	$6d {}^3P_1$	37183.3
$6p {}^3P_2$	61644.6	$6d {}^3P_0$	35779.1
$6p {}^3P_1$	61150.6		

The following is a complete list of the classified lines:—

Table IX.

λ	Int.	ν_{mc}	Combinations.	
			Triplets.	Singlets.
8447	8	11835	$6s^3P_2 - 6p^3D_2$	
7988	10	12515	$5d^1D_2 - 6p^3P_2$	
7772	12	12863	$6s^3P_2 - 6p^3D_2$	
7428	9	13459	$5d^1D_2 - 6p^3P_1$	
7275	9	13742	—	
7194.7	8	13895.2	$5d^1D_1 - 6p^3P_2$	$6s^1P_1 - 6f^1P_1$
6996.4	7	14289.1	$5d^1D_2 - 6p^3P_2$	
6947.3	5	14390.1	$5d^1D_1 - 6p^3P_1$	
6874.3	7	14543.9	$5d^1F_2 - 6p^3D_1$	
6806.2	8	14688.4	$5d^1F_2 - 6p^3D_2$	
6778.3	10	14748.9	$5d^1F_4 - 6p^3D_2$	
6502.5	5	15374.5	$5d^1F_2 - 6p^3D_1$	
6465.2	4	15463.2	$6p^3P_1 - 7s^3P_2$	
6359.5	3	15720.2	$5d^1F_2 - 6p^3D_2$	
6319.2	5	15820.4	$6p^3P_2 - 7s^3P_1$	
6208.1	4	16103.5	$6p^3S_1 - 6d^3D_2$	
6156.8	6	16237.7	$6s^3P_2 - 6p^3D_1$	
6004.6	9	16649.3	$6p^3P_1 - 7s^3P_1$	
5981.0	10	16715.0	$6s^3P_1 - 6p^3F_2$	
5927.6	7	16865.6	$6s^3P_1 - 6p^3D_2$	
5567.0	10	17958.0	—	$6s^1P_1 - 6p^1S_2$
5320.1	4	18791.4	$6p^3P_2 - 6d^3F_2$	
5158.6	5	19379.3	$6p^3P_2 - 6d^3D_2$	
5033.1	3	19882.9	$6p^3S_1 - 6d^3P_1$	
5025.3	7	19893.8	—	$6p^1S_2 - 7s^1P_1$
5000.6	8	19992.0	$6s^3P_1 - 6p^3S_1$	
4947.2	4	20207.8	$6p^3P_1 - 6d^3D_2$	
4914.2	4	20343.5	$6p^3D_1 - 7s^3P_2$	
4895.0	4	20423.3	$6s^3P_1 - 6p^3P_2$	
4877.0	6	20498.7	$6p^3P_2 - 6d^3D_2$	
4829.0	8	20702.5	$6p^3D_2 - 7s^3P_1$	
4779.4	8	20917.3	$6s^3P_1 - 6p^3P_1$	
4734.0	3	21117.9	$6s^3P_2 - 6p^3P_1$	
4704.6	8	21249.9	$6p^3P_2 - 6d^3P_1$	
4700.22	2	21269.6	$6p^3S_1 - 6d^3P_2$	
4643.18	5	21530.9	$6p^3D_1 - 7s^3P_1$	
4597.08	6	21746.9	$6s^3P_1 - 6p^3P_2$	
4544.73	5	21997.4	—	$6p^1P_1 - 6d^1D_2$
4530.84	9	22064.8	$6p^3P_2 - 7s^3P_1$	
4457.14	4	22429.6	—	$6p^1S_2 - 6d^1P_1$
4415.40	4	22641.7	$6p^3D_2 - 6d^3F_2$	
4367.38	3	22890.6	$6p^3P_1 - 7s^3P_2$	
4337.30	2	23049.4	$6p^3D_2 - 6d^3F_2$	
4330.27	3	23140.2	$6p^3P_2 - 6d^3P_1$	
4242.86	3	23562.4	$6p^3D_2 - 6d^3D_1$	
4223.24	4	23671.3	$6p^3D_2 - 6d^3F_2$	
4186.34	4	23880.5	$6p^3D_1 - 6d^3F_2$	
4170.35	4	23972.1	$6p^3P_1 - 6d^3P_1$	
4146.60	7	24109.4	—	$6p^1P_1 - 7s^1P_1$
4141.21	7	24140.7	—	$6p^1D_2 - 6d^1F_2$
4134.17	7	24181.9	$6p^3D_2 - 6d^3F_4$	
4120.89	5	24259.8	$6p^3D_2 - 6d^3D_2$	
4105.86	10	24348.6	$6p^3D_2 - 6d^3D_2$	
4097.87	4	24396.1	$6p^3D_1 - 6d^3D_1$	
4085.93	3	24467.3	$6p^3P_2 - 6d^3P_1$	
3994.90	6	25024.9	$6s^3P_1 - 6p^3S_1$	

Table IX—continued.

λ .	Int.	ν_{vac}	Combinations.	
			Triplets.	Singlets.
3982.05	8	25105.6	$6p\ ^1D_2 - 6d\ ^1P_1$	
3963.95	3	25226.0	$6s\ ^1P_1 - 6p\ ^1S_1$	
3944.58	3	25344.1	—	$6p\ ^1D_2 - 6d\ ^1D_2$
3939.57	4	25376.3	$6p\ ^1D_2 - 6d\ ^1D_2$	
3857.32	10	25917.4	$6p\ ^1D_2 - 7s\ ^1P_1$	
3825.39	4	26133.7	$6p\ ^1D_2 - 6d\ ^1P_1$	
3752.02	6	26649.8	—	$6p\ ^1P_1 - 6d\ ^1P_1$
3710.56	6	26942.5	$6p\ ^1D_2 - 7s\ ^1P_1$	
3640.84	8	27458.4	—	$6p\ ^1D_2 - 7s\ ^1P_1$
3599.62	4	27772.8	$6p\ ^1D_1 - 7s\ ^1P_1$	
3567.98	6	28019.1	$6p\ ^1D_2 - 6d\ ^1P_1$	
3332.64	5	29997.6	—	$6p\ ^1D_2 - 6d\ ^1P_1$
3304.63	2	30251.9	$6p\ ^1D_1 - 6d\ ^1P_1$	

Summary.

The first spark spectrum of antimony has been classified from the data obtained by the author in the region λ 3000 to λ 8500. The classification once more illustrates the usefulness of the method of horizontal comparison developed in this laboratory. The ionisation potential of Sb^+ has been roughly found to be 18.8 volts.

In conclusion I wish to express my sincere thanks to Professor Meghnad Saha, D.Sc., F.R.S., for his advice and guidance in this work, and to Mr. Suresh Chandra Deb for the invaluable help he rendered me throughout the course of this work.

The Development of a High Speed Wind Channel for research in External Ballistics.

By Sir THOMAS E. STANTON, F.R.S.

(Received December 12, 1930.)

[PLATE 6.]

In November, 1918, the British Ballistic Mission paid a visit to the French Government Laboratory in which experiments on stationary projectiles in a high-speed current of air were being carried out at velocities greater than the velocity of sound by MM. Langevin, Hugenard and Ste. Lague.

In these experiments a large reservoir of compressed air (200 cubic feet at 100 lbs. per square inch) was used, the air being released by a very quick-acting valve and allowed to expand into the open air through a circular pipe 10 cm. diameter. The projectile model was mounted in the pipe or near the mouth of it on a torsion balance, by means of which the wind force could be measured.

At the time of the visit no determinations of the air velocity, temperature, and pressure on the jet had been made, but from the results placed before them, the members of the Mission were so convinced of the value of the method in the study of external ballistics, that Captain R. H. Fowler on his return to England drew up, at the request of Major A. V. Hill, a memorandum describing the French experiments and pointing out the desirability of the installation in England of a high-speed wind channel.

This memorandum was forwarded to the Ordnance Committee and was discussed at a special meeting of the Committee on February 18, 1919. Captain Fowler's suggestion was approved and a Ballistic Air Resistance Committee, under the chairmanship of Brigadier-General Hezlet, was appointed to draw up a programme of research.

The preliminary scheme of work approved by the Committee was as follows :

- (1) The design and construction of apparatus on the lines contemplated by the French investigators for the measurement of the force and couple coefficients of projectiles exposed to a momentary air blast of high intensity.
- (2) An investigation into the possibility of carrying out the experiments in a continuous air current on the scale, admittedly small, which could be attained by an air-compressing plant of moderate capacity.

FIG. 1. $P_0 = 46.0$ lb./sq. in.

FIG. 2. $-P_0 = 59$ lb./sq. in.

Distribution of stationary waves in air jet issuing from same orifice under different initial pressures.

For the purpose of the investigation under (1) it was realised that one of the main difficulties would be the construction of a quick-acting valve sufficiently rapid in its action to allow a high velocity of efflux. The design of this valve was undertaken by Mr. Dobrée, a member of the Committee, and its construction by the Cambridge Instrument Company. This valve had a parallel-sided outlet 3 inches by 3 inches, and a diverging rectangular channel of 5° total angle was fitted to it having a maximum section of 12 inches by 12 inches.

The method of measuring the speed of the current in this channel was that previously used by the author in his experiments on continuous flow air jets,* and consisted of the successive measurement at a fixed point of the pressures in a pitot tube and in a static pressure tube, and the calculation of the speed in terms of the velocity of sound at that point by means of the Rayleigh formula.

As this jet was of a momentary character it was, of course, necessary to obtain a record of the variation of the pressures with time, and this was done by Mr. R. W. Fenning, of the National Physical Laboratory, by means of a suitable modification of the recording pressure anemometer which he has devised for his researches on detonation.†

The results of the experiments showed that the quick-acting valve was satisfactory in its action, but in no case observed did the diverging channel run full, with the result that it was not possible to obtain a speed in the channel greater than that of sound. When the diverging cone was removed and a free blast was used, a momentary speed of $1.46a$ was observed at a distance of 20 inches in front of the mouth of the valve.

The characteristics of jets of this type have been studied by the writer in a previous investigation‡ which has shown the existence in them of a complicated system of stationary waves, due apparently to reflections from the edges of the orifice, whose distribution changes to a very marked extent with the initial pressures of the jet. Examples of such a jet showing the changes in the wave pattern due to changes in initial pressure are shown in figs. 1 and 2 (Plate 6) taken from the previous paper. In fig. 3 are also shown the simultaneously existing distributions of pressure and velocity along the axis of the jet.

It will be obvious that the value of the resultant force on a model of a projectile immersed in such a jet must depend on the position of its nose and base relatively to the wave crests, and that any coefficient expressing this value

* 'Proc. Roy. Soc.,' A, vol. 111, p. 306 (1926).

† 'Report of Aeronautical Research Committee,' vol. 2, p. 629 (1923-24).

‡ 'Proc. Roy. Soc.,' A, vol. 111, p. 306 (1926).

in terms of the mean speed and mean density of the jet may be entirely misleading.

For these reasons it was decided not to proceed with the complicated and

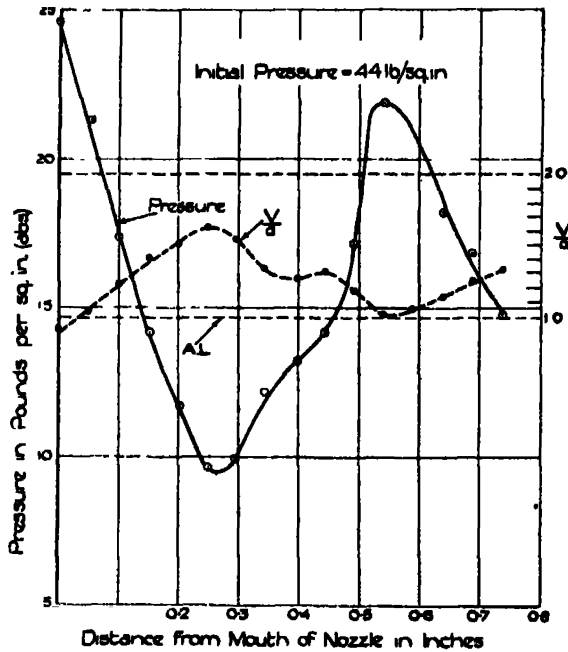


FIG. 3.—Pressure and velocity distribution along axis of air jet issuing into atmosphere. (from 'Proc. Roy. Soc.,' A, vol. 111 (1926)).

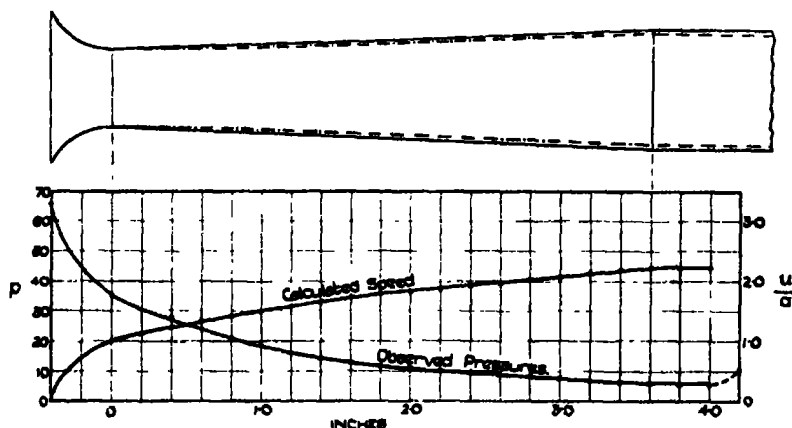
costly mechanism required for the recording of the forces exerted on a model in a momentary jet until the possibilities of the continuous jet had been fully explored.

For the purpose of investigation (2) a 50-h.p. compressor was obtained from Messrs. Peter Brotherhood, Ltd., and installed at the National Physical Laboratory. The capacity of this plant was 200 cubic feet of free air per minute at a working pressure of 120 lbs. per square inch. After a series of preliminary tests, it was found that by allowing the compressed air from the receiver to expand through a converging-diverging nozzle, terminating in a parallel part, to a pressure of about one-twelfth its original value, it was possible to maintain continuously in the parallel part, which was 0.8 inch diameter, an air current moving at above twice the speed of sound. As this speed was of the order required for ballistic experiments, a solution of the problem on these lines appeared hopeful provided that :—

- (1) The air current in the parallel or working part of the channel could be made sufficiently free from stationary waves and variations in speed and density, to enable reliable predictions to be made of the behaviour of projectiles moving in free air.
- (2) Apparatus of sufficient delicacy could be devised for the measurement of the forces on a small scale projectile model in such a channel.

A considerable amount of experimental work was carried out in order to obtain a nozzle which would satisfy the conditions laid down in (1) above, and an illustration of the degree of success attained is shown in fig. 4, in which is plotted the observed pressure distribution throughout the nozzle and the working part of the channel. It will be observed that the flow breaks down at a point not far removed from the end of the parallel channel, but that there is a region of approximately constant velocity and pressure in which a small model of a projectile could be placed for observational purposes. In the same figure is shown a comparison between the actual dimensions of the nozzle and the dimensions of the equivalent nozzle for adiabatic expansion to the observed final pressure with no reduction of velocity at the walls due to friction. The differences in diameter exhibited are what would be expected from the known effect of solid boundaries in reducing speed in their neighbourhood and the conclusion is drawn that the expansion of the air in the nozzle is sensibly adiabatic in character.

It was considered, therefore, that by care in design it would be possible to



Converging-diverging nozzle 0.515 inch to 0.800 inch diameter to give a speed above twice that of sound.

FIG. 4.—Observed pressure distribution (inches of mercury) and calculated speed.
 ———. ———. ———. Dimensions of equivalent nozzle having no wall effect in which adiabatic expansion would give the same pressure distribution.

set up a current of air in a closed channel which would be sufficiently free from the disturbances inherent in an open air jet, to satisfy the purpose of the investigation and that condition (1) could be satisfied. For the estimations of the air forces on the model projectile a simple balance of the type illustrated in fig. 5 was used.

It was found that by using a scale model projectile of diameter not exceeding

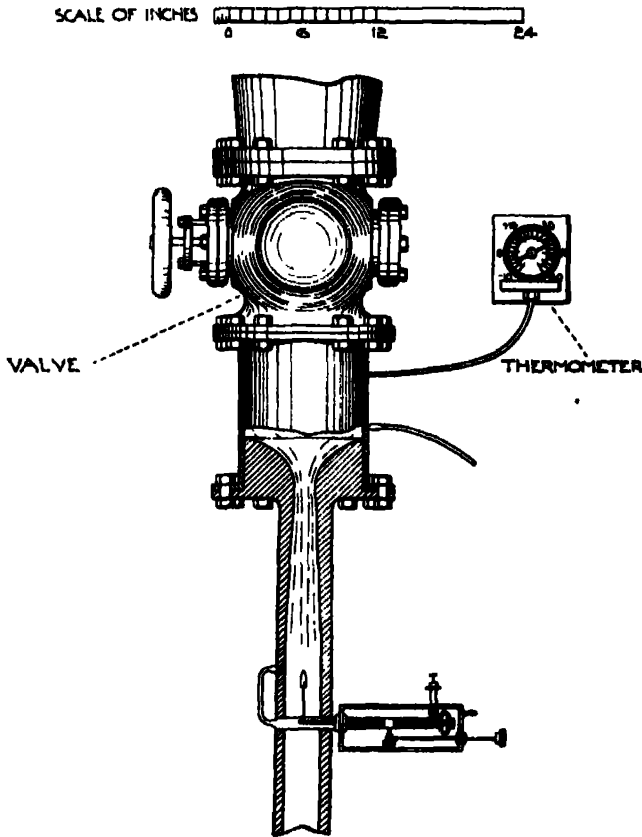


FIG. 5.

0.09 inch, the effect of the walls of the channel on the air flow round the model was small and that the force on the model at twice the speed of sound was of the order of 10 grammes, which could be measured with fair accuracy on the balance. It was concluded that the second condition could be satisfied, and a report was made to the Committee summarising the results of a series of head resistance tests on certain forms of model projectiles at speeds up to twice that of sound.

Shortly after the date of the report (1922), provision was made for equipping the Laboratory with a large air compressing plant which would deal with quantities up to 2800 cubic feet of free air per minute. By this means a considerable increase in the scale of the experiments was possible, and after some preliminary trials a new high-speed wind channel was developed having a diameter of 3.07 inches in which speeds up to $3\frac{1}{2}$ times the velocity of sound could be maintained continuously. This channel is illustrated in fig. 5.

For the purpose of securing a uniform distribution of speed in the approach to the nozzle, a copper box fitted with a honeycomb and guide-blade system is inserted between the stop valve and the nozzle. This box also contains the thermometer for obtaining the initial temperature of the air. The nozzle mouthpiece has a form determined by experience as giving a uniform speed across the throat of the nozzle. In the nozzle illustrated, which represents that by which a speed of $3\frac{1}{2}$ times the velocity of sound is obtained, the total angle of divergences is 6.2° . The distributions of pressure and velocity along and perpendicular to the channel when fitted with this nozzle are shown in fig. 6. It will be seen that in the radial direction outwardly a marked rise in the static pressure takes place at about half radius. This, however, was accompanied by a corresponding rise in the pitot pressure so that the resultant effect on the speed distribution is small.

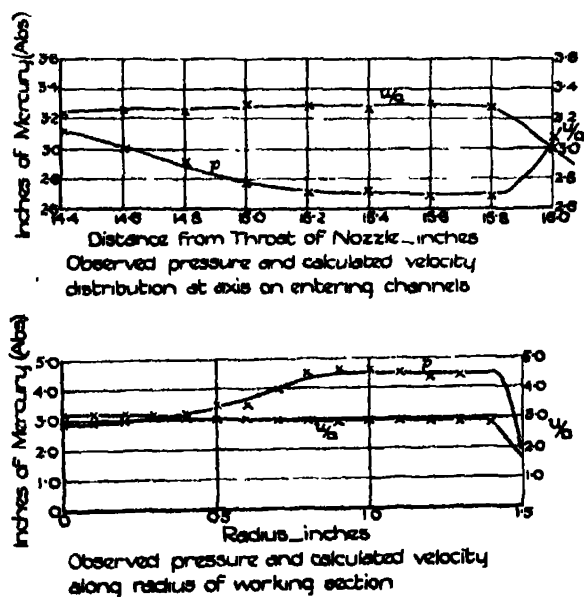


FIG. 6.

In the balance described above constructed for the 0·8-inch channel the outside of the bearings and pivots of the weigh beam were exposed to the air of the room. Owing to abnormally low values obtained for the head resistance of some models at high speeds, in which the static pressure inside the channel was of the order of one-fifth of an atmosphere, it was suspected that there was an appreciable leakage of air through the balance arm bearings into the vertical sleeve which might to an appreciable extent affect the base pressure of the model. For this reason the whole of the balance of the new channel was enclosed in an airtight box with plate-glass windows communicating with the interior of the channel, as shown in fig. 5.

On retesting the models, it was found that at speeds exceeding 1·5*a*, the head resistances were appreciably greater with the box in action than when it was removed and the suspicion of leakage was therefore confirmed. The box was consequently retained as part of the channel equipment.

Several series of investigations for the Ballistic Air Resistance Committee of the Ordnance Committee have been carried out in the 3-inch channel during the last 6 years. These have been chiefly concerned with the determination of the relative merit in reducing head resistance of different methods of stream lining and a typical series of results on a single model is shown in fig. 7. In this figure the ordinate is the value of k^* in the expression for the total head resistance

$$R = k\rho V^2 r^2 = k\rho \gamma \left(\frac{u}{a}\right)^2 r^2, \quad (1)$$

where p is the static pressure in the axis of the wind channel at the position of the model, γ is the ratio of the specific heats of the air, and u/a is calculated from the Rayleigh formula

$$\left(\frac{p_2}{p_0}\right)^{\frac{\gamma-1}{\gamma}} = \frac{(\gamma+1)^2}{4\gamma} \left(\frac{p_1}{p_0}\right)^{\frac{\gamma-1}{\gamma}} \left\{1 + \frac{\gamma-1}{\gamma+1} \frac{p_0}{p_1}\right\}$$

where

$$\frac{p_1}{p_0} = \frac{2\gamma}{\gamma+1} \frac{u^2}{a^2} - \frac{\gamma-1}{\gamma+1}$$

from measurements of the pitot pressure (p_2) and static pressure p_0 taken successively at the position of the model.

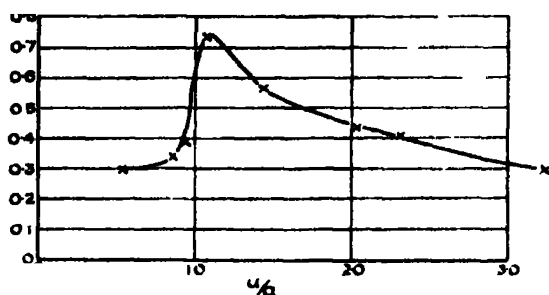
* In works on ballistics this non-dimensional coefficient is commonly written f_R .† In works on aerodynamics it is customary to write the value of the head resistance or 'drag' as $D = k_D \rho V^2 S$,‡ where S is the projected area of the model, so that on this convention

$$k_D = k/\pi.$$

† Fowler, Gallop, Lock and Richmond, 'Phil. Trans.,' A, vol. 221, p. 295 (1921).

‡ Bairstow's "Applied Aerodynamics," p. 119.

In the calculation of k from (1) the accuracy of the Rayleigh formula and the constancy of γ throughout the whole range of the experiments (300° C. to 100° C.



Load resistance Coefficient of Model Projectile

FIG. 7.

absolute) has been assumed. This assumption was verified up to $u/a = 2$ in the author's previous investigation from a comparison of the actual mass discharge from the channel determined by means of a meter, with the integrated value of the mass flow by a measurement of the radial distribution of pitot and static pressures and the assumption of adiabatic expansion of the jet from the initial pressure in the receiver.

An extension of this method up to a value of $u/a = 3.25$ for the purpose of the present paper showed an agreement between the observed and calculated mass discharge within an accuracy of 2 per cent., which is regarded as satisfactory evidence of the approximate accuracy of the assumption made.

In applying the results to the prediction of the ranges of, say, 3-inch projectiles, the difference in linear scale (16.5 to 1) is so great that the existence of a considerable difference in the values of the coefficient for model and full-scale projectiles would not be surprising.

On comparison with the results of firing trials, fairly satisfactory agreement between the values of the coefficients has been found, indicating that the scale effect is small.

It cannot, however, be claimed that the channel has yet reached a stage in its development at which the observations made in it can be regarded as reliable without careful checking in the form of a close examination of the conditions of flow in the region of the model for the following reasons:—

The normal conditions of working of the channel are that the air is drawn from the atmosphere and compressed into two large receivers 12 feet long by 5 feet in diameter, from which it passes through a stop valve to the wind channel

and is discharged into the atmosphere again through an open stand pipe. Due to the heating of the air in the compressor the temperature in the receivers over a run of 1 or 2 hours' duration rises by an amount of the order of 10°C . The initial viscosity of the air admitted to the channel is therefore a variable quantity.

It was noticed at an early stage of the work that the value of the head resistance coefficient k of the same model calculated by means of equation (1) from the results of observations made on different days under different atmospheric conditions varied to a greater degree in the case of the high-speed experiments ($u/a > 2$), than appeared to be consistent with common experience of the effect of the viscosity of the air on projectiles.

In order to investigate this effect the first course which suggested itself was to measure the head resistance of a model over the widest possible range of viscosity. For this purpose a gas-fired furnace was constructed consisting of a nest of pipes through which the air supply to the nozzle was passed. Owing to the large amount of heat required to produce a considerable rise of temperature the experiment was carried out in the 0.8-inch channel developed for the preliminary experiments at a speed of approximately twice that of sound. The range of initial temperature of the air obtained by this means was from 20°C . to 160°C ., equivalent to a change in the value of μ/ρ , at the model, of nearly 100 per cent. On measuring the head resistance of a model over this range, together with the values of the corresponding pitot and static pressures in the channel, small differences in the value of k were obtained, of approximately the same order as those obtained from the 3-inch wind channel tests for differences in viscosity of the order of 5 per cent.

It was clear, therefore, that the effect found in the latter tests could not be due to a purely viscous drag on the projectile model since an increase in viscosity of 20 times the amount observed in the tests had not produced any greater change in the drag. On further experimental study of the matter in the 3-inch channel an added complexity was found in that for some nozzles the head resistance coefficient of the model appeared to rise with increase of viscosity of the air supply and with other nozzles appeared to fall with increase of this viscosity. It appeared practically certain therefore that the effect must be due to the action of the model, or the channel walls, or both, in producing modifications in the flow round the model and in the distribution of pressure over its surface. To investigate this possibility comparisons were made, by means of pitot and static pressure measurements along the axis, of the effect of variations in initial viscosity on the pressure and velocity distribu-

tions in that part of the channel in which the model was exposed to the air stream. In fig. 8 are plotted the variations of static pressure in two sets of

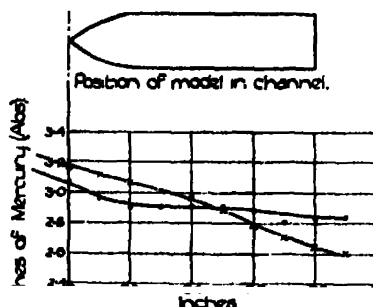


FIG. 8.—Initial pressure in receiver 136 inches Hg.

Initial temperature in receiver,

—x—x—x—x—x 22.0° C., $k = 0.30$; — · · · · · 33.5° C., $k = 0.27$.

observations both made at the same value of u/a ($= 3.25$), but one set with an initial temperature of the compressed air of 22° C. and the other at 34° C. These conditions corresponded with those under which a fall of head resistance from 26.0 to 23.5 grammes had been observed, and since the value of $p\gamma(u/a)^2 r^2$ was the same for each set, the experiments exhibited a similar fall in the value of the coefficient k .

It will be seen from the curves that the effect of a rise in temperature of 15° C. in the initial compressed air, is to change the slope of pressure in the region of the model so that the pressure at the nose of the model is less and that at the base is greater than at the lower temperature. Each of these effects causes a reduction in head resistance and this affords a satisfactory explanation of the differences of the observed forces on the model.

Further investigation showed that by a suitable modification of the initial pressure of admission to the nozzle, it was possible to obtain a much closer agreement between the pressure distributions in the working section of the channel for the same variations in initial temperature. These pressures are shown in fig. 9, and on testing a model under those conditions it was found that the variation of head resistance throughout the temperature range 22° to 35° was less than 5 per cent.

This extreme sensitiveness of the pressure and velocity distribution in the channel at very high speeds to small changes in initial conditions, remains, however, the outstanding difficulty in making accurate predictions of the drag

coefficients of projectiles from wind channel observations, and it has been suggested by the author to the Ballistic Air Resistance Committee that before further attempts at these predictions are made such conditions should be

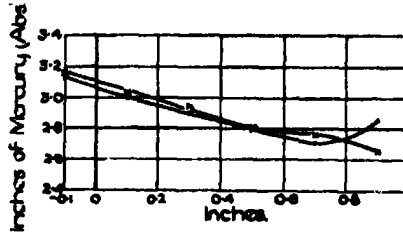


FIG. 9.—Initial pressure in receiver 143.5 inches Hg.

Initial temperature in receiver,

-- —x—x— 21.5° C., $k = 0.30$; — · — · — · — 32.5° C., $k = 0.29$.

brought under control. This suggestion has been approved by the Committee, and it is hoped to put the necessary work in hand at an early date.

In conclusion, the author wishes to express his thanks to Mr. A. Eaton, of the Artificer Staff of the Laboratory, for his valuable assistance in the construction of the apparatus and the carrying out of the experiments.

The Effect of Combined Electric and Magnetic Fields on the Helium Spectrum. —II.

By J. STUART FOSTER, Professor of Physics, McGill University, Montreal.

(Communicated by A. S. Eve, F.R.S.—Received January 19, 1931.)

[PLATES 7, 8.]

Introduction.

This report deals with effects in spectra when the source is subjected to external electric and magnetic fields simultaneously applied in either parallel or perpendicular directions. The helium spectrum has been chosen, owing to the relative ease with which it is usually possible (1) to excite the new combination lines, and (2) to trace the connections between the original lines and the components produced by the external electric and magnetic fields. In hydrogen, the second problem is extremely difficult. Moreover, the introduction of quantum mechanics has greatly reduced the advantage formerly held by the hydrogen atom in theoretical interpretations.

In a recent paper the writer* reported the observation of additive effects in the parhelium spectrum when parallel electric and magnetic fields were applied to the atoms. Additive effects were also found for certain orthohelium lines under an analysis which failed to reveal any of their fine structure. The present report consists of two parts. The first is an extension of the earlier paper, and deals with modifications of the additive law which are found when orthohelium fine structure is studied in the presence of parallel fields. Moreover, in pure Stark effect, the new plates show for the first time a complete analysis in which the two observed fine structure components of an orthohelium line contribute identical patterns. This pattern is exactly that observed for the corresponding line in parhelium, *i.e.*, there is no observed modification arising from electron spin. These facts are consistent with the view that the angular momenta due to orbital motion and to spin are separately resolved along the axis of the electric field, m_l , m_s , and that during transitions m_s remains unchanged, as in high magnetic fields. The addition of a parallel magnetic field greatly weakens or entirely suppresses all but one of the Stark components of the *weaker* member of the fine structure. This component corresponds to the longer wave-length member in the usual Zeeman splitting

* 'Proc. Roy. Soc.,' A, vol. 122, p. 599 (1929).

observed for all other σ components which persist in the two external fields. Thus reduced, the effect is very similar to that observed by Paschen and Back* in the case of other orthohelium lines in pure Zeeman effect. In contrast with this, the electric and magnetic effects are nearly additive for the *stronger* member of the fine structure, the only departure being a definite inequality in the intensities of the two Zeeman components of each σ Stark component. The applied magnetic field was from 14,000 to 15,000 gauss; the electric field, 0-70,000 volts per centimetre.

The second part of the paper is concerned with methods and observations in the study of effects due to crossed electric and magnetic fields. It contains descriptions of sources suitable for the study of the spectra emitted by atoms in external fields crossed at right angles. Employing these, it has been possible to make some preliminary observations on parhelium and orthohelium lines. Some of the effects are of a definitely new character.

The discharge is radial, the cathode lying along the axis of the cylindrical tube, and parallel to the magnetic field. Spectrograms are obtained with a large prism system or a new 30-foot concave grating in Wadsworth (stigmatic) mounting. The experimental conditions are such that in the observed diffuse and combination series, the effects due to the fields taken separately are of the same order of magnitude. With the application of crossed fields, it is found that each member of the above series splits into a structure asymmetric as regards both displacements and intensities. This is true in parhelium as well as in orthohelium. The magnitude of the splitting, and the fine structure (or energy distribution) are very similar for members of a given spectral series, but show wide variations between different series.

Orthohelium Lines in Pure Stark Effect.

A Lo Surdo source of simple type was employed. The cathode itself (fig. 1) is carefully fitted into a short piece of lavite pipe which in turn is sealed into a pyrex glass tube 10 mm. in diameter. The glass and lavite together insulate the magnet (used later) from the high potential terminals. A further advantage is found in the narrow slit which allows the light to pass out to the spectrograph, while the lavite wall offers the glass effective protection from cathode sputtering.

The tube was placed along the axis of the hollow poles of the magnet, the anode being inside one of the poles. It was filled with pure helium at 2 mm.

* 'Ann. Physik,' vol. 39, p. 897 (1912).

pressure, and excited by a 10,000 volt source of direct current, used to the limit of voltage.

Over a period of 2 weeks, 30 plates showing pure Stark effect or effects with parallel electric and magnetic fields were obtained with a total of 60 hours actual operation. The position of maximum field was initially at the cathode. It rose rapidly during the first hour, and thereafter very slowly, until it finally reached a point $\frac{1}{2}$ mm. above the original cathode surface. This was accompanied by the formation of a pit in the cathode, and a heavy metallic coating on the lavite wall which, however, remained insulated from the cathode.

The plates were taken in a glass spectrograph having a dispersion of 2.2 Å./mm. at λ 4026. In the electric field, this diffuse orthohelium line was accompanied by the combination lines $2p - 5p$, $2p - 5f$ and $2p - 5g$.

Owing to the limitations of the spectrograph, this group is the only one in which the (partial) fine structure of orthohelium is clear enough for our purpose. The central line (see Plate 7) $2p - 5f$ clearly exhibits a doublet character with a fine structure separation which remains nearly constant in electric fields up to 70,000 v./cm. In the other lines of this group, the small separation (1 cm.^{-1}) is lost through appreciable variations in the larger displacements of the Stark components. The observed fine structure separations show slight variations from that which represents the difference between the level $2p_0$ and the unresolved levels $2p_{12}$. This is not accounted for by the fine structure of the initial terms, which is much too small to appear in the spectrum.

The π and σ components of the Stark effect in Plate 7 are taken from different plates, since no single plate showed both groups of components in satisfactory focus. Since the displacements have been found to depend almost entirely upon the action of the electric field on the initial term, the observed components may be identified by reference to the initial values of k and m_k . In the lower (σ) image, from which most of the measurements have been taken, the external electric field is 65,800 v./cm.

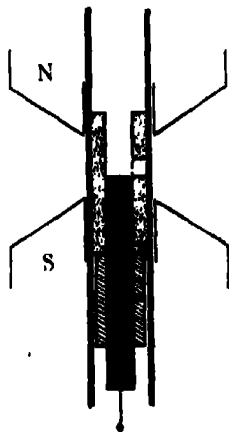


FIG. 1.

Table I.—Displacements from d line in cm^{-1} ; orthohelium group $2p - 5q$ in pure Stark effect.

$\begin{array}{c} m_k \\ k \end{array}$	0.	$\pm 1.$	$\pm 2.$
0	—	—	—
1	(135)	(135)	—
2	(43.0)	43.0	+41.1
3	-10.32	-8.5	-2.5
4	-62.75	-58.75	-46.4

The weaker member of the fine structure, $2p_0 - 5f$ gave the same pattern as $2p_{12} - 5f$. The fine structure separations from the stronger components were as follows at maximum electric field :—

$\begin{array}{c} m_k \\ k \end{array}$	0.	$\pm 1.$	$\pm 2.$
$\frac{\pi}{3}$	1.10 weak	1.00 0.91	— 1.04

Discussion of Stark Effect in Orthohelium.

The Stark effect in orthohelium offers some contrast with the well-known effect in parhelium, which may be described as "normal," since effects attributed to electron spin do not enter. The writer has shown in earlier papers that the observed orthohelium patterns of the Stark effect require a breaking down of the k, s coupling which gives the known j values. The observations just recorded may be explained on the following assumptions, which are valid in *high* magnetic fields : (1) the k and s vectors are separately resolved along the axis of the electric field, making $m = m_k + m_s$ ($\Delta m = 0, \pm 1$), and (2) m_s does not change during a transition. On this basis the patterns should be as observed.

It is noted that the fine structure separation in high electric fields is in some places the same as that found in the normal spectrum. This is probably due to the fact that the original vector model of the final state of the normal atom remains unchanged except for the case $m = m_s + m_k = 1$. The latter arrangement is directly connected with the few appreciable departures from the normal fine structure separation which are recorded in the above table.

Orthohelium Lines in Pure Zeeman Effect.

A few plates were taken showing $2p - 5d$ in a field of 14,000 gauss. The two σ components of $2p_{12} - 5d$ appeared with equal intensity, and separation 1.2 cm.^{-1} . At the side toward longer wave-lengths and not entirely separated from one of these, is the only observed Zeeman component of $2p_0 - 5d$. This is merely an extension to observations of a similar nature made at nearly the same field strength by Paschen and Back (*loc. cit.*) on the strong yellow line $2p - 3d$.

Orthohelium Group $2p - 5q$ in Parallel Electric and Magnetic Fields.

In parallel fields, the magnetic force has the effect of suppressing the π and σ Stark components of $2p_0 - 5f$ characterised by $m_s = 0, \pm 1$ in initial state. There remains only the σ component just mentioned in pure Zeeman effect, viz., that for which the initial m_s value is now known to be -2 (Plate 7). This component can be resolved from its stronger neighbour very readily in parallel fields, whereas in pure Zeeman effect it is much more difficult. The separation is evidently increased by the application of an electric field of 15,000 v./cm. or less; yet thereafter it remains constant over a wide range of higher fields (fig. 2, Plate 7; lower images). The mean value, taken from three plates, is 0.65 cm.^{-1} at 14,400 gauss.

There is also a new feature in the intensities. In low electric fields the two Zeeman components of the lines $2p - 5d$ (or $-5f$) are of equal intensity. At about 15,000 v./cm., however, it becomes clear that the Zeeman component of higher frequency is definitely more intense; and at the same point the component of $2p_0 - 5f$ makes its appearance. Presumably this marks the "high field" condition referred to in the preceding section dealing with pure Stark effect.

The normal Zeeman separation for $2S - 4P$ (3965) is most convenient for the determination of the strength of the magnetic field. Measurements show that at the position of E_{max} , H exceeds by a few hundred gauss its value at $E = 0$. E is found from the separation of the strongest σ components of the d and g lines.

The following displacements and intensities were observed at $E = 62,400$ v./cm. and $H = 14,400$ gauss.

Table III.--Displacements of σ Components from Normal d Line in cm.^{-1} .

Initial k .	
2	- 34.38 - - 38.0 group of components not fully resolved.
3	+ 1.1 (1); [1.86 (4); 3.07 (5)]; [7.16 (2); 9.54 (3)]; 10.94 (1)
4	[+ 43.58 (2); 44.75 (3)]; [54.97 (1); 56.62 (2)]; 60.07 (1)

The estimated intensities are in parenthesis; the square brackets include displacements for Zeeman components of a Stark component. The relative intensities of the central components of $2p$ -- $5f$ are better represented in fig. 2, Plate 7, traced by a Moll photometer.

Since the separation of the component of $2p_0$ -- $5f$ from its strong neighbour is so small, one may reasonably ask whether the remaining components of this line are really suppressed, or merely unresolved. Suppression is suggested by the observations in pure Zeeman effect. It is also supported by the observed differences in the intensities of the Zeeman components of $2p_{12}$ -- $5q$ in parallel fields. The photographs and the photometer curve show that if the component of $2p_0$ -- $5f$ joined its neighbour, the central Zeeman components of $2p_{12}$ -- $5f$ should appear with nearly the same intensity. The fact is, however, that each σ electrical component is split into two of quite different intensities by the magnetic field. This feature makes it appear almost certain that the analysis does not involve an unresolved component from the weaker member of the fine structure.

Electric field strengths have been calculated from the theory, using the observed separations of the strongest components of the d and g lines. When this is done it is found that $2p$ -- $5p$ is displaced too much for the theory, and the discrepancy is too great to be accounted for by a second order effect, or by the fine structure of the lines.

Helium Spectrum in Crossed Electric and Magnetic Fields.

The Lo Surdo source in its original form is extinguished or rendered useless for our present purpose by the action of a magnetic field applied in a direction perpendicular to that of the discharge. These difficulties may be removed by employing a radial discharge between a cylindrical anode and a cathode placed along the axis of the cylinder and parallel to the external magnetic field. The few necessary details of design become clear by a consideration of the problem in pure Stark effect.

The general form of Lo Surdo source just mentioned was first used by Depper-

man.* To secure high electric fields Depperman constricted the discharge at a cathode of small diameter. The tube was made long and was viewed in end-on position in order to secure good intensity of light. This arrangement had one disadvantage in the appearance of diffuse components. The source at constant field was so extended that the light could not be focussed at one point on the slit.

In the present design the discharge is constricted through the use of a short cylinder. The cathode may then be any diameter, and is chosen large enough to prevent overheating. High fields may be established in pure Stark effect, and the components are comparatively intense and well-defined. It is only in connection with crossed fields, however, that the source has marked advantages over other forms.

In fig. 3 it will be seen that the lavite insulation limits the discharge to a cylindrical section only 2 mm. long. The anode and cathode are made perhaps unnecessarily heavy in this first model.

The object was to avoid melting the electrodes under the heavy discharge which one might expect the experiment would require. In the discharge chamber, the lavite is everywhere separated from the electrodes by a small space which prevents or delays electrical contact with the exposed lavite surfaces after they have been made conducting by the discharge. While the magnetic field is somewhat weakened by the use

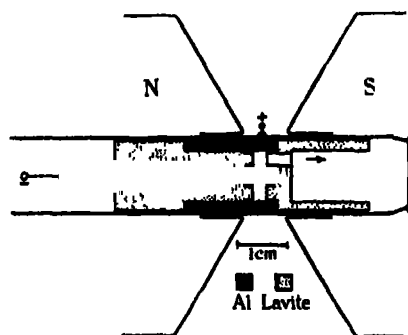


FIG. 3.

of hollow poles, an advantage appears in the automatic adjustment of the discharge chamber accurately perpendicular to the field. The light to be examined is taken out through a fine slit cut along the radius of the tube. Throughout this selected source, the magnetic field has been found nearly constant while the electric field varies from zero to a maximum at the cathode.

Behaviour of Source.

After a thorough roasting with a torch to drive gases out of the electrodes and lavite, the tube was filled with helium at a pressure of 1.5 mm. of mercury. A potential of several thousand volts was applied from a source described elsewhere. High fields were immediately established, as in the more usual

* 'Astrophys. J.,' vol. 63, p. 33 (1926).

forms of Lo Surdo tubes. Upon exciting the magnet, however, the voltage dropped to a value too low for observable Stark effects. From previous experience, I believe that this action is due in part to further small quantities of air driven from the neighbouring lavite walls by the modified discharge. After a run of 20 minutes to half-an-hour, the voltage rose to a moderate value.

All tubes, from the first, have passed through the stages just described. The voltage which could be applied in the final stage remained nearly constant for several hours. With different sources, it ranged from 1200 to 3000 volts. Thus helium tubes, which are relatively "hard" under ordinary conditions, are made very much "softer" through the action of a moderate magnetic field.

Light Intensity.

To develop a light intensity suitable for the examination of the Stark effect alone, a minimum current of 15 mil. amp. would be required. In crossed fields the strong lines were photographed in 20 minutes when the current was only 3 mil. amps. The much longer path taken by a charged particle in the presence of a magnetic field evidently leads to a large increase in the number of excited atoms per unit current.

The maximum magnetic field which could be applied to source (a), fig. 1. was 14,000 gauss. This field was large enough to allow some clear resolutions with the glass spectrograph working near the upper limit of its dispersion. In changing from the glass to the grating spectrograph, it was thought advisable to separate the anode and cathode a little more in order to avoid irregular electric field distributions. The larger holes in the magnetic poles then dropped the field to 10,000 gauss, and the dispersion of the grating instrument (3.9 A./mm.) proved too low for satisfactory analyses under the new conditions.

Further Modification of the Source.

Fig. 4 represents a modified source similar to (a) except that higher magnetic fields may be established with the solid poles. This form requires much smaller electrodes, and these are satisfactory, owing to the small necessary heating effects in all tubes of this type. The parts are placed in a pyrex glass tube which is afterwards drawn down to form flat ends. In this source, the lavite is especially useful, since it provides good insulation between the cathode and the pole of the magnet. A narrow slit in one pole allows the light to pass through to the spectrograph.

While sources of type (a), fig. 1, never failed to operate, the initial trials with type (b) were entirely unsatisfactory. The potential which could be applied did not exceed 500 volts. I think the difficulty lay in the adjustment of the axis of the cylinder accurately along the magnetic lines of force. This could not be done so easily as with type (a). Consequently the discharge attacked the lavite walls more severely. A decided improvement was made by covering the exposed lavite walls with a hard glaze such as is baked on dishes. The resulting smooth surface was much less affected by the discharge, and the source then proved as satisfactory as type (a) in its operation.

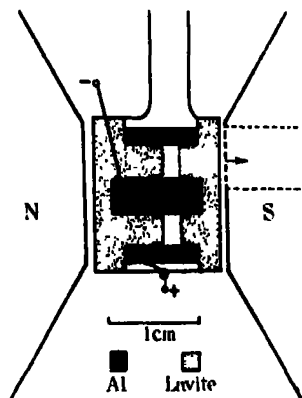


FIG. 4

Analysis of Effects.

The light from source (a) was analysed by the large prism spectrograph. For the present, the observations have been restricted to the group $2p - 5q$; since the electric fields were too low to bring out the full $2S - 4Q$ group, or to produce interesting effects in the principal series line which did appear.

Analyses covering a much greater spectral range can be secured on a single plate with a new stigmatic grating spectrograph. The 30-foot concave grating was recently ruled at Johns Hopkins University, and was secured through the kindness of Professor Wood, who called attention to the remarkable features which made it especially valuable in the Wadsworth mounting constructed at this laboratory. The grating produces an exceptionally weak central image. The first order spectrum on one side is amazingly bright. The second order, also, is much above average intensity. In the stigmatic mounting, this grating is comparable in speed to the glass instrument, if the first order is employed. The dispersion in this order is 3.91 Å./mm. at the setting used in the present work. A region of nearly 1000 Å. can be brought into satisfactory focus by slightly bending the photographic plate.

The ghosts may be described as very much stronger than those obtained with other gratings recently ruled by Professor Wood. This feature has given no trouble, since the main problem is to secure the weaker components themselves, and ghosts of the few strong lines are too far away to introduce any confusion in the analysis.

Temperature Control.

The electro-magnet is placed in a corridor surrounding the room in which the grating is mounted, and here the temperature variation is limited to 2° C. by automatic control of the general heating system of the building. Within the room, a grid of iron wire is stretched on all four walls, and is heated electrically under control of an air thermometer. The temperature variation in the room is reduced to a small fraction of 1° . This condition is maintained over long periods, since it is not necessary to enter the room to change or adjust the photographic plate. These changes may be made by reaching through a small doorway located immediately behind the plate holder.

Results.

From the above experimental arrangement, it will be seen that the electric vector is perpendicular to the magnetic field in all the light examined. A double image prism was introduced into the beam in front of the glass spectrograph. The resulting " π " and " σ " images (e.g., fig. 5, Plate 8) thus represent light with electric vector respectively parallel and perpendicular to the electric field. Polarisation effects are quite pronounced in the fundamental combination series. To avoid loss of light, the double image prism has been omitted in the analyses with the grating.

In low fields, the intensities of many components are sensitive to changes in the electric field. Additional general features and qualitative effects are given in the following paragraphs.

The members of the sharp series of parhelium failed to show any interesting variations due to the increasing electric field, i.e., the Zeeman effect is normal for $\lambda\lambda$ 5047, 4438 and in each case the intensities of the two Zeeman components are equal. An interesting modification occurs in the orthohelium line λ 4713. The original fine structure is filled in so as to form an apparently continuous spectrum of nearly constant intensity, and placed symmetrically with regard to the zero fields structure. The following member of the sharp series, λ 4121, is much weaker, and shows only the usual Zeeman effect.

In the principal series of parhelium the normal Zeeman effect of $\lambda\lambda$ 5015, 3965 persists in moderate electric fields. A slightly greater separation observed at maximum electric field for the line λ 3965 has been attributed to the greater magnetic field which exists at the axis of the poles according to experiments with pure Zeeman effect. Ghosts of the over-exposed orthohelium line λ 3888 showed on one plate a weak unresolved fine structure between the two strong Zeeman components.

Owing to the low electric fields, the combination lines $2P - 4P$, $2P - 5P$ appeared on only a few plates and with low intensity. The corresponding orthohelium lines were absent. The displacements due to the electric field must be very small: hence very little blurring could be produced by variations in the field strength. Nevertheless it has been impossible to resolve the Zeeman components of these lines. The separation therefore is probably less, and certainly not greater than normal.

With the diffuse series, much more interesting effects appear. The measured separations of the strong components are always more than normal; though the exact value (at a constant magnetic field) varies with the electric field and with the exposure. This feature originates in an asymmetric fine structure at least partially revealed on a few plates to be described in detail later. The relative intensities of unresolved components change with the electric field strength, giving on each plate a different energy distribution. This has its effect on the observed separation of the two diffuse Zeeman components.

The above separation is much more than that which appears in pure Stark effect, and is attributed to transitions in which Δm is more than unit. The appearance of new lines of this type in crossed fields was first predicted for the hydrogen atom by Professor Bohr.*

The effects just described are very similar in parhelium and orthohelium, and have been observed for the following lines:— $\lambda\lambda$ 4922, 4388, 4471, 4026.

All the above general features observed in the diffuse series are exaggerated in the fundamental combination series. The lines $2P - 4F$, $2P - 5F$, $2p - 4f$ and $2p - 5f$ all show a very wide separation of the outside strong Zeeman components. Many weaker components are clearly resolved. Most of them, though not all, lie between the strong components. The whole structure of each line is asymmetric both as regards the positions of the components and their intensities.

$2P - 4D$ and $2P - 4F$.†—An analysis of these lines in crossed fields is reproduced, with photometer curve, on Plate 8. The magnetic field, from the separation of the components of λ 5047, is 14,700 gauss. This is believed to be accurate, since the electric field does not disturb λ 5047 appreciably. There are much greater difficulties in the determination of the electric field. An estimate has been made in the following way. The separation of the centres

* "On the Quantum Theory of Line Spectra," Copenhagen (1918).

† In a private communication I have recently learned of an unpublished theoretical paper by K. F. von Weizsäcker, Leipzig, on the helium atom in crossed fields, which includes numerical results for these lines.

of the groups of components for $2P - 4D$ and $2P - 4F$ is 8.6 cm.^{-1} . From Lo Surdo photographs, it is known that the separation of the lines is 5.6 cm.^{-1} at zero field. It is now assumed that the additional separation of the centre 3.0 cm.^{-1} , is due to the electric field. Let us take this as the separation of the $4D$ and $4F$ levels characterised by $m = \pm 1$, the corresponding level of $4P$ being affected very little. This gives $4D$ a displacement of 1.5 cm.^{-1} ; hence the electric field is 8500 v./cm. approximately. This estimate may easily contain an error of 10 per cent.

Displacements of $2P - 4D$ and $2P - 4F$ from the normal D line, in cm.^{-1} , are as follows ($H = 14,700 \text{ gauss}$; $E = 8500 \text{ v./cm.}$ approximately)

$$2P - 4D \dots\dots - 3.36; - 1.1.$$

$$2P - 4F \dots\dots + 4.7; 5.4; 6.1; 6.7; 8.4.$$

$2p - 5d$ and $2p - 5f$.—In a magnetic field of $14,500 \text{ gauss}$ and an electric field less than 1000 v./cm. the displacements from the normal d line are:—

$$\text{"}\pi\text{" comp.} \dots (-0.98, +0.28); (2.77, 3.39, 4.28).$$

$$\text{"}\sigma\text{" comp.} \dots (-0.79, +0.30); (1.50, 2.70, 3.40, 4.20).$$

The components of d and f lines are indicated by the brackets. In addition to the above, an outer " π " component of $2p - 5f$ is found in moderate electric fields at 0.50 cm.^{-1} , and two further components at $10.85, 12.06$, which appear to be foreign to this group. It was thought that the latter might come from the lavite. Arcs with lavite cores failed to show any trace of the line. The σ components corresponding to the above have displacements $0.52, 10.88, 12.00$.

The diffuse components with relatively large displacements indicate that the source was slightly unstable, and produced higher fields during a part of the exposure. From these large displacements the electric field was estimated to be $15,000 \text{ v./cm.}$ in an earlier note.* Doubtless such fields existed, but I believe the main analysis is to be attributed to the joint action of the magnetic field with an electric field of less than 1000 v./cm.

Polarisations in this group are shown on Plate 7. It may be noted that when the " π " and " σ " components are combined, as in the figures at the top of the plate, the "red" group of components of each line is spread out more and is stronger than the "violet" group. But when the two polarisations are separated, this is not generally true of them individually.

The photometer curves for $2p - 4d$ and $2p - 4f$ were taken from the plate

* 'Nature,' vol. 123, p. 414 (1929).

used to illustrate effects in the corresponding parhelium lines. The photograph, however, is from a quite different plate, and represents a much lower electric field. The point illustrated is the great change in the energy distribution in $2p - 4f$ by the change in electric field.

As already mentioned, Professor Bohr first pointed out some new features which might be expected to appear in crossed fields. He also called attention to a photograph of H_β by Paschen and Back in which components of unusually large displacement appeared. These he attributed to the action of a small electric field perpendicular to the applied magnetic field, and developed by the discharge. These components have re-appeared in the present research. In the same investigation, Paschen and Back found a "satellite" of $\text{He } \lambda 4388$ which behaved like $2P - 5F$ on Plate 7 (bottom). Thus there remains not the slightest doubt that the earlier investigation did involve a small electric field. In this connection it is interesting to recall that Urey* has published a theoretical paper in which he gives reasons for expecting a wide magnetic splitting of fundamental lines of helium and lithium under the above conditions.

The work of Paschen and Back has not been extended during the many intervening years, while a need for experimental facts was created from the theoretical side. It is believed that the present method offers a solution to the problem.†

The writer expresses his best thanks to the National Research Council of Canada for grants in aid of this research. His thanks are extended to Dr. Laura Chalk and Mrs. R. Stewart for able assistance.

Summary.

Complete Stark patterns identical with the corresponding normal parhelium patterns (same $nk \rightarrow n'k'$) are observed for each of the two resolved fine structure components of the orthohelium line $2p_{0, 12} - 5f$.

The above observation suggests the view that $m = m_k + m_s$ and $\Delta m_s = 0$ as in high magnetic fields.

The σ Stark components of $2p_{12} - 5q$, all of which persist in parallel electric

* 'Z. Physik,' vol. 29, p. 86 (1924).

† The following additional papers deal with the older quantum theory of the hydrogen atom in crossed fields: Epstein, 'Phys. Rev.,' vol. 22, p. 202 (1923); Halpern, 'Z. Physik,' vol. 18, p. 287 (1923); Klein, 'Z. Physik,' vol. 22, p. 109 (1924). More recently, the same subject has been treated by Pauli, 'Z. Physik,' vol. 36, p. 336 (1926), and Sen, 'Z. Physik,' vol. 56, p. 673 (1929), on the basis of quantum mechanics.

and magnetic fields, are split into two Zeeman components of unequal intensity. In parhelium, these components have equal intensities.

The addition of a parallel magnetic field of 14,000 gauss suppresses the Stark components of the weak fine structure component, $2p_0 - 5f$, with the exception of the one (initial $m_k = -2$) characteristic of pure Zeeman effect.

Sources are developed in which the electric and magnetic fields are crossed at right angles, and separately produce effects of the same order of magnitude.

Effects of crossed fields in the different series of parhelium and orthohelium are observed. In the sharp and principal series there is little variation from the usual Zeeman effect. The magnetic splitting is possibly less than normal in the $2P - nP$ series, since the components remain unresolved. In the diffuse series the splitting is more than normal and the complex components are of unequal intensity. The fundamental lines $2p - nf$ and $2P - nF$ show even greater splitting and more complex structures. Quantitative details of the fine structure are given for $2P - 4F$ and $2p - 5f$. Polarisation effects and changes in relative intensities with increasing electric field are described.

Stark-Effect in Molecular Hydrogen in the Range 4100-4770 Å.

By J. K. L. MACDONALD, Emmanuel College, Cambridge, 1851
Exhibitioner.

(Communicated by A. S. Eve, F.R.S.—Received January 27, 1931.)

[PLATE 9.]

A report on the Stark effect in a violet region of the H_2 spectrum was given by the writer in an earlier communication.* The present paper deals with the effect within the range 4100-4770 Å., and treats certain of the results from a theoretical standpoint.

An adequate summary of the work already done in this field has been published in the paper referred to. The apparatus employed (fig. 1) and the procedure followed in the present experiments are essentially the same as were described in the earlier publication.

A Lo Surdo tube of the type designed by Foster† was used. In this tube

* 'Proc. Roy. Soc.' A, vol. 123, p. 103 (1929).

† 'Phys. Rev.' vol. 23, p. 667 (1924).

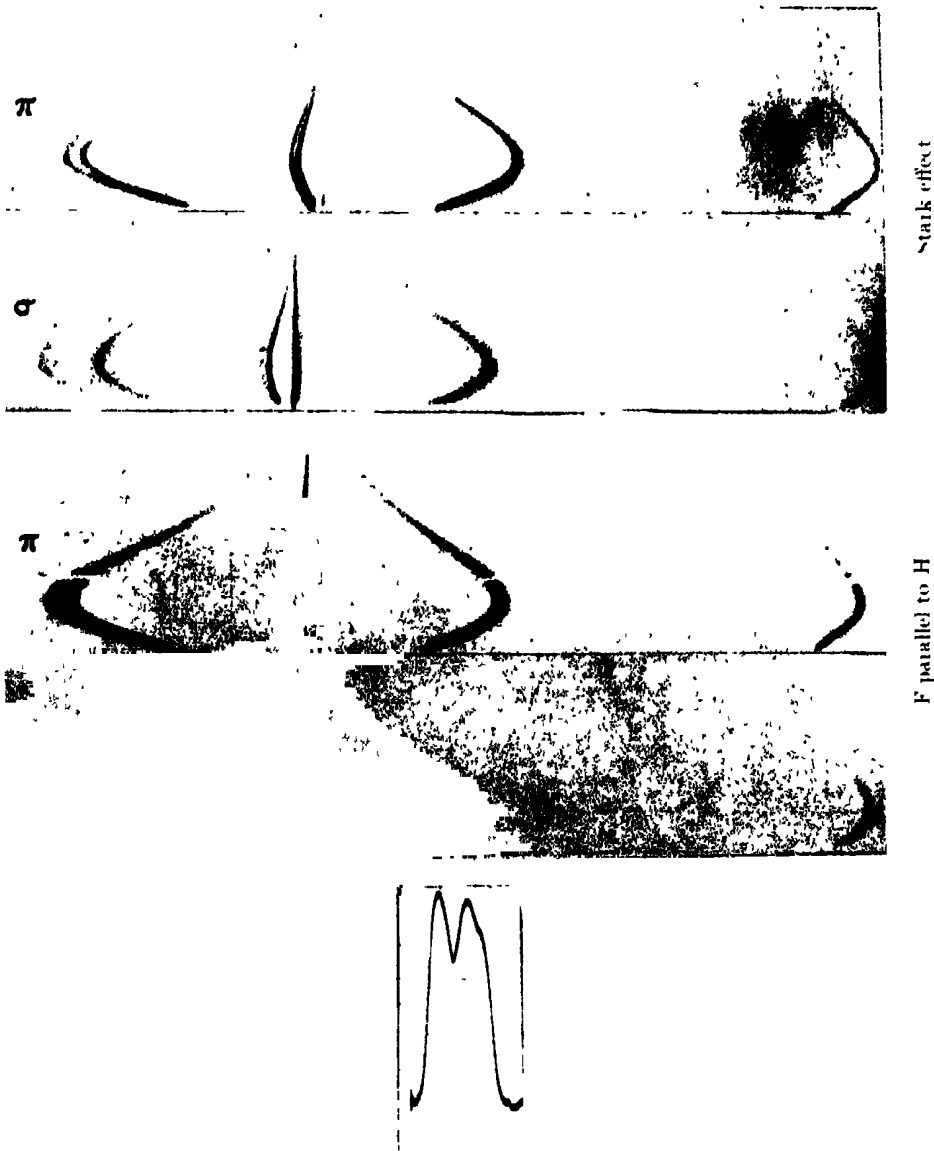


FIG. 2

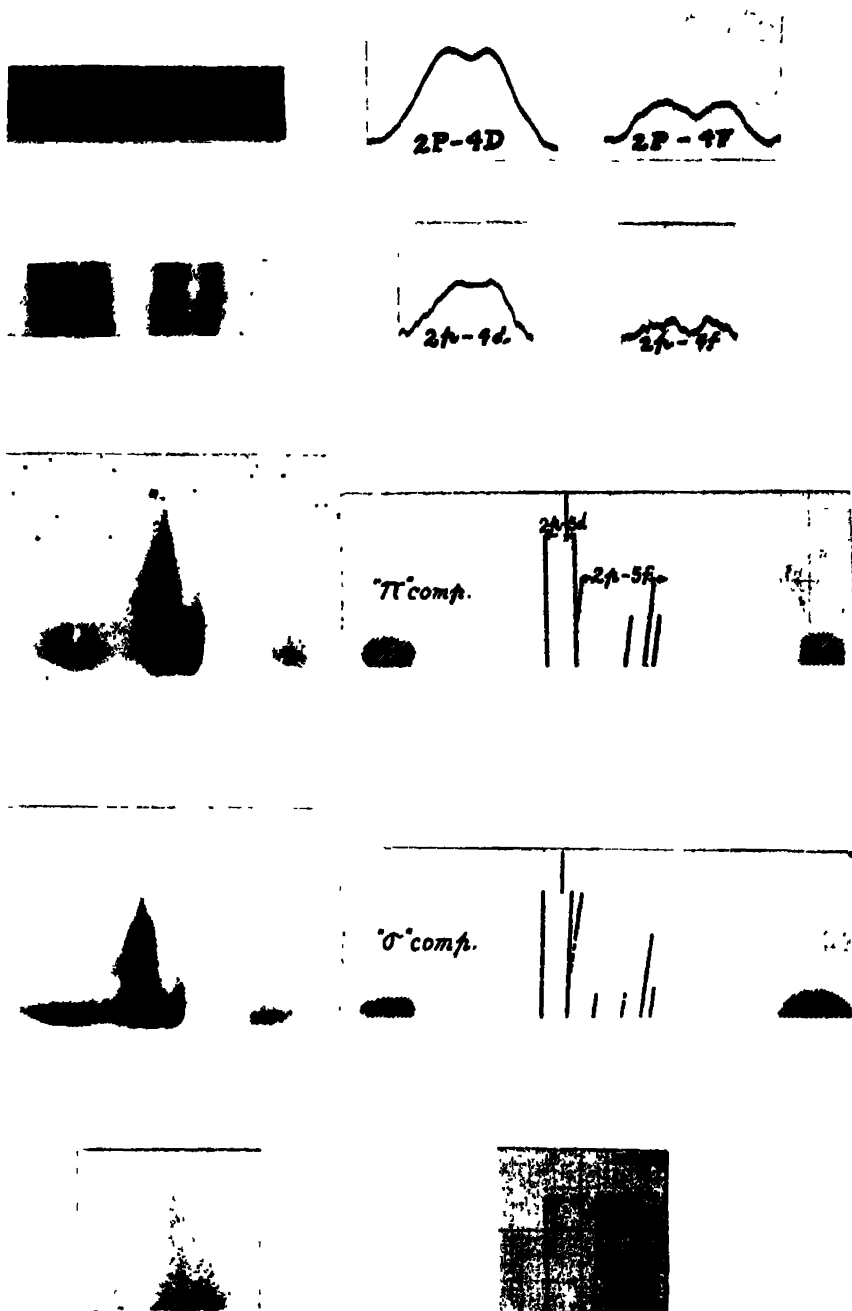


FIG. 5

(T, fig. 1) the discharge takes place between (A), a large anode surface (about 6 cm.²) and (C), a small cathode surface. The cathode is immediately below a hole 1 mm. in diameter drilled parallel to the axis of a cylinder of lavite (L). The lavite is sealed in the pyrex tube. Strong electric fields are developed by the accumulation of positive ions near the cathode. The light from this region, after passing through a slit (S) in the lavite, goes through a lens (L_1) and a double-image prism (D). It is then focussed as a pair of images on the slit of the spectrograph. One of the images is polarised parallel, the other perpendicular to the field.

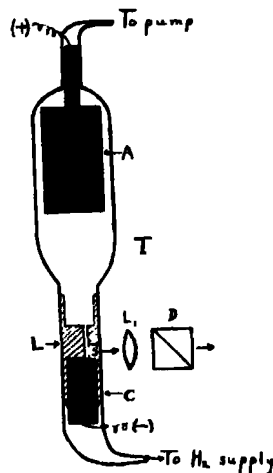


FIG. 1.

In the earlier work great difficulty was experienced in maintaining a steady discharge in purified hydrogen. The remedy for this trouble was found to be a continuous stream of gas through the tube from an inlet below the cathode. The motion of the gas up the discharge channel in some way favoured the production of steady fields. In the attempt to obtain details of the line structures, field strength was sacrificed to steadiness and light intensity.

With the glass spectrograph previously described (*loc. cit.*) 20 spectrograms were obtained. Eight of the plates were satisfactory over a large range and the remaining 12 were useful in verifying data on certain lines. The time of exposure of these plates varied between 20 minutes and 20 hours. Determinations of wave-lengths and displacements were obtained by means of a travelling microscope, kindly loaned by the Cavendish Laboratory. The results were checked on a large graph based on 24 standard lines of an iron comparison spectrum.

Results.

The data obtained from a study of the plates have been arranged in Table I. In the columns headed (λ) and (ν) are indicated the wave-lengths and the wave-numbers of the lines respectively. In cases where nearby lines are not resolved or where the position at zero field strength is ambiguous, two wave-lengths are bracketed. The wave-numbers are those given by Gale, Monk and Lee* except when otherwise indicated. In columns (II) and (I) are shown

* 'Astrophys. J.,' vol. 67, p. 89 (1928).

Table I.

λ	$II d^*$	$I d^*$	ν	Classification
4763.844	- 6.5 III	- 6.5 III	20985.60	$^4(N-2S) P_2$
59.851	-	+ 2.0 ±	21003.21	$^4(N-2S) P_2$
56.948	- 2.5 ±	- 2.5 ±	016.02	$^4(N-2S) P_2$
40.965	-	- 6.5	086.78	$^4(N-2S) P_2$
4613.116	-	-	671.27	$^4(O-2S) P_2$
4572.710	-	- 8.0	862.76	$^4(3B-2S) Q_2$
62.232	- 14.5 III	- 7.5 III	913.02	$^4P_1 Q_2$
57.393	- 12.0 I	- F	931.77	-
54.158	-	-	951.80	$^4P_1 Q_1$
39.163	-	- 5.5 III	22024.83	-
34.627	- 1.5	- 1.5	046.37	$^4(3B-2S) Q_2$
33.055	-	+ 20.5 II	064.01	-
29.079	- 9 ±	(small)	073.37	-
24.139	- 5.5 IV	- 5.5 IV	097.47	$^4(3A-2S) P_2$
15.562	- 7.0 III	- 7.0 III	139.45	$^4P_1 R_2$
15.182	- 5.5 D	- 5.5 D	141.31	$^4(3A-2S) P_2$
11.690	- 14.0 III	- 13.5 III	158.45	$^4(N-2S) P_2$
4498.523	-	-	223.30	$^4P_0 Q_2$
98.108	- 6.0 III	- 6.0	225.34	$^4(3B-2S) Q_2$
97.877	- 6.0 III	- 6.0 III	226.50	-
93.688	- 9.1 I	- 5.5 I	227.98	$^4(3N-2S) P_2$
90.852	- 24.0 III	- 24.0 III	247.21	$^4(K-2S) P_2$ or $^4P_0 Q_2$
90.451	- 4.5 D	- 4.5 D	261.26	$^4(N-2S) P_2$
87.813	- 6.5	- 6.5	262.25	$^4P_0 Q_1$
86.084	- 2.0 D	- 2.0 D	276.33	$^4(M-2S) P_2$
85.832	- 10.0	- 10.0	284.92	-
82.510	- 32.0 I	- 14.0 II	286.17	-
77.823	-	- 3.5	287.77	-
74.261	- 8.75 III	- 8.75 F	326.03	$^4P_0 R_1$
71.608	- 8.75 II	- 8.75 II	329.79	$^4(3A-2S) P_2$
71.516	-	+ 9.5 ±	343.81	-
67.145	-	+ 9.5 I	357.05	$^4(K-2S) R_1$
66.928	-	+ 12.5 F	357.53	$^4P_0 R_1$
			379.40	$^4(O-2S) P_2$
			380.49	-

* Probably a separate line.

(Table I)---(continued).

λ	$H\delta^*$	$L\delta^*$	ν	Classification.
{4400-830}	- 3.75	- 3.75	{22716.63}	$^4(10-2\ 1S)_2P_2$
{00.745}	- 4.25 \pm	- 4.25 \pm	717.07	$^3(3\ 8S-2\ 8S)_2R_1$
4392.093	- 4.5	- 4.5	761.81	—
91.726	—	—	763.71	—
90.900	—	- 8.5	768.00	—
{89.084}	- 8.5	- 6.0	{777.41}	$^1(1N-2\ 1S)_2P_2$
{88.888}	- 16.0	- 8.5	778.43	—
79.955	- 4.0	- 16.0	824.89	—
75.544	- 4.5	- 4.5	847.90	$^1(1N-2\ 1S)_2P_2$
70.766	- 9.25	- 9.25	872.87	—
67.726	- 3.5	- 3.5	888.79	—
61.915	- 14.5	- 14.5	919.29	—
54.540	hidden in $H\gamma$	- 2.5	958.10	$^4(1L-2\ 1S)_2P_1$
4386.637	- 1.75	- 1.75	23272.91	$^4(1K-2\ 1S)_2R_1$
90.114	- 1.0	- 1.0	302.87	$^4(1E-2\ 1S)_2R_2$
87.613	- 2.75	- 2.75	316.46	$^4(1E-2\ 1S)_2R_2$
80.740	- 1.5	- 1.5	353.90	$^4(1E-2\ 1S)_2R_2$
79.416	- 10.0	- 10.0	361.12	$^4(1C-2\ 1S)_2R_1$
55.221	- 4.5	- 4.5	493.95	$^4(1B-2\ 1S)_2P_2$
53.289	- 3.0	- 3.0	504.61	$^4(1N-2\ 1S)_2P_2$
50.20*	—	—	521.71	$^4(1N-2\ 1S)_2P_2$
46.691	—	—	541.14	$^4(1N-2\ 1S)_2P_2$
33.818	—	—	612.71	$^4(1N-2\ 1S)_2P_2$
30.0†	—	—	634.0	$^4(1N-2\ 1S)_2P_2$
24.508	—	—	664.78	$^4(1N-2\ 1S)_2P_2$
22.518	—	—	675.90	$^4(1N-2\ 1S)_2P_2$
19.495	—	—	692.84	$^4(1N-2\ 1S)_2P_2$
{05.098}	—	—	{773.97}	$^4(1N-2\ 1S)_2P_2$
{05.279}	—	—	772.96	$^4(1N-2\ 1S)_2P_2$
{4189-462}	- 10	- 10 \pm	863.34	$^4(1N-2\ 1S)_2P_2$
89.350	—	—	916.10	$^4(1N-2\ 1S)_2P_2$
80.111	—	—	24035.74	$^4(1N-2\ 1S)_2P_2$
59.202	- 5.5	- 5.5	055.98	$^4(1N-2\ 1S)_2P_2$
55.804	—	—	182.88	$^4(1N-2\ 1S)_2P_2$
33.995	—	—	328.22	$^4(1N-2\ 1S)_2P_2$
09.297	—	—	346.40	$^4(1N-2\ 1S)_2P_2$
06.231	—	—	—	—

* Deodhar, 'Proc Roy. Soc.,' A, vol. 113, p. 369.

† Tanaka, 'Proc. Roy. Soc.,' A, vol. 113, p. 429.

displacements in cm.^{-1} of the components of the lines at a field strength of 72 kv./cm. By Roman numerals are roughly indicated the relative intensities of certain components as visually estimated. The letter "D" signifies "disturbed by other lines," "F" means "fuzzy," and a question mark indicates doubt as to the existence of faint components. In the last column the lines are classified according to Richardson's scheme.* A symbol such as ${}_0(3^1A - 2^1S)_1R_1$ expresses the fact that the line is formed by (i) an electron jump between levels 3^1A and 2^1S and (ii) a vibration jump 0 to 1 together with (iii) a rotational jump from 2 to 1 (an R-branch line). Accuracy of measurement is necessarily dependent to a great degree upon the character of the lines. In the majority of cases the error for the displacements should be less than 5 per cent. and in the worst instances should be no more than 10 per cent. Plate 9 is a reproduction of enlargements of the spectrograms. Selected lines are marked.

These observations again make clear the irregular character of the effect, which has already been noted as its distinguishing feature. The patterns depend markedly upon vibration as well as rotation and electron configuration. For example, Table I shows how different are the effects on the lines ${}_0(1O - 2^1S)_0P_3$, ${}_1(1O - 2^1S)_1P_3$, ${}_0(1O - 2^1S)_0P_5$ and ${}_1(1K - 2^1S)_1P_3$ of which the quantum numbers are almost identical.

This irregularity is to be expected from theoretical considerations. It may be shown that the perturbation is a second order effect. The values obtained by accurate measurement of displacements fit closely into a quadratic law. The expression for the effect is as follows :—

$$\Delta E_{N'} = - (Fe)^2 \sum_{N'' \neq N'} \left| \int Z \psi_{N'} \bar{\psi}_{N''} dV \right|^2 / (E_{N''} - E_{N'}).$$

where $(\Delta E_{N'})$ is the energy perturbation of the level $(E_{N'})$ with eigen function $(\psi_{N'})$ and totality of quantum numbers (N') . (F) is the field strength, (e) the electronic charge. Z is the F-directed component of the difference of the electron vectors and the proton vectors as measured from the centre of gravity of the molecule. The integration extends over the entire configuration space and the sum over all sets of quantum numbers (N'') not identically equal to N' .

Any variation in the vibrational, rotational or electronic quantum numbers will affect the value of both the numerators and the denominators of the

* 'Proc. Roy. Soc.,' A, vol. 127, p. 493 (1930).

expression inside the Σ . In cases where a particular set N' is such that $E_{N'} \doteq E_{N''}$ for a certain set N'' , any change in N' may alter this condition considerably. Thus a decrease in the contribution from N'' may result.

The necessity of first determining suitable ψ_N functions makes the quantitative calculations extremely complicated and lengthy. They will be communicated in a later publication.

Certain regularities appear upon examination of Table I. Consider for instance the group associated with the electron jump ($^1N - 2^1S$), viz. :—

		\parallel	\perp
(0, 3) P_3	— 6.5, 0	— 6.5, 0
(0, 3) R_1	0	— 6.5
(0, 2) P_3	— 6.0, 0	— 6.0, 0
(0, 1) P_3	— 4.5, 0	— 4.5, 0

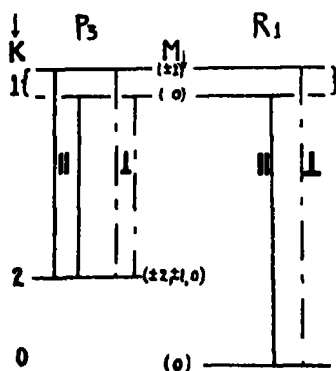
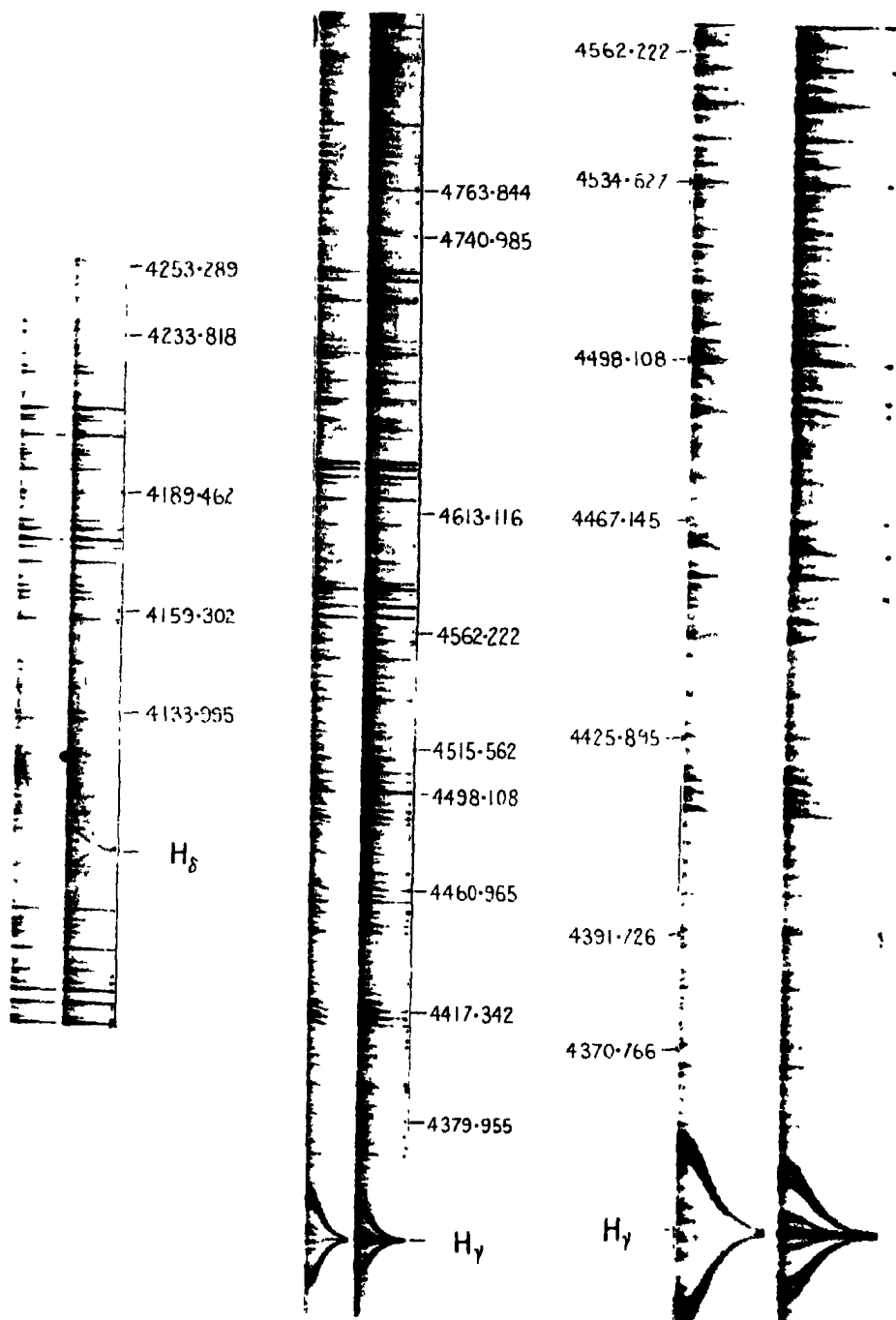


FIG. 2.— $\parallel \Delta M = 0$; $\perp \Delta M = \pm 1$.

These four lines have the same initial level. As the effects are similar, the perturbations in the final levels must be small. Theory supports this conception since, in the final levels, the function $|\psi_N|$ is mainly concentrated near the nuclei where the contributions to the integrals are small (due to a small value of Z). Theory also accounts for the number and polarisations of the components. Fig. 2 illustrates the subdivision of the initial and final rotational levels which give P_3 and R_1 lines. (K) is a theoretical rotation quantum number equal to $(m - 1)$ where (m) is Richardson's equivalent number. (M) is a "magnetic quantum number" associated with the "longitude" of the nuclear axis about the direction of the field. $|M| \leq K$. For \parallel components $\Delta M = 0$ and for $\perp \Delta M = \pm 1$.

Theoretical investigation shows that the sublevels $(\pm M)$ are perturbed in



identical ways. Assuming that the initial levels $M = \pm 1$ are displaced while $M = 0$ is not, an adherence to the rules just stated will produce the observed patterns in the manner indicated in the figure. \parallel transitions are denoted by full lines, \perp transitions by dotted lines. For both \parallel and \perp polarisations the P_3 lines show one undisplaced and one displaced component. For R_1 lines there is only one component in each polarisation the \parallel undisplaced and the \perp displaced.

There are identical initial levels and identical effects in the lines $1(3^1A-2^1S)$ OP_3 and $1(3^1A-2^1S)_0R_3$. The explanation is quite similar to that given above.

Allowing for perturbations in both initial and final M levels, in general, for singlet states, the numbers of possible different components of a line are given by the following :—

$$\begin{array}{ll} \text{for } P_m \dots \dots m \overset{\parallel}{-} 1 & 2m \overset{\perp}{-} 3 \text{ components} \\ \text{for } R_m \dots \dots m & 2m \overset{\perp}{-} 1 \text{ components.} \end{array}$$

In actual cases, two or more components may be nearly coincident, and some may have zero intensity.

All experimental observations made in this investigation conform to the limitations of the above scheme.

A few of the lines described in this paper have probably already been observed by Kiuti.* Comparison of results is made difficult due to the fact that Kiuti uses the tables of Merton and Barratt† for wave-length checking. These tables are considered less reliable than those used in the present paper. Wherever simple patterns are reported by the latter, the results seem to be in agreement with the present work ; but complicated systems, resolved by the author into separate lines, are reported by Kiuti as components of a single line. This difference in treatment is most clearly illustrated in the group of lines near 4498 Å.

The experimental work reported in this paper was performed in the Department of Physics, McGill University, under the direction of Dr. J. S. Foster. The writer takes pleasure in acknowledging his indebtedness to Dr. Foster for encouragement and suggestions. An expression of appreciation is extended to the Canadian National Research Council for the financial aid given in the earlier stages of this investigation. The generosity of the Royal Commission

* 'Jap. J. Phys.,' vol. 4, p. 1 (1925).

† 'Proc. Roy. Soc.,' A, vol. 108, p. 603 (1925).

for the Exhibition of 1851 and of the Governors of Emmanuel College in enabling the writer to complete the work at Cambridge University, is also acknowledged. Thanks are due to Mr. R. H. Fowler for encouragement and suggestions in the theoretical work.

Summary.

The Stark effect in the spectrum of molecular hydrogen in the range 4100–4700 Å. is investigated. Certain complex structures reported by Kiuti are resolved into independent lines. Displacements of line components are measured and the observations are discussed from a theoretical point of view.

Certain groups of P and R lines with common initial levels are found to be adequately described as regards number and polarisation of components by a theory which is briefly discussed.

*Investigations on the Spectrum of Selenium. Part I. --Se IV
and Se V.*

By K. R. RAO, D.Sc., Madras Government Research Scholar, and J. S. BADAMI,
B.Sc., Bombay University Research Scholar, Imperial College of Science,
London.

(Communicated by A. Fowler, F.R.S.—Received January 24, 1931.)

[PLATES 10, 11.]

In continuation of the previous work on germanium and arsenic by one of the writers (K. R. R.), an extensive investigation of the spectrum of selenium has been undertaken in order to analyse the spectra of the atom at successive stages of ionisation and determine the energy levels characteristic of each. In the present part an account is given of the general experimental methods adopted in these investigations and the results* obtained for the spectra of Se IV and Se V. The other spectra of the element, a consideration of which is in progress, will form the subject of succeeding parts.

Of the earlier measurements of the spark spectrum of selenium, those by Messerschmidt† are extensive and range from λ 5898 to λ 2340. McLennan

* A preliminary report of these has been published in 'Nature,' vol. 126, p. 508 (1930).

† Kayser, 'Handbuch,' vol. 6.

and Young* have recorded 12 lines in the spark and 5 lines in the arc between λ 2200 and λ 1850. McLennan, Young and Ireton† have also measured the vacuum arc spectrum in the region λ 2296 to λ 1492. However, in the Schumann region extending to λ 1230, the measurements by Lacroute‡ are more complete. Bloch and Bloch§ have investigated, on two occasions, the spectrum of an electrodeless discharge through selenium vapour by varying the length of the auxiliary gap in series with the discharge and have assigned all the lines of selenium between λ 6783 and λ 2196 to the different stages Se I, Se II, Se III and Se IV.

While experimental studies and measurements of the lines of selenium have been made by various investigators, attempts at analysis appear to have been few. In the arc spectrum of the element, Runge and Paschen|| discovered in 1898 sharp and diffuse series systems of what then were considered to be triplets. Later, McLennan, McLay and McLeod¶ brought these into consonance with predictions from Hund's theory. The published reports on the analysis of the spark spectra of selenium are discussed separately for each stage in the body of the paper.

As the existing measurements do not extend into the ultra-violet below λ 1230 they are not complete enough for any attempt to identify the series in the spark spectra of selenium. Measurements have therefore been made of the spectrum over the wide region extending from λ 7000 to λ 400 in which range most of the prominent groups of Se II, Se III, Se IV, etc., are expected to occur.

For the excitation of the complete arc spectrum of selenium recourse must be had to special methods such as the introduction of a foreign gas like argon, as adopted by Runge and Paschen. But for the production of spectra corresponding to higher excitation, it has been found that the familiar methods are quite suitable. In the present work the lines have been observed mainly with suitably strong discharges through selenium vapour in vacuum tubes of the simple form shown in fig. 1, and have been assigned to the various stages by the method of comparing the intensities of the lines under the action of different discharges. The tube could be replenished with the metal conveniently

* 'Phil. Mag.,' vol. 36, p. 459 (1918).

† 'Proc. Roy. Soc.,' A, vol. 98, p. 103 (1920).

‡ 'J. Physique,' vol. 9, p. 180 (1928).

§ 'C. R.,' vol. 185, p. 761 (1927), vol. 187, p. 562 (1928), and 'Ann. Physique,' vol. 13, p. 233 (1930).

|| 'Astrophys. J.,' vol. 8, p. 70 (1898).

¶ 'Phil. Mag.,' vol. 4, p. 486 (1927).

whenever desired ; on heating the bulb selenium marked its appearance in the tube by a beautiful green discharge.

The spectra obtained with this source have been sharp enough for accurate measurement. Capillary tubes of two different bores, 1 mm. and 0.5 mm., have been used. As a further aid to the classification of lines the methods of varying the self-induction in the secondary circuit and the length of the auxiliary spark gap have been employed.

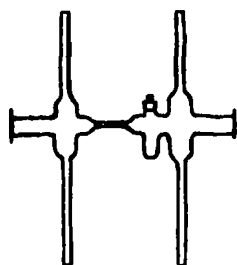


FIG 1.

As selenium is non-conducting the spark in air has been examined by placing it on carbon electrodes, but the lines emitted are extremely diffuse, sometimes extending over 2 to 3 Å, and this source has served only to make a qualitative study of the spectrum. It may

be remarked that lines up to Se III have been observed in this source. In the region λ 2200 to λ 1600 the selenium-in-carbon arc in an atmosphere of nitrogen has also been photographed, in the manner described by Selwyn.* Some of the arc lines of selenium which appeared in discharge tubes could thus be distinguished.

Different instruments have been used for photographing the spectra, depending upon the spectral region to be examined. Those used for purposes of measurement, however, are the first order of a 10-foot concave grating of dispersion about 5.6 Å. per millimetre in the region λ 6600, to λ 2900, and a Hilger quartz Littrow spectrograph between λ 3200 to λ 2200. Below this region down to λ 700, spectra have been taken with a meter vacuum grating spectrograph of dispersion about 18 Å. per millimetre. When using this instrument without a fluorite window considerable difficulty has been met with, owing to the discharges leaking into the spectrograph and fogging the plates ; a small earthed plate having at its centre a hole of about 1 to 2 mm. diameter, mounted between the discharge tube and the slit of the spectrograph was found effective in diminishing this fogging. But fairly good plates, extending to λ 650, have been obtained only when, after prolonged working of the tube, the selenium spectrum could be excited with little heating of the bulb and a high degree of vacuum in the tube. However, owing to the large number of close lines present in the spectrum, particularly in the region below λ 1000, and the smallness of the dispersion available, much progress could not be made in the analysis of the spectra. It must further be observed

* 'Proc. Phys. Soc.,' vol. 41, p. 392 (1929).

that on plates taken with strong discharges, lines belonging even to Se V and Se VI could be traced, so that as a method of excitation of spectra it is believed that this simple discharge tube affords a wider range of ionisation, *i.e.*, Se I to Se VI, of the atom, than the vacuum spark usually employed in the region of short wave-lengths.

The main results presented in this paper have been suggested from photographs of the vacuum spark spectrum of selenium in the region λ 1400 to λ 400 taken by K. R. Rao in the Physical Laboratory at Upsala. The spectrograph employed was designed by Professor Siegbahn and is similar in construction to those described by Edlén and Ericsson* and by Ekefors.† The grating of radius 1.5 metres and of about 30,000 lines per inch is mounted at nearly tangential incidence, the glancing angle being about 7° . The instrument gave lines of excellent definition, and was used by Arvidsson‡ previously with extremely narrow slits for the study of the hyperfine structure of some lines of ionised thallium and bismuth in this region. The dispersion obtained is about 3.4 Å. per millimetre at λ 1400, increasing uniformly to about 2.4 Å. per millimetre at λ 400. Several close lines have been split up under this large dispersion and have helped in working out the present scheme. In determining wave-lengths the usual grating formula

$$m\lambda = e (\sin \phi - \sin \phi')$$

has been used where ϕ and ϕ' are the angles of incidence and diffraction. From fig. 2 the formula may be rewritten thus

$$m\lambda = e \sin \phi - e \sin \left(\phi - \frac{x}{R} \right)$$

where R is the radius of curvature of the grating and x is the distance of a line of wave-length λ from the directly reflected image S' of the slit S .

From a preliminary plate containing the known standard lines of O, N and C, the constants in the above equation are determined by a method of approximations, by measuring the values of x , corresponding to known standards. A table is then constructed which gives the wave-lengths, corresponding to various values of x . By interpolation from this table, the wave-lengths can be evaluated easily. The values thus determined are finally corrected from a correction curve drawn separately for each plate. The method is the one usually practised at Upsala and described in detail by Edlén and Ericsson

* 'Z. Physik,' vol. 59, p. 656 (1930).

† 'Phys. Z.,' vol. 31, p. 737 (1930).

‡ 'Nature,' vol. 126, p. 565 (1930).

(*loc. cit.*). It is expected that a general accuracy of about 0.02 \AA. is attained in this work.

The spark was produced by a 50 kv. transformer rectified by a Kenotron

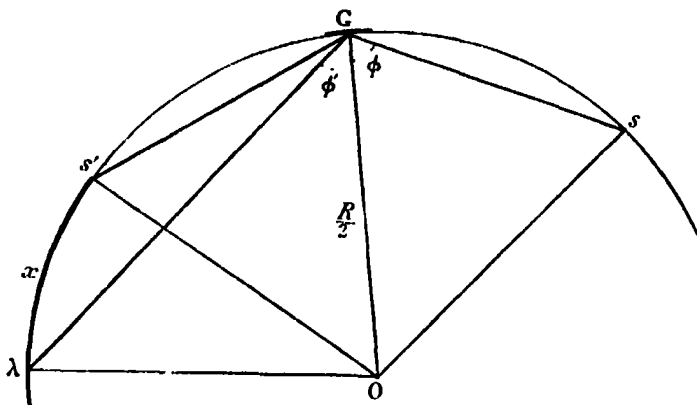


FIG. 2.

valve, condensed by a capacity of about 0.27 mf. About 5 to 20 sparks took place per minute depending on the vacuum obtained in the chamber. The upper electrode was of aluminium; for the lower one, any of three different electrodes could be shifted into position while the vacuum was on; one of these consisted of selenium melted into a small hole at the tip of an aluminium rod while the others were a carbon rod and another aluminium rod containing lithium nitrate at the tip. These latter served to give the necessary standard lines of C, N and O on the plate. The spark was violent enough to excite lines up to Se VI.

The method of employing inductance in series with ordinary sparks in air or hydrogen in order to assign lines in the glass and quartz regions to the various stages of ionisation of the atom, has now been widely used. Fowler* has suggested its usefulness with sparks *in vacuo*; Gibbs, Vieweg and Gartleint† have made a special use of it in clearing up some incorrect classifications made in the spectra of ionised antimony and tin and refer to the method as furnishing generally useful experimental evidence for the classification of lines in this region. Recourse to this method has been taken with successful results in the identification of the spectra of selenium. A coil, 60 cm. in length, 73 cm. in diameter, and consisting of 31 turns of copper wire 0.4 mm. thick, has been inserted, in these experiments, in series with the vacuum spark. Insertion of

* 'Phil. Trans.,' A, vol. 225, p. 1 (1925).

† 'Phys. Rev.,' vol. 34, p. 406 (1929).

self-inductance in the circuit reduces the frequency of oscillation and hence the instantaneous value of the current, so that a relative suppression of the lines of the higher stages is effected. But on account of the diminution in the intensity of such sparks exposures of about 1 to 1½ hours have been necessitated. Plates 10, 11 show the spectra of selenium with and without series inductance in the region λ 1400 to λ 400. Sawyer and Humphreys* have identified the essential groups of Se V and Se VI, mainly by the application of the relativity doublet laws to the respective iso-electronic spectra. The above plates afford clear evidence of the correctness of the identifications. The groups of Se V† and Se VI are either faint or entirely absent in the inductance spectrum, while others, which must be due to Se III and Se II, are relatively much more intense. It was possible by a careful scrutiny of the plates to sort out, with confidence, most of the lines belonging to the various spectra of the element. It may be noted that in working with selenium and some other elements, on occasions when the vacuum was poor and a tension of only about 10 to 20 kv. was obtained, the lines of the lower stages were much in evidence on the plates while those of higher stages were absent.

Analysis of Se IV.

The spectrum of Se IV, being similar to those of Ga I, Ge II, As III, consists essentially of a simple doublet system. The important electron configurations and resultant terms expected in this spectrum are listed in Table I.

Table I.—Term Scheme of Se IV.

3_1 3_2 3_3	4_1 4_2 4_3 4_4	5_1 5_2 5_3 5_4 5_5	6_1 6_2 6_3	Term prefix.	Terms.
2 6 10	2 1			1p	² P
2 6 10	2	1		5s	² S
2 6 10	2 1			4d	² D
2 6 10	2	1		5p	² P
2 6 10	2 1			4f	² F
2 6 10	2		1	5g	² G
2 6 10	1 2			4p ²	⁴ P ² P ² D ² S

The notation used is that proposed by Russell, Shenstone and Turner,‡ the symbol ° which distinguishes the odd terms being omitted as this is considered

* 'Phys. Rev.', vol. 32, p. 583 (1928).

† One line λ 839.43 appears strongly (*cf.* Plate 10) in the inductance spectrum when the other lines, associated with this to form the ²P ²P combination, are considerably suppressed. Possibly it is a blend with another low stage line.

‡ 'Phys. Rev.', vol. 33, p. 900 (1929).

necessary only when the configuration corresponding to any observed term is either not given or unknown. As all terms found in this work are doublets, the numeral denoting the multiplicity is also omitted, in succeeding tables in this section, for convenience in printing.

P. Pattabhiramiah and A. S. Rao* have published an analysis of Se IV in which the difference 4378 cm.^{-1} of $4pP_{\frac{1}{2}} - 4pP_{\frac{3}{2}}$ is arrived at correctly but only three of the pairs suggested appear to be real, the classification of one of them agreeing with the present scheme.

Examination of the plates in the region $\lambda 600$ at once revealed the pairs $4pP - 5sS$ and $4pP - 4dD$ belonging definitely to Se IV. A search for further pairs, with the difference 4378 , among the lines of Se IV has resulted in the detection of the groups arising from the transition $4s^2 4p \rightarrow 4s 4p^2$ in the appropriate region. The secondary series pairs, observed in the quartz region, have given further support to this identification. There is but one isolated pair, $\lambda\lambda 1314, 1307$, on plates taken with violent sparks, which can be assigned the classification $4dD - 4fF$. The situation is similar to that which existed in finding the corresponding member in As III.† The faint component $4dD_{2\frac{1}{2}} - 4fF_{2\frac{1}{2}}$ is unobserved but the detection of $4fF - 5gG$ with the proper separation, -29.8 cm.^{-1} , in keeping with the corresponding interval of -9 cm.^{-1} in As III, and of $4p^2D - 4fF$ in the calculated position has confirmed the assignment.

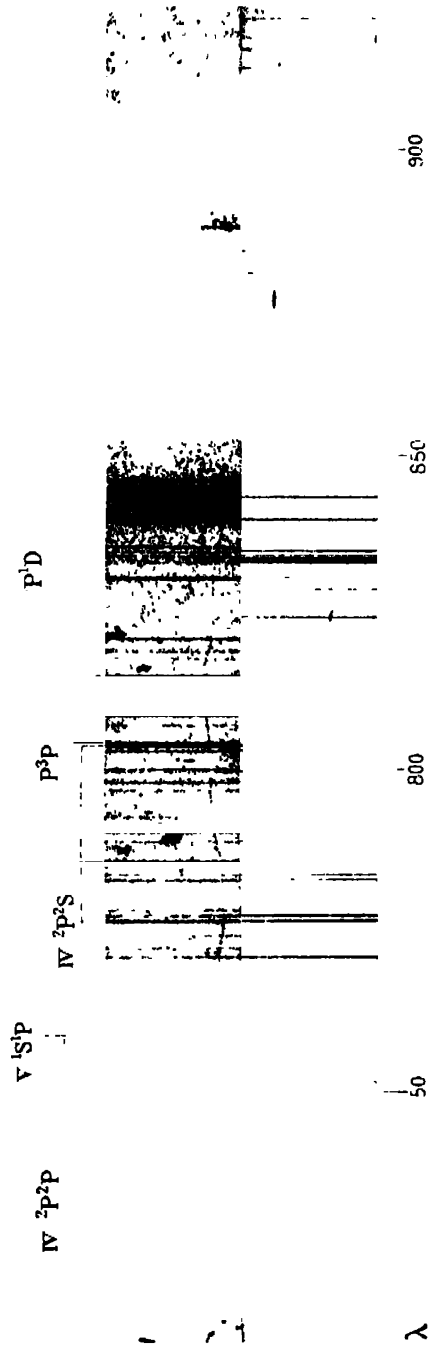
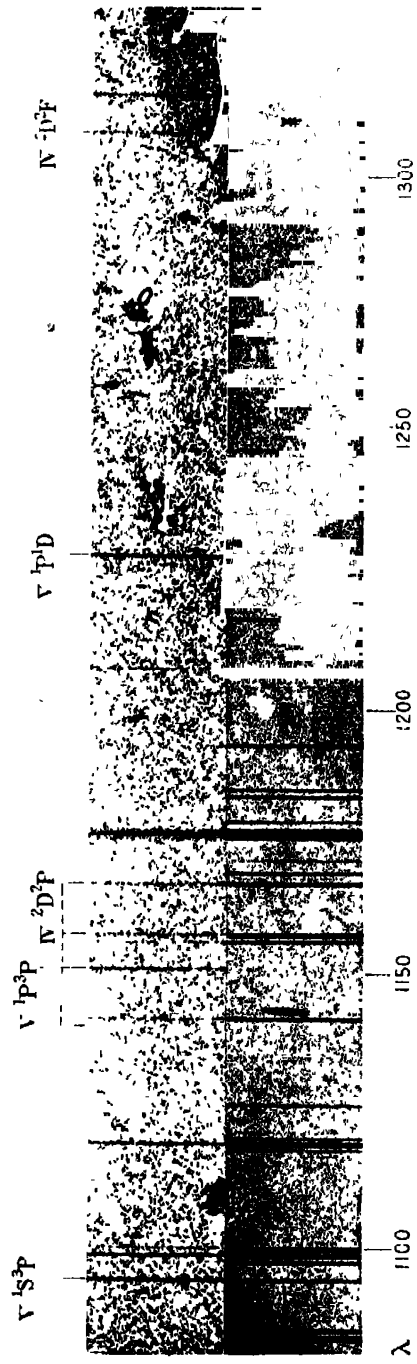
Table II gives the results of the analysis of the spectrum obtained in the course of this work. The wave-lengths above $\lambda 2000$ are in air and the others in vacuum; the intensities are on a scale of 10 for maximum.

Of the terms $^4P, ^2P, ^2D, ^2S$ of the configuration $4s 4p^2$, the term 4P has not been located in any of these Ga I-like spectra. The suggested pair $4pP - 4p^2S$ seems to be the only one available from an examination of the plates; the term $4p^2S$ is of the proper order of magnitude as inferred from the sequence Ga I to Se IV, but the pair $4p^2S - 5pP$, involving a double electron transition, has been located in As III‡ but not in Se IV.

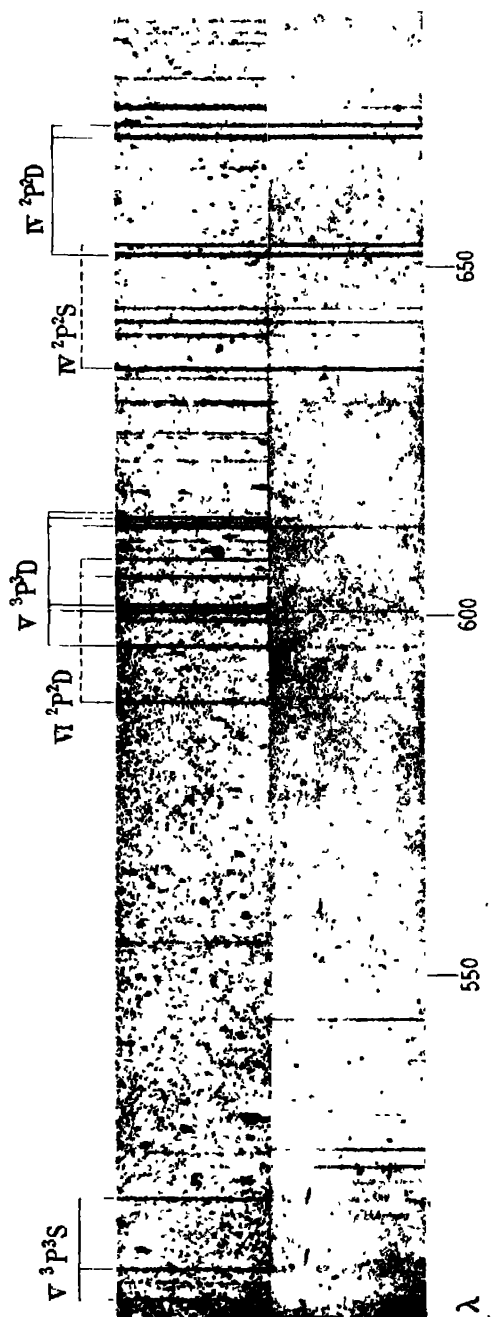
* 'Ind. J. Phys.,' vol. 3, p. 531 (1929).

† K. R. Rao, 'Proc. Phys. Soc.,' vol. 43, p. 68 (1931).

‡ Lang, 'Phys. Rev.,' vol. 32, p. 737 (1928); K. R. Rao, *loc. cit.*



Without inductance. With series inductance. Without inductance. With series inductance.
Spark Spectrum of Selenium taken with a Siegbahn Vacuum Spectrograph



Without inductance. With series inductance.

Spark Spectrum of Selenium taken with a Siegbahn Vacuum Spectrograph.

Table II.—Classified Lines in Sc IV.

Classification.	λ (int.).	ν (vac.).	$\Delta\nu$.
$5s\ S_{\frac{1}{2}} - 5p\ P_{\frac{1}{2}}$	3059.85 (5)	32871.9	1198.3
$S_{\frac{1}{2}} - P_{\frac{1}{2}}$	2951.59 (6)	33870.2	
$4d\ D_{\frac{1}{2}} - 5p\ P_{\frac{1}{2}}$	2724.33 (8)	36095.4	1198.8
$D_{\frac{1}{2}} - P_{\frac{1}{2}}$	2665.50 (9)	37505.3	
$D_{\frac{1}{2}} - P_{\frac{1}{2}}$	2638.14 (3)	37894.2	
$4f\ F_{\frac{7}{2}} - 5g\ G$	2166.64 (6)	46139.9	—29.8
$F_{\frac{7}{2}} - G$	2165.24 (6)	46169.7	
$5p\ P_{\frac{1}{2}} - 5d\ D_{\frac{1}{2}}$	2143.60 (3)	46635.7	151.7
$P_{\frac{1}{2}} - D_{\frac{1}{2}}$	2136.65 (8)	46787.4	
$P_{\frac{1}{2}} - D_{\frac{1}{2}}$	2089.98 (7)	47832.1	
$5p\ P_{\frac{1}{2}} - 6s\ S_{\frac{1}{2}}$	2014.08 (5)	49634.3	1197.6
$P_{\frac{1}{2}} - S_{\frac{1}{2}}$	1967.27 (4)	50831.9	
$4d\ D_{\frac{1}{2}} - 4f\ F_{\frac{5}{2}}$	1314.43 (8)	76079	—30
$D_{\frac{1}{2}} - F_{\frac{5}{2}}$	[1313.01]	[76109]	
$D_{\frac{1}{2}} - F_{\frac{5}{2}}$	1307.24 (7)	76497	
$4p^2\ D_{\frac{1}{2}} - 5p\ P_{\frac{1}{2}}$	1166.84 (4)	85702	1198
$D_{\frac{1}{2}} - P_{\frac{1}{2}}$	1157.35 (5)	86404	
$D_{\frac{1}{2}} - P_{\frac{1}{2}}$	1150.75 (1)	86900	
$5p\ P_{\frac{1}{2}} - 7s\ S_{\frac{1}{2}}$	1030.57 (2) ?	97034	1200
$P_{\frac{1}{2}} - S_{\frac{1}{2}}$	1017.98 (2) ?	98234	
$4p\ P_{\frac{1}{2}} - 4p^2\ D_{\frac{1}{2}}$	1001.63 (4)	99837	496
$P_{\frac{1}{2}} - D_{\frac{1}{2}}$	996.68 (10)	100333	
$P_{\frac{1}{2}} - D_{\frac{1}{2}}$	959.57 (9)	104213	
$4p^2\ D_{\frac{1}{2}} - 4f\ F_{\frac{5}{2}}$	800.13 (5)	124980	—30
$D_{\frac{1}{2}} - F_{\frac{5}{2}}$	[799.94]	[125010]	
$D_{\frac{1}{2}} - F_{\frac{5}{2}}$	796.79 (4)	125504	

Table II—(continued).

Classification.	λ (int.).	ν (vac.).	$\Delta\nu$.
$4p\ P_{1\frac{1}{2}} - 4p^2\ S_{\frac{1}{2}}$	803.79 (8)	124411	4379
$P_{\frac{1}{2}} - S_{\frac{1}{2}}$	776.46 (8)	128790	
$4p\ P_{1\frac{1}{2}} - 4p^2\ P_{\frac{1}{2}}$	758.97 (8)	131758	2220
$P_{1\frac{1}{2}} - P_{1\frac{1}{2}}$	746.39 (10)	133978	
$P_{\frac{1}{2}} - P_{\frac{1}{2}}$	734.58 (8)	136132	4374
$P_{\frac{1}{2}} - P_{1\frac{1}{2}}$	722.79 (7)	138353	2221
			4375
$4p\ P_{1\frac{1}{2}} - 4d\ D_{1\frac{1}{2}}$	671.86 (8)	148841	390
$P_{1\frac{1}{2}} - D_{2\frac{1}{2}}$	670.10 (10)	149231	
$P_{\frac{1}{2}} - D_{1\frac{1}{2}}$	652.66 (9)	153219	4378
$4p\ P_{1\frac{1}{2}} - 5s\ S_{\frac{1}{2}}$	654.16 (8)	152868	4377
$P_{\frac{1}{2}} - S_{\frac{1}{2}}$	635.95 (8)	157245	

The term values of Se IV which have been found are given in Table III. These depend upon a choice of 70240 cm.^{-1} for the term $5g\ ^2G$, which is assumed to be very nearly hydrogenic. There are two members of each of the secondary sharp and diffuse series available for the evaluation of the absolute terms, but it is believed that better values can be obtained by the assumption of the

Table III.—Term Values.

Term.	Term value.	Term.	Term value.
$4p\ P_{\frac{1}{2}}$	346094	$6s\ S_{\frac{1}{2}}$	105349
$P_{1\frac{1}{2}}$	341718	$5g\ G$	[70240]
$4d\ D_{1\frac{1}{2}}$	192877	$7s\ S_{\frac{1}{2}}$	57948 ?
$D_{2\frac{1}{2}}$	192488	$4s\ 4p^2\ D_{1\frac{1}{2}}$	241883
$5s\ S_{\frac{1}{2}}$	188853	$D_{2\frac{1}{2}}$	241338
$5p\ P_{\frac{1}{2}}$	156181	$S_{\frac{1}{2}}$	217307
$P_{1\frac{1}{2}}$	154983	$P_{\frac{1}{2}}$	209900
$4f\ F_{3\frac{1}{2}}$	116410	$P_{1\frac{1}{2}}$	207740
$F_{2\frac{1}{2}}$	116390		
$5d\ D_{1\frac{1}{2}}$	108347		
$D_{2\frac{1}{2}}$	108195		

5gG term as is done here. The limits obtained by a simple Rydberg formula, (with 16R constant) applied to the two above-mentioned series, are 159187 and 156946 respectively, which agree well with the directly determined value 156181. The comparison of the term values of the iso-electronic spectral sequence Ga I to Se IV is shown in Table IV, which is an extension of a similar one given previously by one of the writers ; the terms of Se IV in this table are divided as usual by 16. The bracketed values are assumed.

Table IV.—Comparison of Term Values.

	4p P ₁ .	5p P ₁ .	5s S ₁ .	6s S ₁ .	4d D ₁₁ .	5d D ₁₁ .
Ga I*	48380	[15326]	23592	10795	13598	7577
Ge II†	32159	12408	16559	8464	11950	7138
As III‡	25378	10772	13524	7280	12306	6976
Se IV	21637	9761	11803	6584	12055	6772

	4f F ₂₁ .	4s 4p ² P ₁ .	4s 4p ² S ₁ .	4s 4p ² D ₁₁ .	5g G.
Ga I	—	—	8115	—	—
Ge II	[7080]	9406	13586	15906	—
As III	7144	12719	13400	15900	—
Se IV	7274	13123	13582	15118	[4390]

* Fowler, "Report"; Sawyer and Lang, 'Phys. Rev.', vol. 34, p. 712 (1929).

† Rao and Narayan, 'Proc. Roy. Soc.' A, vol. 119, p. 611 (1928); Lang, 'Phys. Rev.', vol. 34, p. 697 (1929).

‡ K. R. Rao, *loc. cit.*

It is interesting to notice that while the variation of the *msS* and *mpP* terms is regular, the *mdD* terms of small total quantum number ($m = 4$) show a marked irregularity which might have been expected. The values of 4dD relative to 5sS and 5pP in these spectra are also worth observing. Fig. 3 represents the Moseley diagrams for these three terms. While 5sS and 5pP curves are regular, that of 4dD shows a sudden increase in the slope and crosses the 5pP curve after the first stage, and the 5sS curve after the second stage of ionisation.

This sudden change in the D terms is brought out also in the following Table V which shows the results of the application of the irregular doublet law to the wave-numbers of the strongest lines in the multiplets arising from transitions between orbits of the same total quantum number.

Table V.—Irregular Doublet Law applied to corresponding Lines.

Spectrum.	$5s\ S_{\frac{1}{2}} - 5p\ P_{\frac{1}{2}}$ $\Delta\nu$	$5p\ P_{\frac{1}{2}} - 5d\ D_{\frac{3}{2}}$ $\Delta\nu$	$4p\ P_{\frac{1}{2}} - 4d\ D_{\frac{3}{2}}$ $\Delta\nu$	$4p\ P_{\frac{1}{2}} - 4p^3\ D_{\frac{3}{2}}$ $\Delta\nu$	$4p\ P_{\frac{1}{2}} - 4p^3\ P_{\frac{1}{2}}$ $\Delta\nu$
Ga I ...	8374	8589	7649	33961	—
Ge II	16963	8524	20764	79246	63412
As III	25487	8383	33526	114801	82693
Se IV	33870		46787	149231	100333
					90355
					112482
					133978
					22127
					21496

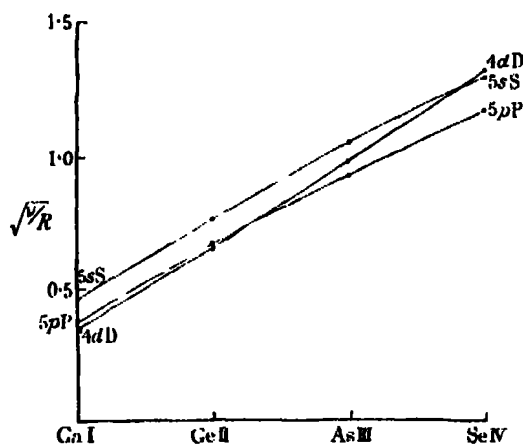


FIG. 3.

The method* of applying this law, when dealing with terms of different total quantum numbers, does not appear to be generally used, but it seems that it might lead to fruitful results in the location of at least the chief members of a spectrum, as the following Table VI shows, in which the method is applied to the member $4p P_{\frac{1}{2}} - 5s S_{\frac{1}{2}}$ of the spectral sequence under consideration; the second difference in the last column exhibits only a slight decrease.

Table VI.

Spectrum.	$4p P_{\frac{1}{2}} - 5s S_{\frac{1}{2}}$	$\nu' = \nu - 2467 \cdot 8(Z - A)^2$	Difference.	2nd Difference.
Ga I . . .	24788	22320		
Ge II .	62399	52528	30208	1748
As III	106694	84484	31956	1321
Se IV .	157245	117761	33277	

The screening constants for the atoms Ga I to Br V† are given in Table VII; they are found to exhibit the familiar slow decrease with increasing ionisation.

* Millikan and Bowen, 'Phys. Rev.', vol. 26, p. 313 (1925).

† From unpublished results of K. R. Rao.

Table VII.—Screening Constants.

Spectrum.	$4p\ P_{\frac{1}{2}} - 4p\ P_{\frac{3}{2}}$	σ .	$\Delta\sigma$.	$\Delta^2\sigma$.
Ga I	828	19.40	1.44	
Ge II	1768	17.96	0.89	0.55
As III	2940	17.07	0.67	0.22
Se IV	4376	16.40	0.52	0.15
Br V	6090	15.88		

A further comparison is made in Table VIII of the intervals of the $4p\ ^3P$ and $4p^2\ ^3P$ terms. It is interesting to see that the ratio gradually

Table VIII.

	$4p\ P_{\frac{1}{2}} - 4p\ P_{\frac{3}{2}}$ $\Delta\nu_1$.	$4p^2\ P_{\frac{1}{2}} - 4p^2\ P_{\frac{3}{2}}$ $\Delta\nu_2$.	$\frac{\Delta\nu_1}{\Delta\nu_2}$.
Ga I			
Ge II	1764	1107	1.59
As III	2940	1487	1.98
Se IV	4376	2220	1.97
Br V*	6090	2855	2.13

* *Loc. cit.*

increases as we pass from Ge II to Br V so that for Ga I the ratio may be predicted to be less than 1.59, indicating the separation $4p^2\ P_{\frac{1}{2}} - 4p^2\ P_{\frac{3}{2}}$ to be somewhat larger than 519 cm.^{-1} .

Spectrum Se V.

The spectrum Se V consists of a singlet and a triplet system, similar to Zn I. The chief triplet terms due to the configurations $4s\ 4p$, $4s\ 4d$, $4s\ 5s$ and $4p^2$ have been already found by Sawyer and Humphreys (*loc. cit.*). In this work the following singlets and intercombinations have been identified.

Classification.	λ (int.).	ν (vac.).
$4p\ ^1P_1 - 4d\ ^1D_2$	1227.58 (10)	81461
$4p\ ^1P_1 - 4p^2\ ^3P_2$	1150.96 (7)	86884
$4s\ ^1S_0 - 4p\ ^3P_1$	1094.68 (9)	91351
$4p\ ^3P_2 - 4d\ ^1D_2$	845.75 (9)	118238
$4p\ ^3P_1 - 4d\ ^1D_2$	820.68 (7)	121850
$4p\ ^1P_1 - 5s\ ^3S_1$	642.28 (2)	155695

Besides the experimental evidence that these are definitely lines of Se V (*cf.* Plates 10, 11) the following progressions of $4p\ ^1P_1 - 4d\ ^1D_2$ and $4s\ ^1S_0 - 4p\ ^3P_1$ in the sequence Zn I to Se V support the assignments made. The data for As IV* included in this table are taken from unpublished results of K. R. Rao.

	$4s\ ^1S_0 - 4p\ ^3P_1$	Difference.	$4p\ ^1P_1 - 4d\ ^1D_2$	Difference.
Zn I	32502	15316	15713	21305
Ga II	47818	14678	37018	16081
Ge III	62496	14466	53099	14441
As IV	76962	14380	67540	13921
Se V	91351		81161	

The following table, written in the multiplet form, gives the above lines, and, for completeness, also the classifications made by Sawyer and Humphreys. For purposes of comparison the intensities of all the lines in this table are from the authors' plates. The relative intensity of the intercombination lines is worth noticing. Of these it is remarkable that while $4p\ ^3P_{1,2} - 4d\ ^1D_2$ are intense, $4p\ ^1P_1 - 4d\ ^3D_{1,2}$ are absent.

* The other intercombinations in As IV are :—

	λ	ν
$4p\ ^3P_1 - 4d\ ^1D_2 =$	974.61 (9)	102605
$\ ^3P_2 - \ ^1D_2 =$	999.25 (9)	100075
$4p\ ^1P_1 - 4p\ ^3P_2 =$	1381.76 (6)	72371
$\ ^1P_1 - \ ^3P_1 =$	1440.00 (2)	69444
$\ ^1P_1 - \ ^3P_0 =$	1472.55 (1)	67909

and the terms $4p\ ^1P_1$ and $4s\ ^1S_0$ are 307190 and 419212 respectively. The latter leads to the ionisation potential 51.7 volts approximately for As IV.

Classifications in Se V.

$4p$	3P_0 500025 1595	3P_1 498430 3610	3P_2 494820	1P_1 458048
$4s\ ^1S_0 \rightarrow 589781$		1094.68 (9) 91351		759.11 (10) 131733
$4p^2\ ^3P_0 \rightarrow 377992$ 2298		830.30 (9) 120438		—
$^3P_1 \rightarrow 375894$ 4528	804.31 (8) 124330	814.77 (7) 122734	839.49 (10) 119120	—
$^3P_2 \rightarrow 371166$		785.78 (8) 127262	808.71 (9) 123654	1150.96(7) 86884
$4d\ ^1D_1 = 332247$ 214	596.01 (8) 167782	608.73 (7) 166188	615.10 (2) 162575	—
$^1D_2 = 332033$ 335		600.95 (8) 166403	614.30 (8) 162787	—
$^1D_3 = 331698$			613.04 (9) 163122	—
$^1D_4 = 376587$		820.68 (7) 121850	845.75 (9) 118238	1227.58 (10) 81461
$5s\ ^3S_1 = 302355$	505.91 (3) 197664	510.02 (4) 196071	519.58 (5) 192463	642.28 (2) 155695

The triplet term values were determined by Sawyer and Humphreys by extrapolation of the Moseley diagrams since no second terms were found; the singlet terms are based on these. The ionisation potential, corresponding to the largest term $4s\ ^1S_0$ found in this work, is about 72.8 volts.

It will be noted that $4d\ ^1D$ is deeper than $4d\ ^3D$. In the corresponding spectra, Sn III,* Sb IV† and Te V†, only one deep 1D_2 term has been found with certainty, but it has been ascribed to the configuration $4p^2$ and not to $4s\ 4d$. The authors think that the 1D_2 term found in all these Zn I-like and Cd I-like spectra arises from the same configuration, presumably $4s\ 4d$, that is adopted in the above scheme.

Summary.

The spectrum of selenium has been investigated from $\lambda\ 7000$ to $\lambda\ 650$ mainly using different intensities of discharge through capillary tubes containing vapour of selenium. Between $\lambda\ 1400$ and $\lambda\ 400$ photographs have been taken also of the spark spectrum of selenium with a Siegbahn vacuum

* Green and Loring, 'Phys. Rev.', vol. 30, p. 574 (1927).

† Gibbs and Vieweg, 'Phys. Rev.', vol. 34, p. 400 (1929).

spectrograph. The use of self inductance with these sparks has proved fruitful in the assignment of lines in the extreme ultra-violet region to the various stages of ionisation of the atom.

With the aid of these experimental data, the doublet system of trebly-ionised selenium has been identified. A term scheme has been proposed, based on a choice of 70240 cm.^{-1} for the term $5g\ ^2G$. The largest term, $4p\ ^3P_1 = 346094$, gives an ionisation potential of about 42.72 volts. A comparison is made of the chief features of the four iso-electronic spectra Ga I, Ge II, As III and Se IV.

A few singlets and intercombination lines in Se V have been added to the triplet system discovered by Sawyer and Humphreys. The largest term $4s\ ^1S_0$ is found to be 589781 cm.^{-1} leading to an approximate ionisation potential of 72.8 volts.

The authors take this opportunity of expressing their deep sense of gratitude to Professor A. Fowler and Professor M. Siegbahn for their kindness and encouragement throughout the course of the investigation.

K. R. Rao is indebted to the Andhra University and the Madras Government for the award of a scholarship, and J. S. Badami to the Bombay University for the same.

A Metrical Theory and its Relation to the Charge and Masses of the Electron and Proton.

By H. T. FLINT, Reader in Physics in the University of London, King's College.

(Communicated by O. W. Richardson, F.R.S.—Received January 26, 1931).

The Five-Dimensional Continuum.

The works of Kaluza* and of O. Klein† have shown that it is possible to give to electromagnetic forces a geometrical interpretation similar to that of gravitational forces in the theory of relativity. It is necessary to assume the existence of a five-dimensional continuum defined by

$$d\sigma^2 = \gamma_{\mu\nu} dx^\mu dx^\nu, \quad (1)$$

where the summation extends over $\left. \begin{smallmatrix} \mu \\ \nu \end{smallmatrix} \right\} = 1, 2, 3, 4, 5$.

The coefficients, $\gamma_{\mu\nu}$ have the values

$$\left. \begin{aligned} \gamma_{mn} &= g_{mn} + \gamma_{55} \alpha^2 \phi_m \phi_n, \\ \gamma_{5m} &= \alpha \gamma_{55} \phi_m, \end{aligned} \right\} \quad (2)$$

where α and γ_{55} are constants, the g 's the Riemannian coefficients and the ϕ 's the components of the electromagnetic potential.

The contravariant components are

$$\left. \begin{aligned} \gamma^{mn} &= g^{mn}, & \gamma^{5m} &= -\alpha \phi^m, \\ \gamma^{55} &= \alpha^2 \phi_m \phi^m + 1/\gamma_{55}. \end{aligned} \right\} \quad (3)$$

The equation of the geodesic in this continuum is

$$\frac{d}{d\sigma} \left(g_{mn} \frac{dx^n}{d\sigma} \right) - \frac{1}{2} \frac{\partial g_{lp}}{\partial x^m} \frac{dx^l}{d\sigma} \frac{dx^p}{d\sigma} = \frac{e}{I} \cdot \frac{dx^n}{d\sigma} \left(\frac{\partial \phi_n}{\partial x^m} - \frac{\partial \phi_m}{\partial x^n} \right), \quad (4)$$

where I is a quantity corresponding to mass in the four-dimensional continuum and is introduced by defining the momentum by means of the relation

$$\Pi_\mu = I \gamma_{\mu\nu} \frac{dx^\nu}{d\sigma}. \quad (5)$$

* 'Sitzungsber. Berl. Akad.,' p. 966 (1921).

† 'Z. Physik,' vol. 36, p. 895 (1926).

For the cases when μ is equal to 1, 2, 3 or 4 we write

$$\begin{aligned}\Pi_m &= I \gamma_m \frac{dx^\nu}{d\sigma} = I \left(\gamma_{mn} \frac{dx^n}{d\sigma} + \gamma_{m5} \frac{dx^5}{d\sigma} \right) \\ &= I \left\{ g_{mn} \frac{dx^n}{d\sigma} + \alpha \phi_m \left(\gamma_{5n} \frac{dx^n}{d\sigma} + \gamma_{55} \frac{dx^5}{d\sigma} \right) \right\} = I g_{mn} \frac{dx^n}{d\sigma} + \alpha \phi_m \Pi_5.\end{aligned}\quad (6)$$

This suggests the following relations

$$\frac{I}{m} = \frac{d\sigma}{ds}, \quad \Pi_{5a} = \frac{e}{c}, \quad (7)$$

where ds is the four-dimensional line element defined by $ds^2 = g_{mn} dx^m dx^n$.

Thus

$$\Pi_m = m g_{mn} \frac{dx^n}{ds} + \frac{e}{c} \phi_m, \quad (8)$$

and is recognised as the generalised momentum familiar in the electromagnetic theory.

The equation of the geodesic (4) now becomes

$$\begin{aligned}\frac{d}{ds} \left(g_{mn} \frac{dx^n}{ds} \right) - \frac{1}{2} \frac{\partial g_{in}}{\partial x^m} \frac{dx^i}{ds} \cdot \frac{dx^n}{ds} &= \frac{e}{I} \left(\frac{d\sigma}{ds} \right) \frac{dx^n}{ds} \left(\frac{\partial \phi_n}{\partial x^m} - \frac{\partial \phi_m}{\partial x^n} \right) \\ &= \frac{e}{m} \frac{dx^n}{ds} \left(\frac{\partial \phi_n}{\partial x^m} - \frac{\partial \phi_m}{\partial x^n} \right),\end{aligned}\quad (9)$$

and is at once recognised as the equation of the path of a mass m carrying a charge e in a gravitational and electromagnetic field.

If we now turn to the fifth of the equations defining the geodesic we find

$$\gamma_{5\nu} \frac{dx^\nu}{d\sigma} = \text{constant},$$

since it is assumed that none of the coefficients $\gamma_{\mu\nu}$ contains x^5 . Let $d\theta$ denote the projection of $d\sigma$ on the fifth axis, i.e.,

$$d\theta = \frac{\gamma_{5\nu}}{\sqrt{\gamma_{55}}} dx^\nu,$$

so that

$$\sqrt{\gamma_{55}} \frac{d\theta}{d\sigma} = \text{constant}. \quad (10)$$

This constant is determined by quantities already introduced for

$$\Pi_5 = I \gamma_{5\nu} \frac{dx^\nu}{d\sigma} = I \sqrt{\gamma_{55}} \frac{d\theta}{d\sigma}$$

or

$$\frac{e}{\alpha c} = I \sqrt{\gamma_{55}} \frac{d\theta}{d\sigma}.$$

We can write $d\sigma^2$ in the form $ds^2 + d\theta^2$ thus

$$\left(\frac{ds}{d\sigma}\right)^2 + \left(\frac{d\theta}{d\sigma}\right)^2 = 1,$$

whence

$$I^2 = m^2 + e^2/\gamma_{55}\alpha^2c^2. \quad (12)$$

The values of γ_{55} and of α have been regarded as constant and we shall for convenience write $\gamma_{55} = -1$. Π_5 will be interpreted as the mass associated with the charge e . We shall suppose that Π_5 , being a component of a vector, can have positive and negative values. It is positive for a positive charge and negative for a negative charge so that α remains constant in sign and has the value e/mc .*

In those parts of the continuum where α has this value, matter of mass m and electric charge of magnitude e are present. The line element $d\sigma$ and the generalised mass I are both zero in these regions, but the ratio $I/d\sigma$ remains definite by (7). Thus in five dimensions matter becomes the exact analogue of the photon in four-dimensions.

If we proceed with this analogy we are led to ask what is the equation corresponding to the wave equation in optics, for associated with the null geodesic in four-dimensions we have the familiar wave equation for light. This analogy leads directly to Schrödinger's equation in the relativistic form for a charged particle in a gravitational and electromagnetic field. It is, however, well known that this equation takes no account of those phenomena which have hitherto been explained by the introduction of electron spin. This difficulty has been removed by Dirac in the discovery of first order equations.

If we remember that the wave equation in optics is a consequence of Maxwell's equations for empty space our analogy can be pushed farther.

We obtain the first order equations of the quantum theory by writing down the equations analogous to Maxwell's for the five-dimensional continuum.† This method of deriving the equations leads to the conclusion that the continuum has a definite metrical property. This property is the same as that previously obtained in an attempt to draw conclusions about the metrics of space from quantum phenomena.‡ Formerly the method was applied to a four-dimensional continuum in which it seems impossible to derive the first order equations except by the introduction of symbolical methods, which appear rather arbitrary in character.

* Fisher, 'Proc. Roy. Soc.,' A, vol. 123, p. 489 (1929).

† 'Proc. Roy. Soc.,' A, vol. 126, p. 614 (1930).

‡ 'Proc. Roy. Soc.,' A, vol. 117, p. 630 (1928).

The method is similar to that of Weyl and Eddington, who suppose that in general the parallel displacement of a vector from a point of a continuum to a neighbouring point results in a change in its length.

The application of this idea to four-dimensions made it possible to recognise in electromagnetic phenomena the expression of space metrics.

Electromagnetic phenomena in the present case are included in the geometry of the continuum and quantum phenomena appear as the expression of the metric.

The Metrics of the Continuum.

The suggestion made in the paper referred to was that Weyl's assumption for the change in length associated with a parallel displacement, viz.,

$$\frac{dl^2}{l^2} = - \phi_m dx^m, \quad (13)$$

where l^2 is the square of the length of the vector, should be replaced by

$$\frac{dl^2}{l^2} = \frac{2\pi ic}{h} \Pi_m dx^m, \quad (14)$$

where Π_m denotes the component of generalised momentum (8) and c is introduced because we have defined Π_m as $mg_{mn} dx^n/ds$ and not as $mg_{mn} dx^n/d\tau$, where τ denotes the proper time.

If we assume the existence of a five-dimensional continuum in which a vector with components A^μ , has length L given by

$$L^2 = \gamma_{\mu\nu} A^\mu A^\nu,$$

we replace (14) by

$$\frac{dL^2}{L^2} = \frac{2\pi ic}{h} \Pi_\mu dx^\mu. \quad (15)$$

With the values of α which we have adopted $\Pi_\mu dx^\mu$ is zero.

Thus the change of length along a null geodesic in the five-dimensional continuum is zero.

(15) can be written

$$\frac{dL^2}{L^2} = \frac{2\pi ic}{h} \Pi_m dx^m + \frac{2\pi ic}{h} \Pi_5 dx^5 = \frac{dl^2}{l^2} + \frac{2\pi i}{h} mc dx^5. \quad (16)$$

Thus the four-dimensional observation dl^2/l^2 is now given by

$$\frac{dl^2}{l^2} = - \frac{2\pi i}{h} mc dx^5. \quad (17)$$

This change of length in a parallel displacement depends only upon dx^5 and not upon the change of any other co-ordinate and is evidently periodic in x^5 with a frequency mc/h . Thus the length returns to its original value after each displacement of h/mc along the fifth axis.

We notice the dependence of the change of length on the mass. From the metrical point of view we could conveniently regard equal lengths along the fifth axis as those associated with the same change in length per unit length.

Thus for two world lines, of masses m and m' , dx^5 is equal to dx'^5 if

$$m dx^5 = m' dx'^5.$$

We could alternatively say that a common unit of length has different values according to the mass with which it is associated.

Let us consider the special case of the proton of mass M_0 carrying a charge ϵ . In this case $\alpha = \epsilon/M_0 c$. Let $\Pi_5 = M_0$.

From (6) we obtain

$$\Pi_m = M_0 g_{mn} \frac{dx^n}{ds} + \frac{\epsilon}{c} \phi_m, \quad (18)$$

which is the usual expression for the generalised momentum of a proton.

If we take the opposite sign for Π_5 and write $\Pi_5 = -M_0$ we obtain

$$\Pi_m = M_0 g_{mn} \frac{dx^n}{ds} - \frac{\epsilon}{c} \phi_m, \quad (19)$$

which is the momentum of a particle of charge $-\epsilon$ and mass M_0 .

We thus pass from the positive to the negative charge merely by changing the sign of the momentum component Π_5 .

This suggests that there is a single constant ϵ not two, $\pm \epsilon$. What we usually describe as the negative charge is merely a mass with negative fifth component of momentum. But there remains a difficulty, for (19) is the momentum of a negative charge with the mass of a proton and no such charged mass is known in physics.

It would appear that with this change in sign of Π_5 we must change the value of α from $\epsilon/M_0 c$ to $\epsilon/m_0 c$, where m_0 is the mass of the electron.

It would be much more satisfactory if we could simplify our geometry by retaining the same value of α in both cases, i.e., recognise only one fundamental mass. We can do this if we are prepared to adopt the above metrical views.

Since we suppose that matter is made up of protons and electrons, any charge e and mass m must consist of a bundle of world lines characterised by the fundamental charge and mass.

Thus we shall adopt for the constant α , the value ϵ/M_0c and Π_5 then has the values $\pm M_0$.

When Π_5 is positive the projection $d\theta$ of the world line along the fifth axis is positive and when Π_5 is negative $d\theta$ is negative and the numerical value is the same in each case. But our discussion of the metric has prepared us for the possibility of a metrical difference in the two cases. We can readily suppose that there is an asymmetry of metric which makes the units of different values in the positive and negative directions of the fifth axis. The asymmetry of mass is then shifted to an asymmetry of metric and we can include in a single metrical and geometrical system the phenomena associated with the proton and electron.

There is only one charge ϵ and one mass M_0 and this mass only occurs when we insist upon considering a five-dimensional world line from the point of view of four-dimensional observers. The constant I is the more fundamental quantity and along the world lines this is always zero.

We have thus a positive length $d\theta^+$ and a negative length $d\theta^-$ metrically equal provided that

$$kd\theta^+ = d\theta^-, \quad (20)$$

where k is the ratio of the mass of a proton to that of an electron and must be regarded as a constant like the constant of gravitation or Planck's constant.

If we describe electrons and protons by the same system of co-ordinates then we must remember that

$$M_0 dx_s^5 = m_0 dx_e^5, \quad (21)$$

when dx_s^5 is equal to dx_e^5 in the sense in which we have defined metrical equality.

In the four-dimensional continuum we make use of a line element ds which, according to our theory, satisfies the relation

$$ds^2 + d\theta^2 = 0.$$

Thus $|ds| = |d\theta|$, and the adoption of a common unit of measurement along ds for world lines with a positive or negative projection along the fifth axis will lead to the introduction of different masses. We must always adjust our equations by applying the factor k when Π_5 is negative. $d\theta_e$ has a smaller value than the $d\theta_p$ which is *apparently* equal to it.

Thus when $d\theta_e$ occurs we must reduce the element in the ratio $m_0 : M_0$.

The expression (19) applies to a negative charge ϵ but is written without the adjustment necessary. The element ds applies to the world line with a negative projection along the fifth axis and if we write the equation in terms of the

same units as are applied to the world line with a positive fifth component, ds must be replaced by $M_0/m_0 ds$.

(19) then becomes

$$m g_{mn} \frac{dx^n}{ds} - \frac{\varepsilon}{c} \phi_n$$

which is the familiar expression for the momentum of the electron.

The same method makes the equation of the geodesic (4) an equation both for the positive and negatively charged particle.

The principles of conservation of momentum and of energy when applied to two masses show that the four-dimensional momentum Π_m is conserved. It seems a natural step from this to suppose that the five-dimensional quantity enjoys the same property of conservation. The Compton effect shows that the principle is applicable in the case of the interaction of electrons and photons.

Since a photon is a particle with zero rest mass, the momentum in this case has a zero fifth component.

According to the views stated here the characteristic differences between the ultimate particles in nature lie in the values of their fifth components of momentum, which may have the values $\pm M_0$ or zero.

The generalisation of the principle of conservation of momentum indicates that it is impossible for radiation to be created by the destruction of matter unless there is a union of two particles with equal and opposite fifth momentum components.

According to our theory this is possible by the union of an electron and proton for these have equal and opposite momenta along the fifth axis. This, of course, implies the adoption of the system of metrics we have described. It is generally accepted that electrons and protons can unite to produce photons, but according to the view taken here, it seems impossible to obtain zero rest mass from the union without adopting the principle that the natural scales of measurement are different in the two cases.

It is from the generation of a photon from the union of an electron and proton that we can hope to calculate the value of the scale constant k , or the ratio of the masses of the proton and electron.*

The occurrence of the length h/m_0c as a natural unit of length has been referred to before.† It appears that this length has a special significance in

* 'Phys. Z.,' vol. 30, p. 895 (1929); 'Proc. Phys. Soc.,' vol. 42, p. 239 (1930).

† 'Proc. Roy. Soc.,' A, vol. 117, pp. 630, 638 (1928).

relation to the world line of the electron and a principle of minimum proper time can be deduced.

This states that no interval of proper time less than h/m_0c^2 has any physical significance in electronic motion.

From this certain deductions can be made which are all in agreement with experiment. From it also a principle of uncertainty follows which, while differing fundamentally from that of Bohr and Heisenberg, gives the same results when applied to dimensions of the order of a few of these natural units of length.

This length may be expected to have some special significance of the nature of a limit, since it is a limiting case of the de Broglie wave-length.

It appears again here as a natural unit of length along the fifth axis of the continuum and is carried over into space time in consequence of the relation $d\sigma^2 = ds^2 + d\theta^2$, which vanishes along the path of the electron or proton.

The Kinetics of Reactions in Solution. Part I. - A Comparison of the Decomposition of Chlorine Monoxide in the Gaseous State and in Carbon Tetrachloride Solution.

By E. A. MOELWYN-HUGHES and C. N. HINSHELWOOD, F.R.S.

(Received February 4, 1931.)

In general the rate of a chemical reaction is profoundly influenced by the solvent in which the reaction takes place. In Menshutkin's experiments* on the combination of tertiary amines and alkyl halides, for example, the reaction velocity in benzyl alcohol was several hundred times greater than that in hexane. While it is clear that the influence of the solvent, which cannot be correlated definitely with any physical properties, belongs to the category of specific chemical effects, it is not easy to see in exactly what it consists. Christiansen† and Norrish and Smith‡ have found that the rate of a bimolecular reaction in solution appears usually to be several powers of 10 smaller than that of a hypothetical reaction occurring in the gaseous phase with the same energy

* 'Z. Phys. Chem.,' vol. 6, p. 41 (1890).

† 'Z. Phys. Chem.,' vol. 113, p. 35 (1924).

‡ 'J. Chem. Soc.,' vol. 131, p. 129 (1928).

of activation. Norrish and Smith therefore suggest that, since each encounter between molecules of the reacting substances takes place with a solvent molecule in very close proximity, and is thus virtually a ternary collision, the influence of the solvent is primarily a deactivating one. On the other hand, the decomposition of nitrogen pentoxide—a unimolecular reaction—takes place at the same rate and possesses the same heat of activation in chloroform, in carbon tetrachloride and a number of similar solvents as it does in the gaseous phase. In certain other solvents, quite different rates and heats of activation are found. Daniels* regards as “normal” those solvents in which the reaction occurs at the same rate as in the gaseous phase, and attributes the deviations found with other, “abnormal,” solvents to a definite formation of complex molecules whose stability differ from that of free nitrogen pentoxide. The isomerisation of pinene† has also been found to take place at the same rate in the gaseous and in the liquid states.

As far as this not very abundant evidence goes, then, it would suggest that bimolecular reactions are usually much slower in solution than in the gaseous phase, while unimolecular reactions tend usually to be uninfluenced by the presence of the solvent. This simple contrast, however, is by no means correct. In the first place, the variation in the rates of unimolecular reactions with change of solvent appears on closer inspection to be not less marked than that of bimolecular reactions. This aspect of the matter is dealt with more fully in the following paper. In the second place, there have hitherto been no data available for comparing the rate of a bimolecular reaction in the gas phase with its rate in solution in one of the relatively inert solvents which had been used for nitrogen pentoxide. It is shown in the present paper, however, that the decomposition of chlorine monoxide, which is essentially bimolecular, although somewhat complex in mechanism, occurs at almost exactly the same rate in carbon tetrachloride as in the gaseous state, and that the heat of activation is substantially the same. Thus it appears that, contrary to first impressions, the kinetic type of the reaction has little to do with the influence of solvents. The chemical nature of the solvent is the determining factor in all cases. Both for bimolecular and unimolecular reactions there appear to exist “ideal” solvents, of which carbon tetrachloride is a good example. This is being confirmed by Mr. Bowen and the writers by measurements on the rate of decomposition of ozone in carbon tetrachloride solution. For reactions

* Eyring and Daniels, ‘J. Amer. Chem. Soc.’ vol. 52, p. 1473 (1930). Cf. Lueck, *ibid.*, vol. 44, p. 757 (1922).

† D. F. Smith, ‘J. Amer. Chem. Soc.’ vol. 49, p. 43 (1927).

that cannot be made to take place in the gas phase at all, and this includes the majority of measurable reactions, the rate in carbon tetrachloride or an analogous solvent would then appear to be a standard or ideal rate equal to that which the gas reaction would possess. Comparison of the rate and the energy of activation of a given reaction in any solvent with the corresponding values for the reaction in carbon tetrachloride thus provides a means of ascertaining whether the solvent has increased or decreased the normal heat of activation, and whether its effect is to be regarded as deactivating or positively catalytic. The similarity of behaviour of chlorine monoxide in the gaseous phase and in carbon tetrachloride solution suggests that, for bimolecular as well as for unimolecular reactions, solvents must be divided into two classes, and that the deactivating influences postulated by Norrish and Smith are as specific as the influence of "abnormal" solvents on unimolecular reactions.

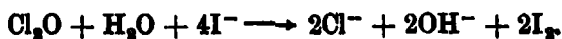
Experimental Procedure.

In studying the thermal decomposition of chlorine monoxide care must be taken to exclude as far as possible any photochemical change, hence the gas was prepared, stored and allowed to react in the dark. A solution of chlorine monoxide in carbon tetrachloride was prepared directly by shaking slightly more than the theoretical amount of mercuric oxide with an approximately normal solution of chlorine in this solvent at room temperature for about half-an-hour.



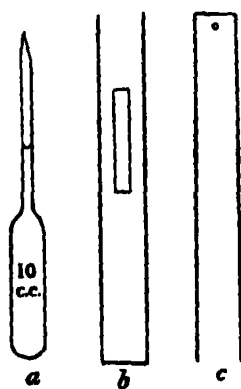
The mercuric oxide, prepared by precipitation, had been thoroughly washed with water, and dried at 300° C. ; chlorine, generated from bleaching powder, had been washed and dried in towers of water and sulphuric acid respectively ; the sulphur-free carbon tetrachloride employed was dried over and distilled from phosphorus pentoxide. The mercury double-salt was removed in a glass filter, and the solution of chlorine monoxide thus obtained was frozen and kept in a vessel surrounded by solid carbon dioxide to prevent decomposition during storage. Solutions thus prepared contained a quite small percentage of free chlorine, which was not removed since subsequent experiments showed it to have no effect on the rate of decomposition of the oxide.

To estimate the relative amounts of chlorine monoxide and free chlorine in solution, a sample is run into an aqueous solution of potassium iodide containing a measured quantity of decinormal sulphuric acid in excess of that demanded by the equation



The iodine liberated is titrated against decinormal sodium thiosulphate, and the excess acid is neutralised with decinormal baryta. If x and y be the number of cubic centimetres of thiosulphate and acid used up, then the concentration of chlorine monoxide is proportional to y , and that of free chlorine proportional to $(x - 2y)$. It may be noted that for all samples originating from the decomposition of a given solution the value $(x - y)$ should be constant, independent of the relative amounts of chlorine monoxide and chlorine; this was verified in all the experiments and served to show that no serious loss of gas occurred during the process of manipulation. (The small disturbances due to the formation of traces of an intermediate oxide were found to be without importance in these experiments.)

The rate of decomposition was measured by analysing in this manner 10 c.c. samples of the solution, which had been kept in an electrically-controlled thermostat for a given time. The reaction vessels were soda-glass tubes of the type shown in the diagram (fig. 1A); after being cleaned with nitric acid



FIGS. 1A. 1B. 1C.

and alcohol, with hot water, and finally with acetone, they were carefully dried, charged with 10 c.c. of solution which partly occupied the narrow portion of the tube, and sealed off. The reaction tube was supported in the thermostat inside a brass cylinder (fig. 1B), possessing a narrow slit which rendered it possible to lower the reaction tube into the thermostat liquid up to the meniscus. Finally, a second brass cylinder (fig. 1C) was slipped inside the cylinder *b* to exclude any light from the reaction tube *a*.

In an investigation of the rate of decomposition of a gas dissolved in a liquid it is clearly most important to be certain that no appreciable change takes place in the gaseous phase above the solution. To reduce the chance of gaseous decomposition, the space above the liquid was made very small compared with that of the solution, and was not heated. Since, however, the pressure developed inside the tube at fairly high temperatures will not permit the air space to be reduced below about 0.5 c.c., it was thought advisable to investigate closely the effect on the reaction rate of a change in the gaseous space above the solution. Accordingly, two experiments were conducted with the same solution at 79.9° C.: in the first series the gas space was about 0.5 c.c.; in the second series the volume of the gas was roughly equal to that of the solution, viz., 10 c.c. Graphs were plotted for both runs, and from these

were read off the times taken for the reaction to proceed from 0 to 25 per cent., 25 to 50 per cent., and 50 to 75 per cent. of the total change. For the first series of experiments these values were 32, 50 and 100 minutes respectively; for the second series they were 34, 56 and 105 minutes. It is thus seen that the reaction proceeds in the vessels with increased gas space at a rate which is actually about 5 per cent. lower than in the ordinary tubes. This small decrease in velocity is due to a certain loss of chlorine monoxide from the solution, for the rate of change is, as will be shown later, dependent on the concentration. There can be little doubt, therefore, that the reaction which we are measuring proceeds in solution, and, under the normal conditions of experiment, only to a negligible extent in the gaseous phase.

The Course of the Reaction.

The curves shown in fig. 2, which have been drawn from the data given in Table I, show the rate of decomposition of solutions of chlorine monoxide in carbon tetrachloride at different temperatures and at slightly different concentrations, and are typical of the results obtained with numerous solutions

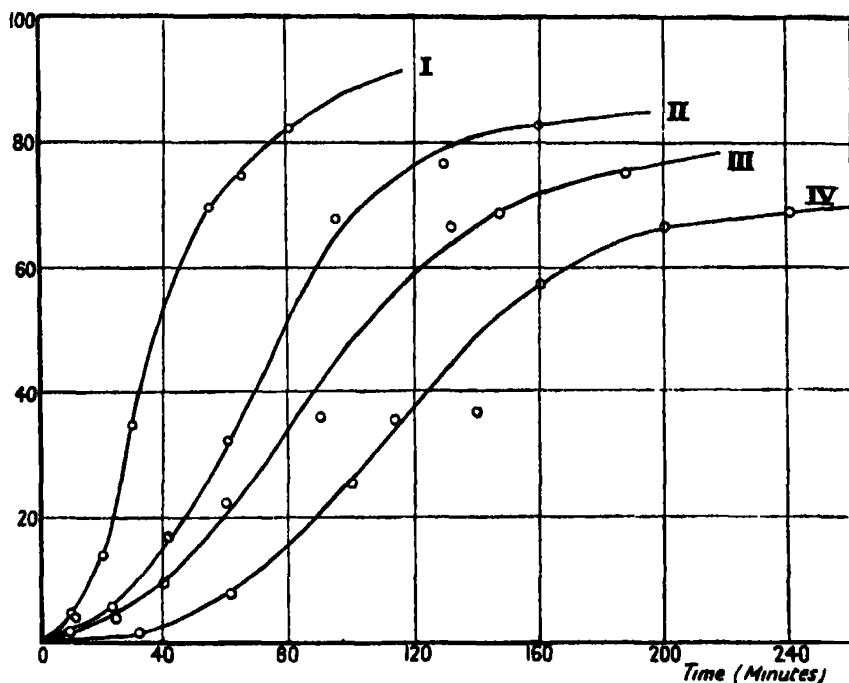


FIG. 2.—Typical Curves showing the decomposition of Chlorine Monoxide in Carbon Tetrachloride Solution. 1, Solution 8 at 89.5° ; 2, Solution 8 at 81.4° ; 3, Solution 5 at 75.3° ; 4, Solution 7 at 69.8° .

Table I.

Solution 8 89.5° C. [Cl ₂ O] = 0.115.		Solution 8 81.4° C. [Cl ₂ O] = 0.115.		Solution 5 75.3° C. [Cl ₂ O] = 0.119.		Solution 7 69.8° C. [Cl ₂ O] = 0.126.	
Time in minutes.	Percentage change.	Time in minutes.	Percentage change.	Time in minutes.	Percentage change.	Time in minutes.	Percentage change.
10	4.2	12	3.8	10	1.8	31	1.2
20	13.6	24	5.5	25	3.9	61	7.7
30	34.8	41	16.8	40	9.2	100	25.1
40	36.1	60	31.9	60	22.4	114	35.4
55	69.5	95	67.6	90	35.6	140	36.6
65	74.6	130	76.5	132	66.3	160	57.2
80	82.2	160	82.8	148	68.7	200	66.7
				188	75.0	240	68.7
				385	90.8	413	84.5

at temperatures varying from 50° to 90° C. The reaction is seen to be markedly accelerated after an initial period of slow change, and in this respect closely resembles the gaseous reaction which has been studied by Hinshelwood and Prichard.* These authors concluded that the gaseous decomposition of chloride monoxide consisted of two consecutive bimolecular reactions, the intermediate compound being possibly an unknown oxide of chlorine. Although the nature of this intermediate compound is not relevant to the present investigation, which is a comparison of the rates of decomposition in the gas and in solution, rather than an attempt at an exact elucidation of the mechanism, it is nevertheless of interest to enquire into the cause of the acceleration, which appears in both cases and is probably attributable to a common intermediate compound. Although the suggestion made by Hinshelwood and Prichard has received no direct proof, there is much circumstantial evidence in its favour. It has been found by Dickinson and Jeffreys† that chlorine peroxide occurs as an intermediate product in the photochemical decomposition of chlorine monoxide. In the present work also it has been found that the addition of small quantities of chlorine peroxide to the system has a marked effect on the reaction rate. With solutions 6 and 7 (containing respectively 0.095 and 0.126 gram-molecules of chlorine monoxide per litre) at 69.7° C., the presence of 0.0002 gram-molecules of chlorine peroxide per litre caused a considerable increase in the rate of decomposition of the monoxide ; addition

* 'J. Chem. Soc.,' vol. 123, p. 2730 (1923).

† 'J. Amer. Chem. Soc.,' vol. 52, p. 4288 (1930).

of 0.0024 gram-molecules of chlorine peroxide per litre eliminated the initial slow period of the uncatalysed reaction.

It should be noted in this connection that curves showing acceleration such as those given in fig. 2 were obtained only after taking great care to eliminate any partial decomposition at room temperatures. The curves obtained for solutions 1 to 4, which had partly decomposed during storage, were of a different shape, corresponding to the latter stages of the complete curves.

Addition to the solution of a small amount of water reduced the rate of reaction. Solution 7, containing 0.126 gram-molecules of chlorine monoxide per litre, at 69.8° C., when dry gave the values 99 and 140 minutes for $t_{1/4}$ and $t_{1/2}$ respectively. When the solvent was saturated with water these numbers became 136 and 200. In all experiments, except those with solution 1, care was taken to use thoroughly dry solutions.

The Order of Reaction.

The thermal decomposition of chlorine monoxide in the gaseous state, in spite of the complication of consecutive stages, appears to be bimolecular over its complete course. That this is also true of the reaction in carbon tetrachloride solution will be seen by an examination of Table II. Column 2 gives the initial concentration of chlorine monoxide, in gram-molecules per litre; and $t_{1/4}$, $t_{1/2}$ and $t_{3/4}$ represent the time, in minutes, taken by the reactant to decompose at 70.7° C. to the extent of 25 per cent., 50 per cent. and 75 per cent. respectively of the total change. The last three columns contain the product of the concentration and the time required for a given fraction of the total reaction. These quantities, although not exactly constant, are

Table II.

Solution.	$a = [\text{Cl}_2\text{O}]$.	$t_{1/4}$.	$t_{1/2}$.	$t_{3/4}$.	$a \cdot t_{1/4}$.	$a \cdot t_{1/2}$.	$a \cdot t_{3/4}$.
9a	0.334	44	57	94	14.7	19.0	31.4
9b	0.224	64	92	146	14.3	20.6	32.7
8	0.117*	112	169	290	13.1	19.8	33.9

* The true concentration (0.115 gram-molecules per litre) of solution 8 has been corrected to this value in order to make approximate allowance for the fact that the temperature in this case was 71.0° C.

probably as near to constancy as the accuracy of the experimental method will permit. That the reaction is bimolecular throughout is highly probable; that it is not unimolecular is certain. In fact, the order given by the van't

Hoff differential method from data relating to the *deteriorated* solutions is actually somewhat higher than the second. These results are, however, not recorded.

The Influence of Temperature.

To determine the heat of activation, experiments were made at five temperatures with an undeteriorated solution containing little free chlorine. Since the decomposition involves consecutive reactions which might have different heats of activation, the values of this quantity are calculated for three different stages of the change. As with the gas, there is little difference between the values found. t_1 , t_2 and t_3 (Table III) are the times, expressed in minutes, required for the decomposition to proceed from 0 to 25 per cent., 25 to 50 per cent. and 50 to 75 per cent. respectively. The calculated values are obtained

Table III.

Temperature.	t_1 (obs.).	t_1 (calc.).	t_2 (obs.).	t_2 (t_2 (obs.).	t_2 (calc.).
° C.						
50.2	663	660	297	331	960	880
59.8	285	282	147	140	300	335
71.0	112	112	58	56	120	116
81.4	52	50	26	24	46	46
89.5	28	28	12	13	23	23

from the Arrhenius equation with the following heats of activation :—

0 to 25 per cent., $E = 18,800$ calories.

25 to 50 per cent., $E = 19,100$ calories.

50 to 75 per cent., $E = 21,500$ calories.

The average value for the range 25 to 75 per cent. is 20,300 calories. The value for the gas reaction in the range 20 to 80 per cent. is 21,000 calories. These values must be regarded as equal within the limits of experimental uncertainty.

Comparison of the Rate of Reaction in Solution with that in the Gaseous Phase.

It is unfortunate that mathematical difficulties render it impossible to evaluate the two individual bimolecular constants for the consecutive reactions. For the present purpose, however, all that is necessary is to compare the time required for the gaseous reaction to proceed to a given extent with the corresponding time for the reaction in solution. The results of Hinshelwood and Hughes* for the gaseous reaction show that at a temperature of 60.2° C. and

* 'J. Chem. Soc.,' vol. 125, p. 1841 (1924).

at a concentration of 0.0113 gram-molecules per litre, the decomposition of chlorine monoxide requires 2215 minutes to proceed from 20 per cent. to 60 per cent. of completion. Combining this with the fact that the corresponding time is 482 minutes at 79.5° C., and with the fact that the time is inversely proportional to the concentration, it is possible to calculate the value of t_{20-60} per cent. for other temperatures and for concentrations other than 0.0113. Values obtained in this manner are given in column 5 of Table IV. Column 4 gives the observed times for solutions of chlorine monoxide of various concentrations (column 2) at different temperatures (column 3). These values

Table IV.

Solution.	Cl ₂ O in gram-mol. per litre.	T° C.	t ₂₀₋₆₀ per cent., in minutes.		$\frac{t_{\text{Solution}}}{t_{\text{Gas}}}$
			For solution.	For gas.	
9b	0.224	70.7	50	47.5	1.05
8	0.115	71.0	105	90.5	1.16
8	0.115	59.8	257	225	1.14
7	0.126	69.8	83	90.5	0.92
6	0.095	69.7	100	122	0.82
5	0.120	80.1	55	44	1.25
5	0.120	75.3	54	61	0.89
5	0.120	65.2	139	137	1.02
5	0.120	60.1	200	211	0.95
4a	0.215	70.2	41	51	0.81
4b	0.127	70.2	88	87	1.01
4b	0.127	79.9	40	53	0.75
4c	0.064	70.2	230	172	1.34
4c	0.064	79.9	91	106	0.86
3a	0.105	70.2	107	105	1.02
3b	0.051	70.2	309	217	1.42
3c	0.024	70.2	421	452	0.93
2	0.061	60.2	267	413	0.65
2	0.061	70.7	158	175	0.91
2	0.061	80.0	66	87	0.76

have been read off from curves of the type shown in fig. 2. It is clear that the rate of reaction in solution is sensibly the same as that in the gaseous phase.

For solutions 5 to 9b, the ratio $\frac{t_{\text{solution}}}{t_{\text{gas}}}$, although not exactly unity, does not vary by more than 25 per cent., and has a mean value of 1.02. We can safely conclude that, within the limits of experimental error, the rate of decomposition in solution equals that in the gas. Solutions 5 to 9 had suffered no deterioration before use, having been stored in solid carbon dioxide, but solutions 2 to

4a were used before the advisability of taking this precaution had been realised. For solutions 2 to 4a this ratio is still, very roughly, equal to unity, but now the mean value is 0.95, which is to be expected from the fact that with these partly decomposed solutions it was possible to measure only the later stages of the reaction.

Summary.

The decomposition of chlorine monoxide in carbon tetrachloride solution proceeds at the same rate, possesses the same temperature coefficient, and apparently takes place by the same mechanism as in the gaseous state.

The retardation of bimolecular reactions by solvents, which has sometimes been revealed by the comparison of the observed rates of reactions in solution with the rates calculated theoretically, thus appears to depend on a specific influence of particular solvents, and need not occur in an "ideal" solution.

The Kinetics of Reactions in Solution. Part II.—The Decomposition of Trinitrobenzoic Acid in Various Solvents.

By E. A. MOELWYN-HUGHES and C. N. HINSHELWOOD, F.R.S.

(Received February 4, 1931.)

There are very few reactions the rate of which can be measured both in the gaseous state and in solution. Several bimolecular reactions have been investigated in solution, and since the rate of a bimolecular gas reaction can be calculated from the equation $\ln k = \ln Z - E/RT$, where E is heat of activation and Z the collision number, the rate of reaction in solution can be compared with that of the hypothetical corresponding gas reaction. The observed velocity constants in solution have usually been found to be smaller by several powers of 10 than the calculated values.* On the other hand, as shown in the previous paper, in the one example where direct comparison has been possible, namely, the decomposition of chlorine monoxide, the rate in solution in carbon tetrachloride is the same as that in the gas phase. Thus it is evident that the retardation of reactions by certain solvents is a specific action and need not occur in an "ideal" solvent.

* Christiansen, 'Z. Phys. Chem.,' vol. 113, p. 35 (1924); Norrish and Smith, 'J. Chem. Soc.,' vol. 131, p. 129 (1928).

The rates of unimolecular gas reactions cannot be calculated, and direct comparison has hitherto been possible only in two examples. The equation $\ln k = 31.69 - 24,710/RT$ has been found* to represent the rate of decomposition of nitrogen pentoxide in the gaseous state and in a series of eight similar, chemically rather inert, solvents. In nitric acid or in propylene dichloride, however, $\ln Z$ increases by several units and E becomes 28,300 calories. Daniels regards as "normal" those solvents which do not produce an alteration in E , and as "abnormal" those which cause a deviation from the value characteristic of the gaseous state. The solvents in which the decomposition of nitrogen pentoxide could be studied were naturally not very varied in character, since most liquids would be attacked chemically. Thus the impression which the results tend to convey, namely, that "normal" or "ideal" behaviour is more common with unimolecular reactions than with bimolecular reactions, may be an illusory one. In the only other known example, the isomerisation of pinene,† the rate of reaction in the gas, in the liquid, and in carbon tetrachloride is the same.

If it is recognised, however, that a reaction in certain ideal solvents such as carbon tetrachloride is almost equivalent to a gas reaction, then data relating to reactions which can only be measured in solution become available for consideration. Here the existing measurements tend to show that "normal" behaviour is not common; but the data are not nearly full enough.

The decomposition of camphorcarboxylic acid‡ exhibits a critical increment which is sensibly the same in three different solvents, namely, acetophenone, water and benzene. The data of von Halban§ and of Corran|| on the other hand, show that E and Z vary from solvent to solvent in the case of the decomposition of triethylsulphonium bromide; and a similar conclusion is evident from Dimroth's values¶ for the kinetics of the conversion of benzylhydroxy-triazole-carboxylic acid ester into the benzylamide of diazomalonic acid in various solvents. The results obtained by Wiig** for the kinetics of the decomposition of acetonedicarboxylic acid in different alcohols show that, although

* Daniels and Johnston, 'J. Amer. Chem. Soc.,' vol. 43, p. 53 (1921); Lueck, *ibid.*, vol. 44, p. 757 (1922); Eyring and Daniels, *ibid.*, vol. 52, p. 1473 (1930).

† Smith, *ibid.*, vol. 49, p. 43 (1927).

‡ Bredig and Balcom, 'Ber. Deuts. Chem. Ges.,' vol. 41, p. 740 (1908); Fajans, 'Z. Phys. Chem.,' vol. 73, p. 25 (1910).

§ von Halban, 'Z. Phys. Chem.,' vol. 87, p. 129 (1909).

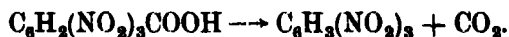
|| Corran, 'Trans. Faraday Soc.,' vol. 23, p. 605 (1927).

¶ Dimroth, 'Annalen,' vol. 373, p. 367 (1910).

** Wiig, 'J. Phys. Chem.,' vol. 32, p. 961 (1928); *ibid.*, vol. 34, p. 596 (1930).

the rates of change in ethyl alcohol and in *iso*-butyl alcohol are almost identical, the critical increments differ by over 5000 calories. An interesting regularity appears in von Halban's work on the rate of decomposition of triethylsulphonium bromide. The solvents fall into two classes—non-hydroxylic and hydroxylic. In a variety of non-hydroxylic solvents, including chloroform, the observed rates showed only small variations. If, according to our present view, these rates can be regarded as approximating to the ideal rate which the reaction would have in the gas phase, then, in the hydroxylic solvents where the rates varied much more and were about a hundred times smaller, the solvent effect appears to be a stabilising influence, analogous to that commonly found with bimolecular reactions. This conclusion must, however, be accepted with reserve, since the experiments described in the present paper show that accidental impurities in non-polar solvents may influence the rate to a very serious extent.

The present paper describes experiments on the decomposition of symmetrical trinitrobenzoic acid into trinitrobenzene and carbon dioxide



Five suitable solvents only could be found. Unfortunately carbon tetrachloride could not be used since the solubility of the acid in it is almost negligible. Nevertheless, the results are of interest in that they exemplify a behaviour which is quite obviously very far from "normal," marked changes in rate and heat of activation being found. The predominating factor with the solvents studied appears to be the presence of accelerating rather than retarding influences, pure dry solvents—especially non-polar ones—tending to give the smallest rates. Moreover, remarkable variations both in rate and heat of activation with solvents of varying purity appear. These suggest that it is dangerous to generalise too much from earlier published experiments carried out without special precautions.

General Experimental Procedure.

Trinitrobenzoic acid was prepared by the oxidation of 2 : 4 : 6 trinitrotoluene. The crystals, after having been washed with samples of nitric acid of diminishing concentrations and finally with water, were precipitated from acetone solution by addition of benzene. After washing with ether and drying at 100° C., the acid melted at $237.5 \pm 1^\circ \text{C. (corr.)}$; the uncorrected melting point of the pure acid is said to be 210° C.* (0.942 gram gave on analysis 0.947 gram of acid).

* Beilstein, "Handbuch."

A sample of trinitrobenzoic acid dissolved in the appropriate solvent was maintained at the required temperature for a measured time, after which it was rapidly added to 50 c.c. of distilled water, shaken, and titrated against N/100 baryta.

The indicator found most suitable for titrating the acid in aqueous and in nitrobenzene solutions was bromothymol blue; when analysing samples in anisole, acetophenone and toluene, phenolphthalein, cresol red and bromocresol purple were used respectively.

Constant temperature was maintained, at intervals between 60° C. and 90° C., by means of an electrically controlled thermostat of the usual type. For higher temperatures, vapour thermostats were employed, containing water, toluene or *m*-xylene, the hydrocarbons having been purified by fractional distillation in the presence of metallic sodium.

Water as Solvent.

The decomposition of trinitrobenzoic acid in conductivity water is unimolecular. Velocity constants such as the specimen values given in Table I were determined in duplicate at intervals of 5° between 70° and 100° C. The average values are summarised in Table II. By plotting $\ln k$ against $1/T$, we obtain the relation

$$\ln k = 32.85 - \frac{29,970}{RT}.$$

Table II shows that this equation represents fairly accurately the kinetics of the reaction in water, except at 60° C., where the observed velocity constant is about one-half of the value given by this equation. Repeated experiments have failed to reveal any error. Why the applicability of the Arrhenius equation should cease in this instance at temperatures below 70° C. remains unexplained. The result is interesting if only as an indication of the unreliability of critical increment values calculated from velocity constants determined at two temperatures only.

Table I.—Unimolecular Velocity Constants for the Decomposition of Trinitrobenzoic Acid in Various Solvents.

Column 1 denotes time, in minutes; column 2 gives cubic centimetres of 0.01N baryta equivalent to reaction sample; column 3 contains unimolecular velocity constants $\times 10^{-6}$ seconds $^{-1}$.

Solvent, water. Temperature, 90° C.			Solvent, 0.0368 N. NaOH. Temperature, 90° C.		
0	55.46	—	0	52.55	—
18	46.43	185	32	40.67	180
31	40.97	163	53	38.15	179
55	31.86	167	66	24.16	183
79	25.37	165	117	12.47	178
157	11.66	166	185	3.83	181
Inf.	0.00	—	Inf.	—3.68	—
165			180		
Solvent, anisole. Temperature, 80.1° C.			Solvent, nitrobenzene (γ). Temperature, 139.6° C.		
0	18.70	—	0	16.64	—
1590	14.03	3.39	20	14.49	116
3055	10.73	3.48	30	13.66	111
4230	9.05	3.35	73	10.14	114
5665	7.05	3.44	93	8.92	113
7115	5.50	3.56	239	3.35	114
8565	4.76	3.39	Inf.	0.12	—
Inf.	1.80	—	114		
3.44					
Solvent, nitrobenzene (α). Temperature, 70° C.			Solvent, acetophenone (α). Temperature, 139.6° C.		
0	37.00	—	0	24.04	—
90	24.03	68.8	3	15.72	2690
140	19.64	68.6	5.25	11.57	2720
190	16.25	67.4	9	7.37	2720
240	13.20	68.2	12.5	5.36	2640
290	10.57	69.4	15	4.36	2650
Inf.	0.24	—	Inf.	2.36	—
68.5			2680		
Solvent, acetophenone (β). Temperature, 70° C.			Solvent, toluene. Temperature, 100° C.		
0	29.43	—	0	22.93	(0.296)
3000	21.50	1.84	1380	22.35	0.302
4000	19.52	1.81	4260	21.17	0.313
5000	17.80	1.77	7560	19.76	0.328
6000	16.03	1.79	9780	18.61	0.356
7000	14.57	1.78	17040	14.47	0.449
8000	13.16	1.80	Inf.	0.00	—
9000	11.90	1.77			
10000	10.69	1.82			
11000	9.56	1.85			
Inf.	1.25	—			
1.80					

$$k_{\infty} = 2.96 \times 10^{-7}.$$

Table II.

Solvent.	Temperature.	Unimolecular constant $\times 10^6$ (seconds ⁻¹).		
		Average for each Expt.	General average.	Calculated value.
Water	60	1.73	(1.74)	3.33
		1.75		
		1.75		
	70	13.5	13.2	12.7
		12.9		
	75	22.0	22.0	23.6
	80	43.8	44.8	43.9
		45.7		
	85	73.7	73.7	79.9
	90	165	161	142
		156		
		430		
	100	420	425	439
Anisole	70	0.84	0.84	0.81
	80.1	0.84		
		3.44	3.36	2.92
	110.4	3.27		
		95.2	95.1	94.6
	139.6	95.0		
		1730	1730	1800
		1730		
Nitrobenzene (α)	60	12.8	(12.9)	27.5
		12.9		
	70	68.5	69.3	69.2
		70.0		
	80.1	185	182	174
	100	179	911	912
		906		
		916		
Nitrobenzene (β)	60	6.24	6.28	6.35
		6.33		
	85	104	104	103
	100	564	564	571
		564		
	110.4	1040	1040	1240
		1040		
Nitrobenzene (γ)	85	0.168	0.168	0.166
	100	1.34	1.34	1.35
	110.9	4.50	4.56	4.68
		4.62		
	139.6	114	114	112
Acetophenone (α)	90	25.4	26.1	26.1
		26.8		
	100	62.3	62.6	64.0
		62.9		
	110.4	159	156	154
		154		
	139.6	2680	(2700)	1470
		2710		
		678		
		680	(679)	

Table II—(continued).

Solvent.	Temperature.	Unimolecular constant $\times 10^4$ (seconds ⁻¹).		
		Average for each Expt.	General average.	Calculated value.
Acetophenone (β)..	70	1.80 1.81	} 1.80	1.79
	100.1	38.8		36.6
	110.4	96.4	} 93.6	94.0
	139.6	90.7		
		1000	1000	1010
Toluene	85	0.0447	0.0447	0.0457
	100	0.296	0.296	0.276
	110.4	0.850	0.850	0.891

Table III below contains the results of experiments conducted on the change in the velocity of decomposition at 90° C. produced by addition of small amounts of hydrochloric acid and of sodium hydroxide. The reaction is catalysed by both acid and base but the effect is very slight. Hydrogen chloride does not influence the rate at which carbon dioxide is evolved from camphorcarboxylic acid,* and picric acid is without effect on the rate of decomposition of trichloroacetic acid in aniline.† Organic bases are, however, moderately good catalysts for the former reaction in various solvents,‡ the magnitude of the catalytic effect being of the same order as that recorded above.

Table III.

Catalyst.	Concentration of catalyst.	$k_{90^\circ \text{C.}} \times 10^4$.
	millimoles/litre.	seconds ⁻¹
HCl	3.75	1.97
HCl	1.25	1.73
Water	0.00	1.61
NaOH	1.23	1.23
NaOH	3.68	1.80

Anisole as Solvent.

10 c.c. samples of a filtered solution of trinitrobenzoic acid in redistilled anisole were delivered into soda-glass tubes, which were drawn out in long

* Bredig and Baloom., *loc. cit.*

† Goldschmidt and Bräuer, 'Berichte,' vol. 39, p. 109 (1906).

‡ Bredig, 'Z. Elektrochem.,' vol. 24, p. 285 (1918).

capillaries and kept, unsealed, in the thermostats. The difficulty of titrating the acid in the presence of anisole was to some extent overcome by allowing the undisturbed reaction samples to stand in the presence of excess alkali, which was subsequently back-titrated against equivalent acid in the usual way.

The kinetics of the reaction, which are summarised thus

$$\ln k = 31.13 - \frac{30,730}{RT}$$

are similar to those in water. At 60° C. the rate of reaction in anisole is 1.95×10^{-7} seconds⁻¹; in water at the same temperature the rate is 3.33×10^{-6} seconds⁻¹. Hence changing the solvent from water to anisole has resulted in a decrease in the velocity coefficient and an increase in the energy of activation.

Nitrobenzene as Solvent.

It soon became evident that the catalytic properties of nitrobenzene were intimately related to its history, for specimens of the solvent which differed only very slightly in their preparation allowed the reaction to proceed at widely different rates. It seemed natural to ascribe this erratic behaviour to the presence of varying amounts of water in the solvent. In the first sample (solvent α), omitting the value of the velocity coefficient for the lowest temperature, the kinetics of the reaction are accurately summarised by the relation

$$\ln k = 22.34 - \frac{21,700}{RT}.$$

In solvent β , however, which differed from the previous one in that it had been stored for weeks over anhydrous calcium chloride before being distilled, the rates of reaction were now invariably lower than those obtained with solvent α (Table II). Furthermore, the Arrhenius equation is now

$$\ln k = 27.97 - \frac{\quad}{RT}.$$

Since drying the solvent in a crude way produced such a marked change in its catalytic properties, it became of interest to study the effect of intensively dried nitrobenzene on the kinetics of the reaction. A series of experiments was made with a sample (γ) of nitrobenzene which had been purified and dried for electrical conductivity purposes.* Recrystallised thiophene-free benzene was nitrated in the cold, and the nitrobenzene frozen out. Different samples, after being dried over and distilled from phosphorus pentoxide under reduced

* Sir Harold Hartley kindly supplied the pure nitrobenzene.

pressure, gave specific conductivity values fluctuating slightly about a mean value of 1.7×10^{-7} ohms $^{-1}$. Dry crystals of the acid were added to this solvent, which was left unfiltered. The reaction was carried out in a soda-glass vessel which was specially designed to enable samples of the solution to be removed without allowing the entrance of atmospheric moisture. A graduated pipette and a long air-inlet tube (which also acted as a reflux condenser) were sealed on to the reaction vessel; both were fitted with ground-in tubes containing phosphorus pentoxide.

In this solvent the reaction proceeded at a rate several thousand times as slow as in the "wet" solvents. Using solution α at 85° C., the time of half completion is 48 minutes; with solution β the reaction is half complete after 2 hours; with solution γ under the same conditions, the reaction, which was at first thought to have been completely inhibited, proved on a careful examination to be proceeding at a rate corresponding to a half-life of 51.5 days. In a few of the experiments with solvent γ , the unimolecular constant exhibited an increase with time—a phenomenon probably attributable to the progressive absorption of impurity, such as tap-grease or moisture. Generally, however, the reaction followed the unimolecular law, and the constants could be duplicated as shown in Table II. The critical increment of the reaction was now 34,990 calories; the kinetics of the decomposition over a range of 55° C. are given by the relation

$$\ln k = 33.75 - \frac{34,990}{RT}.$$

Two questions now present themselves: (1) Does the slight change in the quality of nitrobenzene produce such pronounced changes in the rates at which other reactions proceed in this solvent? and (2) Is the catalytic activity of other organic solvents as sensitive to traces of water as that of nitrobenzene?

Acetophenone as Solvent.

Unimolecular velocity constants were determined in duplicate over a range of 50° C. With acetophenone purified by crystallisation (solvent α) the results conformed to the equation

$$\ln k = 23.00 - \frac{24,130}{RT},$$

except at 139.6° C., where reproduction of results became difficult.

In view of the surprising changes exhibited by nitrobenzene after careful purification and drying, it seemed desirable to subject acetophenone to a similar treatment. It was purified by washing with dilute hydrochloric acid

and with water, and by fractional crystallisation. The fraction melting at 21° C. was dried over and fractionally distilled from phosphorus pentoxide under reduced pressure (72·6° C./6 mm. Hg). With this solvent (solvent β) the velocity constants were determined in duplicate, employing the same apparatus as that used with dry nitrobenzene. Over a range of 70° C. the kinetics of the reaction are accurately represented by the equation

$$\ln k = 24 \cdot 23 - \frac{25,450}{RT}.$$

Purification of the solvent in this case has lowered the velocity to about one-half the previous value, and has increased the critical increment by only 1300 calories. Purification of nitrobenzene, on the other hand, reduced the rate of reaction in the ratio of about 7000 : 1, and increased the value of the critical increment by 13,300 calories. Reverting to question (2) raised above, then, it can safely be stated that, as far as this reaction goes, the catalytic behaviour of nitrobenzene as a solvent is anomalous. Hehlgers* has shown that certain of the physical properties of nitrobenzene (particularly the electrical conductivity) are highly influenced by the merest trace of impurity.

Toluene as Solvent.

Investigation of the rate of decomposition of trinitrobenzoic acid in toluene was rendered somewhat difficult by the small solubility and low rate of reaction, and by the sensitiveness of the change to the presence of impurity. The experimental method was that described in the section on anisole, except that a larger volume of solution (25 c.c.) was used. The chief points of interest are (1) when ordinary toluene, purified by distillation, is used, the reaction is unimolecular although exact duplication of results is difficult. The observed velocity constants are greater than, and the observed heat of activation is less than, the corresponding values for the dry solvent; (2) with both the crude and the dry solvents, water acts as a powerful positive catalyst; (3) when working with toluene which had been fractionally distilled in the presence of sodium, the reaction was in some cases inhibited for an indefinite period. As a rule, however, titre-time curves gave a unimolecular "constant" increasing slightly as the reaction proceeds (see specimen in Table I). In this instance, the true value of k is taken as the extrapolated value corresponding to zero time. This tendency is probably attributable to the accumulation of traces

* Hehlgers, 'Phys. Z.,' vol. 30, p. 942 (1929).

of water; (4) the kinetics of the decomposition in pure toluene are given approximately (see Table II) by the relation

$$\ln k = 27.68 - \frac{31,600}{RT},$$

in which the heat of activation is correct only to within about 2000 calories. The rate of decomposition in toluene at all temperatures is thus several hundred times lower than the speed of the reaction in water.

Discussion.

The results are summarised in Table IV. It is to be noted that the energy of activation is 5000 calories greater in pure nitrobenzene, and 5000 calories less in pure acetophenone, than it is in water. The magnitude of these quantities leaves no doubt whatsoever that, as far as the unimolecular decomposition of trinitrobenzoic acid is concerned, change of solvent can bring about a real, and very considerable, variation in the value of E . In this respect the reaction behaves similarly to those studied by von Halban,* Corran,* Dimroth,* and Wiig,* where the dependence of the value of E on the nature of the solvent is, although not as pronounced as that recorded here, quite definite. Not only E but also $\ln Z$ for this reaction varies from solvent to solvent, and there is a rough proportionality between E and $\ln Z$.

Table IV.

Solvent.	E .	$\ln Z$.	$k_{300^\circ \text{C.}}$
	Calories		Seconds ⁻¹
Water	29,970	32.85	3.33×10^{-4}
Anisole	30,730	31.13	1.97×10^{-7}
Nitrobenzene (α)	21,700	22.34	2.75×10^{-5}
Nitrobenzene (β)	26,320	27.97	6.35×10^{-6}
Nitrobenzene (γ)	34,990	33.75	4.07×10^{-9}
Acetophenone (α)	24,130	23.00	1.25×10^{-6}
Acetophenone (β)	25,450	24.23	5.79×10^{-7}
Toluene	31,600	27.68	1.62×10^{-8}

It is remarkable that there is a greater difference in the rates of reaction in two different samples (α and γ) of nitrobenzene than there is between the rates in any two pure solvents, i.e., the accidental variation in k and E caused by impurity in this solvent exceeds in magnitude any change which can be induced by altering the medium designedly. It is to be observed that the

* *Loc. cit.*

approximate parallelism existing between E and $\ln Z$ for pure solvents is found also for different specimens of the same solvent. The very marked change in the velocity of reaction and in the heat of activation caused by traces of impurity in nitrobenzene, while being important in itself, raises the problem of the mechanism of the catalytic effect. The catalyst may function either (1) by forming a reactive complex with the reactant, thus converting the change into what is really a bimolecular reaction, or (2) by altering the properties of the medium, such as the electrical properties quoted by Hehlhans.* The first explanation will not account for the *gradual* decrease in E with increase in the amount of catalyst, which should merely increase the number of encounters between molecules without progressively changing the heat of activation. The second suggestion thus seems the more probable.

The problems raised here, however, like those which have been previously mentioned, must be further studied by the comparison of data for as many different kinds of reaction as possible.

Summary.

The aim of this investigation has been to determine, by the study of a new reaction, whether constancy of rate and heat of activation with change of solvent can be regarded as the usual characteristic of a unimolecular reaction. Velocity constants have been determined for the decomposition of trinitrobenzoic acid over a temperature range of 70° C. in five solvents, viz., water, anisole, nitrobenzene, acetophenone and toluene. The heats of activation for this reaction in pure dry acetophenone, in water, and in pure dry nitrobenzene are 25,500, 30,000 and 35,000 calories respectively. This very considerable change in E with the nature of the medium is in direct contrast to the behaviour of nitrogen pentoxide, but the contrast is probably due to the difference in the types of solvent which can be used for the two reactions.

The rate of reaction in water is but slightly influenced by either hydrochloric acid or sodium hydroxide. The velocity of decomposition and the energy of activation are dependent on the purity of the solvent, especially with nitrobenzene. Careful purification and drying of acetophenone lowers the rate of reaction to about one-half its previous value, and raises the critical increment by 1500 calories; similar treatment with nitrobenzene causes k to decrease about 7000-fold and E to increase by 13,000 calories. In toluene also, water acts as a powerful positive catalyst. The rate of reaction in toluene is at all temperatures several hundred times lower than in water.

* *Loc. cit.*

We are indebted to Imperial Chemical Industries, Ltd., for a grant by the aid of which apparatus and materials for this investigation have been purchased. One of the authors also desires to express his thanks to the Department of Scientific and Industrial Research for the award of a Senior Research Scholarship.

The Forces on a Solid Body Moving Through Viscous Fluid.

By S. GOLDSTEIN.

With notes in the text by J. M. BURGERS.

(Communicated by H. Jeffreys, F.R.S.—Received October 31, 1930.)

In a previous paper with the same title* a general theorem was stated concerning the resultant force on a solid body of any size and shape moving with uniform velocity U through otherwise still fluid of density ρ . The discussion then given was not sufficiently general. This was pointed out to me by Professor Burgers, to whom I wish to express my thanks for the great interest he has shown in the matter. My thanks are also due to Dr. Jeffreys for valuable criticisms of the first draft of this paper, which has been largely rewritten in consequence.

In the previous discussion the equations (P.4)† give the solution only when the solid body is of revolution,‡ and they are not sufficiently general. To recognise this, it is sufficient to note that they give no component of vorticity about the direction of the stream.

A new discussion is therefore given below. For the connection between this paper and the previous one, see also p. 202, footnote.

As before, we begin with the case of a solid body fixed in a stream of velocity U , and consider the motion, supposed to have become steady, inside a surface S , which is at a great distance from the body in all directions. We take an origin of rectangular co-ordinates (x_1, x_2, x_3) anywhere within the body, with the axis of x_1 in the direction of the velocity U . We denote by $(U + u_1, u_2, u_3)$ the components of fluid velocity at the point (x_1, x_2, x_3) , and, assuming

* 'Proc. Roy. Soc.' A, vol. 123, pp. 216–225 (1929).

† References to the previous paper mentioned above will be given in this way. Thus equation (P.4) and p. P.220 mean equation (4) and p. 220 of that paper respectively.

‡ See Lamb's 'Hydrodynamics,' § 340.

that at a great distance from the body u_1 , u_2 and u_3 are small, and that the squares of small quantities may be neglected, we take the equations of motion at a great distance to be

$$U \frac{\partial u_i}{\partial x_1} + \frac{1}{\rho} \frac{\partial p}{\partial x_i} = \nu \nabla^2 u_i \quad (i = 1, 2, 3), \quad (1)$$

where p is the pressure, and ν the kinematic viscosity. The equation of continuity is

$$\frac{\partial u_i}{\partial x_i} = 0, \quad (2)$$

with the convention that when a general suffix occurs twice, as in (2), summation for the values 1, 2 and 3 of the suffix is implied. It follows from (1) and (2) that

$$\nabla^2 p = 0. \quad (3)$$

We now obtain a particular solution of (1) and (2) if we write*

$$p = -\rho U \frac{\partial \phi}{\partial x_1}, \quad (4)$$

and

$$u_i = \frac{\partial \phi}{\partial x_i}, \quad (5)$$

where

$$\nabla^2 \phi = 0. \quad (6)$$

If the complete solution is

$$u_i = \frac{\partial \phi}{\partial x_i} + w_i, \quad (7)$$

then

$$\left(\nabla^2 - 2k \frac{\partial}{\partial x_1} \right) w_i = 0, \quad (8)$$

and

$$\frac{\partial w_i}{\partial x_i} = 0, \quad (9)$$

where

$$k = U/2\nu. \quad (10)$$

We must now consider at some length the nature of this solution, and, in particular, of the function ϕ .

* Lamb's 'Hydrodynamics,' *loc. cit.*

We first note that the pressure, p , satisfies Laplace's equation, and we take it to have continuous second derivatives in the infinite region bounded by a sphere containing the solid body in its interior,* and to be regular at infinity, so that it may be expanded, in this region, in a uniformly convergent series of solid spherical harmonics of negative degree. A value of ϕ may be found by term by term integration of equation (4) to satisfy the condition (6); but this condition leaves ϕ indeterminate to the extent of an additive function of x_2 and x_3 satisfying Laplace's equation. Further restrictions may therefore be imposed, and since u_i must be continuous in the fluid and tend to zero at infinity,† we might try to make $\partial\phi/\partial x_i$, which is the part of u_i dependent on ϕ , satisfy the same conditions. We should find, however, that these conditions are, in general, too severe to allow of a solution being found at all; and, after consideration of the nature of the solutions of the equation (8) satisfied by the remaining part, w_i , of the u_i , we are led to impose the above conditions on ϕ not everywhere in the fluid, but only outside the wake. Expressed mathematically, the conditions are that $\partial\phi/\partial x_i$ must be continuous in the fluid except when x_1 is positive and x_2 and x_3 zero, and must tend to zero at infinity except in the direction $x_2 = x_3 = 0$, x_1 positive.

Methods of obtaining the general value of ϕ under these conditions are easy to find. In the first place, differentiation of the $(2n - 1)$ solid spherical harmonics of degree $-n$ with respect to x_1 gives $(2n - 1)$ solid spherical harmonics of degree $-(n + 1)$, so that of the $(2n + 1)$ solid spherical harmonics of degree $-(n + 1)$ that p may contain, the terms in ϕ corresponding to all except two of them are themselves solid spherical harmonics (of degree $-n$); and therefore are continuous, with derivatives continuous and regular at infinity. The two exceptional solid spherical harmonics of degree $-(n + 1)$ in p are obtained from those two rational integral harmonics of degree n that are functions only of x_2 and x_3 by dividing them by r^{2n+1} ; and the corresponding terms in ϕ are of degree $-n$ and satisfy Laplace's equation, but are not solid

* We are concerned with the motion not everywhere outside the body, but only at a sufficiently great distance from it to allow of equations (1) being approximations to the equations of motion. Nevertheless, for the sake of brevity, we shall later refer to this region as "in the fluid" without qualification.

† We are, strictly speaking, not entitled to consider what happens at infinity, but only inside a surface in the interior of which the motion has become steady. The surface may, however, be at as great a distance from the origin as we please, if we consider the beginning of the motion to be sufficiently far in the past. The mathematical difficulty persists, but will not affect the physical conclusions.

spherical harmonics of degree $-n$. They are therefore not continuous. They may fairly easily be found as

$$\int_{-\infty}^{x_1} \frac{f(x_2, x_3)}{r^{2n+1}} dx_1,$$

where r is the positive square root of $x_1^2 + x_2^2 + x_3^2$.*

The terms in ϕ may be easily obtained otherwise. For all solid spherical harmonics of negative degree can be obtained by repeated differentiation of r^{-1} , and all the terms in ϕ can therefore be obtained by differentiation of the term corresponding to

$$-p/\rho U = \partial\phi/\partial x_1 = r^{-1}. \quad (11)$$

It will easily be verified that

$$\phi = -\log(r - x_1) \quad (12)$$

satisfies all the required conditions when p is given by (11); and the values of ϕ corresponding to other values of p may now be found by differentiation. A few of these values are given in the table below.

$-p/\rho U.$	$\phi.$
$\frac{\partial}{\partial x_1} \left(\frac{1}{r} \right) = -\frac{x_1}{r^3}$	$\frac{1}{r}$
$\frac{\partial}{\partial x_2} \left(\frac{1}{r} \right) = -\frac{x_2}{r^3}$	$-\frac{x_2}{r(r-x_1)}$
$\frac{\partial}{\partial x_3} \left(\frac{1}{r} \right) = -\frac{x_3}{r^3}$	$-\frac{x_3}{r(r-x_1)}$
$\frac{\partial^2}{\partial x_1 \partial x_2} \left(\frac{1}{r} \right) = \frac{3x_1 x_2}{r^5}$	$-\frac{x_2}{r^3}$
$\frac{\partial^2}{\partial x_1 \partial x_3} \left(\frac{1}{r} \right) = \frac{3x_1 x_3}{r^5}$	$-\frac{x_3}{r^3}$
$\frac{\partial^2}{\partial x_1^2} \left(\frac{1}{r} \right) = \frac{3x_1^2 - r^2}{r^5}$	$-\frac{x_1}{r^3}$
$\frac{\partial^2}{\partial x_2 \partial x_3} \left(\frac{1}{r} \right) = \frac{3x_2 x_3}{r^5}$	$\frac{x_2 x_3}{r^3} \left[\frac{1}{r(r-x_1)} + \frac{1}{(r-x_1)^2} \right]$
$\frac{\partial^3}{\partial x_1^3} \left(\frac{1}{r} \right) - \frac{\partial^3}{\partial x_2^3} \left(\frac{1}{r} \right) = \frac{3(x_1^3 - x_2^3)}{r^5}$	$\frac{x_1^3 - x_2^3}{r^3} \left[\frac{1}{r(r-x_1)} + \frac{1}{(r-x_1)^2} \right]$

* A fairly simple physical interpretation of these potentials can be given. For $f(x_2, x_3)/r^{2n+1}$ will be the potential of a certain system of doublets at the origin, and since

$$\int_{-\infty}^{x_1} \frac{f(x_2, x_3)}{r^{2n+1}} dx_1 = \int_{-\infty}^{x_1} \frac{f(x_2, x_3)}{(\xi^2 + x_2^2 + x_3^2)^{\frac{2n+1}{2}}} d\xi_1 = \int_0^\infty \frac{f(x_2, x_3)}{((x_1 - x)^2 + x_2^2 + x_3^2)^{\frac{2n+1}{2}}} dx,$$

the integral gives the potential of the corresponding line distribution of doublets stretching

The value of ϕ corresponding to any value of p may be found in this way, and it will be seen that ϕ is single-valued,[†] and, in general, discontinuous.

The pair of corresponding values of p and ϕ given by (11) and (12) were used as fundamental values, from which all others can be derived by differentiation; but these values themselves cannot occur. For according to (12) we should have $\partial\phi/\partial r = -r^{-1}$, and this term in the radial velocity component would give infinite inflow through a large sphere. Further, as we shall see, the inflow calculated from the w -terms must always be finite.

Before passing to a consideration of w , it remains to point out that the solution for ϕ corresponding to a given p is unique. This we prove as follows. If ϕ' is the difference of two solutions, $\partial\phi'/\partial x_1$ is zero, and ϕ' is a function only of x_2 and x_3 . If x_1 tends to minus infinity, x_2 and x_3 remaining constant, $\partial\phi'/\partial x_2$ and $\partial\phi'/\partial x_3$ must tend to zero; but since they are independent of x_1 they will remain constant, and must therefore be identically zero, so that ϕ' must be independent of x_1 , x_2 and x_3 .

We must now consider the w , and we note first that $u_i = w_i + \partial\phi/\partial x_i$ must be finite and continuous in the fluid (with finite and continuous derivatives) and tend to zero at infinity. Hence w_i may be divided into two parts, w_i' and w_i'' , each of which satisfies (8) and (9), and of which the latter, w_i'' , satisfies the conditions of continuity and the conditions at infinity separately, while the former, w_i' , cancels out the discontinuities in $\partial\phi/\partial x_i$.

Now w_i'' , being a continuous solution of (8) tending to zero at infinity in all

along the x_1 -axis from the origin to plus infinity. In particular, x_3/r^2 gives the potential of a simple doublet along the x_3 -axis at the origin, and the corresponding value of ϕ , namely, $x_3/(r - x_1)$, is the potential of the corresponding line doublet stretching from the origin along the x_1 -axis to plus infinity. Again, a doublet has the same potential as a vortex filament bounding an infinitely small plane area if the strength of the doublet is equal to the product of the area and the strength of the vortex, and the doublet is along the normal to the area. It follows that a line doublet, stretching to infinity in one direction, has the same potential as a "horse-shoe" vortex (of the type encountered in approximate aerofoil theory), of infinitesimal breadth, if the strength of the doublet per unit length is equal to the product of the strength of the vortex and the breadth of the "horse-shoe"; and $x_3/(r - x_1)$ is the potential of such a "horse-shoe" vortex, with the "trailing" vortices along the axis of x_1 from the origin to plus infinity, and the "bound" vortex of infinitesimal span, along the x_3 -axis. This last result was communicated to me by Professor Burgers without proof.

[†] Since ϕ is single-valued, it follows from the discussion in the previous paper that for flow past a body of revolution with its axis along the stream, there would be no circulation round a circuit at a great distance cutting the wake at right angles, and no lift in steady motion, or no average lift in quasi-periodic or turbulent motion (which is what we should expect for a body of revolution).

directions, is of order $e^{-k(r-x_1)}/r$ at infinity, just as, if there are no sources of sound at infinity, the solution of the equation of sound propagation is of order $e^{\pm ikr}/r$. Thus w_i'' is insensible except when $r - x_1$ is small or moderate. Also the outflow through a large sphere calculated from this part of the fluid velocity must be finite, and could not balance an infinite inflow calculated from $\phi = -\log(r - x_1)$.

We shall now show how to calculate w_i' term by term so that its discontinuities cancel out those in $\partial\phi/\partial x_i$; and we shall begin with the case in which $\phi = -\log(r - x_1)$, and derive the solutions corresponding to other values of ϕ by differentiation, as before. We have, however, already stated (and the proof of the statement will be completed below) that the term $-\log(r - x_1)$ cannot occur in ϕ , so that the solution in this case will not be completed.

Now if

$$-\int_s^\infty \frac{e^{-ks}}{s} ds, \quad (13)$$

where

$$s = r - x_1, \quad (14)$$

then

$$\frac{\partial\psi}{\partial x_1} = -\frac{e^{-k(r-x_1)}}{r}, \quad \frac{\partial\psi}{\partial x_2} = \frac{x_2}{r} \frac{e^{-k(r-x_1)}}{r-x_1}, \quad \frac{\partial\psi}{\partial x_3} = \frac{x_3}{r} \frac{e^{-k(r-x_1)}}{r-x_1}, \quad (15)$$

so that if

$$w_i' = \partial\psi/\partial x_i, \quad (16)$$

the singularities in w_i' cancel out the singularities in $\partial\phi/\partial x_i$, when ϕ is $-\log(r - x_1)$.

Also

$$\left(\nabla^2 - 2k \frac{\partial}{\partial x_1}\right)\psi = 0, \quad (17)$$

so that w_i' satisfies (8), but

$$\frac{\partial w_i'}{\partial x_i} = \nabla^2\psi = 2k \frac{\partial\psi}{\partial x_1} = -2 \frac{ke^{-k(r-x_1)}}{r}, \quad (18)$$

so that (9) is not satisfied. To complete the solution we should have to add on to w_i' a continuous solution of (8), with $\partial w_i'/\partial x_i$ equal and opposite to the value given by (18). This we shall not do, nor shall we consider the question of the existence of such a solution, for the reason given above.

Now, corresponding to the first three values of ϕ in the table on p. 201, we should begin by writing,

$$w_i' = \partial^2\psi/\partial x_j \partial x_i, \quad (19)$$

with $j = 1, 2$ or 3 respectively. This would satisfy (8), and would give

$$\frac{\partial w_i'}{\partial x_j} = - \frac{\partial}{\partial x_j} \left(\frac{2ke^{-k(r-x_1)}}{r} \right), \quad (20)$$

so that the solution is completed by adding on to (19)

$$w_j' = 2ke^{-k(r-x_1)}/r, \quad (21)$$

which also satisfies (8). It is to be noticed that in this way we have obtained Oseen's fundamental solution, quoted by Professor Burgers below (p. 206). Solutions for w_i' corresponding to other values of ϕ may now be found by differentiating (19) and (21). It will be seen that part of w_i' is the gradient of a single-valued function (cp. (19)); that the remaining part is continuous in the fluid (cp. (21)); and that w_1' and its derivatives and the x_1 -derivatives of w_2' and w_3' are also continuous in the fluid.

Lastly, we remark that w_i' is of order $e^{-k(r-x_1)}/r$ at infinity, and that the term in w_i' necessary to complete the solution begun in equations (13) to (18), being a continuous solution of (8) vanishing at infinity, would in any case be of this order; so that the outflow through a large sphere calculated from w_i' would be finite. This completes the proof of the statement previously made, that the term $-\log(r-x_1)$ in ϕ cannot occur.

We now turn to the formula for the lift. We shall denote the vorticity components by ξ_i ; the resultant of the fluid pressures on the solid in the direction x_i by F_i ; and the angle made by the radius vector with the axis of x_1 by θ . We are going to integrate over the surface S , which is at a great distance from the origin in all directions.

Then from equations (P.44), (P. 45) and (P.46)

$$F_2 = \int (-n_2 p + \mu n_1 \xi_3 - \mu n_3 \xi_1 - \rho U n_1 u_2) dS. \quad (22)$$

Now ξ_i is of order $e^{-k(r-x_1)}/r$ at infinity. If S cuts the wake at right angles, n_2 and n_3 vanish with θ . Hence

$$\int n_3 \xi_1 dS \quad (23)$$

vanishes in the limit. Also

$$\int n_1 \xi_3 dS = \int n_1 \left(\frac{\partial w_3}{\partial x_1} - \frac{\partial w_1}{\partial x_3} \right) dS, \quad (24)$$

and, since $\partial w_3/\partial x_1$ contains terms of order $e^{-k(r-x_1)}/r^2$ and $(1 - \cos \theta)e^{-k(r-x_1)}/r$ at infinity,

$$\int n_1 \frac{\partial w_3}{\partial x_1} dS \quad (25)$$

vanishes in the limit. Again, in the limit,

$$\int n_2 \frac{\partial w_1}{\partial x_1} dS \quad (26)$$

vanishes, so that

$$-\int n_1 \frac{\partial w_1}{\partial x_2} dS = \int \left(n_2 \frac{\partial w_1}{\partial x_1} - n_1 \frac{\partial w_1}{\partial x_2} \right) dS, \quad (27)$$

which vanishes identically, w_1 being continuous and single-valued (cp. equations (P.31) to (P.33)). Thus, in the limit,

$$\int (n_1 \xi_3 - n_3 \xi_1) dS = 0. \quad (28)$$

Again

$$p = -\rho U \partial \phi / \partial x_1 = -\rho U (v_1 - w_1), \quad (29)$$

and

$$\int n_2 w_1 dS = 0 \quad (30)$$

in the limit, so that

$$F_2 = -\rho U \int (n_1 u_2 - n_3 u_1) dS. \quad (31)$$

This is the result required. In calculating the integral we may omit the terms in $\partial \phi / \partial x_i$ together with that part of the w_i which is the gradient of a single valued function, since for these terms the integral vanishes. And since

$$\int n_2 w_1 dS \quad (32)$$

vanishes, we may write

$$F_2 = -\rho U \int n_1 w_2 dS, \quad (33)$$

where the discontinuous part of w_2 is to be omitted.

We may also briefly notice the revised calculation of the drag. From equations (P.28), (P.29) and (P. 35)

$$F_1 = \int (-n_1 p + \mu n_3 \xi_2 - \mu n_2 \xi_3 - \rho U n_1 u_1) dS, \quad (34)$$

since

$$\int n_1 u_1 dS = 0. \quad (35)$$

As before,

$$\int (n_2 \xi_3 - n_3 \xi_2) dS \quad (36)$$

vanishes in the limit if S cuts the wake at right angles. Substituting

$$-\rho U \partial \phi / \partial x_1$$

for p , we find

$$F_1 = -\rho U \int n_1 w_1 dS, \quad (37)$$

which is the result required. For the inflow along the wake is

$$-\int n_1 w_1 dS \quad (38)$$

and

$$\int (n_2 w_2 + n_3 w_3) dS \quad (39)$$

vanishes in the limit.

In the previous paper the solution adopted made $\xi_1 = 0$. In this connection Professor Burgers wrote, "According to the Lanchester-Prandtl theory, lifting force is always connected with the appearance of vortices stretching out in the direction of the x_1 -axis (i.e., of the general flow U).

Oseen's expressions, on the other hand, give such a system of vortices, as will be seen when we look at the formulæ

$$u_i = A_n \left\{ \delta_{ik} \nabla^2 \Phi - \frac{\partial^2 \Phi}{\partial x_i \partial x_k} \right\}, \quad (40)$$

$$\Phi = \frac{1}{k} \int_0^{k(r-a)} \frac{1-e^{-\alpha}}{\alpha} d\alpha, \quad (41)$$

$$\left. \begin{aligned} \delta_{ik} &= 1 & (i=k) \\ &= 0 & (i \neq k) \end{aligned} \right\}, \quad (42)$$

which constitute a special solution of Oseen's equations (Oseen's 'Hydrodynamik,' pp. 31-33). They describe the motion that will arise when a force with components equal to $8\pi\mu A_n$ acts in the fluid at the origin. Let us take, for instance, $A_1 = 0$, $A_2 = 0$, $A_3 \neq 0$. Then

$$\xi_1 = -A_3 \frac{\partial}{\partial x_3} \nabla^2 \Phi. \quad (43)$$

Now

$$\nabla^2 \Phi = 2e^{-k(r-a)}/r; \quad (44)$$

hence we find approximately (neglecting terms of order r^{-2}):

$$\xi_1 = 2A_3 k x_3 e^{-k(r-a)}/r^2. \quad (45)$$

For a negative force A_2 (the reaction of a lifting force), we have $\xi_1 > 0$ for x_2 negative and $\xi_1 < 0$ for x_2 positive, so that we get a distribution of vortices of a general type reminding us immediately of the Lanchester-Prandtl system."

The general formula for the lift may be illustrated from the case discussed by Professor Burgers, when a force $8\pi\mu$ acts at the origin in the direction of the axis of x_2 . For then, according to (33),

$$F_2/\rho U = - \int n_1 \nabla^2 \Phi \, dS. \quad (46)$$

Taking S to be a sphere, we have

$$F_2/\rho U = - \int_0^{2\pi} \int_0^\pi 2e^{-kr(1-\cos\theta)} r \cos\theta \sin\theta \, d\theta \, d\varpi. \quad (47)$$

The integrand is sensible only when θ is small, and on working out the integral by the method on p. P.220, we find

$$F_2/\rho U = -4\pi/k, \quad (48)$$

or

$$F_2 = -8\pi\mu, \quad (49)$$

the reaction of the force acting on the fluid at the origin.

Professor Burgers writes, concerning this last calculation and the similar calculation for the drag: "It shows that the theorem is true for a single force. Hence it also applies to a system of forces, provided the surface S is taken so great that the points of application of all forces lie within it. Now the hydrodynamical equations can be written

$$U \frac{\partial u_i}{\partial x_1} + \frac{1}{\rho} \frac{\partial p}{\partial x_i} = \nu \nabla^2 u_i + Y_i, \quad (50)$$

where

$$Y_i = X_i - u_j \frac{\partial u_i}{\partial x_j}. \quad (51)$$

Here the X_i represent the external forces. As, however, on account of the equation of continuity

$$u_j \frac{\partial u_i}{\partial x_j} = \frac{\partial}{\partial x_j} (u_j u_i) \quad (52)$$

and therefore

$$\int Y_i \, d\tau = \int X_i \, d\tau, \quad (53)$$

the resultant of the "apparent forces" Y_i which appear in Oseen's equations is equal to the resultant of the (real) external forces X_i . So, with the aid of

some suppositions regarding a sufficiently fast convergence of the integrals, the theorem can be extended to the case when the real (quadratic) equations are applied.

Lastly, the action of a body on a fluid can be represented by a system of forces acting on its surface, the interior of the body being replaced by fluid at rest. The system of forces will be rather intricate (it may be that we have to introduce infinitely great positive and negative tangential forces, acting infinitely near to each other, in order to prevent any diffusion of the motion to the interior), but the resultant of the system at any rate is equal and opposite to the resistance. As now we have the case of an unlimited field, the former considerations can be applied. This gives a second proof of the theorem."*

One last remark—about turbulent motion in the wake. Miss L. M. Swain has pointed out† that according to Prandtl's theory of turbulence the width of the wake behind a body of revolution at large distances from the body varies as $r^{\frac{1}{2}}$ and the velocity in the wake as $r^{-\frac{1}{2}}$, whereas on the theory considered here and in the previous paper the width of the wake varies as $r^{\frac{1}{2}}$ and velocity in the wake as r^{-1} . The discrepancy is not surprising, for whereas Prandtl neglects the purely viscous drag and retains only the "apparent turbulent stresses," quadratic in the velocities, what has been assumed here is that if we go far enough away we must eventually come to a region where the purely viscous drag, being linear in the velocities, must predominate. The distance required for this will be enormous.

* "It may be pointed out that the analogue in two-dimensional motion of the drag formula here obtained (first given by Filon) seems to be in contradiction with a result obtained by Zeilon ('K. Svenska Vetensk. Handl.,' vol. 1, No. 1, p. 17 (1924)). Zeilon gives for the drag $\frac{1}{2}\rho \iint v^2 dx_2 dx_3$, where v is the velocity in the wake at a great distance from the body, measured relative to the fluid at infinity, and the integration is to extend over a section of the wake. For the circular cylinder Zeilon obtains for the drag $0.657 \cdot 2\rho a V^2$, where a is the radius of the cylinder, whereas the inflow along the wake is found to be $(\pi - 2) \cdot 2aV$. The discrepancy will form the subject of a future paper." (See 'Proc. Acad.,' Amsterdam, vol. 33, p. 504 (1930).) (J. M. B.)

† 'Proc. Roy. Soc.,' A, vol. 125, p. 656 (1929).

The Magnetic Susceptibility of Binary Systems of Organic Liquids.

By Miss V. C. G. TREW, Ph.D., and JAMES F. SPENCER, D.Sc., Ph.D., Bedford College, University of London.

(Communicated by W. Wilson, F.R.S.—Received December 23, 1930.)

Introduction.

From the results of a large number of measurements with organic compounds Pascal* has shown that the magnetic susceptibility of straight chain substances may be calculated from the susceptibilities of the constituent atoms, except in those cases where double or treble linkings occur. In such cases the susceptibility may be calculated if due allowance is made for the constitutive effect of the multiple bonds. It would therefore appear that the magnetic susceptibility of a mixture of two organic liquids should be capable of calculation, by the mixture law, from the values of its components.

It has, however, been shown by many investigators, dealing with widely differing properties of organic liquids, that mixtures of these substances do not in most cases obey the simple mixture law. On the contrary, it is very difficult to find two liquids, which on mixing give a value for any physical property that is exactly the mean of those of its constituents. Several physical properties of organic liquids are similar to magnetic susceptibility, in that the property of the compound is largely an additive function of those of the constituent atoms and the linkings in the molecule. The investigation of many properties of liquid mixtures, such as vapour pressure, density, refractive index, dielectric constant, specific heat and other thermal quantities has shown that in the case of a large number of binary mixtures of organic liquids the value of a particular property differs from that calculated by the mixture law because of the influence of other factors such as, for example, intermolecular forces which bring about association, dissociation, and, in some cases, molecular compound formation. The examination of curves in which the value of the property under consideration is plotted against the molecular composition of the mixture frequently furnishes evidence of the existence of association, dissociation, and compound formation in such binary mixtures.

The present investigation has been carried out with the object of ascertaining whether or no magnetic susceptibility is a property from which conclusions,

* Pascal, 'Ann. Phys. Chem.,' vol. 16, p. 531 (1909); 'Compt. Rend.,' vol. 149, pp. 342, 508 (1909); 'Bull. Soc. Chim.,' vol. 5, pp. 1150 (1909); and vol. 7, p. 17 (1910).

similar to those indicated above, may be drawn, and also, in the event of such deductions being possible whether magnetic susceptibility is a property peculiarly suitable for such determinations.

Method of Measurement and Preparation of Materials.

The measurements of the susceptibility were made by means of a slightly modified Curie-Cheneveau magnetic balance,* as described previously. Water was the substance of comparison and was taken as having a mass susceptibility at room temperature of -0.72×10^{-6} . The density measurements were made by means of a small stoppered pyknometer of either 2 c.c. or 10 c.c. capacity. All the recorded results are the mean of five closely agreeing experimental values. The materials used were the purest obtainable and in every case were submitted to a rigorous purification and fractional distillation. The density of the fraction of correct boiling point was then determined and, if on redistillation the density was sensibly unchanged, the fraction was accepted as pure and used for the preparation of the mixtures. Ethyl acetate and diethyl ether were specially prepared from pure materials and purified as above. Table I gives the boiling point and density of the pure substances.

Table I.

	Boiling point.	Density.
Acetone	56.15°-56.25° (760 mm.)	$d(15^{\circ}-4^{\circ}) = 0.79724$
Benzene	79.9°-80.1° (756 mm.)	$d(18.5^{\circ}-4^{\circ}) = 0.8763$
Bromoform	150.3°-150.5° (759 mm.)	$d(19^{\circ}-4^{\circ}) = 2.8937$
Carbon tetrachloride ..	76.70° (754 mm.)	$d(19^{\circ}-4^{\circ}) = 1.5961$
Chloroform	61.1°-61.2° (760 mm.)	$d(15^{\circ}-4^{\circ}) = 1.4985$
Di-ethyl ether	34.3° (760 mm.)	$d(14^{\circ}-4^{\circ}) = 0.7213$
Ethyl acetate	77.3°-77.5° (754 mm.)	$d(22^{\circ}-4^{\circ}) = 0.8966$
Ethylene dichloride	83.0°-83.5° (754 mm.)	$d(15^{\circ}-4^{\circ}) = 1.2596$
Pyridine	116.0°-116.2° (760 mm.)	$d(18.5^{\circ}-4^{\circ}) = 0.9851$
Trichloroethylene	88.0° (756 mm.)	$d(15^{\circ}-4^{\circ}) = 1.4726$

The mixtures used in the measurements were made in a progressive series starting with the pure constituent A and passing through mixtures containing approximately 10, 20, 30, etc., per cent. of B and finishing with the pure constituent B. The liquids were added to one another in approximately the required amounts from burettes and the actual weight obtained by two weighings. The mixtures, after preparation, were preserved for a few days before they were measured to allow equilibrium to establish itself. Table II contains the mass susceptibilities of the pure liquids used.

* John and Spencer, 'Proc. Roy. Soc.,' A, vol. 116, p. 61 (1927).

Table II.

	$-\chi \cdot 10^6$	$-\chi_M \cdot 10^6$	$-\chi \cdot 10^6$	$-\chi_M \cdot 10^6$	$-\chi_M \cdot 10^6$
Acetone	1.229	71.3	0.581 (15°)†	33.7	35.3
Benzene	0.732	57.1	0.712 (16.8°)*	55.5	57.3
Bromoform	0.300	75.9	0.316 (15°)†	79.9	101.1
Carbon tetrachloride	0.542	83.5	0.429 (15°)†	66.1	86.6
Chloroform	0.596	71.2	0.488 (15°)†	58.2	69.6
Di-ethyl ether	0.817	60.5	0.766 (15°)†	56.7	60.1
Ethyl acetate	0.656	57.7	0.607 (6°)*	53.4	57.4
Ethylene dichloride	0.657	65.0	0.602 (15°)†	59.9	64.9
Pyridine	0.851	67.2	0.623 (15°)†	—	—
Trichloro-ethylene ...	0.577	75.9	—	—	70.2

* Ishwara, 'Sci. Rep. Tôhoku Imp. Univ.,' vol. 3, p. 303 (1914), vol. 5, p. 53 (1916), and vol. 9, p. 233 (1920).

† Pascal, 'Compt. Rend.,' vol. 152, pp. 862, 1010 (1911); 'Bull. Soc. Chim.,' vol. 9, pp. 6, 79, 134, 177, 336 (1911) and vol. 10, pp. 809, 868 (1911).

‡ Pascal, 'Compt. Rend.,' vol. 147, pp. 56, 242, 742 (1908), vol. 148, p. 413 (1909), vol. 150, p. 1167 (1910); 'Bull. Soc. Chim.,' vol. 7, pp. 17, 45 (1910); 'Ann. Chim. Phys.,' vol. 19, p. 10 (1910).

The mass or specific susceptibilities are given in the first column as determined by us; the second column contains the molecular susceptibilities calculated from the values in column 1, the third and fourth columns contain the same quantities determined by other observers and the last column contains the values of the molecular susceptibility calculated from Pascal's atomic susceptibility values. With the exception of acetone the present values are much closer to the calculated values than those of other observers, whilst there is considerable agreement between our value for bromoform and that of Pascal, but a great divergence from the calculated value.

Benzene-Ethylene dichloride Mixtures.

Both density and mass susceptibility are plotted against molecular composition in fig. 1 and straight line curves obtained, which indicates that this

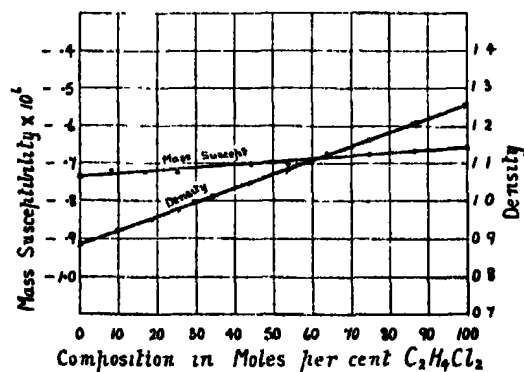


FIG. 1.

pair of liquids obeys the mixture law at the experimental temperature (18° to 20°). In this case, therefore, ideal mixtures are formed, from which it is to be deduced that neither liquid influences the density or the susceptibility of the other to a measurable extent. The property-composition curves for refractive index,* heat of vaporisation,† specific heat,‡ compressibility,§ and vapour pressure* are all straight lines and therefore confirm the conclusion that benzene and ethylene dichloride form ideal mixtures.

Carbon Tetrachloride-Ethyl acetate Mixtures.

Density and susceptibility are, as before, plotted against molecular composition and again, fig. 2, straight line curves are obtained, which would

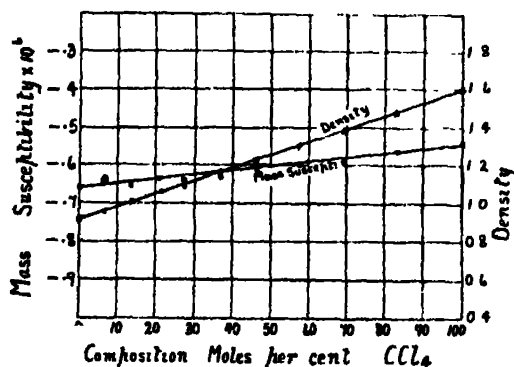


FIG. 2.

appear to show that this pair of liquids form ideal mixtures. The evidence, however, from measurements of other physical properties is not so definite. The curves for refractive index,|| density,¶ and dielectric constant¶ deviate slightly from the straight line whilst the vapour pressure curve|| deviate widely. The evidence taken as a whole indicates that solutions of carbon tetrachloride and ethyl acetate are not strictly ideal, although almost so, with respect to certain properties. It is probable that the mixture deviates slightly from the mixture law and the molecules of the two substances on mixing

* Zawidzki, 'Z. Phys. Chem.,' vol. 35, p. 129 (1900).

† Faust, 'Z. Phys. Chem.,' vol. 113, p. 482 (1924).

‡ Schulze and Hock, 'Z. Phys. Chem.,' vol. 86, p. 445 (1919).

§ Dolezalek and Spiedel, 'Z. Phys. Chem.,' vol. 94, p. 72 (1920).

|| Zawidzki, *loc. cit.*

¶ Krehma and Williams, 'J. Amer. Chem. Soc.,' vol. 49, p. 2408 (1927).

exert a small attractive or repulsive force on one another which is reflected in some of the physical properties more than in others.

Benzene-Ethyl acetate Mixtures.

Susceptibility and density values when plotted against molecular composition give curves, fig. 3, which deviate markedly from the straight line to

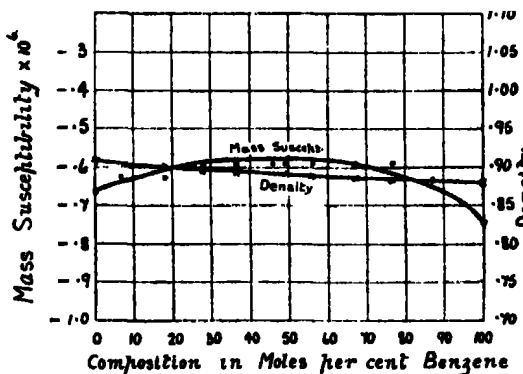


FIG. 3.

which an ideal solution should conform. The divergence is much greater in the case of susceptibility than in the case of density, consequently it would appear that susceptibility is a property more suitable for examining the change which has occurred on mixing than density, and since the effect is a decrease in the diamagnetism of the mixture, it would appear that in some way the electronic orbit systems of one or both of the constituents is, in the mixture, in a more unbalanced condition than it is in the pure liquid. The density curve agrees well with that obtained by Lineberger* when note is taken of the fact that his values were obtained at 25°.

Measurements of viscosity, and dielectric constant show similar deviations from the mixture law, consequently all the physical properties measured point to the same result, namely, that the mixtures of this pair of liquids are non-ideal.

Benzene-Carbon tetrachloride Mixtures.

The curves for mixtures of benzene and carbon tetrachloride, fig. 4, show a marked deviation from the straight line curves, this deviation from the ideal is shown also in a decided manner by the composition-property curves for

* Lineberger, 'Amer. J. Sci.' vol. 2, p. 331 (1896).

viscosity,* dielectric constant,† specific heat,‡ heat of mixing,§ compressibility|| and vapour pressure,¶ whereas the refractive index** gives an almost straight

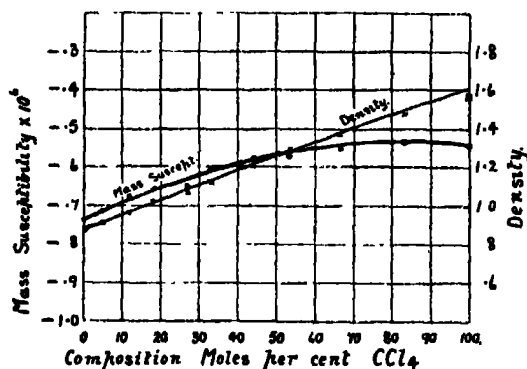


FIG. 4.

line curve. Hence it appears that these liquids are in no sense normal liquids, the fact that the refractive index curve would seem to point to the contrary is relatively unimportant for the refractive index is somewhat insensitive to the changes which may occur on mixing liquids except in those cases where there is the formation of compounds. None of the liquid systems described so far show any signs of compound formation.

Pyridine-Water Mixtures.

Plotting the susceptibility and density respectively against the molecular composition, fig. 5, gives curves deviating widely from those calculated by the mixture law. Both curves show a decided maximum at 25 moles per cent. of pyridine. Before considering the significance of these maxima it will be well to consider the work done on other physical properties of mixtures of pyridine and water. Dunstan, Thole and Hunt†† measured the densities at 25° C. and obtained a curve showing a series of definite breaks; they also obtained a viscosity-composition curve showing the same breaks. The breaks were taken,

* Thorpe and Rodger, 'J. Chem. Soc.,' vol. 71, p. 360 (1897).

† Lineberger, 'Z. Phys. Chem.,' vol. 31, p. 131 (1896).

‡ Schulze, 'Z. Phys. Chem.,' vol. 86, p. 309 (1914).

§ Baud, 'Bull. Soc. Chim.,' vol. 17, p. 328 (1915).

|| Dolezalek and Spiedel, *loc. cit.*

¶ Haywood, 'J. Amer. Chem. Soc.,' vol. 2, p. 994 (1899).

** Zawidzki, *loc. cit.*; Hubbard, 'Z. Phys. Chem.,' vol. 74, p. 207 (1910).

†† Dunstan, Thole and Hunt, 'J. Chem. Soc.,' p. 1728, vol. 91 (1907).

by them, to indicate the existence of a series of hydrates in aqueous solutions of pyridine. Hartley, Thomas and Appleby* repeated the density and

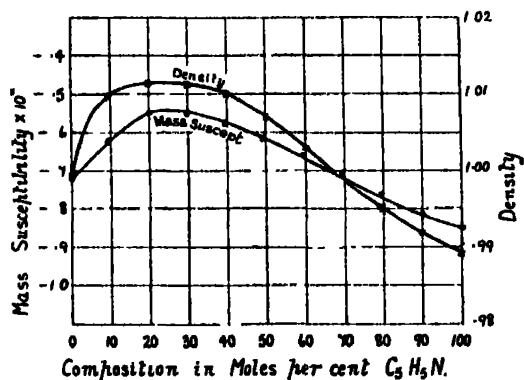


FIG. 5.

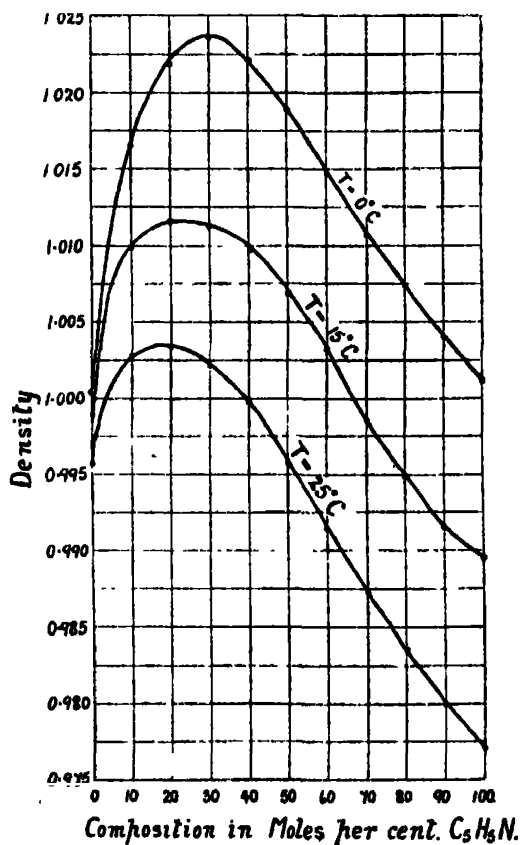


FIG. 6.

* Hartley, Thomas and Appleby, 'J. Chem. Soc.,' p. 538 vol. 93 (1908).

viscosity measurements of aqueous solutions of pyridine and obtained unsymmetrical smooth curves showing no breaks (fig. 6) and from their results deduce the existence of a single hydrate of pyridine, $C_5H_5N \cdot 2H_2O$ in the solutions at $0^\circ C.$ and $25^\circ C.$, the experimental temperatures. The density curve in the present work shows no breaks and it also shows a single maximum; there is also a single maximum and no breaks in the susceptibility curve. The evidence for the existence of a single hydrate and against the view of Dunstan, Thole and Hunt* is therefore very strong. The maximum on the density and susceptibility curves lies, however, at 25 moles per cent. pyridine, which does not, at first sight, appear to correspond with the formula $C_5H_5N \cdot 2H_2O$ as established by Hartley, Thomas and Appleby.† Such a compound would require 33.3 moles per cent. pyridine. Considerable light is thrown on this divergence by plotting the density at $0^\circ C.$, $15^\circ C.$ and $25^\circ C.$ when it will be seen (fig. 6) that the maximum shifts toward lower pyridine content with elevation of temperature. At $0^\circ C.$ the maximum almost corresponds with the compound $C_5H_5N \cdot 2H_2O$, whilst at $25^\circ C.$ it corresponds with less than 20 moles per cent. pyridine. A clearer indication of the composition of the compound to which the maximum is due is obtained by plotting the deviation of the density and susceptibility from the value calculated by the mixture law against the composition. In this way the effect of the relative temperature coefficients of water and pyridine is eliminated. This was done by reading the density and susceptibility values from the straight line joining the values for the two constituents and subtracting the value from the experimental value.

The density curves at $0^\circ C.$ and $25^\circ C.$ are plotted from the values of Hartley, Thomas and Appleby, and those at $15^\circ C.$ are newly determined values. It will be seen that the maximum divergence lies above 30 moles per cent. pyridine

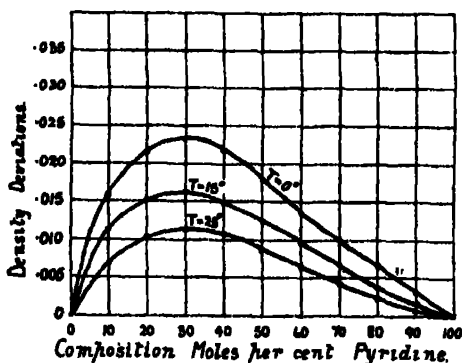


FIG. 7.

* Dunstan, Thole and Hunt, 'J. Chem. Soc.', p. 1728, vol. 91 (1907).

† Hartley, Thomas and Appleby, 'J. Chem. Soc.', p. 538, vol. 93 (1906).

and on plotting the values (fig. 7) the maximum is seen to correspond, within the limits of experimental error, with the compound $C_5H_5N \cdot 2H_2O$. The susceptibility values are known for one temperature only, $15^\circ C.$; on calculating the deviation of these values, as in the case of the density, figures are obtained which, when plotted against the molecular composition, give a curve (fig. 8) with a maximum at the composition corresponding with $C_5H_5N \cdot 2H_2O$. The

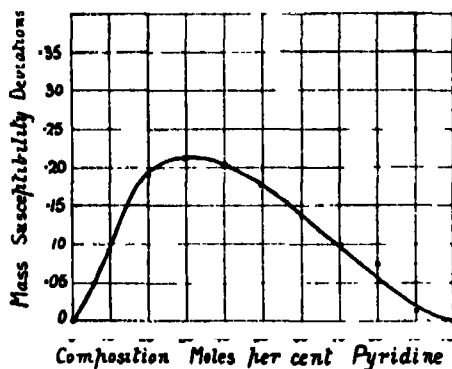


FIG. 8.

results obtained from the density and susceptibility curves are confirmed by the property-composition curves for refractive index,* volume contraction,† vapour pressure,* and viscosity deviation,† all of which have a maximum at 33.33 moles per cent. pyridine. Consequently the evidence for the existence of the compound $C_5H_5N \cdot 2H_2O$ in solution is exceedingly strong.

Acetone-Chloroform Mixtures.

Both the density and susceptibility curves (fig. 9) for mixtures of acetone and chloroform show a marked deviation, the divergence from the value calculated on the basis of the mixture law is 2.56 per cent. in the case of the density, whilst in the case of the susceptibility the value changes from diamagnetic to paramagnetic with changing composition, indicating that a fundamental change has taken place in the solution. The maximum for both density and susceptibility lies at 50 moles per cent., thus pointing to the presence of a compound formed from one molecule of acetone and one molecule of chloroform. Since a considerable amount of heat was evolved in the preparation of the mixtures it appears likely that a definite chemical reaction has taken place

* Zawidski, *loc. cit.*

† Denison, 'Trans. Faraday Soc.,' vol. 8, p. 20 (1912); de Lattre, 'J. Chim. Phys.,' vol. 24, p. 289 (1927).

between the constituents. In 1881 Willgerodt* caused these two substances to combine in the presence of potassium hydroxide to form a very pale yellow

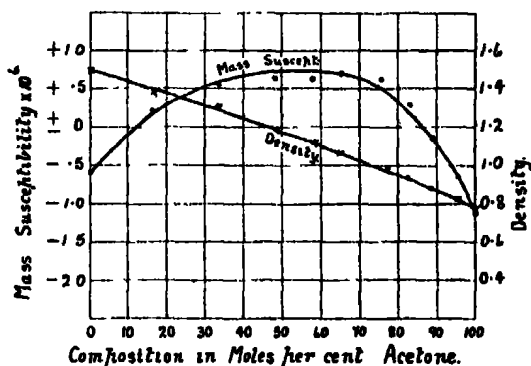


FIG. 9.

crystalline solid to which he attributed the formula $(\text{CH}_3)_2 \cdot \text{C}(\text{OH})\text{C} \cdot \text{Cl}_2$. A quantity of this compound was prepared and examined. It was found to melt at 97°C . and to have a density $d(15^\circ-4^\circ) = 0.666$ and a specific susceptibility $+2.564 \times 10^{-6}$. The strongly paramagnetic character of the compound indicates that its presence in mixtures of acetone and chloroform is likely, for these mixtures have already been shown to be paramagnetic. Assuming, for the moment, that this and no other compound is present in the mixtures, since the specific susceptibility of all three constituents is known and also the specific susceptibility of the mixture, it becomes a mere matter of arithmetic to calculate the composition of each mixture.

From these figures a mass action constant may be calculated; the average value of k is 27.5, and whilst the value obtained cannot be regarded as really constant, still the values are all of the same order, and considering the very approximate nature of the calculation the figures may be looked upon as constant. An attempt was made to isolate the compound from the mixtures by distillation, but only acetone and chloroform distilled over leaving no residue. To test whether or no Willgerodt's compound is present in the mixtures a quantity of the compound was dissolved in a mixture of acetone and chloroform and distilled, when the solvents both passed over leaving the compound unchanged. From which it is to be concluded that whatever the nature of the acetone-chloroform compound in the mixture, it is most certainly not Willgerodt's compound. The evidence shows that both compounds have the same empirical formula, and the fact that a mass action constant can be

* Willgerodt, 'Ber. Chem. Ges.,' vol. 14, p. 2451 (1881); *ibid.*, vol. 16, p. 1585 (1883).

deduced by using the susceptibility value of Willgerodt's compound would seem so indicate that both compounds have the same susceptibility. Hence it would appear that in the mixture of acetone and chloroform we have a co-ordination compound of one molecule of acetone with one molecule of chloroform which decomposes on distillation and that Willgerodt's compound, having a different structure, is stable. Willgerodt assigns the formula $(\text{CH}_3)_2\text{C} \cdot (\text{OH})\text{C} \cdot \text{Cl}_3$ that is α, α, α , trichloro- β -hydroxy- β dimethyl propane, to his compound. The molecular susceptibility of a compound of this formula, calculated on the basis of Pascal's atomic susceptibilities is $\chi_M = -116.4 \times 10^{-6}$, whereas the measured value is $\chi_M = +454.7 \times 10^{-6}$. The difference between these two values can only be explained by the compound having a constitution different from that assigned to it by Willgerodt. The fact that the susceptibility is paramagnetic indicates that the compound has an unbalanced electron orbit system. It may also be remarked here that very few paramagnetic organic compounds are known, and this compound has the largest paramagnetic susceptibility of any organic compound yet measured.

Property-composition curves of mixtures of acetone and chloroform for boiling point,* heat of vaporisation† and vapour pressure* also indicate the existence of a molecular compound. Further, cryoscopic measurements‡ show that a compound is present in mixtures of acetone and chloroform.

Acetone-Bromoform.

Since a compound is formed between acetone and chloroform on mixing it is to be expected that acetone and bromoform should form a similar derivative. Both density and susceptibility curves for mixtures of acetone and bromoform (fig. 10) confirm this view. The divergence of the density-composition curve for these mixtures from the straight line is greater than that of any other system examined, amounting to 5 per cent. at the maximum. The maximum in both the density and susceptibility curves lies at 50 moles per cent., indicating the existence in the solution of a compound of one molecule of acetone with one molecule of bromoform. A compound of this type has been described by Willgerodt,§ but we were unable to prepare the compound in a sufficiently pure condition to determine its susceptibility and density. Other physical

* Thayer, 'J. Phys. Chem.', p. 38 (1899).

† Faust, 'Z. Phys. Chem.', vol. 113, p. 482 (1924).

‡ Madgin Peel and Briscoe, 'J. Chem. Soc.', p. 707 (1928).

§ Willgerodt, 'Ber. Phys. Ges.', vol. 14, p. 2451 (1881).

properties of this series of mixtures do not appear to have been investigated and are now under investigation in this laboratory.

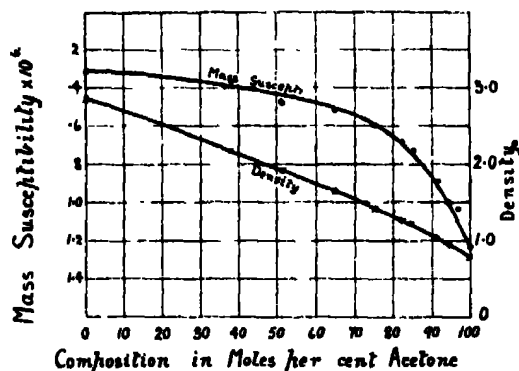


FIG. 10.

Diethyl Ether-Chloroform.

The curves (fig. 11) representing the change of density and magnetic susceptibility for mixtures of ether and chloroform are similar to those obtained for acetone and chloroform. The density curve deviates at the maximum 3.6 per cent. from the straight line, but in this case the deviations are in the opposite direction, being less than the value calculated from the mixture law. The susceptibility curve shows a very pronounced maximum which may be

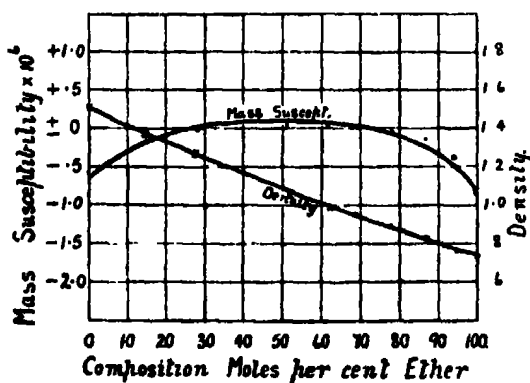


FIG. 11.

taken to indicate the existence of a compound in solution. The maximum lies at the equi-molecular composition, hence it would appear that the compound is formed by the co-ordination of one molecule of ether with one molecule of

chloroform. Since di-ethyl ether is known to be highly polymerised* it would appear that the density curve indicates that a dissociation of complex ether molecules takes place on mixing with chloroform. Further evidence of the formation of a compound is furnished by the fact that the susceptibility curve passes into the paramagnetic region. The existence of a compound in these mixtures is also indicated by the composition-property curves in the case of the dielectric constant and the volume contraction† on mixing.

Acetone-Trichloroethylene.

The constituents of these mixtures are a highly reactive and unsaturated substance, trichloroethylene and a reactive substance, acetone. Consequently it would appear likely that a molecular compound of the two substances should be formed. The density curve, fig. 12, shows a considerable deviation

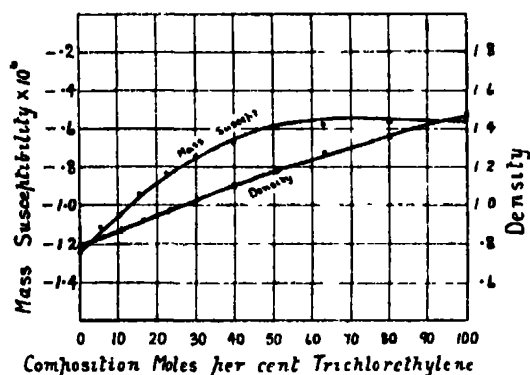


FIG. 12.

from the calculated curve, the amount at the maximum being 3.0 per cent. Heat was generated on mixing the liquids. The susceptibility curve also shows a marked maximum. The maximum in both curves lies at the composition 50 moles per cent. The evidence points, therefore, to the presence of a compound of one molecule of acetone with one molecule of trichloroethylene in the solutions. The physical properties of trichloroethylene have been little investigated and no measurements are recorded of the properties of the system acetone-trichloroethylene, consequently there is no support from other work on the present conclusion.

* Holmes, 'J. Chem. Soc.,' vol. 89, p. 791 (1906), vol. 91, p. 1608 (1907), vol. 95, p. 1919 (1909), vol. 103, p. 2147 (1913).

† Dolezalek and Schulze, 'Z. Phys. Chem.,' vol. 83, p. 45 (1913).

Table III.—Diethyl Ether-Acetone.

	Percentage composition moles.		Density.	Mass susceptibility.
	$\text{CH}_3\text{CO} \cdot \text{CH}_3$	$\text{C}_2\text{H}_5 \cdot \text{O} \cdot \text{C}_2\text{H}_5$	d ($15^\circ-4^\circ$).	$\chi \cdot 10^6$.
Acetone	100.00	0.00	0.7972	-1.229
Mixture I	94.04	5.96	0.7899	-1.215
" II	86.86	13.14	0.7840	0.000
" III	74.36	25.64	0.7737	+0.159
" IV	64.99	35.01	0.7682	+0.193
" V	55.15	44.85	0.7585	+0.195
" VI	44.19	55.81	0.7516	+0.162
" VII	34.73	65.27	0.7429	+0.129
" VIII	24.99	75.01	0.7370	+0.006
" IX	11.47	88.53	0.7280	-0.442
Ether	0.00	100.00	0.7213	-0.817

The density curve, fig. 13, for this mixture shows a maximum deviation of 0.7 per cent., whilst the susceptibility curve shows a much greater deviation

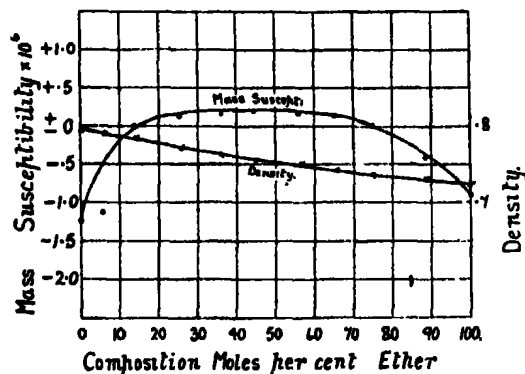


FIG. 13.

and passes into the paramagnetic region. Both curves indicate that some very fundamental change has taken place on mixing the constituents. The fact that the density curve lies below the straight line calculated from the mixture law indicates a dissociation of one or both of the constituents and since they are both associated in the unmixed state* this is not unlikely. The susceptibility curve, however, since it has its maximum in the paramagnetic region, suggests something more fundamental than a dissociation, and since the maximum occurs at 50 moles per cent. it would appear likely that a co-

* Holmes, *loc. cit.*

ordinated compound is formed between one molecule of acetone and one molecule of ether. Most of the property-composition curves for this pair of liquids deviate widely from the straight line curve, particularly the heat of mixing* and the volume contraction, both of which have a maximum at 50 moles per cent. Specific heat,† boiling point‡ and vapour pressure‡ curves confirm the conclusion of compound formation.

Diethyl Ether-Bromoform.

A series of mixtures of ether and bromoform were prepared in which a reaction commenced, bromine being liberated, as soon as the two liquids were mixed. This reaction occurred also when the mixture was protected from light, but not so rapidly as in daylight. After keeping one of the yellow solutions in the dark for 24 hours the bromine had disappeared but in its place hydrogen bromide had appeared. Consequently no measurements were made of either density or susceptibility for this series of mixtures. The chemical action is being examined by a study of the velocity of the process.

Conclusions.

The results recorded show that, in general, the magnetic susceptibility of mixtures of organic liquids does not follow the simple mixture law, although in a few cases a straight line is found to represent the relationship between molecular composition and mass susceptibility. Hence it follows that measurements of the specific susceptibility furnish evidence from which deductions may be drawn as to whether or no physical and chemical changes occur on mixing two organic liquids. The mixtures examined fall into three groups exactly as in the case of measurements of other physical properties (i) ideal pairs, which obey the mixture law and which undergo neither chemical or physical change on mixing; (ii) pairs which deviate slightly from the mixture law, and in which a physical change occurs on mixing; and (iii) pairs which deviate markedly from the mixture law and in which chemical changes occur on mixing.

Magnetic susceptibility is a property which is very sensitive to small changes in the physical and chemical nature of a substance and consequently when a marked change occurs very large deviations are obtained from the mixture law. Although this property is considered by Pascal to be additive, so much

* Sameshima, 'J. Amer. Chem. Soc.,' vol. 40, p. 1482 (1918).

† Schulze, 'Z. Phys. Chem.,' vol. 97, p. 388 (1921).

‡ Haywood, 'J. Phys. Chem.,' vol. 3, p. 317 (1899).

so that the susceptibility of a compound may frequently be calculated from the atomic susceptibilities of its constituent atoms, it is evident that in solutions other forces come into play and cause deviations so that in the majority of cases the susceptibility of mixtures cannot be calculated from that of the constituents. The calculation is only possible for ideal mixtures and in those cases where there is a slight deviation only from the mixture law the divergence is to be attributed to physical forces, whilst where there is a large divergence the formation of compounds, which will change the electron orbit system, is to be taken as the modifying cause. There does not appear to be any close relationship between the deviation of the density and those of the susceptibility although an approximate parallelism exists.

The expenses of this research have been met by a grant from the Government Grant Committee of the Royal Society, to whom the authors desire to express their thanks. Acknowledgment is also made to the Department of Scientific and Industrial Research for a grant which enabled one of us (V. C. G. T.) to engage in this work.

The Study of the Magnetic Properties of Matter in Strong Magnetic Fields.—I.—The Balance and its Properties.

By P. KAPITZA, F.R.S., Messel Research Professor of the Royal Society.

(Received January 26, 1931.)

[PLATE 12.]

Introduction.

In several previous communications* the author has described a method by which magnetic fields up to 300,000 gauss could be obtained for a duration of time of the order of $1/100$ of a second. It was shown that these magnetic fields, in spite of the shortness of their duration, can be applied to the study of different phenomena such as the change of resistance, the Zeeman effect, and others. The present paper describes a number of investigations which have been made on different substances, extending the application of intense magnetic fields to the study of magnetic susceptibility and magnetostriction.

The interest in measuring the susceptibility of different substances in strong

* 'Proc. Roy. Soc.' A, vol. 105, p. 691 (1924), and vol. 115, p. 658 (1927).

magnetic fields lies mainly in seeing whether the linear law of magnetisation for ordinary para- and diamagnetic substances holds for higher fields, and also in the investigation of the saturation of paramagnetic bodies at low temperatures, with a view to determining the elementary magnetic moments. In the present communication a method of measuring the magnetic susceptibility is described and experimental results are given which verify the linear law of magnetisation for several paramagnetic and diamagnetic substances. The saturation of iron and nickel in strong fields is also studied. As will be seen later, the possibility of making these measurements in such a small fraction of time results from the increased magnitude of the phenomenon itself. The most direct method for measuring the magnetic susceptibility is to record the force on a magnetised body in an inhomogeneous magnetic field. In the usual experiments at room temperature this force is only a few hundred dynes, but when fields reach the magnitude of 300 kilogauss the force becomes several grams, and is then sufficiently large to be measured with fair accuracy even in short times of the order of $1/100$ of a second. In this paper a special type of balance will be described by which these measurements are made possible.

The principle of the balance can also be used for an extensometer for studying magnetostriction. In the study of magnetostriction in ordinary magnetic fields it was only possible to detect and measure these phenomena in ferromagnetic substances. In our present experiments we have been able to increase the scope of investigation up to a field of 300,000 gauss, and in this field we have observed magnetostriction in several diamagnetic substances such as bismuth, antimony and graphite. Of these substances the magnetostriction of bismuth was found to be the greatest, and in fields of 300 kilogauss the change in length reached the same magnitude as that observed, for instance, in nickel which shows the most marked magnetostriction of the ferromagnetic substances. This magnetostriction, however, has quite a different character from that observed in ferromagnetic substances where the phenomenon is closely related with the magnetic saturation.

We have chosen bismuth for the careful study of this magnetostriction, and have found how it depends on the temperature, crystal orientation, and impurities. The large influence which all these factors exert on this interesting phenomenon shows its complicated character and indicates a close connection with the peculiar magnetic properties of this metal.

The methods and results of these investigations will be described in a series of papers with the same heading. In the first part the balance used will be

described in detail ; in the second part the experimental arrangements for the measurement of the magnetisation, and the results of measurements of the magnetisation of iron, nickel, some ferrous alloys, gadolinium sulphate, manganese and bismuth will be given ; in the subsequent parts the apparatus for measuring the magnetostriction, and the results of measurements for iron, nickel, bismuth, antimony, graphite, gallium and some other substances will be described.

All these investigations were carried out with the continuous and valuable assistance of Mr. E. Laurmann to whom I wish to express my thanks. The balance and other apparatus required for this research needed particularly accurate and skilful workmanship, and were made in this laboratory by Mr. H. Pearson. I am also indebted to Dr. J. D. Cockcroft for the correction of this MS. and for looking through the calculations. My thanks are also due to Lord Rutherford for his kind interest shown during the progress of this work.

(i) *Description of a Type of Spring Balance for Measuring the Magnetisation.*

The most practical method for measuring the magnetic susceptibility (χ) of para- and diamagnetic bodies of mass m is to measure the force (F) which they experience when placed in a magnetic field (H) having a known gradient dH/dx

$$F = \chi m H \frac{dH}{dx}. \quad (1)$$

In our case H is of the order of 300,000 gauss, and we may take for dH/dx a value of 30,000 gauss per centimetre. Since χ , the susceptibility, is for most substances of the order of 10^{-6} , we get for a gram weight of the substance $F = 9000$ dynes $\simeq 9$ grams ; about 100 times more than the force obtained in experiments with an ordinary electromagnet.

If we choose a spring balance for measuring this force, the most important requirement is that the natural period of the balance must be shorter than the time during which the magnetic field is applied, i.e., about 0.025 second. As will be shown, if we wish to make this measurement with an accuracy of about 1 to 0.5 per cent. the natural frequency of the balance used must be about 1000 to 2000 per second. Further, it can be shown that in the most efficiently designed balance the inertia of the moving parts must be of the same order as the inertia of the mass of the investigated body ; the balance must be critically damped, and finally the strong magnetic fields must have no direct disturbing effects on the balance.

The main difficulty in designing a balance which fulfils these requirements lies in the extremely large linear magnification of the displacement of the magnetised body required. From the classical formula of oscillation it is known that the restoring force of a balance per unit of displacement is

$$f = M(2\pi/T)^2 \text{ dyne/per centimetre,} \quad (2)$$

so when T has the value $1/2000$ second, and M is 6 grams, we find $f = 9.3 \times 10^9$.

Since
$$z = F/f \quad (3)$$

and F is about 9000 dynes, we find the displacement z is 10^{-5} cm. This very small displacement of the point where the body is attached has to be magnified about 100,000 times for it to be easily measurable.

In our first attempts to make a balance with such a magnification power, we attached the investigated magnetic body to a rigid spring (the best type of which was found to be a horizontally stretched wire), and then by means of a system of very light levers, magnified the motion of the spring 40 or 50 times, thus tilting a very small mirror, which, by means of an optical lever, gave us another 2000 times magnification. Several balances of this type were constructed, but not a single one proved wholly satisfactory. The main trouble arose from the vibration of the levers, and also from the thermal expansion of the levers due to accidental temperature variations which shifted the zero position of the balance. Finally, the damping of this complicated system offered great difficulties. After a number of unsuccessful attempts, quite a different method of magnification, based on a hydraulic principle, was successfully adopted. This will now be described in its final form.

The detailed drawing of the balance is shown on fig. 1. The main body of it consists of a brass ring (1) fitted to a brass base (2), which has in the bottom a

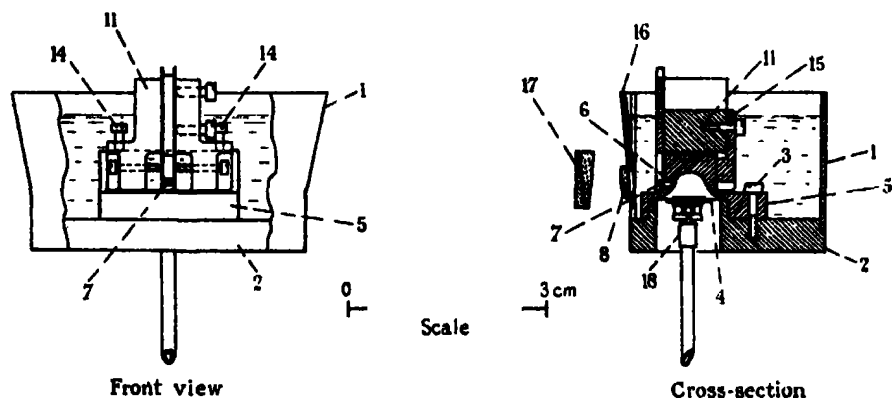


FIG. 1.—The Balance.

circular hole. A circular diaphragm (4) made of a thin sheet of hard rolled constantan covers this hole and acts as the spring in the balance, to which the force produced by the attraction of the body in the magnetic field is applied. The diaphragm (4) is pressed to the hole by a brass cover (5) by means of three screws (3), the joint being made tight by using two very thin, ring-shaped paper washers on both sides of the diaphragm. The cover (5) forms above the diaphragm an enclosure quite separated from the surrounding space except for the circular opening (6) about 1 mm. in diameter and 1 mm. in length, made on one side of the cover. All the space above the diaphragm and above the cover is filled with oil. It is evident that when the diaphragm is displaced by a force, the oil is moved through the little hole (6) into the space outside the cover (5) and the displacement of the oil close to the hole (6) is larger than the displacement of the diaphragm. The magnification is of the order of the ratio of the surface of the hole to the surface of the diaphragm. A small square mirror (7) 0.9 mm. \times 0.7 mm. is suspended close to the hole (6) in such a way that it can pivot freely about a horizontal support attached to its upper edge. It is evident that the oil moving out of the circular channel (6) will tilt the mirror (7), and if a beam of light is thrown through the opening in the case fitted with a glass window (8), the spot of light obtained from the deflection of the mirror will be displaced. The magnification of this optical lever, if the plate is placed at a distance of 78 cm. from the mirror, is about 2000, and combined with the hydraulic magnification of 50 due to the oil system, will give the required figure of 100,000.

This arrangement provides a most suitable tool for measuring force during the required short intervals. The position of the mirror is mainly controlled by gravity which tends to restore it to the vertical position. If it is displaced it moves only very slowly in oil. It appears that during 1/100 of a second the tilt of the mirror is completely controlled by the motion of the oil. On the other hand, thermal expansion in the metal parts of the balance or of the oil itself produces only extremely slow currents of oil round the mirror which do not affect its zero position. Thus, since the temperature during 1/100 of a second remains constant, this type of balance which excludes all thermal disturbances, makes it possible to take full advantage of the short time of experiment.

In order to develop an accurate balance on these lines, several technical difficulties had to be surmounted before good results could be obtained. The main difficulty is in the suspension of the mirror. This suspension must be as frictionless as possible and must have a well-defined pivoting axis. In the

first balance, we used for suspending the mirror a strip of silver tissue foil stuck by one end to the edge of the mirror, the other end being clamped. This provided in many respects quite an efficient suspension, but it had the following disadvantages. First, it was very difficult to fix accurately, since to have a definite pivoting axis the three parts of the silver foil have to be made not longer than 0.2 mm., and even then, after a large displacement of the mirror, the sensitivity of the balance could change considerably. Secondly, the fixing of the mirror was a very difficult task, since a little shellac flowing on the suspension made it stiff, and the mirror would not follow the motion of the oil. Thirdly, the zero of the balance was not constant, as even the thin silver foil still possessed a certain elastic controlling power which might alter the displacement of the mirror considerably. This led us to another method of suspending the mirror which proved to be more satisfactory. The details of it are shown on fig. 2. The mirror (7) is fixed by means of a very small amount

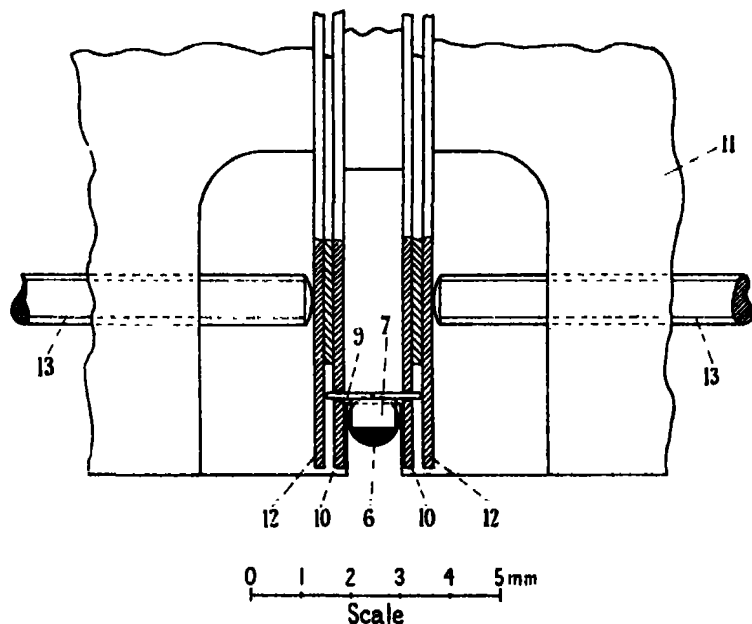


FIG. 2.—Detailed drawing of the suspension of the mirror in the balance.

of shellac to the middle of the glass rod (9) which is 0.13 mm. in diameter and about 2 mm. long. The rod, which is used as an axis, has its ends slightly smoothed by melting in a flame, and is placed in bearings made in two vertical constantan strips (10) 0.2 mm. thick, fixed in a holder (11). Owing to the small size of the mirror we found it necessary to carry out all this work under a

binocular microscope. The two circular holes which form the bearings have a diameter only 0.02 mm. larger than the axis and have to be made accurately circular and smooth. Two constantan strips (12) 0.2 mm. thick placed by the sides of the strips (10) prevent the mirror from moving sideways. The thrust surfaces are well polished. The strips (10) and (12) are fixed in the holder (11) by means of two screws as shown on fig. 1. The two screws (13) are used for pressing together the strips (10) and (12) which are necessary to fix the mirror in the holder and adjust the distance between the thrust surfaces of the strips (12) so that the axis (9) cannot move sideways in either direction.

The holder (11) to which the mirror and the strips are fixed has a small projecting plate which shields the axis and the top of the mirror and protects it from the direct stream of the moving oil from the hole (6). This we found necessary, since if the axis is exposed to a direct stream of oil it might either bend slightly or move in the bearings, thus affecting the proportionality of the balance.

The holder (11) is placed on the cover (5), fig. 1, which has a rectangular top fitting the holder (11). By means of the screw (14), the mirror with the holder can be adjusted to lie opposite the hole (6) at the proper height. The clamp (15) prevents the holder (11) from sliding sideways on the cover (5) after the mirror is adjusted in the middle of the hole. The sensitivity of the balance is not much affected by the height of the mirror, but the best results were obtained when the bottom edges of the mirror were just slightly below the centre of the hole (6). The front wall of the balance (16) is made with a hole to which a convex lens (8) is fixed. The whole wall (16) can be slightly tilted round its bottom edge in such a way that the inside flat plane of the lens is made parallel to the plate of the mirror. This is necessary to get an achromatic spot from the mirror in order to obtain a well-defined line on the photographic plate.

For zero adjustment of the spot a set of achromatic prisms (17) is used, which are placed in front of the lens, so that by choosing a suitable prism it is possible to bring the image on to the required part of the photographic plate.

Care must be taken in putting the balance together to use only clean and dry oil, and more important still to see that no air bubbles are left in the side of the cover (5), as this can completely upset the working of the balance. The oil is therefore boiled, and then, keeping it at a temperature of about 50°, all the parts of the balance assembled together are placed in the oil. This is advisable since, owing to the reduced viscosity of the warm oil, the air bubbles leave the parts of the balance and the oil itself quite easily.

(ii) *The Design of the Balance.*

As the motion of the oil above the diaphragm and the way in which it tilts the mirror is a very complicated hydrodynamical problem, it is useless to attempt to study it theoretically. The method which we have chosen to design the most efficient balance is based on the principle of similarity; thus, at first a balance was designed from approximate calculation, and afterwards its properties have been studied experimentally. From these data a balance to suit any experimental requirements could be accurately designed.

Let us call the diameter of the constantan diaphragm a , and the diameter of the opening before the mirror d . The displacement of the bottom edge of the mirror is then proportional to the displacement of the diaphragm Z magnified E' times, where

$$E' = A' \frac{a^2}{d^2}, \quad (3)$$

A' being a coefficient of proportionality which depends in a complicated way on the motion of the oil. The magnification due to the optical lever E'' is, if we take the width of the mirror e to be proportional to the diameter of the hole and call this coefficient of proportionality α ,

$$E'' = 2L/e = 2L/\alpha d, \quad (4)$$

where L is the distance from the mirror to the photographic plate. The complete magnification power of the balance E will then be

$$E = \frac{2A'L}{\alpha} \cdot \frac{a^2}{d^2} \quad (5)$$

In the balance used we had the following dimensions: $a = 1$ cm., $L = 78$ cm., $e = 0.07$ cm., $d = 0.1$ cm. By a method to be given in Part III where the extensometer is described, we find $E = 1.02 \times 10^5$. We thus find $A' = 0.46$ and $E' = 46$.

If a mass m' of the substance is suspended and the force per unit mass is F' , the total force is equal to $F = F'm'$ dynes, and the displacement of the diaphragm will be

$$z = B \frac{F'm'a^3}{h^3}, \quad (6)$$

h is the thickness of the diaphragm (in our balance 0.011 cm.), whilst the coefficient B only depends on the elastic constants of the material of the diaphragm and the ratio of the outer diameter, a , of the diaphragm to the diameter, b , of the inside brass disc, which is soldered to the middle of the diaphragm

and to which the force is applied. This ratio a/b in our balance was equal to 1.8, and if we keep it constant the value of B will be independent of the size of the balance. The value of B can be estimated from the theory of elasticity,* but a more accurate determination can be made experimentally. By loading the balance by known weights and measuring the deflection on the plate Z , and dividing by the magnification power E we get z and from (6) we get B . In our balance $B = 6.2 \times 10^{-15}$ cm./dynes. The sensitivity of the balance is given by the following equation, relating the deflection of the spot on the plate to F'

$$Z = E_z z = \frac{B \cdot 2A'LF'}{\alpha} \cdot \frac{m'a^4}{h^3 d^3}. \quad (7)$$

The next point to consider is the natural frequency n of the balance, which is, after (2)

$$n^2 = 1/T^2 = f/4\pi^2 M. \quad (8)$$

The restoring force f of the balance is evidently $m'F'/z$ which can be obtained from (6)

$$f = \frac{1}{B} \cdot \frac{h^3}{a^2}. \quad (9)$$

The inertia mass M is the sum of the mass m' of the body M' , the mass m'' of the suspension and the inertia m''' of the oil in the balance. It can be shown that to obtain the maximum efficiency of the balance the following relation between these masses must hold: $m'' = m'''$, and $m' = m'' + m'''$, when we get

$$M = 4m''' \quad m' = 2m'''. \quad (10)$$

The inertia of the moving oil, m''' , cannot be accurately estimated unless we can solve the hydrodynamical problem of the motion of the oil. To this very complicated problem only an approximate solution can be obtained. It is evident that if the motion of the oil were uniform in the space above the diaphragm the contribution of different layers of oil to the inertia of the balance would be inversely proportional to their cross section; thus most of the inertia mass is contributed by the oil in the circular channel before the mirror. The effective mass in the channel may be written $\frac{\gamma \pi p}{4} a^2$, where γ is the specific weight of the oil and p is the effective length of the channel. (We take it to be twice the length of the channel which is, in our balance, 0.1 cm.) The

* See Prescott, "Applied Elasticity," p. 405.

effective mass will then be $m''' = \frac{1}{4}E'^2 \gamma \pi \rho d^2$ or, replacing E' from (3), we get

$$m''' = \frac{\pi}{4} A'^2 \gamma p \frac{a^4}{d^2}. \quad (11)$$

For our balance m''' is estimated to be between 2 and 3 gm. From the equations (7), (8), (9), (10) and (11) we get

$$Z = \left(\frac{\pi B A'^3 L p \gamma}{\alpha} \right) F' \cdot \frac{a^8}{h^3 d^6} \quad (12)$$

and

$$n^2 = \left(\frac{1}{4\pi^2 B A'^2 \gamma p} \right) \cdot \frac{h^3 d^2}{a^6} \quad (13)$$

The term in the brackets in formulæ (12) and (13) may be regarded as constant for a definite family of balances and their numerical values can be determined from an experimental examination of one balance. We shall call them K and N so that we get

$$Z = K F' \cdot \frac{a^8}{h^3 d^6} \quad (12B)$$

$$n^2 = N \frac{h^3 d^2}{a^6}. \quad (13B)$$

In designing a balance we are free to choose the value of h , the thickness, a , the diameter of the diaphragm, and d , the diameter of the hole (6), fig. 1. We have to do it in the following way: the deflection Z is fixed by the size of the photographic plate and the accuracy of measurement required. On the other hand n , the frequency, has to be made as large as possible. Of the three quantities, h , a and d , h may be eliminated from the equations since in practice we are not limited in its choice, and we get

$$n^2 = \left(\frac{K F' N}{Z} \right) \cdot \frac{a^2}{d^2}. \quad (14)$$

From this we see that to make n as large as possible, having fixed values for the terms in the bracket, it is preferable to make a balance with a large diameter diaphragm and a small mirror and hole. Thus we must choose the mirror to be as small as is practical to make. In our choice of a we are limited by the fact that large values of a require a large mass for the magnetised body m' , as appears from equations (10) and (11). The formulæ (12) and (13), combined with the experimental data for b and a obtained for one balance give us all the necessary data to design a balance of any dimensions and to answer the requirements of a particular experiment.

In practice it is impossible to fulfil strictly the condition of equality of the masses given by (11), as the same balance has to be used for studying the magnetisation of a number of bodies which may have a large variation of susceptibility. For instance, in our investigation of iron, we used only 0.005 gram compared with 0.4 gram for bismuth. Also the glass rod which connects the studied body with the diaphragm must be made sufficiently rigid to prevent vibration. If the rod was taken too thin, longitudinal oscillations were set up which could be seen on the oscillograms; this requires a minimum weight for the rod of the order of 2 to 3 grams. Thus all the results deduced from these formulæ actually only give the general method for the design of a balance, and each case has to be considered in more detail on its merits.

The next point to consider is the damping of the natural vibration of the balance. It appears that the main part of the damping is due to the motion of the oil through the small hole (6), fig. 1, opposite the mirror. To have the motion of the balance as nearly critically damped as possible we can only adjust the viscosity of the oil since the dimension of the hole is usually fixed. We found it always possible to make an oil of the required viscosity if we mixed two kinds of paraffin oil, one of high viscosity and the other of low viscosity. The oil used in our balance had a viscosity equal to 0.63.

(iii) *The Examination of the Balance.*

Before use in magnetisation research, the balance was carefully studied to determine its constant and to clear up several doubtful points. For this purpose a weight was suspended from the diaphragm by a silk thread and then suddenly lifted by means of an electromagnetic device which was timed with the falling plate of the oscillograph. Three of the oscillograms so obtained are shown. The oscillograms Nos. 1 and 2 are taken for weights of 2.382 and 4.740 grams respectively; the oil in the balance was of such a viscosity that the motion was very nearly critically damped. Oscillogram No. 3 was taken with the balance filled with less viscous oil, in order to estimate the natural frequency of the balance from the few oscillations which appear on the oscillogram. The natural frequency will be somewhat higher than that directly measured on the oscillogram as the damping increases the time of oscillation. From similar oscillograms we first verified that the deflection of the balance is proportional to the weight which is lifted within the limits of the errors of measurements of the oscillogram, namely, 0.5 per cent. Secondly, experiments were made with very small weights to verify that there was no static friction in the motion of the mirror which would make it unresponsive

to small displacements of the oil. No such effect could be traced. As can be seen on the oscillograms, after the deflection is reached, the mirror remains stationary on the plate, showing that the influence of the gravity control on the mirror is excluded as a possible source of error. The other possible source of error is that the acceleration force due to the inertia mass of the glass of the mirror having a higher density than the surrounding oil, may retard the motion of the mirror relative to that of the oil during a rapid deflection. A simple calculation shows that this acceleration force is in most cases much larger than the possible friction of the axis of the mirror in the bearings or the force of the gravity control. To reduce this inertia force to the smallest possible value, the mirrors used in the balance had a thickness of only $40\ \mu$, but to make sure that the influence of this accelerating force is excluded the following check experiment was made: the same weight was unloaded from the balance, first more or less gradually and then very rapidly. If such an effect was large the final deflections ought to be different, but in the two experiments the deflections were found to be equal within limits of 1 to 2 per cent. It is thus clear that the influence of this effect on the accuracy of the balance when used for magnetisation measurements, where the curves are much smoother, must be negligibly small.

The other possible source of error is that the shape of the stream lines of the flow of the oil from the hole depends on the way velocity of the oil changes. This would mean that in equation (3) A' could not be regarded strictly as a constant. The results of the experiment with slow and quick unloading given above, also seem to exclude the possibility of this error being appreciable.

By measuring the amplitude of the deflection, and dividing by the weight in the experiments of unloading the balance, we find the sensitivity of our balance to be about 0.50 cm. deflection on the photographic plate per gram load. The natural frequency of the balance estimated from (8), using (11) to give the approximate value for the mass of the oil, was 1300 per second unloaded, and with a load of about 3 grams 900 per second. The natural frequency was also measured approximately from oscillograms similar to that on fig. 3 taken with less viscous oil, and as might be expected, it agrees closely with the frequency deduced from the approximate theory.

Finally, it is worth mentioning a few other properties of the balance. When the diaphragm is pressed up, the oil is forced out of the cover by means of the compression force, but when the diaphragm is pressed down, the oil is forced into the chamber by the atmospheric pressure. No vacuum can be formed in the chamber unless a sudden force is applied to the diaphragm exceeding

that of the atmospheric pressure (800 gr.) and it is evident that this force is far larger than that for which the balance is designed (10 gr.), and we can thus be quite sure that the oil follows the motion of the diaphragm whether it is displaced upwards or downwards.

In working with the balance it was found essential to bring it to its "natural zero" before starting to experiment. After the balance is assembled and the weight is suspended and slight kicks are given to the balance the spot makes oscillations and the zero gradually shifts. Finally it comes to a position at which it does not shift any more, and this position we call the "natural zero." If this precaution is not taken, then the shift of the zero may occur during the experiment. It took some time to discover that this precaution was necessary, and it can be seen that on some of the oscillograms there is a slight displacement of the zero position after the experiment.

It may also be mentioned that it is rather important to have the strips (12), fig. 2, which form the thrust surface, as close as possible, so as to restrict the sideways motion of the mirror, but not so close as to produce a pressure on the axis and introduce a friction. This adjustment is made by the screws (13).

A troublesome property of the balance is that when a weight is attached to the diaphragm the balance acts as a most sensitive seismograph, recording even the most minor disturbances in the room. In order to avoid these disturbances we found it essential to place the balance on a massive slate plate suspended from the ceiling by means of four thin bronze wires. It is possible that advantage can be taken of this property of the balance to use it as a simple and very sensitive seismograph. The formulæ and data given above supply all the information necessary to design a balance suitable for use in recording seismological disturbances.

(iv) *The Influence of the Inertia of the Moving Part on the Accuracy of recording of the Balance.*

As the full natural period of the balance T is $1/900$ second, it is only about twenty times smaller than the time, 0.0215 second, during which the force is applied to the balance, and during which the whole of the curve of the deflection of the balance is traced. The accuracy of the experiment may therefore be affected by the influence of the inertia of the moving masses of the balance. In this section we shall discuss this question and show how, by measuring the oscillograms in an appropriate way, this effect may be practically eliminated. The problem may be stated as follows: a force F , as given by the equation (1), acts on the diaphragm of the balance. This force

produces a deflection Z of the spot on the photographic plate which is E (the magnification) times z , the displacement of the diaphragm.

$$Z = Ez. \quad (15)$$

Now, in an ideal case, when the inertia of the balance would not interfere we should have from (3)

$$z = F/f, \quad (16)$$

where f is the restoring force of the diaphragm. We have then $F = \frac{f}{E} Z$ so that by measuring Z on the plate for different values of the magnetic field, we determine F as a function of H . Actually instead of (16) we get a more complicated connection between F and z as they are both functions of time. We have the classical equation for the forced motion of an elastic system, namely,

$$M \frac{d^2 z}{dt^2} + V \frac{dz}{dt} + fz = F(t), \quad (17A)$$

where M is the effective mass of the balance and the suspended body (see (10)), and V the coefficient of friction. This equation can be solved when $F(t)$ is a simple function of time, but in our case this is more difficult, for if the body is, for instance, paramagnetic and below saturation, then $F(t)$ is proportional to H^2 , namely,

$$F(t) = \gamma H^2. \quad (18)$$

In a stronger field the body gets saturated, and we have $F(t)$ proportional to H , that is

$$F(t) = \delta H. \quad (19)$$

Between these limits $F(t)$ is a most complicated function of H . On the other hand, H can be represented approximately by a sine curve during the impulse of the current in the coil

$$H = H_0 \sin(2\pi t/\tau). \quad (20)$$

Thus the complete solution of the equation (17) applicable to experimental conditions is very complicated. However, as the influence of the inertia is small, we can obtain a general solution which will enable us to estimate the corrections to the solution (16) for any practical function $F(t)$.

First, we simplify (17) in the usual way by dividing both sides by M and by introducing the following standard abbreviations

$$F(t)/M = U(t); \quad V/M = 2\lambda; \quad f/M = \kappa^2. \quad (21)$$

We then get

$$\frac{d^2 z}{dt^2} + 2\lambda \frac{dz}{dt} + \kappa^2 z = U(t). \quad (17B)$$

We limit ourselves to our practical case where the balance is critically damped, when

$$\kappa^2 - \lambda^2 = 0. \quad (22)$$

The general integral of (17) can be written

$$z = e^{-\kappa t} (C_1 t + C_2) + e^{-\kappa t} \int_0^t e^{\kappa \xi} (t - \xi) U(\xi) d\xi, \quad (23)$$

where C_1 and C_2 are constants of integration. To evaluate the integral we introduce the following new variable

$$y = \xi - t. \quad (24)$$

and obtain for the integral term

$$I = \int e^{\kappa y} y U(y + t) dy. \quad (25)$$

Integrating by parts, and taking into account that

$$\int e^{\kappa y} (\kappa y - n) dy = \frac{1}{\kappa} e^{\kappa y} [\kappa y - (n + 1)] \quad (26)$$

we get

$$I = \frac{1}{\kappa} \left[\frac{\kappa y - 1}{\kappa} U(y + t) - \frac{\kappa y - 2}{\kappa^2} U'(y + t) \dots (-1)^n \frac{\kappa y - n}{\kappa^n} U^n(y + t) \right] e^{\kappa y}. \quad (27)$$

Introducing the limits of integration, we get

$$z = e^{-\kappa t} (C_1 t + C_2) + \left[\frac{1}{\kappa^2} U(t) - \frac{2}{\kappa^3} U'(t) + \frac{3}{\kappa^4} U''(t) \dots \right] \\ - e^{-\kappa t} \left[\frac{\kappa + 1}{\kappa^2} U(0) - \frac{\kappa + 2}{\kappa^3} U'(0) + \frac{\kappa + 3}{\kappa^4} U''(0) \dots \right]. \quad (28)$$

If we assume that the initial conditions are that $t = 0$, $z = 0$ and $dz/dt = 0$, and return to our original function F by (21), we get

$$zf = F(t) - \frac{2}{\kappa} F'(t) + \frac{3}{\kappa^2} F''(t) \dots \\ - e^{-\kappa t} \left[(\kappa + 1) F(0) - \frac{\kappa + 2}{\kappa} F'(0) + \frac{\kappa + 3}{\kappa^2} F''(0) \dots \right]. \quad (29)$$

We see that the correction consists of two terms, the second being an exponential one in which evidently $F(0) = 0$, as in the beginning $H = 0$, and there is no force acting on the balance. This correction is thus reduced to

$$\Delta F_{\text{exp.}} = e^{-\kappa t} \left[\frac{t\kappa + 2}{\kappa} F'(0) - \frac{t\kappa + 3}{\kappa^2} F''(0) \dots \right], \quad (30)$$

and as will be shown later by numerical examples, owing to the exponential $e^{-\kappa t}$, ΔF_{exp} is negligibly small very soon after the beginning of the deflection. The main error is produced by the part which does not contain the exponential and this, using the Taylor expansion formula, can be written from (29) with sufficient approximation

$$zf = F\left(t - \frac{2}{\kappa}\right) + \frac{1}{\kappa^2} F''(t). \quad (31)$$

This formula gives us a very important general result of great practical value for our measurements. Apart from a small correction term

$$\Delta F = \frac{1}{\kappa^2} F''(t) \quad (32)$$

the curve drawn by the ordinate z relative to the abscissa time t is the same as that of the force F , but is shifted by the time $\Delta t = 2/\kappa$ independently of the way in which the force F depends on the time (provided, of course, that the series (20) converges, which is the case for most physical problems). Actually, from (19) and (2) we find that

$$\Delta t = 2/\kappa = T/\pi. \quad (33)$$

This means that the shift of the curve is approximately one-third of the complete period of natural oscillation of the loaded balance. On the oscillogram No. 3, Plate 12, we see that the full period of damped oscillation occupies about 2 mm. on the plate. The actual period is evidently less, so that the shift of the curve on the oscillogram will be less than 0.7 mm.

Before considering a general case let us consider the two cases (18) and (19) mentioned above. For a paramagnetic body we get from (18) and (20)

$$F_p = \gamma H_0^2 \sin^2(2\pi t/\tau), \quad (34)$$

where $\tau = 0.043$ second, twice the time of our impulse. Then we get from (15), (31) and (33) by differentiating (34)

$$Z_p = \frac{E\gamma H_0^2}{f} \left[\sin^2\left(\frac{2\pi}{\tau}t - \frac{2T}{\tau}\right) + \frac{2T^2}{\tau^2} \cos \frac{2\pi}{\tau}t \right]. \quad (35)$$

Taking $T = 0.0011$ second we find that the shift $2T/\tau$ is equal to 3° .

For the sake of clearness the curve Z_p is graphically represented in fig. 3 as it actually occurs in practice in our oscillograms. The abscissa is the time

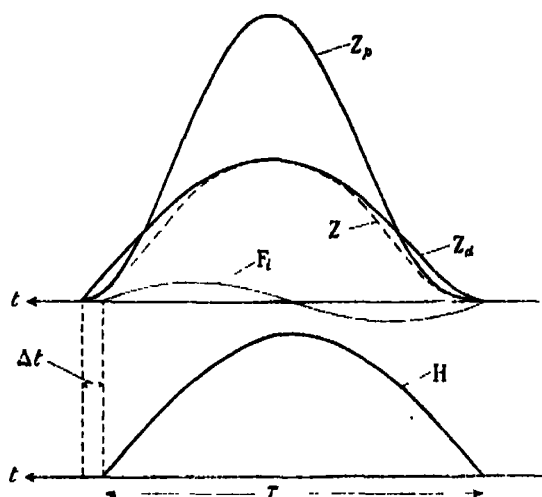


FIG. 3.

running from the right to the left; the line below represents the magnetic field as recorded by the oscillogram of the current in the coil; the curve Z_p is shifted in phase by Δt which is exaggerated about three times for the sake of the clearness of the drawing. In the following Table I we have calculated the ratio of the correction term ΔF_p to the applied force F_p for values of H ranging from 0.1 of the maximum H_0 so that $F_p/F_{p\max.}$ varies from 0.01 to unity.

Table I.

H/H_0	0.1	0.2	0.3	0.4	0.5	0.6	0.7	0.8	0.9	1.0
$F_p/F_{p\max.}$	0.01	0.04	0.09	0.16	0.25	0.36	0.49	0.64	0.81	1.0
$\Delta F_p/F_p \times 100$	+13	+3.1	+1.2	+0.57	+0.27	+0.12	+0.01	-0.06	-0.1	-0.13
$\Delta F_{p\exp.}/F_p \times 100$	+1.7	<+0.001	—	—	—	—	—	—	—	—

We see that if we limit ourselves to measurements on the oscillograms where the range of H/H_0 varies between 0.3 and unity, the error in measuring F_p will not exceed 1.2 per cent. Actually, when the field is 0.3 of the maximum, the amplitude of Z_p is only 0.09 of its maximum value, and the error in measuring such a small deflection on the oscillogram sets the limit of accuracy. Thus if the maximum field is 280 kilogauss (as in most of our present experi-

OSCILLOGRAM 1. The unloading of the balance with a weight of 2.382 gm., the balance being critically damped. The small kicks on the curve after unloading are due to the oscillation of the weight after it has been lifted suddenly, which slightly pulls the thread attaching it to the balance.

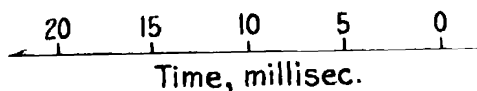


OSCILLOGRAM 2 The same as 1, but the weight is 4.740 gm

20



OSCILLOGRAM 3. The unloading of the balance when the viscosity of the oil is small and the balance is underdamped.



ments) we can study the magnetisation from one single oscillogram within an accuracy of 1 per cent. in the range between 85 and 280 kilogauss. In cases where the magnetisation in lower fields had to be studied, another oscillogram with a smaller maximum value of H_0 was taken.

To justify our assumption about the smallness of the exponential correction ΔF_{exp} as given by (30), we have also included its numerical values in Table I, and we see that even for small values of H it is negligible in comparison with the correction ΔF_s .

If we consider the force F_s on a ferromagnetic or a saturated paramagnetic substance, we have from (19) and (20)

$$F_s = \delta H_0 \sin(2\pi t/\tau) \quad (36)$$

and we get from (31)

$$Z_s = \frac{E \delta H_0}{f} \left[\sin\left(\frac{2\pi t}{\tau} - \frac{2T}{\tau}\right) - \frac{T^2}{\tau^2} \sin \frac{2\pi t}{\tau} \right], \quad (37)$$

in this case we see that the correction follows the same curve as F_s , and throughout the curve is equal to 0.05 per cent. The correction due to the exponential term ΔF_{exp} is in this case practically the same as in the previous paramagnetic case.

This case is represented by the curves Z_s in fig. 3, in a similar way to the previous one.

We may consider now the most general case for $F(t)$. From the expression (31) we see that the correction term ΔF is closely related to the curvature of F plotted against t as in fig. 3. The radius of curvature of our curve $F(t)$ is given by

$$\frac{1}{\rho} = \frac{F''(t)}{[1 + F'^2(t)]^{3/2}},$$

and from expression (32) we get

$$\frac{1}{\rho} = \frac{\kappa^2 \Delta F}{[1 + F'^2(t)]}. \quad (38)$$

This shows that in the part of the curve where $F'(t) = 0$, namely, at the top and at the ends of the curve, the radius of curvature is inversely proportional to the correction ΔF . This also means that when the radius of curvature is large and the curve approaches a straight line, there are no corrections to introduce. Expression (38) also indicates that the largest corrections are to be expected in places where the curvature of the line is the greatest, and a

more accurate estimate of the correction term may be made by measuring the slope and the radius of curvature of the curve on the oscillogram at a definite point. However, in practice this is found to be unnecessary. The cases in which we are practically interested, namely, a transition from a paramagnetic to a saturated state, lie in between the two just considered, and are approximately represented by the curve Z .

It is evident that the process of saturation must be a gradual one. The curvature of the line Z must be less than if the substance, instead of becoming saturated, should follow the paramagnetic curve Z_p . As we have seen that in the above range of magnetic fields the inertia correction for paramagnetic cases fulfils the required accuracy for the experiment, we can be sure that in the case of saturation the error due to the inertia of the system will be even smaller.

Another way to apply the expression (31) to estimate the error in Z , when $F(t)$ is any function of the time, is to develop the function F in a Fourier series

$$F(t) = \sum A_n \sin \frac{2\pi n t}{\tau}.$$

The coefficient A may be determined either graphically or analytically, when Z may at once be obtained from (31)

$$Z = \frac{E}{f} \sum A_n \left[1 - \left(\frac{nT}{\tau} \right)^2 \right] \sin n \left(\frac{2\pi t}{\tau} - \frac{2T}{\tau} \right).$$

From this expression it is evident that to a first approximation all the terms of the Fourier series will have the same phase shift $2T/\tau$, and the coefficient A_n will be diminished. The correction will depend on the order of the term, and gradually increases as the term becomes of higher order, and, as we should expect, for high harmonics when the period of time approaches that of the balance the formula will not hold any more. If the coefficients in the Fourier series converge sufficiently rapidly and only a limited number of terms are required to represent the function F with the required accuracy, the formula (31) can still be successfully used. From these formulæ it is also evident that the accuracy of the experiment will in all cases depend on the square of the ratio of the period of the balance to the period of the harmonics examined.

In the later sections of our paper we shall show how the general results of this section are used for actual measurements of the oscillograms.

(1) A high frequency, damped, sensitive type of balance is described by means of which it is possible to measure forces of a few grams in a time of the order of a hundredth of a second.

(2) A general formula for the design of this balance to suit any practical requirement is given.

(3) The results of the examination of the balance are described.

(4) A general theory is given for estimating and correcting for the inertia of the moving part of the balance.

The Study of the Magnetic Properties of Matter in Strong Magnetic Fields. Part II.—The Measurement of Magnetisation.

By P. KAPITZA, F.R.S., Messel Research Professor of the Royal Society.

(Received January 26, 1931.)

[PLATE 13.]

(i) *The Experimental Arrangements.*

The balance described in Part I of this paper was found to be quite suitable for measuring the magnetisation of most substances. The experimental arrangement, by which it was used for measuring magnetisation in strong magnetic fields, is shown in fig. 4.*

A thin-walled quartz or glass tube (19) is suspended below the diaphragm (4) of the balance; the tube is divided into two parts by a small neck, the top part being filled with the substance to be investigated (20). The lower part of the tube was introduced merely to compensate the magnetic force which acts on the top part; in this way the corrections due to the magnetic properties of the suspension were reduced to a minimum. If the substance (20) was diamagnetic it was placed below the centre of the coil; if paramagnetic it was placed above the centre; thus the force to be measured by the balance always acts downwards. This is necessary as in most cases, even with weakly dia-

* Cf. 'Proc. Roy. Soc.,' A, vol. 115, p. 678 (1927).

magnetic substances, the force was larger than the weight of the glass tube with the substance.

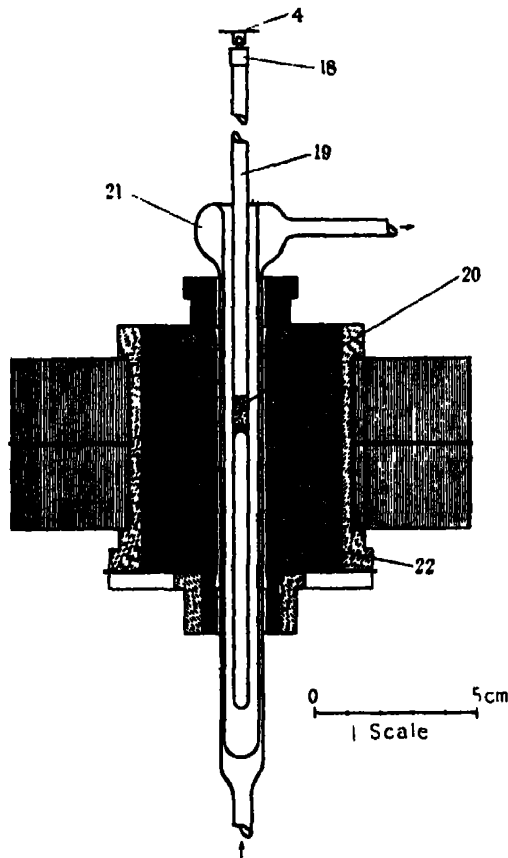


FIG. 4.—The coil, and the suspension of the magnetised body.

The rod (19) was attached to the diaphragm of the balance by means of a small brass ball made in one piece with a brass cap (18) which was shellaced to the glass rod. This brass ball fitted into a slot made in a brass appendix soldered to the diaphragm (4), thus providing a universal joint so that the glass rod always took up a vertical position. The balance itself (not shown in fig. 4) was placed above the coil on a solid slab of slate by means of levelling screws which made it possible to adjust the height of the balance above the coil. The slab was suspended by four phosphor-bronze wires making a vibrationless suspension which was necessary, because, as before stated, the balance acts as a very sensitive seismograph. The glass rod (19) is surrounded by double walled glass tubing (21); water was kept running between the walls

of this glass tube thus keeping the inside of the coil round the substance examined at a constant temperature, and protecting the substance from being heated after the experiment, when the temperature of the coil may rise to 140° C.

Later on we made a few measurements at lower temperatures, and in this case, instead of the water jacket, the glass rod was surrounded by a similarly shaped vacuum tube, the bottom of which was open and connected to a Dewar vessel which contained liquid nitrogen. By means of an electric heater, cooled nitrogen gas was evaporated and made to flow round the substance, thus cooling it down to within 2° or 3° of the temperature of liquid nitrogen (the complete description of this method will be given in Part III of this paper). The use of a gas cryostat was found to be necessary, since if the tube was directly immersed in liquid nitrogen, the shaking produced by the boiling seriously disturbed the deflection of the balance.

The coil (22) used for this set of experiments was different from that used for resistance measurements and described in a previous paper.* The general design was very similar, but we found it convenient to increase the inside space in the coil where the field was produced. In our new coil the inside diameter was 1.4 cm. instead of 1 cm. as before. This necessarily lowered the range of magnetic fields which could be produced, the maximum field obtainable with this coil being 280 kilogauss instead of the previous 320 kilogauss.

The image from the mirror of the balance is directed on to a horizontally moving photographic plate, on which the displacement of the light spot from the balance is recorded (see curve F of the oscillograms, No. 4 to No. 9 on Plate 13). By means of an electrical release and a certain timing apparatus the plate passes the place where the images are thrown at the correct moment in the experiment. On the same plate the current through the coil is also recorded (see curve I on the oscillograms). The current was recorded by means of an oscillograph similar to that used in our previous experiments,† the only difference being that the magnetic field in this oscillograph was produced with a permanent magnet made of tungsten steel. A fraction of the beam from the arc which supplied the light to the balance was deflected by means of a mirror on to the oscillograph, from which the reflected light was thrown by another mirror on to the photographic plate. The oscillograph was so adjusted that the spot of light produced on the plate moved in the same

* 'Proc. Roy. Soc.,' A, vol. 115, p. 678 (1927).

† 'Proc. Roy. Soc.,' A, vol. 105, p. 701 (1924).

line as the spot produced by the balance ; in this way, having the two curves on the same photographic plate it was quite easy to measure the deflection of the balance, and the corresponding simultaneous deflection of the current oscillograph as they were both on the same vertical line.

The Performance of the Experiments and Measurements.—The general way in which the experiments were conducted was as follows : the required amount of the substance was first cleaned from all possible traces of iron on the surface ; in most cases when it was possible this was done by washing the substance in diluted hydrochloric acid. The substance was then placed in the tube which had been carefully cleaned of any traces of iron. The tube was weighed on a microbalance before and after insertion of the substance, and in this way the amount of the substance used was determined.

The tube was then connected to the balance which was placed on the slate above the coil. The glass rod was adjusted centrally in the opening of the coil by moving the balance on the slate table. The zero of the spot of light from the balance was adjusted on the photographic plate by means of prisms, and made to move in the same line as the spot from the oscillograph. Before using the maximum magnetic fields available the experiments were made with smaller fields (about 70 kilogauss) ; this was necessary in order to adjust the deflection which will occur when the maximum field is used. If in this preliminary experiment it was found that the deflection was too small or too large it was always possible, by lowering or lifting the balance by means of the levelling screws, to move the balance into the region of the coil where the gradient of the magnetic field was either larger or smaller. The gradient of the field inside the coil is zero exactly at the centre, and increases gradually towards the ends of the coil. In practice we found that it was not advisable to work in fields with a small gradient close to the centre of the coil, as in this region the variation of the gradient is rather large, and a small shift of the substance may easily bring it to a place which has a different gradient, and in case the rod has to be removed and replaced, it is very difficult to ascertain that it has been put back in exactly the same place.

The oscillograms taken were measured in the way described previously.* The measurements of the deflections were made by an ordinary rule after the oscillograms had been magnified about three times. The maximum amplitude of the magnified oscillograms was about 100 mm. and the accuracy of measurement was within about $\frac{1}{2}$ mm. This gives, in the region of the deflection between the maximum and $1/10$, an accuracy ranging from

* 'Proc. Roy. Soc.,' A, vol. 123, p. 293 (1929).

0.25–2.5 per cent.; this was considered to be sufficient because, as was shown in the previous part, owing to the inertia of the moving parts of the balance, the estimated accuracy in the above region of deflection was of the same order.

In the measurement of the oscillograms, account was also taken of the phase shift which occurs as described in the last section of the previous part. The phase shift was very small, and could be traced graphically; as a matter of fact, it was not found to be constant, this being mainly due to the error in setting the two images from the oscillograph and the balance to move in a line. Any inaccuracy in the adjustment would also produce a phase shift. By taking account of the phase shift graphically, the correction was introduced for rectifying the phase shift occurring from both sources. The graphical method of finding the phase shift was to find for two equal values of the current, slightly before and after the maximum current, two equal deflections of the balance which would be displaced by the same amount. This phase shift was then taken in the measurement of the whole of a single oscillogram. The slight difference in the values of the balance deflection for the same current, obtained on the rising and falling parts of the oscillograms were averaged, and the mean deflection was obtained in this way for different magnetic fields. From them the variation of the magnetisation with the magnetic field could be studied.

At present only relative changes of the magnetisation with the magnetic field have been studied; it is evident that there is no special interest attached to making absolute measurements, as they can be made much more conveniently by experiments in permanent fields obtained by means of electromagnets, and the absolute values of magnetisation can, in this way, be measured for fields up to 30 kilogauss. Taking this value as a starting point, we can extend by means of our methods the study of magnetisation changes to fields 10 times stronger.

(ii) *Sources of Error.*

In order to check the accuracy of the experiments a careful study of the sources of error had to be made, particularly as the performance of the experiments in such a short time necessarily involved some difficulties. We will first consider the general errors which depend only on the actual experimental arrangements used.

In the first place, it was possible that the balance itself might be influenced by the magnetic field; this was easily checked by taking oscillograms of the deflection of the balance when the glass tube (19) was removed. The oscillograms showed that there was no trace of deflection, indicating that no error

arose from this cause. A possible error may arise from a displacement of the substance in the field during the experiment; this can easily be shown to be negligible as the maximum value of the displacement was only 10^{-4} mm., and the variation of the magnetic field and of the gradient in such a small length is so small that the error produced comes well within the limits of accuracy of our experiments. The proportionality of the deflection of the balance to the force applied has already been examined and described in Part I (iii), and it has been shown that if the balance is properly set, this error is also within the limits of the accuracy of the measurements of the oscillograms. In the case of the balance not being brought to the "natural zero" as happened in some of our earlier experiments when all the properties of the balance were not sufficiently known, a small zero shift occurred which can be traced on some of the reproduced oscillograms. Even in this case, if the zero line be taken as the straight line connecting the beginning and the end of the curve of the oscillogram, it appears that the accuracy of the measurement is still within 1 per cent.

One of the sources of error which appeared to be of great importance was the influence of the magnetic field on the oscillograph. As has already been described, the current oscillograph traces a line on the same plate as the balance, and this made it impossible to keep the oscillograph sufficiently far from the coil, and we found that the magnetic field of the coil affected the magnetic field of the permanent magnet of the oscillograph during the time when the current wave was recorded. The magnitude of this effect was easily determined from an oscillogram which was taken while a constant current was passing through the oscillograph, and the magnetic field was produced in the coil. In this way, it was found that the magnetic field in the oscillograph was slightly increased, and this increase was proportional to the magnetic field in the coil; as this error was apparently quite constant for a definite position of the coil and the oscillograph, the deflections of the current oscillograms were easily corrected, the correction being proportional to the magnetic field, and at its maximum value, in the worst cases, reached a value of about 4 per cent. With this correction we estimate the accuracy of the measurements of the magnetic fields to be within 0.5 to 1 per cent.

The next important source of error to be considered was the magnetic effect of the glass or quartz rod (19). As has been previously stated, the shape of the rod was chosen to be such as to produce as small an effect as possible, and actually, at room temperature, the effect from the rod was never more than 1 or 2 per cent. of that produced by the substance under examination. The correction could, therefore, be accurately determined by measuring the force

on the rod without the substance. However, at low temperatures the correction for the rod in certain cases was quite considerable, especially where a glass rod was used instead of quartz. It appears that our glass was paramagnetic, and its susceptibility depends on the temperature. When the rod is cooled down, with the gas cryostat used it was impossible to get a uniform temperature along the whole of the rod, the lower part being slightly cooler than the upper; therefore the magnetisation of the lower half of the rod was not equal to the magnetisation of the upper half, so that the forces on the two did not cancel out. Using glass rods, this produced a considerable effect at low temperatures. However, after realising this effect the use of glass rods was discontinued and quartz rods only were used in their place. Even in the cases when glass rods were used the correction was easily made since it was found that the force on the glass rod was strictly proportional to the square of the magnetic field.

From a general consideration of all possible errors, combined with the error due to the inertia of the moving masses in the balance, the relative error of measurement for one single oscillogram could be quite fairly estimated to be within 1 or 2 per cent. in the range of magnetic fields before indicated. In comparing different oscillograms taken for the same substance the accuracy is probably lower, as in this case the general conditions of the experiments may vary. Thus, in comparing two different oscillograms of the same substance when no special precautions had been taken to keep the conditions the same, the error in most cases was not higher than 2 to 4 per cent.

Stray Effects.—Two main stray effects have to be considered. The first is the influence of the presence of impurities in the form of ferro-magnetic substances, mainly iron, in the substance used for experiment. It is well known that even a small amount of such impurity, if it is in a free condition, may completely alter the magnetic properties of a weakly magnetic substance. However, in our experiment, the influence of a definite amount of iron is much smaller than in a corresponding experiment made in the weaker field produced by an electromagnet. In the range of our magnetic fields, namely between 20 to 300 kilogauss, the stray magnetisation not only has a smaller value relative to the total magnetisation compared with that in weak fields, but, as the iron present in the substance remains fully saturated all the time, its stray contribution to the magnetisation remains constant, and this makes its elimination comparatively simple. It will be seen from the description of the experiments on some ferrous, non-magnetic alloys, how it was possible to separate the paramagnetic and the ferro-magnetic parts of the magnetisation.

Another important stray effect arises from the eddy currents produced in the substance by the variable magnetic field when the substance under investigation is a metal with a high electrical conductivity. The influence of these eddy currents is manifested in two ways: first, a dynamic effect is produced, and secondly a thermal effect which heats the substance. The first effect is a force on the substance resulting from the interaction of the magnetic field and the eddy currents. We shall call this force F_i .

To estimate the magnitude of F_i we shall assume, as before, that the magnetic field H changes as a sine function of the time, and the magnetised body we take to be a cylinder of outside radius r and height h , placed in the coil with its axis parallel to the axis of the coil. We consider an elementary ring of cross section $dx \cdot dr$. If I is the density of the induced current and H_r is the radial component of the magnetic field, this ring will be submitted to a usual force equal to

$$dF_i = IH_r 2\pi r \cdot dx \cdot dr. \quad (38)$$

If we assume that in the plane of the ring considered the variation of the magnetic field is small, and no skin effect occurs in the range of frequency of our experiments, we get for the density of the induced current

$$I = \frac{r}{2\rho} \frac{dH}{dt}, \quad (39)$$

where H is the axial component of the magnetic field, and ρ the specific resistance of the metal. In case of axial symmetry a simple relation between H_r and H can be deduced from the standard properties of the potential field.

$$H_r = -\frac{r}{2} \frac{dH}{dx}. \quad (40)$$

Then, from (38), (39), (40) and (20), after performing the integration for all the cylinder, and writing $v = \pi hr^2$ for the volume of the cylinder, we get

$$F_i = -\frac{\pi v r^2}{4\rho r} H_0 \frac{dH_0}{dx} \frac{\pi}{\tau} \sin \frac{2\pi t}{\tau} \cos \frac{2\pi t}{\tau}. \quad (41)$$

On fig. 3 we have plotted the curve F_i which represents the force F_i .

It can be seen from (41) as well as from the curve on fig. 3 that the force F_i due to the induction effect is zero when the magnetic field reaches its maximum value, but before this maximum value is reached, when the current in the coil is increasing, the force F_i has a negative value; this means that the stray effect in this region has the appearance of an additional diamagnetism. After the maximum field when the current through the coil decreases, the curve of F_i

has the same general shape as before the maximum, but with the opposite positive sign. This shape of the function F_s makes it possible to eliminate it from the total force, when the force is small, by taking the mean value of the balance deflection for equal magnetic fields measured on the increasing and the decreasing sides of the current wave. As has already been mentioned in the previous section, this was the standard procedure adopted for measuring the oscillograms.

In certain cases where the metal has a large conductivity it is difficult to eliminate this stray effect sufficiently accurately by this method, and in this case it is much more convenient to diminish its magnitude. This can be done by a proper choice of the shape of the examined substance. From (4) it is evident that the magnitude of F_s does depend on the shape of the body, as in two cylinders of equal volume v , but with different cross section, the force F_s will be proportional to the area of cross section; this indicates that for metals of high conductivity, thin wires should be taken in order to reduce the stray effect.

The magnetic force on a body of volume v and susceptibility χ and density d will be, from (1) and (20),

$$F = v d \chi H_0 \frac{dH_0}{dx} \sin^2 \frac{2\pi t}{\tau}. \quad (42)$$

If we compare it with (41) we get

$$\frac{F_s}{F} = -r^2 \frac{\pi}{4\rho\chi\tau} \cot \frac{2\pi t}{\tau}. \quad (43)$$

This ratio evidently diminishes with decreasing values of r . For the metallic substances which we have examined so far, we have been able to make r , the radius, small enough to keep the ratio of the stray effect to the total force, as given by (43), under 1 or 2 per cent. in the region of magnetic fields in which we were interested. However, in the case of a highly conducting metal like copper which is at the same time very weakly magnetic, we can see from (43) that the radius of the wire required to keep the stray effect small in comparison with the magnetic force, will have an impracticably small value. In such a case another way of eliminating the stray effect is possible, namely by compensation. This could be done by using two differently shaped metal specimens of different volume; one, for instance, being a flat ring of large diameter but with a smaller volume; the other being a long cylinder having a small radius and a larger volume. They would have to be attached to the same rod (19), fig. 4, but placed one above and one below the centre of the coil. It is evident that it would be

possible to find such a position of the rod in the coil that the forces F , due to the induced effect, having opposite directions in the two specimens, will balance each other, while the magnetisation effect will be the same as for a similar substance having a volume equal to the difference between the volumes of the two specimens.

The second stray effect due to the eddy currents results from the heating produced, which may in certain cases alter the susceptibility of the substance under examination. The magnitude of this effect can easily be calculated from (39) by integrating the square of the density of the current over the whole volume of the substance and the time of the experiment. The mean value of the total heat produced in the substance per unit volume during the experiment will be

$$W = \frac{\pi^2}{8} \frac{r^2}{\rho} \frac{1}{\tau} H_0^2 \text{ ergs.} \quad (44)$$

Evidently the heating effect also diminishes with the square of the radius of the wire. Numerical evaluation shows that in general this stray effect is too small to be of any practical significance; for instance, if we take copper, which has the highest conductivity, in the form of a wire 1 mm. in diameter, it can be shown from (44) that the rise of temperature after an experiment with a field reaching a maximum value of 300 kilogauss is only 0.1°C . for experiment at room temperatures. At lower temperatures, owing to the decrease in the specific heat and increase in conductivity, the effect becomes considerably larger. This effect is actually only of importance at very low temperatures (liquid hydrogen), but in this case we also have to consider the rapid increase of resistance of the metal in magnetic fields which will considerably reduce the rise in temperature.

(iii) *The Adiabatic Magnetisation.*

Langevin* was the first to show theoretically that a paramagnetic gas when magnetised must increase its temperature. It can also be shown on general thermodynamical grounds that any substance in which the magnetisation depends on the temperature, will also change its temperature while being magnetised. This temperature change in weak magnetic fields as obtained by electromagnets is negligibly small in most cases, but since in general the temperature increases as the square of the magnetic field, in the range of magnetic fields used in our experiments it reaches a value about 100 times larger and has to be considered very carefully, especially in cases where the

* 'Ann. Physik,' vol. 5, p. 123 (1905).

magnetisation of the substance depends a great deal on the temperature, since this change in temperature may considerably change the magnetisation. The importance of the phenomenon at once becomes evident when we think of the brief time space in which our experiments were made. In the experiments made in steady fields as produced by permanent magnets the observations are always on isothermal magnetisation, as the initial change of temperature of the magnetised body disappears very soon as it gets into thermal equilibrium with the surroundings. In our case, owing to the shortness of the time of the experiments we have an adiabatic magnetisation and the temperature change will not be dissipated. A knowledge of this change of temperature is essential for the interpretation of our experimental results. We shall now give a deduction, on purely thermodynamic grounds, of formulæ which will enable us to calculate this change for para-, ferro- and diamagnetic substances.

If the magnetisation of the body changes by dI in a magnetic field H , the work done by the external system will be $-jHdI$ expressed in calories, where j is the heat equivalent. If the internal energy of the body changes by dU , and a heat dQ is supplied we have

$$dQ = dU - jH dI. \quad (45)$$

Taking the temperature and the magnetic field as independent variables we have

$$dQ = \left(\frac{\partial U}{\partial H} - jH \frac{\partial I}{\partial H} \right) dH + \left(\frac{\partial U}{\partial T} - jH \frac{\partial I}{\partial T} \right) dT. \quad (46)$$

If, in the usual way, we divide both sides of this equation by T , and note that in this case (46) must be a complete differential, we get from the properties of its coefficients

$$jT \frac{\partial I}{\partial T} = \frac{\partial U}{\partial H} - jH \frac{\partial I}{\partial H}. \quad (47)$$

In the case of an adiabatic magnetisation, dQ in (46) is equal to zero, and combining (46) with (47) we get

$$dT = - \left[jT \frac{\partial I}{\partial T} / \left(\frac{\partial U}{\partial T} - jH \frac{\partial I}{\partial T} \right) \right] dH. \quad (48)$$

This formula is a fundamental relation from which we can calculate the rise of temperature for the adiabatic magnetisation of any substance, provided we know the value of the coefficients. At first we see that, in general, a temperature change will always occur if $\partial I / \partial T \neq 0$; thus only in substances

in which we have a magnetisation completely independent of the temperature, as for instance in most of the diamagnetic substances, will the temperature be unchanged by magnetisation.

In the expression (48) the differential can be eliminated if first we know how I , the magnetisation, depends on the magnetic field and the temperature; secondly, we must know the value of U , which, in general, is a function of T and H ; the way in which U depends on H can be obtained from (47) if I is a known function of T and H . The way in which U depends on the temperature can only be obtained from the theory of specific heats. However, with a temperature which is not too low the main part of the internal energy U is contributed by the heat motion, and $\partial U/\partial T$ may be taken as equal to the specific heat C

$$C = \partial U/\partial T. \quad (49)$$

Let us take the case of a paramagnetic substance, the magnetisation of which follows the generalised Curie-Langevin law.

$$I = \chi H = \frac{I_0^2}{3R(T + \theta)} H. \quad (50)$$

If we take the approximation (49) we get

$$dT = \left[j\chi \frac{T}{T + \theta} / \left(C + j\chi \frac{H^2}{T + \theta} \right) \right] dH. \quad (51)$$

At ordinary temperatures where C is large compared with its neighbouring term, and when θ is small or equal to zero, we get, after integrating

$$T = j \frac{X}{2C} H^2. \quad (52)$$

This result is similar to that obtained for an ideal paramagnetic gas by Langevin (*loc. cit.*).

At low temperatures, close to absolute zero, when C , according to the Debye-Einstein theory tends to zero, the relation between the magnetisation and the applied magnetic field becomes more complicated due to the saturation. Equations (49) and (51) are then no longer a sufficient approximation, and we must take account of U being a function of H and T . Our present experiments were limited to temperatures not lower than that of liquid air, and the case of C being small in comparison with its neighbouring term did not occur. However, this case must be most carefully considered when we extend our work to the very low temperatures at which we propose to determine the saturation

value of paramagnetic substances. A more complete analysis indicates that the large rise in temperature which must occur close to the absolute zero due to adiabatic magnetisation, makes the magnetic field less efficient in magnetising the body to saturation than in cases of an isothermal process. The adiabatic magnetisation at temperatures very close to the absolute zero for a paramagnetic substance which follows the Langevin law of magnetisation have been worked out theoretically by Debye.* He has shown that at this temperature the Langevin law involves a contradiction with the Nernst law, and that at low temperatures the Langevin law of magnetisation can only be regarded as approximate. Debye's work is of great interest to us as it reveals the general character of adiabatic magnetisation of a paramagnetic substance at low temperatures.

Ferro-magnetic bodies also alter their temperature when they are magnetised. By the Langevin-Weiss theory of magnetisation of ferro-magnetic substances, the magnetisation I is given by

$$I/I_0 = \coth a - 1/a, \quad (53)$$

where a is

$$a = I_0 (\lambda I + H)/RT \quad (54)$$

and I_0 is the intensity of magnetisation for complete saturation. λI is the molecular field, in most ferro-magnetic substances of the order of 6000 kilogauss. If we attempt to find an exact value for $\partial I/\partial T$ from these two last expressions we shall meet with considerable mathematical complications; we shall therefore limit ourselves to finding out the magnitude of dT which can easily be estimated fairly accurately if we make the following approximations. As shown by Weiss, from the formulæ (53) and (54), below a certain temperature T_0 which is called the critical temperature, we have the spontaneous magnetisation characteristic of ferro-magnetic substances. Below this critical temperature we have the value of a always larger than 3, and it can be expressed in the following approximate way

$$a = 3T_0/T. \quad (55)$$

Thus we find that, at room temperature (300° K.), a will be about 9 for iron and about 6 for nickel. When a is large, then with a sufficiently close approximation we get from (53)

$$\frac{\partial I}{\partial T} = \frac{I_0}{a^3} \frac{\partial a}{\partial T}. \quad (56)$$

* 'Ann. Physik,' vol. 81, p. 1154 (1925).

By differentiating (54) and making some further approximations in which we neglect the applied field in comparison with the molecular field λI , we find

$$\frac{\partial I}{\partial T} = \frac{I_0}{3T_0 - T}, \quad (57)$$

and finally, for the rise of temperature, we get

$$dT = \left[\frac{T}{3T_0 - T} / \left(C + j \frac{I_0 H}{3T_0 - T} \right) \right] j I_0 dH. \quad (58)$$

As before, by neglecting the neighbouring term to the specific heat we get, approximately,

$$\Delta T = \frac{T}{C(3T_0 - T)} j I_0 H. \quad (59)$$

We see that the rise of temperature in the case of ferro-magnetic substances is linear with the field and diminishes as the temperature becomes lower. At very low temperatures when C approaches zero the calculations are again complicated as in the paramagnetic case, the internal energy U being a function of H . However, it appears that the general result expressed by (58) will still give the right order of rise of temperature for ferro-magnetic substances, even when the temperature is very low.

In some diamagnetic substances the susceptibility changes with the temperature. For instance, in bismuth over a considerable range of temperature the diamagnetic susceptibility increases according to the following empirical law

$$I = \chi H = -|\chi_0(1 - \alpha T)| H. \quad (60)$$

Using this expression we get from (58) for the rise in temperature

$$dT = -j \frac{T |\chi_0| \alpha H}{C - j |\chi_0| \alpha H} dH. \quad (61)$$

If the temperature is not very low and we neglect the neighbouring term to C , we get

$$T = -j \frac{|\chi_0| \alpha T}{2C} H^2. \quad (62)$$

We see that in this case, contrary to the ferro- and para-magnetic cases, the temperature will diminish with the magnetic field.

As will be seen later, the change of temperature, which occurred in our magnetic fields, and in the range of temperatures used (room temperature to the temperature of liquid air), was never more than 1° or 2° for any measured

substance. Such small changes in temperature do not appreciably affect the magnetic properties of the substances, and, as will be shown, have very little influence on our present results. However, it is very important to give careful consideration to this change of temperature in studying the magnetostriction, where the increase is sufficient to produce a well-marked phenomenon due to the thermal expansion.

(iv) *The Magnetisation of Ferro-magnetic Substances.*

Iron.—For the study of the magnetisation of iron we used some exceptionally pure metal kindly given to us by Dr. Rosenhain; it contains only 0.01 per cent. of impurity, consisting chiefly of carbon. A small piece of wire, 0.36 mm. in diameter and 5.7 mgm. in weight was fixed in a quartz tube similar to that shown on fig. 4 (19), except that the tube was only 2.6 mm. in diameter.

Measurements were made only at room temperature, and a number of oscillograms were taken, one of which for a field of 260 kilogauss is reproduced on Plate 13, No. 4. For a number of deflections of the balance, corresponding deflections of the current oscillograph were measured, and corrections were made in the way previously described to deduce the magnetic field. The values obtained are plotted on fig. 5, where the abscissæ are the magnetic

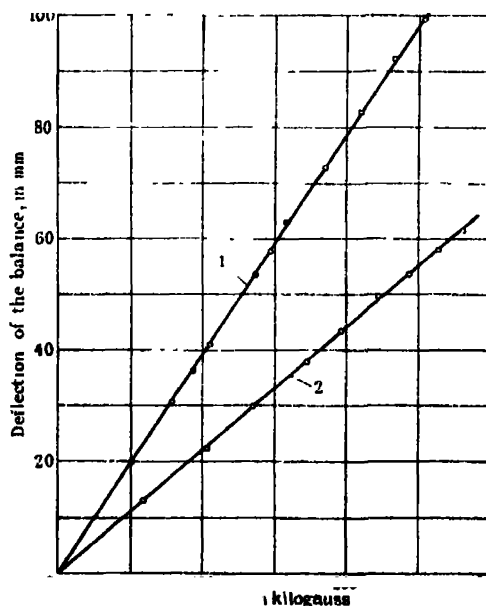


FIG. 5.—The magnetisation of ferro-magnetic substances at room temperature. Curve 1, Iron. Curve 2, Nickel.

field in kilogauss, and the ordinates represent the corresponding deflection of the balance in millimetres as measured on the enlarged oscillogram. On curve I the data for two oscillograms have been plotted, one for a field strength up to 260 kilogauss shown by plain circles, the other for a field strength up to 158 kilogauss shown by blackened circles. It is evident that when the magnetisation of the body remains constant, the deflection must be proportional to the strength of the magnetic field; and it can be seen from this curve that the points lie well on a straight line, showing that the magnetisation of iron remains constant within the limits of experimental error up to field strengths of 260 kilogauss.

Nickel.—The nickel used was kindly given to us by the Research Department of the Mond Nickel Company and was 99·964 per cent. pure, the impurities being :—

Fe	Mg	Co	Ca	C	N
0·01	0·003	0·002	0·001	0·015	0·005
per cent.	per cent.	per cent.	per cent.	per cent.	per cent.

A piece of nickel wire 0·62 mm. in diameter and weighing 11·2 mgm. was placed in the same quartz holder as used for the iron. Experiments were made only at room temperature. One of the oscillograms obtained with a maximum field of 287 kilogauss is shown on Plate 13, No. 5. The corresponding curve is plotted on fig. 5, curve 2; and since the deflection is again proportional to the strength of the field we deduce that the magnetisation of nickel remains constant within the limits of experimental error up to field strengths of 287 kilogauss.

Oscillograms were also taken with weaker magnetic fields, and each of these showed a constant magnetisation. As no special precautions were taken to keep the temperature and the position of the specimen the same for all individual experiments of this series, they could not be compared on the same curve.

Error of Experiments.—The experimental errors for iron and nickel were small. The induction effect is negligible owing to the high magnetisation value, and the temperature rise due to induction currents only amounts to about 0·01° C. The temperature rise due to the adiabatic magnetisation was calculated from formula (59) to be 1·5° C. for iron and 0·5° C. for nickel for a magnetic field of 300 kilogauss; this small temperature change cannot alter the magnetisation more than a fraction of a per cent. which is well within the limits of experimental error.

Discussion of Results.—From curves 1 and 2 on fig. 5 for iron and nickel, we

see that the magnetisation in the fields used, and at room temperature, cannot vary more than the error of our experiments, namely, about 1 per cent. Thus, if we take I , the specific magnetisation at saturation, to be 216 for iron and 58 for nickel, since our experiments show that in the range of fields up to H_{\max} , it does not change more than 1 per cent., we get the possible limits for the absolute value of the magnetic susceptibility of these two metals after saturation. Thus for iron, χ the specific susceptibility cannot be larger than

$$|\chi_{Fe}| < 0.01 \times I/H_{\max} = 0.01 \times 216/260.10^3 = 8 \times 10^{-6},$$

and for nickel

$$|\chi_{Ni}| < 0.01 \times 58/287.10^3 = 2 \times 10^{-6}.$$

We can also estimate the value of the susceptibility after saturation from the Weiss-Langevin theory. If we differentiate formula (53) with respect to H , we get, with the same approximations used in obtaining (56)

$$\chi = \frac{dI}{dH} = \frac{I_0}{a^2} \frac{da}{dH}. \quad (63)$$

Using again an approximation similar to the one used in calculating the rise of temperature, and which holds when the applied magnetic field is smaller than the molecular field, and the temperature well below the critical temperature, we get the value

$$\chi = I_0 T / 3 T_0 H_0, \quad (64)$$

where H_0 is the molecular field, and T_0 is the critical temperature. We see that in these cases we get a peculiar type of paramagnetism which increases with increasing temperature. This can easily be understood since at lower temperatures the spontaneous magnetisation approaches complete saturation, and the applied external field is less efficient in increasing it any further. If we take values of 5.56×10^6 and 5.35×10^6 for the molecular fields H_0 of iron and nickel respectively, and critical temperatures T_0 of 1042° K. and 629° K. respectively, we get for the susceptibilities after saturation at room temperature (288° K.)

$$\chi_{Fe} = 3.1 \times 10^{-6}$$

$$\chi_{Ni} = 1.4 \times 10^{-6}.$$

Thus our results from the magnetic saturation experiment do not contradict the values deduced from the Weiss-Langevin theory of magnetisation. With our present experimental arrangements it is difficult to obtain values for the susceptibility with the greater accuracy necessary to verify the

theory of ferro-magnetism more precisely. It may, however, be possible in the future, when we propose to resume this experiment with a view also to determining the absolute value of saturation for different temperatures, to use a differential method by which the component of the force on the iron specimen in the magnetic field due to its spontaneous magnetisation, will be compensated by a force on a small coil, attached to the glass rod, through which a constant current is passed. Evidently the differential effect recorded by the balance will give a more precise measure of the value of magnetisation after saturation.

It is interesting to note that in the many attempts which have been made to measure the magnetisation of iron after saturation, the results obtained are not in complete agreement. The reason for this is evidently the well-known difficulties encountered in measuring the magnetisation of ferro-magnetic substances in the fields of about 30 kilogauss to which one is limited with electro magnets.

In a recent paper, Weiss and Forrer* give an experimental proof of the hyperbolic law of magnetisation, namely

$$I = I_{\infty}(1 - \alpha'/H). \quad (65)$$

This was found to be correct up to 20 kilogauss, and the values of the constant α' were found to be 6.3 and 20 for iron and nickel respectively. If we write (65) in the form

$$(I_{\infty} - I)/I_{\infty} = \alpha'/H \quad (66)$$

we easily see that in the region of our fields, from 50,000 to 300,000 gauss, the variation in magnetisation for iron will be less than 0.01 per cent., and for nickel less than 0.04 per cent., thus coming well below our 1 per cent. Thus our results are in general agreement with the work of Weiss and Forrer; for some specimens of nickel, however, they found a parasitic magnetisation which occurs after saturation and is proportional to the field, the susceptibility being about 11×10^{-6} .† Our experiments do not seem to confirm this phenomenon when using strong magnetic fields, as this parasitic effect would give a change in the magnetisation of about 5 per cent. and could be easily traced in our experiments. As Weiss and Forrer mention that this phenomenon was only observed with a few particular samples of nickel, and as the nickel used, according to the analysis,‡ seems to have been less pure than the sample used in our

* 'Ann. Physik,' vol. 12, p. 279 (1929).

† *Loc. cit.*, p. 316.

‡ *Loc. cit.*, p. 324.

experiments, this parasitic phenomenon is probably due to some impurities, and does not appear to have any direct bearing on the theory of magnetisation after saturation.

(v) *Ferro-Magnetic Alloys.*

Among the ferro-magnetic alloys we selected for study was a peculiar nickel-chromium steel which was kindly given to us by Sir Robert Hadfield. This steel, as was found by Sir Robert, is non-magnetic at room temperature; but on hammering, it acquires quite distinct ferro-magnetic properties. The composition of this steel was :—

C	Si	Cr	Ni	Mn	Fe
0.12	0.43	18.80	8.10	0.24	72.31
per cent.	per cent.	per cent.	per cent.	per cent.	per cent.

The heat treatment consisted in heating up to 1150° C. and then cooling in air. 130 mgm. of this alloy was carefully ground out and placed in the same quartz tube as used before for iron. The results of the measurements of the magnetisation before hammering are given on fig. 6 where the abscissæ represent the field in kilogauss, and the ordinates represent the magnetisation in arbitrary units obtained by dividing the deflection of the balance on the magnified oscillogram, measured in millimetres, by the field in kilogauss, and multiplying by 100. It can be seen from fig. 6, curve 1, that in this case we have a constant

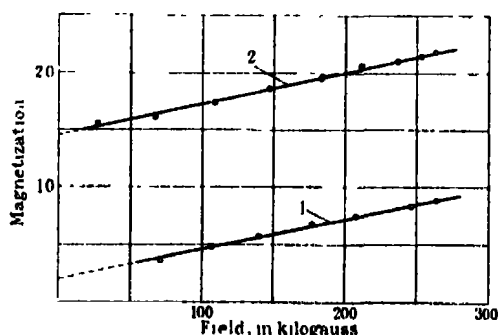


FIG. 6.—The magnetisation of ferro-magnetic alloys. Hadfield nickel-chromium steel at room temperature. Curve 1, before hammering. Curve 2, after hammering.

magnetisation equal to that at zero field, together with a magnetisation which increases linearly with the magnetic field. The constant magnetisation is about 0.1 per cent. of that of iron and the increase in magnetisation corresponds to a susceptibility of about 5×10^{-6} .

After hammering, the sample slightly increased its length, and curve 2

fig. 6, was obtained. It is quite evident from this that the constant magnetisation increases about 10 times but the magnetic susceptibility remains practically the same. This experimental result may throw some light on the actual mechanism of the transition of the alloy from the non-ferro-magnetic to the ferro-magnetic state, particularly when more experiments are made at different temperatures combined with metallographical analyses of the specimens. It may be possible that this alloy is in a state of unstable equilibrium at room temperature, and is changed to its normal ferro-magnetic state by hammering. From experiments initiated by Osmond* on nickel-iron alloys, and later made by a number of other investigators on chromium-iron and manganese-iron alloys, we know that these alloys may have "two Curie temperatures," and it is therefore possible to have them in ferro- or non-ferro-magnetic states at the same temperature. The transition to the ferro-magnetic state may sometimes be produced simply by cooling to low temperatures, and it is possible that some analogous transition is produced in this case by hammering.

The great advantage of our method in studying such alloys lies mainly in the fact that by means of our strong magnetic fields it is very easy to separate the para- and ferro-magnetic parts of the magnetisation.

It would be most interesting to study the variation of the paramagnetic susceptibility with temperature for these alloys for the two states. In our present experiments, as curve 1 runs practically parallel to curve 2, it appears that the paramagnetic susceptibility of the hammered specimen is the same as before hammering. This, however, may be due to the fact that the specimen has not been sufficiently hammered, since, from Sir Robert Hadfield's data, we may expect a considerably larger increase in the ferro-magnetism. If in this case also, the paramagnetic part remains the same, it means that the change from the non-ferro- to the ferro-magnetic state is not made at the expense of the paramagnetic component of the alloy.

We also studied a manganese alloy of iron, kindly given to us by Sir Robert Hadfield. The composition was :—

C	Si	Mn	Fe
1.2 per cent.	0.33 per cent.	13.38 per cent.	85.09 per cent.

It was heated to 1000° C. and quenched in water. The alloy was supposed to be non-magnetic, but actually we found that the ferro-magnetic part of the magnetisation was 0.1 per cent. of that of iron, and the paramagnetism was

* 'C. R.,' vol. 118, p. 532 (1894).

3.5×10^{-6} —again a very small value which is surprisingly smaller than the paramagnetism of manganese itself.

These experiments on alloys were only intended as a preliminary study with a view to finding out the possibilities of using our methods for this line of research.

(vi) *Paramagnetic Substances.*

Gadolinium Sulphate.—Among the paramagnetic substances which we chose for experiment was gadolinium sulphate ($\text{Gd}_2(\text{SO}_4)_3 \cdot 8\text{H}_2\text{O}$), which has been most carefully examined at all temperatures, particularly by Kamerlingh Onnes and L. C. Jackson.* This substance appears to follow very closely at all temperatures the classical law of magnetisation given by Curie and Langevin. The gadolinium sulphate which we used was kindly given to us by Lord Rutherford and was prepared by Dr. Welsbach. On this substance, we have made measurements at room temperature and also at the temperature of liquid nitrogen. Two sets of experiments were made at room temperature; in the first, the quartz tube (19) fig. 4, was filled with 167 mgm. of the salt. In this case the deflection of the balance reached the maximum amplitude permitted by the size of the photographic plate at 120 kilogauss, and from these experiments we found that, within the experimental error of 1 per cent., no deviation from the linear law of magnetisation occurred in this region of magnetic field. The amount of substance was then reduced to 74 mgm. and the magnetisation was studied up to the full field strength. The oscillogram on Plate 13, No. 6, was obtained with a field strength up to 271 kilogauss, and the results of the measurements are given on curve 1, fig. 7. As in the previous case, the abscissæ represent the field in kilogauss, and the ordinates the magnetisation in arbitrary units (obtained by measuring the deflection of the balance on the enlarged oscillogram in millimetres, dividing by the field in kilogauss, and multiplying by 100). From the examination of the points on this curve it is evident that at room temperature the magnetisation is proportional to the field strength within the limits of experimental error of 1 per cent.

The experiments at lower temperatures were carried out in the gas cryostat described before. The tube and the specimen were moved into a region of smaller gradient of the magnetic field, closer to the centre of the coil, as otherwise the deflection of the balance was thrown out of the range of the photographic plate. Oscillogram No. 7, Plate 13, was obtained with a field strength of 265 kilogauss, and the results are plotted on curve 2, fig. 7. From this

* 'Leiden Com. Sup.,' vol. 167c, p. 38 (1923).

curve it will be seen that the law of magnetisation is no longer linear, and as we should expect from the theory, we have the beginning of saturation.

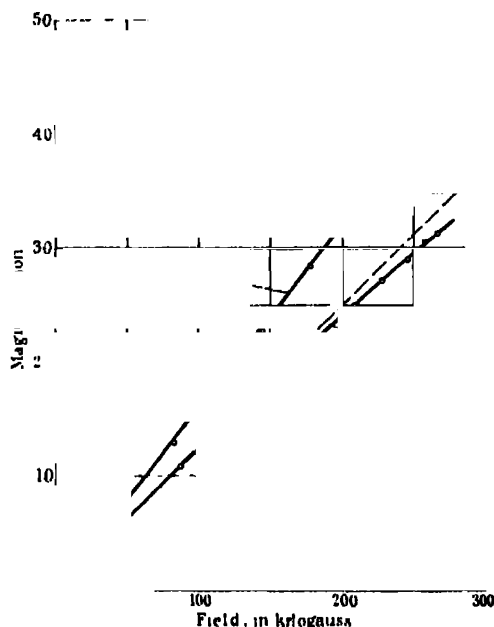


FIG. 7.—The magnetisation of gadolinium sulphate. Curve 1, at room temperature. Curve 2, at temperature of liquid nitrogen.

Errors of Experiments.—The errors in this case were rather small as no induction phenomenon occurred, the only one which we had to consider being due to the change in temperature of the substance which was caused by the adiabatic magnetisation. At room temperature, as we can obtain from (52), taking the value of the specific heat of gadolinium sulphate to be 0.83, the increase of temperature in a field of 271 kilogauss is only 0.04° C. At the temperature of liquid nitrogen the specific heat of gadolinium sulphate is 0.40, and the temperature rise in a field of 265 kilogauss about 0.25° C. In both cases the changes of temperature are too small to affect the value of the magnetisation by more than a fraction of 1 per cent.

Discussion of Results.—On the Langevin theory, the magnetisation I' of gadolinium sulphate approaches its saturation value I_0 according to the following formula

$$I'/I_0 = (\coth a - 1/a), \quad (67)$$

where

$$a = I_0 H / RT.$$

When the value of a is small we have the well-known approximation which gives the Curie linear law

$$I/I_0 = a/3 = I_0 H/3RT. \quad (68)$$

For gadolinium sulphate at room temperature, the value of a in formulæ (67) and (68) is equal to 0.29 for a field strength of 271 kilogauss, and the difference between I'/I_0 and I/I_0 is only 0.7 per cent. At the temperature of liquid nitrogen, however, a reaches a value of 1.06 at a field strength of 265 kilogauss, and the magnetisation, as given by (67), is 0.328 instead of 0.354 as given by (68), which should be the value if the magnetisation followed the linear law. Thus the deviation from the linear law of magnetisation is about 8 per cent. This result is confirmed within the limits of experimental error by our experiments, as can be seen from fig. 7. Here the broken straight line represents the tangent to the curve of magnetisation 2 as given by the experiment, and evidently represents the law of magnetisation as given by the approximate formula (68). It can be seen that at 271 kilogauss the difference in the ordinate for the broken and experimental curve is actually about 8 per cent. of the magnetisation. It is interesting to note that at 271 kilogauss the magnetisation is 0.328 of the complete saturation and is actually about the same as for nickel.

Woltjer and Kamerlingh Onnes* have measured the saturation of gadolinium sulphate at 1.3° K., where they approached to within about 85 per cent. of a saturation value with a field of 23 kilogauss, and found good agreement with the Langevin law. With our magnetic field strengths we should expect a much closer approach to saturation at low temperatures, and we shall probably be able to check the Langevin law of magnetisation fairly accurately over a greater range, since, owing to the shortness of the time, we have the great advantage of the absence of any temperature disturbances. From the position of the points on the curve of fig. 7, the fair precision of our experiments may easily be judged.

Manganese.—The manganese used in the experiments was kindly given by Dr. Rosenhain, and was prepared at the National Laboratory by Dr. Marie Geyler. It had been melted *in vacuo* and contained only 0.01 per cent. of impurities. It was used in small fragments of about 1 to 1½ mm. in size. 0.345 gm. of the manganese was placed in the quartz tube, all the usual precautions being taken, and the experiments were carried out at room temperature. The oscillogram obtained in the strongest field (275 kilogauss) is shown on Plate 13, No. 8. The results of the measurements have been plotted in the

* 'Leiden Com. Sup.,' vol. 167c, p. 38 (1923).

same way as for gadolinium. On fig. 8 the curves are obtained from two oscillograms; the points from one before mentioned are indicated by plain circles,

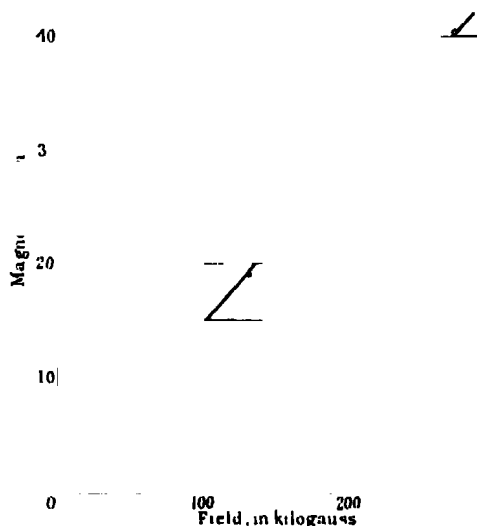


FIG. 8.—The magnetisation of manganese at room temperature.

and the others using a field up to 210 kilogauss, are indicated by blackened circles. It will be observed that the magnetisation is strictly proportional to the magnetic field.

Discussion of Results.—Owing to the small conductivity of manganese, no eddy currents or stray effects occurred. Also, as it appears that the paramagnetism of manganese is independent of the temperature, no change in temperature due to adiabatic magnetisation will be expected.

We have chosen manganese for study because several investigators have found that the magnetisation of manganese is dependent on the field strength.* In later researches,† however, it has been shown that the variation in the susceptibility of manganese with the magnetic field is probably due to impurities. It is well known that manganese, when combined with certain elements, has the unique magnetic property of becoming ferro-magnetic. It appears that nitrogen is one of the elements which is capable of producing this change, and owing to this, the experimental determination of the magnetic properties of manganese is exceptionally involved; this probably accounts for the number

* Ihde, 'Ann. Physik,' vol. 41, p. 829 (1913); Lepke, 'Ver. Phys. Ges.,' vol. 16, p. 369 (1914).

† T. Ishiwara, 'Sci. Rep. Tokyo Univ.,' vol. 1, p. 51 (1916).

of anomalies observed by different workers. As is shown on the curve on fig. 8 the magnetisation of manganese is proportional to the magnetic field up to 275 kilogauss, within the experimental error. From the curve of fig. 8 we may be certain to within 0.5 of the divisions of the ordinates that the curve starts from the zero of the co-ordinates, and, taking the value of the susceptibility of manganese to be 9.66×10^{-6} , we may conclude from simple calculations that the constant specific magnetisation of our specimen of manganese, should it exist at all, must be less than

$$I < 9.66 \times 10^{-6} \times 1.45 \times 10^4 \times 0.5 = 0.07$$

or less than 0.033 per cent. of that of iron. Thus at room temperature manganese seems to behave as a perfect paramagnetic substance. It must be remembered that we were lucky to be able to use the exceptionally pure manganese prepared by Dr. Geyler which had been melted *in vacuo*, and in this case there does not appear to be any nitrogen or other ingredient to turn it into the ferro-magnetic state.

(vii) *Diamagnetic Substances.*

Bismuth.—For reasons which we will state later, we have investigated the susceptibility of bismuth in particular detail. The metal used was obtained from Messrs. Adam Hilger, and, according to their analysis, was 99.993 per cent. pure, the chief impurities being lead 0.005 per cent. and silver 0.0014 per cent.

Rods about 0.6 mm. in diameter were extruded and carefully washed in dilute hydrochloric acid to remove any traces of iron from the surface. Crystals of different orientations were then grown in the rod by the method described previously by the author in detail.* The rod was placed freely in a small glass tube and slowly pulled through a heated platinum spiral which only melted the rod over a short length. The rod was inoculated with a seed crystal to get the required orientation. In our present experiments we improved the method by evacuating the glass tube, and thus the growth was made *in vacuo*, ensuring that practically no oxide coating is formed on the surface of the crystal. In previous experiments the coat of oxide was necessary to keep the shape of the crystal, but in this experiment, as before stated, we passed the glass rod through a very short heater which only melted a very short length of the crystal so that the bismuth did not collect in drops.

* 'Proc. Roy. Soc.,' A, vol. 119, p. 370 (1923).

We used rods with two orientations of the crystal axes, one in which the axis of the crystal was parallel, and one in which the axis was perpendicular to the length of the rod. After growth, the crystal rods were cut into pieces 1 cm. long, and 14 such pieces were placed in a bunch in the glass holder, a tiny piece of paraffin wax being used to keep the rods close together in the same position. The amount of bismuth placed in the tube was approximately the same for the two orientations of the crystals and for extruded multicrystalline rods. The measurements were made at room temperature and at the temperature of liquid nitrogen. At the temperature of liquid nitrogen, we were particularly interested in the magnetisation when the crystal axis was perpendicular to the direction of the magnetic field; this is shown on oscillogram No. 9, Plate 13. The result for the magnetisation of bismuth at room temperature (about 290° K.) is shown on fig. 9; and the result for a temperature close to that of liquid nitrogen (85° K.) on fig. 10. On both drawings, curve 1 is for the case when the axis of the crystal is perpendicular to the field; in curve 2 the axis of the rod is parallel to the field; curve 3 is for an extruded rod; that is, the crystal axes were distributed more or less at random. The data for figs. 9 and 10 are plotted in the same way as for manganese and gadolinium sulphate; they were also corrected for the magnetisation due to the suspension, which at the temperature of liquid nitrogen was quite considerable as we were

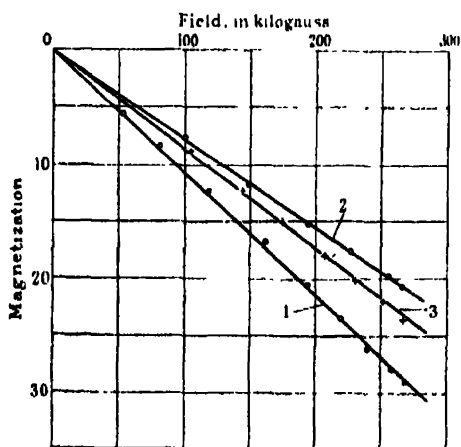


FIG. 9.—The magnetisation of bismuth at room temperature. Curve 1, crystal axis perpendicular to the field. Curve 2, crystal axis parallel to the field. Curve 3, extruded rod.

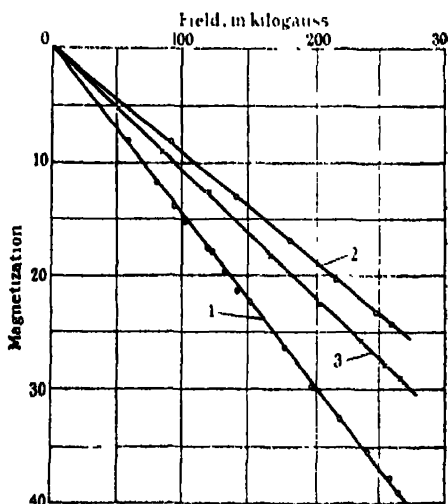


FIG. 10.—The magnetisation of bismuth at the temperature of liquid nitrogen. Curve 1, crystal axis perpendicular to the field. Curve 2, crystal axis parallel to the field. Curve 3, extruded rod.

using a glass instead of a quartz tube. The deflections were also reduced in proportion to the weights of bismuth used. By using the same holder and the same shape of bismuth, and by placing the specimen as nearly as possible in the same position in the coil, we kept the conditions of the experiments identical, as far as possible, for the three specimens of bismuth. We were thus able to obtain from the corrected and reduced deflection of the balance, the relative magnetisations and susceptibilities of the three specimens of bismuth by measuring the slope of the curves on figs. 9 and 10.

Errors of Experiments.—The principal stray effects which occurred in the study of bismuth were due to the induction currents. We chose the diameters of the bismuth rods to be as small as was practicable for growing crystals. As can be shown from (43), the ratio of the force F_i due to the eddy current, to the measured force F , in the range of fields between 60 and 270 kilogauss, taking into account the increased resistance of bismuth in magnetic fields, at room temperature, was about 2 per cent. at its maximum, and about five times less at the temperature of liquid nitrogen. This small stray effect may easily be eliminated, as described before, by averaging the balance deflections before and after the maximum amplitude, and it appears that this eddy current effect has no appreciable influence on the accuracy of our experiments. However, in one particular case, we may have a new stray effect intervening due to the peculiar properties of bismuth. This effect is due to the e.m.f. which is developed in a bismuth crystal placed in a magnetic field when a current is flowing. The e.m.f. produces a considerable phase shift in curve F_i relative to the force F , making the averaging method of excluding the eddy current effect invalid. This e.m.f. has been studied by the author in a previous paper,* where it was shown that it has a considerable value only at room temperature and when the current is parallel to the axis of the crystal. Thus this stray effect will only intervene when we study the magnetisation perpendicular to the axis at room temperature, namely the case shown by curve 1, fig. 9, and it is the only curve on which the point seems to show a slight deviation from the linear law of magnetisation. This deviation can probably be accounted for by this stray effect.

The heating of the bismuth due to the induction effect was very small, amounting to less than 0.01° C. The change of temperature due to the adiabatic magnetisation can be estimated from formulæ (62) and (68) by using the data given in the table below for the values of χ and α , and can be shown to be largest for the case when the magnetic field is perpendicular to the crystal

* 'Proc. Roy. Soc.,' A, vol. 119, p. 402 (1928).

axis. At room temperature, for this case, there is a drop of 0.22°C. , and at the temperature of liquid nitrogen a drop of only 0.05°C. This change in temperature evidently cannot appreciably affect the magnetisation of bismuth.

Discussion of Results.—We were particularly interested in the study of the magnetic properties of bismuth in strong magnetic fields, in view of some experimental results obtained from the detailed study of the magnetostriction of bismuth crystals which will be described in the next part of this paper.

It appears that in the case when the axis of the crystal is perpendicular to the magnetic field, the magnetostriction is strongly affected by the temperature, and at the temperature of liquid nitrogen tends to reach a saturation value. The simplest explanation of this phenomenon, as will be shown later, would be that the magnetic susceptibility of bismuth undergoes a similar change. The corresponding case for the magnetisation perpendicular to the crystal axis at the temperature of liquid nitrogen is given by curve 1, fig. 10. The curve was obtained from two oscillograms with different maximum field strengths, one being plotted with plain circles, and the other by blackened circles. From this curve it may be seen that, within the limits of experimental error, the magnetisation of bismuth is proportional to the magnetic field. The same result holds for all other orientations and temperatures which we have studied, the results for which are given on the remaining curve on figs. 9 and 10.

The linear dependence of the magnetic susceptibility of bismuth on the temperature was first experimentally obtained by Curie and confirmed by Honda. It can be written in the following form

$$\chi = \chi_0 (1 - \alpha T). \quad (69)$$

The experiments of Kamerlingh Onnes and Perriere* seem to show that at temperatures close to that of liquid hydrogen the change is smaller than indicated by (69), but apparently from the melting point to this low temperature (69) is a good approximation. Formula (69) was apparently only verified for multi-crystalline bismuth and I have been unable to trace in the literature on the subject, any data about the change of magnetic susceptibility of single bismuth crystals with temperature. If we assume that the linear law is also correct for the monocrystal of bismuth we may get the coefficients α and χ from our data. For this we must adopt an absolute value for the susceptibility for some particular orientation of the bismuth crystal. In recent investigations, Focke† has examined very carefully at room temperature the magnetisa-

* 'Leiden Comm.,' No. 122a, p. 9 (1911).

† 'Phys. Rev.,' vol. 3, p. 319 (1930).

tion of bismuth for the two positions of the crystal axes. For the case of the crystal axis perpendicular to the magnetic field he has obtained for the magnetic susceptibility of bismuth a value of $\chi = 1.49 \times 10^{-6}$. We took this value as a basis for an estimate of the susceptibility in absolute units for other orientations and temperatures from the data obtained in our experiments. The values for χ , χ_0 and α in the formula (69) calculated in this way are given in the following table :—

	Axis parallel to field.	Axis perpendicular to field.	Extruded rod.
$-\chi \cdot 10^6$ at 290° K.	1.08	1.49	1.21
$-\chi \cdot 10^6$ at 85° K.	1.295	2.04	1.52
	0.76×10^{-3}	1.191×10^{-3}	0.94×10^{-3}
$-\chi_0 \times 10^6$	1.39	2.27	1.66

Comparing the value of $\chi = -1.08 \times 10^{-6}$ for the case of magnetisation parallel to the axis as given in the table, with the value given by Focke of $\chi = -1.05 \times 10^{-6}$, we see that the difference is about 3 per cent. Considering that our present method is not well suited to this kind of measurement, since in comparing the data for different specimens of bismuth we cannot be sure that the experimental conditions remain identical, this agreement must be considered quite satisfactory. The main object in calculating the values in the table was to obtain data for the interpretation of experiments on magnetostriction for which we had to know the value of α .

Conclusions.

The main object of the experiments described in this paper has been to develop a method of measuring the magnetic susceptibility in strong magnetic fields during the brief interval of time available. The experimental results for different substances, as described here, seem to prove that the method given makes the investigation of the magnetisation for most substances quite possible with an accuracy of about 1 to 2 per cent., and there are no obvious reasons why this accuracy should not, if required, be increased further.

The substances for this first series of experiments were chosen as being typical examples of ferro-, para-, and diamagnetic substances. Our investigations have shown that within the range of temperature used, the laws of magnetisa-

tion as given by the modern theories and verified in magnetic fields up to 30 kilogauss, apply also in a region of fields up to 10 times larger.

As has already been stated, the main interest of this method lies in the possibility of obtaining saturation values for different paramagnetic substances, and the present experimental results show that there is every hope that this may be done with fair accuracy. This experiment will be started as soon as the necessary equipment and facilities for using liquid hydrogen and helium are developed.

(1) The experimental arrangements for measuring the magnetisation of substances in short times are described.

(2) Different stray effects and errors arising from the shortness of the time of experiment are discussed.

(3) The change of temperature during adiabatic magnetisation is estimated.

(4) A description of the measurement of magnetisation for iron and nickel after saturation is given. It is shown that the magnetisation remains practically constant up to fields of 280 kilogauss within the limits of experimental error (1 per cent.). This result is in agreement with the Weiss-Langevin theory of ferro-magnetism.

(5) The separation of the ferro- and paramagnetic parts of the magnetisation in some ferro-magnetic alloys is described.

(6) The measurements of the magnetisation of gadolinium sulphate and manganese is described. For gadolinium sulphate a deviation from the linear law of magnetisation at the temperature of liquid nitrogen is observed, the magnitude of which agrees with the value given by the Langevin theory.

(7) The magnetisation of bismuth for different crystal orientations at room temperature and the temperature of liquid nitrogen is measured, and found to be proportional to the magnetic field. The dependence of the magnetic susceptibility on the temperature is estimated for different crystal orientations.

EXPLANATION OF PLATE 13.

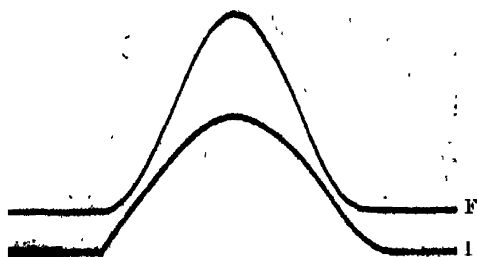
In the oscillograms the time is increasing from right to left. The bottom curves marked I represent the current through the coil, the curve marked F represents the deflection of the balance.

OSCILLOGRAM 4.—The magnetisation of *iron*, room temperature, maximum field, 260 kilogauss.

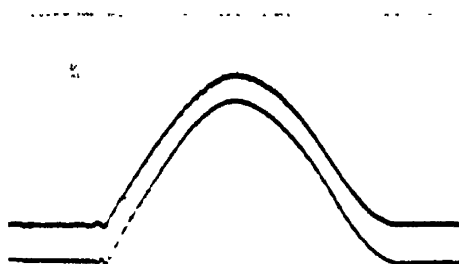
OSCILLOGRAM 5.—The magnetisation of *nickel*, room temperature, maximum field 287 kilogauss.



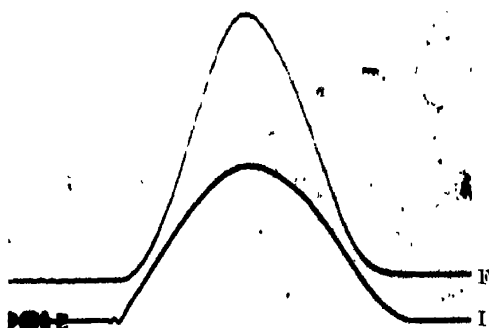
OSCILLOGRAM 4. Iron, room temp.: 260 kilogauss.



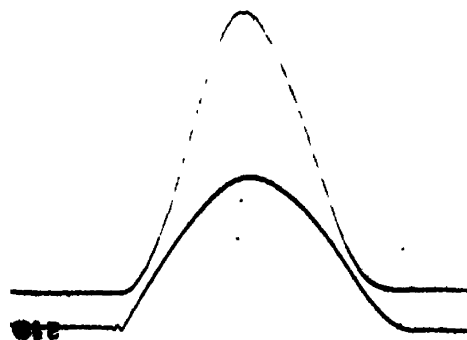
OSCILLOGRAM 7. Gadolinium sulphate, low temp.: 265 kilogauss.



OSCILLOGRAM 5. —Nickel: room temp.: 287 kilogauss.



OSCILLOGRAM 8. —Manganese: room temp.: 275 kilogauss.



OSCILLOGRAM 6.—Gadolinium sulphate: room temp.: 271 kilogauss.



OSCILLOGRAM 9. —Bismuth: low temp.: 265 kilogauss.

← 25 20 15 10 5 0
Time, millisec.

OSCILLOGRAM 6.—The magnetisation of *gadolinium sulphate*, room temperature, maximum field 271 kilogauss.

OSCILLOGRAM 7.—The magnetisation of *gadolinium sulphate*, temperature of liquid nitrogen, maximum field 265 kilogauss.

OSCILLOGRAM 8.—The magnetisation of *manganese*, room temperature, maximum field 275 kilogauss.

OSCILLOGRAM 9.—The magnetisation of *bismuth*, crystal axis perpendicular to the field, temperature of liquid nitrogen, maximum field 285 kilogauss.

The Antiseptic and Trypanocidal Action of certain Styryl and Anil Benzthiazole Derivatives.

By C. H. BROWNING, F.R.S., J. B. COHEN, F.R.S., S. ELLINGWORTH, and R. GULBRANSEN, Medical School, Leeds; the Pathological Department of the University and Western Infirmary, Glasgow.

(Abstract.)

The antiseptic and trypanocidal actions of anil and styryl benzthiazole compounds have been investigated. The substances examined are analogues of the more active members of the anil and styryl quinoline series previously reported on. The anil benzthiazole derivatives are relatively weakly antiseptic for *staphylococcus* and *B. coli*, as compared with the quinoline analogues which are highly active in this respect. Several benzthiazole styryl compounds have produced cure of mice infected with *Trypanosoma brucei* and the same relationships between chemical constitution and trypanocidal action have been found to hold as in the styryl quinoline series. Thus the maximum effect is produced when one nucleus contains a basic group and the other an acetyl amino group. The anil benzthiazole series, in general, possesses some trypanocidal action, but cure has only exceptionally been produced.

[The full paper appears in 'Proceedings,' Series B, vol. 108, pp. 119-129.]

Some Aliphatic and Aromatic Amino Derivatives of α -Quinoline Methiodide.

By J. B. COHEN, F.R.S., K. E. COOPER, and P. G. MARSHALL,
Medical School, Leeds.

(Abstract.)

Many of the amino and acylamino compounds obtained by the condensation of derivatives of α -methyl quinoline with nitroso-acylamines possess active antiseptic and in some cases mild trypanocidal properties. It appeared interesting to examine the physiological effect of substances obtained by attaching a basic aliphatic or aromatic side-chain directly to the α -carbon of the quinoline nucleus. A variety of these substances were prepared and submitted to Professor Browning, of Glasgow University, but they exhibited no marked antiseptic or trypanocidal character. Similar reactions have been carried out with diamino compounds of aliphatic and aromatic series with basic groups at both ends of the chain in the hope that they might exhibit antimalarial action, but no such effect was observed.

[*The full paper appears in 'Proceedings,' Series B, vol. 108, pp. 130-137.*]

The Wave Resistance of a Spheroid.

By T. H. HAVELOCK, F.R.S.

(Received February 20, 1931.)

1. A method which has been used to calculate the wave resistance of a submerged solid is to replace the solid by a distribution of sources and sinks, or of doublets, the distribution being the image system for the solid in a uniform stream. The cases which have been solved hitherto have been limited to those in which the image system is either a single doublet or a distribution of doublets lying in a vertical plane parallel to the direction of motion. It is shown here how to obtain the solution for an ellipsoid moving horizontally at given depth below the surface of the water, and with its axes in any assigned directions. The present paper deals specially with prolate and oblate spheroids moving end-on and broadside-on, the general case of an ellipsoid with unequal axes being left for a subsequent paper.

In § 2 it is shown that the image system for an ellipsoid in a uniform stream is a certain surface distribution of parallel doublets over the elliptic focal conic, the direction of the doublets being in general inclined to the direction of motion; if the motion is parallel to a principal axis, the doublets are in the same direction. For a spheroid the image system reduces to either a line distribution or to a surface distribution over a certain circle; explicit expressions are given in § 3 for prolate and oblate spheroids when moving either in the direction of the axis of symmetry or at right angles to that axis.

The calculation of the wave resistance is considered in § 4. An expression has been given previously for the wave resistance associated with two doublets at any points in the liquid with their axes in any assigned directions; this can be generalised to cover continuous line, surface or volume distributions of doublets. Incidentally, it is shown how by integration we may pass from a three-dimensional doublet, corresponding to a submerged sphere, to a two-dimensional doublet, corresponding to a circular cylinder. In § 5 expressions for the wave resistance are developed for the particular cases of moving spheroids of § 3. In the final section these results are illustrated by numerical and graphical calculations for certain series of models. In each case the axis of the spheroid is supposed horizontal, and to make the calculations definite the depth of the axis is taken to be twice the radius of the central circular section. The models consist of a sphere, radius b ; an oblate spheroid

with semi-axis $a = 4b/5$; and prolate spheroids with $a = 5b/4$, $5b/2$ and $5b$ respectively. Graphs are given for the variation of wave resistance with velocity for these five models (i) when moving in the direction of the axis of revolution, (ii) when moving at right angles to that axis; these illustrate respectively the effect of increased length, and the effect of increased beam and area of cross-section. It is of interest to note that increase of length gives diminished resistance at low speeds, with a subsequent rapid increase; while increasing beam in the second series gives increased resistance at all speeds.

2. Consider the motion of a solid bounded by the ellipsoid

$$\frac{x^2}{a^2} + \frac{y^2}{b^2} + \frac{z^2}{c^2} = 1, \quad (1)$$

in an infinite liquid, the velocity being u parallel to Ox .

It is well known that if V is the gravitational potential of a uniform solid of unit density bounded by (1), then the velocity potential of the fluid motion is given by

$$\phi = \frac{u}{2\pi(2 - \alpha_0)} \frac{\partial V}{\partial x}, \quad (2)$$

where

$$\alpha_0 = abc \int_0^\infty \frac{du}{(a^2 + u)^{3/2} (b^2 + u)^{1/2} (c^2 + u)^{1/2}}. \quad (3)$$

Since

$$V = \iiint \frac{dx' dy' dz'}{\{(x - x')^2 + (y - y')^2 + (z - z')^2\}^{1/2}}, \quad (4)$$

taken throughout the ellipsoid, it follows from (2) and (4) that the velocity potential of the fluid motion is that due to a uniform volume distribution of doublets throughout the ellipsoid, with their axes parallel to Ox , and of moment per unit volume equal to $u/2\pi(2 - \alpha_0)$.

Similarly for motion parallel to Oy or Oz we have a like result with a corresponding quantity β_0 or γ_0 taking the place of α_0 . For motion in any other direction we resolve the velocity along the three axes and combine the

The gravitational potentials of two solid homogeneous ellipsoids, bounded by confocals, at any point external to both are proportional to their masses. Hence in the hydrodynamical problem we may replace the distribution of doublets throughout the ellipsoid (1) by a uniform distribution through any interior confocal, increasing the moment per unit volume by the factor

$$abc/\sqrt{\{(a^2 + \lambda)(b^2 + \lambda)(c^2 + \lambda)\}}, \quad (5)$$

where λ is the parameter of the confocal.

In particular, we obtain the simplest system by taking the confocal which reduces in the limit to the elliptic focal conic

$$z = 0; \frac{x^2}{a^2 - c^2} + \frac{y^2}{b^2 - c^2} = 1, \quad (6)$$

with $a > b > c$. In this case the volume distribution of doublets reduces to a surface distribution over the plane area bounded externally by (6). The moment per unit area is found by putting $\lambda^2 = -c^2 + \delta$ and taking limiting values as $\delta \rightarrow 0$, taking into account the factor (5) and the limiting thickness of the confocal at each point. We may refer to the distribution found in this way as the image system for an ellipsoid in a uniform stream.

If the motion is parallel to Ox , the doublets are parallel to Ox and are distributed over (6) with a moment per unit area given by

$$\frac{abcu}{\pi(2 - \alpha_0)(a^2 - c^2)^{1/2}(b^2 - c^2)^{1/2}} \quad /, \quad x^2 \quad y^2 \quad \sqrt{1/2} \quad (7)$$

There are similar expressions for motion parallel to Oy , Oz with β_0 , γ_0 respectively in place of α_0 .

3. We shall specify now the particular results for spheroids, using the known values of α_0 , β_0 , γ_0 . We take Ox to be the axis of symmetry, with $c = b$; and consider first motion parallel to the axis of symmetry.

For a prolate spheroid, the focal conic reduces to the line joining the foci of the generating ellipse. The image system reduces to a line distribution along Ox , from $x = -ae$ to $x = ae$, of moment per unit length

$$Au(a^2e^2 - x^2), \quad (7)$$

where

$$A^{-1} = 4e/(1 - e^2) - 2 \log \{(1 + e)/(1 - e)\}, \quad (8)$$

with $e^2 = 1 - b^2/a^2$.

For an oblate spheroid under the same conditions, the system is a surface distribution of doublets parallel to Ox , over the circle

$$x = 0; \quad y^2 + z^2 = b^2e'^2, \quad (9)$$

where $e'^2 = 1 - a^2/b^2$; and the moment per unit area is

$$Bu(b^2e'^2 - y^2 - z^2)^{1/2}, \quad (10)$$

with

$$B^{-1} = \pi(\sin^{-1} e' - e' \sqrt{1 - e'^2}). \quad (11)$$

For motion at right angles to the axis of symmetry, we take Oy as the direction

of motion. For a prolate spheroid the system is a line distribution along Oz between $x = \pm ae$, with axes parallel to Oy , and of moment per unit length

$$A'u (a^2e^2 - x^2), \quad (12)$$

where

$$A'^{-1} = 2e (2e^2 - 1)/(1 - e^2) + \log\{(1 + e)/(1 - e)\}. \quad (13)$$

For an oblate spheroid the system consists of doublets parallel to Oy , over the circle

$$x = 0; \quad y^2 + z^2 = b^2e'^2, \quad (14)$$

and of moment per unit area

$$B'u (b^2e'^2 - y^2 - z^2)^{\frac{1}{2}}, \quad (15)$$

where

$$B'^{-1} = \pi \{e' (1 + e'^2)/(1 - e'^2)^{1/2} - \sin^{-1} e'\}. \quad (16)$$

For $e = 0$, all these distributions reduce to the finite doublet at the origin appropriate to the motion of a sphere.

4. Consider now the wave resistance when an ellipsoid is wholly immersed at some depth in water and is moving with constant horizontal velocity; we obtain the first approximation for the resistance by replacing the ellipsoid by the image system which was discussed in the preceding section. The resistance is derived from the doublet system by expressions which have been given previously; in particular, reference may be made to an expression for the wave resistance corresponding to two doublets at any points in the water with their axes in any given directions.* We shall not quote the general result, as we require here only the case in which the doublets have their axes parallel to the direction of motion. Take the origin O in the free surface of the water, Oz vertically upwards; for a doublet of moment M at the point $(h, k, -f)$ and a doublet M' at $(h', k', -f')$, both axes being parallel to Oz , the direction of motion, the wave resistance is given by

$$R = 16\pi\rho\kappa_0^4 \int_0^{\pi/2} \{M^2 e^{-2\kappa_0 f \sec^2 \theta} + M'^2 e^{-2\kappa_0 f' \sec^2 \theta} + 2MM' e^{-\kappa_0 (f+f') \sec^2 \theta} \cos A \cos B\} \sec^5 \theta \, d\theta, \quad (17)$$

with

$$\kappa_0 = u^2/g; \quad A = \kappa_0 (h - h') \sec \theta; \quad B = \kappa_0 (k - k') \sin \theta \sec^2 \theta.$$

This can easily be extended to continuous distributions. For distributions

* 'Proc. Roy. Soc.,' A, vol. 118, p. 32 (1928).

in a vertical plane parallel to the direction of motion, to which previous work has been limited, we have

$$R = 16\pi\rho\kappa_0^4 \int_0^\infty df \int_0^\infty df' \int_{-\infty}^\infty dh \int_{-\infty}^\infty dh' \int_0^{\pi/2} M(h, f) M(h', f') \\ \times e^{-\kappa_0(f+f')\sec^2\theta} \cos\{\kappa_0(h-h')\sec\theta\} \sec^5\theta d\theta, \quad (18)$$

where we have taken $y = 0$ as the plane of distribution. This expression can be written as

$$R = 16\pi\rho\kappa_0^4 \int_0^{\pi/2} (P^2 + Q^2) \sec^5\theta d\theta, \quad (19)$$

where

$$P + iQ = \int_0^\infty df \int_{-\infty}^\infty dh \cdot M(h, f) \cdot e^{-\kappa_0 f \sec^2\theta + i\kappa_0 h \sec\theta}. \quad (20)$$

When the distribution is in a plane perpendicular to the direction of motion, say the plane $x = 0$, it is easily seen that we have the same expression (19) for R , but now

$$P + iQ = \int_0^\infty df \int_{-\infty}^\infty dk \cdot M(k, f) \cdot e^{-\kappa_0 f \sec^2\theta + i\kappa_0 k \sin\theta \sec^2\theta}. \quad (21)$$

If the doublets are distributed along a line, the suitable forms for R may readily be deduced from these expressions.

Before proceeding to apply these results to spheroids, we may notice a simple case of (21). The first problem in wave resistance to be solved was that of a two-dimensional doublet corresponding to the motion of a circular cylinder with its axis horizontal and moving at right angles to the axis; the next problem was the three-dimensional doublet for the motion of a sphere. By means of (19) and (21) we may pass from the second problem to the first by integration.

Write down the velocity potential of a uniform distribution of three-dimensional doublets of moment M per unit length over a straight line of finite length, the axes of the doublets being at right angles to this line; evaluate the expression in the limit when the length of the distribution becomes infinite, and we obtain the velocity potential of a two-dimensional doublet of moment $2M$. Consider now the expression for the wave resistance for the same process; if $2l$ is the length of the distribution, (21) gives

$$P + iQ = \int_{-l}^l M e^{-\kappa_0 f \sec^2\theta + i\kappa_0 k \sin\theta \sec^2\theta} dk. \quad (22)$$

Evaluating the integral and using (19) we have

$$R = 64\pi\rho\kappa_0^2 M^2 \int_0^{\pi/2} \frac{\sin^2(\kappa_0 l \sin \theta \sec^2 \theta)}{\sin^2 \theta \cos \theta} e^{-2\kappa_0 f \sec^2 \theta} d\theta. \quad (23)$$

The wave resistance for the corresponding two-dimensional doublet is for unit length perpendicular to the plane of motion, and should be given by $\lim (R/2l)$ as $l \rightarrow \infty$. From (23), this is

$$\begin{aligned} \lim_{l \rightarrow \infty} 32\pi\rho\kappa_0^2 M^2 e^{-2\kappa_0 f} \int_0^{\infty} \sin^2(\kappa_0 u \sqrt{1+u^2/l^2}) e^{-2\kappa_0 f u^2/l^2} u^{-2} \sqrt{1+u^2/l^2} du \\ = 16\pi^2 \rho \kappa_0^3 M^2 e^{-2\kappa_0 f}, \quad (24) \end{aligned}$$

and this is the known expression for the wave resistance of a two-dimensional doublet of the corresponding moment $2M$.

5. We proceed now to the wave resistance of a submerged spheroid, taking in each case the axis of the spheroid to be horizontal and at a depth f below the surface of the water.

Prolate Spheroid in Direction of Axis.—From (7) and (20) we have

$$\begin{aligned} (P + iQ)/Aue^{-\kappa_0 f \sec^2 \theta} &= \int_{-ae}^{ae} (a^2 e^2 - h^2) e^{i\kappa_0 h \sec \theta} dh \\ &= (8\pi a^3 e^3 / \kappa_0^3 \sec^3 \theta)^{1/2} J_{3/2}(\kappa_0 a e \sec \theta), \quad (25) \end{aligned}$$

where J denotes the usual Bessel function. Hence from (19),

$$R = 128\pi^2 g \rho a^3 e^3 A^2 \int_0^{\pi/2} e^{-2\kappa_0 f \sec^2 \theta} \{J_{3/2}(\kappa_0 a e \sec \theta)\}^2 \sec^2 \theta d\theta, \quad (26)$$

a result which was obtained previously by a different method.* For purposes of numerical calculation it is convenient to change the variable in the integration from θ to $\tan \theta$; we then have

$$R = 128\pi^2 g \rho a^3 e^3 A^2 e^{-p} \int_0^{\infty} e^{-pt} \{J_{3/2}(\kappa_0 a e \sqrt{1+t^2})\}^2 dt, \quad (27)$$

where $p = 2\kappa_0 f = 2gf/u^2$, and A is given in (8).

Oblate Spheroid in Direction of Axis.—Here we have a surface distribution given by (10), and remembering that the centre of the circular distribution is at a depth f , (21) gives

$$(P + iQ)/Bue^{-\kappa_0 f \sec^2 \theta} = \iint (\delta^2 e^2 - y^2 - z^2)^{1/2} e^{i\kappa_0 x \sec^2 \theta + i\kappa_0 y \sin \theta \sec^2 \theta} dy dz, \quad (28)$$

taken over the circle $y^2 + z^2 = b^2 e^2$.

* 'Proc. Roy. Soc.,' A, vol. 95, p. 365 (1919).

Taking the integration with respect to y first, we obtain, after integration by parts,

$$(\kappa_0 \sin \theta \sec^3 \theta)^{-1} \int_{-(b^2 e'^2 - z^2)^{1/2}}^{(b^2 e'^2 - z^2)^{1/2}} y (b^2 e'^2 - y^2 - z^2)^{-1/2} \sin (\kappa_0 y \sin \theta \sec^3 \theta) dy \\ = \frac{\pi (b^2 e'^2 - z^2)^{1/2}}{\kappa_0 \sin \theta \sec^3 \theta} J_1 (\kappa_0 \sqrt{b^2 e'^2 - z^2} \sin \theta \sec^3 \theta). \quad (29)$$

The integration with respect to z now becomes

$$\int_{-be'}^{be'} (b^2 e'^2 - z^2)^{1/2} e^{\kappa_0 z \sin \theta \sec^3 \theta} J_1 (\kappa_0 \sqrt{b^2 e'^2 - z^2} \sin \theta \sec^3 \theta) dz, \quad (30)$$

and this is equivalent to evaluating

$$\int_0^{\pi/2} \cosh (\alpha \cos \phi) J_1 (\beta \sin \phi) \sin^3 \phi d\phi, \quad (31)$$

where $\alpha = \kappa_0 b e' \sec^3 \theta$, $\beta = \kappa_0 b e' \sin \theta \sec^3 \theta$.

The integral (31) may be evaluated as a special case of Sonine's integral, or by expanding $\cosh(\alpha \cos \phi)$ in powers of $\cos \phi$, integrating term by term, and summing the resulting series. The latter expression for (31) is found to be

$$\sum_{n=0}^{\infty} \frac{\alpha^{2n}}{2n!} \frac{2^{n-1/2} \Gamma(n + \frac{1}{2})}{\beta^{n+1/2}} J_{n+3/2}(\beta). \quad (32)$$

Noting that in the present problem, $\alpha \gg \beta$, the value of (32), or of the integral (31), is

$$\left(\frac{\pi}{2}\right)^{1/2} \frac{\beta}{(\alpha^2 - \beta^2)^{3/4}} I_{3/2} \{(\alpha^2 - \beta^2)^{1/2}\}, \quad (33)$$

where the Bessel function is given by

$$I_{3/2}(x) = \left(\frac{2}{\pi x}\right)^{1/2} \left(\cosh x - \frac{\sinh x}{x}\right). \quad (34)$$

Collecting these results, we obtain

$$(P + iQ)/Bu e^{-\kappa_0 f \sec^3 \theta} = (\pi^{3/2} b^3 e'^3 / 2 \kappa_0^3 \sec^3 \theta)^{1/2} I_{3/2} (\kappa_0 b e' \sec \theta). \quad (35)$$

Finally, from (19) we find

$$R = 8\pi^4 \rho \kappa_0 b^3 e'^3 B^2 u^2 \int_0^{\pi/2} e^{-2\kappa_0 f \sec^3 \theta} \{I_{3/2} (\kappa_0 b e' \sec \theta)\}^2 \sec^3 \theta d\theta, \quad (36)$$

or in the same form as (27),

$$R = 8\pi^4 g \rho b^3 e'^3 B^2 e^{-\nu} \int_0^{\infty} e^{-\nu t} \{I_{3/2} (\kappa_0 b e' \sqrt{1+t^2})\}^2 dt, \quad (37)$$

where B is given in (11).

Prolate Spheroid at Right Angles to its Axis.—The distribution is given in (12), and in this case we use (21) instead of (20); apart from this, the calculation follows the same course and we obtain finally

$$\begin{aligned} R &= 128\pi^3 g \rho a^3 e^3 A'^2 \int_0^{\pi/2} e^{-2\kappa_0 f \sec^2 \theta} \{J_{3/2}(\kappa_0 a e \sin \theta \sec^2 \theta)\}^2 \cos \theta d\theta / \sin^3 \theta \\ &= 128\pi^3 g \rho a^3 e^3 A'^2 e^{-p} \int_0^\infty e^{-t^2} \{J_{3/2}(\kappa_0 a e t \sqrt{1+t^2})\}^2 t^{-3} dt, \end{aligned} \quad (38)$$

with A' given in (13).

Oblate Spheroid at Right Angles to its Axis.—The distribution given in (15) lies in a plane parallel to the direction of motion, so we now use (20); the integrals are, however, of the same type as those already discussed and the analysis need not be given in detail. Using (15), (19) and (20), we obtain after some reduction

$$R = 32\pi^4 g \rho b^3 e'^3 B'^2 e^{-p} \int_0^\infty e^{-t^2} \{I_{3/2}(\kappa_0 b e' t \sqrt{1+t^2})\}^2 t^{-3} dt, \quad (39)$$

where B' is given in (16).

Sphere.—It may easily be verified that in the limit when e , or e' , becomes zero, all these expressions (27), (37), (38) and (39), reduce to the known result for a sphere, namely

$$\begin{aligned} R &= 4\pi g \rho \kappa_0^3 b^3 e^{-p} \int_0^\infty (1+t^2)^{3/2} e^{-p^2 t^2} dt \\ &= \pi g \rho \kappa_0^3 b^3 e^{-1/2} \left\{ K_0\left(\frac{1}{2}p\right) + \left(1 + \frac{1}{p}\right) K_1\left(\frac{1}{2}p\right) \right\}, \end{aligned} \quad (40)$$

where K_n is the Bessel function defined by

$$K_n(x) = \int_0^\infty e^{-x \cosh u} \cosh nu du. \quad (41)$$

6. The resistances for prolate and oblate spheroids have been worked out independently in the preceding section. It is of interest to note that the results have the same analytical form and may, in fact, be deduced from each other by taking the eccentricity to be imaginary instead of real. For the prolate spheroid, $e^2 = 1 - b^2/a^2$; while for the oblate spheroid, $e'^2 = 1 - a^2/b^2$. It may be verified that if in (27) we write $e = ie'b/a$, the expression transforms precisely into (37); and the same relation holds between (38) and (39).

7. The integrals in the various expressions can be transformed into alternative forms, or expressed in infinite series in several ways; but either the series do not converge rapidly enough for the values of the parameters which are of interest, or else the functions involved have not been tabulated. It

has been found simpler to make numerical calculations directly from the integrals as given, although a considerable amount of work is involved in any case.

The calculations have been carried out for a set of five spheroids, including the sphere, the radius b of the central circular section being supposed constant and the semi-axis a varied. The following are the data for the series:—A, oblate, $a = 4b/5$, $e' = 0.6$; B, sphere, $a = b$; C, prolate, $a = 5b/4$, $e = 0.6$; D, prolate, $a = 5b/2$, $e = 0.9165$; E, prolate, $a = 5b$, $e = 0.9798$. The axial sections of these forms are shown in fig. 1, drawn to scale, the diagram showing one quarter of the section in each case.

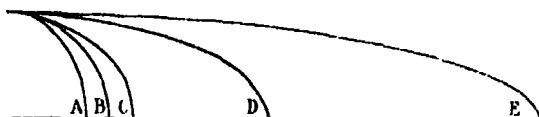


FIG. 1.

We suppose the axis horizontal in each case and at the same depth f below the free surface. To make a definite case for numerical calculation we take

$$f = 2b, \quad (42)$$

that is, the depth twice the radius of the central circular section. We consider the models in two series, (i) with the axis in the direction of motion, (ii) with the axis at right angles to the motion. Our object is to show the variation of wave-resistance with velocity for each model, and to see how the graph varies, in (i) with increasing length, and in (ii) with increasing beam. To give one example of the calculations, when $a = 5b/2$, (27) gives

$$R = 17.47\pi g \rho b^3 e^{-p} \int_0^\infty e^{-pt} \{J_{3/2}(0.5728\sqrt{1+t^2})\} dt. \quad (43)$$

For velocities which are of special interest, the parameter p ranges from about 1 to 8. A graph of the Bessel function $J_{3/2}$ was drawn on a large scale and values were taken from it, except for small values of the argument when they were calculated from tables of $J_{1/2}$ and $J_{-1/2}$. Values of the integrand were calculated for values of t at intervals of 0.1, and the numerical integration carried out by the usual methods. Owing to the exponential factor, it was unnecessary to go beyond $t = 2$ in any case; and for the larger values of p , a smaller range of t was sufficient. This process was carried out for seven or eight values of p , and so a graph could be drawn for the variation of R with p , that is, with velocity u .

A similar method was used for the integrals in (37) and (38). For (39), the Bessel function was expanded in powers of $(1 + t^2)$, and integration carried out term-by-term; the integrals involved are then of the form

$$\int_0^\infty (1 + t^2)^{\frac{2n+1}{2}} e^{-pt^2} dt, \quad (44)$$

which can be expressed in terms of the Bessel function K_n defined in (41). By recurrence formulæ, the terms can be reduced to expressions involving K_0 and K_1 , and tables of these functions are available. In all these calculations no attempt was made to obtain any high degree of numerical accuracy; the object was to obtain sufficient values to enable graphs to be drawn showing the nature of the results and the main differences between the two series.

The graphs are shown in figs. 2 and 3; the scale is the same throughout, the ordinates being $R/\pi gpb^3$, and the abscissæ $u/\sqrt{(gf)}$.

The nature of the results is obvious from the graphs. Fig. 2 shows the curves for the end-on motion. The curve B, which is the same in both

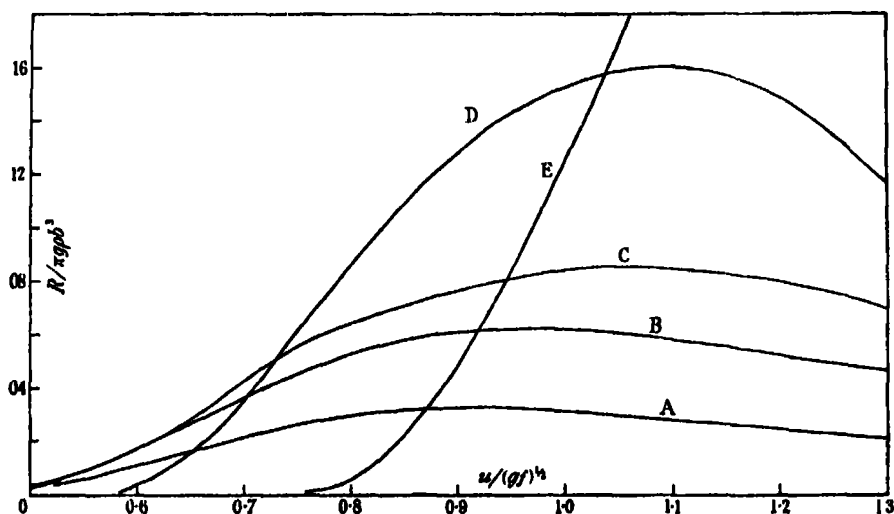


FIG. 2.

diagrams, is for the sphere and shows the maximum just before the velocity $(gf)^{1/2}$. The graphs for C, D, E show how much the resistance is diminished at the lower velocities by increasing length in this way; but this is followed by a rapid increase at higher velocities. The latter effect may be described, roughly, as due to the final interference between bow and stern system giving a prominent hump on the resistance curve; the interference effects at lower

speeds were found in the calculations for curve E, but could not be shown on the scale of the diagram.

The graphs in fig. 3 for the broadside motion are in striking contrast to those in fig. 2. Here we have increased resistance at all velocities as we go up the series of models ; the values for E were calculated, but could not be shown on

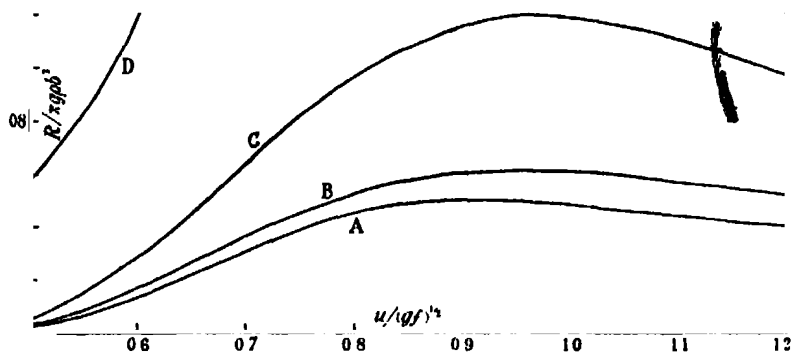


FIG. 3.

the scale of the diagram. It appears from the curves of fig. 3 that a rough empirical rule for this series is that the resistance per unit volume of displacement is proportional to the area of the midship section.

On Twisted Cubic Curves which satisfy Twelve Conditions.

By J. A. TODD, Trinity College, Cambridge.

(Communicated by H. F. Baker, F.R.S.—Received December 18, 1930.)

Introduction.

In ordinary space the freedom of twisted cubic curves is 12, so that a finite number of such curves can be drawn to satisfy a set of 12 independent conditions. The aim of the present paper is to determine this number in all the possible cases which arise by combination of elementary conditions of certain types. These types are three in number, and are as follows :—

- (a) The simple condition that the curve should meet a line. We shall denote this condition by the symbol l .
- (b) The double condition of meeting a given line in two points, or of having the line as a chord ; this we denote by B .
- (c) The double condition of passing through an assigned point, which we denote by P .

Any combination of these conditions can be expressed symbolically as a product ; the condition that the curve should pass through α given points, have β given lines as chords, and meet, in a single point, γ further lines, being represented symbolically by the expression $P^\alpha B^\beta l^\gamma$. The power of this condition is clearly

$$2\alpha + 2\beta + \gamma.$$

When the condition is of power 12 there is in general a finite number of cubic curves which satisfy it ; and it is convenient to denote this number by the same symbol as is used for the condition. Thus the fact that one cubic curve passes through six given points is expressed symbolically by the relation $P^6 = 1$.

In the course of the present paper the numbers corresponding to all possible conditions of power 12, made up of combinations of these symbols, are determined, with the exception of those elementary cases in which only the conditions P and B occur, which are referred to below. Some of these have been obtained before, but it is believed that most of the more complicated results are here treated in a simpler manner than heretofore. Some new results are also included.

Using the letters α, β, γ in the sense previously adopted, the present state of knowledge may be summarised as follows.

The cases in which γ is zero were investigated by Cremona, who obtained the results

$$P^6 = 1, P^5B = 1, P^4B^2 = 0, P^3B^3 = 1, P^2B^4 = 1, PB^5 = 1, B^6 = 6,$$

the condition P^4B^3 being a poristic one. Proofs of these may be found in Baker, 'Principles of Geometry,' vol. 3, chap. 3, where previous references will also be found.

The cases in which $\gamma = 2$, and the case P^4B^4 , were considered by Sturm,* mostly by methods different from the present.

Many of the remaining cases in which $\gamma = 4$ are discussed in a recent paper by van Kol.† His methods are similar to those of Sturm, and are different from those employed here.

The cases in which $\beta = 0$ were first considered by Schubert in his "Kalkül der abzählende Geometrie" (Teubner, 1879), with a symbolic calculus largely based on the degeneration method. The present treatment, though involving degeneration arguments, is throughout purely geometrical; and no symbolic calculations are necessary.

In the course of the paper two subsidiary conditions are involved, namely :—

The triple condition Q that a cubic curve should pass through an assigned point and have a given line through this point as a chord.

The quadruple condition R that a cubic curve should pass through a given point and have two assigned lines through it as chords.

The numbers of cubics satisfying conditions of this type in combination with those already discussed will be required in the second half of the paper.

The paper divides naturally into two parts, the first consisting of those cases which are readily soluble without the use of degeneration arguments, and the latter part containing the more complicated cases in which the use of the degeneration method is of considerable value. We consider the more elementary direct methods first.

Part I.—Direct Methods.

With few exceptions all the cases in which γ is not greater than 4 are easily amenable to direct treatment. The most useful direct methods employ

* 'J. Mathematik,' vol. 79, p. 99 (1875), and vol. 80, p. 128 (1875).

† 'Proc. R. Acad. Sci., Amsterdam,' vol. 32, p. 625 (1929).

certain transformations of space which are described below ; but three of the cases are readily soluble without use of these.

The simplest of all is the case $P^3B^2l^2$, in which we are to determine the cubic curves which pass through three points P , have two given lines B as chords, and which meet two further lines l in one point each. The curves which satisfy the tenfold condition P^3B^2 are ∞^3 in aggregate, and clearly all lie on the quadric which contains the three points P and the two lines B ; belonging all to one system on this quadric. One such curve is known to pass through five points on the quadric ; and in particular one of the ∞^3 curves of the system passing through the points P will pass through two further points of the quadric. We can, in four ways, select these two points to lie one on each of the lines l . We thus have four curves satisfying the required condition ; whence $P^3B^2l^2 = 4$.

The cubics which pass through five points P and meet two lines l_1, l_2 , can also be determined without difficulty. The pencil of quadrics containing the points P and the line l_1 meet further in a cubic curve, c , which has l_1 as a chord and passes through the points P ; let this meet l_1 in the points M_1, M_1' . There is similarly a cubic curve c_2 passing through P and meeting l_2 in two points M_2, M_2' . Consider the transversal lines of the curves c_1, c_2 and the lines l_1, l_2 . In general there are 18 such lines, by a well-known theorem. These include, however—

- (a) the transversal from a point P to the lines l_1, l_2 ;
- (b) the four lines joining one of M_1, M_1' to one of M_2, M_2' ;
- (c) the join of M_1 to the third intersection of the plane M_1l_2 with the curve c_2 ;

and three similar lines ; which have not four distinct points of intersection with the four curves. As there are five lines of type (a) this accounts for 13 of the 18 transversals of l_1, l_2, c_1, c_2 . There remain then five others. If l is one of these, which meets the four curves c_i, l_i , in distinct points, the points P , the line l and the line l_1 lie on a quadric containing c_1 , while Pl_2 lie on a quadric through c_2 . The two quadrics meet in the line l and a twisted cubic through the points P which has l as a chord and which therefore meets l_1, l_2 each in one point. From the five lines l we get five such curves. Thus $P^5l^3 = 5$.

The value of P^4l^4 may be obtained by means of the principle of correspondence, as follows. Consider the cubic curves which pass through four points P and meet four lines l_1, l_2, l_3, l_4 . Through a point P_1 of l_1 and the points P can be drawn five cubics to meet l_2, l_3 ; and through each of the points Q in which one of these cubics meets l_2 can be drawn five cubics which pass through the points

P and meet the lines l_1l_4 . If P_1' be one of the intersections of such a curve with l_1 it is clear that each point P_1 of l_1 gives rise to 5 or 25 points P_1' , while conversely, the point P_1' arises from 25 points P_1 . Thus in the correspondence between the points P_1, P_1' of l_1 , set up by this construction, there are 50 points of l_1 for which pairs of corresponding points coincide. This can happen in two ways. Either there is a cubic through the points PP_1Q meeting l_3 and l_4 (hence satisfying the conditions of the problem), or else there exist two distinct curves through the points PP_1Q , one meeting l_3 and the other meeting l_4 . This can only happen if the curves in question degenerate, since two proper cubics cannot intersect in six points. This will happen if the line P_1Q passes through one of the points P, or again if the points P_1Q are coplanar with three of the points P. In the former case the cubics are completely determined, their residual part consisting of a conic passing through the three remaining points P (and hence lying in the plane of these) and meeting the line P_1Q and the line l_3 or l_4 as the case may be. In the latter case each cubic has two possibilities, the rest of it, other than a prescribed conic in the plane of three of the points P, consisting of either of the two transversals drawn from the fourth point to the conic and the line l_3 or l_4 as the case may be. The pair of cubics through the six points can thus be selected in four ways, and the coincidence must count four times among the 50. Thus the degenerate cases account for $4 \cdot 1 + 4 \cdot 4$ or 20 of the 50 coincidences; the remaining 30 must arise from proper cubics which satisfy P^4l^4 . Hence $P^4l^4 = 30$.

We shall now describe the relevant properties of four Cremona transformations of space which are of value in the solution of many of the simpler cases. These transformations are all well known, but only two of them appear to have been used for the solution of enumerative problems in the manner which will be described below, and one of these seems to have been used only for the simple cases already mentioned as having been dealt with by Cremona. These transformations all have the property of changing cubic curves satisfying a certain eightfold condition into straight lines. It is clear that such cubics must possess the property that one of them passes through two arbitrary points. Now it is clear from Cremona's results that the cubics satisfying any one of the four eightfold conditions P^4, P^3B, PB^3, B^4 are of this type. We seek accordingly transformations of space which transform such systems of cubics into straight lines.

(i) The first of these transformations is the well-known involutorial transformation of space defined by replacing each co-ordinate by its reciprocal.

Geometrically considered, the transformation is symmetrical and transforms a general plane of space into a cubic surface having four fixed nodes at the vertices of the fundamental tetrahedron. The lines of space are transformed into cubic curves passing through these four points, and conversely every cubic curve through these points is transformed into a line. The lines which pass through one of the four points are invariant under the transformation i.e., a line through one of the points P is transformed into another line through P . In this way we can transform the quadruple infinity of cubics satisfying the condition P^4 into the lines of space.

The values of $P^3/2$ and $P^4/4$ are calculated in this way by de Vries.*

(ii) The next transformation is defined by the system of quadric surfaces in space which pass through a line and three points not lying on it. These quadrics form a homaloidal system, and determine a quadri-cubic transformation of space. The planes are transformed into cubic scrolls having a fixed double directrix and three fixed generators in common; lines are transformed into conics which meet these three lines and the directrix, and cubics which pass through the base points of the system of quadrics, and have the base line as chord, are transformed into straight lines. This transformation is well known,† and has been applied to certain problems by Wren,‡ but no use of it in the present connection appears to have been made. It clearly transforms cubics which satisfy the condition P^3B into lines.

(iii) The third transformation is defined by cubic surfaces which contain three fixed lines and have a fixed node, containing then the three transversals from the node to pairs of the three lines. These are a homaloidal system and correspond to the planes of the transformed space. The planes of the original space are transformed into cubic surfaces passing through a fixed twisted cubic curve and having three fixed nodes on this curve. The lines of the first space become cubics through these three points which have two further intersections with the cubic curve, c ; and cubics in the original space which pass through the fixed node and have the three fixed lines as chords are transformed into lines. The equations of the transformation can be reduced to the form

$$\begin{aligned}x' &= yz(y - t), y' = zx(z - t), z' = xy(x - t), t' = xyz, x = t'(t'^2 + t'z' + y'z'), \\y &= t'(t'^2 + t'x' + z'x'), z = t'(t'^2 + t'y' + x'y'), t = t'^3 - x'y'z'.\end{aligned}$$

This transformation can obviously be used to transform cubics satisfying PB^3 into lines.

* 'Proc. R. Acad. Sci., Amsterdam,' vol. 11, p. 84 (1908).

† Hudson, "Cremona Transformations," p. 287 (Cambridge, 1927).

‡ 'Proc. Lond. Math. Soc.,' vol. 15, p. 144 (1916).

(iv) The last of the transformations is the symmetrical one defined by means of cubic surfaces passing through four lines and their two transversals. This converts the lines of either space into cubic curves with the four fixed lines as chords and *vice versa*. This transformation is well known and has been extensively applied to problems dealing with cubic curves by Wakeford* and others, it yields the neatest proof of the last three of Cremona's results already quoted, for which see Baker, *op. cit.*, *antea*, p. 143.

All of these transformations may be regarded as degenerations of the general cubo-cubic transformation of space defined by cubic surfaces through a sextic curve of genus three, with the exception of the second, which is of lower order.

We shall now proceed to apply these transformations to our problem. Consider the first transformation. The conditions which involve P^4 are three in number, namely, $P^5/2$, $P^4B/2$, $P^4/4$.

Consider the cubics which satisfy $P^5/2$ and apply the first transformation with four of the points P as fundamental. The cubics become lines passing through the transform of the fifth point and meeting the two cubic curves into which the two lines are transformed. These curves pass through the four points which are base points of the reverse transformation. Of the nine lines through P which intersect these two cubics, four join P to these points and are not the transforms of cubic curves; there remain five lines which meet the two curves in distinct points. These are the transforms of cubics satisfying the required conditions. Hence we have $P^5/2 = 5$, verifying the previous result.

In a similar way the cubics which satisfy $P^4B/2$ become lines which are chords of one cubic and secants of two others, the three curves all having four common points. Let c be the former curve, c_1, c_2 the latter two, and let P_i ($i = 1, \dots, 4$) be the common points. The chords of c meeting an arbitrary line l form a quartic scroll on which c is double. This meets c_1 in four points other than P_i . The secants of c_1 which are chords of c thus form a quartic scroll. If l' is a line through P_1 the chords of c meeting l' lie on a quadric surface and this has two intersections with c_1 not lying at any of the points P_i . Thus two lines, chords of c , meet l' and c_1 . This means that P_1 is multiple on the scroll of chords of c meeting c_1 to order $4-2$ or 2 . Thus c_2 meets the scroll in $3.4 - 4.2$ or 4 points. The four generators of the scroll through these points are the transforms of the cubics required, so that $P^4B/2 = 4$.

Finally $P^4/4$ is the number of lines which intersect four cubic curves c_i ($i = 1, \dots, 4$) passing through the four points P_i . The transversals of c_1 and

* 'Proc. Lond. Math. Soc.' vol. 21, p. 98 (1923).

two arbitrary lines form a sextic surface on which the cubic curve is simple (one line passing through each point of c_1), this has 14 points in common with c_2 which do not coincide with the points P_i . Thus the transversals of c_1, c_2 , and one arbitrary line l form a surface of order 14. By choosing the second line to pass through a point P_i it is easy to see, by a similar process of reasoning, that on this surface the points P_i are 5-ple, the general point of c_1 being only triple. Thus c_3 meets the surface in $3 \cdot 14 - 4 \cdot 5$ or 22 variable points. The transversals of c_1, c_2, c_3 , thus form a scroll of order 22. Considering special positions of the line l and arguing as in the previous case it is easy to show that the four points P_i are 9-ple on this surface. The surface has, therefore, $22 \cdot 3 - 4 \cdot 9$ or 30 free intersections with c_4 , so that there are 30 lines meeting the four curves in distinct points. This verifies the result already proved, that $P^4_4 = 30$.

The cases which involve the condition P^3B are the three $P^4B^{1/2}$, $P^3B^{3/2}$, $P^2B^{5/2}$, and these cases are simplified and reduced to problems of lines by means of the second of the four transformations mentioned above.

We observed that the lines of the original space were transformed by this transformation into conics which meet three skew lines l_1, l_2, l_3 , and a transversal λ of these. Apply the transformation, with the base elements consisting of three points and a prescribed chord; the cubics satisfying $P^4B^{1/2}$ are easily seen to be transformed into lines which pass through the transform of the fourth point and meet two of these conics; there are clearly four such lines. Hence $P^4B^{1/2} = 4$, as before. The curves satisfying $P^3B^{3/2}$ are transformed into chords of one such conic which meet two others; of such lines there are clearly four, so that we have $P^3B^{3/2} = 4$, again verifying a previous result. Finally the curves which satisfy $P^2B^{5/2}$ become the transversal lines of four such conics. Recalling the theorem (which has already been quoted) that four curves of degrees m, n, p, q , have $2mnpq$ common transversals, we see that the four conics in question have 32 common transversals. Four of these, however, are the lines l_1, l_2, l_3, λ , and are not the transforms of cubics satisfying the conditions of the problem. There remain 28 transversals corresponding to such cubics. Hence $P^2B^{5/2} = 28$. This is one of the results obtained by van Kol, who, however, does not make use of the simplification afforded by this transformation.

Passing to the third transformation, we consider the cases $P^2B^{3/2}$, $P^2B^{5/2}$, $P^2B^{7/2}$, which all involve the condition P^2B^3 ; and apply the transformation with the point and the three base lines chosen from among the prescribed chords and points. The lines of space become, as we have seen, cubics passing

through three points and having two further intersections with a definite cubic, c , passing through these points. The cubics in the original space which satisfy $P^2B^{3/2}$ then become lines through a point meeting two such cubics; of the nine such lines the joins of the point to the three intersections of the curves with c which are fixed in the transformation do not correspond to cubic curves, so that there remain six others. Hence $P^2B^{3/2} = 6$. The cubics satisfying $PB^{4/2}$ become the chords of one such cubic which meet two others. By argument parallel to that used in the corresponding case of the first transformation it appears that there are nine such lines which have their intersections with the curves distinct. Hence $PB^{4/2} = 9$. Finally, the cubics satisfying $PB^{3/4}$ become lines meeting four such curves and, by the process of reasoning used in the first transformation for a similar case, we find there are 54 lines with distinct intersections. Thus $PB^{3/4} = 54$.

In the last two results the fact that the cubic curves concerned have each two variable intersections with the curve c does not in any way affect the argument.

The last transformation, namely, the symmetrical one determined by cubic surfaces containing four skew lines, is applicable to the solution of those problems in which the condition B^4 is involved. These are $PB^{4/2}$, $B^{5/2}$, and $B^{4/4}$. In the first case the cubics satisfying the conditions of the problem are transformed into lines which pass through a point and meet two cubic curves, there are nine such so that we verify the previous result $PB^{4/2} = 9$. The cubics satisfying the condition $B^{5/2}$ are transformed into the chords of one cubic curve which meet two others, the three curves having four common chords (the base lines) irrelevant among the solutions. Now, considering the two congruences of lines formed, (a), of the chords of the first cubic and, (b), of the secants of the other two, and applying Halphen's theorem, it is easy to see that the number of such lines is in general 36. Of these, in our case, each of the four lines occurs as a fourfold solution, so that there remain 20 relevant solutions. Hence $B^{5/2} = 20$. In a similar way the cubics satisfying $B^{4/4}$ become lines meeting four cubics which have four common chords; in general there are 162 solutions to this problem, but in our case each of the four common chords must count $2 \cdot 2 \cdot 2$ or 16 times, so that there remain only 98. Thus $B^{4/4} = 98$.

These exhaust the cases of the problem we consider in which by means of one of these transformations we can transform the curves we require into lines. In some other cases the curves in question could be transformed into conics, but it is in general simpler to use the degeneration method to which we presently

proceed. There will be noted, incidentally, the ease with which most of the above results are obtained. In the degeneration method we shall frequently require the number of solutions of problems involving the condition Q defined previously,* in which a curve is constrained to pass through a point and have a given line through the point as chord. It is therefore necessary to obtain the more elementary results for such conditions before proceeding further. The results enumerated below all can be proved very easily, either directly or by very simple applications of the transformations described, and for reasons of space it is not necessary to give detailed proofs. It can in fact be verified that

$$\begin{aligned} QP^4I &= 2, \quad QP^3BI = 2, \quad QP^2B^2I = 2, \quad QPB^3I = 3, \quad QB^4I = 6; \\ Q^2P^3 &= 1, \quad Q^2P^2B = 1, \quad Q^2PB^2 = 1, \quad Q^2B^3 = 2, \quad Q^3PI = 3, \quad Q^3BI = 4, \quad Q^4 = 2. \end{aligned}$$

Other results may be obtained by consideration of the transformations already given, and as we have already given examples of the use of such transformations, it will be sufficient to mention the transformation, and the results obtained by its use. The work is in all respects similar to that which precedes. Thus by means of the first transformation we can deduce the results $Q^2P^2I^2 = 6$, $QP^3I^3 = 13$; from the second transformation we deduce $Q^2PBI^2 = 7$, $QP^2BI^3 = 14$; while from the fourth can be obtained $Q^2B^2I^2 = 10$ and $QB^3I^3 = 30$. For the two latter cases the only necessary remark is that in this transformation the neighbourhood of a point on one of the base lines becomes the set of points of a transversal line of three out of the four base lines in the second space.

The elementary conditions which involve the condition R † can also be obtained similarly, they are tabulated in the table at the end of this paper.

Part II.—Degeneration Methods.

The degeneration method is perhaps the most powerful method at present available for obtaining the number of solutions of geometrical problems in which this number is large. In the hands of Schubert the method ultimately resolved itself into a series of symbolic calculations, in which the geometrical nature of the initial problem was lost sight of. It seems however, at any rate in the present case, that little is lost in brevity, and much is gained in simplicity, by keeping the geometrical ideas foremost, and making all the calculations ultimately geometrical ones. We are thus able to solve all the problems with which we are concerned with no reference whatever to symbolic calculation.

* See the Introduction, above.

† Defined above, in the Introduction.

The principle on which the degeneration method rests is that the number of solutions of a geometrical problem, if finite, is independent of the existence of particular relations between the given entities in the problem. The solutions of a problem in the general case will accordingly be the same in number as those in any particular case we choose to investigate, provided only that this number does not become infinite in the process of specialisation. In our particular case, we allow the given points and lines to have certain mutual relations such as letting two lines intersect or letting a line and two points become coplanar. It frequently happens that if we choose this specialisation properly the cubic curves which satisfy the required conditions are thereby forced to satisfy certain other conditions, rendering them enumerable by means of results we have already obtained, or they may degenerate. In general we find it is convenient to specialise as little as possible consistently with the curves we require reducing to those which can be determined by applying simpler cases.

It is necessary to examine the manner in which a cubic in space can degenerate and to ascertain in what way conditions are satisfied when it does so. In the first place a degenerate cubic can consist of a conic and a line intersecting it but not lying in its plane. As there are ∞^{11} such systems and ∞^{12} cubics in all we infer that this degeneration imposes a simple condition on the curve. It is important to note that in this case an arbitrary line which passes through the double point of the curve is not to be regarded as a chord of the curve; for if the cubic tend to its limiting position the chord of the cubic which passes through an arbitrary point P clearly tends, for general position of P , to the transversal which can be drawn from P to meet the line and the conic. As a consequence, the condition that a cubic should have a given line as a chord is *not* satisfied when the cubic degenerates into a line and a conic which intersect on the prescribed line. If the conic of this case split up further into two straight lines further conditions are imposed on the cubic, and this case will not arise in our work save in the last few cases. Another degeneration of the cubic is, however, possible; it may degenerate into a rational cubic lying in a plane, possessing then a node. In this case every line through the node is the limit of a chord of the twisted cubic, and indeed the only chord of the degenerate cubic passing through a point is the join of the point to the node unless the point lies in the plane of the cubic.

Apart from three complicated cases which arise at the end, all the cases which arise from conditions of our kind admit of solution by means of comparatively elementary degenerations, many of which can be used for several different problems. We shall work out in detail only samples of the cases,

the general procedure being always the same. The more elementary cases will be given in greater detail, but one complicated calculation is worked out as a model.

Consider first the cubics which satisfy the condition $P^2B^2l^4$. This affords an example of a degeneration which is very useful for other cases. Let P_1P_2 denote the two prescribed points, b_1b_2 the prescribed chords, and l_1, l_2, l_3, l_4 the four secants. Suppose the position of the lines to be specialised so that $b_1l_1l_2$ lie in a plane π . They thus meet in pairs, let l_1l_2 meet in X and let b_1 meet l_1l_2 in L_1L_2 respectively. If a cubic which satisfies the required conditions is undegenerate it can only have three points in common with the plane π , and as it must meet b_1 twice and l_1l_2 each once this requires it to pass through one of the points X, L_1, L_2 . If it passes through X it satisfies the conditions of meeting l_1l_2 , so that the remaining conditions on the curve are those of having b_1b_2 as chords, passing through P_1P_2 and meeting l_3l_4 , i.e., the curves are those which satisfy the condition $P^2B^2l^2$, and we have seen that there are four such curves. Similarly if the curve passes through L_1 it must satisfy the condition QP^2Bl^3 , there are 14 such curves, similarly 14 more arise from cubics through L_2 ; but the curves which pass through both L_1 and L_2 , whose number is P^4Bl^3 , or 4, have been counted twice, once as passing through L_1 and once for L_2 . The total number of undegenerate curves obtained is thus

$$4 + 2 \cdot 14 - 4 = 28.$$

There remains the possibility that the curve degenerates and a part of the degenerate curve lies in π . Now the curve has to pass through the points P_1P_2 and have b_2 as a chord, the points and line not lying in π , whence it is easily seen that the portion of the curve lying in π is a line, and the rest of the curve is a conic through P_1P_2 meeting this line. If b_2, l_3, l_4 meet π in the points Y, L_3, L_4 respectively the possible cases which arise are the following.

(i) There are four conics through P_1, P_2 which meet b_1, b_2, l_3, l_4 , let K be a point in which one of these meets π . Then the conic together with the line KY is a degenerate cubic satisfying the conditions of the problem. There are four such solutions.

(ii) The line in π may be the line YL_3 . In this case the rest of the cubic must consist of a conic through P_1P_2 meeting l_4, b_1, b_2 and this line; of the four conics which satisfy this condition one passes through each of the points in which the line meets b_1, b_2 , and these do not give rise to solutions of our problem since we have seen that a degenerate cubic does not have as chord an arbitrary line through the node when the cubic consists of a line and a conic.

Thus only two of the conics lead to proper solutions, and two more arise by considering the line YL_4 . In all we get four of this type.

The total number of cubics satisfying the problem is thus

$$28 + 4 + 4 = 36,$$

and we infer that generally $P^2B^2L^4 = 36$. This result has been obtained otherwise by van Kol in the paper already cited.

We shall give less detail in subsequent computations. It is necessary to quote four results concerning conics in space, which were first obtained by Lüroth.*

- (a) Four conics pass through two points and meet four lines.
- (b) Eighteen conics pass through one point and meet six lines.
- (c) Ninety-two conics meet eight lines.
- (d) Eight conics meet six lines and lie in a plane through a seventh.

Any degenerate cubic which meets k times a line which it is only required to meet once will be a k -ple solution of the problem, and must be so reckoned in the enumeration. Similarly if the cubic degenerates into a plane cubic it meets an arbitrary line of the plane in three points, and if this line is a prescribed chord of the curve it counts triply among the solutions.

Consider now the cubics which satisfy QPB^2L^3 , where Q , as before, is the condition that the curve should pass through a point and have a fixed line through the point as chord, and suppose that the line in the condition Q is met by one of the prescribed chords. It is then easy to see that the undegenerate curves are those which satisfy $QP^2B^2L^3$. Degenerate curves consist of conics lying in the plane of these two lines and a line through the point P , three cases arising if the line is a transversal to the second chord and one of the three secants, and one if the conic passes through the three points in which these lines meet the plane, the intersection of the plane with the second chord, and the point of the condition Q . The total number of curves is thus $14 + 3 + 1$ or 18. Thus $QPB^2L^3 = 18$.

Consider now the curves satisfying Q^2L^3 . A simple determination of this number is obtained by letting the three lines of the conditions Q be met by one of the secants, so that the four lines lie on a quadric, the cubic then either lies entirely on the quadric or else it passes through one of the three points of intersection of the secant with one of the lines. Of the former category there are easily seen to be four cubics; the cubics which pass through one of the three

* 'J. Mathematik,' vol. 68, p. 185 (1868).

intersections satisfy the condition $Q^3P^2l^3$ and are thus six in number, whence we have $Q^3l^3 = 4 + 3 \cdot 6 = 22$.

The cases Q^2Pl^4 and Q^2Bl^4 may be solved by supposing the two lines Q to intersect, the solutions are as follows :—

(a) For Q^2Pl^4 —

- (i) Proper cubics in number P^4l^4 .
- (ii) A line through a point P meeting two of the lines l , together with a determined conic in the plane of the lines Q .
- (iii) A conic in the plane meeting three of the lines l and a transversal from P to this and the fourth line.

Thus we get, using previous results, $Q^2Pl^4 = 30 + 6 + 4 \cdot 2 = 44$.

(b) For Q^2Bl^4 —

- (i) Proper cubics in number P^3Bl^4 .
- (ii) Conic in plane of lines Q through intersection with chord and two of the secants, together with a determined line.
- (iii) Line meeting the chord and three secants, with a determined conic in the plane.
- (iv) Plane cubic having node at the intersection of the plane and chord, passing through the points Q and the intersection of the plane with the four secants; as this meets each line Q in two points other than the prescribed one it counts as a quadruple solution. Hence $Q^2Bl^4 = 28 + 6 \cdot 3 + 4 \cdot 2 + 4 = 58$.

In any particular case, given the degeneration, the curves can be determined by a perfectly straightforward process. In order then to save space we shall simply state suitable degenerations for the cases which follow, and the results, omitting details of the working except in one typical complicated case. Most of the results can be obtained by several different degenerations, and this serves as a check on the accuracy of the work.

The value of P^3l^6 is found by letting the three points lie in a plane with one of the lines, whence we easily verify Schubert's result that $P^3l^6 = 190$.

QP^2l^6 can be obtained in three ways :—

- (i) By supposing the line Q and the two points P coplanar.
- (ii) By supposing the line Q , a point P and a line l coplanar.
- (iii) By supposing the point Q , the two points P and a line l coplanar.

In all cases we are led to the result $QP^2l^6 = 92$.

QPB¹⁵ arises by supposing—

- (i) Point P, line Q, line l coplanar.
- (ii) Lines Q, B coplanar.
- (iii) Line B, points P, Q coplanar.
- (iv) Line B and two lines l coplanar.

giving in all cases the result QPB¹⁵ = 112.

QB²¹⁵ arises by supposing—

- (i) A line B and two lines l coplanar,
- (ii) A line B and line Q coplanar,

and we find QB²¹⁵ = 168.

Using these results we find, by letting a chord and two secants lie in a plane, the results P²B¹⁶ = 220, PB²¹⁶ = 320, B³¹⁶ = 536; of which the first has been obtained by van Kol. The first of these may be verified by supposing the line B and the points P to be coplanar, the second by supposing the point P, a line B and a line l to be coplanar. The third admits of a simple verification by supposing the lines B all to be met by one of the lines l , we then get 32 cubics lying on the quadric containing these lines and 168 passing through each of the three points of intersection of the secant with a line B, this being the number QB²¹⁶; and $536 = 32 + 3 \cdot 168$. We can then obtain:—

Q²¹⁶ = 348 by supposing the lines Q to meet or by supposing the plane joining one of the lines Q to the point of the other line to contain a line l .

QP¹⁷ = 682 by supposing the line Q and two lines l coplanar, or the line Q, the point P and one line l coplanar.

QB¹⁷ = 964 by supposing B and two lines l coplanar, or B, a line l , and the point Q coplanar, or the line Q and two lines l coplanar.

PB¹⁸ = 1820 by supposing B and two lines l coplanar, or P, B, and a line l coplanar.

B²¹⁸ = 2976 by supposing a line B and two lines l coplanar. A second degeneration leading to this result arises by letting the lines B intersect, but this introduces conditions of the type R mentioned previously. These may be dealt with by the same methods as heretofore, and a second verification of the result stated obtained. The results for conditions of type R are given in the table at the end of the paper, and may be verified by methods similar to the present.

As an example of a complicated calculation the terms in the first degeneration of this case may be worked out.

Let π be the plane of the line b_1 and the lines l_1, l_2 , and let b_2, l_3, \dots, l_8 be the other lines. It may then be verified that we have :—

(i) Proper cubics in number $PB_2^{2/6} + 2QB_1^{1/7} - P^2B_1^{1/6}$	2028
(ii) Line in π joining intersection with b_2 and l_1 , and a conic ($i = 3, \dots, 8$)	336
(iii) Line joining intersections with l_i and l_j , and a conic	105
(iv) Conic meeting $b_1, b_2, l_3, \dots, l_8$ and line in π	92
(v) Conic with chord b_2 meeting b_1 , and five lines l_i , and line in π	48
(vi) Conic in π through intersection with b_2 and four lines l_i , with a line	180
(vii) Line meeting b_2 and three lines l_i , and conic in π	160
(viii) Cubic in π with node on b_2 meeting l_3, \dots, l_8	27

2976

In order to obtain the value of $P^2B_1^{1/6}$ it is necessary to investigate a different kind of degeneration, somewhat more complicated than the previous ones. We suppose the two points P and the eight lines l to be so specialised that they lie on a cubic surface,* on which, in the usual notation, the lines are identified with four skew lines a_1, \dots, a_4 , the two transversals b_5, b_6 of these, and two lines c_{12}, c_{34} which intersect each other and of which c_{12} meets a_1 and a_2 while c_{34} meets a_3 and a_4 . A cubic curve through the points P which meets these eight lines in distinct points has 10 points in common with the cubic surface and hence lies wholly or in part upon it. The curves we require must thus either lie wholly or in part on the surface or else pass through one or more of the intersections of the lines.

Now the rational cubic curves which lie on the cubic surface are either the tangent plane sections, or else are twisted cubics of one of 72 systems on the surface, each curve having the six lines of a row of a double six as chords and intersecting in one point the 15 lines which do not belong to the double six. Of the 36 double sixes on the surface four only are associated with cubics which satisfy the conditions of our problem, a typical one being

$$\begin{array}{cccccc} a_1, & a_5, & a_6, & c_{34}, & c_{24}, & c_{23}, \\ c_{56}, & c_{16}, & c_{15}, & b_2, & b_3, & b_4, \end{array}$$

* It is easily verified that in general they lie on only one such surface. Similar remarks apply to the cases considered below.

and the curves which have the first row of this as chords satisfy the conditions of the problem, since one such curve passes through the two points P . As the curves meet two of the prescribed lines in two points they count each for four solutions. Thus we have in all 16 solutions arising in this way.

Twelve solutions arise from the 12 nodal cubics lying in tangent planes to the cubic surface which pass through the line joining the points P .

If the cubic consist of two curves, one of which lies on the surface, it is easy to see that the latter must consist of a conic passing through one of the points P and lying in a plane through a_5 or a_6 ; the rest of the cubic then consists of the transversal drawn from the second point P to meet b_5 (or b_6) and the conic. Thus we have eight such curves in all. The total number of cubics which do not pass through an intersection of two of the lines l is accordingly

$$16 + 12 + 8 = 36.$$

The cubics which pass through one of the intersections of a pair of the prescribed lines satisfy the condition $P^{2/6}$ and in general would be 190 in number. From the 13 such points we would then get $13 \cdot 190$ or 2470 curves; in this, however, a curve passing through two of the intersections which lie on four different lines is counted twice, once for each intersection, it is easily verified that there are 48 such pairs of points, so the total deduction on this account is $48 \cdot P^{4/4} = 48 \cdot 30$. Similarly we must add a correction $P^{5/2}$ for each of the 52 triads of intersections which lie on six different lines, and deduct P^6 for the eight tetrads of points lying between them on all the lines. In all then we obtain a contribution

$$13 \cdot 190 - 48 \cdot 30 + 52 \cdot 5 - 8 \cdot 1 = 1282.$$

This includes all the curves of this type once only, except those curves which consist of the line b_5 (or b_6) taken with a conic through the points P to meet the two lines b and the two lines c . It remains to investigate the multiplicity of these degenerate solutions in our enumeration and also in the problem.

We may make here the following remark. If we have five lines in space, of which one meets the other four, a curve of order n (supposed rational) will satisfy the condition of meeting these five lines if it degenerate into the transversal line and a rational curve of order $n - 1$ meeting this; if the original curve be subjected to a further condition which makes it determinate, the same thing will be true of the curve of order $n - 1$. This solution of the problem will be a multiple one. By its nature, however, it seems clear that the multiplicity of the solution in question is simply a characteristic of the

special position of the five lines, and is independent either of the order of the curve or of the remaining condition. Assuming this, we can find the multiplicity in question by applying it to a simple case; taking for example the problem of finding the conics which pass through a point and meet six lines in the case when five of the lines possess this property it is easily verified that the condition in question gives a triple solution.

Consider now the cubic curves which degenerate into b_5 and a conic through the points P meeting the two lines b and the two lines c . There are four such conics, one of which passes through the intersection of the lines c . Each such conic, together with the line, forms a degenerate solution of the problem which, in virtue of what has just been said, we must regard as triple. If the conic do not pass through the point C in which the lines c intersect, it has been counted four times among the 1282 solutions, namely, once for each of the four points on the line b_5 , as a triple solution is all which is required we must deduct one from the computed total on this account. There are three such conics arising for either of the lines b_5, b_6 . On the other hand, if the conic pass through C it has been counted simply among the curves passing through each of the four points on b , as a triple solution among the curves passing through C, and once negatively for each of the pairs consisting of C and a point of b_5 . In all it is thus counted $4 + 3 - 4$ or three times, which is right. No correction is, therefore, necessary here.

It follows that the number P^{276} is equal to

$$36 + 1282 - 6 = 1312,$$

which agrees with Schubert's result obtained symbolically. By letting two of the secant lines lie in a plane with the line B or the line Q we can obtain from this the results

$$Q^{79} = 5384, \quad BI^{10} = 15864.$$

The case P^{120} may be dealt with similarly. Here we suppose nine of the lines and the point to lie on a cubic surface, the nine lines being those of a Steiner trihedral, for example $a_1, a_2, a_3, b_1, b_2, b_3, c_{23}, c_{31}, c_{12}$. Calling a set of n points skew if they lie on $2n$ distinct lines of the figure, it is easy to see that the intersections of the nine lines contain 18 points, 99 skew pairs, 180 skew triads, and 72 skew tetrads. A cubic curve passing through P and meeting the nine lines either lies wholly or partially on the surface or passes through one or more of the intersections. Of the former class of curve there are 36 which arise from tangent plane sections of the surface passing through P and one of

the three points in which the tenth line meets the surface; and 18 curves associated with double sixes, these being of the form

$$\begin{array}{cccccc} a_4, & b_4, & c_{15}, & c_{25}, & c_{35}, & c_{65}, \\ a_5, & b_5, & c_{14}, & c_{24}, & c_{34}, & c_{64}. \end{array}$$

As before, the curves passing through the intersections of the lines number $18 \cdot 1312 - 99 \cdot 130 + 180 \cdot 30 - 72 \cdot 5 = 9846$, and these are subject to correction for curves which contain one of the lines. Such a curve has for residual a conic which passes through P, meets the tenth line, the line considered, and the four lines not meeting this, which form a quadrilateral. Of the 18 such conics, two pass through the pairs of opposite vertices of the quadrilateral, three more through each vertex, and four through neither. It is easy to verify, by a method similar to that used for the previous case, that in the 9846 curves the first 14 of these conics have been counted triply, while the last four have been reckoned quadruply, as all must count triply in the final solution we have a deduction of four to make. There being nine lines the total deduction is 36, whence

$$PI^{10} = 36 + 18 + 9846 - 36 = 9864,$$

again in agreement with Schubert's result.

The result P^{276} may be verified by taking the eight lines to be eight lines of this configuration, equally with the method already used.

To obtain the value of I^{12} we suppose 10 of the lines to lie on a cubic surface and form a double five thereon, say, $a_1, \dots, a_5, b_1, \dots, b_5$. The configuration contains 20 points, 130 skew pairs, 320 skew triads, 265 skew tetrads, and 44 skew pentads.*

The curves which give rise to multiple solutions consist either of one of the 10 lines together with a conic, a solution which we have seen must be counted three times, or else of two of the lines paired in the double five, and a transversal of these and the last two lines. The multiplicity of this solution we do not at present know, but as in the other case, it is independent of the particular problem under consideration. We shall therefore determine it by considering the problem PI^{10} , solved above, in the case when the 10 lines form a double five on the surface and the point does not lie on it. In this case the only cubics which consist of a part lying on the surface and not passing through an intersection of two of the lines are one of the lines a_6 or b_6 taken with a conic through the point P meeting all the six lines a_i (or b_i); there are 18 such conics in each case, but the particular cubic curve consisting of a_6, b_6 , and

* The same figure may be used to verify the value of BP^{10} determined above.

the transversal from P to these lines arises in each case, and only corresponds to a simple solution of the problem. The contribution under this head is thus 35.

The cubics which pass through the intersections of the lines give rise in the usual manner to

$$20 \cdot 1312 - 130 \cdot 190 + 320 \cdot 30 - 265 \cdot 5 + 44 \cdot 1 = 9859$$

solutions, in which we have to take into account the degenerate ones.

If the cubic consist of a line a_1 and a proper conic through P it must count as a triple solution of our problem. Such a conic must meet the line b_1 and the five lines $a_1, \dots a_5$. Of the 18 conics which in general exist, the line b_1 and the transversal from P to a_1, b_1 , counts as a triple solution, three pass through each of the points on b_1 , and there are three others passing through none of these points; these 15 proper conics with the line a_1 must be triple solutions of our problem. The first 12 of these, repeating an old argument, have been counted once for each point on a_1 , triply for the point on b_1 and negatively once for each pair consisting of the point on b_1 and a point of a_1 ; in all triply, similarly the other three conics have been counted quadruply. On account of these non-degenerate conics we must thus deduct 30 solutions in all, three for each of the 10 lines. Again, the degenerate cubic which consists of a_1, b_1 and a line through P has been counted triply for each of the eight points these lines contain, and negatively once for each of the 16 skew pairs involved, or eight times in all. If x is the required multiplicity of this solution for the general problem we must deduct a further $8 - x$ for each of the five pairs a_i, b_i . The total number of solutions is thus

$$35 + 9859 - 30 - 5(8 - x)$$

and this must equal the number previously found, namely, 9864, whence it follows that $x = 8$ and the curves in question are to be regarded as 8-ple solutions of the problem.

We can now deal with the problem of calculating I^{12} . The cubics which do not pass through any of the intersections, and which thus lie wholly or in part upon the surface, are easily seen to be :—

(a) Tangent plane sections passing through two of the intersections of the last two lines with the surface, in number 9 . 12 or 108.

(b) Curves associated with double sixes of the form

$$\begin{array}{cccccc} a_1, & b_1, & c_{26}, & c_{36}, & c_{46}, & c_{56}, \\ a_6, & b_6, & c_{13}, & c_{13}, & c_{14}, & c_{15}, \end{array}$$

in number 9 . 5 . 4 or 180.

- (c) The line a_6 (or b_6) together with a transversal conic of the two last lines and the six lines a_i (or b_i); the 92 conics include the degenerate ones b_6u , u being one of the two transversals of the last two lines and a_6 , b_6 , so that this gives only $2 \cdot (92 - 1)$ or 182 distinct curves.
- (d) Conics of the surface passing through one of the intersections of the last two lines with the surface and lying in planes through c_{16} , together with a line, of this type there are $6 \cdot 5 \cdot 4$ or 120.

The total number of such curves is thus 590.

Passing through the intersections of the lines we have

$$20 \cdot 9864 - 130 \cdot 1312 + 320 \cdot 190 - 265 \cdot 30 + 44 \cdot 5 = 79790.$$

If a cubic consist of the line pair a_i , b_i , together with a transversal of these and the last two lines, it is an eightfold solution of the problem, and reasoning as before we can show that it has been counted precisely eight times in the enumeration.

If the cubic contain a_1 , the two degenerate conics containing b_1 associated with it count triply among the 92 conics meeting the last two lines and the lines a_i ; of the remaining 86 conics, which with a_1 form cubics corresponding to triple solutions of the problem, 16 pass through each of the four points on b_1 , and 22 pass through none of these points. Each of the former 64 conics gives with a_1 a cubic which we have counted three times in the 79790, the last 22 give cubics we have counted four times. We must, therefore, have a deduction of 22 for each of the 10 lines, or 220 in all, hence

$$I^3 = 590 + 79790 - 220 = 80160,$$

which again verifies Schubert's result.

This completes the investigation of all possible combinations of the symbols P, B, l, Q ; the conditions which involve R can be treated by similar methods, the elementary degenerations being quite adequate.

A further set of results is easily deducible from the foregoing. Consider cubic curves passing through a point P and meeting a line l , and satisfying any other condition of power nine, and let the line move in the plane Pl until it passes through P . In the limit the conditions of the problem are satisfied if (i) the curve passes through P and meets the limiting position of the line in a further point; (ii) if the curve touches the plane at P . Denoting the latter condition by ρ , we have the symbolic relation

$$Pl = Q + \rho,$$

by means of which conditions involving ρ , are reduced to others previously discussed.

306 *Twisted Cubic Curves which satisfy Twelve Conditions.*

The table below contains a list of the number of solutions for all possible conditions involving P, B, *l*, Q, R and ρ_p . Results already known are indicated as follows :—

- (1) Cremona, 'J. Mathematik,' vol. 60, p. 191 (1862).
- (2) Sturm, *ibid.*, vol. 79, p. 99, and vol. 80, p. 128 (1875).
- (3) Schubert, "Kalkül der abzählende Geometrie" (1879).
- (4) van Kol, 'Proc. Acad. Sci., Amsterdam,' vol. 32, p. 625 (1929).

The remaining results are believed to be new.

Table showing the number of twisted cubic curves satisfying conditions compounded of P, Q, R, B, and *l*.

(1) $P^4 = -$	(1) $P^3l = 5$	(1) $P^2l^2 = 30$	(2) $P^3l^2 = 190$	(2) $P^2l^3 = 1312$	(3) $P^2l^3 = 9864$
(1) $P^3B = -$	(1) $P^2B^2 = 4$	(1) $P^2B^2l = 28$	(1) $P^2B^2l^2 = 220$	$P^2B^2l^3 = 1820$	$l^7l^3 = 15864$
(1) $P^2B^3 = -$	(1) $P^2B^3l = 4$	(1) $P^2B^3l^2 = 36$	$P^2B^3l^3 = 320$	$B^2l^3 = 2976$	
(1) $P^2B^3l = -$	(1) $P^2B^3l^2 = 6$	$P^2B^3l^3 = 54$	$B^2l^3 = 536$		(3) $l^4 = 90160$
(1) $P^2B^3l^2 = -$	(1) $P^2B^3l^3 = 9$	$B^2l^3 = 98$			
(1) $P^2B^3l^3 = -$	(1) $B^2l^3 = 20$				
(1) $R^4 = 6$					
$QP^4l = 2$	$QP^3l^2 = 13$	$QP^2l^3 = 92$	$QPl^7 = 682$	$Q^2P^3 = 1$	$Q^2P^2l^3 = 6$
$QP^3B^2l = 2$	$QP^2B^3l^2 = 14$	$QPl^7l^3 = 112$	$QB^2l^7 = 964$	$Q^2P^2B = 1$	$Q^2P^2B^2l^3 = 7$
$QP^2B^3l^2 = 2$	$QPB^3l^3 = 18$	$QB^2l^3l^3 = 168$		$Q^2PB^2 = 1$	$Q^2B^2l^3 = 58$
$QPB^3l^3 = 3$	$QB^3l^3 = 30$		$Ql^9 = 5384$	$Q^2B^2l^3 = 10$	$Q^2l^3 = 22$
$QB^3l^3 = 6$				$Q^2B^3 = 2$	$Q^2l^3 = 348$
					$Q^4 = 2$
$RP^4 = 0$	$RP^3l^2 = 4$	$RP^2l^3 = 35$	$RP^2l^3 = 293$	$RQP^2l^2 = 2$	$RQl^3 = 148$
$RP^3B^2l = 1$	$RP^2B^3l^2 = 6$	$RPB^3l^3 = 49$	$RBl^3 = 442$	$RQPB^2l = 3$	$R^2PB^2l = 1$
$RP^2B^3l^2 = 1$	$RPB^3l^3 = 8$	$RB^2l^3 = 78$		$RQB^2l^3 = 5$	$R^2PB^2l^3 = 3$
$RPB^3l^3 = 1$	$RB^3l^3 = 15$		$Rl^9 = 2504$	$RQ^2P^2 = 1$	$R^2Ql^3 = 4$
$RB^3l^3 = 4$				$RQP^2l^3 = 17$	$RQ^2B^2 = 2$
				$RQB^2l^3 = 26$	$RQ^2l^3 = 9$
					$R^2PB^2l^3 = 12$
					$R^3 = 2$

Table showing the numbers for conditions involving ρ_p .

(1) $P^4\rho_p = 3$	$P^3\rho_p = 17$	$P^2l^2\rho_p = 98$	$Pl^7\rho_p = 630$	$QP^3\rho_p = 1$	$QP^2\rho_p = 7$	$QPl^3\rho_p = 48$	$Q^2Pl^3\rho_p = 3$
$P^3B\rho_p = 2$	$P^2B^2\rho_p = 14$	$P^2B^2l^3\rho_p = 108$	$B^2l^7\rho_p = 856$	$QP^2B\rho_p = 1$	$QPB^2\rho_p = 7$	$QB^2l^3\rho_p = 54$	$Q^2B^2l^3\rho_p = 3$
$P^2B^3\rho_p = 2$	$P^2B^3l^2\rho_p = 18$	$B^2l^3\rho_p = 152$		$QPB^2l^3\rho_p = 1$	$QB^2l^3\rho_p = 8$		$Q^2l^3\rho_p = 22$
$PB^3l^3\rho_p = 3$	$B^3l^3\rho_p = 24$		$l^9\rho_p = 4480$	$QB^2\rho_p = 1$		$Ql^9\rho_p = 334$	$Q^3\rho_p = 1$
$B^3l^3\rho_p = 3$							
$P^3\rho_p = 2$	$P^2\rho_p = 10$	$QPl^3\rho_p = 4$	$Pl^7\rho_p = 6$	$\rho_p^4 = 4$	$RP^4\rho_p = 2$	$RQP\rho_p = 1$	$RP\rho_p^3 = 1$
$P^2B\rho_p = 1$	$P^2B^2\rho_p = 7$	$QB^2l^3\rho_p = 4$	$B^2l^3\rho_p = 3$		$RPB^2\rho_p = 3$	$RQB^2\rho_p = 1$	$RB\rho_p^3 = 2$
$P^2B^2\rho_p = 1$	$B^2l^3\rho_p = 10$	$Ql^9\rho_p = 26$			$RB^2l^3\rho_p = 3$		
$B^2\rho_p = 2$	$Pl^7\rho_p = 50$		$l^9\rho_p = 24$		$RP^2\rho_p = 18$	$RQ^2\rho_p = 8$	$Rl^9\rho_p = 10$
	$B^2l^3\rho_p = 54$	$Q^2\rho_p = 2$			$RB^2\rho_p = 23$		
	$l^9\rho_p = 296$	$Q\rho_p = 2$			$Rl^9\rho_p = 145$	$Rl^9\rho_p = 3$	

P is the condition that the curve should pass through a fixed point.

B is the condition that it should have a fixed line as chord.

l is the condition that it should meet a fixed line once.

Q, R are the conditions that it should pass through a fixed point and have respectively one, two, fixed lines through the point as chords.

ρ_p is the condition that the curve should touch a given plane at a given point.

The symbols P, B, ρ_p , follow Schubert, but *l* replaces the symbol ν of Schubert. The conditions Q, R, were not considered by Schubert.

On the Transmission of Light by Thin Films of Metal.

By S. RAMA SWAMY, Ph.D., University College, London.

(Communicated by W. Wilson, F.R.S.—Received December 17, 1930.)

[PLATE 14.]

1. *Introduction.*

It is a matter of common knowledge that an ordinary gold leaf appears green by transmitted light while silver leaf appears blue. Faraday* found that the gold leaf lost all its colour if heated on glass. T. Turner† found that this change occurs at about 550° C. in the case of gold and about 240° C. in the case of silver. Faraday obtained thinner films from the “deflagration” of gold wire by the discharge of a Leyden jar battery. These were red and violet in places and green in others. They turned red on heating, but the green colour could be brought back by rubbing with a rounded piece of agate. The gold films used by Beilby,‡ obtained from paints used for ceramic gilding, behaved in a similar manner. One of his thin purple films turned rose-pink on annealing, and his thicker green films became transparent at a temperature above 400° C. R. W. Wood§ obtained purple, blue and green films of gold by sputtering. He found that films of all other colours could be turned green by heating, as opposed to the observations of Faraday and Beilby.

Maxwell Garnett|| has explained the colours observed by Beilby, Faraday and R. W. Wood by considering the films as made up of minute spherical particles of metal. He finds that the transmission-coefficient T , of films for which $\pi d/\lambda$ is very small, is given by

$$T = 1 - 4\pi d n^2 k / \lambda,$$

where d is the thickness of the film, k the absorption coefficient, n the refractive index, and λ the wave-length of the light used.

For thick films he finds

$$T = \frac{16n^2(1+k^2)}{(1+n)^2 + n^2k^2} e^{-4\pi d n k / \lambda}.$$

* Bakerian Lecture, ‘Phil. Trans.’ vol. 147, p. 145 (1857).

† T. Turner, ‘Proc. Roy. Soc.’ A, vol. 81, p. 301 (1908).

‡ Beilby, ‘Proc. Roy. Soc.’ A, vol. 72, p. 226 (1903).

§ R. W. Wood, ‘Phil. Mag.’ vol. 4, p. 425 (1902).

|| Maxwell Garnett, ‘Phil. Trans.’ A, vol. 203, pp. 385–420 (1904); also vol. 205, pp. 237–288 (1905).

On the other hand, Houston and George Moore* found that the transmission curves for sputtered gold and silver films are essentially independent in character of the thickness of the films. They found that for gold the transmission is maximum at 5000 Å., whereas for silver it is greatest at 4600 Å. (in the visible range) and decreases to a little more than half that value at 7000 Å.

More recently, since this work was begun, Dreisch and Rutten† have found that the infra-red absorption curves for thin films of metals are similar in shape to those of colloidal substances. They obtained, by sputtering, gold films which were red-blue, bright blue and green-blue, and silver films which were red and reddish yellow.

As the observations on the colour of the films in most of the above experiments are qualitative, it seemed desirable to carry the matter further by making strictly quantitative observations on the colour variation of sputtered metal films on heating. For this purpose the absorption spectra were photographed and the plates obtained measured with a photometer. The transmission coefficient was obtained from the photometric measurements. Films which were initially of two colours were examined, viz., green and blue-green in the case of gold and blue and violet in the case of silver. The gold films were heated up to a temperature of 600° C., the silver to 400° C. Finally the films were mounted on microscope slides and examined under a microscope.

2. Sputtering, Weighing and Measurement of Electrical Resistance of the Films.

The gold and silver films used were sputtered on thin microscope cover glasses $\frac{3}{4}$ inch in diameter in a discharge tube shown in fig. 1. It consisted of a glass tube D 17 cm. long and about 4 cm. in diameter, closed at both ends by aluminium discs A and B. Circular grooves were cut in A and B to take the glass tube as shown in figure. The cathode K, consisted of an aluminium rod to which a disc G (3 cm. in diameter) of the metal to be sputtered was suitably fixed as shown in figure, and passed through the disc B. It was fixed to B in position by a sealing wax joint, after adjusting the height of the plate G above A. The aluminium rod was enclosed in a glass tube and all aluminium parts inside the tube were screened off with mica. A suitable stand of glass was constructed on the disc A as shown in figure, for holding the cover glasses to

* Houston and George Moore, 'J. Opt. Soc., Amer.,' vol. 16, p. 174 (1928).

† Dreisch and Rutten, 'Z. Physik,' vol. 60, p. 69 (1930).

be sputtered. A glass ring made by drilling a hole $\frac{3}{4}$ inch in diameter in a thin microscope coverglass (3 cm. in diameter) was stuck on to the top of the glass stand and the cover glass to be sputtered kept in it. A mica disc with a hole 1.15 cm. in diameter was placed over it so as to leave a rim of unsputtered glass round the edge of the cover glass. After these adjustments the glass to metal joints between B and D, and D and A were sealed and made vacuum tight with sealing wax. A water cooling device, as shown in fig. 1, was adopted for the cathode to prevent softening of the wax joints by the heat produced during sputtering. The tube was evacuated by connecting the brass tube T to a mercury diffusion pump backed by a Hyvac pump. Two traps, one of liquid air and the other of a silver-tin alloy (73 per cent. silver), were included between the sputtering tube and the pump in order to prevent back diffusion of mercury vapour into the former. One or two blue gold films obtained before insertion of traps had several green patches in them, surrounding what appeared under the microscope to be minute globules of mercury. These patches were found to spread steadily. The films obtained after the insertion of the traps were free from all contaminations of this kind. For insertion and removal of the cover glasses, it was only necessary to warm the disc A and remove it, leaving the upper part of the sputtering tube intact. The under side of the cover glass was in contact with a strip of aluminium foil connected to the anode A, in order to maintain it sufficiently anodic in charge for sputtering to take place. Dewhurst* has also had recourse to this device. The length of the dark space was maintained constant for any particular film by continuously adjusting the vacuum by suitable taps.

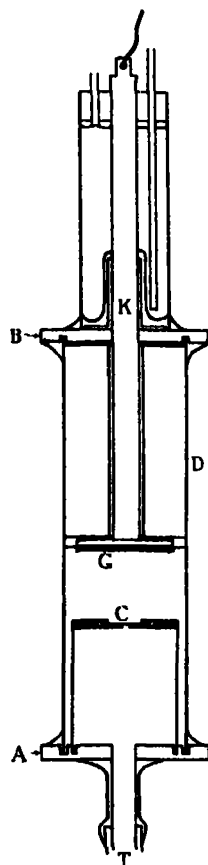


FIG. 1.

For sputtering, the discharge was produced by an induction coil with a mercury interrupter connected to the 220 D.C. mains. It was found unnecessary to use a rectifier in the secondary circuit, to prevent contamination of the cathode. Since all exposed metal parts in the anode were of aluminium and since aluminium does not sputter ordinarily, the cathode was found to be

* Dewhurst, 'Proc. Roy. Soc.,' A, vol. 39, p. 7 (1926).

uncontaminated. Richtmyer and Curtiss* have also dispensed with a rectifier for the same reason.

Films of two colours were obtained for each metal, viz., green and blue-green for gold, and blue and violet for silver. The colour of the film for any particular metal was found to depend on the length of the dark space, other things being the same, as shown by Table I. The electrical resistance of the films was measured approximately by keeping them in series with an accumulator and a microammeter, a suitable shunt being used when necessary. An ebonite holder was used to keep the films in position while measuring their resistance. Two light springs with polished brass knobs (gilded or silvered) were used as electrodes. The electrodes were kept at the ends of a diameter of the sputtered deposit. The deposits of gold and silver on the cover glasses all had the same diameter, since the same mica mask, already mentioned, was used in all cases. Thus the measured resistance was that between the ends of a diameter of a circular film 1.15 cm. in diameter. The resistance measurements taken both before and after heating the films are given in Table I.

Table I.

No.	Metal.	Colour.	Primary current.	Length of dark space.	Distance from cathode.	Time of sputtering.	Thickness.	Result before heating.	Result after heating.
			amps.	mm.	cm.	min.	cm.	ohm.	ohm.
C ₁	Gold	Green	6	4	2.5	60	5×10^{-6}	8.8	7.3
D ₁	„	Blue-green	6	3	2.5	65	0.5×10^{-6}	100.9	Very high
E ₁	Silver	Blue	6	3	2.3	30	3×10^{-6}	7.5	Very high
E ₂	„	Violet	6	2	2.3	60	$< 0.5 \times 10^{-6}$	Very high	Very high

N.B.—In the cases marked "very high" even 220 volts in series with the film and microammeter (not shunted) failed to produce a visible deflection of the needle.

3. Heating the Films and Photographing their Absorption Spectra.

The arrangement of the apparatus used for photographing the absorption spectra of the films at different temperatures is shown in fig. 2. P, a 500-c.p. pointolite lamp was the source of light used for the experiment, I being an iron arc, the spectrum of which was photographed alongside the absorption spectra for wave-length setting. R consisted of two right-angle prisms mounted one above the other with their reflecting faces at right angles; by raising or

* Richtmyer and Curtiss, 'Phys. Rev.', vol. 15, p. 465 (1920).

lowering this arrangement either of the two sources of light P and I could be thrown on to the lens L, which served to focus the light on the metal film G.

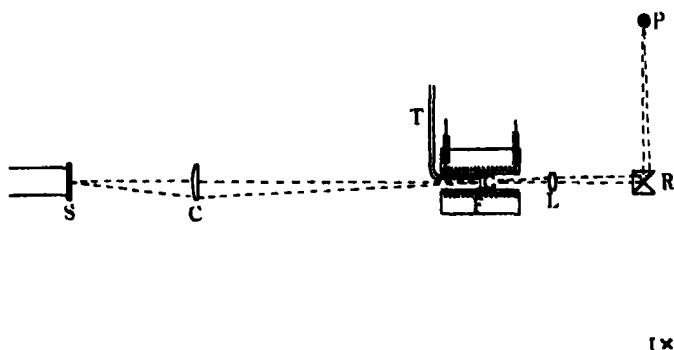


FIG. 2.

The cylindrical lens C served to obtain a line image of the former pointolite image on the slit of the spectrograph, S. The distance from R of the pointolite and the iron arc wave were the same so that the latter were both in focus on the film and on the slit. The heights of P and I above the table on which the apparatus was mounted were adjusted to equality, and the axis of the optical system lay in the same horizontal plane as P and I. This was done by first adjusting the spectrograph and the optical system with one of the sources of light, viz., the iron arc, and then adjusting the height of P to suit the optical system.

The metal film was kept in a brass holder to which could be screwed at the end, small brass tubes of equal length. This was placed in the electric furnace F, which itself was mounted horizontally as shown in fig. 2. The brass tube occupied the full length of the furnace, which was constructed of nichrome wire wound over an alundum tube 5 inches in length. The furnace was open at both ends and was rigidly fixed to a brass base which, by means of a geometrical device, could rest in either of two fixed positions on a brass table, the two positions corresponding to a shift normal to the axis of the optical system. The brass table itself was constrained to adopt a fixed position on the table by another geometrical device. By this arrangement the furnace could adopt two definite positions only so that in all cases two definite parts of the metal film, 2 mm. apart, could be examined. Even after removing the furnace for photographing the iron arc or the pointolite spectrum separately, one could be sure of bringing the same part of the film as before under examination. The two portions examined in each film were equally distant from its centre. These

parts were actually 2 mm. long and 0.05 mm. wide, as was calculated from a knowledge of the width of the image on the slit, the diameter of the pointolite image on the film and the width of the slit in use. These readings are given below in Table II.

Table II.

	mm.
Diameter of image on metal film	2
Width of image on slit	1
Width of slit	0.023
Width of metal film examined	0.046
Length of metal film examined	2

The examination of two different parts of the film was made to guard against local irregularities, should such exist. The two sets of readings obtained with two different portions of the same metal film agreed quite closely, proving that the films were fairly uniform and also that experimental errors were very small.

Only the central part of the lens L was used, the angle of convergence of the pencil of light falling on the gold film being consequently very small (3° to 4°). Thus the pencil could be treated as approximately parallel and the passage of light through the film could be taken to be normal. Wellington spectrum plates were used along with a photometric bluish filter (Wratten No. 78A). The temperature of the film was measured with a platinum platino-rhodium thermocouple kept in contact with it.

The following procedure was adopted. The furnace unit was removed with the film in position and the iron arc spectrum photographed once at the top and once at the bottom of the plate. A neutral screen or pair of wedges was kept in the position of the film, the photometric filter was interposed and the pointolite image obtained on the slit. Its spectrum was then photographed with a suitable exposure just below the upper iron arc spectrum. The correct exposure was found by test plates. The neutral screen was then removed, the furnace put back, with the metal film in it, and the spectrum photographed under the former one giving the *same exposure* as before. The furnace was then moved to its second position and the spectrum photographed, giving the *same exposure*. The film was then heated to 200° C. in the furnace and the absorption spectra of the two parts of the film corresponding to the two positions of the furnace photographed again. The rise in the furnace temperature during the time occupied by the photographing of the spectra was never more than 3° or 4° C. The same procedure was adopted for temperatures of 300° , 400° ,

500° and 600° C. in the case of gold, and 250°, 300°, 350° and 400° C. in the case of silver. The exposures were constant for each film and the spectra of the iron arc and pointolite were obtained on each plate exposed. The exposure was measured correct to a fifth of a second. The filter was interposed for all exposures except those of the iron arc spectra.

The purpose of using the neutral screen (or wedges) was to cut down the intensity of the pointolite by a known fraction. If this was not done the pointolite spectrogram was found to be much too dense. By using a properly chosen screen the density of the pointolite spectrum could be made favourable for measurement and comparison with that of the absorption spectra. Several neutral screens were made by fogging slow lantern plates uniformly and subsequently developing them. Only a small circular part (3 mm. in diameter) was used in these screens, their transmission-coefficient being measured in a photometer. The most suitable screen for use with each metal film, as also the correct exposure for obtaining easily measurable spectra were found out by means of test plates, by trial and error. One of the spectrogram plates obtained is reproduced in fig. 3. 1 and 7 are the iron arc spectra, 2 is the pointolite spectrum, 3 and 4 are the absorption spectra of two parts of the same metal film at atmospheric temperature and 5 and 6 are those at 200° C. The plateholder of the spectrograph was loaded in absolute darkness, and during development the safelight was turned away from the plate, in order to prevent undue and uneven fogging of the plate. The remaining background fog was merely that known as chemical fog, and was made fairly even by uniform development of the plate. Uniform development was secured by continually brushing the sensitive surface of the plate during development with a wide soft camel hair brush. This method, used by Dr. Clark* of the British Photographic Research Association, was found to be quite satisfactory. After development and fixation the plates were washed for 4 or 5 hours in running water, in a tank reserved for this purpose, in order to remove all traces of hypo and the dye with which the plates are coated to render them panchromatic. They were dried in air, no effort being made to accelerate their drying, in order to prevent small differences in density due to uneven drying.† An idea of the evenness of the background fog can be obtained from Table III in which are set out photometric readings at five different unexposed parts of one of the plates, obtained for the determination of average density of fog.

* Dobson, Griffith and Harrison, "Photographic Photometry," p. 76.

† Dobson, Griffith and Harrison, "Photographic Photometry," p. 80.

Table III.

Part of plate.	Mean rotation of photometer nicol.	Density of fog.
	° ' ''	
1	37 58	0.21
2	37 47	0.20
3	37 41	0.20
4	37 52	0.21
5	37 52	0.21
	Mean	0.21

4. Measurement of Density of the Plates.

A slightly modified form of the photometer described by Dobson* was used for measuring the density of the plates prepared as mentioned before. The modification consisted of getting a fine line image with a cylindrical lens instead of a point image as in Dobson's instrument. A pair of nicols were substituted for the wedge for measuring density. The line image was divided along its length into three parts, AC, CD, and DB (fig. 3) by pasting narrow strips of black paper horizontally on the cylindrical lens. The part CD had the same length as the width of the spectra to be measured (about 1 cm.). The window of the photoelectric cell was restricted to such dimensions as to admit only the light from the central part CD of the line image. In order to measure the density of any one of the spectra at some particular wave-length the plate was moved horizontally and adjusted so as to make the ends of the line image AB coincide with lines of the chosen wave-length in the iron arc spectra. The plate was then moved vertically and adjusted so that the part CD of the line image just covered the width of the spectrum to be measured. Thus in fig. 3 the plate is set for measuring the fifth spectrum from the top, at a wave-length 4528.6 Å. Only one setting of wave-length was used for all the spectra on a plate for any particular wave-length, thus eliminating any possible errors in density due to errors in the wave-length setting. Since the dispersion of the spectrograph used was not very large, a small error in setting the line image would lead to a larger error in wave-length. Thus if different wave-length settings were made for each spectrum the densities measured would not all correspond to the same wave-length. But if a single wave-length setting was used for all of them the densities would all correspond to the same wave-length.

* Dobson, 'Proc. Roy. Soc.,' A, vol. 104, p. 248 (1923); see also Dobson, Griffith and Harrison, "Photographic Photometry,"

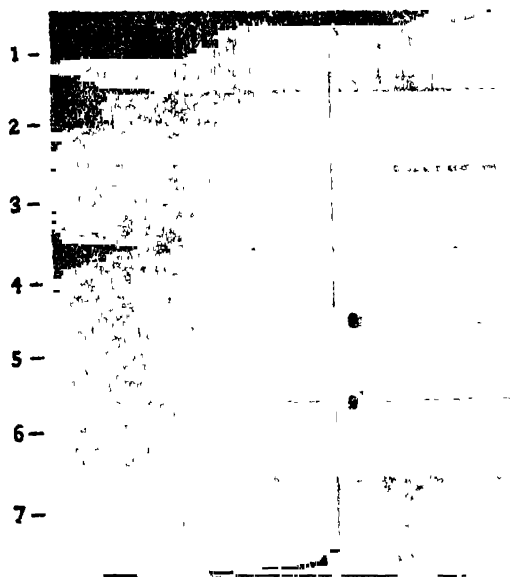


FIG. 3.

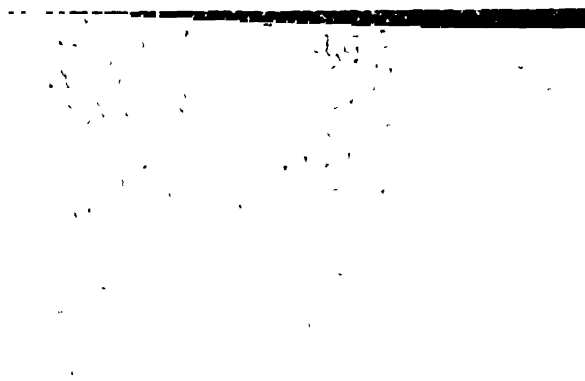


FIG. 4.—Microphotograph of Gold Film C₁ after heating.
Magnification 1,000 diameters.

The error would then be only in the wave-length measurement and would not introduce one in the density measurements.

The density of a photographic plate is defined as $\log_{10} I_0/I_t$, where I_0 is the intensity of the light falling on the plate and I_t is the intensity of the light transmitted by it. In the above measurements I_t is the same as the light transmitted by the nicols and hence

$$I_t = I_0 \cos^2 \theta,$$

where θ is the rotation of the analysing nicol. Hence

$$I_0/I_t = \sec^2 \theta$$

and

$$\text{density} = \log_{10} \sec^2 \theta.$$

The mean density of fog of the plate was subtracted from the measured density in order to get the actual density. By appropriate use of neutral screens (or wedges) all densities were arranged to be nearly of the same value. The range of intensities being thus made small the assumption of a linear direct proportion cannot lead to appreciable error. Therefore the transmission coefficient was taken to be the ratio of the densities of the absorption

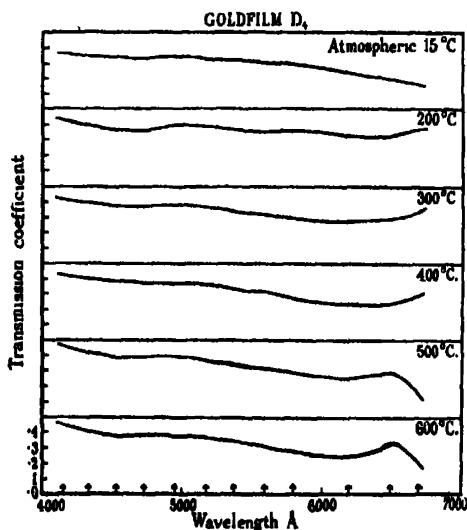


FIG. 5.

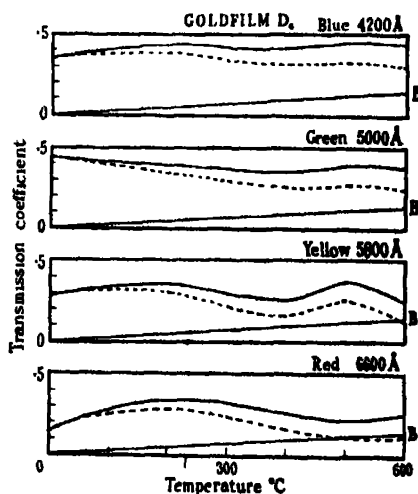


FIG. 6.

Not.—The arrow marks in fig. 5 correspond to the wave-lengths of the iron arc lines used for reference.

In fig. 6, the line joining B and the origin in the above diagrams represents the variation of the transmission coefficient due to the development of "windows." The dotted curves have been corrected for this effect.

spectra and of the pointolite spectra multiplied by the transmission coefficient of the neutral screen (or wedges) used. A typical set of curves obtained for the gold film D_4 are reproduced in fig. 5. In fig. 6 the transmission coefficient is plotted against temperature at four different wave-lengths of light.

5. Discussion of Results.

In his theoretical paper Maxwell Garnett* considers the films as composed of small metal spheres whose diameters are small compared to the wave-length of light used, and, treating these as Hertzian oscillators, calculates the transmission coefficient of such films for various values of μ , the volume of metal per unit volume of the film. He divides the theory into two sections, one dealing with thick films and the other with thin ones. For thick films, for which the thickness exceeds two-thirds the wave-length of light used, the transmission-coefficient is given by†

$$T = M_0 e^{-4\pi d n k / \lambda}, \quad (1)$$

where $M = 16n^2(1 + k^2)/\{(1 + n)^2 + n^2k^2\}$, n = the refractive index of the film, k = the absorption coefficient, and λ = wave-length of light used.

If, however, the thickness of the film is less than $\lambda/25$ a simplification can be made in the calculation by assuming higher powers of $\pi d/\lambda$ as negligible. This leads finally to the result‡

$$T = 1 - 4\pi d n^2 k / \lambda. \quad (2)$$

In this paper comparison is made between theoretical curves giving transmission coefficient against μ , and the experimental curves giving transmission coefficient against temperature at various values of λ . For this purpose the transmission coefficient of the films examined were calculated using the values of M_0 , nk/λ and n^2k given by Maxwell Garnett,§ and the values of the thickness d obtained by weighing the films. Equation (1) for thick films was applicable to C_1 and equation (2) for E_3 and D_4 . The curves obtained thus were compared with the experimental ones (transmission-temperature) and a fair measure of agreement was found to exist on making the following assumptions:—

- (1) μ diminishes steadily in a linear manner as temperature rises.

* Maxwell Garnett, 'Phil. Trans.,' A, vol. 203, p. 385 (1904).

† *Ibid.*, p. 409.

‡ *Ibid.*, p. 408.

§ *Ibid.*, p. 406; vol. 205, pp. 269, 272-273.

- (2) On heating, the film breaks up and becomes non-uniform, some parts increasing in thickness at the expense of others where the film becomes very thin or disappears totally. The latter parts would then act as transparent or semi-transparent "windows" with the result that increasing temperature dilutes the true absorption effect with increasing amounts of white light.
- (3) The open area of these windows is a linear function of temperature. (All the four films were heated at approximately the same rate in order to maintain constant any time factor which may exist.)

Maxwell Garnett considers that μ diminishes with increase of temperature. The truth of assumption (2) is substantiated by the microscopic evidence obtained after heating the films. The visual observations of Turner (*loc. cit.*) and others mentioned in the beginning of this paper that gold leaf and silver leaf became transparent at *certain temperatures* (550° C. for gold and 240° C. for silver) agrees also with assumptions (2) and (3). The opening of the windows in the *initial stages* of heating may be smaller than the effect of variation of μ , and hence may have escaped notice in the visual observations. Assumption (2) is further justified by the enormous increase in electrical resistance of D_4 , E_1 and E_3 on heating. In one case, viz., C_1 , no increase in resistance was noted, but that can be explained by assuming that the elements into which the film broke up formed an interconnected network system, as shown by the microphotograph taken after heating it (fig. 4). This film was much thicker than the others and may therefore have had enough gold to permit of the formation of a network. Another gold film 10 times as thick behaved similarly. The theoretical and the experimental curves for C_1 , D_4 and E_3 are given in figs. 7, 8 and 9. The horizontal axes for the curves for yellow, green and blue have each been shifted upward to avoid overlapping, by 0.1, 0.2 and 0.3 of a unit respectively in fig. 7, by 0.4, 0.8 and 1.2 units in fig. 8, and by 0.5, 1.0 and 1.5 units in fig. 9. In fig. 6 the line AB in the experimental curves, drawn by inspection, is suggested as representing the variation in the transmission coefficient due to the windows developed in the film. The curve drawn in broken lines is the corrected curve (*i.e.*, corrected for window opening). The experimental curves in figs. 7, 8 and 9 have been corrected for this effect in a similar manner. The part of the μ scale to correspond to the experimental temperature scale is selected so as to give most agreements. $\mu = 1$ corresponds to a homogeneous metal film and decreasing μ to increasing collection of gold due to rise of temperature. The corrected curves are found to agree to some

extent with the corresponding theoretical curves for the films C_1 and D_4 in the range $\mu = 1$ to about $\mu = 0.6$ or 0.7 . The slight initial rise between 0° C.

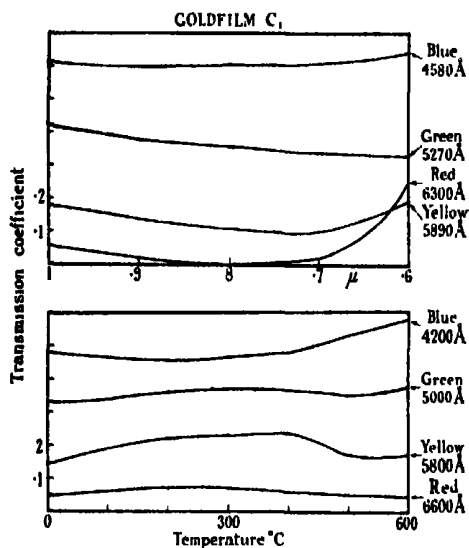


FIG. 7.

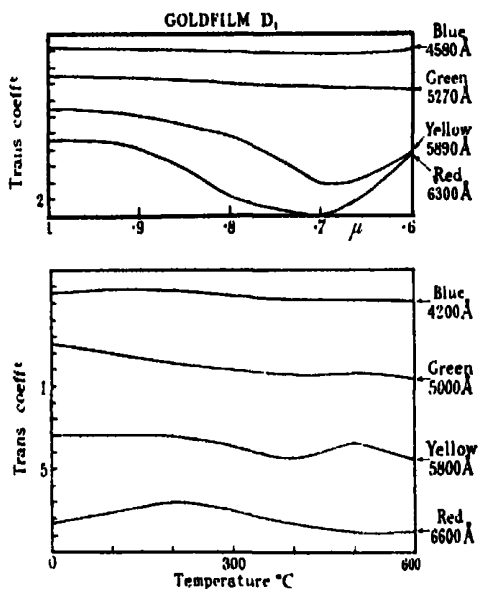


FIG. 8.

and 200° C. in the curves for C_1 , and the initial rise in the red and the maximum at 500° C. in the yellow for the film D_4 , are, however, not indicated in the theoretical curves. The film C_1 was originally green and became slightly bluer beyond about 400° C. D_4 was originally blue-green (like the 4916 mercury line) in colour, whereas it turned definitely blue on heating. This film was first noticed to scatter red light at about 300° C., and this phenomenon was present right through at all temperatures after its first appearance.

In the theoretical curves for the silver film E_3 (fig. 9) the transmission coefficient becomes negative in the neighbourhood of $\mu = 0.8$ in the red and yellow and lower values in the blue and green. Such negative values cannot actually exist and these parts of the curves merely correspond to absorption bands, the transmission being zero. If we assume the curves for red and yellow to start from $\mu = 1$ and remain fairly horizontal till they reach the right-hand branches, there is found to be a reasonable agreement between them and the experimental curves. The range of the negative values in the blue and the green may be taken to correspond to the minima at 200° and 250° C. in the experimental curves for these colours.

Two other silver films of thickness 3×10^{-8} cm. (E_1 , see Table I) and

5×10^{-5} cm. (E_4) and a gold film of thickness 5×16^{-5} cm. were also examined. The thinner one of these did not fall clearly in either of the ranges

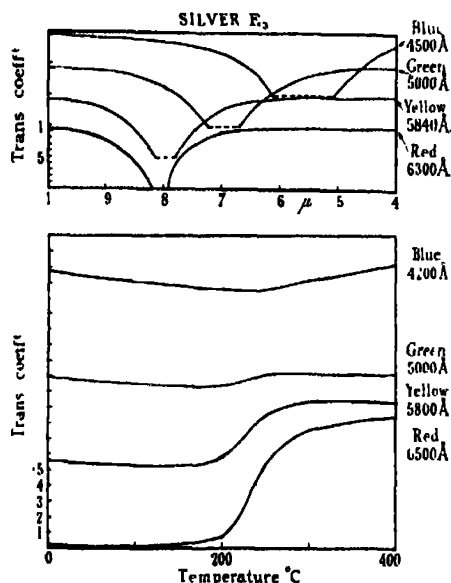


FIG. 9.

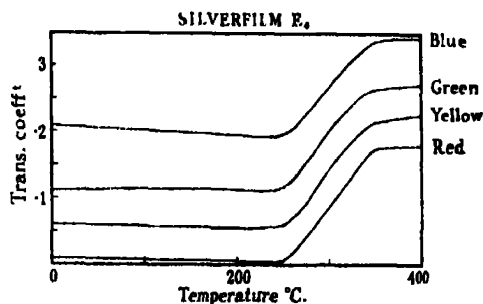


FIG. 10.

of thickness dealt with by Maxwell Garnett while the transmission coefficient for the other two was found to be not appreciably different from zero theoretically. Experimentally, however, it was quite measurable and thus their curves could not be compared with theory. The experimental curves for the silver film E_4 (thickness 5×10^{-5} cm.) are given in fig. 10.

The transmission coefficient-wave-length curves for the gold and silver films obtained from the results of Houston and George Moore (*loc. cit.*) are similar in shape to those of the thicker films at atmospheric temperature dealt with in this paper. The intense scattering of red light by the film D_4 perhaps corresponds to the change in colour from green and violet to rose-pink of the gold films examined by Faraday. R. W. Wood, however, finds that gold films of *all other colours* could be turned *green* by heating. None of the films examined by the present writer turned green on heating. The thickness of the films examined by R. W. Wood may have been of a different order to those dealt with here. This may, perhaps, be the reason for the difference in their behaviour in the two cases. The edges of some of the gold films examined were violet in colour and turned reddish after heating. The observations of Faraday and

Turner that gold and silver leaf become transparent on heating justifies one of the assumptions in this paper as already mentioned.

Thus Maxwell Garnett's theoretical results agree in some particulars with the experimental results discussed in this paper after making the assumptions given above. Slight disagreement may be due to the fact that the law of variations of μ , the relative volume of metal in the film, with temperature, as also that of the opening of the "windows" on heating, may not be as simple as those assumed here.

It is with much pleasure that I take this opportunity to express my gratitude to Professor E. N. da C. Andrade for the keen interest with which he has supervised this work, and for many valuable suggestions which have so considerably helped me in its execution. I must also thank Professor A. W. Porter for suggesting the work and Dr. R. E. Gibbs for the various valuable suggestions he has given me in carrying out this work.

On the Thermal Conductivity of some Metal Wires.

By W. G. KANNULUIK, B.Sc., University of Melbourne.

(Communicated by Lord Rutherford, O.M., F.R.S.—Received January 19, 1931.)

Introduction.

The methods of investigating thermal conduction in metals and alloys in which the steady state is employed fall into two groups (1) thermal, (2) electrical.

In a previous paper* use was made of the thermal method of which a brief critical account was given in that paper. In the present investigation the electrical method has been used. All the variants of this method employ a thin uniform cylinder heated by passing a steady electrical current through it, both ends of the cylinder being kept at the one constant temperature, that of the surrounding medium. The electrical method has several advantages:—

- (a) It is available for use with metals obtainable only in the form of a wire.
- (b) It enables a direct comparison of the electrical and the thermal conductivity to be made under the same conditions.
- (c) It can be used over a wide range of low temperatures.

* Kannuluik and Laby, 'Proc. Roy. Soc.,' A, vol. 121, p. 640 (1928).

The principal electrical methods are those of (1) Callendar,* (2) Kohlrausch,† and (3) Knudsen.‡

(1) *Callendar's Method*.—In this the lateral loss of heat from the surface of the wire just balances the extra heat developed in it by the increase in resistance due to the positive temperature coefficient of resistance of the wire.

(2) *Kohlrausch's Method*.—In the theory of this method, zero lateral loss of heat is assumed in an electrically heated rod. The ends which are at a potential difference of V volt are at approximately equal temperatures, θ_1 and θ_3 . The ratio of thermal to the electrical conductivity is given by

$$\lambda/\kappa = V^2/8 [\theta_2 - \frac{1}{2}(\theta_1 + \theta_3)],$$

where θ_2 is the temperature of the middle of the rod. In the application of this method by Jaeger and Diesselhorst§ the lateral loss of heat from the rod by convection and by radiation was eliminated by a lagging of cotton wool. By a calculation they showed that if the temperature of the surroundings was less than θ_2 by $\frac{1}{6}(\theta_2 + \frac{1}{2}\theta_1 + \theta_3)$ the effect of the lateral loss by conduction was approximately eliminated. With the high vacuum technique now available, a substance of the indefinite properties of cotton wool would not be used. A modification of this method for use between 20° and 373° K. based on a formula given by Diesselhorst|| was employed by Meissner¶ in 1915. Wire specimens were employed and the lateral loss of heat was made small by evacuating the nickel silver tube in which they were mounted.

(3) *Knudsen's Method*.—In this the ratio of the lateral to the longitudinal losses was made very small by using a short fine wire and a high vacuum.

Theory.

Verdet in 1872 was the first to suggest using the electrical method, and he obtained an expression for the distribution of temperature along an electrically heated wire subject to lateral loss of heat, equivalent to relation (3) below. As in Verdet's analysis we consider a straight uniform cylinder of length $2l$ cm., cross-section q cm.², perimeter p cm., and resistance ρ ohm cm.⁻¹, heated by a steady current of I amp. The ends of the wire are held at the same steady

* 'Ency. Brit.' (1929), vol. 11, p. 313, article "Heat" (§ 35).

† 'Ann. Physik,' vol. 1, p. 132 (1900).

‡ 'Ann. Physik,' vol. 34, p. 593 (1911); also S. Weber, 'Ann. Physik,' vol. 54, p. 165 (1917).

§ 'Wiss. Abh. Phys. Techn. Reichsanst.,' vol. 3, p. 269 (1900).

|| 'Z. Inst. Techn.,' vol. 22, p. 115 (1902).

¶ 'Ann. Physik,' vol. 47, p. 1001 (1915).

temperature as the walls of the tube in which it is mounted. Taking this temperature as an arbitrary zero, we have for the equation of heat flow in the wire

$$\lambda q \frac{d^3 \theta}{dx^3} = hp\theta - \frac{I^2 \rho}{J}, \quad (1)$$

where λ cal. cm.⁻¹ sec.⁻¹ deg.⁻¹ is the thermal conductivity; h is the loss of heat from the wire per square centimetre per second, when the temperature of the surface is one degree higher than that of the surrounding medium; θ is the temperature excess at any point x cm. from the middle of the wire, and J is the electrical equivalent of heat. The quantity h cal. cm.⁻² sec.⁻¹ deg.⁻¹ is complex.* Under the conditions of the experiments described below, the loss by conduction through and convection in the surrounding gas was small; h was mainly a small loss by radiation. This is discussed fully later.

If ρ_0 be the resistance per centimetre of the wire at 0° and α the temperature coefficient of resistance, then for a short range of temperature θ , $\rho = \rho_0(1 + \alpha\theta)$, and, substituting in (1) we get

$$\lambda q \frac{d^3 \theta}{dx^3} = hp\theta - \frac{I^2 \rho_0}{J} (1 + \alpha\theta). \quad (1A)$$

After setting $\mu^2 \equiv ph/\lambda q$; $k \equiv I^2 \rho_0/J\lambda q$; $\beta^2 \equiv k\alpha - \mu^2$, and $v \equiv \theta + k/\beta^2$ in succession, (1A) reduces to

$$\frac{d^2 v}{dx^2} + \beta^2 v = 0. \quad (2)$$

There are two forms of the solution of (2):

$$\text{and } \left. \begin{aligned} \theta + k/\beta^2 &= A \sin \beta x + B \cos \beta x & \text{if } k\alpha > \mu^2 \\ \theta + k/\beta^2 &= A \sinh \beta' x + B \cosh \beta' x & \text{if } k\alpha < \mu^2 \end{aligned} \right\}, \quad (3)$$

and A and B are arbitrary constants to be evaluated by means of the boundary conditions $x = \pm l$, $\theta = 0$.

The mean resistance \bar{R} of the wire is given by

$$\bar{R} = R_0 \frac{1}{2l} \int_{-l}^{+l} (1 + \alpha\theta) dx, \quad (4)$$

where $R_0 = 2\rho_0 l$.

* For a discussion of this see the papers of Smoluchowski, 'Wied. Ann.,' vol. 64, p. 101 (1898); and 'Ann. Physik,' vol. 35, p. 983 (1911); and Knudsen, *loc. cit.*

On evaluating A and B and using (4) we get

$$\text{and } \left. \begin{aligned} \frac{\bar{R} - R_0}{R_0} &= \frac{k\alpha}{\beta^2} \left(\frac{\tan \beta l}{\beta l} - 1 \right) \\ \frac{\bar{R} - R_0}{R_0} &= \frac{k\alpha}{\beta'^2} \left(1 - \frac{\tanh \beta' l}{\beta' l} \right) \end{aligned} \right\} \quad (5)$$

The last two equations can be written

$$\lambda = \frac{R_0^2 I_c^2 \alpha l}{2Jq(\bar{R} - R_0)} \cdot f, \quad (6)$$

where f is one or other of the expressions

$$\left(\frac{1}{\beta l} \right)^2 \left(\frac{\tan \beta l}{\beta l} - 1 \right) \quad \text{or} \quad \left(\frac{1}{\beta' l} \right)^2 \left(1 - \frac{\tanh \beta' l}{\beta' l} \right)$$

according as

$$k\alpha \geq \mu^2.$$

Relation (6) is true whether h be large or small. Callendar and Knudsen have given important special cases of it.

(1) *Callendar's Case*.—The lateral loss just equals the extra heat developed in the wire by the increase of resistance in it. This condition is complied with when $k\alpha = \mu^2$; equivalent to adjusting the current I to the critical value I_c given by

$$I_c^2 = 2Jphl/R_0\alpha.$$

In this case (6) reduces to

$$\lambda = R_0^2 I_c^2 \alpha l / 6Jq(\bar{R} - R_0). \quad (7)$$

If only a rough adjustment of the current to the critical value I_c is possible the following more accurate formula replaces (7)

$$\lambda = \frac{R_0^2 I_c^2 \alpha l}{6Jq(\bar{R} - R_0)} \left\{ 1 + \frac{2}{5} \left(\frac{\rho_0 I_c^2 \alpha}{J\lambda q} - \frac{ph}{q\lambda} \right) l^2 \right\}, \quad (8)$$

for $I = I_c$.

This condition that I must be approximately equal to the critical current, I_c , for relation (8) to hold, becomes less and less stringent, the smaller h is made. With wires of the dimensions used and with the heating currents employed, it may be dispensed with when h approximates to zero. In this case (8) simplifies to (9) below.

(2) *Knudsen's Case*.—The lateral loss is small compared to the longitudinal. For this case*

$$\lambda = \frac{\bar{R}R_0I^2\alpha l}{6Jq(\bar{R} - R_0)} \left(1 + \frac{R_0I^2\alpha l}{30J\lambda q} \right). \quad (9)$$

Possibility of Simultaneously determining λ and h .

It might be thought that relation (6) which is true for any steady conditions in the wire could be used to determine λ and h from a set of observations of \bar{R} and I . The electrical method would then become quite generally applicable, and no adjustment of the ratio of the lateral to the longitudinal loss of heat from the wire would be necessary. Relation (6) would be useful at elevated temperatures (100° to 500° C.) where the lateral loss of heat by radiation and by molecular conduction must be considerable.

The writer made a number of unsuccessful attempts to solve two equations of the type (6) for λ and h using a pair of corresponding values of \bar{R} and I as widely different as possible. It is, however, not feasible to heat the wire first by a small current and then by a current so large that the alteration in the value of the factor f in (6) is rendered sufficiently great to give a determinate solution of the problem. As the theory assumes both λ and h to be independent of the temperature, which is not the case, the allowable mean rise of temperature in the wire is small and was not greater than 20° in any of the writer's experiments. The magnitude of the largest current which can be used to heat the wire is thus limited by the permissible rise of temperature in it. The writer is also indebted to Professor T. M. Cherry, of this University, for suggesting an elegant mathematical determination of λ and h , using a set of observations of \bar{R} and I . This, also, failed to give a solution of the problem, as the degree of accuracy experimentally obtainable in the observations was not great enough.

Determination of λ at the Ice Point.

The same reasons that two equations of the type (6) cannot be solved for λ and h , also apply in respect to the solution of two equations of the type (8). It is therefore necessary to make a separate determination of the lateral heat losses in order to determine the thermal conductivity of an electrically heated wire. This is the writer's conclusion after many attempts to make a simultaneous determination of λ and h by using a range of heating currents.

In the experiments at the ice point to determine λ , the lateral loss of heat was made very small and an approximate value of h was obtained by the

* Weber, *loc. cit.*

calculation of the radiation loss from the surface of the wire. The lateral loss of heat was always so small that the effect of neglecting it entirely would introduce in λ an error of the order of 1 per cent. This correction was made by obtaining an uncorrected value λ' of λ from (8) by putting $h = 0$, and then multiplying λ' by the factor $(1 - \frac{2}{3}phl^2/q\lambda)$ to get λ . In calculating this factor the uncorrected value λ' may be substituted for λ .

Description of Conductivity Apparatus.

Mounting of Wires.—As the theory given above is applicable only when the temperature of the ends of the wire is the same as that of the walls of the tube in which it is mounted, it is important to construct, if possible, an apparatus in which this is realised. In the experiments of Knudsen and of Weber (*loc. cit.*) very thin short wires were necessary with the method of mounting the wires employed, and in Weber's work a small correction had to be applied as the temperature of the ends of the wire was slightly in excess of the temperature of the walls of the tube.

Several types of apparatus were designed in which no restrictions on the dimensions of the wires were imposed and consequently no "end" correction was necessary. In each of these the same principle was kept in view, namely, that of mounting the wire axially in a copper tube, and gold- or silver-soldering it through the thin copper cups with plane ends closing the tube and by some device providing for the electrical insulation of one end of the metal tube from the other.

In fig. 1 a section of an all-metal tube of copper is shown. It is 17.5 cm. long and constructed of $\frac{1}{4}$ -inch tubing, the end caps and walls being about 1 mm. thick. The tube was constructed in two portions, a flanged nickel steel sleeve being brazed to the open end of each part. One of the sleeves had a thread cut in it to engage a union nut by means of which the plane faces of the flanges could be screwed tightly together. To insulate the wire from the tube a thin washer *W* of mica or red fibre was inserted between the flanges and the mica washer *w* between the nut and the sleeve. Thick current leads *C* and *C* were soldered to the tube while the free ends of the wire itself were used for potential leads.

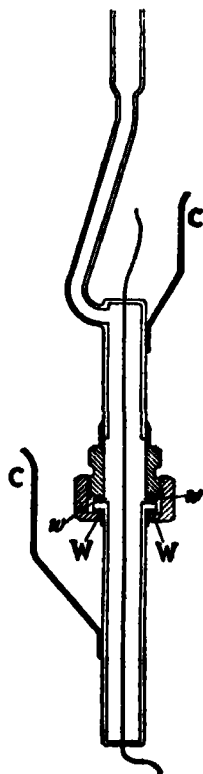


FIG. 1.

In this way a vacuum tight tube having an insulation resistance of several megohms was constructed. It was exceedingly robust and there were no "end corrections." A small disadvantage of this tube was that it had to be immersed in a tube containing oil to protect the insulation of the tube and not directly into an ice or a steam bath. Provision had to be made to stir the oil as well as the ice and water in which the tube containing the oil was immersed.

A mechanism driven by a small motor was used to move the glass tube containing the oil vertically up and down through a distance of a couple of inches, thus stirring both the oil and the ice and water simultaneously. By means of a copper-constantan couple it was shown that the oil and the ice water or steam were at the same temperature.

A section of a simpler tube of similar overall dimensions is shown in fig. 2. Copper-to-lead glass joints JJ are used in constructing this. The two portions of the copper tube were insulated from each other by the central section G of glass tube. This form of tube could be immersed directly in ice and water or in steam, and was used for molybdenum and tungsten wires. The vacuum properties proved to be quite satisfactory.



Fig. 2.

Measurements.

The determination of λ involves the measurement of the diameter and the length of the wire; the fixed electrical constants R_0 and α and a series of values of \bar{R} and I under steady conditions of temperature and pressure. All the electrical quantities were obtained by the potentiometer method using the three-dial pattern of the "thermokraftfrei" potentiometer made by Wolff (Berlin). A diagram of the circuit used is shown in fig. 3. The quantities \bar{R} and I were obtained by comparing the p.d. across the ends of the wire with that across a standard resistance of 0.01 ohm. A similar procedure gave R_0 when the current in the wire was a very small one and the tube was open to the atmosphere.

The value of α used was the mean for the range of temperature of the experiments. When the resistance is a linear function of the temperature which is very nearly the case in silver and in gold, the resistance was obtained at 0° and 100° C. and the value of α was $(R_{100} - R_0)/100R_0$. When the resistance is a quadratic function of the temperature, as in molybdenum and tungsten,

the mean value of α for the short range of temperature t was used, namely, $\alpha = (R_t - R_0)/R_0 t$. The value of α in the last formula was calculated from

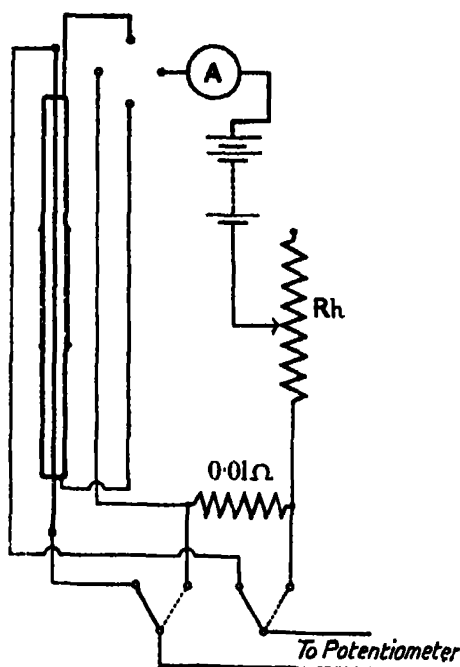


FIG. 3.

the quadratic formula $R_t = R_0 (1 + \alpha' t + \beta t^2)$ where α' and β were calculated from observations of the resistance at the three temperatures 0° , 100° C., and the boiling point of naphthalene, 217.96° C.

Metals Used.

The thermal conductivities of silver, gold, molybdenum and tungsten were obtained at 0° C., the tube being immersed in an ice bath. Two specimens of silver wire were employed, one, Ag I, being commercially pure electrolytic silver, and the other, Ag II, a wire drawn from a rod of spectroscopically pure silver. The latter proved to be the less pure, which can be attributed only to contamination during the process of drawing. For gold a wire by Heraeus containing 99.99 per cent. Au was used. Very pure molybdenum wire,*

* Some very pure monocrystal wires of tungsten of hexagonal section were also presented by the same firm, but unfortunately were broken to fragments in transit from Holland to Australia.

Mo I, was kindly presented by N. V. Philips Gloeilampenfabrieken te Eindhoven (Holland). A less pure wire, Mo II, by the General Electric Company (Schenectady) was also used. For tungsten a wire from the latter firm was used, but was relatively impure, and its electrical properties were not greatly improved by annealing at 1300° C.

Lateral Heat Loss by Molecular Conduction.

A good vacuum was obtained in the tube by pumping it out by means of a rotary oil pump, and simultaneously activating an attached charcoal tube by heating it to about 400° C. for 5 or 6 hours. The pump was then cut off and the charcoal tube immersed in liquid air.

The pressure obtained by the rotary oil pump alone was of the order 10^{-3} mm. Hg, and with the charcoal tube and liquid air was less than 10^{-4} mm. Hg, as no discharge whatever could be obtained in an attached tube with plane aluminium electrodes connected to an induction coil giving a p.d. of 60,000 volts.

It can readily be shown from a relation obtained by Knudsen (for which see Lorentz, 'Lectures on Theoretical Physics,' vol. 1, p. 144) that the loss of heat per cm.² per second from a wire at t° C. to a coaxial surrounding cylinder at the temperature 0° C., and which contains air at a pressure p dyne cm.⁻², is

$$W = 2.97 \cdot 10^{-6} \cdot p t.$$

This gives for the part h_s of h due to molecular conduction

$$h_s < 3.9 \times 10^{-7} \text{ cal. cm.}^{-2} \text{ sec.}^{-1} \text{ deg.}^{-1}$$

for air at 273° K. at a pressure of 10^{-4} mm. of mercury.

Lateral Heat Loss by Radiation.

The problem of radiation from metal surfaces is treated in detail in a valuable article by Lax and Pirani.* The radiation per cm.² per second from a metal surface is

$$S = l_s \sigma T^4,$$

where σ is Stefan's constant, T the absolute temperature, and l_s the emissive power of the metal surface. From the above fourth power law it follows that the part h_R of h due to radiation is given by

$$h_R = 4 l_s \sigma T^3.$$

* See Geiger-Scheel, 'Handb. Physik.,' vol. 21, p. 190, article "Temperatur Strahlung fester Körper."

The value of l_e for a given metal was obtained from the experimental curves in the above article representing l_e as a function of the wave-length. The value of l_e used was that corresponding to a wave-length of 100×10^{-5} cm. which is the position of the energy maximum given by the Wien Displacement Law for the temperature 273° K. The following are the values of l_e from the curves, and the corresponding values of h_R at 273° K.

Metal.	Silver.	Gold.	Tungsten.	Molybdenum.
l_e	0.013	0.02	0.035	0.03*
h_R	1.4	2.2	3.9	3.3

* Calculated from the electrical conductivity.

The loss of heat by molecular conduction being of the order 1/10 that by radiation, h_e was neglected. As the correction to λ on account of heat losses is of the order 1 per cent. only, we may put $h = h_R$ without appreciably affecting λ .

To obtain λ , the uncorrected value λ' calculated from (8) by putting $h = 0$ is multiplied by the factor

$$\left(1 - \frac{2}{3} \frac{ph}{q\lambda} l^2\right) \equiv \lambda/\lambda'.$$

In Tables I, II, III and IV are given details of the geometrical, the electrical constants, the value of λ/λ' , and the corrected values of λ for the different wires used at the mean temperature θ° C. of the wire.

Table I.—Silver.

Ag I: $R_0 = 0.0124430$ ohm; $\alpha = 0.004060$; $2l = 17.63$ cm.;
diameter = 0.05286 cm.; $\lambda/\lambda' = 0.997$.

I amp.	2.17398	2.49238	2.80819
λ cal. cm. ⁻¹ sec. ⁻¹ deg. ⁻¹ ..	0.981	0.980	0.981
θ° C.	10.0	13.4	17.2

$\lambda_{\text{mean}} = 0.981$ cal. cm.⁻¹ sec.⁻¹ deg.⁻¹ at 0° C.

Ag II: $R_0 = 0.0141917$ ohm; $\alpha = 0.003967$; $2l = 17.47$ cm.;
diameter = 0.05059 cm.; $\lambda/\lambda' = 0.996$.

I amp.	1.37840	1.50114	1.81606	2.02648
λ cal. cm. ⁻¹ sec. ⁻¹ deg. ⁻¹	0.984	0.983	0.985	0.985
θ° C.	5.01	5.85	8.65	10.80

$\lambda_{\text{mean}} = 0.984$ cal. cm.⁻¹ sec.⁻¹ deg.⁻¹ at 0° C.

Table II.—Gold.

$R_0 = 0.00856311$ ohm; $\alpha = 0.003958$; $2l = 20.12$ cm.;
diameter = 0.07960 cm.; $\lambda/\lambda' = 0.994$.

I amp.	2.34962	2.58390	3.73953	4.37903
λ cal. cm. ⁻¹ sec. ⁻¹ deg. ⁻¹ .	0.733	0.730	0.731	0.733
θ° C.	5.28	6.44	13.86	18.40

$$\lambda_{\text{mean}} = 0.732 \text{ cal. cm.}^{-1} \text{ sec.}^{-1} \text{ deg.}^{-1} \text{ at } 0^\circ \text{ C.}$$

Table III.—Molybdenum.

Mo I annealed at 220° C.:

$$R_0 = 0.0128865 \text{ ohm}; \quad R = R_0 (1 + 0.004497t + 0.0^5 132t^2)$$

[0° — 220° C.];

$\alpha_{0-10^\circ} = 0.004510$; $2l = 19.83$ cm.; diameter = 0.09983 cm.; $\lambda/\lambda' = 0.984$.

I amp.	1.32137	1.48560	1.59288	1.78510	2.13786
λ cal. cm. ⁻¹ sec. ⁻¹ deg. ⁻¹ .	0.3323	0.3337	0.3323	0.3348	0.3336
θ° C.	3.45	4.34	5.06	6.34	9.28

$$\lambda_{\text{mean}} = 0.333, \text{ cal. cm.}^{-1} \text{ sec.}^{-1} \text{ deg.}^{-1} \text{ at } 0^\circ \text{ C.}$$

Mo I annealed at 900° C.:

$$R_0 = 0.0128585 \text{ ohm}; \quad R = R_0 (1 + 0.004557t + 0.0^5 107t^2)$$

[0° — 220° C.];

$\alpha_{0-10^\circ} = 0.004568$; $2l = 19.83$ cm.; diameter = 0.09983 cm.; $\lambda/\lambda' = 0.984$.

I amp.	1.55098	1.89013	2.11695	2.27679	1.47252*	1.68255*
λ cal. cm. ⁻¹ sec. ⁻¹ deg. ⁻¹ .	0.3433	0.3430	0.3436	0.3422	0.3430	0.3420
θ° C.	4.59	6.90	8.76	10.20	4.13	5.42

$$\lambda_{\text{mean}} = 0.343 \text{ cal. cm.}^{-1} \text{ sec.}^{-1} \text{ deg.}^{-1} \text{ at } 0^\circ \text{ C.}$$

* Repeated readings.

Mo II annealed at 220° C.:

$$R_0 = 0.0131148 \text{ ohm}; \quad R = R_0 (1 + 0.003990t + 0.0^5 125t^2)$$

[0° — 220° C.];

$\alpha_{0-10^\circ} = 0.004003$; $2l = 20.28$ cm.; diameter = 0.1069 cm.; $\lambda/\lambda' = 0.984$.

I amp.	1.44479	1.79831	1.92596	2.16117
λ cal. cm. ⁻¹ sec. ⁻¹ deg. ⁻¹ .	0.3153	0.3170	0.3164	0.3182
θ° C.	3.92	6.08	7.05	8.96

$$\lambda_{\text{mean}} = 0.316 \text{ cal. cm.}^{-1} \text{ sec.}^{-1} \text{ deg.}^{-1} \text{ at } 0^\circ \text{ C.}$$

Table IV.—Tungsten.

Annealed at 220° C.:

$$R_0 = 0.0128316 \text{ ohm}; \quad R = R_0(1 + 0.003878t + 0.0^5 109t^3) \\ [0^\circ\text{--}220^\circ \text{ C.}];$$

$$\alpha_{0-10^\circ} = 0.003889; \quad 2l = 17.63 \text{ cm.}; \quad \text{diameter} = 0.1022 \text{ cm.}; \quad \lambda/\lambda' = 0.988.$$

I amp.	1.39506	1.71087	1.84928	2.21305
λ cal. cm. ⁻¹ sec. ⁻¹ deg. ⁻¹ ..	0.3919	0.3933	0.3908	0.3937
° C. ...	2.73	4.12	4.82	7.03

$$\lambda_{\text{mean}} = 0.393 \text{ cal. cm.}^{-1} \text{ sec.}^{-1} \text{ deg.}^{-1} \text{ at } 0^\circ \text{ C.}$$

Annealed at 1300° C.:

$$R_0 = 0.0137647 \text{ ohm}; \quad R = R_0(1 + 0.004143t + 0.0^6 63t^3) \\ [0^\circ\text{--}220^\circ \text{ C.}]$$

$$\alpha_{0-10^\circ} = 0.004150; \quad 2l = 19.96 \text{ cm.}; \quad \text{diameter} = 0.1022 \text{ cm.}; \quad \lambda/\lambda' = 0.985.$$

I amp.	1.35045	1.49799	1.82122	2.31653	2.68107	1.28889*	1.56864*
λ cal. cm. ⁻¹ sec. ⁻¹ deg. ⁻¹ ..	0.3956	0.3949	0.3938	0.3918	0.3919	0.3957	0.3955
° C.	3.15	3.83	5.77	9.52	12.85	2.80	4.17

$$\lambda^\dagger = 0.397 \text{ cal. cm.}^{-1} \text{ sec.}^{-1} \text{ deg.}^{-1} \text{ at } 0^\circ \text{ C.}$$

* Repeated readings.

† Slightly extrapolated.

The Lorenz Coefficient.

As the resistance and the dimensions of the wires are known, the electrical conductivity κ ohm⁻¹ cm.⁻¹ can be obtained, and thence also the quantity $\lambda/\kappa T$, known as the Lorenz coefficient, T being the absolute temperature. The experimental values of κ , λ , and $\lambda/\kappa T$ for $T = 273^\circ \text{ K.}$ obtained in this investigation are given in Table V.

Table V.

Metal.	κ ohm ⁻¹ cm. ⁻¹ .	λ watt cm. ⁻¹ deg. ⁻¹ .	$\lambda/\kappa T$ watt ohm deg. ⁻¹ .
Ag I ..	64.6×10^4	4.10	2.32×10^{-4}
Ag II ..	61.2	4.03	2.41
Au ..	47.0	3.06	2.39
Mo I*	19.6	1.39	2.60
Mo I†	19.7	1.43	2.67
Mo II*	17.2	1.32	2.81
W*	16.7	1.64	3.58
W†	17.7	1.66	3.44

* Annealed at 220° C.

† Annealed at 900° C.

‡ Annealed at 1300° C.

Matthiessen's Rule.

It has been shown by Geiss and van Liempt* that the metals molybdenum, tungsten, and their alloy system Mo—W obey Matthiessen's rule which states that the product of the specific resistance σ , at a given temperature and the temperature coefficient, α , of the resistance is a constant. In Table VI are given five values of $\sigma_{18} \times \alpha_{0-100}$ obtained for the tungsten and the molybdenum employed in this work.

Table VI.

Metal.	σ_{18} , ohm cm.	α_{0-100}	$\sigma_{18} \times \alpha_{0-100}$
W*	6.39×10^{-4}	0.003987	254.7×10^{-10}
W†	6.07 ₈	4206	255.5
Mo I*	5.50 ₈	4629	254.8
Mo I†	5.50	4664	256.6
Mo II*	6.22	4115	255.9
		Mean	255.5×10^{-10}

* Annealed at 220° C.

† Annealed at 900° C.

‡ Annealed at 1300° C.

A more exact test of the above rule can be made by replacing the average value of α (e.g., α_{0-100} used in Table VI) by the actual value of α at 0° C. (say), and multiplying it by σ_0 . It was found on calculating the products $\sigma_0 \alpha_0$, that the mean departure of $\sigma_0 \alpha_0$ from the mean value was appreciably greater than that of $\sigma_{18} \times \alpha_{0-100}$ of Table VI.

Discussion of Results.

Comparatively few determinations of the thermal conductivity at room temperature of the four metals studied in this paper have been made. A summary of the available data is given below in Table VII, the values of both λ and $\lambda/\kappa T$ being for the temperature T° K. quoted.

* 'Z. Metallkunde,' vol. 17, p. 194 (1925).

Table VII.

Metal.	α_0-100°	λ cal. cm. ⁻¹ sec. ⁻¹ deg. ⁻¹	$\lambda/\kappa T$ watt ohm deg. ⁻²	T° K.	Authority.
Silver	0.00410	0.981	2.32×10^{-8}	273	Author.
Silver (99.98 per cent.)	400	1.006	2.36	291	Jaeger and Diesselhorst.*
Silver (99.90 per cent.)	—	0.974	2.33	291	Loes.†
Gold (99.999 per cent.)	400	0.744	2.35	273	Meissner.‡
Gold (99.99 per cent.)	396	0.732	2.39	273	Author.
Gold	368	0.700	2.43	291	Jaeger and Diesselhorst.*
Gold	356	0.705	2.45	290	Barratt and Winter.§
Molybdenum	467	0.346	3.08	290	Barratt and Winter.§
Molybdenum	466	0.343	2.67	273	Author.
Tungsten	464¶	0.383	2.88	273	S. Weber.
Tungsten	453	0.476	3.79	290	Barratt and Winter.§
Tungsten	415	0.397	3.44	273	Author.

* Jaeger and Diesselhorst, *loc. cit.*

† 'Phil. Trans.,' A, vol. 208, p. 381 (1908).

‡ Meissner, *loc. cit.*

§ 'Proc. Phys. Soc.,' London, vol. 26, p. 347 (1913-14).

|| Weber, *loc. cit.*

¶ α_0-100° .

As any impurities present always depress the thermal conductivity of a metal, the degree of purity where it was specified by the investigator has been included in the table. The writer has also stated the temperature coefficient of the resistance, as it is possibly the best available measure of the amount of the effective impurity present. Taking α as the criterion of purity, the metals are given in descending order of purity. The writer's value of λ for gold accords better with that of Meissner than with the values obtained by Jaeger and Diesselhorst and by Barratt and Winter, the specimens of the latter investigations being less pure than those of the former. The commonly accepted value of the thermal conductivity of gold at 18° C., that of Jaeger and Diesselhorst, is probably 4 to 5 per cent. too low. While the two values of λ for molybdenum are in very fair agreement, those of tungsten are entirely discordant. The value $\lambda = 0.383$ at 273° K. obtained by S. Weber might appear to be the most probable, as the value of $\lambda/\kappa T$ corresponding to it is much the nearest to the theoretical value of this quantity. On the other hand the writer does not think his value of $\lambda = 0.397$ at 273° K. for impure tungsten can be subject to experimental error of more than 2 per cent.; if that is the case, Weber's value is in error. The thermal conductivity of pure tungsten is thus a matter for further experimental investigation. It is to be noticed also that the silver

wire used by the writer is purer than the silver used by Jaeger and Diesselhorst, but has a conductivity 2 per cent. less.

The theoretical value of the Lorenz coefficient deduced from the Sommerfeld-Fermi theory of conduction is $\lambda/\kappa T = 2.43 \times 10^{-8}$ watt ohm deg.⁻². The experimental values of $\lambda/\kappa T$ for 273° K. lie between 2.3 and 2.6×10^{-8} for the metals excluding iron, bismuth, antimony, molybdenum, and tungsten. It appears to have been accepted by some writers that the Lorenz coefficient is the same for alloys as for pure metals. The values of $\lambda/\kappa T$ in Table V do not bear this out, as the Lorenz coefficients for metals containing a small amount of impurity (*e.g.*, tungsten and molybdenum in Table V) are much greater than for pure metals. As it is now possible to obtain both tungsten* and molybdenum in a state of great purity, the possibility of these metals being real exceptions to Lorenz's rule is a matter for further experiment. The value of 2.67×10^{-8} for $\lambda/\kappa T$ at 273° K. for pure molybdenum obtained by the writer is roughly an upper limit of the range of values of $\lambda/\kappa T$ hitherto obtained for pure metals. It may be noted that the much higher value of 3.08×10^{-8} for $\lambda/\kappa T$ at 290° K. obtained by Barratt and Winter may be due to an error in the measurement of κ or of α , as with their values of these quantities Matthiessen's rule is not satisfied. The data given by them appears to make $\sigma_{18} \times \alpha_{0-100} \doteq 2.9 \times 10^{-10}$, which does not agree with the constant value of 2.55×10^{-10} obtained by the writer.

The author desires to acknowledge his indebtedness to Professor T. H. Laby, M.A., Sc.D., for many helpful suggestions, for the design of the all-metal tube used in the investigation, as well as for his continued interest in the work. The molybdenum and the tungsten wires used were kindly presented by the N. V. Philips Gloeilampenfabrieken te Eindhoven (Holland) and by the General Electric Company of Schenectady.

A research scholarship by the University of Melbourne, and a grant by the Commonwealth Council of Scientific and Industrial Research made it possible to carry out the work.

Summary.

An electrical method of determining the thermal conductivity, λ , of some metals in wire form is described and the theory is discussed. The method is applicable provided that the ratio of the lateral to the longitudinal heat loss

* See note p. 327.

from the wire is made small. When this ratio is not small, λ cannot be determined unless the surface emissivity, h , be known independently.

A simple form of conductivity apparatus was used, and although long thick wires were mounted in it, no "end" corrections were necessary. A small lateral loss of heat by radiation which involved a correction in λ of the order of 1 per cent. was allowed for by calculation.

The thermal conductivity, λ , the electrical conductivity, κ , and the Lorenz coefficient, $\lambda/\kappa T$, T being the temperature in degree K., are given in Table V, p. 331, of this paper for silver, gold, molybdenum and tungsten.

Material and Radiational Waves.

By A. M. MOSHARRAFA, Ph.D., D.Sc., Professor of Applied Mathematics in the Egyptian University, Cairo.

(Communicated by O. W. Richardson, F.R.S.—Received January 26, 1931.)

§ 1. In what follows the Maxwellian equations of electromagnetic and electron theory are derived from one set of basic relations, in a manner which throws some light on the relationship between material and radiational waves, and accounts for the existence of exactly three types of physical entities, namely, positive electricity, negative electricity, and radiation. We assume the existence of two vectors \mathbf{A} and \mathbf{n} and of a scalar quantity θ and identify \mathbf{n} with a unit normal to the wave surface associated with the observable entity (whether material or radiational), and θ with the normal speed of propagation of the surface, so that

$$\theta \mathbf{n} = \frac{d\mathbf{n}}{dt}. \quad (1)$$

If E_1, E_2, E_3 are the components of the electric vector \mathbf{E} in a Cartesian system of co-ordinates (x_1, x_2, x_3) the set of relations from which all equations are derivable may be written

$$\left. \begin{aligned} \frac{\partial E_\mu}{\partial x_\nu} &= \cos(n x_\nu) A_\mu, & \mu, \nu &= 1, 2, 3 \\ \frac{\partial E_\mu}{\partial t} &= \theta A_\mu, & \mu &= 1, 2, 3 \end{aligned} \right\}, \quad (2)$$

where $\cos (nx_r)$ stands for the cosine of the angle between \mathbf{n} and the axis of x_r .

§ 2. First, let it be supposed that the vector \mathbf{A} is normal to the wave surface so that

$$\mathbf{A} = \pm |\mathbf{A}| \mathbf{n}, \quad (3)$$

where $|\mathbf{A}|$ is the absolute value of \mathbf{A} , the positive or negative sign to be taken according as \mathbf{A} and \mathbf{n} are in the same or in opposite directions. We then have from (2)

$$\operatorname{div} \mathbf{E} = \rho, \quad (4)$$

where

$$\rho = \pm |\mathbf{A}|. \quad (5)$$

We identify ρ with the electric density. Further from (2) we get

$$\begin{aligned} \frac{\partial E_3}{\partial x_2} - \frac{\partial E_2}{\partial x_3} &= A_3 \cos (nx_2) - A_2 \cos (nx_3) \\ &= \pm [\cos (nx_2) \cos (nx_2) - \cos (nx_2) \cos (nx_2)] |\mathbf{A}| \\ &= 0, \end{aligned}$$

and similarly for the other two components of $\operatorname{curl} \mathbf{E}$, so that

$$\operatorname{curl} \mathbf{E} = 0. \quad (6)$$

Again from (2) we have

$$\frac{\partial \mathbf{E}}{\partial t} = \theta \mathbf{A},$$

which, on account of (1), (3) and (5) may be written

$$\frac{\partial \mathbf{E}}{\partial t} + \rho \mathbf{V} = 0, \quad (7)$$

where

$$\mathbf{V} = -\theta \mathbf{n} = -\frac{d\mathbf{n}}{dt}, \quad (8)$$

and we identify \mathbf{V} with the velocity of the charge. From (7) we get, on operating with div and using (4)

$$\frac{\partial \rho}{\partial t} + \operatorname{div} (\rho \mathbf{V}) = 0. \quad (9)$$

§ 3. Next, let it be supposed that \mathbf{A} is tangential to the wave surface so that

$$\sum_1^3 A_\mu \cos (nx_\mu) = 0, \quad (10)$$

we then have from (2)

$$\operatorname{div} \mathbf{E} = 0, \quad (11)$$

denoting the absence of electric charge. Further we get

$$\frac{\partial E_1}{\partial x_2} - \frac{\partial E_2}{\partial x_1} = [\cos(Ax_3) \cos(nx_3) - \cos(Ax_2) \cos(nx_3)] |A|,$$

with two similar equations for the other two components of curl E . Let n' be a unit vector perpendicular both to n and to A . It is seen that

$$\text{curl } E = |A| n'$$

so that if we define a vector H by means of the equation

$$n' |A| = -\frac{1}{c} \frac{\partial H}{\partial t}, \quad (12)$$

where c is the fundamental velocity, we have

$$\text{curl } E = -\frac{1}{c} \frac{\partial H}{\partial t}. \quad (13)$$

We identify H with the magnetic vector. Operating on both sides of (13) with the operator curl, we have

$$\text{curl curl } E = -\frac{1}{c} \frac{\partial}{\partial t} (\text{curl } H),$$

or since

$$\text{curl curl } E \equiv \text{grad div } E - \nabla^2 E$$

we obtain an account of (11)

$$\nabla^2 E = \frac{1}{c} \frac{\partial}{\partial t} (\text{curl } H),$$

hence substituting from (2) we have for the x_1 components

$$\begin{aligned} & \left[\cos(nx_1) \frac{\partial}{\partial x_1} + \cos(nx_2) \frac{\partial}{\partial x_2} + \cos(nx_3) \frac{\partial}{\partial x_3} \right] A_1 \\ & + A_1 \left[\frac{\partial \cos(nx_1)}{\partial x_1} + \frac{\partial \cos(nx_2)}{\partial x_2} + \frac{\partial \cos(nx_3)}{\partial x_3} \right] = \frac{1}{c} \frac{\partial}{\partial t} [\text{curl } H]_1, \end{aligned} \quad (14)$$

if now we suppose the vector n to be solenoidal so that

$$\frac{\partial \cos(nx_1)}{\partial x_1} + \frac{\partial \cos(nx_2)}{\partial x_2} + \frac{\partial \cos(nx_3)}{\partial x_3} \equiv \text{div } n = 0, \quad (15)$$

we may write

$$\frac{dA}{dn} = \frac{1}{c} \frac{\partial}{\partial t} (\text{curl } H),$$

which on introducing the speed $\theta = dn/dt$ gives

$$\frac{\partial A}{\partial t} = \frac{\theta}{c} \frac{\partial}{\partial t} (\text{curl } H). \quad (16)$$

If now we put

$$\theta = \pm c \quad (17)$$

we get from (2)

$$\frac{\partial \mathbf{A}}{\partial t} = \frac{1}{\theta} \frac{\partial^2 \mathbf{E}}{\partial t^2},$$

which in conjunction with (16) and (17) yields

$$\frac{\partial \mathbf{E}}{\partial t} = c \operatorname{curl} \mathbf{H}. \quad (18)$$

§ 4. Equations (4), (6), (7) and (9) are seen to be the Maxwellian equations in the absence of radiation,* whereas equations (11), (13) and (18) are the equations in the absence of charge. The first set is obtained on the assumption that the vector \mathbf{A} is longitudinal and the velocity dn/dt of wave propagation variable and equal to minus the velocity of the charge, the second set is obtained on the assumption that \mathbf{A} is transverse and dn/dt constant and equal to the fundamental velocity. Thus a material entity is associated with the propagation of a longitudinal vector, whereas a radiational entity is associated with the propagation of a transverse vector. Since a longitudinal vector may have either of two directions of opposite signs, we have exactly two types of material entities, namely, positive and negative electricity. Radiation corresponds to a mid-way position, so to speak, between positive and negative electricity.

§ 5. In the general case, the vector \mathbf{A} will possess a longitudinal and a transverse component, corresponding to the existence of matter and radiation. If we assume the longitudinal component to be propagated with a variable speed $-v$, and the transverse component with a constant speed c , so that θ is given one or the other of these two values according as it is associated with the one type of component or with the other, the Maxwellian equations may now be obtained in their general form

$$\begin{aligned} \operatorname{div} \mathbf{E} &= \rho & (i) \\ c \operatorname{curl} \mathbf{E} &= -\frac{\partial \mathbf{H}}{\partial t} & (ii) \\ c \operatorname{curl} \mathbf{H} &= \frac{\partial \mathbf{E}}{\partial t} + \rho \mathbf{V} & (iii) \\ \frac{\partial \rho}{\partial t} + \operatorname{div} (\rho \mathbf{V}) &= 0 & (iv) \end{aligned} \quad \left. \begin{array}{l} \\ \\ \end{array} \right\} \quad (20)$$

* All radiation is characterised by the existence of a magnetic vector. A so-called "steady" electromagnetic field is an idealistic conception of a limiting form of radiation, namely, when the frequency is supposed to be vanishingly small.

Of these (i) and (ii) follow as in (4) and (13) above, (iii) is obtained from (ii) by operating with curl as in deriving (18) above, but with $\text{div } \mathbf{E} = \rho$ instead of 0, and (iv) follows from (iii) on operating with div.

Summary.

The Maxwellian equations of electromagnetic and electric theory are derived from one set of basic relations, in a manner which throws some light on the relationship between material and radiational waves, and accounts for the existence of exactly three types of physical entities, namely, positive electricity, negative electricity and radiation. It is shown that a physical entity may be associated with the propagation of a vector \mathbf{A} in a direction \mathbf{n} . If \mathbf{A} and \mathbf{n} are in the same direction, the entity is recognised as positive electricity, if in opposite directions as negative electricity, and if mutually perpendicular as radiation. In the general case \mathbf{A} will have a longitudinal and a transverse component corresponding to the existence of matter and radiation.

The Chemical Constant of Chlorine Vapour and the Entropy of Crystalline Chlorine.

By T. E. STERN, Trinity College, Cambridge.

(Communicated by R. H. Fowler, F.R.S.—Received February 24, 1931.)

Introduction.

In a recent paper* the writer calculated the vapour pressure of hydrogen crystals, using the Einstein-Bose statistics for the gaseous phase. The work was an extension of that of R. H. Fowler,† who had used the slightly less accurate classical statistics for the hydrogen gas.

In this paper we propose to apply similar methods of investigation to chlorine. The investigation will have to be different in some respects, however. Hydrogen was considered to consist of a mixture of two gases, para- and ortho-hydrogen, which retained their individuality over long periods of time at low temperatures. Due to the existence of two isotopes of chlorine, we shall here have five gases to consider instead of two. Further, hydrogen molecules almost

* 'Proc. Roy. Soc.,' A, vol. 130, p. 367 (1931).

† 'Proc. Roy. Soc.,' A, vol. 118, p. 52 (1928).

certainly can rotate quite freely in the crystals of hydrogen; on the other hand, molecules of chlorine almost certainly can not rotate at all in crystals of chlorine.

We shall consider chlorine at ordinary temperatures to consist of three sorts of molecules, namely, $\text{Cl}_{35}\text{Cl}_{35}$, $\text{Cl}_{35}\text{Cl}_{37}$, and $\text{Cl}_{37}\text{Cl}_{37}$; which we shall denote respectively by A, B, and C. The work of Elliott* on the absorption band spectrum of chlorine makes it seem extremely likely that the Cl_{35} nucleus has a $5/2$ quantum spin. Elliott was unable to determine the magnitude of the nuclear spin of Cl_{37} . In any case, however, we would expect chlorine A and C at ordinary temperatures to consist of two sorts of chlorine: para-chlorine molecules represented by wave functions with even rotational quantum numbers and antisymmetric in the nuclear spins, and ortho-chlorine molecules with wave functions with odd rotational quantum numbers and symmetric in the nuclear spins. The normal state of a chlorine molecule is a $^1\Sigma$. If the $5/2$ quantum spin for Cl_{35} is correct, then there will be 15 pairs of simultaneous eigenvalues of the resultant nuclear angular momentum and of the z component of this, in the case of para-chlorine A molecules; and 21 pairs in the case of ortho-chlorine A molecules. At ordinary temperatures we would therefore expect para- and ortho-chlorine A molecules to exist in chlorine gas in the ratio of 5 : 7.

Before we investigate the vapour pressure of chlorine, we shall investigate by statistical mechanics the composition of chlorine gas—the relative numbers of molecules of the different sorts present in the ordinary gas. This has never been measured experimentally; from the atomic weight of chlorine we can obtain directly merely the relative numbers of atoms of the two isotopes. It is necessary to use statistical methods to calculate, from this ratio, the proportions between the molecules of sorts A, B and C. We shall perform this calculation rigorously, using the Einstein-Bose statistics; and our results will be found to differ only trivially from the results obtained by the simple assumption that any atom of chlorine is equally likely to combine with any other atom present to form a molecule of chlorine. But our investigation will show that the composition of chlorine is independent of the magnitudes of the nuclear spins.

In calculating the vapour pressure of chlorine crystals we shall carry through the analysis in a general fashion applicable not only to chlorine but also to other diatomic homopolar gases which may consist of two or more isotopes. We denote the nuclear angular momentum of Cl_{35} (sort 1) by $n_1\hbar/2\pi$, and that

* 'Proc. Roy. Soc.,' A, vol. 130, p. 638 (1930).

of Cl_{27} (sort 2) by $n_2 k/2\pi$, where k is Planck's constant. We shall find that the values of n_1 and n_2 are without effect on the vapour pressure; and we shall obtain a value for the chemical constant of chlorine vapour in satisfactory agreement with experiment.

Finally, we shall calculate by statistical mechanics the entropy of crystalline chlorine at the absolute zero of temperature. Here n_1 and n_2 are important.

§ 1. *The Statistical Mechanics of Assemblies containing Free Atoms of Types X_1 and X_2 , and Molecules of Types Para- X_1X_1 , Ortho- X_1X_1 , X_1X_2 , Para- X_2X_2 , and Ortho- X_2X_2 .*

The wave function of the entire assembly must be symmetrical in any two similar particles. There are in all seven types of particles present. We denote the total number of atoms in the assembly of sorts X_1 and X_2 by X_1 and X_2 respectively. The numbers of free atoms of these sorts we denote by M_1 and M_2 respectively. The numbers of molecules of sorts para- X_1X_1 , ortho- X_1X_1 , X_1X_2 , para- X_2X_2 , and ortho- X_2X_2 present in the assembly we denote by N_1 , N_2 , N_3 , N_4 and N_5 respectively. We assume that the reader is familiar with the methods of enumerating wave functions developed by Fowler in his "Statistical Mechanics."* We denote the five sorts of molecules enumerated above by the numbers 1, 2, 3, 4, and 5 respectively; we denote the two sorts of atoms by 1 and 2. If the total energy of the molecules of type 1 is E_1 , then these molecules contribute to the total number of linearly independent wave functions capable of describing the entire assembly a factor equal to the coefficient of $x_1^{2N_1} z^{E_1}$ in $\Pi 1/(1 - x_1^2 z^{e_1})$. Here the e_1 's are the energy levels of a molecule of sort 1. The product is taken over all the energy levels, with as many factors for any degenerate level as there are linearly independent wave functions which represent it. Similarly, the molecules of sort 2 if their total energy is E_2 contribute a factor equal to the coefficient of $x_1^{2N_2} z^{E_2}$ in $\Pi 1/(1 - x_1^2 z^{e_2})$. The molecules of sort 3, if their total energy is E_3 , contribute a factor equal to the coefficient of $(x_1 x_2)^{N_3} z^{E_3}$ in $\Pi 1/(1 - x_1 x_2 z^{e_3})$. Those of sort 4, if their total energy is E_4 , contribute a factor equal to the coefficient of $x_2^{2N_4} z^{E_4}$ in $\Pi 1/(1 - x_2^2 z^{e_4})$. Those of sort 5, if their total energy is E_5 , contribute a factor equal to the coefficient of $x_2^{2N_5} z^{E_5}$ in $\Pi 1/(1 - x_2^2 z^{e_5})$. Finally, the free atoms of sort 1, if their total energy is E_1' , contribute a factor equal to the coefficient of $x_1^{M_1} z^{E_1'}$ in $\Pi 1/(1 - x_1 z^{e_1'})$.

* Chapter 21.

And the free atoms of sort 2, if their total energy is E_2' , contribute a factor equal to the coefficient of $x_2^{M_2} z^{E_2'}$ in $\Pi 1/(1 - x_2 z^{E_2'})$.

If the total energy of the assembly is E , we must have

$$E = \sum_1^5 E_r + \sum_1^2 E_r',$$

and also

$$X_1 = 2N_1 + 2N_2 + N_3 + M_1,$$

$$X_2 = 2N_4 + 2N_5 + N_3 + M_2.$$

Thus the total number of linearly independent wave functions capable of representing the entire assembly of energy E , corresponding to all possible partitions of the X_1 atoms of sort 1 and the X_2 atoms of sort 2 among the different sorts of particles, is equal to the coefficient of $x_1^{X_1} x_2^{X_2} z^E$ in the product of all of the Π 's. Hence this number W is given by

$$W = \left(\frac{1}{2\pi i}\right)^3 \iiint \frac{dx_1 dx_2 dz}{x_1^{X_1+1} x_2^{X_2+1} z^{E+1}} \Pi_1 \Pi_2 \dots \Pi_5 \Pi_1' \Pi_2',$$

where the Π_1, Π_2 , etc., are the seven Π 's of this discussion.

A slight extension of the usual arguments* leads to the following mean values of N_1, N_2, N_3, N_4 and N_5 :

$$\left. \begin{aligned} \bar{N}_1 &= -\xi_1^2 \frac{\partial}{\partial \xi_1^2} \sum_i \log(1 - \xi_1^2 \theta^{1'i}) \\ \bar{N}_2 &= -\xi_1^2 \frac{\partial}{\partial \xi_1^2} \sum_r \log(1 - \xi_1^2 \theta^{2'r'}) \\ \bar{N}_3 &= -\xi_1 \xi_2 \frac{\partial}{\partial (\xi_1 \xi_2)} \sum (1 - \xi_1 \xi_2 \theta^{3'i}) \\ \bar{N}_4 &= -\xi_2^2 \frac{\partial}{\partial \xi_2^2} \sum_i (1 - \xi_2^2 \theta^{4'i}) \\ \bar{N}_5 &= -\xi_2^2 \frac{\partial}{\partial \xi_2^2} \sum_{r'} (1 - \xi_2^2 \theta^{5'r'}) \end{aligned} \right\} \quad (1.0)$$

Here the parameters ξ_1, ξ_2 and $\theta (= \exp[-1/kT])$ corresponding to the partial potentials and to the temperature, are determined by the unique position of the saddle-point of the integrand of W , given by the vanishing of its three partial differential coefficients.

If we now set

$$N_1 + N_2 = N_A, \quad N_3 = N_B, \quad N_4 + N_5 = N_C,$$

* Fowler, *loc. cit.*, p. 532.

so that A, B and C denote the three types of molecules without regard to the symmetry properties of their wave functions, we have

$$\begin{aligned}\bar{N}_A &= -\xi_1^2 \frac{\partial}{\partial \xi_1^2} \left[\sum_i \log (1 - \xi_1^2 \theta^{1'i}) + \sum_i' \log (1 - \xi_1^2 \theta^{2'i}) \right] \\ \bar{N}_B &= -\xi_1 \xi_2 \frac{\partial}{\partial (\xi_1 \xi_2)} \sum_i \log (1 - \xi_1 \xi_2 \theta^{3'i}) \\ \bar{N}_C &= -\xi_2^2 \frac{\partial}{\partial \xi_2^2} \left[\sum_i \log (1 - \xi_2^2 \theta^{4'i}) + \sum_i' \log (1 - \xi_2^2 \theta^{5'i}) \right]\end{aligned}\quad (1.01)$$

Now \bar{N}_A , \bar{N}_B , and \bar{N}_C are the same as the mean numbers of molecules of types A, B and C calculated on the assumption that free transitions occur between the para- and ortho-types. Although we assumed that the non-combining groups of wave functions existed, we obtained the same result that we should have obtained had we neglected entirely these non-combining properties. The explanation, of course, is that although we supposed that our ortho- and para-molecules retained their individualities in so far as direct transitions between the groups were impossible, we supposed that both sorts were able to dissociate into atoms—hence, in effect, their non-combining properties were lost, since the atoms could recombine to form molecules of both groups. But if free atoms were absent (which would be the case at very low temperatures) then any original proportion between the ortho- and para-types would never alter, and the appropriate statistical discussion would then provide for this by requiring the use of different x 's and hence of different ξ 's, for the ortho- and para-types. In this case the expressions for \bar{N}_1 and \bar{N}_2 on the one hand, and for \bar{N}_4 and \bar{N}_5 on the other in the equations corresponding to (1.0) would no longer be additive.

The equations (1.0) and (1.01) are awkward to work with; at ordinary temperatures and pressures we may use Fowler's arguments (the temperature as well as the molecular weight is much greater in the case of chlorine than in that of hydrogen which Fowler considers) on pp. 534–537 of his "Statistical Mechanics," and obtain the above relations in the simpler and very nearly accurate forms (the classical approximations to the Einstein-Bose statistics) corresponding to (1.0) and (1.01):

$$\left. \begin{aligned}\bar{N}_1 &= \xi_1^2 F_1(\theta) \\ \bar{N}_2 &= \xi_1^2 F_2(\theta) \\ \bar{N}_3 &= \xi_1 \xi_2 F_3(\theta) \\ \bar{N}_4 &= \xi_2^2 F_4(\theta) \\ \bar{N}_5 &= \xi_2^2 F_5(\theta)\end{aligned}\right\}, \quad (1.1)$$

where the $F(\theta)$'s are the classical partition functions for the different sorts of molecules; and

$$\left. \begin{aligned} \bar{N}_A &= \xi_1^2 F_A(\theta) \\ \bar{N}_B &= \xi_1 \xi_2 F_B(\theta) \\ \bar{N}_C &= \xi_2^2 F_C(\theta) \end{aligned} \right\}, \quad (1.11)$$

where we have put $F_1 + F_2 = F_A$, $F_3 = F_B$, $F_4 + F_5 = F_C$. We could have obtained these expressions directly by the use of the classical approximation to the Einstein-Bose statistics.

§ 2. The Calculation of the Ratios $\bar{N}_A : \bar{N}_B : \bar{N}_C$.

At ordinary temperatures, the number of atoms present in the gas will be trivial. We have, therefore,

$$\left. \begin{aligned} X_1 &= 2\bar{N}_A + \bar{N}_B \\ X_2 &= 2\bar{N}_C + \bar{N}_B \end{aligned} \right\} \quad (2.0)$$

effectively.

Let a , b and c be three numbers proportional to \bar{N}_A , \bar{N}_B and \bar{N}_C ; and such that $a + b + c = 1$. Let it be given that $X_2 = sX_1$. We wish to calculate a , b and c . In (1.11) we are interested only in the ratios between the left-hand members, so we may arbitrarily set ξ_1 equal to unity. From (1.11) and (2.0) we then find

$$\xi_2 = [(s-1)F_B + \sqrt{(s-1)^2 F_B^2 + 16sF_A F_C}] / 4F_C. \quad (2.1)$$

We may neglect factors in the three partition functions common to all of them, in calculating a , b and c . We take as the zero of energy of a molecule the energy which it has when completely dissociated with its component atoms at rest at infinity in their lowest quantum states. The complete partition functions, including translational, rotational and nuclear orientational factors, are, very nearly,

$$F_j(T) = V e^{x'/kT} \frac{(2\pi m_j kT)^{3/2}}{h^3} \frac{8\pi^2 I_j kT}{h^2} J_j, \quad (2.2)$$

where j takes the values A, B and C, and where

$$J_A = \frac{1}{2} (2n_1 + 1)^2; \quad J_B = (2n_1 + 1)(2n_2 + 1); \quad J_C = \frac{1}{2} (2n_2 + 1)^2.$$

We have assumed the temperature to be such that nuclear vibrations are not important and may be neglected in the partition functions. Actually, even in the lowest states of nuclear vibration there will be a slight additional difference between the three partition functions because of the vibrational isotope

effect, which causes χ' to differ slightly from type to type. The quantity V is the volume, and χ' is the energy required to bring a molecule in a state of zero nuclear rotation and minimum vibration, to the zero of energy defined above. Also, k is Boltzmann's constant, and m_j and I_j are the mass and moment of inertia of molecules of the j th type.

From equations (1.11), (2.1), and (2.2) we can calculate a , b and c . Inspection of these equations shows that these last quantities are independent of n_1 and n_2 , even if χ' varies from type to type. Actually, the variations of χ' are quite insignificant.

§ 3. *The Composition of Chlorine.*

From the international value of the atomic weight of chlorine, 34.457; and from Aston's atomic weights of the isotopes, namely, 34.979 and 36.976 (Aston's values are 34.983 and 36.980 respectively, referred to a scale where O_{16} is 16), we find that the quantity s in the last section is equal to 0.315, with a possible error of about 1 per cent. If we take the masses of the three sorts of molecules to be proportional to 70, 72 and 74 respectively; and if we take the moments of inertia to be proportional to 114, 118 and 121,* we then find for the relative numbers of chlorine molecules in ordinary chlorine the values $a = 0.5779$, $b = 0.3650$, $c = 0.0571$.

If we had assumed simply, at the start, that any one atom of chlorine was equally likely to combine with any other atom present in the assembly to form a molecule, this simple assumption would have led to the results $a' = 0.5783$, $b' = 0.3643$, $c' = 0.0574$; which differ only trivially from the results of the rigorous investigation above. Without the rigorous investigation, however, we could not be sure that the simple analysis would be correct, since it is certainly not obvious *a priori* that the nuclear spins are without effect upon the constitution of chlorine.

§ 4. *The Statistical Mechanics of Assemblies containing Gaseous Molecules of Types Para- X_1X_1 , Ortho- X_1X_1 , X_1X_2 , Para- X_2X_2 , and Ortho- X_2X_2 ; as well as Mixed Crystals of these Molecules.*

We shall use the classical approximation to the Einstein-Bose statistics for the gases, since they are sufficiently accurate for our purpose, but we shall, of course, keep the wave functions for the entire assembly symmetrical in all pairs of similar molecules.† We denote the number of molecules of the s th

* From Elliott, *loc. cit.*, and from Aston's values of the masses.

† Stern, *loc. cit.*

type in the crystal by P_r , and we suppose that the total number $X_r = P_r + N_r$ of molecules of the sort r in the assembly remains constant. We define a set of quantities D_r by the equations $D_r/X_r = \text{const.}$, $\sum D_r = 1$, $r = 1, 2, 3, 4, 5$. We consider that the molecules retain their identity in the crystal and form a molecular lattice, as they certainly do in the case of iodine. There will be normal modes of oscillation of the crystal as a whole, considered in the usual Debye analysis of specific heats. In addition, the molecules themselves can be in various eigenstates of spherical oscillation or rotation.* We consider that a complete wave function for the crystal is of the form $\psi_m \psi_A \psi_B \psi_C$ to the first approximation; where ψ_m is a wave function representing a normal mode of vibration (we assume that there is one such wave function for each normal mode) of the crystal lattice, where ψ_A is a wave function† representing a set of rotational or spherical oscillational states of the molecules of sort A, symmetric in all of them; and where ψ_B and ψ_C are similar functions for molecules of sorts B and C respectively. Then the normal modes contribute to the total number of linearly independent wave functions capable of representing the assembly a factor equal to the coefficient of z^Q in $[\kappa(z)]^P$, if the total energy of these modes is Q . We have considered that the partition function for the normal modes of vibration of the entire crystal, containing P molecules in all, is of the form $[\kappa(z)]^P$. Let a partition function for a molecule of the r th type for rotations or spherical oscillations be $f_r(z)$. Then these motions, if their total energy for the whole crystal is S , contribute to the total number of wave functions of the entire assembly a factor equal to the coefficient of z^S in $P! \prod_1^5 [f_r(z)]^{P_r} / \prod_1^5 P_r!$. Thus the whole crystal, if its energy is U , contributes a factor equal to the coefficient of $z^U \prod_1^5 x_r^{P_r}$ in

$$1/[1 - \kappa(z) \sum_1^5 x_r f_r(z)].$$

The gaseous phase, if its total energy is F , contributes a factor equal to the coefficient of $z^F \prod_1^5 x_r^{N_r}$ in $\Pi_1, \Pi_2, \Pi_3, \Pi_4, \Pi_5$, where now

$$\Pi_r = \Pi_r / (1 - x_r z^{e_r}).$$

Hence the whole assembly, if its energy is E , and if we allow all possible parti-

* L. Pauling, 'Phys. Rev.', vol. 36, p. 430 (1930); T. E. Stern, 'Proc. Roy. Soc.', A, vol. 130, p. 551 (1931).

† This wave function will be a permanent similar to those considered by T. E. Stern, first reference.

tions of the molecules between the different phases,* can be represented by a number of linearly independent wave functions, symmetric in all the molecules, equal to

$$W = \left(\frac{1}{2\pi i}\right)^6 \iiint \frac{dz \prod_1^5 dx_r \Pi_1 \Pi_2 \Pi_3 \Pi_4 \Pi_5}{z^{E+1} \prod_1^5 x_r^{x_r+1} \left[1 - \kappa(z) \sum_1^5 x_r f_r(z)\right]}. \quad (4.0)$$

For the same reasons as in § 1, we may replace the product of the Π_r 's in the numerator of the integrand if the above expression by

$$\exp \sum_1^5 x_r F_r(z),$$

thus obtaining the classical approximation to the Einstein-Bose statistics as far as the gas molecules are concerned, with sufficient accuracy.

By the usual methods, we find for the mean values

$$\bar{P}_r = \xi_r f_r(\theta) \kappa(\theta) / [1 - \kappa(\theta) \sum_1^5 \xi_r f_r(\theta)]; \quad \bar{N}_r = \xi_r F_r(\theta). \quad (4.1)$$

If \bar{P} is large, then we have very nearly

$$\kappa(\theta) \sum \xi_r f_r(\theta) = 1. \quad (4.2)$$

If, further, nearly all of the molecules are in the crystal, then, very nearly,

$$\bar{P}_1 : \bar{P}_2 : \bar{P}_3 : \bar{P}_4 : \bar{P}_5 = D_1 : D_2 : D_3 : D_4 : D_5. \quad (4.3)$$

It follows from these equations that

$$\bar{N}_r = D_r F_r(\theta) / \kappa(\theta) f_r(\theta), \quad (4.4)$$

and the total number of molecules in the vapour

$$\bar{N} = \sum_1^5 \bar{N}_r = \sum_1^5 D_r F_r(\theta) / \kappa(\theta) f_r(\theta). \quad (4.5)$$

§ 5. The Vapour Pressure of Chlorine.

We have the relation $pV = \bar{N}kT$, where p is the pressure. It follows that the vapour pressure

$$p = \sum_1^5 D_r p_r, \quad (5.0)$$

where

$$p_r = F_r(\theta) kT / f_r(\theta) \kappa(\theta) V, \quad (5.1)$$

* . . . and of the sets of molecules A, B and C between the lattice points. For an analysis of the legitimacy of this procedure, see section 6. The sets of molecules are not constrained to condense on definite sets of lattice points.

which is not the partial pressure of the r th species, but is the vapour pressure of a crystal made up wholly of the r th sort of molecules. We take as the zero of energy the state when all the molecules are in their lowest quantum states in the lattice in the crystalline phase, at the absolute zero, and at zero pressure. We suppose the partition functions $f_r(\theta)$ to be of the form

$$f_r(\theta) = \sum_j \omega_{r,j} e^{-\epsilon_{r,j}/\theta},$$

where $\omega_{r,j}$ is the number of linearly independent wave functions capable of representing the j th eigenstate of a molecule of the r th species in the crystal, and $\epsilon_{r,j}$ is the energy of the state. We denote by C_r the specific heat per gram molecule at constant pressure of a crystal made up wholly of the r th sort of molecules. Then we may readily show* that

$$\int_0^T \frac{dT'}{RT'^2} \int_0^{T'} C_r dT'' = \log K(T) f_r(T) - \log \omega_{r,0}. \quad (5.15)$$

* *Added March 23, 1931.*—This is not shown correctly in Fowler's "Statistical Mechanics." To do it correctly, we consider a gram molecule of crystal, having N molecules, with the complete partition function $H(V, T)$. We take the same zero of energy as that in the text above. We suppose for complete generality that the pressure acting on the crystal, p , is kept some definite function of the temperature, and is zero at $T = 0$; this is equivalent to supposing that the volume V of the crystal is a definite function of the temperature $V(T)$. Then the energy of the crystal at a temperature T will be

$$E[V(T), T] = \int_0^T (C dT - p dV) = kT^2 \frac{\partial}{\partial T} \log H(V, T).$$

Here C is the specific heat measured under the conditions specified above. Now

$$p = kT \frac{\partial}{\partial V} \log H(V, T),$$

and

$$\frac{d}{dT} \log H(V, T) = \frac{\partial}{\partial T} \log H(V, T) + \frac{\partial}{\partial V} \log H(V, T) \frac{dV(T)}{dT}.$$

Hence

$$\int_0^T \frac{dT'}{T'^2} \int_0^{T'} C dT'' = k \log \frac{H[V(T), T]}{H[V(0), 0]} + \int_0^T \frac{dT'}{T'^2} \int_0^{T'} p dV - \int_0^T \frac{p}{T} dV.$$

This can be reduced to

$$\int_0^T \frac{dT'}{T'^2} \int_0^{T'} C dT'' = k \log \frac{H[V(T), T]}{H[V(0), 0]} - \frac{1}{T} \int_0^T p dV.$$

If the pressure p is always zero, then the last term vanishes and the equation in the text follows as a special case. The reader can readily verify the fact that the errors, due to the pressure being not zero but equal to the vapour pressure, when C_p is measured, are trivial.

Here R is the gas constant per gram molecule. It follows from this last relation and (5.1), if we make use of the gaseous partition functions similar to (2.2) which should be very nearly accurate at ordinary temperatures (since only the nuclear vibrations are neglected), that

$$\log p_r = -\frac{\chi}{kT} + \frac{7}{2} \log T - \int_0^T \frac{dT'}{RT'^2} \int_0^{T'} C_r dT'' + \log \frac{(2\pi m_r)^{3/2} k^{7/2} 8\pi^2 I_r}{h^5} + \log \frac{G_r}{r\omega_0}. \quad (5.2)$$

Here G_r is a number which appears as a factor in front of $8\pi^2 I_r kT/h^2$ in the rotational partition function for a gas molecule of the r th sort, due to nuclear spins. Its values are

$$G_1 = \frac{1}{2}n_1(2n_1 + 1); \quad G_2 = \frac{1}{2}(n_1 + 1)(2n_1 + 1); \quad G_3 = (2n_1 + 1)(2n_2 + 1); \\ G_4 = \frac{1}{2}n_2(2n_2 + 1); \quad G_5 = \frac{1}{2}(n_2 + 1)(2n_2 + 1).$$

The quantity χ , which we have taken to be the same for all five sorts of molecule (the differences are trivial) is the work which must be done on a molecule in the crystal, in a state of zero energy defined above, in order to put it in a state of rest, in its lowest quantum state, at infinity.

It now becomes necessary to investigate in detail the nature of the energy states of the molecules of chlorine in the crystalline phase. In the paper of Pauling (*loc. cit.*) criteria are given for determining when the motion of molecules in crystals approximates to "rotation," and when to "oscillation" about positions of equilibrium. In the writer's paper (*loc. cit.*) on the same subject, the criterion is put in the simpler form: that "rotation occurs if $T > 2V_0/k$, and "oscillation" if $T < 2V_0/k$. Here V_0 is a potential energy which appears in the potential function $V_0(1 - \cos 2\theta)$ of the homopolar molecule, free from axial spin, with two positions of equilibrium. For its determination, the reader is referred to Pauling's paper. Pauling states that it may be obtained from the expression

$$V_0 = I(v_0\pi)^2$$

and from the consideration that $h\nu_0/k$ is equal to approximately three times the absolute temperature at which the specific heat of the crystal becomes equal to 5 calories per gram molecule. It should also be equal approximately to twice the total heat change accompanying transitions and fusion, per molecule. In the case of chlorine the specific heat of the solid becomes equal to

5 calories per gram molecule at approximately* 34° K. By the first method, then, we find that V_0 is equal approximately to 5.2×10^{-13} ergs. Taking the heat of fusion (there are no transitions) to be 1615 calories per mole, from the same experimental source, we find by the second method that V_0 is approximately 2.2×10^{-13} ergs. In either case, rotation ought not to occur for absolute temperatures lower than about 3000° . Thus we may be sure that chlorine molecules in crystalline chlorine at temperatures at which the latter can exist are not rotating; but are vibrating about orientations of equilibrium with a set of energy levels much like those of a two-dimensional harmonic oscillator. X-ray analysis of the structure of iodine crystals shows that iodine molecules possess definite orientations (presumably a pair in opposite directions) and are not rotating. It is plausible to guess that chlorine, when its crystal structure is investigated, will be found to be similar to iodine. If the Raman spectrum of chlorine crystals could be studied, we should then have definite experimental evidence to clinch the matter; since the molecular rotations, if they existed, would give lines in the Raman spectrum separated by only a few wave numbers, whereas the spherical oscillations would give rise to frequencies, easily distinguished from the former, of the order of 60 per cm.

Since it seems so likely that chlorine molecules in chlorine crystals oscillate instead of rotating, we assume that they oscillate. We can then apply the analysis developed by the writer (*loc. cit.*). Taking V_0 for chlorine to be about 3.7×10^{-13} ergs., we find that λ in that paper is about equal to 120. Thus the analysis developed to deal with the case of large λ ought to apply quite well in the case of chlorine. In the case of a chlorine molecule made up of two atoms of the same sort with nuclear angular momenta $n\hbar/2\pi$ each, the lowest eigenstate of the molecule in the crystal can be represented by $n(2n+1)$ wave functions antisymmetric in the nuclear spins, and by $(n+1)(2n+1)$ wave functions symmetric in the nuclear spins. In the case of a chlorine molecule of sort B the lowest eigenstate can be represented by two oscillational wave functions each of which corresponds to $(2n_1+1)(2n_2+1)$ complete wave functions after nuclear spins are considered—since in this case we are not concerned with the exclusion principle. The statistical weight of this molecule in its lowest quantum state is then $2(2n_1+1)(2n_2+1)$.

After the above digression, we can evaluate the last terms in the five expressions (5.2). We find that in all cases the last term reduces to $\log \frac{1}{2}$.

A detailed examination of the terms in equations (5.15) and (5.2) shows that

* Eucken and Karwat, 'Z. Phys. Chem.,' vol. 112, p. 478 (1924).

the different p_r 's only differ by less than about one part in seven from each other. We can show that in this case

$$\log p = \log \Sigma D_r p_r = \Sigma D_r \log p_r \quad (5.3)$$

very nearly; with an error of less than 2 per cent. in p .* Further, we can show by using the complete crystalline partition function that if C_{sol} is the specific heat at constant pressure of the mixed crystal, per mole, then

$$C_{\text{sol}} = \sum_1^5 C_r D_r. \quad (5.4)$$

Hence, from (5.2), (5.3), and (5.4),

$$\log p = -\frac{\chi}{kT} + \frac{7}{2} \log T - \int_0^T \frac{dT'}{RT'^2} \int_0^{T'} C_{\text{sol}} dT'' + i, \quad (5.5)$$

where

$$i = \sum_1^5 D_r i_r,$$

or, since

$$D_1 + D_2 = a, \quad D_3 = b, \quad D_4 + D_5 = c, \quad i_1 = i_2,$$

and

$$i_4 = i_5,$$

we have

$$i = ai_1 + bi_3 + ci_4.$$

Here

$$i_r = \log \frac{8\pi^2 I_r k^{7/2} (2\pi m_r)^{3/2}}{2h^5}. \quad (5.6)$$

The quantity i in equation (5.5) is by definition the chemical constant of chlorine vapour. We know the masses from Aston's measurements and from a knowledge of Avogadro's number; we know the moments of inertia of chlorine A and B from the work of Elliott (*loc. cit.*) to be 114×10^{-40} and 118×10^{-40} C.G.S. units respectively. We take as the moment of inertia of chlorine C molecules 121×10^{-40} C.G.S. units, obtained from the former value by a simple proportion involving the masses, since the nuclear distances may be supposed to be the same for all the molecules. It is usual to use common logarithms, and to express pressures in atmospheres. When this is done, and we calculate the constant i' in the new and slightly different equation for the vapour pressure which results, we find for chlorine the value†

$$i' = 1.35.$$

* Define a set of quantities A_r small compared with unity such that $p_r = p(1 + A_r)$, $\Sigma D_r A_r = 0$. Then $\Sigma D_r \log p_r = \log p + \Sigma D_r \log(1 + A_r)$. If the logarithms in the last term are expressed as power series the truth of (5.3) follows at once, since terms in A disappear.

† The writer has also calculated the chemical constant of chlorine vapour upon the different assumption, that non-combining groups of terms do not exist at all for chlorine molecules, and has obtained the same value $i' = 1.35$.

This is in satisfactory agreement with Eucken's experimental value*

$$i' = 1.51 \pm 0.16.$$

§ 6. *The Entropy of Crystalline Chlorine at the Absolute Zero.*

We unfortunately do not know the precise value of the nuclear spin of Cl_{37} . The spin of the Cl_{35} nucleus is apparently a $5/2$ quantum spin; this is the conclusion of Elliott (*loc. cit.*) after an analysis of the absorption band spectrum of chlorine. The values of the spins did not concern us in evaluating the chemical constant of chlorine vapour, but they are of importance in calculating the entropy at the absolute zero† of crystalline chlorine. We shall therefore assume in this section that n_1 is $5/2$, but leave the value of n_2 unassigned.

We consider a gram molecule of the crystalline chlorine, possessing N molecules in all, at the absolute zero. We may neglect the normal modes of vibration of the crystal lattice, since they contribute a factor of unity simply to the total number of linearly independent wave functions capable of representing the crystal. We suppose that the five sorts of molecules are in the ratios $D_1 : D_2 : D_3 : D_4 : D_5$ of the last section. Each molecule of sort 1 in its lowest quantum state can be represented by $n_1(2n_1 + 1)$ wave functions, of sort 2 by $(n_1 + 1)(2n_1 + 1)$ wave functions, of sort 3 by $2(2n_1 + 1)(2n_2 + 1)$ wave functions, of sort 4 by $n_2(2n_2 + 1)$ wave functions, and of sort 5 by $(n_2 + 1)(2n_2 + 1)$ wave functions. Hence the total number of linearly independent wave functions capable of representing the gram molecule of mixed crystal is

$$\begin{aligned} W = & [n_1(2n_1 + 1)]^{D_1 N} [(n_1 + 1)(2n_1 + 1)]^{D_2 N} \\ & \times [2(2n_1 + 1)(2n_2 + 1)]^{D_3 N} [n_2(2n_2 + 1)]^{D_4 N} [(n_2 + 1)(2n_2 + 1)]^{D_5 N} \\ & \times \left[N! / \prod_1^5 (D_i N)! \right]. \quad (6.0) \end{aligned}$$

* Eucken, Karwat and Fried, 'Z. Phys.,' vol. 29, p. 1 (1924).

† Added March 23, 1931.—Strictly speaking, we refer to conditions not at *precisely* the absolute zero, but at temperatures which, while close to the absolute zero, are still large when compared with the differences in energy, divided by Boltzmann's constant, of the "lowest" quantum states of the molecules in the crystal. These differences in energy can be due to the differences between the energies of symmetrical and antisymmetrical spherical oscillational states, as well as to differences due to the differing configurations of the nuclei. A rough calculation of the former effect shows that it may be neglected unless the temperature is smaller than 10^{-5} °K. Unfortunately there have been no measurements of hyperfine structure in band spectra; but rough calculations show that differences of the second sort would not be significant unless the temperature of the crystal were so low that it was of the order of 0.01 °K. Needless to say, our calculations,

Now the expression (6.0), it will be noted, represents the number of linearly independent wave functions, symmetric in all pairs of similar molecules, capable of representing the crystal when each type of molecule is in its lowest quantum state and when account is taken of all possible partitions of the five types of molecule between the different lattice points. In modern statistical theory, the entropy appears as the product of Boltzmann's constant and the logarithm of the number of linearly independent wave functions capable of representing the assembly, plus an arbitrary constant which we take to be zero. But what is the assembly, in this case? Is it merely a gram molecule of crystal at the absolute zero, in which case (6.0) is correct, or is it rather a gram molecule of crystal with the further specification that definite sets of lattice points are occupied by the five different types of molecules? In the latter case (6.0) would be in error by the last factor, involving factorials. It appears that the number of wave functions, and hence the entropy at the absolute zero as we have defined it, is relative to our knowledge of the crystal. What do we know about the specification of the crystal? The answer seems to be that in the case of a mixed crystal of chlorine we know nothing about the type of molecule occupying any particular set of lattice points, so that (6.0) is correct. Looked at broadly, an exact wave equation might be set up for an entire crystal, involving all of the potential energy terms due to the fields of the other molecules in the crystal. Theoretically, the actual crystal corresponds to the various possible solutions of this wave equation—the lattice points of the crystal corresponding to a definite set of eigenvalues of some observables. That is, any particular configuration corresponds to a specification of a set of quantum numbers. The quantum numbers denoting which types of molecule occupy certain lattice points cannot be regarded as known, if we know merely that we have a gram molecule of crystalline chlorine obtained by cooling from higher temperatures or by condensation from the gas, any more than the nuclear orientational quantum numbers can be regarded as known for particular molecules of a diatomic gas.

That this is the correct view to take in the case of chlorine may be verified by referring back to section 4 above, where we based our calculation of the vapour pressure upon the assumption that all possible wave functions, corresponding to all possible distributions of the molecules among the lattice

applying to temperatures higher than this, apply to all conditions of practical importance. Heat capacity measurements do not extend below a few degrees absolute; and physical chemists, in evaluating entropies, suppose that at lower temperatures the heat capacity of crystals is accurately zero.

points, were to be counted. Had we imagined the molecules of each of the sets A, B and C to be somehow constrained to occupy a definite set of lattice points, we should have been led to a value for the chemical constant greater than that obtained by* $\log 3$. Eucken's measured value can hardly be in error by that amount; so that we have definite experimental evidence for the correctness of our treatment.†

Hence, using Stirling's asymptotic formula for factorials, if we put $n_1 = \frac{1}{2}$, and if we remember that $D_1 = n_1 a / (2n_1 + 1)$, $D_2 = (n_1 + 1) a / (2n_1 + 1)$, $D_3 = b$, $D_4 = n_2 c / (2n_2 + 1)$, $D_5 = (n_2 + 1) c / (2n_2 + 1)$, we find that the entropy of a gram molecule of crystalline chlorine at the absolute zero of temperature is

$$S_0 = k \log W = R [a \log 36 + b \log 12 + (b + 2c) \log (2n_2 + 1) - a \log a - b \log b - c \log c]. \quad (6.1)$$

In calories per °C,

$$S_0 = 7.60 + 0.95 \log (2n_2 + 1)$$

if we use the values of a , b and c obtained in § 3.

The writer's thanks are due to Mr. R. H. Fowler for his criticisms and encouragement.

* Instead of the last factor in the denominator of the integrand of (4.0) we should then have had the product of three factors

$$\{1 - \kappa(z) [x_1 f_1(z) + x_2 f_2(z)]\} \{1 - x_2 f_3 \kappa(z)\} \{1 - \kappa(z) [x_4 f_4(z) + x_5 f_5(z)]\},$$

and we should have thus found three times the vapour pressure that we did find.

† In the case of mixed crystals of other molecules than chlorine, it is, of course, possible that certain configurations will be unstable, and will not be eigenstates of the exact wave equation for the whole crystal; so that in dealing with these crystals we should have to omit the corresponding wave functions in our count. Further, even in the case of chlorine, it is possible that after a long time at the absolute zero certain configurations, with lower energies than the others, would be arrived at regardless of the original configuration of the crystal. Expression (6.0) would not be accurate in this case. The entropy of the crystal would gradually diminish, at a rate depending upon the rate at which molecules could migrate in the crystal. Our present calculations would then be for a "metastable" state, but one which would still very probably be the only state of real importance.

The Velocity of Corrosion from the Electrochemical Standpoint.

By U. R. EVANS, L. C. BANNISTER, and S. C. BRITTON, Chemical Laboratory,
Cambridge.

(Communicated by Sir Harold Carpenter, F.R.S.—Received February 28, 1931.)

Introduction.

It is now agreed that the wet corrosion of metals is usually an electrochemical process, accompanied by the flow of electric currents over measurable distances. Direct combination, without appreciable flow of current, is indeed met with in some cases, for instance, in corrosion by a solution of a halogen. But direct attack by dissolved oxygen would lead to the production of a film of oxide, which, being sparingly soluble, would restrain further action. Indirect electrochemical action by oxygen, in the presence of a salt, will, however, often yield soluble bodies as the primary products; thus iron in sodium chloride solution containing oxygen, yields ferrous chloride at the anodic areas and sodium hydroxide at the cathodic areas. Where these primary products meet, in presence of oxygen, they yield a mixture of hydrated iron oxides known as "rust"; but such secondary products—although almost insoluble—are usually precipitated at a sensible distance from the metal, and do not protect it from further attack. In cases where electrochemical action would lead to a sparingly soluble salt as the direct product, the attack does not develop; thus lead, although rapidly attacked by a nitrate solution in presence of oxygen, is hardly affected by a sulphate solution.*

The electric currents involved in the corrosion-process may be set up:—

- (a) By differences in the *metallic object* (e.g., on a "bimetallic" specimen, where one metal serves as cathode and the other as anode; or on iron partly covered with mill-scale, which serves as cathode, the exposed metal acting as anode).
- (b) By differences in the *liquid*, notably differences in oxygen-concentration, which cause the "aerated" part of the metal to be cathodic and the "unaerated" to be anodic.

These "differential aeration currents"† can themselves, however, be referred to differences in the state of repair of an "invisible" oxide-film present on

* J. A. N. Friend and J. S. Tidmus, 'J. Inst. Met.,' vol. 31, p. 182 (1924).

† J. Aston, 'Trans. Amer. Electrochem. Soc.,' vol. 29, p. 449 (1916); U. R. Evans, 'J. Inst. Met.,' vol. 30, p. 239 (1923).

the metallic surface.* On some materials (aluminium or stainless steel) this film confers definite protection from many liquids. Even ordinary iron or steel exhibits passivity to certain reagents after oxidising treatment, but the film produced by exposure to air gives no permanent protection. For such films tend to break down locally, and only at places where oxygen (or an oxidising agent) is present in excess do they remain "in repair."† Thus the film on ordinary iron, although not "protective" in any real sense, does serve to *divert* corrosion to the parts least accessible to oxygen. The potential is slightly higher at the "aerated" places, where the film is kept in good repair;‡ these parts are therefore cathodic towards the "unaerated places," and electric currents flow between the aerated and unaerated areas; corrosion only continues so long as oxygen is supplied to the cathodic region, but the attack actually occurs at the anodic parts which are relatively inaccessible to oxygen.

Qualitatively, the electrochemical character of corrosion may be said to have been definitely proved, since the currents have been tapped, the cathodic and anodic products have been identified, and the invisible skin responsible for the differential aeration currents has been isolated and thus rendered visible. On the quantitative side considerable progress has been made, through the very accurate measurements of Bengough, Stuart and Lee,§ and the very extensive studies of the hydrogen-evolution type of attack conducted under Palmaer.|| Approaching the matter from another side, one of the authors¶ has tapped a considerable proportion of the electric current passing under differential aeration conditions, and has showed, by applying Faraday's law, that, in the case of iron, this current accounted for 93 per cent. of the attack actually observed on the "unaerated" area; part of the current could not be tapped, and presumably this accounted for the remaining 7 per cent.,

* Although invisible whilst in optical contact with the bright metal, it becomes visible when separated from it. See U. R. Evans, 'J. Chem. Soc.,' p. 1020 (1927); U. R. Evans and J. Stockdale, 'J. Chem. Soc.,' p. 2651 (1929).

† Recent work by L. C. Bannister and U. R. Evans, ('J. Chem. Soc., p. 1361 (1930)) suggests that the repair of the film at the well-aerated places is largely due to the fact that the hydrated ferric oxide, produced by electrochemical action between the iron exposed at faults in the film and the oxide film around, is precipitated so close to the surface as to repair the faults.

‡ A. McAulay and F. P. Bowden, 'J. Chem. Soc.,' vol. 127, p. 2605 (1925); U. R. Evans, 'J. Chem. Soc.,' p. 103 (1929).

§ G. D. Bengough, J. M. Stuart and A. R. Lee, 'Proc. Roy. Soc.,' A, vol. 116, p. 425 (1927); vol. 121, p. 88 (1928); vol. 127, p. 42 (1930).

|| W. Palmaer, "Corrosion of Metals," 1929.

¶ U. R. Evans, 'J. Inst. Met.,' vol. 30, p. 267 (1923).

although that could not be proved. A general correspondence of the same kind has been obtained by Tödt* for a bi-metallic system.

It seemed essential to attempt the measurement of the whole current flowing, in order to correlate it with the corrosion velocity. In the *first* part of the present paper, it is established experimentally (both with bi-metallic specimens and also under differential aeration conditions) that the corrosion produced corresponds closely to the current actually tapped. It is therefore only necessary to ascertain the laws defining the strength of this current in order to understand quantitatively the principles governing the velocity of corrosion.

It is generally recognised† that polarisation is an important factor in determining the strength of current that can be maintained. Polarisation depends on the current strength; the higher the current, the more nearly will the cathodic and anodic potentials be brought together. Clearly under any conditions there is a certain current which would render the cathodic and anodic potentials equal, and so reduce the e.m.f. to zero; the limiting "*equipotential*" values of the current and corrosion-rate may be approached, when the resistance of the circuit becomes very low, but clearly they can never be exceeded, however high the conductivity of the solution. In the *second* part of the present paper it is shown experimentally that "*equipotential conditions*" are in fact approximately obtained with fairly concentrated solutions, thus simplifying the position. In the *third* part, a number of the "*polarisation-curves*" connecting current-density and potential, under controlled conditions of oxygen-supply, have been traced, and the principle governing the ratios of the cathodic and anodic areas, under conditions of differential aeration, has been ascertained. It is found that the anodic areas spread (or contract) until the current flowing is of such a strength that the cathodic current density just reaches the "*protective*" value. The establishment of this point is essential to a quantitative understanding of corrosion, for it is the current per unit area, not the total current, which defines the polarisation. Since the "*protective value*" of the current density has been studied in earlier work, it is felt that the essential electrochemical principles governing the strength of the corrosion-current—and therefore the velocity of corrosion—are now understood, although much work will be required in applying them to concrete cases.

Materials.—The electrolytic iron sheet (E28) and mild steel (H28) were

* F. Tödt, 'Z. Elektrochem.,' vol. 34, p. 853 (1928).

† H. J. Donker and R. A. Dengg, 'Korr. Met.,' vol. 3, pp. 217, 241 (1927); E. Liebreich, 'Korr. Met.,' Beiheft, p. 20 (1929); U. R. Evans, 'J. Chem. Soc.,' p. 111 (1929).

those used in previous researches; they were kindly prepared by Dr. W. H. Hatfield. Analysis showed:—

	Iron E 28.	Steel H 28.
Carbon	0.03	0.26
Silicon ...	Trace	0.15
Manganese	0.04	0.57
Sulphur	0.005	0.014
Phosphorus	0.020	0.018
Thickness (mm.)	0.34	0.32

The electrolytic zinc was kindly provided by Mr. H. C. Lancaster, and was rolled from spelter of 99.97 per cent. purity. The copper was Kahlbaum's electrolytic foil. Before use the specimens were abraded with French emery paper No. 1, degreased with carbon tetrachloride, and cut into the required shapes.

EXPERIMENTAL PORTION.

I.—*Correlation between Corrosion Velocities and Current Flowing between Anodic and Cathodic Areas.*

In the preliminary experiments, attempts were made to tap the current generated by bi-metallic specimens, since this presents less difficulty than the case of currents set up by differential aeration. A specimen of zinc (4×1.5 cm.) was weighed, and clamped beside a similar specimen of copper in a vertical position in N potassium chloride; the immersed area of each metal was 2.0×1.5 cm. The pair was supposed to represent an article composed half of zinc and half of copper; but, actually, instead of being in contact at their edges, the two metals were separated by a gap of 1 mm. and were joined by low-resistance leads through a milli-ammeter. The current was measured at intervals and after 25 hours the zinc was freed from corrosion-products and re-weighed. It was found that the current tapped represented only about 82.4 per cent. of the total corrosion of zinc. Another experiment, conducted for 7 hours, gave 85.3 per cent. Examination of the specimens revealed the reason why the whole of the current had not been tapped. The part of the zinc near the water-line was quite unattacked, and had all the appearance of a typical cathodic area; evidently not only the copper surface, but also the aerated portion of the zinc surface had functioned as cathode. The only way to prevent this complication was to exclude oxygen from the anodic surface by means of a membrane. This did not really introduce an artificial condition,

since in "natural corrosion," a membrane of metallic hydroxide appears at the boundary of the cathodic and anodic areas, and plays a real part in excluding oxygen from the latter. The method adopted was applicable to the study, not only of bimetallic specimens, but also to cases of differential aeration, where the anode and cathode are different portions of the same metal, respectively shielded from oxygen, and exposed to it.

In order to shield the anode from oxygen, porous tubes of cellulose acetate of diameter 2 cm. and length 9 cm. were employed. These were made by covering the interior surface of a test-tube with a solution of cellulose acetate in acetone, pouring off the excess, and after drying, flooding with water; the cellulose acetate lining was then removed and thoroughly washed. The cellulose tube thus produced was attached at its mouth to a glass tube by means of a rubber band. It was filled with N potassium chloride and clamped in an outer vessel containing N potassium chloride. The two pieces of metal taken to represent the anodic and cathodic parts of the "article" to be exposed to corrosion were introduced; the former, after being weighed, was placed in the cellulose tube, whilst the latter formed its prolongation outside the tube. They were joined by low-resistance leads to a milliammeter, or alternatively to a silver coulometer. To protect the anode from air, the solution in the tube was covered with viscous paraffin.

It was necessary to consider the effect of diffusion of oxygen through the cellulose into the tube. Clearly when the current passing is high, the error caused by leakage of oxygen should be small. In some of the preliminary experiments, with stagnant liquids, 95 per cent. of the Faraday current was obtained from the combination zinc-copper, and 100 per cent. from the combination iron-copper.* But the combination iron-nickel generated only half the current of the iron-copper combination, and this only accounted for 66 per cent. of the total corrosion. When the specimens were both iron, the strength of current was also small, and the amount of current tapped was only 59 per cent. of that corresponding to the weight-loss. In these preliminary experiments, no special attention was paid to the position of the electrodes, or to the renewal of oxygen at the lower parts of the outer electrode. It was decided in the main series to keep the electrodes as close together as the tube thickness permitted, and to bubble air or oxygen through the liquid in the outer compartment, so as to increase the current. Clearly a state of affairs must be aimed at in which the supply of oxygen outside is made adequate,

* Special experiments showed that iron passed into solution as ferrous ions; ferric salts were quite absent from the liquid in the tube.

without the leakage inwards becoming excessive. Special experiments in which there was no metal outside the tube showed that an isolated iron specimen placed inside the tube developed rust very rapidly when oxygen was bubbled through the liquid outside the tube, but very much more slowly when air was used instead of oxygen. On the other hand, in two-electrode experiments, the current was only decreased slightly when air was used instead of oxygen. It was, therefore, decided to use a stream of air in order to provide adequate aeration of the cathode without involving danger of serious aeration of the anode.

Experiments made with this arrangement gave results for iron and steel anodes shown in Table A.

Table A.

Experiment No.	Anode.	Cathode.	Weight loss.	Total coulombs as percentage of coulombs corresponding to weight loss.
1	Iron E28	Iron E28	grams. 0.01383	per cent. 102.1
2	Iron E28	Copper	0.05060	101.1
3	Steel H28	Steel H28	0.01652	97.6
4	Steel H28	Steel H28	0.01183	100.8
5	Steel H28	Steel H28	0.01281	98.9

The duration of each experiment was about 6 hours. It will be seen that the current actually tapped was always within 2.5 per cent. of the value calculated from the weight-loss. It would appear, therefore, that no appreciable fraction of the corrosion was connected with either (a) untapped current, or (b) evolution of hydrogen, or (c) direct chemical attack.

Any variation of the standard procedure which reduced the current flowing between the outer and inner electrodes was found to favour the formation of local cathodic areas on the inner metal, and thus decreased the concordance between measured current and corrosion-loss. For instance, in one experiment an attempt was made to protect the edges of the outer electrode with nitro-cellulose in order to avoid rust on the cathode, and thus utilise to a greater extent the supply of oxygen. Actually, however, the production of rust was merely diverted to the central parts of the face, and the effective cathode area was diminished; accordingly the current strength was abnormally low (about one-tenth of its usual value), and the current tapped represented only 90 per cent. of the total corrosion of the inner specimen. Clearly "local currents"

which, under standard conditions, would represent, say, only 1 per cent. of the total corrosion (an amount less than experimental error) may come to represent 10 per cent., when the oxygen supply to the aerated portion is reduced in the manner described.

Under standard conditions the corrosion corresponded closely to the current tapped. There is little doubt that the correspondence obtained with iron was due to the fact that ferrous hydroxide, which is formed by interaction between the cathodic and anodic products, is itself an excellent oxygen-absorbent. It was found impossible to obtain accurate results in analogous experiments on zinc, owing to the already well-known difficulty of removing the corrosion-product,* but there was evidence that some local cathodic action took place on the unaerated area. Certainly there were portions of the surface within the tube which had not undergone corrosion; with iron and steel the etching had been much more uniform. This accords with the observation of Bengough, Stuart and Lee that the corrosion of zinc is not wholly of the oxygen-absorption type, some hydrogen being liberated even from neutral solutions. It is doubtful whether any metal other than iron is suitable for testing the correspondence between current and weight-loss. But since, in the case of iron and steel, the corrosion velocity is determined solely by the current flowing between the aerated and unaerated areas, the problem of the kinetics of corrosion here resolves itself into finding the laws which govern the strength of this current. Even on metals, like zinc, where a second type of corrosion is superimposed, it is clear that, in neutral solutions, the main part of the corrosion is due to differential aeration currents, and a realisation and knowledge of these laws is of the first importance; the laws governing the subsidiary (hydrogen-evolution) type of attack, which is superimposed, are already to a large extent understood.

II.—*Study of the Potentials at the Anodic and Cathodic Areas.*

In Part I it was shown that the corrosion-velocity is equivalent to the current flowing; the next step is to study the principles which determine the strength of the current generated. Here again it appeared useful to commence with a study of bimetallic specimens. Strips of zinc and copper were fixed side by side in a vertical position, being cemented above the water-line to a strip of glass; the lower portion (2×2 cm.) was immersed in potassium chloride of different concentrations. The object was to represent an article half zinc

* Cf. G. D. Bengough, J. M. Stuart and A. R. Lee, 'Proc. Roy. Soc.,' A, vol. 116, p. 447 (1927); U. R. Evans, 'J. Chem. Soc.,' p. 121 (1929).

and half copper. The two metals were only separated by a gap of about 1 mm., and were joined by low resistance leads to mercury cups; these were at first disconnected, but could be short-circuited at will, or joined through a milliammeter. Two glass tubuli were fixed opposite the central points of the immersed areas of zinc and copper, and led, through saturated potassium chloride as intermediate liquid, to two calomel electrodes. The general arrangement and the method of measuring the potential by means of a thermionic voltmeter has been described in a previous paper.† The precautions taken to exclude the atmosphere and keep the temperature constant were the same as in that work.

The results are shown in Table B. The initial potentials measured before the zinc and copper were short-circuited were naturally far apart; after short-circuiting, the copper potential rapidly dropped towards that of the zinc, and in the case of the normal solutions became practically equal to the zinc value within 2 minutes. After this time, there was merely a slow sinking of both potentials, just as had been found in previous work on monometallic specimens; but the potentials of the two metals kept close together. In the N/10 solution the approach of the copper potential to the zinc value was slower, and even after a longer period was less complete, whilst in N/100 solution, the difference between the two values was still considerable even after 44 minutes, although both potentials had, after this time, sunk very low.

Table B.

Concentration (grm. equiv. per litre).	Initial potentials (hydrogen scale).		Time of experiment needed for constancy of acting e.m.f.	Final potentials (hydrogen scale).		Final acting e.m.f.
	Zinc.	Copper.		Zinc.	Copper.	
			minutes.			volts.
{ 1.0	-0.792	+0.030	1.4	-0.795	-0.795	0.000
{ 1.0	-0.802	+0.018	0.7	-0.807	-0.807	0.000
{ 0.1	-0.752	+0.123	2.5	-0.752	-0.742	0.010
{ 0.1	-0.742	+0.108	2.1	-0.745	-0.720	0.025
{ 0.01	-0.742	+0.158	44*	-1.002*	-0.912*	0.090*
{ 0.01	-0.892	+0.048	6*	-1.042*	-0.927*	0.115*

* Potentials still changing slowly.

Thus when a normal solution is considered, it is legitimate to say that the current flowing between anodic and cathodic areas is that which will cause

† L. C. Bannister and U. R. Evans, 'J. Chem. Soc.', p. 1361 (1930).

sufficient polarisation to make the cathodic potential approximately equal to the anodic value. But equipotentiality was not attained when the liquid was more dilute. No doubt the gap between the final values in dilute solutions represents the residual e.m.f. needed to force the current through the quite appreciable resistance of the circuit.

It will be observed that *practically the whole of the polarisation is cathodic*; no rise in the anodic value is obtained;* frequently in fact, the potential at the zinc slightly falls, owing, no doubt, to the exhaustion of oxygen (the presence of which is unfavourable to the anodic reaction). The observations on an iron-copper couple recorded in a previous paper† suggests that with zinc-copper specimens an upward movement of the zinc potential might be obtained if the area of the zinc was made smaller than that of the copper. Some experiments carried out in N/10 concentration with variation of area-ratio are shown in Table C. Even when the zinc area was only a quarter of that of the copper, there was practically no movement of the zinc potential. The value of the current flowing also suggested that it was controlled by the cathodic polarisation, not by the anodic polarisation. When the breadth of the zinc was decreased (that of the copper remaining constant), the current obtained was practically the same as when the zinc was as large as the copper; but when the breadth of the copper was decreased (that of the zinc being constant), the current was diminished.

Table C.

Breadth of electrode.		Copper potentials.		Zinc potentials.	
Zinc.	Copper.	Initial.	Final.	Initial.	Final.
cm.	cm.				
{ 0.5	2.0	+0.118	-0.722	-0.745	-0.747
{ 0.5	2.0	+0.118	-0.727	-0.744	-0.747
{ 2.0	2.0	+0.113	-0.712	-0.742	-0.747
{ 2.0	2.0	+0.123	-0.742	-0.752	-0.752
{ 2.0	2.0	+0.108	-0.720	-0.742	-0.745
{ 2.0	2.0	+0.103	-0.752	-0.752	-0.752
{ 2.0	0.5	+0.113	-0.750	-0.740	-0.750
{ 2.0	0.5	+0.118	-0.738	-0.740	-0.742

* For couples in acid solution E. Liebreich ('Korr. Met.,' Beiheft, p. 20 (1929)) has also found that nearly all the polarisation occurs at the cathode metal; here the polarisation is no doubt of a different type.

† L. C. Bannister and U. R. Evans, 'J. Chem. Soc.,' p. 1361 (1930).

Another series of experiments, conducted in normal solution, included couples other than zinc-copper. Here the potential was measured after the current passing had become constant. At this stage, approximately equilibrium conditions had been reached in the case of zinc-copper, iron-copper and lead-copper combinations; indeed, frequently, the copper showed in the end a slightly *lower* potential at the point studied than the other electrode, although the direction of the current flowing always indicated that the copper was acting predominantly as cathode. In spite of lack of perfect reproducibility, the general trend of the results is not in doubt. Where, as in zinc, the initial potential is low (-0.79 volts), the copper potential must be greatly reduced before the acting e.m.f. vanishes, and thus a considerable current flows under polarisation conditions (actually 1.27 m.a. and 1.21 m.a. in two experiments); in such cases corrosion is naturally rapid. Where the initial potential is higher, as on lead (-0.347 volts), the copper potential has not so far to descend, and the resulting current is lower (actually 0.25 m.a.), the corrosion also being less rapid. It should be noted that the lead potential appears to rise slightly after short-circuiting, namely, to -0.252 volts. Whether this rise is mainly due to *true* anodic polarisation may be doubted; more likely it is caused by the protective skin which restricts the attack to a few points, so that a considerable part of the liquid resistance falls between the tip of the tubulus and the exposed part of the metal. The same principle explains the lack of reproducibility, since it will be a chance whether the tubulus happens to be close to a weak spot or not. This matter has been considered in detail in another research.*

A rise in the anodic potential was also noticed in experiments with copper-aluminium couples; this is easily understood since it is well-known that a non-conducting oxide-film is present on aluminium. The dimensions of the immersed area were 1.5×1.7 . The numbers obtained are shown in Table D.

Table D.

Copper potentials.		Aluminium potentials.	
Initial.	Final.	Initial.	Final.
+0.048	-0.482	-0.512	-0.486
+0.053	-0.487	-0.517	-0.492
+0.043	-0.485	-0.517	-0.485

* S. C. Britton and U. R. Evans, 'J. Chem. Soc.,' p. 1773 (1930).

The next question to be considered is whether the same principles apply to a specimen of a single metal under conditions of differential aeration. The testing of the matter is made difficult by the fact, noticed by McAulay and Bowden,* that—even within the predominantly cathodic or anodic areas—small local variations of potential exist. Consequently, it was decided to measure the potential at several places on each area. Specimens of electrolytic iron (fig. 1) were fixed vertically in potassium chloride solution of chosen

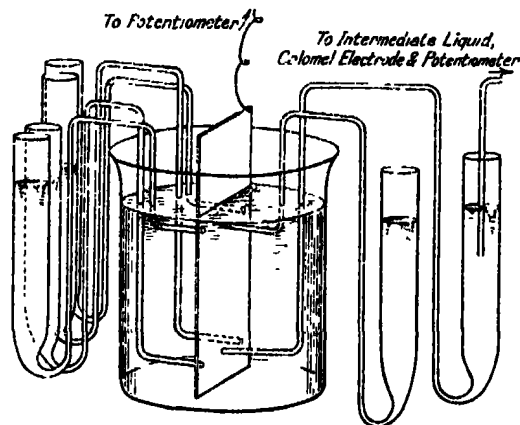


FIG. 1.

concentration; the immersed area was 4.0×4.0 cm. Six tubuli opened opposite to each specimen, three being fixed just below the water-line, whilst the other three were fixed close to the bottom. From the broad end of any one of these, connection could be made through an intermediate vessel containing saturated potassium chloride to a calomel electrode. Two experiments were conducted at each concentration. The potential at any given point fluctuated with time, as found in previous work, owing no doubt to alternate breakdown and repair of the skin. Table E shows for each pair of tubuli the difference between the potential at the water-line zone and that at the bottom measured after different intervals; a negative sign indicates an abnormal polarity, the potential near the water-line being negative towards that measured lower down.

Here also the potentials at the cathodic and anodic parts remain far apart when the concentration is low, but come close together when it is high; the limiting, equipotential conditions are approximately reached in normal solution. But it must not be forgotten that where (as in materials like aluminium or

* A. L. McAulay and F. P. Bowden, 'J. Chem. Soc.,' vol. 127, p. 2605 (1925).

Table E.

Differences of potential between upper and lower zones after

Concentration.	2 hours.	6 hours.	24 hours.	48 hours.
M/1 A—				
(i)	Zero	Zero	-0.005	Zero
(ii)	+0.005	Zero	+0.005	-0.005
(iii)	+0.005	-0.005	Zero	-0.020
M/1 B—				
(i)	+0.030	Zero	Zero	Zero
(ii)	+0.010	+0.005	Zero	-0.005
(iii)	Zero	Zero	+0.005	-0.005
M/10 A—				
(i)	+0.015	Zero	+0.005	+0.015
(ii)	Zero	-0.010	Zero	+0.015
(iii)	-0.005	+0.005	+0.010	+0.015
M/10 B—				
(i)	+0.005	+0.010	+0.010	+0.010
(ii)	+0.010	-0.005	+0.010	+0.010
(iii)	+0.005	+0.005	+0.005	+0.015
M/100 A—				
(i)	+0.010	+0.055	+0.035	+0.020
(ii)	+0.010	+0.035	+0.030	+0.025
(iii)	+0.010	+0.030	+0.040	+0.035
M/100 B—				
(i)	Zero	+0.060	+0.030	+0.035
(ii)	+0.010	+0.055	+0.030	+0.035
(iii)	+0.010	+0.045	+0.030	+0.035
M/1000 A—				
(i)	+0.005	+0.040	+0.145	+0.120
(ii)	+0.005	+0.030	+0.160	+0.150
(iii)	+0.030	+0.035	+0.155	+0.160
M/1000 B—				
(i)	+0.010	+0.040	+0.130	+0.115
(ii)	-0.010	+0.005	+0.150	+0.115
(iii)	+0.040	+0.050	+0.170	+0.170

NOTE.—The letters A and B denote the two experiments conducted at each concentration; the numbers (i), (ii) and (iii) denote the three pairs of tubuli.

stainless steel), the anodic areas remain mere pores in the highly protective skin, the circuit resistance may be high even when a solution of high specific conductivity is employed; in such cases, true equipotentiality is not to be expected, even in concentrated solutions, although in any ordinary method of measurements the potential drop over the pores in the skin would be included in the "apparent anodic polarisation."

III.—*The Determination of Potential-current Curves and the Significance of Cathodic Protection.*

Since the corrosion-current is largely controlled by cathodic polarisation, it is necessary to study the alteration of cathodic potential with current density

in the presence of dissolved oxygen. Cathodic polarisation curves have already been plotted by numerous experimenters, notably by Liebreich and Wiederholt;* none of the researches, however, give quite the information needed. It was decided to carry out measurements, using cathodes of different metals in N/10 potassium chloride solution with controlled stirring, so as to supply oxygen in a regulated manner to the cathode surface. For this purpose, the apparatus previously used for tracing the corresponding anodic curves† was found suitable. The specimen constituted the cathode and a platinum anode was placed parallel to it at a distance of 3.5 cm.; the orifice of a tubulus, leading through saturated potassium chloride as intermediate liquid to a calomel electrode, was placed close to the cathode surface; the immersed area of the electrode was 2×2 cm. The stirrer was a vertical glass rod of diameter 0.52 cm., describing a circle of diameter 2.2 cm. centrally between the two electrodes; the speed of rotation was 15 revolutions per minute. The whole was kept at a temperature of 20.0°C ., by means of the double-walled thermostat described elsewhere.‡

A fairly high e.m.f. was first employed. When the cathode potential and current density had become constant, the e.m.f. was reduced slightly, and a new correlation between potential and current density was obtained. This process was continued until the whole curve was completed. During the first part of each experiment no corrosion occurred, and the curve rose smoothly; but below a certain value of the current density (the "protective" value), corrosion was seen to start on the specimen, and the curve became horizontal. Typical curves are shown in figs. 2 and 3, the potential of a N/10 KCl calomel electrode being taken as zero. Experiments were also conducted with steel H28, which gave curves similar to electrolytic iron, and with stainless steel, from which a horizontal branch was obtained at a higher potential, namely, at -0.53 volts. Curves were also traced for steel in potassium chloride of other concentrations and also in N/10 potassium sulphate; these had a similar form to those obtained with N/10 potassium chloride.

After each alteration of the e.m.f. the current and potential moved only slowly towards their new values; on fig. 3 the direction of these time-movements is indicated by arrows; the movements take place in a different direction on the two parts of the curve; this accords with previous work,§ which indi-

* 'Z. Elektrochem.,' vol. 30, p. 263 (1924); vol. 31, p. 6 (1925).

† S. C. Britton and U. R. Evans, 'J. Chem. Soc.,' p. 1773 (1930).

‡ U. R. Evans, 'Chem. Ind.,' vol. 50, p. 66 (1931).

§ L. C. Bannister and U. R. Evans, 'J. Chem. Soc.,' p. 1361 (1930). Compare W. J. Muller and K. Konopicky, 'Monats. Chemie.,' vol. 52, p. 463 (1929).

cated that, during film-repair, the potential rises with the time, and that during film-breakdown it falls with the time. The fact is useful, since it helps in

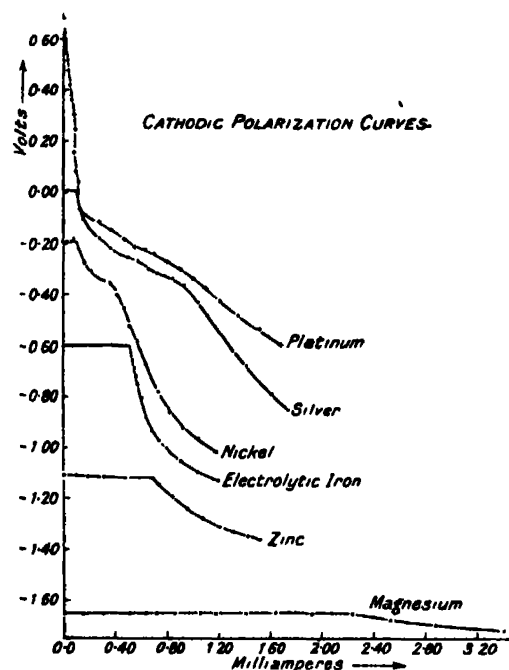


FIG. 2.

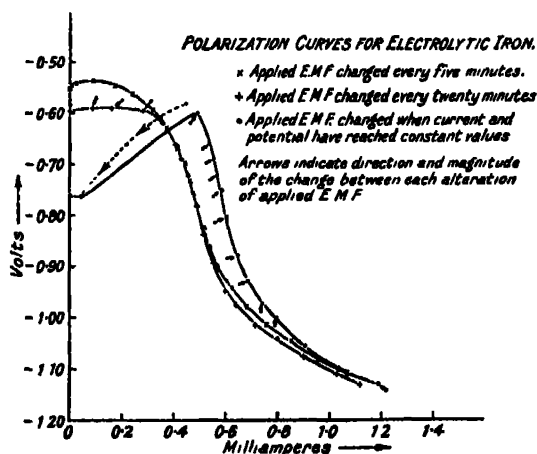


FIG. 3.

obtaining the exact point at which the horizontal portion begins. The time needed to reach a state of constancy for the first point taken varies greatly

with the metal, being about 20 minutes for zinc and about 4 hours for platinum, magnesium and silver. The time needed for attaining constancy after each alteration of e.m.f. also varies somewhat; if insufficient time is allowed, the portion which should be horizontal naturally slopes upwards to the left. This was illustrated by the curves obtained with iron (fig. 3); when 5 minutes' interval was allowed between alterations of current density, the portion in question sloped upwards; if 20 minutes was allowed, it was truly horizontal. Even after 20 minutes a slow movement continues, but this was apparently due to another cause; ferrous hydroxide is a good oxygen-absorbent, and the accumulation of rust shuts off the supply of oxygen from the cathode, so that if time be allowed, the current density finally sinks almost to zero, and the potential to a value similar to the potential attained in unstirred liquid. Iron is exceptional in this respect. The other metals do not show this slow movement due to oxygen-absorption, and give well-marked horizontals, whatever the interval chosen (see fig. 2).

The "stagnant potentials" were measured both for zinc (-1.30 volts) and for iron (-0.76 volts); they are naturally a little lower than the potentials corresponding to the horizontals obtained under conditions of stirring (-1.10 volts and -0.59 volts respectively).

The meaning of the curves may now be considered. If the current flowing depends solely on *depolarisation by oxygen*, then the oxygen used up in unit time by current i is equal to i/F , where F is Faraday's number. The rate of renewal of oxygen by diffusion to the surface is equal to $(C_0 - C)k_1/h$, where C_0 is the oxygen concentration in the body of the solution, C that at the iron surface, h the thickness of the diffusion layer and k_1 a constant indicating that diffusivity for oxygen inwards. Evidently $i/F = (C_0 - C)k_1/h$, whence

$$C = C_0 - \frac{h}{Fk_1} i.$$

Assuming the electrode to be reversible, and the potential to be fixed by the oxygen concentration alone, then the polarisation, measured from the potential of a reversible oxygen electrode of oxygen concentration C_0 , is equal to

$$\frac{RT}{nF} \ln \frac{C}{C_0} = \frac{RT}{nF} \ln \left(1 - \frac{h}{Fk_1 C_0} i \right) = k_2 \ln (1 - k_3 i),$$

where k_2 represents RT/nF and k_3 represents $h/Fk_1 C_0$. (R is the gas constant, T the absolute temperature, and n the electron-transfer). The curve I (fig. 4) represents this equation; a limiting value of the current is set by the fact that

the rate of diffusion of oxygen to the metal can never exceed the value $C_0 k_1/h$ corresponding to complete exhaustion of oxygen at the metal surface.

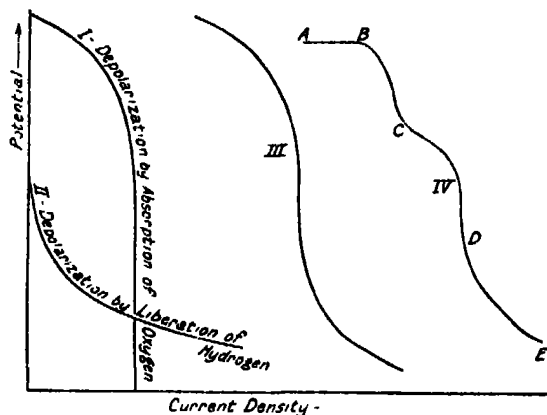


FIG. 4.

If the current depends on production of *free hydrogen*, then there is no limiting value to the current. If C_0' and C' represent respectively the concentrations of free hydrogen in the body of the solution and at the metal surface, it is clear that now $i/F = (C' - C_0')k_1'/h$, where k_1' is the constant indicating the diffusivity for hydrogen outwards. Thus

$$C' = C_0' + \frac{h}{Fk_1'} i$$

and the polarisation, measured from the potential of a reversible hydrogen electrode of hydrogen concentration C_0' is equal to

$$\frac{RT}{nF} \ln \frac{C'}{C_0'} = \frac{RT}{nF} \ln \left(1 + \frac{h}{Fk_1'C_0'} i \right) = k_s \ln (1 + k_s' i),$$

where k_s' represents $h/Fk_1'C_0'$. The curve II of fig. 4 represents such an equation.

Actually, it is known that the current depends on oxygen-depolarisation at high potentials, but on the evolution of hydrogen when the potential is sufficiently depressed to permit the production of this gas. In such a case, the complete polarisation curve should have the form shown in curve III (fig. 4). The general type of curve obtained experimentally is shown in curve IV. The position is not the same for all metals, and therefore the potential cannot depend merely on the oxygen and hydrogen concentration in the bulk of the solution. There is little doubt, however, that the branch BC represents depolarisation by oxygen, and the branch DE evolution of hydrogen, which

can be seen rising in bubbles. Except in the platinum curve, there is also a horizontal branch (AB) the meaning of which is discussed later ; on magnesium, zinc and iron, this horizontal comes so low as to cut off the portion BC. On the curves for platinum, silver and nickel (where the horizontal appears at a high level), there exists between the typical oxygen and hydrogen portions an intermediate feature (CD) which may, perhaps, correspond to depolarisation by some less active form of oxygen, only capable of removing hydrogen at a depressed potential. This portion (CD) was invariably obtained on curves with platinum, silver and nickel, which were repeated sufficiently to ensure that the peculiar shape was not due to some chance irregularity.

It may be interesting to note that metals yielding curves with the horizontals cutting the oxygen part of the curve (nickel and iron) are those which normally suffer the oxygen-absorption type of corrosion in neutral solution.* Magnesium which gives a curve with a horizontal cutting the hydrogen portion, readily liberates free hydrogen gas from neutral salt solution. Zinc, whose horizontal is not far from the place where the oxygen and hydrogen portions pass into one another, is attacked partly by absorption of oxygen and partly by liberation of hydrogen. Platinum, which suffers practically no corrosion, appears to give no horizontal.

The existence of the horizontal portions is of the greatest importance. The current density at the corner point B, represents the "protective current density" just sufficient to prevent attack ; this was verified in the case of steel by special experiments using ferricyanide as indicator. If, at this point, no corrosion is proceeding, there is no local current, and therefore the whole of the current flowing must pass through the ammeter, the reading of which is an accurate measure of the protective current density. At A, the potential is the same as at B, hence (since the potential depends on the current density), the current density developed on the cathodic portions of freely corroding specimens, must also become equal to the protective value. Now in these specimens, the cathodic area represents almost the whole area of the specimen. Hence it is proved that, in the absence of an applied current, the corrosion, starting at weak points, will extend out until the current density on the cathodic portions reaches the protective value, which will prevent further development of the attack. Thus the law defining the limit of extension of the anodic areas is established.

* Iron actually liberates a considerable amount of hydrogen when "rusting" in a neutral solution, but G. Schikorr ('Z. Elektrochem.,' vol. 35, p. 65 (1929)) has shown that this may arise in part from the decomposition of water by ferrous hydroxide.

The fact that different cathodes give different polarisation curves shows clearly that the electrode is *not* acting as a simple oxygen electrode, as some of those who have discussed differential aeration have supposed. Evidently the oxide-film is not impervious to the ions present in the solution, and the nature of the metal below it exerts as great an influence in determining the potential reached as the oxygen-concentration in the solution; the metal is, in effect, "exposed" to the solution at the weak points which occur at intervals in time and space, and this is true, not only over the horizontal parts of the curves, but also over the sloping portions. It may be asked why no corrosion is seen on the sloping portion. The explanation is that—at current densities above the protective value—potassium hydroxide is produced sufficiently close to the weak points to ensure that any iron salts which diffuse through the film are precipitated at the surface itself, thus healing up the weak points in question; this healing is indicated by the rise of the potential with time. The precipitation of hydrated ferric oxide close to surface is not merely an *ad hoc* hypothesis; in some special experiments with rotating iron cathodes, interference tints were obtained on the sloping portion of the polarisation curves.

Similar interference tints, undoubtedly due to hydrated ferric oxide, were noted, in earlier work, on the "cathodic zone" of half-immersed specimens in stagnant potassium chloride solution, without applied current, and also on the weakest parts of steel specimens in chloride-chromate solution, when the chromate concentration is adjusted so as to be just insufficient to stop all visible change. The anti-corrosive action of chromate—like that of an externally applied cathodic current—is to ensure that the rust is produced close to the film, thus healing its defects. In the absence of chromate, the renewal of oxygen to the circle of oxide-skin immediately surrounding the weak point is insufficient to maintain the cathodic area close up to the anodic point (which would ensure precipitation *in situ*, and healing of the defect). A ring of rust is formed at an appreciable distance from the point of origin, and such rust is not protective (it actually stimulates attack by screening from oxygen). In the presence of a sufficient supply of soluble chromate, depolarisation can continue very close to the defect; the cathodic ring is actually in contact with the pore in the skin, and precipitation occurs where it will heal the defect. This may occur even in the absence of chromate if the pores in the primary skin are very small, so that the current flowing is small; for instance in some of the special steels containing large amounts of chromium, no corrosion develops, and the rise in potential points to healing.

The idea that, in essential features, the anti-corrosive effects of chromates

and of cathodic treatment are identical is confirmed by some recent measurements of the protective current density.* It was found that the addition of chromates to a chloride solution, although enormously influencing the distribution of free corrosion, does not sensibly affect the current density which must be applied from an external source to prevent attack altogether. If chromate-protection depended on a different principle to cathodic protection (*e.g.*, if the effect of chromate were to reduce the defects of the primary film by direct oxidation) one would expect that in presence of chromate a smaller cathodic current density would be needed to stop the attack entirely. If, however, the function of large amounts of chromate is to facilitate depolarisation of the local currents, thus causing the cathodic area to extend to within molecular distance of the cracks, smaller amounts of chromate (insufficient to prevent corrosion by themselves) will not reduce the externally applied current density to prevent attack completely, for at the limiting current density when corrosion vanishes, the current contributed by the local circuit also vanishes. No doubt the chromate, as a depolariser, will reduce the *e.m.f.* required to produce the protective current density; but the protective value of the current in the chloride-chromate solution will be no lower than in the absence of chromates.

A similar principle is involved in several methods of preventing the corrosion of iron. The formation of an insoluble product close to the weak spots in the primary oxide-film (thus automatically healing these defects) can be brought about in various ways :—

- (1) A salt like sodium phosphate can be added so that the immediate anodic product is a sparingly soluble body.
- (2) The article may be subjected to a cathodic treatment from an external source of *e.m.f.*; in this way, the cathodic areas on the specimen are made to extend right to the edges of the microscopic defects which at first form the anodic points, and thus allow the rust to be precipitated where it will seal the defects.
- (3) An excess of a depolariser may be added which will permit the cathodic areas of the local circuits to extend up to the edge of the defects and thus seal them with rust. For this purpose a chromate is commonly employed;† but other oxidising depolarisers, like hydrogen peroxide‡

* U. R. Evans, "Metals and Alloys," February, 1931.

† It is possible, that, with chromate, the co-precipitation of hydrated chromic oxide may assist in the healing, but this has never been proved.

‡ H. Wieland and W. Franke, 'Liebigs Ann. Chemie,' vol. 469, p. 257 (1929).

and even oxygen, which promote corrosion at low concentrations, act as inhibitors if supplied in sufficient quantity. In the case of oxygen, which has a low solubility, it is difficult to ensure rust-production sufficiently close to the point of attack to seal the defect entirely; but the rate of attack definitely falls off when the oxygen-pressure is made very high,* or when the flow-rate (and therefore the rate of renewal of oxygen) is made very rapid.†

In all these cases, no change will be visible when the anti-corrosive agent (or current) has been applied in sufficient strength. It is only when the treatment is just insufficient that the rust thickens sufficiently to give interference tints; if the strength is made still more insufficient, the tints indicate a still thicker film, and in extreme cases pass into typical rust blisters.

One of the authors (L. C. B.) gratefully acknowledges the assistance afforded by a Fellowship of the Salters' Institute of Industrial Chemistry.

SUMMARY AND CONCLUSIONS.

It has been shown experimentally that—under conditions favourable for the complete tapping of the electric currents flowing between the anodic and cathodic portions of corroding metal—the currents measured are equivalent to the corrosion produced; this is true not only (a) in cases when the anodic and cathodic areas consist of different metals, but, also (b) in cases where the whole specimen consists of one metal, the anodic and cathodic areas being determined by differences in oxygen-concentration. Thus the problem of corrosion velocity resolves itself into a study of the electrochemical factors which determine the strength of this current.

Owing to polarisation, the cathodic and anodic potentials tend to approach one another as the current flowing is increased. It is obvious that the strength of current can never exceed the value which would cause the two potentials to meet. This sets a limiting value for the corrosion-rate under any particular conditions, which can never be exceeded, however low the resistance of the circuit is made; the current-strength cannot be obtained by assuming a fixed value for the e.m.f. and dividing this by the resistance. Experiments shows that there is an approximation to "equipotential conditions" at fairly high concentrations, but that the anodic and cathodic potentials remain far apart

* G. Schikorr, 'Korr. Met.', vol. 4, p. 242 (1928).

† E. Heyn and O. Bauer, 'Mitt. K. Materialprüfungsamt,' vol. 28, pp. 93, 130 (1910); J. A. N. Friend, 'J. Chem. Soc.,' vol. 119, p. 932 (1921).

in dilute solutions, where, owing to the low specific conductivity, an appreciable residual e.m.f. is needed to force even the small corrosion-current round the circuit. Some caution is needed in interpreting the experimental results, since it is possible that in certain cases the part of the circuit between the anodic circuit and the anodic tubulus may have an appreciable resistance; this may occur for instance (1) when the primary skin has only occasional weak points (as on stainless steel), (2) if the anodic surface becomes covered with an undissolved layer of the anodic product (which may conceivably occur with ordinary iron or steel in concentrated solutions).

In most cases, the polarisation which limits the corrosion-rate, occurs at the *cathodic area*, and is due to *limitations in the rate of oxygen-supply*. Cathodic polarisation curves, under controlled conditions of oxygen-supply, have been traced for a number of metals. These curves end at high potentials in a horizontal branch which serves to indicate the law governing the ratio of anodic and cathodic areas. When corrosion starts at a weak point in the invisible film covering the surface of a metal, *the area undergoing attack extends (or contracts) until the cathodic current density on the part remaining unattacked is equal to the "protective value"*; the current flowing under these conditions will define the rate of corrosion. The protective value is the current density which will cause any incipient attack on a weak point within the area in question to lead to the precipitation of rust so close to the surface as to seal the defect.

This principle is utilised in the cathodic method of preventing corrosion, and several other methods of protection depend on what is really the same principle.

*On a Night Sky of Exceptional Brightness, and on the Distinction
between the Polar Aurora and the Night Sky.*

By LORD RAYLEIGH, For. Sec. R.S.

(Received March 12, 1931.)

[PLATE 15.]

For more than seven years past I have had in progress systematic photometric measurements on the brightness of the night sky as seen through certain colour filters.*

These filters are designed to isolate separate portions of the spectrum in the red, green, and blue. The green one isolates as nearly as possible the light of the green auroral line due to oxygen, but the isolation is very imperfect, and, in fact, the continuous background of the spectrum often contributes more to the transmitted light than does the auroral line.†

Considerable variations in each of the components have been found from time to time, but the primary object of this note is to describe an extreme case when the intensity was something altogether beyond the common, and in my experience unexampled. The accompanying magnetic conditions will be discussed, and it will then be considered whether this case in particular, and the light of the night sky in general, can be classified with the polar aurora. It may be stated at once that the conclusion will be in the negative.

The observations were at my home in Essex (latitude 52° N.) and the exceptional conditions were first noticed at 11.25 p.m. on the evening of Friday, November 8, 1929. The moon had set, and the sky was clear, which it had not been on several previous nights. On looking out from a north window it was noticed at once without instrumental aid that the sky was exceptionally bright, and on going out into the open the exceptional brightness was seen all over the visible hemisphere, no direction being obviously favoured.

Although the sky was apparently quite clear, and the brighter stars gave the impression of being very bright, the luminous background was strong enough to make it difficult to distinguish the Milky Way, which, it was judged, was invisible for the same reason that it is invisible when the moon is up—namely, that there is too much “false light” superposed upon it.

* ‘Proc. Roy. Soc.,’ A, vol. 106, p. 117 (1924); vol. 109, p. 428 (1925); vol. 119, p. 11 (1928).

† ‘Proc. Roy. Soc.,’ A, vol. 129, p. 465 (1930).

On examining the spectrum of the sky in various directions with a spectro-scope, specially designed for this kind of work,† it seemed to be continuous, and could be observed with a much narrower slit than can ordinarily be used on the night sky. To my surprise, however, I was not able to see the aurora line distinctly. It has often been well seen when the general illumination of the sky was much lower, and was probably concealed on this occasion by the exceptional brightness of the continuous spectrum. Unfortunately I had no suitable spectrograph in adjustment ready to take a photograph, for there had been no kind of warning that it would be needed.

The sky was next examined with the photometric instruments which are in regular use and in which the filtered light is compared in intensity with a self-luminous radioactive source of potassium uranyl-sulphate.

The following table gives the readings on the standard scale formerly explained.‡ The scale is such that when we pass up one unit the intensity is multiplied by the anti-logarithm of 0.1 or 1.259. Three units on the scale are equivalent to an intensity factor of $(1.259)^3$, or approximately a doubled intensity. The readings are usually taken to the nearest unit, but fractions are introduced by correcting from the instrument actually used to the master standard instrument (*loc. cit.*). In the table, the abnormal period is included between the two horizontal lines. I have given, for the sake of comparison, readings for the nearest observation before and after the abnormal period, also the general mean for the period 1925-26 formerly published, and the lowest values that have ever been observed.

Date (1929).	Hour.	Red.	Green (auroral).	Blue.
Thursday, October 31	8.15 p.m.	-2.3	+2.7	+6.7
Sunday, November 3	9.55 p.m.	-1.3	+2.7	+6.7
Friday, November 8	11.25 p.m.	+2.7	+6.7	+12.7
Saturday, November 9	0.15 a.m.	—	—	+12.7
Saturday, November 9	2.15 a.m.	—	—	+12.7
Saturday, November 9	5.40 a.m.	—	+6.7*	+12.7*
Saturday, November 9	10.55 p.m.	+0.7	+4.7	+9.7
Sunday, November 10	12.0 midnight	+0.7	+4.7	+9.7
Wednesday, November 20	6.15 p.m.	-1.3	+0.7	+6.7
General mean, 1925-1926		-2.5	+0.5	+6.4
Lowest observed so far		-5.3	-2.3	+4.2

* Doubtful, owing to possible influence of daylight. (See below.)

† Gerland's 'Beiträge der Geophysik,' vol. 19, p. 292 (1928).

‡ 'Proc. Roy. Soc. 'A, vol. 119, p. 11 (1928).

While, therefore, the relative intensities of the various components remained much as usual, the absolute intensities were about four times the ordinary, and about eight times the minimum that has ever been observed.

The same conditions prevailed unchanged until 2.15 a.m. on the morning of November 9. It was my intention to observe again before dawn, but unfortunately being overtired I was not quite up to time, and did not get the observation until 5.40 a.m., when there may have been a trace of daylight. The actual measurement was still unchanged at the high value of the previous night, but owing to the possible effect of daylight, it cannot be relied upon.

On the evening of November 9 it was not possible to observe till late, because the moon was up. At 10.55 p.m. the intensities were still very high, but no longer unprecedented. They were about equal to the highest recorded in earlier years.

On November 10 the values were the same as on November 9.

I was not able to get another observation until November 20, when the conditions were found to have returned to normal.

It is much to be regretted that the stations in the southern hemisphere which are observing with instruments of the same kind, namely, the Cape Observatory and Canberra Solar Observatory, did not observe on November 8 owing to the unfavourable phase of the moon.

A large number of stations in all parts of the British Isles report to the Meteorological Office the clearness or otherwise of the sky, and the occurrence of aurora, if any. It is remarkable that no station in England reported aurora on November 8, though there was clear sky over practically the whole of England south of the Humber. It is evident at least that the bright sky which I observed is not what the meteorological observers are accustomed to call an aurora, though it is to me surprising that none of them seem to have drawn attention to it in any way as a noteworthy phenomenon.

Max Wolf* describes a bright night sky for two or three nights early in July, 1908, which did not show the aurora line, and which he attributed to dust in the higher atmosphere which gradually sank. So far as can be judged from his description this does not seem to have been the same phenomenon as the one here recorded.

We have now to consider whether this exceptionally brilliant night sky showed any of the characteristics of the polar aurora. My answer is that it did not. The reasons for this opinion will be best brought out by contrasting it with the only undoubted polar aurora that I have seen extending to the

* 'Ast. Nach.,' vol. 178, p. 4266 (1908).

zenith in the same place of observation (latitude 52° N.).* This was the world-wide aurora of May 13-14, 1921. The features in these two cases are tabulated below for comparison.

At Terling (latitude 52° N.).

November 8, 1929.

Luminosity extends uniformly over the sky.

Intensity perfectly constant by photometric measurement for 2 hours, and possibly much more.

Visual spectrum continuous, aurora line not definitely seen.†

Range of horizontal magnetic force 16γ from first observation till morning.‡

Range of declination 1 minute of arc from first observation until morning.

Chromatic constitution of light nearly the same as on ordinary nights.

May 14, 1921.

Luminosity very patchy. Extended beyond zenith, but more intense north than south.

In constant flickering movement every few seconds with change of colour and intensity.

Visual spectrum consists mainly of the aurora line.†

Range of horizontal magnetic force off scale of instrument but at least 550γ .

Range of declination off scale of instrument. At least $1^{\circ} 50'$, thus more than 110 times as great as on night of November 8, 1929.

Light far more actinic than on ordinary nights. Actinic quality due to nitrogen bands.

Although the methods of investigation in use were not altogether the same at the times of these two events (separated by 8 years) the contrast between the two cases stands out very clearly. I have tried in the above table to formulate specific differences. In addition to these a certain general impression is left on the observer's mind which is very strong and may have some independent weight. It is to the effect that the phenomena of May 14, 1921, were of an essentially different nature from those of November 8, 1929.

In my experience the most striking distinction between the light of the ordinary night sky and that of the polar aurora is that the latter alone shows the negative nitrogen bands.

* Auroras low down in the north have been seen comparatively often.

† The visual observations are not adapted to decide whether the negative bands of nitrogen are present or not, as the stronger of these are too far in the blue.

‡ There was a disturbance of 40γ about $1\frac{1}{2}$ hours before the first sky observation.

It must, of course, be admitted that no actual observation can do more than set a limit to the possible intensity of these bands. The statement that the bands are absent in a periphrasis, merely indicating that a severe test does not give rise to any suspicion of their presence. This has been my own experience, and was set out as one of the grounds for regarding the night sky luminosity as a phenomenon of different origin from the polar aurora.* L. A. Sommer† has contested this conclusion and finds reason to think that the nitrogen bands are normally present in the night sky, at any rate over Göttingen.

It remains, however, that my own long exposure photographs‡ do not show any trace of these bands, while they do show two bright lines or (possibly) band heads which I may refer to as X_1 and X_2 , the wave-lengths of which were given as 4435 and 4210. As Sommer is unable to find any features corresponding with these, it would seem that the difference between us cannot be altogether explained by insufficient exposure of my own plates, and that it remains to be cleared up in some other way.

To assist in an objective judgment I was anxious to reproduce one of the two spectrograms on which these were recorded. Unfortunately neither of them was quite strong enough for the purpose, though the lines mentioned were evident enough on both, an opinion in which I understood my friends, Professors A. Fowler and T. R. Merton, to concur. As a better alternative I here reproduce (in negative, with the bright lines showing black) a photograph of the night sky spectrum taken by Dr. V. M. Slipher at the Lowell Observatory, and mentioned in my previous paper (*loc. cit.*, p. 51). It shows essentially the same features as my own plates, with better intensity. I am unable to see the nitrogen bands upon it, though the bright aurora line 5577, the unidentified bright lines marked X_1 and X_2 , and the dark lines G, H, K and H_2 come up well. For comparison, my own photograph of the aurora of May 14, 1921, is reproduced below on approximately the same scale. It shows the green line 5577 in about the same intensity as the upper photograph. If we compare the nitrogen bands in the lower photograph with the places where they should appear in the upper one, I think we shall see good ground for making a distinction. The night sky alone shows the lines X_1 and X_2 , and the auroral spectrum alone shows the nitrogen bands.

For further evidence of the same kind reference may be made to a paper by MacLennan and Ireton§ in which are reproduced a large number of spectro-

* 'Proc. Roy. Soc.,' A, vol. 106, p. 136 (1924).

† 'Z. Physik.,' vol. 57, p. 582 (1929).

‡ 'Proc. Roy. Soc.,' A, vol. 103, p. 51 (1923).

§ 'Canadian Journal of Research,' vol. 2, p. 279 (1930).

K H X₂ G X₁ 5578
✓ ✓ ✓ ✓ ✓

Night Sky.
Polar Aurora.

3914 4278 4709 5578

grams taken in England and in various parts of Canada. Study of these and of the accompanying text clearly shows that while the green line 5577 comes up strongly in the normal night sky, the nitrogen bands only accompany it when the geographical locality and the distribution of the light into streamers and other characteristic forms indicates that the polar aurora is present.

This is entirely in agreement with my own experience in comparing photographs taken in Shetland and in the south of England.* Sommer† mentions that V. M. Slipher has photographed the nitrogen bands in the west, before the last glimmer of daylight has disappeared, and Professor MacLennan informs me that he has confirmed this observation. But, apart from the evidence brought forward by Sommer himself, there seems to be no confirmation of their presence when night conditions are fully established.

Since Slipher's photograph of the night sky spectrum was on a better scale than my own *very* small spectra, it was measured to give a value for the wave-length of the unknown lines or band heads X_1 and X_2 . After trial of various methods, it was found that the measurement was best made with an ivory scale divided into 1/50ths of an inch, estimating to 1/10 division.

A Cornu-Hartmann interpolation formula was calculated, using the dark Fraunhofer lines H and G, and the bright auroral line 5577·3 as fiducial wave-lengths. X_1 came out as 4419 and X_2 as 4168. As a check H_α was measured, and the wave-length found was less than 2 Å. in excess of the true value. These values are regarded as considerably more trustworthy than the old ones, from the smaller and less well-exposed photographs. The climate of England is very unfavourable for work of this kind.

Summary.

An exceptionally bright night sky on November 8, 1929, is described, with photometric observations. It was of about four times the ordinary brightness, and eight times the minimum ever observed. It was of the same chromatic constitution as usual, and the aurora line was not conspicuous. There was no accompanying magnetic disturbance. This is contrasted in detail with the aurora of May 14, 1921.

Spectra of the aurora and of the normal night sky are reproduced for comparison. Nitrogen bands are absent in the latter.

Two unidentified bright lines in the night sky spectrum are remeasured. The wave-lengths found are 4419 and 4168.

* 'Proc. Roy. Soc.,' A, vol. 101. p. 312 (1922).

† *Loc. cit.*, p. 598, footnote.

The Behaviour of Electrolytes in Mixed Solvents. Part III.—The Molecular Refractivities and Partial Molar Volumes of Lithium Chloride in Water-Ethyl Alcohol Solutions.

By J. A. V. BUTLER, D.Sc., and A. D. LEES, B.Sc., University of Edinburgh.

(Communicated by J. Kendall, F.R.S.—Received March 5, 1931.)

The Refractivities.

It is well known that the molecular refractivity of most salts, as calculated by the Lorentz-Lorenz formula, is nearly independent of the concentration in moderately dilute aqueous solutions. Walden* determined the refractivities of tetra-ethyl-ammonium iodide and other similar salts in a variety of solvents and found that, while the molecular refractivity was approximately independent of the concentration in each solvent, it varied from one solvent to another, the greatest variation from the value in water, amounting to about 2 per cent., being obtained in nitro-methane. Schreinert† has recently determined the molecular refractivity of hydrogen chloride and lithium chloride in methyl and ethyl alcohols, and found that in the case of lithium chloride the value is independent of the concentration up to a concentration of about 3 M. His values for R_D^{20} for lithium chloride are: 8.73 in water, 8.55 in methyl alcohol and 8.38 in ethyl alcohol. The difference between the values in water and ethyl alcohol appeared to make it just possible to determine the variation of the refractivity with the composition of the solvent in mixtures of water and the alcohol. It is possible that a solvent might be found, miscible in water in all proportions, in which the value of R is further removed from that in water. Such a substance would be more suitable than alcohol for the investigation of this effect, but in order to correlate the results with the measurements recorded in Part II of the activities of alcohol and water in water-alcohol-lithium chloride solutions, it seemed desirable to investigate this case in the first instance.

The variation of the refractivity of a salt with the composition of a mixed solvent may be expected to give some indication of the composition of the solvent in the immediate vicinity of the ions. For the refractivity of a salt is determined by (1) the polarisability of the ions themselves and (2) the change in the polarisability of the solvent produced by their presence. The molecular

* 'Z. Phys. Chem.,' vol. 59, p. 385 (1907).

† 'Z. Phys. Chem.,' vol. 135, p. 461 (1928).

refractivity of a salt in a solution containing m grams of a salt in w grams of the solvent is taken as

$$R = \frac{M}{m} \left(\frac{n^2 - 1}{n^2 + 2} \cdot \frac{w + m}{d} - \frac{n_0^2 - 1}{n_0^2 + 2} \cdot \frac{w}{d_0} \right), \quad (1)$$

where n , and d and n_0 , d_0 are the refractive index and density of the solution and of the solvent, respectively, and M the molecular weight of the salt. According to the Lorentz-Lorenz theory

$$\frac{n^2 - 1}{n^2 + 2} \cdot \frac{w + m}{d} = \frac{4}{3}\pi [\sum_s v_s \alpha_s + \sum_i v_i \alpha_i],$$

where v_s is the number of molecules of solvent in the weight w for which the coefficient of polarisability by externally applied fields is α_s and v_i is the number of ions in m grams of the salt having the coefficient of polarisability α_i . Similarly

$$\frac{n_0^2 - 1}{n_0^2 + 2} \cdot \frac{w}{d_0} = \frac{4}{3}\pi \sum_s v_s' \alpha_s',$$

so that we may write

$$R = R_{\text{ions}} - \Delta R_{\text{solvent}},$$

where

$$R_{\text{ions}} = \frac{4}{3}\pi \frac{M}{m} \sum v_i \alpha_i,$$

and

$$\Delta R_{\text{solvent}} = \frac{4}{3}\pi \frac{M}{m} [\sum v_s' \alpha_s' - \sum v_s \alpha_s].$$

The molecular refractivity (R_D^{18}) of lithium chloride when completely ionised, in the gaseous state, according to Fajans and Joos* is 9.2. On the basis of this value, $\Delta R_{\text{solvent}}$ is 0.5 in water and 0.8 in ethyl alcohol. Without laying any stress on these values, it is evident that since the molecular refractivities of water and alcohol are 3.7 and 12.8, $\Delta R_{\text{solvent}}$ is only a small fraction of the total refractivity of the molecules which are in actual contact with the ions. Since the electric field decreases rapidly with the distance from any ion, it is reasonable to assume that only those molecules which are in contact with an ion have a lower polarisability than those which are not so situated. Then in the case of a mixed solvent containing molecules of two kinds, we shall have

$$\Delta R_{\text{solvent}} = \frac{4}{3}\pi [v_1 (\alpha_1' - \alpha_1) + v_2 (\alpha_2' - \alpha_2)],$$

where v_1 and v_2 are the numbers of molecules of the two kinds which are in contact with the ions of a gram molecule of the salt and $\alpha_1' - \alpha_1$ and $\alpha_2' - \alpha_2$,

* 'Z. Physik,' vol. 23, p. 1 (1924).

the average difference of polarisability produced by the ions in these molecules. Thus if we write

$$\Delta R_W = \frac{4}{3}\pi v_1^{\circ} (\alpha_1' - \alpha_1),$$

$$\Delta R_A = \frac{4}{3}\pi v_2^{\circ} (\alpha_2' - \alpha_2),$$

for the solvent effect of a gram molecule of the ions in alcohol and in water respectively, we have

$$\frac{R_W - R_S}{R_W - R_A} = \frac{\Delta R_W - \Delta R_S}{\Delta R_W - \Delta R_S} = f_A,$$

where the suffixes W, A and S refer to solutions in water, alcohol and a mixed solvent and $f_A = v_2/v_1^{\circ}$ is the ratio of the number of alcohol molecules in contact with the ion in the given solvent to the corresponding number in alcohol.

We have determined the refractivities of lithium chloride in a number of mixed solvents of water and alcohol. The materials and solutions were prepared by the methods described in Part II of this series. The refractive indices of the solutions were determined by means of a Pulfrich refractometer. In order to obtain greater accuracy than is given by direct readings of the divided circle, we used a divided cell containing the solution on one side and the corresponding solvent on the other. The difference of refractive index of these two liquids was obtained from the reading on the small drum of the angular separation of the two lines visible in the field of view. In this way the refractive index difference between the solution and its solvent can be measured within ± 0.00002 . The refractive indices of the solvents were measured directly at 18° C., but great accuracy is not essential, for a considerable variation in the value does not affect the calculated refractivity of the salt. All measurements were made with the mercury green line ($\lambda = 5461$ A.U.). The densities of the solutions were determined at 18.1° C. in a silica pyknometer, the capacity of which was about 15 c.c.*

The experimental data and the molecular refractivities of lithium chloride, calculated by formula (1), are given in Table I. The density measurements of the more dilute solutions recorded in this table are used below in connection

* When the measurements were completed, we found that an error in the calibration of the thermometer had been made and that the density measurements had been made at 18.1° C. and not at 18.0° C., as we intended. The molecular refractivity depends ultimately on the difference of refractive index and of density between the solvent and the solution and so long as the differences are measured when the solvent and the solution have the same temperature, a small difference between the temperature at which the densities and the refractive index differences are measured does not affect the value of R.

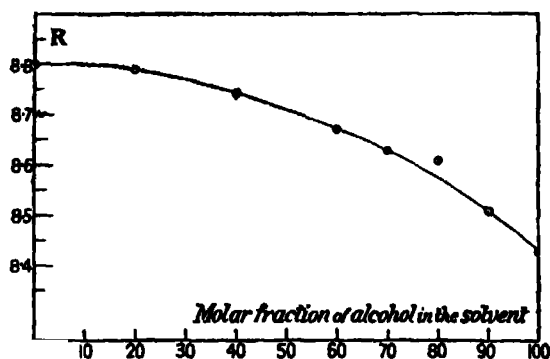
Table I.—Refractive Indices and Densities of Solutions of Lithium Chloride in Water-Alcohol Mixtures.

Molar fraction of alcohol.	Concentration of lithium chloride (m).	$d_4^{18.1}$	n_{D461}^{18}	R_{5461}^{18}	$V - V_e$
0.00	0.0000	0.99860	1.33410	—	—
	0.3980	1.00814	1.33762	8.81	7.34
	0.4611	1.00972	1.33824	8.81	8.33
	0.6839	1.01494	1.34021	8.81	12.45
	0.7264	1.01597	1.34055	8.81	13.28
	0.9654	1.02123	1.34250	8.78	17.48
	1.1235	1.02500	1.34392	8.79	20.69
0.20	0.0000	0.93817	1.35911	—	—
	0.1432	0.94173	—	—	2.42
	0.2206	0.94352	—	—	3.87
	0.3559	0.94672	1.36208	8.82	6.31
	0.6318	0.95306	1.36426	8.81	11.46
	0.7989	0.95692	1.36556	8.79	14.51
	1.2812	0.96801	1.36936	8.77	23.26
0.40	0.0000	0.88633	1.36538	—	—
	0.2402	0.89220	—	—	3.08
	0.3456	0.89470	1.36813	8.74	5.82
	0.4747	0.89757	1.36905	8.74	8.30
	0.5098	0.89840	1.36932	8.75	8.91
	1.2312	0.91484	1.37472	8.75	21.90
0.60	0.0000	0.84713	1.36696	—	—
	0.1693	0.85217	—	—	2.44
	0.3800	0.85699	1.37013	(8.50)	5.21
	0.6436	0.86326	1.37225	8.69	9.57
	0.9056	0.86919	1.37411	8.68	14.19
	1.5207	0.88330	1.37857	8.66	24.55
	1.9770	0.89212	1.38108	8.64	34.43
0.70	0.0000	0.83097	1.36678	—	—
	0.0833	0.83324	—	—	1.02
	0.1361	0.83481	—	—	1.38
	0.2442	0.83754	1.36896	8.60	2.92
	0.6830	0.84869	1.37264	8.65	9.00
	1.0173	0.85679	1.37522	8.63	14.08
0.80	0.0000	0.81664	1.36601	—	—
	0.2093	0.82267	—	—	1.81
	0.3786	0.82714	1.36958	8.64	3.85
	0.8023	0.83839	1.37330	8.60	8.81
	1.7392	0.86164	1.38078	8.59	21.66
0.90	0.0000	0.80321	1.36485	—	—
	0.1359	0.80745	—	—	0.60
	0.2800	0.81168	1.36780	8.50	1.63
	0.5188	0.81854	1.37013	8.50	3.56
	0.7426	0.82476	1.37225	8.53	5.66
	1.2301	0.83751	1.37645	8.52	11.30
1.00	0.0000	0.79084	1.36322	—	—
	0.1450	0.79584	—	—	-0.22
	0.2030	0.79776	—	—	-0.18
	0.3008	0.80082	—	—	+0.17
	0.4954	0.80683	1.36893	8.44	0.98
	0.7334	0.81397	1.37140	8.43	2.31
	1.0230	0.82224	1.37422	8.44	4.47
	1.2339	0.82808	1.37615	8.42	6.32

Table II.—Molecular Refractivities and Partial Molar Volumes of Lithium Chloride in Water-Alcohol Solutions.

Molar fraction of alcohol.	R^{18} .	$100f_A = \frac{R_W - R_{\infty}}{R_W - R_A}$	Partial molar volumes of lithium chloride.	
			0.5 m.	1.0 m.
0.00	8.80	0	18.3	18.6
0.20	8.79	3	18.1	18.4
0.40	8.74	16	17.8	17.9
0.60	8.67	36	16.1	16.8
0.70	8.63	46	14.2	15.1
0.80	8.61	51	11.6	13.5
0.90	8.51	78	9.1	11.6
1.00	8.43	100	5.2	8.1

with the partial molar volumes. The refractivity of lithium chloride is constant, within the experimental error, in each solvent. The mean values for the different solvents are given in Table II, and are shown plotted against the molar fraction of alcohol in the solvent in fig. 1. It can be seen that there

FIG. 1.—Molecular Refractivities (R_{5461}^{18}) of Lithium Chloride in Water-Alcohol Solvents.

is little change in the value of R until the molar fraction of alcohol is greater than 0.2. Beyond this point it falls off steadily, as the proportion of alcohol is increased, to the value for pure alcohol. We may therefore conclude that the ions are surrounded almost entirely by water molecules until the molar fraction of alcohol in the solvent reaches about 0.2. From this region, the number of alcohol molecules in contact with the ions increases steadily as the proportion of alcohol is increased. This is in agreement with the conclusions

drawn by Shaw and Butler in Part II* from the effect of lithium chloride on the vapour pressures of similar solutions.

The Partial Molar Volumes.

The variation of the density of the solutions with the lithium chloride concentration is greatly affected by the proportion of alcohol present. This may be illustrated by fig. 2, which shows the change of volume produced by the addition of lithium chloride to 1000 grams of the various solvents. Whereas

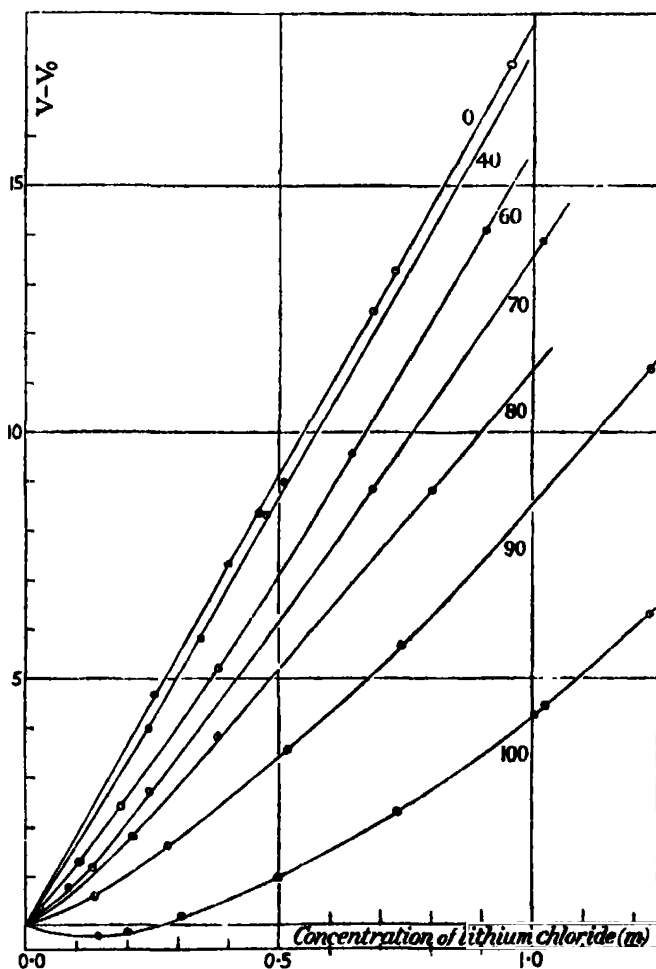


FIG. 2.—Differences between the Volumes of Solutions of Lithium Chloride in Water-Alcohol Mixtures and the Volume of the Solvent, plotted against the Concentration of Lithium Chloride. (Molar fractions of alcohol in the solvent are given by the figures in the diagram.)

* 'Proc. Roy. Soc.,' A, vol. 129, p. 519 (1930).

the addition of lithium chloride to water gives rise to a nearly linear increase of volume, in alcohol it causes a decrease in the total volume at small concentrations and an increase at greater concentrations.

The change of volume of the solution is calculated as follows: The volume of 1000 grams of the solvent (density d_0) is $V_0 = 1000/d_0$, and that of a solution (density d) containing Mm grams of lithium chloride in 100 grams of the solvent is $V = (1000 + Mm)/d$. The increase of volume of the liquid on the addition of the salt is therefore

$$\Delta V = V - V_0 = (1000 + Mm)/d - 1000/d_0.$$

The partial molar volume of lithium chloride $\bar{V} = (dV/dm)$ at a given concentration is determined by taking the slope of the curve of m at the corresponding value of m . The values obtained at $m = 0.5$ and $m = 1.0$ are given in Table II and are shown graphically in fig. 3.

We may first observe that the partial molar volumes of the salt in 100 per cent. alcohol are much smaller than in water. The molecular volume of solid lithium chloride at 18° is 20.5 .* Its partial molar volume at $m = 1$ is 18.6 in water and 8.1 in 100 per cent. alcohol. Since the partial molar volume in a given solution is the increase of volume of the solution, per gram of salt added, when a small quantity of the salt is added to the solution, the difference between the molecular volume of the solid and its partial molar volume represents the contraction, per gram molecule of salt, when a small quantity of the latter is added to the given solution. There is thus a contraction of 1.9 mls. per gram molecule when lithium chloride is added to the solution in water ($m = 1$), and of 12.4 mls. per gram molecule when added to the solution in alcohol of the same strength. We have no means of determining how much of this change of volume is due to a change in the intrinsic volume of the lithium chloride, and how much is due to the contraction of the solvent caused by the presence of the salt. But since it is entirely improbable that the intrinsic volume of lithium chloride in alcoholic solution is little more than a third of the volume of the solid salt, we must conclude that the contraction of the solvent (electrostriction) produced by the salt is considerably greater in alcohol than in water. We think that the determination of the partial molar volumes of a salt in a series of solvents would reveal some interesting effects.

Secondly, whereas in water an increase in the concentration of the salt causes only a small increase in the partial molar volume, in 100 per cent. alcohol it produces a very great change. The partial molar volume of lithium

* Baxter and Wallace, 'J. Amer. Chem. Soc.,' vol. 38, p. 70 (1916).

chloride in 100 per cent. alcohol, as can be seen from fig. 2, is negative at small concentrations and increases rapidly with the concentration becoming 5.2 at $m = 0.5$ and 8.1 at $m = 1$. Baxter and Wallace (*loc. cit.*), who determined the "apparent molar volumes" ($\Delta V/m$) of the halogen salts of all the alkali metals in aqueous solution, suggested that the increase with concentration might be due to an increase in the proportion of unionised molecules. If this were the true explanation, it would imply a considerable change in the degree of ionisation in alcoholic solution between $m = 0$ and $m = 1$. Unless the undissociated salt and its ions have the same molecular refractivity, which is unlikely, such a change might be expected to cause variations in the molecular refractivity, which have not been observed. It may be suggested that a possible cause of the effect might be found in collisions between two ions, which become more frequent as the concentration is increased, and cause a certain amount of disorientation of the sheaths of solvent molecules carried by them, and thus give rise to an increase of volume. This effect would be greater when the ions are surrounded by alcohol molecules, than in water. A more detailed discussion, however, would be unprofitable with the data at present available.

Thirdly, we may consider the change in the partial molar volume with the composition of the solvent, at a constant concentration of lithium chloride. The form of the curves (fig. 3) is very similar to the variation of the molecular refractivities with the composition of the solvent. The presence of alcohol up to a molar fraction of about 0.4 causes only a small change in the partial

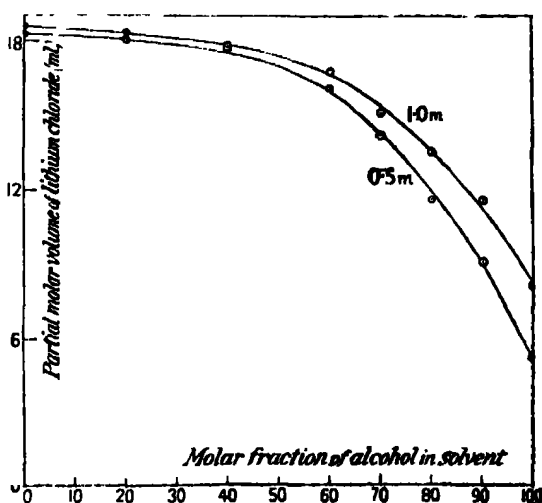


FIG. 3.—Partial Molar Volumes of Lithium Chloride in Water-Alcohol Solvents.

molar volume, but in solvents containing a greater proportion of alcohol the value decreases steadily.

It is noteworthy that whereas Walden (*loc. cit.*) found that the refractivity of tetra-ethyl-ammonium iodide varied inversely as its apparent molecular volume in a series of solvents, in the case of lithium chloride the refractivity decreases in the same direction as, but to a much smaller extent than, the change of volume. Walden's relation, therefore, cannot be generally true.

Summary.

(1) The molecular refractivities and partial molar volumes of lithium chloride have been determined in a series of water-alcohol mixtures.

(2) The molecular refractivity in each solvent is constant over the range of concentrations investigated. It is hardly affected by the presence of alcohol until the molar fraction of the latter is over 20 per cent. With greater proportions of alcohol it falls off steadily to the value for pure alcohol.

(3) On certain assumptions, the proportions of water and alcohol molecules in contact with the ions have been calculated. The proportion of water molecules in contact with the ions is always greater than their proportion in the solvent.

(4) The partial molar volume of lithium chloride is much smaller in 100 per cent. alcohol than in water, and increases rapidly with the concentration. Its variation with the composition of the solvent, at a constant concentration of the salt, is similar to that of the refractivity.

We are indebted to the Earl of Moray Fund of the University of Edinburgh for a grant for the purchase of apparatus. One of us (J. A. V. B.) has also to acknowledge a Carnegie Teaching Fellowship, held while the work was in progress.

*Valve Methods of Recording Single Alpha-Particles in the
presence of Powerful Ionising Radiations.*

By C. E. WYNN-WILLIAMS, Ph.D., Exhibition of 1851 Senior Student, and
F. A. B. WARD, Ph.D., Goldsmiths' Senior Student.

(Communicated by Lord Rutherford, O.M., F.R.S.—Received February 16, 1931.)

Introduction.

In 1926, Greinacher* showed that it was possible to detect single α -particles by linearly amplifying the ionisation current due to an α -ray by means of thermionic valves. Subsequently, he was also able to detect single H-particles by the same method. Other workers† have since applied the method to various radio-active problems in which the counting would otherwise have had to be done by means of scintillation screens or Geiger counters, etc. The present writers, working in conjunction with H. M. Cave,‡ also employed the method for determining the mean rate of emission of α -particles from radium C, by counting accurately the number of particles emitted within a defined solid angle.

While the problem of counting α - or H-particles can be a comparatively simple matter under certain conditions, there are many experiments necessarily carried out under conditions which render it utterly impossible to employ the Greinacher method in its original form. These experiments involve the counting of comparatively few particles in the presence of disturbances caused by powerful β - or γ -radiation, or by large groups of α -particles which it is not desired to count.

After the conclusion of the work described in Paper I, in July, 1929, the present writers spent considerable time in developing and modifying the original method, with the result that it is now possible to apply it to many problems which were previously out of the question. Such problems are the study of long and short-range α -particles emitted by various radio-active bodies, and of artificial disintegration phenomena.

* 'Z. Physik,' vol. 36, p. 364 (1926), and vol. 44, p. 319 (1927).

† Ortner and Stetter, 'Phys. Z.,' vol. 28, p. 70 (1927), and 'Z. Physik,' vol. 54, p. 449 (1929); Schmidt and Stetter, 'Z. Physik,' vol. 55, p. 467 (1929); Chadwick, Constable and Pollard, 'Proc. Roy. Soc.,' A, vol. 130, p. 463 (1931).

‡ 'Proc. Roy. Soc.,' A, vol. 125, p. 713 (1929). Hereafter referred to as Paper I.

In a recent paper by Lord Rutherford* and the present writers an account was given of the successful application of the method to the analysis of the short-range α -rays emitted from radium C, thorium C and actinium C. Similar work is now in progress with the long-range particles, and the results will be published shortly. The method is also being applied in the laboratory by Chadwick, Constable and Pollard, to problems connected with the artificial disintegration of elements.

For convenience, details of the amplifying and recording system, and of the methods employed for reducing the disturbance, were omitted from Paper II. It was felt that they would be of sufficiently general interest to warrant a separate description, particularly as valve methods of counting are now being adopted for general use. In the present paper, therefore, are described the apparatus and the methods which we have found to be successful in reducing the disturbances, together with precautions which must be observed. For the sake of completeness, a few points are recalled which are either well known in wireless practice, or which have already appeared in print elsewhere.

With regard to the reduction of the disturbances, it may be remarked that the methods we have found to be successful are almost identical with those described in a paper by Fränz,† which appeared while our experiments on the analysis of α -ray groups (Paper II) were in progress. Fränz, however, worked with a Geiger ball counter and a three-stage amplifier, and larger charges could therefore be given to the first valve grid than when a simple ionisation chamber is used, as in our experiments. This rendered the problem of reducing the magnitude of the disturbance a little simpler in his experiments.

General Considerations.

In view of the numerous papers that have already appeared bearing on this subject, little need be said concerning the mechanism of the process of amplification. Briefly, the ionic charge collected after the entry of a particle into the ionisation chamber is driven on to the insulated grid of the first valve, from which it eventually leaks away. The sudden rise and fall of grid potential is amplified with as little distortion as possible, until the corresponding anode current surge of the last valve is about 10 or 20 milliamperes, and sufficient to operate a recording device.

Experiments made with the Greinacher arrangement of amplifying and recording system used for the research described in Paper I showed that

* 'Proc. Roy. Soc.,' A, vol. 129, p. 211 (1930). Hereafter referred to as Paper II.

† 'Phys. Z.,' vol. 30, p. 810 (1929), and 'Z. Physik,' vol. 63, p. 370 (1930).

sufficient sensitivity was available to detect H-particles with ease, in the absence of β - or γ -radiation. The presence of powerful β - and γ -ray sources near the counter, however, rendered the zero so unsteady that it was impossible to draw definite conclusions as to the numbers or sizes of the H-particle deflections. This was also the case when attempts were made to study the long-range α -particles emitted from radium C and thorium C. As has already been pointed out by Fränz, the ionisation due to a single β -particle, being only of the order of 1/20th to 1/200th of that of an α -particle, is too small to give rise to an appreciable deflection. The disturbance produced by γ -ray ionisation is due to the superposition of the effects of such single β -particles (released by photo-electric or Compton effects). If, therefore, each β -ray could be completely and instantaneously recorded, the trouble would disappear.

In the experiments on the short-range α -rays described in Paper II, the strengths of the sources were such that no disturbance was caused by β - or γ -rays. A disturbance was, however, introduced by what we may term the "residual α -ray" effect. A special "differential" type of chamber had to be used in order to detect and measure a small group of short-range α -particles which were present only in the ratio of 1 : 4000 of a main group of particles of longer range, which passed through the chamber. This main group of particles entering the chamber at a rate of about 100,000 per minute were not recorded in the normal way, but each particle gave rise to an exceedingly small *negative* deflection. The superposition of these small deflections produced a disturbance very similar to that caused by β - or γ -rays. Fortunately, both kinds of disturbance can be reduced by the same method—by sharpening up the processes of recording the deflections, so as to reduce the probability of superposition of small neighbouring deflections.

Reduction of β - and γ -ray Disturbances.

The primary β -rays can be bent away from the counter by means of a magnetic field. The first valve of the amplifier, however, must be placed where the stray field is small, otherwise the electrons emitted from the filament will also suffer deflection. Variations in the magnetic field might thus introduce unwanted deflections on the record. In our experiments, the first valve is situated 30 cm. from the counter, and the grid lead consists of a fine wire, screened by a metal tube 3.5 cm. in diameter.

The γ -ray disturbance can be reduced in two ways. In the first place, the number and lengths of β -ray tracks crossing the chamber per second must be reduced to a minimum. Secondly, in order to avoid superposition, the process

of recording each particle must be speeded up as much as possible. To comply with the first condition, the wall surfaces of the chamber and the idle volume of gas should be kept low. To secure this, the design of chamber finally adopted was of the guard ring type. Some experiments carried out by J. E. R. Constable and E. C. Pollard, who were engaged upon a similar problem and using an amplifier and recording system of the same type as ours, showed that it should be possible to reduce the γ -ray disturbance by using a thin walled aluminium chamber. This conclusion is drawn from the observation that the ionisation within a gold-leaf electroscope (caused by γ -rays from a radium tube) could be reduced by a factor of four if the walls of the electroscope were made of thin aluminium.

Attention has been concentrated by the writers on the second method of reducing the disturbance—the sharpening up of individual deflections to avoid superposition. To secure this, the rise and fall of the first valve grid potential must be as rapid as possible, *i.e.*, the rate of collection of ions must be high, and there must be a rapid leak away of the charge after collection. Further, the resulting sharp rise and fall of grid potential should be amplified without serious distortion, and recorded by an instrument capable of responding immediately to the rapid current changes.

“Shape” of a Deflection.

As stated by Ortner and Stetter, the grid potential change of the first valve during the recording of a particle is given by the two equations

$$E = rq/T (1 - e^{-t/rC})$$

from $t = 0$ to $t = T$, and

$$E = rq/T (1 - e^{-T/rC}) e^{-(t-T)/rC}$$

for t greater than T . (E = grid potential; q = collected charge; T = time of collection; r and C = resistance and capacity to earth of chamber and first valve grid (see fig. 1A).)

In fig. 1B the rise and fall of grid potential is shown plotted for various values of the time constant rC , $-rC$ being taken, for convenience, as multiples of the ion collection time T . In practice, C will be fixed at the lowest possible value (about 10 cm.) to secure high sensitivity, and T will be made as small as possible to approximate to the ideal case, by employing a high collecting field. One is therefore left with one variable, r , the value of which can considerably modify the “shape” of the deflections.

It is evident that as r is made small, the time of recording is reduced, and the probability of the superposition of neighbouring deflections is decreased. A

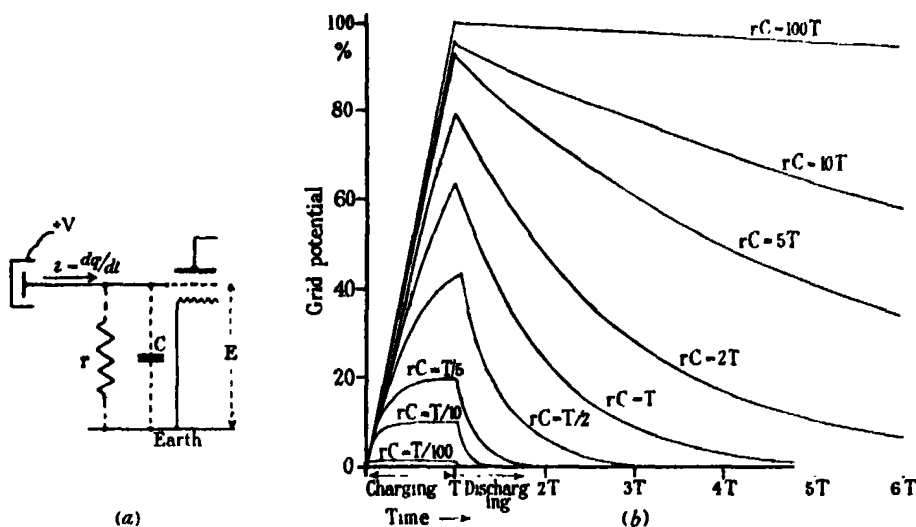


FIG. 1.—Characteristics of first valve grid system.

reduction, however, occurs in the peak value of the grid potential. A compromise must therefore be made between rapid clearing of the grid of its accumulated charge, and high sensitivity. This, we find, is best done by trial and error under working conditions. One might conclude from the curves, however, that a good compromise would be attained when $rC = T$ or $rC = 2T$, provided, of course, that the recording instrument could respond sufficiently rapidly.

A high value of r must not be employed for two other reasons. Firstly, if fast counting is contemplated, the first valve mean grid potential may not attain equilibrium rapidly, but may fluctuate about a value higher than the normal, and possibly cause changes in the sensitivity of the system as a whole. Secondly, as in the case of the first valve grid potential, the zero position of the recording instrument may fluctuate, and deflections may move off the scale.

"Johnson Effect."—In our experiments, the ions were collected by a field of about 800 volts per centimetre in a time of about 0.0002 seconds (the field could be raised to about 4000 volts per centimetre if necessary). An oscillogram showed that the value of rC was of the order of 1/200th to 1/400th of a second. This was too high for our purpose, and attempts were made to reduce it by means of an external grid leak connected between the grid and the filament. Unfortunately, such a leak creates a large disturbance, caused by the so-called "Johnson effect."

Johnson* has shown that a random fluctuating e.m.f. exists between the two ends of a resistance R , the root mean square value of which is proportional to $(RT)^{\frac{1}{2}}$ (where T is the absolute temperature of the resistance) and is independent of the nature of the resistance. For a resistance of the order of 10 megohms at room temperature, the e.m.f. is of the order of 30 micro-volts, which is a large disturbance when compared with the 100 to 150 micro-volt changes of grid potential produced by α -particles. Fränz, who used an external grid leak in connection with the first valve, does not seem to have experienced this trouble. As, however, he used a Geiger ball counter instead of an ionisation chamber, the potential changes due to the Johnson effect would be much smaller in his case than those due to α -particles, and could probably be ignored. In practice, we found it impossible to work with an external leak connected to the first valve grid, and the effect of a "quick leak" on the first valve grid had to be obtained in another way, as described below.

Artificial Distortion.—Owing to the type of inter-valve coupling employed (resistance-capacity), it is a simple matter to introduce the necessary "quick leak" in a later stage of the amplifier without incurring the disadvantage of the Johnson effect. Suppose the "shape" of the deflection in the early stages of the amplifier corresponds to, say, the curve for $rC = 50T$ in fig. 1B; at a certain stage in the amplifier—usually the second—artificial distortion is deliberately applied, so that the amplified shape of the deflection now corresponds to, say, the curve for $rC = T$. The subsequent amplification is made as linear as possible, so that the recorded deflection still corresponds (in this hypothetical case) to $rC = T$. It is thus possible to defer the sharpening up process from the first stage, where trouble would arise from the Johnson effect, to a later stage, without introducing any serious disadvantage. Fränz has also made use of this method of artificial distortion for sharpening the deflections by employing a coupling circuit of small time constant in one of the later stages of the amplifier.

It can be shown that the equations from which the curves of fig. 1B are drawn correspond to a particular case of resistance-capacity coupling. The "shape" of the amplified deflection can therefore be modified very simply by suitably choosing the time constant of an appropriate coupling stage (*e.g.*, by giving suitable values to r_1 and C_1 in fig. 2). By making this small, the deflection can be sharpened to any desired degree; the peak value of the grid potential of the next valve, however, is reduced in exactly the same way as when a rapid leak is applied to the grid of the first valve. As already men-

* 'Phys. Rev.', vol. 29, p. 367 (1927), and vol. 32, p. 97 (1928).

tioned, the optimum value for the time constant of the distorting stage is best determined by trial and error under working conditions. In our particular case, we found that a value of 0.0015 second, given by $r_1 = 250,000$ ohms, and $C_1 = 0.006$ μ fd., was very suitable. A smaller value might be necessary in some cases. For comparison, it may be noted that the ion collection time was about 0.0002 second, and the oscillograph period about 0.0003 second (i.e., natural frequency about 3000). The time constants of the remaining stages were made large (about 0.2 second; $r = 2$ megohms; $C = 0.1$ μ fd.). Falling plate oscillograms showed that, while in the ordinary way an α -particle deflection was over in a time of the order of 20×10^{-3} seconds, when a distorting stage of very small time constant was introduced, the deflection was completely over in a time of the order of 0.8×10^{-3} seconds.

Characteristics of Remaining Stages.—Ortner and Stetter have discussed in great detail the form of distortion introduced by transformer and by resistance-capacity coupling circuits. They showed that, in general, a surge of the form illustrated in fig. 1B is distorted into a surge followed by several slow oscillations, the time periods of which depend upon the coupling circuit constants. For this reason they adopted for their work a battery-coupled amplifier, which introduces no such distortion. While such an amplifier is undoubtedly the best, the numerous separate batteries required are a drawback when many stages and a large power output are needed for recording with a high frequency oscillograph. We find that the more convenient resistance-capacity coupling is quite satisfactory for most purposes, provided the coupling circuits (with the exception, of course, of the distorting stage) are given large time-constants (i.e., $-r$ and C (fig. 2) made large) compared with the time of recording. Under these conditions, the sudden impulse corresponding to the "sharpened" deflection is amplified fairly faithfully, and the subsequent oscillation is of so small an amplitude, and at so low a frequency, that it is almost imperceptible on the record, and causes no confusion.

When using coupling circuits of large time constants, a precaution well known in wireless practice must be observed. If the time constant is too large, the phenomenon known as "grid-choking" may occur during fast counting. This is caused by the grid of a valve being subjected to a large positive swing. Grid current flows, and the grid is finally left with a large negative charge, which leaks off slowly, during which time the amplifier ceases to function properly. For this reason, the artificial distorting stage should be situated early in the amplifier to avoid excessive grid swings occurring in the later stages during fast counting.

Characteristic of Recording System.—It is necessary to ensure that the sharp deflections are not superposed by the recording instrument. If the natural frequency of the recording oscillograph is too low, sharp “peaks” will be recorded as blunt peaks, which are much more liable to be superposed. This form of distortion is the result of the higher frequency components of the deflections (considering the latter capable of analysis into Fourier components) being recorded on a smaller amplitude scale than the low frequency components. As is well known, the natural frequency of a critically damped oscillograph should be several times higher than that of the highest frequency to be accurately recorded. (Approximately, an amplitude loss of 4 per cent. is incurred when the factor is 5, and a 50 per cent. loss when the two frequencies are equal.)

As a falling plate oscillogram shows that the deflection is over in a time of the order of a thousandth of a second, the natural frequency of the oscillograph should be raised to as high a value as possible (i.e., several thousand per second), bearing in mind the fact that for a given instrument, critically damped, the sensitivity is inversely proportional to the square of the natural frequency.

An experiment showed that α - and H-particle deflections could be distinguished easily from the γ -ray background when a cathode-ray oscillograph was used. For several reasons, however, this type of instrument was unsuitable, and a mechanical oscillograph (described later) had to be used.

“Shot Effect.”

Each stage of a distortionless amplifier magnifies to the same degree both the particle deflections and the “shot effect” fluctuations of the first valve (i.e., the probability variations in the anode current of the first valve due to the random arrival of electrons at the anode). If the latter are already apparent on the record, no further *resolution* is obtained by the addition of an extra stage of amplification, as both the particle deflections and the shot effect fluctuations will still appear in the same ratio. More *power*, however, is available to operate a less sensitive recording instrument.

The ratio of the magnitudes of particle deflections to shot effect disturbances is found to be highest (for a dull-emitter valve such as the “D.E.V.”) when practically the full filament voltage is applied. It is further increased by using a low anode potential, which also minimises disturbances which may be caused by the ionisation of residual gas in the first valve.

The shot effect also imposes a practical limit to the process of sharpening

up the deflections. When the distorting stage is used and the natural frequency of the oscillograph made high, the low frequency components of the particle deflections are reduced in magnitude relatively to the high frequency components. The shot effect fluctuations then become relatively more important, and with a distorting stage of time constant 10^{-4} seconds, the fluctuations become comparable in magnitude to α -ray deflections. In our particular experiments, where α -particles were recorded in the presence of γ -rays emitted from sources of 5 to 10 milligrammes equivalent strength placed near the chamber, an oscillograph frequency of about 3000, and a time constant for the distorting stage of 0.0015 second, seemed fairly satisfactory. A higher frequency and smaller time constant would probably have been better, but this would have necessitated an extra stage of amplification to compensate for the reduced sensitivity.

Design of Ionisation Chambers.

The type of chamber to be employed naturally depends upon the problem to be investigated. In some cases, simple deep chambers may advantageously be used, for the mere counting of particles; in others, very shallow chambers, of the single or differential type, may be required to secure adequate "resolution" in analysing a complex beam of radiation. Whatever type is employed, however, one or two precautions must be observed which would be comparatively unimportant were the chamber to be used with an electrometer instead of a valve. Owing to the low capacity of the valve grid, the electrostatic capacity of the chamber and its screened connecting lead must be kept down to a bare minimum in order to obtain maximum sensitivity, and as little solid dielectric as possible should be employed. In order to reduce the effect of the γ -rays to a minimum, it should be arranged that there is little idle volume in the chamber, and that unnecessary wall surfaces are avoided. Further, to secure uniformity in the shapes and sizes of the deflections, the electrodes should be so arranged that ions from all parts of the chamber are collected at as uniform a rate as possible; as before mentioned, this rate should be made high.

Diagrams of single and differential chambers which have been employed in the present work are shown on pages 213, 217 and 220 of Paper II, and also in fig. 2 of the present paper. A description of the mode of action and the characteristic curve of the differential chamber are also given on p. 218 of Paper II. Here it suffices to point out that whereas with the single chamber *all* particles entering or passing through it are recorded, only the particles

which stop within the front half of the differential chamber give rise to positive deflections, thus enabling differential counting to be carried out.

In these chambers, the idle volume (and hence the γ -ray effect) is reduced by employing the "guard-ring" type of construction. The collecting electrode consists of the central zone of an earthed metal plate, from which it is insulated by a narrow ring of sulphur or sealing wax. The collecting field being sensibly uniform over the whole plate, ions formed within a cylinder defined by a diameter slightly greater than that of the collecting electrode will be collected. Those formed outside this cylinder, however, will be driven on to the earthed concentric portion of the plate, and will give rise to no deflections. The "chamber" is thus defined by a minimum of boundaries, viz., bounded at each end by an electrode, and laterally by an imaginary cylinder passing through the insulating ring supporting the collecting electrode from the earthed portion of the plate.

Microphonic Effects.—For high resolution, very shallow chambers, which include only a few millimetres of track, may have to be used. The shallowest chamber with which we were able to work had a depth of 2.5 mm. Apart from constructional difficulties, the disadvantages of too shallow a chamber are: (1) Deflections may be small and difficult to count in the presence of shot effect fluctuations; (2) the electrostatic capacity may be unduly increased, thus reducing sensitivity; (3) when—as is usually the case—thin foil electrodes and high collecting fields are used, the chamber behaves as a condenser microphone.* The trouble arises from the movement of the foils under the influence of air currents or sound waves; the foils being at different potentials, alternating voltages are induced on the collecting electrode, which are magnified by the amplifier and recorded. The effect can be reduced by the use of sputtered mica in place of thin foils, but the use of this material is attended by two drawbacks—that it cannot be obtained as thin as foils, and that in time its conductivity decreases. For certain experiments, grids of 25 μ wire, spaced $\frac{1}{2}$ mm. apart, might be employed, as this form of electrode is practically non-microphonic. An uncertainty exists, however, as to the magnitudes of the "shadow ratio" and the scattering of particles by the wires. Further, the end of the chamber is not sharply defined by the grid, as ions formed 2 mm. outside the grid can be driven on to the collector.

With a single chamber, the microphonic effect can be considerably reduced

* This effect, which can be very troublesome, should not be confused with the "valve microphonic" effect; the latter is caused by mechanical vibration of valve filaments or other electrodes, and is very much easier to cure than "chamber microphonics."

by employing as far as possible a skeleton form of construction, and using wire gauze for the earthing cap instead of solid metal. Freer air circulation is thus obtained round the electrodes, so that air currents and sound waves produce less effect. With the differential chamber more elaborate precautions are necessary. In addition to ensuring free air circulation between the electrodes, the whole chamber (and if necessary, the source and absorbing screens, etc.) should be enclosed in a vessel which can be made practically gas tight. If air or gas is to be circulated during an experiment, sudden pressure changes and eddies should be avoided by using aspirators, and leading the gas in and out of the vessel by narrow capillary tubes.

The Amplifier.

The amplifier employs five stages of resistance-capacity coupling, and is generally similar to an ordinary audio-frequency amplifier. In certain essential points, however, departures are made from the usual design.

Choice of Valves.—The first valve, which serves as a low period electrometer, consists of an Osram "D.E.V." valve, as was used by Ortner and Stetter. The normal characteristics of this valve are: filament voltage = 2.8, filament current = 0.2 amp., $\mu = 6$, $R_a = 24,000$ ohms, anode voltage = 60. The grid insulation is fairly high, and the grid-earth electrostatic capacity low (about 2.5 cm.) on account of the peculiar construction. As used in this apparatus, the valve is operated at normal filament voltage, but with a high-tension battery voltage of only 20. With an anode resistance of 100,000 ohms the anode potential is then only about 10 volts, and the anode current about 20 or 30 micro-amperes. Other ordinary valves and specially designed types have been tried as first valves, but we found none to be superior for our particular purpose to the D.E.V. Further, in all cases, the measured grid capacity was appreciably higher than that of the D.E.V.

The second, third and fourth valves serve as voltage amplifiers. Valves of large amplification factor are therefore used. In our case, these consisted of Osram "H 610" valves, having the following characteristics: filament voltage = 6, filament current = 0.1 amp., $\mu = 40$, $R_a = 65,000$ ohms, anode voltage = 150. Other valves having a value of μ about 40 should, however, be suitable. These valves were operated under normal conditions, with an anode resistance of 250,000 ohms, and high-tension supply of 160 volts, and separate grid bias cells.

The choice of the fifth (output) valve is governed by the type of recording instrument to be employed. If this is of the current-operated type (and there-

fore of comparatively low impedance), a low impedance "power" or "super power" valve, having a high "slope" or "mutual conductance" should be used. On the other hand, if the recorder is of the potential operated type (and therefore of high impedance) a valve of correspondingly high impedance and high amplification factor may be used with advantage. For a reason given later, a pentode valve is at present employed, viz., an Osram "PT625" having characteristics: filament volts = 6, filament current = 0.25 amps., R_a = about 43,000 ohms, mutual conductance = 1.85 milliamperes per volt, anode voltage = 250, grid base, about 20 volts.

It is perhaps needless to draw attention to the fact that in the last valve, or even the last valve but one, care must be taken to observe that the length of the operating slope is sufficient to accommodate large grid swings. As, however, the grid swings are usually confined to one side of the mean value, valves may conveniently be biased to points near the *ends* of the straight portions of their characteristics, thus enabling larger grid swings to be dealt with than if the valves were biased to points near the *middle* of their characteristic curves, as is usually done.

Construction.—A detailed diagram of the amplifier, showing the values of the various components, is given in fig. 2. The ionisation chamber and first valve form one unit, while the remaining four valves and associated apparatus form the other. This form of construction enables the ionisation chamber to be conveniently moved to any desired position. The first valve ("D.E.V.") is weighted with lead and rests on a pad of soft rubber sponge, in order to reduce "valve microphonics" set up by mechanical shock. The remaining valves are supported, bulb downwards, by rubber sponges in compartments in the main amplifier.

The anode resistances, decoupling resistances, condensers, grid leaks, etc., consist of high quality wireless components. Mica dielectric condensers should be used for $C_1, 2, 3, 4$ and for K_c , but paper condensers suffice for $K_1, 2, 3, 4, 5$. The resistances $R_1, 2, 3, 4$ and $S_1, 2, 3, 4, 5, c$ are of the "wire-wound" type. All connections, with only one or two unavoidable exceptions, are firmly soldered, no reliance whatever being placed on clamped connections. This may seem a very trivial point to mention, but it is our experience that time after time, an unsteady zero has been traced eventually to a badly made connection—usually in the filament circuit—which seemed on first examination to be perfectly satisfactory. For this reason, no valve holders are used, wires being soldered directly to the valve pins instead. Large low-tension and high-tension accumulators are used to minimise battery voltage variations,

and two separate high-tension batteries are employed to prevent self-oscillation.

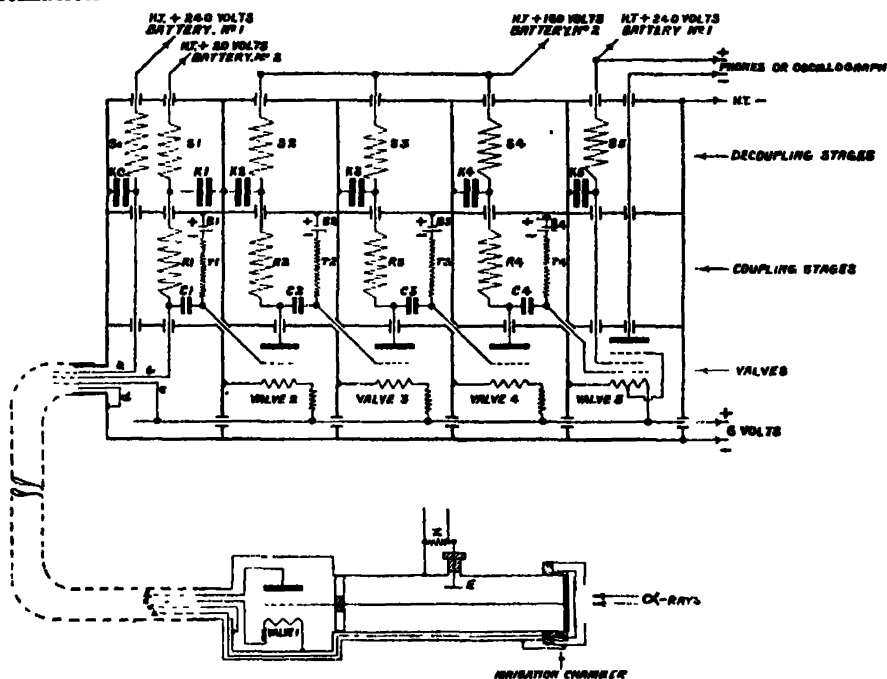


FIG. 2. —Diagram of amplifier and ionisation chamber.

($R_1 = 100,000$ ohms; $R_{2,3,4} = 250,000$ ohms; $r_1 = 250,000$ ohms; $r_{2,3,4} = 2$ megohms; $S_1 = \frac{1}{2}$ megohm; $S_{2,3,4} = 30,000$ ohms; $S_5 = 5,000$ ohms; $C_1 = 0.006 \mu\text{fd.}$; $C_{2,3,4} = 0.1 \mu\text{fd.}$; $K_1 = 0.25 \mu\text{fd.}$; $K_{2,3,4,5} = 2 \mu\text{fd.}$; $B_1 = -0.9$ volt; $B_2 = -1.5$ volts; $B_3 = -24$ volts; valve 1 = "D.E.V."; valves 2, 3, 4 = "H610"; valve 5 = "PT625.")

Screening.—High-frequency disturbance from induction coils or similar apparatus may be picked up and recorded unless adequate screening is provided. It should be emphasised that the screening of the apparatus in this kind of work must be much more thorough than screening employed in electrometer work. Lack of attention in this respect is a very fruitful cause of trouble. The reason for the extra care needed lies in the fact that the first valve in virtue of its free grid, functions as a rectifier. Consequently, unless *electromagnetic waves* are cut off, as distinct from electrostatic fields, disturbances will be picked up and recorded. It is not sufficient merely to observe that all separate sections of the screen are connected to a common earth. Gaps between sections should be avoided as far as possible, and where they exist should be bridged over with a short wire link.

The main amplifier is completely enclosed in a multi-partitioned tinplate case in order to reduce to a minimum any possible interaction between stages, which can be very troublesome when many stages are employed. The leads connecting the first valve with the main amplifier are screened by a flexible metal tube. It should be observed that flexible metallic gas piping (coiled metal and rubber), while forming an excellent electrostatic screen, is quite useless in cutting out high-frequency disturbances, as electric vectors parallel to the enclosed leads are *not* cut off by the insulated coils of the tube. The tube employed must be electrically continuous in all directions.*

To prevent high-frequency surges from being carried into the amplifier along the high tension supply wires, filter circuits, consisting of 30,000 ohm resistances and 2 μ fd. condensers (K and S in fig. 2) are inserted in each lead at its point of entry into the amplifier. Surges travelling along the leads are thus short-circuited to earth by the condensers. This filter circuit also serves as a "decoupler," such as is now the custom to incorporate in amplifiers to check self-oscillation. No need has so far arisen for including such filters in the low-tension supply leads. Pick-up of high-frequency surges by outside wires (such as high-tension battery leads) can be greatly reduced in the first place by avoiding inductive loops as far as possible (*i.e.*, by using twin conductors, one wire of which serves as the earth wire).

Recording Apparatus.

As has already been pointed out, a recording instrument of high natural frequency must be employed. While the frequency of an Einthoven galvanometer (such as was used in the experiment described in Paper I) can be made high by using a metal fibre, the records are much easier to obtain with the paper travel speeds employed, and more satisfactory, if a spot of light is used for recording in place of a moving shadow. The available current changes, being only about 10 to 20 milliamperes, are too small to give reasonable deflections with oscillographs of the Duddell type, and it is undesirable to use a step-down transformer. Experiments made with a balanced armature loud-speaker unit converted into a simple oscillograph of natural frequency about 1000 indicated the lines on which a simple type of oscillograph could be constructed which would be suitable for our purpose. In passing, it may be mentioned that an oscillograph made from a modified loud-speaker unit, while unsuitable for many purposes, forms an excellent demonstration instrument.

* The tubing at present used is obtainable from Messrs. W. Edwards, and is known commercially as "Tombac." This is jointless copper tubing used for vacuum work, and is sufficiently flexible in long lengths.

Oscillograph.—The oscillograph is similar in principle to the balanced armature loud-speaker unit. A soft iron armature is constrained by control

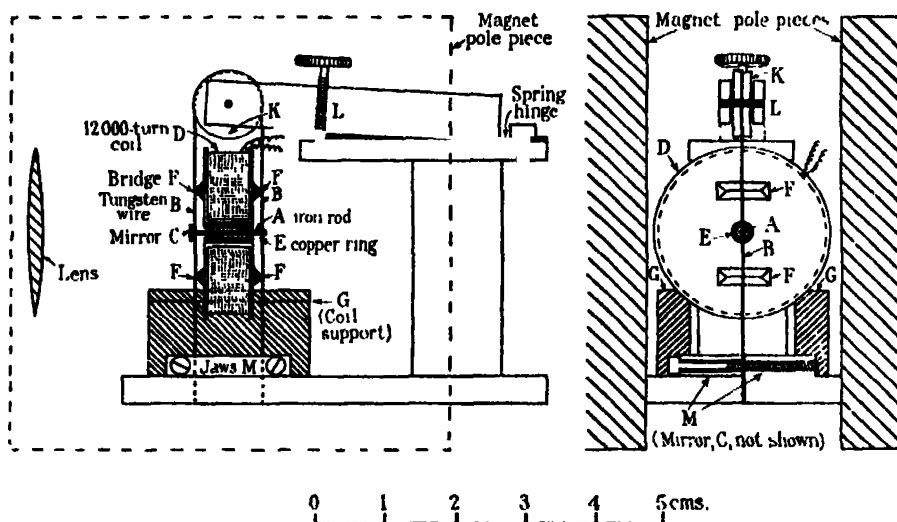


FIG. 3.—Constructional details of oscillograph.

forces to lie in a direction perpendicular to a steady magnetic field. Changes in the current flowing through a coil surrounding the armature vary the magnetic moment of the iron, which in virtue of the field in which it is situated is thus subjected to a deflecting couple, and to a restoring couple due to the control forces. The constructional details are given below, and in fig. 3.

The armature is a soft iron rod A, about 5 to 10 mm. long, and about $\frac{1}{2}$ to 1 mm. diameter. The control forces are supplied by two tungsten wires, BB, 40 μ in diameter, forming the sides of a loop, the ends of which are firmly gripped by jaws M, and which is tensioned by a screw and pulley device, K, L. The ends of A are slightly grooved and firmly attached to the mid points of BB, by fused shellac. The mirror C is a 2-mm. square of thin silvered cover-slip, very little wax being used in attaching it, to avoid distorting the glass. The current coil D, consists of 12,000 turns of No. 47 enamelled copper wire, wound on a thin ebonite bobbin supported from the base so that the armature A passes through the centre of the bobbin, without touching it during a deflection.

The instrument is placed between the poles of an electromagnet, so that A is situated in a uniform field of about 2000 gauss, perpendicular to the plane containing A and BB. Soft iron pole pieces may, if necessary, be added to concentrate the field near the ends of the armature. For small changes of

current through the coil, the angular rotation of the rod and mirror in the horizontal plane is proportional to the current change. Limitations are, of course, imposed by saturation, hysteresis, etc., but reasonably large deflections (about 2 cm. at 60 cm. distance) can be obtained before departure from the linear relation becomes serious.

A natural frequency of about 3000 can be obtained without much difficulty, by tensioning the wires BB, and by shortening the operating length of the wires by small bridges (F). Electromagnetic damping is applied by giving the bobbin a copper centre (E), in which eddy currents are induced by the movement of the iron rod in the field. For best working conditions, the instrument should be just critically damped.

Owing to the large number of turns, the inductance of the coil D is not negligible. The result is that, if a sudden change is made in the grid potential of the last valve, the anode current change will not be sudden, but will rise exponentially with time constant L/R , where L and R are the inductance and resistance of the output circuit. This may increase the probability of superposition of deflections. The lag can be reduced in the usual way by means of a large series "swamping" resistance. A better way of achieving the same result, however, is to use a valve of high impedance and high mutual inductance for the output stage. Valves of this type are found in the "pentode" class.* As already stated, for our purpose, an Osram "PT625," for which R_a is about 43,000 ohms, and the mutual conductance 1.85 milliamperes per volt, was suitable, though other pentodes might be preferable under different conditions.

In conjunction with the pentode, the instrument forms a potential oscillograph of natural frequency about 3000, which can be deflected by about 10 to 20 volts (and negligible current) applied to the pentode grid. It is suggested that it might be found useful for laboratory purposes other than that described here. It has the advantages of being cheap, fairly robust, and easily constructed.

Photographic Arrangements.—A 60-cm. focal length lens is placed before the plane oscillograph mirror, and an image, 60 cm. away is formed of a vertical slit, $\frac{1}{2}$ mm. wide, illuminated by a 12-volt 48-watt filament lamp, overrun at 17 to 18 volts. A cylindrical lens, 2.5 cm. focal length, with its axis horizontal condenses the image to an intense spot which moves horizontally along a slit $1/15$ th mm. wide, behind which a strip of Kodak "Cine-bromide" paper $1\frac{1}{2}$ inches wide is drawn smoothly by rollers at speeds of 4 to 50 mm. per second.

* The use of high impedance pentode valves in connection with an oscillograph has been described by Matthews, 'Journal of Scientific Instruments,' vol. 6, p. 220 (1929).

By suitably masking the aperture of the camera, it is possible to reduce the exposure near the zero position of the spot, while still enabling full exposure to be given at points where the spot is moving with high velocities. Reproductions of records are shown in Plates 11 and 12 of Paper II, but considerable loss of detail has unfortunately occurred in the printing processes.

Calibration.—To allow for small changes in the overall amplification of the system, “standard sizes” are recorded before and after each record of particles. A predetermined and constant current flowing through the resistance Z (fig. 2) is suddenly started and stopped a few times; the potential of the electrode E is thus altered, and definite potential surges are induced on the first valve grid thus giving a deflection of standard size with which particle deflections can be compared. To prevent high-frequency pick-up, Z should be small, non-inductive, and have very short connecting leads.

Test for Linearity.—The ionisation-deflection ratio must be linear over the whole working range of the deflections. The linearity of the amplifying system and oscillograph as a whole can be tested by inducing known voltage surges on the first valve grid (as described above) and plotting the recorded deflection as a function of the voltage surge. From the resulting curve, which is straight for some distance from the origin, the maximum working deflection can be determined. The curve shows that the centre of the zero line (which shows slight fluctuations caused by the shot effect) is the correct point from which to measure deflections.

Effect of Different Times of Ion Collection.—Ions formed by particles which only just penetrate into the chamber are collected in very much shorter times than those formed by particles passing right across the chamber. Owing to the leakage from the grid, therefore, the ratio of the grid potential rise to the number of ions collected will be greater in the former case than in the latter. It can be shown, however, that in our experiments, where the shape of the recorded deflection is of the form corresponding to a value of rC in the neighbourhood of 5T to 10T (fig. 1B), the maximum error introduced in this way does not exceed 7 per cent.—which is not serious in experiments of the kind described in Paper II.

Amplification Obtainable.—The theoretical voltage amplification factors (estimated from the valve and coupling circuit constants) for the first four stages are 3, 32, 32, 32. The values determined experimentally are 3.3, 30, 24, 32. The fifth valve is not used as a voltage amplifier, but its voltage amplification factor can be determined if the impedance of the recording instrument is known. Assuming this to be, say, 5000 ohms (probably a low value)

and the mutual conductance of the pentode to be 1.85 milliamperes per volt and practically independent of the output circuit impedance, the voltage amplification factor for the whole system is given by $3.3 \times 30 \times 24 \times 32 \times 1.85 \times 10^{-3} \times 5000$ or about 7×10^6 . This represents the ratio of the voltage developed across the oscillograph to the voltage surge produced at the first valve grid, and while only an approximate value, serves to form an idea of the amplification factor. The charge amplification factor (i.e., ratio of charge passed through the oscillograph during deflection to charge collected in the chamber) depends among other things, upon the constants of the distorting stage. Under our conditions, however, a factor of the order of 10^9 to 10^{11} is obtainable.

Automatic Counting.

Sufficient power is available to enable automatic mechanical counting of α - or H-particles to be carried out, provided the relay and meter mechanism is sufficiently rapid in action to respond and reset itself before a second particle arrives. Automatic counting is therefore possible when particles are arriving at a mean rate sufficiently small to ensure a low probability of pairs occurring too close to be separately recorded. This method of counting was demonstrated with the present apparatus just over a year ago, a simple relay constructed from a loud-speaker movement and a step by step cyclometer being used. α - and H-particles could, however, only be counted when the background disturbance was small. For this reason, automatic counting was not attempted in the experiments described in Paper II, except for trial experiments prior to photography.

Summary.

The recording of α - or H-particles by means of the original Greinacher counter is rendered difficult or impossible if they are accompanied by powerful β - or γ -radiations, owing to the disturbances caused by the latter. Difficulties of a similar nature are also introduced in some experiments by unwanted α -rays, when differential counting methods are employed. In the present paper, methods are described whereby these difficulties can be overcome to a great extent, by speeding up the recording processes as much as possible to avoid the superposition of the small deflections produced by the unwanted radiations responsible for the disturbances. Details are given of the apparatus used and the necessary precautions to be observed.

With the present apparatus, it was possible to carry out an analysis of the

short-range α -particles emitted from various radio-active bodies—an account of which has already appeared. This necessitated the recording of single short-range α -particles entering the chamber simultaneously with a main group of particles 4000 times as large, which it was not desired to record. It should now be possible to extend the application of these methods to problems connected with long-range α -particles and artificial disintegration.

It is our pleasure to thank Lord Rutherford for his interest and encouragement during the course of the work, and Dr. Chadwick for many helpful suggestions. We also wish to thank Mr. G. R. Crowe, who prepared the necessary radio-active sources, and gave us valuable assistance.

Viscosity and Rigidity in Suspensions of Fine Particles.

I.—Aqueous Suspensions.

By C. M. McDOWELL and F. L. USHER, The University, Leeds.

(Communicated by R. Whytlaw-Gray, F.R.S.—Received October 10, 1930.)

The variation of the coefficient of viscosity of many colloidal liquids with the rate of shear has been extensively studied and discussed, chiefly in connection with substances—such as gelatin or rubber—which are soluble or dispersible in the liquids in which they are examined. The observation of Humphrey and Hatschek* that a similar variation is shown by suspensions of starch grains in a liquid exercising no solvent or dispersing action on them suggests that a common factor may operate in both instances, and it appeared possible that an examination of systems of the second type, in which the nature and condition of the physical units of the dispersed phase are more open to investigation, might give some information about one or more of the factors which cause viscosity to vary. The systems available for this purpose are (1) suspensions of electrically charged particles in an aqueous liquid and (2) suspensions, like those studied by Humphrey and Hatschek, of electrically

* 'Proc. Phys. Soc.,' vol. 28, p. 274 (1916); Hatschek and Jane, 'Kolloid Z.,' vol. 40, p. 53 (1926).

uncharged particles in neutral organic liquids. The present communication deals with the former.

The viscosity of systems of this type has been measured from time to time for specific purposes; thus Odén* found a linear relation between viscosity and concentration in sulphur sols, in agreement with Einstein's equation, but showed also that sols with smaller particles possessed a higher viscosity than those of the same total concentration with larger particles. Ishizaka,† Gann,‡ and Fernau and Pauli§ used measurements of viscosity as an index of the degree of coagulation reached by sols of metal oxides, and in particular Ishizaka observed that stable sols of aluminium hydroxide showed the same coefficient of viscosity whether measured by the oscillating disc or the capillary viscometer method, but that in coagulating sols the former gave higher viscosities than the latter, a result which he attributed to the different rates of shear incidental to the two methods.

The experiments recorded below (out of a large number all pointing to the same conclusion) show clearly that sols of copper ferrocyanide, when stable, possess a constant viscosity coefficient differing little from that of water, and one which increases with decreasing rate of shear when rendered unstable by the addition of an electrolyte. Under certain conditions these sols and those of cadmium sulphide are definitely rigid. The aspects of the problem more particularly studied have been the possible connection between variable viscosity and elasticity toward shearing forces, and the conditions of physical stability or instability under which each of these properties may be exhibited. The two substances chosen for study—cupric ferrocyanide and cadmium sulphide—are, unlike gelatin and other “emulsoids,” definitely insoluble in water, and form with it typical fine suspensions sensitive to electrolytes, which in suitable concentrations cause the primary particles to coalesce. It is unlikely that either of them attracts water to an extent capable of explaining the behaviour observed.

EXPERIMENTAL.

Cupric potassium ferrocyanide, prepared by precipitation in the presence of excess of potassium ferrocyanide, was washed centrifugally until it began

* ‘Z. Phys. Chem.,’ vol. 80, p. 709 (1912).

† ‘Z. Phys. Chem.,’ vol. 83, p. 97 (1913), and vol. 85, p. 398 (1913).

‡ ‘Kolloid-Chem. Beih.,’ vol. 8, pp. 64, 81 (1910).

§ ‘Kolloid-Zeitschrift,’ vol. 20, p. 20 (1917).

to form a stable suspension, and was then dialysed until neither sulphate nor ferrocyanide could be detected in a filtrate from the coagulated substance. The cadmium sulphide was made by the action of hydrogen sulphide on a thoroughly washed precipitate suspended in water.

Measurements of Viscosity.

Experiments on viscosity were done in a concentric cylinder apparatus in which the inner cylinder was a glass tube with a hemispherical bottom, of outer diameter 1.23 cm., whilst the outer rotating cylinder has an internal diameter 5.49 cm., and was mounted on a worm-driven table operated by an electric motor through suitable reducing gear. The inner cylinder was suspended by a quartz fibre having a torsional modulus of 6.6 dyne-cm. The dimensions of the cylinders and the rigidity of the suspending fibre were chosen so as to allow the use of low rates of shear, and although the sensitiveness of the apparatus made the individual measurements liable to a rather large experimental error, this latter was of a much smaller order of magnitude than the variations in viscosity observed at the different velocity gradients, and it was possible with this arrangement to demonstrate the existence of variable viscosity in suspensions of very low concentration. The quartz fibre was protected throughout its length by a glass tube cemented to a torsion head, and the whole of the rotating system was contained in a strawboard housing provided with a window. Deflexions of the inner cylinder were observed by means of a beam of light reflected from a mirror attached to a thin copper rod connecting the cylinder to the lower end of the quartz fibre. The liquids examined were always introduced to a mark on the inner cylinder, the "equivalent height" of which was found by independent measurements to be 3.7 cm. The stock suspension of copper ferrocyanide contained 0.57 per cent. by volume of solid, and preliminary experiments showed that the difference between the coefficient of viscosity of this suspension and that of water was within the experimental error. In Tables I to V the rate of shear is the radial gradient of velocity in centimetres per second per centimetre at the wall of the outer cylinder, and the coefficient of viscosity is in arbitrary units obtained by dividing the observed deflexion by the rate of shear. The concentration of the various suspensions is expressed throughout as a volume percentage, the density of the solid having been found to be 1.58. The experiments were done at the room temperature, which was controlled so as to vary as little as possible (generally not more than 1°) during a series of measurements.

Table I.—Viscosity of Copper Ferrocyanide, 0.57 per cent., without Electrolyte.

Rate of shear $\times 10^4$.	Deflexion.	Viscosity.
	cm.	
29	0.25	87.6
51.1	0.46	90.5
74.6	0.65	86.9
94	0.80	84.8
109	0.90	82.7
116	1.00	86.9
152.	1.36	86.9
163.2	1.55	93.5
176	1.48	84.0
233	2.00	85.6
256	2.27	87.6
312	2.65	84.0
345	2.95	84.8
	Average ...	86.6

Table II.—Viscosity of Copper Ferrocyanide, 0.033 per cent., with N/15 Sodium Chloride. Put in apparatus at 5.30 p.m.

Time.	Rate of shear $\times 10^4$.	Deflexion.	Viscosity.
p.m.		cm.	
5.45	330	2.70	81.1
5.55	31	0.4	129.0
6.5	45	0.57	126.8
6.30	62	0.90	143.3

In these experiments the outer cylinder was rotated at speeds varying between 18.5 and 730 seconds for one revolution. The extreme rates of shear at the outer wall were in the ratio 40 : 1, and the lowest used was 0.0009 sec.^{-1} , much lower than the rates (varying from 11.6 to 0.83 sec.^{-1}) used by Humphrey and Hatschek.

The tables show clearly that the addition of sodium chloride in certain concentrations causes the otherwise "normal" sols to exhibit variable viscosity, that the phenomenon requires a definite time to make its appearance, and that this time is the longer, the weaker the suspension with respect to either electrolyte or copper ferrocyanide. The variation is more marked in the more concentrated sols, in which a very little electrolyte produces an enormous increase of viscosity at low rates of shear, and in these it is associated

Table III.—Copper Ferrocyanide, 0·14 per cent., with N/25 Sodium Chloride.
Made up and put into apparatus 12 noon Friday and allowed to stand.
First showed signs of variable viscosity at 4 p.m.

Time.	Rate of shear $\times 10^4$.	Deflexion.	Viscosity.
Friday.			
p.m.		cm.	
4.15	24	0·55	230
4.30	63	1·55	246
4.45	25	0·80	315
5.0	345	7·3	216
5.15	44	1·65	377
5.30	349	8·4	239
6.15	28	1·4	500
6.30	29	1·95	664
6.40 to 6.55	345	14·5 to 7·6	420 to 220
7.10	23	1·30	581
Saturday.			
a.m.			
9.30	Suspension had partly settled out. Stirred gently, and found hour later that viscosity at a low rate of shear was considerably lower.		
10.30	17	0·20	110

with gelatinisation (see observations in body of Table V). Such high viscosities at a particular rate of shear are diminished by previous rapid rotation of the outer cylinder (Table IV). On the other hand, it was noticed (as illustrated by the results at the end of Table V) that very gentle stirring of the suspension facilitates "setting." Contrary to the experience of Humphrey and Hatschek and of Hatschek and Jane, the deflexions were never steady when the liquid possessed variable viscosity, but the inner cylinder oscillated irregularly about a mean position. The discrepancy is probably due to the difference in sensitiveness of the suspended systems used in the two sets of experiments; the relative coarseness of the fibre and the high moment of inertia of the metal cylinder used by the other observers would tend to smooth out irregularities which could be individually registered by the much more sensitive apparatus employed for the present experiments.

No experiments on variable viscosity were done with cadmium sulphide, because the gradual loss of hydrogen sulphide (used as a stabiliser) from the sols during the measurements would have led to a corresponding alteration in the viscous behaviour which could not have been distinguished from changes effected by time or mechanical treatment.

Table IV.—Copper Ferrocyanide, 0·15 per cent., with N/25 Sodium Chloride.
Made 9.30 a.m. Monday and put into cylinder at 3 p.m.

Time.	Rate of shear $\times 10^4$.	Deflexion.	Viscosity.
Tuesday. a.m.	cm. Suspension had settled half-way down cylinder. Stirred up and obtained following readings :—		
9.45	14	0·20	138
10.0	51	0·65	127
10.15	82	1·10	133
10.30	142	1·30	91
10.40 to 11.40	342	5·45	168
12.0 noon	24	0·75	300
	43	1·28	265
	85	2·00	235
	353	5·83	164
p.m.			
2.25	17	1·05	603
	45	1·60	354
2.35	87	2·50	254
2.40 to 3.0	124	2·85	228
3.5	195	3·80	195
3.40	366	5·70	155
3.45	Suspension had begun to settle. Stirred up.		
	19	15·0	8050
	55	29·8	5390
	Allowed to run at the highest speed for 45 minutes.		
6.10	85	31·3	3660
6.25	81	23·0	2840
6.35	45	17·0	3830
6.50	15	9·0	6040
7.2	49	22·0	4510
7.15	77	28·0	3650
	No sign of settling at this stage.		

Table V.—Copper Ferrocyanide, 0.56 per cent., with N/50 Sodium Chloride.

Time.	Rate of shear $\times 10^4$.	Deflexion.	Viscosity.
Saturday.			
a.m.		cm.	
11.30	312	2.90	90
p.m.			
2.15	22	0.35	161
2.22	330	3.30	100
3.30	19	0.30	153
6.10	17	0.25	144
7.30	18	0.30	164
Sunday.			
p.m.			
3.0	No measurements possible as cylinder was turned through more than 90° at the lowest speed. The outer cylinder was, therefore, rotated for 30 minutes at full speed.		
3.30	135	28.0	2110
3.40	12	5.50	4730
3.55	77	24.5	3160
Monday.			
a.m.			
9.30	Again "set." No sign of coagulation. Stirred and allowed to stand for 15 minutes.		
10.20	17	3.40	2000
	71	9.20	1310
	128	16.7	1328
11.10	188	22.0	1166
11.30	9.5	21.7	22640
11.55	9.5	27.2	28300
p.m.			
12.10	9.4	27.8	29100
12.25	9.3	28.2	30200
2.15	9.4	31.5	33300
2.30	9.5	31.2	32800
2.50	9.5	31.0	32500

Experiments on Rigidity.

The apparatus used in the experiments on variable viscosity was found convenient also for the observation of elastic properties. For this purpose a mirror was attached to the lower end of the glass sleeve protecting the quartz fibre and was adjusted so that the images of the source of light were received on the scale from both mirrors simultaneously. Since the glass sleeve was cemented rigidly at its upper end to the torsion head it was possible to observe on the scale the response of the inner cylinder when the former was rotated through a known angle. It was often necessary to rotate the torsion head through angles much larger than could be read by means of the scale; these were measured by the movement of a horizontal arm attached to the torsion head over a scale of degrees of arc.

With this apparatus experiments of three different types were carried out. In the first, the torsion head was turned and the subsequent behaviour of the inner cylinder was noted ; in the second, measurements were made of the rate at which the stress excited by a given strain decreased—that is to say, the “relaxation” of the sols was studied in the same way as Hatschek and Jane had done with their lyophilic sols ; and in the third the relation between stress and strain was observed. A few of the observations made in the first way are recorded in Tables VI to IX, in which the positions of the torsion head (T) and inner cylinder (C) are given as scale readings in centimetres. The mirrors were adjusted so that the images of the light source were close together but did not coincide. The differences in the positions ($C - T$) are denoted by “D,” and the value of D in water (*i.e.*, for zero stress) is given at the head of each table.

The behaviour of glycerol, a highly viscous but inelastic liquid, was observed in the apparatus. The scale readings were : $T = 6.8$, $C = 5.0$, giving $D = -1.8$. The torsion head was turned so as to bring T to 22.6, when the inner cylinder moved slowly and without jerking until C reached 20.8, where it remained, giving the same “zero” value of D. With a suspension containing a little over 1 per cent. of copper ferrocyanide without electrolyte between the cylinders the inner one oscillated freely and regularly as in water, and gave a similar period of oscillation, 20.9 seconds, compared with 20.6 seconds for water. Reproducible zero values of D were obtained as in water or glycerol. Very different behaviour was observed with sols containing electrolyte. The results are summarised below.

Table VI.—Copper Ferrocyanide, 0.035 per cent., with N/15 Sodium Chloride.

Made and put into cylinder at 3.30 p.m. Period of oscillation in water, 20.6 seconds. $D(\text{water}) = 1.7$.

Time.	Period.	Time.	Period.	Remarks.
3.40	20.5	4.24	26.0 21.2	(a) Where two values are given, the second is that obtained from the later oscillations of smaller amplitude.
3.43	21.2 21.8(a)	4.28	26.0 27.0	
3.45	20.2 25.6	4.32	26.5 17.4	
3.48	26.2	4.35	24.4 26.5	
4.0	25.0	4.45	26.8 19.0	
4.15	24.0			
4.20	26.0 21.3	4.52	27.2 18.6	
Time.	T.	C.	D.	Remarks.
5.5	27.1	28.4	1.3	Cylinder oscillated slightly about a false zero position.
5.20	27.1	28.2	1.1	
	26.6	28.2	1.6	
5.45	24.2	26.1	1.9	External vibrations here caused cylinder to move toward its true equilibrium position.
6.5	26.75	26.90	0.15	
6.20	26.75	27.3	0.55	
6.45	26.75	27.8	1.05	
6.58	13.85	16.5	2.65	
At this stage the suspension was rigid but in a very sensitive condition, slight outside disturbances causing the cylinder to creep toward the equilibrium position. It was removed and examined. Flocculation had begun. The suspension was thoroughly shaken and replaced in the apparatus. The inner cylinder swung freely and evenly with a large amplitude, and no trace of rigidity could be detected.				
7.16	26.8	28.6	1.8	
7.40	Period 20.4 seconds.			
8.8	Period 20.5 seconds.			
8.30	11.5	13.4	1.9	

Table VII.—Copper Ferrocyanide, 0·10 per cent., with N/15 Sodium Chloride.
D = 2·0. Put into apparatus at 2.12 p.m.

Time.	Period.	Time.	Period.	Remarks.
2.14	20·8	2·31	19·2	Apparently very low viscosity, less than that of water. The amplitudes of these swings were very small, and there were indications that the oscillations were being confined between narrow limits.
2.19	21·1	2·35	18·2	
2.21	21·5	2·37	17·7	
2.23	25·0	2·40	16·4	
2.25	27·8	2·46	14·8	
2.26	24·4	2·53	14·6	
2.29	20·6		14·3	The suspension was examined without disturbing it, and showed no signs of coagulation.
		3·12	13·0	
Time.	T.	C.	D.	Remarks.
3.18	33·7	35·7	2·0	The movement of the cylinder was very slow and jerky. The suspension was stirred vigorously.
	32·75	33·45	0·7	
3.34	33·65	33·3	-0·35	The cylinder followed the movement of the torsion head, but not completely; it then oscillated about a position which was not the true zero. The suspension, in contrast to the one described in Table VIII, was not obviously thixotropic, probably because the time of "setting" was very short with these particular concentrations of copper ferrocyanide and salt.
	21·1	22·7	1·6	
3.45	33·6	31·5	-2·15	
3.50	33·6	31·8	-1·8	

Table VIII.—Copper Ferrocyanide, 0·7 per cent., N/50 Sodium Chloride.
Made up and put into apparatus at 7 p.m. D = 2·4. Cylinder oscillated freely with period of 21·4 seconds. The suspension was allowed to stand overnight.

Time.	T.	C.	D.	Remarks.
a.m.				The cylinder could not now be made to move by turning the torsion head, i.e., the suspension was rigid. It was taken out and shaken vigorously. When replaced in the apparatus the cylinder swung freely. D = 2·3.
10.0	26·3	30·8	4·5	
10.30	19·1	30·8	11·7	
10.50	19·1	30·7	11·6	

Table VIII—(continued).

Time.	Period.	Time.	Period.	Remarks.
12.12	21.1	12.37	23.4	At 12.46 the cylinder had become fixed and could not be made to oscillate by moving the torsion head. The suspension thus became rigid again after shaking. Its "setting" time was about 30 minutes.
12.22	21.4	12.39	24.1	
12.30	21.9	12.40	24.6	
12.34	22.45	12.45	25.6	

Table IX.—Copper Ferrocyanide, 1.04 per cent., N/50 Sodium Chloride. Made up and put into apparatus at 7 p.m. D (water) = 1.55.

Time.	T.	C.	D.	Remarks.
a.m.				The cylinder could not be made to move by hard thumping on the bench nor by tapping the supporting rod.
2.20	15.9	18.6	2.7	
2.22	19.8	18.6	-1.2	
2.27	4.5	18.55	14.05	
2.37	4.5	18.55	14.05	
2.40	Turned outer cylinder counter-clockwise through 360°. Inner cylinder responded by moving through about 2°. Although D now corresponded with 1180 scale centimetres there was no sign of movement in 35 minutes.			

Table X.—Cadmium Sulphide, 0.77 per cent., N/15 Sodium Chloride. Made up and put into apparatus on Tuesday at 1.30 p.m. Cylinder oscillated freely, period 20.8 seconds. D = 1.5.

Time.	Period.	Remarks.		
Tuesday.				
p.m.				
3.15	21.0			
3.41	22.6			
4.0	24.0			
4.26	Moved very slowly and jerkily over about 1 cm., and could not be made to swing by moving torsion head.			
Time.	T.	C.	D.	Remarks.
p.m.				
6.38	12.5	13.5	1.0	
7.0	21.3	13.6	-7.7	
Wednesday.				
a.m.				
9.30	21.3	17.6	-3.7	
	5.4	17.6	12.2	Quite rigid.

Table XI.—Cadmium Sulphide, 1.26 per cent., N/20 Sodium Chloride. Made up and put into apparatus on Monday at 10.35 a.m. $D(\text{water}) = 1.0$.

Time.	Period.	Time.	Period.	Remarks.
Monday. a.m.				
10.45	20.7	11.43	16.2	
11.15	36.0	11.51	15.0	
11.25	19.0	p.m.		
11.35	15.0	12.3	14.4	
(Readings during next 24 hours omitted.)				
Time.	T.	C.	D.	Remarks.
Tuesday. a.m.				
11.40	15.4	15.95	0.55	
p.m.				
12.50	15.4	15.90	0.50	
	4.2	15.80	11.60	
1.0	4.2	15.75	11.55	
1.25	4.2	15.40	11.2	
3.0	4.2	15.30	11.1	
Wednesday. a.m.				
9.20	Settling had occurred. Suspension was stirred up at 12.40 p.m., and showed rigidity in 16 minutes.			
p.m.				
12.56	3.6	19.3	15.7	During these observations, lasting nearly 5 hours, the stress was reduced by only one-fourteenth of its initial value. The movement of the cylinder occurred in slight jerks, and was almost certainly due to external vibrations.
1.4	3.6	19.0	15.4	
3.15	3.6	18.5	14.9	
4.0	3.6	18.45	14.85	
4.42	3.6	18.15	14.55	
5.45	3.6	17.85	14.25	

A characteristic feature of the observations recorded above, and indeed of all the work done with suspensions containing electrolyte, was their extreme sensitiveness to slight mechanical disturbance. By carrying out experiments during the "small hours" and by the scrupulous avoidance of unnecessary movement on the part of the observer it was possible to show that some of the sols were able—apparently permanently—to support small stresses without yielding, whereas exactly similar sols under ordinary working conditions were mechanically unstable. The significance of this well-defined property will be discussed at a later stage.

Experiments on Relaxation.

Some of the sols which observations of the kind just described showed to possess a very high viscosity bordering on rigidity were used for "relaxation" experiments such as were done by Hatschek and Jane with gelatin and certain colloidal dyestuffs. The results are shown in fig. 1, in which the abscissæ

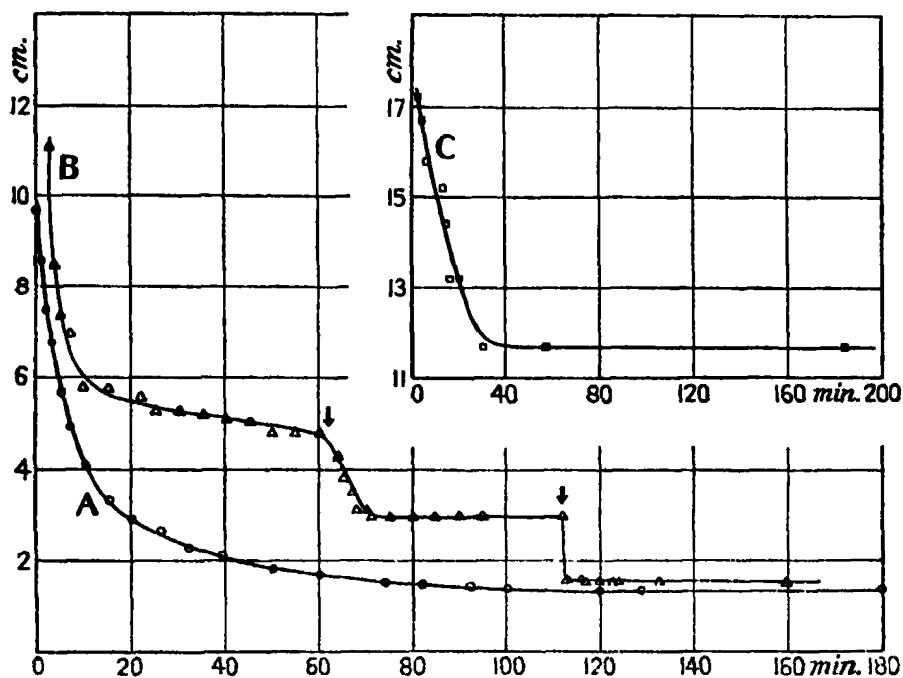


FIG. 1.—Relaxation Curves of Copper Ferrocyanide Sols. A and B: 0.26 per cent. with N/32 NaCl; C: 0.23 per cent. with N/25 NaCl. Arrows indicate times when external vibrations occurred. Ordinates: distance in centimetres from position of zero stress.

are times and the ordinates are proportional to the stress. In the first experiment (A) the torsion head was rotated, and the slow creep of the inner cylinder toward its new equilibrium position was watched and timed. In succeeding experiments the cylinder was prevented from moving by progressive backward movement of the torsion head so as to diminish the torque (B and C). It is evident that in no case did the inner cylinder regain, or show any signs of ever regaining, its initial equilibrium position; that is to say, the suspensions were able to support a stress indefinitely when that stress had reached a small enough value. Curve B is of special interest in showing the effect of accidental mechanical vibrations on the course of the relaxation curve. There is a clear

suggestion that in the absence of such disturbances the final equilibrium position would have been quite different.

Relation between Stress and Strain.

With sols more rigid than those referred to in the preceding section, observations of the relation between stress and strain were made by a method similar to that used by Schwedoff* for determining the rigidity of gelatin solutions. The results of some of these measurements are shown in fig. 2. It will be seen

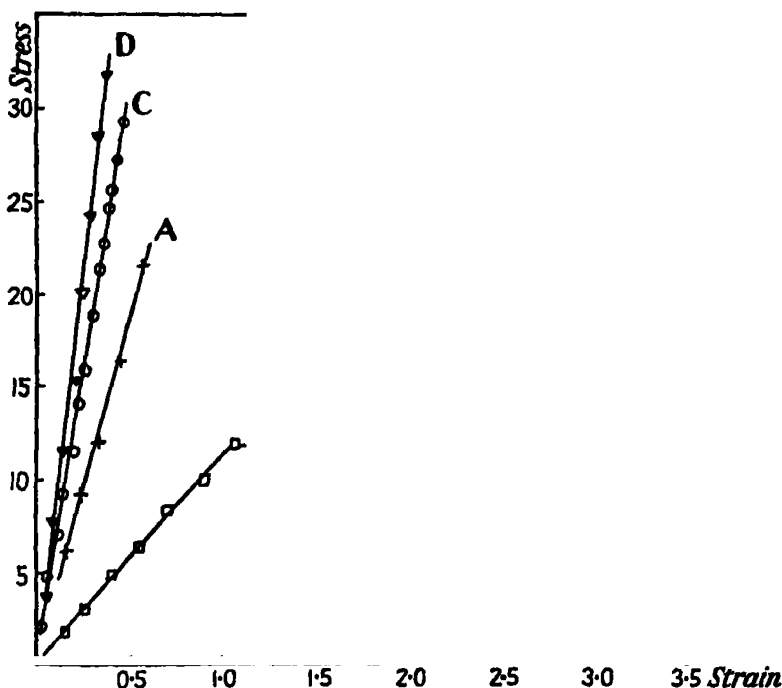


FIG. 2.—A and B : $\text{Cu}_2\text{Fe}(\text{CN})_6$, 0.24 per cent., N/25 NaCl ; C : $\text{Cu}_2\text{Fe}(\text{CN})_6$, 0.37 per cent., N/40 NaCl ; D : CdS, 0.77 per cent., N/20 NaCl. Stress and strain in arbitrary units.

that the stress-strain curves are practically rectilinear, and that the liquids therefore behave as perfectly elastic bodies within the time taken for the experiments. Curve B is of interest because an accidental disturbance in the course of the measurements caused the inner cylinder to move in such a way as apparently to reduce the strain whilst the stress remained almost unchanged. The continuation of the curve after the break is, however, parallel with the first part, suggesting a slipping of the cylinder in the liquid rather than a shearing of the liquid itself.

* 'J. Physique,' vol. 8, p. 341 (1889).

§ The moduli of rigidity (E) of the liquids studied have been calculated from the constants of the apparatus and are given in Table XII, together with those of some typical emulsoid sols for comparison.

Table XII.—Moduli of Rigidity (E) of Liquids.

Substance.	E.	Observer.
Copper ferrocyanide, 0.24 per cent., N/25 NaCl	0.86	M. & U.
" " 0.24 per cent., N/25 NaCl	0.50	"
" " 0.24 per cent., N/25 NaCl	0.95	"
" " 0.24 per cent., N/25 NaCl	1.4	"
" " 0.30 per cent., N/32 NaCl	0.57	"
" " 0.37 per cent., N/40 NaCl	2.7	"
Cadmium sulphide, 0.30 per cent., N/50 NaCl	9.1	"
" " 0.30 per cent., N/50 NaCl	8.8	"
" " 0.77 per cent., N/20 NaCl	3.7	"
Gelatin, 0.15 per cent.	0.5	R. & S.*
" 0.2 per cent.	0.7 to 3	"
" 0.2 per cent.	0.86	H. & J.†
Cotton yellow, 0.5 per cent.	2.3 to 15.7	"
Benzopurpurin, 0.3 per cent.	0.75	"
Mercury sulphosalicylic acid, 1.5 per cent.	2.3 to 18.8	"
Ammonium oleate	0.43 to 2.9	"

* Rohloff and Shinjo, 'Phys. Z.', vol. 8, p. 442 (1907).

† Hatschek and Jane, 'Kolloid-Z.', vol. 39, p. 300 (1926).

Other Methods of Detecting Rigidity in Suspensions.

When it is required to test a number of liquids, or a given liquid at short intervals, for rigidity, the apparatus described above is unsuitable on account of the length of time often needed to distinguish rigidity from very high viscosity. Two other methods were therefore used for this purpose. In the first, a cylindrical glass tube, 7 cm. long and 2.8 cm. in diameter, closed at the bottom, was weighted with lead shot and floated to a height of about 6 cm. in the liquid to be examined. A cork in the mouth of the tube carried a short vertical wire to which a light mirror was attached and which had also a pair of aluminium vanes fixed transversely to it. A magnetised needle was inserted vertically in the centre of the cork. The apparatus was enclosed in a draught-free housing, through the walls of which projected two glass jets directed toward the aluminium vanes in opposite directions. Outside the housing the jets were connected to the limbs of a T-piece through which air could be blown at the vanes, thus producing a torque which caused the floating tube to rotate through a small angle which could be measured by means of a lamp and scale. Translatory movement was prevented by a bar magnet fixed vertically in the roof

of the housing. Thus when the tube was rotated there was no restoring moment excepting that due to any elasticity in the liquid. Observations were made by measuring the rotation of the tube caused by blowing through the jets, and noting any subsequent reversal of this movement. Stable suspensions, and a normal but viscous liquid (glycerol), showed no reversal of the rotation, whereas suspensions of copper ferrocyanide containing 0.7 per cent. with N/50 and 0.35 per cent. with N/25 sodium chloride were shown to be perfectly elastic for strains up to those corresponding respectively with 10 cm. and 1.5 cm. movement on the scale.* The backward movement observed was a pronounced "spring," recalling the return of a piece of stretched elastic.

In the second method, a beaker was half filled with the liquid and placed centrally on a card marked in degrees of arc, whilst a glass plate marked with crossed reference lines covered the beaker. Some cork dust was floated on the surface of the liquid, which was then given a rotary movement either by turning the beaker or by gentle stirring. The subsequent behaviour of the liquid was observed by watching the movement of a selected particle of cork dust. In the case of a normal liquid the particles came to rest very slowly, and remained at rest; but with elastic liquids they rotated for a much shorter time in the direction in which the liquid had been stirred, and then came to rest and rotated in the opposite direction through an angle which could be roughly measured and which indicated the extent to which the liquid had been strained. The rapidity with which the original movement died down gave some idea of the degree of rigidity. Examples of observations made in this way are given in Tables XIII and XIV.

Table XIII.—Copper Ferrocyanide, 0.052 per cent., N/15 Sodium Chloride.

Time in minutes.	Backward movement in degrees.
5	Nil
15	More than 90
25	60
35	Just detectable
50	Nil

The sol was quite clear at the end of the experiment. No coagulation or precipitation had occurred.

* 10 cm. on the scale corresponds with an integral shear strain of about 0.1, or an actual strain of 0.13 at the wall of the inner cylinder.

Table XIV.—Copper Ferrocyanide, 0·10 per cent., N/15 Sodium Chloride.

Time in minutes.	Backward movement in degrees.	
5	Nil	
9	5	
14	10	
17	10	
29	10	
36	10	
41	Very slight	The suspension had started to settle. It was stirred up.
46	Nil	
53	5	
57	10	
63	5	Stirred vigorously.
92	Slight	
95	10	
253	20	The process appeared to be reversible. Between the last two readings the sol had been set aside and had settled only 4 mm. in 3 hours. It was left overnight and stirred again.
1140	5	
1148	7	

The observations quoted above show that a dilute suspension of copper ferrocyanide containing a little electrolyte may be perfectly elastic for small strains and under stresses of short duration. The cork dust experiments illustrate the important fact that, whilst elasticity requires a certain time to develop, yet the property may vanish after a still longer time, provided the suspension is sufficiently dilute; thus the 0·05 per cent. suspension had lost its elasticity after standing for about 1 hour, whereas one of double this strength retained the property for 19 hours.

Discussion.

The general results obtained with the two substances examined are in agreement so far as comparison is possible; the chief difference observed was that the development of rigidity in suspensions of cadmium sulphide required a greater volume percentage of solid than with copper ferrocyanide.

All the experiments agree in emphasising the importance of the time factor in the production both of variable viscosity and of rigidity. The appearance of these two properties in the order named is clearly seen from the measurements of the oscillation period given in Table VI. The period at the beginning of the experiment was almost the same as in water, but after about 15 minutes began to increase, becoming, however, higher for oscillations of small than for those of large amplitude; and this behaviour corresponds with a higher viscosity at low rates of shear. Still later, the period became considerably

smaller than in pure water, especially when the amplitude was small. The phenomenon is shown still more strikingly in Tables VII and XI. This behaviour can only be explained by assuming that the liquid possesses rigidity, since it is impossible for the suspension to be only half as viscous as water. The rotating cylinder produces a strain in the surrounding liquid, and this excites a stress the moment of which is added to the torque of the fibre, thus increasing the restoring moment and shortening the period of oscillation. It is evident, from a detailed examination of the experiments with the weaker suspensions, that variable viscosity is shown sometimes when rigidity is absent, and always when it is present.

The origin of these effects may be looked for either in the condition of the dispersion medium or in that of the solid. The relative adequacy of theories embodying respectively these two points of view will be discussed when the results of similar experiments with non-aqueous systems have been presented in a later communication. At present it may be pointed out that the addition of an electrolyte such as sodium chloride in concentrations up to decinormal to the suspensions studied is not known to produce any such change in the dispersion medium (water) as would account for the transformation of a mobile liquid with a normal viscosity coefficient into one possessing measurable rigidity. On the other hand, such an addition is known to cause the formation of aggregates from the initially independent particles of the disperse phase, and if this action is taken into account it becomes easy to explain all the phenomena observed. It has already been shown* by one of us that, in the case of a stable aqueous suspension of particles individually visible under the microscope, the first effect of the addition of sodium chloride in concentrations insufficient to cause precipitation is to promote the formation of open or dendritic aggregates. When the concentration of electrolyte exceeds a certain limiting value these aggregates gradually become more compact; and if the original volume percentage of solid is high enough these processes lead to the production of jellies which afterwards undergo syneresis—that is, the solid material retains its coherence and shrinks as a whole. If, on the other hand, the concentration of disperse phase is small, a coherent jelly may not be formed at any stage, and if it does form the subsequent consolidation may lead to the formation of separate aggregates rather than a single coherent structure, owing to the lack of solid material required to form connecting links.

The production of elastic systems with a measurable coefficient of rigidity is a natural consequence of the processes referred to above, on the reasonable

* 'Proc. Roy. Soc.,' A, vol. 125, p. 143 (1929).

assumption that the addition of electrolyte produces the same effects in stable suspensions of amicroscopic particles as have been directly observed in those with visible ones. In those cases where the inner suspended cylinder was firmly "held" by the liquid a continuous structure must have extended between the walls of the two cylinders. It is the rigidity of this solid network that is determined in measurements of the stress-strain type. Such a structure is disintegrated by mechanical disturbance, and when this happens the rigidity vanishes until a sufficient time has elapsed for the structure to be rebuilt. It may also be rendered discontinuous by later consolidation (syneresis) leading to rupture of its weaker parts. Thus the presence of a continuous solid structure throughout the liquid is a necessary and a sufficient condition for rigidity. If aggregates are formed but not linked up to a continuous structure—whether by reason of too small a proportion of solid or because the process of shrinkage has ruptured the weaker parts and left isolated masses—there can be no elasticity to shearing forces, but such a system may still possess variable viscosity on account of the large proportion of liquid entrained in the separate aggregates. At low rates of shear the effective volume concentration of solid is very high and leads to high viscosities, whilst the disintegration of the aggregates brought about by higher rates of shear causes the previously held liquid to be liberated and thus reduces the effective volume concentration of solid. This effect is progressive, and at sufficiently high rates of shear may lead to a complete breakdown of the aggregates and to a viscosity corresponding with the actual proportion of dry solid.

Optical and Equivalent Paths in a Stratified Medium, Treated from a Wave Standpoint.

By D. R. HARTREE, Ph.D., Beyer Professor of Applied Mathematics,
University of Manchester.

(Communicated by E. V. Appleton, F.R.S.—Received January 20, 1931.)

§ 1. *Introduction.*

In a series of recent papers,* Appleton has examined various methods of investigating the structure of the Heaviside layer, laying particular stress on the exact nature of the information which can be obtained from the experimental observations made by different methods.

One particular point of importance in the interpretation of the observations emerges from this examination, namely the distinction between the "optical path" or "phase path" $\int \mu ds = c \int ds/V$ and the "equivalent path" or "group path" $c \int ds/U$, where V , U are the wave and group velocities and the integrations are taken along the geometrical ray between transmitter and receiver. The analysis also shows clearly that the latter is the quantity which is observed by most methods, and in particular by the frequency-change method used by Appleton himself in his observational work.*

In his discussions, Appleton has used a ray treatment of the refraction by the ionised layer, that is to say a treatment based on rays obeying the laws of geometrical optics as expressed in a general form in Fermat's principle, together with the idea of interference between different rays. In many cases this treatment gives a good approximation, but it is certainly inadequate in two particular cases, both of which may be of practical importance, and its application to another commonly occurring case seems to need justification.

It is well known that the rays of geometrical optics are not adequate to give an account of phenomena when the refractive index μ varies appreciably in a distance of the order of wave-length in the plane of the wave front (e.g., diffraction grating formed by alternate strips of different refractive index†)

* E. V. Appleton, 'Proc. Phys. Soc., Lond.,' vol. 41, p. 43 (1928), vol. 42, p. 321 (1930); 'Proc. Roy. Soc.,' A, vol. 126, p. 542 (1930); E. V. Appleton and J. A. Ratcliffe, 'Proc. Roy. Soc.,' A, vol. 128, p. 133 (1930); E. V. Appleton and A. L. Green, 'Proc. Roy. Soc.,' A, vol. 128, p. 159 (1930).

† Cf. the "laminary grating," R. W. Wood, 'Physical Optics,' p. 211.

and it may be expected that geometrical optics would also be inadequate to deal with the propagation in a medium in which there is an appreciable variation of μ in a wave-length (in the medium), in a direction normal to the wave front. Now for total reflection at normal incidence (which may actually occur with radio waves) the wave-length in the medium becomes indefinitely large as $\mu \rightarrow 0$, that is, at the "totally reflecting" layer, so for such total reflection it is never true that the change of μ in a wave-length is everywhere small. This is the case in which the use of the ray treatment needs justification.

Secondly, geometrical optics is inadequate to give an account of partial transmission through a thin layer at an angle of incidence greater than the critical angle for "total reflection." Now one conclusion from Appleton's observations is that there are two regions at different heights in which the ionisation may be enough to cause reflection. If we consider the frequency varied through the frequency necessary to give appreciable penetration of the lower layer, the reflected wave, over part of this range, will depend essentially on partial transmission through the lower layer, although it is "totally reflecting" in the sense of geometrical optics; and the details of the transition from negligible to effectively complete penetration of the lower layer cannot be described in terms of rays at all. Further, a pure ray treatment cannot give an account of the partial reflection by a sharp boundary between two media of different μ , and still less of the partial reflection by a medium of continuously varying μ . Consequently on a ray treatment the reflection from the lower ionised region will be "all or none"; if the ionisation in the lower region increases, there will be a discontinuous transition from complete reflection from the upper region to complete reflection from the lower region; on a wave treatment the transition will be continuous, with simultaneous reflection from both regions in the intermediate stages. Actually observation indicates a rapid but not discontinuous change, and simultaneous reflections from both regions has been observed. Clearly a wave treatment is necessary to give an account of these observations.

Thirdly, in a stratified medium, waves polarised in and perpendicular to the plane of incidence are propagated differently (apart from any effect due to an external magnetic field); the difference is related to the difference between the reflection coefficients of a sharp boundary for the two waves, and the ray treatment gives no account of it.

For application to these cases it is desirable to give a wave treatment of the phenomena discussed by Appleton. The object of the present paper is to investigate the first case and find the magnitude of the errors of the ray treat-

ment in the case of total reflection, and in general to find precisely the conditions under which the ray treatment is applicable, and also to carry out the necessary work preliminary to an investigation of the second and third cases mentioned. It will appear that in most examples of the first case, the use of the ray treatment can be justified.

We will consider a refracting medium stratified in layers perpendicular to the z axis, which in view of applications we will take as being vertically upward; that is, we consider μ a function of the height z only. The propagation of plane waves in such a medium had been investigated by the writer in two other papers.* For simplicity the medium will here be taken as optically isotropic.

§ 2. Optical and Equivalent Paths.

We must first enquire what are the quantities which in a wave treatment correspond to the optical and equivalent paths.

$$P = \int \mu ds, \quad P' = \int c ds/U \quad (1)$$

of the ray treatment.

If λ_0 is the wave-length *in vacuo*, and λ the wave-length in the medium, then

$$P/\lambda_0 = \int \mu ds/\lambda_0 = \int ds/\lambda. \quad (2)$$

If μ is constant, $\int ds/\lambda$ can validly be called the number of waves in the range of integration, and it would seem at first sight that the same interpretation could be given when μ (and so λ) is varying along the path of integration. But on closer consideration it is rather difficult to assign this meaning to $\int ds/\lambda$ when μ varies so rapidly that the change of μ (and so of λ) in a wave-length in the medium is considerable; the space variation of the electric field in the wave is no longer simple harmonic, and there is some liberty of choice in defining the "phase" at any point, and therefore in specifying the fraction of a wave-length lying in a range small compared to λ . Also the interpretation fails entirely when μ^2 becomes negative, whereas we know that waves can be partially transmitted through a layer in which μ^2 is negative, and that even in

* D. R. Hartree, 'Proc. Camb. Phil. Soc.,' vol. 25, p. 97 (1929); vol. 27, p. 143 (1931). These will be referred to as I and II.

the case when the reflection is complete, the wave disturbance does not fall to 0 immediately at the point where $\mu^2 = 0$.

But although usually expressed in terms of optical path, what is observed in the experiments is effectively the phase difference Φ between the upgoing wave at the transmitter and the downcoming wave at the receiver, and in particular what is observed in the frequency-change method is the change of this phase difference with change of frequency ; and although the optical path $\int \mu ds$ integrated along a ray has not always a precise meaning, this phase difference between upgoing and downcoming waves has a precise meaning, and can be found from the solution of the equations of wave propagation in the medium considered.

Except in the cases of reflection at vertical incidence (*i.e.*, transmitter and receiver on the same vertical), we have to remember that, speaking in terms of rays, the angles of incidence and the path of the ray may be different for different frequencies, or in terms of waves, that the wave is divergent ; a direct solution of the equations of a stratified medium for a divergent wave would be difficult to obtain and probably too complicated to use, so we consider the emitted wave resolved into trains of plane waves ; each plane wave train gives rise to a reflected wave train which will reach the receiver, but only those for which the phase is stationary with respect to the direction of the wave normal will contribute appreciably to the resultant field there.

Leaving out of account the effect of an external magnetic field (the earth's field in the application considered), propagation is symmetrical round the normal to the stratified medium, and we need only consider waves whose normals are in vertical plane containing transmitter and receiver ; if for one of these component plane waves θ is the angle of incidence (angle between vertical and wave normal in region where $\mu = 1$), and ϕ the phase difference between the incident wave at the transmitter and reflected wave at the receiver, then the plane waves which contribute to the effect at the receiver are those for which the θ is in the neighbourhood of the root of

$$\partial\phi/\partial\theta = 0. \quad (3)$$

The phase Φ of the *resultant* field at the receiver will not necessarily be the same as at the phase ϕ of the component plane wave at angle of incidence given by (3). The details of the analysis of the transmitted wave into component plane wave trains travelling in different directions depends on the particular directional properties of the transmitter, but assuming all the component

plane waves to be in phase at the transmitter it can be shown* that the phase difference between Φ and ϕ is in general independent of the frequency. The ray treatment gives no account of this difference.

If the component plane waves are not in phase at the transmitter, the relation between them and the resultant at the transmitter may give an additional contribution to $\Phi - \phi$; if it exists its variation with frequency is likely to be very small, and it will be neglected.

We will write

$$k = 2\pi/\lambda_0 = 2\pi f/c$$

where f is the frequency, and take

$$P = \phi/k, \quad (4)$$

for the value of θ given by (3), as the definition of P ; when the ray treatment is applicable, this is equivalent to (2), and (3) is then a special case of Fermat's principle; (4) will serve as an extension when the ray treatment is inapplicable.

We will find that the value given by the formula for ϕ in terms of the solution of the equations of propagation is undetermined to the extent of an arbitrary multiple of 2π . This corresponds to the impossibility pointed out by Appleton of determining the optical path, and to the well-known fact that by observation on one wave-length alone, it is impossible to determine the whole number of periods in the phase difference between two waves, though the fractional part of the number of periods is often easily determined.†

In the frequency-change method the *change* of Φ for a given *change* of k is measured. If $\Delta\Phi = 2\pi\Delta n$ is the change of Φ for a given frequency change Δf , the quantity which Appleton calls the equivalent path is $c\Delta n/\Delta f = \Delta\Phi/\Delta k$. We will define the equivalent path P' by

$$P' = \frac{\partial\Phi}{\partial k},$$

where for each k , Φ is taken for such a value of θ that (3) is satisfied. But since firstly $\Phi - \phi$ is independent of k , and secondly ϕ is stationary with respect to θ , this is equivalent to

$$P' = \frac{\partial\phi}{\partial k}, \quad (5)$$

* The analysis is similar to the evaluation of the predominant group in the propagation of a wave group in a dispersive medium (see, for example, Havelock, 'Camb. Math. Tracts,' No. 17, §§ 10, 12) with the difference that instead of the frequency as single independent variable there are now two independent variables θ and azimuth ψ . The value of $\Phi - \phi$ may be 0 or $\pm \pi/2$ according to the signs of $\partial^2\phi/\partial\theta^2$ and $\partial^2\phi/\partial\psi^2$.

† Cf. measurement of wave-length of light by Fabry-Perot plates.

where $\partial\phi/\partial k$ is taken for θ constant and equal to a root of (3). We will further define the mean equivalent path for a finite change Δk of k by

$$\bar{P}' = \frac{\Delta\phi}{\Delta k}, \quad (6)$$

It will appear that in some cases, when Δk is such that $\Delta\phi/2\pi$ is an integer, the expression for the mean equivalent path is simpler than that for the equivalent path; the mean equivalent path also corresponds more closely with the quantity actually observed.

If the equation (3) for θ has more than one root, we get the phenomenon described on a ray treatment as interference between the rays emitted with the corresponding values of θ (e.g., interference between ray reflected from Heavyside layer and ground ray).

§ 3. Phase Difference in Terms of Solutions of Equations of Propagation.

Taking the xz plane as plane of incidence, the equations of propagation of plane waves, incident from below at angle of incidence θ , in a stratified medium are*

$$\frac{\partial^2 L_y}{\partial z^2} = -k^2 (\mu^2 - \sin^2 \theta) L_y, \quad (7)$$

(cf. I, (23)) for waves in which L is perpendicular to the plane of incidence, and

$$\sin \theta \frac{\partial L_x}{\partial z} = ik (\mu^2 - \sin^2 \theta) L_x, \quad (8)$$

$$\frac{\partial}{\partial z} (\mu^2 L_x) = ik \sin \theta \mu^2 L_x, \quad (9)$$

(cf. I, (26), (27)) for waves in which L is in to the plane of incidence; the x and t variations of all components of L are expressed by a factor $e^{ik(x - z \sin \theta)}$.

As emphasised in I, § 5, we can only define precisely the optical properties of a *finite* layer of stratified medium if it is bounded on both sides by a homogeneous medium; and in this case the solution of the equations required is that corresponding to a wave travelling in the $+z$ direction only above the layer; this gives the boundary condition necessary to define the appropriate

* The notation is that of I and II, in which E is used for the electric field actually acting on an element of the refracting medium; L is a derived vector introduced for mathematical convenience, and is shown in I (§ 3) to be the field in a needle cavity, that is the "electric field E " in Maxwell's equations of a material medium as usually written μ^2 may be real, of either sign, or complex.

solution of the equations. The problem is also definite when we have a *semi-infinite* slab of stratified medium, either with μ^2 complex (absorbing medium), or with $\mu^2 < \sin^2 \theta$ (totally reflecting medium), for all sufficiently large z , and bounded below by a homogeneous medium; in this case the boundary condition $L = 0$ at $z = \infty$ is sufficient to define the solution.

In either problem, the wave in the lower homogeneous medium (which we will take to have $\mu = 1$) is

$$L = e^{ik(ct - x \sin \theta)} (\alpha e^{-ikz \cos \theta} + \beta e^{ikz \cos \theta}) \quad (10)$$

the first term representing the upgoing (incident) and the second the downcoming (reflected) wave. If the transmitter is at $(0, z_0)$, and the receiver at $(2x_0, z_0)$ the phase of the upgoing wave at the transmitter is

$$\arg \alpha + k(ct - z_0 \cos \theta)$$

and that of the downcoming wave at the receiver is

$$\arg \beta + k(ct - 2x_0 \sin \theta + z_0 \cos \theta),$$

so the phase difference between upgoing wave at the transmitter and downcoming wave at the receiver is

$$\phi = \arg(\alpha/\beta) + 2kx_0 \sin \theta - 2kz_0 \cos \theta. \quad (11)$$

We can put this into two different forms, for use according as we find it more convenient to use two general independent solutions of the equations of the stratified medium, which have to be combined to give the solution of the problem with the particular boundary conditions, or to use directly the appropriate solution.

The former method is probably the most convenient for a finite layer of stratified medium; the analysis follows closely that of I, § 5. If G, H are two independent solutions, and suffixes 0, 1 refer respectively to the height at which the phase difference is required and to the upper homogeneous medium,* and

$$n_1 = [\mu_1^2 - \sin^2 \theta]^{\frac{1}{2}} \quad (12)$$

the root for which the real part is positive being taken, and

$$\begin{aligned} \Delta_{\pm} = & \quad G_1' + ikn_1 G_1 & H_1' + ikn_1 H_1 \\ & G_0' \pm ik \cos \theta G_0 & H_0' \pm ik \cos \theta H_0 \end{aligned} \quad (13)$$

* This use of the suffixes 0 and 1 is the reverse of that made in I; it is adopted here as being more convenient.

then from (I, (33), (35))

$$(\alpha/\beta) e^{-2ikz_0 \cos \theta} = \Delta_-/\Delta_+, \quad (14)$$

so

$$\phi = 2kx_0 \sin \theta + \arg (\Delta_-/\Delta_+). \quad (15)$$

The latter method is probably the most convenient for a semi-infinite medium for which the boundary condition, for waves incident from below, is $L = 0$ at $z = \infty$; in this case, with examples of which we will mainly be concerned, the particular solution of the equation which fits the boundary conditions is supposed known. Differentiating (10) with respect to z , and forming $ikL \cos \theta \pm \partial L/\partial z$, we find

$$\phi = 2kx_0 \sin \theta + \arg \left[\left(-\frac{\partial L}{\partial z} + ikL \cos \theta \right) / \left(\frac{\partial L}{\partial z} + ikL \cos \theta \right) \right]_0. \quad (16)$$

If μ^2 is always real, the equations have a real solution* satisfying the boundary conditions $L = 0$ at $z = \infty$; in this case we get complete reflection (i.e., the reflection coefficient $|\alpha/\beta|^2$ is 1), the wave system is a pure stationary wave without a travelling wave superposed, and since L is then real,

$$\phi = 2kx_0 \sin \theta + 2 \tan^{-1} \left[\frac{\partial L/\partial z}{kL \cos \theta} \right] \quad (17)$$

this can be expressed in terms of the phase of the stationary wave, but is most useful as it stands. Clearly ϕ is indeterminate to the extent of an arbitrary multiple of 2π , as noted in § 2.

Formula (17), it must be emphasised, only holds for a stratified medium whose reflection coefficient is 1, i.e., for total reflection by a perfectly transparent medium; in order for this to occur, it is strictly necessary that $\mu^2 < \sin^2 \theta$ for all sufficiently large z ; it will be approximately the case if $\mu^2 - \sin^2 \theta$ is negative and not very small over a range of z of several wave-lengths.

§ 4. Vertical Incidence. General Expression for Equivalent Path.

The case of vertical incidence is particularly simple, as, speaking in terms of rays, the ray is the same for all k , or in terms of waves the solution of (3) is $\theta = 0$ by symmetry, and we are not further concerned with the variation of ϕ with θ ; and also we avoid having to consider the different propagation of waves polarised in and perpendicular to the plane of incidence.

If we have two general solutions of the equations of propagation or the one

* For μ^2 real, and L perpendicular to plane of incidence, the solution of (8) and (9) gives a stationary wave for which L_x and L_z are in quadrature; either can be taken as real.

particular solution satisfying the required boundary conditions, we can find the optical path ϕ/k by the methods of § 3. Further, for a medium of reflection coefficient unity we can find an expression for the equivalent path in terms of the particular solution as follows.

Putting $\theta = 0$ in (17), which is applicable to the case, and distinguishing the value of quantities, at the height z_0 at which we require the phase difference, by the suffix 0 we have

$$\phi = 2 \tan^{-1} \left[\frac{\partial L / \partial z}{kL} \right]_0. \quad (18)$$

The equation of propagation is

$$\frac{\partial^2 L}{\partial z^2} = -k^2 \mu^2 L, \quad (19)$$

and we are concerned with the solution for which $L = 0$ at $z = +\infty$.

Suppose this equation solved for one value of k ; we require the variation of ϕ at a given z_0 for a variation of k , remembering that μ^2 is a function of k . Let the symbol δ prefixed to any quantity mean the first order variation in that quantity at a given height z , for a variation δk of k (δk being independent of z). Then

$$\frac{\partial^2 (\delta L)}{\partial z^2} = -k^2 \mu^2 \delta L - L \delta (k^2 \mu^2).$$

If we write

$$\delta L = L\gamma, \quad (20)$$

we find

$$\frac{\partial}{\partial z} \left(L^2 \frac{\partial \gamma}{\partial z} \right) = -L^2 \delta (k^2 \mu^2). \quad (21)$$

But differentiating (20) we have

$$L^2 \frac{\partial \gamma}{\partial z} = L \frac{\partial (\delta L)}{\partial z} - \frac{\partial L}{\partial z} \delta L,$$

and as L and $L + \delta L$ are both solutions of (19) for which $L = 0$ at $z = \infty$, we have $L^2 \frac{\partial \gamma}{\partial z} = 0$ at $z = \infty$, so integrating (21).

$$\left(L^2 \frac{\partial \gamma}{\partial z} \right)_0 = \left(L \frac{\partial (\delta L)}{\partial z} - \frac{\partial L}{\partial z} \delta L \right)_0 = \int_{z_0}^{\infty} L^2 \delta (k^2 \mu^2) dz. \quad (22)$$

Further, from (18) the first order variation $\delta \phi$ of ϕ is

$$\delta \phi = \frac{2}{[(kL)^2 + (\partial L / \partial z)^2]_0} \left[k \left(L \frac{\partial (\delta L)}{\partial z} - \frac{\partial L}{\partial z} \delta L \right) - L \frac{\partial L}{\partial z} \delta k \right]_0,$$

so by using (22)

$$\frac{\partial \phi}{\partial k} = \frac{2}{[(kL)^2 + (\partial L/\partial z)^2]_0} \left[k \int_{z_0}^{\infty} L^2 \frac{\partial (k^2 \mu^2)}{\partial k} dz - L_0 \left(\frac{\partial L}{\partial z} \right)_0 \right]. \quad (23)$$

Now $z = z_0$ is in a region in which μ is constant and equal to 1. If in this region Λ is the maximum amplitude of the stationary oscillation, then

$$(kL)^2 + (\partial L/\partial z)^2 = k^2 \Lambda^2, \quad L_0 \left(\frac{\partial L}{\partial z} \right)_0 = \frac{1}{2} k \Lambda^2 \sin \phi,$$

$$P' = \frac{\partial \phi}{\partial k} = 2 \int_{z_0}^{\infty} \frac{L^2}{\Lambda^2} \frac{\partial (k^2 \mu^2)}{k \partial k} dz - \frac{\sin \phi}{k}, \quad (24)$$

Now when μ is real the group velocity U is given by

$$c/U = \partial (k\mu)/\partial k,$$

and we can take this as the definition of U when μ^2 is negative ; so

$$\partial (k^2 \mu^2)/\partial k = 2k\mu c/U. \quad (25)$$

Also, if we take a finite variation Δk giving a variation $\Delta \phi$ of ϕ over a number of periods, the first term in (24) remains approximately constant, while the second term oscillates in sign ; hence the *mean* equivalent path is given very nearly by

$$\bar{P}' = \frac{\Delta \phi}{\Delta k} = 2 \int_{z_0}^{\infty} \frac{2\mu L^2}{\Lambda^2} \frac{c}{U} dz. \quad (26)$$

§ 5. Vertical Incidence, Example. Finite Slab of Refracting Medium backed by Total Reflector.

The method of the previous section enables us to find the equivalent path for any frequency from the solution of the equation of propagation for that frequency and the dispersion formula for the medium alone.

In some particular cases, an exact formula for ϕ in terms of known functions can be obtained, and in such cases it may be easier to obtain an expression for ϕ as an explicit function of k , and to differentiate it to give the equivalent path.

We will consider some such cases, which will illustrate various points of difference between the wave and ray method of treatment.

The first example is that of a finite slab of homogeneous transparent refracting medium backed by a perfect reflector ; that is, a variation of μ^2 shown in

fig. 1. We take the heights of the lower and upper faces of the slab as z_1 , z_2 , and require the value of ϕ for $z = z_0 < z_1$.

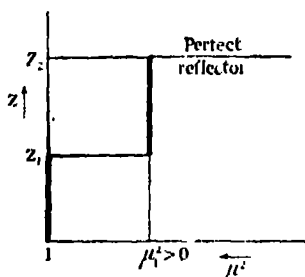


FIG. 1.

We need, therefore, a solution of

$$\frac{\partial^2 L}{\partial z^2} = -k^2 \mu^2 L,$$

with

$$\left. \begin{aligned} L &= 0 \text{ at } z = z_2 \\ \mu^2 &= \mu_1^2, \quad z > z_1; \quad \mu^2 = 1, \quad z < z_1 \\ L, \partial L / \partial z &\text{ continuous at } z = z_1 \end{aligned} \right\}. \quad (27)$$

Putting

$$\begin{aligned} L &= A \sin k\mu_1 (z - z_2), \quad L' = Ak\mu_1 \cos k\mu_1 (z - z_2); \quad z > z_1 \\ L &= B \sin (kz - \alpha), \quad L' = Bk \cos (kz - \alpha); \quad z < z_1 \end{aligned}$$

the boundary conditions at $z = z_1$ give at once

$$\tan (kz_1 - \alpha) = \frac{1}{\mu_1} \tan k\mu_1 (z_1 - z_2), \quad (28)$$

so that at $z = z_0$

$$\begin{aligned} \phi &= 2 \tan^{-1} \left[\frac{\partial L / \partial z}{kL} \right]_0 = 2 [\pi/2 - (kz_0 - \alpha)] \\ &= \pi + 2k(z_1 - z_0) + 2 \tan^{-1} [\mu_1^{-1} \tan k\mu_1 (z_2 - z_1)], \end{aligned} \quad (29)$$

The ray treatment gives

$$\phi = k \int \mu \, ds = 2k(z_1 - z_0) + 2k\mu_1(z_2 - z_1). \quad (30)$$

The difference of π between these two expressions represents the phase change on reflection from a perfect reflector. The difference in the term depending on the thickness of the slab ($z_2 - z_1$) arises from the fact that the ray treatment takes no account of the partial reflection of the incident wave at the lower face,

or multiple reflection between the upper and lower faces. A ray treatment of the interference between all the reflected waves could be given, similar to the ray treatment of the Fabry-Perot plates, but it would have to use a reflection coefficient derived from a wave treatment, and also there would be no unique ray for which we could put $\phi = k \int \mu ds$ for the phase of the resultant downcoming wave, so that it would no longer be a pure ray treatment based on Fermat's principle. As pointed out in I, § 5, the infinite system of reflected waves is only a device for obtaining the result without solving the equation of propagation; by using the solution with the necessary boundary condition we have been able to avoid use of the system of reflected waves. If $\mu_1 - 1$ is small the reflection coefficient at the lower boundary $(\mu_1 - 1)/(\mu_1 + 1)$ is small, and correspondingly $\tan^{-1}[\mu_1^{-1} \tan k\mu_1(z_2 - z_1)]$ is nearly equal to the value $k\mu_1(z_2 - z_1)$ of the simple ray treatment.

Despite the difference, if we take a *finite* change Δk of k , such that $k\mu_1(z_2 - z_1)$ changes from $n\pi$ to $(n + 1)\pi$, where n is an integer, $\tan^{-1}[\mu_1^{-1} \tan k\mu_1(z_2 - z_1)]$ also changes by π , so

$$\bar{P}' = \Delta\phi/\Delta k = (z_1 - z_0) + [\Delta(k\mu_1)/\Delta k](z_2 - z_1) \quad (31)$$

exactly as for the ray formula; neglecting the change of μ_1^{-1} factor in $\mu_1^{-1} \tan k\mu_1(z_2 - z_1)$, the same is true for *any* change Δk giving a change of π in $k\mu_1(z_2 - z_1)$. Thus the *mean* equivalent path is very nearly if not exactly equal to that calculated by the ray treatment.

The simplification of the formula on taking the mean rate of change over a number of periods is similar to that which we have already noted in (26); the present case is complicated by an oscillation in the value of the integral in (26) as the phase of the wave at the lower boundary of the slab varies; the average over a number of periods takes the average over the oscillations.

§ 6. Vertical Incidence. Linear Variation of μ^2 .

We will take two examples of continuous variation of μ^2 for which we can obtain exact expressions for ϕ , and take first a linear variation (fig. 2),

$$\left. \begin{aligned} \mu^2 &= 1 - \frac{z}{z_1} & z > 0 \\ \mu^2 &= 1 & z < 0 \end{aligned} \right\}, \quad (32)$$

and find the phase difference between upgoing and downcoming waves in the homogeneous medium at $z = 0$. If we take any value of z_0 less than 0, a

corresponding addition will be made to ϕ , corresponding to the term $2k(z_1 - z_0)$ in formula (29) of the previous example.

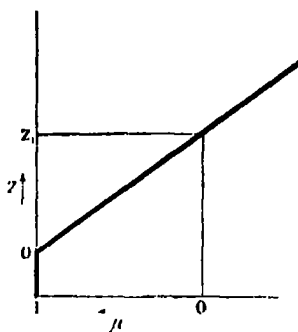


FIG. 2.

Putting

$$\zeta = \left(\frac{k^2}{z_1}\right)^{1/3} (z_1 - z), \quad (33)$$

the equation for wave propagation becomes for this case

$$\frac{\partial^2 L}{\partial \zeta^2} + \zeta L = 0. \quad (34)$$

We will write $L = A(\zeta)$ for the solution of this equation which tends to 0 as $\zeta \rightarrow -\infty$ ($z \rightarrow +\infty$), namely,*

$$\left. \begin{aligned} A(\zeta) &= \zeta^{1/3} [J_{1/3}(\frac{2}{3}\zeta^{3/2}) + J_{-1/3}(\frac{2}{3}\zeta^{3/2})] & (\zeta > 0) \\ &= |\zeta|^{1/3} [-I_{1/3}(\frac{2}{3}|\zeta|^{3/2}) + I_{-1/3}(\frac{2}{3}|\zeta|^{3/2})] & (\zeta < 0) \end{aligned} \right\}, \quad (35)$$

the asymptotic behaviour of $A(\zeta)$ for large positive ζ is

$$A(\zeta) \sim 3\pi^{-1} \zeta^{-1/2} \cos \left[\frac{2}{3}\zeta^{3/2} - \frac{1}{4}\pi \right]. \quad (36)$$

The value of ϕ at $z = 0$ [i.e., at $\zeta = (kz_1)^{2/3}$] is given by†

$$\tan \frac{\phi}{2} = \left[\frac{\partial L / \partial z}{kL} \right]_{z=0} = - \left[\zeta^{-1/2} \frac{1}{A} \frac{dA}{d\zeta} \right]_{\zeta = (kz_1)^{2/3}}. \quad (37)$$

When $kz_1 \gg 1$, the thickness of the medium in which μ^2 is positive is a large number of wave-lengths (*in vacuo*), and, speaking roughly, we may say

* See J. W. Nicholson, 'Phil. Mag.,' Series 6, vol. 18, p. 6 (1909); G. N. Watson, 'Treatise on Bessel Functions,' § 6.4.

† This can be expressed in terms of $J_{\pm 1/3}$, $J'_{\pm 1/3}$, but the form given is more convenient.

that μ^2 is "slowly varying"; in this case we can use the asymptotic expression (36) for A in (37) and find

$$\phi \sim \frac{4}{3}kz_1 - \frac{1}{2}\pi. \quad (38)$$

The ray treatment gives

$$\phi = k \int \mu ds = 2k \int_0^{z_1} [1 - z/z_1]^{\frac{1}{2}} dz = \frac{4}{3}kz_1, \quad (39)$$

so that for this case of a medium with μ^2 slowly varying, the expressions agree except for the term $-\pi/2$ in ϕ which can be interpreted as the sum of $-\pi$ for total reflection* and $+\pi/2$, the contribution to $\int \mu ds$ from the exponential "tail" of the wave in the region in which $\mu^2 < 0$.

In order to obtain the group path $P' = \partial\phi/\partial k$, it is not enough to differentiate (37) with respect to k for z_1 constant, as on account of dispersion μ^2 at each height may vary with k , and the variation of μ^2 with z may not remain linear, or if it does the value of z_1 may change.

If we take an ionised medium with electron density $N(z)$ varying with the height z , and assume a dispersion formula

$$\mu^2 = 1 - 4\pi N(z) e^2/mc^2 k^2, \quad (40)$$

then the algebraic form of variation of μ^2 with z (linear, quadratic, etc.) is the same for all k , and also the group velocity U is given by the simple formula $c/U = 1/\mu$. For these reasons it is often convenient to use this dispersion formula in order to get approximate quantitative results, and in fact it has been usually taken in work on the Heaviside layer. But the correct formula is†

$$\mu^2 = 1 - k_0^2/(k^2 + \frac{1}{3}k_0^2), \quad k_0^2 = 4\pi N(z) e^2/mc^2, \quad (41)$$

and in this case a distribution of electron density which gives a linear variation of μ^2 with z for one frequency will not give a linear variation of μ^2 with z for any other frequency. We could not then find the equivalent path by differentiation of (37), but would have to use the solution $L = A(\zeta)$ in the general formula (24) or (26) for the equivalent path.

However, to illustrate the difference between the type of results obtained by the wave and ray treatments, we will assume first that the variation of

* Since ϕ is indeterminate to a multiple of 2π , the change of phase on reflection can be taken as $+\pi$ or $-\pi$. If the arbitrary multiple of 2π in ϕ is chosen so as to give the asymptotic formula (38), then $\phi = -\pi$ for $z_1 = 0$ (sharp reflector).

† See II, § 8.

μ^2 with z remains linear as k is changed. Then differentiating (37) and substituting for $d^2A/d\zeta^2$ from the differential equation satisfied by A , we find

$$\begin{aligned} P' &= \frac{\partial \phi}{\partial k} = \frac{4}{3} \frac{\partial(kz_1)}{\partial k} \left[1 + \frac{1}{2\zeta} \frac{A dA/d\zeta}{\zeta A^2 + (dA/d\zeta)^2} \right]_{\zeta = (kz_1)^{\frac{1}{2}}} \\ &= \frac{4}{3} \frac{\partial(kz_1)}{\partial k} \left[1 - \frac{1}{4kz_1} \sin \phi \right]. \end{aligned}$$

If we write P_r' for the equivalent path calculated on the ray treatment

$$P_r' = \frac{4}{3} \frac{\partial(kz_1)}{\partial k},$$

so the difference between the equivalent path calculated by the wave and ray treatment is

$$P' - P_r' = -\frac{P_r'}{4kz_1} \sin \phi.$$

This difference, rather than its ratio to P_r' is the interesting quantity; we cannot evaluate it without knowing the relation between P_r' and z_1 , and this depends on the relation between k and z_1 . We will, therefore, assume further that the dispersion is given by (40); then $z_1 \propto k^2$, $P_r' = 4z_1$, and

$$P' - P_r' = -\frac{\sin \phi}{k} = -\frac{\lambda_0}{2\pi} \sin \phi. \quad (42)$$

This formula gives the difference, in vacuum wave-lengths, between the equivalent path calculated by the wave and ray treatments, under the assumptions stated. The maximum value of this difference is clearly $\lambda_0/2\pi$. This result depends on the particular dispersion formula (40), but the difference is likely to be of the same order of magnitude whatever dispersion formula is used.

The difference given by (42) oscillates, and if a finite frequency change is taken so that the change of ϕ at the lower boundary of the medium (not at the receiver) is a period or number of periods, $\bar{P}' - \bar{P}_r'$ will be very small on account of the oscillation. This justifies the use of the ray treatment in this case.

§ 7. Vertical Incidence. Quadratic Variation of μ^2 .

An exact solution can also be found for the case when we have a quadratic variation of μ with z above a certain height, joining smoothly to the homogeneous medium as shown in fig. 3; that is

$$\left. \begin{aligned} \mu^2 &= 1 - \left(\frac{z}{z_1}\right)^2 & z > 0 \\ &= 1 & z < 0 \end{aligned} \right\}. \quad (42)$$

We will calculate the phase difference between upgoing and downcoming waves at $z = 0$.

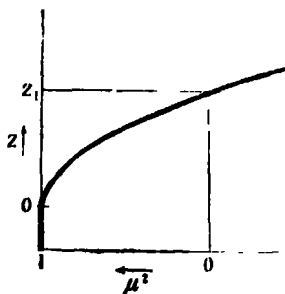


FIG. 3.

Putting this function for μ^2 into the equation of propagation we get

$$\frac{\partial^2 L}{\partial z^2} + [k^2 - (k/z_1)^2 z^2] L = 0, \quad (43)$$

which can be reduced to the standard form used by Whittaker and Watson*

$$\frac{\partial^2 L}{\partial \zeta^2} + (n + \frac{1}{2} - \frac{1}{4}\zeta^2) L = 0 \quad (44)$$

by the substitutions

$$\zeta = (2k/z_1)^{\frac{1}{2}} z, \quad n = (kz_1 - 1)/2. \quad (45)$$

The solution of (44) which tends to 0 as $\zeta \rightarrow \infty$, Whittaker and Watson* write $D_n(\zeta)$; so the solution of (43) we require for waves incident from below is

$$L = D_{\frac{1}{2}(kz_1-1)} [(2k/z_1)^{\frac{1}{2}} z].$$

The phase difference ϕ at $z = 0$ is given by

$$\tan \frac{\phi}{2} = \left[\frac{\partial L / \partial z}{kL} \right]_{z=0} = \frac{1}{(n + \frac{1}{2})^{\frac{1}{2}}} \frac{D_n'(0)}{D_n(0)} \quad (46)$$

with the value of n given by (45).

Now from the results given by Whittaker and Watson*

$$D_n(0) = \frac{\Gamma(\frac{1}{2}) 2^{in}}{\Gamma(\frac{1}{2} - \frac{1}{2}n)}, \quad D_n'(0) = \frac{\Gamma(-\frac{1}{2}) 2^{in-1}}{\Gamma(-\frac{1}{2}n)},$$

so

$$\frac{D_n'(0)}{D_n(0)} = -2^{\frac{1}{2}} \frac{\Gamma(\frac{1}{2} - \frac{1}{2}n)}{\Gamma(-\frac{1}{2}n)} = +2^{\frac{1}{2}} \tan \frac{\pi n}{2} \frac{\Gamma(\frac{1}{2}n + 1)}{\Gamma(\frac{1}{2}n + \frac{1}{2})},$$

* E. T. Whittaker and G. N. Watson, 'Modern Analysis,' § 16.5.

so finally from (46), and the value of n given by (45)

$$\tan \frac{\phi}{2} = \frac{2}{(kz_1)^{\frac{1}{2}}} \frac{\Gamma[\frac{1}{4}(kz_1 + 3)]}{\Gamma[\frac{1}{4}(kz_1 + 1)]} \tan \frac{\pi}{4} (kz_1 - 1). \quad (47)$$

Expanding by Stirling's theorem we have for kz_1 large

$$\tan \frac{\phi}{2} \sim \tan \frac{\pi}{4} (kz_1 - 1),$$

so

$$\phi \sim \frac{1}{2}\pi kz_1 - \frac{1}{2}\pi. \quad (48)$$

The ray treatment gives

$$\phi = k \int \mu dz = 2k \int_0^{z_1} [1 - (z/z_1)^2]^{\frac{1}{2}} dz = \frac{1}{2}\pi kz_1, \quad (49)$$

so that again for a slowly varying μ^2 we have agreement, apart from contributions $-\pi$ for total reflection and $+\frac{1}{2}\pi$ from the tail of the wave in the medium where $\mu^2 < 0$.

We note that for $kz_1 = 0$ (sharp reflector), the factor $(kz_1)^{-\frac{1}{2}}$ in $\tan \frac{1}{2}\phi$ gives $\phi = -\pi$, the usual change of phase at reflection.

§ 8. Vertical Incidence. μ^2 slowly varying.

We have seen that in the two previous examples that when the variations of μ^2 through the refracting layer is slow enough, the phase difference between upgoing and downcoming waves calculated by the wave treatment agrees with that calculated by the ray treatment, apart from a constant addition which we can think of as the sum of a change of phase of $-\pi$ due to the reflection and a contribution $\frac{1}{2}\pi$ to $\int \mu ds$ from the exponential tail of the wave in the part of the medium for which $\mu^2 < 0$.

We will now show that this is true for any medium in which μ^2 varies slowly enough, and will find more precisely the conditions under which it holds.

Jeffreys* has considered the solution of

$$\frac{d^2y}{dx^2} - \chi y = 0,$$

where χ is a slowly varying function of x , with a single zero at $x = x_0$, at which $\frac{d\chi}{dx} < 0$, so that $\chi > 0$ for $x < x_0$, and $\chi < 0$ for $x > x_0$. He first finds two asymptotic solutions for $x \rightarrow +\infty$ and for $x \rightarrow -\infty$, and then relates these

* 'Proc. Lond. Math. Soc.,' ser. 3, vol. 23, p. 428 (1924), particularly § 1.4.

asymptotic solutions to one another by using an approximate solution in Bessel functions of order $\pm \frac{1}{2}$ in the region near $x = x_0$, and joining the asymptotic expansions of the Bessel functions to the asymptotic solutions of the equation. For the solution zero at $x = -\infty$, he finds the asymptotic solution for $x > x_0$ to be

$$(-\chi)^{-\frac{1}{2}} \cos \left[\frac{\pi}{4} - \int_{x_0}^x (-\chi)^{\frac{1}{2}} dx \right].$$

If we consider a medium in which $\mu^2 > 0$ below $z = z_1$ and $\mu^2 < 0$ above, our equation is

$$\frac{\partial^2 L}{\partial (kz)^2} + \mu^2 L = 0,$$

and this corresponds to Jeffreys' case if we take $x = -kz$, $\chi = -\mu^2$; so the solution we require, namely that which becomes 0 at $z = -\infty$ has for $z < z_1$ the asymptotic form

$$L \sim \mu^{-\frac{1}{2}} \cos \left[\frac{\pi}{4} - k \int_z^{z_1} \mu dz \right]. \quad (50)$$

If we extend this solution into a region in which $\mu = 1$ and is constant, L only depends on z through the lower limit of $\int_z^{z_1} \mu dz$, and we have

$$\tan \phi/2 = \left(\frac{\partial L / \partial z}{kL} \right) \sim -\tan \left(\frac{\pi}{4} - k \int_z^{z_1} \mu dz \right), \quad (51)$$

$$\phi \sim 2k \int_z^{z_1} \mu dz - \frac{\pi}{2},$$

which is the expression obtained on the ray treatment for total reflection at height z_1 , plus contributions $-\pi$ from the total reflection and $+\frac{1}{2}\pi$ from the exponential tail.

The conditions under which this result holds depend firstly on the possibility of obtaining an approximate solution in the form $\mu^{-\frac{1}{2}} e^{ik \int \mu dz}$ in the region not near $z = z_1$, and secondly on the solution in Bessel functions of order $\pm \frac{1}{2}$ near $z = z_1$ being valid for $|z - z_1|$ large enough to use the asymptotic expansions of the Bessel functions in order to join on to the asymptotic solutions of the form $\mu^{-\frac{1}{2}} e^{ik \int \mu dz}$.

The first requirement demands that $\mu^{-3} d(\mu^2)/d(kz) \ll 1$, or, since $1/k\mu = \lambda/2\pi$ where λ is wave-length in the medium,

$$\frac{\lambda}{2\pi} \frac{d}{dz} (\log \mu^2) \ll 1, \quad (52)$$

that is to say the proportional change in μ^2 in $1/2\pi$ of a wave-length in the medium must be small compared to 1. The second demands that μ^2 should not vary appreciably from a linear dependence on $(z - z_1)$ for values of $|z - z_1|$ less than that at which the asymptotic expansions for the Bessel functions are used to join on to the asymptotic solutions $\mu^{-1} e^{ikz}$. This requires that at $z = z_1$

$$\frac{d^2(\mu^2)}{d(kz)^2} \ll \left[\frac{d(\mu^2)}{d(kz)} \right]^{4/3}, \quad (53)$$

if the effect of higher derivatives of μ^2 are neglected, for the use of the asymptotic expansions of the Bessel functions requires that

$$\frac{d(\mu^2)}{d(kz)} [k(z - z_1)]^3 \gg 1,$$

at the point where they are joined to the asymptotic solutions $\mu^{-1} e^{ikz}$, and in order that the Bessel functions should still be a good approximation to the actual solution, it is necessary that the proportional change in $\frac{d\mu^2}{d(kz)}$ in this range of z should be small compared to 1, that is,

$$k(z - z_1) \frac{d^2\mu^2}{d(kz)^2} / \frac{d\mu^2}{d(kz)} < 1;$$

if the inequality (53) is satisfied it is possible to find a value of $z - z_1$ satisfying both these conditions.

If Λ is the amplitude of the oscillation in the stationary wave in the region where $\mu = 1$, then from (50) it follows that the mean value of $2\mu L^2$ over a period of the stationary wave is equal to Λ^2 ; when μ is slowly varying, the mean over a period is approximately equal to the mean with respect to z , and the group velocity is approximately constant over a period. Thus in formula (26) for the mean equivalent path \bar{P}' , namely,

$$= 2 \int_{z_1}^{\infty} \frac{2\mu L^2}{\Lambda^2} \frac{c}{U} dz,$$

the contribution from the range of z in which the solution (50) holds is $2 \int (c/U) dz$ for this region; the solution (50) does not hold for μ^2 very small, or negative, but μL^2 is small in both these regions, so they give only small contributions to the integral. Thus

$$\bar{P}' = 2 \int_{z_1}^{z_2} (c/U) dz,$$

approximately, in agreement with the formula of the ray treatment.

The method used in this section is clearly *not* applicable without modification when μ^2 has two (or more) zeros; a similar method would be applicable if the zero were widely separated so that the asymptotic solutions could be used between them, but not when the two zeros are close together, when the second condition (53) would not be satisfied.

This case of two zeros close together is of particular interest in connection with the transition from reflection from the upper (F) to reflection from the lower (E) of Appleton's two reflecting regions. If we have a variation of μ^2 such as shown in fig. 4 (the upper medium is taken as a sharp reflector for simplicity), and μ_m^2 , the minimum values of μ^2 , varies with the frequency, the variation in P and P', as the frequency passes through the critical frequency for which $\mu_m^2 = 0$, will depend essentially on transmission through the thin "totally reflecting" layer when μ_m^2 is small and negative. This case is now under investigation.

Perfect
reflection

FIG. 4.

§ 9. Oblique Incidence. General Formula for Equivalent Path.

When the receiver and the transmitter are not on the same vertical, we have seen (§ 2) that the equivalent path is given by $\partial\phi/\partial k$ for plane waves at an angle of incidence such that $\partial\phi/\partial\theta = 0$ (the medium is assumed to be optically isotropic, see § 2).

We can obtain a general expression for the equivalent path in a way similar to that used in § 4 for vertical incidence.

We will take waves with L in the plane of incidence; the equation of propagation is then (cf. (7))

$$\frac{\partial^2 L}{\partial z^2} = -k^2 (\mu^2 - \sin^2 \theta) L,$$

and the phase difference ϕ between upgoing wave at the transmitter and downcoming wave at the receiver, on the same horizontal plane and distant $2x_0$ from the transmitter, is, by (17)

$$\phi = 2kx_0 \sin \theta + 2 \tan^{-1} \left[\frac{\partial L / \partial z}{kL \cos \theta} \right]_0.$$

If small variations are made in k and θ , then the first order variation in L is given by the equation

$$\frac{\partial^2}{\partial z^2} \delta L = -k^2 (\mu^2 - \sin^2 \theta) \delta L - L \delta [k^2 (\mu^2 - \sin^2 \theta)],$$

and following the same argument as in § 4 for the similar equation with $\theta = 0$, we find

$$\left[L \frac{\partial}{\partial z} \delta L - \delta L \frac{\partial L}{\partial z} \right]_0 = \int_{z_0}^{\infty} L^2 \delta [k^2 (\mu^2 - \sin^2 \theta)] dz. \quad (54)$$

Also the first order variation in ϕ is

$$\delta \phi = 2x_0 \delta(k \sin \theta) + \frac{2}{[(kL \cos \theta)^2 + (\partial L / \partial z)^2]_0} \left[k \cos \theta \left(L \frac{\partial}{\partial z} \delta L - \delta L \frac{\partial L}{\partial z} \right) - L \frac{\partial L}{\partial z} \delta(k \cos \theta) \right]_0. \quad (55)$$

As before, $z = z_0$ is in a region in which $\mu = 1$, and if Λ is the maximum magnitude of the stationary oscillation in that region, and

$$\phi' = 2 \tan^{-1} \left[\frac{\partial L / \partial z}{kL \cos \theta} \right]_0 = \phi - 2x_0 \sin \theta,$$

we have

$$(kL \cos \theta)^2 + (\partial L / \partial z)^2 = k^2 \Lambda^2 \cos^2 \theta, \quad (L \partial L / \partial z)_0 = \frac{1}{2} k \Lambda^2 \cos \theta \sin \phi',$$

and using this and (54) we find

$$\delta \phi = 2x_0 \delta(k \sin \theta) + 2 \left[\int_{z_0}^{\infty} \frac{L^2}{k \Lambda^2 \cos \theta} \delta [k^2 (\mu^2 - \sin^2 \theta)] dz - \frac{\delta(k \cos \theta)}{2k \cos \theta} \sin \phi' \right].$$

The condition $\partial \phi / \partial \theta = 0$ then gives

$$x_0 \cos \theta = 2 \left[\int_{z_0}^{\infty} \frac{L^2}{\Lambda^2} dz - \frac{\sec \theta \sin \phi'}{4k} \right] \sin \theta. \quad (56)$$

The value of the integral here depends on θ , and the value (or values) of θ satisfying (56) gives the angle of incidence of the mean plane wave of the group contributing to the total effect at the receiver, or in terms of rays, the angle of incidence of the ray from transmitter to receiver. The first term in the bracket is of order of magnitude of the total path, while the second is of the order $\lambda_0/4\pi$, so that the second is negligible and we have approximately

$$x_0 = 2 \tan \theta \int_{z_0}^{\infty} \frac{L^2}{\Lambda^2} dz. \quad (57)$$

If $x_0 = 0$ (transmitter and receiver on same vertical), (56) gives $\theta = 0$, as has been assumed from symmetry considerations in § 4.

Taking now a variation of ϕ with k for θ constant, and eliminating x_0 by (56) we find for the equivalent path

$$P' = \partial\phi/\partial k = 2 \int_{z_0}^{\infty} \frac{L^2}{k \cos \theta \Lambda^2} \frac{\partial(k^2 \mu^2)}{\partial k} dz - \frac{\sin \phi'}{k} \sec^2 \theta. \quad (58)$$

Again neglecting the second term, and introducing the group velocity (cf. (25), this gives

$$P' = 2 \int_{z_0}^{\infty} \frac{2\mu L^2}{\Lambda^2 \cos \theta} \frac{c}{U} dz, \quad (59)$$

the integral being evaluated for the function L for the angle of incidence given by (57).

If $c/U = 1/\mu$, then from (56), (58) we find $P' \sin \theta = 2x_0$; that is, if we think of the reflection as being due to a perfect reflector in a non-refracting region, the heights of this reflector deduced from the equivalent path and by triangulation from the angle of incidence agree. This has already been deduced by Breit and Tuve* and by Appleton† from the ray treatment, for those cases to which this treatment applies; the present result shows that it is general if the dispersion formula is such that $c/U = 1/\mu$.

§ 10. Oblique Incidence. μ^2 slowly varying.

The relation of (59) to the formula of the ray treatment becomes clearer when we consider a medium in which μ^2 is "slowly varying." The solution of (7), and the conditions under which it is valid, are given by substituting $\mu^2 - \sin^2 \theta$ for μ^2 in § 6; the solution is

$$L = \Lambda (\cos \theta)^{\frac{1}{2}} (\mu^2 - \sin^2 \theta)^{-\frac{1}{2}} \cos \left[\frac{\pi}{4} - \int_{z_1}^{z_2} (\mu^2 - \sin^2 \theta)^{\frac{1}{2}} dz \right], \quad (60)$$

where z_1 is the height at which $\mu^2 = \sin^2 \theta$ (i.e., the height of the "totally reflecting layer" for the angle incidence θ); the coefficient has been chosen so that $L = \Lambda$ in the region where $\mu = 1$.

As μ is slowly varying, we replace L^2 in (57), (59) by the mean value of L^2 over a period, which, from (60), is $\frac{1}{2}\Lambda^2 \cos \theta / (\mu^2 - \sin^2 \theta)^{\frac{1}{2}}$ so that to this approximation

$$P' = 2 \int_{z_1}^{z_2} \mu (c/U) dz / (\mu^2 - \sin^2 \theta)^{\frac{1}{2}}. \quad (61)$$

Now if ψ is the angle between the vertical and the tangent to the geometrical ray at any point (see fig. 5)

$$\mu |\sin \psi| = \sin \theta, \quad \mu \cos \psi = (\mu^2 - \sin^2 \theta)^{\frac{1}{2}},$$

* G. Breit and M. A. Tuve, 'Phys. Rev.', vol. 28, p. 554 (1926), (see particularly p. 572).

† O. V. Appleton, 'Proc. Phys. Soc., Lond.', vol. 41, p. 93 (1928), § 2 (b).

and if ds is an element of length of the ray, $dz = ds \cos \psi$, so (61) becomes

$$P' = \int (c/U) ds$$

as in the ray treatment.

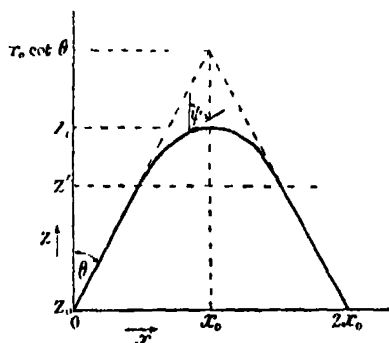


FIG. 5.

Summary.

The limitations of a ray treatment of reflection of electromagnetic waves by a stratified medium are discussed and it is shown that a wave treatment is essential for the interpretation of some of the phenomena of reflection from the Heaviside layer. The object of this paper is to lay the foundations for such a treatment.

General expressions for the optical and equivalent paths in terms of the solutions of equations of wave propagation are obtained both for normal and oblique incidence, and the exact expressions are obtained for the optical path for normal incidence on stratified media with certain specified simple variations of refractive index, and it is shown that for a totally reflecting medium (for which $\mu^2 < 0$ for all sufficiently large heights) the difference between the optical path deduced from a wave and from a ray treatment is not likely to be greater than a vacuum wave-length, although at the height at which $\mu^2 = 0$ the conditions for application of a ray treatment are not satisfied.

Approximate expressions for the optical and equivalent paths are obtained for any stratified totally reflecting medium in which μ^2 varies sufficiently slowly.

In conclusion the writer wishes to thank Professor E. V. Appleton for his interest and encouragement, and for much helpful discussion.

The Scattering of Light by Turbid Media.—Part I.

By J. W. RYDE, Research Laboratories of the General Electric Co., Ltd.,
Wembley.

(Communicated by R. H. Fowler, F.R.S.—Received February 26, 1931.)

Introduction.

The investigation which follows was undertaken with the object of arriving at a theory of the scattering of light by dense turbid media, which would be applicable, in particular, to opal diffusing glasses. The theory is developed on fairly general lines and applies to a system composed of a large number of similar spherical particles of a dielectric suspended in any medium, provided the relative refractive index is not far from unity. The expressions derived show how the total transmission and reflection of a sheet of a medium containing the particles depends on the following variables; the refractive index of the medium, the size and number of the particles and their refractive index, the wave-length of the incident light and its distribution, that is whether it is diffuse or in the form of a parallel beam, the absorption coefficient of the medium in which the particles are suspended, and the thickness of the sheet.

In Part I the general theory is developed, and in Part II numerical values of the necessary coefficients are computed. As a check on the theory, the size and number of the particles in a certain opal glass are deduced from photometric observations of its transmission and reflection. These calculated values are shown to be in agreement with those obtained by direct observation.

(1) *The Light Scattered by a Single Particle.*

The late Lord Rayleigh* has determined the intensity of the light scattered from a spherical particle of any diameter D , provided that the relative refractive index of the particle and the surrounding medium is not far from unity. His results show that the intensity at a distance r from the particle in a direction making angles χ , ϕ , with the directions of incidence and vibration respectively may be expressed, as follows:—

$$\frac{\pi \alpha^4 D^2 \eta}{8 r^2 m^3} \{1 - \sin^2 \chi \cos^2 \phi\} J_{3/2}^2(m), \quad (1)$$

* 'Proc. Roy. Soc.,' A, vol. 90, p. 219 (1914), and Sci. Papers, vol. 6, p. 220.

where

$$\left. \begin{aligned} \alpha &= \frac{\pi D n_0}{\lambda} & m &= 2\alpha \cos \frac{1}{2}\chi \\ \eta &= 9 \left(\frac{n^2 - 1}{n^2 + 2} \right)^2 \div (n^2 - 1)^2 & n &= n_1/n_0, \end{aligned} \right\} \quad (2)$$

in which n_1 is the refractive index of the particle and n_0 that of the medium. Also r is supposed to be very great compared with the wave-length λ and $(n^2 - 1)D/2\lambda$ is to be small.

For incident light of unity intensity, the total quantity of light scattered (per unit time) by the particle was also shown by Rayleigh to be, in the above notation,

$$E \left[\frac{5}{2} + 2\alpha^2 - \frac{\sin 4\alpha}{4\alpha} - \frac{7}{16\alpha^2} (1 - \cos 4\alpha) + \left(\frac{1}{2\alpha^2} - 2 \right) \{ \gamma + \log 4\alpha - \text{Ci}(4\alpha) \} \right], \quad (3)$$

in which γ is Euler's constant,

$$E = \frac{\pi D^2 \eta}{16}, \quad (4)$$

and Ci is the cosine integral defined by

$$\text{Ci}(x) = - \int_x^\infty \frac{\cos u}{u} \cdot du.$$

If the incident light is unpolarised, the intensity of the light scattered in any direction making an angle χ with the direction from which the light is incident will be from (1).

$$f(\chi) = \frac{\alpha^4 D^2 \eta}{8r^2 m^3} \cdot J_{3/2}^2(m) \int_0^\pi (1 - \sin^2 \chi \cos^2 \phi) d\phi,$$

hence, expressing the Bessel function in terms of circular functions,

$$f(\chi) = \frac{\alpha^4 D^2 \eta}{36r^2} \psi(\chi), \quad (5)$$

where

$$\psi(\chi) = \frac{2}{3} (1 + \cos^2 \chi) \left\{ \frac{\sin m - m \cos m}{m^3} \right\}^2, \quad (6)$$

so that $\psi(\pi) = 1$.

The quantity of radiation scattered between the limits $\chi = \pi$ and $\chi = \theta$ will thus be

$$r^2 \int_\theta^{2\pi} d\phi \int_0^\pi f(\chi) \sin \chi \cdot d\chi = \frac{\pi \alpha^4 D^2 \eta}{8} \int_0^\pi \left\{ \frac{2}{m^5} - \frac{1}{\alpha^2 m^3} + \frac{1}{4\alpha^4 m} \right\} M \cdot dm, \quad (7)$$

where

$$M = 1 + m^2 + (m^2 - 1) \cos 2m - 2m \sin 2m,$$

and

$$q = 2\alpha \cos \frac{1}{2}\theta.$$

Integrating, we obtain,

$$\frac{\pi D^2 \eta}{8} \left[\left(\alpha^2 - \frac{1}{4p^2} + 1 + \frac{p^2}{2} \right) - \frac{(1 - \cos 4\alpha p)}{8\alpha^2} \left(\frac{1}{4p^4} - \frac{1}{p^2} + \frac{1}{2} \right) \right. \\ \left. + \frac{\sin 4\alpha p}{2\alpha} \left(\frac{1}{4p^3} - \frac{1}{p} + \frac{p}{2} \right) + \left(\frac{1}{4\alpha^2} - 1 \right) (\gamma + \log 2q - \text{Ci}(2q)) \right], \quad (8)$$

where $p = \cos \frac{1}{2}\theta$.

We shall require expressions for the quantities of light B' and F' which are scattered backwards and forwards respectively, that is, the amounts scattered in directions making angles from $\frac{1}{2}\pi$ to 0 and from $\frac{1}{2}\pi$ to π with the direction of incidence.

The total scattered light $F' + B'$ will be obtained by putting $\theta = 0$, that is $p = 1$, in (8) which then reduces to (3).

In order to obtain F' , the quantity scattered forwards, we must put $\theta = \frac{1}{2}\pi$ that is, $p = 1/\sqrt{2}$. We then find,

$$F' = E \left[\frac{1}{2} + 2\alpha^2 - \frac{\sin 2\sqrt{2}\alpha}{2\sqrt{2}\alpha} - \frac{3}{8\alpha^2} (1 - \cos 2\sqrt{2}\alpha) \right. \\ \left. + \left(\frac{1}{2\alpha^2} - 2 \right) \{ \gamma + \log 2\sqrt{2}\alpha - \text{Ci}(2\sqrt{2}\alpha) \} \right]. \quad (9)$$

Subtracting from (3) we obtain B' , the quantity scattered backwards,

$$B' = E \left[1 - \frac{\sin 4\alpha}{4\alpha} + \frac{\sin 2\sqrt{2}\alpha}{2\sqrt{2}\alpha} + \frac{7}{16\alpha^2} \cos 4\alpha - \frac{3}{8\alpha^2} \cos 2\sqrt{2}\alpha \right. \\ \left. - \frac{1}{16\alpha^2} + \left(\frac{1}{2\alpha^2} - 2 \right) \{ \log \sqrt{2} + \text{Ci}(2\sqrt{2}\alpha) - \text{Ci}(4\alpha) \} \right]. \quad (10)$$

When α is very much less than unity, we find on expansion, neglecting powers of α above the fourth,

$$F' = B' = \frac{1}{2} E \alpha^4. \quad (11)$$

On the other hand, if α is very large we obtain

$$F' = 2E\alpha^2 \quad (12)$$

$$B' = (1 - 2 \log \sqrt{2}) E. \quad (13)$$

Now consider a plane passing through the particle, which is illuminated by light falling equally from all directions on one side of the plane. We shall

next require the quantities of light B and F which will be scattered by the particle in directions respectively behind and in front of the plane, when the intensity of the incident diffuse light is unity and there are random phase relationships between the energy coming from different directions.

Let θ be the angle which an incident ray makes with the normal to the plane. Then taking polar co-ordinates θ, γ with the particle as origin, γ being measured in the plane, the amount of radiation received by the particle from directions between θ and $\theta + d\theta$ and between γ and $\gamma + d\gamma$ will be $\sin \theta \cdot d\theta \cdot d\gamma$. Now if β be the angle which an emergent ray of scattered light makes with the normal to the plane, the corresponding amount of radiation scattered backwards will be

$$2r^2 \sin \theta \, d\theta \cdot d\gamma \int_0^{\frac{1}{2}\pi} d\beta \int_0^\pi \sin \beta \cdot f(\chi) \, d\gamma,$$

where $f(\chi)$ is the intensity of the scattered light at a distance r from the particle, in a direction making an angle χ with the incident ray.

The total quantity of radiation B which will be scattered backwards when the particle is illuminated equally from all directions making angles between 0 and $\frac{1}{2}\pi$ with the normal, will thus be

$$B = 2r^2 \int_0^{\frac{1}{2}\pi} d\theta \int_0^{\frac{1}{2}\pi} d\beta \int_0^\pi \sin \theta \sin \beta \cdot f(\chi) \, d\gamma, \quad (14)$$

where $f(\chi)$ is given by (5) and χ itself is a function of γ, β and θ whose form is given by

$$\cos \chi = \cos \theta \cos \beta + \sin \theta \sin \beta \cos \gamma. \quad (15)$$

Expanding $f(\chi)$ in powers of m we find

$$2r^2 f(\chi) = E \left[\frac{1}{3} \alpha^4 H_0 + \sum_{n=1}^{\infty} \{ k_{n+1} \alpha^{2(n+2)} - \frac{1}{2} k_n \alpha^{2(n+1)} + \frac{1}{2} k_{n-1} \alpha^{2n} \} H_n \right], \quad (16)$$

in which

$$H_n = \frac{2}{\pi} \left(\frac{m}{\alpha} \right)^{2n} = \frac{2^{n+1}}{\pi} (1 + \cos \chi)^n. \quad (17)$$

$$k_n = \frac{(-1)^{n+1} n \cdot 2^{2(n+1)}}{(2n+1)! (n+1)(n+2)}, \quad (18)$$

and E is given by (4).

Hence from (14)

$$B = E \left[\frac{1}{3} \alpha^4 K_0 + \sum_{n=1}^{\infty} \{ k_{n+1} \alpha^{2(n+2)} - \frac{1}{2} k_n \alpha^{2(n+1)} + \frac{1}{2} k_{n-1} \alpha^{2n} \} K_n \right] \quad (19)$$

which may be reduced to the more compact form

$$B = E \sum_{n=1}^{\infty} \{K_{n-1} - \frac{1}{2}K_n + \frac{1}{8}K_{n+1}\} k_n \alpha^{2(n+1)} \quad (20)$$

where

$$K_n = \frac{2^{n+1}}{\pi} \int_0^{i\pi} d\theta \int_0^{i\pi} d\beta \int_0^\pi \sin \theta \cdot \sin \beta \{1 + \cos \theta \cos \beta + \sin \theta \sin \beta \cos \gamma\}^n d\gamma. \quad (21)$$

Integrating, we find $K_0 = 2$ and

$$K_n = \sum_{q=0}^{i^n, i^{n-1}} \sum_{r=0}^{n-2q} \frac{n! 2^{n+1}}{r! (n-2q-r)! \{(r+1)(r+3) \dots (r+2q+1)\}^2}, \quad (22)$$

which reduces to

$$K_n = \frac{2^{n(n+1)}}{n+1} - \frac{2}{n+1} \binom{2n+1}{n}. \quad (23)$$

Again since

$$F = 2r^2 \int_{i\pi}^\pi d\theta \int_0^{i\pi} d\beta \int_0^\pi \sin \theta \cdot \sin \beta \cdot f(\chi) \cdot d\chi, \quad (24)$$

we find that (20) will give F instead of B if K_n is replaced by

$$\frac{2}{n+1} \binom{2n+1}{n}. \quad (25)$$

Similarly, since

$$B' = 2\pi r^2 \int_0^{i\pi} \sin \chi \cdot f(\chi) \cdot d\chi \quad (26)$$

$$F' = 2\pi r^2 \int_{i\pi}^\pi \sin \chi \cdot f(\chi) \cdot d\chi, \quad (27)$$

series for B' and F' may be obtained by replacing K_n by

$$\frac{2^{n+1}}{n+1} (2^{n+1} - 1), \quad (28)$$

and

$$2^{n+1}/(n+1) \quad (29)$$

respectively.

It will be seen that since the sum of the coefficients (23) and (25) is equal to that of (28) and (29) we have

$$F + B = F' + B'. \quad (30)$$

That this must be so is obvious, since if unit quantity of either diffuse or collimated radiation falls on a spherical particle, the total amount scattered will be the same in each case.

If the diameter of the particle is very small compared with the wave-length,

so that powers of α above the fourth may be neglected, we find that $B = B'$. The reason is that in this case (5) reduces to

$$f(\chi) = \frac{\alpha^4 D^2 \eta}{72r^2} (1 + \cos^2 \chi), \quad (31)$$

so that $f(\chi) = f(\pi - \chi)$; hence $F' = B'$ and $F = B$. It then follows from (30) that B will be equal to B' .

Values of B'/E , B/E , etc., have been computed from the above expressions, for various values of α and will be given in Part II. These values apply only to dielectric spheres when the relative refractive index of the particles and medium is not far from unity. The developments in the sections which follow are, however, in no way restricted to the particular values of the four scattering coefficients derived in this section.

(2) *The Transmission and Reflection of a Layer containing a Large Number of Particles.*

Suppose that a parallel beam of light of unit intensity falls normally upon a layer of scattering material of thickness X , composed of N similar particles per unit volume, suspended in some medium. We shall assume for the moment that they are suspended in air, or that the medium extends indefinitely in all directions, so that reflection does not occur at the boundaries of the layer.

The intensity of the parallel beam passing through a plane parallel to the front surface of the layer and at a distance x below it, will be some fraction I_{\parallel} , owing to loss by scattering and absorption. Let the combined absorption coefficient of the particles and medium be μ ; that of the particles alone will be N times the absorption per particle.

The light scattered from the parallel beam will travel in all directions and will be continually rediffused. Let t be the diffuse flux passing through the plane in the forward direction and s be that travelling through it in the backward direction towards the surface of incidence. Then we have,

$$dt/dx = NF'I_{\parallel} - \mu t - NBt + NBs \quad (32)$$

$$-ds/dx = NB'I_{\parallel} - \mu s - NBs + NBt \quad (33)$$

for the diffuse flux and

$$-dI_{\parallel}/dx = [\mu + N(F' + B')] I_{\parallel} \quad (34)$$

for the parallel beam. It follows that

$$I_{\parallel} = e^{-q'x} \quad \text{where} \quad q' = \mu + N(F' + B'). \quad (35)$$

The effect of interference between the primary wave and that part of the light scattered directly forwards, is here neglected. When the particles are small, this will mainly produce a change in the phase of the primary wave. If, however, the particles are of large diameter and of high relative refractive index, the effect on q' may become considerable, as was shown to be the case with sulphur particles in water by Raman and Ray.* Even in this case, however, it is easily seen that the effect on the total transmission and reflection will be very small.

We now obtain from (32) and (33)

$$\frac{d^2 t}{dx^2} = K^2 t - \{N F' (NB + \mu + q') + N^2 B' B\} e^{-q'x}, \quad (36)$$

$$\frac{d^2 s}{dx^2} = K^2 s - \{N B' (NB + \mu - q') + N^2 F' B\} e^{-q'x}, \quad (37)$$

in which

$$K = \sqrt{\mu(\mu + 2NB)}. \quad (38)$$

The solution may be shown to be of the form

$$\left. \begin{aligned} t &= g k_1 e^{Kx} + h k_2 e^{-Kx} - Q e^{-q'x} \\ s &= h k_1 e^{Kx} + g k_2 e^{-Kx} - P e^{-q'x} \end{aligned} \right\}, \quad (39)$$

where $g = 1 - \mu/K$, $h = 1 + \mu/K$. Also, remembering (30)

$$Q = \{2\mu F' + N(B + F')(F' + B')\} / \{2\mu F + N(F' + B')^2\} \quad (40)$$

and

$$P = N(B - B')(F' + B') / \{2\mu F + N(F' + B')^2\}. \quad (41)$$

If T' is the fraction transmitted, including both the diffuse light and the residue I' of the parallel beam, and R' is the fraction reflected, the boundary conditions are, for

$$x = 0, \quad t = 0 \quad \text{and} \quad s = R',$$

and for

$$x = X, \quad t = T' - IX \quad \text{and} \quad s = 0.$$

We then find

$$T' = \frac{QK + P e^{-q'X} NB \sinh KX}{(\mu + NB) \sinh KX + K \cosh KX} - (Q - 1) e^{-q'X} \quad (42)$$

and

$$R' = \frac{P e^{-q'X} K + QNB \sinh KX}{(\mu + NB) \sinh KX + K \cosh KX} - P, \quad (43)$$

also

$$I' = e^{-(\mu + N(F' + B'))X} = e^{-q'X}. \quad (44)$$

* 'Proc. Roy. Soc., A, vol. 100, p. 102 (1922).

As the thickness increases indefinitely, (43) tends to the limiting value

$$\lim_{\lambda \rightarrow \infty} R' = \frac{QNB}{\mu + NB + K} - P. \quad (45)$$

The above expressions for P and Q are somewhat complicated but they reduce to much simpler forms when the coefficient of absorption is small compared with that of the scattering. This is almost always the case with opal glasses, for example. Thus if μ is small compared with $N(F' + B')$ we have, remembering (30),

$$Q = (F' + B)/(F + B). \quad (46)$$

Similarly,

$$P = (B - B')/(F + B), \quad (47)$$

so that,

$$P = Q - 1. \quad (48)$$

If μ is not only small compared with the scattering coefficient $N(F' + B')$ but is absolutely negligible, the expressions for T' and R' reduce to the simple forms

$$T' = \frac{(F' + B) - I'(B - B')}{(F' + B')(1 + NBX)} \quad \} \quad (49)$$

and

$$R' = I - T'$$

(3) *The Transmission and Reflection Coefficients when the Incident Light is Diffuse.*

If, instead of being a parallel beam, the incident light is diffuse, (42) and (43) reduce to much simpler expressions, for now B must be substituted for B' and F for F'. We then find from (40) and (41) that $Q = 1$ and $P = 0$. Hence if T and R are respectively the fractions transmitted and reflected in the case of diffuse incident light, we obtain

$$T = \frac{K}{(\mu + NB) \sinh KX + K \cosh KX}, \quad (50)$$

$$R = \frac{NB}{(\mu + BN) + K \coth KX}, \quad (51)$$

and

$$I = e^{-(\mu + N(F+B))X}, \quad (52)$$

where I is the fraction of the incident light which emerges without having been scattered. It is to be remembered that T is the total fraction transmitted including I.

Equivalent forms of these three expressions have been derived previously by A. Schuster,* who first introduced the conception of the two diffuse fluxes s and t , travelling in opposite directions, and also by Channon, Renwick and Storr† and L. Silberstein.‡ In each case, however, the scattering coefficients B and F were left as constants to be determined by observation.

Schuster considered the case when the diameter of the particles is very small compared with the wave-length, so that $B = F$. He supposed also that the particles themselves emitted light. For no emission, his expressions reduce to (50) and (51). The more general case when the incident light is a parallel beam was not considered.

Silberstein treated the case of a collimated incident beam, but he did not allow for the fact that the amounts scattered in the forward and backward directions are different for the diffuse flux and for the collimated light. Since he used the same constants for both, that is he took $B' = B$ and $F' = F$, his expressions are equivalent to (50) and (51), which apply only to diffuse incident light. Also in the case of very small particles they reduce to Schuster's equations for no emission.§

Let T_1, R_1 be the values of T and R for unit thickness and T_2, R_2 the values for double this thickness. Then, considering two layers placed in contact, it is easily seen that

$$\left. \begin{aligned} T_2 &= T_1^2 \sum_{n=0}^{\infty} R_1^{2n} = T_1^2 / (1 - R_1^2) \\ \text{Similarly,} \quad R_2 &= R_1 (1 + T_2) \end{aligned} \right\}. \quad (53)$$

The expressions (50) and (51) may be shown to obey these relations and, in fact, may be derived from them by finite difference methods, as was done by Channon, Renwick and Storr (*loc. cit.*). In applying their results to opal glasses and in calculating Schuster's absorption and scattering coefficients, they did not, however, take into account the effects of reflection at the glass-air interfaces.|| We shall see later that, in the case of opal glasses, the effective reflection coefficient r_2 of the inside surfaces of a sheet of glass is as high as 0.4 for the internal diffuse light. On account of this the observed transmission and

* 'Astrophys. J.,' vol. 21, p. 1 (1905).

† 'Proc. Roy. Soc.,' A, vol. 94, p. 222 (1918).

‡ 'Phil. Mag.,' vol. 4, p. 1291 (1927).

§ In spite of his assertion to the contrary, the expression (12) on p. 1295 of his paper may, for small particles, readily be shown to be equal to that of Schuster quoted in the footnote to the same page.

|| It is true that when dealing with a pile of plates they introduced oil between them, but this does not eliminate the internal reflection at the two outside surfaces of the pile.

reflection τ and ρ , for a layer of a medium whose refractive index differs from that of air, will not be the same as T and R , which only refer to the case when r_s is zero. As will appear later, this difference is often considerable. It follows that their results, which are equivalent to (50) and (51), apply only to particles suspended in air and not to opal glasses or to other diffusing media.

In the following section we shall develop equations relating the observed values of the transmission and reflection, which include the effects of the boundary reflections, to the expressions already obtained. Before leaving the present case we shall, however, derive a few further relations which will be of use later. Eliminating KX from (50) and (51) we obtain the following interesting relation connecting T and R , which is valid for any thickness,

$$T^2 = (1 - R)^2 - 2R \mu/NB. \quad (54)$$

From equations (42) and (43), which apply when the incident light is a parallel beam, it will be seen that, when the thickness is sufficiently great for I' to be negligible, that is when practically none of the incident beam is transmitted unscattered

$$T' = QT \quad (55)$$

and

$$R' = QR - P \quad (56)$$

where P and Q are given by (40) and (41).

When, in addition, the absorption coefficient is small compared with the scattering coefficient, as in all opal glasses, we may use the simple expressions for P and Q given by (46) and (47). We now have $Q = P + 1$ and it follows that, under the above conditions, the following simple relation holds between the transmission and reflection for parallel and diffuse incident light

$$T'/T = (1 - R')/(1 - R) = Q = (F' + B)/(F + B). \quad (57)$$

(4) *The Effects of the Boundary Reflections.*

Up to the present we have considered the medium containing the layer of scattering particles to extend indefinitely in all directions. If, however, it is of finite dimensions and it is placed in some other medium, generally air, having a lower refractive index, the effects of reflection at the boundaries may, as mentioned above, be considerable. We shall suppose that the medium containing the particles is in the form of a sheet with parallel sides, and also that the particles are uniformly distributed throughout the whole of the sheet. Let the coefficients of reflection for incident parallel and diffuse light falling

on the outside surface of the sheet be r_0 and r_1 respectively, also let the coefficient for scattered light falling on the inside surfaces be r_2 . If the particles were absent, no light could strike the surface internally at a sufficient angle to be totally reflected; but since the particles re-diffuse the light inside the sheet, an appreciable fraction of it will undergo total reflection. It follows that r_2 will be greater than r_1 . We shall consider the actual values of these coefficients in the next section.

If the incident light is a parallel beam falling normally on the surface of the sheet, let the values of its transmission and reflection including the effects of the boundary reflections be τ' and ρ' respectively. These are thus the quantities which are actually observed by photometric measurements. Similarly let τ and ρ be the corresponding values for diffuse incident light. Taking into account all the successive internal multiple reflections, it may readily be shown that for parallel incident light

$$\tau' = (1 - r_0)(1 - r_2) \frac{T'(1 - r_2 R) + r_2 R' T}{(1 - r_2 R)^2 - r_2^2 T^2} \quad (58)$$

and

$$\rho' = r_0 + (1 - r_0)(1 - r_2) \frac{R'(1 - r_2 R) + r_2 T' T}{(1 - r_2 R)^2 - r_2^2 T^2}, \quad (59)$$

provided that I' is small compared with unity. With the same restriction, we can obtain the corresponding expressions for diffuse incident light by substituting T for T' , R for R' , and r_1 for r_0 so that

$$\tau = \frac{(1 - r_1)(1 - r_2)T}{(1 - r_2 R)^2 - r_2^2 T^2} \quad (60)$$

and

$$\rho = r_1 + (1 - r_1)(1 - r_2) \frac{R(1 - r_2 R) + r_2 T^2}{(1 - r_2 R)^2 - r_2^2 T^2}. \quad (61)$$

The relation corresponding to (54) may be shown to be as follows

$$\tau^2 = \frac{k^2 - 2k(\rho - r_1)(1 + \mu/NB) + (\rho - r_1)^2}{1 - 2r_2(1 + \mu/NB) + r_2^2} \quad (62)$$

where

$$k = 1 - r_1 - r_2(1 - \rho). \quad (63)$$

Remembering (57), we derive the following important relation between the values of the transmission and reflection for parallel and diffuse incident light, which holds provided the absorption coefficient μ is small compared with the

scattering coefficient $N(F+B)$ and that I' is very small compared with unity,

$$\frac{\tau'}{\tau} = \frac{1-\rho'}{1-\rho} = \frac{1-r_0}{1-r_1} \{r_2 + Q(1-r_2)\} \quad (64)$$

and Q is given by (46).

We shall finally consider the general case for parallel incident light, when I' can no longer be neglected. If τ_p' and τ_d' are the fractions of the incident light which are transmitted as a parallel beam and as diffuse light respectively, we find

$$\tau' = \tau_p' + \tau_d' \quad (65)$$

where

$$\tau_p' = (1-r_0)^2 I' / (1-r_0^2 I'^2) \quad (66)$$

$$\tau_d' = (1-r_0) (w + v r_0 I') / (1-r_0^2 I'^2) \quad (67)$$

in which

$$w = (1-r_2) \frac{(T' - I')(1-r_2 R) + r_2 R' T}{(1-r_2 R)^2 - r_2^2 T^2}, \quad (68)$$

$$v = (1-r_2) \frac{R'(1-r_2 R) + r_2 (T' - I') T}{(1-r_2 R)^2 - r_2^2 T^2}. \quad (69)$$

Similarly, if the fractions reflected as parallel and diffuse light are ρ_p' and ρ_d' respectively,

$$\rho' = \rho_p' + \rho_d', \quad (70)$$

where

$$\rho_p' = r_0 + r_0 (1-r_0)^2 I'^2 / (1-r_0^2 I'^2) \quad (71)$$

and

$$\rho_d' = (1-r_0) (v + w r_0 I') / (1-r_0^2 I'^2). \quad (72)$$

When either X or N is small, so that the fraction of the incident light which is transmitted without being scattered is fairly large, the internally scattered light will no longer be uniformly diffuse, so that the values of the constants will change somewhat. This will affect τ_d' but not τ_p' . As soon as this effect becomes appreciable, however, τ_d' will have become relatively unimportant compared with τ_p' , so that the value of their sum τ' will remain sensibly correct and approaches τ_p' , as it should do, in the limiting case when X or N becomes zero. A similar argument applies to ρ' . In other words, as soon as the effect of the change in the constants on v and w becomes appreciable, the terms through which they enter into τ' and ρ' become negligible.

(5) The Boundary Reflection Coefficients.

In order to complete the solution of the general problem, it now only remains to show how the boundary reflection coefficients may be determined. The

coefficient r_0 for parallel light falling normally on the front surface of the sheet, will be given by the simple Fresnel formula,

$$r_0 = \left(\frac{n-1}{n+1} \right)^2, \quad (73)$$

where n is the refractive index of the medium containing the particles relative to the surrounding medium, generally air.

The corresponding coefficient r_1 , for diffuse incident light, will be

$$r_1 = \frac{\int_0^{\frac{1}{2}\pi} \sin \theta \cdot \cos \theta \cdot f(\theta, n) \cdot d\theta}{\int_0^{\frac{1}{2}\pi} \sin \theta \cdot \cos \theta \cdot d\theta} \quad (74)$$

in which $f(\theta, n)$ is the general Fresnel expression,

$$f(\theta, n) = \frac{1}{2} \left[\frac{\sin^2(\theta - \phi)}{\sin^2(\theta + \phi)} + \frac{\tan^2(\theta - \phi)}{\tan^2(\theta + \phi)} \right],$$

where $n \sin \phi = \sin \theta$.

The integration has already been performed by Walsh.* The result is

$$r_1 = \frac{1}{2} + \frac{(n-1)(3n+1)}{6(n+1)^3} + \left\{ \frac{n^2(n^2-1)^2}{(n^2+1)^3} \right\} \log \left(\frac{n-1}{n+1} \right) \\ - \frac{2n^3(n^2+2n-1)}{(n^2+1)(n^4-1)} + \left\{ \frac{8n^4(n^4+1)}{(n^2+1)(n^4-1)^2} \right\} \log n. \quad (75)$$

From these expressions, values of r_0 and r_1 have been computed for various values of n from 1.0 up to 1.9. These will be given in Part II.

When we come to r_2 , the reflection coefficient for the scattered light falling on the inside surfaces, we cannot obtain this by integrating (74) over the range for which total reflection does not take place and then adding the totally reflected fraction. This is because the total reflection occurs at the large angles of incidence and it follows that any slight deviation of the diffuse light from perfect uniformity at these angles will have a considerable effect on the value of r_2 . This coefficient must, therefore, be determined experimentally. Its value will vary somewhat with the thickness of the sheet and with its opacity. It appears, however, that the change is only appreciable when I' is large and then, as shown at the end of the last section, its effect is unimportant. One method of determining this coefficient is as follows.

Let ρ_b be the value of ρ when the rear surface of the sheet is backed by an

* "Dept. Sci. Ind. Res. Illumination Research Tech. Pap.," 2, p. 10 (1926).

absorbing material in contact with it, so that the light reaching it is not reflected back to the particles. It may then be shown that ρ_b is given by (61), in which T has been put equal to zero. Now it is easily seen from (60) and (61) that if $T = R$ then $\tau = \rho - r_1$. It follows that if τ , ρ and ρ_b are measured, for a thickness such that $\tau = \rho - r_1$, then

$$\frac{1}{r_2} = 1 + \tau \frac{(\rho_b - r_1)}{(1 - r_1)(\rho - \rho_b)}, \quad (76)$$

so that r_2 may be found. A similar expression, which however involves Q , may be found if the incident light is parallel.

This completes the general theory. We are now in a position to calculate the effects of all the variables upon the transmission, reflection, and thence the absorption, of diffusing media of the type considered.

The Scattering of Light by Turbid Media.—Part II.

By J. W. RYDE and B. S. COOPER, Research Laboratories of the General Electric Company, Ltd., Wembley.

(Communicated by R. H. Fowler, F.R.S.—Received February 26, 1931.)

Introduction.

In Part I it was shown how the values of the transmission and reflection of a sheet of a medium containing particles in suspension can be calculated. First the amounts of light scattered in the forward and backward directions from a single particle were determined; from these results the transmission T and reflection R for diffuse incident light were found for a layer of the diffusing medium, when the effects of boundary reflections are negligible. At this stage, the expressions developed apply to a mist or fog consisting of particles suspended in air. Finally it was shown how, if the particles are suspended in some other medium, having a different refractive index from that of air, the transmission and reflection τ and ρ can be expressed in terms of T and R and the surface reflection coefficients. The more general expressions, for the case when the incident light is a parallel beam, were also developed.

We shall now show how the absorption coefficient μ can be determined from photometric observations. As a check on the theory, we shall deduce the

diameter D of the particles and the number N present per unit volume and compare these calculated values with those found by direct observation. Finally, the necessary modifications of the theory will be made to cover the case when the diffusing medium is in the form of a spherical shell.

First of all it will be necessary to determine numerical values of the coefficients introduced in Part I.

(1) *Computation of the Coefficients F , B , F' and B' , and the Reflection Coefficients r_0 and r_1 .*

From the closed expressions (3) and (19) given in Part I, values of $(F' + B')/E$ and B'/E were computed* for values of α up to 12.4. These are given in Table I.

The coefficient B/E can be determined from the series (20), but the following, which is rather more convenient for numerical computation, may be derived from (23) and (28).

$$\frac{B - B'}{2E} = \sum_{n=1}^{\infty} \left\{ -H_{n-1} + \frac{1}{2}H_n - \frac{1}{8}H_{n+1} \right\} k_n \alpha^{2(n+1)}, \quad (77)$$

where

$$H_n = \frac{1}{n+1} \left[\binom{2n+1}{n} - 2^n \right]. \quad (78)$$

From this, B/E may be derived immediately, since we have already found B'/E from the closed expression (10). Then since we have shown that,

$$F + B = F' + B'$$

the value of F/E is also determined. Table II gives the values of B/E and the important ratios

$$(F' + B)/(F + B) \quad \text{and} \quad (F + B)/B = f(\alpha). \quad (79)$$

The first of these is the form (46), to which the exact expression for Q reduces, under the conditions generally realised in opal glasses. The second ratio, which we shall call $f(\alpha)$, can be deduced from experimental data and the table thus allows the corresponding value of α to be derived. This in turn, as we shall see later, leads to a determination of the diameter of the particles.

Table II could not be extended to such high values of α as the last, because the series then become unmanageable. It will be found, however, to cover a sufficiently large range for most purposes.

The coefficients F'/E and F/E are not very often needed, but whenever they are required, they may readily be derived from those tabulated.

* Values of $C_i(\alpha)$ are given by Glaisher, 'Phil. Trans.,' vol. 160, p. 367 (1870). They have been considerably extended in the 'Report of the British Association,' p. 248 (1927).

Table I.

a	$\frac{F'+B'}{E}$	$\frac{B'}{E}$	a	$\frac{F'+B'}{E}$	$\frac{B'}{E}$	a	$\frac{F'+B'}{E}$	$\frac{B'}{E}$	a	$\frac{F'+B'}{E}$	$\frac{B'}{E}$
0	0	0	3.2	16.88	0.341	6.4	76.84	0.368	9.6	178.4	0.296
0.2	0.00187	0.00093	3.4	19.42	0.421	6.6	81.99	0.354	9.8	186.1	0.316
0.4	0.0285	0.0138	3.6	22.09	0.443	6.8	87.28	0.317	10.0	194.0	0.326
0.6	0.133	0.0612	3.8	24.88	0.412	7.0	92.72	0.271	10.2	202.0	0.325
0.8	0.379	0.161	4.0	27.84	0.354	7.2	98.31	0.239	10.4	210.2	0.321
1.0	0.813	0.313	4.2	30.99	0.298	7.4	104.1	0.235	10.6	218.6	0.317
1.2	1.437	0.476	4.4	34.35	0.268	7.6	110.0	0.263	10.8	227.1	0.316
1.4	2.245	0.605	4.6	37.89	0.265	7.8	116.2	0.311	11.0	235.8	0.319
1.6	3.201	0.666	4.8	41.60	0.279	8.0	122.5	0.355	11.2	244.7	0.316
1.8	4.285	0.605	5.0	45.46	0.293	8.2	128.9	0.380	11.4	253.7	0.310
2.0	5.499	0.471	5.2	49.45	0.297	8.4	135.5	0.372	11.6	262.8	0.290
2.2	6.872	0.306	5.4	53.57	0.295	8.6	142.2	0.337	11.8	272.1	0.276
2.4	8.441	0.171	5.6	57.87	0.301	8.8	149.1	0.297	12.0	281.6	0.274
2.6	10.23	0.111	5.8	62.34	0.308	9.0	156.2	0.267	12.2	291.2	0.267
2.8	12.26	0.140	6.0	66.99	0.330	9.2	163.4	0.259	12.4	301.1	0.311
3.0	14.49	0.233	6.2	71.84	0.357	9.4	170.8	0.271	∞	∞	0.3069

Table II.

a	$\frac{B}{E}$	$\frac{F'+B}{F+B}$	$f(a)$	a	$\frac{B}{E}$	$\frac{F'+B}{F+B}$	$f(a)$
0	0	1.000	2.00	4.0	3.943	1.129	7.06
0.5	0.0321	1.007	2.09	4.5	4.621	1.120	7.81
1.0	0.356	1.053	2.28	5.0	5.354	1.111	8.49
1.5	0.964	1.119	2.81	5.5	6.15	1.105	9.08
2.0	1.466	1.181	3.75	6.0	7.00	1.100	9.57
2.5	1.951	1.196	4.77	6.5	7.85	1.096	10.1
3.0	2.677	1.169	5.41	7.0	8.71	1.091	10.6
3.5	3.381	1.142	6.13	7.5	9.62	1.087	11.1

The external surface reflection coefficients r_0 and r_1 , for parallel and diffuse incident light respectively, were computed from the expressions (73) and (75) and are given in Table III, for values of n_0 from unity up to 1.9.

Table III.—Values of r_0 and r_1 .

n_0	r_0	r_1	n_0	r_0	r_1
1.00	0.0000	0.000	1.45	0.033	0.085
1.10	0.0023	0.028	1.60	0.040	0.092
1.15	0.0049	0.035	1.55	0.047	0.100
1.20	0.0083	0.045	1.60	0.053	0.107
1.25	0.012	0.053	1.65	0.060	0.114
1.30	0.017	0.061	1.70	0.067	0.121
1.35	0.022	0.069	1.80	0.082	0.134
1.40	0.028	0.077	1.90	0.096	0.146

As regards the value of r_2 , the internal surface reflection coefficient for the scattered light, the methods described in section (5) of Part I show that, in the case of opal glasses, its value is not far from 0.4. It has been found that deviations from this value, between the limits 0.35 and 0.45, make comparatively little difference in the final results. In what follows, we shall always take the value as 0.4 for opal glasses whose refractive index is in the neighbourhood of 1.5. A direct measurement of this coefficient, not depending on the expressions developed here, has been made recently by J. S. Preston,* at the National Physical Laboratory, who finds values sensibly the same as that given here.

(2) *Methods of Determining the Particle Size and Number from Observations on Transmission and Reflection.*

It will be remembered that, if the incident light is diffuse, τ and ρ are the observed values of the total transmission and reflection, while T and R are the values that would be obtained in the absence of boundary reflections. In order to eliminate the effects of these reflections from the observed values, we shall need T and R in terms of τ and ρ . From (60) and (61) it may be shown that, if

$$k = 1 - r_1 - r_2(1 - \rho)$$

then

$$T = \frac{(1 - r_1)(1 - r_2)\tau}{k^2 - r_2^2\tau^2} \quad (80)$$

and

$$R = \frac{k(\rho - r_1) - r_2\tau^2}{k^2 - r_2^2\tau^2}. \quad (81)$$

The substitution of these expressions in (54) gives

$$z = 4 \frac{k(\rho - r_1) - r_2\tau^2}{(1 - r_2)^2 \{(1 - \rho)^2 - \tau^2\}} \quad (82)$$

where

$$z = 2NB/\mu. \quad (83)$$

Then from (51) it follows that

$$\mu = \frac{1}{X\sqrt{1+z}} \coth^{-1} \left\{ \frac{(1-R)z - 2R}{2R\sqrt{1+z}} \right\} \quad (84)$$

where X is the thickness of the sheet. Thus the combined absorption coefficient

* "The Properties of Diffusing Glasses with special Reference to surface Effects." To be published shortly in the 'Proceedings of the International Commission on Illumi-

μ and the product NB are determined. If μ is quite negligible, (82) cannot be used to determine NB; in this case, however, we have the simple relation

$$NB = (1 - T)/TX. \quad (85)$$

In order to find N and B separately, one further observation is needed. It will now be shown, that an observation of τ_p' , the fraction of an incident parallel beam which is transmitted unscattered through a sheet of the diffusing material, will suffice for this purpose.

From (66) and (44) we have

$$\tau_p' = \frac{(1 - r_0)^2 e^{-\sigma'x}}{1 - r_0^2 e^{-2\sigma'x}} \quad (86)$$

where, remembering (30)

$$q' = \mu + N(F + B). \quad (87)$$

A very simple method of determining τ_p' and therefore q' , will be described in the next section; q' may therefore be considered as known.

In the case of opal glasses, the total scattering coefficient $N(F + B)$ is of the order of some hundred times the absorption coefficient μ . We can therefore write with sufficient accuracy

$$q'/NB = (F + B)/B = f(\alpha). \quad (88)$$

From $f(\alpha)$ the corresponding values of α and B/E are then found by means of Table II. The diameter D of the particles then follows immediately, since from (2)

$$D = \alpha\lambda/\pi n_0, \quad (89)$$

where λ is the wave-length of the incident light and n_0 the refractive index of the medium containing the particles. If the refractive index n_1 of the particles is known, we then find η from (2) and E from (4). Finally, knowing B/E and NB, the number N of particles per unit volume is determined.

If the absorption coefficient is not small compared with the total scattering coefficient, then we must use, in place of (88),

$$NB \cdot f(\alpha) = q' - \mu. \quad (90)$$

If, instead of τ and ρ , the values observed are τ' and ρ' , which are the corresponding values when the incident light is parallel, we must proceed as follows. An equation of the form of (82) will, as may be seen from (64), contain Q, whose value at this stage is unknown. We therefore rely on the fact that the difference produced by changing from diffuse to parallel light is not large. This can easily be seen to be the case from (64). It follows that by treating the observations as if they had been made with diffuse light we can get approxi-

mate values of μ and NB and thence of α . Now we have shown in (64) that if μ is small compared with $N(F + B)$, then, provided I' is small,

$$\frac{\tau'}{\tau} = \frac{1 - \rho'}{1 - \rho} = \frac{1 - r_0}{1 - r_1} \left\{ r_2 + (1 - r_2) \frac{F' + B}{F + B} \right\}. \quad (91)$$

A glance at Table II will show that $(F' + B)/(F + B)$ varies comparatively slowly with α . So that, from the approximate value of α , we obtain values of τ and ρ from (91) which will differ but slightly from the values that would have been found if diffuse incident light had been used initially. When substituted in (82) they lead to a much more accurate value of z and thence of α . If this new value differs considerably from the first approximate value found, the process may be repeated; it will, however, seldom be found necessary to do this. Once a sufficiently accurate value of α has been determined, N and D then follow as before.

In the case when the particles are not uniform in size, we see that if we divide them into m classes, such that the i th class contains a number N_i of particles, whose diameter can be considered constant, there will be equivalent values of $N(F + B)$ and NB, for the mixture, given by

$$N(F + B) = \sum_1^m N_i(F + B)_i, \quad (92)$$

$$NB = \sum_1^m N_i B_i. \quad (93)$$

These will lead to corresponding equivalent values of N and D , such that a medium containing N particles of diameter D would have the same transmission and reflection as the one considered. It will be seen that it is these equivalent values which will be found, if N and D are derived from photometric observations of media containing particles of non-uniform size. It follows that the theory may still be applied to media containing particles of mixed sizes, provided that the equivalent values of N and D are used.

(3) *The Experimental Determination of τ, ρ .*

Let the medium containing the particles be held at some distance from a small bright source of light, rendered approximately monochromatic by means of a filter. The distance must be sufficiently great for the brightness of the surrounding field, due to the transmitted scattered light, to be negligible compared with that of the source as seen through the sheet. Then it will be seen that the ratio of the brightness of the source thus viewed, to its actual

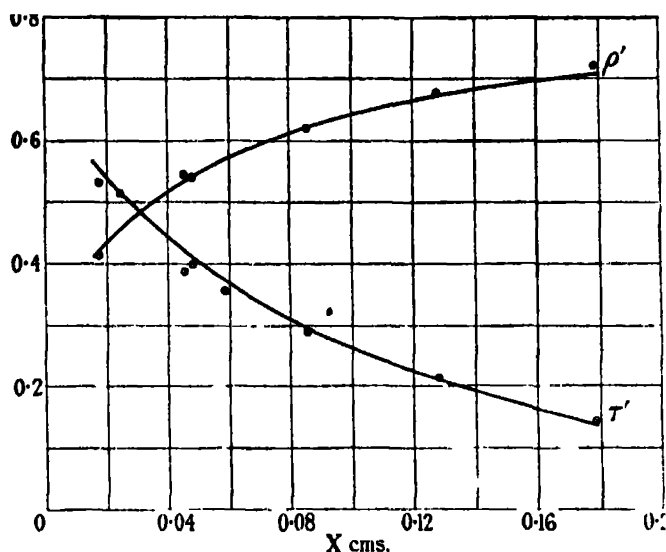
brightness will equal τ_p' , which is the fraction of an incident parallel beam which would be transmitted unscattered. It follows that by choosing a thickness such that the brightness of the source is reduced to a convenient value, τ_p' may be determined by comparing this brightness, as seen through the medium, with that seen through a calibrated neutral wedge. With a series of filters, τ_p' and thence q' may readily be obtained as functions of the wave-length.

(4) *Comparison of the Theory with Observation on Opal Glasses.*

Opal diffusing glasses are generally made by introducing cryolite, $\text{AlF}_3 \cdot 3\text{NaF}$, into the batch mixture. Their diffusing properties have been shown* to be due to the separation, on cooling, of large numbers of spherical particles composed of calcium and sodium fluorides. The relative refractive index of the particles is only about 1.1, and their average diameter may vary, in different glasses, from below 0.25×10^{-4} cm. up to about 1.0×10^{-4} cm. In some glasses the particles are very nearly all of the same size, but in others a considerable range of size may be present. The number of particles per cubic centimetre varies from about 10^8 up to 10^{14} according to the type of glass. Some opal glasses are occasionally made in other ways, for example, by the introduction of phosphates. The separated material in these also, is generally in the form of spherical particles.

We shall first apply the theory to a cryolite glass in which the particles were known to be fairly uniform in size. Fig. 1 shows a series of measurements of τ' and ρ' made on this glass, using parallel incident light. The observations were made several years ago by A. S. Radford in the Photometry Department of these Laboratories. His results are shown by the circles and they are plotted against corresponding values of the thickness. Unfiltered light from a gas-filled lamp was used, but since, however, τ' and ρ' vary comparatively slowly with λ , we may take as an effective wave-length the peak of the curve corresponding to the product of the energy distribution of the source and the sensitivity curve of the eye. This comes out to be 5.7×10^{-5} cm. The refractive index of the glass was found to be 1.51 so that, interpolating the values given in Table III, we find $r_0 = 0.04$ and $r_1 = 0.093$. Also, as discussed previously, $r_2 = 0.4$. The value of q' , determined for the above wave-length, was found to be 195.

* J. W. Ryde and D. Yates, 'Trans. Soc. Glass. Tech.,' vol. 10, p. 274 (1926).



Applying the method of successive approximations described in section (2), we find as the final values, $\mu = 0.6$, $NB = 35$ and $\alpha = 3.13$. By means of the six expressions (50), (51), (60), (61), (46) and (64), we may now calculate values of τ' and ρ' for different thicknesses. The results are shown by the curves drawn in the figure. It will be seen that the one set of constants μ , NB and α well represents the experimental data for both τ' and ρ' .^{*} Now since n_0 and λ are known, we find from (89) that $D = 3.75 \times 10^{-5}$ cm.

An X-ray examination of the glass showed that the composition of the particles was about 40 per cent. CaF_2 , and 60 per cent. NaF . The refractive indices of these compounds are 1.43 and 1.33 respectively. There is some evidence that the compounds exist in the particles as mixed crystals, and not separately. An ambiguity thus arises in the exact value of η to be used. It will be remembered that from (2)

$$\eta = 9 \left(\frac{n_1^2 - n_0^2}{n_1^2 + 2n_0^2} \right)^2, \quad (94)$$

where n_1 is the refractive index of the particles and n_0 that of the medium. The effective value is, however, almost certain to lie between the value obtained by substituting

$$n_1 = 0.4(1.43) + 0.6(1.33), \quad (95)$$

^{*} If diffuse light had been used, only the two constants μ and NB would be necessary, provided that I' is small.

in the expression for η , which leads to $\eta = 0.031$, and the value $\eta = 0.035$ obtained from

$$\eta = 0.4\eta_1 + 0.6\eta_2, \quad (96)$$

where the first η on the right-hand side refers to CaF_2 and the second to NaF . Corresponding to these two values we find from (4) two values of E . From Table II we find that B/E corresponding to the above value of α is 2.9, so that already knowing NB we arrive at two limiting values of N . On the assumption (95) we get $N = 1.1 \times 10^{12}$ per cubic centimetre and according to (96), $N = 9.4 \times 10^{11}$ per cubic centimetre. The difference is thus unimportant.

The above calculated values of D and N may now be compared with the results of a direct approximate determination of these quantities by a microscopical examination of the glass. The value of D was estimated from measurements on photomicrographs of extremely thin sections of the glass. Then by direct counts on the photographs, knowing the magnification and the effective depth of focus of the instrument, the number of particles per cubic centimetre was derived. The values obtained in this way are compared with the calculated values in the following table.

Table IV.—Calculated and Observed Values of N and D .

	By theory from observations on τ' and ρ' .	By direct measurements (approximately).
N	9.4×10^{11} by (96) 1.1×10^{12} by (95)	1.0 to 2.0×10^{12}
D	3.75×10^{-8} cm.	3.5×10^{-8} cm.

The agreement is seen to be extremely good and better than may be expected to hold generally. This question will be discussed in section (6).

Knowing the value of α for $\lambda = 5.7 \times 10^{-5}$ cm. we can now calculate its value for other wave-lengths by means of (89). This leads, by Table II, to the corresponding values of q' at the new wave-lengths. In this way q' was calculated for two other values of λ . These values are compared with the means of direct determinations in the following table.

Let us now consider the ratio of the transmission when the incident light is parallel, to that when it is diffuse. Using the values $r_0 = 0.04$, $r_1 = 0.09$ and $r_2 = 0.40$, which apply, at least approximately, to the majority of opal glasses, we can calculate the ratio τ'/τ as a function of α by means of (91) and

Table V.—Values of q' .

λ . cms.	Values of q' .	
	Observed.	Calculated.
5.3×10^{-5}	232	230
5.7×10^{-5}	195	—
6.3×10^{-5}	147	150

Table II. The values obtained are given in Table VI. It will be seen that this ratio rises at first, passes through a maximum and then steadily falls.

Table VI.—Values of τ'/τ assuming $r_0 = 0.04$, $r_1 = 0.09$ and $r_2 = 0.40$.

α .	τ'/τ .	α .	τ'/τ .	α .	τ'/τ .
0	1.057	4	1.139	8	1.110
1	1.089	5	1.127	9	1.106
2	1.173	6	1.120	10	1.103
3	1.164	7	1.115	11	1.100

The maximum occurs at $\alpha = 2.35$ and the value of the ratio is then 1.182. Since for most opal glasses α lies between 2 and 15, we should expect that τ'/τ should lie between the limits 1.06 and 1.18. Observations of the ratio were made on seven different opal glasses and the values obtained were found to lie between 1.10 and 1.17, which are within the theoretical limits.

(5) *The Transmission of Spherical Shells of Diffusing Media.*

Up to the present we have only considered flat sheets of diffusing material, but it is of some importance to consider also the transmission of spherical shells, as this has direct application to the design and specification of illumination fittings. We shall therefore develop, very briefly, the necessary expressions applicable to this case.

If the diffusing medium is in the form of a thin spherical shell of thickness X , with a point source at its centre, the transmission σ may be found as follows. It will be seen that the direct light falling on the inside surface of the shell may be considered to be parallel, while that scattered back by the particles will be diffuse. If Y' is small compared with unity, it may be shown that

$$\sigma = h + r_0 h + r_0^2 h + \dots$$

where

so that
$$h = \tau' + (\rho' - r_0) \tau + (\rho' - r_0) \rho \tau + (\rho' - r_0) \rho^2 \tau + \dots,$$

$$= \left\{ \tau' + \frac{\tau(\rho' - r_0)}{1 - \rho} \right\} / (1 - r_0). \quad (97)$$

Under the conditions such that the absorption coefficient μ is small compared with $N(F + B)$, we get from (64), still provided that I' is small,

$$\tau' / (1 - \rho') = \tau / (1 - \rho). \quad (98)$$

Substituting this in (97), we obtain the useful relation

$$\sigma = \tau / (1 - \rho). \quad (99)$$

If I' cannot be considered small compared with unity, the more general expression may, remembering (71) and (72), be shown to be

$$= \left\{ \tau' + \frac{\tau \rho_d'}{1 - \rho} \right\} / (1 - \rho_p'). \quad (100)$$

This refinement is, however, seldom necessary. It follows that, if σ and ρ are given instead of τ and ρ , the value of τ is immediately derivable from (99), so that we can proceed as in section (2).

In this way the theory has been applied to the determination of N and D from observations of σ and ρ made on a series of opal globes of different thicknesses. In this case the problem was complicated by the fact that the particle diameters were known, from a microscopical examination, not to be uniform. Using the equivalent values of N and D , however, reasonably good agreement with observation was obtained. Details of this, together with results of applying the theory to suspensions of particles in liquids, will be published elsewhere.*

(6) Discussion.

In the example discussed in section (4), the value of $(n^2 - 1) D / 2\lambda$, which must be small, was 0.07. When this is appreciably larger, we should no longer expect to be able to calculate N and D even approximately. This is because the numerical values given in Tables I and II will cease to apply and also, owing to the effect of interference between part of the forward scattered light and the primary beam, discussed in section (2) of Part I, we can no longer

* J. W. Ryde and B. S. Cooper, "The Theory and Specification of Opal Diffusing Glasses," to be published in the 'Proceedings of the International Commission on Illumination' (1931).

determine $N(F + B)$ from the observed value of q' . The determination of N and D is, however, not the main purpose of the present investigation, which is more concerned with the calculation of the total transmission and reflection when the number and diameter are known. Now, as long as the diameter and the relative refractive indices are not too large, so that the values in Tables I and II still apply, the expressions for the total transmission and reflection will remain sensibly correct even when the above interference effect vitiates the expression for I' . Finally, when $(n^2 - 1) D/2\lambda$ is comparatively large so that the numerical values in the tables cannot be used, several of the above results still remain of practical value. For example, from suitable observations of τ and ρ , we may always determine μ and NB ; also r_2 can be found from ρ , or by direct methods. Turbid diffusing media of various kinds can then be classified by means of the corresponding values of these constants, and when they are given, the total transmission and reflection can be calculated from them for any thickness. Applications of the theory to the design and specification of illumination fittings and to the assessment of the intrinsic goodness of different opal glasses, will be considered in a subsequent paper elsewhere.

In conclusion, the authors wish to express their thanks to Mr. R. H. Fowler for his kindness in reading and criticising the paper.

X-Ray Nondiagram Lines.

By G. B. DEODHAR, M.Sc., King's College, London.

(Communicated by O. W. Richardson, F.R.S. Received February 19, 1931.)

Introduction.

In a previous paper* an account of the measurements of the K satellites of the elements 14 (Si) to 17 (Cl) was given. In the same paper the various existing hypotheses regarding the origin of the X-ray nondiagram lines were examined and a conclusion arrived at that no theory at present available seems to satisfactorily account for the emission of these lines.

In addition to accurate measurements of these lines it is necessary to present the available experimental material in a form which may bring out new relationships as they would prove helpful for a theoretical discussion.

The present paper is written with this aim in view. As will be seen, interesting empirical relations in the K and L series are obtained which seem to throw some light on the nature of the nondiagram lines.

The following lines are discussed: α^i , α_s , α_4 , α_3 and α_2 for the elements 11 (Na) to 17 (Cl); β_s line for the elements 11 (Na) to 28 (Ni); β^{II} line for the elements 19 (K) to 26 (Fe); β^{III} line for the elements 19 (K) to 39 (Y) and η line for the elements 23 (Va) to 32 (Ge). In the L series the lines recently measured by Richtmyer† are discussed. These are the satellites of the L_{α_1} , L_{β_1} and L_{β_2} principal lines for the elements 37 (Rb) to 49 (In). Out of the six satellites of the L_{α_1} line mentioned by Richtmyer, two (α^i , α^{II}) seem to have been measured earlier by Coster.‡ Of the four satellites of L_{β_1} given by Richtmyer, two are already measured by Coster for the elements $z = 37$ to $z = 51$. These are in Coster's terminology β_1^i and β_{13} lines. Out of the four L_{β_1} satellites measured by Richtmyer, two, β_2^i and β_2^{II} (Druyvesteyn and Richtmyer), or β_{11} and β_{12} (Coster), have been measured earlier. Druyvesteyn§ even follows the unresolved β_2^i and β_2^{II} up to $z = 82$. It must be noticed that the measurements of the three authors vary for some elements by as much as 3 to 4 X.U.

* Deodhar, "On some Investigations in Röntgen Spectra" (*in course of publication*).

† 'Phys. Rev.', vol. 34, p. 574 (1929).

‡ 'Phil. Mag.', vol. 43, p. 1070 (1922).

§ 'Z. Physik,' vol. 43, p. 719 (1927).

Manipulation of Data.

In Table I are collected the differences of the $\sqrt{\nu/R}$ values of the K_{α} satellites and the principal diagram line K_{α_1} . The values of K_{α_1} are taken from Siegbahn's spectroscopy of X-rays. In fig. 1 the data are plotted against atomic number.

Table I. $\Delta \sqrt{\nu/R} (\sqrt{\nu_s/R} - \sqrt{\nu_{\alpha_1}/R})$.

Element.	α'_1	α_2	α_3	α_4	α_5
11 Na....	0.017	0.030	0.036	0.062	0.073
12 Mg	0.021	0.033	0.041	0.068	0.081
13 Al..	0.022	0.034	0.044	0.070	0.083
14 Si	0.024	0.034	0.042	0.072	0.086
15 P..	0.028	0.039	0.050	0.083	0.094
16 S	0.026	0.040	0.047	0.079	0.093
17 Cl	0.031	0.045	0.048	—	—
19 K	—	0.047	0.052	—	—
20 Ca	—	0.049	0.055	—	—

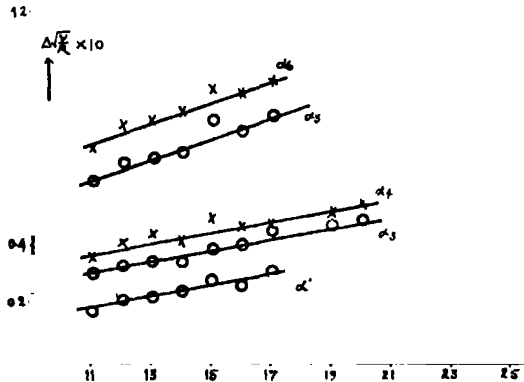


FIG. 1.

In Table II are collected similar values for the K_{α_1} nondiagram lines with reference to the principal diagram line K_{α_1} . In fig. 2 these values are plotted against atomic number.

Table II. $\Delta \sqrt{\nu/R} (\sqrt{\nu_s/R} - \sqrt{\nu_{\beta_1}/R})$.

Element.	β_s^* .	η .	β_{α_1} .	β_{α_2} .
11 Na	0.043	—	—	—
12 Mg	0.057	—	—	—
13 Al	0.067	—	—	—
14 Si	0.052	—	—	—
15 P	0.033	—	—	—
16 S	0.033	—	—	—
17 Cl	0.018	—	—	—
19 K	—	—	0.010	0.102
20 Ca	0.021	—	0.011	0.101
21 Sc	0.083	—	0.020	0.103
22 Ti	0.032	—	0.030	0.098
23 V	0.037	0.144	0.032	0.098
24 Cr	0.028	0.155	0.038	0.099
25 Mn	0.026	—	0.090	0.103
26 Fe	0.024	0.173	—	0.099
27 Co	0.021	0.178	—	0.102
28 Ni	0.017	0.180	—	—
29 Cu	—	0.183	—	—
30 Zn	—	0.162	—	0.112
31 Ga	—	0.180	—	0.111
32 Ge	—	0.090	—	0.115
33 As	—	—	—	—
34 Se	—	—	—	0.120
35 Br	—	—	—	0.120
37 Rb	—	—	—	0.128
38 Sr	—	—	—	0.128
39 Y	—	—	—	0.140

* Calculated from "International Tables of Critical Constants," vol. 6, p. 36.

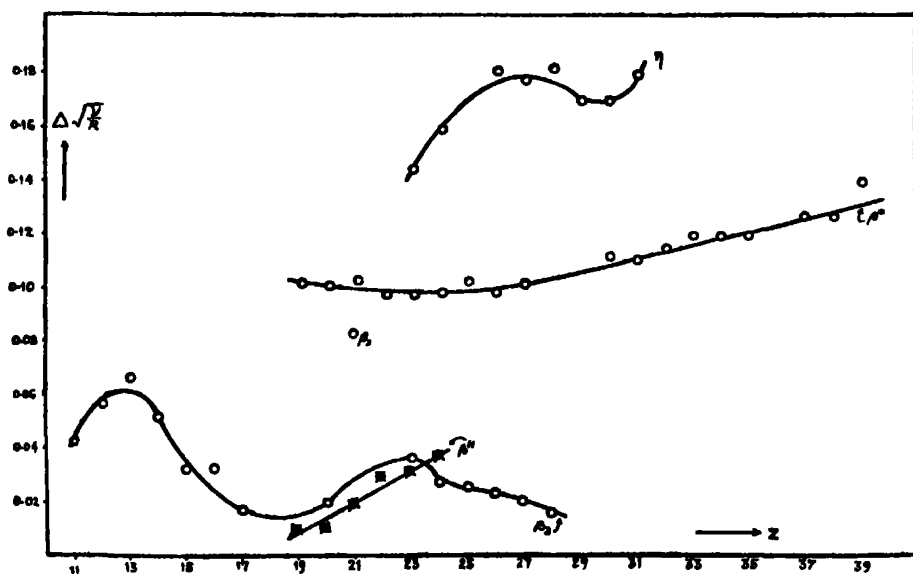


FIG. 2.

In Table III are given similar values for the β_3 , η and β_{III} lines with reference to the α_1 instead of the β_1 line. In fig. 3 these are plotted against atomic number.

Table III. $\Delta \sqrt{\nu/R} (\sqrt{\nu_3/R} - \sqrt{\nu_{\alpha_1}/R})$.

Element.	β_3 .	η .	β_{II} .	β_{III} .
11 Na	0.067	—	—	—
12 Mg	0.110	—	—	—
13 Al	0.180	—	—	—
14 Si	0.254	—	—	—
15 P	0.337	—	—	—
16 S	0.400	—	—	—
17 Cl	0.485	—	—	—
19 K	—	—	0.646	0.738
20 Ca	0.682	—	0.714	0.804
21 Sc	—	—	0.790	0.873
22 Ti	—	—	0.863	0.929
23 Va	—	0.753	0.928	0.994
24 Cr	—	0.804	0.997	1.057
25 Mn	—	0.846	1.112	1.124
26 Fe	—	0.912	—	1.184
27 Co	—	0.967	—	1.247
28 Ni	—	1.025	—	—
29 Cu	—	1.100	—	—
30 Zn	—	1.163	—	1.437
31 Ga	—	1.210	—	1.501
32 Ge	—	1.366	—	1.571
33 As	—	—	—	1.641
34 Se	—	—	—	1.709
35 Br	—	—	—	1.778
37 Rb	—	—	—	1.918
38 Sr	—	—	—	1.981
39 Y	—	—	—	2.062

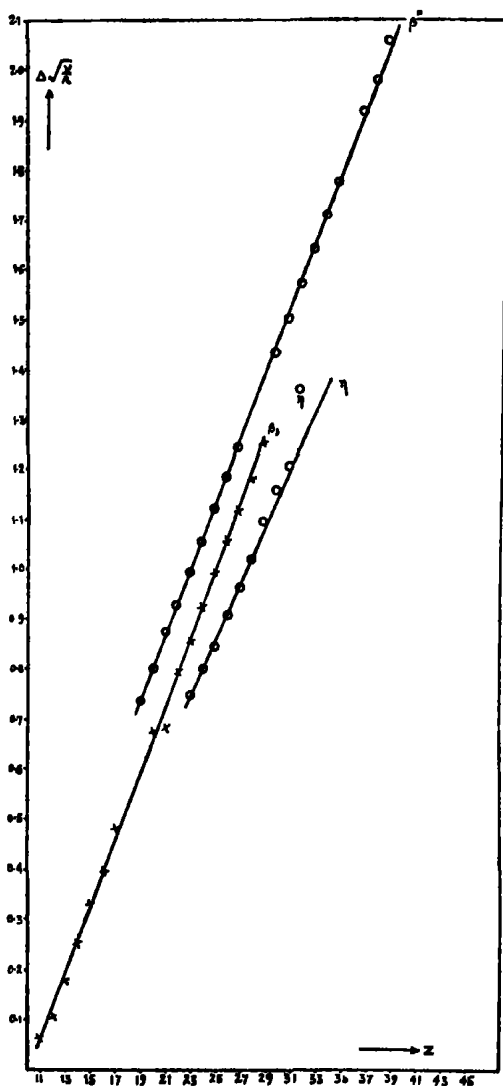


FIG. 3.

In Tables IV, V and VI are collected $\Delta\sqrt{v/R}$ values of the satellites of the principal lines L_α , L_β , and L_γ ; and in figs. 4, 5 and 6 these are plotted against atomic number.

Table IV. $\Delta\sqrt{v/R}$ values of the Satellites of K_{α} .

Element.	$\alpha^I - \alpha_1$ (Richtmyer).	$\alpha^II - \alpha_1$ (Coster).	$\alpha^III - \alpha_1$ (Richtmyer).	$\alpha^I - \alpha_1$ (Coster).	$\alpha^III - \alpha_1$ (Richtmyer).	$\alpha^II - \alpha_1$ (Coster).	$\alpha^IV - \alpha_1$ (Richtmyer).	$\alpha^V - \alpha_1$ (Richtmyer).	$\alpha^{VI} - \alpha_1$ (Richtmyer).
37 Rb	0-017	0-025	0-022	—	0-030	0-042	0-039	0-047	—
38 Sr	0-017	0-024	0-022	—	0-028	0-043	0-040	0-046	—
40 Zr	0-017	0-027	0-024	—	0-030	0-043	0-041	0-048	—
41 Nb	0-018	0-030	0-024	—	0-030	0-045	0-043	0-049	0-056
42 Mo	0-018	0-028	0-025	—	0-031	0-045	0-042	0-052	0-061
44 Ru	0-018	0-028	0-025	—	0-033	—	0-044	0-055	0-067
45 Rh	0-018	0-026	0-025	0-036	0-033	0-045	0-044	0-055	—
46 Pd	0-019	0-027	0-025	0-038	0-035	0-046	0-046	0-058	0-071
47 Ag	0-019	0-026	0-027	0-036	0-036	0-047	0-048	0-060	—
48 Cd	0-019	—	0-027	0-037	0-036	—	0-049	0-062	—
49 In	0-019	—	0-027	0-040	0-037	—	0-050	0-060	0-070
50 Sn	—	—	—	0-041	—	—	—	—	—
51 Sb	—	—	—	0-043	—	—	—	—	—
55 Cs	—	—	—	0-047	—	—	—	—	—
56 Ba	—	—	—	0-048	—	—	—	—	—

TABLE V. $\Delta\sqrt{v/R}$ values of the Satellites of L_{β_1} .

Element.	β_{1^I} (Coster).	β_{1^I} (Richtmyer).	β_{1^II} (Coster).	β_{1^II} (Richtmyer).	β_{1^III} (Richtmyer).	$\beta_{1^{IV}}$ (Richtmyer).
37 Rb	0.016	—	0.032	—	—	—
38 Sr	0.017	—	0.032	—	—	—
39 Y	—	—	—	—	—	—
40 Zr	0.017	—	0.032	—	—	—
41 Nb	0.018	0.016	0.036	0.033	—	—
42 Mo	0.020	0.016	0.035	0.033	0.042	0.051
44 Ru	—	0.016	—	0.034	0.045	0.059
45 Rh	0.023	0.018	0.037	0.034	0.047	0.060
46 Pd	0.022	0.019	0.036	0.037	0.050	0.062
47 Ag	0.026	0.023	0.039	0.038	0.052	0.064
48 Cd	0.024	0.021	0.039	0.037	0.055	0.071
49 In	0.020	0.018	0.040	0.036	0.055	—
50 Sn	0.027	0.020	0.043	0.040	0.055	—

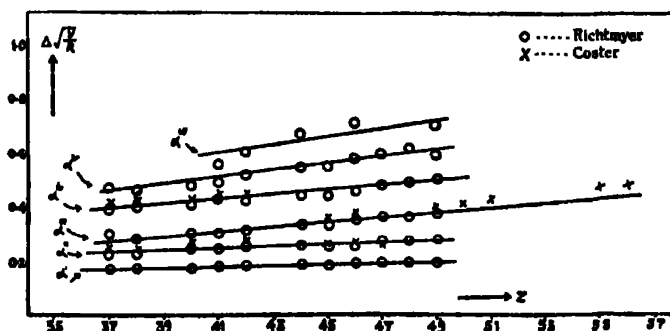


FIG. 4.

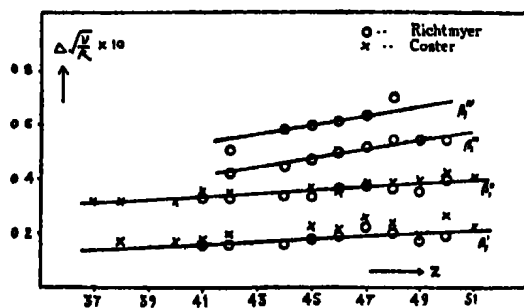


FIG. 5.

Table VI. $\Delta\sqrt{\nu}/R$ values of the Satellites of L_{β_1} .

Element.	$\beta_2(a)$ (Richtmyer).	β_2^1 (Druyvesteyn) (Richtmyer).		$\beta_2(b)$ (Richtmyer).	β_2^{π} (Druyvesteyn) (Richtmyer).		$\beta_2(c)$ (Richtmyer).
		(Druyvesteyn)	(Richtmyer).		(Druyvesteyn)	(Richtmyer).	
40 Zr	—	—	0.061	0.068	—	—	—
42 Mo	—	0.065	0.063	0.073	0.086	0.081	0.092
44 Ru	—	0.064	0.061	0.072	0.088	0.083	0.095
45 Rh	0.010	0.063	0.061	0.071	0.083	0.084	0.098
46 Pd	0.010	0.063	0.062	0.073	0.085	0.084	0.099
47 Ag	0.010	0.065	0.064	0.074	0.086	0.085	0.100
48 Cd	0.012	0.064	0.067	0.077	0.083	0.088	0.101
49 In	0.013	0.068	0.067	0.078	0.088	0.087	0.100
50 Sn	0.015	0.068	0.068	0.078	0.089	0.089	0.100

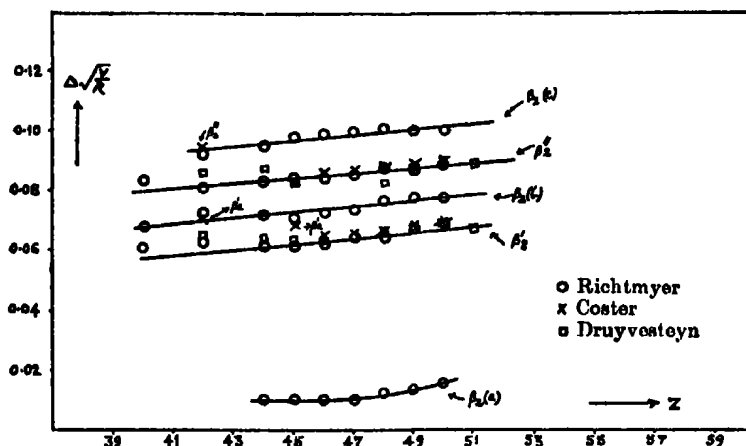


FIG. 6.

Discussion.

The outstanding feature of these graphs is that the $\Delta \sqrt{v/R}$ values keep a linear relation with the atomic number and that pairs are usually found out for which the graphs run parallel to each other. Thus in fig. 1, α^I , α_3 and α_4 are parallel to each other and so are α_5 and α_6 .

In fig. 2 no such relationship is observable; but in fig. 3 the case is different. The same lines are here referred to the α_1 instead of the β_1 line. The immediate consequence of this shift of reference line is that the behaviour of the β_3 , η and β^{III} lines becomes regular. It is also seen from this figure that the course of the β_3 line is very nearly parallel to that of the β^{III} line. It thus appears that the β^{III} , η and β_3 lines are in some way associated with the α_1 instead of the β_1 line, although in the X-ray spectrum they seem to lie closer to the β_1 line.

This circumstance shows that care must be taken in the choice of a diagram line with which a given nondiagram line is to be associated.

Examination of fig. 4 shows that the α^I and α^{II} lines run parallel to each other and so also the α^{III} and α^{IV} lines. Similarly the α^V and α^{VI} lines run parallel to each other. Moreover, the inclination of these three pairs of lines with the axis of atomic number increases with higher v/R values.

Inspection of fig. 5 shows that the β_1 satellites fall into two pairs, $\beta_1^I \beta_1^{II}$ and $\beta_1^{III} \beta_1^{IV}$, for which $\Delta \sqrt{v/R}$ values are approximately constant.

Scrutiny of fig. 6 shows that all the lines, with the exception of $\beta_2(a)$, run parallel to each other approximately. Thus the four satellites can be taken in pairs having more or less constant $\Delta \sqrt{v/R}$ values.

Coster (*loc. cit.*) appears to think that in the case of α_3 , α_4 , β_{11} , β_{12} and γ_7 lines in the L series of certain elements, $\Delta\sqrt{\nu/R}$ values when referred to the corresponding principal diagram lines show constancy. Actually, however, they appear to vary systematically with atomic number and are representable by a straight line inclined to the axis of atomic number. And this is found to be true for the majority of nondigram lines as the foregoing figures show. However, as seen above, pairs of nondigram lines are obtained which closely satisfy the constancy of $\Delta\sqrt{\nu/R}$ values.

Taking the pair $\alpha^I\alpha^{\pi}$ for our discussion, the line α^I may be represented as a first approximation by the equation

$$(\nu/R)_{\alpha^I} = (Z - \sigma_1)^2/n_1^2 - (Z - \sigma_2)^2/n_2^2, \quad (1)$$

where Z is the atomic number, n_1 , n_2 the total quantum numbers, and σ_1 and σ_2 the screening constants corresponding to the initial and final condition of the atom emitting the line in question. From equation (1) we get, neglecting the terms involving in the denominator second and higher powers of Z ,

$$\left(\sqrt{\frac{\nu}{R}}\right)_{\alpha^I} = Z\left(\frac{1}{n_1} - \frac{1}{2}\frac{n_1}{n_2^2}\right) - \left(\frac{\sigma_1}{n_1} + \frac{1}{2}\frac{\sigma_1 n_1}{n_2^2}\right) + \frac{n_1}{n_2^2}\sigma_2. \quad (2)$$

Combining this with the empirical relation

$$\left(\sqrt{\frac{\nu}{R}}\right)_{\alpha^{\pi}} - \left(\sqrt{\frac{\nu}{R}}\right)_{\alpha^I} = \text{constant} \quad (3)$$

we are led to the equation

$$\left(\sqrt{\frac{\nu}{R}}\right)_{\alpha^{\pi}} = Z\left(\frac{1}{n_1} - \frac{1}{2}\frac{n_1}{n_2^2}\right) - \left(\frac{\sigma_1'}{n_1} + \frac{1}{2}\frac{\sigma_1' n_1}{n_2^2}\right) + \frac{n_1}{n_2^2}\sigma_2'. \quad (4)$$

Equations (1) and (4) go to point out that to a first approximation the nondigram lines α^I , α^{π} result from transitions between two states characterised by the same initial and final total quantum numbers, but different screening constants. It is easy to see that the same is the case with the other pairs of nondigram lines satisfying relation (3).

It can be easily shown from the foregoing relations that

$$\begin{aligned} \left(\frac{\nu}{R}\right)_{\alpha^{\pi}} - \left(\frac{\nu}{R}\right)_{\alpha^I} &= \left[\frac{2}{n_1^2}(\sigma_1 - \sigma_1') - \frac{2}{n_2^2}(\sigma_2 - \sigma_2') \right] Z \\ &\quad - \left\{ \frac{1}{n_1^2}(\sigma_1^2 - \sigma_1'^2) - \frac{1}{n_2^2}(\sigma_2^2 - \sigma_2'^2) \right\} \\ &= mZ + c. \end{aligned} \quad (5)$$

Thus pairs of satellites having constant $\Delta\sqrt{\nu/R}$ values should satisfy equation (5). We shall proceed to see how far this deduction is realised in the case of the lines discussed above.

Tables VII to XI give $\Delta \nu/R$ values for the pairs of nondiagram lines which appear to show constancy of $\Delta \sqrt{\nu/R}$ values. The data are plotted in figs. 7 to 11.

Table VII. $\Delta \nu/R$ values of the K Series Satellites.

Element.	$\alpha^1 - \alpha_2$	$\alpha^1 - \alpha_4$	$\alpha_2 - \alpha_4$	$\alpha_2 - \alpha_6$
11 Na	0.22	0.36	0.14	0.20
12 Mg	0.24	0.39	0.15	0.24
13 Al	0.27	0.47	0.20	0.27
14 Si	0.34	$\left\{ \begin{array}{l} 0.48 (\alpha^1 - \alpha_4^1) \\ 0.40 (\alpha^1 - \alpha_4) \end{array} \right\}$	$\left\{ \begin{array}{l} 0.25 (\alpha_2 - \alpha_4^1) \\ 0.15 (\alpha_2 - \alpha_4) \end{array} \right\}$	0.34
15 P	0.35	0.54	0.19	0.30
16 S	0.37	0.58	0.21	0.34
17 Cl	0.40	0.63	0.23	—

Table VIII. $\Delta \nu/R$ values.

Element.	$\beta_{III} - \beta_2$	Element.	$\beta_{III} - \beta_2$
20 Ca	4.57	24 Cr	5.27
21 Sc	6.73	25 Mn	5.60
22 Ti	5.01	26 Fe	5.53
23 V	5.45	27 Co	5.75

Table IX. $\Delta \nu/R$ values.

Element.	$\alpha^I - \alpha^{II}$	$\alpha^{III} - \alpha^{IV}$	$\alpha^V - \alpha^{VI}$
37 Rb	0.11	0.19	—
38 Sr	0.12	0.27	—
40 Zr	0.15	0.27	—
41 Nb	0.16	0.35	0.17
42 Mo	0.18	0.29	0.24
44 Ru	0.20	0.32	0.31
45 Rh	0.21	0.32	—
46 Pd	0.20	0.32	0.39
47 Ag	0.23	0.33	—
48 Cd	0.23	0.40	—
49 In	0.23	0.41	0.30

Table X. $\Delta \nu/R$ values.

Element.	$\beta_{I^1} - \beta_{I^{II}}$	$\beta_{I^{III}} - \beta_{I^{IV}}$
41 Nb	0.43	—
42 Mo	0.46	0.25
44 Ru	0.51	0.40
45 Rh	0.57	0.39
46 Pd	0.53	0.35
47 Ag	0.47	0.36
48 Cd	0.51	0.49
49 In	0.57	—

Table XI. $\Delta \nu/R$ values.

Element.	$\beta_1^I - \beta_2(b).$	$\beta_2(b) - \beta_2^{II}.$	$\beta_2(c) - \beta_2^{II}.$
40 Zr	0.18	0.39	—
42 Mo	—	0.32	0.30
44 Ru	0.33	0.47	0.34
45 Rh	0.30	0.32	0.42
46 Pd	0.33	0.34	0.46
47 Ag	0.34	0.35	0.49
48 Cd	0.35	0.18	0.44
49 In	0.36	0.34	0.45
50 Sn	0.33	0.38	0.39

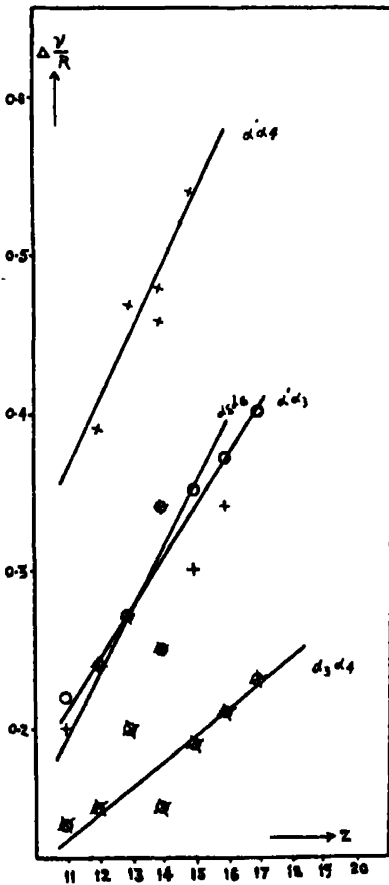


FIG. 7.

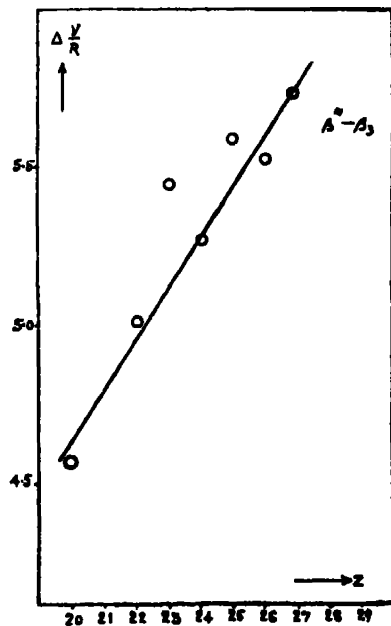


FIG. 8.

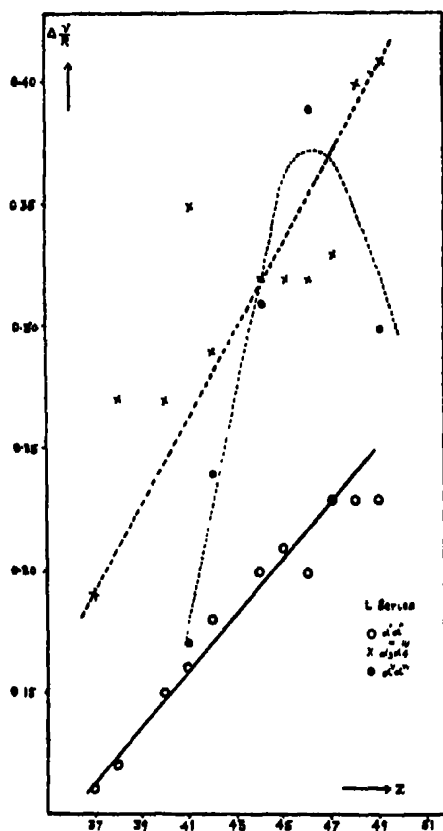


FIG. 9.

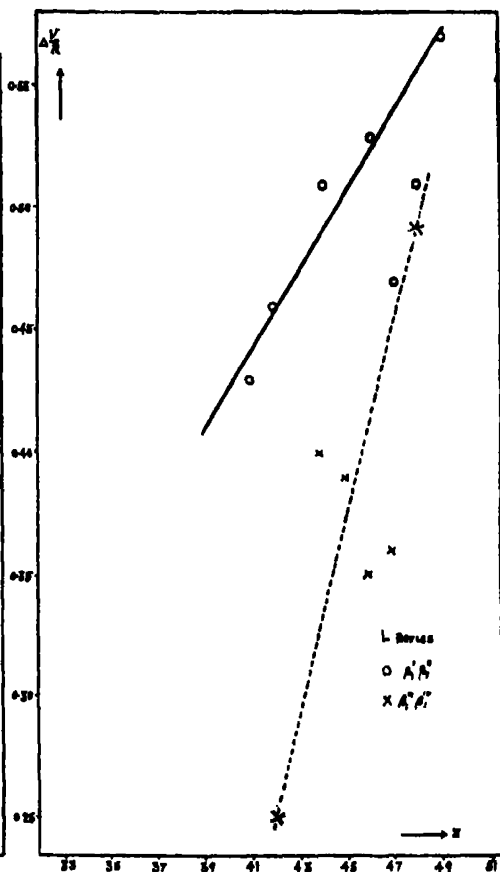


FIG. 10.

It appears that the relation (5) is more or less realised in the case of the pairs in the K series and the $L \alpha' \alpha''$ and $L \beta_1' \beta_1''$ pairs in the L series. In the other cases it is not obvious. In fact, for the pairs $L \alpha' \alpha''$ and $L \beta_2 (c) \beta_2''$ the curve appears to decline after reaching a maximum.

The cause of this discrepancy is not obvious. It may be pointed out that in the case of the usual screening doublets in the L absorption spectra also the $\Delta \nu/R$ values do not seem to be governed by a linear relation in spite of the more or less constancy of $\Delta \sqrt{\nu/R}$ values.

We shall return now to the case of the β_3 , β_3'' and η lines in the K series, which, as remarked above, are connected in some way with the α_1 instead of the β_1 line.

Richtmyer* has pointed out that the square root of the difference of frequency

* 'Phil. Mag.', vol. 6, p. 64 (1928); 'Phys. Rev.', vol. 34, p. 574 (1929).

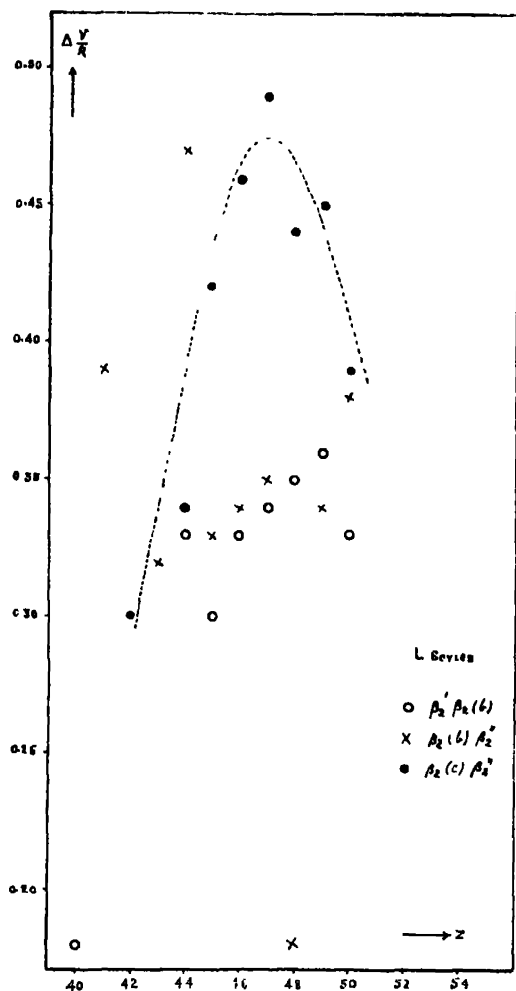


FIG. 11.

of the parent line and its satellite holds a linear relation with atomic number like Moseley's law.

If the β_3 , β^m and γ lines have really something to do with the α_1 rather than the β_1 line as observed above, the graphs plotted after Richtmyer with the α_1 and β_1 lines taken in turn as parent line should show striking differences.

In Tables XII to XIV are given the $\sqrt{(v_s - v_p)/R}$ values for the three lines β_3 , β^m and γ , where v_s means the frequency of a satellite and v_p that of a parent line.

Table XII.

Element.	$\sqrt{\left(\frac{\nu}{R}\right)_{\beta_3} - \left(\frac{\nu}{R}\right)_{\alpha_1}}$	$\sqrt{\left(\frac{\nu}{R}\right)_{\beta_1} - \left(\frac{\nu}{R}\right)_{\beta_2}}$
11 Na	1.091	0.866
12 Mg	1.456	1.054
13 Al	1.946	1.200
14 Si	2.406	1.114
15 P	2.865	0.910
16 S	3.253	0.959
17 Cl	3.700	0.728
20 Ca	4.788	0.837
21 Sc	4.930	1.721
22 Ti	5.455	1.118
23 Va	5.819	1.221
24 Cr	6.166	1.073
25 Mn	6.519	1.073
26 Fe	6.873	1.044
27 Co	7.214	1.010
28 Ni	7.558	1.910

Table XIII.

Element.	$\sqrt{\left(\frac{\nu}{R}\right)_{\eta} - \left(\frac{\nu}{R}\right)_{\beta_1}}$	$\sqrt{\left(\frac{\nu}{R}\right)_{\eta} - \left(\frac{\nu}{R}\right)_{\alpha_1}}$
23 Va	2.385	5.445
24 Cr	2.538	5.722
25 Mn	—	—
26 Fe	2.803	6.359
27 Co	2.902	6.692
28 Ni	2.982	7.004
29 Cu	2.992	7.403
30 Zn	2.934	7.745
31 Ga	3.162	8.039
32 Ge	2.268	8.692

Table XIV.

Element.	$\sqrt{\left(\frac{\nu}{R}\right)_{\beta_{\text{in}}} - \left(\frac{\nu}{R}\right)_{\beta_1}}$	$\sqrt{\left(\frac{\nu}{R}\right)_{\beta_{\text{in}}} - \left(\frac{\nu}{R}\right)_{\alpha_1}}$
19 K	1.900	4.891
20 Ca	1.987	5.244
21 Sc	1.942	5.571
22 Ti	1.934	5.894
23 Va	2.020	$\left. \begin{array}{l} 6.240 \\ 6.250 \end{array} \right\}$
24 Cr	2.032	6.580
25 Mn	2.126	6.940
26 Fe	2.124	7.267
27 Co	2.198	7.609
30 Zn	2.437	8.633
31 Ga	2.462	8.982
32 Ge	2.569	9.343
33 As	2.655	9.703
34 Se	2.693	10.053
35 Br	2.755	10.417
37 Rb	2.933	11.144
38 Sr	2.950	11.495
39 Y	3.131	11.879

In figs. 12 and 13 the data in Tables XII to XIV are plotted against atomic number. These figures immediately bring out the fact that whilst the behaviour of these lines when referred to the β_1 line as the parent line is complicated, the same when referred to the α_1 as the parent line becomes remarkably simple; in the case of all the three lines the graphs come out to be straight lines.

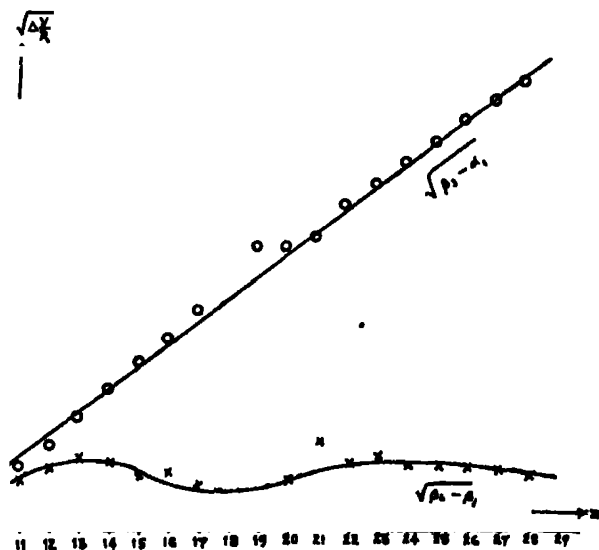


FIG. 12.

There is thus evidence from two different directions in favour of choosing α_1 as the principal diagram line for the three lines in question.

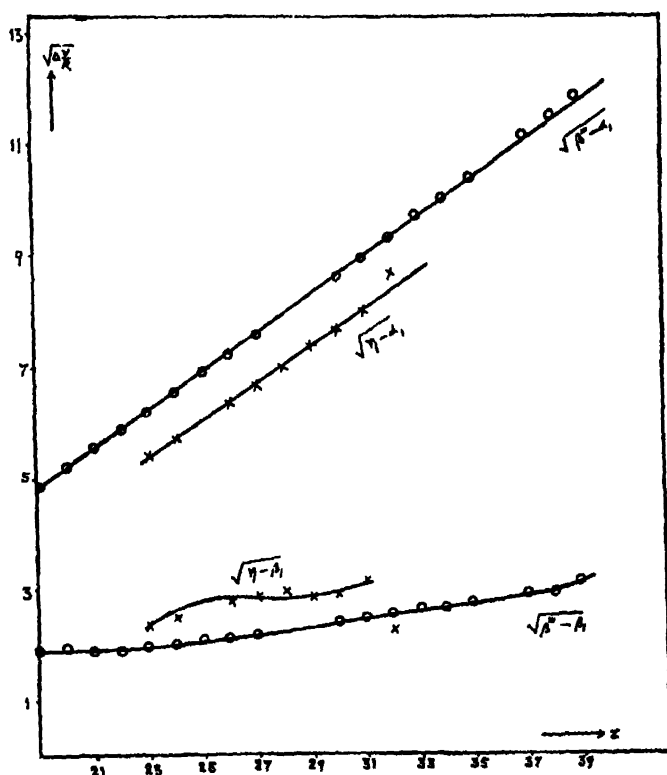


FIG. 13.

This linear relation is interesting and perhaps suggests the existence of double electron transfers in the inner levels of the excited atom. The possibility of such a process has been demonstrated by the author in Part I of his paper on "Some Investigations in Röntgen Spectra" in the case of the $L\gamma'_{23}$ line as resulting from the double jump $N_{IV} \rightarrow M_{II}$ and $M_{II} \rightarrow L_I$. The probability of the β''' line as resulting from the double jump $L_{III} \rightarrow K$ and $M_{IV,V} \rightarrow L_{III}$ seems to have been demonstrated by Beuthe.* The β_3 line probably arises from the double jump $M_I \rightarrow L_{III}$ and $L_{III} \rightarrow K$.† Unfortunately the M_I levels are not directly known. They have been calculated indirectly by Mukerjee and Ray.‡ Their figures have been used in computing column 2

* 'Z. Physik,' vol. 60, p. 603 (1930).

† Beuthe suggests that this double jump represents the line η ; but the discrepancies between the calculated and observed values seem comparatively to be rather too large.

‡ 'Z. Physik,' vol. 57, p. 345 (1929).

of Table XV, which demonstrates the probable origin of the β_3 line. The data in column 3 of this table are taken from Siegbahn's spectroscopy of X-rays.

Table XV.

Element.	ν/R $M_I \rightarrow L_{II, III}$	ν/R $L_{III} \rightarrow K$	ν/R $M_I \rightarrow L_{II, III}$ + $L_{III} \rightarrow K$	ν/R β_3	δ obs. - cal.
11 Na ..	1.782	76.68	78.462	77.87	-0.59
12 Mg ..	3.049	92.34	95.389	94.46	-0.93
13 Al ...	3.954	109.53	113.484	113.32	-0.16
14 Si ..	5.585	123.18	133.765	133.97	+0.21
15 P ..	7.479	148.37	155.849	156.58	+0.73
16 S ..	10.040	169.98	180.020	180.56	+0.54
17 Cl ..	12.653	193.14	205.793	206.83	+1.04
19 K ...	18.722	244.07	262.792	—	—
20 Ca ..	21.720	271.88	293.600	294.81	+1.21
21 Sc	25.276	301.24	326.516	325.55	-0.97
22 Ti	28.922	332.20	361.122	361.95	+0.83
23 V ..	32.866	364.38	397.246	398.23	+0.98
24 Cr ..	37.087	398.83	435.917	436.85	+0.93
25 Mn ..	41.547	434.49	476.037	476.98	+0.94
26 Fe ..	46.081	471.60	517.681	518.81	+1.13
27 Co ...	50.912	510.44	561.352	562.48	+1.13
28 Ni ..	55.842	550.75	606.592	607.88	+1.29

The discrepancy in the last column of this table may partly be attributed to changes in the M_I orbits as a result of multiple ionisation. Nothing more definite can be said in the absence of accurate experimental data.

Summary.

In the present paper it has been shown that in the K and L series nondiagram lines, pairs are found which show approximately constant $\sqrt{\nu/R}$ differences. These seem to resemble the usual screening doublets in the X-ray absorption spectra.

It seems that the components of such pairs arise from transitions in multiply ionised atoms characterised by the same initial and final total quantum numbers but different screening constants.

In spite of the more or less constant $\Delta\sqrt{\nu/R}$ values all the pairs do not show the required linear variation of $\Delta\nu/R$ with atomic number. In this matter also these pairs appear to have analogy with the usual screening doublets.

It has been shown that behaviour of the β_3 , η and β''' lines in the K series becomes more regular when they are associated with the K_{α_1} instead of the K_{β_1} line. It is demonstrated that the β_3 line probably arises from the double jump $M_I \rightarrow L_{III}$ and $L_{III} \rightarrow K$.

The Theory of Metallic Corrosion in the Light of Quantitative Measurements.—Part IV.

By G. D. BENGOUGH, A. R. LEE, and F. WORMWELL, Chemical Research Laboratory, Teddington.

(Communicated by Sir Harold Carpenter, F.R.S.—Received February 9, 1931.)

[PLATES 16-22.]

The present paper includes some experiments suggested by criticisms of Part III of the research, and describes work upon the effect of depth of immersion on the corrosion of zinc in potassium chloride solutions. Some of the factors which influence the distribution of corrosion over the metallic surface are discussed with particular reference to the effect of differential aeration. Curves are given showing the effect of concentration of potassium chloride and potassium sulphate on the initial corrosion rate of zinc in tranquil conditions. The experimental methods used are those described in previous papers, supplemented by micrographic work and a few potential measurements.

The criticism has been made that the tranquil conditions in which the present series of experiments is being conducted cause abnormally slow rates of oxygen supply which dictate the corrosion rates; these, therefore, are not considered characteristic of the metal under test, but merely of the rate of penetration of oxygen through the liquid and any corrosion products which cover the metal. It has also been suggested that much faster rates of oxygen supply would be required to bring out the true corrosion characteristics of a metal or even to differentiate between two fairly reactive metals.

Some special experiments have been made to test the effect of faster and slower rates of oxygen supply than the authors' normal rate, which for zinc in N/10 KCl in the standard apparatus is about twice as fast as that for immersed specimens in similar open non-thermostated vessels exposed to air. The rates tested vary from about one-quarter to six times the normal rate, as shown in Table I. This range is obtained by the use of different depths of immersion and oxygen partial pressures. Only the effect of reducing the partial pressure of oxygen from one to one-fifth of an atmosphere is now recorded, but experiments are proceeding with pressures up to 20 atmospheres.

The results in Table I include the corrosion due to oxygen absorption at the

Table I.—Oxygen Corrosion (milligram equivalents) in N/10 KCl.

Conditions of experiments.	Time (days).	I Zinc.	II Mild steel.	III Zinc Steel	IV Corrosion in O Corrosion in air		V Initial rate for zinc (mgm. per day).
					Zinc.	Steel.	
A. Purified air at 25° C.	100.72	5.17	2.31	2.24	7.1	4.4	1.7
B. Purified oxygen at 25° C.	100.72	36.92	10.14	3.64			7.6
C. Laboratory air, protected from dust	24.75	2.87	2.04	1.41	2.4	1.4	3.8
D. Purified oxygen at 25° C.	24.75	6.75	2.93	2.30			7.6
E. Purified oxygen at 25° C. (shallow immersion, 0.35 mm.)	24.71	24.86	18.8	1.30			44.5

Note.—Results in column V are in milligrams (not milligram-equivalents) per day. For sets A and C the results were obtained by dividing the total oxygen corrosion by the time of corrosion; for sets B, D and E they represent the maximum slopes of the corrosion-time curves. The air used in set A was purified by passage through sulphuric acid, caustic potash, distilled water and a filter of blotting paper.

end of a given time and the initial corrosion rates in four sets of conditions, three of which were essentially the authors' standard conditions. In set A these were modified by the use of purified air instead of oxygen in the apparatus shown in fig. 1 which has the same cross-section, holds the same volume of liquid and gives the same depth of immersion as the standard apparatus. It can be immersed so that evaporation and the consequent convection currents are eliminated. The tap is so arranged that the oxygen pressure (which falls owing to corrosion) can be restored to normal from time to time. The total corrosion is determined by loss of weight which has already been shown to agree closely with the oxygen absorption determination. In set E the top surfaces of the specimens were immersed at a depth of 0.35 mm. instead of 15 mm. In set C the experiments were performed in open bottom vessels of the usual apparatus exposed to the laboratory air but covered with large inverted beakers supported on wooden blocks; the vessels were placed on a shelf in the laboratory and the corrosion rates were affected by changes of temperature and pressure and correspond to those of the ordinary type of corrosion test, but using the standard size of vessel and depth of immersion.

All steel specimens were turned from a rolled rod of $1\frac{1}{4}$ inches diameter with a composition of carbon 0.13 per cent., silicon 0.20 per cent., manganese 0.46, sulphur 0.034, phosphorus 0.034, chromium 0.04, and copper 0.02. A more detailed account of this steel, which was taken from a specially homogeneous part of a large ingot tested and selected for the authors by Mr. J. H. S. Dickenson, will be given in a separate paper on the corrosion of iron and steel.

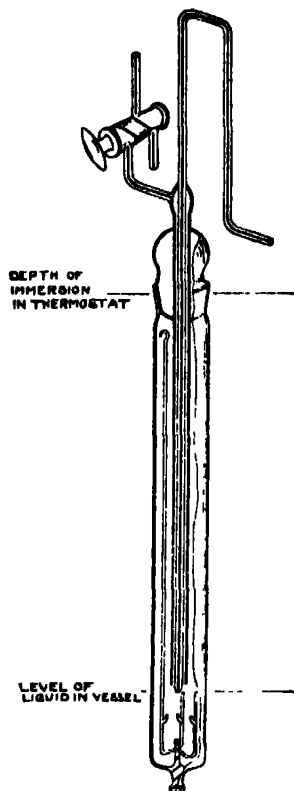


FIG. 1.—Simple Corrosion Apparatus.

Throughout the range of Table I the corrosion rates of zinc and mild steel are different, as shown in column III. It is probable that these differences are mainly due to the respective rates of penetration of oxygen through the corrosion products, but it has been found that accumulations of loose zinc hydroxide and of the voluminous loose yellow-brown ferric hydroxide have very little effect on the corrosion rates of zinc and steel; they may be shaken off in the middle of an experiment without noticeable effect on the corrosion-time curves. Any possible effect on corrosion rates is confined to thin continuous films or adherent nodules of corrosion product, such as the well-known yellowish film on zinc and the adherent part of the dark purple-black layer on iron.

Such partially protective layers of corrosion products are found in many types of corrosive conditions, including some in flowing water, and the study of their effects is an important branch of corrosion study. These effects will probably vary with the conditions, and so, in the present state of knowledge, prevent precise calculations of corrosion rates in conditions other than those in which they were obtained. Therefore the rates found in this research should not be used to calculate probable rates in widely different industrial conditions. Close imitation of any particular set of industrial conditions has not been sought, but rather constant and reproducible conditions which constitute the necessary, initial stage of the work.

The true interpretation of such results as those of Table I, which consist mainly of corrosion measurements made at the end of a given time, can only be

based on a knowledge of corrosion-time curves of the individual metals. The table shows that the relative amounts of corrosion of zinc and mild steel varied with the conditions and that the difference between them increases with time, owing to divergence of the corrosion-time curves. The curve for zinc usually turns upwards after 30 to 40 days owing to increased hydrogen gas evolution, and that for steel becomes less steep after about 20 days; the result is a change in the ratio of the corrosion rates of zinc and steel from 2.30 at 25 days to 3.64 at 100 days. The ratio in oxygen is somewhat greater than in air and always exceeds 2.20 except with very shallow immersion, so there is little likelihood of masking differences between the metals in the authors' standard apparatus. The effect of changing from air to oxygen is to multiply the corrosion of steel determined at the end of 100 days by 4.4; the reason why a value 5 was not obtained will be explained when the corrosion time curves for steel are published. The figure for zinc, 7.1, was unexpected, and differs from the ratio obtained from column V, namely, 4.5, because the corrosion-time curve in air is practically linear throughout 100 days whereas the curve in oxygen shows a considerable increase in slope after 50 days owing to hydrogen gas evolution as explained in Part III.

From partial pressure considerations the ratio of corrosion rates in oxygen and air would be expected to be 5 instead of 4.5 actually found for zinc, but measurements recorded on p. 62 of Part III of this research showed that corrosion rates were proportional to the square of the solubility of oxygen in solutions over the range $N/2$ to 4 N . From these results a ratio of 25 would be expected. It seems, therefore, that the same effect is not produced by varying the oxygen supply by means of alteration of partial pressure as by alteration of KCl concentration which affects oxygen solubility.

To investigate this matter further a series of experiments were performed in the simple form of corrosion vessel, beneath an atmosphere of purified air, with five solutions in the range $N/10$ to 4 N . The corrosion rates are plotted against salt concentration in fig. 2 and against oxygen solubility in fig. 3. The curve shown in the latter is a straight line instead of the parabola obtained in similar solutions in an atmosphere of oxygen. The explanation of the effect of changing the atmosphere is not at present known.

Several results in Table I cannot be explained at present, particularly the relative rates of zinc and steel with shallow immersion.

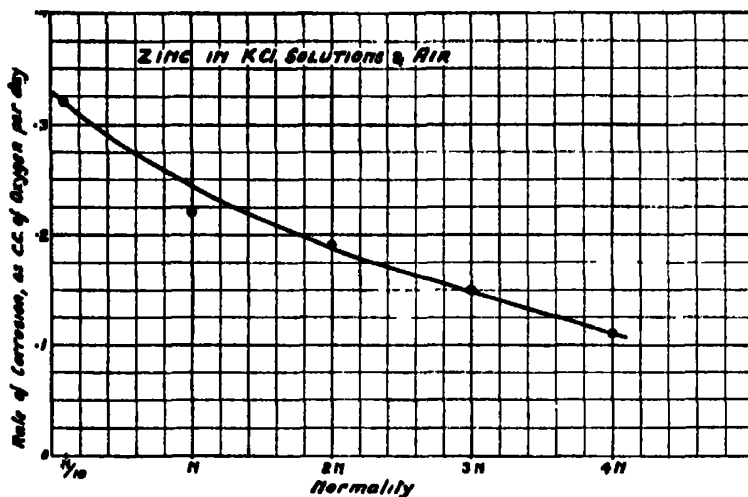


FIG. 2.—Variation of Corrosion Rate with Concentration of Salt.

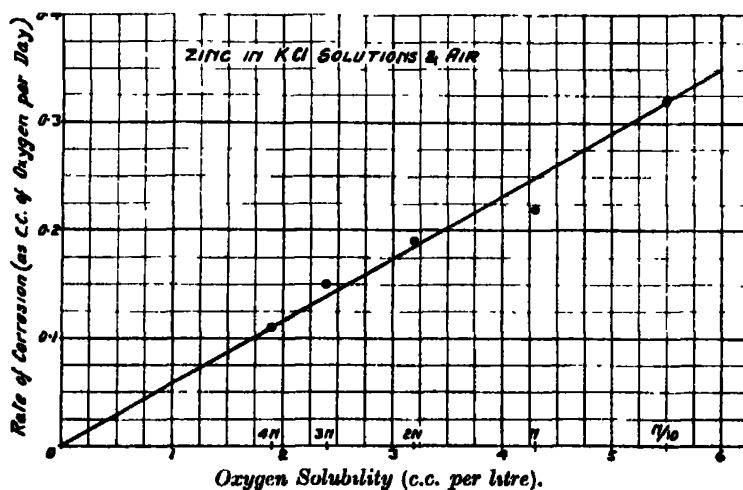


FIG. 3.—Variation of Corrosion Rate with Oxygen Solubility.

The Effect of Concentration of Salt on Corrosion.

In Part III curves were given in fig. 8 showing the relations between the rate of oxygen absorption and the concentrations of potassium chloride and potassium sulphate. It was stated that the experimental results had probably been affected by slight vibration, and some of them were redetermined for truly stagnant conditions and recorded in fig. 11 of Part III. The redeterminations have now been completed and correct curves are given in fig. 4. The point at

—6.7 on the log scale of concentration corresponds to the conductivity of the distilled water used in the experiment, 0.044×10^{-6} mhos., on the

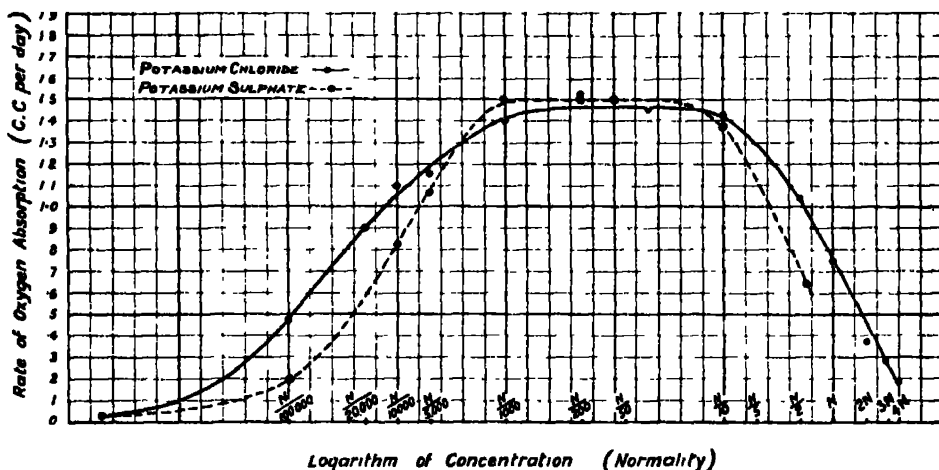


FIG. 4.—Variation of Corrosion Rate with Concentration of Salt.

assumption that this conductivity is due wholly to chloride or sulphate and so measures the concentration. The curves are practically flat between $N/1000$ and $N/10$. Consequently the main experimental support is withdrawn from the view¹³ adopted in Parts II and III that corrosion rates in this range are controlled by the rate of oxygen supply to restricted cathodic areas which increase in size with the concentration. The increase in the narrow range $N/5000$ to $N/1000$ is probably due to the fact that in the weaker solutions the maximum rate of oxygen absorption is not observed for 2 or 3 days, and in the meantime the concentration of chlorine or sulphate ions has been reduced sufficiently to affect it. This range may be regarded as a transition between those zones in which the concentration of anions and oxygen respectively control corrosion rates from the beginning of the experiments.

The flat portions of the curves between $N/1000$ and $N/10$ are probably characteristic of the cross-section of the corrosion vessel which has a diameter of 4.4 cm. This determines the maximum rate of oxygen supply to the metal; increases in cross-section would allow gradually diminishing increases in oxygen supply, which would finally be too small to affect appreciably the corrosion rates. In a vessel sufficiently wide to fulfil this condition the corrosion rate-concentration curve would consist mainly of two branches; one would correspond with the lower concentrations, and would cover the range

of chlorine ion control ; the other, corresponding with the higher concentrations which appreciably affect oxygen solubility, would cover the range of oxygen control. Such a curve, for a specimen of definite area, would give the effect of concentration independently of the cross-section of the apparatus, and of the depth of immersion between depth limits of 2 cm. and 10 cm., as shown below. Preliminary experiments suggest that the necessary cross-section could be about 15 cm.

The corrosion rates indicated in fig. 4 are initial rates which persist for times which, in the authors' conditions, are dependent on the salt concentration and other factors discussed later. Therefore, the relative amounts of corrosion that would occur at the end of a given time cannot be deduced directly from fig. 4, but must be judged from the complete corrosion-time curves given elsewhere.

The Influence of Depth of Immersion.

Fig. 5 shows groups of curves obtained for oxygen-corrosion of zinc in N/10 KCl in which the depth of immersion of the top surface of the specimens is varied

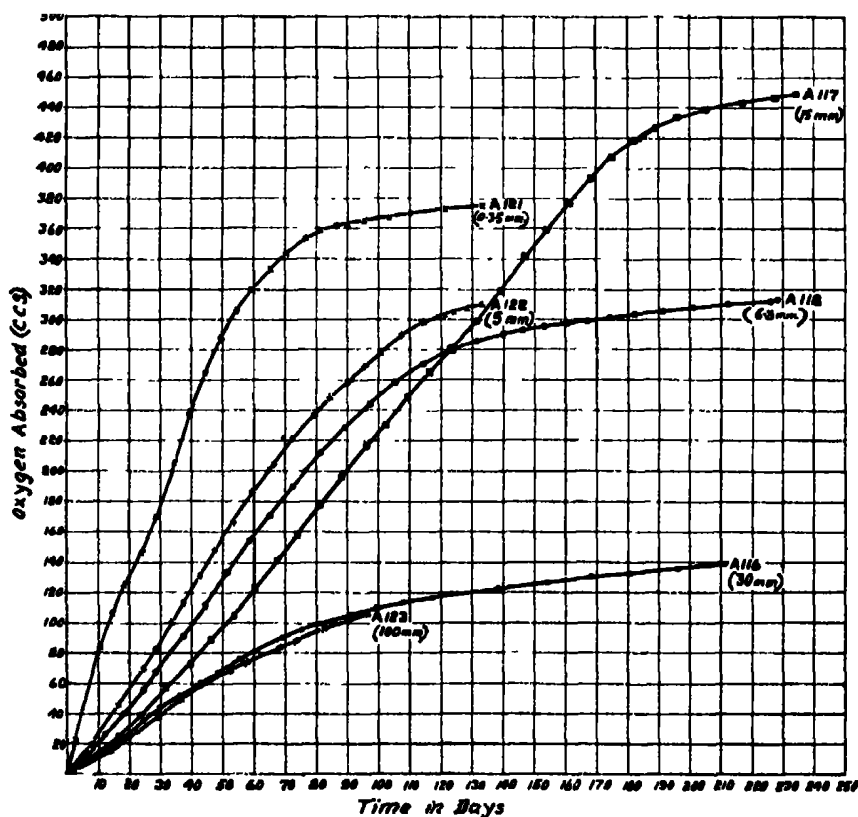


FIG. 5.—Influence of Depth of Immersion in N/10 KCl on True Oxygen Absorption.

from 0.35 mm. to 100 mm. It includes a curve obtained at the standard depth of 15 mm. used in previous work. The composition and preparation of the specimens and the experimental methods were similar to those described in previous papers. Fig. 6 shows a curve in which the rates of oxygen absorption

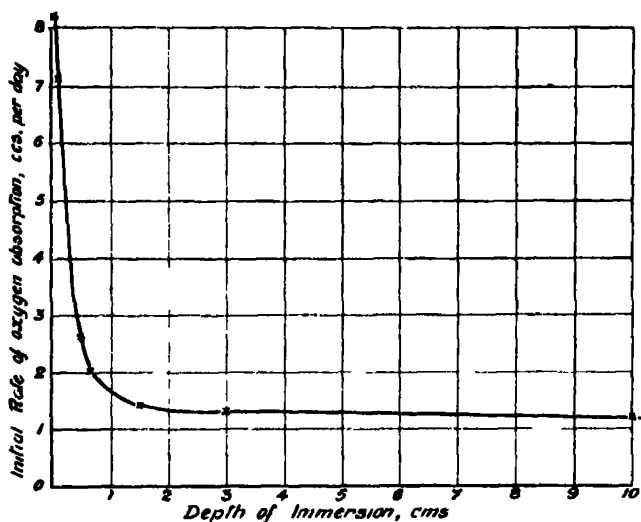


FIG. 6.—Influence of Depth of Immersion in N/10 KCl.

obtained from the initial straight line portions of the curves given in fig. 5 are plotted against the respective depths. At a depth of immersion of about 0.35 mm. the rate of oxygen absorption is nearly six times that at the standard depth, but this rate falls off rapidly with depth till it reaches a nearly constant value, which persists over the range from the standard depth to the greatest studied.

Throughout the whole range the rate of corrosion is limited by the rate of oxygen supply to the metal surface, and the peculiar form of the curve seems to be due to the relative influence of diffusion and convection on this oxygen supply. At very shallow depths the oxygen is conveyed to the metal surface mainly by diffusion which is a very effective carrier over the short distances required, owing to the abrupt difference of concentration between oxygen-saturated solution at the liquid surface and oxygen impoverished solution at the metal surface. Over longer distances, although a similar absolute difference of concentration occurs, the gradient is lessened proportionately to the distance and the rate of conveyance correspondingly reduced. The effectiveness of diffusion is further reduced as depth is increased by the occurrence of convection currents the origin of which is not quite clear, but which

may possibly be set up by the slightly higher density of the oxygen-saturated surface layers of the solution which tend to fall and carry oxygen with them and so reduce differences of concentration available for diffusion. At the standard depth of 1.5 cm. these convection currents seem to have almost completely replaced diffusion since the rate of oxygen supply has become nearly constant, whereas it would fall off in inverse proportion to the depth if it depended mainly on diffusion.

The approximate constancy of oxygen supply and corrosion rate over a considerable range of depth is not peculiar to the authors' condition. It was noted with surprise, and over a greater range, by Heyn and Bauer* in their report on the corrosion of steel in open beakers exposed to the atmosphere. The matter was left unexplained by them, probably because their work was finished before Adeney and his co-workers had shown the predominating importance of convection currents in conveying oxygen to the interior of solutions.

It has been suggested to the authors that the supply of oxygen to the metal in the standard conditions of this research is by diffusion only. If this were the case a straight line relation should hold between the rate of corrosion and the reciprocal of the depth. The experimental results do not give this relation. Another objection to the diffusion view is that Hufner's† value for oxygen diffusion only allows about 0.5 c.c. of oxygen per day to reach the metal, whereas about 1.5 c.c. reaches it in N/10 KCl in the corrosion experiments. Tor Carlson's‡ measurements confirm those of Hufner and both these authors accept the earlier views of Wroblewsky and Stefan that downward oxygen-streaming occurs into the body of solutions contained in vessels much greater in cross-section than 1 mm. The movement is so great that diffusion measurements can only be made in tubes of capillary section and is believed to be due to the increased density of gas-saturated surface layers of the solution. In the corrosion experiments there is an alternative mechanism due to the movement of corrosion products.

Departure from Linear Corrosion Rates in Strong KCl Solutions.

In previous papers the statement has been made that the slopes of the steeply inclined linear portions of corrosion-time curves are determined by the rate of oxygen supply and that departure from the linear form implies departure

* 'Mittel. König. Materialprüfungsamt,' vol. 26, p. 14 (1908).

† 'Ann. Phys. Chim.,' vol. 60, p. 134 (1897).

‡ 'J. Amer. Chem. Soc.,' vol. 33, p. 1027 (1911).

from oxygen control. Since doubt had been expressed about this view the following experiments were tried.

The corrosion vessel containing specimen A117 was taken out of the thermostat at the end of 111 days and placed for 4 hours and 20 minutes in another so that only the bottom part of the corrosion vessel was kept at 25° while the top was at about 21°. Convection currents due to temperature differences were thus produced in the vessel, and the rate of oxygen absorption rose from 1.42 c.c. per day to 1.8 for the particular day of the experiment. The corrosion-time curve for A117 is given in fig. 5 and shows the linear form up to the time of the experiment and afterwards as soon as the effect of the temporarily altered conditions had worn off (the disturbed readings are not plotted).

To test the view that oxygen control no longer holds after the corrosion-time curves have left the steeply inclined linear form, the corrosion vessel containing specimen A116 in N/10 KCl (see fig. 5) was taken out of the thermostat at the end of 110 days and shaken vigorously. The rate of oxygen absorption, 0.25 c.c. per day was not changed by this treatment. The vessel containing specimen A120 in N/10 KCl was treated similarly to A117 above, but convection currents were maintained for 4 hours only. The rate of oxygen absorption, which was 0.52 c.c. per day and slowly falling, was not increased even temporarily by the treatment.

The causes of the departure from the linear form of corrosion-time curves such as are shown in fig. 5 have not hitherto been discussed in detail. It has been found that both the time and the amount of corrosion at which this inflection occurs varies in supposedly duplicate experiments, and seriously reduces reproducibility at the end of long periods of corrosion. Burnishing and, to a lesser extent, turning and increased depth of immersion usually hasten inflection as shown by experiments A120, A119 and by fig. 5 of the present paper; A117 maintained the steeply inclined straight line form for 170 days, whereas most of the other curves in the figure began to bend in less than 100 days.

It was suggested in Part III (pp. 57 and 58) that the inflection "in strong solutions which still contain a considerable concentration of chlorine and sulphate ions is apparently due to the gradual accumulation of corrosion products which increase the electrical resistance of the corrosion current." There are difficulties about this view which the authors attempted to meet in the following paragraph, perhaps unsuccessfully. Further investigation has shown that considerable alkalinity has developed in experiments which have been continued long enough to give an appreciable diminution of corrosion

rates and of chlorine ion concentration. Some results are recorded in Table II.

Table II.—Concentration of Cl' and (OH') at the End of Corrosion Experiments in N/10 KCl.

No. of specimen.	Time of experiment.	I Cl found in 100 c.c.	II Cl abstracted from 100 c.c.	III OH equivalent to Cl abstracted.	IV OH found in 100 c.c.	Remarks.
A115	93 days	283.7 mgr.	70.9 mgr.	34.0 mgr.	38.2 mgr.	Immersed at 1.5 cm.
A116	212	269.5	85.1	40.8	36.3	" 3 cm.
A117	250	260.2	94.4	45.3	53.8	" 1.5 cm.
A118	246	262.4	92.2	44.2	42.5	" 6.3 mm.
A119	179	265.9	88.6	42.5	43.0	" 1.5 cm.
A120	146	283.7	70.9	34.0	38.2	" "
A121	134	276.6	78.0	37.3	45.8	" 0.35 mm.
A122	153	265.9	88.6	42.5	43.9	" 5 mm.
A123	109	319.1	35.5	17.0	15.8	" 10 cm.
A124	100	347.5	7.1	3.4	4.5	Atmosphere of purified air. 1.5 cm. depth, Immersed at 0.9 mm.
A125	45	294.3	60.3	28.9	29.6	

The figures in column II are obtained by subtracting those in column I from the total amount of Cl' ions present at the beginning of the experiment. The calculated equivalent of hydroxyl and the amount actually found experimentally are given in the following columns. There is a general correspondence between these two, the principle divergence occurring with very shallow immersion which sets up special conditions and with A117 which gave a linear corrosion-time curve for an unusually long time.

Founded upon the figures of Table II, an experiment was performed in which the total corrosion of zinc at the end of 25 days was determined in 100 c.c. of mixed solution which was 1/40N with respect to KOH and 3/40N with respect to KCl. It was found to be 30 mgr. as compared with 229 mgm. in N/10 KCl. The corrosion-time curve showed the final rate to be less than 0.1 c.c. of oxygen absorption per day, which is of the same order as that corresponding to the flattened portions of the curves obtained in N/10 KCl, e.g., A117 and A118 in fig. 5. It was thought possible that the actual alkalinity beneath mounds of corrosion product might differ from the general alkalinity and attempts were made to estimate them by the use of the B.D.H. Universal Indicator. Liquid was removed from inside domes on specimen A118 after 228.7 days in N/10 KCl and the hydrogen ion concentration appeared to be at

least p_H 11—approximately the same as the general concentration. A test carried out on Al28 which had been in N/50 KCl for 21.73 days gave a value close to p_H 7 for the liquid inside the dome and at least p_H 11 outside, but the corrosion-time curve was linear at the time of the test. The alkalinity inside the dome appears to be an important factor in determining the slopes of curves.

The Distribution of Corrosion.

The corroded surfaces of all specimens used for corrosion-time curves throughout the research have been examined both before and after removal of corrosion products. In conductivity water and dilute solutions of KCl and K_2SO_4 corrosion is concentrated upon isolated areas, round which rings of interference colours are usually found. Even when experiments are continued for long periods parts of the metals, particularly on the top surface, suffer relatively little attack and become covered with transparent films which show interference colours and, later, yellowish tints to which no definite order of interference colour can be assigned (see fig. 7 which shows turning marks through such a film). In solutions stronger than N the uncorroded areas are larger on the bottom than on the top surface. In moderately strong solutions the corroded areas are covered with white "domes" of zinc hydroxide which sometimes terminate in long tubes extending upwards to the liquid surface, or downwards deep into the solution as shown in Plate 16, figs. 7 to 9; all photographs in this paper were taken at a magnification of 2.5 diameters with oblique illumination, unless otherwise stated. In reproduction the magnification has been reduced to 1.6.

The "domes," according to the current view, are considered to screen oxygen away from the underlying metal, which is thought to be the anode of an electrolytic cell set up by differential aeration, the corresponding cathodes being the relatively unattacked areas covered with the yellow film, *e.g.*, the centre of fig. 7, to which oxygen has free access.

A comparison between the corrosion-time curves and the distribution of corrosion on a series of specimens tested in N/10 KCl suggested that there were difficulties in the way of this view. Specimens A114, A113 and A96 were corroded for 17, 50 and 112 days respectively, and were giving linear corrosion-time curves when the experiments were stopped. Their surfaces, cleared of corrosion products, are shown in Plate 17, figs. 11, 13 and 15, representing top surfaces and figs. 12, 14 and 16 bottom surfaces. Corrosion has evidently begun at many scattered areas which have gradually spread till the whole of the bottom surface and a large part of the top and sides have been attacked.

In strong solutions it is not uncommon for 90 per cent. of the metal surface to be attacked, and in an extreme case the whole of the specimen has been heavily corroded as shown in Plate 18, figs. 17, 18 and 18A, which are photographs of the top, bottom and side of specimen A91 in 2N KCl, the corrosion-time curve of which was linear throughout the experiment. The whole specimen was covered with an interlaced system of domes similar to those shown in Plate 16, fig. 8. These domes consist at first of gelatinous "zinc hydroxide," which seizes chlorine and gradually "ages"; at the end of about 100 days it has become hard, difficult to break away from the specimen and only slowly soluble in 10 per cent. acetic acid. In the aged and dried state the walls of the domes on specimen A116 had an average thickness of about 0.015 mm.; the thinnest portion examined was 0.004 mm. and a specially thick part 0.026 mm. Thus the dense-looking domes on zinc are merely very thin shells, as indicated in fig. 50.

It is clear from Plates 17 and 18, figs. 11 to 18, that unattacked areas which were film-covered when in the solution, and were supposed to be cathodes, have greatly decreased in size with increased period of corrosion; in A91 they have disappeared altogether. Consequently they cannot be the *sole* cathodes for the oxygen absorption process, since corrosion can continue at a constant rate notwithstanding their gradual reduction and final disappearance. It follows also that oxygen must be able to penetrate through the white domes to maintain the constant corrosion rate.

To test this point directly and to ascertain whether the departure of corrosion-time curves from linear form was due in any way to domes of corrosion product, the following experiment was tried. The apparatus containing specimen A118 in N/10 KCl was removed from the thermostat and opened after 229 days' corrosion, when the rate of oxygen absorption had fallen from an initial rate of 1.42 c.c. per day to 0.16 c.c. per day. The hard white domes of corrosion product on the specimen were then broken down by a glass rod and removed as far as possible. The apparatus was then sealed up again, swept out with pure oxygen and replaced in the thermostat. The subsequent daily readings for oxygen absorption were 0.24, 0.21 and 0.09 c.c., i.e., of the same order as before the removal of the domes. This result confirms the conclusion that the hard variety of zinc hydroxide has but little effect on the rate of oxygen supply to the metal.

Several varieties of "zinc hydroxide" have been met with during the research. The most distinct occurred in experiments carried out in KCl solutions stronger than N in an atmosphere of purified air; it was crystalline

with one well-marked cleavage similar to that of mica, and others much less well-marked suggesting a hexagonal structure; it seems to correspond with the mineral zincite (ZnO). In similar strong solutions beneath an atmosphere of oxygen the corresponding substance was powdery and without noticeable cleavage; the difference is not due to carbon dioxide, etc., since the air was purified by passage through caustic potash, sulphuric acid, distilled water and a filter.

Figs. 11 to 16 of Plate 17 show that in $\text{N}/10$ KCl much larger areas were attacked on the bottom surfaces than on the top; the penetration was also deeper. It was thought that this might be due to differential aeration since access of oxygen may reasonably be supposed to be more rapid to the top. To test this possibility the apparatus shown in fig. 23 was made. The liquid entirely fills the inner cap and the tube above the specimen, which rests on the points of the glass tripod. The liquid level is half-way up the outside of the inner cap, so that oxygen reaches first the bottom surface of the specimens; this should, therefore, be less corroded than the top if differential aeration is the main determining factor influencing the distribution of corrosion in the authors' conditions. Experiments were conducted at 25°C . with all the usual precautions, in $\text{N}/200$, $\text{N}/10$ and 2N KCl ; results are shown on Plate 18 in which figs. 19 and 21 represent the top, and figs. 20 and 22 the bottom, surfaces respectively in $\text{N}/200$ and 2N solutions.

In all three solutions corrosion has penetrated more deeply, but was rather less widely distributed, on the bottom than on the top.

These experiments suggest that though differential aeration of the top and bottom surfaces of the specimen may have some effect on the distribution of corrosion, it is not the sole, nor even the principal, factor which determines it.

Further study of the distribution of corrosion on the standard-sized metal specimens was made with a microscope mounted on the top of a circular glass trough in which the specimen is supported in the usual manner, and which can be evacuated and subsequently filled with any desired atmosphere and solution,

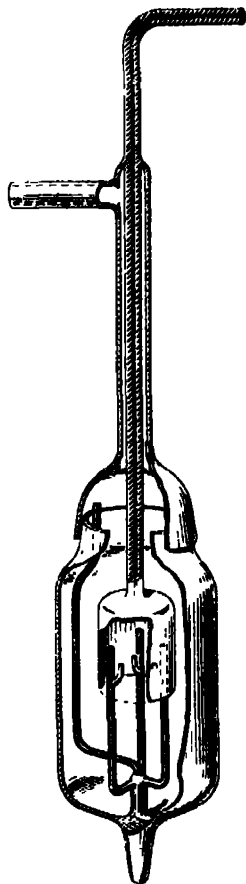


FIG. 23.

similarly to the standard corrosion apparatus. To keep the depth of immersion at the usual value of 1.5 cm. about 350 c.c. of solution must be used instead of the usual 100 c.c. The specimen is viewed through a disc of plate glass held in a tube of stainless steel fixed in the top one of two stainless steel discs between which the glass trough can be clamped by bolts. Rubber bands are interposed between the steel discs and the glass to enable sufficient pressure to be exerted to give a vacuum tight joint without danger of fracture of the glass. For very low-power work a camera carrying a Zeiss Tessar photographic lens is substituted for the microscope.

The top surface only of the specimen can be observed ; it is illuminated by the glancing incidence of two beams of light reflected from two mirrors arranged at opposite ends of a diameter of the trough. The sources of light are two pointolite lamps used with 4-inch condensers and water-cooling troughs.

The apparatus cannot conveniently be placed in a thermostat and is merely shielded from draughts in a room with double door and shutters. It is hoped shortly to thermostat the room, which varies in temperature over the range 20° to 23° C. At present, therefore, notable convection currents occur in the trough.

Figs. 24 to 29 (Plate 19) illustrate the progress of corrosion of annealed zinc in N/10000 KCl during 11 days, and figs. 30 to 35 (Plate 20) corrosion in N/10000 K_2SO_4 during 6 days. In the early stages of corrosion the distribution is nearly sporadic on both top and bottom surfaces in both solutions and in conductivity water, as shown by figs. 24, 38 and 10, the last two representing turned specimens ; under higher powers of the microscope the initial corrosion centres are seen to be very numerous. Irregularity soon sets in on the top surface, accompanied by obvious movement of corrosion products, which is well shown by comparing fig. 25 with fig. 27 and fig. 32 with fig. 34. Many of the initial centres of corrosion soon cease to function, as shown by comparison of figs. 38 and 39. The cessation seems to be due to the formation of a film of zinc hydroxide which stops action at many of the less active centres as suggested by fig. 30. The persistent corrosion centres occur as groups surrounded by conspicuous white walls which result from a re-arrangement and increase of zinc hydroxide (see figs. 28 and 34). There is no corrosion beneath the walls (see figs. 29 and 28, and figs. 34 and 35), and only a part of the enclosed area is attacked in the early stages. Corrosion spreads from the original centres outwards, especially in strong solutions, but spreading can be seen even in N/10000 K_2SO_4 in Plate 20, figs. 31 and 32, in which corroded areas are indicated by white or half-tone patches within the walls. Spreading is, of course, stopped in dilute solution by the exhaustion of

anions when only a small proportion of the surface has been attacked as shown in figs. 29 and 35.

It has been found that nearly all the corrosion centres observable on a specimen stripped of corrosion products after 11 days' immersion in N/10000 KCl, coincided with centres which were visible after only 10 minutes' immersion, i.e., no new centres were formed after a very early stage of the corrosion process; the final distribution is the result of the cessation of activity at certain of the initial centres and the persistence and spreading of others.

The position at which corrosion actually begins in N/20000 KCl was sometimes decided by the crystal structure of the metal discs used. This normally consisted of a system of large radial crystals surrounding a thin core of others axially arranged. The discs were turned to definite size and annealed for a week at 260° to 270° C.; a superficial network of polygonal crystals could then be seen without etching, similar to those shown in figs. 46 and 47. This evidently consisted of a very thin recrystallised layer, overlying the coarse radial crystals formed during casting which are revealed by turning or better by corrosion as shown in fig. 16. Before these can be attacked the surface layer of small crystals must be removed and this removal is sometimes selective in dilute solutions such as N/20000 KCl. Fig. 46 shows selective attack on two crystals, a large one near the lower right-hand corner, and another near the top left-hand corner; the other crystals are sparsely covered with tarnish films.

It was thought desirable to determine whether corrosion would occur at the same positions on a metal after it had been removed from a corrosive solution, stripped of corrosion products by dilute acetic acid, thoroughly washed with distilled water and replaced in a similar solution. An experiment was tried with N/10000 K_2SO_4 and the distribution of the first corrosive attack is shown in Plate 20, fig. 35. Fig. 36 (Plate 21) shows the state of affairs at the end of 5 hours during the second attack. The isolated black spots are the corroded areas produced by the first period of corrosion. The new positions of attack are enclosed by the usual white sinuous walls and the distribution is either actually reversed or perhaps independent of the original one, a result that was quite unexpected. The final distribution at the end of the second immersion, lasting 5 days, is shown in fig. 37, which should be compared with fig. 35. Possibly a slight deposition of metallic impurity may cause the original attacked areas to be slightly cathodic, and so produce an approximate reversal of the first distribution. The differential aeration effect which is generally assumed to occur when crevices are present in a metal did not cause the original pits to become anodic.

The special action that often takes place in the neighbourhood of the glass points of support of the specimens is clearly shown in several micrographs, *e.g.*, figs. 20 and 22. This action was originally thought to be due to differential aeration. Sometimes, however, the metal seemed to be actually protected instead of attacked over a small area round the points, especially in sulphate solution. Another curious feature of the glass point action was that it could never be detected when much corrosion had occurred, *i.e.*, the points never bored deeply into the metal; figs. 16 and 18, for instance, do not show any sign of this special attack. The action of the glass points is confined to the initial stages of corrosion in strong solutions and does not seem to be due to differential aeration, but no alternative explanation can be proposed for it at present.

One of the most definite phenomena shown by the micrographic work was the vigorous selective attack on the crystal boundaries as shown, for instance, in fig. 16 (Plate 17). The metal used for most of the work was selected cast Australian electrolytic zinc, turned to shape in a lathe and finally annealed for a week at 260° to 275° C., in an atmosphere of argon. It contained only about 0.01 per cent. of total metallic impurity, mainly lead and iron, so that little segregation would be expected. Etch pits of definite shape were rare in any of the solutions used, but occasionally hexagons were found. A few experiments were carried out with highly purified American zinc supplied by the New Jersey Zinc Company, but this metal behaved differently from the Australian metal. It was received as cast rods, 0.75 cm. in diameter, enclosed in glass tubes, and was broken to the desired length and used in the unannealed state. Care was taken that it never touched the fingers; spectroscopic examination showed it to be practically free from any metallic impurity. No attack along a crystal boundary in this metal was ever detected, either in N/10 or N/10000 KCl, the only two solutions used. Well-developed etch pits were found in large numbers, particularly in the more dilute solution, as shown in figs. 42 to 45 (Plate 22). The first shows hexagonal pits characteristic of the basal pinakoid of the hexagonal system. Other types of pit seem to be characteristic of first and second order prisms ($10\bar{1}0$ and $11\bar{2}0$ forms respectively) and first and second order pyramids ($10\bar{1}1$ and $11\bar{2}1$ forms) since they closely resemble the well-known pits in the mineral apatite.

An important factor in deciding the regional arrangement of corrosion over a specimen is the distribution of strong convection currents.* This was shown by experiments carried out in a trough placed in an air thermostat and

* 'Proc. Roy. Soc.,' A, vol. 121, p. 103 (1928).

illuminated from the sides by two pointolite lamps, the radiation from which was focussed on the specimen by a four-inch lens without intervention of cooling jackets. Convection currents due to temperature differences could be seen by the streaming of corrosion products, their direction being from the circumference of the specimen to the centre and then upwards. The corresponding distribution of corrosion of a standard sized specimen in distilled water in air is shown in fig. 40, which is a photograph taken at the end of 4.5 hours from the start of the experiment with corrosion product *in situ*. The radial distribution of the little pits, situated in the dark areas, is markedly different from the initial sporadic and final irregular distribution which occur in the absence of the strong convection currents. It was noticed that the streaming of corrosion products had ceased at 22 hours from the start of the experiments, apparently because temperature equilibrium had been reached in the trough; nevertheless the initial radial distribution persisted.

Fig. 41 shows the distribution of corrosion on a specimen contained in a trough 12 cm. in length placed in an air-thermostat; the two ends of the trough differed in temperature by 0.1°C ., the two sides were 5 cm. apart and at closely similar temperatures. The arrangement of the corroded areas is approximately along the steepest temperature gradient. In this experiment the illuminating beam was passed through cooling jackets so that the radial type of convection currents obtained in the last experiment was eliminated. The least corroded metal appears to be that which is in contact with the more rapidly moving liquid. The explanation of the distribution of corrosion seems to be that the convection currents decide the distribution of corrosion products and consequently of temporarily protected areas.

Experiments on Differential Aeration.

The fact that the differential aeration principle fails to explain many of the results obtained in the authors' conditions suggested the desirability of some special experiments to elucidate the matter. Much of the previous work has been carried out by U. R. Evans and his associates, who usually produced differential aeration either by bubbling air or oxygen through the solution surrounding one of two electrodes enclosed by a diaphragm, or by partial immersion. Such methods produce large differences of oxygen supply, e.g., partial immersion may produce a difference of at least 7 to 1 between different parts of the metal, if one may judge from results of the depth of immersion curve. In stagnant conditions it was thought that the difference of oxygen concentration between any two parts

of a totally immersed metal would be far less than this, especially since it has been established that oxygen can freely penetrate deposits of zinc hydroxide. To test the effect of different concentrations of oxygen the apparatus shown in fig. 48 was used. It consisted of two glass tubes, A and B, one of which carries

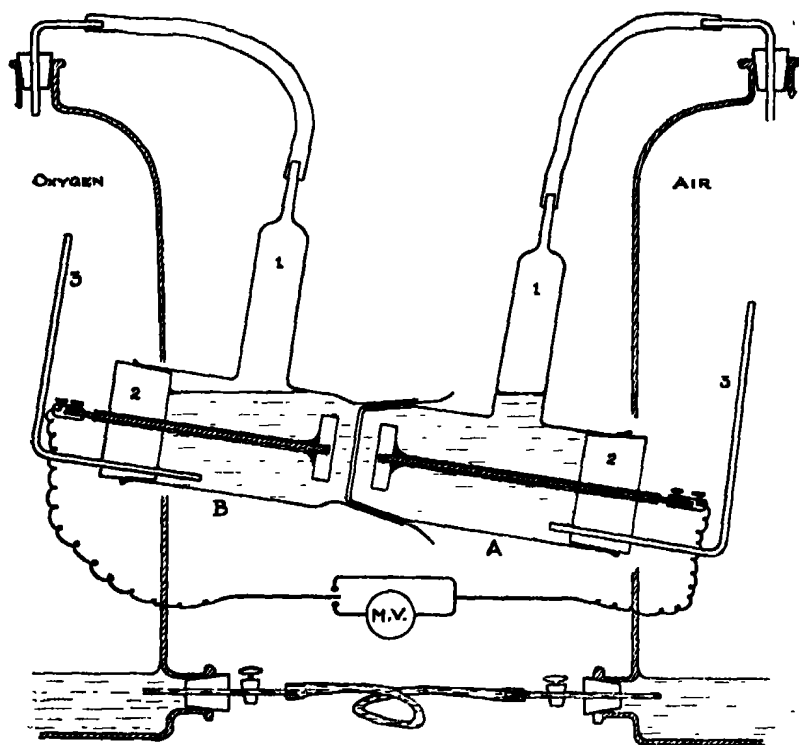


FIG. 48.—Differential Aeration Cell.

a diaphragm formed by wrapping a sheet of parchment over its end. It is then ground into the other and the joint made water-tight by vacuum wax. A and B each carry a side tube (1) which can be connected to a large gas reservoir, a rubber bung (2) which carries a weighed electrode and a filling tube (3) for introducing solutions. An atmosphere of oxygen was maintained on one side of the diaphragm and air on the other and the oxygen actually in solution near each electrode was determined by Winkler's method at the beginning and end of each experiment. In order to prevent different pressures occurring over the two liquid surfaces the two gas reservoirs were connected together as shown and protected from draughts, but they were not thermostated. The apparatus was tilted so as to allow the liquid-oxygen interface

to be larger than the liquid-air interface in the proportion, roughly, of 7 : 1. Before beginning an experiment, one compartment of the apparatus was swept out with oxygen and the other with purified air. Periodical potential measurements were made, but the electrodes were normally short circuited. The experimental results are collected in Table III, and some typical potential curves in fig. 49.

The experiments were tried in four different strengths of solution. In all

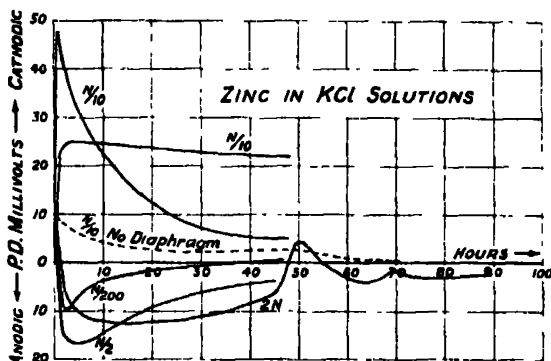


FIG. 49.—Potential Difference of Oxygenated Electrode relative to Aerated Electrode.

of them the oxygenated electrode (called hereafter the O electrode) was cathodic at first, and remained so throughout some of the experiments in $N/10$ and $N/2$; in the others a reversal of potential occurred and persisted for long periods in $N/200$ and $2N$, but in $N/10$ and $N/2$ a zero potential or another reversal occurred.

The O electrode always suffered more corrosion than the aerated electrode in stagnant conditions except in $N/10$ solution; even in this solution it lost nearly as much if the diaphragm was removed. In $N/2$ the O electrode lost more than twice the weight of the A electrode even when the oxygen concentration was three times that at the A electrode.

If oxygen were bubbled round the O electrode in $N/2$ solution, as in experiment X of the table, a high cathodic potential was reached and the O electrode lost only one-ninth of the weight lost by the A electrode, although the ratio of oxygen concentration was 3 to 1. In a repeat experiment, XI of the table, the losses of weight were much greater, but their ratio was less than 1 to 2. In the bubbling experiments slight supersaturation with oxygen occurred near the O electrode; also a foaming effect which in the later stages caused part of the electrode to be wetted by only a film of moisture. A temporary cessation of bubbling caused an immediate drop of potential, and if bubbling was carried

Table III.

Experiment No.	Time in days.	Concentration of KCl.	Loss of weight in mgn.		Oxygen concentration, c.c. per litre.						Conditions.	Remarks on potential differences.
			Oxygen.	Air.	Initial.		Final.					
					Oxygen.	Air.	Oxygen.	Air.				
I	2	N/200	8.8	3.4	24.1	8.4	16.8	6.1	Stagnant	O electrode cathodic for 2.5 hours; then continuously anodic.		
II	2	N/200	27.8	22.6	20.7	7.6	14.0	7.3	"	O electrode cathodic for 0.5 hours; then anodic for 1 day; then nearly zero potential.		
III	2	N/10	7.6	12.3	—	—	—	—	"	O electrode cathodic throughout.		
IV	2	N/10	10.9	20.2	26.0	5.9	8.4	2.8	"	O electrode cathodic throughout.		
V	2	N/10	17.2	18.2	20.8	—	10.6	—	Stagnant	O electrode cathodic for 1 hour; then slightly anodic; then no P.D.		
VI	3	N/10	15.8	23.7	26.3	5.0	10.1	3.9	"	O electrode cathodic throughout.		
VII	5	N/2	26.5	20.6	19.1	8.4	13.4	3.9	no parchment	O electrode cathodic throughout. Several changes of direction of potential.		
VIII	2	N/2	13.6	6.6	22.9	8.4	13.4	3.9	"	O electrode cathodic for 10 minutes; then anodic; finally no P.D.		
IX	8	N/2	59.4	3.6	22.4	6.7	11.2	5.0	"	O electrode cathodic for 0.5 hours; then anodic throughout. Electrodes 1 cm. apart (about).		
X	2	N/2	10.2	89.4	18.5	8.2	28.0	10.1	O bubbled	O electrode cathodic throughout. Maximum P.D. 220 mv.		
XI	2	N/2	101.5	188.9	20.7	7.3	25.7	11.0	"	O electrode cathodic throughout.		
XII	1	N/2	43.9	13.1	22.4	6.7	29.7	13.4	O and A bubbled	O electrode cathodic throughout. Maximum P.D. 180 mv.		
XIII	2	2N	5.4	2.4	11.6	4.4	3.8	2.5	Stagnant	O electrode cathodic 1 hour; then anodic.		
XIV	5	2N	11.6	5.2	14.1	6.9	11.2	5.0	"	O electrode cathodic for 0.5 hours; then anodic for 4 days; then no P.D.		



FIG. 7. —Top surface of A 117 after 250 days in N 10 KCl



FIG. 8. —Bottom surface of A 117

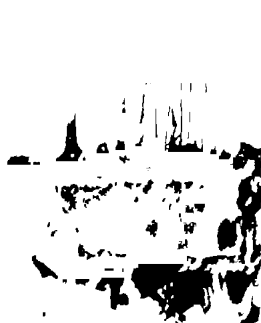


FIG. 9. —Side view of A 116 after 211 days in N 10 KCl



FIG. 10. —Zinc after 3 hours in conductivity water

TOPS.

BOTTOMS.



FIG. 11.

A 114, 17 days.

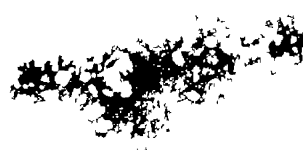


FIG. 12

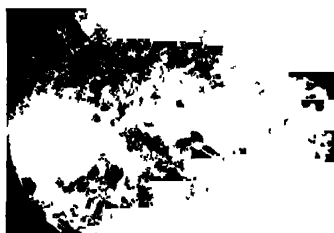


FIG. 13

A 113, 50 days

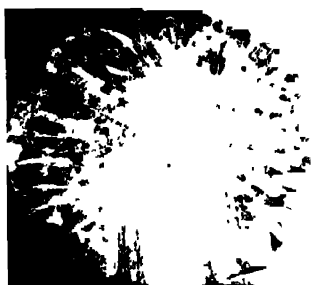


FIG. 14

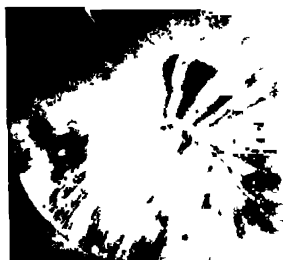


FIG. 15.

A 96, 112 days.

Zinc in N/10 KCl.



FIG. 16.

TOP

BOTTOM.



FIG. 17. —A 91

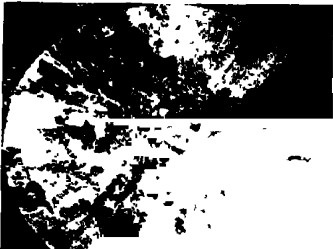


FIG. 18. —A 91



FIG. 18A. —A 91, side.

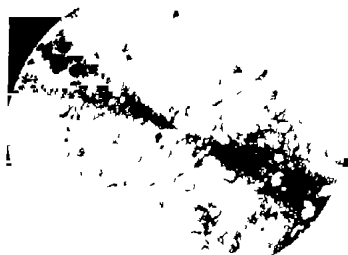


FIG. 19.

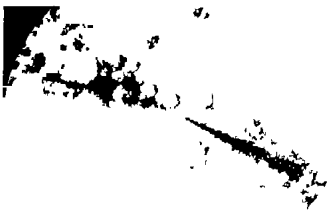


FIG. 21.

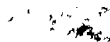


FIG. 22

FIG. 24



FIG. 25

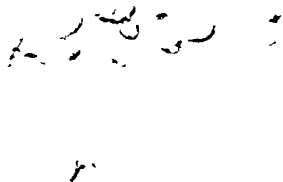


FIG. 26

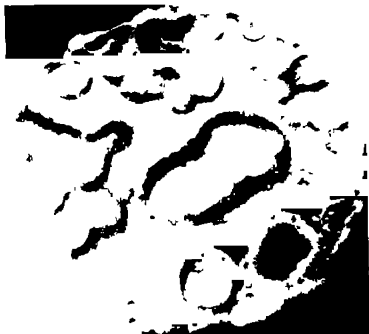


FIG. 27

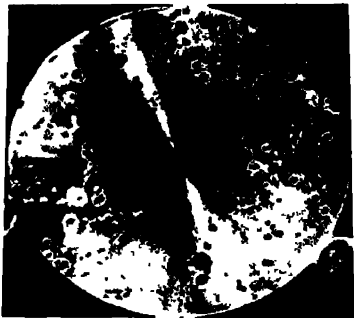


FIG. 28

FIG. 29

Zinc, in N/10,000 KCl.

Figure	24	25	26	27	28	29
Time of corrosion	30 mins.	2½ hours	1 day	2 days	8 days	11 days



FIG. 31

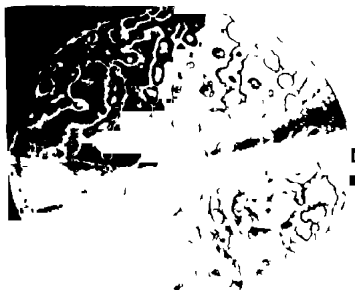


FIG. 32



FIG. 34.

FIG. 35.

Zinc in N 10,000 K_2SO_4 .

Figure	30	31	32	33	34	35
Time of corrosion	17 mins	2 hours	3 hours	1 day	6 days	6 days

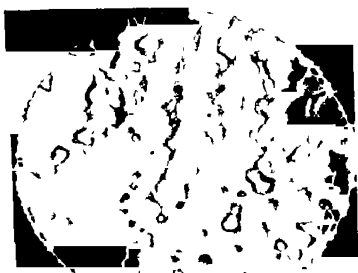


FIG. 36.



FIG. 37



FIG. 38

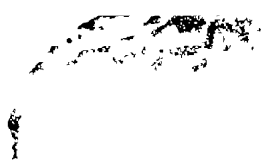


FIG. 39.

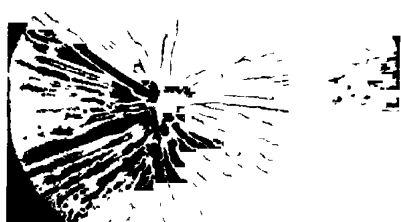


FIG. 40

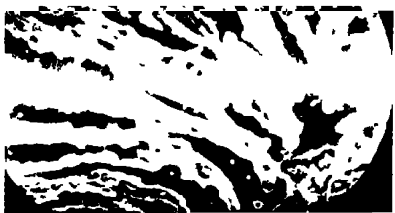


FIG. 41

Figure	36	37	38	39	40	41
Liquid		$\frac{N}{10,000} K_2SO_4$			Distilled water	
Time of corrosion	5 hours	5 days	27 mins	5 days	4½ hours	1 day



FIG. 42 - 0001 face ($\times 25$)



FIG. 43 (A). 1010 face ($\times 25$)



(B) ($\times 200$).



FIG. 44 - 1120 face ($\times 75$)



FIG. 45 - 1121 face ($\times 75$).



FIG. 46. ($\times 600$).

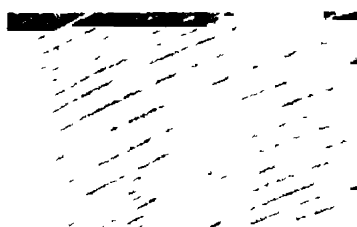


FIG. 47. ---($\times 70$).

on at both electrodes and that at the A electrode stopped, a drop also occurred ; these drops were 20 to 30 mvs., i.e., small fractions of the total potentials, and may possibly be due to subsidiary factors such as the accumulation of hydrogen and zinc ions at the two electrodes in the absence of bubbling. In experiment XII in which both the oxygen and air were bubbled near their respective electrodes the O electrode was cathodic throughout, sometimes to the extent of 55 mvs., but lost more than three times the weight of the A electrode.

A complete explanation cannot be given for the bubbling experiments. The rate of bubbling was not accurately controlled, but was approximately similar in the three experiments. Possibly the conditions for the maximum effect of bubbling are easily upset and require investigation by more sensitive methods.

All the above experiments except numbers V and VI were performed with the electrodes at an average distance apart of 3.3 cm. To find out the effect of the resistance of the electrolyte experiment number IX was carried out in N/2 KCl with electrodes 1.0 cm. apart. The O electrode lost more proportionately than in any other experiment. In experiments VII and VIII the calculated resistance of the electrolyte was less than 6 ohms ; the internal resistance of the cell was found to vary from 40 to 240 ohms.

Table III shows that the experiments were not reproducible in detail, and caution must, therefore, be exercised in drawing conclusions. It is possible that they do not present a close analogy to the corrosion of a single specimen, but it is upon somewhat similar experiments that the differential aeration theory has been largely built up. Nevertheless, it is quite clear that a more highly oxygenated electrode generally suffers more corrosion than one less highly oxygenated ; only in N/10 solution did the reverse hold, and then only to an important extent when a parchment diaphragm was used.

The differences of potential set up when the two electrodes were differentially oxygenated seem to be due mainly to films of corrosion product such as precipitated " zinc hydroxide " rather than to directly formed zinc oxide. Bubbling oxygen evidently has a specific action apart from oxygen concentration ; for instance, in experiment No. X the maximum potential difference was 220 millivolts although the ratio of the oxygen concentrations was only 3 to 1 ; this ratio without bubbling usually gave a potential difference of about one-tenth of that amount.

The Mechanism of Corrosion.

The general conclusion to be drawn from many of the experiments described in this paper is that the distribution of corrosion on zinc cannot be adequately accounted for by differences in oxygen concentration as postulated by the "differential aeration" theory, which states, broadly, that oxygen is needed for corrosion, but the attack occurs at places relatively inaccessible to oxygen. A modified view of the mechanism is given below.

The initial behaviour of zinc when placed in a salt solution which does not form a passifying film, either general or local, is to displace hydrogen at a multiplicity of points. Neglecting the possibility of the production of hydrogen gas, a polarising layer is formed at the metal surface. No regional distinction can at first be made into anodes and cathodes, which are probably adjacent and constantly changing, as in an acid solution; at any instant the point-anodes are probably sporadically distributed and corrosion will proceed uniformly except in so far as it is affected by factors related to crystal structure and method of preparing the surface, provided that supplies of oxygen and suitable anions are available.

The oxygen is required for depolarisation, and the anions must be such that they form a soluble salt with the metal; corrosion will then proceed at a rate directly proportional to the oxygen supply, so long as the concentration of anions is sufficient and no protective films are formed. An example of this kind of action is the initial attack of ammonium chloride on zinc.

With zinc, corrosion will not *usually* be regularly distributed over the whole surface, notwithstanding the initial sporadic attack, because :—

- (1) Insoluble substances produced by corrosion may be irregularly distributed and give local protection.
- (2) The supply of oxygen may not be uniform.

Vernon's* work suggests that any air-formed film on zinc will not be an influencing factor owing to its lack of protective power except, perhaps, in influencing the initial, nearly sporadic, distribution of attack.

The most important insoluble substance formed during corrosion in the presence of potassium chloride or sulphate is zinc hydroxide, part of which forms a thin film closely adherent to the metal and is impervious to oxygen and zinc ions but not to electrons, but much of which forms loose masses which are permeable to oxygen, as indicated in fig. 50, which shows a "dome" of the permeable form and films of the inhibitive form.

* 'Trans. Faraday Soc.', vol. 19, p. 840 (1924); vol. 23, pp. 135–137 (1927).

Assuming the presence of only the permeable type of zinc hydroxide, corrosion will be nearly uniformly distributed and proportional to the rate; of

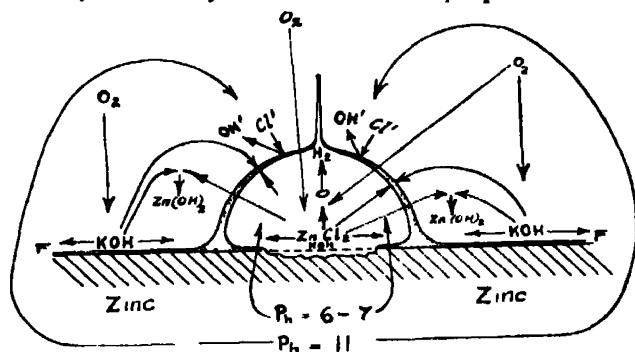


FIG. 50.—Section through Dome of Corrosion Product.

oxygen supply. If oxygen be not uniformly distributed *most corrosion will usually occur where the concentration is greatest*, just as most corrosion occurs on the upper part of zinc partially immersed in ammonium chloride solution. If the inhibitive type of hydroxide is formed over a part of the metal, corrosion can only take place elsewhere, but the average rate of corrosion over the whole specimen need not alter since it is dependent on the rate of oxygen supply to the whole surface, which is not altered by the presence of the inhibitive film. Nevertheless, the rate of corrosion per square centimetre of the attacked area will be increased since the oxygen there present can be reinforced by that present over the inhibitive film which forms a part of the total area available for depolarisation. Corrosion at the portions of the metal covered by "domes" is not due mainly to a potential difference set up by difference of oxygen concentration, but to the fact that ions can freely enter solution there. Other portions are covered with a precipitated protective film which prevents local solution of the metal, but allows depolarisation of hydrogen displaced by metal entering solutions elsewhere. Actually more oxygen reaches the *metal* beneath the domes than where it is covered with a precipitated protective film.

The authors wish to acknowledge the help they have received in the experimental work from Mr. J. M. Stuart and Miss Ruth Pirret. The research was carried out for the Corrosion of Metals Research Committee of the Department of Scientific and Industrial Research, and the thanks of the authors are due to the Chairman, Professor Sir Harold Carpenter and to Professor G. T. Morgan for many facilities afforded and for permission to publish.

On Periodicity in Series of Related Terms.

By Sir GILBERT WALKER, F.R.S.

(Received January 22, 1931.)

An important extension of our ideas regarding periodicity was made in 1927 when Yule* pointed out that, instead of regarding a series of annual sunspot numbers as consisting merely of a harmonic series to which a series of random terms were added, we might suppose a certain amount of causal relationship between the successive annual numbers. In that case the system might be regarded as a physical system possessing one or more natural oscillations of its own, all subject to damping; and the effect of annual random disturbances would be to produce a fairly smooth curve with periods varying in amplitude and length, essentially as the sunspot numbers vary. If we call the departures from their mean of our series u_1, u_2, \dots , Yule showed that the consequence of a single natural period is an equation like

$$u_x = k'u_{x-1} - u_{x-2} + v_x,$$

where v_x represents the "accidental" external "disturbance"; and if there are two natural periods,

$$u_x = k_1(u_{x-1} + u_{x-3}) - k_2u_{x-2} - u_{x-4} + v_x.$$

He considered also the effect of the relation

$$u_x = g_1u_{x-1} - g_2u_{x-2}. \quad (A)$$

which leads to a damped harmonic vibration

$$u_x = e^{-\lambda x} (A \cos \theta x + B \sin \theta x),$$

where $\exp. (-\lambda \pm i\theta)$ are the roots of the equation

$$y^2 - g_1y + g_2 = 0.$$

Yule determined his constants by applying the equation (A) to the successive terms of the u series and using the method of least squares.

2. We shall now consider such serial correlation coefficients as r_1, r_2, \dots , where r_1 is that between consecutive terms of u 's and r_p that between terms

* 'Phil. Trans.,' A, vol. 226, pp. 267-298 (1927).

separated by p intervals. The use of such coefficients in connection with periodicities is old, but it has recently been more widely employed.*

If the equation connecting successive terms in the absence of disturbance is

$$u_x = g_1 u_{x-1} + g_2 u_{x-2} + \dots + g_s u_{x-s}, \quad (\text{B})$$

then the equation for the terms as disturbed is obtained by adding a term v_x to the right-hand side. Let us multiply this equation by u_{x-s-1} and sum for all values of x from $(s+2)$ to n ; we get, ignoring the sums of product terms in uv as relatively insignificant because the v 's are accidental,

$$\sum_{s+2}^n \{u_x u_{x-s-1} - (g_1 u_{x-1} u_{x-s-1} + \dots + g_s u_{x-s} u_{x-s-1})\} = 0. \quad (\text{C})$$

In order to simplify the analysis we treat the number of terms as so large that we may neglect errors due to its finiteness;† then if the S.D. of the series is d , we can neglect the differences between the S.D.'s of n terms and of $(n-s)$ terms, so that (C) becomes

$$(n-s-1)d^2 \{r_{s+1} - (g_1 r_s + g_2 r_{s-1} + \dots + g_s r_1)\} = 0,$$

or

$$r_{s+1} = g_1 r_s + g_2 r_{s-1} + \dots + g_s r_1.$$

Similarly on multiplying by u_{x-s-2} and adding,

$$r_{s+2} = g_1 r_{s+1} + g_2 r_s + \dots + g_s r_2;$$

and in general

$$r_v = g_1 u_{v-1} + g_2 u_{v-2} + \dots + g_s r_{v-s},$$

which is analogous with (B) and shows that the relationships between the successive u 's and the successive r 's are, in the limit when n is very large, identical.

If the roots of the equation

$$z^s = g_1 z^{s-1} + \dots + g_s \quad (\text{D})$$

are $h_1, h_2 \dots h_s$, the solution of (B) will be

$$u_p = U_1 h_1^p + U_2 h_2^p + \dots + U_s h_s^p$$

* See, for example, Dinsmore Alter in the Washington 'Monthly Weather Review,' June, 1927; and a derivation of a criterion of reality applicable to H. H. Turner's "chapters" of continuous oscillations, separated by breaks due to outside interference, in paragraph 11, pp. 340, 341 of a paper "On Periodicity," 'Q.J.R. Met. Soc.,' vol. 51 (1925).

† For instance, it is customary, if seeking a 13-year period with 120 annual values available, to consider 117 years out of the 120, and to assume that ignoring 3 terms will not seriously affect the result.

where the U 's are constants ; and of (D) will be

$$r_p = R_1 h_1^p + R_2 h_2^p + \dots + R_s h_s^p$$

where the R 's are constants.

3. Thus the r 's must have the same periods as the u 's. This is obvious in slightly damped simple oscillations each occupying say q of the intervals between the u 's ; for then $r_{q+1}, r_{q+2} \dots r_{2q}$ will tend to be the same as $r_1, r_2, \dots r_q$; the r 's will thus have a period of q intervals and will be damped if the u 's are damped. One advantage of using the values of $r_1, r_2 \dots$ for getting the relationship (B) over using the u 's is that the former, being based on the whole series, are much less influenced by accidental effects.

4. We shall first of all consider in somewhat greater detail the effect of the simplest type of dependence of each term on the previous ones, that of the tendency of a departure to persist ; and we shall suppose that any term u_s is made up of tu_{s-1} (where t is a fraction less than unity) and of an external 'disturbance' v_s . Also, since we may write $u_s = tu_{s-1} + v_s$ in the form $u_s - u_{s-1} = -(1-t)u_{s-1} + v_s$, we might regard "persistence" as equivalent to "damping" in a mechanical system, the diminution being proportional to the magnitude of the previous term. If now we write the equations

$$u_2 = tu_1 + v_2, \quad u_3 = tu_2 + v_3, \quad \dots \quad u_n = tu_{n-1} + v_n,$$

and assume that n is so large that the S.D.'s d and d' of the u 's and v 's may be treated as unaffected by cutting out a term, we realise (1) that t is the correlation coefficient that we have previously denoted by r_1 , and (2) that by the ordinary theorem

$$d'^2 = (1 - r_1^2) d^2. \quad (\text{E})$$

Now for the Fourier terms of the u series

$$\frac{n}{2} (a_q + ib_q) = \sum_{k=1}^n u_k e^{i(k-1)q\alpha},$$

where $\alpha = 2\pi/n$; and for the Fourier terms of the series of disturbances, which terms are distinguished by dashes, inasmuch as u_0 is unknown, v_1 is indeterminate ; but when n is large enough we may make any hypothesis we like regarding v_1 without appreciably affecting the Fourier terms ; and we choose it as equal to $u_1 - r_1 u_n$. Thus

$$\frac{n}{2} (a_q' + ib_q') = \sum_{k=1}^n v_k e^{i(k-1)q\alpha},$$

and, on substituting $u_k - r_1 u_{k-1}$ for v_k , it is easily seen that this becomes

$$(1 - r_1 e^{i q \alpha}) \sum_{i=1}^n u_i e^{i(i-1)q\alpha}, \text{ or } \frac{n}{2} (1 - r_1 e^{i q \alpha}) (a_q + i b_q).$$

So multiplying by the corresponding equation with the sign of i changed, if $c'^2 = a'^2 + b'^2$ and $c^2 = a^2 + b^2$,

$$c_q'^2 = c_q^2 (1 - 2r_1 \cos q\alpha + r_1^2). \quad (F)$$

Also if $c'/2^{\frac{1}{2}}d'$, the amplitude ratio,* is denoted by f' and $c/2^{\frac{1}{2}}d$ by f , we have using (E)

$$f_q^2/f_q'^2 = (1 - r_1^2)/(1 - 2r_1 \cos q\alpha + r_1^2). \quad (G)$$

It would appear that if we had two physical systems, one in which the successive values were independent and a second system in which persistence produced a relationship r between successive terms, and if the same disturbances were imposed on the systems, then, by (F), when the oscillations had gone on so long that a fairly steady mean amplitude had been attained in the persistent system, the amplitude c' of the first or free system would average $(1 - 2r \cos q\alpha + r^2)^{\frac{1}{2}}$ times that of the second or persistent system, and the persistence would alter the amplitude ratio of the oscillations set up in the ratio $(1 - r^2)^{\frac{1}{2}}/(1 - 2r \cos q\alpha + r^2)^{\frac{1}{2}}$.

It may be noted that q lies between 1 and $n/2$, and $q\alpha$ between $2\pi/n$ and π , and so between 0 and π . Thus the ratio f^2/f_1^2 lies between $(1 + r)/(1 - r)$ and $(1 - r)/(1 + r)$; it is unity when $\cos q\alpha = r$. In practice q does not in general exceed $n/6$, so $q\alpha$ is not in general greater than $\pi/3$. For instance, with 120 annual values, for a period of 20 years $q\alpha = \pi/10$, and for 8 years it is $\pi/4$.

The result that "persistence" or inertia will diminish the amplitudes of oscillations of short period, but may increase the relative importance, and therefore the amplitude ratio, of those of long period, by destroying quick oscillations, is in accordance with expectation.

5. Let us now consider the oscillations set up in a system which has natural periods of its own. Corresponding to (D), with $s = 3$ for brevity, we have the equations

$$\left. \begin{aligned} u_4 &= g_1 u_3 + g_2 u_2 + g_3 u_1 + v_4 \\ u_3 &= g_1 u_4 + g_2 u_3 + g_3 u_2 + v_3 \\ u_n &= g_1 u_{n-1} + g_2 u_{n-2} + g_3 u_{n-3} + v_n \end{aligned} \right\}. \quad (H)$$

* The amplitude ratio of a Fourier term is the ratio of its amplitude to $2^{\frac{1}{2}}$ times the standard deviation of the terms analysed, see (c) p. 26 of 'Q.J.R. Met. Soc.,' vol. 54 (1928). If a series consists accurately of a single sine series the ratio is unity.

and we may define quantities v_1, v_2, v_3 by the equations

$$\left. \begin{aligned} u_1 &= g_1 u_n + g_2 u_{n-1} + g_3 u_{n-2} + v_1 \\ u_2 &= g_1 u_1 + g_2 u_n + g_3 u_{n-1} + v_2 \\ u_3 &= g_1 u_2 + g_2 u_1 + g_3 u_n + v_3 \end{aligned} \right\}, \quad (I)$$

which would be continuous with (H) if the u series repeated itself after n terms, so that $u_{n+1} = u_1, u_{n+2} = u_2$, etc. Then the typical Fourier terms of the u and v series will be

$$a_q \cos qx + b_q \sin qx \quad \text{and} \quad a'_q \cos qx + b'_q \sin qx$$

where

$$\begin{aligned} a_q + ib_q &= \frac{2}{n} \sum_{p=0}^{n-1} u_{p+1} e^{ipqa} \\ &= \frac{2}{n} \sum_0^{n-1} \{g_1 u_p e^{ipqa} + g_2 u_{p-1} e^{ipqa} + g_3 u_{p-2} e^{ipqa} + v_{p+1} e^{ipqa}\} \\ &= (a_q + ib_q) \{g_1 e^{iqqa} + g_2 e^{2iqqa} + g_3 e^{3iqqa}\} + a'_q + ib'_q. \end{aligned}$$

Therefore

$$a_q + ib_q = (a'_q + ib'_q) / (1 - g_1 e^{iqqa} - g_2 e^{2iqqa} - g_3 e^{3iqqa})$$

so

$$\begin{aligned} c_q^2 &= c'_q{}^2 / \{1 + g_1^2 + g_2^2 + g_3^2 + 2(g_1 g_2 + g_2 g_3 - g_1) \cos \alpha \\ &\quad + 2(g_1 g_3 - g_2) \cos 2\alpha - 2g_3 \cos 3\alpha\}. \end{aligned} \quad (J)$$

6. Further it may be seen that if there is a natural period of the u 's corresponding to this Fourier term in the accidental disturbances and the damping is small, the amplitude set up will be relatively large. For if there is a natural period of the u 's, in view of which they repeat after n/q terms, we have to consider n/q in conjunction with the solution $\exp. (-\lambda \pm i\theta)$ of the equation $x^3 - g_1 x^2 - g_2 x - g_3 = 0$, the undisturbed u terms being got by giving values 1, 2, 3, ..., to p in $e^{-\lambda p}$ ($A \cos p\theta + B \sin p\theta$). Thus, if λ is small, $2\pi/\theta$ must be n/q . But as $\exp. (-\lambda \pm i\theta)$ satisfied the cubic equation the value of

$$e^{\pm 3i\theta} - g_1 e^{\pm 2i\theta} - g_2 e^{\pm i\theta} - g_3$$

will be small, and as $\theta = 2\pi q/n = qa$ the equation preceding (J) shows that c_q will be relatively large; thus the u system will, if its damping is not too large, act like a resonator and respond, in its own periods, to relatively small accidental external disturbances.

7. If we want the ratio of the mean magnitudes of the accidental disturbances v to the u 's of the original series, we realise that the equations (H) and (I)

may be interpreted algebraically as a regression equation with coefficients g_1, g_2, g_3 by means of which the terms of the series $u_4, u_5, \dots u_n, u_1, u_2, u_3$ are expressed as linear functions of the terms in the three series (u_3, u_4, \dots, u_2) , $(u_2, u_3, \dots u_1)$, and $(u_1, u_2, \dots u_n)$; so the joint correlation coefficient R , between the first series u_x and the series of which the general term is

$$(g_1 u_{x-1} + g_2 u_{x-2} + g_3 u_{x-3}),$$

is given by*

$$R^2 = g_1 r_1 + g_2 r_2 + g_3 r_3,$$

and then, as v_4 is independent of u_1, u_2, u_3 and v_5 of u_2, u_3, u_4 , etc., we have the same algebraic relation as in ordinary statistics,

$$\sum_1 v_x^2 = (1 - R^2) \sum_1 u_x^2$$

or

$$d'^2 = (1 - g_1 r_1 - g_2 r_2 - g_3 r_3) d^2. \quad (K)$$

8. In a practical application of the method we work out the series of values of r_p and, if their graph clearly contains oscillations with certain periods, it is conceivable that instead of these being all natural periods of the original system some might be due to periodicities in the external disturbances which would no longer be purely accidental. Accordingly we shall examine the case in which the external disturbances indicated by v_p are made up of two portions, one f_p a periodic function of p and the other w_p a purely "accidental" element. We may then express u_p as given by the relation

$$u_p = g_1 u_{p-1} + g_2 u_{p-2} + \dots + g_s u_{p-s} + f_p + w_p.$$

Let the roots of the equation

$$y^s = g_1 y^{s-1} + \dots + g_s$$

be $\alpha_1, \alpha_2, \dots, \alpha_s$ and let the oscillation denoted by f_p be governed by a similar equation

$$y^t = h_1 y^{t-1} + \dots + h_t$$

with roots $\beta_1, \beta_2, \dots, \beta_t$. Then f_p is of the form $B_1 \beta_1^p + B_2 \beta_2^p + \dots + B_t \beta_t^p$; and if the equation whose roots are all the α 's and all the β 's is

$$y^{s+t} = k_1 y^{s+t-1} + k_2 y^{s+t-2} + \dots + k_{s+t}$$

we shall have the relations

$$u_p = k_1 u_{p-1} + \dots + k_{s+t} u_{p-s-t} + w_p$$

and

$$r_p = k_1 r_{p-1} + \dots + k_{s+t} r_{p-s-t}.$$

* 'Indian Meteorological Memoirs,' vol. 20, p. 122, equation 2 (1908).

Thus when we plot the r_p graph we shall see in it the oscillations of both the internal and external systems. Now it often happens that from the nature of the case the oscillations of the external disturbing system are undamped, while those of the disturbed system must be damped; and then the interpretation of the graph should be possible.

9. Some light is thrown by this analysis on the utility of a series of values of r_p , a "correlation-periodogram," as a substitute for the ordinary Fourier-Schuster periodogram when there is no question of damped oscillations.

We shall first consider the relations between the r 's of the former and the f 's, the amplitude-ratios, of the latter. If the number of departures $u_1, u_2, \dots u_n$ be $2m + 1$, as usual

$$u_p = a_0 + a_1 \cos p\alpha + \dots + a_m \cos m p\alpha \\ + b_1 \sin p\alpha + \dots + b_m \sin m p\alpha,$$

and $a_0 = 0$ since the series consists of departures from the mean. Thus in general when n is large enough for the S.D. d to be unaffected by modifying a few u terms

$$r_s = \sum_{p=1}^{n-s} u_p u_{p+s} / (n-s) d^2.$$

Also as n is supposed large while s remains finite we may as a first approximation replace this expression by

$$r_s = \sum_{p=1}^n u_p u_{p+s} / n d^2,$$

it being assumed, as before, that $u_{n+1} \equiv u_n$; thus

$$r_s = \frac{1}{n d^2} \sum_{p=1}^n \left[\begin{array}{l} a_1 \cos p\alpha + \dots + a_m \cos m p\alpha \\ + b_1 \sin p\alpha + \dots + b_m \sin m p\alpha \end{array} \right] \left[\begin{array}{l} a_1 \cos (p+s)\alpha + \dots + a_m \cos m (p+s)\alpha \\ + b_1 \sin (p+s)\alpha + \dots + b_m \sin m (p+s)\alpha \end{array} \right] \\ = \frac{1}{n d^2} \{ (a_1^2 + b_1^2) \cos s\alpha + (a_2^2 + b_2^2) \cos 2s\alpha + \dots \} \frac{n}{2} \\ = f_1^2 \cos s\alpha + f_2^2 \cos 2s\alpha + \dots + f_m^2 \cos m s\alpha. \quad (L)$$

A partial check is easy; for if the series forms an accurate cosine curve with a period of n/q or s terms, let us say, where s is an integer, the property of amplitude-ratios tells us that $f_q = 1$, all the other f 's vanishing; and as the series repeats itself completely after s terms we shall have $r_s = 1$.

Thus any period of q terms with an amplitude ratio f will produce as graph for r_p a cosine curve with maxima of at f_p at $p = q, 2q, 3q, \dots$, and equal and opposite minima half-way between.

Accordingly if there are only one or two periods and they are well-marked, inspection of the correlation-periodogram will reveal them; but if there are three or four periods or they are ill-marked, Fourier analysis of the r_p curve will be necessary.

10. We will now apply these ideas to the pressure at Port Darwin, one of the most important centres of action of "world weather," which, like the closely related station of Batavia, displays surges of varying amplitude and period with irregularities superposed, suggesting that pressure in this region has a natural period of its own, based presumably on the physical relationships of world-weather, but that the oscillations are modified by external disturbances. The data examined have been the 177 quarterly pressure values from 1882 to 1926, and as a first experiment we have considered the amplitude ratio f of the 26 Fourier harmonics* from the 5th to the 30th, covering periods from 9 years to $1\frac{1}{2}$ years, which will be found in Table I; the pressure curve and the

Table I.—Periodogram of Port Darwin Pressure 177 quarters.

Order of harmonic.	Fourier period.	Period examined.	Amplitude ratio.	Amplitude ratio corrected.
	Quarters.	Quarters.	f .	f' .
5	35.4	35	0.19	0.08
6	29.5	30	0.06	0.03
7	25.3	25	0.19	0.09
8	22.1	22	0.24	0.13
9	19.7	20	0.14	0.08
10	17.7	17.5	0.21	0.13
11	16.1	16	0.12	0.08
12	14.7	14.7	0.18	0.12
13	13.6	13.5	0.29	0.21
14	12.6	12.5	0.07	0.05
15	11.8	11.7	0.29	0.23
16	11.1	11	0.24	0.20
17	10.4	10.5	0.15	0.13
18	9.8	10	0.08	0.07
19	9.3	9.3	0.14	0.13
20	8.8	8.8	0.06	0.06
21	8.4	8.3	0.02	0.02
22	8.0	8	0.11	0.12
23	7.69	7.66	0.14	0.16
24	7.38	7.33	0.07	0.08
25	7.08	7	0.10	0.12
26	6.80	6.67	0.04	0.05
27	6.56	6.5	0.03	0.04
28	6.32	6.29	0.05	0.07
29	6.10	6.12	0.16	0.22
30	5.90	5.90	0.07	0.10

* The periods examined are sufficiently close to the Fourier periods; see pp. 119, 120, 'Memoirs of R. Met. Soc.,' I, No. 9, 1927.

periodogram are in figs. 1 and 2. It will be seen that the 8th, 13th, 15th and 16th harmonics have the largest ratios; their periods are 22, 13½, 11½ and 11

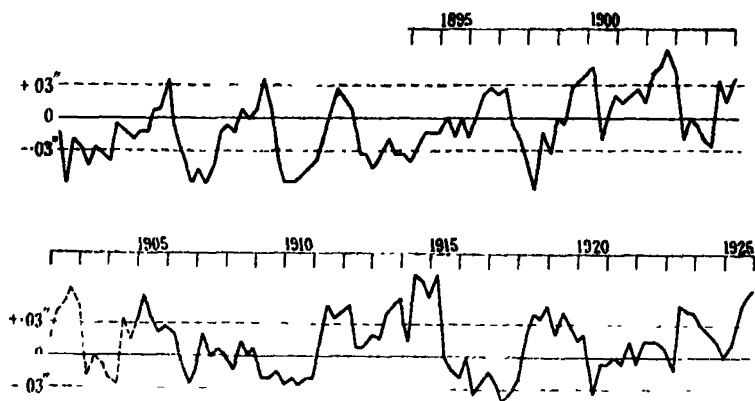


FIG. 1.—Port Darwin Pressure.

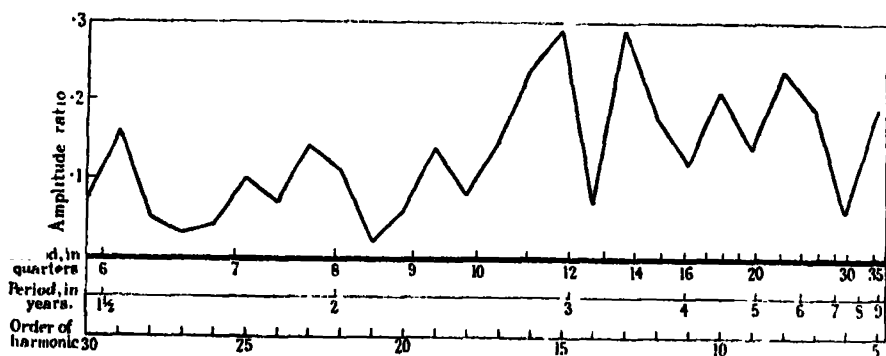


FIG. 2.—Periodogram.

quarters, and their f 's are 0.24, 0.29, 0.29 and 0.24, the amplitude ratio for a pure sine curve being unity. The probable value of a single f is 0.088, and the probable value* of the greatest of 26 of these, if they had been independent, would have been 0.20. But inasmuch as the correlation coefficient r_1 between successive quarterly pressures is 0.76, the terms of the series to be analysed are far from independent; and we cannot compare the results directly with those derived by Fourier analysis of a random series. It may be noted that the amplitudes of the 15th and 16th harmonics point to a single natural period of intermediate length, say, 11½ quarters or 2.8 years, while the length of the 13th harmonic is 3.4 years.

11. But granted the persistence we naturally interpret the pressure variations

* 'Q.J.R. Met. Soc.,' para. 6, p. 338, vol. 51 (1923).

in one of two ways. Either (a) the pressure is like a mechanical system, with persistence but without natural periods and acted on by a series of disturbances; in this case it is the periodicity of the disturbances that must be examined. Or (b) the pressure behaves like a mechanical system with persistence and natural periods, and then these periods interest us. In the first case having found $r = 0.76$ for Port Darwin we may* use equation (G) above and deduce the amplitude ratio f' of the disturbances from the ratios f of the original series. These are given in the last column of Table I† and plotted in fig. 3; we have four ratios, corresponding to the 13th, 15th, 16th and 29th

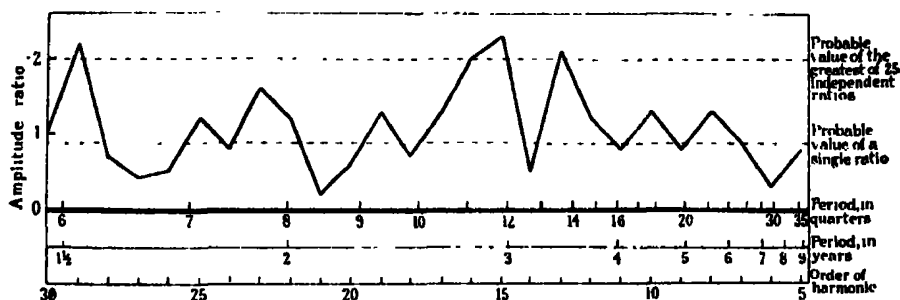


FIG. 3.—Periodogram of Disturbances, when Persistence alone is allowed for.

harmonics, which reach the limit of 0.20 that we should expect as the largest produced by mere chance. The ratio of the 14th harmonic is only 0.07. Regarding the amplitudes of the 15th and 16th harmonics as due to a single period of about $11\frac{1}{2}$ quarters, this interpretation suggests that while belief in the reality of three periods, of about 3.4 years, 2.8 years and 1.53 years, is permissible, it is far from inevitable.

12. We shall now consider the second interpretation and examine the idea that Port Darwin pressure has natural periods of its own, maintained by non-periodic disturbances from outside. The values of the correlation coefficients between quarterly pressures separated by an interval of p quarters are given in Table II from $p = 1$ to $p = 147$; but, before discussing these in full, it may be well to gain experience of the method in a preliminary trial of a simpler problem, and consider the first 40 coefficients which are plotted in fig. 4 in the continuous curve A. In this first experiment, then, we have to determine r_p ,

* It will be seen that in paragraph 4 above it has not been assumed that the disturbances are accidental.

† As a check the values of the successive v 's have been tabulated, and 10 of their amplitude ratios calculated; these all agreed with those derived as above within 0.03, i.e., within the limit of probable error.

Table II.—Correlation Coefficients of Port Darwin Pressure one Quarter with another after various intervals, (a) using all data, (b) using only 77 pairs.

Interval.	All data.	77 pairs.	Interval.	All data.	77 pairs.	Interval.	All data.	77 pairs.	Interval.	All data.	77 pairs.	Interval.	All data.
0	1.00	1.00	31	0.12	0.22	62	-0.22	-0.20	93	0.22	0.12	124	-0.30
1 <i>qr.</i>	0.76	0.80	32	0.06	0.22	63	-0.22	-0.26	94	0.12	0.04	125	-0.44
2	0.56	0.58	33	0.10	0.24	64	-0.14	-0.18	95	0.08	0	126	-0.62
3	0.36	0.34	34	0.10	0.16	65	-0.10	-0.20	96	-0.04	-0.10	127	-0.68
4	0.18	0.12	35	0.12	0.08	66	-0.08	-0.22	97	-0.16	-0.22	128	-0.60
5	0.08	0.02	36	0.08	-0.06	67	0.02	-0.10	98	-0.16	-0.20	129	-0.58
6	0.02	-0.02	37	0.06	-0.16	68	0.06	-0.04	99	-0.30	-0.32	130	-0.48
7	0.02	-0.02	38	0.06	-0.18	69	0.06	-0.06	100	-0.34		131	-0.38
8	-0.02	0.04	39	0.02	-0.22	70	-0.04	-0.14	101	-0.34		132	-0.38
9	0.08	0.20	40	0.08	-0.18	71	-0.08	-0.18	102	-0.24		133	-0.24
10	0.16	0.34	41	0.04	-0.14	72	-0.12	-0.24	103	-0.10		134	-0.12
11	0.22	0.48	42	0.14	0	73	-0.06	-0.16	104	-0.06		135	-0.04
12	0.24	0.46	43	0.24	0.10	74	-0.10	-0.20	105	0		136	0
13	0.28	0.48	44	0.26	0.20	75	-0.10	-0.18	106	-0.02		137	0.08
14	0.22	0.38	45	0.28	0.24	76	-0.16	-0.24	107	-0.04		138	0.06
15	0.18	0.30	46	0.22	0.16	77	-0.14	-0.20	108	0		139	-0.14
16	0.08	0.18	47	0.20	0.10	78	-0.04	-0.12	109	-0.10		140	-0.22
17	0.08	0.16	48	0.16	0.02	79	-0.02	-0.08	110	-0.20		141	-0.36
18	0.06	0.10	49	0.12	-0.14	80	0	-0.10	111	-0.24		142	-0.44
19	0.04	0.08	50	0.02	-0.20	81	-0.10	-0.20	112	-0.30		143	-0.56
20	0.14	0.24	51	-0.04	-0.22	82	-0.12	-0.26	113	-0.32		144	-0.60
21	0.12	0.30	52	0.08	-0.26	83	-0.20	0.40	114	-0.40		145	-0.60
22	0.18	0.34	53	-0.02	-0.16	84	-0.20	-0.38	115	-0.36		146	-0.48
23	0.20	0.36	54	0.04	-0.10	85	-0.22	-0.40	116	-0.34		147	-0.36
24	0.20	0.28	55	0.12	0.04	86	-0.24	-0.36	117	-0.30			
25	0.18	0.14	56	0.08	0.02	87	-0.20	-0.30	118	-0.22			
26	0.10	0	57	0.04	0.04	88	-0.14	-0.22	119	-0.28			
27	0.06	-0.12	58	0	0.06	89	-0.10	-0.18	120	-0.30			
28	0.04	-0.10	59	-0.14	-0.08	90	0	-0.06	121	-0.22			
29	0.10	0	60	-0.16	-0.08	91	0.12	0.04	122	-0.16			
30	0.12	0.12	61	-0.22	-0.16	92	0.16	0.04	123	-0.22			

as the sum of such terms as $e^{-\alpha p} \cos (\beta p + \gamma)$ in such a way as to give a fair approximation to the curve.

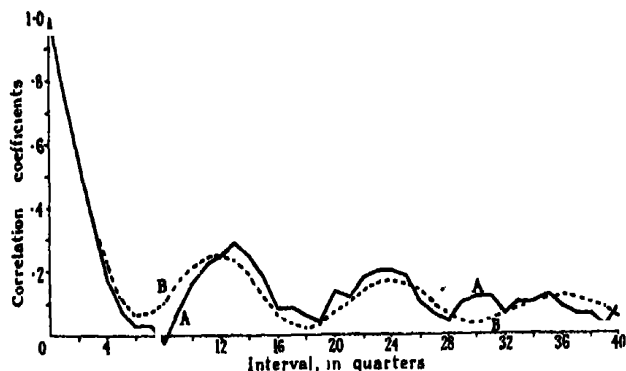


FIG. 4.—Preliminary Experiment. Serial Correlation Coefficients of Port Darwin Pressure, —, A, actual values of r_1, r_2, \dots ---, B, sum of the ordinates P, Q, R, of fig 5.

Now inspection shows a rapid descent from unity at $p = 0$ followed by maxima near $p = 13$ and 23 ; the natural interpretation is in terms of a damped harmonic curve with a period of about 12 quarters, producing maxima of diminishing amplitudes for $p = 12$ and 24 ; so we take $r_p = 0.19 (0.96)^p \cos 2\pi p/12$, plotted as curve P in fig. 5, as a first approximation. But this

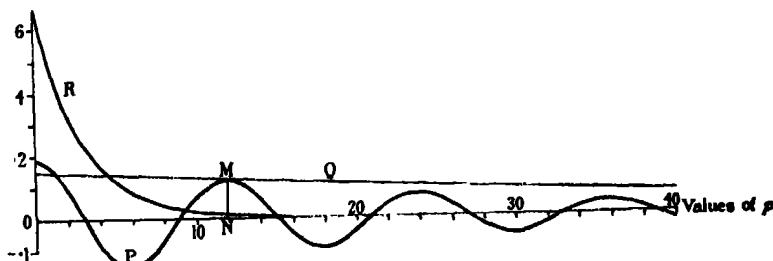


FIG. 5.— $P = 0.19(0.96)^p \cos (2\pi p/12)$. $Q = 0.15(0.98)^p$. $R = 0.66(0.71)^p$.

oscillates about the zero line, while in fig. 4 the r curve has only one negative value; accordingly we interpret r_p as the sum of two terms, the first being that indicated by the P curve and the second a curve like Q whose co-ordinates diminish gradually; that plotted as Q is $r_p = 0.15 \times (0.98)^p$, which we may regard as a slightly damped oscillation of infinite period. Corresponding to this there must be a similar term in the expression for u_p , the typical term in the pressure curve, and a sloping line there would mean what is sometimes called a "secular change" in the pressure. The existence of such a change is obvious from fig. 1 and the correlation coefficient 0.43 of pressure with time is one of the largest in the world.*

The sum of these two terms gives fair agreement except that from $p = 0$ to $p = 6$ the curve has not large enough co-ordinates and does not descend fast enough. So we add a strongly damped curve R of which the ordinate is $0.66 (0.71)^p$, the effect of which is to increase the amount of "persistence" in the pressure; the coefficient 0.66 is chosen so as to make $r_0 = 1$. The sum of P, Q, R is indicated by the dotted graph B in fig. 4, which is a fair approximation. Thus we find

$$r_p = 0.19 (0.96)^p \cos 2\pi p/12 + 0.15 (0.98)^p + 0.66 (0.71)^p, \quad (M)$$

and the equation corresponding to equation (D) in paragraph 2 above is

$$z^p = 3.35z^{p-1} - 4.43z^{p-2} + 2.71z^{p-3} - 0.64z^{p-4}. \quad (N)$$

* It may be that this change is partly due to some change of barometric correction, but its effect on periodicity will be insignificant.

Apart from external disturbances the corresponding solution for the u series would be of the form

$$u_p = (0.96)^p (A \cos 2\pi p/12 + B \sin 2\pi p/12) + C(0.98)^p + D(0.71)^p$$

and the effect of disturbances v_1, v_2, \dots , is to give a typical equation

$$u_p = 3.35u_{p-1} - 4.43u_{p-2} + 2.71u_{p-3} - 0.64u_{p-4} + v_p \quad (O)$$

so, as in paragraph 7 above, if the joint correlation coefficient of u_p with its expression in terms of preceding terms is R , we have

$$R^2 = 3.35r_1 - 4.43r_2 + 2.71r_3 - 0.64r_4 = 0.92,$$

and hence $R = 0.96$ and $d' = 0.28d$. Accordingly this preliminary interpretation of the pressure variations as resembling the damped natural oscillations of a mechanical system maintained by external disturbances would explain a very large fraction of the variations, the magnitude of the disturbances averaging only about a quarter of that of the oscillations. As we shall see, however, further extension leads to a different result, and shows the danger of an incomplete examination.

13. Regarding the periods of the natural oscillations it will be seen that the curve A of fig. 4 is not capable of resolving the difference between the damped oscillations of 2.8 and 3.4 years. A Fourier analysis of it would have a third harmonic with a period of $3\frac{1}{2}$ years and a fourth of $2\frac{1}{2}$ years; the intermediate amplitudes would, as Turner showed, not be independent of these. On this account and in order to discuss the period of between 11 and 12 years suggested by the values of 4 near $p = 44, 93$ and 137 we must extend our examination of the values of r_p , as in curve A, fig. 6; here when p is 20 we have 157 pairs of correlates, but as p grows the number of correlates diminishes until when $p = 140$ it is only 30. A glance shows outstanding oscillations near $p = 44, 93$ and 137 with three smaller oscillations between 0 and 44, three between 44 and 93, and two between 93 and 137; the general downward slope is maintained. The obvious interpretation is that we have an oscillation with eight periods in 92 quarters, fitting well with the intermediate maxima; superposed on this there is evidence of a rise up to maxima near 46, 92 and 137 with minima in between, or of an oscillation with a period of about 46 quarters. But far from showing damping the oscillations grow with p , and the explanation seems to lie in the contrast between the number $(177 - p)$ of correlates when p is small and the number when p exceeds 100. Thus for the last 40 terms the number of values correlated averages 50, covering $12\frac{1}{2}$ years, and we have the first 12 or 13 years correlated, with different lags, with the last 12 or 13 years;

as fig. 1 shows, each has well-marked waves and it is obvious that there will be relative positions in which the waves correspond; so there will be big oscillations in r_p on a scale that would not arise if the number of years correlated were longer. In order to verify this the columns in Table II headed "77 pairs" have been computed, giving the values of r_p derived by correlating the first 77 quarters with the groups of 77 quarters which occur 1, 2, 3, ..., 100 quarters later; in this way each correlation coefficient is based on 77 pairs of terms. The resulting curve B in fig. 6 contains the main features of A and

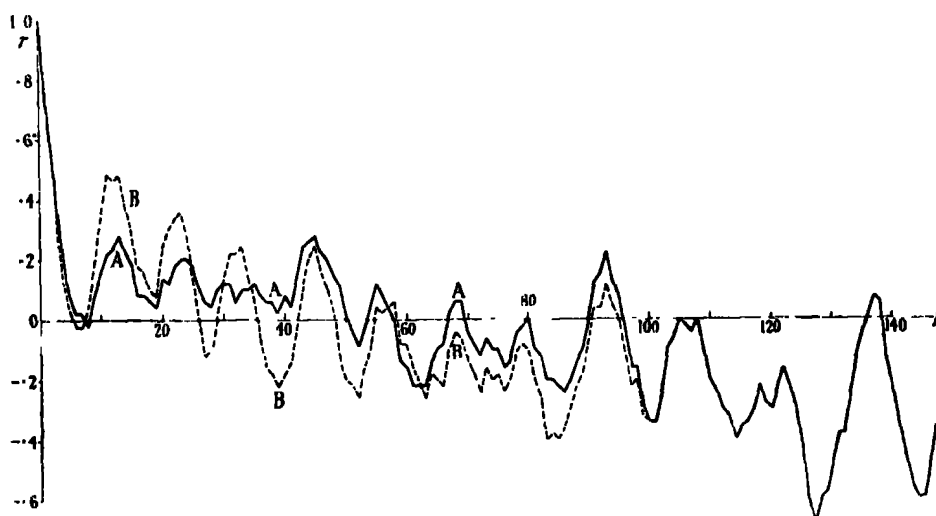


FIG. 6.—Serial Correlation Coefficients.

—, A, coefficients r_p based on all the available material. - - - B, coefficients r_p based on 77 pairs of correlates.

shows the reduction in amplitude due to damping that we should expect. It appears wiser therefore to ignore values of r_p for which p is greater than about 100 in fig. 6; but the differences between curves A and B show that the error due to sampling (i.e., to an inadequate number of pairs of terms) is probably as great as 0.1 and the apparent damping in B may be largely due to a greater amplitude in the $11\frac{1}{2}$ quarters oscillation in the first half of the data of 177 quarters than in the second.

14. On the whole then it is safer not to attempt a very precise interpretation. There appears to be a periodicity of about $11\frac{1}{2}$ quarters with an amplitude (or half-range) of something like 0.12, corresponding to an amplitude-ratio in the Fourier series of about 0.35; but the evidence that it is damped is not conclusive. There are also indications of a periodicity of about 46 quarters,

or $11\frac{1}{2}$ years, with an amplitude of the order of 0.05 (and amplitude ratio 0.22); of damping in this no trace is visible; this oscillation appears, therefore, to be superposed from without and is presumably solar in origin. The general downward slope of the graphs is due to the general trend of the pressure data. There is clear evidence of strong persistence.

The negative conclusions are more definite. Of the periodicities of 6.5 quarters and 13.5 quarters doubtfully suggested by the periodogram there is no visible trace; nor do I see any evidence of the other periods, such as 2 years, 4 years and 7 years, which have from time to time been suggested by students of Australian meteorology.

15. Finally I would express my indebtedness to Mr. E. W. Bliss for the care with which he has done the whole of the computing involved in this paper.

Summary.

In 1927 Yule developed the idea that a series of numbers u_1, u_2, \dots, u_n expressing the condition of a physical system, such as successive annual sunspot numbers, might be regarded as due to a series of accidental disturbances from outside operating on some dynamical system with a period or periods of its own, probably subject to damping. The consequent oscillations would vary both in amplitude and in period. In this paper it is shown that if Yule's equation defining the relationship between successive undisturbed terms of the u series is

$$u_n = g_1 u_{n-1} + g_2 u_{n-2} + \dots + g_s u_{n-s},$$

then, provided n is large, a similar equation holds very approximately between successive values of r_p , the correlation coefficient between terms of u separated by p intervals, i.e.,

$$r_n = g_1 r_{n-1} + g_2 r_{n-2} + \dots + g_s r_{n-s}.$$

Thus the graph expressing the r_p 's, which is much smoother than that of the u 's, may be used to read off the character of the natural periods of the u 's; further various relationships are found between the amplitude of the corresponding terms in the Fourier periods and those of the correlation coefficients.

The analysis is illustrated by applying it to the quarterly values of pressure at Port Darwin, a key-centre of world weather, which proves to have a strong persistence and to show evidence of not very strongly developed periods of about $34\frac{1}{2}$ months and of about four times this length or $11\frac{1}{2}$ years; the series of data is not long enough to settle whether the former oscillations are damped and are free oscillations, but the latter appear to be imposed from without and are presumably solar in origin.

Ethyl Alcohol, A Product of High Pressure Syntheses.

By GILBERT T. MORGAN, F.R.S., and RAYMOND TAYLOR, Chemical Research Laboratory, Teddington, Middlesex.

(Received March 4, 1931.)

In opening the "discussion on catalytic reactions at high pressures,"* one of us (G. T. M.) referred to experiments made in the Chemical Research Laboratory of the Department of Scientific and Industrial Research which had led to the isolation of notable quantities of ethyl alcohol among the condensation products from carbon monoxide and hydrogen interacting at high temperatures and pressures in presence of catalysts. These experiments were first described in March, 1928,† and since that date statements have appeared in the scientific press to the effect that ethyl alcohol is a possible exception to the whole sequence of higher alcohols which can be produced by such interactions.‡ Moreover during the above-mentioned discussion Mr. M. P. Appleby, speaking on behalf of the Imperial Chemical Industries, Ltd., Billingham, said "that in our experience we have never succeeded in obtaining, with any catalyst whatsoever, more than a mere trace of ethyl alcohol."

To the latter statement we take no exception whatever. It is a record of personal experience. But we felt that it was desirable to substantiate our earlier experiments by such corroborative evidence as would leave no doubt that ethyl alcohol is a product of high pressure synthesis.

An entirely new set of experiments has been carried out, the products have been examined in detail, and the results of this examination have confirmed our original statements both in regard to the identity of ethyl alcohol and to the proportions in which this compound is formed under our experimental conditions.

Preparation and Composition of Catalyst.

Two parts by weight of cobalt nitrate were mixed with one part of commercial zinc permanganate, a little water was added, the mixture evaporated to dryness and gently roasted until no more nitrous fumes were evolved. The black mass was ground to a fine powder and about 10 per cent. by weight of a potter's clay added; the mixture was made into a paste with water and

* 'Proc. Roy. Soc.,' A, vol. 127, p. 246 (1930).

† 'J. Soc. Chem. Ind.,' vol. 47, p. 117T (1928); compare Eng. pat. 313061.

‡ Compare E. K. Rideal, 'Nature,' April 12, p. 584 (1930).

extruded through a die into a vermiform mass; this material was dried at 130° and broken up into granules which were reduced in hydrogen at a temperature not exceeding 350° and then placed in the catalyst chamber. The commercial zinc permanganate used in making this catalyst contained a considerable quantity of potassium permanganate and an analysis of the granules after use in the converter gave the following composition:—ZnO, 7.9; MnO, 26.34; Co, 29.9; alkalis, 7.4; SiO₂, 8.8; Al₂O₃, 2.5; CaO, 0.4; Fe, 0.3; free C, 8.9 per cent. (92.4). That these values do not add up to 100 is due to the uncertainty in regard to the state of oxidation of the whole of the manganese and of part of the cobalt.

An analysis of the clay used in making up the catalytic granules gave the following data:—Loss on ignition, 7.76; SiO₂, 67.80; Al₂O₃, 19.90; Fe₂O₃, 0.54; CaO, 0.70; MgO, 0.30; Na₂O, 0.90; K₂O, 1.96 per cent. (99.86).

Apparatus and Experimental Conditions.

The synthesis was carried out in the 1½-inch by 3-foot converter system described in detail by Mr. H. Tongue.* The catalyst was heated at 380° to 410°, while the pressure of the circulating gases was maintained at 200 atmospheres by regulated admission of a mixture of hydrogen and carbon monoxide (2 parts and 1 part by volume respectively). Employing 75 c.c. of catalyst we obtained an hourly yield approximating to 75 c.c. of liquid product of which 4 litres were prepared.

This crude liquid product consisted of a mixture of alcohols, aldehydes, acetals, organic acids and water from which it was essential to remove all organic products except alcohols before the latter could be separated by fractional distillation. By boiling the mixture under reflux with aqueous caustic alkali the organic acids were fixed as salts and the free aldehydes were resinified, but the distillate from this treatment still contained acetals. These aldehydic ethers, which are only hydrolysable in acid media, were decomposed by the use of 2:4-dinitrophenylhydrazine, a reagent already employed by O. L. Brady and G. V. Elsmie.† The mixture of alcohols and acetals, after heating under reflux with excess of this reagent in presence of dilute sulphuric acid, gave a distillate entirely free from either acetals or aldehydes. The alcoholic content of this distillate was determined both by direct fractional distillation and by conversion of the alcohols into alkyl acetates which are readily separated by fractional distillation.

* 'Trans. Inst. Chem. Eng.,' vol. 8 (1930).

† 'Analyst.,' vol. 51, p. 77 (1926).

Fractional distillation as a method of quantitative analysis is described by S. Young,* who states that in the case of a mixture of two liquids which on distillation separate normally into the original components, the weight of distillate passing over below the "middle point" is as a rule almost exactly equal to that of the more volatile component, even when a separation is very far from complete. The "middle point" is defined as the temperature midway between the boiling points of the two components, whether single substances or mixtures of constant boiling point into which the original mixture tends to separate, or in the case of more complex mixtures the boiling points of any two consecutive fractions of constant boiling point. The still-head selected for fractionations was a Dufton column 150 cm. long, with inner tube of 13 mm. external diameter, and outer tube of 16 mm. internal diameter, since this type of column is designed for the efficient distillation of small quantities of liquid.†

The separation of alcohols was found to be more effective the less the amount of water in the mixture, and in our experiments alcohols were freed from water as far as possible by a preliminary distillation. The liquid under examination was weighed, as were also the various fractions derived therefrom, and the percentage of carbon and hydrogen was determined in each case by combustion in oxygen over copper oxide. The results of two separate examinations "A" and "B" are tabulated on p. 536.

A separate portion of the crude liquid product was neutralised with sodium carbonate and the volatile non-acidic constituents removed by distillation. The carbon content of these neutral compounds (alcohols and acetals) was found to be 85.2 per cent. of total carbon in the crude liquid product, so that by difference the carbon value for the non-volatile acid constituents was equal to 14.8. The carbon content of aldehydes, either free or combined as acetals, was obtained by deducting the alcoholic mean value 70.6 from that of the foregoing distillate 85.2, giving a value of 14.6 per cent.

Acetaldehyde, a probable intermediate in the synthesis of ethyl alcohol, was distilled from the crude liquid product, after acidification with dilute sulphuric acid. This separation was effected in experiment "B" before resinification of the remaining aldehydes by aqueous caustic potash, and again in a special experiment "C" when the following concordant yields were obtained: 1.73 and 1.76 grams of acetaldehyde per 100 grams of product.

The carbon distribution in the total products of reaction both gaseous and liquid was as follows: Alcohols, 35.3; acids, 7.4; aldehydes, 7.3; methane,

* "Distillation Principles and Processes," 1922, chap. 16, p. 170.

† 'J. Soc. Chem. Ind.,' vol. 38, p. 45T (1919).

Alcohols as Estimated by Fractional Distillation.

Description of liquid.	Experiment A.				Experiment B.			
	Weight in grams.	Carbon per cent.	Carbon content in grams	Percentage of total carbon in liquid product present as alcohols.	Weight in grams.	Carbon per cent.	Carbon content in grams.	Percentage of total carbon in liquid product present as alcohols.
Crude liquid product	717	23.65	169.5	—	700	23.65	165.6	—
Total alcohols (distillate from 2:4- dinitrophenylhydrazine)	307	38.9	119.4	70.4	297.0	39.4	117.0	70.7
Alcohols taken for fractionation (after removal of sample)	279	38.9	108.5	—	289.0	39.4	113.9	—
Fraction I (up to 71°)	128	39.9	51.1	33.2	121.0	39.1	47.3	29.4
Fraction II (71° to 83°)	69	44.0	30.4	19.7	69.5	44.9	31.2	19.4
Fraction III (above 83°)	80	33.2	26.6	17.3	96.0	35.2	33.8	21.0

50 per cent. ; of these percentages ethyl alcohol accounted for 9.8 and acetaldehyde 2.0 per cent.

The accuracy of the distillation method of analysis as applied to this particular alcoholic mixture was now checked by a chemical process. Experiment showed that a uniform 93 per cent. conversion to alkyl acetates was obtainable by treating alcohols under reflux with excess of acetic anhydride in the presence of a trace of concentrated sulphuric acid. Accordingly fraction II (experiment "B") was converted to alkyl acetates from which methyl and ethyl acetates were readily separated by fractional distillation. The corresponding fractions I and III which necessarily contained some ethyl alcohol were also acetylated and ethyl acetate again separated by fractional distillation. Ethyl alcohol calculated from ethyl acetate produced by acetylation of :—

	grams.
(1) Fraction I	= 9.4
(2) Fraction II	= 39.0
(3) Fraction III	= 7.3
	—
Total	= 55.7
Ethyl alcohol calculated from carbon content of	
fraction II	= 59.9

Now since acetylation gives only 93 per cent. conversion of alcohol to alkyl acetate, 55.7 grams of ethyl acetate corresponds with $55.7 \times 100/93 = 59.9$ grams of ethyl alcohol originally present in the three fractions, an amount equal to that calculated from the carbon content of fraction II. The ethyl acetate collected together from various fractions was finally purified by fractional distillation and its purity verified by determination of the following physical constants : Boiling point, $77.1^{\circ}/759.6$ mm. ; density, $D^{20.3}_{4} 0.9002$, compare $D^{20.4}_{4} 0.9005^{*}$ which corresponds with $D^{20.3}_{4} 0.9001$; refractive indices, $n^{20}_{D} 1.37060$; $n^{20}_{D} 1.37694$; compare $n^{20}_{D} 1.37060$ and 1.37068 , $n^{20}_{D} 1.37690$ and 1.37709 .†

About 200 g. of ethyl acetate prepared from synthetic alcohol were hydrolysed by strong aqueous caustic potash and on fractionation of the liberated alcohol the first drop distilled at 77.7° , but the temperature quickly rose to 78.0° , with barometric pressure 757.7 mm. This alcohol was then dried by boiling under reflux for 6 hours with quicklime and submitted to ultimate

* Lowry, 'Trans. Chem. Soc.,' vol. 105, p. 81 (1914).

† Landolt, 'Pogg. Ann.,' vol. 122, p. 552 (1864).

analysis* with the following results: Found, C, 51.9, 52.1, 52.4, 52.0; H, 12.9, 13.1, 13.2, 13.1; C_5H_9OH requires C, 52.1; H, 13.1 per cent.

The following physical constants of this alcohol were determined:—Boiling point, $78.6^\circ/770$ mm.; specific gravity, D^{25}_4 , 0.7861, compare D^{25}_4 , 0.7851†; refractive indices n^{20}_D 1.35966, n^{20}_D 1.36148, compare n^{20}_D 1.36050‡. An authentic specimen of ethyl alcohol dried in the same manner gave D^{25}_4 0.7861 and n^{20}_D 1.35952, n^{20}_D 1.36132.

In addition to the foregoing determinations made on a specimen of synthetic ethyl alcohol purified through its acetate, experiments were also carried out on a sample of this alcohol obtained directly by rectification of fraction II after dehydration over quicklime.

Ultimate analysis furnished the following values:—C, 52.2, 51.8, 51.9; H, 13.01, 13.04, 13.08 per cent. This specimen had a boiling point $78.5^\circ/765.3$ mm.; D^{25}_4 , 0.7860; n^{20}_D , 1.361.

Characteristic Chemical Properties.

Both preparations of synthetic alcohol were converted into the following crystalline esters:—

Ester.	Synthetic ethyl alcohol purified.		Authentic specimen.
	(a) Through acetate.	(b) By rectification.	
2:4-dinitrobenzoate $C_6H_3(NO_2)_2.CO_2.C_2H_5$	91	91	91
Ethyl phenylcarbamate $C_6H_5.NH.CO_2.C_2H_5$	51	51	51
Ethyl p-xenylcarbamate $C_{11}H_9.NH.CO_2.C_2H_5$...	118-119	118-119	118-119

Mixed melting points of the three different preparations of each of the three foregoing esters confirmed the identity of the derivatives from the synthetic alcohol (two samples) with those of an authentic specimen of this compound.

In addition to the catalyst employed in the foregoing detailed study of the high pressure synthesis of ethyl alcohol, the following mixtures have been

* The first accurate ultimate analysis of ethyl alcohol was accomplished by N. T. de Saussure ('Ann. Chim.' vol. 89, p. 273 (1814)) who, operating on an aqueous alcohol, found after making due allowance for water that his values were—C, 51.98; H, 13.70; and O, 34.32 per cent.

† Munch, 'J. Amer. Chem. Soc.' vol. 48, p. 996 (1926).

‡ Landolt, 'Pogg. Ann.' vol. 122, p. 548 (1864).

examined and found to induce the formation of appreciable quantities of this alcohol :—

- (1) Zinc chromate, 1 part ; cobalt nitrate, 2 parts ; copper formate, 0.3 part, by weight.
- (2) Basic zinc chromate, 5 parts ; manganese nitrate, 2 parts ; copper nitrate, 1 part ; cobalt nitrate, 4 parts, by weight.
- (3) Copper nitrate (1 grm. mol.) ; manganese nitrate (1 grm. mol.) ; cobalt nitrate (0.01 grm. mol.).
- (4) Copper nitrate (1 grm. mol.) ; manganese nitrate (1 grm. mol.) ; cobalt nitrate (0.05 grm. mol.).
- (5) Copper nitrate (1 grm. mol.) ; manganese nitrate (1 grm. mol.) ; iron nitrate (0.1 grm. mol.).
- (6) Cobalt nitrate (1 grm. mol.) ; manganese nitrate (0.7 grm. mol.) ; zinc nitrate (0.35 grm. mol.).

A catalyst produced by ignition of mixture (3) gave a liquid product which contained only traces of aldehydes and organic acids ; the carbon distribution in the total product was approximately :—Methyl alcohol, 54 ; ethyl alcohol, 8 ; higher alcohols, 8 ; methane, 30 per cent.

When, however, a catalyst was made by precipitation with caustic potash from a solution of the same mixture of nitrates, it induced the production of almost pure methyl alcohol and no methane.

The catalyst made by ignition of mixture (4) gave a product very similar to that obtained in the large preparation which was studied in detail ; the carbon distribution being—Acids, 4 ; aldehydes, 11 ; methyl alcohol, 22 ; ethyl alcohol, 12 ; higher alcohols, 5 ; methane, 45 per cent.

The catalyst obtained by ignition of mixture (6) gave a product in which the carbon distribution was as follows :—Acids, 1.2 ; aldehydes, 8.2 ; methyl alcohol, 6.0 ; ethyl alcohol, 4.7 ; higher alcohols, 2.0 ; methane, 78 per cent.

Identification of Two Acetals in the Crude Liquid Product.

Throughout this communication the term acetal has been used in a generic sense to indicate aldehydic ethers (aldehydals) of types $X \cdot CH(OR) \cdot OH$ and $X \cdot CH(OR)_2$, where X is either hydrogen or an alkyl group (methyl, ethyl, propyl, etc.) and R is an alkyl group and predominantly methyl since in the foregoing experiments methyl alcohol is the main constituent. One would expect this alcohol to furnish most of the aldehydic ethers, and two such acetals have been identified in the following manner :—

Free aldehydes were removed from the crude product of catalysis by boiling with caustic potash under reflux and by subsequent distillation when the fraction boiling below 64° was collected separately and shaken with saturated aqueous caustic potash. The mixture separated into two layers, the upper consisting mainly of acetals, the lower containing most of the methyl alcohol. Any alcohol or water remaining in the acetal layer was removed by mixing with phenylcarbimide, the acetals being then redistilled on to solid caustic potash. Distillation from this alkali gave a mixture of acetals free from phenylcarbimide. Fractional distillation separated this mixture into two individual acetals, one boiling at 63° to 65° and the other above 85° .

Each acetal was identified by mixing with excess of 2 : 4-dinitrophenylhydrazine which combined with the aldehydic radical of the compound and formed the corresponding 2 : 4-dinitrophenylhydrazone. The alcohol liberated by this process was distilled into phenylcarbimide and combined to form an alkyl phenylcarbamate. The more volatile acetal was thus shown to be *ethylidene dimethyl ether*, for it furnished acetaldehyde 2 : 4-dinitrophenylhydrazone m.p. 158° to 162° and giving a mixed m.p. 159° to 162° with an authentic specimen of the hydrazone (m.p. 162°). The liberated methyl alcohol combined with phenylcarbimide yielding methyl phenylcarbamate m.p. 48° and giving a mixed m.p. 48.5° with an authentic specimen (m.p. 48.5°). The specimen of synthetic ethylidene dimethyl ether has b.p. 63° to $65/760$ mm. and refractive index $n_{20}^{20:D}$ 1.366, an authentic specimen giving $n_{20}^{20:D}$ 1.366 with b.p. 64° . The less volatile acetal was *propylidene dimethyl ether*, for it yielded propaldehyde 2 : 4-dinitrophenylhydrazone m.p. 147° to 149° and mixed m.p. 153° to 155° with an authentic specimen of this hydrazone (m.p. 155°). The methyl alcohol obtained by hydrolysis of this acetal furnished methyl phenylcarbamate identified by comparison with an authentic specimen.

We desire to express our thanks to Mr. W. H. Withey of the National Physical Laboratory, who analysed the catalyst; to Dr. J. S. Anderson of the same Laboratory, who determined the refractive indices; and to our colleague, Mr. A. J. Bunce, who made the ultimate analyses.

The Decay Constant of Uranium II.

By C. H. COLLIE.

(Communicated by F. A. Lindemann, F.R.S.—Received January 3, 1931.)

The relations between the radioactive elements which occur in "uranium" have attracted attention since Boltwood's* discovery that uranium gave two α -particles for each α -particle emitted by the radioactive elements in equilibrium with it. As is well known, Geiger and Rutherford,† Marsden and Barrett‡ and Geiger and Nuttall,§ proved that this was due to the existence of two uraniums with separate decay constants. The primary relationships having been established, it was not until recently that attention was again turned to the group of radioactive elements in "uranium." Clearly, no advance can be made in elucidating the relationships between the various branches, or series starting with unknown isotopes of uranium, until the decay constant of UII is well established. Also, until this constant is known, no information of theoretical value can be drawn from the atomic weight of uranium; quite different conclusions being arrived at if uranium II exists in a measurable or negligible proportion in uranium.|| Three estimates have been made of the range of the α -particles from uranium II, and so, using the Geiger-Nuttall rule, three estimates of its period of half life. These are:—

- (a) Geiger and Nuttall (*loc. cit.*) = 2×10^6 years.
- (b) Gudden¶ = 10^8 years.
- (c) Laurence** = 1.3×10^4 years.

The values given by Geiger in a later paper†† for uranium I and II are only recalculated values and do not represent new measurements. Gudden's measurements are much more accurate, but, as they depend on the measurement of pleochroic haloes, they are not suitable for giving an absolute value of the range, since the density of the fluorspar in immediate contact with the uranium

* 'Nature,' December, 1906.

† 'Phil. Mag.,' vol. 20, p. 691 (1910).

‡ 'Proc. Phys. Soc.,' vol. 23, p. 367 (1911).

§ 'Phil. Mag.,' vol. 23, p. 439 (1912).

|| Stefan Meyer, 'Mitteilung des Institutes für Radium Forschung,' No. 226.

¶ 'Z. Physik,' vol. 26, p. 110 (1924).

** 'Phil. Mag.,' vol. 5, p. 1027 (1928).

†† 'Z. Physik,' vol. 8, p. 45 (1921).

inclusion is not measured. They are, however, eminently suitable for determining the ratio of the ranges of α -particles of nearly the same range, since whatever the mechanism of the formation of pleochroic haloes may be, it is one which depends essentially on the very intense ionisation produced by the α -particle at the end of its range. It is thus possible to measure the difference in range between two groups of α -particles more accurately than would be possible using the ordinary method with an ionisation chamber of finite depth.

Laurence's Wilson chamber method is the most direct and his results are supported by measurements on the atomic weight of uranium,* and on the total ionisation of the α -particles from uranium,† and have been adopted by Rutherford in his theory of radioactive disintegration.‡

No direct measurement of the period of uranium II has hitherto been made, but the introduction of the valve amplifier has made this possible. In principle the method is extremely straightforward and consists in preparing a known number N atoms of uranium II, observing the number of α -particles emitted from them and thus observing directly $N\lambda$ where λ is the decay constant. Experimentally the method may be divided into four parts:—

- (1) The preparation of a large quantity of uranium X acetate, uncontaminated by any radioactive material.
- (2) Estimating the number of atoms of uranium X present by comparing its β -ray activity with that of the UX in radioactive equilibrium with a known weight of uranium. Thus, if the prepared source has p times the β -ray activity of the uranium X in equilibrium with 238 grm. of uranium it contains $p \frac{\lambda_1}{\lambda_2} N$ atoms of UX, where N is Avogadro's number and λ_1, λ_2 the decay constants for uranium I and uranium X respectively.
- (3) The known number of atoms of uranium X is allowed to decay for a known time, thus producing a known number of atoms of uranium II.
- (4) This quantity of uranium II is separated from the solution containing the remaining uranium X and the number of α -particles emitted per second observed.

* Stephan Meyer, *loc. cit.*

† H. Ziegert, 'Z. Physik,' vol. 46, p. 668 (1928).

‡ 'Phil. Mag.,' vol. 4, p. 580 (1927).

Preparation of Uranium X.

The uranium X must be concentrated from uranyl nitrate by a method which is capable of being used for large quantities of uranyl nitrate (10 to 50 kg.), but which does not involve the crystallisation of large volumes of solution, which would make the avoidance of contamination with thorium almost impossible; nor are the usual methods, which involve the solution of large quantities of uranium carbonate in ammonium carbonate,* or the addition of a non-radioactive base not easily separable from uranium, at all suitable.

After considerable preliminary work in Dr. Russell's laboratory, the following method was adopted:—

The saturated solution of the nitrate in ether† is shaken with 2 per cent. by volume of distilled water, and the whole allowed to stand for 12 hours. The aqueous layer is then separated off and contains at least 90 per cent. of the uranium X present in the original solution. The separated aqueous layer is then warmed to distil off the dissolved ether and evaporated‡ after the addition of a small quantity of nitric acid until the temperature of the boiling solution is about $112\frac{1}{2}^{\circ}$ C. When the solution is allowed to crystallise, the uranyl nitrate, for the most part, forms large well-formed crystals covered with a small amount of yellow powdery basic uranyl nitrate and leaves a few cubic centimetres of mother liquor.

The contents of the dish are transferred to a Büchner funnel (no filter paper), and well drained at the pump. The crystals (which are large enough not to pass through the perforations in the funnel) are washed with about 100 c.c. of strong nitric acid, when the adhering mother liquor and basic nitrate are completely removed. In this way 90 per cent. of the uranium X is transferred to the acid filtrate. For example, in small scale experiments, using 100 gm. of uranyl nitrate, all the UX was found in the acid filtrate, while in two large scale experiments, using about 60 kg. of uranyl nitrate, 80 per cent. and 95 per cent. respectively was found in the acid filtrates.

In this way the uranium X in equilibrium with about 20 kg. of uranyl nitrate is concentrated into a 100 c.c. of nitric acid and solution containing about 20 grammes of uranyl nitrate. The acid solution is transferred to a platinum dish, most of the nitric acid removed by evaporation and the volume made up to about 50 c.c. with water. To the boiling solution is added strong redistilled hydrofluoric acid until further addition causes a permanent precipitate of hydrogen uranyl fluoride. The uranium X is now precipitated on a nucleus of cerium fluoride (free from thorium) by adding enough cerium nitrate solution to give a visible precipitate (about 10 mg. of cerium nitrate is enough). The whole is kept hot for half an hour and is then filtered through a 2 cm. diameter filter paper in a porcelain filter, and the filtrate returned at once to the platinum dish while the precipitated cerium fluoride is washed with boiling water. Only part of the cerium is precipitated under these conditions, and it is best to carry out the precipitation three times. Usually

* G. and A. S. Russel, 'J. Chem. Soc.,' vol. 123, p. 2626 (1923).

† W. Crooks, 'Proc. Roy. Soc.,' A, vol. 66, p. 409 (1900).

‡ If the ether solution has been standing for some time there may also be a sudden evolution of inflammable vapour at 80° C.

90 per cent. of the UX is in the first precipitate, 5 per cent. in the second, and 1 per cent. in the third, but these figures are very variable and it is essential to control the precipitation by measuring the uranium X adsorbed with a β -ray electroscope.

The cerous fluoride at this stage is usually pale green owing to the presence of small quantities of uranous fluoride formed by the reduction of the uranyl salts by the ether in the first part of the process.

The wet filter papers are now transferred to a small silica crucible (2 c.c. capacity), and carefully ignited. The residue is fused before the blowpipe with potassium hydrogen sulphate, when the whole goes into solution forming a bright orange melt. The crucible and its contents are transferred to a small beaker of water, and filtered from any silica. The acid solution is made alkaline with sodium carbonate and the precipitated cerous carbonate, which is now quite white, digested with the alkaline solution to remove any uranium present as sodium uranyl carbonate. After filtration the cerous carbonate is well washed with boiling water and then dissolved on the filter in dilute nitric acid. This process of purification can be carried out with very little loss and in this way most of the uranium X in equilibrium with a large quantity of uranyl nitrate can be concentrated into 5 c.c. of solution containing only a few milligrammes of cerous nitrate.

Separation of the Uranium II.

It is well known* that uranium is deposited electrolytically as oxide from weakly acid (2 c.c. of glacial acetic acid per litre) solutions at 70° C. This method of separation is very suitable, since it yields the uranium in a thin film suitable for measurement and can be carried out in a closed vessel, so that the risk of radioactive contamination is very much decreased.

Since under the most favourable conditions one could not obtain more than 10^{-7} grm. of uranium II, it is essential to make sure that the small quantity of uranium II which is formed from the UX is actually deposited on the cathode, since the principle of the method is to count the α -particles emitted by all the uranium II formed in a given time. The simplest way of ensuring that this very small quantity of uranium II is deposited is to raise the concentration of the uranyl ion present by adding a known amount of the electrochemically identical but much less radioactive isotope, uranium I (as "uranium" UI and UII). If it can be shown that at this higher concentration all the added isotope has been deposited, then it follows that the whole of the uranium II has also been deposited.

Preliminary experiments were carried out in which a small weighed quantity of uranyl acetate was added to a cerous nitrate solution similar to that which would contain the UX, UII mixture and the amount separated electrolytically measured by counting the α -particles from it. The electrolytic cell used is shown in fig. 1, and consisted of an electrically heated glass vessel with a small

* Smith's "Electrochemistry."

platinum anode sealed through the bottom, a removable cathode made by sealing a stout platinum plate to a glass stem so that only one side was exposed, and a ground stopper to prevent the entrance of dust and loss by evaporation.

For measurement the cathode was placed in the ionisation chamber shown in fig. 2. This consisted of an insulated cylindrical chamber A which could be raised to a high negative potential, carrying at one end the platinum cathode. The ions formed by an α -particle emitted into the chamber from the cathode were collected by the insulated disc B which was connected directly to the grid of a 6-stage resistance capacity amplifier. The sudden potential change of the plate of the last valve caused by the passage of an α -particle through the chamber was recorded photographically on a cinematograph film. It was found that if all the surfaces of the chamber were nickel plated, using a bath from which radium emanation had been removed by boiling, the "natural contamination" was not more than 1 α -particle in 2 minutes. No spontaneous emission of ionising particles by the platinum plate was noticed.*

For an experiment the cathode was first thoroughly cleaned, washed, dried, transferred to the chamber, and the number of α -particles emitted in 1 to 2

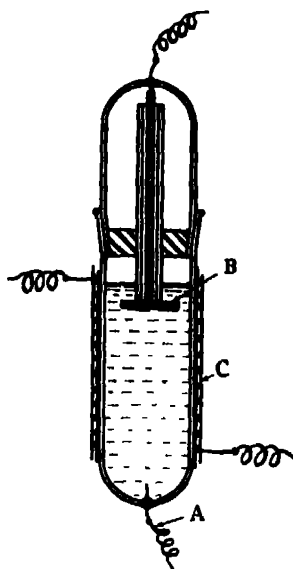


FIG. 1.—Electrolytic Cell.
A, anode; B, removable cathode; C, heating element.

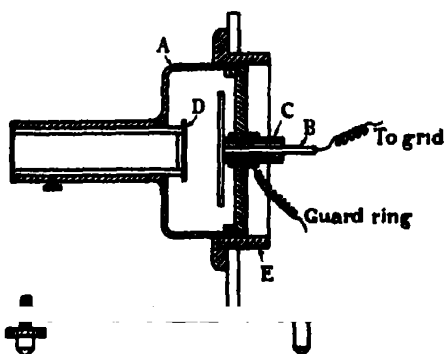


FIG. 2.—Ionisation Chamber. A, insulated cylinder at high potential; B, electrode connected to amplifier; C, silica insulation; D, platinum cathode; E, ebonite insulation.

* Hoffmann, 'Z. Physik,' vol. 7, p. 254 (1921).

hours counted. This blank was subtracted from the number emitted after the electrolysis, and was always determined separately for each experiment. It varied between $\frac{1}{2}$ and 1 α -particle per minute according to the thoroughness of the cleaning process.

The apparatus was now standardised by taking a cerium nitrate solution differing from that in which the UII was growing only by the absence of the minute concentrations of UX and UII. To this was added a known quantity of uranium. The added uranium was then deposited electrolytically on the platinum cathode and the number of α -particles emitted compared with the theoretical number which would have been emitted if all the added uranium had been deposited.

The results of the actual experiment are given below and show that all the added uranium is deposited when the amount added is more than 0.01 mg.

20 c.c. of acetic acid solution containing 40 mg. of crystalline cerium nitrate were electrolysed at 70° C. to remove any impurities, and the platinum plate cleaned and a blank taken. A weighed quantity of standard uranyl acetate solution was then added from a small weight pipette and the electrolysis repeated. The platinum plate was then removed, washed, dried, and the number of α -particles it emitted counted. The platinum cathode was then cleaned, a further weighed quantity of uranium added to the same solution, and the electrolysis repeated.

In this way the following results were obtained.

Number of electrolysis.	Weight of solution added.	Weight of uranium added.	Number of particles per minute.	Number per 0.01 grm. solution.
	grm.	grm.		
1	0.0704	2.01×10^{-5}	10.2	1.45
2	0.0608	1.73 "	12.1	1.99
3	0.0568	1.62 "	8.7	1.54
4	0.0423	1.21 "	5.13	1.21
5	0.0471	1.34 "	5.12	1.09
6	0.0487	1.39 "	5.66	1.16
7	0.0325	0.93 "	3.44	1.06
8	0	—	0.2	—

Since the standard solution contained 500 mg. of uranyl acetate (57 per cent. U) per litre, 0.01 c.c. contained 2.85×10^{-6} grm. of uranium, while each gramme of uranium gives about 2.4×10^4 α -particles per second.

Therefore each 0.01 c.c. of solution should give $2.85 \times 10^{-6} \times 60 \cdot 2.4 \times 10^4 = 4.10$ α -particles per minute; but half of these are emitted backwards into the plate so that the maximum number of α -particles to be expected from

0.01 grm. of solution is 2.05 per minute. The reason why less than this number (on an average 1.36) is found is to be accounted for by the deposition of the uranium oxide in patches and small holes in the surface of the plate which prevent all the particles emerging into the ionisation chamber. If it were due to incomplete deposition of the uranium the numbers in the last column would rise steadily and No. 8 which contained no added uranium would show practically no drop in the number of α -particles emitted. In the calculations which follow the experimentally found factor 0.331 for the ratio

$$\frac{\alpha\text{-particles observed after electrolysis}}{\text{total number of } \alpha\text{-particles emitted by the added uranium}}$$

has been adopted; the difference between this factor and the theoretical factor 0.5 is not more than can be accounted for by the shielding effect of a sensibly rough plate.

Three separate experiments were made to determine the period of UII. The first was done with a small quantity of uranium X to make sure that no unforeseen errors had been overlooked. It revealed a chemical difficulty which prevented the result obtained from being quite conclusive, and which was avoided in the subsequent experiments. The condition essential for the electrolytic deposition of uranium is a very small hydrogen ion concentration (2 c.c. of acetic acid per litre). If the solution has considerably higher hydrogen ion concentration, small quantities of uranium remain in the solution and are not deposited.

The uranium X cerous nitrate solution, as prepared, contains free nitric acid which must be removed. This was done by evaporating the solution to dryness and dissolving the crystalline cerous nitrate in acetic acid of the appropriate strength. It was found that solutions so prepared were cloudy owing to the formation of a small amount of oxide which could however be removed by filtration. In neutral (or slightly acid) solution UX is extremely easily absorbed on filter paper, and with the small quantity of uranium X it was not feasible to filter the solution. An unknown proportion of the UX was therefore in the solid state, and it is possible that the UII atoms formed by its decay might be entangled in the interior of the solid and not find their way into the solution from which they were being removed electrolytically. No way of avoiding this difficulty was discovered except to prepare so strong a source of UX that one could afford to neglect the loss on filtering the weak acetic acid solution.

In the second experiment about 15 kg. of uranyl nitrate were used as starting

material, which had been used 4 years before as a source of UX, and had at that time been freed from thorium; however, it contained some ionium which had grown in the meantime. This solution was extracted three times to remove the UX, Io mixture, and the UX allowed to grow, and concentrated as described. In the electrolysis of this solution it was found that a small quantity of UX (and therefore of the isotopic ionium) was adsorbed on the deposited uranium oxide. The original uranyl nitrate had not been freed entirely from ionium, and thus an additional source of α -particles was introduced. Since this was proportional to the amount of UX deposited, the magnitude of this contribution could be estimated by measuring the β -ray activity of the deposited uranium. But, as the number of α -particles due to uranium II is obtained by difference, this contamination reduces the accuracy of the method. For this reason great care was taken in the third experiment to free the uranyl nitrate as completely as possible from ionium so that this source of error should be avoided. In the second and third determination the slightly acid UX cerium solution was filtered directly into the electrolytic cell and the quantity of UX introduced obtained by measuring the β -ray activity of an aliquot part (1 c.c.) of the solution. There can, therefore, be no doubt that all the UII formed was in solution.

The third determination was carried out in the same way as the second, but using UX which had grown for 29 days in 10 kg. of uranyl nitrate which had been previously completely freed from all isotopes of UX.

The actual results obtained are given below.

Experiment I.—The uranium X solution was twice electrolysed so as to free it from any traces of uranium, a small quantity of uranium being added at the second electrolysis so as to make sure that the conditions were suitable for the deposition.

The UX had a β -ray activity of 20.5 d.p.m.* an amount in equilibrium with 172 grm. of uranium.

After 26 days 0.0574 grm. of standard uranyl acetate solution ($1.64 \cdot 10^{-5}$ grm. of U) was added, and the uranium separated electrolytically.

0.23 d.p.m. of β -ray activity were adsorbed.

The blank gave 0.41 α -particles per minute.

After electrolysis 571 α -particles were counted in 97 minutes 25 seconds = 5.41 ± 0.25 particles per minute from $1.64 \cdot 10^{-5}$ grm. of uranium.

* Since only relative all β -ray activities are expressed at the rate of collapse in divisions per minute of a gold leaf β -ray electroscope with a 100 μ aluminium foil base.

After $27\frac{1}{2}$ days 0.0566 gm. of uranyl acetate solution ($1.61 \cdot 10^{-5}$ gm. of U) were added, and the electrolysis repeated.

Blank = 1.2 per minute.

β -ray activity adsorbed = 0.00.

589 α -particles were counted in 102 minutes 27 seconds or 4.55 ± 0.25 α -particles per minute from $1.61 \cdot 10^{-5}$ gm. of uranium.

Experiment II.—(a) The uranium X, which was known to contain a small quantity of ionium, was dissolved in the appropriate acetic acid solution and filtered into the cell, the solution cleaned by a preliminary electrolysis and then a weighed quantity of standard uranium acetate added. Time = 0.

The uranium X introduced had a β -ray activity of 57.7 d.p.m., a quantity in equilibrium with 483.4 gm. of uranium.

Blank = 0.75 α -particles per minute.

β -ray activity adsorbed = 1.27 d.p.m.

Weight of solution added = 0.0379 gm. ($1.08 \cdot 10^{-5}$ gm. of uranium).

2172 particles were emitted in 172 minutes 44 seconds or 11.8 ± 0.25 particles per minute from $1.08 \cdot 10^{-5}$ gm. of uranium.

(b) Time = 28 days.

A further 0.0560 gm. of uranium acetate solution ($1.60 \cdot 10^{-5}$ gm. of U) were added and separated electrolytically.

Blank = 0.75 α -particles per minute.

β -ray activity adsorbed = 0.57 d.p.m.

2593 particles were emitted in 166.8 minutes = 14.8 ± 0.3 α -particles per minute from $1.60 \cdot 10^{-5}$ gm. of uranium.

(c) Time = 37 days.

A further 0.0515 gm. of uranium solution ($1.47 \cdot 10^{-5}$ gm. of U) were added and separated.

Blank = 0.64 α -particles per minute.

β -ray activity carried down = 0.39 d.p.m.

2644 particles were counted in 185 minutes 55 seconds = 13.7 ± 0.25 particles per minute from $1.47 \cdot 10^{-5}$ gm. of uranium.

The counted α -particles had three separate sources: (a) The added uranium, (b) the adsorbed ionium, (c) the extra UII produced by the decay of the UX. (c) is only present to an appreciable extent in the second source.

Experiment III.—About 10 kg. of uranyl nitrate dissolved in ether were freed from isotopes of thorium, UX being used as a radioactive indicator.

After 29 days the UX which had grown was separated and freed from all uranium as previously described.

(a) The uranium X introduced at time $t = 0$ had β -ray activity of 37.5 d.p.m., a quantity in equilibrium with 356 grm. of uranium.

(b) $t = 39\frac{1}{2}$ days.

Blank = 1.48 α -particles per minute.

β -ray activity absorbed 0.77 d.p.m.*

0.0624 grm. of uranyl acetate ($1.78 \cdot 10^{-5}$ grm. of U) were added to the solution, and separated electrolytically.

1679 α -particles were counted in 115 minutes 39 seconds = 13.06 ± 0.3 α -particles per minute from $1.78 \cdot 10^{-5}$ grm. of uranium.

(c) $t = 46.6$ days.

Blank = 1.70 α -particles per minute.

β -ray activity adsorbed = 0.43 d.p.m.

0.0623 grm. of uranyl acetate of uranium solution ($1.78 \cdot 10^{-5}$ grm. of U) were added and separated by electrolysis.

1470 α -particles were counted in 119 minutes 43 seconds = 10.59 ± 0.3 α -particles per minute from $1.78 \cdot 10^{-5}$ grm. of uranium.

Discussion of the Results.

In this discussion the following numerical values are used:—

The decay constant for uranium I	= $\lambda_1 = 4.9 \cdot 10^{-18} \text{ s}^{-1}$
„ uranium X	= $\lambda_2 = 2.81 \cdot 10^{-2} \text{ d}^{-1}$
„ ionium	= $\lambda_3 = 2.4 \cdot 10^{-13} \text{ s}^{-1}$
Avogadro's number	= $N = 6.06 \cdot 10^{23}$.
Amount of uranium X in equilibrium with unit quantity of uranium	= $1.4 \cdot 10^{-11}$

(a) The number of α -particles emitted from the uranium II formed by the decay of the uranium X in equilibrium with 100 grm. of uranium.

There are $100/238.6 \cdot 0.6 \cdot 10^{23} \cdot 1.4 \cdot 10^{-11} = 3.53 \cdot 10^{12}$ atoms of UX in equilibrium with 100 grm. of uranium, and when n of this has decayed it will form $3.53 \cdot 10^{12} n$ atoms of uranium II which will emit $3.53 \cdot 10^{12} n \lambda$ α -particles per second, where λ is the decay constant of uranium II. Using the experimentally found factor 0.331, one will expect actually to observe $7.0 \cdot 10^{13} \lambda \cdot n$ α -particles per minute in the ionisation chamber after electrolysis.

* These values, though measured on a more sensitive electroscope, have been converted to the same scale as the original measurement of the β -ray activity taken for the experiment.

- (b) If λ were $1.7 \cdot 10^{-12} \text{ s}^{-1}$, which corresponds to a half life period for uranium II of $1.3 \cdot 10^6$ years, one would have observed in experiment I, 103, in experiment II, 312, in experiment III, 283 α -particles per minute. Since no such number was found in any of the experiments it is clear that the period of uranium II cannot be of the order 10^6 years, but may be as small as 10^6 years.
- (c) It will now be shown that both in experiment II and experiment III if a correction be made for the α -particles emitted by the ionium, then it is not necessary to attribute more than one α -particle per minute to uranium II in order to account for the results obtained.

Experiment II.—In this experiment the uranium X was mixed with an unknown amount of the isotopic ionium, but the ratios of the quantities of the ionium adsorbed in the three separations can be calculated from the measured amounts of uranium X adsorbed.

Using the results from the first and last separations at $t = 0$ and $t = 37$ days, which do not contain any important quantity of uranium II, it is possible to make a rough estimate of the number of α -particles due to adsorbed ionium. Using this figure one finds that 14 ± 2 α -particles per minute were contributed to the second separation from the added uranium and the adsorbed ionium, while 14.8 were observed. If the uranium II present had contributed 4 α -particles per minute these would have been detected in spite of the ionium, so that the maximum value of λ consistent with this experiment is given by

$$7 \cdot 10^{13} \cdot \lambda \cdot 4.8 \cdot 0.545 < 4 \quad \text{or} \quad \lambda < 2.2 \cdot 10^{-14} \text{ s}^{-1},$$

so that the half life period of uranium II $> 1.0 \cdot 10^6$ years.

Experiment III.—If no correction is applied for the ionium one has $13.06 - 10.59 = 2.47$ α -particles per minute to be attributed to uranium II. Thus, using the uncorrected result we have $7.0 \cdot 10^{13} \lambda \cdot 3.56 \cdot 0.636 = 2.5$, since 0.636 of the uranium X used had decayed when the separation was made. This gives $\lambda = 1.58 \cdot 10^{-14} \text{ s}^{-1}$ or $T = 1.3 \cdot 10^6$ years. Since the uranyl nitrate used in this experiment was initially free from ionium it is possible to calculate the number of α -particles contributed by the ionium. If 238 grm. of uranium are left for a time t , $(1 - e^{-\lambda t})$ of the equilibrium amount of UX will have grown together with $N\lambda_1 t$ atoms of ionium which will emit $N\lambda_1 t \lambda_2$ α -particles per second. It may thus be calculated that the uranium X grown in 29 days from 238 grm. of uranium initially free from ionium would be in equilibrium with 133 grm. of uranium and would emit 1.79 α -particles per second from the ionium formed during its growth.

Since the UX in equilibrium with 100 grm. of uranium showed a β -ray activity of 10.5 d.p.m., each unit of β -ray activity in this experiment will also emit $\frac{1.79}{1.33 \cdot 10.5} = 0.128$ α -particles per second when originally separated from the uranium. The beginning of the experiment $t = 0$ was 14 days after the original separation of the uranium X from the uranium, so that each unit of β -ray activity then emitted is 0.189, i.e. $0.128/e^{-\lambda_1 \cdot 14}$ α -particles per second = 11.4 α -particles per minute.

During the experiment the uranium X continued to decay so that the ionium associated with each division of β -ray activity emitted after 39.5 days 31.25, after 46.6 days 42.1 α -particles per minute. If we assume that the ratio

$$\frac{\alpha\text{-particles observed}}{\alpha\text{-particles theoretically emitted}}$$

is 0.331, as was obtained experimentally, we would expect in the first electrolysis $0.331 [0.77 \cdot 31.25 + 4.1 \cdot 6.24] = 15.9$ α -particles per minute, in the second electrolysis $0.331 [0.43 \cdot 42.1 + 4.1 \cdot 6.23] = 14.5$ α -particles per minute. For an absolute calculation of this type the agreement between the observed and calculated values is extremely good, the difference being no more than would be expected from the uncertainty in the factor 0.331.

The conclusion to be drawn from this calculation is that of the 2.5 α -particles per minute difference between the two separations $15.9 - 14.5 = 1.4$ are to be attributed to differences in the amount of adsorbed ionium, so that only 1.1 can be attributed to uranium II. This correction raises the lower limit for the half life period of uranium II to about $2.5 \cdot 10^6$ years.

The results of the three concordant experiments show that the half life period of uranium II is not less than a million years, thus definitely excluding the value $1.3 \cdot 10^4$ years deduced by applying the Geiger-Nuttall rule to a range of 3.28 cm. for the α -particle from uranium II.

It is, of course, impossible to distinguish whether the error lies in the measurement of the range or in the application of the Geiger-Nuttall rule, but the following facts also indicate a long period of uranium II :—

- (a) In the original determination of the range of the α -particles from uranium by Geiger (*loc. cit.*), some ionium was intentionally mixed with the uranium oxide and there was no evidence that the range of the α -particles from uranium exceeded that of those from ionium (3.19 cm.).
- (b) The deviations from the Geiger-Nuttall rule indicated by theory increase the range of the α -particle from uranium II, associated with a given

period. Using the original value $R_{15} = 3.07$ cm. for the α -particles from uranium II, Gamov and Houtermans* calculations lead to a half period value of $7 \cdot 10^7$ years. Although these calculations are admittedly approximate, they have hitherto indicated deviations from the simple Geiger-Nuttall rule in the same sense as experience.

- (c) It was shown by Soddy, 'Phil. Mag.', vol. 19, p. 343 (1910), that the product of uranium X, if it underwent α -particle disintegration, had a period of half life greater than $3.5 \cdot 10^4$ years.

The method described in the present paper is not suitable without modification for measuring a half life period of uranium II much greater than a million years, and further experimental work is in progress. The important result obtained is that this period is not of the order ten thousand years and is probably more than one million years.

In conclusion, I have to thank Professor Lindemann for his continued interest, for many helpful suggestions and for extending to me the facilities of his laboratory.

Summary.

The half life period of uranium II is shown to be at least a million years and not ten thousand years as has been recently suggested. The method used was to separate electrolytically the uranium II formed by the decay of a known quantity of uranium X mixed with a small known weight of ordinary uranium. The α -particles from this source were counted electrically, and those due to the uranium II obtained by difference.

* 'Z. Physik.', vol. 52, p. 453 (1928).

The Reflection of Vapour Molecules at a Liquid Surface.

By T. ALTY, D.Sc., Ph.D., Professor of Physics, University of Saskatchewan,
Canada.

(Communicated by Sir Joseph Thomson, F.R.S.—Received February 4, 1931.)

[PLATE 23.]

Introduction.

The rate of evaporation of a liquid may be calculated from the kinetic theory of gases if it be assumed that all vapour molecules which strike the surface enter the liquid and that, as a first approximation, the vapour behaves as a perfect gas. Under these circumstances, it follows from the kinetic theory of gases that

$$\begin{aligned} m &= \text{mass of molecules leaving unit area per minute} \\ &= \text{mass of molecules striking unit area per minute from the saturated} \\ &\quad \text{vapour} \\ &= 14.63 P_s / \sqrt{T}, \text{ gram/sq. cm./min.}, \end{aligned} \tag{1}$$

where P_s is the saturated vapour pressure in millimetres of mercury at the surface temperature T , ° A.

So far as can be found, this equation has not been verified for water. It will be valid only if there is no reflection of vapour molecules at the surface so that every incident molecule enters the liquid. Before the use of the equation is justified in connection with the evaporation from a water surface, it is therefore necessary to show that there is no such reflection at this surface.

Previous work bearing on this subject has been published by Rideal* and by Langmuir.† Both these observers were particularly interested in the effects of insoluble films on the rate of evaporation of water, rather than in testing the validity of equation (1).

Rideal placed the water to be evaporated in one arm (A) of an inverted U-shaped vessel, the other arm (B) being maintained at 0° C. by immersion in a bath of melting ice. The arm (A) was surrounded by a water bath whose temperature could be varied. The vessel was exhausted so that the water could distil from the warm arm to the cold arm, and the rate of evaporation

* 'J. Phys. Chem.,' vol. 29, p. 1585 (1925).

† 'J. Phys. Chem.,' vol. 31, p. 1719 (1927).

was determined by weighing the cold arm from time to time. Under these conditions the pressure above the evaporating surface would not be zero as is required by equation (1). If the actual pressure were p mm. then a number of vapour molecules would strike the liquid and return to the latter. The net rate of evaporation into a space at pressure p might therefore be taken to be $m = (\text{mass leaving the liquid}) - (\text{mass returning to it})$

$$= 14 \cdot 63 (P_s - p) / \sqrt{T_s}. \quad (2)$$

Again, this equation will hold only if there is no reflection at the liquid surface.

The rate of evaporation under the conditions of Rideal's experiments was measured by him for pure water and for water covered by a monomolecular film of various substances. In the case of pure water Rideal found that the rates of evaporation measured experimentally were very much smaller than those given by equation (2). Now, in his calculation the pressure p of equation (2) was taken as the saturated vapour pressure at the temperature of the cold arm. As the pressure just above the evaporating surface must be greater than that in the cold arm to which the vapour is flowing, this assumption leads to a value of m which is too large. Also the temperature T_s in equation (2) is not exactly equal to the temperature of the water bath, but strictly should be taken as the temperature of the evaporating surface. If there is any pronounced evaporation from the surface the temperature of the latter must fall considerably, so that T_s must be smaller than the temperature of the bath. Since P_s decreases rapidly with T_s , the calculation of m for the temperature of the bath, instead of for that of the surface, will lead to a result which is too large.

It thus appears that the theoretical rate of evaporation as calculated by Rideal is considerably too large, while his experimental rate was smaller than the rate of evaporation into a vacuum. Hence, although the results shown in his paper give definite indication that the resistance to evaporation is increased when an insoluble film is placed on the water, they are not suitable for use as a test of equation (1).

Langmuir (*loc. cit.*) defines the "resistance to evaporation" as the reciprocal of the rate of evaporation. In Rideal's experiment, after allowing for condensation from the cold arm, he assumes that there are two such resistances :—

- (a) The surface resistance R_r .
- (b) The resistance due to diffusion of the evaporated molecules from the warm arm of the U tube to the cold arm.

In order to calculate the resistance R_f for film-covered water, Langmuir assumes that R_f for pure water is given by the reciprocal of equation (1) above, thus assuming that there is no reflection of vapour molecules at the liquid surface.

A test of the validity of equation (1) in the case of water therefore appears to be necessary, and the object of the experiments described below was to examine this equation as carefully as possible. The results obtained suggest that there may be very considerable reflection at the surface, so that only a fraction of the incident vapour molecules get into the liquid.

Let this fraction be f .

Then the mass of water evaporating per minute into a vapour space at pressure p will be

$$m = 14.63 (P_s - p) f / \sqrt{T_s} \quad (3)$$

while if the mass evaporating per minute into a perfect vacuum could be measured, then

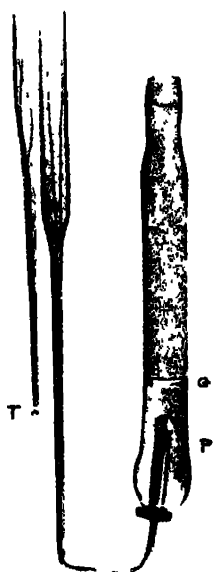
$$f = m \sqrt{T_s} / 14.63 P_s. \quad (4)$$

Experimental.

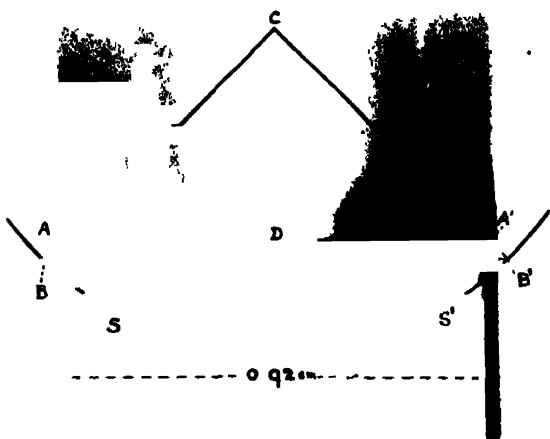
Preliminary work showed that, when the rate of evaporation is large, the surface temperature is very much reduced. When the evaporating water was placed in a water-bath at room temperature it was found possible to freeze the water by rapid evaporation. At higher temperatures this rapid evaporation will not cause the water to freeze, but it produces large temperature gradients in the liquid so that the latter boils instead of evaporating steadily. For this reason the temperature gradients were reduced as far as possible by supplying heat to the evaporating water at the greatest possible rate.

This was done by using a glass experimental cell with very thin walls, and immersing it in a mercury thermostat so as to increase the rate of heat transfer to the water. With these precautions it was possible to obtain large rates of evaporation without causing the liquid to boil or freeze.

The thin-walled experimental cell C (fig. 1b) was connected directly to the manometer M and through a leak L to a vacuum pump of large capacity. A set of these leaks, offering various resistances to the vapour flow, was constructed and the apparatus was arranged so that they could be interchanged with ease. In this way the pressure p above the evaporating surface could be controlled and the rate of evaporation for different values of p could be measured.



A.



B.

A tilted mercury manometer was used for the pressure measurements, the angle of inclination being decreased with the temperature of the bath so that

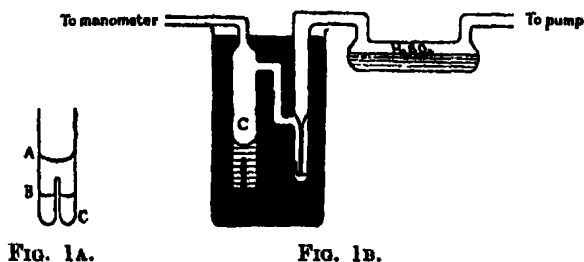


FIG. 1A.

FIG. 1B.

the sensitivity remained sufficiently great at all the temperatures considered. In order to minimise the chance of boiling, all water used was freshly distilled and boiled to remove air.

The experiment was performed in two parts.

First the temperature difference (ΔT) between the evaporating surface and the surrounding mercury bath was obtained as a function of p and the graph $\Delta T - p$ plotted. Then the rate of evaporation (M) was obtained as a function of p and the graph $M - p$ plotted. These graphs were extrapolated to cut the axis $p = 0$ at $\Delta T = \Delta T_0$ and $M = M_0$ respectively. M_0 is then the rate of evaporation into a vacuum* from a surface at the temperature ($T_B - \Delta T_0$), if T_B is the temperature of the bath. Under these conditions equation (4) should apply if we place

$$T_s = (T_B - \Delta T_0).$$

$$m = M_0/A.$$

$$P_s = \text{saturated vapour pressure at the temperature } T_s.$$

$$A = \text{surface area of the evaporating water.}$$

Consequently it should be possible to determine whether or not there is any reflection at the surface.

In order to measure the surface temperature a thermocouple was introduced into the experimental cell as shown in Plate 23, A, the other junction T being immersed in the mercury thermostat. The cell was filled up to a point A (fig. 1A) and the pump started. The temperature difference was measured every minute until the water had evaporated to a point B (fig. 1A) and the levels A and B were measured by means of a reading telescope. The time at which the thermocouple was in the surface was calculated from the total

* Assuming that the pressure fall between the liquid surface and the manometer connection is negligible, as is the case in these experiments.

change in level in the course of the experiment, and the thermocouple reading at this time was then taken as ΔT . This was repeated with each of the different leaks L and the $\Delta T - p$ graph plotted as above described.

It is clear that when the thermocouple sheath projects through the evaporating surface, the area of the latter will be slightly altered and the rate of evaporation will be altered correspondingly. Measurements of the rate of movement of the meniscus first in the position A and then in the position B show that this change is small so that there will be little error in the above estimation of ΔT .

In the measurement of M , however, it is advisable to eliminate this change in the surface area and for this reason each such experiment was commenced with the meniscus in a position such as A (fig. 1A) and ended before the thermocouple sheath penetrated the surface.

For this determination of M , a weighed quantity of water was placed in the cell and the evaporation was allowed to proceed for a known time so that M was obtainable from the loss of weight. During the course of all these experiments a small stopper was placed in the lower end of the thermocouple sheath so as to prevent the ascent of the mercury to varying levels up the sheath in different experiments.

Results.

The curves of $\Delta T - p$, and $M - p$ for the cases in which the thermostat temperatures were 60°C ., 40°C . and 18°C . are shown in figs. 2, 3, and 4, respectively. It will be seen that these curves approach the pressure axis at a relatively sharp angle so that a fair estimate of the ordinates corresponding to $p = 0$ seems possible.

Before the fraction of molecules entering the liquid can be calculated from the values of $(\Delta T)_0$ and M_0 obtained from these curves, it is necessary to measure the area of the evaporating surface. The external diameter of the experimental cell was 0.92 cm. , so that the water surface was neither large enough to be treated as plane nor small enough to be approximately hemispherical. The area was therefore obtained from a photograph of the meniscus. In order to eliminate distortion, the cell, about half full of water, was lowered into a water-filled rectangular glass vessel until the meniscus was submerged. The latter was then photographed through the sides of the rectangular vessel and the photograph enlarged as in Plate 23, B. It will be noted that when photographed through the water in this way, the meniscus is clearly defined almost to its point of contact with the glass walls of the experimental cell.

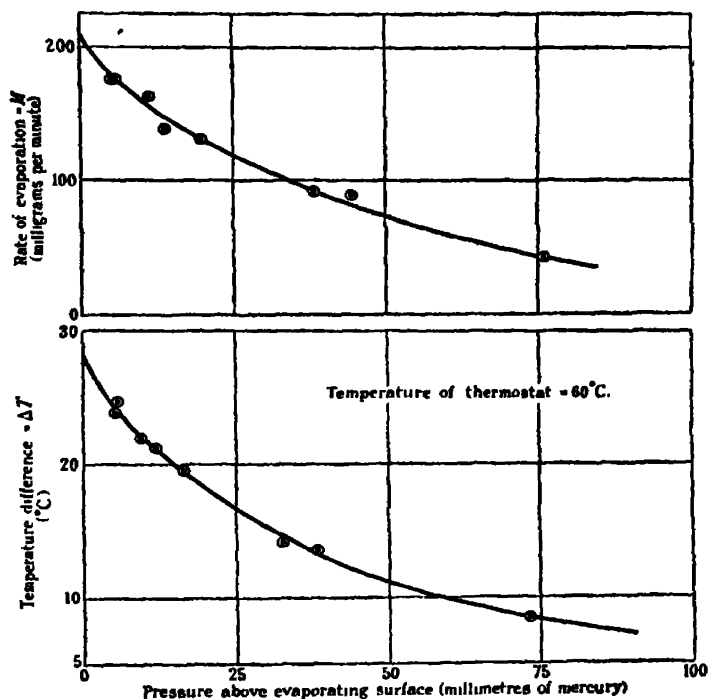


FIG. 2.

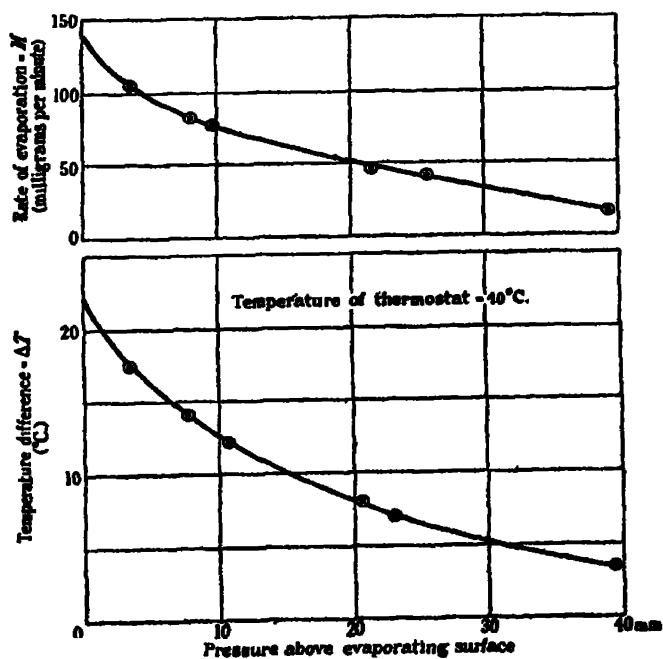


FIG. 3.

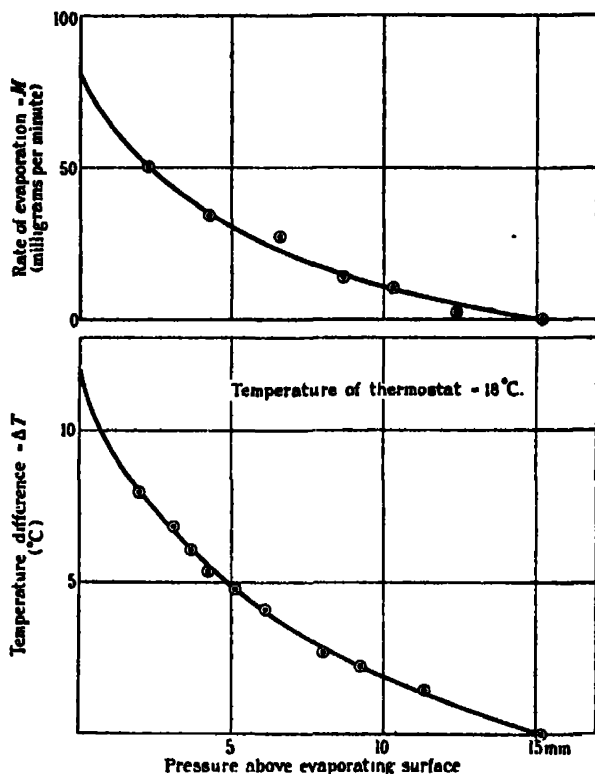


FIG. 4.

The area was estimated by fitting to the actual meniscus the spherical cap BSB'. These two curves fit very well except near the edges of the glass tube and the area of the evaporating surface was taken as being equal to the area of the spherical cap BSB', the length of whose arc BB' is equal to the total length AA' of the liquid surface, i.e.,

$$\text{arc BS} = \text{arc AS}$$

and

$$\text{arc B'S'} = \text{arc A'S'}.$$

Calculation of the area of this cap gives

$$A = 0.84 \text{ sq. cm.}$$

The fraction of molecules incident on the liquid surface which are able to enter the liquid may now be obtained from equation (4).

The values of ΔT_0 and m as deduced from figs. 2, 3 and 4, and the fractions f calculated from them, are given in the following table.

Table I.

T_s , °C.	$(\Delta T)_0$, °C.	T_r , °C.	$\frac{m_0}{\text{gram/sq. cm/min.}}$	P_r , mm. Hg.	f .	F .	t , sec.
60	28.0	32.0	24.9×10^{-3}	35.32	8.3×10^{-3}	0.8	6.00×10^{-4}
40	22.5	17.5	16.9×10^{-3}	14.86	13.1×10^{-3}	1.3	8.53×10^{-5}
18	12.1	5.9	9.53×10^{-3}	6.96	15.5×10^{-3}	1.5	15.7×10^{-5}

In this table $F = 100 f$ = percentage of incident molecules entering the liquid.

It therefore appears that only about 1 per cent. of the incident vapour molecules is able to enter the liquid, so that there must be very considerable reflection at the surface of the latter.

Relation between ΔT and M .

When the liquid is evaporating and the pressure of the vapour above it is p mm. there will be associated with this value of the pressure, a definite rate of evaporation (M) and temperature difference (ΔT) between the surface and its surroundings. A simple relation might be expected to exist between these sets of corresponding values of M and ΔT .

When the evaporation is proceeding, heat is supplied to the cooler surface layers of the liquid by the mass of liquid below it. The rate of heat supply to the surface will be proportional to the temperature difference between the surface and the thermostat and may be written as $k \cdot \Delta T$, k being considered constant.

If L is the latent heat of evaporation at the temperature of the surface, the rate of loss of heat by the surface will be ML , and, since the surface temperature remains constant, these two quantities of heat must balance so that

$$M = (k/L) \cdot \Delta T.$$

Hence, ignoring the small changes in L , M will vary as ΔT . The relation between M and ΔT for various values of p is shown in fig. 5, which represents the experiment at 40° C. and indicates clearly that the above relationship between these quantities holds good throughout the range of pressure from the saturated vapour pressure $p = 54.8$ mm. to $p = 3$ mm.

Further evidence in favour of the suggestion that there is very pronounced reflection at the liquid surface is obtainable from this graph if we make the assumption that ΔT will remain proportional to M for all values of the pressure

up to $p = 0$. There appears to be no reason to doubt the truth of this assumption in view of the wide range of pressures considered in fig. 5.

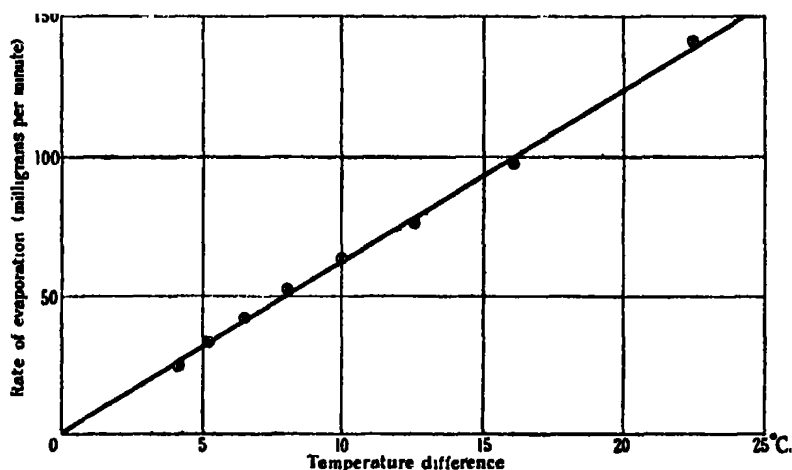


FIG. 5.

The straight line graph of fig. 5 may be represented by the equation

$$M = \frac{5 \times 10^{-3}}{8} \Delta T = \frac{5 \times 10^{-3}}{8} (T_B - T_s),$$

$$= 6.25 \times 10^{-3} (40 - T_s) \text{ gram per minute,}$$

if T_s is in degrees Centigrade, or

$$m = M/A = 7.45 \times 10^{-3} (40 - T_s) \text{ gram per square centimetre per minute.} \quad (5)$$

Hence m will increase linearly with decrease of T_s .

On the other hand, the mass evaporated per square centimetre per minute on the assumption that there is no reflection at the surface is

$$m = 14.63 P_s / \sqrt{T_s}, \quad (6)$$

so that this mass decreases with T_s .

There therefore remains a possibility of avoiding the conclusion that vapour molecules are reflected at the liquid surface. This is that, between the pressures $p = 3$ mm. and $p = 0$, the surface temperature decreases by more than the amount shown in fig. 3. If this decrease is sufficiently great the actual amount evaporating per minute as given by (5) may agree with the theoretical amount as given by (6), in which case there would be no reflection of molecules at the surface.

The necessary temperature difference ΔT for no reflection may be obtained by plotting the quantities m , as derived from (5) and (6), against T_s , the surface temperature. The point of intersection of the resulting curves then gives the surface temperature at which the amount actually evaporated per minute will agree with that theoretically possible when there is no reflection. Fig. 6 shows graphs of equations (5) and (6). They intersect at $T_s = -26.5^\circ \text{C.}$ or $\Delta T = 66.5^\circ \text{C.}$

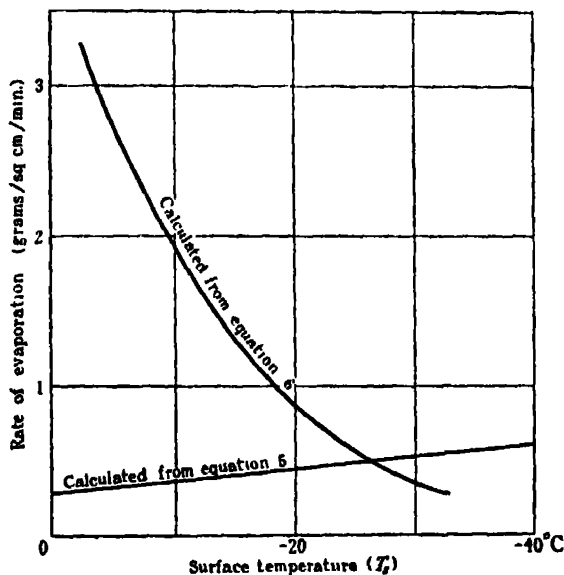


FIG. 6.

If therefore the water obeys equation (1) even approximately, it is necessary to suppose either that not all the vapour molecules striking the liquid surface are able to enter the liquid, or that in reducing the pressure above the liquid from $p = 3 \text{ mm.}$ to $p = 0$, the surface temperature is reduced by almost 50°C. from $T_s = +22^\circ \text{C.}$ to $T_s = -26.5^\circ \text{C.}$ This latter supposition seems improbable, and it is therefore assumed that the curves of figs. 2, 3 and 4 have approximately the form indicated and that there is pronounced reflection at the liquid surface.

Average Life of a Liquid Molecule in the Surface.

If it is assumed as a rough approximation that the water molecule in the surface acts as a sphere of radius $2 \times 10^{-8} \text{ cm.}$ (cf. Debye, "Polar Molecules," p. 85), the average period (t) which any one evaporating molecule spends in the surface can be calculated from the above results. The values of t so obtained

are shown in Table I from which it appears that the life of a surface molecule is not greater than about 10^{-5} seconds.

Summary.

The rate of evaporation from a water surface is measured as a function of the vapour pressure above the evaporating surface. By extrapolation to zero pressure the rate of evaporation into a vacuum is deduced.

On comparison of this experimental result with the formula of the kinetic theory of gases for the number of vapour molecules striking a water surface per second from the saturated vapour, it appears that only about 1 per cent. of the molecules incident on the surface are able to enter the liquid. This result is taken to indicate that there must be very pronounced reflection of water vapour molecules at the liquid surface.

Viscosity and Rigidity in Suspensions of Fine Particles.

II.—Non-Aqueous Suspensions.

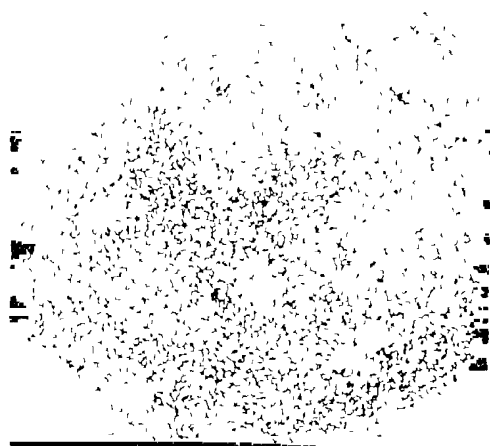
By C. M. McDOWELL and F. L. USHER, The University, Leeds.

(Communicated by R. Whytlaw-Gray, F.R.S.—February 14, 1931.)

[PLATES 24–26.]

In the first part* of this investigation evidence was presented for the view that the shear-variable viscosity exhibited by aqueous suspensions containing suitable amounts of an electrolyte is due to the formation of loosely packed aggregates which enclose varying quantities of the dispersion medium. The progressive liberation of liquid as the aggregates are broken up by increasing shear gradients is equivalent to a gradual diminution of the volume concentration of solid, and accounts qualitatively for the variation of viscosity observed; whilst a complete linking up of the aggregates throughout the liquid gives rise to a structure possessing rigidity, a property which was demonstrated in suspensions containing a high enough proportion of solid. The conclusions reached were speculative in so far as the association of microscopic particles to form any but gross aggregates cannot be directly observed. The present

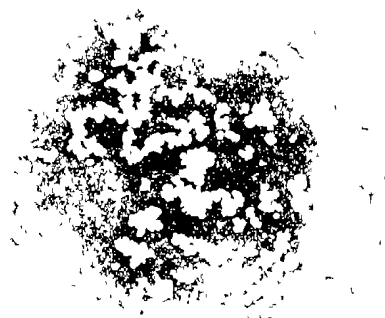
* 'Proc. Roy. Soc.,' A, vol. 131, p. 409 (1931).



(c) More concentrated suspension of starch protected by cellulose nitrate.



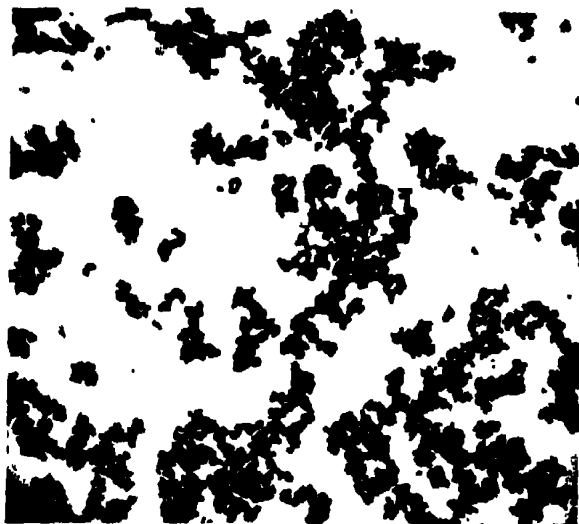
(b) Starch in mixture of equal density protected with 0.05 per cent rubber



(a) Unprotected starch in mixture of equal density (amylose acetate + tetrachloroethane).

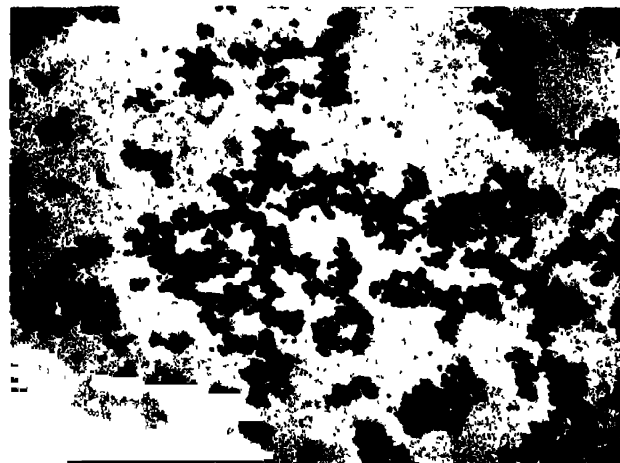
FIG. 1.

(Facing p. 564.)



(a) Ferric oxide in amyl acetate, unprotected.

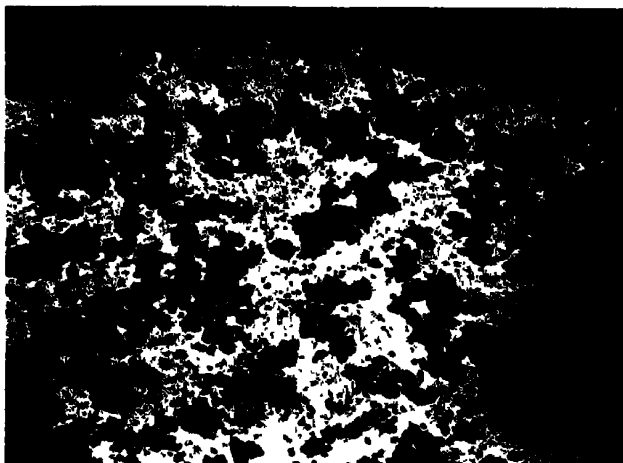
(b) Ferric oxide in amyl acetate protected by
cellulose nitrate.



(a) Gas black in amy! acetate, unprotected.



(b) Gas black in amy! acetate, protected by
0.5 per cent. cellulose nitrate.



(c) Gas black in bromoform mixture of equal
density, unprotected.

FIG. 3

communication describes evidence of a more complete character, provided by the microscopic examination of suspensions of visible particles in inert organic liquids, and the correlation of these observations with the results of parallel experiments on viscosity and rigidity.

EXPERIMENTAL.

Microscopic Observations.

Specimens of white lead, ferric oxide (rouge), rice starch, lampblack, and "gas black" were severally ground up with toluene, amyl acetate, or chlorinated hydrocarbons, and examined under a microscope by transmitted light. The appearance of all of them was very similar, consisting of loosely packed arboriform masses with patches of clear liquid. A careful and prolonged examination of starch was made with material which had been fractionally sedimented in water so as to contain particles of 2 to 3 μ equivalent diameter. The fractionated starch was dried at 100° and ground thoroughly in an agate mortar with a mixture of amyl acetate and tetrachloroethane of the same density, 1.515, as the solid. Fig. 1 (a) (Plate 24) shows a photograph of this, using an 8-mm. Leitz fluorite objective. The individual grains of the aggregates were at first in Brownian movement, and the filamentous texture was seen to become gradually more compact by collisions between its parts. The structure, once formed, was never observed to disintegrate spontaneously, but pressure on the cover glass caused it to break up into isolated grains and small aggregates which, however, collected together again when left undisturbed. The presence of branched aggregates in starch suspensions similar to those used by Hatschek and his co-workers is thus established by direct observation.

Another portion of the starch was ground up with the same liquid mixture containing 0.05 per cent. of raw rubber dissolved in it. The rubber served to "protect" the starch grains, and the starch so protected gave quite a different appearance, as shown in fig. 1 (b) (Plate 24). The distribution was seen to be remarkably uniform, and the starch grains were separate and showed no tendency to form aggregates, although in the more concentrated suspensions collisions were frequent. Fig. 1 (c) (Plate 24) shows a photograph of a concentrated suspension in amyl acetate containing a little cellulose nitrate as protective.

Although there was little doubt that the protective was actually adsorbed by the solid under the conditions of these experiments, the fact was definitely

ascertained by mixing a measured volume of dilute rubber solution (in which the content of rubber was known in terms of a standard solution of bromine in the mixed liquids) with a weighed quantity of starch. After adding a little amyl acetate to alter the density the starch was removed by centrifuging and the concentration of rubber in the remaining liquid was again determined. It was found that 18 per cent. of the rubber had been taken up by the starch, corresponding with about 0.001 gm. of rubber per 1 gm. of starch.

Fig. 2 (Plate 25) shows ferric oxide in amyl acetate, (a) unprotected and (b) protected by cellulose nitrate.

From the various substances examined starch and "gas black" were selected for experiments on viscosity and rigidity, on account of the fairly regular shape and convenient size of their particles and their low density. Gas black is of special interest in that the particles are very much smaller than those of starch, many of them being below the limit of microscopic resolvability. Two specimens were used (referred to as A and B), of which one (B) had grains considerably larger than the other. We are indebted to Messrs. Reckitt and to Messrs. Binney and Smith and Ashby for kindly supplying this material. The density of the black was found to be 1.81, and the liquid used to suspend it was a mixture of tetrachloroethane ($D = 1.60$) with bromoform ($D = 2.89$). Since the cellulose nitrate used for protection was not soluble in this liquid, the microscopic examination and measurements of viscosity of the protected material were made with suspensions in amyl acetate. As is evident from the photographs (fig. 3, (a) and (c), Plate 26) the behaviour of the unprotected gas black is not affected by this interchange of liquids, and it is therefore justifiable to conclude that the viscous behaviour of gas black in amyl acetate (which cannot be used for the unprotected substance on account of the difference in density) would be substantially the same as that observed in the mixture of equal density. Fig. 3 (b) shows the gas black in amyl acetate protected with 0.5 per cent. of cellulose nitrate and it is clear that, although on account of their small size some of the original aggregates have escaped grinding, the particles are fairly uniformly distributed. They were seen to be in vigorous Brownian movement which, together with their smallness, made it impossible to obtain a clear photograph of the individual particles.

Viscosity Measurements.

The concentric cylinder apparatus used for measuring the viscosity was the same as that already described in Part I. The starch (or gas black) was ground in a ball mill with the dispersion medium for 12 to 24 hours, and afterwards

diluted, if necessary, and re-ground for a shorter time. The solids were dried by heating at 100° , and the liquids by means of calcium chloride.

Starch.—Fig. 4 shows the viscosities at different rates of shear of (a) a mixture of amyl acetate and tetrachloroethane of density 1.515; (b) the mixed liquids

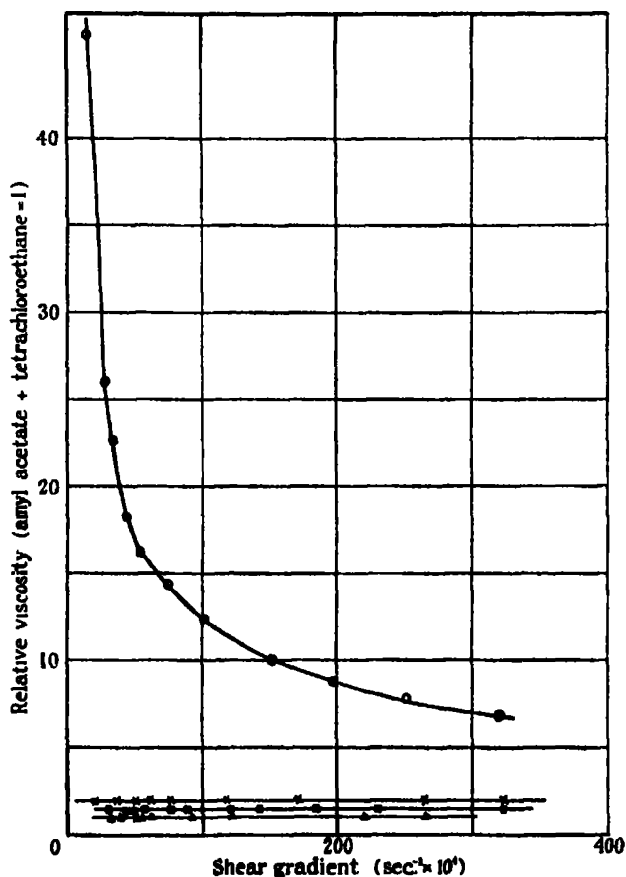


FIG. 4.—Viscosity of mixture of amyl acetate and tetrachloroethane (Δ); mixture + 0.05 per cent. rubber (\square); 6 per cent. suspension of starch protected with 0.05 per cent. rubber (\times); 6 per cent. suspension of starch unprotected (\circ).

with 0.05 per cent. of rubber; (c) a 6 per cent. suspension of starch in the mixed liquids with 0.05 per cent. of rubber; and (d) a 6 per cent. suspension of unprotected starch. (A trace of quinol was dissolved in the liquids containing rubber in order to retard its oxidation, since it was found that after a time varying from a few days to 2 or 3 weeks the starch ceased to be protected unless an anticatalyst was present.) The viscosities are relative, that of the dispersion medium being taken as 1. All the liquids excepting the unprotected

starch gave an approximately constant value for the coefficient of viscosity, whereas the unprotected starch showed a large increase at low rates of shear.

Gas Black.—For the measurements of viscosity of this material an outer cylinder of diameter 6.40 cm. was used, and a new quartz fibre of torsional modulus 0.285 dyne-cm. The apparatus was further modified by using a gramophone motor in place of the electric motor for driving the rotating table, and additional reducing gear was introduced. In this way the apparatus was made 23 times as sensitive as previously, and rates of shear as low as 9×10^{-6} sec.⁻¹ could be used. The extreme shear gradients were in the ratio 11400 : 1. In this, as in the previous series, the viscosity of liquids of normal behaviour could not be measured at very low rates of shear owing to the smallness of

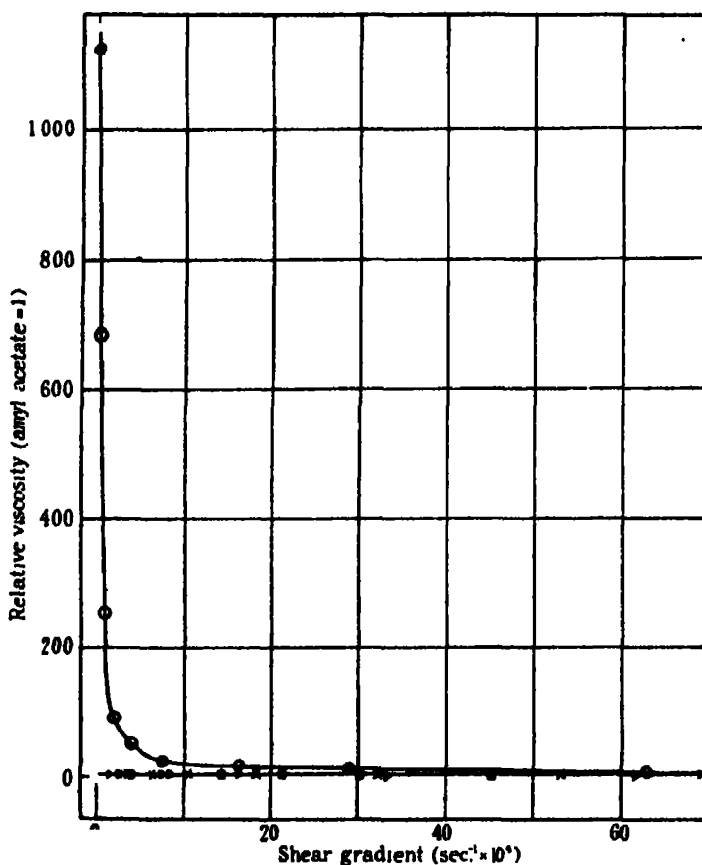


FIG. 5.—Viscosity of mixture of bromoform and tetrachloroethane (□); amyl acetate + 0.5 per cent. cellulose nitrate (×); 0.13 per cent. gas black in amyl acetate protected with 0.5 per cent. cellulose nitrate (Δ); 0.13 per cent. gas black in mixture unprotected (○).

the torque produced. The curves in fig. 5 show the relation between shear gradient and viscosity of (a) a mixture of bromoform and tetrachloroethane of density 1.81; (b) the same mixture containing 0.13 per cent. of unprotected gas black (sample B); (c) amyl acetate with 0.5 per cent. cellulose nitrate; and (d) amyl acetate containing 0.13 per cent. of gas black protected by 0.5 per cent. cellulose nitrate. The results are similar to those obtained with starch and show clearly that suspensions of these materials exhibit a rapidly increasing viscosity at low rates of shear when aggregates are present, but a constant viscosity when the particles are separate.

The deflection readings were quite steady in the case of the liquids with constant viscosity coefficients, but very irregular when the viscosity was variable. This behaviour was also noticed with aqueous suspensions showing variable viscosity. The following table shows the variation of the relative viscosities of the respective protected and unprotected suspensions at the extreme rates of shear used for each.

Table I.

(A = amyl acetate, T = tetrachloroethane, B = bromoform.)

Suspension.	Range of shear gradient ($\text{sec.}^{-1} \times 10^4$).	Corresponding relative viscosities (amyl acetate = 1).
A + T + 6 per cent. starch with 0.05 per cent. rubber	323-16.6	2.0-1.7
A + T + 6 per cent. starch without protective	320-15.2	6.8-45.8
A + 0.03 per cent. gas black with 0.5 per cent. cellulose nitrate	295-7.4	3.1-3.2
T + B + 0.03 per cent. gas black without protective	303-6.2	2.5-36.2
A + 0.13 per cent. gas black with 0.5 per cent. cellulose nitrate	942-1.2	2.9-3.4
T + B + 0.13 per cent. gas black without protective	1025-0.09	2.3-1125
T + B + 0.5 per cent. gas black without protective	1505-0.47	6.4-2960

It is interesting to note that, for a given rate of shear, the viscosity of the 6 per cent. starch was roughly only three times that of the 0.03 per cent. gas black (A), although the proportion of solid was 200 times as great and the viscosity of the 0.03 per cent. gas black (A) was slightly higher than that of the 0.13 per cent. (B) suspension. This behaviour is evidently connected with the size of the particles, and is what would be expected if the effect of shearing is to disintegrate aggregates, since the force acting on a particle must, *ceteris paribus*, vary directly with its linear dimensions.

A striking difference between the behaviour of starch or gas black and that of the aqueous suspensions was the relative unimportance of a time factor in the former. In general, neither the amount of the variation nor the magnitude of the viscosity at a given rate of shear showed any increase with time. With gas black, particularly at low concentrations, the effects tended rather to become smaller, or even to vanish, when the suspensions were allowed to stand, and if then examined the latter were seen to contain granules visible to the naked eye. These granules could not be dispersed again completely even by violent shaking.

The form of the curve showing the relation between angular deflection and rate of shear is of special interest. For normal liquids it is a straight line passing through the origin, whereas for liquids showing variable viscosity it is generally convex to the deflection axis, and with the rates of shear hitherto employed an extrapolation to zero rate of shear is too uncertain to give definite information about the ultimate value of the deflection. Bingham* has expressed the opinion that suspensions of rigid particles are plastic, and can exhibit viscous flow only when the shear gradient exceeds a certain "yield" value. His experimental curves connecting pressure with rate of flow in capillary tubes for suspensions such as oil paints are approximately straight lines which, if produced, would cut the pressure axis. Actually, the curves are always found to bend toward the origin at the lowest pressures used. This behaviour is attributed by Bingham to an independent flow of the dispersion medium through the solid, or to movement of the whole suspension due to viscous flow in a thin layer of liquid in contact with the walls of the tube; and since it is in the nature of an experimental accident it should not be taken into account in extrapolating the curves. Hatschek,† on the other hand, holds the opinion that the curvature at low pressures represents the normal behaviour of suspensions, and considers that the data available are consistent with the occurrence of true viscous flow down to zero pressure.

Shear gradient—deflection curves given by the concentric cylinder apparatus are equivalent to flow—pressure curves in the capillary tube method, and the very low rates of shear used in the present experiments make it possible to perform the extrapolation with greater confidence, and to say that the curves would probably not pass through the origin but would cut the deflexion axis.

In fig. 6 the relation between rate of shear and deflexion is shown for two of the suspensions already referred to. The curves show two interesting features :

* Bingham and Green, 'Proc. Amer. Soc. Testing Materials,' vol. 19, p. 640 (1919).

† "Viscosity of Liquids," 1928, pp. 207, *et seq.*

firstly, if extrapolated only from the higher rates of shear they would pass naturally through the origin ; secondly, the addition of points at sufficiently

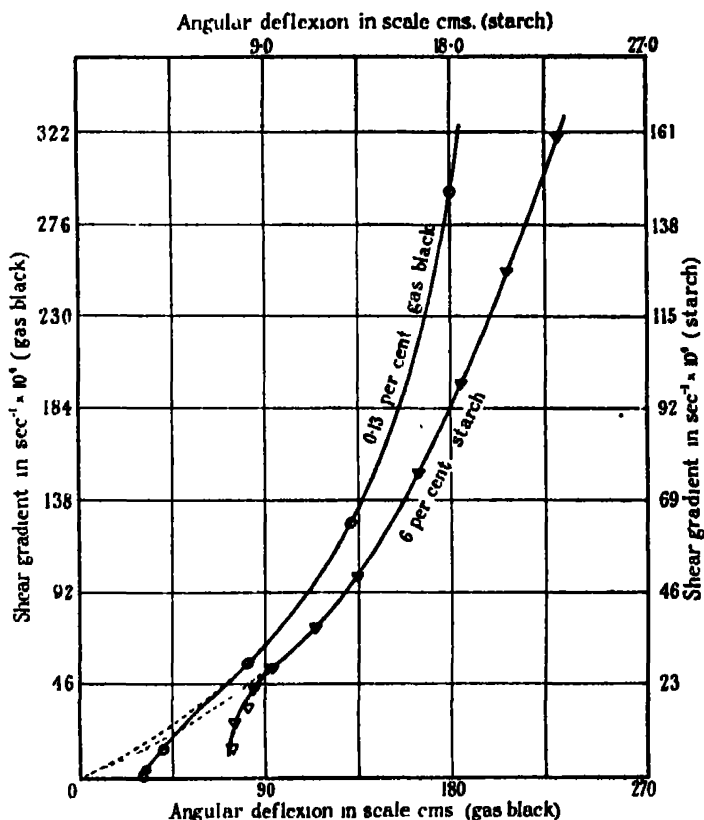


FIG. 6.

low rates of shear alters the course of the curves so as to make it nearly certain that the fluidity of both suspensions would be zero at a vanishingly small shear gradient. The curves serve to reconcile the view that the curvature at moderately low shear gradients is normal with the contention that the suspensions are essentially plastic, although it is only at shear gradients as low as $2 \times 10^{-2} \text{ sec}^{-1}$ that the latter property becomes apparent.

Experiments on Rigidity.

Suspensions of starch and of gas black in liquids of the same density as the solids were examined by the methods described in Part I. The actual observations so closely resembled those previously recorded for the aqueous suspensions that it is unnecessary to give them in detail. The chief differences noted were

the larger proportion of solid required in the present case to give rigidity to a suspension, and the still greater sensitiveness to mechanical disturbance. Both these differences may be attributed to the larger average size of the particles in the non-aqueous systems. Protected suspensions showed no trace of rigidity.

Rigidity could not be detected with certainty in starch suspensions containing less than 8 per cent. of solid. An 8 per cent. suspension, however, was perfectly elastic for small strains of the order 0.005. When the solid occupied 12 to 20 per cent. of the total volume rigidity was pronounced; for example, a 13.7 per cent. suspension was subjected to a stress corresponding with 7 cm. on the scale, and no relaxation was observed from 1.45 to 4.45 a.m., a period when there were no external disturbances. (During the daytime some diminution of the stress occurred at frequent intervals, for instance at the banging of a door in a distant part of the building.)

Examples of stress-strain curves for starch and for gas black, obtained in the manner described by Schwedoff,* are shown in fig. 7. Values of the modulus

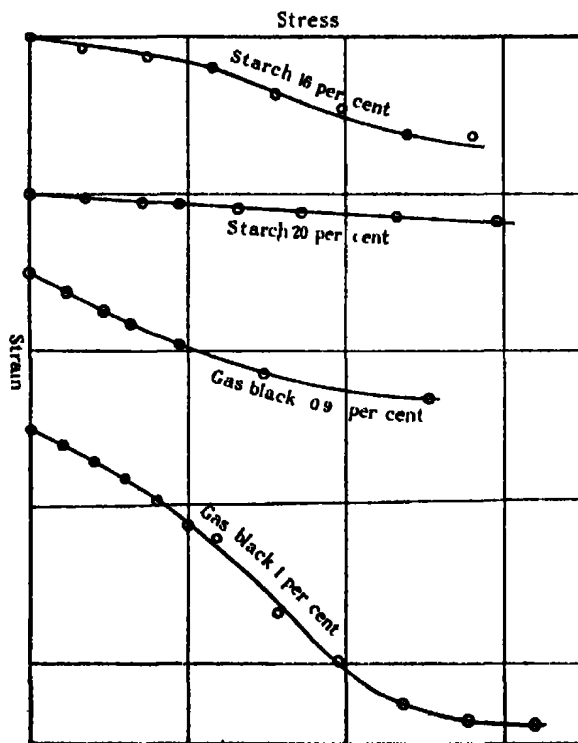


FIG. 7.—Stress-strain curves for starch and gas black.

* 'J. Physique,' vol. 8, p. 341 (1899).

of rigidity derived from the curves by means of the constants of the apparatus are of the same order of magnitude as those of the aqueous suspensions previously described, for example, 0.25 to 1.1 for 0.9 per cent. gas black, and 5.2 to 10.9 for 20 per cent. starch.

In many instances, especially with the lower concentrations, an immediate response to a change of stress was followed by a slow "creep." Some of the curves were sinuous, being slightly convex to the stress axis for small strains; but nearly all were concave to the stress axis at the larger strains, and usually throughout their length, indicating an increase of the modulus with strain. This behaviour, which is being further investigated, has also been observed in the jellies of gelatin and of cellulose acetate studied by Poole,* who considered that it implied the existence in them of a connected fibrillar structure.

Electrical Conductivity.

Both the starch and the gas black were examined in an electric field and no cataphoresis could be detected in either. It may therefore be concluded that the particles were uncharged in the liquids used.

The fact that gas black consists of particles with a fairly high electrical conductivity suggested a simple means of detecting the presence of a continuous solid structure. A small quantity of suspension was placed in a glass cell in which were two copper electrodes of area 3.7 sq. cm. and 0.5 cm. apart, and the current flowing when 110 volts were applied was noted at frequent intervals. The observations are recorded in Table II.

The figures show that, whilst the conductance of a 1 per cent. suspension protected with cellulose nitrate was too small to be detected (less than 0.1 micro-amp.), the unprotected suspensions allowed currents as large as 60 micro-amp. to pass, so long as they remained at rest. Tapping or violent shaking always reduced the conductance greatly. This result appears to furnish direct proof that the carbon particles in the undisturbed and unprotected suspensions are actually in contact and form a continuous structure between the electrodes. The figures for the conductance were not reproducible, nor would one expect them to be in view of the great diversity possible in the fortuitous structure built up.

* 'Trans. Faraday Soc.,' vol. 21, p. 114 (1925), and vol. 22, p. 82 (1926).

Table II.—Conductance of Suspensions of Gas Black in a Mixture of Bromoform and Tetrachloroethane of Density 1.81.

Time in minutes.	Current in micro-amps.	Time in minutes.	Current in micro-amps.
(a) 0.25 per cent.		(c) 1 per cent.	
0	1.2	0	27.0
11	4.2	0 (shaken)	6.0
11 (shaken)	0†	5	36.0
50	4.8	5 (shaken)	6.0
50 (shaken)	0†	10	30.0
		10 (shaken)	1.2
(b) 0.5 per cent.		15	28.2
0	60	15 (shaken)	1.2
2	21	20	28.8
2 (stirred)	10.5	20 (shaken)	1.2
2 (shaken)	3.6	25	27.0
9	9.0	30	63.0
12	9.0		
12 (tapped)	4.5	(d) 1 per cent. with cellulose nitrate.	
15	7.2	—	0†
15 (shaken)	3.0		
990	15.0	† "0" equals less than 0.1 micro-amp.	
990 (rotated gently)	18.3		
990 (tapped)	6.0		

Conclusions.

Theories of variable viscosity (or rigidity) depending respectively on an assumed structure of the disperse phase or on solvation of its discrete physical units have been discussed, chiefly with reference to lyophilic colloids, by McBain* and by Hatschek.† In estimating their relative adequacy, it must be admitted that the existence of a sufficiently thick layer of solvent around discrete particles would account for viscosity increasing with decreasing rate of shear, and even for rigidity. The sensitiveness of suspensions to mechanical disturbance could be attributed to the shearing and temporary mobilisation of some of the liquid in these layers. A theory based on the existence of a structure of particles in contact can explain the effects equally well, and is free from two objections which make the hypothesis of extensive solvation difficult to accept. Briefly, these objections are (1) that in an aqueous suspension (of a lyophobic substance) the electrical forces usually considered responsible for holding a layer of oriented water molecules around the particles are inadequate to explain rigidity, since an aqueous solution of a strong electrolyte, the ions of which are surrounded by far more intense fields of

* 'Journ. Physical Chem.,' vol. 30, p. 239 (1926).

† *Ibid.*, vol. 31, p. 383 (1927).

force, is hardly more viscous than pure water; and (2) that the liquid layer around uncharged lyophobic particles necessary to impart rigidity to a suspension would sometimes (as in an 8 per cent. suspension of starch grains $3\ \mu$ in diameter) require to be as much as $0.005\ \text{mm.}$, or about 10,000 molecules, thick, an extremely improbable value.

The experiments described above provide direct evidence of a close connection between rigidity and the formation of a continuous structure, and between variable viscosity and the formation of loose aggregates. Taken in conjunction with the observations recorded in Part I, they also support the belief that any solvation which may occur does not sensibly contribute either to variable viscosity or to rigidity. In an aqueous suspension of charged particles the effects attributed in the "solvation" theory to a layer of water are only developed when the electric charge is reduced by the addition of an electrolyte; and rigidity is developed in a stable sol of copper ferrocyanide by adding alcohol to it, a treatment which ultimately produces coagulation, but which certainly cannot increase the hydration of the particles. In the non-aqueous suspensions both variable viscosity and rigidity are abolished when the lyophobic particles are surrounded by a film of a lyophilic protective, under which conditions solvation must be increased rather than diminished; and visual evidence of the absence of a rigid layer of liquid of a thickness comparable with the size of the particles is afforded by the appearance of starch grains in close contact, in a suspension which can be shown to possess variable viscosity. Again, contact between carbon particles in unprotected suspensions which possess variable viscosity is demonstrated by their conductance, but when the particles are surrounded by a protective film both the variable viscosity and the conductance disappear. Thus it is possible to form a clear and consistent picture of the behaviour of both types of suspension; the stable aqueous sols exhibit variable viscosity or rigidity when aggregation of their particles is made possible by the addition of an electrolyte, and the inherently unstable suspensions in organic liquids cease to exhibit these properties when their particles are prevented from forming aggregates. The noticeable operation of a time factor in suspensions of the former class and its almost complete absence in the latter is to be expected in view of the slowness with which particles are known to form aggregates when the concentration of electrolyte is much below that needed to cause rapid visible coagulation.

McBain's contention,* that the existence of elasticity in sols is "a specific

* McBain, *loc. cit.*

positive test for the presence of ramifying aggregates," although unsupported by direct experimental evidence at the time when it was published, appears to hold good for suspensions of a lyophobic character. The variation with strain of the tensile modulus of gelatin or cellulose acetate jellies finds, according to Poole,* a simple explanation in the presence of a similar branched fibrillar structure; but whether, or to what extent, solvation contributes to variable viscosity in solutions of lyophilic substances must remain a question of opinion until new experimental methods are devised. At present one generalisation seems to be permissible: if rigid particles suspended in a liquid in which they are insoluble are not prevented from cohering—whether by an electric charge or by an envelope of a soluble substance—they will in time form aggregates, the presence of which will always cause the viscosity to be a function of the rate of shear; and which, if they are completely interlinked, will also impart rigidity to the suspension as a whole.

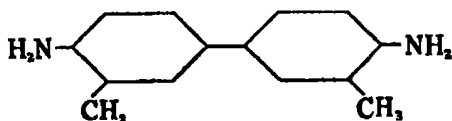
The Colloid Chemistry of Dyes: the Aqueous Solutions of Benzo-purpurine 4B and its Isomer prepared from m-Tolidine.—Part I.

By CONMAR ROBINSON and HAROLD A. T. MILLS, University College, London, and Imperial Chemical Industries.

(Communicated by F. G. Donnan, F.R.S.—Received February 19, 1931.)

Introduction.

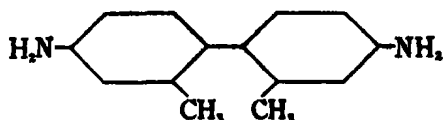
Substantive cotton dyes may be prepared from such para diamines as benzidine, diamidoazobenzene, diamidostilbene, etc., and also from homologues of these compounds containing the substituting group in the ortho position to the amido group. It is a well-known fact, however, that if the substituting group is in the meta position to the amido group the compound does not yield azo dyes which are substantive to cotton.† Thus, although substantive dyes may be prepared from *o*-tolidine,



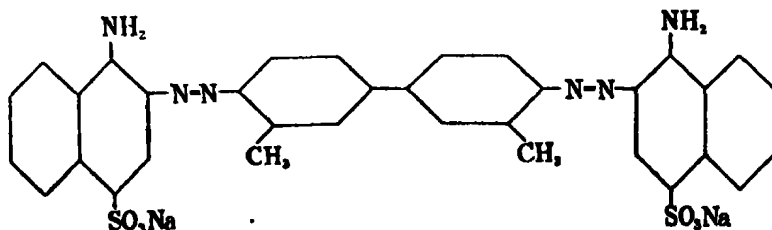
they cannot be prepared from *m*-tolidine.

* *Loc. cit.*

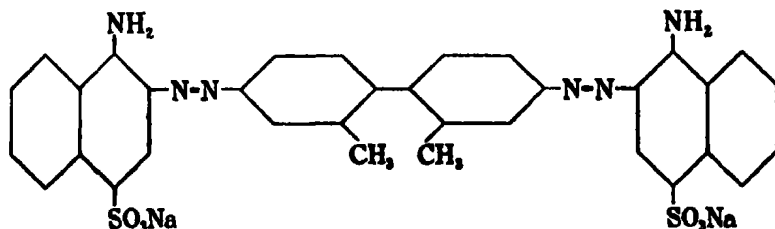
† "The Synthetic Dyestuffs and Intermediate Products," J. C. Cain and J. F. Thorpe (1923), p. 58, *et seq.*



So that while we have the well-known substantive dye benzopurpurine 4B, which is prepared from *o*-tolidine and sodium naphthionate,



we find that the corresponding substance prepared from *m*-tolidine



has not sufficient affinity for cotton for it to be of practical use as a dyestuff.

No obvious explanation of this marked change in properties with the change of the position of the methyl groups can be put forward on organic chemical lines. As the dyeing of cotton with substantive dyes is generally considered to be a process in which colloidal phenomena play a large part—if not a predominant one—it was thought that a thorough investigation of the physico-chemical and colloidal properties of such a pair of azo compounds might throw some light on this problem as well as on the more general problem of the mechanism of dyeing with substantive cotton dyes and the determination of the factors which decide the dyeing properties of a compound.

The research which is described in this report was therefore carried out on benzopurpurine 4B and the corresponding isomer prepared from *m*-tolidine (for convenience these two substances will be referred to subsequently as the "4B" dye and the "meta" dye respectively). The field of work was at first intentionally limited to only two substances and, further, to a study of their properties in solution (as distinct from their dyeing properties). It is

intended later to extend the work to a study of other dyes, as the results here obtained might suggest, and to a study of the mechanism of adsorption of the dyes on cotton and other substances and the factors which control it. The object of the work here described was therefore a complete investigation of the solutions of these two substances differing greatly in dyeing properties but only slightly in chemical constitution, and the development of methods suitable for this investigation.

Purification.

In general the cotton substantive dyes cannot be recrystallised from water.* Their purification is therefore not easy, and many investigators who have studied the colloid properties of these dyes have worked with impure specimens, with the consequence that their results, as well as being impossible to reproduce, are often quite misleading. The samples of the two dyes with which we worked were specially prepared by the British Dyestuffs Corporation, Ltd., from pure intermediates, the products so obtained containing considerable quantities of electrolytes (sodium chloride and probably sodium naphthionate with traces of sodium acetate and sodium carbonate). Their further purification (freedom from electrolytes) was undertaken in this laboratory.

Several methods have been used for the purification of benzidine dyes, to most of which there are objections. Dialysis gives rise to the formation of the acid dye as Donnan and Harris have pointed out.† Dialysis with sodium hydroxide as the outside liquid (to prevent membrane hydrolysis) will give a product containing alkali—further the method is very slow and, owing to the low solubility of benzopurpurine 4B, unsuitable for preparing large quantities.

Azuma and Kameyama‡ salted out congo red with ammonium carbonate and then volatilised the ammonium carbonate. We found that this method gave the ammonium salt of the dye, and their statement that they obtained a sample which gave no reaction with Neasler's solution must have been due to an error. A sample of congo red treated in the way they describe was obtained chloride-free, but on analysis was shown to contain 96 per cent. ammonium and 4 per cent. sodium, as a percentage of the total alkali radicles present.

* Pelet-Jolivet in his book "Die Theorie des Färbeprozesses" states, without comment, that he purified benzopurpurine 4B by recrystallisation from water. It can only be assumed that he did not actually obtain crystals. The cooling of a 2 per cent. benzopurpurine 4B solution gives rise to the separation of a tectosol ('Zocher, Kolloidchem. Beihefte,' vol. 28, p. 167 (1929)).

† 'J. Chem. Soc.,' vol. 99, p. 1554 (1911).

‡ 'Phil. Mag.,' vol. 50, p. 1264 (1925).

Overbeck,* in Zaigmondy's laboratory, purified congo red by continued washing in the pressure ultrafilter (this is fitted with an electromagnetic stirrer and pressures up to 125 atmospheres can be applied) until the conductivity of the ultrafiltrate was of the same order as that of the distilled water used. We tried this method, using the same apparatus, but found that with benzo-purpurine 4B the filtration, even when using the electromagnetic stirrer, was so extremely slow that the method was not practical for preparing the quantities of this dye required

Several workers have used the method of precipitating the acid dye and neutralising it with the theoretical amount of sodium hydroxide. This method does not seem very reliable as, firstly, there is a difficulty in preparing the pure acid dye (prolonged washing peptises it) and, secondly, the acid dye being insoluble it is doubtful if the equivalent quantity of caustic soda would neutralise all of it, so that the final product might be expected to contain occluded acid dye.

The method finally decided on was repeated, salting out with sodium acetate and washing out the sodium acetate with absolute alcohol (potassium acetate, although more soluble in alcohol, cannot be used if the sodium salt of the dye is required). The sodium acetate used was British Drug Houses' "A.R." product, recrystallised. A 40 per cent. solution of this was made up. 40 grams of the impure dye was stirred up with 75 c.c. of distilled water and heated until boiling with constant stirring. 75 c.c. of the sodium acetate was now added and the whole allowed to stand. The dye was then filtered off by suction on a Buchner funnel, a colourless filtrate being obtained. The dye was again stirred up with water and the salting out process continued. This procedure was carried out five times, the filtrate and the dye itself were then found to be free from chloride.

The dye was now boiled with alcohol, transferred to the Buchner and washed two or three times with hot alcohol. The boiling and washing with alcohol was carried out five or six times. The dye, after this, no longer gave the caodyl test for acetate. It was then dried at 105° C. Care was taken not to let the temperature go above this, as at a temperature of about 120° C. there was some decomposition accompanied by a darkening of the dye. All vessels used during the purification were of Jena or Pyrex glass.

The sodium content of the two dyes was determined, the following

* W. Overbeck, "Verbesserungen an Methoden zum Untersuchung von kolloiden Farbstoffen" ('*Diis*,' Göttingen, 1926).

results being obtained. This determination was made as accurately as possible.

	Sodium found.	Sodium theoretical.	Percentage pure dye calculated on sodium found.
Meta dye	per cent. 6.32	per cent. 6.34	99.7
4B dye	6.34	6.34	100.0

The sodium content of both dyes agreed with the calculated values within the limits of the experimental error of the method of determination.

Titration of a weighed quantity of the purified dyes gave with titanous chloride in the presence of sodium citrate 101 per cent. This high result is probably due to a methodical error, accurate absolute values being difficult to obtain owing to the precipitation of the dye before reduction is complete.

Preparation of Solutions.

As the dyes were found to be hygroscopic, solutions were made up by weighing off approximately the amount of the dye required and dissolving in the necessary amount of distilled water, boiling for 1 minute, to ensure complete solution, and filtering through an ash-free filter paper. The exact concentration of the dye was determined by evaporating 25 c.c. of the solution in a wide-mouthed weighing bottle on a water bath until the residue of dye just began to flake off the bottom, the weighing bottle then being transferred to an oven and heated at 105° C. until its weight remained constant.

All solutions were made up and preserved in pyrex flasks fitted with ground-glass stoppers.

Viscosity and Ageing of Solutions.

The viscosity of benzopurpurine 4B is said to depend on the method of preparation and the age of the solution. Thus Ostwald* found that the viscosity of a 0.3 per cent. benzopurpurine solution prepared cold was from 1.041 to 1.075, depending on the pressure applied to the capillary viscometer, while dissolved hot the viscosity was from 1.239 to 1.723. He does not mention purifying the dye. Similarly Hatschek† found the modulus of elasticity and the viscosity (measured in the Couette viscometer) dependent on the history of solution, a 1 per cent. solution having a low viscosity if

* 'Z. Phys. Chem.,' vol. 111, p. 62 (1924).

† 'Kolloid Z.,' vol. 39, p. 300 (1926).

prepared cold, and 100 times that of water if prepared hot. Liepatoff,* using the Ostwald viscometer, found for 0.5 per cent. solution a relative viscosity of 1.68 at 18° C.

As the dependence of any property of the dye solution on either the method of preparation or the age of the solution would have to be taken into account in the study of these dyes, we carried out some measurements with an Ostwald viscometer. Bungenberg de Jong† has fully described the conditions under which an Ostwald viscometer should be used so as to obtain reliable results with an accuracy of 0.1 to 0.2 per cent. The viscometer we used was therefore constructed (out of durosil) in accordance with these principles. The diameter of the capillary was 0.34 mm. and the length of the capillary was so chosen as to conform with the formula of Grüneisen.‡

The ends of the capillary opened out gradually into the wider parts of the tube, this reducing the tendency to form eddy currents. The time of flow with 10 c.c. of water in the viscometer was 95.4 seconds. The stand recommended by de Jong was not found necessary, as no difficulty was found in obtaining readings checking within 1/5 second for several different settings up of the viscometer in the thermostat when using an ordinary clamp and plumb line. The measurements were made at 25° C., the temperature at no time being allowed to vary more than 1/40° C. The influence of ageing is shown in the following measurements made on solutions of the respective dyes prepared hot by the method described.

Table I.

	Meta dye.	4B dye.
Concentration (grams per 100 c.c.)	0.569	0.571
η at 25° after 1 day	1.035	1.035
" 12 days	1.036	1.036
" 6 weeks	—	1.037
" 6 months	1.040	1.041

We also made up two solutions of the 4B dye of the same concentration (0.57 grams per 100 c.c.), one of which was prepared cold, and the other hot, and measured their viscosities. The viscosity of the one prepared cold, which

* 'Kolloid Z.,' vol. 39, p. 230 (1926).

† 'Rec. Trav. Chim., Pay-Bas.,' vol. 42, p. 1 (1923).

‡ 'Wiss. Abh. Phy. Tech. R. Anst.,' Berlin, vol. 4, p. 151 (1905).

had to be shaken vigorously to obtain solution, was measured after 20 hours, while the one prepared hot was measured after 3 hours. The results were :—

Prepared hot.	Prepared cold.
1.034	1.034

Freundlich and Shalek* using the Hess viscometer and also the Couette viscometer, showed that the viscosity of a benzopurpurine solution varied with the rate of shear, i.e., the solution did not obey Poiseuille's law. Ostwald† showed that similar results could be obtained with the Ostwald viscometer if varying pressure, positive or negative, were applied to the capillary of the viscometer. We therefore carried out some experiments to see if the viscosity of our dye solution was also dependent on the rate of flow through the capillary. Pressure, positive or negative, was applied to the Ostwald viscometer by means of an aspirator fitted with a water manometer. The viscometer was first filled with water and the rate of flow measured for different readings of the manometer varying from -3 to $+10$ cm. of water. From the results a curve was plotted and subsequently when the rate of flow for a dye solution at a certain pressure was measured, the corresponding rate of flow for water could be read from this curve. The results are given as the ratio of the time of flow for the dye (T_D) to the time for water (T_W), this differing by less than the experimental error from the relative viscosity of the dye (the density of the dye solution being only 1.002). It will be seen that within the range of pressure used the viscosity does not vary by more than 0.005. The experimental error was rather greater than with the Ostwald viscometer as ordinarily used, but the results were reproducible to within about 0.004.

Table II.—Viscosity of a 0.5 per cent. "Meta" Dye Solution at various Rates of Flow (at 25° C.).

T_D .	T_W .	T_D/T_W .
seconds	seconds	
145.6	141.0	1.033
121.4	117.0	1.038
108.4	104.5	1.038
99.1	95.5	1.038
83.4	81.2	1.035
55.4	53.4	1.038
52.4	50.6	1.036

* 'Z. Phys. Chem.,' vol. 108, p. 152 (1924).

† 'Z. Phys. Chem.,' vol. 111, p. 62 (1924).

Table III.—Viscosity of a 0.5 per cent. "4B" Dye Solution at various Rates of Flow (at 25° C.).

T_D .	T_W .	T_D/T_W .
seconds	seconds	
138.6	134.5	1.032
136.2	131.3	1.035
133.2	128.5	1.036
95.7	98.8	1.032
57.2	55.2	1.036
51.8	50.2	1.031

We may therefore conclude from these experiments that viscosities of these two dyes are the same within the experimental error and are of the same order as that of a typically lyophobic solution (i.e., they do not greatly exceed the viscosity of water). The particles are therefore either unhydrated or only slightly hydrated. Also the viscosity is independent of the method of preparation and age of the solution. Further, the viscosity obeys Poiseuille's law and does not vary with the rate of shear—in other words, there is no structural viscosity. The much higher and varying viscosities obtained for benzopurpurine 4B by the other workers were due to either the solutions with which they worked being in a state of incipient coagulation due to the presence of electrolytes, or due to the concentration of the dye being above the saturation point, or both these causes.

Flocculation with Electrolytes.

In determining the flocculation values of a solution for a certain electrolyte, it is usual to determine the minimum concentration of electrolytes which will bring about complete flocculation in a given time. In the case of benzopurpurine 4B this was quite possible to determine as there was a fairly sharp point where complete flocculation was obtained, giving a bulky gelatinous precipitate of the dye with a quite clear colourless liquid above this. Thus, when two portions of sodium chloride solution were added to one portion of a 0.5 per cent. benzopurpurine 4B solution, this was brought about when the final concentration was 0.16 moles. of sodium chloride per litre. The meta dye, however, behaved differently, even when under the same conditions, the final concentration of sodium chloride was 2.30 moles., complete flocculation was not brought about; the liquid above the precipitate being still coloured (it should be noted that a very small quantity of dye is necessary to give a con-

siderable colour, as one part of dye in 10 million of water can be easily detected). The precipitate for the meta dye was not gelatinous like that of the benzo-purpurine 4B and was far less bulky. Since for our purpose it was more important to obtain results for the two dyes which could be compared, we determined the minimum concentration of electrolyte which would cause the solution to become cloudy.

Experimental.

The experiments were carried out in flat-bottomed pyrex test-tubes, which had previously been carefully cleaned with chromic acid and then steamed out. 2 c.c. of a solution of dye containing 5 grams per litre were placed in a number of these, and 4 c.c. of various concentrations of sodium chloride solution were added and the tube shaken. The large volume of salt solution added is necessary in the case of the meta dye, as here we have to add quantities of sodium chloride which are near the saturation point of that salt. By only adding an equal volume of salt solution the necessary final concentration could not be attained. Care was taken in each case to follow exactly the same procedure for adding the electrolyte and shaking in the tube. After 24 hours the concentration of sodium chloride which made the contents of the tube so cloudy that they could not be seen through was noted, as well as the lower concentration which did not give this cloudiness. A second series of tubes was then set up containing concentrations ranging between these two concentrations, and finally a third series, so that the limiting value is obtained as accurately as possible. The results are given in Table IV. We also show the results obtained for calcium chloride and aluminium chloride. It is, however, doubtful if these two salts do not introduce other complications as both have an acid reaction. In the case of the aluminium chloride in particular, the colour of the precipitate suggested that some of the insoluble blue acid dye had been formed. Washing the precipitate given by aluminium chloride repeatedly with distilled water, redissolved it however. The results for NaCl were quite sharp and easily reproducible for both dyes. The results are accurate to about 5 per cent. Repeating the experiments 6 weeks later gave the same results within 5 per cent., so that here also, as with the viscosity experiments, there seemed to be no appreciable ageing effect. The results obtained with NaOH were similar to those for NaCl, the flocculation values being somewhat higher.

Table IV.—Flocculation by Electrolytes.

	4B dye.	Meta dye.
	moles./litre.	moles./litre
NaCl	0.072	2.23
CaCl ₂	0.0037	0.063
AlCl ₃	0.0004 (about)	0.004 (about)
NaOH	0.083	2.60

The small amount of sodium chloride necessary to bring about the complete precipitation of benzopurpurine 4B would seem to suggest that we were here dealing with the flocculation of a typical lyophobic solution, where flocculation is brought about by the added electrolytes lowering the potential at the surface of the colloidal particle to a critical potential at which coagulation can take place. On the other hand, the high concentration necessary to bring about a precipitate in the case of the meta dye and the fact that this precipitate increases in quantity with increasing quantities of sodium chloride added (up to a point where we are adding a saturated solution of sodium chloride to the dye solution), suggests that the precipitation here is more of the nature of the "salting out" of a soluble substance. To throw further light on this we determined the flocculation values for different concentrations of dye. If the precipitate was merely a "salting out," or lowering of the solubility of a substance it would be expected that on diluting the dye considerably more electrolyte would be needed to bring about precipitation, while in the case of a true colloidal flocculation, the increase of the flocculation value on dilution would not be so great and there might in fact be a decrease* (as in the case for BaCl₂ and AlCl₃ with the As₂S₃ solution). Our results were as follows:—

Table V.—Variation of Flocculation Values with Concentration of Dye.

Concentrations.	NaCl (moles. per litre).	
	4B.	Meta.
20.0 gm. per litre	—	1.77
5.0 "	0.072	2.23
1.25 "	0.090	2.53

* Krulyt and van der Spek, 'Koll. Z.,' vol. 25, p. 1 (1919); also H. R. Krulyt, Jerome Alexander, "Colloid Chemistry," vol. 1, p. 306.

These results then point to colloidal flocculation, especially in the case of the 4B dye. It is most likely that both factors (lowering of potential and "salting out") play a part in each of these dyes, but that in the case of benzopurpurine 4B the colloidal precipitation predominates. These results then suggest that in the "4B" dye solution the particles are big enough for the charge at the surface of the particle to be of significance while the "meta" is either in true solution or more nearly in true solution. For comparison we give the flocculation values for sodium chloride for four dyes obtained by Frl. Beger* (the method of determining the end point is not stated).

Table VI.

	Concentration of dye	Flocculation value for NaCl.
	grams per litre	millimoles. per litre
Congo rubin	1.0	105
Benzopurpurine 4B	1.0	105
Benzopurpurine 10B	1.0	480
Congo red	1.0	980

From these results it would seem that benzopurpurine 10B and congo red are cases intermediate between the "4B" and "meta" dyes.

Ultramicroscopic Examination and Streaming Double Refraction.

It is generally stated in the literature that solutions of benzopurpurine 4B when looked at in the ultramicroscope are found to contain ultramicros which are non-spherical. Fräulein Beger† says that although a 0.01 per cent. solution of benzopurpurine 4B is almost optically empty, ageing phenomena can be plainly observed and after 3 months the same solution shows numerous needle-shaped particles.

We found that a solution made up from the dyes that had not been freed from electrolytes gave these ultramicros, their long shape being plainly seen if a suitable dilution was chosen. A 0.5 per cent. solution of the purified dye, however, showed no ultramicros (that is, the solution only contained a quantity of ultramicros comparable to that in the distilled water) when examined either undiluted or diluted 50 times. The six-month-old solution showed somewhat more particles, but still very few, no needle-shaped particles

* 'Z. Phys. Chem.,' vol. 111, p. 227 (1924).

† Beger, 'Diss.,' Göttingen (1923); Zeigmondy, 'Z. Phys. Chem.,' vol. 111, p. 223 (1924).

being observed in either solution. The addition of sodium chloride to the benzopurpurine was found to give ultramicros as observed by other workers. Thus, if two volumes of sodium chloride solution were added to one volume 0.5 per cent. dye solution so that the final concentration of sodium chloride was 0.05 moles. per litre, this mixture was found to contain masses of ultramicros which gave the scintillating effect associated with non-spherical particles. The occurrence of needle-shaped particles on ageing, described by other workers, may therefore have been due to impurities in the dye solutions.

All the solutions of benzopurpurine 4B which were shown to contain ultramicros were also found to give streaming double refraction. This was observed by the "vortex" method of Zocher.* The dye to be examined is placed in a flat-bottomed cylindrical tube. A beam of polarised light enters the tube at the bottom, parallel to the axis of the cylinder. The dye is then observed from above using a Nicol prism as analyser. The nicol being crossed so that darkness is obtained, the cylinder is rotated about its axis, whereupon when the dye settles down to a steady motion four light quadrants are seen and a dark maltese cross between the quadrants, this figure disappearing again as soon as the solution has come to rest. This streaming double refraction, as Schuster has pointed out, is also observed at concentrations of electrolytes which are insufficient to give rise to ultramicros. The method is very sensitive, it being possible to see the double refraction in extremely dilute solutions.

With the "meta" dye, however, in no case did we obtain ultramicros (that is in any considerable quantity), or streaming double refraction, either with small quantities of sodium chloride or with concentrations which were nearly sufficient to bring about flocculation (i.e., over 2.00 moles. per litre). When 2.00 moles. per litre of sodium chloride were present a certain number of ultramicros could be seen, but these, unlike those obtained with the "4B" dye, did not scintillate. In no case was there any streaming double refraction observed, this applying also to additions of calcium chloride and aluminium chloride.

The difference in the behaviour of the two dyes is here very marked.

Solubility.

The solubility of benzopurpurine 4B is difficult to determine accurately owing to the difficulty of separating the undissolved dye from the saturated solution. Thus W. C. Holmes† who determined the solubilities of a number of

* 'Z. Phys. Chem.,' vol. 98, p. 293 (1921).

† 'Stain Tech.,' vol. 3, p. 12 (1928).

dyes, found that in the case of benzopurpurine 4B "extremely colloidal solutions" were formed, and he found no means of separating the dye. For these reasons we made no attempt to obtain an accurate value of the solubility, but only arrived at a method that would bring out any marked difference in the solubilities of the two dyes.

The solubility was determined at room temperature in two ways: A, the dye was shaken for 12 hours with distilled water and then the undissolved dye allowed to settle for days until a clear solution was obtained; B, a super-saturated solution was kept at room temperature until the precipitate forming from it had settled. The result in the case of the "4B" was only very approximate, owing to the difficulty found in separating the saturated solution.

	A.	B.
Meta dye	5.97 grm./100 c.c.	5.58 grm./100 c.c.
4B dye	0.8 ,,	0.8 ,,

These results are sufficiently accurate to bring out the marked contrast in the solubilities of these two dyes.

Hydrogen Ion Concentration.

The p_H of solutions of each of the dyes as well as that of congo red (similarly purified) were measured electrometrically, using a hydrogen electrode. The following results were obtained for 0.5 per cent. solutions:—

Meta dye	7.13
4B dye	7.10
Congo red	7.18

Hydrolysis in these dye solutions may, therefore, be considered negligible. Zsigmondy found the degree of hydrolysis to be negligible for congo red, benzopurpurine 4B and benzopurpurine 10B.

Ultrafiltration.

This was carried out in the Zsigmondy* pressure ultrafilter, using the Zsigmondy "ultrafeinfilters."† The apparatus, which is made by Membranfilter G.m.b.H., of Göttingen, is described fully elsewhere.*

With this apparatus it is possible to use pressures up to 125 atmospheres. The electromagnetic stirrer was removed for these and the subsequent con-

* Brukner and Overbeck, 'Koll. Z.,' vol. 36, "Zsigmondy Festschrift," p. 192 (1925).

† 'Z. Anorg. Chem.,' p. 398 (1926); 'Biochem. Z.,' vol. 171, p. 198 (1926).

ductivity experiments, as it was found to be superfluous for the dye solutions used, and only added to the difficulty of cleaning the apparatus. All parts of the apparatus with which the solution comes in contact were heavily tinned.

The ultrafilters are made of nitrocellulose, and can be obtained of various pore sizes. The numbers of the filters here given are those given by the makers and refer to the time (in minutes) taken to filter 100 c.c. of water through a filtering surface of 100 sq. cm. under a pressure of 60 to 70 cm. of mercury. Using a 0.5 per cent. solution of each dye, we determined the filter of largest pore size which would just prevent the dye particles from passing through. The apparatus was washed very thoroughly with distilled water before use, and, after setting up, several lots of distilled water were filtered through the apparatus, the final ultrafiltrate having a conductivity comparable to that of distilled water.

Table VII.

Filter.	Appearance of filtrate.	
	Meta dye.	4B dye.
min. sec.		
16 0	Colourless	Colourless
10 0	Distinctly coloured	"
7 0	Coloured	"
3 0	Passes through unchanged	"
2 0	"	"
1 25	"	Passes through unchanged

The results were reproducible. They also were independent of the order in which the dye solutions were filtered, so that the results were not due to dye particles adsorbed in the pores of the filter preventing the passage of the "4B" dye. The method of graduation of these filters gives, of course, only the mean pore size of the filter. Even, however, if there is some doubt about the exact pore size of the filters here used, there seems no doubt that there is a very big qualitative difference in the ultrafilterability of these two dyes.

Conductivity.

The conductivity of a dye solution is the sum of the conductivity of the dye particles and the conductivity of the intermicellar liquid. For the purpose of this research we are more interested in the conductivity of the dye particles, and to find the value of this it is necessary to know the conductivity of the

intermicellar liquid. This can be obtained by ultrafiltering the dye and measuring the conductivity of the ultrafiltrate, a procedure which was followed by Willy Oberbeck* in studying the conductivity and mobility of congo red. For this purpose then we used the Zsigmondy pressure ultrafilter and ultrafeinfilters described in the last section. As the determination of the conductivity of the dye particles is obtained by a different method, it is necessary, especially when studying the more dilute dye solutions, to have a conductivity apparatus with which highly accurate measurements can be made and which will be suitable for the measurement of the conductivity of very dilute solutions.

Apparatus.

The conductivities of the solutions were measured by means of a Wheatstone bridge. The source of alternating current was an oscillating circuit giving a current of about 1000 cycles, to which frequency the ear is most sensitive. The metre scale was graduated in millimetres and fitted with a vernier, so that readings correct to a tenth of a millimetre could be made. The wire was carefully standardised before use. The conductivity cell was an ordinary Kohlrausch cell, made of Jena glass. The variable resistance in the other arm was a non-inductively wound four-dial resistance box, which had been standardised by the National Physical Laboratory. A variable capacity was put in parallel with the resistance box and "tuned" until silence was obtained in the telephones at the null point.

All connecting wires were of lead shielded cable. The resistance box, metre scale, etc., were laid out as symmetrically as possible and placed on sheet iron. The oscillating circuit was shielded by being placed in a copper box. This copper box, the leaden shielding of the wire, the copper of the thermostat, and all other shieldings, were connected together by soldered wires and earthed. This apparatus was found to be very sensitive and the null point could be determined correct to 0.1 mm. For determining the null point, a pair of 2000 ω ear-phones were used. The thermostat was kept at 25° C. and did not vary by more than 0.005° C. throughout the experiments.

The Solutions.

An approximately 0.5 gram per 100 c.c. solution of the dye was made as described already, and the exact concentration determined by evaporating 25 c.c. to dryness. The more dilute solutions were made up from this by successive dilution. The distilled water was used (sp. conductivity, 3.6×10^{-6} reciprocal ohms) as it came from the still. No attempt was made

* 'Diss.,' Gottingen (1926).

to use CO_2 free water, as the conductivity of the water when passed through the ultrafilter became considerably higher than the ordinary water and the use of the ordinary distilled water reproduced more closely the conditions of the solutions used for other experiments, where they came in contact with the atmosphere.

To obtain a sample of the ultrafiltrate, a 16-minute "ultrafeinfilter" was placed in the pressure ultrafilter and successive quantities of distilled water filtered through until the conductivity of the water which had passed through the filter remained constant and was of the same order as the conductivity of the water before filtering. Very prolonged washing was sometimes necessary for this. 30 c.c. of the dye solution was then placed in the filter and the conductivity of the ultrafiltrate was measured, rejecting, of course, the first few cubic centimetres that passed through. A second sample of the dye was then filtered and another measurement made, the mean of these two values being taken. All the filtrates were quite colourless.

The results obtained are shown in Tables VIII and IX. The specific conductivity of the intermicellar liquid was obtained by subtracting from the observed conductivity of the ultrafiltrate a correction factor C, which was the

Table VIII.—Conductivities of Meta Dye Solutions.

	Solution number.						
	1.	2.	3.	4.	6.	8.	10.
$K_{WI} \times 10^4$	3.62	—	—	3.59	3.62	3.62	3.62
$K_{WII} \times 10^4$	6.84	—	—	4.49	4.81	4.45	4.02
$C \times 10^4$	3.22	—	—	0.90	1.19	0.83	0.40
$K_s \times 10^4$	1017.4	593.9	317.1	169.85	46.394	14.61	6.872
$K_u \times 10^4$	35.85	—	—	10.19	6.58	5.22	4.66
$K_i \times 10^4$	32.63	(21.0)	(13.8)	9.29	5.39	4.39	4.26
$K_m \times 10^4$	984.8	572.9	303.28	160.56	41.0	10.22	2.61
$\eta \times 10^4$	145.7	72.85	36.43	18.22	4.554	1.136	0.284
$\frac{\eta}{\Lambda} \times 1000$	2.441	1.938	1.538	1.222	0.7693	0.4844	0.3051
Λ	67.60	78.5	83.24	88.10	89.03	89.97	91.89

K_{WI} = Specific conductivity of the water before filtration.

K_{WII} = Specific conductivity of the water after filtration.

K_s = Specific conductivity of the dye solution.

K_u = Specific conductivity of the ultrafiltrate.

$K_{WII} - K_{WI} = C$ = Correction factor.

$K_i = K_u - C$ = Specific conductivity of intermicellar liquid.

$K_m = K_s - K_i$ = Specific conductivity of the dye.

η = Equivalent concentration.

Λ = Equivalent conductivity.

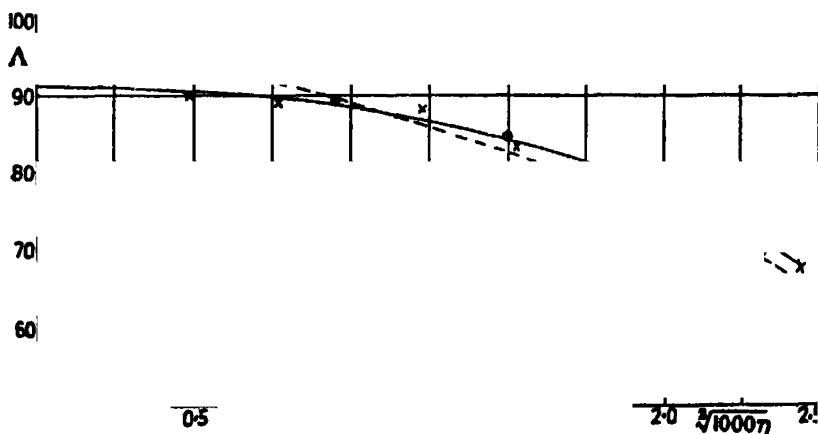
The figures for K_i for solutions Nos. 2 and 3 were obtained by interpolation.

Table IX.—Conductivities of "4B" Dye Solutions.

	Solution numbers.					
	1.	2.	3.	5.	7.	9.
$K_w I \times 10^6$	3.21	3.21	3.08	3.31	3.21	3.21
$K_w II \times 10^6$	4.15	4.90	6.11	3.84	4.56	4.11
$C \times 10^6$	0.94	1.69	3.03	0.63	1.35	0.90
$K_s \times 10^6$	956.5	521.5	293.8	85.64	27.61	12.68
$K \times 10^6$	23.3	14.88	13.18	11.45	8.88	8.62
$K_i \times 10^6$	22.4	13.19	10.15	10.82	7.33	7.72
$K_m \times 10^6$	934.1	508.3	283.7	74.79	20.28	4.96
$\eta \times 10^4$	133.84	66.92	33.46	8.365	2.092	0.5228
$\sqrt[3]{1000\eta}$	2.313	1.885	1.496	0.9420	0.5933	0.3739
Λ	69.79	75.91	84.82	89.39	96.96	94.84

amount that the conductivity of the distilled water increased by on filtering through the apparatus. The specific conductivity of the intermicellar liquid was then subtracted from that of the dye solution, this giving a value which represents the specific conductivity due to the dye itself. From this value we obtain the equivalent conductivity of the dye Λ , the equivalent concentration being taken as twice the molecular concentration. The equivalent conductivity of the *dye* determined in this way we find approaches a limiting value with progressive dilution, while the equivalent conductivity of the *dye solution* increases with increasing dilution.

In the figure we show the equivalent conductivity of both dyes plotted against $\sqrt[3]{1000\eta}$, where η is the equivalent concentration. For the "meta" the



curve runs almost horizontal for the more dilute solution and we obtain by extrapolation a value of 92 reciprocal ohms for the equivalent conductivity

at infinite dilution, Λ_{∞} . The conductivity of the 4B dye (broken line) does not differ by more than 1 or 2 per cent. from that of the meta dye in the more concentrated solutions. The curve, however, is not so regular as for the meta dye and the value for Λ_{∞} obtained by extrapolation is therefore more doubtful.

This is partly because the conductivity of the intermicellar liquid for the more dilute solutions was greater for the meta dye than in the case of the 4B dye, which renders the values for the last two solutions less reliable and hence throws doubt on the final direction of the curve. By extrapolation we obtain a value of 98 reciprocal ohms for Λ_{∞} . There seems, however, to be no great difference between the conductivity concentration curves of these two dyes. The curve for benzopurpurine 4B agrees very closely with the curve obtained by Frl. Beger, which is reproduced by Zsigmondy* except that for the very dilute solutions ($\sqrt[3]{1000\eta} < 0.1$) Frl. Beger's curves show a much more rapid increase of equivalent conductivity with dilution. By extrapolation they obtain $\Lambda_{\infty} = 105$.

From the similarity of the values for Λ_{∞} we must conclude that the values for the mobilities of the anion cannot greatly differ. This, however, does not necessarily mean that the anions are of the same size. Thus McBain† has found in his researches on the soaps that a more complex anion may actually have a greater mobility than the sum of the mobilities due to the simpler anions which constitute it—the more complex ion, containing the same number of charges as the sum of the constituent ions offering less resistance to the motion than do the single ions.

The value of the mobility of the anion (u) for a 0.1 per cent. benzopurpurine 4B solution has been determined by Frl. Beger‡ with Galecki's§ modification of the Coehn U-tube and found to be 47.9. The value of v being 50.9 this would mean that the mobility of the anion does not alter greatly between this concentration and infinite dilution since we have obtained a value of 92 for Λ_{∞} .

In calculating the equivalent concentration for obtaining values for the equivalent conductivity, we have taken the equivalent as being half the molecular weight of the dyestuff. The "electroequivalent" (by which term Zsigmondy|| denotes the number of molecules associated with one electric

* 'Z. Phys. Chem.,' vol. 111, p. 216 (1924).

† 'Z. Phys. Chem.,' vol. 76, p. 179 (1911).

‡ 'Diss.,' Göttingen (1923).

§ 'Z. Anorg. Chem.,' vol. 74, p. 174 (1912); cf. Zsigmondy, "Kolloid Chemie," 3rd ed., p. 61.

|| "Kolloidchemie," 3rd ed., p. 173.

charge) will, however, not be equal to the chemical equivalent if all the sodium of the dyestuff is not dissociated. For this reason W. Overbeek, in the dissertation already referred to, attempts to calculate the electro-equivalent of congo red by the method of Wintgen* using the formula

$$A_e = \frac{G}{M} \cdot \frac{u + v}{1000 K_m},$$

where A_e = electro-equivalent, G = number of grams of the colloid per litre, M = simplest molecular weight of the dissolved substance, $u + v$ = the sum of the mobilities, K_m = specific conductivity of the micelle; and then calculates the equivalent conductivity using this value. He obtained a value for A_e in the higher concentrations, determining u by the U-tube method at this concentration. For the more dilute solutions it was not possible to determine u , and he assumed that A_e did not change greatly with dilution. His evidence for this assumption being that with Bordeaux extra, while it was found possible to determine u for a large range of concentrations, A did not vary by much. To assume that other dyes behave as Bordeaux extra seems to us, however, not justified, Bordeaux extra, as we shall point out later (Part II) being probably much nearer to a condition of true solution than either congo red or benzopurpurine 4B.

We give, however, as a matter of interest the value for A_e calculated from Frl. Beger's result for u already referred to :—

G.	M.	u .	v .	$u + v$.	$1000 K_m$.	A_e .
1.00	726.1	47.9	50.9	99.8	0.240	0.57

A study has been made of the solutions of benzopurpurine 4B and the isomer prepared from meta tolidine.

(1) A method has been devised for the purification of these and similar dyestuffs.

(2) It has been shown that the phenomenon of ageing which takes place in impure solutions of benzopurpurine 4B does not appear in either of these dye solutions when pure.

(3) The viscosities of solutions of these dyes (if not supersaturated) are the

* Wintgen, 'Z. Phys. Chem.,' vol. 103, p. 254 (1922).

same and are of the order to be expected in an unhydrated (lyophobic) colloid. The viscosity does not vary with the rate of shear.

(4) p_H determinations have shown hydrolysis to be negligible.

(5) The "solubility" of the "meta" dyes is much greater than the "4B" dye.

(6) Flocculation experiments with electrolytes point to the particle size of the "4B" dye being of colloidal dimensions, while that of the "meta" is more nearly in true solution.

(7) Ultrafiltration experiments with graduated ultrafilters show that the particle size of the "4B" is larger than the "meta."

(8) While solutions of the pure dyes show no particles in the ultramicroscope, non-spherical ultramicros are obtained by the addition of small quantities of electrolyte to the "4B." In the meta dye ultramicros could not be produced.

(9) Streaming double refraction which can be observed in solutions of the "4B" to which electrolytes had been added was in no case observed in the "meta."

(10) Conductivity measurements showed the conductivities of the two dyes to be almost the same. The conductivities were measured over a large range of concentrations. By subtracting the conductivity of the ultrafiltrate, that of the "micelle" was obtained. The similarity of the results for the two dyes is, however, not evidence that the (multiple) anions are of the same degree of complexity.

It will be seen, therefore, that there is a marked difference in the properties of the solutions of these two dyestuffs, which could be explained on the assumption that the 4B dye forms larger aggregates than the meta dye. This will be further discussed in Part II.

The authors desire to express their best thanks to Professor F. G. Donnan, C.B.E., F.R.S., for his very kind interest in this work.

*The Colloid Chemistry of Dyes: The Aqueous Solutions of Benzo-
purpurine 4B and its Isomer prepared from m-Tolidine.—Part II.*

By CONMAR ROBINSON and HAROLD A. T. MILLS, University College, London,
and Imperial Chemical Industries.

(Communicated by F. G. Donnan, F.R.S.—Received February 19, 1931.)

OSMOTIC PRESSURE.

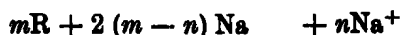
Introduction.

A number of investigators, including Knecht, Bayliss, Biltz and von Vegesack, Pelet-Jolivet, Donnan and Harris, and Zsigmondy* and his co-workers have made measurements of the conductivity and osmotic pressures of benzidine dyes, congo red in particular having been much studied. From these results it appears that although the conductivities of the dyes have a high absolute value suggesting a highly dissociated or completely dissociated electrolyte, the osmotic pressure approximately corresponds to the pressure calculated from the molecular weight, that is to say, the pressure is that which would be expected if we assume the dye to exist in solution in single undissociated molecules.

A number of attempts have been made to explain this very striking anomaly. Thus Donnan and Harris point out that although the observed values for the osmotic pressure could be explained by assuming complexes dissociated somewhat as follows



this cannot account for the values obtained for the conductivities. Zsigmondy, in a paper in which he goes very thoroughly into the whole matter, also points out that it is quite impossible to correlate the results obtained by conductivity measurements if the classical theory of electrolytes is used, even if the existence of molecular aggregates such as



* Knecht, 'Soc. Dyers & Colourists,' vol. 25, No. 7 (1909); Bayliss, 'Proc. Roy. Soc.,' B, vol. 81, p. 269 (1909), 'Koll. Zeit.,' vol. 6, p. 23 (1910), 'Proc. Roy. Soc.,' B, vol. 84, pp. 81, 229 (1911); Biltz & von Vegesack, 'Z. Phys. Chem.,' vol. 73, p. 481 (1910); Pelet Jolivet, "Die Theorie des Färbeprozesses" (Dresden), 1910, p. 27; Donnan & Harris 'J. Chem. Soc.,' vol. 99, p. 1554 (1911); Zsigmondy, 'Z. Phys. Chem.,' vol. 111, p. 211 (1924); Beger, 'Diss.,' Göttingen (1923); Meier, 'Diss.,' Göttingen (1925); Overbeck, 'Diss.,' Göttingen (1926).

is assumed. He here also takes into consideration the fact shown by the researches of himself and his co-workers that in the osmotic pressure results (obtained by both direct measurements and lowering of freezing point) the product $P.V.$ is almost constant. The evidence for this is not quite convincing. Thus the lowering of freezing point experiments were done with the ordinary Beckmann apparatus and the experimental error is such a large percentage of the observed (very small) lowering that one hesitates to conclude much from the results. As for the osmotic pressure measurements, they may be fairly reliable in the case of Bordeaux extra, but it is difficult to know how accurate they were from the data given.

One possible explanation which Zaigmondy suggests is that some of the dissociated sodium ions are enclosed in a sponge-like micelle in such a way that they partake in the transport of electricity on the passage of an electric current, but are not osmotically active.

Another explanation can be put forward on the basis of the Debye and Hückel theory, assuming that the anions (possibly with cations) are aggregates in polyvalent micelles and that the low osmotic pressure is due not only to the reduction of the number of particles by aggregation, but also due to the electrical attraction between the micelles and the sodium ions.

Dr. E. Hückel is quoted (private communication) by Zaigmondy* as saying that it is possible by suitably choosing the composition and size of the micelles to calculate that $P.V.$ will be constant over a large range of concentrations and to bring it into agreement with the observed values for the osmotic pressure. Thus making the simplest assumptions (for congo red), that is assuming that no sodium is included in the complex anion (a suggestion which is in accordance with the high conductivity) and that the composition of the micelle is independent of the concentration, then one must assume a micelle with 10 to 20 elementary charges and a radius of about 10^{-7} cm.

From the theory it will also follow that for smaller concentrations the value of the product $P.V.$ increases and at infinite dilution reaches a limiting value which is greater than that calculated from the formula weight and which is determined by the number of the anion micelles and the sodium ions.

By means of the Debye and Hückel theory it is only possible from the osmotic pressure measurements to foretell the order of the change of conductivity with concentration, as according to this theory the change of the conductivity depends not only on the change in the number of free charges, but also on the decrease in the velocity of the migration of the ions with increasing concentra-

* 'Z. Phys. Chem.,' vol. 111, p. 221 (1924).

tion. Zsigmondy considers that the postulation of a micelle consisting of 10 to 20, or 20 to 40 molecules is much more in accordance with the properties of the solutions of these dyes than that of the existence of the dye in simple molecules and ions.

A quite different possibility is introduced by Linderstrøm-Lang,* who suggests that the anomalous osmotic pressure exhibited by some colloidal electrolytes (the soaps, dyes, etc.) can be explained without postulating the existence of a micelle, the low osmotic pressure being due to an unusually large interionic attraction which comes into play when one ion is very much larger than the oppositely charged ion and when it is easily "deformable" as in the case of the soaps; in other words, he explains the anomalous osmotic pressure purely from the low activity coefficients of the ions, basing his belief in this low activity coefficient on thermodynamical grounds. It should be pointed out that Linderstrøm-Lang does not deny the possible existence of the micelle, but only shows (particularly in the case of the soaps) that the postulation of its existence is not necessary to explain the observed results.

From what has been said it will be seen that our knowledge of the state of solution of these dyestuffs (and for that matter of the other colloidal electrolytes exhibiting anomalous osmotic pressure) cannot be considered complete until this problem has been finally elucidated. In studying the osmotic pressure of these substances we have tried therefore, as well as to obtain values for their osmotic pressures, to throw as much light as possible on this more general problem.

Experimental.

The apparatus used for the measurement of the osmotic pressure was a modification of the osmometer used by Sørensen† (see figure). The osmotic pressure is determined by finding the pressure which will just keep the level of the dye meniscus from either rising or falling, thus enabling the concentration of the dye solution to remain constant throughout the experiment. The apparatus was so designed that CO₂ could be entirely excluded and further so that the dye solution and the liquid on the other side of the membrane only came in contact with the membrane itself and pyrex glass (*e.g.*, the rubber ring used by Sørensen for holding on the membrane was avoided).

Collodion membranes were used. These were prepared from a solution containing 10 grams of pyroxyline in 60 c.c. of ether and 40 c.c. of absolute alcohol. A large test-tube was filled with this substance, the solution then

* 'C. R. Trav. Lab. Carlsberg,' vol. 16, p. 47 (1927).

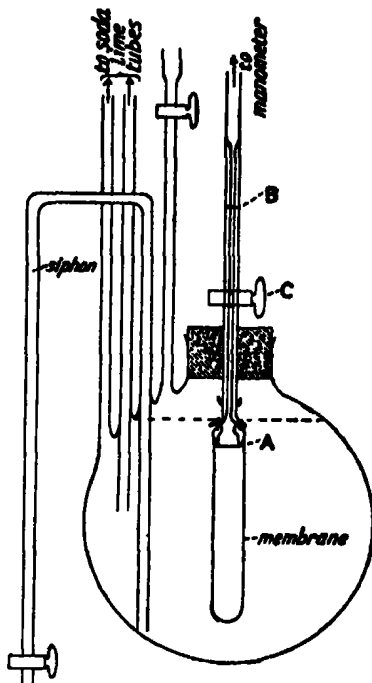
† 'C. R. Trav. Lab. Carlsberg,' vol. 12, p. 1 (1917).

being poured out slowly while rotating the tube and the tube left inverted to drain. After about 10 minutes, the tube was again filled, the process of filling and pouring out being repeated three times. The tube was then filled with distilled water. After a few minutes the membrane could then be pulled out without difficulty. Strong membranes could be obtained in this way, which were quite impervious to the dyes studied. The rigidity of the membrane depends, of course, on its thickness, and although very thick membranes could be obtained by slight modification of the above method, they were not considered desirable owing to the longer times necessary for equilibrium pressures to be reached. As will be explained later, a slight distortion of the membrane does not introduce appreciable errors.

The elaborate precautions taken by Sørensen to prepare suitable membranes (including the spinning of the tube while drying) were found to be unnecessary.

To attach the membrane to the lower part of the osmometer tube (A) we first used the method of Sørensen, using a rubber ring and outside this a glass ring. This was not found satisfactory, the membrane sometimes being forced off by the comparatively high pressures which were reached. Eventually, after a number of experiments, we found it best to prepare a membrane which was of such size that it could be pulled about half way up the tapering part of A. By moistening the end of the membrane with alcohol, it was then gradually worked over the shoulder of A. It was then allowed to shrink on by letting the part in contact with the glass dry, while that below the glass was kept immersed in water. This method was found very satisfactory, it being possible to attach the membrane very firmly without obtaining the creases which give rise to leaks.

The osmometer was filled with the dye solution at the temperature at which the experiment was to be made (25° C.) as described by Sørensen, the solution being brought to the mark B by means of a capillary pipette. The tap C was then closed so as not to allow the level of the dye solution to change while



fitting up the rest of the apparatus. The vessel in which the outside liquid was contained consisted of a litre pyrex flask with the neck cut short, into which had been sealed four glass tubes which served as inlet and outlet for CO_2 free air, a syphon for emptying the vessel and a tube for filling the vessel. The osmometer was set up in the outside vessel, using a rubber stopper to close the neck of the vessel. A segment of the rubber stopper was cut so as to be removable and allow the placing of the osmometer in position. After replacing the segment it was fixed in position by means of copper wire, the stopper placed in the neck of the vessel and sealed with a suitable wax so as to be water-tight and air-tight. The apparatus, as soon as the wax had set, was placed in a retort stand and the retort stand sunk in the thermostat so that the meniscus of the dye was under water and could be seen through the glass side of the thermostat. Connection was then made to the soda lime tubes by means of the ground-glass joints, and finally the osmometer was attached to the mercury manometer by another ground-glass joint. Any CO_2 present in the apparatus was now swept out by sucking CO_2 free air through the vessel. The outside liquid was prepared in a pyrex flask fitted with a rubber stopper through which passed a syphon with a ground-glass end which could be connected to the tube on the osmometer vessel used for filling it, a second tube with a glass tap through which the alkali could be added, and a third ending in a soda lime tube. By this means the solution of alkali used could be prepared and put into the vessel without it coming into contact with the atmosphere.

The tap C was kept closed until the first reading was made (this being generally 24 hours after starting the experiment). To obtain a reading, the mercury reservoir was raised until a reading on the manometer equal to the expected osmotic pressure was obtained. The tap was then cautiously opened and if any marked rise or fall was noticed, the manometer was adjusted until the motion of the meniscus was small. The rate of movement at this pressure was then found by measuring the distance travelled in 10 minutes by means of a cathetometer. The pressure was then raised or lowered sufficiently and the motion in the opposite direction measured. Two such readings having been obtained, one of which gave a slight upward movement and one a slight downward movement, the pressure at which there would be no movement was then obtained by interpolation. The observed osmotic pressure was then obtained from this value by adding the pressure of the dye column supported above the level of the outside liquid and subtracting the pressure due to the column of dye which would be supported by the capillary rise in the osmometer tube (this

last value being obtained by a direct experiment of the capillary rise in the actual osmometer tube used).

A typical reading was as follows :—

Manometer reading.	Movement.	Time.	Pressure for no movement (by interpolation).
cm. 16.00 16.64	mm. Up 0.26 Down 0.22	minutes 10 10	} 16.35

Height of dye column = 15.5 cm. = 1.14 cm. mercury.

Capillary rise = 0.07 „

Hence observed osmotic pressure = 16.35 + 1.14 - 0.07
= 17.42 cm. of mercury.

In this way readings reproducible to about 0.03 cm. were obtained.

The Outside Liquid.

Donnan and Harris* have shown that if an attempt is made to measure the osmotic pressure of a dye such as congo red with pure water as the outside liquid of the osmometer, a membrane hydrolysis will take place and some of the acid dye will be formed. In the case of congo red, where the acid dye is insoluble, this will be precipitated and consequently the membrane hydrolysis will continue with a progressive lowering of the observed osmotic pressure; we therefore find that the observed osmotic pressure rises rapidly to a maximum and then falls.

Donnan and Harris also found that if sufficient caustic soda is put into the original outside liquid no hydrolysis will take place and steady osmotic pressures are obtained—thus with a 0.5 per cent. solution of congo red they find with concentrations of NaOH above N/800, once the maximum osmotic pressure was reached, it remained constant for days, while below this concentration constant pressures were not obtained.

From the Donnan theory of membrane equilibria we may calculate the minimum concentration of NaOH which should be necessary to prevent membrane hydrolysis (CO₂, of course, being excluded).

At equilibrium we have

$$\frac{[\text{Na}^+]_{\text{inside}}}{[\text{Na}^+]_{\text{outside}}} = \frac{[\text{OH}^-]_{\text{outside}}}{[\text{OH}^-]_{\text{inside}}}.$$

* 'J. Chem. Soc.,' vol. 99, p. 1545 (1911).

The terms in the square brackets represent activities. Owing to the low concentrations here considered we may write the activity as being equal to the concentration in all but the case of $[\text{Na}^+]_{\text{inside}}$.

Let the concentration of the dye correspond to a sodium ion activity of $1/70$,* and let us assume that the original $[\text{H}^+]$ of the dye solution is 10^{-7} , hydrolysis being negligible. Then for no membrane hydrolysis to take place we must choose a concentration of NaOH so that no OH ions diffuse through the membrane. For this condition Na ions will also not diffuse through. Hence we have

$$\frac{1/70}{[\text{Na}^+]_{\text{outside}}} = \frac{[\text{OH}^-]_{\text{outside}}}{10^{-7}},$$

$$[\text{Na}^+]_{\text{outside}} \times [\text{OH}^-]_{\text{outside}} = 10^{-7}/70 = 14.3 \times 10^{-10}.$$

Hence concentrations of caustic soda required outside

$$= [\text{Na}^+]_{\text{outside}} = [\text{OH}^-]_{\text{outside}} = \sqrt{14.3 \times 10^{-10}} = 3.781 \times 10^{-5}$$

$$= (\text{about}) \text{ N}/26,000.$$

Hence above this figure no membrane hydrolysis will take place, but sodium hydroxide will diffuse into the dye solution. If, however, the concentration of caustic soda is less than this membrane hydrolysis will take place. This minimum concentration is independent of the relative volumes of the inside and outside liquids. If the sodium ion activity was less than the above figure, the necessary concentration of caustic soda would be still less.

We at first tried to obtain constant pressures with N/20,000 sodium hydroxide, using the "meta" dye. It was found, however, that the pressure after 48 hours was always considerably lower than the maximum. N/10,000 sodium hydroxide gave similar results, a fall in the pressure always being observed.

On measuring the p_{H} of the outside liquid by means of indicators, it was found that not only had the OH ion concentration fallen during the experiments, but that the initial concentrations were much less than that calculated from the number of times the N/10 NaOH from which the solution was made had been diluted. The solutions were therefore in future made up so as to give a p_{H} of 10.0 ($= \text{N}/10,000$), the amount of N/10 NaOH required to do this being found by experiment, thymol phthalein being used as an indicator. This concentration of NaOH is more than twice that shown to be necessary by the calculation, a considerable margin being necessary, as will be realised when it

* This being the approximate concentration of the sodium in the (approximate) 0.5 per cent. solutions used.

is pointed out that 1 litre of N/20,000 NaOH would be neutralised by 2.24 c.c. of carbon dioxide. The back osmotic pressure due to N/10,000 NaOH would be less than 0.19 cm. of mercury, so that results not differing greatly from the true osmotic pressure should be obtained in this way; there is therefore nothing to be gained by replacing the outside liquid by distilled water before taking the final reading.

The rate of fall after the maximum reading was reached may be seen from the following figures (Table I). The concentration of the dye was in all cases approximately 0.5 per cent.

Table I.

Outside liquid.	Dye.	Fall of pressure.
Distilled water	Congo red	16.90 to 15.20 in 3 days.
N/8000 NaOH	"	16.68 to 16.03 in 8 days.
N/16,000 NaOH	" Meta "	16.74 to 15.94 in 4 days.
N/8000 NaOH	"	16.96 to 15.67 in 4 days.
		16.96 to 14.79 in 10 days.
		16.96 to 11.47 in 20 days.
N/16,000 NaOH	" 4B "	17.15 to 16.83 in 2 days.
N/8000 NaOH	"	15.70 to 13.15 in 5 days.
p_H 10.0 NaOH	"	15.97 to 15.80 in 3 days.
		15.97 to 15.62 in 10 days.
		15.97 to 15.46 in 20 days.

"N/8000 NaOH" in this table refers to the concentration of the NaOH as calculated from the number of times the N/10 NaOH was diluted. " p_H 10.0" NaOH was made by diluting 2.5 c.c. N/10 NaOH to 1 litre and is therefore stronger than the "N/8000" solution.

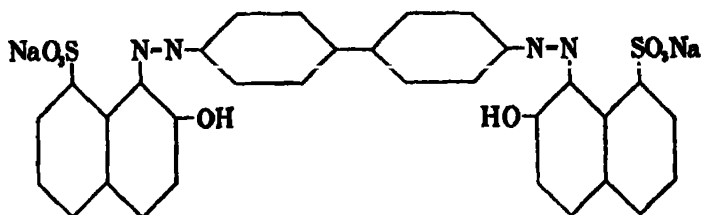
From these figures it will be seen that at p_H 10.0 we have results sufficiently constant to assure us that the maximum pressure after 24 hours is equal to the true osmotic pressure less the small "back" osmotic pressure due to a solution of p_H 10 NaOH. If, however, less alkali is used, the fall is so rapid that we cannot feel certain that the maximum observed has ever reached this value.

We suggest that this procedure of using the minimum amount of alkali or acid sufficient to prevent membrane hydrolysis as determined by calculation and experiment should always be followed in measuring the osmotic pressure of a colloidal electrolyte, the errors arising from the Donnan equilibrium phenomena being in this way reduced to a minimum.

It is difficult to understand why Donnan and Harris could not obtain constant pressure for 0.5 per cent. congo red solutions with less than N/800

NaOH, unless we assume that the presence of small amounts of CO_2 had affected the results.

The fall in osmotic pressure will, of course, be to a great extent determined by the degree of insolubility of the acid dye which is formed by the hydrolysis, a greater rate of fall probably being due to a more insoluble acid dye. Meier* has made a number of osmotic pressure measurements on Bordeaux extra,



the acid dye of which is soluble and (according to his measurements) has an osmotic pressure of the same order as that of the sodium salt. This probably accounts for the ease with which he was able to obtain reproducible results over a wide range of concentrations even when using distilled water as the outside liquid.

The fall in osmotic pressure seems to be irreversible. Thus if the osmotic pressure has fallen considerably, due to membrane hydrolysis, and the outside liquid is replaced by sodium hydroxide of p_H 10.0, the osmotic pressure does not rise appreciably. Experiments in which stronger concentrations of sodium hydroxide were added also failed to restore the osmotic pressure to anything like its original value. This will be seen from the following example:—

Table II.

		Manometer reading.
Day.	Experiment commenced. Outside liquid N/8000 NaOH ...	cm.
1st	...	—
2nd	...	16.99
18th	...	13.90
19th	Outside liquid replaced by fresh N/8000 NaOH	14.03
20th	Outside liquid replaced by N/1000 NaOH	11.04
21st	Outside liquid replaced by N/8000 NaOH	13.47

Thus although a solution of NaOH eight times as strong as that originally used was added, and then this replaced by fresh N/8000 NaOH, the original pressure of 16.99 cm. was not restored.

* 'Diss.' Göttingen (1925).

Results.

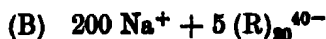
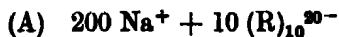
In the following table are shown some of our results, determined in this way:—

Table III.

Dye concentration grams/100 c.c.	Outside liquid.	P observed (cm. of Hg).	P calculated from M. wt.	$\frac{P \text{ observed}}{P \text{ calculated}} \times 100.$
<i>Meta Dye</i> —				
0.529	N/16,000	18.10	13.54	133.7
0.529	N/8000	18.01	13.54	133.0
0.529	N/8000	17.97	13.54	132.7
<i>Benzopurpurina 4B</i> —				
0.486	N/8000	16.34	12.44	131.4
0.523	N/8000	16.99	13.39	127.0
0.523	N/10,000 ($p_H = 10.0$)	17.26	13.39	128.9
<i>Congo Red</i> —				
0.524	N/8000	16.74	13.97	119.8
0.524	N/8000	16.70	13.97	119.8

The value given in the third column is in each case the highest pressure observed (generally after 24 hours), corrected for the height of the dye column supported and the capillary rise. No correction has been made for the back pressure due to the sodium hydroxide.

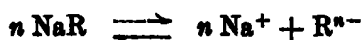
From these results we see that the osmotic pressure of the two dyes under investigation do not differ to any great extent. At first sight we might be led to conclude that this means that the two dyes have the same size of micelle. Such a conclusion is, however, not justified if we admit the possibility of complex micelles. Thus we could have two dyes A and B dissociated as follows:—



and their osmotic pressure would be in the ratio of 210 to 205, a difference of 2.5 per cent., although the micelle of B is twice as large as that of A.

It is therefore necessary to try and obtain evidence as to how much of the osmotic pressure is contributed by the non-diffusible ion. This we can do since we can calculate the ratio of the observed osmotic pressure in the presence of a certain concentration of sodium chloride to the real osmotic pressure. This ratio may be calculated as follows:—

If the dye dissociates as



let c_1 be the concentration of R^{n-} , nc_1 the concentration of Na^+ , and c_2 the concentration of $NaCl$ added.

Then if (as the simplest case) the volumes of the liquids on either side of the membrane are equal, we have :—

Initial distribution.				Equilibrium distribution.				
Inside.		Outside.		Inside.			Outside.	
Na^+ nc_1	R^{n-} c_1	Na^+ c_2	Cl^- c_2	Na^+ nc_1+x	R^{n-} c_1	Cl^- x	Na^+ c_2-x	Cl^- c_2-x

$$\text{The real osmotic pressure} = P = (n+1)c_1 RT. \quad (1)$$

$$\begin{aligned} \text{Opposing pressure of NaCl} &= P_1 = [2(c_2 - x) - 2x] RT \\ &= 2(c_2 - 2x) RT \end{aligned}$$

$$\begin{aligned} \text{Observed pressure} &= P_0 - P - P_1 = (n+1)c_1 RT - (2c_2 - 4x) RT \\ &= [(n+1)c_1 - 2c_2 + 4x] RT. \end{aligned} \quad (2)$$

From Donnan's theory

$$(nc_1 + x)x = (c_2 - x)^2,$$

hence

$$x = c_2^2 / (nc_1 + 2c_2).$$

From (1) and (2)

$$\frac{P_0}{P} = \frac{(n+1)c_1 - 2c_2 + 4x}{(n+1)c_1} = \frac{(n+1)c_1 - 2c_2 + 4c_2^2 / (nc_1 + 2c_2)}{(n+1)c_1}.$$

hence

$$\frac{P_0}{P} = c_1 + \frac{2}{n(n+1)} c_2 \left/ \left(c_1 + \frac{2}{n} c_2 \right) \right.$$

As c_2 becomes very large as compared to c_1 , this approaches the limiting value

$$P/P_0 = n+1,$$

or, in other words, we will be measuring the osmotic pressure due to the non-diffusible ion. This, of course, will only hold good if the concentration of the sodium chloride used does not affect the degree of aggregation of the dye. We have already shown in Part I that in the case of the meta dye a concentration of over 2.0 N is necessary to bring about precipitation and that with concentrations below this particles are not even observed in the ultramicroscope.

Hence by taking a concentration of 0.25 N or less we should expect no change in particle size.

The results so obtained with the meta dye were as shown in the table.

Table IV.

Concentration of NaCl added.	P.	P_0 .	P/P_0 .
N			
0.25	16.74	0.90	18.6
0.25	16.74	0.80	20.9
0.10	16.74	1.22	13.3
0.10	16.74	1.16	14.4
0.0143	16.74	3.78	4.4
0.0143	16.74	3.77	4.4

If we take 21 as the limiting value of P/P_0 ($= n + 1$) then $n = 20$ or the micelle contains 10 disulphonate anions. Assuming $n = 20$, we can calculate what should be the value of P/P_0 for 0.0143 N NaCl. In this actual case the ratio of the outside volume to the inside volume equals 50, hence we have

Initial distribution.				Equilibrium distribution.				
Inside.		Outside.		Inside.		Outside.		
Na^+ nc_1	R^{n-1} c_1	Na^+ c_2	Cl^- c_2	Na^+ nc_1+x	R^{n-1} c_1	Cl^- x	Na^+ c_2-x	Cl^- c_2-x

when 0.0143 N NaCl is used $nc_1 = (\text{approx.}) c_2$.

Assuming $n = 20$ we have (in arbitrary units)

Initial distribution.				Equilibrium distribution.				
Inside.		Outside.		Inside.			Outside.	
Na ⁺ 20	R ⁿ⁻ 1	Na ⁺ 20	Cl ⁻ 20	Na ⁺ 20+50x	R ⁿ⁻ 1	Cl ⁻ 50x	Na ⁺ 20+x	Cl ⁻ 20-x

Then

$$P = 21 RT,$$

$$P_1 = [2(20 - x) - 100x] RT = [40 - 102x] RT,$$

$$P_0 = P - P_1 = (102x - 19) RT.$$

From Donnan's theory we have at equilibrium

$$(20 + 50x) 50x = (20 - x)^2,$$

therefore

$$x = 0.243.$$

Hence

$$P_0 = 24.78 - 19 RT = 5.78 RT,$$

$$\frac{P}{P_0} = \frac{21}{5.78} = 3.63.$$

Since we find 4.4 it would seem that n must be bigger than 20. It is very improbable that the 0.0143 N NaCl has brought about this aggregation. Although the data are at present insufficient to tell us the exact value of n , the experiments point to a micelle containing about 10 (or more) anions.

The possibility of Na ions being included in the micelle must not be excluded. The fact that the osmotic pressures of the two dyes are the same can, however, best be explained if we assume all the Na ions to be free.

The Activity of the Sodium Ions.

A value for the activity coefficient of the sodium ions of the dye may be obtained if we use the Donnan theory of membrane equilibria in its simplest form and make certain assumptions. Thus we may write

$$[\text{Na}^+]_{\text{inside}} = \frac{[\text{Cl}^-]_{\text{outside}}}{[\text{Cl}^-]_{\text{inside}}} \times [\text{Na}^+]_{\text{outside}}.$$

The concentration of the chlorine inside and outside may be obtained by analysis, then assuming complete dissociation and taking the activity coefficient of the chlorine ions inside as equal to that of the chlorine ions outside, we may obtain a value for $[\text{Na}^+]_{\text{inside}}$.

Also we may write

$$(\text{Na}^+)_{\text{dye}} = (\text{Na}^+)_{\text{inside}} - (\text{Na}^+)_{\text{due to NaCl inside}},$$

and hence

$$(\text{Na}^+)_{\text{dye}} = (\text{Na}^+)_{\text{inside}} - (\text{Cl}^-)_{\text{inside}},$$

where the terms in round bracket represent ionic concentrations.

Then, if we write in activities,

$$[\text{Na}^+]_{\text{dye}} = [\text{Na}^+]_{\text{inside}} - [\text{Na}^+]_{\text{due to NaCl inside}}.$$

On the simplest assumption of complete ionisation and that the activity coefficient of the sodium due to the NaCl inside equals the activity coefficient of the chlorine inside, we may write

$$[\text{Na}^+]_{\text{dye}} = [\text{Na}^+]_{\text{inside}} - [\text{Cl}^-]_{\text{inside}}$$

and so obtain a value for $[\text{Na}^+]_{\text{dye}}$. This came to 0.0050 for 0.5 per cent. "meta" dye solution, the concentration of the sodium of which would be about 0.0143. This would give an activity coefficient for the sodium of about 0.35. Values which were not in agreement with this figure but higher, were, however, obtained when higher concentrations of sodium chloride were used, which seems to show that the simplifications made above introduce large errors. This may be due to several factors which we cannot by this method evaluate. The activity coefficient of the chlorine ions inside the membrane may, for instance, be very much lowered by the presence of the dyes.

Discussion.

The osmotic pressure measurements in the presence of electrolytes have shown us that the "meta" dye is not in true solution, but probably has a micelle consisting of at least 10 elementary anions. It was not possible to carry out similar experiments with the "4B" dye, owing to its great sensitivity to electrolytes. The evidence from the other experiments, described in Part I, however (flocculation by electrolytes, ultrafiltration, the ease with which ultra-microns are formed) points to the micelle of this dye being larger than that of the meta dye. If, however, the micelle of the meta dye is so large that the osmotic pressure is almost all due to the sodium ions, the micelle of benzo-purpurine 4B being still larger would not give it an appreciably higher osmotic pressure. In this connection it is of interest to compare the results obtained by Meier for Bordeaux extra. This dye he found to have an osmotic pressure of 172 to 186 per cent. of the value calculated from the molecular weight, this remaining fairly constant over a range of concentration from 0.044 to 1.82 grams per litre. By adding 0.005 N NaCl to 0.000126 N dye he obtained 2.8 for P/P_0 . Assuming this to be the limit value (he omits to say what was the ratio of inside volume to outside volume in his osmometer), then $n = 1.8$, say about 2, that is to say the dye is in true solution. The osmotic pressure of these three dyes could then be explained as follows:—

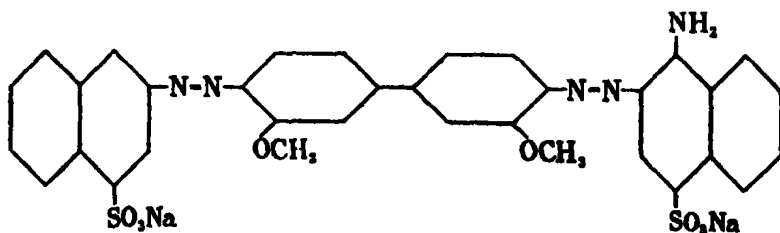
Bordeaux Extra.—In true solution. Activity coefficient of sodium ions 0.6. Osmotic pressure 120 (due to sodium) + 60 (due to R) = 180 per cent. of that given by the molecular weight.

"Meta" Dye.—Micelle containing 10 ions. Activity coefficient of sodium ions = 0.6. Osmotic pressure 120 + 6 (due to R) = 126 per cent.

"4B" Dye.—Micelle containing considerably more than 10 ions. Sodium ion activity coefficient = 0.6. Osmotic pressure = 120 + less than 6 = 120 to 126 per cent.

In the above the activity coefficients have been taken as equal to the osmotic coefficients.

An activity coefficient of this order is not unusually low. Thus the activity coefficient of $N/50 \text{ K}_2\text{SO}_4$ is 0.614. If the activity coefficient is of this order and is about the same for these and other dyes of the same class, the figures 120 to 180 would represent the limits of the osmotic pressures to be expected (cf. our figure of 122 per cent. for congo red and Zeigmondy's figures of 127 to 143 for benzopurpurine 10B). Probably the CH_3O groups in benzopurpurine 10B with their greater affinity for water reduce the micelle formation, just as do the OH groups in Bordeaux extra.



Benzopurpurine 10B.

Zeigmondy found "10B" passed through ultrafilters more readily than "4B."

As we have already pointed out (p. 598), Linderstrøm-Lang considers that the anomalously low osmotic pressures similar to those obtained for these dyes can be equally well explained without assuming the existence of a micelle. Although we consider that the sum of the evidence obtained in this research points to the existence of a micelle, it would be of great interest to determine the particle size by other method that gave less ambiguous results. This, we believe, could be done in the Svedberg ultracentrifuge.

Summary.

The study of the solutions of benzopurpurine 4B and its isomer prepared from meta tolidine has been continued.

(1) Osmotic pressure measurements have been made, the errors arising from membrane equilibria being reduced to a minimum. It has been shown how the minimum amount of alkali necessary to prevent membrane hydrolysis can be calculated.

(2) The osmotic pressures of the two dyes are almost the same. It has been shown how this can be accounted for in spite of the difference in particle size shown by the other experiments.

(3) In the case of the meta dye, the size of the anion has been calculated from the fall in the observed osmotic pressure when a concentration of sodium chloride, large compared with the concentration of these anions, but not large enough to bring about coagulation, is present. From this it would be seen that the micelle of the "meta" dye consists of about 10 anions, while that of the "4B" must therefore be assumed to contain considerably more.

(4) Attempts have been made to measure the activity of the sodium ions, by applying Donnan's theory of membrane equilibria. Owing to complications not fully understood this has not so far been successful.

(5) Although we have at present no direct evidence that all the sodium is in the form of free ions, we can most easily explain the high absolute value of the conductivity, and the fact that it is the same for both dyes and the absolute values of the osmotic pressure and the fact that they are also almost the same in each, although the complexity of the anion is not the same, on the assumption that no sodium, or very little sodium, is included in the multiple anion.

We conclude from the results described here and in Part I that both these dyes exist in solution as totally dissociated colloidal electrolytes, hydrolysis being negligible. The anion of each dye is an unhydrated, or only slightly hydrated, multiple anion, that of the "meta" dye consisting of about 10 elementary anions, while that of the "4B" is considerably larger. The larger anion allows the "4B" to exhibit properties generally associated with colloids, while the smaller anion of the "meta" gives it properties which might be mistaken for those of a true solution.

In conclusion, we would like to thank Professor F. G. Donnan, C.B.E., F.R.S., for the interest with which he has followed this research and the valuable advice which he has given.

The Molecular Symmetry of Hexa-aminobenzene in the Crystalline State, and certain other Properties of the Substance.

By I. ELLIE KNAGGS, Ph.D., F.G.S.

(Communicated by Sir William Bragg, F.R.S.—Received February 25, 1931.)

[PLATE 27]

Introduction.

A benzene derivative in which six like radicles replace the six hydrogen atoms is of rare occurrence, and because of its molecular symmetry of peculiar interest in the study of organic molecules in the crystalline state. Therefore, when Flürscheim and Holmes ('J. Chem. Soc.,' 1929, p. 330) succeeded in preparing hexa-aminobenzene, $C_6H_6H_{12}$, the opportunity of investigating the crystals by X-rays was specially welcomed, though there were certain factors which made the crystals rather undesirable for the work. Most important, the crystals were unavoidably of so minute a size as to be suitable only for powder photographs. Further, the substance was difficult to obtain pure and was comparatively unstable in air. As will be seen in what follows, these drawbacks were partially or wholly overcome.

Experimental.

Some of the first specimens, which Flürscheim and Holmes submitted consisted of crystals, which though not large enough for a single crystal X-ray method, were yet large enough to be seen under the microscope with a $\frac{1}{4}$ -inch objective, as perfect little cubic octahedra, transparent and pale yellow in colour and showing complete extinction between crossed nicols. From these observations it follows that the crystals belong to one of the following three cubic classes :—

The hexakis octahedral (O_h) ;

The dyakis dodekahedral (T_h) ; or

The pentagonal icositetrahedral (O).

A number of photographs (see 1 and 2, Plate 27) of the crystalline powder were taken with copper K_α radiation ($\lambda = 1.539$) from a Shearer X-ray tube. The first photographs were confused by lines due to impurities or decomposition. Holmes, however, was eventually successful in eliminating all impurities and it was found that by sealing the pure substance in a thin-walled

glass tube it was possible to arrest decomposition indefinitely. Measurements of lines obtained from the pure substance showed the space lattice to be a simple cubic one Γ_1 and the smallest cubic cell to be one with sides 15.14 A.U. in length.

N , the number of molecules in this unit cell may be found from the equation

$$\rho = N \times 168 \times 1.65/15.14^3,$$

where ρ = the density and 168 is the molecular weight of $C_6 N_6 H_{12}$ referred to oxygen as 16.

The density could not be determined by the usual methods, but was found by Holmes to be greater than 1.1, since the crystalline powder is precipitated in a liquid of that density. Now N may be 1, 2, 4, 6, 12, 16, 24 or 48. Only if $N = 16$ is a reasonable value, namely 1.27, obtained, for ρ . It may be concluded, therefore, that there are 16 molecules in the unit cell. From this, combined with a Γ_1 lattice, it follows that the molecule must have threefold symmetry.

In Table I are given the calculated spacings, d , for planes $\{hkl\}$ in a simple cubic cell of side 15.14 A.U., and also the spacings corresponding to the lines on the photographs.

The lines corresponding to the planes $\{310\}$ and $\{320\}$ establish the lattice as Γ_1 , since for a face-centred lattice both would be absent and for a body-centred lattice $\{320\}$ would be absent. Except for planes of low indices, there are generally so many planes having the same or nearly the same spacings, that there is much ambiguity in the identification of the lines. If it had been possible to obtain a single crystal of sufficient size, this ambiguity could have been avoided by taking oscillation photographs. However, in spite of this inability to identify unequivocally all the lines, it has still been possible (excluding "association" of the molecules) to determine the space-group. There are eight space-groups with a Γ_1 lattice, belonging to the three crystal classes O_h , T_h and O . Of these, there are only three, namely, O_h^3 , O_h^2 and O_h^4 , which allow of 16 molecules to the unit cell.

In O_h^3 and O_h^4 odd orders of $\{hkl\}$ planes, where $(h+k)$ is odd must be absent. But this condition is not satisfied since $\{310\}$ and $\{320\}$ are present. The only space-group left then is the O_h^2 in which $\{hkl\}$ planes are halved when l is odd. There is no line on the photographs, which is certainly due to an odd order of such a plane and all the lines observed can be accounted for otherwise. The space-group O_h^2 , therefore, appears to be established and with it the molecular symmetry of hexa-aminobenzene in the crystalline

Table I.

Planes.	$d_{\{hkl\}}$ in Å.U.		Approximate intensities.
	Calculated.	Observed.	
100	15.14	—	
110	10.7	—	
111	8.74	—	
200	7.57	—	
210	6.70	—	
211	6.18	—	
220	5.35	5.36	Very strong.
221, 300	5.04	—	
310	4.76	4.75	Very very weak.
311	4.56	—	
222	4.36	—	
320	4.20	4.22	Medium strong.
321	4.05	—	
400	3.78	3.78	Strong.
410, 322	3.66	—	
411, 330	3.56	—	
331	3.47	—	
420	3.38	3.39	Very very weak.
421	3.30	—	
332	3.22	—	
422	3.09	3.09	Strong.
430, 500	3.03	—	
431, 510	2.97	—	
511, 333	2.91	—	
520, 432	2.81	2.78	Very very weak.
521	2.76	—	
440	2.67	2.67	Strong.
441, 522	2.63	—	
433, 530	2.59	—	
531	2.55 (5)	—	
442, 600	2.52	2.51	Very weak.
610	2.48	—	
611, 532	2.45	—	
620	2.38	2.39	Very very weak.
443, 621, 540	2.36	—	
541	2.34	—	
533	2.31	—	
622	2.28	2.29	Weak.
542, 630	2.25	—	
631	2.23	—	
444	2.18	—	
632, 700	2.16	—	
543, 560, 710	2.14	—	
551, 711	2.12	—	
640	2.10	—	
641, 720	2.08	—	
552, 633, 721	2.06	2.07	Fairly weak.
642	2.02	—	
544, 722	2.00	—	
730	1.96	—	
553, 731	1.97	1.97	Very weak.
643	1.94	—	
732	1.92	—	
800	1.89	—	
740, 810	1.88	—	
554, 741, 811	1.86	—	
733	1.85	—	
644, 820	1.83	1.83	Very weak.
742, 821	1.82	—	

state. For since it requires 48 asymmetric molecules per unit cell to build up this space-group and it has been found that there are actually 16 molecules in the unit cell, the molecules must each possess threefold symmetry. This will be a trigonal axis, which from stereo-chemical considerations will evidently be perpendicular to the general plane of the six carbon ring of the molecule and in the crystal must necessarily be perpendicular to the {111} planes. So the molecules will lie with their centres four on each of the trigonal axes, which in this space-group intersect in the centre of the cell.

Examination at Low Temperature.

Besides the photographs at room temperature, a photograph at liquid air temperature was taken and from it a determination of the linear coefficient of expansion between -183° and $+15^{\circ}$ C. for the crystal was made.

Table II gives a list of spacings obtained from the lines observed on the low temperature photograph and these are compared with the corresponding spacings at ordinary room temperature. In agreement with the symmetry of the crystal, the ratios obtained are found to be very constant. Neglecting the line in brackets, which is a very weak one, the ratio of the mean value of the spacing at 15° C. to that at -183° C. is 1.02 ± 0.004 . This leads to a value 14.84 A.U. for the length of the side of the unit cell at -183° C. and the linear coefficient of expansion between -183° and $+15^{\circ}$ C.

$$0.3/(14.84 \times 198) = 0.000102.$$

Table II.

d at 15° C.	d at -183° C.	$d_{15^{\circ}}/d_{-183^{\circ}}$
5.36	5.27	1.018
4.23	4.13	1.024
3.78	3.72	1.017
3.09	3.03	1.02
2.67	2.63	1.016
2.51	2.46	1.018
2.29	2.24	1.022
2.07	2.03	1.02
(1.97)	1.96	1.005
1.83	1.79	1.022

The Rate of Decomposition in Air.

From a chemical point of view, it was thought of importance to obtain some measure of the rate at which the substance decomposes in air. X-ray photographs of the powder crystals contained in a thin-walled open glass

tube were taken at intervals. After 3 days signs of decomposition began to show in the blurring of the lines on the photograph. At the end of 6 days the change was very marked and at the end of 17 days the substance had broken down completely, the photograph showing only one rather diffuse ring. Exactly the same photograph is obtained from material kept exposed to air for more than a year.

The theoretical importance of the degree of stability of the substance will not be discussed here, as it is dealt with fully by Flürscheim and Holmes (*loc. cit.*). It will be sufficient to say that the X-ray evidence is in agreement with the view of Flürscheim and Holmes that the stability of hexa-aminobenzene is greater than has hitherto been supposed.

Theoretical.

In the absence of single crystal photographs and accurate intensity measurements, a determination of the structure will not be attempted. Nevertheless, it may be of interest to consider the facts available and to try to arrive at some conclusions as to a possible structure.

First some remarkable absences of reflections may be noted. The {100} planes are quartered and were it not for the moderately strong reflection from {320} and the extremely weak one from {310}, the cell dimensions could be halved. That is, the crystal approximates to one built on a cube of side 7.57 and containing only two molecules instead of the 16 of the larger cell. The reflecting planes referred to this smaller cell would be 110, 200, 211 and 220, etc., thus indicating a centred cube. This approximate structure may be represented as in fig. 1, in which O and X represent groups of atoms, of which the X groups are so nearly like the O groups as regards the scattering of X-rays that there is no 100 reflection. The two kinds of groups O and X cannot, of course, be exactly alike or there would be no reflections {310} and {320}, as referred to the larger cell.

These groups O and X must each possess four axes of trigonal symmetry, in accordance with the cubic symmetry of the cell. The two molecules of the approximately realised small cell cannot therefore be identified with O and X, for a benzene ring with four trigonal axes is inconceivable, though it may very well, and evidently does in this case, possess one such axis. O and X must, therefore, consist of groups of atoms drawn from different molecules.

Considering now the full-sized cube of side 15.14 A.U., the 48 asymmetric units of the space-group O_h^3 can be divided into two sets of 24. If one set is grouped round each corner of the cube, the second is grouped round the centre,

being derived from the first by reflection across 110 and a displacement along the cube diagonal equal to half its length.

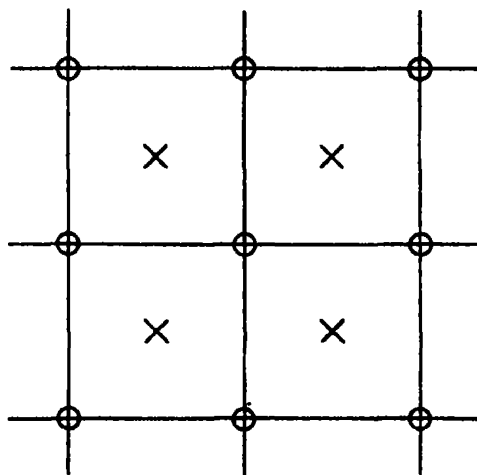


FIG. 1.

Each set has four trigonal axes, three diagonal axes, symmetry about {100} and a centre, that is T_h symmetry. Since there are 16 molecules of $C_6(NH_2)_6$ per unit cell, each of the sets consists of eight molecules. The trigonal symmetries must, therefore, be provided by the molecules themselves, which evidently lie with their centres one on each of the semi-diagonals radiating outwards from the centre of the set of eight. Referred to this point, the eight rings of the one set of molecules may be represented by the following sets of three co-ordinates

$$\begin{array}{ll}
 xyz, & yzx, & zxy; & x\bar{y}\bar{z}, & \bar{y}\bar{z}\bar{x}, & \bar{z}\bar{x}\bar{y}; \\
 xy\bar{z}, & y\bar{z}x, & \bar{z}xy; & \bar{x}y\bar{z}, & y\bar{z}\bar{x}, & \bar{z}\bar{x}y; \\
 x\bar{y}z, & \bar{y}zx, & zxy; & \bar{x}\bar{y}z, & \bar{y}z\bar{x}, & z\bar{x}y; \\
 \bar{x}yz, & yz\bar{x}, & z\bar{x}y; & \bar{x}\bar{y}\bar{z}, & \bar{y}\bar{z}\bar{x}, & \bar{z}\bar{x}\bar{y}.
 \end{array}$$

While the eight rings of the other set will be represented similarly by co-ordinates

$$yxz, zyx, xzy, \text{ etc. ;}$$

referred to its own centre, or

$$\frac{1}{2} + y, \frac{1}{2} + x, \frac{1}{2} + z; \frac{1}{2} + z, \frac{1}{2} + y, \frac{1}{2} + x; \frac{1}{2} + x, \frac{1}{2} + z, \frac{1}{2} + y, \text{ etc.}$$

referred to the centre of the first set.

Fig. 2 shows the relative positions of these cubic sets of eight molecules.

The centres of the eight outlying cubes are the corners of the unit cell of side 15.14 \AA.U. , while the centre of the middle cube is, of course, the centre of that

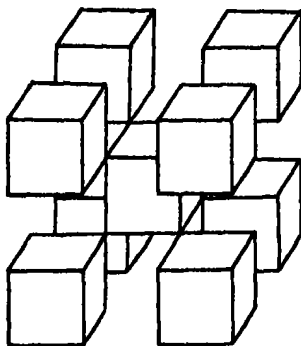


FIG. 2.

unit cell. The first of the two kinds of sets of eight molecules, whose coordinates are given above is related to the centre cube, while a set of the other kind is related to each of the outlying cubes.

In fig. 3 let ACB represent a diagonal of the unit cell, A and B being its extremities and C the centre of cell. The length AB is 26.2 \AA.U. and along it lie b_1, b_2, b_3, b_4 , the centres of four molecules with their benzene rings perpendicular to it. Suppose b_1 and b_2 , as also b_3 and b_4 are 3.5 \AA.U. apart (a

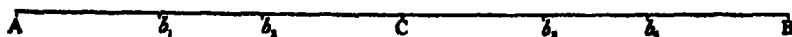


FIG. 3.

value in agreement with the dimensions found for anthracene and other benzene ring compounds) the distance Cb_3 will be

$$\frac{1}{2} (CA - 3.5) = \frac{1}{2} (13.1 - 3.5) = 4.8 \text{ \AA.U.}$$

In accordance with the symmetry all the planes of the rings in one set are at the same distance from the centre of the set. It will be seen that there is just room for them to clear each other. For let CA_1 and CA_2 (fig. 4) be two semi-diagonals of the set making an angle of 70° with each other. Let m and n be the centres of two rings Cm and Cn will then each be 4.8 \AA.U. Suppose the rings arranged so that, in each case, the narrowest cross-section, which is found in other benzene ring compounds to be about 2.6 \AA.U. , lies in the plane CA_1A_2 . Then the rings will extend to P and Q respectively making mP and $nQ = 1.3 \text{ \AA.U.}$ From this the distance PQ may be calculated and it is found to be approximately 3.38 \AA.U. So that placing the rings 3.5 \AA.U.

apart along the cube diagonal, leaves only just enough space between the rings on adjacent diagonals. In fact, the positions of the rings are fixed within

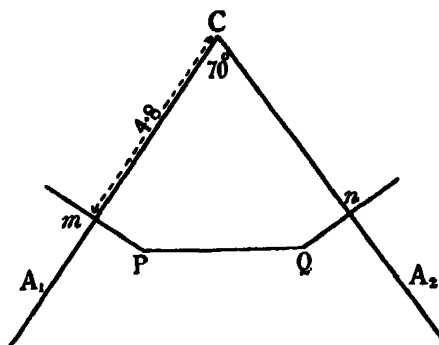


FIG. 4.

narrow limits. In fig. 5 is shown a projection of the rings on a cube face, the rings being represented by ellipses, of which the major axis is 3 Å.U.

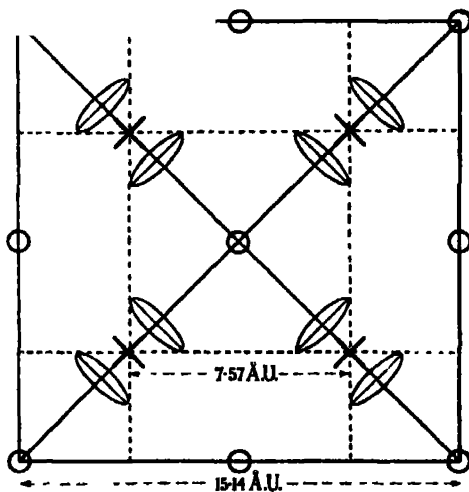


FIG. 5.

The positions of the nitrogen atoms have next to be considered. Now it is clear that nitrogen atoms cannot lie between adjacent carbon rings, such as b_1 b_2 in fig. 3, for there is no space available. They must, therefore, either ring the carbon rings in some way or be drawn away from the carbon rings, so as to form groups of their own inside the small cubes, which have a carbon ring at each corner, such as the small cube of side 7.57 Å.U., whose centre is the centre in fig. 5. In any case the packing will be very tight.

Returning to fig. 1, on this view, the groups of two carbon rings may be

regarded as represented by the crosses, while the nitrogen groups are represented by the noughts. Since the scattering power of the nitrogens is not very different from that of the carbons, the arrangement is in accordance with the non-appearance of the 200 reflection and the approximation to a smaller centred cubic cell of side 7.57 \AA.U.

Photograph 3 (Plate 27) is of a model built to scale to show a corner of one of the small cubes of side 7.57 \AA.U. The elliptical disc is intended to represent a ring of carbon atoms. It will be seen that behind the disc, that is between carbon rings adjacent to one another along a diagonal of the large cube, there is no space into which nitrogen atoms could be packed, but they could be grouped inside the small cell as suggested above.

The structure described is admittedly only a suggestion and in any case approximate, but it does appear to fit in with the experimental observations. One point, however, is firmly established and that is the trigonal symmetry of the $\text{C}_6(\text{NH}_2)_6$ molecule. Whether the molecule really possesses any more symmetry than a threefold axis cannot be said, but, at any rate, it only uses a threefold axis in building up the symmetry of the cell.

Summary.

Hexa-aminobenzene has been examined by the powder X-ray method.

The space group has been found to be O_h^3 with therefore a Γr lattice.

There are 16 molecules in the unit cell of side 15.14 \AA.U. and the molecules possess a threefold axis of symmetry.

The spacings of the planes at -183° C. have been measured and compared with those at 15° C. and the change in spacing, in accordance with the cubic symmetry, has been found to be uniform in all directions measured.

The coefficient of linear expansion between -183° C. and $+15^\circ \text{ C.}$ has been estimated as 0.000102 .

The stability of hexa-aminobenzene in air has been studied by means of X-rays.

A possible structure has been outlined.

Acknowledgments.

It is with much pleasure that I record my thanks to Sir William Bragg for the interest which he has taken in these results and for many helpful suggestions when discussing the structure of hexa-aminobenzene. My thanks are also due to Mr. E. L. Holmes for his co-operation in preparing samples of the crystals and to the Managers of the Royal Institution for giving me the opportunity of carrying out the work in the Davy Faraday Laboratory.



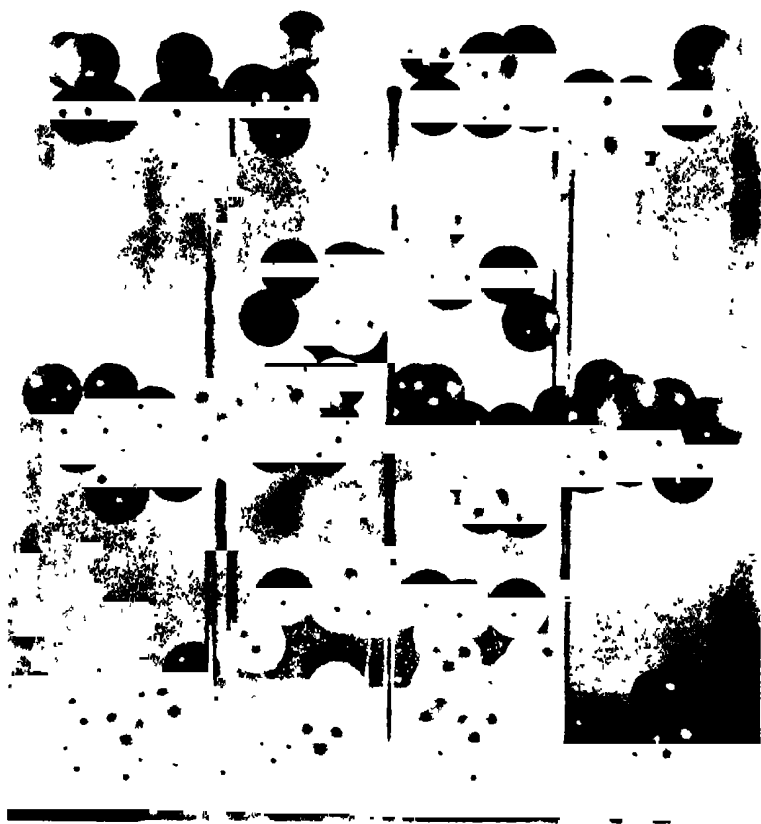
Photograph 1. Hexa-aminobenzene



Photograph 2. -Hexa-aminobenzene



Photograph 3.



Mannitol. (001) Face

An X-Ray Study of Mannitol, Dulcitol, and Mannose.

By THORA C. MARWICK, Textile Physics Laboratory, The University,
Leeds.*

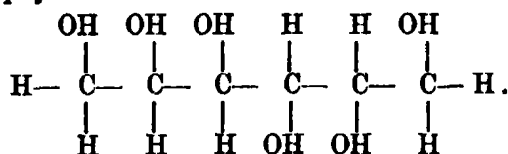
(Communicated by Sir William Bragg, F.R.S.—Received March 5, 1931.)

[PLATE 28.]

The present work was undertaken in the hope that a convenient avenue of approach to the structure of the sugars might be opened up by the two hexose alcohols, mannitol and dulcitol, which give excellent crystals at ordinary temperatures. It is not unreasonable to expect that isomers such as these, with very similar densities, might show in the dimensions of their unit cells certain similarities suggestive of some form of molecule common to the hexose alcohols, as the long-chain configuration is common to the hydrocarbons and the fatty acids. In addition, a collateral examination of mannose might equally well be expected to yield some evidence as to the nature of the change which takes place when a sugar is formed from the corresponding alcohol, and hence to supply data of fundamental importance in correlating the structures of the sugars and of their derivatives.

d-Mannitol and Dulcitol.

The Space-Group of Mannitol.—Structural formula



Class.—Orthorhombic bisphenoidal.

Unit cell.— $a = 8.65$ A.U. $\left. \begin{array}{l} b = 16.90 \text{ A.U.} \\ c = 5.56 \text{ A.U.} \end{array} \right\} \text{error 1 per cent.}$

Density.— 1.497 gms./c. cm. (determined by flotation method).

Number of molecules per unit cell.—4.

Volume per molecule.— 203 A.U.³.

* The experimental work discussed in this paper was carried out at the Davy Faraday Laboratory of the Royal Institution of Great Britain.

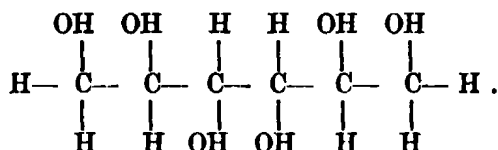
Axial ratio.—

$$\begin{array}{l} a : b : c \\ 0.511 : 1 : 0.329 \text{ (X-ray measurements)} \\ 0.5121 : 1 : 0.6557 \text{ (Groth).}^* \end{array}$$

The values quoted from Groth are for the β -form of mannitol and are due to Zepharovich,[†] whose measurement of the ratio b/c is based on the observation of two faces which he called (012) and (112). The X-ray evidence shows that these planes must be given the true indices (011) and (111).

Space-group.—A careful investigation of many oscillation photographs failed to reveal any of the odd orders from ($h00$), ($0k0$), and ($00l$). The ($00l$) reflections are very weak and could not be traced beyond the sixth order, but the ($h00$) reflections were examined as far as the tenth, and the ($0k0$) as far as the twentieth order. In the absence of any general "halvings" this indicates that the crystal belongs to the space-group Q_4 .[‡] The lattice is simple orthorhombic and the four molecules in the unit cell are without symmetry.

The Space-group of Dulcitol.—Structural formula



Class.—Monoclinic prismatic.

Unit cell.— $a = 8.61 \text{ \AA.U.}$
 $b = 11.60 \text{ \AA.U.}$
 $c = 9.05 \text{ \AA.U.}$ } error 1 per cent.
 $\beta = 113^\circ 45'.$

Density.—1.466 gms./c. cm.

Number of molecules per unit cell.—4.

Volume per molecule.—216 \AA.U.^3 .

Axial ratio.—

$$\begin{array}{l} a : b : c \\ 0.74 : 1 : 0.78 \text{ (X-ray measurements)} \\ 0.737 : 1 : 0.774 \text{ (Groth).}^\S \end{array}$$

* 'Chem. Kristal.,' vol. 3, p. 431 (1910).

† 'Z. Kristal.,' vol. 13, p. 145 (1888).

‡ $P2_12_12_1$ in the new nomenclature. Astbury and Yardley, 'Phil. Trans.,' A, vol. 224, p. 221 (1924).

§ *Loc. cit.*, p. 434.

Space-group.—Long-exposure oscillation photographs showed no trace of the odd-order reflections from the $(0k0)$ planes as far as $(0.13.0)$. Further, reflections from the $(h0l)$ planes were absent when l was odd. The crystal was, therefore, assigned to the space-group C_{2h}^2 , the glide being parallel to the c -axis.* This is in agreement with the fact that the alcohol is not optically active.

The Relationship between Mannitol and Dulcitol.

The two cells, at first sight apparently very different, show obvious dimensional similarities when viewed as in fig. 1.

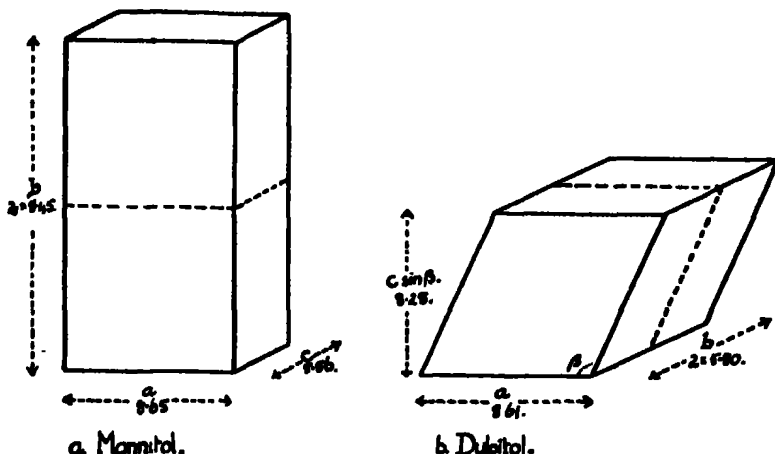


FIG. 1.

The most striking feature is the occurrence in both crystals of the length 8.6 Å.U., which is almost exactly equal to that of the unit cell of hexane, 8.55 Å.U.† This suggests that the molecules are based on a zig-zag carbon chain, similar to that of the hydrocarbons and fatty acids, lying along the a -axis in each case.

This hypothesis is supported by the equality of cross-section of the two cells; the values, in each case for four molecules, are for mannitol, 94 Å.U.², and for dulcitol, 96 Å.U.². A separate investigation, described in detail at the end of this paper, gives for the area of cross-section of the $(CH_2.OH)$ end-group a value 22 Å.U.². Taking into account the presence of the oxygen atoms along the chain as well as in the end-groups, the area 96 Å.U.² corresponds reasonably well with what might be expected for four such long-chain molecules. Figs. 2, 3 and 4 show the suggested arrangement of the molecules in the two crystals.

* $P2_1/c$ in the new nomenclature.

† Müller, 'Proc. Roy. Soc.,' A, vol. 127, p. 417 (1930).

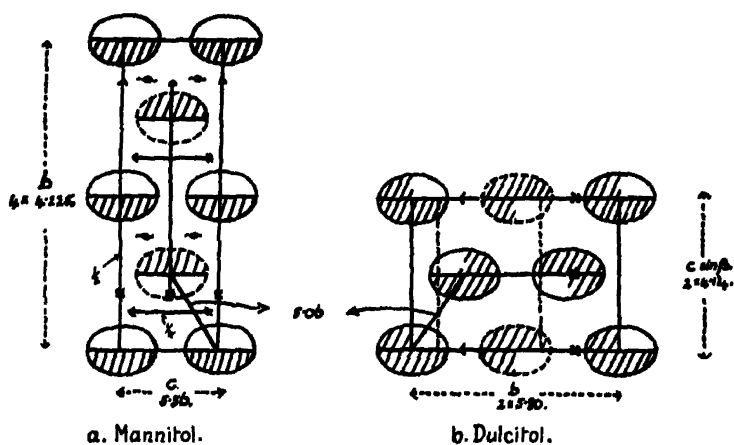


FIG. 2.

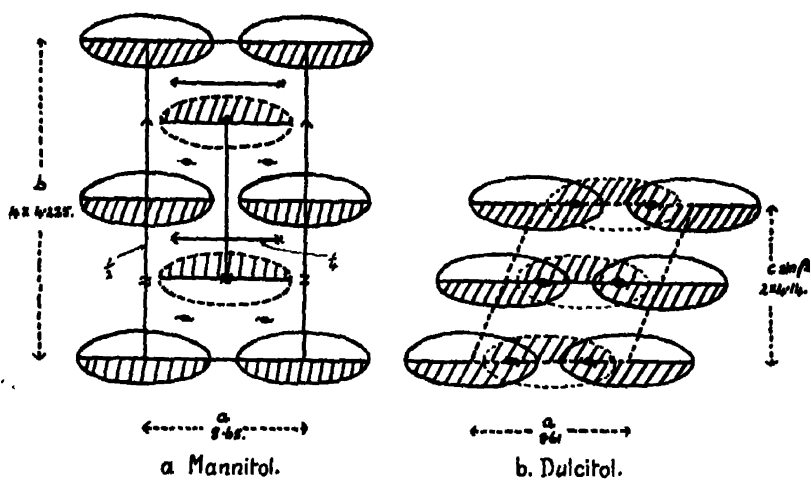


FIG. 3.

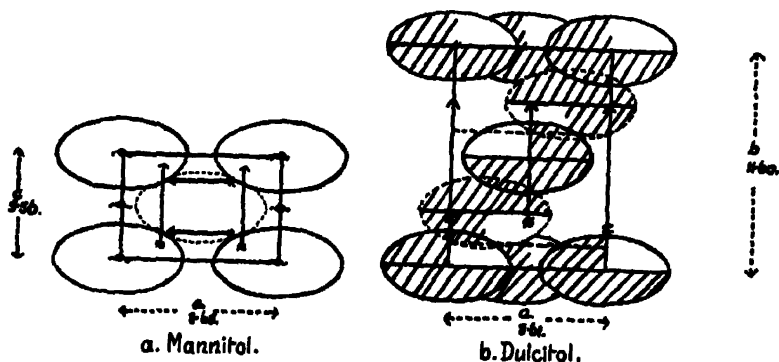


FIG. 4.

From fig. 2 it is seen that in this arrangement the shortest distance between the chain axes is exactly the same in the two cases, 5.06 Å.U. Taken alone, this might be merely a coincidence, but when taken in conjunction with the fact that photographs of both substances just above their respective melting points show a single ring with a mean spacing of about 4.9 Å.U., it becomes highly significant. This ring, which almost certainly indicates the distance of closest approach of the molecules, is indistinct at the edges as are most liquid rings, but is located approximately between the limits 4.2 and 5.5 Å.U., in both mannitol and dulcitol. Fig. 5 shows how these two quantities occur in the two rectangular parallelepipeda with which the molecules of mannitol and dulcitol may be considered to be associated in the crystalline state.

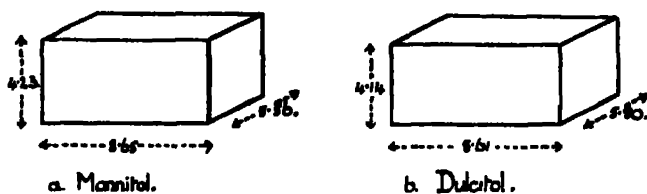


FIG. 5.

Another feature of this system is that it correlates the very perfect cleavage parallel to (010) in mannitol with the perfect cleavage parallel to (021) in dulcitol. Both these cleavages are parallel to the a -axis and, according to the postulated arrangement, involve a splitting along the sides of the chains, a behaviour which might appear unlikely in view of the fact that the fatty acids cleave between the ends of the chains. But if we consider the cleavage plane of the fatty acids not simply as the plane which passes through the ends of the molecules, but as the plane in which the carboxyl groups are concentrated, the apparent disharmony between the two cases disappears. The molecules are overlapping in their long directions, with the consequence that there is no cleavage transverse to this direction in dulcitol, and only an imperfect one in mannitol. The cohesion in both structures is purely a function of the configuration of the hydroxyl groups lying along the sides of the molecules, and for this reason, too, since the two alcohols have different hydroxyl configurations, it is not a strictly legitimate objection that mannitol does not show a cleavage parallel to (021), and dulcitol a cleavage parallel to (001) corresponding to the (010) in mannitol. The most that one can expect is that the two crystals should cleave in an analogous manner; and this is precisely what is found.

When scale models are constructed in accordance with the schemes shown

diagrammatically in figs. 2, 3 and 4, it is seen that mannitol possesses the characteristics of a "layer lattice," the alternate sheets of molecules parallel to (010) being held together by strong and weak forces in turn. One side of each molecule carries four hydroxyl groups and the other side two hydroxyl groups, so that the resultant effect of the three dyad screw-axes is to bring about a clinging together of the heavily loaded sides, but little or no interaction between the remaining pairs of hydroxyl groups on the opposite sides. The figures illustrate this point well, but the photograph of the proposed mannitol model brings it out very clearly. The model of dulcitol suggests a similar strong attraction between the (001) planes, but the alternating planes of minimum attraction are absent and there is no (001) cleavage. In mannitol each molecule is associated with a width of 5.56 Å.U. in the plane of the zig-zag and a distance of 4.23 Å.U. normal to the plane of the zig-zag. The corresponding quantities for dulcitol are 5.8 and 4.14 Å.U.

In dulcitol, also, it is true that there are four hydroxyl groups on one side of the chain and two on the other, but they are more symmetrically disposed than in the case of mannitol, with the result that, with the aid of two enantiomorphous molecules, an equilibrium arrangement is attained by sliding the parallelepipeda of fig. 5, *b*, in a direction parallel to the *a*-axis to the positions implied by the β -angle of the monoclinic cell. With the molecules in the positions given by figs. 2, 3 and 4, the model shows a striking uniformity of structure of such a kind that each molecule is linked by pairs of hydroxyl groups to its neighbours in the (021) planes. The principle of this simple molecular interlocking is shown in fig. 6.

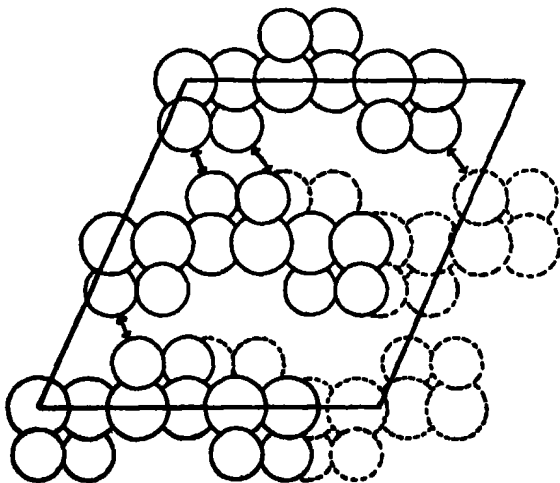


FIG. 6.

It is directly across the paired hydroxyl groups that the crystal cleaves, in a manner reminiscent of the fatty acids. A cleavage parallel to (001) would involve rupture of all the hydroxyl junctions and does not take place; what apparently does happen is that the crystal cleaves so that one half of its junctions are broken, while the other half remain to bind together the molecules of the cleavage plane (021).

The value of the β -angle of dulcitol, $113^\circ 45'$, seems also to be determined by the simple pairing of hydroxyl groups described above and shown diagrammatically in fig. 6. The hydroxyl groups lie in planes perpendicular to the length of the molecule, so that for any two chains in adjacent layers a direct cross-linking would involve a translation of twice the distance between two consecutive carbon atoms. Such a displacement would give rise to a β -angle (acute) of $\tan^{-1} 4.14/2 \times 1.26 \approx 59^\circ$, instead of the observed $66^\circ 15'$. Owing to the counter-attractions of the other chains, however, the molecule is forced to take up an equilibrium position corresponding to the observed angle.

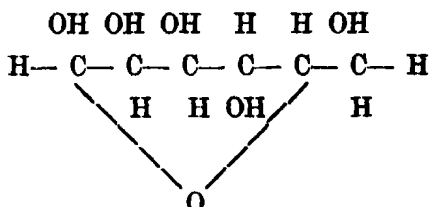
Finally, from the positions of the molecules suggested, it would be expected that in mannitol (020) should be weak and (021) strong, whereas in dulcitol (002) and (021) should both be strong; such is indeed the case.

The dimensions of the unit cell of mannitol $(2 \times 8.45) \times 5.56 \times (2 \times 4.3)$, and of dulcitol, $9.05 \sin 66^\circ 15' \times (2 \times 5.8) \times (2 \times 4.3)$, suggest that some arrangement of the molecules other than that described above might be possible, in fact that they should lie along the b -axis in mannitol and in some way bridging the (001) planes in dulcitol. Three positions only need be considered for dulcitol: (a) the molecules lie along the c -axis; (b) the molecules are perpendicular to the a -axis; (c) the molecules lie along the (101) planes. Since the glide is $c/2$, it seems inevitable that the first possibility, if it gave rise to any cleavage at all, would give rise to one parallel to (011), instead of to the observed (021), while the second arrangement would make the maximum possible distance between the chains equal to 2.9 A.U., if the (021) cleavage is to be retained. The third suggestion is consistent with the observed cleavage, but would involve a molecular length of 9.7 A.U., which is not only excessive in comparison with the length of hexane (8.55 A.U.), but which has no parallel in the dimensions of mannitol. Thus, however tempting may appear the hypothesis that the molecules do *not* lie approximately along the a -axis, it does not seem to be at all possible to obtain such a striking degree of correlation between the structures of mannitol and dulcitol by any other arrangements than those described above. If a cleavage across the ends of the molecules is

to be insisted upon, then all attempts at dimensional correlation appear to be fruitless.

d-Mannose.

The Space-group of Mannose.—Structural formula



Class.—Orthorhombic bisphenoidal.

Unit cell.— $a = 7.62$ Å.U.
 $b = 18.18$ Å.U.
 $c = 5.67$ Å.U. } error 1 per cent.

Density.—1.501 gms/c.cm. This was determined by the flotation method in a mixture of α -monobrom-naphthalene (S.G. 1.488 at 16° C.) and methylene iodide (S.G. 3.33 at 15° C.).

Number of molecules per cell.—4.

Volume per molecule.—196 Å.U.³.

Axial ratio.—

$$\begin{array}{l}
 a : b : c \\
 0.419 : 1 : 0.312 \text{ (X-ray measurements)} \\
 0.826 : 1 : 0.319 \text{ (Groth.)}^*
 \end{array}$$

Groth's values are due to Mohr.† The only face observed from which the ratio a/b could be determined is given as (110). This must now be given the true indices (120), and Mohr's value for a/b then becomes 0.413 as compared with 0.419 from X-ray measurements.

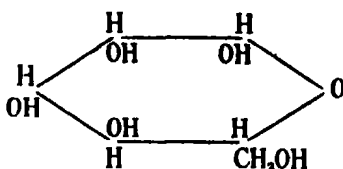
Space-group.—As in mannitol, no general "halvings" were observed, neither was any trace found of the odd order reflections from the ($h00$), ($0k0$) and ($00l$) planes, although these were examined in each case as far as possible, i.e., the ($h00$) planes to the seventh order, the ($0k0$) planes to the fifteenth order, and the ($00l$) planes to the fifth order. The crystal therefore belongs to the space-group Q_4 . The four molecules are asymmetric.

* *Loc. cit.*, p. 441.

† 'Z. Kristal.' vol. 30, p. 642 (1899).

The Relationship between Mannose and other Saccharides.

In view of the results obtained for mannitol, the dimensions of the unit cell of mannose are at once suggestive. They are $7.62 \times 5.67 \times (4 \times 4.55)$, while for mannitol we have $8.65 \times 5.56 \times (4 \times 4.23)$. The dimensions of the mannose cell are just of the order that would be expected for a structure built up of manno-pyranose rings, in which five carbon atoms and one oxygen atom form a "crumpled" hexagon to which are attached four hydroxyl groups and a side-chain, CH_2OH . In particular, from what has been said of the



The Mannose Ring.

mannitol structure above, the thickness of the ring must be something greater than 4.23 \AA.U. , because of the "crumpling" of the hexagon. Thus it seems clear that the dimension of the mannose cell which arises from the thickness of the ring is (4×4.55) . Similarly, from the known dimensions of the carbon atom and of hexagon rings which are based on it, 5.67 corresponds to the normal width of the ring, and 7.62 to the width in the direction of the side-chain.

This hypothesis is the only one so far suggested which shows not only the connection between the alcohols and the sugars, but more important still, the close similarity underlying the apparently widely divergent results obtained for the isomers in both the hexoses and the hexose alcohols. In order to test it more thoroughly, an examination was made by Astbury and Marwick* of the known crystallographic data for cellulose and the sugars. The results, which have already been published in 'Nature,' may be quoted here directly.

"From an examination of the available data for cellulose and the sugars, we have formed the conclusion that the six-atom sugar ring is associated in the crystalline state with certain linear dimensions which are approximately constant, and that at least one of these dimensions usually corresponds to

* 'Nature,' vol. 127, p. 12 (1931).

one of the axial lengths of the unit cell. The existing crystallographic data are as follows :—

	a.	b.	c.	Density.
Native cellulose	8.3	10.3	7.9, $\beta = 84^\circ$	1.52
Hydrate cellulose	8.14	10.3	9.14, $\beta = 62^\circ$	1.56
Cellobiose	5.0	13.2	11.1, $\beta = 90^\circ$	1.556
Sucrose	11.0	8.7	7.65, $\beta = 103\frac{1}{2}^\circ$	1.588
Mannose	7.62	18.18	5.67	1.501
Glucose	10.40	14.99	4.99	1.544
Fructose	8.06	10.06	9.12	1.598
Sorbose	6.12	18.24	6.43*	1.654

* Calculated from the density, crystal class, and axial ratios.

"The most striking feature of the above list is the small variation in density shown by these saccharoses. This in itself strongly suggests an approximate close-packing of some molecular unit, but when we arrange the data as in the following table, it becomes still more apparent how the dimensions of this unit—undoubtedly the sugar ring with its side-chain—impress themselves on the dimensions of the various unit cells.

	Axial dimension.	Cross-sectional product.
Native cellulose	10.3	$8.3 \times 7.9 \sin 84 = 65.2$
Hydrate cellulose	10.3	$9.14 \times 8.14 \sin 62 = 65.7$
Cellobiose	11.1	$5.0 \times 13.2 = 66.0$
Mannose	5.67	$(\frac{1}{2} \times) 18.18 \times 7.62 = 69.3$
Sucrose	11.0	$8.7 \times 7.65 \cos 13\frac{1}{2} = 64.7$
Sucrose	7.65	$(\frac{1}{2} \times) 11.0 \times 8.7 \cos 13\frac{1}{2} = 46.5$
Glucose	$(2 \times) 7.45$	$10.40 \times 4.99 = 51.9$
Mannose	7.62	$5.67 \times (\frac{1}{2} \times) 18.18 = 51.5$
Mannose	$(4 \times) 4.55$	$5.67 \times 7.62 = 43.2$
Fructose	$(2 \times) 4.56$	$(2 \times) 5.03 \times 8.06 = 40.6$
Sorbose	$(4 \times) 4.56$	$6.12 \times 6.43 = 39.3$

"Putting $xy = 66.6$, $yz = 51.7$, and $xz = 41.0$, in order to determine the mean values of x , y and z respectively, gives $x = 7.27$, $y = 5.64$, and $z = 2 \times 4.58$. We suggest that the interpretation of these results is that, on the average, the sugar ring takes about $4\frac{1}{2}$ A. normal to the ring, about $5\frac{1}{2}$ A. across the ring in the direction of the cellulose chains, and about $7\frac{1}{2}$ A. across the ring in the direction of the side-chain, $-\text{CH}_2 \cdot \text{OH}$."

Returning now once more to the question of the details of the mannose and

alcohol structures, it may be mentioned that the intensities of a large number of reflections have been estimated by eye; but in consequence of the complexity of the molecules, their lack of symmetry, and the fact that carbon and oxygen are little different in weight, it would be dangerous to lay too much stress on evidence deduced from such estimations alone. The more outstanding features appear to support the conclusions arrived at above, but the complete analysis must await accurate photometric measurements. Since the author is unable to continue the work, this task has been undertaken by Dr. J. Robertson, of the Davy Faraday Laboratory of the Royal Institution.

Measurement of the Area of Cross-section of the Alcohol End-group, CH₂OH.

It has been shown by A. Müller* that in crystals the effect of replacing the (CH₃) end-group of a hydrocarbon by an acid group (COOH) or an alcohol group (CH₂OH) is to cause a tilt of the long chains until the area of the end is sufficiently large to accommodate it. The cross-section of the cell, however, remains constant. This is illustrated in fig. 7. The monoclinic angle, β , has therefore a definite value depending on the constitution of the molecular end-groups. From the diagram it is clear that while the cross-section of the cell and therefore the side-spacings characteristic of the hydrocarbon photographs remain the same, or approximately so, there will be a decrease in the long spacing from d_1 to d_1' , when a change is made in the end-group. This decrease can be measured; hence β and therefore the area of the end-group can be determined. A slight error may be introduced, since the exact difference produced in the length of the chain has yet to be determined.

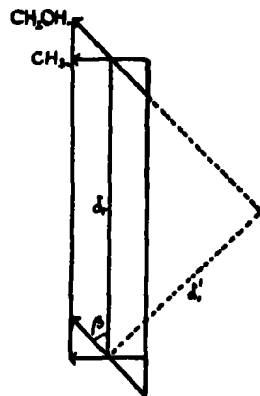


FIG. 7.

In order to measure the area of the (CH₂OH) group the alcohol docosanol, C₂₂H₄₅OH, was chosen, the corresponding hydrocarbon having been previously measured by A. Müller. The photographs of docosanol showed the two characteristic side-spacings, d_2 and d_3 , and a long spacing, d_1 , which could be measured to the tenth order. The results are:—

Substance.	d_1 .	d_2 .	d_3 .
Docosanol (C ₂₂ H ₄₅ OH)	50.0	4.15	3.69 A.U.
Hydrocarbon (C ₂₂ H ₄₆)	($\frac{1}{2} \times$) 59.8	4.08	3.67 A.U. (Müller).

* 'Proc. Roy. Soc.,' A, vol. 114, p. 542 (1927).

To avoid the possibility of errors in measurements arising out of different conditions, Dr. Müller kindly took a companion photograph of docosanol under conditions identical with those of the hydrocarbon measurement. The same value, 50 Å.U., of the long spacing was obtained. Assuming the total change to be due to the tilt of the molecule, this gives for β , the angle of tilt caused by an alcohol group, the value $56^\circ 43'$. The cross-section of the hydrocarbon cell is approximately a constant, 37 Å.U.², and this, as Müller's theory requires, is the same as the cross-section of docosanol as calculated from the values of d_2 and d_3 given above. The base of the unit cell of the alcohol has thus an area 44.2 Å.U., or 22.1 Å.U. for the (CH₂OH) group. This is in very fair agreement with the value obtained by N. K. Adam in his work on monomolecular films. For alcohols of the form R.CH₂OH (where R = C_nH_{2n+1}), he obtained for the area of the end-group (CH₂OH) the value 21.5 Å.U.* Considering the widely different methods of measurement, the agreement between these two results is very gratifying.

In conclusion, the author wishes to express her sincere thanks to Sir William Bragg for his kindness, to the Managers of the Royal Institution for permission to work in the Davy Faraday Laboratory, and to the members of the staff for their assistance and advice. She is also very much indebted to Mr. W. T. Astbury, of the Textile Physics Laboratory, the University, Leeds, for his valuable criticism and suggestions.

For the crystals used her thanks are due to Professor Sir James Irvine, of St. Andrews University, Dr. H. S. Gilchrist, of the Davy Faraday Laboratory, Dr. K. C. Roberts, of King's College, London, and Dr. G. M. Moir, of the Dairy Research Institute, Reading.

The above paper is based on a thesis submitted to the University of London for the degree of Doctor of Philosophy.

Summary.

(1) X-ray investigation of mannitol, dulcitol and mannose gives the following results for these three substances :—

Mannitol.—Space-group, Q_4 ; $a = 8.65$ Å.U., $b = 16.90$ Å.U., $c = 5.56$ Å.U.; density, 1.497 gm. per cubic centimetre; number of molecules per cell, 4.

* Adam, 'Proc. Roy. Soc.,' A, vol. 101, p. 452 (1922).

Dulcitol.—Space-group, C_{2h}^5 ; $a = 8.61$ Å.U., $b = 11.60$ Å.U., $c = 9.05$ Å.U.; $\beta = 113^\circ 45'$; density, 1.466 gm. per cubic centimetre; number of molecules per cell, 4.

Mannose.—Space-group, Q_4 ; $a = 7.62$ Å.U., $b = 18.18$ Å.U., $c = 5.67$ Å.U.; density, 1.501 gm. per cubic centimetre; number of molecules per cell, 4.

(2) A study of the X-ray data suggests that in all three cases the long dimension of the molecule corresponds to the a -axis; in the alcohols, the molecules appear to have the long-chain configuration; in the sugar, that of the manno-pyranose ring, with the longest dimension in the direction of the a -axis.

(3) The relationship is traced between the structures of mannitol and dulcitol, and between the structures of mannose and other saccharides.

(4) An account is given of a measurement of the area of cross-section of the alcohol end-group, CH_2OH .

Some Investigations in Röntgen Spectra. Part I.—X-Ray Spark Lines.

By G. B. DEODHAR, M.Sc., Allahabad University.

(Communicated by O. W. Richardson, F.R.S.—Received October 31, 1930.)

[PLATE 29.]

Introduction.

As is now well known there are certain lines in Röntgen spectra which cannot be fitted up into the usual energy level diagram even after violating the selection rules $\Delta j = \pm 1, 0$ and $\Delta l = \pm 1$. These are called "non-diagram" lines or "spark" lines although the latter designation is somewhat anomalous in as much as the usual diagram lines are, regularly, lines due to transitions in an atom deprived of one of the electrons of the completed groups. They are found on the short as well as on the long wave-length side of the principal diagram lines, and consequently it has been customary to describe them as "satellites" of the principal lines. After their first discovery by Siegbahn

and Stenström* their number has rapidly grown large.† Recently Beuthe‡ has measured the β''' line for elements V (23) to Y (39) and has also discovered a new line η for some of these elements.

The problem of X-ray spark lines is little understood, and it is desirable to study closely the satellites of the principal lines for many elements in the several series. As a first step towards the achievement of this end a close study of $K\alpha$ and $K\beta$ satellites of the elements Si (14) to Cl (17) was undertaken. The results obtained go to show that the structure of the satellites is complex and that their nature is highly dependent upon the state of chemical combination of the atom which emits them.

Apparatus and General Procedure.

The apparatus used mainly consists of a high vacuum spectrometer of Professor Siegbahn's design made in the laboratory workshop. A metallic X-ray tube is joined to the main body of the X-ray spectrometer by conical ground joints. The anticathode is of copper and has got four sides. As a source of cathode rays either a cold cathode or a hot cathode could be used. The cathode was cooled by cold water running through a series of glass tubes and the anticathode by another system of tubes. The anticathode as well as the body of the spectrometer were kept earthed whilst the cathode was insulated from the metallic parts of the X-ray tube by a porcelain insulator.

The source of high tension was an oil transformer the primary of which was fed from alternating mains of 127 volts 50 \sim . The high tension was rectified by two kenotrons and smoothed by two condensers. The current through the X-ray tube was measured by a milliammeter of varying ranges and the tension was estimated by an electrostatic voltmeter of Abraham and Villard. The primary current could be regulated by a rheostat.

The body of the spectrometer together with the X-ray tube was evacuated by a Siegbahn pump backed with an oil pump. The pumping system was so efficient that the whole apparatus could easily be evacuated within 5 minutes. The X-rays generated were limited before falling on the crystal face by means of two slits, the first one of which was 0.08 mm. in width. The second slit was covered by thin aluminium leaf to stop ordinary light from falling upon the photographic plate.

The crystal to be used was first mounted upon the crystal table so that its

* 'Phys. Z.,' vol. 17 (1916).

† Lindh's "Report."

‡ 'Z. Physik,' vol. 60 (1930).

face was parallel to the axis of rotation. This was done by clamping a plane parallel glass plate to the surface and observing through a telescope the image of a scale kept at a distance of about 2 metres. The coincidence of the face of the crystal with the axis of rotation could be made by observing the image of a movable fine ivory point in a microscope mounted upon the rim of the spectrometer body. The general method for both of these adjustments has been outlined in Siegbahn's "Spectroscopy of X-rays" (see p. 67). The second adjustment could easily be made accurate to less than 0.002 mm. As the spectrometer was used for relative measurements an error in this adjustment will not affect the measurements of the wave-lengths to an appreciable degree. After these adjustments were made the frame carrying the photographic plate was moved parallel to itself in its grooves so that the perpendicular distances of the middle of the plate and the middle of the slit from the axis of rotation were equal. This was done to satisfy the Bragg focussing condition. As a mean of several measurements it was found that the distance between the centre of the plate and the axis of rotation was $r = 137.98$ mm. The maximum difference of this from an individual measurement was ± 0.04 mm. This error is of no consequence in the computation of glancing angles. After the plate holder was thus adjusted it was finally clamped. A fine tungsten wire was then fixed in front of the frame in the form of a cross the shadow of which could be recorded upon the photographic plate. The zero positions of the plate holder and the crystal were next determined and read upon the fine and rough scales. Suitable lines were used as standard for the relative measurements of the lines of the spectrum to be measured. A list of such lines has already been published by Siegbahn* and as far as possible one of these was taken as standard.

The substance to be investigated was pressed on three sides of the copper anticathode, the fourth one being reserved for the material which was selected for the suitable reference lines.

The exposure time and the tension and the current through the X-ray tube were adjusted to suit the particular conditions. During exposure the crystal was rotated by steps to have sharp lines. The plates were measured on a projection comparator which was found particularly suitable for weak and diffuse lines. In all cases Imperial Eclipse plates were used.

* 'Arkiv. Mat. Ast. Fys.,' vol. 21, A (1929).

Results of Measurements.

Silicon.—For investigation of $K\alpha$ and $K\beta$ satellites of this element crystalline and amorphous silicon, quartz and sodium silicate were used. Crystalline and amorphous silicon gave identical spectra. The spectra of quartz and sodium silicate although identical with each other were different in appearance from those of crystalline and amorphous silicon.

Before exposing for another substance the anticathode surfaces were thoroughly cleaned. The X-ray tube was worked at about 18 kv. and 50 ma. and the exposure for a measurable record of some of the faint lines of $K\alpha$ and $K\beta$ groups was as much as 6 hours. The $K\alpha$ group is reproduced in fig. 1 (Plate 29).

In the $K\alpha$ group it is seen that α' and α_4 are doublets and that a new line between α_5 and α_6 is found. The doublet nature of α_3 was shown earlier by Bäcklin.* The line between α_5 and α_6 which I have named α_7 is of interest. There seems to be no doubt that it is due to silicon since its diffuse nature is just in conformity with the neighbouring lines α_5 and α_6 . Besides its wave-length does not coincide with any multiple of copper or calcium lines. Moreover it is obtained from crystalline as well as amorphous silicon. That it is hardly noticeable on SiO_2 plates need not indicate that it is a line due to impurity, since SiO_2 modification shows not only different wave-lengths of the $K\alpha_1$ $K\alpha_2$ doublet† but it also enormously influences the whole structure of $K\alpha$ and $K\beta$ satellites as fig. 2 (Plate 29) shows.

In the β group on the long wave-length side of $K\beta_1$ a faint line is seen. I have designated it by β_4 . As it is seen with difficulty in the comparator it is measured by a glass scale (0.5 mm.). The error may not be more than ± 2 X.U. The line β_2 for pure silicon is very broad. Consequently its two edges are measured and from that the value corresponding to the middle is computed. The spark lines of silicon are rather broad and diffuse and consequently the accuracy of measurement is not very high. The maximum error can be ± 1 X.U.

In computing the glancing angle for an unknown line the glancing angle for the reference line was calculated at the temperature of the experiment, due allowance being made for the deviations from the Bragg law whenever higher orders were used and the grating constant was known for the higher orders. The correction to be applied to get the glancing angle for the unknown line is

* 'Z. Physik,' vol. 38, p. 221 (1926).

† Bäcklin, 'Z. Physik,' vol. 33, p. 547 (1925).

Table I.—Quartz Crystal. Order I. Reference $\text{CaK}\alpha_1$ (ord. II) $\log 2d_1 = 3.92908$.

Line.	Silicon.*	Silicon oxide.
a'	7080.1	7081.6
a''	7085.8	—
a_3	7087.5	7084.5
a_4	7058.1	7055.5
a_4'	7054.0	—
a_5	7021	—
a_7	7011.2	—
a_8	7003	—
β_1	6753.0	6752.9
β_2	6739	—
β_2'	6802	6803.8
β_4	6824†	6823†

* Probably some of the lines here listed are due to some chemical combination. See discussion ahead.

† Measured with glass scale (0.5 mm.) error may be $\pm 2 \text{ X.U.}$

$\tan^{-1} a/2r$, a being the distance of the unknown line from the reference line, and r the distance from the centre of the plate to the axis of rotation. The value of glancing angle thus obtained was further referred to 18° C. In this way the wave-lengths calculated were all reduced to 18° C.

Phosphorus.—For investigating the $\text{K}\alpha$ and $\text{K}\beta$ groups of this element P_2O_5 was used. The anticathode was for a few plates aluminium but in the majority of cases it was copper. Two different crystals were used to suit the special purpose in view. In the first order quartz was found to give a feeble but clearly noticeable impression of α_5 and α_4 lines (fig. 5). On some plates a faint line on the long wave-length side of β' was noticed. As it was not possible to measure it in a comparator it was roughly measured with a glass scale. The error in the wave-length was estimated not to exceed $\pm 2 \text{ X.U.}$ One important point in connection with the β group must be mentioned here. On changing the anticathode from copper to aluminium a dark band on the short wave-length side of β_1 and just in continuation with it appeared. This was altogether absent when the copper anticathode was used. I have called this β_1' . The middle of this band was measured. The tube was worked at 16 kv. and 50 ma. and the exposure time varied from 1 to 6 hours. During exposure the crystal was rotated discontinuously to get sharp lines.

To get good dispersion which was found necessary to study the possible

double nature of α' , α_3 and α_4 lines as well as to measure α_1 and α_2 accurately mica in the third order was used. As reference line Cu $K\alpha_1$ in the 12th order was used. It was found that α_3 and α_4 were not resolved but a faint line on the long wave-length side of α' was clearly seen. It is called α'' . Its wave-length was estimated in the same way as that of Si and P β_4 , the order of error being the same. The wave-lengths have been reduced to 18° C. as in the case of silicon. The deviation from the Bragg law is also taken into account in the case of mica.*

Sulphur.—The general procedure of working with this element was the same as described before. Pure crystalline sulphur was used on a copper anticathode. The mica crystal used in the case of phosphorus was found to give too low a dispersion so it was replaced by calcite. In the α group the observation was made that the line α_3 is double. On exposing for about 6 hours at 12 kv. and 50 ma. two lines in the expected positions of α_5 and α_6 were clearly seen (Plate 29, fig. 3). It was, however, not possible to measure these lines with the comparator. Their wave-lengths were calculated from rough measurements with a glass scale. The error cannot be more than ± 2 X.U. The line 5262.6 listed by Hjalmar as α_5 (see Siegbahn's X-rays, p. 106) was not found. The wave-length of the line α_4 was calculated with reference to α_1 from four plates. This mean value was used in calculating the wave-lengths of the rest of the α group lines which were measured with reference to α_4 . This was necessary as α_1 and α_2 lines were over-exposed on all plates taken for the lines α' , α_3 , α_3' , α_5 and α_6 .

The reference line for the β group was Ni $K\alpha_1$ in the third order. In the β group it was seen that no other lines except β_1 and β_2 are obtained from pure sulphur.

Chlorine.—For the investigation of $K\alpha$ and $K\beta$ groups of this element pure sodium chloride on copper was used. The α'' line recorded by Dolejssek was not seen at all even after a long exposure of 12 hours at 9 kv. and 30 ma. A faint dark band in the expected position of ($\alpha_5\alpha_6$) was seen (fig. 3, Plate 29). The two extremities of this were measured with a glass scale (0.5 mm.). The α_3 line was found to be a little broader and stronger than α_4 . The α_3 had the appearance of a doublet; but for want of higher resolution it could not be seen whether α_3 is actually double. As a reference line Cl $K\alpha_2$ ($\lambda = 4718.21$) was used; and as a control the wave-lengths of the $\alpha_3\alpha_4$ lines were also determined with reference to Cu $K\alpha_1$ in the third order. In the β group no other lines except

* For values of the grating constant in different orders see Larsson, 'Diss. Upsala' (1929).

β_1 and β_2 were seen even on plates exposed for 6 hours. The β lines were not measured. It is of interest to note that the β_3 line listed by Dolejšek is not emitted by pure sodium chloride nor by the chloride of zinc.

In Tables II, III and IV are collected the mean values of λ , ν/R and $\sqrt{\nu/R}$ respectively for the four elements. Values in brackets are taken from earlier measurements.

Table II.— λ Values.

Line.	Element.			
	14 Si.	15 P.	16 S.	17 Cl.
α_1	} [7111]	{	[5361]	[4718]
α_2			—	—
α_2''			—	—
α_2'			—	—
α_3			5341.5	4701.5
α_3'			5330.0	4691.8
α_3''			5327.8	—
α_4			5323.3	4686.2
α_4'			—	—
α_5			5297	4661
α_7			—	—
α_8			5286	4654
β_4			—	—
β_1			—	—
β_2			5021.1	—
β_2'			5013.0	—
β_1'			—	—

Table III.— ν/R Values.

Line.	Element.			
	14 Si.	15 P.	16 S.	17 Cl.
α_1	} [128.15]	{	[160.98]	[193.14]
α_2			—	—
α_2''			—	—
α_2'			—	—
α_3			170.60	193.82,
α_3'			170.97	194.22,
α_3''			171.04	—
α_4			171.18,	194.46
α_4'			—	—
α_5			172.04	195.50,
α_7			—	—
α_8			172.38	195.79,
β_4			—	—
β_1			—	—
β_2			181.49	—
β_2'			181.78	—

Table IV.— $\sqrt{v/R}$ Values.

Line.	Element.			
	14 Si.	15 P.	16 S.	17 Cl.
α_1	} [11·320] {	12·181	[13 038]	[13·897]
α_2''		12·178	—	—
α_3'		12·196	—	—
α_4'		12·204	13·061	13·922
α_5'		12·218	13·076	13·937
α_6'		—	13·078	—
α_7'		12·226	13·084	13·945
α_8'		—	—	—
α_9'		12·259	13·116	13·982
α_{10}'		—	—	—
α_{11}'		12·270	13·130	13·993
β_1		12·487	—	—
β_2		12·507	—	—
β_3		12·547	13·472	—
β_4		—	13·483	—

Discussion.

The doublet character of the $K\alpha$ spark lines of silicon shown in fig. 4 comes as a surprise in view of the fact that it was not obtained on the spectrogram taken by Bäcklin (*loc. cit.*) who worked with this substance in connection with the subject of X-ray spectra and chemical combination. The present results though agreeing to some extent regarding the complexity of the α_3 line are in surprising variance with the earlier ones of Bäcklin regarding what I have called α_2'' , α_4' and α_7 lines. This author worked with the same specimen of silicon but instead of an ion-tube he used an electron tube as a source of X-rays. On a close examination of the plates taken by this author who kindly lent them to me for my inspection I found a very faint indication of a line between α_5 and α_6 ; but the α_3' and α_4 lines were single.

It is possible that these three extra lines are given out by some foreign matter which originally was not present along with the silicon when it was put upon the anticathode, but which later on came in from somewhere during the working of the tube. Another possibility may be put forward and that is that these lines may be due to a partial conversion of silicon into its oxide during the process of the X-ray generation in the ion-tube. Still another possibility is that silicon is somehow modified in the ion-tube during the process of electron bombardment due to the deposition of sputtered particles on the anticathode.

The first possibility does not seem to appear since these lines are not obtained

when the oxide of silicon is used on the anticathode. There is no obvious reason why such a foreign matter should show preference to the anticathode when silicon is put on it.

The second possibility seems to be not probable since (see Table I) the lines in the spectra of the two substances shows small differences in the measured wave-lengths.

As observed before, the wave-length of the strong line α_7 also does not coincide with the L or higher order K lines of the heavy elements concerned. It, however, coincides with the $K\beta_1$ of iron in the fourth order. There is no obvious source of any traces of iron on the anticathode. Moreover this line is not recorded on silicon oxide plates.

The question regarding the possibilities mentioned above must be answered by a detailed examination of the spectrum under varying working conditions. For want of time I had to postpone the investigation of this point which I intend to take up in the near future.

The line α'' of phosphorus is very faint and was seen only on two plates. It is necessary to confirm it. The absence of the α'' line listed by Dolejšek when sodium chloride is used probably indicates that it is a line resulting from electronic transitions in levels which may arise when one atom is in close proximity with another in a solid substance. The case of the β_3 line of sulphur and chlorine appears to be similar.

From the foregoing considerations it appears that the nature of the non-diagram lines is very complex.

The simple doublet structure found for the α_3 line of sulphur may become complex for some elements as in the case of silicon.

Various hypotheses have been offered to explain the origin of the X-ray spark lines. The chief among these are (1) Wentzel's multiple ionisation* ; (2) Coster and Druyvesteyn's empirical relations† ; (3) double jump hypothesis‡ ; (4) application of the laws of complex spectra to the X-ray field.§

The difficulties in the way of accepting theory (1) have been indicated by the experiments of Bäcklin on aluminium $K\alpha$ and of Siegbahn and Larsson on molybdenum $L\alpha$ satellites.|| More recently Du Mond and A. Hoyt raise the same point on the basis of their experiment on $K\alpha_3$ of copper.¶ As an indirect

* 'Ann. Physik,' vol. 66 (1921).

† 'Z. Physik,' vol. 40 (1927) and vol. 43 (1927).

‡ Wentzel, 'Z. Physik,' vol. 31 (1925); Richtmayer, 'J. Franklin Inst.,' vol. 208 (1929).

§ Saha and Ray, 'Phys. Z.,' vol. 28 (1927); Ray, 'Phil. Mag.,' vol. 8 (1929).

|| Siegbahn, "X-rays," p. 184.

¶ 'Phys. Rev.,' vol. 36 (1930).

support of this theory it has been pointed out that for the elements (11) Na to (14) Si the relations $(\alpha_3 - \alpha_1) = (\alpha_5 - \alpha_3) = (\alpha_7 - \alpha_5)$ and

$$[(\nu/R)_{\alpha_3} - (\nu/R)_{\alpha_1}]_{s+1} = [(\nu/R)_{\alpha_5} - (\nu/R)_{\alpha_3}]_s$$

approximately hold good.* From the foregoing pages it will be seen that the data for α_3 and α_5 lines for P, S and Cl are now available to a fair degree of accuracy to allow us to see how far the above relations are true for elements Si to Cl. The following table shows the result.

Table V.

	11 Na.	12 Mg.	13 Al.	14 Si.	15 P.	16 S.	17 Cl.
$\alpha_3 - \alpha_1$	0.52	0.64	0.71	0.83	0.91	0.99	1.09
$\alpha_5 - \alpha_3$	0.57	0.67	0.76	0.91	1.02	1.07	1.28
$\alpha_7 - \alpha_5$	0.65	0.76	0.83	0.94	1.13	1.20	1.34

The discrepancy for P, S and Cl is rather high and appears to be unexplainable by the errors in the measurement of α_3 and α_5 . It is impossible to make any final statement about this so long as accurate measurements of α_3, α_5 lines for these three elements are not made. In any event it seems difficult to accept Wentzel's theory in the face of the direct experimental evidence against it noted above nor does the indirect evidence seem to be satisfactory.

Druyvesteyn proposes certain relations to represent the results of his observations on K and L satellites of certain elements. For example, the relation $(KL - LM)_s - (K - M)_s = (L_{s+1} - L_s) - (M_{s+1} - M_s)$ is shown to govern his measurements of the β''' line of the elements 19 K to 26 Fe. Here KL means an atom state in which one K and one L electron are removed and so on for the other pairs. It must be noticed that the right-hand side of this equation is not stated precisely inasmuch as the multiplicity of the L and M levels is not taken into consideration by Druyvesteyn. Assuming that the levels in question are L_{II} and $M_{II, III}$ we shall see how the above relation of Druyvesteyn holds for the line β''' up to 39 Y. Recently Beuthe† has measured this line from 23 V to 39 Y. It is easy to see from Table VI that the line β_y of Beuthe is the same as the line β''' of Druyvesteyn. In future, consequently, it will always be described as β''' .

* Wetterblad, 'Z. Physik,' vol. 52, p. 613 (1927).

† 'Z. Physik,' vol. 60 (1930).

Table VI.

Element.	Line.	Druyvesteyn.	Beuthe ($\beta\gamma$).
		λ	λ
22 Ti	β'''	2483.6	—
23 Va	"	2257.7	2256.8
24 Cr	"	2061.7	2061.1
25 Mn	"	1888.8	1890.4 ($\beta\gamma_1$)
26 Fe	"	1737.1	1885.8 ($\beta\gamma_2$)
			1737.7

The right-hand side of the above relation can be put in the form

$$(L_{II} - M_{II, III})_{s+1} - (L_{II} - M_{II, III})_s = (K\beta_1 - K\alpha_2)_{s+1} - (K\beta_1 - K\alpha_2)_s.$$

In Table VII are collected the several values. The last column gives the difference (δ) between the calculated and observed values of β''' .

The values of δ are plotted against atomic number in fig. 4. The curve shows

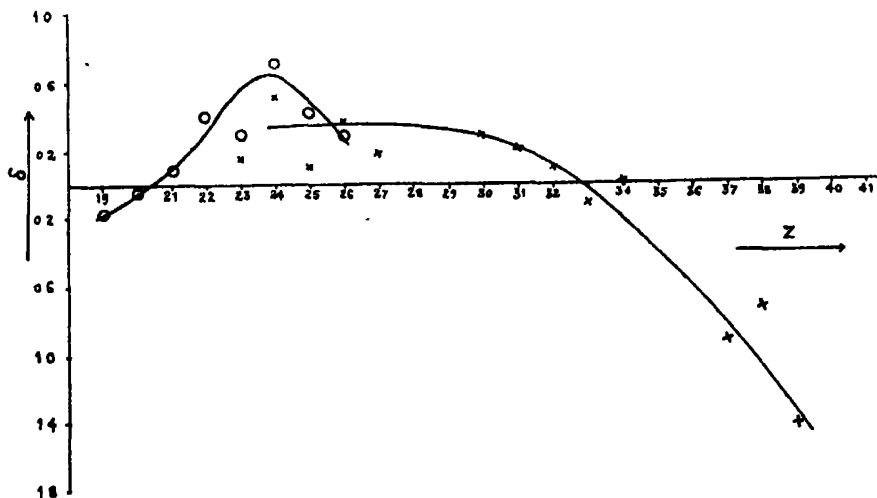


FIG. 4.—Variation of δ with Z for β''' measurements by Druyvesteyn and Beuthe.

that the agreement is not good. In fact there seems to be a systematic variation of this difference with increasing atomic number changing sign at two places, once nearly at atomic number 20 and then at about atomic number 32. It is noteworthy that near these regions the process of building new shells just begins.

Table VII.

Element.	$(\nu/R)_{\text{cr}}$	$(\nu/R)_{\beta_1}$	$(L_{II} - M_{II, III})$	$(L_{II} - M_{II, III})_{\beta_1 + 1}$ $-(L_{II} - M_{II, III})_{\beta_1}$	Benthe $\beta'' - \beta_1$	Drayvestoy $\beta'' - \beta_1$	δ
19 K	243.84	264.38	20.54	3.36	—	3.52	-0.16
20 Ca	271.61	285.51	23.90	3.71	—	3.76	-0.04
21 Sc	300.90	328.51	27.61	3.83	—	3.74	+0.09
22 Ti	331.775	363.215	31.44	4.09	—	3.68	+0.41
23 V	364.166	399.717	35.53	4.24	4.08	3.94	+0.30
24 Cr	398.22	437.99	39.77	4.66	4.14	3.94	+0.16
25 Mn	433.63	478.06	44.43	4.70	4.59 (βy_1)	4.27	+0.72
26 Fe	470.70	519.83	49.13	4.95	4.58	4.66	+0.52
27 Co	509.32	563.40	54.08	5.12	4.94	—	0.43
28 Ni	549.51	608.71	59.20	5.49	—	—	0.11
29 Cu	591.25	655.94	64.60	5.65	—	—	0.37
30 Zn	634.65	704.99	70.34	6.17	—	—	0.18
31 Ga	679.61	756.12	76.51	6.27	5.88	—	—
32 Ge	725.99	808.77	83.78	6.87	6.06	—	+0.29
33 As	773.97	863.62	89.65	6.98	6.77	—	+0.21
34 Se	823.61	920.24	96.63	7.47	7.08	—	+0.10
35 Br	874.88	978.98	104.10	—	7.46	—	+0.01
36 Kr	928.27	1101.88	119.61	8.00	8.92	—	—
37 Rb	1038.44	1166.05	127.61	8.63	9.36	—	-0.92
38 Sr	1096.36	1232.60	136.24	8.99	10.32	—	-0.73
39 Y	1155.70	1300.93	145.23	9.23	—	—	-1.33
40 Zr						—	—

The hypothesis of double jumps taking place simultaneously to give a new quantum was supported by Richtmyer on the empirical relation

$$\sqrt{(\nu_s - \nu_p)/R} \propto Z,$$

where ν_s is the frequency of a satellite and ν_p that of the parent line. It is probable that the doublet nature of Si K α satellites may be explained by such processes. But the transitions in outer shells of a silicon atom in close associations with others are hardly known, and thus it is difficult to obtain a quantitative test of this hypothesis.

Instead of one of the jumps taking place in the outermost shell as supposed by Richtmyer both of them may occur in the inner levels. Thus the $L\gamma_{23}'$ line for the elements Zr, Nb, Mo, Rh and Ag measured by Druyvesteyn may be explained as resulting from $N_{IV} \rightarrow M_{II}$ and $M_{II} \rightarrow L_I$ jumps taking place simultaneously. Table VIII shows the result of such calculations.

Table VIII.

Element.	ν/R $M_{II} \rightarrow L_I$ ($L\beta_4$)	ν/R $N_{IV} \rightarrow M_{II}$	ν/R ($M_{II} \rightarrow L_I$) + ($N_{IV} \rightarrow M_{II}$) = $L\gamma_{23}'$ calculated.	ν/R $L\gamma_{23}'$ observed.	Difference calc. - obs.
40 Zr	161.21	25.4	186.61	186.16	+0.45
41 Nb	170.93	27.3	198.23	198.23	0.00
42 Mo	180.96	30.0	210.96	210.80	+0.16
45 Rh	213.02	36.9	249.92	249.87	+0.05
47 Ag	236.01	42.4	278.41	278.68	-0.27

The discrepancy in column 6 may be due partly to the uncertainty in the measurement of the line $L\gamma_{23}'$ which according to Druyvesteyn is rather faint and very broad, and partly to the want of knowledge of exact values of the N_{IV} level when one of the electrons of the M_{II} level is already missing. It is not possible to say whether the change of sign at 47 Ag is of any significance unless $L\gamma_{23}'$ is measured for some elements beyond silver.

The question of the application of the laws of complex spectra to X-ray field cannot be discussed here. It may be pointed out, however, that the terms arrived at by Ray† from the hypothetical transition $1s' 2s' 2p^6 \rightarrow 1s^2 2s' 2p^5$ do not seem to fit in with the doublet character of the K α satellites described above.

* 'Z. Physik,' vol. 43, p. 721 (1927).

† 'Phil. Mag.,' vol. 8 (1929).

From the foregoing it is seen that the explanation of the X-ray satellites on the short wave-length side of the main diagram lines is rather vague. The case with the long wave-length side satellites appears to be similar.

Summary.

(1) The $K\alpha$ and $K\beta$ groups of the elements silicon, phosphorus, sulphur and chlorine are studied.

In the $K\alpha$ group of silicon new lines α'' , α_4' and α_7 are observed and measured. Their possible origin is discussed.

In the $K\beta$ group of this element a new faint line β_4 has been recorded and roughly measured.

For silicon oxide compared to the pure element considerable changes in the spectral structure are found.

In the case of phosphorus the hitherto unmeasured lines $K\alpha_1$, $K\alpha_2$ and $K\alpha'$ are measured. A very faint line on the long wave-length side of α' called α'' has been recorded on two plates and its wave-length roughly estimated. The α_3 and α_6 lines are recorded and roughly measured.

In the $K\beta$ group a new faint line β_4 is recorded and roughly measured.

In the case of sulphur the $K\alpha_3$ line has been found to be double. The two components are measured. The α_5 and α_6 lines have also been recorded and roughly measured. Even after special search Hjalmar's doubtful line $\lambda 5262.6$ has not been found.

In the $K\beta$ group of pure sulphur the $K\beta_3$ line listed by Hjalmar has not been found.

For chlorine using pure sodium chloride the $K\alpha''$ and $K\beta_3$ lines listed by Dolejssek have not been found. A faint $\alpha_5\alpha_6$ band has been recorded and roughly measured. The α_3 , α_4 and α' lines are re-measured.

(2) Various suggestions for the origin of X-ray spark lines are examined.

(3) The probability of the $L\gamma_{23}'$ line of Druyvesteyn as resulting from the double jump $N_{IV} \rightarrow M_{II}$ and $M_{II} \rightarrow L_I$ or as a forbidden direct transition $N_{IV} \rightarrow L_I$ is demonstrated.

This work has been carried out in the Physics Institute of the University of Upsala; and I take this opportunity of expressing my most sincere thanks to Professor M. Siegbahn who suggested to me this work and placed his valuable time at my disposal, not only all the time the work was being carried on but also when it was written out. I am also thankful to the staff of the workshop

for showing me many courtesies. I am also indebted to the Executive Council of the University of Allahabad for giving me an opportunity to carry out this research. My sincere thanks are also due to the High Commissioner for India for allotting me a grant-in-aid from the Government of the United Provinces, which has partially met the cost of this research.

Some Investigations in Röntgen Spectra. Part II.—X-Ray Spectra and Chemical Combination. Sulphur.

By G. B. DEODHAR, M.Sc., Allahabad University.

(Communicated by O. W. Richardson, F.R.S.—Received October 31, 1930.)

[PLATES 30, 31.]

Introduction.

A large amount of experimental work has been done to show an effect of chemical combination on X-ray absorption edges.* After the first attempt of Wentzel,† Kossel and others, and still more recently Pauling,‡ have tried to explain the effect; but at the present time it remains far from being clearly understood.

The question must be attacked from the side of the emission spectrum also. About the year 1923 Lindh and Lundquist in Professor Siegbahn's laboratory at Lund showed an influence of chemical combination on the wave-lengths and structure of the β lines of phosphorus, sulphur and chlorine. Later Bäcklin§ and Ray|| showed an effect of chemical combination on the $K\alpha$ doublet of some light elements. Most surprising shifts in the positions of the components of the doublet were then observed. Recently Lundquist¶ has studied the $K\beta$ group of sulphur in different chemical compounds of this element. This author finds that no other line except β_1 and β_2 is emitted by any of the compounds. It is interesting to note that Hjalmar has definitely listed a third

*For bibliography see Lindh's Report and Siegbahn's "Spectroscopy of X-rays."

† 'Naturwiss.', vol. 10 (1922).

‡ 'Phys. Rev.', vol. 34, p. 959 (1929).

§ 'Z. Physik,' vol. 33 (1925) and vol. 38 (1926).

|| 'Phil. Mag.', vol. 49 (1925) and vol. 50 (1925).

¶ 'Z. Physik,' vol. 60 (1930).

line β_2 for sulphur. The following investigation was therefore taken up to clarify this point. As will be seen, some interesting facts regarding this question have been brought to light.

Apparatus and General Procedure.

The apparatus has already been described in Part I. The general method of working with silicon has also been described there and the results of measurements tabulated in Table I.

In the case of sulphur different compounds of this element were used. They were taken from the firm of Kahlbaum in Berlin, except the two compounds : silver sulphide and silver sulphate. These latter were made by me from pure silver nitrate. The following substances were used :—

- (1) CuS, ZnS, CaS, SrS, BaS, CdS, MgS, HgS, PbS, MoS, Na₂S, K₂S and Ag₂S.
- (2) Li₂SO₄, Na₂SO₄, K₂SO₄, Rb₂SO₄, Cs₂SO₄, Ag₂SO₄, ZnSO₄, CuSO₄, HgSO₄ and MgSO₄.

Nickel $K\alpha_1$ in the third order was taken as reference line. The crystal used was calcite. The slit width was 0.08 mm. In all cases a copper anticathode having four sides was used. Three of these sides were used for the compound under investigation and the fourth one was reserved for nickel powder. Each side was exposed for about 20 minutes. Thus at a time a total exposure of 1 hour could be given. When the duration of exposure was more than this, as was usually the case, it was necessary to admit air into the apparatus and to recharge the surfaces with the substance under investigation. This process was repeated till the desired exposure was given. Finally the surface with nickel powder was used to record the reference line. For each substance several plates were taken. Before using another compound the surfaces were thoroughly cleaned with a fine file. The plate holder was kept fixed in one position for all the plates. The tension used was about 10 kv. and the current through the tube was about 35 ma. A cold cathode was used in all cases. A minimum exposure of 5 hours was found to be necessary to have a measurable record of the faint lines under investigation. During exposure the crystal was rotated by steps through the desired angle. The temperature in the spectrometer was read by a mercury thermometer and the wave-lengths were all reduced to 18° C. as described in Part I. This correction is, however, small. The error in the relative measurement of β_1 and β_2 is about ± 0.2 X.U. and of β_3 less than ± 1 X.U.

Results of Measurements.

In fig. 1 (Plate 30) are reproduced the β lines of pure sulphur and also those of a typical sulphur compound giving the β_3 line. In Table I are collected the wave-lengths of β_1 , β_2 and β_3 lines. Column 5 of this table gives a qualitative relation between the intensities of β_1 and β_2 lines. For the remaining compounds β_1 , β_2 and β_3 are not measured. Table II simply describes the state of the β_3 line in relation to the relative intensities of β_1 and β_2 lines.

Table I.— λ Values of β_1 , β_2 and β_3 .

Substance on the anticathode of copper.	β_2 .	β_1 .	β_3 .	Remarks.
S	5013.0	5021.1	Absent	$I_{\beta_1} > I_{\beta_2}$
Na ₂ S	5014.7	5020.6	5043.0	$I_{\beta_1} < I_{\beta_2}$
Na ₂ SO ₄	5014.8	5020.7	5043.0	"
K ₂ S	5014.6	5020.7	5042.9	"
K ₂ SO ₄	5014.7	Very faint	5042.7	"
Li ₂ SO ₄	5014.7	5020.6	5043.0	"
Rb ₂ SO ₄	5014.3	5020.8	5042.9	"
Cs ₂ SO ₄	5014.1	—	5043.0	"
Ag ₂ SO ₄	5012.9	5021.1	Faint	$I_{\beta_1} > I_{\beta_2}$
Ag ₂ S	5013.2	5021.1	Absent	"
MoS	5012.7	5021.3	"	"
SrS	5015.0	5020.6	5043.1	"
BaS	5014.7	Faint	5043.0	$I_{\beta_1} < I_{\beta_2}$
CdS	5016.7	5021.5	5043.0	β_3 obtained $I_{\beta_1} < I_{\beta_2}$ $\lambda_{\beta_3} = 5032.6$

Table II.

Substance on the anticathode of copper.	β_2 .	β_1 and β_3 .
PbS	Absent	β_1 and β_3 not separated
ZnS	"	"
MgS	"	$I_{\beta_1} > I_{\beta_2}$
CuS	"	"
CaS	Very faint	"
CuSO ₄	"	"
ZnSO ₄	"	"
MgSO ₄	"	"
HgSO ₄	Strong	$I_{\beta_1} < I_{\beta_2}$
HgS	Absent	$I_{\beta_1} > I_{\beta_2}$

From the inspection of Tables I and II it is readily seen that β_3 appears in measurable intensity whenever β_2 is stronger than β_1 , the only exception to this statement being SrS, in which case as visually estimated β_1 and β_2 appear to be equally strong.

Some Fainter Lines.

*Line λ 5033 (β_2).—*Besides this β_2 line of wave-length 5043 some more lines of varying degree of intensity are obtained in the case of certain sulphur compounds. For example for the sulphide of cadmium after 8 hours of exposure at 10 kv. and 30 ma. a measurable doublet on the long wave-length side of the β_1 line could be recorded and measured. The wave-lengths of the components of this doublet are λ 5043 and λ 5033 X.U. It is obvious that one of this doublet is the β_2 line, whilst the second one is a new line. I have called this β_5 . This line was also obtained for silver sulphate on the silver anticathode.

Line λ 5065 (β_4).—*This line measured in the same way as the line λ 4994 was obtained for silver sulphate on the silver anticathode, and for the sulphides of calcium and strontium on the copper anticathode. As none of these lines are found to be multiples of the known strong lines of the heavy elements concerned, and besides as each of them is obtained from different compounds of sulphur it seems that they belong to sulphur. Fig. 2 (Plate 31) shows these lines.

*Line λ 4994 (β_6).—*This line is recorded on plates taken for the sulphides of calcium, strontium and barium on the copper anticathode and also for silver sulphate on the silver anticathode. As the line is faint it was found possible to obtain only an approximate measurement with a glass scale (0.5 mm.). The error may be ± 4 X.U. I have called this line β_6 . Its wave-length is 4994 X.U. It should be noted that the value of the absorption line falls near this.

Besides the peculiarities regarding the emission of distinct lines, an inspection of the photographs for various sulphur compounds brings to light considerable changes in the relative intensities and sharpness of the β doublet. It seems as if each compound has got its own characteristic structure of these lines. Thus as one goes from lithium to caesium the β_2 line becomes sharper and the β_1 line fainter, till at the last element it is hardly seen on the plate. The case with the sulphides of calcium, strontium and barium is somewhat similar. Here, however, both the lines grow sharper as we go towards barium. For CaS β_1 is stronger than β_2 , whilst for BaS the reverse is the case. For SrS the state appears to be intermediate. It is worthy to note here that Lundquist† could not resolve this doublet for the sulphides of strontium, barium and cadmium

* For silicon and phosphorus see Part I.

† 'Z. Physik,' vol. 60, pp. 646, 647 (1930).

and consequently could not observe these intensity changes. A change from sulphide to sulphate also sometimes changes the appearance of the β doublet. Thus magnesium sulphide gives a broad β_1 and a faint narrow β_2 , whilst for magnesium sulphate they grow sharper. On changing from sulphide of mercury to the sulphate β_2 becomes more intense than β_1 .

Influence of Anticathode Material.

This effect was first observed by Lindh and Lundquist for certain compounds of sulphur and phosphorus.* During the course of my study of the $K\beta$ lines of sulphur I have made some interesting observations in this connection. The compounds used were sulphides of copper and silver and sulphate of silver on copper and silver anticathodes. Fig. 3 (Plate 30) shows the effect of the reaction of the anticathode material on the relative intensities of β_1 and β_2 lines. For Ag_2S , Ag_2SO_4 and CuS β_1 is stronger than β_2 when a copper anticathode is used; but the condition is reversed immediately on changing the anticathode material to silver. The wave-lengths of β_1 and β_2 for Ag_2S and Ag_2SO_4 also show considerable alterations far beyond experimental error. Table III gives the results of the measurements.

Table III.

Substance.	β_1 .				β_2 .			
	Cu anticathode.		Ag anticathode.		Cu anticathode.		Ag anticathode.	
	Author.	Lindh.	Author.	Lindh.	Author.	Lindh.	Author.	Lindh.
Ag_2S	5021.1	5021.0	5024.6	--	5013.2	5013.4	5014.9	--
Ag_2SO_4	5021.1	5020.9	5023.9	--	5012.9	5012.7	5014.5	--

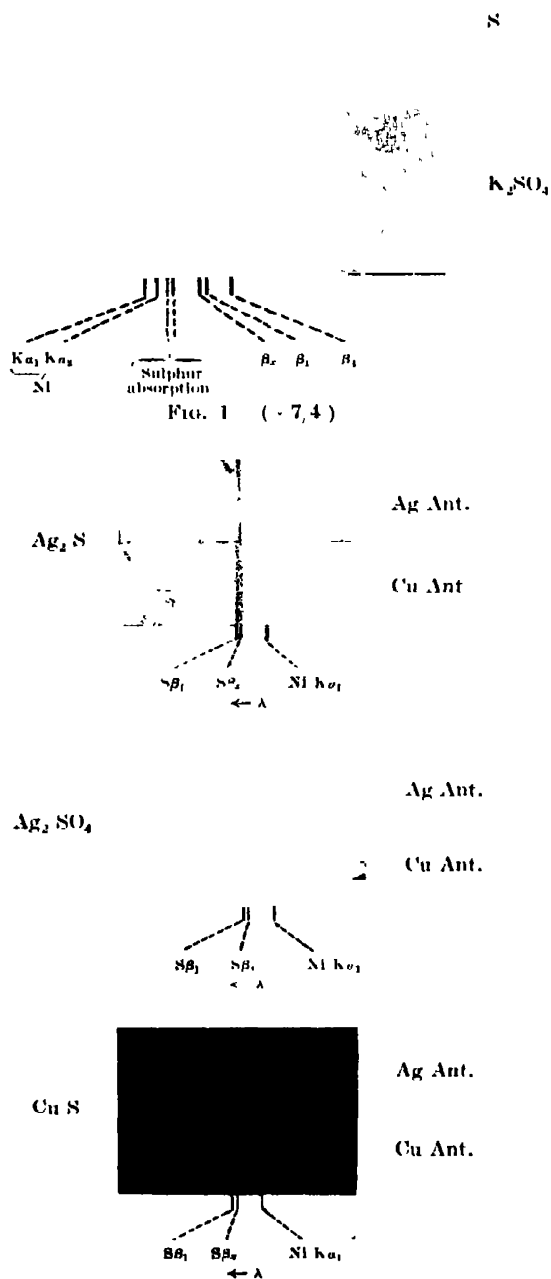
One more point must be mentioned before closing this description and it is regarding the emission of β_2 . When Ag_2SO_4 on a silver anticathode is used a very long exposure (about 10 hours at 30 ma. and 10 kv.) is needed to have a noticeable β_2 line, whilst when the same salt on a copper anticathode is used β_2 line appears pretty strong after about half this exposure.

These intensity and wave-length changes indicate that the substance of the anticathode reacts under cathodic bombardment on the molecule of the sulphur

* Siegbahn's "Spectroscopy of X-rays," p. 99.

compound causing alteration in the electron distribution of the peripheral levels of the sulphur atom. It is difficult to make a more precise statement than this. As a matter of fact a substance, *e.g.*, sulphur, emitting X-rays is in a solid form where one atom is in close proximity with another. This is bound to cause some alteration in the energy of the outer shells which may reach the deeper lying K shells. A change in the nature of the surrounding atoms should be thus expected to cause a redistribution of the electron and energy contents of these outer shells. Such a process cannot be entirely local but must reach the innermost shells. The remarkable changes found in K absorption edges for different chemical compounds of the same element (see references given above) as well as the changes in $K\alpha$ and $K\beta$ emission lines for lighter atoms, clearly go to show that such redistribution really takes place throughout the atom. In this connection it is interesting to recall the facts regarding the astonishing difference between the spectra of pure silicon and silicon oxide. These have been already described in Part I. Perhaps the most interesting fact is that of the almost total suppression of the β_n line by silicon oxide. Suppression of only one of the β doublet lines indicates that the distribution of the external electrons between the silicon and oxygen atoms is not a very simple process. At least it definitely goes to show that the oxide of silicon is not a polar compound formed by a silicon atom giving over its four valence electrons to oxygen, for otherwise no β_1 line should be emitted as remarked by Bäcklin. It is not easy to see how the term giving the β_n line is suppressed. Similar suppression of one of the lines of the β doublet is observed in some sulphur compounds especially prominently in the case of the sulphate of caesium, only the line affected here is β_1 . Besides this partial or total suppression of the β_1 line by some sulphur compounds, some more surprising facts are revealed by the examination above. New lines β_3 , β_4 , β_5 , β_6 are obtained from some sulphur compounds. Of these new lines β_3 is the strongest and is emitted by a majority of compounds. Scrutiny of Tables I and II brings to light the interesting fact that in the majority of cases the line β_3 appears when β_n is stronger than β_1 , the exceptions being $MgSO_4$, $ZnSO_4$, $CuSO_4$ and CaS when β_3 is very weak. The case of SrS is rather unique inasmuch as both the components appear to be equally strong. It is very probable that β_3 and the other faint lines noted above result from electronic transitions in the *molecule* of the sulphur compound. Extensive investigation of this class of lines is expected to throw considerable light on the electron orbits in a molecule.

It is to be noted here that the β_3 line of chlorine should belong to the above-mentioned class. Detailed study of this line will be taken up at a suitable time.

FIG. 3.—Influence of anticathode material on $K\beta$ lines of sulphur. ($\times 7/8$)

(Facing p. 652.)

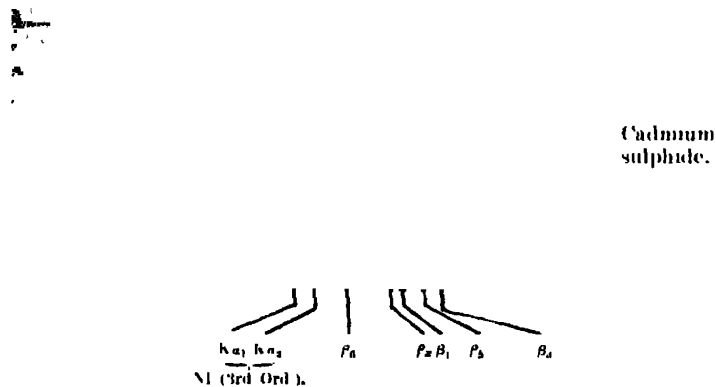
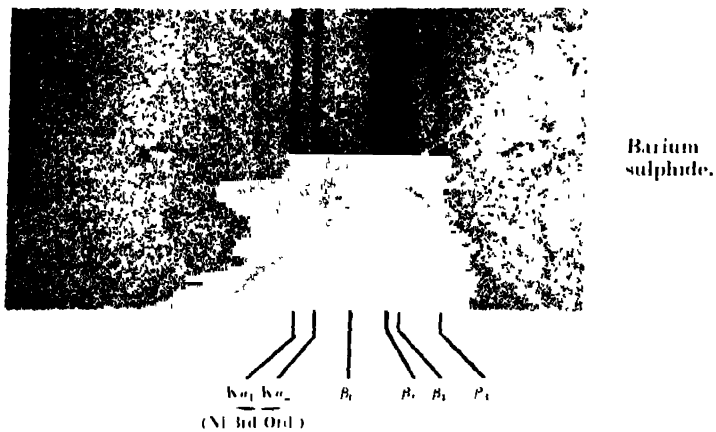
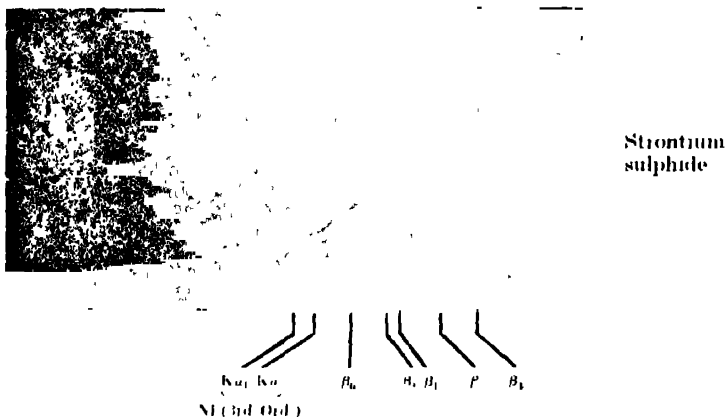


FIG. 2 ($\times 3$.)

Summary.

(1) A large number of sulphur compounds are examined and it is found that considerable changes in the relative intensities of β_1 and β_n lines take place from substance to substance.

(2) The line β_3 already listed by Hjalmar is suppressed by pure sulphur and other sulphur compounds whilst it is given out by some others. It is observed that in the majority of cases β_3 appears in measurable intensity whenever β_n is stronger than β_1 . Within the limits of error the wave-length of this line is the same for all compounds.

(3) Some new faint lines called β_6 , β_7 and β_4 have been observed for a few compounds.

(4) It has been observed that for the compounds Ag_2S and Ag_2SO_4 considerable changes in the wave-length and intensity relations of β_1 and β_n lines take place on changing the anticathode material from copper to silver.

(5) It is suggested that some X-ray lines may possibly result from electronic transitions within a *molecule*.

This investigation has been carried out in the Physics Institute of the University of Upsala, and I desire to record my most sincere thanks to Professor M. Siegbahn for suggesting to me the problem, and for putting his valuable time at my disposal throughout its execution.

Some Investigations in Röntgen Spectra. Part III.—Fine Structure of K-Absorption Edge of SiO_2 .

By G. B. DEODHAR, M.Sc., Allahabad University.

(Communicated by O. W. Richardson, F.R.S.—Received October 31, 1930.)

It is now well known from the works of Lindh,* Fricke† and others that the principal K or L edge is attended on its short wave-length side by a number of secondary edges. The usual method of obtaining this structure consists in putting absorbing screens in the path of X-rays before or after they are analysed by a suitable crystal. The chief difficulty in this is the preparation of absorbing screen of suitable thickness. Fricke as well as Lindh have used this method for the study of absorption spectra of several substances. The former author failed to obtain any K-absorption limit at all for silicon. This was probably due to his using thick absorbing screens coupled with the low dispersion which he obtained with a sugar crystal. Later Lindh succeeded in obtaining K-limits for both silicon and silicon oxide, and showed that as in so many other cases the K-edge of pure silicon is softer than that of the compound. He, however, did not succeed in getting any fine structure. The probable cause of this was again the use of screens of unsatisfactory thickness. This difficulty may be avoided by using the analysing crystal itself as an absorber when a suitable crystal is available. Lindsay and Van Dyke‡ used this method successfully to study the fine structure of the calcium K-edge in calcite, gypsum and fluorite crystals. Nuttall§ has made partial use of this method in his study of structure of K-absorption edges of potassium and chlorine. Later Lindsay and Voorhees|| made use of this method to study the fine structure for different crystals containing iron.

Following the same method the fine structure for silicon oxide was photographed and measured by using quartz as the analysing and absorbing crystal. The apparatus used was a high vacuum spectrograph of Professor Siegbahn's design made in the laboratory workshop. Its adjustment and use is described in Part I. The continuous radiation was obtained from a tungsten anticathode formed by dovetailing a plate of this material on the copper anticathode which

* 'Z. Physik,' vol. 31 (1925).

† 'Phys. Rev.,' vol. 16 (1920).

‡ 'Phys. Rev.,' vol. 28 (1926).

§ 'Phys. Rev.,' vol. 31 (1928).

|| 'Phil. Mag.,' vol. 6, p. 913 (1928).

as already described had four sides. One of these was scratched with a sharp knife and a small quantity of pure silicon was pressed on it. The tension was about 6 kv. and the current through the X-ray tube was about 40 ma. Imperial Eclipse plates were found to be quite suitable for photographing the spectrum. After the desired exposure was given, which was of about 20 to 24 hours' duration, the surface with silicon was brought in by turning the anticathode and an exposure was given for the Si $K\alpha$ line with suitable tension and current density. During both the exposures the crystal was turned by steps through the desired angle. The $M\beta$ line of tungsten was also recorded on the plate.

The plates were measured with a projection comparator which was found to be particularly suitable for lines of low intensity. The principal characteristics of the darkening of the plate are shown diagrammatically in fig. 1. Table I

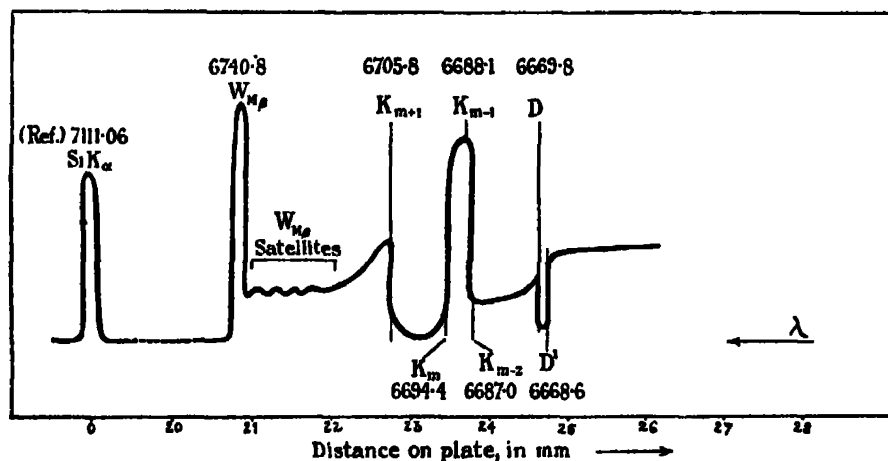


FIG. 1.

gives λ and ν/R values of the edges. As reference line Si $K\alpha$ λ 7111.06 X.U.† was used.

Table I.

Line or edge.	λ .	ν/R .
$W_{M\beta}$	6740.8	135.19
K_{m+1}	6705.8*	135.90
K_m	6694.4	136.12
K_{m-1}	6688.1	136.25
K_{m-2}	6687.0	136.28
D	6669.8	136.63
D'	6668.6	136.65

* Lindh, 'Z. Physik,' vol. 31, p. 213 (1925), gives the following values: SiO_2 , λ 6707.5, and Si, λ 6731.0; but the tungsten $M\beta$ line was not much separated from the edge on the plates taken by this author.

† Larsson, 'Dis. Upsala,' p. 51 (1929).

The error in the measurement is not more than 1 X.U. for the different edges. The boundaries of the white line DD' are pretty sharp and consequently their wave-lengths cannot be in error by more than 0.4 X.U. The line W_{ms} serves as a control for these measurements, inasmuch as its wave-length as measured here agrees with the value $\lambda 6741$ found earlier by Lindberg* on a different occasion and with a different apparatus. Table II gives the comparison in wave-length between the principal edge K_{m+1} and the other two secondary edges.

Table II.

Edges.	$\Delta V.$	$\Delta \nu/R.$
$K_{m-2} - K_{m+1}$	5.17	0.38
$K_{m-1} - K_{m+1}$	4.87	0.35
$K_m - K_{m+1}$	3.13	0.22

The white line DD' has got only 0.054 mm. width whilst the slit width was 0.091 mm. This line as well as two more faint ones on its short wave-length side appear not to be constituents of the fine structure. The other two lines were not measured because of their feeble intensity. The explanation for these lines must be sought in the geometry of the atomic planes of the quartz crystal. The discontinuity at DD' may arise as fig. 2 shows in the process of

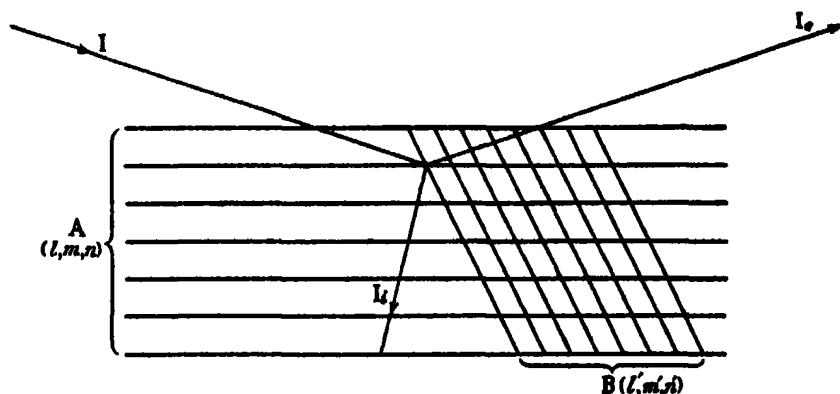


FIG. 2.

division of the incident energy I corresponding to wave-length λ into two parts ; one I_e regularly reflected towards the photographic plate by a system of atomic planes A (l, m, n) and the other I_i simultaneously reflected inwards by another system of atomic planes B (l', m', n'). Similar light lines having the appearance

* 'Z. Physik,' vol. 50 (1928).

of absorption lines were observed in the case of rocksalt by Wagner,* O. Overn† and later on by Berg‡ who extended the observations to other cubic crystals. Their origin was explained on the lines indicated above.

On examining Table II it is seen that the extreme difference between the principal edge and the limit of the fine structure designated by K_{m-2} is only 5.17 volt and the corresponding $\Delta\nu/R$ only 0.38. This circumstance precludes at once the possibility of double ionisation. According to this theory which was first put forward by Wentzel§ to account for the so-called non-diagram lines, the differences between the principal edge (K_{m+1}) and other edges should be of the order of the energy necessary to remove an electron from one of the L or M groups. In the present case if it is supposed that K_{m+1} corresponds to complete removal of a K-electron and K_m to an additional removal of one of the M electrons, then, assuming that the two acts are not simultaneous, $K_{m+1} - K_m$ should be of the order of the first ionisation potential of P_1 which is known to be about 13.29 volt. Here, of course, it is assumed that in SiO_2 silicon acts as a neutral atom rather than as an ion, an assumption which seems to be justified by the consideration of $K\beta$ emission lines of silicon and quartz (see Part I).

If, on the other hand, the ejection of one K and one M electron is effected in one and the same act, then $K_{m+1} - K_m$ should be of the order of the first ionisation potential of Si_1 which according to Fowler|| is 8.12 volts. Nor does it seem to be probable that the M-electron is ejected after having reached one of the metastable states $1D_2$ and $1S_0$ corresponding to 7.3 and 6.3 volts respectively. It is unnecessary to consider the possibility of ejection of an L electron since in that case the extreme difference should be still more as a consequence of the deeper position of L levels.

Nor is the above difficulty solved by following Kossel's line of reasoning according to which the principal or the softest K-edge corresponds to removing the electron to the surface of the atom, and the frequency of the limiting edge corresponds to its complete removal since the extreme difference of 5.17 volts is much too low.

It must, however, be remembered that the silicon atom is in a crystal lattice and it is probable that the work done to remove an M electron is more than in

* 'Phys. Z.,' vol. 21, p. 632 (1921).

† 'Phys. Rev.,' vol. 16 (1920) and vol. 18 (1921).

‡ 'Naturwiss.,' vol. 14 (1926).

§ 'Ann. Physik' vol. 66 (1921) and vol. 73 (1924).

|| 'Proc. Roy. Soc.,' A, vol. 123 (1929).

the case of a free atom. That it is definitely more for a K-electron is easily seen from the fact that the K-edge for silicon is softer than that for quartz. Consequently, speaking qualitatively, the objections pointed out above still hold good.

It is possible that the K-electron is not at all removed outside the influence of the silicon atom, but simply occupies virtual electron orbits in the *molecule* SiO_2 and thus gives rise to secondary edges. The possibility of such transitions has been already indicated in connection with the emission of β_3 , β_4 , β_5 and β_6 lines by the molecules of some sulphur compounds (see Part II).

In conclusion I wish to express my most sincere thanks to Professor M. Siegbahn who suggested to me this problem and gave me facilities to carry it out.

The Spectrum of H_2 .—The Bands Ending on $2p^3\Pi$ Levels.

By O. W. RICHARDSON, F.R.S., Yarrow Research Professor of the Royal Society, and P. M. DAVIDSON, Ph.D., Lecturer in Physics, University College, Swansea.

(Received March 11, 1931.)

§ 1. *Introduction.*

Rather more than a year ago it was announced that the bands which go down to the two $2p^3\Pi_{\infty}$ levels had been found,* but owing to the inclusion of a considerable number of wrong lines little progress in understanding them has been made until quite recently. The discovery of these bands is important for several reasons, of which we shall mention one at this stage. It proves that a system of triplet states analogous to the states of the orthohelium line spectrum really exists in the spectrum of H_2 and to that extent confirms the view we have taken of the structure of this spectrum.* This follows since the singlet $2p^1\Pi_{\infty}$ levels have now been firmly identified* with the C level of Dieke and Hopfield; the final levels of the present band systems are undoubtedly $2p\Pi_{\infty}$ levels, and there is no room for any other $2p\Pi$ level in the singlet system.

The notation here used is that proposed by Mulliken. It has been described

* O. W. Richardson: 'Trans. Faraday Soc.,' vol. 25, p. 691 (1929); 'Proc. Roy. Soc.,' A, vol. 126, p. 501 (1930).

by one of us in the 'Transactions of the Faraday Society,' vol. 25, p. 628. It is assumed that in all the electronic states of H_2 with which these bands are concerned only one electron gets excited, the other being in an s state ($l = 0$). Thus the resultant azimuthal quantum number L of the two electrons is equal to that of the azimuthal quantum number l of the excited electron. The magnitude of both these quantities is thus expressed by the letters s (for $l = 0$), p (for $l = 1$), d (for $l = 2$), etc., in such symbols as $2p^3\Pi$. In addition we have to specify Λ the resolved part of L about the molecular axis. This is indicated by the symbols Σ for $\Lambda = 0$, Π for $\Lambda = 1$, Δ for $\Lambda = 2$, etc. The first number, such as 2 in $2p^3\Pi_{ab}$, indicates the principal quantum number n and the second such as s^3 shows that the level is believed to be a triplet level. The suffixes $_{ab}$ distinguish the double character of Π , Δ , etc., levels which arise according to whether the value of Λ is positive or negative.

The selection rules are (1) $\delta L = \delta l = \pm 1$, (2) $\delta K = 0$ or ± 1 , where $K = |\Lambda| + R$, R being the quantum number of the nuclear rotation, and (3) $a \leftrightarrow a$ and $s \leftrightarrow s$ but not $a \leftrightarrow s$. If, as it will appear from the analysis of the bands, the final state is a $p\Pi$ state the first selection rule $\delta l = \pm 1$ shows that the initial states must be $d\Sigma$, $d\Pi$, $d\Delta$ or $s\Sigma$ states. Except near the origin of a band, the second rule allows every upper rotational level to make a transition to three consecutive lower levels giving rise to P, Q and R lines respectively. In connection with this it is necessary to consider the third selection rule. This arises out of the fact that the nuclei are indistinguishable apart from their spins. This causes each consecutive set of rotational levels to consist of two alternating sets of non-intercombining levels with a weight ratio of 3 to 1. The stronger levels are denoted by a and the weaker levels by s . In a Σ level either the levels for which $K = 0$ (a), 1 (s), 2 (a), 3 (s), etc., or alternatively those for which $K = 0$ (s), 1 (a), 2 (s), 3 (a), etc., are alone present, according to the symmetry structure of the level. In Π , Δ , etc., levels owing to the so-called rotational doubling which arises from the positive and negative values of Λ , both the above sets of values of K are present. The lowest value of K is 0 for a Σ level, 1 for a Π level, 2 for a Δ level, and so on. This fact, together with the second and third selection rules, requires that the first band lines in transitions down to $p\Pi$ states are:—

- (1) From Σ states.— $Ra1$, $Rs2$, $Ra3$, ..., $Qs1$, $Qa2$, $Qs3$, ..., $Pa1$, $Ps2$, $Pa3$, ..., or $Rs1$, $Ra2$, $Rs3$, ..., $Qa1$, $Qs2$, $Qa3$, ..., $Ps1$, $Pa2$, $Ps3$, ..., according as the initial set of states are $0a$, $1s$, $2a$, $3s$, ..., or $0s$, $1a$, $2s$, $3a$, ...
- (2) From Π states.— $Ra1$, $Rs2$, $Ra3$, ..., $Qs1$, $Qa2$, ..., $Pa2$, $Ps3$, ..., and $Rs1$, $Ra2$, $Rs3$, ..., $Qa1$, $Qs2$, ..., $Ps2$, $Pa3$, ...

- (3) From Δ states.— $Ra1, R\alpha2, R\alpha3, \dots, Q\alpha2, Q\alpha3, \dots, Pa3, Pa4, \dots$, and $R\epsilon1, R\epsilon2, R\epsilon3, \dots, Q\epsilon2, Q\epsilon3, \dots, P\epsilon3, Pa4, \dots$

These various requirements which, taken together, are rather stringent, are all fulfilled by the bands to be described.

In describing the bands we propose to use dashed letters for transitions between s (weak) levels and undashed for transitions between a (strong) levels. Thus successive lines of the *same* band are $R1, R'2, R3, \dots, Q'1, Q2, Q'3, \dots, P1, P'2, P3, \dots$, and so on. This notation is not usual, but it seems convenient for these bands.

Although we believe these band systems to be correct in their main outlines, some of the details cannot be fixed with the same degree of certainty as was the case with the band systems described previously. We are doing further work which may modify them and make them more certain.

§ 2. The Bands of the System $3d^3\Sigma \rightarrow 2p^3\Pi$.

The lines of the $0 \rightarrow 0$ band of $3d^3\Sigma \rightarrow 2p^3\Pi_{ab}$ are:—

Table I.

				Properties.			R.T.	L.A.	V.
R'1	16884.94	†22.3	4	†LP++	†CD+	†Z=0	†35	†30	
R2	16834.27*	37.7	10	HP++	He++	CD+	Z	81	60
R'3	16774.97	U	4	†HP+	†He+	†CD+	†Z	†46	†27
R4	16710.63*	23.5	6	HP++	He++	CD+	Z	43	21
Q1	16854.86*	37.5	10	HP++	He++	Z	77	60	11.75
Q'2	16764.12	12.0	4	HP+	He++	CD+	Z	19	16
Q3	16654.24*	18.1	9	HP++	He++	CD+	Z	39	30
Q'4	‡16544.31	18.5	2	HP+	He++	Z=0	15‡	10	11.68
P'1	16870.70	10.5	2	CD++					
P2	16734.20	11.0	4	HeO	CD+				
P'3	16580.34	..	0	CD+					
P4	16416.35	..	2	He++					

† These data are for a blend with 16885.83 (5) = $3d^3\Delta_5 \rightarrow 2p^3\Pi_1 \rightarrow 1Q'3$?

‡ These data are for a blend with possibly two other lines.

§ Coincident with $0 \rightarrow 0$ $3p^3\Pi \rightarrow 2s^3\Sigma^+ Q4$ which requires nearly all the strength.

|| Data for a blend with a stronger unclassified line.

Possible alternative: R'3 might be covered by 16802.37* (10) (Z=0) and Q'4 by 16572.33 (0) = $1 \rightarrow 6$ of $3d^3\Pi_6 \rightarrow 2p^3\Sigma$. This is improbable.

In this and succeeding tables the first column gives the designation of the line, the second its wave-number,† the third its intensity as measured by Kapuscinsky and Eymers,* the fourth the eye estimate of Gale, Monk and Lee,†

* 'Proc. Roy. Soc.,' A, vol. 122, p. 58 (1928).

† 'Astrophys. J.,' vol. 67, p. 89 (1928).

the fifth the response to high pressure (H.P.), low pressure (L.P.), helium (He) or condensed discharge as recorded by Merton and Barratt,* the sixth the effect of a magnetic field as recorded by Dufour† or Croze,‡ the seventh, under R.T. and L.A., the intensities at room temperature or with the tube immersed in liquid air as given by McLennan, Grayson-Smith and Collins,§ and in the last column under V the excitation potential of the final level of the line as determined by Finkelnburg, Lau and Reichenheim.|| An asterisk denotes interferometer measures of Gale, Moll and Lee.

The lines of the $1 \rightarrow 1$ band of $3d^3\Sigma \rightarrow 2p^3\Pi$ are given in Table II.

Table II. $3d^3\Sigma v' = 1 \rightarrow 2p^3\Pi v'' = 1$.

							R.T.	L.A.	V.
R' 1	16630.47	8.4	3				14	13	
R2	16584.72*	34.7	10	HP++		Z	63	52	
R' 3	16536.89	8.7	1	CD+	He++	Z=0	21	12½	
R4	16469.93	22.6	8	HP++		Z	47	30	12.48
Q1	16603.20	27.0	9	HP++	CD++	Z	56	50	
Q' 2	16515.45	15.0	5	HP+	CD++				
Q3	16413.37	26.1	7	HP++	CD++	Z	47	38	12.25
Q' 4	16307.76		0						
? Q5	16187.50		1		‡CD++				
P' 1	16615.98		0						
P2	16488.15*	30.6	8	HP++		Z=0	26	16	
P' 3	†16344.13	9.7	1						
P4	16186.63	15.5	3						
? P' 5	16027.77		0		‡CD++				

† Claimed also as P3 of $v' = 0$ $1N \rightarrow v'' = 7$ $2p^1\Sigma$, in which band it seems too strong.

‡ This observation refers to a blend of Q5 and P4.

§ Possible (but very improbable) alternative R' 3 = 16532.87 (0a) and Q' 4 = 16303.84 (1). This weak R' 3 line is claimed by two others.

The non-diagonal bands of all the systems which end on $2p^3\Pi$ are very weak indeed and no lines involving transitions between the weak s levels have been found. The following are the lines of the $v' = 1 \rightarrow v'' = 0$ band of $3d^3\Sigma \rightarrow 2p^3\Pi$:—R2 coincident with 18918.02 (9) (= R0 of $v' = 1$ $3p^3\Pi \rightarrow v'' = 0$ $2s^3\Sigma$), R4 = 18783.54 (0), Q1 = 18942.00 (1), Q3 = 18737.96 (1), P2 = 18821.41 (1), P4 = 18499.91 (0).

A striking feature of this band system is that nearly all the strong lines respond to the Zeeman effect.

* 'Phil. Trans.,' A, vol. 222, p. 1.

† 'Ann. Chim. Physique,' vol. 9, p. 361 (1906); 'J. Physique,' vol. 8, p. 259 (1909).

‡ 'Ann. Physique,' vol. 1, p. 58 (1914).

§ 'Proc. Roy. Soc.,' A, vol. 116, p. 277 (1927).

|| 'Z. Physik,' vol. 61, p. 782 (1930).

Another is the marked tendency of the lines to be enhanced at higher pressures and by the condensed discharge. It will be seen from an examination of Kapuscinski and Eymers' intensity measures that the weights of alternate rotational α and s states are very close to 3 : 1. In any one branch of a band the ratio of R.T. to L.A. should increase as the rotational quantum number m increases. This is seen to be the case. The value of V for the $1 \rightarrow 1$ band should be about 0.3 volt more than for the $0 \rightarrow 0$ band. The difference is greater than this, but not beyond the possible errors which may be involved in these numbers. It might be that the band in Table II is $v + 2 \rightarrow v + 2$, that in Table I being $v \rightarrow v$. In that case there should be another band $v + 1 \rightarrow v + 1$ in the neighbourhood. We have looked for such a band but find no evidence of it. We have also been unsuccessful in finding a band at $v - 1 \rightarrow v - 1$. These facts seem to us good reasons for calling the first band $0 \rightarrow 0$ and the second $1 \rightarrow 1$.

For any band we can write

$$Qm - P'm = Fe' + Fv' + F'(m + \frac{1}{2}) - Fe'' - Fv'' - F''(m + \frac{1}{2}) \\ - fe' - fv' - f'(m - \frac{1}{2}) + fe'' + fv'' + f''(m + \frac{1}{2}), \quad (1)$$

where $F(m + \frac{1}{2})$, say, represents the contribution to the respective term arising from the rotational energy, Fv or fv that from the vibrational energy and Fe or fe the remainder of the energy, single and double dashes referring to initial and final terms respectively. Capital letters are used for α levels and small letters for s levels. For any one band we put $Fe' = fe'$, $Fv' = fv'$, $Fe'' = fe''$, and $Fv'' = fv''$. This assumes* that the nuclear spin has no perceptible influence on the electronic frequency and on the vibrational frequency. It is difficult to see how it can influence the vibration frequency appreciably and the smallness of the fine structure separations even for heavy elements justifies the assumption about electronic frequency.

We then have, for a $\Sigma \rightarrow \Pi$ band,

$$Q1 - P'1 = F'(1\frac{1}{2}) - f'(\frac{1}{2}) - [F''(1\frac{1}{2}) - f''(1\frac{1}{2})]. \quad (2)$$

There is no means of ascertaining the doublet separation $[F''(1\frac{1}{2}) - f''(1\frac{1}{2})]$ of the two lowest final Π levels. Let us denote it by x . The numerical values of the final terms indicate that it is small. We then have

$$F'(1\frac{1}{2}) - f'(\frac{1}{2}) = Q1 - P'1 + x. \quad (3)$$

* It assumes also that these quantities are the same for the α and b states in the lower level. The equivalent assumption seems to be justified for the upper levels of the α , β bands (*cf.* Richardson and Das, 'Proc. Roy. Soc. A', vol. 122, p. 716 (1929)).

By a similar process

$$\begin{aligned}
 f'(2\frac{1}{2}) - F'(1\frac{1}{2}) &= R'1 - Q1 - x \\
 &= Q'2 - P2 + [R'1 - Q'2 - (Q1 - P2)] - x \\
 F'(3\frac{1}{2}) - f'(2\frac{1}{2}) &= R2 - Q'2 - [R'1 - Q'2 - (Q1 - P2)] + x \\
 &= Q3 - P'3 + [R2 - Q3 + Q1 - P2 \\
 &\quad - (Q'2 - P'3 + R'1 - Q'2)] + x \\
 f'(4\frac{1}{2}) - F'(3\frac{1}{2}) &= R'3 - Q3 - [R2 - Q3 + Q1 - P2 \\
 &\quad - (Q'2 - P'3 + R'1 - Q'2)] - x \\
 &= Q'4 - P4 + [R'3 - Q'4 + Q'2 - P'3 + R'1 \\
 &\quad - Q'2 - (Q3 - P4 + R2 - Q3 + Q1 - P2)] - x
 \end{aligned} \quad (4)$$

and so on.

For the bands with $R1, R'2, R3$, etc., we have to interchange F and f , also the dashed and undashed PQR 's and to reverse the sign of x in these formulæ.

As will be seen later, the final terms $R'(m) - Q'(m+1)$, $Rm - (Qm+1)$, $Q'm - P'(m+1)$, $Qm - P(m+1)$ are known with considerable accuracy; so that these equations enable us, by using the appropriate combinations of the final terms occurring in equation (4), to make two independent determinations of each initial rotational level difference such as $F'(m+\frac{1}{2}) - f'(m-\frac{1}{2})$. However, it is quicker to use equation (3) to determine the lowest level difference and then to evaluate the others by using the successive equations

$$f' \text{ or } F'(m+\frac{1}{2}) - f' \text{ or } F'(m-\frac{1}{2}) = R' \text{ or } Rm - P' \text{ or } Pm \quad (5)$$

starting with $m=1$. Equations (5), which give the differences between successive pairs of alternate initial levels directly, involve no assumptions of the kind which were made in deducing (3) and (4). Thus we subtract the value of $F'(1\frac{1}{2}) - f'(\frac{1}{2}) - x$ given by (3) from the value of $f'(2\frac{1}{2}) - f'(\frac{1}{2}) = R'1 - P'1$ given by (5) and so obtain $f'(2\frac{1}{2}) - F'(1\frac{1}{2}) + x$. This in turn is subtracted from $F'(3\frac{1}{2}) - F'(1\frac{1}{2}) = R2 - P2$, giving $F'(3\frac{1}{2}) - f'(2\frac{1}{2}) - x$, and so on. The initial terms thus extracted, together with their successive differences denoted by Δ , are given in the first two rows of Table III.

It will be seen that the rotational terms of both initial levels are very similar and tend to be a little less for the $v=1$ than for the $v=0$ level. They are also very like the corresponding levels* of $3d^1\Sigma$ which are set out in the two

* Richardson and Davidson, 'Proc. Roy. Soc.,' A, vol. 123, p. 75 (1929). For these singlet levels the x 's in the headings are to be omitted.

Table III.—Initial Terms of $nd\ ^3\Sigma \rightarrow 2p\ ^3\Pi$.

Term \rightarrow value of n \downarrow v' \downarrow	$F'(1\frac{1}{2})$ $-f'(1\frac{1}{2})-x.$	$f'(2\frac{1}{2})$ $-F'(1\frac{1}{2})+x.$	$F'(3\frac{1}{2})$ $-f'(2\frac{1}{2})-x.$	$f'(4\frac{1}{2})$ $-F'(3\frac{1}{2})+x.$	$F'(5\frac{1}{2})$ $-f'(4\frac{1}{2})-x.$
3 0	-15.84				
3 $\Delta \rightarrow$ 1	-12.78	45.92	39.91	45.05	63.00
4 0	-9.23	40.05	42.03	54.16	36.38
4 $\Delta \rightarrow$ 1		32.85	52.50	44.60	
3d $^1\Sigma 0$	-7.53	22.70	65.24	112.48	164.38
3d $^1\Sigma 1$	-13.74?	30.23	42.54	47.24	51.90
d \rightarrow		29.25?	31.72	39.43	51.66

last rows of Table III. This similarity in the uncoupling phenomena is sufficient to identify the initial electronic level as $d\ ^3\Sigma$ and it is confirmed by the strong Zeeman response. The identification as $3d\ ^3\Sigma$ is required by the value of v_0 for the level. This will be considered later. There is an irregularity in Table III which lies either in the $v=0$ or in the $v=1$ level. This is discussed in § 8.

§ 3. The Bands of the Systems $3d\ ^3\Pi_{ab} \rightarrow 2p\ ^3\Pi_{ab}$.

The lines of the bands of $3d\ ^3\Pi_b \rightarrow 2p\ ^3\Pi_{ab}$ are set out in Table IV.

Table IV.

$3d\ ^3\Pi_b\ v' = 0 \rightarrow 2p\ ^3\Pi_{ab}\ v'' = 0.$								R.T.	L.A.	V.
R1	17672.31*	34.6	10	HP+	HeO	CD++	61	51	11.88
R' 2	17691.22	19.4	4			CD++			
R3	17693.01	15.0	3		He++	CD++			
Q' 1	17498.65	U2						
Q2	17451.59*	30.7	10	HP+	HeO	CD++	Z = 0	61	49
Q' 3	17416.51	3			CD+		9 $\frac{1}{2}$	7
Q4	17355.14	16.2	6	HP+	HeO	CD++	Z	29 \rightarrow 21 48 \rightarrow 41	21
P' 2	17377.85	1						
P3	17271.56	13.9	4		He+	CD++		18 \rightarrow 14 32 \rightarrow 27	14
P' 4	17186.00	8.9	2						

Table IV—(continued).

$3d\ ^3\Pi_b\ v' = 1 \rightarrow 2p\ ^3\Pi_{ab}\ v'' = 1.$							R.T.	L.A.	V.
R1	..	17426.25*	40.3	10	CD++	Z=0	39	38	12.28
R'2	..	17431.57	17.1	6	CD+				
R3	.	17411.21	.	5	CD+		11½a→10½		
R'4							27→24		
Q'1		17347.97	9.4	3	CD++		6½	6a	
Q2		17311.08*	37.0	9	†LP++	†CD++	42→43	58	12.47
Q'3		17260.69	17.1	4	LP++	He++	26→17½		
Q4		17184.46	10.7	3	CD++		40→30		
P'2	...	17233.19	10.3	2h	He++	CD++	12½→9		
P3	..	17139.77	17.6	5	†CD++		21→16		
P'4		17031.67		1a	†CD++		24a→21		
							29→26		
$3d\ ^3\Pi_b\ v' = 1 \rightarrow 2p\ ^3\Pi_{ab}\ v'' = 0.$									
R1	.	19765.11	.	0h					
Q2	.	19644.35	..	0					

† These observations are for a blend with $3p\ ^3\Pi v' = 5 \rightarrow 2s\ ^3P v'' = 4Q1$

‡ These observations are for blends with weak unclassified lines.

The lines of these bands show a weaker response in the Zeeman effect than those which come from $3d\ ^3\Sigma$. The strength of corresponding lines is about the same and the 3 : 1 weight ratio is evident from the intensities. The high pressure feature is not so evident, but all the lines are enhanced in the condensed discharge. The R.T. : L.A. ratio increases with increasing m and the value of V is higher for the $1 \rightarrow 1$ band than for the $0 \rightarrow 0$ band by about the amount expected.

The lines of the system $3d\ ^3\Pi_a \rightarrow 2p\ ^3\Pi_{ab}$ are set out in Table V.

Table V.

$3d^3\Pi_a v' = 0 \rightarrow 2p^3\Pi_{ab} v'' = 0.$						R.T.	L.A.
R' 1	†17591.23	19.4	4		CD++		
R2	17669.81	3.3	2	He+	CD++	21	→ 40
R' 3	17739.54	.	1				
or							
R' 3	17743.02	...	1				
Q1	17463.59		0				
Q' 2	17470.40		1				
Q3	17489.90	9.6	3	He+	CD++	20	→ 12
Q' 4	†17508.99	12.1	5		CD++	20	→ 27
or							
Q' 4	‡17512.41		2				
P2	17342.83	.	1				
P' 3	17295.44		0				
P4	17251.99		0a				
$3d^3\Pi_a v' = 1 \rightarrow 2p^3\Pi_{ab} v'' = 1.$							
R' 1	17456.16	12.4	3				
R2	17529.00	12.0	5	HP+	CD++		
R' 3	¶17586.73	5.7	1				
Q1	17344.17		1				
Q' 2	††17341.26		1				
Q3	17357.64	15.6	5	HP+	CD++		
Q' 4	17357.64		1				
P2	.. ††17229.24	.	0				
P' 3	[17170.24]		ab				
P4	17130.78	3a				

† This is also R' 2 of $3d^3\Pi_b v' = 0 \rightarrow 2p^3\Pi_{ab} v'' = 0$, where it is too strong.

‡ Coincident with $3d^1\Sigma v' = 0 \rightarrow 2p^1\Sigma v'' = 3$ P5 where it is a little too strong.

§ Misprinted as 17512.71 in Gale, Monk and Lee's Tables.

|| Coincident with $^1N v' = 0 \rightarrow 2p^1\Sigma v'' = 6$ P3, which requires most of the strength.

¶ Coincident with $^1N v' = 0 \rightarrow 2p^1\Sigma v'' = 6$ R3, for which it seems rather strong.

†† Coincident with $3d^1\Sigma v' = 1 \rightarrow 2p^1\Sigma v'' = 5$ P5, a doubtful line in that system.

‡‡ Coincident with a P2 line in $3p^3\Sigma \rightarrow 2s^3\Sigma$.

The fact that the bands coming from $3d^3\Pi_a$ are much weaker than those which come from $3d^3\Pi_b$ and $3d^3\Sigma$ is not surprising. In the corresponding singlet band complex the bands coming from $3d^1\Sigma$ and $3d^1\Pi_b$ which go down to $2p^1\Sigma$ are very strong, and much stronger than those going from $3d^1\Pi_a$ to $2p^1\Sigma$.

The initial rotational terms of $3d^3\Pi_a$ and $3d^3\Pi_b$ are given in Table XIII. Consideration of these will be deferred until some other systems of bands have been described.

§ 4. The Bands of the Systems $3d^3\Delta_{ab} \rightarrow 2p^3\Pi_{ab}$.

The lines of the system $3d^3\Delta_b \rightarrow 2p^3\Pi_{ab}$ are set out in Table VI. The $0 \rightarrow 0$ band is rather doubtful as the accuracy of the combinations is below the average.

Table VI.

$3d^3\Delta_b v' = 0 \rightarrow 2p^3\Pi_{ab} v'' = 0.$									
							R.T.	L.A.	V.
R1	.. †17588.00	5.7	5		CD++	He++	47	29	
R' 2	.. 17638.60	..	0		‡CD++	‡He++	‡ 9	‡ 7‡	
R3	.. 17671.44		1						
or R3	.. 17679.32	9.7	2						
Q2	.. 17467.13	10.0	6	HP+	CD++	HeO	24	20	
§Q' 3	.. 17463.59	..	0						
Q4	.. 17433.50	..	1						
or Q4	.. 17441.32	19.6	8	HP++	CD++	HeO	25 → 18‡ 52 → 40		
P3	.. 17287.27	9.3	2		CD++	He+			
P' 4	.. 17233.19	10.3	2h		CD++	He++ Z=0	12‡ → 9 21 → 16		
$3d^3\Delta_b v' = 1 \rightarrow 2p^3\Pi_{ab} v'' = 1.$									
R1	.. 16978.52	28.0	10	HP++	CD+	Z	57 → 43 41 → 32		12.13
R' 2	.. 17056.70†	9.3	1						
R3	.. 17068.60	..	1		CD+	He++	6‡ → 5 5‡ → 4‡		
Q2	.. 16863.40	1		CD++				
Q' 3	.. 16885.83?	22.3	5	LP++		He+	Z=0	35 → 30	
Q4	.. 16841.63	10.3	4			HeO	Z=0	20a → 19‡a	
P3	.. 16692.00	14.0	5	HP++	CD+	Z=0			
P' 4	.. [16656.60]?	ab							
$3d^3\Delta_b v' = 1 \rightarrow 2p^3\Pi_{ab} v'' = 0.$									
R1 = 19317.37(0) Q2 = 19196.60(00) P3 = 19016.55(0).									

† Coincident with $3d^1\Sigma \rightarrow 2p^1\Sigma \rightarrow 5 R1$.

‡ These data refer to a blend with a weak unclassified line.

§ Coincident with Q1 of the band in Table V.

|| These properties are for a blend with $3d^3\Sigma \rightarrow 2p^3\Pi R' 1$.

The lines of the system $3d^3\Delta_a \rightarrow 2p^3\Pi_{ab}$ are set out in Table VII.

Table VII.

$3d^3\Delta_a v = 0 \rightarrow 2p^3\Pi_{ab} v = 0.$						R.T.	L.A.	V.
R' 1	17657.88	14.8	3					
R2	17717.06	5.9	3a					
R' 3	17767.43	2.5	2					
Q' 2	17537.02	9.6	4	CD++ He++				
Q3	17537.02							
Q' 4	17537.02							
P' 3	17362.40		0					
P4	17299.30	14.6	4	HP++	CD++	He++	Z=0	19 → 12 34 → 24
$3d^3\Delta_a v = 1 \rightarrow 2p^3\Pi_{ab} v = 1.$								
R' 1	17031.67	1a					
R2	17086.67	9.2	2					
R' 3	17130.78		3a					
Q' 2	16916.57	13.0	0					
Q3	16915.33		3					
Q' 4	16901.67		1					
P' 3	16745.48		0					
P4	16688.40	19.0	4	HP+			Z=0	30 → 24
$3d^3\Delta_a v = 0 \rightarrow 2p^3\Pi_{ab} v = 1.$								
Q3 = 15212.66 (1A).								

The properties of a good many lines in this table have not been inserted as they are due to mixtures and are thought to be misleading. The Q branch of $0 \rightarrow 0$ is obviously open to objection. It can be changed by substituting $R' 3 = 17778.92$, 14.2 (4) and $Q' 4 = 17548.63$, $3.2(0a)$. However, the combinations are quite good with 17537.02 in the place of all three lines.

The transitions to $2p^3\Pi$ from the $3d^3\Delta$ levels when compared with those from $3d^3\Sigma$ and $3d^3\Pi$ levels are relatively stronger than the transitions to $2p^1\Sigma$ from $3d^1\Delta$ in comparison with those from $3d^1\Sigma$ and $3d^1\Pi$ levels. In He_2 the $3d^3\Delta \rightarrow 2p^3\Pi$ transitions seem to have a fair amount of strength. In both the $3d^3\Delta \rightarrow 2p^3\Pi$ systems only one line is recorded as giving the Zeeman effect and five are recorded definitely as not affected by a magnetic field. The testimony of two of these lines is open to question. $Q' 3$ of Δ , $1 \rightarrow 1$ is much too strong and $P' 4$ of Δ , $0 \rightarrow 0$ is recorded by Gale, Monk and Lee as probably double. However, we can conclude that the $3d^3\Delta \rightarrow 2p^3\Pi$ transitions certainly show a weaker Zeeman response than $3d^3\Sigma \rightarrow 2p^3\Pi$ and probably one which is weaker than that of $3d^3\Pi \rightarrow 2p^3\Pi$. The initial rotational terms of these bands are set out in Table XIII and will be considered later.

We have also found the $0 \rightarrow 0$ bands of the whole d complex $4d^3\Sigma\Pi\Delta \rightarrow 2p^3\Pi$. The lines are set out in Table VIII. These bands are in the blue between H_2 and H_7 , whereas the foregoing bands lie in the yellow and orange, except the very weak $1 \rightarrow 0$ fragments which lie in the green.

§ 5. The $4d^3\Sigma\Pi\Delta \rightarrow 2p^3\Pi$ Complex.

Table VIII.

$4d^3\Sigma v = 0 \rightarrow 2p^3\Pi_{ab} v = 0.$				R.T.	L.A.	V.
R' 1	22646.10	5.2	1			
R 2	22601.50	21.1	3	15	14	
R' 3	22647.31	2.7	1			
Q 1	22622.48		0			
Q' 2	22525.32	4.5	3	He++	Z	6 $\frac{1}{2}$ 5
† Q 3	22421.63	20.0	3	He+	Z	15 $\frac{1}{2}$ 10
Q' 4	22316.72	4.1	2			
P' 1	22631.71	47.0	5	He++	Z	22 14
P 2	22501.76	9.4	2			
P' 3	22350.47	..	0/1	Finkelburg*		
P 4	22183.74	..	00			
$4d^3\Pi_b v = 0 \rightarrow 2p^3\Pi_{ab} v = 0.$						
R 1	22657.81	86.0	8	He++	Z	35 \rightarrow 30
R' 2	22656.64	10.6	2			
R 3	22631.71	47.0	5	He++	Z	22 \rightarrow 14
or						
R 3	22657.81	86.0	8			
Q' 1	22586.89	...	0			
Q 2	22537.10	4.6	1	He++		
Q' 3	22481.71	3.0	0			
Q 4	22394.07	8.6	2			
or						
Q 4	22419.69	...	2			
P' 2	22466.06	28.3	6	HP+		14 $\frac{1}{2}$ \rightarrow 10
P 3	22357.05	...	1	§LP+		
P' 4	22251.41	...	1			
$4d^3\Pi_a v = 0 \rightarrow 2p^3\Pi_{ab} v = 0.$						
R' 1	22699.42	6.7	1			
R 2	22758.54	..	00a			
R' 3	22807.41	..	0			
Q 1	22584.34	3.3	1			
Q' 2	22578.51					
Q 3	22578.51	6.3	oa			
Q' 4	22578.98	2.5	00			
P 2	22463.85	3.2	0			
P' 3	[22403.71]	...	ab			
P 4	22340.76	...	o/1 F*			

* 'Z. Physik,' vol. 52, p. 27 (1928).

† The properties given for this are for a blend of three lines, one of which is $4p^3\Pi \rightarrow 2s^3\Sigma$ $0 \rightarrow 0$ R3, and the other unclassified.

‡ Coincident with $3d^1\Pi_b \rightarrow 2p^1\Sigma$ $3 \rightarrow 4$ Q4, for which it is too strong.

§ Refers to a blend with R1 of $1 \rightarrow 1$ $^1K \rightarrow 2p^1\Sigma$.

|| Coincident with R1 of $3 \rightarrow 4$ $3d^1\Sigma \rightarrow 2p^1\Sigma$.

Table VIII—(continued).

$4d\ ^3\Delta_5\ v=0 \rightarrow 2p\ ^3\Pi_{ab}\ v=0.$						R.T.	L.A.	V.
R1	... †22778·43	4·3	1	He++		9	→ 7	
R' 2	22826·33	..	o/F					
R3	22833·89		oo/F					
Q2	... †22657·81	86·0	8	He++	Z	35	→ 30	11·74
Q' 3	22651·41	12·8	2	He++				
Q4	... 22596·04	..	0					
P3	... 22477·97	66·7	9	He++	Z	38	→ 39	11·75
P' 4	... 22420·99	13·0	3	He+	Z	15‡	→ 10	
$4d\ ^3\Delta_5\ v=0 \leftarrow 2p\ ^3\Pi_{ab}\ v=0.$								
R' 1	... 22777·41	13·6	3	He++		9	→ 7	
R2	22827·77	20·3	4	He++	Z=0	11	→ 7‡	11·78
R' 3	22866·48	2·4	1					
Q' 2§	22656·64	10·6	2					
Q3	22647·73	33·3	4	He++	Z=0	26	→ 16	
Q' 4	22636·12	7·1	1					
P' 3	22481·71	3·0	0					
P4	[22409·88]	...	ab					
<i>Alternative in $^3\Delta_5$—</i>								
R3	... 22881·78		o/F					
Q4	... 22643·75	21·5	3	He++	Z			

† Coincident with P7 of $1 \rightarrow 3\ ^1N \rightarrow 2p\ ^1\Sigma$.‡ Most of the strength of this is required in $4d\ ^3\Pi_b \rightarrow 2p\ ^3\Pi_{ab}\ 0 \rightarrow 0$.§ Coincident with R' 2 of $4d\ ^3\Pi_b\ v=0 \rightarrow 2p\ ^3\Pi_{ab}\ v=0$.|| Coincident with Q' 3 of $4d\ ^3\Pi_b\ v=0 \rightarrow 2p\ ^3\Pi_{ab}\ v=0$.

In this complex the only system for which the Zeeman effect is definitely established is $4d\ ^3\Delta_5\ v=0 \rightarrow 2p\ ^3\Pi\ v=0$. In $d\ ^3\Sigma$ and $d\ ^3\Pi_b$ the lines marked Z are probably all blends and the lines of Π_a are all too weak for observation of this effect. The strong lines of $d\ ^3\Delta_5 \rightarrow 2p\ ^3\Pi$ definitely do not respond to the magnetic field. This property is also possessed by the $0 \rightarrow 0$ and $1 \rightarrow 1\ 3d\ ^3\Delta_5 \rightarrow 2p\ ^3\Pi$ bands. Another feature which is common to the $n=3$ level is the weakness of the Π_a bands. In fact, the relative strength of each system at $n=4$ is very much the same as at $n=3$. The line P' 2 of Π_b is much too strong. The excitation potentials of the final levels of three of the strongest lines as measured by Finkelnburg, Lau and Reichenheim are all identical and the same as those of $3d\ ^3\Sigma\Pi\Delta\ v=0$ to $2p\ ^3\Pi\ v=0$, as they should be if the final levels are identical.

§ 6. *The Final Rotational Levels.*

The most satisfactory test of the identity of the final levels as well as of the genuineness of the bands is afforded by the values of the final terms. The final rotational terms of all the bands which have been described are collected together in Table IX. In this table an asterisk denotes a value which is affected by a line which is either a known blend or which is obviously much too strong.

It will be seen that for all the $0 \rightarrow 0$ bands the following pairs of differences have the same values: $-Q_1 - P_2 = R_1 - Q_2$, $R_2 - Q_3 = Q_2 - P_3$, $Q_3 - P_4 = R_3 - Q_4$, $R'_1 - Q'_2 = Q'_1 - P'_2$, $Q'_2 - P'_3 = R'_2 - Q'_3$ and $R'_3 - Q'_4 = Q'_3 - P'_4$. The same statement is true for the $1 \rightarrow 1$ bands but here the values are different. The terms set out in Table IX are not differences between consecutive rotational levels of a single electronic level. There are two separate final electronic levels $2p^3\Pi_a$ and $2p^3\Pi_b$. The successive rotational levels of a given electronic level such as $2p^3\Pi_a$ have alternately *a* (weight 3) and *s* (weight 1) character. If we define a band as a sequence of rotational transitions from one given electronic and vibrational level to another single electronic and vibrational level, the lines of a single band such as $3d^3\Sigma v' = 0 \rightarrow 2p^3\Pi_b v'' = 0$ are $P_s 1, P_a 2, P_s 3, P_a 4, \dots, R_s 1, R_a 2, R_s 3, R_a 4, \dots$, and the lines $Q_a 1, Q_s 2, Q_a 3, Q_s 4, \dots$, belong to another band namely, $3d^3\Sigma v' = 0 \rightarrow 2p^3\Pi_a v'' = 0$. It is to be remembered that in the present paper the notation $P_s 1, P_a 2, P_s 3, P_a 4, \dots$, etc., has been shortened to $P' 1, P_2, P' 3, P_4, \dots$, etc., to avoid the repetition of so many suffixes. The meaning of the intervals in Table IX will be made quite clear by reference to fig. 1, which shows, but not to scale, the rotational structures of $d^3\Sigma, d^3\Pi_{ab}, d^3\Delta_{ab}$ and $p^3\Pi_{ab}$ together with the transitions from the first three to the last level. To avoid confusion only the first line of each branch is indicated for $\Pi \rightarrow \Pi$ and $\Delta \rightarrow \Pi$ transitions.

The detailed structure of the final levels is not as regular as it is shown in fig. 1. It is set out roughly, with the doublet distances exaggerated, for the two vibrational levels in fig. 2. x_0 and x_1 in this diagram have the opposite sign to x as defined on p. 662. The j values in these figures have the same meaning as those in our former papers. We have decided that more confusion than help would be created by modernising this notation at this stage.

The actual rotational term values as they would more usually be written, that is to say, the separation of successive rotational levels of a given electronic level such as $2p^3\Pi_b$, are set out towards the bottom of Table XIII. These can only be given subject to $\pm x_0$ and $\pm x_1$, the doublet distance at the lowest

Table IX.

Final Rotational Terms of $d^3 0 \rightarrow 0$ Bands.

	Q1-P2	R1-Q2	R2-Q3	Q2-P3	Q3-P4	R3-Q4	R'1-Q'2	P'1-P'2	Q'2-Q'3	P'3-R'3	Q'3-Q'4	P'4-Q'3-P'4
3 Σ	120.66	120.72	180.03	180.03	237.89	237.87	120.82	120.82	174.78	174.71	230.65*	230.51
3 Π_b	120.76		179.91		237.91		120.82	120.82	174.96*		230.55*	230.61
3 Π_a		120.87*		179.86		237.94				175.01*		230.40
3 Δ_b			180.04		237.72	238.00*	120.86		174.62*		230.41	
Means	120.71	120.72	179.99	179.95	237.84	237.90	120.83	120.80	174.78	174.71	230.51	230.45
4 Σ	120.72		179.87		237.89		120.78		174.85		230.59	
4 Π_b		120.71		180.05		237.64*		120.83		174.90		230.30
4 Π_a	120.49*		180.03		237.75	238.12*	120.91				230.43	
4 Δ_b		120.62	180.04	179.84		237.85	120.77		174.93	174.92	230.36	230.42
4 Δ_a			179.98	179.95	237.82	237.85	120.82	120.83	174.89	174.91	230.46	230.36
Means	120.72	120.66										
Total means ..	120.70		179.97		237.85		120.82		174.85		230.44	

	$d^3 1 \rightarrow 1$ Bands.									
3 Σ	115.05		171.35		228.74		115.02		171.32*	230.13
3 Π_b				171.31		228.75		114.78*		229.03
3 Π_a	114.93*		171.36		228.86		114.90*		170.88	229.02
3 Δ_b		115.12	171.40			228.97			170.87*	
3 Δ_a			171.34		228.93		115.10		171.09	229.11
Means	115.05	115.14	171.35	171.35	228.84	228.86	115.01		171.09	229.09
Total means ..	115.11		171.35		228.85		115.01		170.98	229.08

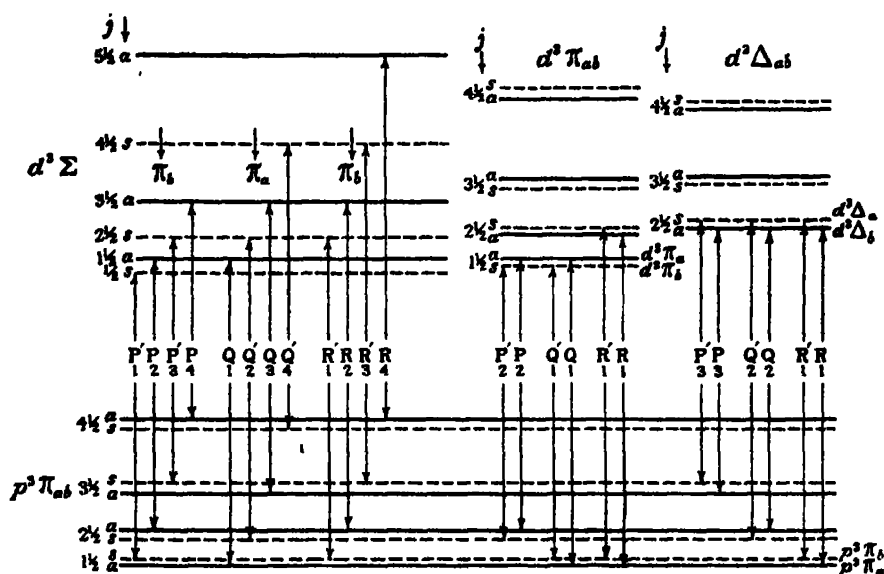
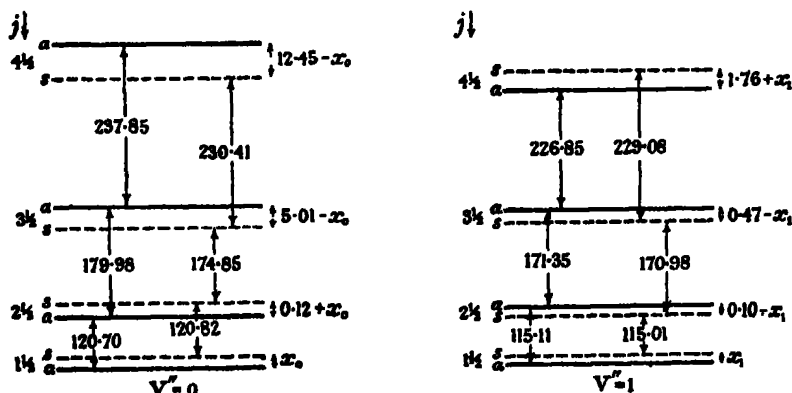
Fig. 1.—Structure and transitions of $d^3\Sigma II \Delta$ complex to $p^3\Pi$.

Fig. 2.—Rotational structure of final levels.

($j = 1\frac{1}{2}$) level for $v'' = 0$ and $v'' = 1$ respectively. Whether x_0 or x_1 has to be added or subtracted depends on whether the upper level of the two is an s or an a level. This is indicated by the formulæ at the top of each column. The numbers inserted in fig. 2 suggest that no very serious risk will be run if x_0 and x_1 are assumed to be negligible.

The final term differences as given in Table XIII are too irregular to fit any simple formula for the terms such as

$$F(j) = Bj^2 + \beta j^4, \quad (6)$$

nor is it really legitimate to assume in bands of this type that the deviation from the formula is small for the lowest j values. If, however, we make this assumption, we can calculate the values of $2B$ and β for each of the lower states, using only the first two rotational intervals, and assuming that x is zero and j exactly $1\frac{1}{2}$ in the lowest level. At $v = 0$ the $2^3\Pi_g$ level is too irregular even for this procedure.

The results of these computations are given in the column under $n = 2$ in Table X.

Table X.
Rotational Constants of $np^3\Pi$ Levels.

	$n \rightarrow$	Values of $2B$.				Values of $-\beta$.		
		2	3	4		2	3	4
$n^3\Pi_a$ $v = 0$..	60.8	59.09	58.80		0.023	0.018	0.019
$n^3\Pi_b$ $v = 0$..		59.65	58.575			0.020	0.02
$n^3\Pi_a$ $v = 1$.	57.8	56.5	55.63		0.02	0.02	0.0175
$n^3\Pi_b$ $v = 1$.	58.1	57.0			0.03	0.0225	

Under $n = 3$ and $n = 4$ in Table X are given the corresponding constants for the upper levels of the α and β bands. The values for the $v = 0$ level are those published by Richardson and Das.* The actual values at the $v = 1$ level of $n = 3$ cannot be deduced directly from the bands owing to a perturbation at this level. Those given in the table have been calculated by interpolation from the values published by Richardson and Das for the $v' = 1, 3$ and 4 levels. These interpolated values of $2B_1$ are probably correct to about 0.1 and those of β_1 to about 10 per cent. The values for $4^3\Pi_g$ $v' = 1$ have been got from the relation $f'(j) - F'(j-1) = Q(j) - Q(j-1) + f''(j) - F''(j-1)$ from the Q lines of the β bands using the known final intervals $f''(j) - F''(j-1)$, the intervals $f'(j) - F'(j-1)$ being then used to calculate B and β as for the final states of the present bands. There is not enough information to determine $2B$ and β for the upper $v = 1$ level of the β bands using the P, R branches which correspond to Π_g . It is evident that the values of $2B$ for the final levels of the present band systems are just what would be expected for the next lower electronic level to the upper level of the α bands. At $v = 1$ the value for Π_g is a little greater than for Π_u , just as for the upper levels of the α bands. The value of α , the constant in $B_n = B_0 - \alpha n$, is evidently very nearly the same for these final levels as for the upper level of the α bands. For $2p^3\Pi_g$ it is 1.5, whereas for $3p^3\Pi_g$ it is 1.295, and for

* 'Proc. Roy. Soc.,' A, vol. 122, p. 688 (1929).

$3p^3\Pi$, it is 1.325. The values of β are as good as can be expected. It is something to get the correct sign and order of magnitude of this quantity from such data. As a matter of fact the value of $-\beta$ comes out larger for Π , than for Π_g just as in the other bands, and if a composite average of all values of $-\beta$ for the final states is taken, which should tend to increase the accuracy, it is quite near what would be expected from the values for the upper levels of the α and β bands. The values of β also agree with the final vibrational interval which will be found in § 7. Substituting this in the equation $-\beta = 4B_0^2/\omega_0^2$ we get $-\beta = 0.02$. Evidently Table X affords good evidence for making the levels considered an electronic sequence.

§ 7. *The Vibrational Intervals.*

The magnitude of these is settled by the lines of the non-diagonal $1 \rightarrow 0$ bands. These are so weak that only the lines representing transitions between the strong intervals ($a \rightarrow a$) can be found, and even these are only represented by faint lines whose strength ranges between (00) and (1). These lines are important for the interpretation of the bands—in fact, there is no other avenue to the vibrational constants—and as they are so very weak the criteria for their genuineness must be regarded critically.

In the lower state the intervals between the individual a levels at $v'' = 0$ are known, and so are the intervals at $v'' = 1$. It is only the interval between the two sets which is not known. Now any one a line of a non-diagonal band fixes this unknown interval. It also fixes the position of the upper sets at $v' = 0$ and $v' = 1$, which are known separately for all the $3d$ states. Thus a single non-diagonal a line enables all the a lines of the $1 \rightarrow 0$ and $0 \rightarrow 1$ bands to be predicted, and determines the vibrational intervals in Table XI. We find only about a dozen non-diagonal lines, all belonging to $1 \rightarrow 0$ bands; but since they correspond to the strongest lines of the diagonal bands, and since they are very accurately in the positions predicted from any one of them, we believe them to be genuine.

In Table XI are set out in the columns under $n = 2$ the final vibrational intervals of the present bands. For $m = 1, 2$ and 3 these are the means of the following individual values:—For $m = 1$, 2338.80, 2338.86, 2338.85; for $m = 2$, 2333.30, 2333.26, 2333.27, 2333.20; and for $m = 3$, 2324.59, 2324.55. For $m = 4$ there are two values, 2313.28 and 2313.61, which do not agree very well. The value 2313.61 is preferred as it gives better combinations. In the columns under $n = 3$ and $n = 4$ are given the values of the corresponding vibrational intervals for the upper levels of the α and β bands

Table XI.

1 \rightarrow 0 Vibrational Intervals of $n^3\Pi_{ab}$ Levels.

		$np^3\Pi_a$ levels.			$np^3\Pi_b$ levels.		
		$n = 2.$	$n = 3.$	$n = 4.$	$n = 2.$	$n = 3.$	$n = 4.$
at j \downarrow	m \downarrow	Final levels of present band systems.	Upper levels of α bands Q branches.	Upper levels of β bands Q branches.	Present bands.	α R'P' branches.	β R'P' branches.
1 $\frac{1}{2}$	1	2338.84	2240.21	2209.60	—	2239.45	—
2 $\frac{1}{2}$	2	—	2234.23	2203.55	2333.26	2231.23	2204.9
3 $\frac{1}{2}$	3	2324.57	2225.28	2194.57	—	2216.28	—
4 $\frac{1}{2}$	4	—	2213.44	—	2313.61	2196.79	—

respectively. It will be seen that in all cases the present final intervals are about 100 w. numbers higher than the corresponding intervals in the upper level of the α bands and these in turn are about 30 w. numbers higher than those in the β bands. The relative magnitudes are just about what would be expected if these levels were three successive electronic levels of the same type with principal quantum number $n = 2, 3$ and 4 respectively. The vibrational data therefore afford a good confirmation of the inference which has already been drawn from the rotational data.

The initial vibrational intervals $\Delta V'm$ calculated from these final intervals and equations of the type $\Delta V'm = \Delta V''(m+1) + P(m+1)(1 \rightarrow 1) - P(m+1)(0 \rightarrow 0)$ are collected in Table XII. The individual determinations are shown in the top part of the table. The letter alongside each value of m' shows whether it has been got from an R, Q or P branch.

The mean values of the intervals are set out in the bottom part of the table. As only the values for the strong α levels are known, the successive values of m' jump by 2 in each band. The successive differences for this change in m are set out, in brackets, under each set of values of the intervals. The large value of this jump in the case of the Π_a and Π_b levels is noteworthy. A precisely similar occurrence is found in the $3d$ complex in the singlet systems where it is most marked in the $3d^1\Pi_a$ level, is very definite in the $3d^1\Sigma$ level and is not noticeable in the $3d^1\Pi_b$ level. These phenomena arise from the uncoupling effects which are very pronounced in both singlet and triplet systems at the d complex. Perhaps the most surprising feature in Table XII

Table XII.

1 \rightarrow 0 Vibrational Intervals of $3d^3\Sigma$, $3d^3\Pi_{ab}$, $3d^3\Delta_{ab}$.

$m' \rightarrow$ level	3R	5R	1Q	3Q	1P	3P
$3d^3\Sigma$	2083.71	2072.91	2087.18	2083.70	2087.21	2083.56
$m' \rightarrow$	2R	4R	2Q	4Q	2P	
$3d^3\Pi_b$	2192.78	2142.77	2192.75	2142.83	2192.78	
$m' \rightarrow$	3R	1Q	3Q	1P	3P	
$3d^3\Pi_a$	2192.45	2219.42	2192.31	2219.67	2192.40	
$m' \rightarrow$	2R	4R	2Q	4Q	2P	
$3d^3\Delta_b$	1729.36	1721.73	1729.53	1721.74	1729.30	
$m' \rightarrow$	3R	3Q	3P			
$3d^3\Delta_a$	1702.87	1702.88	1702.71			
$m' \rightarrow$	1	2	3	4	5	
$3d^3\Sigma \rightarrow$	2087.20		2083.71		2072.91	
(Δ) \rightarrow		(3.49)		(10.80)		
$3d^3\Pi_b \rightarrow$		2192.77		2142.80		
(Δ) \rightarrow			(49.97)			
$3d^3\Pi_a \rightarrow$	2219.54		2192.38			
(Δ) \rightarrow		(27.16)				
$3d^3\Delta_b \rightarrow$		1729.40		1721.73		
(Δ) \rightarrow			(7.67)			
$3d^3\Delta_a \rightarrow$			1702.87			
(Δ) \rightarrow						

is the low value of the vibrational intervals at the $3d^3\Delta_b$ and $3d^3\Delta_a$ levels. One would expect them to be much nearer the value of $w_0 - w_0x$ for H_2+ , which is 2220, at these levels. However, it may be that w_0x , which is unknown, has an abnormally high value for these $3d^3\Delta$ levels. The other levels compare with the following values of $w_0 - w_0x$ for the corresponding levels in the singlet systems. $3d^1\Sigma$ 2225.75, $3d^1\Pi$, 2097.22, $3d^1\Pi_a$ 2102.67. In both singlets and triplets Π_b values look to be slightly less than the values for Π_a . The $3d^1\Pi$ values are about 100 lower than those for $3d^3\Pi$, whereas the $3d^1\Sigma$ value is rather more than 100 higher than that for $3d^3\Sigma$. The vibrational intervals for the $3d^1\Delta_{ab}$ levels are unknown.

§ 8. The Initial Rotational Levels.

These have been extracted in the manner described in § 2 where an example was worked out in detail for the initial levels of the $3d^3\Sigma \rightarrow 2p^3\Pi$ bands. The results, together with similar data for the final levels, denoted by $2p^3\Pi_{ab}$, and for the upper levels of the α bands, denoted by $3p^3\Pi_{ab}$, are collected together in Table XIII. The magnitude of the terms of a given type of initial level decreases in going from $v' = 0$ at $n = 3$ to $v' = 1$ at $n = 3$, and also to $v' = 0$ at $n = 4$. Looking at the figures broadly this is true of the general trend throughout. If there are some isolated exceptions, this is not surprising

when we consider the complicated nature of these terms which arises from the uncoupling phenomena. The general character and trend of the terms is closely parallel to that of the $d^3\Sigma$, $d^3\Pi_a$ and $d^3\Delta_a$ terms of He_2 and also, so far as the Σ and Π terms are concerned, to the $d^1\Sigma$ and $d^1\Pi_a$ terms of H_2 . Very little is known with certainty as to the structure of the $^1\Delta_a$ terms of H_2 . This correspondence is the main justification for the identification of the nature of the levels as $d^3\Sigma$, $d^3\Pi$, and so on, given in the last column. In our opinion it is sufficient. Such peculiar types of rotational structure are known only in connection with levels of the types designated and so far have only

Table XIII.

Initial and Final Rotational Terms of the $nd^3\Sigma\Pi\Delta \rightarrow 2p^3\Pi$ Complex.

Term \rightarrow	$F1\frac{1}{2}-f\frac{1}{2}-x$	$f2\frac{1}{2}-F1\frac{1}{2}+x$ $F2\frac{1}{2}-f1\frac{1}{2}-x$	$F3\frac{1}{2}-f2\frac{1}{2}-x$ $f3\frac{1}{2}-F2\frac{1}{2}+x$	$f4\frac{1}{2}-F3\frac{1}{2}+x$ $F4\frac{1}{2}-f3\frac{1}{2}-x$	$F5\frac{1}{2}-f4\frac{1}{2}-x$ $f5\frac{1}{2}-F4\frac{1}{2}+x$	Electronic level
value of v						
0	-15.84	+30.08	69.99	115.64	178.64	$3d^1\Sigma$
1	-12.78	+27.27	69.30	123.46	159.84	$3d^1\Sigma$
0	-9.23	+23.63	76.12	120.72		$4d^1\Sigma$
0		73.66	139.71	181.74		$3d^3\Pi_b$
1		78.28	120.10	151.34		$3d^3\Pi_b$
0		70.92	119.63	*155.03 or 181.13 244.75		$4d^3\Pi_b$
0		127.63	199.35	or 247.93		$3d^3\Pi_a$
1		111.99	187.77	228.72		$3d^3\Pi_a$
0		115.08	179.61	224.09 212.58		$4d^3\Pi_a$
0			171.59	or 220.46		$3d^3\Delta_b$
1			193.20 ?	183.40 ?		$3d^3\Delta_b$
0			168.64	187.28 225.11		$4d^3\Delta_b$
0			179.92	or 236.60		$3d^3\Delta_a$
1			170.20	215.10		$3d^3\Delta_a$
0			171.01	213.76		$4d^3\Delta_a$
0		120.70	174.97	242.86		$2p^3\Pi_b$
1		115.11	170.88	227.22		$2p^3\Pi_b$
0		120.82	179.86	225.40		$2p^3\Pi_a$
1		115.01	171.45	228.61		$2p^3\Pi_a$
0		118.61	176.69	233.30	287.95,	$3p^3\Pi_b$
1		114.42,	161.72	213.77		$3p^3\Pi_b$
0		117.80	175.51	231.92	286.62,	$3p^3\Pi_a$
1		111.75	166.63	220.22	271.96	$3p^3\Pi_a$

* More probable alternative.

been found in He_2 and H_2 . The levels which are most alike are those attributed to Δ_a and to Π_a . It is possible that by a little reconstruction these levels might be interchanged. The weakness of all the bands which go from $^3\Pi$.

levels to $2p\ ^3\Pi$ would be in favour of this. We are inclined to prefer the designations as set out in the table, but the matter must be regarded as uncertain.

There are a few points of detail in connection with the table that should be referred to. Owing to the complex nature of the initial levels and to irregularities in the final levels it is impossible to ascertain the doublet distance x at the lowest of these final levels, although we have seen that there is a presumption that it is very small. As a result we can only specify the intervals within a quantity $\pm x$. The correct formula for what the numbers represent is given at the top of each column. In these formulæ F denotes an a level and f an s level. For a level which gives rise to a band containing a Q_2 line (i.e., a Q_a2 line) the formulæ to use are those in the lower row. If the Q line at $m = 2$ is $Q'2$ (i.e., Q_a2) then the formulæ to use are those in the upper row. $d\ ^3\Sigma$ is the only level which has an $m = 0$ rotational level and this level is an s level, so the expression $f1\frac{1}{2} - F\frac{1}{2} + x$ is not applicable to any band.

There seems to be an irregularity in the $v' = 1$ level of $3d\ ^3\Sigma$. The value 123.46 seems high and 159.84 low in comparison with the others. It is as though the $R'3$ line of this band were about 10 units too high. There is, however, no line which could be substituted for the present $R'3$ which would rectify this irregularity. It may be that the irregularity is really in the $0 \rightarrow 0$ band and that 115.64 is too low. All that seems really certain is that there is an irregularity somewhere in the $3d\ ^3\Sigma$ level. Another irregularity is in the $3d\ ^3\Delta_s$ level at $n = 1$. Here the successive level differences appear to fall with rising m instead of behaving in the same way as in all the other cases. However, the disparity in the succeeding level differences is not very marked in the other two Δ_s levels. It would be possible to reconstruct the three $d\ ^3\Delta_s \rightarrow 2p\ ^3\Pi$ bands so as to make the initial intervals much larger, but if this were done the similarity with the corresponding helium levels would be reduced. Compared with the others the structure of the $^3\Delta_s$ levels must be regarded as relatively uncertain. It is a curious coincidence that at the $v' = 0$ level of $3d\ ^3\Pi_a$, $3d\ ^3\Delta_s$ and $3d\ ^3\Delta_a$ there is a choice of possible values of the interval with differences almost in the ratio 1 : 2 : 3. These alternative values are bracketed in the table.

The similarity with the structure of the corresponding He_2 levels can be exhibited in a rather different way. In the He_2 spectrum every alternate rotational level is missing, the weight ratio being 1 : 0 instead of 3 : 1 as in H_2 . Consequently, only the double intervals for the strong pairs of alternate levels are known for this spectrum. Owing to the heavier molecule of He_2

these intervals are much smaller than in H_2 , but they become comparable when multiplied by a factor of 4. Accordingly in Table XIV we have collected the double rotational intervals of H_2 and the corresponding intervals of He_2 , these multiplied by 4, which fall on the same quantum numbers. The last have only been given to a whole integer as the decimal would probably not be correct after the multiplication by 4. It will be seen that the hydrogen numbers for the two $d^3\Sigma\Pi\Delta$ complexes are uniformly a little lower than the helium numbers. The similarity of the trend of the two sets of numbers is unmistakable. For the $2p^3\Pi_{ab}$ levels the hydrogen numbers are all about equal to the corresponding quadrupled helium values.

Table XIV.

Double Rotational Intervals for H_2 and He_2 Levels.

$$\Delta j = F(j+1) - F(j-1).$$

State $j \rightarrow$	Hydrogen.				Helium ($\times 4$).		
	$1\frac{1}{2}$	$2\frac{1}{2}$	$3\frac{1}{2}$	$4\frac{1}{2}$	$2\frac{1}{2}$	$3\frac{1}{2}$	$4\frac{1}{2}$
$3d^3\Sigma$ $v=0$	14.24	100.07	185.63	294.28	180		357
$3d^3\Sigma$ $v=1$	14.49	96.57	192.76	293.30			356
$4d^3\Sigma$ $v=0$	14.39	99.74	196.84		108		310
$3d^3\Pi_b$ $v=0$		213.37	321.45			368	
$3d^3\Pi_b$ $v=1$		198.38	271.44			343	
$4d^3\Pi_b$ $v=0$		190.55	300.76			342	
$3d^3\Pi_a$ $v=0$		326.98	447.58 or 444.10		358		613
$3d^3\Pi_a$ $v=1$		299.76	416.49		346		584
$4d^3\Pi_a$ $v=0$		294.69	403.70		367		588
$3d^3\Delta_b$ $v=0$			392.05 or 384.17			420	
$3d^3\Delta_b$ $v=1$			376.60			400	
$4d^3\Delta_b$ $v=0$			355.92			452	
$3d^3\Delta_a$ $v=0$			405.03				542
$3d^3\Delta_a$ $v=1$			385.30				521
$4d^3\Delta_a$ $v=0$			384.77				
$2p^3\Pi_b$ $v=0$		295.67	417.83			407	
$2p^3\Pi_b$ $v=1$		285.99	398.20			396	
$2p^3\Pi_a$ $v=0$		300.68	405.26		292		526
$2p^3\Pi_a$ $v=1$		286.46	400.06		288		512

§ 9. Energy of the Electronic Levels.

For consistency with previous papers dealing with other hydrogen levels, we define v_0 in terms of the old quantum mechanics; it is the wave-number of a hypothetical line of the $0 \rightarrow 0$ band having no rotation either in the upper or lower state. For Π and Δ states we have to make a considerable extra-

polation from the trend of the existing rotational levels. As there are not many of them, and they do not obey a simple formula, there is a certain degree of arbitrariness about this process; but it is believed that the values of ν_0 so obtained are not in error by more than about 10 wave-numbers, even for the Δ states.

Taking $3d^3\Sigma \rightarrow 2p^3\Pi$ as an example, we have $\nu_0 = P' 1 + f''(1\frac{1}{2}) - f'(1\frac{1}{2})$. The rotational intervals require that $f'(1\frac{1}{2})$ shall be about $\frac{3}{2}B$, which is about 15. Similarly $f''(1\frac{1}{2})$ is about 60. Thus since $P' 1$ is 16870.70, we have $\nu_0 = 16915$. The various values of ν_0 obtained in this manner are set out in the second column of Table XV.

Table XV.

Electronic level.	ν_0 of $0 \rightarrow 0$ band.	ν_0 .	Denominator.	Total negative energy.	Heat of dissociation (volts).
$3d^3\Sigma$	16915	12392	2.976	17.690	2.644
$3d^3\Pi_b$	17545	11762	3.054	17.616	2.570
$3d^3\Pi_a$	17461	11846	3.046	17.624	2.578
$3d^3\Delta_b$	17458	11849	3.046	17.624	2.578
$3d^3\Delta_a$	17528	11779	3.052	17.617	2.571
$4d^3\Sigma$	22676	6615	4.072	16.978	2.590
$4d^3\Pi_b$	22636	6671	4.055	16.984	2.596
$4d^3\Pi_a$	22589	6718	4.041	16.991	2.603
$4d^3\Delta_b$	22585	6722	4.041	16.992	2.604
$4d^3\Delta_a$	22637	6670	4.055	16.984	2.596
$2p^3\Pi$		29307	1.935	19.77	2.843

To determine the electronic ν_0 of the levels we proceed as follows. The values of each pair of ν_0 's, e.g., for the two Σ or for the two Π , levels, are all very much alike and also they are quite close to the ν_0 's of the α and β bands. Accordingly for each pair we put

$$\nu_0 = A - \frac{109678.3}{(n+x)^2}, \quad (9)$$

where $n = 3$ for the yellow bands and 4 for the blue bands. If the electronic frequencies obey such a Rydberg formula exactly then A will be a constant equal to the ν_0 of the final states and x will be a positive or negative fraction which will be different for each pair. On applying the equation to each successive pair we find:—from $d^3\Sigma \rightarrow 2p^3\Pi$ $A = 29833$, $x = -0.0868$; from $d^3\Pi$, $A = 29316$, $x = +0.052$; from $d^3\Pi_a$, $A = 29294$, $x = +0.0444$; from $d^3\Delta$, $A = 29290$, $x = +0.0447$; and from $d^3\Delta_a$, $A = 29328$, $x = +0.0485$. From the appearance of these numbers it looks as if the Σ level did not follow a Rydberg formula as accurately as the remaining four.

It is also possible that the blue Σ band is incorrect. There is an alternative arrangement, which, however, does not look so good in itself, which would give a value of A in better agreement with the others. However this may be, there is enough agreement among the others to settle the value of A . The values are, in fact, as near alike as we can expect them to be from determinations based only on the first two terms of a Rydberg formula. Taking the mean, we find

$$\nu_0'' = A = 29307.$$

This compares with a value* 29503 extrapolated from the Rydberg-Ritz formula for the α , β , γ bands, *i.e.*, assuming these bands have ν_0 's given by $A' - 109678 \cdot 3 / (n + x + z/n^2)^2$, $n = 3, 4, 5$, the value of the fraction extrapolated to $n = 2$ is 29503. This is another confirmation of the conclusion that the lower level of these bands is the continuation at $n = 2$ of the series of electronic states which constitute the upper levels of the α , β , γ bands, which are Π levels with $n = 3, 4, 5, \dots$. Another estimation of ν_0'' which has been published† is 29500.0. This was from a faulty preliminary analysis of part of the present bands and must now be abandoned in favour of the more accurate value 29307.0. As a matter of fact, this ν_0'' is also practically identical with the ν_0 for the $2s\Sigma$ state which constitutes the final level of the α , β , γ bands‡ which is 29340.0.

There is a confirmation of the correctness of this determination of ν_0'' in the experimental results of Finkelburg, Lau and Reichenheim,§ who have measured the excitation potential of nine of the stronger lines ending on the $\nu'' = 0$ level of these systems. The values they find, in volts, are: for $3d^3\Sigma \rightarrow 2p^3\Pi$, $R_2 = 11.76$, $R_4 = 11.78$, $Q_1 = 11.75$, $Q_3 = 11.68$; $3d^3\Pi, \rightarrow 2p^3\Pi$, $R_1 = 11.88$, $Q_2 = 12.18$; $4d^3\Delta, Q_2 = 11.74$, $P_3 = 11.75$; $4d^3\Delta, R_2 = 11.78$. The mean of these, after subtracting the small amount of rotational energy, average 0.032 volt, present in the final levels of the lines, is 11.78. The high value from Q_2 of the Π , band for some unknown reason differs from the mean by an amount which exceeds the errors of the measurements. If this is taken out the average of the remainder, after subtracting the rotational energy, is 11.73. The value|| of ν_0 for the ground state

* O. W. Richardson, 'Proc. Roy. Soc.,' A, vol. 113, p. 399 (1926).

† O. W. Richardson, 'Trans. Faraday Soc.,' vol. 25, p. 692 (1929); 'Proc. Roy. Soc.,' A, vol. 126, p. 501 (1930).

‡ O. W. Richardson, 'Proc. Roy. Soc.,' A, vol. 113, p. 399 (1926).

§ 'Z. Physik,' vol. 61, p. 782 (1930).

|| Cf. Richardson and Davidson, 'Proc. Roy. Soc.,' A, vol. 125, p. 35 (1929).

1, $^1\Sigma$ of H_2 is 124569. If we subtract 29307 from this we get 95262 w. numbers or in volts 11.76. The value determined from Finkelburg, Lau and Reichenheim's results is identical with this to the accuracy of their measurements.

The values of ν_e for the upper levels of the bands set out in Table XV are obtained immediately by subtracting the ν_0 of the $0 \rightarrow 0$ bands from the final $\nu_e = 29307$. The denominators are the values of d in the equation $\nu_e = R/d^2$, where R is Rydberg's constant. They are all so close to 3, 4 or 2 that they obviously settle the principal quantum numbers of the various levels. In the $3d$ complex the trend of these denominators is quite similar to that of the corresponding helium bands* where the denominators rise from 2.935 at $3d\ ^3\Sigma$ to 3.013 at $3d\ ^3\Delta_e$. Except at the Σ levels, in which it has been noted already that there is something exceptional at $n = 4$, the trend of the denominators, and of the ν_e 's, at $n = 3$, is parallel to that at $n = 4$.

The values of the total negative energy in the last column but one of Table XV are based on Burrau's†‡ value 16.16 volts of the negative energy of H_2+ . If this theoretical value were changed there would need to be a corresponding change in the figures in this column of the table. These figures are, in fact, simply 16.16 plus the corresponding value of ν_e in equivalent volts.

The heats of dissociation in the last column of Table XV are got by subtracting $R \left(1 + \frac{1}{n^2}\right)$ in equivalent volts from the values of the total negative energy in the preceding column. This is equivalent to assuming that when a molecular state of principal quantum number n dissociates, it breaks up into an unexcited H atom and an H atom excited to principal quantum number n . This type‡ of dissociation has been shown to occur for several H_2 molecules. These heats of dissociation also, of course, rest on Burrau's value 16.16.

§ 10. Other Bands.

In addition to the bands described in this paper, we think we have some coming from $s\ ^3\Sigma$ levels, also the $1 \rightarrow 1$ bands of $4d\ ^3\Sigma\Pi\Delta$ and some others, all going down to the final levels of the present bands. These are all weak and mixed up with stronger unclassified lines. This makes the details difficult to decipher with much certainty. We have, therefore, decided not to publish an account of them for the time being.

* W. E. Curtis, 'Trans. Faraday Soc.', vol. 25, p. 695 (1929).

† Cf. Richardson and Davidson, 'Proc. Roy. Soc.,' A, vol. 123, p. 485 (1929).

‡ Richardson and Davidson, 'Proc. Roy. Soc.,' A, vol. 125, p. 31 (1929).

Analysis of the Long Range α -Particles from Radium C.

By Lord RUTHERFORD, O.M., F.R.S., F. A. B. WARD, Ph.D., Goldsmiths
Senior Student, and W. B. LEWIS, B.A.

(Received April 28, 1931.)

In a previous paper,* an account has been given of a new method of detection of groups of α -rays expelled from a radioactive substance, even when these are present in small quantity compared with the main group or groups. In this way we were able to show that the α -rays from actinium C were complex, and to prove the presence of a group of α -rays arising from the dual disintegration of radium C, although present in numbers about 1 in 3000 of the main group of α -rays of longer range.

The method depends on the linear magnification of the ionisation current, due to a few millimetres of the track of an α -particle, by means of valves and the recording of the momentary current on a photographic film by a special oscillograph. By the use of a differential method, it was found possible to record only those α -particles which were stopped in the shallow ionisation chamber. In this way a type of straggling curve for the α -rays was obtained, the maximum of which corresponded to the mean range of the group of α -particles in the air or other gas employed. By comparison with a standard range, this mean range could be fixed with precision when isolated homogeneous groups of α -rays were present.

The valve and recording system was specially developed in order to count α -particles in the presence of a strong γ -radiation with a view to its use in analysing the long range α -particles from radium C, thorium C and actinium C. While a number of experiments have been made on the long range α -particles from thorium C and actinium C, we shall confine our attention in this paper to the analysis of the long range α -particles from radium C, which will be shown to consist of a large number of groups of α -particles expelled with definite characteristic velocities. An examination of this kind is not only of importance in itself in showing the complexity of the modes of disintegration of the radioactive atom, but, as we shall see, is of great value in throwing new light on the origin of the γ -rays from radium C.

It is not necessary to give a detailed discussion of the numerous experiments that have been made to fix the numbers, range and nature of the groups of

* Rutherford, Ward, Wynn-Williams, 'Proc. Roy. Soc., A, vol. 129, p. 211 (1930).

long range particles from radium C, which were first noted by Rutherford in 1919.* It suffices to say that about 17 in a million of the α -particles from radium C have a range of about 9 cm. in air, while about 5 in a million have a greater range extending to about 12 cm. The most accurate analyses of the long range α -particles have been made by the Wilson expansion chamber method by Nimmo and Feather† and by Philipp and Donat.‡ The results obtained by Nimmo and Feather are given in fig. 1, which shows the distribution of the ranges of about 200 long range α -particles from radium C. There appears to be a well-defined group of mean range 9.08 cm. in air and a fairly general distribution of particles with ranges between 7.5 and 12 cm. The

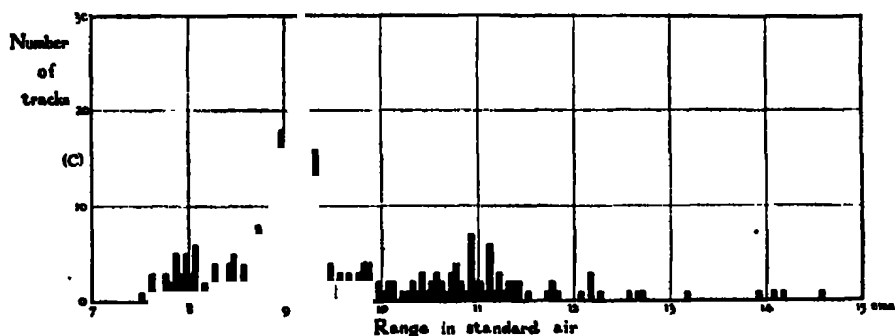


FIG. 1.

number of particles counted was too small, however, to show with certainty the presence of other definite groups besides the sharply marked group of range 9 cm. Moreover, it was difficult in some cases to distinguish between the tracks of α -particles and of protons, which are always present under the experimental conditions.§ For example, our experiments indicate that the tracks of range greater than 12 cm. shown in fig. 1 must be ascribed to protons, not α -particles. The results obtained by Philipp and Donat are in substantial agreement with those of Feather and Nimmo referred to.

If we use a single counting chamber of depth 3 mm. and count the number of particles recorded for different distances in air from the source, we should obtain a curve of the type shown in fig. 2. It is difficult to fix such a curve

* See "Radiations from Radioactive Substances" (Rutherford, Chadwick and Ellis), Camb. Univ. Press, 1930, pp. 87-95.

† Nimmo and Feather, 'Proc. Roy. Soc.,' A, vol. 122, p. 668 (1929).

‡ Philipp and Donat, 'Z. Physik,' vol. 52, p. 759 (1929).

§ These protons are for the most part due to the collision of the main group of α -particles with any hydrogen present in the source or absorbing screens.

with accuracy for a number of reasons. In the first place, any protons near the end of their range would give a record similar to a swift α -particle, while

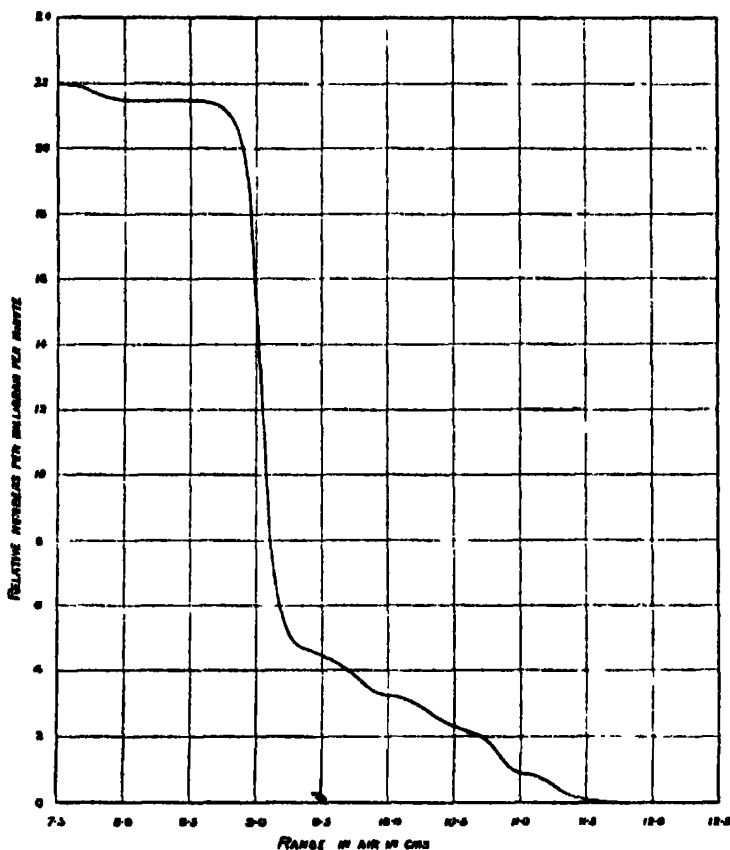


FIG. 2.

the disturbance due to the γ -rays emitted from the source makes it difficult to count α -particles near the end of their range when the ionisation is small. Also the probability fluctuations in the number of α -particles counted makes it difficult to locate small rises in the curve. For these reasons, only a preliminary examination was made by the single chamber method, and the more complete analysis was carried out by the differential method. By restricting the counting to particles which give a kick of not less than 60 per cent. of the maximum, the error due to the presence of protons is entirely eliminated, for it was found that, under the experimental conditions, the maximum kick due to a proton near the end of its range was never greater than 40 per cent. of the maximum due to an α -particle. In a similar way, the disturbance due to the γ -rays is not serious unless very intense sources are used.

Experimental Method.

The general experimental arrangement was similar to that described in the previous paper and is shown in fig. 3. The differential ionisation chamber is shown on the left. The front F_2 of the first chamber and the aperture of the central electrode F_1 were both covered with thin gold foil of stopping power about 0.4 mm. of air. The defining diaphragm of copper with an opening 8.50 mm. in diameter was attached to the front of the chamber F_2 . As before, a film of collodion of stopping power about 0.3 cm. of air separated the counting chamber from the source. Arrangements were also made for introducing mica plates of known stopping power at A. In some of the experiments the number of α -particles to be counted was small, and to increase the number for a given absorption mica screens were introduced. In no case, however, was the source brought closer than 4 cm. from the collodion, corresponding to about 4.7 cm. from the front of the counting chamber. The arrangement for adjusting the position of the source is seen in the figure. In order to reduce the effect of β - and γ -rays, the tube containing the source was placed between the pole-pieces of a powerful electromagnet.

However much care is taken in the preparation of the source, a small amount of emanation is released during the experiment. This easily diffuses through the collodion and may contaminate the counting chamber. To avoid this difficulty a slow steady current of air was circulated through capillary tubes and along the source tube in order to carry any emanation away. Even under the best conditions, a number of experiments had to be abandoned owing to contamination either by emanation or due to the appearance of active deposit on the collodion film. In order to obtain as clean sources as possible, nickel discs 8 mm. in diameter were exposed to emanation. After removal from the emanation, they were cleaned and heated in the usual way. The edge effects were much reduced by rubbing the rim of the disc on rouge paper.

These experiments differed from those described in the previous paper in the fact that much stronger sources of radium C were used, corresponding in activity in some cases to 50 milligrammes of radium. Such sources emitted a strong γ -radiation. The strength and distance of the source from the chamber were so adjusted that the disturbance of the oscillograph zero due to the γ -rays did not exceed a practicable value.*

* A full account of the development of the counting mechanism used in these investigations has been published by Wynn-Williams and Ward ('Proc. Roy. Soc.,' A, vol. 131, p. 391 (1931)).

Check experiments on the 8.6-cm. range of α -particles from thorium C', made in the presence of γ -rays from 6 mgm. of radium enclosed in a glass tube

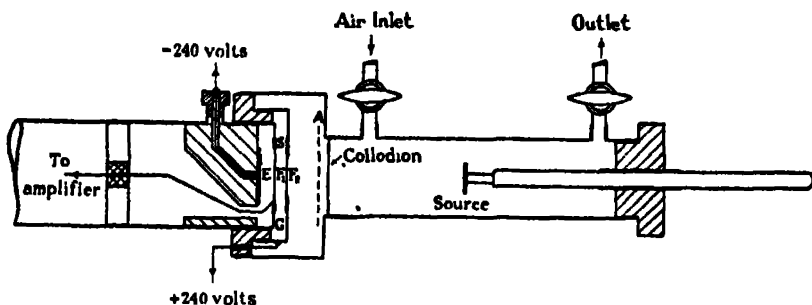


FIG. 3.

placed alongside the source, showed that the height and breadth of the straggling curve obtained was slightly affected by the presence of strong γ -rays. This was traced to an increase of amplification by the first valve. Normally the grid of the first valve floats at a potential just over 2 volts negative with respect to the negative end of the filament to which the earthed screens were connected. The grid therefore collects positive ions from the air inside the screening tube, when this is ionised by the γ -radiation. This ionisation current may alter the floating potential of the grid by as much as $1/3$ volt. Owing to the curvature of the valve characteristic this is sufficient to alter the amplification of the minute (100 microvolt) potential changes due to the α -particles by 20 per cent. The change of grid potential produced a change of anode current, which was measured, and the change of amplification was allowed for. It has now been arranged that the negative end of the filament of the first valve is 2 volts positive with respect to the earthed screens, so that the effect is no longer appreciable. Under these conditions, the form of the straggling curve obtained is not noticeably altered by the presence of γ -radiation.

About 20,000 long range α -particles have been counted under sufficiently good conditions to be included in the results presented, though nearly double that number have been counted in all the experiments. Particular attention has been directed to the complicated distribution curve for the α -rays between the ranges 9 to 12 cm. of air. Since the intensity of the source of α -particles and the distance from the source to the counting chamber varied in different experiments, the results were expressed in terms of the number of α -particles per milligramme per minute for a standard distance (10 cm.) of the source from the counting chamber. The stopping power of the air was corrected for changes of temperature and barometric pressure.

The results of the analysis of the whole region between 7 cm. and 12 cm. of air are shown in fig. 4, where the ordinates represent the relative number of

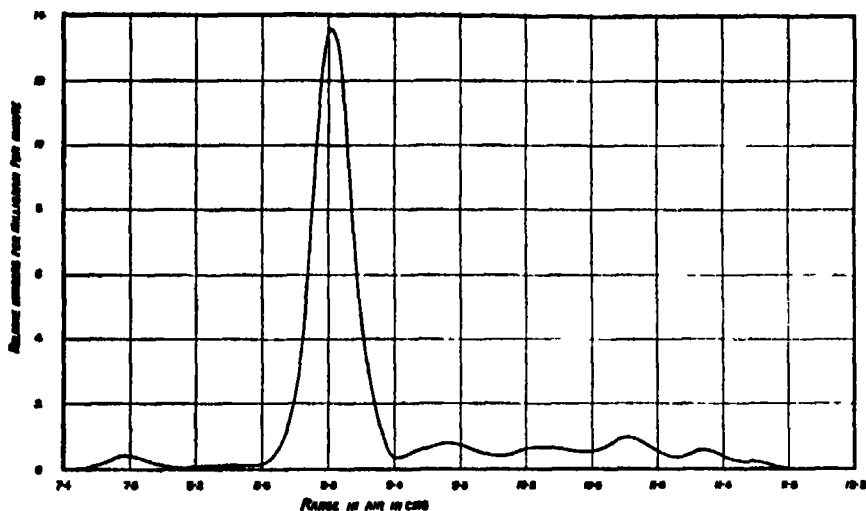


FIG. 4.

α -particles observed at the various ranges. The ordinates also represent the number of α -particles counted at each point corresponding to one million α -particles from radium C'.

It will be seen that while the peak at 9 cm. is predominant, a well-defined peak is observed at 7.8 cm., and between 9 and 12 cm. an approximately continuous distribution with clear evidence of maxima.

This distribution of particles is more clearly brought out in figs. 5 and 6. Fig. 5 shows the distribution between 7 cm. and 9 cm. with the vertical scale magnified 10 times. Only the lower edge of the straggling curve for the relatively very strong group of range 9 cm. can be shown in the figure. In order to bring out the peak at 7.8 cm., the experiments were made without any mica in the path of the rays. This reduced the straggling of the main group of 7 cm. particles sufficiently to show clearly the new group. The reduction of the straggling made it practicable to count with a narrower effective slit width;* this explains why the 7.8 cm. peak appears narrower than those in the other figures. No certain evidence of any other group was observed in this region, but it would be difficult to detect the presence of a weak group which might be present in the region 8.4 to 9 cm., for it would be

* For explanation of this term see Rutherford, Ward and Wynn-Williams, 'Proc. Roy. Soc.,' A, vol. 129, p. 211 (1930). See page 220, etc.

obsured in the marked tail of the strong 9 cm. group. In a similar way it would not be expected that any weak group of α -rays could be detected within

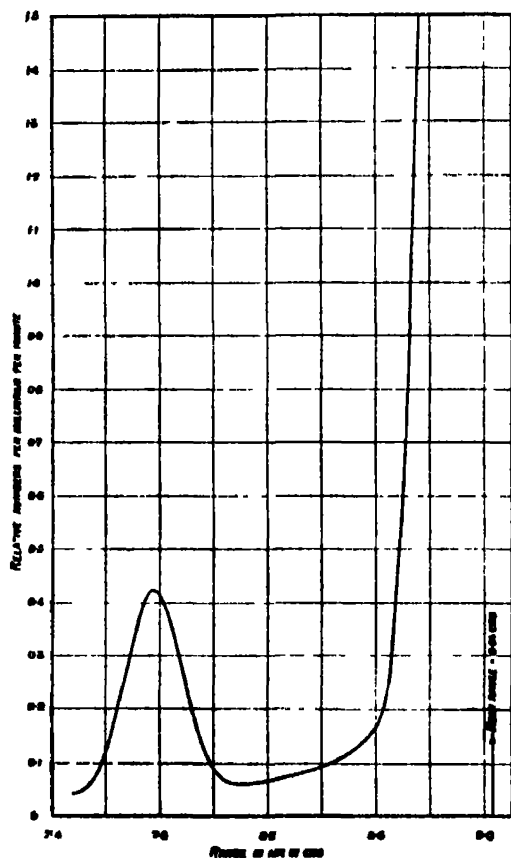


FIG. 5.

the tail of the main 7 cm. group, which is about 60,000 times stronger even than the 9 cm. group.

The shape of the straggling curve of the 9 cm. group was carefully determined and compared with that of the 7 cm. group and of the well-known group of α -rays from thorium C' of range 8.6 cm. Making allowance for the increase of straggling due to the increase of velocity of the α -particles, the curve obtained agreed closely with that to be expected from a homogeneous group of α -rays of mean range 9.04 cm. in air at 760 mm. and 15° C. Such a result does not preclude the possibility of the presence of relatively weak groups of α -rays of ranges between 8.6 and 9.5 cm.

The distribution curve of the long range particles between 9 cm. and 12 cm.

is shown in fig. 6. It is seen that the curve shows definite maxima at 9.8, 10.3, 10.8 and 11.3 cm. It is natural to suppose that this complex distri-

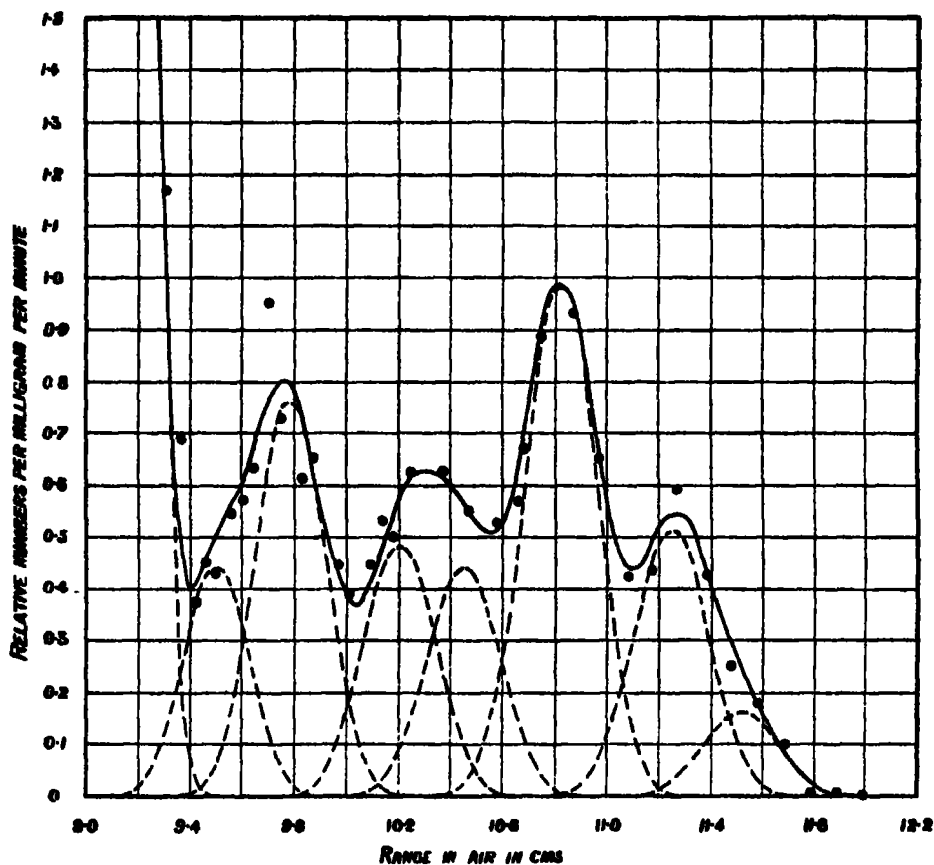


FIG. 6.

bution is due to the presence of a number of distinct groups of α -rays similar to those of range 7.8 and 9 cm. but so close together that their straggling curves are only partially separated. A preliminary inspection indicates the probable presence of about seven groups.

When an attempt is made to fix the range of any group with precision a difficulty is encountered. It was found experimentally that the shape and position of a peak is noticeably affected by the slightest tarnish on the source. For instance, the breadth of the 9 cm. peak was increased by 0.4 mm. and the mean range decreased by 0.3 mm. when a source was used which had a slight tarnish in the centre. The 7 cm. peak obtained with the same source was similarly affected. The nickel source is normally exposed in a strong concen-

tration of radon mixed with residual gases at atmospheric pressure. For some reason there often appears, after long exposures, a slight tarnish of the nickel disc, the result probably of some type of chemical action. The results shown for the ranges between 7.4 and 9.6 cm. have been obtained using only the cleanest sources. The results for the longer ranges are averaged for a number of sources which on the whole were not so free from tarnish.

In order to analyse the curve, the effective slit width under the experimental conditions of counting was determined from the straggling curve of allowable shape which best fitted the experimental points for the 8.6 cm. range of α -rays from thorium C'. An approximate value for the straggling coefficient for this range was simultaneously determined, and found to be in fair agreement with that determined by an extrapolation of the curve given by Briggs.* From measurements at various parts of the range of the 7 cm. α -particles from radium C', Briggs obtained a curve giving the square of the straggling coefficient for mica for α -particles of range between 0 and 7 cm. The curve is very nearly linear over the first two centimetres and we have extended this part of the curve backwards beyond the origin in a straight line to include ranges up to 12 cm. The possible error involved in this extrapolated curve should not seriously affect our results. The effective straggling coefficient for any range was calculated from this extrapolated curve, taking as a basis our experimental value for the 8.6 cm. range. From the straggling coefficient and the effective slit width, the correct shape of the straggling curve at any range was determined. The complex distribution curve of fig. 6 was analysed by reconstructing it by trial and error methods from a minimum number of straggling curves of correct shape.

The results of the analysis are shown by the dotted curves in the figure, each representing a homogeneous group of α -particles. The full line curve is the resultant obtained by adding up the dotted curves. The points represent the averaged experimental observations at the particular ranges. The part of the curve between 9.3 and 9.7 cm. was very carefully examined in special experiments and it was concluded that, in order to fit the experimental results, a group of α -particles of mean range about 9.5 cm. must be present. On account, however, of the great difficulty of fixing with the required accuracy the end of the tail of the strong 9 cm. group, neither the range nor the number of α -particles in this 9.5 cm. group can be found with certainty.

Our analysis of the curve is based on the probable assumption that the

* G. H. Briggs, 'Proc. Roy. Soc.,' A, vol. 114, p. 313 (1927), see fig. 8.

observed distribution results from the mixture of a small number of homogeneous groups of rays. Some of the groups stand out obviously, but the inner groups are deduced to fit the distribution curve. In any case it would be difficult to be certain that some of the groups, supposed homogeneous, may not in fact be complex, consisting of a mixture of two or more groups of slightly different ranges. Such uncertainty can only be removed by using a method of much higher resolving power. For example, it may prove possible to produce the required resolution by the use of the focussing method used for α -rays by Rosenblum, but it may be difficult to obtain sufficiently clean and intense sources of α -rays for the purpose.

The results of the analysis are included in the following table. Column 1 gives the number of the group and column 2 the mean range of the group, column 3 the value of the extrapolated range ordinarily employed, which is deduced from the mean range by adding a correction varying from 0.7 to 1.2 mm. Column 4 gives the corrected velocity of the α -particle in terms of V_0 , (1.922×10^9 cm./sec.) the velocity of the main 7 cm. group from radium C'. Column 5 gives the energy of the α -particle in each group in electron volts. This is calculated from the velocity range curve discussed in the next section, taking the energy of the α -particle of the 7 cm. group from radium C' as 7.683×10^6 electron volts. In column 6 is given the number of particles in each group corresponding to 10^6 α -particles of the 7 cm. range. This number is not the same as the peak height shown in the figures, but is deduced from it by taking into account the effective slit width and the straggling coefficient for the range concerned. It is seen that nine groups have been detected varying in energy between 8.30 and 10.62 million volts. The mean range of the strongest group (9.04 cm.) agrees well with that

(1) Number of group.	(2) Mean range cm. of air 15° C., 760 mm.	(3) Extrapolated range, cm. of air, 15° C., 760 mm.	(4) Velocity of α -particle in terms of V_0 .	(5) Energy of α -particle in electron- volts $\times 10^{-6}$.	(6) Relative number of α -particles.
1	6.88	6.95	1.0000	7.683	10^6
2	7.79	7.87	1.0395	8.303	0.49
3	9.04	9.13	1.0891	9.117	16.7
4	9.50	9.60	1.1065	9.412	0.53
5	9.78	9.88	1.1166	9.585	0.93
6	10.21	10.31	1.1316	9.843	0.60
7	10.46	10.56	1.1400	9.992	0.56
8	10.83	10.94	1.1527	10.215	1.26
9	11.25	11.37	1.1667	10.466	0.67
	11.52	11.64	1.1754	10.623	0.21

(9.08 cm.) deduced by Nimmo and Feather (see fig. 1). As already pointed out, the number of long range α -particles observed by them was far too small except to fix the energy of the main group.

We made a number of experiments to test for the presence of α -particles of range greater than 12 cm. but without success. If such α -particles are present, they are certainly less than 1 in 1000 of the main 9 cm. group. It is thus clear that the tracks of range greater than 12 cm. observed by Nimmo and Feather must be ascribed to protons rather than to α -particles.

It is of interest to note a type of repeating pattern shown by groups of α -rays 4, 5, 6 and 7, 8, 9, clearly shown in fig. 6. In each set of three, the head of the set is the strongest and the two following of decreasing height. It is of interest to note that the difference of energies between corresponding groups (viz., 4 to 7, 5 to 8, 6 to 9) in these series are nearly the same, being 6.4 , 6.4 and 6.5×10^5 volts. There is some reason to believe that this represents a repeating pattern in the system of energy levels, which shows itself also in other ways. This important point will be discussed in more detail in a subsequent paper by Rutherford and Ellis.

Velocity-Range Relation.

It is now necessary to consider how the velocities and energies of the long range α -particles can be deduced from the measured ranges. It has long been known that the relation between the extrapolated range of a group of α -rays and the velocity is expressed approximately by Geiger's rule $V^3 = kR$ for ranges of particles between 3 cm. and 8.6 cm. in air. The accuracy of this relation has been carefully examined in recent years by comparing the relative deflections in a magnetic field of the α -particles emitted by thorium C, thorium C' and polonium with the deflection for the α -particles from radium C' taken as a standard. The extrapolated ranges of these groups of α -particles have also been measured as precisely as possible. From these data, the departure from Geiger's rule for α -particles of different velocity can be deduced. No direct information is available of the relation between velocity and range for α -particles of range greater than 8.6 cm. It would require an extensive research to measure directly with the necessary precision the velocity, for example, of the strongest known group of long range particles, namely, the group of range about 11.7 cm. from thorium C'. In the absence of such direct measurement, it is necessary to construct an extrapolated curve to allow a close estimate to be made. This

question has been discussed by Laurence,* Harper and Salaman,† and Feather by taking Geiger's rule as a basis and using a difference curve to give the necessary corrections to be applied for α -particles of different velocities. This general method, which seems likely to give a trustworthy estimate, will be employed, using the latest data which will now be considered. The extrapolated ranges in air at 760 mm. and 15° C. of the α -particles under consideration found by different observers, are given in the following table :—

	Ranges in cm. of air at 15° C., 760 mm.			
	Thorium C'.	Radium C'.	Thorium C.	Polonium.
Henderson*	8.616	6.953	4.778	—
Geiger†	8.617	6.971	4.787	3.925
Harper and Salaman‡	8.61	6.94	4.72	3.87
I. Curie§	—	—	—	3.87
Probable values	8.61	6.95	4.73	3.87

* G. H. Henderson, 'Phil. Mag.', vol. 42, p. 538 (1921).

† Geiger, 'Z. Physik,' vol. 8, p. 45 (1921).

‡ G. I. Harper and E. Salaman, 'Proc. Roy. Soc.,' A, vol. 127, p. 175 (1930).

§ I. Curie, 'Ann. Physique,' vol. 3, p. 299 (1925).

The most probable values of these constants are given in the last row.

The relative velocities of these groups of α -particles in terms of the velocity of the α -particles from radium C', corrected for relativity changes of mass, are given in the following table :—

	Velocities.			
	Radium C'.	Thorium C'.	Thorium C.	Polonium.
Briggs*	1	1.068	0.896	—
Laurence†	1	1.0679	0.8885	0.8277
Rosenblum‡	1	1.0706 \pm 0.0015	0.889§	—
Most probable value	1	1.069(5)	0.888	0.828

* G. H. Briggs, 'Proc. Roy. Soc.,' A, vol. 118, p. 549 (1926).

† G. C. Laurence, 'Proc. Roy. Soc.,' A, vol. 122, p. 543 (1929).

‡ Rosenblum, 'C. R. Acad. Sci. Paris,' vol. 190, p. 1124 (1930).

§ Mean value.

* Laurence, 'Proc. Roy. Soc.,' A, vol. 122, p. 543 (1929).

† G. I. Harper and E. Salaman, 'Proc. Roy. Soc.,' A, vol. 127, p. 175 (1930).

Briggs and Laurence estimated that the ratios of the velocities were correct to about 1 in 1000. Rosenblum, using the large electromagnet of the Academy of Sciences, Paris, was able to bend the α -particles into a semicircle and so use the well-known focussing method. Although the actual deflections of the bands due to the α -particles from radium C' and thorium C' were much greater, yet, owing to the uncertainty of the magnetic field, the accuracy is not estimated to be greater than ± 1.5 parts in 1000. The general evidence indicates that the value of the velocity 1.0706 found by him for the α -rays from thorium C' is slightly high. The most probable value is estimated to be 1.069 or 1.0695, within the experimental error estimated by Rosenblum. It should be mentioned that a special difficulty arises in the case of the α -particles from thorium C of range about 4.73 cm.; for Rosenblum has shown that the radiation is complex, consisting of at least five groups of α -particles. Taking the velocity of the strongest line α as 1, the velocity of the second group α_1 of intensity about 0.3 is 1.0034, while three other weak lines have been observed of velocities 0.976, 0.964, 0.962, of the group α . It can be shown that the extrapolated range of this complex group of α -rays, measured in the usual way, must very nearly correspond to the weighted mean of the ranges of the two strong groups α and α_1 , if they could be measured independently. The observed extrapolated range corresponds to α -particles of velocity 1.0008 when the velocity of the strongest group is taken as unity. From this, it follows from Rosenblum's data that the observed extrapolated range 4.73 cm. corresponds to a velocity 0.889 V_0 .

Taking the velocity V_0 of the α -particles from radium C' as a standard, on Geiger's rule, $V_0^3 = kR_0$, where R_0 is the extrapolated range. Suppose that a correction ΔV has to be subtracted from the velocity V of the α -particles to fit in with Geiger's rule, then $(V - \Delta V)^3 = kR$, where R is the range of the group.

Consequently

$$\frac{V - \Delta V}{V_0} = \left(\frac{R}{R_0}\right)^{\frac{1}{3}} \quad \text{or} \quad \frac{\Delta V}{V_0} = \frac{V}{V_0} - \left(\frac{R}{R_0}\right)^{\frac{1}{3}}.$$

Taking the most probable values given in the tables above for the velocities and ranges, the values of $\Delta V/V_0$ are found to be 5.3×10^{-3} , 8.4×10^{-3} and -4.5×10^{-3} ($V/V_0 = 1.0695$) or -5.0×10^{-3} ($V/V_0 = 1.069$) for the α -rays from polonium, thorium C and thorium C' respectively. The value for the α -rays from radium C' is by assumption zero. By plotting $\Delta V/V_0$ as ordinates and the extrapolated ranges as abscissae we obtain the correction

curve shown in fig. 7 which is extrapolated in an obvious way to include the probable corrections for ranges up to 12 cm. The range of extrapolation is not great as regards velocity, viz., from about $1.07 V_0$ to $1.19 V_0$, a ratio of 1.11 in velocity. The corresponding ratio of velocities between the α -rays from polonium and thorium C', for which observational data are available, is much greater, viz., 1.29. It seems probable that the extrapolation curve should give the velocities and energies of the long range α -particles with considerable accuracy.

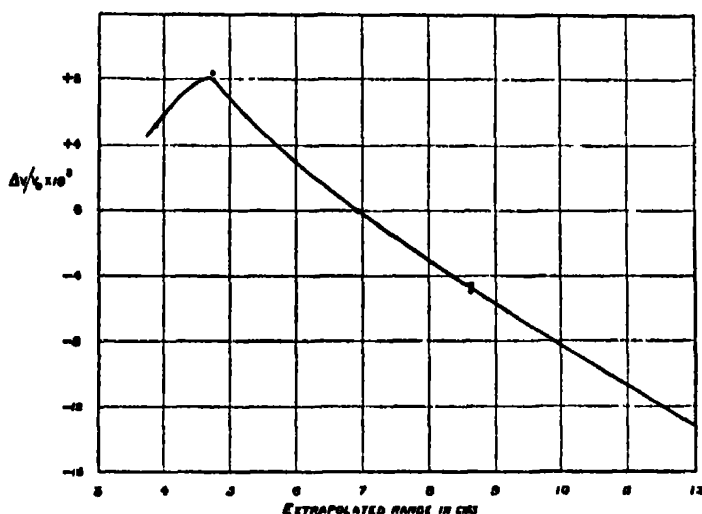


FIG. 7.

Connection of Long Range α -Particles with the Emission of γ -Rays.

It has for some time been supposed that there must be a close connection between the emission of long range α -particles from radium C' and thorium C' and the emission of γ -rays from these bodies. This question has been examined by N. Feather* and discussed in some detail by Gamow,† with a special application to the emission of the complex group of α -rays from thorium C. In our experiments we have obtained evidence of at least nine different groups of long range α -rays from radium C', and their relative energies and abundance have been measured. It seems simplest to suppose that these groups of α -particles of high energy represent different modes of disintegration of the radium C' nucleus, indicating that some of the atoms of radium C' are left in different excited states as a consequence of the β -ray disintegration of the parent product

* Feather, N., 'Phys. Rev.', vol. 34, p. 1558 (1929).

† Gamow, G., 'Nature,' vol. 123, p. 397 (1930).

radium C. Suppose, for example, that the α -particles in the normal or ground level of the nucleus of radium C' have an energy E_0 and that the normal particles of range 7 cm. have their origin in this level. Following Gamow, we may suppose that a fraction p of the α -particles in the radium C' nucleus after the β -ray disintegration of radium C, occupy an excited level of higher energy E_1 in the nucleus. If T be the average duration of the α -particles in the level before falling to a lower level or the ground level, there will be a certain chance that in the interval T some of the α -particles will penetrate the potential barrier and appear as long range α -particles. The fractional number N of such long range particles will be given by $N = p\lambda T$, where λ is the transformation constant corresponding to α -particles escaping from the excited level. The energy liberated in the transition of the α -particle to the ground level will be $E_1 - E_0$ and this energy may appear in the γ -ray form or be communicated directly to the outer electrons of the atom due to some type of coupling with the nucleus.* In such a case, the energy may appear in the form of a β -particle liberated from the outer atom. A similar argument applies to all possible excited levels and also to a transition of an α -particle from a higher to a lower level. It should be pointed out that the time T is normally so short—of the order of 10^{-15} second—that in general only a minute fraction of the α -particles in an excited level escape as long range α -particles. The main number fall to the ground level and escape from this level in the form of the normal α -particles from radium C'.

Feather† first drew attention to the important point that, in estimating the energy emitted in a β - or γ -ray form as a consequence of a transition from a higher to a lower level, it is necessary to take into account not only the observed difference of energy of the α -particles escaping from these levels, but also the energy liberated in the recoil of the main nucleus. It can easily be shown that the total change of nuclear energy E involved in the escape of an α -particle of energy E^* is given by

$$E = E^* \left(1 + \frac{M}{m - M} \right)$$

where M is the mass of the α -particle and m the mass of the disintegrating nucleus. Consequently the evolution of energy E either in the β - or γ -ray form, corresponding to the fall of an α -particle of energy E_2^* to a lower level from which the α -particle escapes with an energy E_1^* is given by

$$E = (E_2^* - E_1^*) \left(1 + \frac{M}{m - M} \right).$$

* Cf. R. H. Fowler, 'Proc. Roy. Soc.,' A, vol. 129, p. 1 (1930).

† Feather, "Thesis Ph.D. Degree, Camb. University," 1930.

Since $M = 4$, and m in this case 214, the energy evolved is nearly 2 per cent. greater than the difference between the observed energies of emission of the two groups of α -particles.

In the following table is given the energy liberated in the fall of an α -particle from each of the observed α -ray levels to the ground level of radium C'. The energy of the α -particle escaping from the ground level is taken as 7.683×10^6 electron volts.

Column 1 gives the number of the group, column 2 the energy of the α -particles in the group and column 3 the energy liberated by the α -particle in falling to the ground level. The relative abundance of the groups is added for convenience in the last column.

(1) Number of group.	(2) Energy of α -particle in electron-volts $\times 10^{-6}$.	(3) Energy liberated by α -particle transition to ground level electron-volts $\times 10^{-6}$.	(4) Relative number of α -particles.
1	8.303	6.3	0.49
2	9.117	14.6	16.7
3	9.412	17.6	0.53
4	9.585	19.4	0.93
5	9.843	22.0	0.60
6	9.992	23.5	0.56
7	10.215	25.8	1.26
8	10.466	28.4	0.67
9	10.623	30.0	0.21

There is one striking fact that at once emerges from a consideration of the table. If the γ -rays from radium C arise from transitions of the α -particle between the excited levels and the ground level, the maximum energy of a probable γ -ray (or corresponding β -ray) must be only slightly greater than 3 million volts. In this connection it is probably very significant that Ellis finds that no β -ray line in the magnetic spectrum of radium C can be observed of energy greater than 3 million volts, while Gurney* found by electrical methods that the β -ray spectrum became very weak at about the same point. Dr. Ellis informs us that he has recently made special experiments to test the point. The highest energy of a β -ray line he has been able to observe is about 2.94×10^6 volts, corresponding to a possible γ -ray of energy 3.03×10^6 electron volts. This general agreement affords strong corroborative evidence that the emission of γ -rays or corresponding β -rays is closely connected with the long range α -rays.

* Gurney, 'Proc. Roy. Soc.,' A, vol. 109, p. 541 (1925).

It should be mentioned that Yovanovitch and d'Espine* have observed the presence of a weak band of β -rays of still higher energy, viz., 4.0 to 7.6 million volts. The origin and number of these swift β -rays are at present unknown. They may represent an abnormal method of transformation of some of the atoms.†

We shall now consider whether the energy differences shown in the table are connected with the energy of the known γ -rays from radium C. The strongest γ -rays from radium C found by Ellis are shown in the table below, where the second column gives the number of quanta per disintegration and is thus a measure of the intensity of the γ -rays. The relative intensity of these γ -rays has also been determined by Skobelzyn by another method and with results in fair accord with those found by Ellis (see 'Nature,' vol. 127, p. 125 (1931))

$h\nu$ of γ -ray in volts $\times 10^{-6}$.	Average number of quanta emitted per disintegration.
6.12 S	0.658
7.73	0.065
9.41	0.067
11.30 S	0.206
12.48	0.063
13.89	0.064
14.26 S	—
17.78 S	0.256
22.19	0.074

It is seen that for some of the stronger α -rays marked S, one quantum is emitted for every two to four disintegrations.

It is at once seen that the energy liberated in falling from the first observed level, viz., 6.3×10^5 volts is in fair accord with the energy of the strongest γ -ray from radium C, viz., 6.12×10^6 volts. The agreement is quite as good as could be expected since an error of only 1/1000 in estimating the relative velocity of this α -particle group results in an error of over 3 per cent. in the energy of the γ -ray, which depends on the difference of two large numbers.

Similarly it is seen that the energy liberated in falling from the second level, viz., 14.6×10^5 volts, is in fair accord with the energy given in the table of 14.26×10^6 volts.‡ In this case no γ -ray has been detected, although the

* Yovanovitch and d'Espine, 'J. Physique,' vol. 8, p. 276 (1927).

† See "Radiations from Radioactive Substances" (Rutherford, Chadwick and Ellis), Camb. Univ. Press, p. 381, 1930.

‡ It is not necessarily to be expected that the energy difference calculated in the way described should agree exactly with the observed energy of a γ -ray. Apart from possible errors of measurement, it is not unlikely that other factors have to be taken into account

corresponding β -ray line is one of the strongest in the magnetic spectrum. R. H. Fowler* has suggested that for this transition the energy for some reason cannot be emitted in the form of a γ -ray, but is directly communicated to one of the electrons outside the nucleus and appears as a swift β -ray. It is noteworthy that the level, corresponding to α -particles of range 9.13 cm., gives rise to much the strongest group of long range α -particles, probably indicating that the time required for the transition is abnormally long.

We have already pointed out that it is difficult for experimental reasons to fix with precision the energy and abundance of the third observed level. The value found, 17.6×10^5 volts, is not very different from the energy of the strong γ -ray 17.78×10^5 volts, and in all probability fixes the origin of this γ -ray. It may be pointed out that an error of 1 per cent. in the energy of this level corresponds to an error in range of about 0.2 mm.

It should be noted also that the energy of the level 22.0×10^5 electron volts is in good accord with the value of the γ -ray 22.19×10^5 . This γ -ray may have its origin in the transition of the α -particle from this level to the ground level.

Careful experiments were made to test whether a group of α -rays was present corresponding to the strong γ -ray 11.30×10^5 volts. If it originated in falling to the ground level, the range of the α -particles should be 8.6 cm. It is to be anticipated that the height of the α -ray peak should not be more than one-half of the first group. Unfortunately, such a group would be masked by the marked tail of the strong 9.13 cm. group (see fig. 4). Although special precautions were taken to prepare very clean sources to reduce the straggling to a minimum, we could obtain no certain evidence of the presence of this weak group. At the same time, the experimental evidence was too uncertain to disprove its existence. A similar argument applies to the difficulty of detecting the still weaker groups of α -rays to be expected corresponding to the weak γ -rays 7.73, 9.41, 12.48, 13.89×10^5 volts if they arise from transitions to the ground level, in which case the corresponding ranges should be 8.08, 8.32, 8.80 and 9.02 cm.

We have seen that the γ -ray of highest energy observed, viz., 22.19×10^5 volts, is not very different from level 5 of energy 22.0×10^5 volts. It must arise in a transition from this level or from 7, 8 or 9. It may, for example,

for a precise deduction. For example, the energy of rotation of the nucleus may in some cases be changed in a transition from one level to another. It can be estimated that for a quantum number 1, the energy of the nuclear rotation is of the order of 10^4 volts.

* R. H. Fowler, 'Proc. Roy. Soc.,' A, vol. 129, p. 1 (1930).

arise in the transition from the level 8 to level 1, giving an energy difference of $28.4 - 6.3 = 22.1 \times 10^5$ volts. There are certain other possible transitions in fair numerical accord with the energy of this γ -ray, but the evidence is too uncertain to warrant a detailed discussion.

There is another interesting agreement. The difference in energy between levels 3 and 1 is 11.3×10^5 electron volts corresponding to a strong γ -ray.

It is to be noted that no strong γ -rays are observed corresponding directly to the energy levels 4, 6, 7, 8 and 9, but there are several transitions between observed levels which are in numerical accord with the energies of observed γ -rays. For example, the sum of the energies of the γ -rays 7.73×10^5 and 17.78×10^5 volts, viz., 25.51×10^5 volts is in fair agreement with level 7 of energy 25.8×10^5 volts. Similarly the sum of the energies of the two γ -rays 9.41×10^5 and 12.28×10^5 is 21.89×10^5 volts, and thus not very different from the energy of level 5 of energy 22.0×10^5 volts. While the sum of the energies of the γ -rays 7.73×10^5 and 22.19×10^5 , viz., 29.9×10^5 is about the energy of the last level 30.0×10^5 volts. While these rough numerical agreements are worthy of mention, we cannot be at all certain at this stage that these γ -rays originate in the transitions mentioned. The accuracy is not sufficient to decide between these and other obvious possibilities. In addition there may be radioactive transitions of the same type as the transition of energy 14.26×10^5 volts. A consideration of the β -ray spectrum shows a number of numerical coincidences for transitions between the observed levels, but without a very careful consideration of existing data it is very difficult to draw decisive conclusions. In particular, it is necessary to consider carefully the relative intensities of the β -ray lines and the relation of the radioactive constant λ to the average time of transition T for the whole series of levels. This difficult question will be discussed in more detail in a subsequent paper by Rutherford and Ellis in the light of existing data on the α -ray levels and of new data on the β -ray spectrum of radium C.

Considering the evidence as a whole, there can be no doubt that there is a close connection between the emission of long range α -particles and the emission of the high frequency γ -rays from radium C. On this view, the γ -rays are not due to electrons but arise from a transition of an α -particle from one excited level to one of lower energy. It was pointed out by Kuhn* some years ago that on general grounds the observed degree of homogeneity of the γ -rays could only be accounted for on the assumption that they arose not from transitions of the light electron in the nucleus but from transitions between massive units

* Kuhn, 'Z. Physik,' vol. 43, p. 56 (1927).

like the α -particle or proton within the nuclear structure. As has been pointed out, it is reasonable to suppose that the emission of the disintegration electron from radium C for some reason leaves the resulting nucleus radium C' in an abnormal or excited state, some of the α -particles being distributed in a number of energy levels much higher than the normal. The energy liberated in the fall of the α -particle from a higher to a lower level appears in the form of a γ -ray or corresponding β -particle of high energy. It is clear that, on these views, the energy of the long range α -particles emitted during the average life of these α -particles in these excited levels allows us to determine for the first time the actual values of, at any rate, some of the energy levels in the excited nucleus. As we have seen, the energy of some of the stronger γ -rays can be satisfactorily accounted for by α -ray transitions between the different levels, and, no doubt, with further and still more accurate experimental information, an explanation may ultimately be given along these lines of the complicated β -ray spectrum of radium C.

Our thanks are due to Mr. G. A. R. Crowe, for his care in the preparation of the sources, and his help in the experiments, and to the Department of Scientific and Industrial Research for a grant to one of us (W.B.L.).

Summary.

An analysis of the distribution of the long range α -particles from radium C of ranges between 7 cm. and 12 cm. has been made using the new counting methods. It is concluded that at least nine homogeneous groups of α -particles are present for which the ranges and numbers have been measured. By means of an extrapolation curve, the velocity and energy of the α -particles for each of these groups have been deduced. No α -particles of range greater than 12 cm. in air have been detected. Their number must be certainly less than 1/1000 of the number in the main group of range 9 cm.

Evidence is given that the emission of γ -rays from radium C is intimately connected with the appearance of these groups of long range particles. It is concluded that the γ -rays arise from a transition of the α -particle in an excited nucleus between two levels of different energies. The energies of these levels can be determined from the energy of the α -particles and it is shown that the differences of energy between these levels and the normal or ground level are in several cases in good accord with the energies of some of the stronger γ -rays.

OBITUARY NOTICES.

CONTENTS.

	PAGE
ALFRED BARNARD BASSET	i
LORD MELCHETT (with portrait)	ii
SIR CHARLES PARSONS (with portrait)	v

ALFRED BARNARD BASSET—1854–1930.

ALFRED BARNARD BASSET was born on July 25, 1854. He was educated at Trinity College, Cambridge, and graduated in 1877 as 13th wrangler, a position which could hardly have represented his real mathematical attainments. He appears to have at first contemplated a legal career, and was called to the Bar at Lincoln's Inn in 1879, but having succeeded to a considerable estate, he soon abandoned the law, and apart from the duties incidental to his private station, devoted himself mainly to mathematical research.

From 1883 onwards Basset produced a succession of papers on applied mathematics, mainly on topics suggested by current discussions. The "classical" hydrodynamics was at that time beginning, after a long interval, to exercise a great fascination on a number of rising mathematicians, and Basset's own contributions in this kind to the 'Proceedings' of the Cambridge Philosophical Society, and the London Mathematical Society, and to the 'Philosophical Transactions' were of distinct originality and merit, and led to his election into the Royal Society in 1889. He was for many years an active member of the Mathematical Society and made many contributions to its 'Proceedings.' He was Vice-President in 1892–93.

Among the numerous subjects which he treated we may mention the dynamical theory of the motion of solids in a fluid, inaugurated by Kirchhoff and Kelvin, the equilibrium of fluid masses revolving under their mutual gravitation, and its stability, and the theorems of Dirichlet and Dedekind, the interest in which had been revived by Bryan, Greenhill, and Love. At a somewhat later period he became interested in elasticity, and wrote extensively on the theory of elastic plates and shells, which was then a matter of some controversy. In this connection he was led to recognise independently the true explanation of an apparent paradox. Mention must also be made of his work on viscosity, and in particular on Boussinesq's problem of the variable (slow) motion of a sphere in viscous fluid. He made some valuable contributions to electrostatics, and wrote also on various developments of the electromagnetic theory of light.

Basset's work was distinguished throughout by a remarkable command of analytical methods, and it may even be fair to say that it was the analytical aspect, as much as the physical content of the theories on which he wrote, which attracted him. As an instance of his mathematical resources, he was an expert in the use of Bessel functions, and discovered new results in connection with them, at a time when the theory was only beginning to be familiar to English applied mathematicians.

Basset was also the author of several able treatises. A book on hydro-

dynamics, in which he incorporated much of his own work, was published in 1888, and did much to sustain the interest in the subject. This was followed in 1892 by a treatise on physical optics, another of his favourite subjects, on which he bestowed immense pains, but which scarcely met with the recognition which it undoubtedly deserved.

At a later period Basset turned his attention to pure mathematics and produced two text-books, on cubic and quartic curves, and on solid geometry. But his interest in current mathematical topics, and his relations with mathematical contemporaries, seem gradually to have faded, partly, no doubt, owing to failing health, and he lived in great retirement at his seat in Berkshire. He died on December 5, 1930, at the age of seventy-six years.

H. L.

LORD MELCHETT—1868-1930.

ALFRED MORITZ MOND, first Baron Melchett of Landford, was born on October 23, 1868, at Farnworth, in Lancashire, within smell of the famous alkali works. His father, Dr. Ludwig Mond, was at that time a chemist at the Hutchinson Alkali Works; it was not until five years later that he founded the firm of Brunner Mond in partnership with John Brunner, an accountant at Hutchinsons. Mrs. Ludwig Mond has described to me the Farnworth days as very happy ones—they preceded some very strenuous times at Winnington. When the new enterprise was started, their capital was very insufficient, their optimism very great. The process was an unknown one and it was laughed at by those who understood the industry; the operations were continuous and Ludwig Mond and a small band of loyal helpers often worked for 36 hours at a stretch.

Alfred Mond in his lifetime has thus seen the founding of the B.M. Works, as it is familiarly called in the North, the overcoming by strenuous effort of its early difficulties both technical and financial, its growth to become the most important chemical firm in Britain and its disappearance as an entity on absorption into Imperial Chemical Industries. Although he was associated closely with the management of the firm in early days, after the retirement to London and death of Ludwig Mond, the active management at Winnington passed into the hands of Sir John Brunner and his two sons, and Alfred Mond's energies were largely spent in other directions.



LORD MELCHETT.



SIR CHARLES PARSONS, 1854 1931.

man has gone further in politics under greater personal handicaps. Latterly it is as a politician, a leader of industry and an Empire builder combined in one man that he has won notoriety and fame. He had the gift of going to the root of any question, grasping the realities and unmasking the shams—his extraordinary power of quick thinking enabled him to see round the corner of the problems of the day. Underlying most of his public utterances it is possible to discern the spirit of science and it is for the electors of the future to see that more men of his type represent them in Parliament. Alfred Mond made use to the utmost of those gifts which he acquired by heredity and by training, and his boundless energy enabled him to attain the very top in every field of endeavour; he passed away on December 27, 1930, at the very height of his career. His loss is one that the Nation, Science and Industry can ill afford.

E. F. A.

THE HON. SIR CHARLES PARSONS, O.M., K.C.B.—1854–1931.

CHARLES ALGERNON PARSONS, whose genius as inventor and engineer has opened up a new era in the production and application of power, was born at 13, Connaught Place, London, on June 13, 1854. A life notable for its intense and sustained creative activity was closed by his death at sea, after a brief illness, on February 11, 1931. He was the youngest of six sons of William Parsons, third Earl of Rosse, and spent his boyhood at the family seat, Birr Castle, Parsonstown, Ireland. The father was a distinguished astronomer and mechanic, whose great reflecting telescope, designed and mainly made by himself, was for long among the wonders of the astronomical world. Its 6-foot speculum of copper-tin alloy was the culmination of work in the casting and polishing of specula on which Lord Rosse had been engaged from 1827. Erected in the grounds of Birr Castle in 1845, the Rosse telescope had then, and for many years after, no rival. The Earl's services to astronomy were recognised by his election as President of the Royal Society for the period 1848–1854. As early as 1844 he had been President of the British Association, and at later meetings he presided over Section G as well as Section A.

He died in 1867, and his eldest son Laurence, who was born 14 years before Charles, succeeded to the earldom. Laurence shared his father's tastes and

had been an active collaborator in the astronomical work. A memoir by him on the great nebula in Orion was published in the 'Philosophical Transactions' of that year; and another, on radiation from the moon, formed the Bakerian Lecture of 1873.

Of the other sons, the second and third died in early boyhood. The fourth, Randal—now the only survivor—was for many years Rector of Sandhurst and is an Honorary Canon of Christ Church. In the fifth son, Richard Clere, who was three years senior to Charles, the family talent took a somewhat different course. He had a successful career as a civil engineer and died in 1923, after carrying out many schemes of water supply and drainage, especially in the cities of South America.

"We never attended any school," writes Canon Parsons. "Everything was provided at home to develop natural ability and mechanical taste, which my brothers, not myself, possessed to a great degree. They had workshops, foundries—iron and brass—for everything was made at the Castle—and my father was always with them. He was a first-class mechanic and could do almost everything with his hands. My brothers were practical engineers before they reached the age for leaving home or attending college, and the theoretical part of their training was imparted by the tutors who, in succession, lived with the family and were our greatest friends personally. Charles showed a strong practical taste for mechanics very early. He was perfectly happy if only cardboard, hat-pins, sealing-wax could be obtained, and one of his child-delights was to make cardboard clocks. These were in time discarded for mechanical toys, home made. I remember one day his running in to my mother with a splinter of steel hanging in the white of an eye from the lock of an air-gun he had made himself. She had the courage to draw it out and no harm was done. Another time he had the whole of his eyebrows taken off by an explosion of gunpowder." The family motto was never "safety first."

One gathers that in this remarkable education the mother had no unimportant share. She was Mary Field, daughter of a Yorkshire squire, who married the astronomer in 1836 and kept up a lively sympathy in his pursuits. Her own aptitude for handicraft made her a delightful companion to mechanically-minded sons. After describing the workshops, forge, foundry, and chemical laboratory which the third Earl established in the moat and keep of the old Castle, Canon Parsons remarks, "My mother was deeply interested in these works and took her part. She was skilled in modelling in wax and made all the moulds for the ornamental work of the large bronze gates at the entrance of the front hall of the Castle. . . . When photography was invented she had a photographic room fitted up adjoining the workroom and spent much time there."

The third Earl's death left her in sole charge of the three younger sons;

Charles, the youngest, was then 13. The process of education at home went on until it was time for each boy in turn to go to the University. "She made a home for us boys after my father's death, at first at Birr, then at Dublin, and afterwards in London, until her death. The family life continued even after Charles went to Cambridge and the vacations were spent together. . . . She was the best of mothers; her influence affected all our lives. She was highly intellectual and simply gave herself for her children."

The family habit, as long as the father lived, was to spend most of the summer in a capacious yacht, the *Titania*. The boys' tutor was always of the party; they had regular hours of study which were strictly kept. Thus Charles learnt not a little of seamanship and navigation before entering his teens.

After their father's death, Randal, Clere and Charles went with their mother each year for a tour in Switzerland, North Italy or the Tyrol. When Charles proceeded to Cambridge in 1873 his mother left Dublin and settled in London for the rest of her life. She died in 1885, having survived long enough to see Charles produce his first steam turbine.

The tutors were mathematicians to whom the great telescope offered a special inducement to join the Earl's household. Among them, in the double capacity of astronomer and tutor, was Sir Robert Ball, whose published *Reminiscences* tell of service at Birr from 1865 to 1867. He claims "the great honour of instilling the elements of algebra and Euclid into the famous inventor who has revolutionised the use of steam. . . . It would seem that he inherited his father's brilliant mechanical genius, with an enormous increase in its effect on the world." He describes Charles as constantly resorting to a little workshop where he made all sorts of machines, among them a sounding gauge which measured the depth of water by registering the pressure of air confined in a glass tube, much as Kelvin did some years later in a well-known device.

Another exploit on the part of Charles and Clere was to build, with much toil, a steam road-carriage. This was long before any form of motor vehicle had come to challenge the supremacy of the horse. On a flat base, like that of a lorry, with four wheels, the front pair of which could be steered, they mounted a boiler and a vertical engine which drove the after pair through a cardan shaft, giving the carriage a speed of some 7 miles an hour. There was a cross bench to carry passengers. The experiment came to a tragic end. One day in 1869 when Clere was driving, Charles stoking and Randal running behind, they had a cousin of the family, Lady Bangor, seated with her husband on the bench. She made a sudden movement, overbalanced, and, falling on the road, was instantly killed.

Enough has been said to show how heredity and environment combined to make Charles Parsons a scientific engineer. From his father and probably from both parents he inherited qualities which were fostered by every part of his training. His nursery was a workshop, his toys were tools, or the things

he could himself use tools to create. Nature and acquired habit alike led him, in maturity as in childhood, to think unconventionally, to seek the solution of problems in ways that had not been attempted before. With Parsons life was a sort of hurdle race: a difficulty was simply a thing to be overcome. An obstacle was never a bar; it was a challenge, an incentive to effort. He revelled in accomplishing what to most men seemed impossible. Untiring, amazingly fertile of ideas, infinitely patient when he had to deal only with the caprices of inanimate things, he found no finality in failure. It meant no more than that another scheme should be tried. His schemes were always carefully planned. He passed from experiment to experiment, assiduous, undiscouraged, until at length he could admit success. But in measuring success he was his own severest critic. A machine of his devising might seem to function very well; his concern, however, was always with the defects and the possibilities of improvement. At every stage in his long development of an invention the better was the enemy of the good. This attitude towards his own work must often have distressed his colleagues—he would find reasons for scrapping what they thought ready for the market. But, looking back now, we see that his passion for improving what was already good was in truth the secret of his finest achievements.

Parsons used in after life to say that he had missed much through not being sent to school. He did, undoubtedly, miss something. Shy, self-contained, inexpressive, he never wholly shook off certain characteristics which a public school might have masked or cured. To the last, even in the universal celebrity of his riper years, he kept an air of self-effacement, an exaggerated though wholly natural modesty which puzzled strangers as much as it endeared him to his friends. Could this seemingly casual person with the passive handshake, the hesitating fragmentary utterance, be the world-famous inventor, the dreamer who compelled his dreams to come true, the man of indomitable will who removed mountains by works no less than by faith? In the early stages of his career it must have been a handicap to appear at first sight so curiously ineffective, to belie so completely the force which a closer acquaintance gradually discovered.

But if a public school had run him into a common mould, would the gain have been worth the cost? He might have been easier with men who did not wish him to have his own way—a more acquiescent colleague, less sensitive to criticism, less impatient of interference, more tolerant and less exacting. But there would have been grave loss had he thus become standardised, had his uncompromising individualism been shaken, had he been schooled into accepting the guidance of other minds. He was not made to be a member of a team. It was better for the world that he should have his head and be allowed to go his own way. That way was not always easy to understand, and he had little ability—perhaps little wish—to explain it. But men came

to see what the goal was, when, as generally happened, they found it had been reached.

What is standard bread for the average boy may be pernicious fare for the budding genius. To Parsons, in any case, school would have been at best a poor substitute for the rarely congenial surroundings in which he spent his boyhood. It is safe to say that the actual home training, both of brain and hand, was ideal for the work he was afterwards to do.

The family tradition was that the boys should go on to Trinity College, Dublin, where their father had been Chancellor, and thither Charles went in 1872. After reading mathematics in Dublin for a year he entered St. John's College, Cambridge, where he became a pupil of Routh. In 1877 he passed out as eleventh wrangler—a place which his College friends did not think a proper measure of his powers. Sir Donald MacAlister, who was senior wrangler of that year, says that Parsons beat him in "problems" but was comparatively weak in "bookwork." There was no Engineering School in the Cambridge of those days, but the table in Parsons' room, with its litter of models, bore witness to his continued interest in matters which the tripos did not touch. He was scheming then a quickly rotative epicycloidal engine to which he gave practical form during the apprenticeship which followed his college course. His contemporaries describe him as very quiet and shy, liked for his modesty, sociable and even convivial on occasion. The shyness which they all remarked was broken down by the intimacies of the Lady Margaret Boat Club where, being very strong, he pulled an effective oar. His last appearance on the river was in the May races of 1877 when he took part in a Homeric struggle, the Iliad of which still lives in college story. The Lady Margaret boat bumped First Trinity; but their bows were smashed in and the boat sunk. A quick repair was completed by working on it all night, and next evening they bumped Third Trinity. Canon Prior writes: "I well recollect his great long back on which it was my job to keep my eye fixed. He was 3 and I was bow, and I also recollect how when we were all in the water together he got me out of the muddle of oars and wreckage and helped me to the bank. He was enormously delighted that we had bumped Trinity." In the diffident youth from Birr new contacts had bred new loyalties. Long after, when loaded with distinctions, it gave Parsons particular pleasure to be made an Honorary Fellow of his College. In 1920 he collected as many survivors of the boat's crew as could be found to meet at dinner one of their number, Sir James Allen, who was then in London as High Commissioner for New Zealand.

It was curious to notice, in Parsons' professional life, how little direct use he made of mathematical calculation. Algebra was a tool for which he did not seem to care. While his assistants were busy with their pencils working out a stated problem, he would find a result by some mental process which he made no attempt to formulate, but in which he appeared to trust more than in

symbols. None the less, the intellectual discipline of the Cambridge days had left its mark. It had given him a sound working knowledge of dynamics which experience converted into something like an instinct. It had bred a definite, if non-formal, mathematical habit of mind in which the principles of physics and mechanics were the only accepted guide in interpreting experience and controlling design. Its influence could be traced in the precision and order of his written statements, in the clearness of his prognosis when he was about to make an experiment, in the selection of methods and the analysis of results. With Parsons experiment was never haphazard; it was planned to clear up some dark spot, and it was turned on that with the concentration of one of his own searchlights.

At the end of his Cambridge course he went to Elswick as a pupil-apprentice in the Armstrong Works. There he spent three or four years, improving his skill in handicraft, learning the ways of workmen, and seeing how an establishment was run in which engineering output proceeded on a grand scale under conditions where design and production had to take account of cost. His mind was in a ferment of invention and he was allowed to bring some of his ideas to the test. A contemporary remarks that he made a name for being the most industrious apprentice the Elswick works had ever known. While still a pupil there Parsons put into working form the epicycloidal engine he had devised and modelled in his college rooms. Its object was to produce rotary motion at a high speed with but little action of reciprocating parts. In this it might be called a precursor of the steam turbine where the object was completely attained of getting very high speed with no reciprocation. He also began experiments on driving torpedoes by means of rockets. By the time he left Elswick his brother Clere had joined the firm of Messrs. Kitson at the Airedale Foundry in Leeds, and for about two years Charles, under an agreement with the firm, continued the manufacture of his engine there along with much experimental work. The torpedo trials went on, permission being given to carry them out in Roundhay Lake. They had fair success; speeds up to 20 knots were reached; but the rockets were found to be uncertain and unsafe.

Writing many years afterwards of the incidents of that period (1884) Parsons says: "I was married and wanted to settle down and start business in earnest, and there was a good opening with Clarke, Chapman & Co., of Gateshead, as junior partner. At Gateshead it was at first contemplated to go on with the rocket experiments, but Messrs. Clarke, Chapman being much interested in electric light and having decided on an electrical department, including the manufacture of incandescent lamps, I put aside the rocket experiments, and steam turbine experiments were started, as the turbine appeared very suitable for the electric lighting of ships."

On April 23, 1884, he took out his first patent for the steam turbine, or rather

two patents of the same date (Nos. 6734 and 6735). From these it is clear that the primary motive was to find a means of giving very rapid rotation to the armature of a dynamo. No. 6734 begins thus:—

“My invention is designed to produce an electrical generator which may be driven at a very high rate of speed, several or many times as fast as such machines are now driven, the object being to obtain a large current or a high electromotive force, or both, from a small machine, and also to obtain an increased efficiency.”

The specification goes on to describe the dynamo in detail and claims, among other things, the driving of it by the turbine which, in its more general aspect forms the subject matter of Patent No. 6735. The dynamo, he used to say, gave him quite as much trouble as the turbine. In those days dynamo design was largely a matter of trial and error; it was not till 1886 that John and Edward Hopkinson formulated the principle of the magnetic circuit. For Parsons the problem was complicated by the enormous centrifugal forces which the armature had to bear.

During the partnership with Clarke, Chapman & Co., which lasted from 1884 to 1889, the manufacture of the combined steam turbine and dynamo was developed mainly for the electric lighting of ships, but only on a small scale. An early model was shown at the Inventions Exhibition in 1885, where it attracted much attention as a new departure in the use of steam for motive power. Parsons was dissatisfied with what seemed meagre progress. He wished to embark on costly experiments, having a faith in the future of the turbine which nobody was disposed to share. His temperament made any partnership irksome. It is not surprising that, after five years, this one was dissolved. With the financial help of a few friends he then set up works of his own at Heaton in Newcastle-upon-Tyne for the manufacture of turbines and dynamos. It was an ambitious venture; the works were by no means small, and his zeal for experiment added to the risk. There were years of waiting for a dividend; some lost heart, himself never. In the end his own faith and his friends' faith found ample reward.

A curious tangle added to the difficulty of that trying time. By the deed of partnership with Clarke, Chapman & Co., all patents taken out by any partner became the property of the firm. The value of Parsons' patents was still highly problematical at the date when the partnership was dissolved. To settle the question—not an easy one—of what Parsons should pay for the right to hold them, recourse was had to arbitration; but before it was completed an agreement was come to under which the patents were left in his late partners' hands. This arrangement lasted for about five years, and although Parsons continued to develop the turbine during that period, he could do so only with modifications which were designed to keep it outside

of the lines specified in his own early patents. The restriction thus imposed was a serious impediment, nevertheless he made notable advances which went far to establish the reputation of the turbine and to pave the way for its ultimate success.

In 1894 he recovered possession of the early patents and was free to return to the original lines of his invention which were, on the whole, definitely better. In his first turbine the general direction of flow of the steam had been parallel to the axis. In the modified form, to which he was for some years limited, he made the flow radial. On recovering the patents he reverted to axial flow, and this feature is retained in nearly all modern turbines. Later the term of validity of the fundamental turbine patent was extended for six years, in recognition of the great value of the invention and the smallness of the reward it had at that time received.

To understand the genesis of Parsons' early inventions, it may be useful to recall the trend of applied science in the eighteen-eighties when his work began. It was a time of exceptional stir and change. The engineering world was teeming with untried notions. Explorers were busy in a country of whose landmarks they knew next to nothing. From being little more than the servant of the telegraph, electricity had suddenly become a part of engineering. It was an agent with unlimited possibilities. Clearly it might serve for distributing light and power, but how that was to be done involved many questions which were still to be settled. To manufacture electricity was the initial problem; to apply it to novel uses offered a vista of further problems which inventors were eager to attack. The magneto-electric generator had led up to the invention of the self-exciting dynamo; small dynamos of the types introduced by Gramme and by Siemens were already serving to illuminate open spaces by means of arc lamps. In 1879 and 1880 Edison and Swan were separately at work on the incandescent filament, and nervous holders of gas stock were being assured by their chairmen that there was nothing to fear from the electric light. At the end of 1881 Sir William Thomson's lighting of his house by Swan lamps was a notable event. Such an installation was isolated and experimental; as yet there was nowhere in Britain a public electric supply. A year later, and we read of "almost daily" flotations of supply companies and find a hot controversy going on over the terms of an Electric Lighting Bill which was hastily promoted to safeguard the interests of local authorities.

Into this welter came Parsons, realising that an urgent mechanical need of the moment was an engine that might be directly coupled to the armature of a dynamo, with the very high speed of rotation which would best suit the electrical element in the combination.

For such a purpose reciprocating motion was out of place. The motion of the armature was purely rotary: the motion of the engine should be purely rotary too. Moreover, the speed of the armature must be high and might with

advantage be very high. Parsons, as his first patent shows, realised the special merit for this purpose of a speed much greater than any to which engine builders were accustomed, even when they increased it by using a belt and pulley between engine and dynamo. Rapid driving of a dynamo armature was his primary concern.

To escape all reciprocating movement meant recourse to some type of steam turbine. The essence of a steam turbine is that the pressure of the steam, instead of pushing a piston, pushes some of the steam itself through an orifice or nozzle, setting up a jet, and the jet gives up its energy either by impulsive action on moving vanes, as in a windmill, or by the reaction that it exerts on the orifice from which it issues. Both of these modes of obtaining motion, by the impulse or the reaction of a jet, were found in ancient philosophical toys; and long before Parsons began to think about the turbine they had been embodied in various proposals of inventors who had failed to give them practical effect. The fundamental difficulty was that a jet escaping under pressure acquired a very high velocity and this needed a correspondingly high velocity in the vanes or the nozzles if they were to take up the energy of the jet. Parsons saw that the right solution lay in dividing the whole drop of pressure into many stages, with the result that in each stage the velocity acquired by the jet is so moderate that it is practicable to make vanes or nozzles move fast enough to absorb nearly all the available energy.

On these lines he built, in 1884, his first compound steam turbine which is now preserved in the Science Museum at South Kensington. Steam flowed through a long annulus between a rapidly revolving shaft or drum and a fixed outer casing in the form of a larger cylinder. On its way the steam passed through a series of many turbines arranged as rings in the annular space. Each of these turbines consisted of a ring of fixed guide-blades projecting inwards from the casing, and a ring of moving blades projecting outwards from the drum and turning with it. Thus the whole annular space between drum and casing was occupied by a series of alternate rings of fixed blades and moving blades, placed near together, with no more clearance over the tips than was needed to escape contact. In each ring the blades were set obliquely; the fixed ones formed, as it were, a ring of nozzles, and delivered jets of steam against the next ring of blades, which served as moving vanes. But the action on these was not one of pure impulse, for in streaming through the passages between the moving blades the steam acquired a new relative velocity; hence the force which it exerted on these blades was due partly to reaction. The fixed and moving blades of a Parsons' turbine are in fact exactly alike, which gives the whole construction a remarkable simplicity. In the earliest turbine the steam entered at the middle of the length and flowed both ways towards the ends, thereby causing no end thrust; but in most designs the steam enters at one end only and a lengthwise balance is obtained in other ways. The

blades are made longer as the exhaust end is approached, in order to provide a bigger passage for the expanded steam.

Nothing, in a sense, could be simpler than this compound steam windmill with the whole series of fixed and moving blades co-operating to make the shaft revolve at a prodigious velocity when the blast of steam was turned on. But to secure that it would run smoothly and without excessive waste of steam was no simple matter. Notwithstanding the division of the whole pressure-drop into many stages the blade-speed had still to be high. In the first turbine, which drove a shunt-wound dynamo and developed about 10 horse-power the shaft made 18,000 revolutions per minute, giving the blade tips a velocity of about 300 feet per second. The dynamical problem of so constructing and supporting the shaft and armature that they could spin without shake at such a pace required much inventive design.

And later, when steam turbines grew and their uses multiplied, every stage in the development made further demands on the inventor's ingenuity and courage and resource. There were many technical advances to be made and much prejudice to be overcome before Parsons convinced other engineers and industrial experts that in this new type of prime-mover they had a convenient, unfailing, and highly economical apparatus for producing power, capable of operating on a scale and with a concentration never before approached. Throughout the whole evolution of the steam turbine he continued to be the active and incessant *deus ex machina*. Other inventors appeared and made their contributions, which led in some cases to more or less different designs. But they would be the first to acknowledge that it is to Parsons, far more than to any other man, that credit is due not only for the first conception and the initial experiments, but for the subsequent improvements which have produced the gigantic turbines of to-day and have made them the chief means of generating central-station power and of propelling the biggest ships. All large modern turbines adopt his fundamental plan of multi-compound action by dividing the whole drop of pressure into many successive stages.

Only a few salient points in the history of the steam turbine can be noticed here. In the early models, all of which were small, the steam was discharged into the atmosphere; there was no provision for condensing it. But Parsons was not long in seeing that the addition of a condenser would do even more for the steam turbine than it did for the engine of Watt. For in the turbine it was easy to extend the system of rings of blades and so allow the steam to expand down to the lowest pressure obtainable in a condenser, doing work all the way; whereas in any engine of the piston type there is a practical limit to the useful expansion, a limit which is set by considerations of cylinder size and of piston friction. This in fact is the chief reason why a condensing turbine can become a greatly more efficient device for converting into work the heat

that is supplied in the steam. It was not until a condenser was introduced that the consumption of steam per horse-power-hour became less in the turbine than in the piston engine ; after that the thermodynamic superiority of the turbine was manifest. The addition of the condenser marks an epoch : the turbine then entered on what may be called, with no exaggeration, a course of conquest.

By chance it fell to me to make the earliest independent tests of a condensing turbine. In 1891, when Parsons had established his works at Newcastle, a scheme was under discussion for setting up an electric supply station in Cambridge. Somebody made the suggestion that it should be equipped with Parsons' turbines. The turbine was a novel and little-tried appliance about which there was much scepticism ; it was said to be a notorious steam-eater. A member of the Cambridge Corporation, who shared this scepticism, asked me to report on it, much as Balaam was asked to report on the Children of Israel. Parsons gave me every facility to make exhaustive trials ; they convinced me that the turbine was the engine of the future, and, like Balaam, I came back blessing where I had been expected to condemn.*

That was the first of several such occasions. A few months later Parsons had me come again to test the effect of certain changes, one of which was the use of superheated steam. From time to time a new development gave opportunity for further trials. It was no small privilege to come in contact with the working of so exceptional a mind and to note some of the milestones in his astonishing career. The friendship thus begun continued without a break or cloud. If to some people Parsons seemed difficult, it is right to say that many others—I for one—found him wholly delightful.

One of the occasions of tests was when a turbine, bigger and more efficient than any turned out before, had been built to the order of the City of Elberfeld, and a group of distinguished German engineers came over to conduct the official trials which Parsons commissioned me to witness. The trials began badly, for in a preliminary run there was some rather serious stripping of the turbine blades. But Parsons met the emergency with his usual resource, and the visitors had an opportunity of seeing how quickly the defect could be repaired. After that all went well, and as the testing proceeded to a more than satisfactory finish it was amusing to observe the scarcely repressed astonishment that an invention so admirable should spring from a non-German source.

Another occasion was in 1897 when Parsons had fitted up his little experimental vessel, the *Turbinia*, to investigate the suitability of the turbine

* The turbine then tested, which was the first to be fitted with a condenser, was of the radial-flow type. It was installed at the Cambridge Electric Supply station in 1892, and, after many years' service there, it is also now preserved in the Science Museum at South Kensington.

for driving ships. This famous craft, 100 feet long and of 9 feet beam, was built at Wallsend in 1894. She was originally fitted with a single propeller-shaft driven by a radial-flow turbine. The results were disappointing on account of the phenomenon of cavitation, to which fuller reference will be made below. Many different propellers were tried, but their action was unsatisfactory until, in 1896, Parsons substituted a three-shaft arrangement in which each shaft was driven by an axial-flow turbine. The turbines, which developed more than 2,000 horse-power, formed a compound series; steam passed through all three in succession, their dimensions being adapted for high, intermediate and low pressures respectively. Further experiments were then made with various forms of propeller. These changes led to a great improvement in the propulsive efficiency, and in April 1897 trials were carried out which convincingly demonstrated the success of Parsons' long and persistent efforts.* After we had been cruising for several days at various speeds over a measured mile on the north-east coast, observing the relation of steam-consumption to speed in weather which was too rough to allow the engines to be worked at their full power, we were returning up the Tyne at the modest pace allowed by local regulations. The river, as it happened, was nearly empty, the tide slack and the water smooth. Passing the posts of a measured mile on the river bank below Wallsend, Parsons was tempted and said, "What about a full-power run here?" to which I replied, "She's your ship." In a few minutes we were tearing through the water at a speed which, in those days, was a "record" for any vessel. A little later Parsons took the *Turbinia* round to the Solent where she amazed the Fleet at the Diamond Jubilee Review. He had a permit to run between the lines, but the midshipmen whose duty it was to keep the course did not know this and were outraged to have an intruder ignore their protests and—what was worse—utterly outpace their patrol-boats.

Lord Rayleigh tells some stories of Parsons' handiness. In the early days of motoring he had a small car which was too lightly built and was apt to give trouble. One day he was on the Northumberland moors, far from anywhere, when a shaft got so badly bent in bumping on a rough track that the car would not go. Parsons took it to pieces, lighted a fire to serve as forge, and with stones for hammer and anvil straightened the damaged part, put all together again, and went his way. That was motoring as he understood and enjoyed it.

* Part of the hull of the *Turbinia*, including the engines of 1897, is now in the Science Museum, and near it is the original engine of 1894. An historical account of the early application of the steam turbine to marine propulsion, written by Parsons in 1903, will be found in 'Trans. Inst. Nav. Architects,' vol. 45, p. 284; it contains as an appendix a copy of my report describing the *Turbinia* trials of 1897.

Another time, when the operation of fixing the blades in a turbine was a rather novel job, a dispute arose as to how it should be treated in the reckoning of piece-work. At the dinner hour Parsons and one of his staff went in, locked the door, and took off their coats. When the men came back they admitted they must revise their notions of the amount of blading that would constitute a fair day's work. His men had unbounded respect for a chief who not only had the obvious qualities of master, but could say, "I have served my time as well as you," and could show, as he did, that the time served in the "shops" had not been misspent, and had given him a skill in craftsmanship equal to their own.

In early experiments with the *Turbinia* a problem presented itself which gave Parsons much trouble. It was already known that a screw-propeller, if turning too fast, might waste its effort by creating vacuous spaces in the water which afterwards collapsed. The phenomenon had been noticed a few years before by Sir John Thornycroft and Mr. Barnaby and had been called by them "cavitation." When Parsons began marine propulsion he found that this imposed a sharp limit on the permissible rate of revolution. The speed had to be a compromise; a high speed was to the advantage of the turbine; on the other hand, if too high it would lead to much cavitation. Accordingly he made a careful study of the conditions under which cavitation would occur, using for the purpose an experimental tank with glass sides where he could observe the action of the screw-blades under momentary illumination and note the effects of varying their speed, pitch, diameter and blade-surface. By the help of such experiments he was able to design turbines and propellers, directly coupled, which could serve effectively for all kinds of fast ships, however large. It was on these lines that turbine propulsion came quickly into favour.

The Admiralty, after trying turbines in destroyers and the cruiser *Amethyst*, were so well satisfied as to adopt them in the *Dreadnought* (1905) and in all new ships. Before long other navies were following the British lead. In the merchant service the first turbine-driven vessel was the Clyde steamer *King Edward* (1901), which was found to consume 15 per cent. less coal than a sister ship with triple-expansion engines. This was followed by the *Quern* and other cross-Channel packets, and soon by several Atlantic liners. The advantages were so conspicuous that in 1904, when plans were under discussion for building the two great Cunarders *Lusitania* and *Mauritania*, then unprecedented in size and power, it was recommended by a committee of experts that turbines should be employed. The decision was a bold one, remarkable as evidence of the faith already felt in Parsons' ability to adapt his invention to untried conditions. As everybody knows, it was amply justified by the event. Turbines developing 70,000 shaft horse-power were provided for each ship and were entirely successful. The turbine had established its position as the normal means of propelling the largest ships both in the Navy and the mercantile marine.

Up to that time, and for some years after, the practice was to couple the turbine directly to the propeller shaft. Parsons, however, was dissatisfied with the compromise of speeds which this entailed. He saw that to secure the best effect the turbine should run fast and the propeller slow. This meant that some form of gearing should be put between them. Moreover, so long as direct coupling was retained, the turbine was suitable only for high-speed ships; with gearing it could be applied as well to cargo boats and slow craft generally. From the first he had contemplated gearing as a possible feature; his earliest patent for marine propulsion (No. 394 of 1894) contains the following comprehensive claim:—

“(1) Propelling a steam vessel by means of a steam turbine, which turbine actuates the propeller or paddle shaft directly or through gearing.”

He decided to try a simple mechanical gear, by putting a small pinion on the turbine shaft which should drive a large wheel on the propeller shaft, through cut teeth of helical form. Accordingly in 1909 the Parsons Marine Steam Turbine Company (a concern which had been formed to take over the marine side of the business) bought an old cargo steamer, the *Vespasian*, the engines of which were of the triple-expansion type. These were taken out and a turbine was substituted with a reducing gear which let the turbine shaft run nearly twenty times as fast as the propeller shaft. The gear worked smoothly; it was found that the loss of power in transmission was almost negligible; and the consumption of fuel was much less than with the old engines. This experiment marks another epoch. Before long it led to the complete abandonment of direct driving in marine turbines and to the universal use of some form of reducing gear, even in the fastest ships. In some instances double-reduction gear, with an intermediate shaft, has been used, but as a rule there is only one step down.

To transmit many thousands of horse-power through the teeth of gear wheels was a new problem. Parsons solved it successfully by his devices for cutting the teeth with extreme accuracy, and by suitable selection and heat-treatment of the steel in which the teeth are cut. Occasionally an electrical transmission of power from the turbine to the propeller shaft is resorted to, but the simple mechanical connection by toothed wheels is much more usual both in naval and mercantile practice. A large-scale example is to be found in the battle-cruiser *Hood* where 144,000 horse-power is transmitted to the propellers through single-reduction gearing. In a fast new Cunarder of some 75,000 tons, the building of which is now in progress (1931), it is understood that the engines will be single-g geared Parsons turbines developing about 175,000 horse-power.

Concurrently with its adoption as a marine engine the steam turbine has become the chief means of generating electricity in countries which depend

for power upon the use of fuel. For this purpose, apart from its high efficiency as a converter of heat into mechanical effect, there is a marked advantage in a prime-mover which gives very fast rotary motion, with no vibration, and can be built in compact units each with an immense concentration of power. The requirements of great electric stations are met by turbo-alternators, often developing 50,000 kilowatts or more. In these machines the turbine gives rapid rotation to a two-pole or four-pole field-magnet and thereby generates alternating currents in the coils of the surrounding stator, which are insulated to stand a high potential and are kept cool by a forced circulation of air. The speed is commonly either 3,000 or 1,500 turns per minute, to suit the now usual frequency of 50 cycles per second. Alternators of this type were built by Parsons as early as 1905, generating current at 11,000 volts. In a recent paper* he describes one designed to generate 25,000 kilowatts at 33,000 volts, this exceptionally high potential being made possible by a novel method of winding the stator coils. In the whole development of the modern alternator Parsons took from the first a prominent part.

Another of his services has been to advocate high steam-pressure and high superheat, and to design his turbines for such conditions. His influence did much to promote these features of present-day practice. He urged their importance at the first World Power Conference in London in 1924, and again at the second Conference in Berlin in 1930. He gave an effective demonstration of them in the Clyde river steamer *King George V* which was placed on service in 1926, and this has led to their application in various large ships. He had already supplied to a power station in Chicago a turbo-alternator of 50,000 kilowatts in which the steam-pressure was 600 lb. per square inch and the temperature 750° F., but to apply similar conditions on board ship was a new departure. These examples will sufficiently indicate how Parsons kept his position to the last as an active leader in the progress of steam engineering.

The steam turbine, like any other heat-engine, has its efficiency determined by the range of temperature through which the working substance is carried in its cycle of operations, and by the degree to which its action conforms to the ideal cycle of Carnot. From the thermodynamic point of view, Parsons' work may be summarised by saying that he brought the actual steam cycle nearer to the cycle of Carnot, and also that he enlarged the effective range of temperature both by raising the limit at which heat is received and by lowering the limit at which heat is rejected. The steam turbine made these changes practicable. It raised the limit of reception by facilitating the use of high

* "Direct generation of alternating current at high voltages," by Sir Charles Parsons and J. Rosen, 'J. Inst. Elect. Eng.' September, 1929. Particulars of other modern turbo-alternators, some of which generate over 150,000 kilowatts, will be found in a paper read by Mr. C. D. Gibb, of the Parsons Company, at the Institution of Mechanical Engineers, in April, 1931.

pressure and high superheat. At the other end, it let the steam expand usefully all the way down to the pressure of the condenser ; and, in addition, one of Parsons' subsidiary inventions—the " vacuum augments "—reduced the temperature of condensation nearly to that of the condensing water. The turbine brings the action of the working substance closer to the Carnot ideal in several respects ; it avoids the alternate give and take of heat between steam and metal which is a cause of loss in all reciprocating steam engines ; it also allows regenerative feed-heating to be adopted, by which the condensed water has its temperature gradually raised before it is returned to the boiler. The general effect of Parsons' inventions has been to double, and more than double, the efficiency with which heat is converted into other forms of energy through the agency of steam.

In his later life Parsons gave much attention to work of another type. For many years he had carried on at Heaton a manufacture of parabolic reflectors for searchlights—an offspring, one may say, of his father's interest in specula. The searchlight mirrors were made from selected plate glass which was softened and formed over moulds of suitable shape ; then carefully annealed to prepare them for the subsequent process of grinding and polishing which was carried out on a special machine devised by Parsons to preserve the parabolic form of the mirror. Finally the back surface received a deposit of highly reflecting silver. By this process Parsons produced mirrors of great efficiency and moderate cost, remarkable not only for their reflecting power but also for the accuracy of their parabolic figure. Made in many sizes ranging up to a diameter of 7 feet, they have found, and still find, wide application. They bear the fierce heat of the arc-lamp without damage, and their lightness makes manipulation easy. In one form the mirror is divided vertically in halves which can be adjusted to split the beam of light into two parts with a dark space between—an arrangement particularly serviceable in certain cases, as, for example, in assisting the passage of a ship through the Suez Canal.

Since about 1890, when the Heaton works were started, these reflectors have been a minor but by no means unimportant product. For long they were the only item which could be said to represent Parsons' concern with optics. But after the death of his son, who was killed in the last year of the war, a friend who saw his need of distraction suggested that there was much useful work to be done in the manufacture of optical instruments and optical glass. This led Parsons to acquire a controlling interest in the business of Ross, Limited, of which firm he became Chairman. As his interest in optical matters grew he went on to think about the construction of large lenses, and because he had ideas as to possible methods of making the necessary large discs of glass, he felt it would be advisable to be in a position to control the manufacture of the optical glass which he would require. It happened at the time that there was an opportunity of purchasing the Derby Crown Glass Works, which were

instituted during the war and were producing optical glass of high quality. He bought them, and the firm has become well known as the Parsons Optical Glass Company. Experiments in making large discs at Derby were brought to a successful issue as a result of Parsons' ingenuity in devising new methods which are now in operation and are considered by experts to be of particular value. In the meantime he arranged for a partnership with Sir Howard Grubb & Co., the well-known makers of astronomical instruments, and established at Heaton a workshop in which telescopes of any size could be built, a site being selected close to the turbine works so that their machinery might serve for any heavy operations. This business was rapidly growing when he died. Using the glass made at his works in Derby, the firm had already completed a 36-inch reflecting equatorial for the Royal Observatory at Edinburgh, and was engaged on one of 74 inches for Toronto, as well as many more. In these multifarious activities there was no sign of waning interest or failing powers. Parsons could still bend his mind to unaccustomed tasks and find fresh solutions of old problems.

A pursuit which cost him much both in money and effort was the attempt to make diamonds. Under what conditions would carbon crystallise? The question attracted him as a physicist, and he brought to bear on it the resources of the engineer, with all his own skill and daring in experiment. As early as 1888 he described ('Proc. Roy. Soc.,' vol. 44) researches on carbon at high temperatures and under great pressures, the primary object then being to obtain forms of carbon which would be specially suitable for the electric arc and for incandescent lamps. Incidentally he obtained minute particles of a very hard substance, "some compound of lime, silica, and carbon, or perhaps pure carbon only." Further results were given in a paper of 1907 ('Proc. Roy. Soc.,' A, vol. 79) and in his Bakerian Lecture of 1918 ('Phil. Trans,' A, vol. 220). Using a press which was placed for safety in an armoured chamber, he applied large electric currents to bring carbon to an intensely high temperature under pressures ranging up to 15,000 atmospheres; but it showed no sign of melting. Changing the mode of attack, he produced still more extreme conditions through the impact of a bullet fired into a hole in a steel block. In another series of experiments he tried to crystallise carbon *in vacuo*. So far as the formation of diamonds was concerned, all his attempts gave negative results.

If Parsons ever approached an admission of defeat it was here. Only a few days before he left England on his last voyage, he showed me—rather wistfully it seemed—a collection of natural diamonds he had lately acquired, in which each stone projected from its matrix of blue clay. Here was Nature's work. What was her method? He was as far as ever from being able to tell. But I think he hoped to try again.

It was no doubt in connection with this enquiry that he suggested, in a

Presidential Address to Section G of the British Association in 1904, the desirability and feasibility of sinking a deep bore-hole to examine the earth's crust. He discussed the procedure that might be adopted in boring to a depth of 12 miles, and the probable cost. Reverting to the subject in his address as President of the Association at the Bournemouth meeting in 1919, he remarked :—

“ The expense seems trivial as compared with the possible knowledge that might be gained by an investigation into this unexplored region of the earth. It might indeed prove of inestimable value to science, and also throw additional light on the internal constitution of the earth in relation to minerals of high specific gravity. In Italy, at Lardarello, bore-holes have been sunk which discharge large volumes of high-pressure steam, which is being utilised to generate about 10,000 horse-power by turbines. . . . It seems, indeed, probable that in volcanic regions a very large amount of power may be, in the future, obtained directly or indirectly by boring into the earth, and that the whole subject merits the most careful consideration.”

The address also refers to another of his scientific enquiries. It had been noticed that the propellers of ships were liable to a species of erosion which took the form of a pitting of the blades. In 1915 a committee was appointed by the Admiralty to examine this matter. Parsons, who was Chairman of the committee, ascribed the action to the “ water-hammer of collapsing vortices,” when the propellers were producing cavitation ; in other words, to the intense blows which are struck upon minute areas of the surface of the metal when vacuous cavities in the adjacent water suddenly close. He compares the phenomenon to the well-known fact that nearly all the energy of the arm that swings a whip is finally concentrated in the tag. At a later date, a pitting action which is observed in condenser tubes was found to be a possible consequence of the same cause.*

In 1926 Parsons collected and republished the scientific papers of his father, giving an account of the great telescope at Birr and of observations made with it. The volume includes certain letters written in 1854, urging on the naval authorities the practicability of constructing a “ floating battery ” or ironclad, an idea then apparently new.

The fertility of Parsons as an inventor is shown by the list of his British patents which number over 300. Turbines, electrical machines and their parts are the chief subjects ; but there are many more.

* For accounts of these investigations see papers on “ Investigations into the causes of corrosion or erosion of propellers ” by Sir Charles Parsons and S. S. Cook, ‘ Trans. Inst. Naval Architects,’ 1919, and “ Some investigations into the cause of erosion of the tubes of surface condensers,” by Sir Charles Parsons, ‘ Trans. I.N.A.,’ 1927 ; also “ Erosion by water-hammer,” by S. S. Cook, ‘ Proc. Roy. Soc.,’ A., vol. 119 (1928).

Among his minor devices was the Auxetophone, better known in the domestic circle as the Bellowphone. It was a loud speaker which could greatly reinforce the sound of a gramophone or musical instrument, the vibration being magnified by means of an air-valve relay. A mention of it will be found in recollections by Lady Parsons which are quoted below.

Another early toy of particular interest was a little flying machine with a spirit engine working a propeller. This was made by Parsons in 1893; he gave an account of it in 'Nature' of June 18, 1896, along with photographs which show the machine at rest and in flight. A feature of the engine was that the spirit vapour, after doing work in the cylinder, was not discharged into the air, but passed to a combustion chamber under the boiler where it served as fuel to evaporate more spirit. The machine had a tail and wings made of cane framework covered with silk; the span of the wings was 11 feet. When gently launched by hand it would fly for 100 yards or so, coming down only when all the spirit was consumed.

In 1884 Parsons married Katharine, daughter of Mr. W. F. Bethell, of Rise Park, East Yorkshire. She shared his anxieties and his triumphs and was with him in his last journey. They had two children, a son—Major A. G. Parsons, R.A.—who was killed in action in 1918 at the age of 31, and a daughter who inherited more than a little of her father's taste for mechanics. Lady Parsons writes :—

"I first knew Charles in 1883. He was then working at Kitsons in Leeds where his brother Clere was a director; he had recently left the Elswick firm where he had been a premium pupil. At Kitsons he had a small workshop and a mechanic and was experimenting with a torpedo. Charles had the character of being an extraordinary and weird young man socially but it was understood he was a great genius. We were married in January 1884, and, after a few days' honeymoon, went into lodgings in Leeds. Charles was immensely keen about the torpedo and used to take the mechanic and me to Roundhay Lake at 7 a.m. There they spent hours trying the torpedo while I shivered on the bank.

"Charles was already thinking out the turbine idea. He made models from cotton reels with cardboard blades stuck on with sealing-wax. He was also trying new ways of winding dynamos. The turbine idea developed very rapidly and soon small experimental machines were constructed. But at that time Clarke, Chapman & Co. were building up a business on other lines and could not encourage expensive experiments."

And later: "Charles used to make all sorts of amusing toys. 'The Spider,' a little spirit engine, carried on three wheels, that careered at a great pace round our lawn, with the two children, Charles and three dogs rushing and shouting after it. A very pretty toy was a little flying machine with a spirit boiler. It was photographed in full flight, and the photograph has often been reproduced in 'flying' papers.

"About that time Charles, who had never ridden a horse, thought he would come out hunting with me. He bought a hunter, knew nothing at all of horses or riding, and out he came. He was perfectly undaunted, galloped as hard as he could and charged everything that came in his way. That particular hunt still talks with amusement and wonder at his courage.

"We always had a workshop in our house where Charles spent most of his time at home, working till 2 or 3 a.m. The most trying time for the family was when he was producing the 'Bellowphone.' Strange and weird were the noises through the nights. The finished Bellowphone was a very sweet and beautiful instrument when played by him at home, with the sound coming through a gigantic trumpet. He used to place it in the garden, and people from miles round came flocking into our park to hear it. After that many experiments on the making of diamonds were undertaken both at home and in the works. He had immense faith in the possibility of making diamonds, and microscopic particles claiming to be diamonds were often shown us. In later years Charles, with his usual courage, admitted his diamonds were not the real thing.

"The outstanding feature to me of his whole life was his power of concentration; nothing disturbed him when he was absorbed in a problem—no noises, no discomfort, no time and no meals. He was perfectly oblivious to them all. The other great feature was his sublime courage. He never admitted defeat; he was always hopeful about any concern he undertook, and looked forward, even in his last days, to making a success of the new kind of work he had undertaken when well over the age of 70 years."

As was to be expected, the achievements and the personality of Parsons brought a host of honours and rewards. He was made C.B. in 1904, K.C.B. in 1911, and was admitted to the Order of Merit in 1927. He was elected F.R.S. in 1898, was a vice-president 10 years later, and was Bakerian Lecturer in 1918. He received the Rumford medal in 1902 and the Copley medal—the Society's highest award—in 1928. He was an honorary Doctor of many universities, including Cambridge, Oxford, Edinburgh, Glasgow, Dublin, Durham, Leeds, Liverpool, Toronto and Pennsylvania. Other recognitions were the Albert Medal of the Royal Society of Arts, the Kelvin Medal, the Faraday Medal of the Institution of Electrical Engineers, the Franklin Medal of the Franklin Institute of Philadelphia, and the Bessemer Medal of the Iron and Steel Institute which was given him in acknowledgment of his services to metallurgy. He was President of the British Association in 1919. He served also as President of the Institute of Physics, and of the North-East Coast Institution of Engineers and Shipbuilders. In 1914 he received the freedom of the City of Newcastle.

He was a generous donor to the funds of many learned societies, especially to the British Association, the Royal Institution, the Royal Society, and the

Royal Society of Arts. Shortly after the Department of Scientific and Industrial Research was established he became a member of its Advisory Council. Before that, he had been an original member of the Board of Invention and Research which was set up by the late Lord Balfour in 1915 for the purpose of finding applications of Physics, Chemistry, and Engineering of a kind that would be of service during the war. Sir Joseph Thomson, who was another active member of the small central committee of that Board, bears witness* to the whole-heartedness with which Parsons threw himself into the work, and adds this appreciation :—

“ Besides being by far the greatest and most original engineer this country has had since the time of Watt, he was one of the kindest and most steadfast of friends, and his death has made in the lives of many a gap which will not be filled.”

With these words, as true as they are authoritative, this notice may appropriately close.

In preparing it I have had much help from Lady Parsons, Canon Randal Parsons, the Master of St. John's, Sir Joseph Larmor, Mr. Pendlebury, Lieut.-Col. Kitson Clark, Sir Dugald Clerk, Lord Rayleigh, Sir Herbert Jackson, Professor Sampson, Mr. J. H. Barker, and Mr. Stanley S. Cook. The portrait is from a painting by Sir William Orpen : its date is 1922.

J. A. E.

* ‘ The Times,’ February 16, 1931.

INDEX to VOL. CXXXI. (A)

- Acetylene and electrolytic gas, explosions (Bone and others), 1.
 Alpha-particles, analysis of long-range (Rutherford and others), 684.
 Alpha-particles, valve methods of recording (Wynn-Williams and Ward), 391.
 Alty (T.) The Reflection of Vapour Molecules at a Liquid Surface, 554.
- Badami (J. S.) *See* Rao and Badami.
 Bannister (L. C.) *See* Evans and others.
 Basset (A. B.) Obituary, i.
 Bengough (G. D.), Lee (A. R.) and Wormwell (F.) The Theory of Metallic Corrosion in the Light of Quantitative Measurements, IV, 494.
 Bone (W. A.), Fraser (R. P.) and Lake (F.) Explosions of Mixtures of Acetylene and Electrolytic Gas, 1.
 Britton (S. C.) *See* Evans and others.
 Browning (C. H.), Cohen (J. B.), Ellingworth (S.) and Gulbransen (R.) The Antiseptic and Trypanocidal Action of certain Styryl and Anil Benzthiazole Derivatives. (Abstract), 273.
 Butler (J. A. V.) and Lees (A. D.) The Behaviour of Electrolytes in Mixed Solvents, III, 382.
- Chlorine monoxide, decomposition, kinetics (Moelwyn-Hughes and Hinshelwood), I, 177.
 Chlorine vapour, chemical constant (Stern), 339.
 Circular shafts, torsion problem (Thom and Orr), 30.
 Cohen (J. B.) *See* Browning and others.
 Cohen (J. B.), Cooper (K. E.) and Marshall (P. G.) Some Aliphatic and Aromatic Amino Derivatives of α -Quinoline Methiodide. (Abstract), 274.
 Colborne (D. C.) The Diurnal Tide in an Ocean bounded by Two Meridians, 38.
 Collie (C. H.) The Decay Constant of Uranium II, 541.
 Cooper (K. E.) *See* Cohen and others.
 Cooper (B. S.) *See* Ryde and Cooper.
 Corrosion, theory of metallic (Bengough and others), 494.
 Corrosion, velocity, from electrochemical standpoint (Evans and others), 355.
 Cubic curves, twisted (Todd), 286.
- Davidson (P. M.) *See* Richardson and Davidson.
 Deodhar (G. B.) Some Investigations in Röntgen Spectra, I, 633.
 Deodhar (G. B.) X-Ray Nondigram Lines, 476.
 Dhavale (D. G.) The Spectrum of Singly Ionised Antimony, 109.
 Diurnal tide in ocean bounded by two meridians (Colborne), 38.
 Dulcitol, X-ray study (Marwick), 621.
 Dyes, colloid chemistry (Robinson and Mills), 576, 596.
- Electrolytic gas, explosions with acetylene (Bone and others), 1.
 Electrolytes, behaviour in mixed solvents (Butler and Lees), 382.
 Electron and proton, metrical theory (Flint), 170.

- Ellingworth (S.) *See* Browning and others.
- Ethyl alcohol (Morgan and Taylor), 533.
- Evans (U. R.), Bannister (L. C.) and Britton (S. C.) The Velocity of Corrosion from the Electrochemical Standpoint, 355.
- Flint (H. T.) A Metrical Theory and its Relation to the Charge and Masses of the Electron and Proton, 170.
- Foster (J. S.) The Effect of Combined Electric and Magnetic Fields on the Helium Spectrum, II, 133.
- Fraser (R. P.) *See* Bone and others.
- Fuller's earth, adsorption (Phelps), 17.
- Goldstein (S.) The Forces on a Solid Body Moving through Viscous Fluid, 198.
- Gulbransen (R.) *See* Browning and others.
- Hartree (D. R.) Optical and Equivalent Paths in a Stratified Medium Treated from a Wave Standpoint, 428.
- Havelock (T. H.) The Wave Resistance of a Spheroid, 275.
- Helium spectrum, electric and magnetic fields (Foster), 133.
- Hexa-aminobenzene, molecular symmetry (Knaggs), 612.
- Hinshelwood (C. N.) *See* Moelwyn-Hughes and Hinshelwood.
- Hydrogen, molecular, stark-effect (MacDonald), 146.
- Jenkin (C. F.) The Pressure Exerted by Granular Material : an Application of the Principles of Dilatancy, 53.
- Kannuluik (W. G.) On the Thermal Conductivity of some Metal Wires, 320.
- Kapitza (P.) The Study of the Magnetic Properties of Matter in Strong Magnetic Fields, I, II, 224, 243.
- Knaggs (I. E.) The Molecular Symmetry of Hexa-aminobenzene in the Crystalline State, and certain other Properties of the Substance, 612.
- Lake (F.) *See* Bone and others.
- Lee (A. R.) *See* Bengough and others.
- Lees (A. D.) *See* Butler and Lees.
- Lewis (W. B.) *See* Rutherford and others.
- Light, scattering by turbid media (Ryde and Cooper), 451, 464.
- Light, transmission by metal films (Rama Swamy), 307.
- Lithium chloride, molecular refractivities (Butler and Lees), 382.
- MacDonald (J. K. L.) Stark-Effect in Molecular Hydrogen in the Range 4100-4770 Å, 146.
- Magnetic properties in strong magnetic fields (Kapitza), 224, 243.
- Mannitol, X-ray study (Marwick), 621.
- Mannose, X-ray study (Marwick), 621.
- Marshall (P. G.) *See* Cohen and others.
- Marwick (T. C.) An X-ray Study of Mannitol, Dulcitol and Mannose, 621.
- McDowell (C. M.) and Usher (F. L.) Viscosity and Rigidity in Suspensions of Fine Particles, I, II, 409, 564.
- Melchett (Lord) Obituary, ii.
- Mills (H. A. T.) *See* Robinson and Mills.

Moelwyn-Hughes (E. A.) and Hinshelwood (O. N.) The Kinetics of Reactions in Solution, I, II, 177, 186.

Mordell (L. J.) The Arithmetically Reduced Indefinite Quadratic Form in n -Variables, 99.

Morgan (G. T.) and Taylor (R.) Ethyl Alcohol, A Product of High-pressure Syntheses, 533.

Mosharrafa (A. M.) Material and Radiational Waves, 335.

Night sky of exceptional brightness (Rayleigh), 376.

Obituary Notices :—

Basset (A. B.), i.

Melchett (Lord), ii.

Parsons (Sir Charles), v.

Optical and equivalent paths in a stratified medium (Hartree), 428.

Organic liquids, binary systems (Trew and Spencer), 209.

Orr (J.) See Thom and Orr.

Parsons (Sir Charles) Obituary, v.

Periodicity in series of related terms (Walker), 518.

Phelps (H. J.) The Adsorption of Substances by Fuller's Earth, 17.

Polar aurora and the night sky, distinction (Rayleigh), 376.

Pressure exerted by granular material (Jenkin), 53.

Quadratic form in n -variables (Mordell), 99.

Radium C, analysis of long-range α -particles (Rutherford and others), 684.

Radium E, spectrum (Terroux), 90.

Rama Swamy (S.) On the Transmission of Light by Thin Films of Metal, 307.

Rao (K. R.) and Badami (J. S.) Investigations on the Spectrum of Selenium, I, 154.

Rayleigh (Lord) On a Night Sky of Exceptional Brightness, and on the Distinction between the Polar Aurora and the Night Sky, 376.

Richardson (O. W.) and Davidson (P. M.) The Spectrum of H_2 , 658.

Robinson (C.) and Mills (H. A. T.) The Colloid Chemistry of Dyes, I, II, 576, 596.

Rutherford (Lord), Ward (F. A. B.) and Lewis (W. B.) Analysis of the Long-range α -Particles from Radium C, 684.

Ryde (J. W.) The Scattering of Light by Turbid Media, I, 451.

Ryde (J. W.) and Cooper (B. S.) The Scattering of Light by Turbid Media, II, 464.

Selenium spectrum (Rao and Badami), 154.

Spectrum of antimony (Dhavale), 109.

Spectrum of H_2 (Richardson and Davidson), 658.

Spectrum of radium E (Terroux), 90.

Spectrum, selenium (Rao and Badami), 154.

Spectra, röntgen, investigations (Deodhar), 633.

Spencer (J. F.) See Trew and Spencer.

Stanton (Sir Thomas) The Development of a High-speed Wind Channel for Research in External Ballistics, 122.

- Stern (T. E.) The Chemical Constant of Chlorine Vapour and the Entropy of Crystalline Chlorine, 339.
- Taylor (R.) *See* Morgan and Taylor.
- Terroux (F. R.) The Upper Limit of Energy in the Spectrum of Radium E, 90.
- Thermal conductivity of some metal wires (Kannuliik), 320.
- Thom (A.) and Orr (J.) The Solution of the Torsion Problem for Circular Shafts of Varying Radius, 30.
- Todd (J. A.) On Twisted Cubic Curves which Satisfy Twelve Conditions, 286.
- Torsion problem for circular shafts (Thom and Orr), 30.
- Trew (V. C. G.) and Spencer (J. F.) The Magnetic Susceptibility of Binary Systems of Organic Liquids, 209.
- Trinitrobenzoic acid, decomposition, kinetics (Moelwyn-Hughes and Hinshelwood), 186.
- Uranium II, decay constant (Collie), 541.
- Usher (F. L.) *See* McDowell and Usher.
- Vapour molecules, reflection at liquid surface (Alty), 554.
- Viscosity and rigidity of fine particles (McDowell and Usher), 409.
- Viscous fluid on a solid body (Goldstein), 198.
- Walker (Sir Gilbert) On Periodicity in Series of Related Terms, 518.
- Ward (F. A. B.) *See* Rutherford and others.
- Ward (F. A. B.) *See* Wynn-Williams and Ward.
- Wave resistance of a spheroid (Havelock), 275.
- Waves, material and radiational (Mosharrafa), 335.
- Wind channel, development of high-speed (Stanton), 122.
- Wormwell (F.) *See* Bengough and others.
- Wynn-Williams (O. E.) and Ward (F. A. B.) Valve Methods of Recording Single Alpha-Particles in the Presence of Powerful Ionising Radiations, 391.
- X-ray nondiagram lines (Deodhar), 476.
- X-ray study of mannitol, dulcitol and mannose (Marwick), 621.

IMPERIAL AGRICULTURAL RESEARCH
INSTITUTE LIBRARY
NEW DELHI

Date of issue.	Date of issue.	Date of issue.
24.5-857		
1 MAY 1967		
24 NC	9	